Bionatura

Latin American journal of Biotechnology and Life Sciences

VI CONGRESO INTERNACIONAL DE BIOTECNOLOGÍA Y BIODIVERSIDAD 2022
BIOTECNOLOGÍA Y BIODIVERSIDAD PARA EL DESARROLLO
SOSTENIBLE DE NUESTRA SOCIEDAD

Scopus publons

BUCO
Universidad Católica de Oriente

UNAH
UNIVERSIDAD NACIONAL
AUTÓNOMA DE HONDURAS

clinicalbiotec.com

Es el momento de los que se atreven a soñar y luchan por alcanzar sus metas.

En la UCO te acompañamos

UCO
Universidad Católica de Oriente
Acreditación Institucional en
ALTA CALIDAD
Resolución 8869 03/06/2019 del Ministerio de Educación Nacional

Vigilada Mineducación

Pregrados

> ### Tecnología en Operaciones Financieras
SNIES 104841 Registro Calificado - Res. 12903 del 21-06-2015 M.E.N.
95 créditos - A distancia tradicional - Rionegro Ant.

> ### Contaduría Pública
SNIES 13016 Registro Calificado - Res. 9256 del 07- 06- 2018
Acreditación de Alta Calidad 4610 del 21 - 03 - 2018 M.E.N.
165 créditos Presencial - Rionegro

> ### Comercio Exterior
SNIES 1854 Registro Calificado - Res. 14314 del 11-12-2019 M.E.N.
159 créditos - Presencial - Rionegro Ant.

> ### Administración de Empresas
SNIES 55096 Registro Calificado - Res. 7658 del 18-04-2017 M.E.N.
152 créditos - Presencial - Rionegro Ant.

> ### Tecnología Agropecuaria
SNIES 1850 Registro Calificado - Res. 8684 del 10-07-2013 M.E.N.
113 créditos - Presencial - Rionegro Ant.

> ### Agronomía
SNIES 4443 Registro Calificado - Res. 8087 del 17-05-2018
Acreditación de Alta Calidad N° 29149 del 26-12-2017
157 créditos - Presencial - Rionegro Ant.

> ### Zootecnia
SNIES 53037 Registro Calificado - Res. 14466 del 04-09-2014 M.E.N.
156 créditos - Presencial - Rionegro Ant.

> ### Psicología
SNIES 8562 Registro Calificado - Res. 9902 del 31-07-2013 M.E.N.
Acreditación de Alta Calidad N° 17227 del 24 - 10 - 2018
175 créditos - Presencial - Rionegro Ant.

> ### Comunicación Social
SNIES 53045 Registro Calificado - Res. 14892 del 11-09-2014 M.E.N.
146 créditos - Presencial - Rionegro Ant.

> ### Trabajo Social
SNIES 106586 Registro Calificado - Res. 26741 del 29-11-2017 M.E.N.
141 créditos - Presencial - Rionegro Ant.

> ### Derecho
SNIES 53639 Registro Calificado - Res. 10542 del 14-07-2015 M.E.N.
166 créditos - Presencial - Rionegro Ant.

> ### Nutrición y Dietética
SNIES 104601 Registro Calificado - Res. 7823 del 01-06-2015 M.E.N.
166 créditos - Presencial - Rionegro Ant.

> ### Gerontología
SNIES 1853 Registro Calificado - Res. 14639 del 22-10-2013 M.E.N.
138 créditos - A distancia con apoyo virtual - Rionegro Ant.

> ### Enfermería
SNIES 91027 Registro Calificado - Res. 12600 del 03-08-2018 M.E.N.
166 créditos - Presencial - Rionegro Ant.

> ### Licenciatura en Filosofía
SNIES 106542 Registro Calificado - Res. 22108 del 24 - 10 - 2017 M.E.N.
164 créditos - Presencial - Rionegro Ant.

> ### Licenciatura en Lenguas Extranjeras con énfasis en Inglés
SNIES 106647 Registro Calificado - Res. 29529 del 29-12-2017 M.E.N.
164 créditos - Presencial - Rionegro Ant.

> ### Licenciatura en Educación Física, Recreación y Deportes
SNIES 106438 Registro Calificado - Res. 17481 del 31-08-2017 M.E.N.
164 créditos - Presencial - Rionegro Ant.

> ### Licenciatura en Educación para la Primera Infancia
SNIES 105359 Registro Calificado - Res. 02846 del 16-02-2016 M.E.N.
164 créditos - Presencial - Rionegro Ant.

> ### Licenciatura en Ciencias Naturales
SNIES 105896 Registro Calificado - Res.19869 del 18-10-2016 M.E.N.
164 créditos - Presencial - Rionegro Ant.

> ### Licenciatura en Educación Religiosa
SNIES 106705 Registro Calificado - Res. 2084 del 13 - 02 - 2018 M.E.N.
164 créditos - Presencial - Rionegro Ant.

> ### Técnico Profesional en Programación Web
SNIES 103704 Registro Calificado - Res.14454 del 04-09-2014 M.E.N.
67 créditos - Presencial - Rionegro Ant.

> ### Ingeniería Ambiental
SNIES 4361 Registro Calificado - Res. 3654 del 02-03-2018 M.E.N.
Acreditación de Alta Calidad No. 6543 del 18 - 04 - 2018
173 créditos - Presencial - Rionegro Ant.

> ### Ingeniería de Sistemas
SNIES 1855 Registro Calificado - Res. 0178 del 05-01-2019 M.E.N.
164 créditos - Presencial- Rionegro Ant.

> ### Ingeniería Industrial
SNIES 1856 Registro Calificado - Res. 1293 del 04-02-2019 M.E.N.
160 créditos - Presencial- Rionegro Ant.

> ### Ingeniería Electrónica
SNIES 20271 Registro Calificado - Res. 24646 del 14-11-2017 M.E.N.
178 créditos - Presencial- Rionegro Ant.

> ### Teología
SNIES 103450 Registro Calificado - Res. 10638 del 09-07-2014 M.E.N.
130 créditos - A distancia - Rionegro Ant.

¡HAGAMOS QUE PASE!

www.uco.edu.co @uconiano universidad catolica de oriente 322 569 90 90

SOMOS UNA
MACROUNIVERSIDAD
RECTORA DEL NIVEL DE EDUCACIÓN SUPERIOR EN HONDURAS

APROXIMADAMENTE:
100,000 Estudiantes
4,000 Docentes
10 Facultades
9 Centros regionales

DICIHT
DIRECCIÓN DE INVESTIGACIÓN CIENTÍFICA, HUMANÍSTICA Y TECNOLÓGICA

UNAH
UNIVERSIDAD NACIONAL AUTÓNOMA DE HONDURAS

Index in directory of open access journals

Instrucciones para los Autores

Los Trabajos serán Inéditos: Una vez aprobados, no podrán someterse a la consideración de otra revista, con vistas a una publicación múltiple, sin la debida autorización del Comité Editorial de la Revista. La extensión máxima será 8 cuartillas para los trabajos originales, 12 las revisiones y 4 las comunicaciones breves e informes de casos, incluidas las tablas y figuras. Los artículos se presentarán impresos (dos ejemplares). Todas las páginas se numerarán con arábigos y consecutivamente a partir de la primera. Estos deben acompañarse de una versión digital (correo electrónico o CD) en lenguaje Microsoft Word, sin sangrías, tabuladores o cualquier otro atributo de diseño (títulos centrados, justificaciones, espacios entre párrafos, etc.). Siempre se ha de adjuntar la carta del consejo científico que avala la publicación y una declaración jurada de los autores.

Referencias Bibliográficas. Se numerarán según el orden de mención en el texto y deberán identificarse mediante arábigos en forma exponencial. Los trabajos originales no sobrepasarán las 20 citas; las revisiones, de 25 a 50 y las comunicaciones breves e informes de casos.

En las Referencias en caso de que las publicaciones revisadas esten online se debe proveer un enlace consistente para su localización en Internet. Actualmente, no todos los documentos tienen DOI, pero si lo tienen se debe incluir como parte de la referencias. Si no tuviese DOI, incluir la URL.

Tablas, modelos y anexos: Se presentarán en hojas aparte (no se intercalarán en el artículo) y en forma vertical numeradas consecutivamente y mencionadas en el texto. Las tablas se ajustarán al formato de la publicación se podrán modificar si presentan dificultades técnicas.

Figuras: Las fotografías, gráficos, dibujos, esquemas, mapas, salidas de computadora, otras representaciones gráficas y fórmulas no lineales, se denominarán figuras y tendrán numeración arábiga consecutiva. Se presentarán impresas en el artículo en páginas independientes y en formato digital con una resolución de 300 dpi. Todas se mencionarán en el texto. Los pies de figuras se colocarán en página aparte. El total de las figuras y tablas ascenderá a 5 para los trabajos originales y de revisión y 3 para las comunicaciones breves e informes de casos.

Abreviaturas y siglas: Las precederá su nombre completo la primera vez que aparezcan en el texto. No figurarán en títulos ni resúmenes. Se emplearán las de uso internacional.

Sistema Internacional de Unidades (SI): Todos los resultados de laboratorio clínico se informarán en unidades del SI o permitidas por este. Si se desea añadir las unidades tradicionales, se escribirán entre paréntesis. Ejemplo: glicemia: 5,55 mmol/L (100 mg/100 mL).

Para facilitar la elaboración de los originales, se orienta a los autores consultar los requisitos uniformes antes señalados disponibles en: http://www. fisterra.com/recursos_web/mbelvancouver. htm#ilustraciones%20 (figura)

Los trabajos que no se ajusten a estas instrucciones, se devolverán a los autores. Los aceptados se procesarán según las normas establecidas por el Comité Editorial. El arbitraje se realizará por pares y a doble ciego en un período no mayor de 60 días. Los autores podrán disponer de no más de 45 días para enviar el artículo con correcciones, se aceptan hasta tres reenvíos. El Consejo de Redacción se reserva el derecho de introducir modificaciones de estilo y /o acotar los textos que lo precisen, comprometiéndose a respetar el contenido original.

El Comité Editorial de la Revista se reserva todos los derechos sobre los trabajos originales publicados en esta.

Bionatura

La **Revista Bionatura** es un medio especializado, interinstitucional e interdisciplinario, para la divulgación de desarrollos científicos y técnicos, innovaciones tecnológicas, y en general, los diversos tópicos relativos a los sectores involucrados en la biotecnología, tanto en Ecuador como en el exterior; así mismo, la revista se constituye en un mecanismo eficaz de comunicación entre los diferentes profesionales de la biotecnología.

Es una publicación sin ánimo de lucro. Los ingresos obtenidos por publicidad o servicios prestados serán destinados para su funcionamiento y desarrollo de su calidad de edición. (http://revistabionatura.com/media-kit.html)

Es una revista trimestral, especializada en temas concernientes al desarrollo teórico, aplicado y de mercado en la biotecnología.

Publica artículos originales de investigación y otros tipos de artículos científicos a consideración de su consejo editorial, previo proceso de evaluación por pares (peer review) sin tener en cuenta el país de origen.

Los idiomas de publicación son el Español e Inglés.

Los autores mantienen sus derechos sobre los artículos sin restricciones y opera bajo la política de Acceso Abierto a la Información, bajo la licencia de Creative Commons 4.0 CC BY-NC-SA (Reconocimiento-No Comercial-Compartir igual).

Esta revista utiliza Open Journal Systems, que es un gestor de revistas de acceso abierto y un software desarrollado, financiado y distribuido de forma gratuita por el proyecto Public Knowledge Project sujeto a la Licencia General Pública de GNU.

ÍNDICE / INDEX

EDITORIAL

Biotechnology and biodiversity for the sustainable development of our society

Julio Andres Bonilla Jaime
Escuela Superior Politecnica del Litoral, CIBE. Guayaquil, Ecuador.
Corresponding author: jabonill@espol.edu.ec

1

Biotechnology has the potential to play a significant role in the sustainable development of our society. This technology involves using living organisms or their products to develop or modify products or processes for specific use. It is a broad term that encompasses a range of technologies, including genetic engineering, tissue culture, and fermentation. While it has many potential benefits, it must be compatible with biodiversity. Biodiversity refers to the variety of life on Earth, including the different plants, animals, and microorganisms that make up our ecosystems. It is essential for the health and functioning of these ecosystems and the sustainable development of our society[1,2].

Events like the VI Biotechnology and Biodiversity International Congress ("CIBB" for its Spanish name) provide an appropriate space for the industry and biotechnology and biodiversity field scholars to showcase and exchange knowledge. With the participation of top scientists, the VI CIBB 2022 delivered their most recent discoveries and highlighted the close relationship between biotechnology and biodiversity for the sustainable development of our society. During the event's four days, topics relevant to biotechnology development and biodiversity were discussed. Researchers from more than seven countries participated and shared their results in impressive dynamic sessions with more than 200 attendees of the event. These areas were discussed within the themes of scientific advances in banana and cocoa, biotechnology and biodiversity, bioproducts, bioremediation and phytopathology.

Biotechnology can positively impact society by improving the efficiency and sustainability of agricultural practices. For example, genetically modified crops can be developed to be more resistant to pests and diseases, reducing the need for pesticides and herbicides[3]. This can lead to improved crop yields and a reduced environmental impact. In addition, biotechnology can be used to develop more nutritious crops or have longer shelf lives, which can help address food insecurity and waste[4,5].

Advancements in biotechnology can also be used to improve environmental conservation efforts. For example, bioremediation involves using microorganisms to clean up contaminated soil and water. This technology can be used to remove pollutants from the environment, making it safer for plants and animals. In addition, biotechnology can be used to develop renewable energy sources, such as biofuels, which can help to reduce our reliance on fossil fuels and combat climate change[6]. The design of high-value-added biobased goods using clean technologies, such as food additives, agricultural bio inputs, crop biofortification, and engineered microorganisms, is currently proving to be fertile ground for collaboration between scientists and the corporate sector (Figure 1).

The most excellent strategy for attaining the goals of academics and the industrial sector is teamwork, despite many obstacles to overcome. This will be accomplished only by creating a solid coalition between the society, industrial and academic sectors[8]. I urge the replication of events like the VI CIBB and encourage our society to get involved and participate more than ever in choosing the course that research should take in our regions.

Overall, biotechnology plays a significant role in the sustainable development of our society. Through the development of new medical treatments, improved agricultural practices, and environmental conservation efforts, biotechnology can help to improve the lives of individuals and communities around the world. All of these, without ignoring the potential impacts of biotechnology on biodiversity, ensure that it is used in a sustainable and responsible way.

Bibliographic references

1. "What is biodiversity? | Pages | WWF." https://www.worldwildlife.org/pages/what-is-biodiversity (accessed Dec. 06, 2022).
2. "Biotechnology: effective solutions for sustainable development | UNESCO." https://www.unesco.org/en/articles/biotechnology-effective-solutions-sustainable-development (accessed Dec. 06, 2022).
3. J. A. Anderson et al., "Genetically engineered crops: Importance of diversified integrated pest management for agricultural sustainability," Front Bioeng Biotechnol, vol. 7, no. FEB, p. 24, Feb. 2019, doi: 10.3389/FBIOE.2019.00024/BIBTEX.
4. S. S. e. A. Zaidi, A. Mahas, H. Vanderschuren, and M. M. Mahfouz, "Engineering crops of the future: CRISPR approaches to develop climate-resilient and disease-resistant plants," Genome Biology 2020 21:1, vol. 21, no. 1, pp. 1–19, Nov. 2020, doi: 10.1186/S13059-020-02204-Y.
5. L. T. Hickey et al., "Breeding crops to feed 10 billion," Nat Biotechnol, vol. 37, no. 7, pp. 744–754, Jul. 2019, doi: 10.1038/s41587-019-0152-9.
6. "Biotechnology for the Environment in the Future : Science, Technology and Policy | OECD Science, Technology and Industry Policy Papers | OECD iLibrary." https://www.oecd-ilibrary.org/science-and-technology/biotechnology-for-the-environment-in-the-future_5k4840hqhp7j-en (accessed Dec. 06, 2022).

2
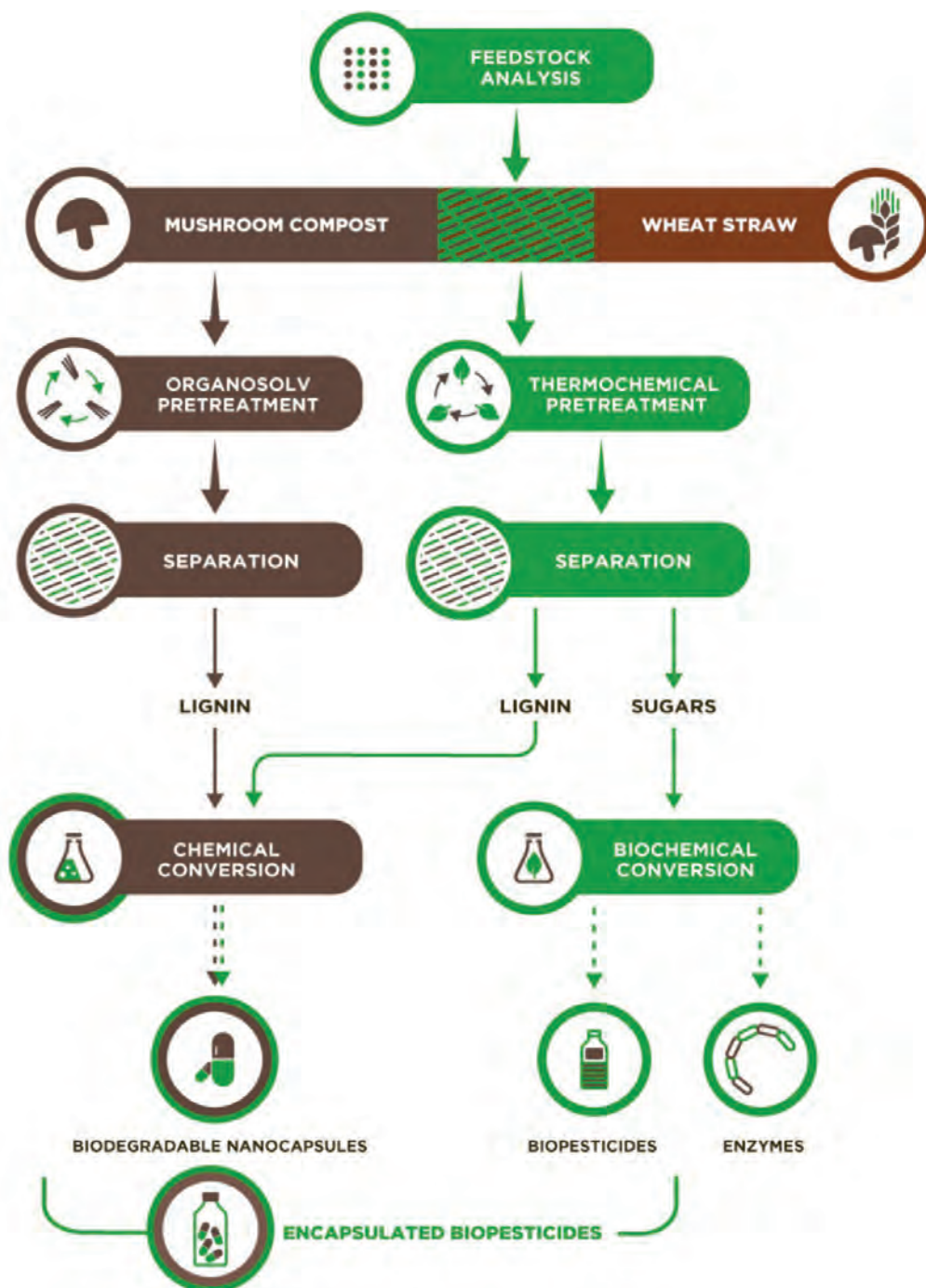
Figure 1. The BIOrescue project developed and tested a resource-efficient biorefinery concept for mushroom compost and other underutilized agricultural feedstocks, allowing their transformation into valuable bio-based products, such as bio-pesticides, biodegradable nano-carriers for drug encapsulation, as well as new enzymes[7].

7. "Research results - Biorescue Project." https://biorescue.eu/research-results/ (accessed Dec. 06, 2022).
8. L. Lange et al., "Developing a Sustainable and Circular Bio-Based Economy in EU: By Partnering Across Sectors, Upscaling and Using New Knowledge Faster, and For the Benefit of Climate, Environment & Biodiversity, and People & Business," Front Bioeng Biotechnol, vol. 8, p. 1456, Jan. 2021, doi: 10.3389/FBIOE.2020.619066/BIBTEX.

ARTICLE / INVESTIGACIÓN

Development of enhanced primer sets for detection of Norovirus and Hepatitis A in food samples from Guayaquil (Ecuador) by reverse transcriptase-heminested PCR

E. J. Salazar[1,2]*, M. J. Guerrero[3], J. A. Villaquiran[3], K.S. Suárez[4], and J.M. Cevallos[1,5]

[1] Centro de Investigaciones Biotecnológicas del Ecuador, Escuela Superior Politécnica del Litoral, Guayaquil, Ecuador.
[2] Facultad de Ciencias Agropecuarias, Universidad Técnica de Babahoyo, Km 7.5 Vía Babahoyo - Montalvo, Ecuador.
[3] Facultad Ciencias de la Vida, Laboratorio para Investigaciones Biomédicas, Escuela Superior Politécnica del Litoral, Guayaquil, Ecuador.
[4] Facultad de Ingeniería Mecánica y Ciencias de la Producción, Escuela Superior Politécnica del Litoral, Guayaquil, Ecuador.
[5] Facultad Ciencias de la Vidas, Escuela Superior Politécnica del Litoral, Km 30.5 Vía Perimetral, P.O. Box 09-01-5863, Guayaquil, Ecuador.
Corresponding author: enriquesalazarll27@hotmail.com

Abstract: Norovirus (NV) is an infectious biological agent that causes gastrointestinal problems of the original nonbacterial appearance of foodborne illnesses. The genotype of NV responsible for the most frequent NV disease outbreaks is GII, accounting for 60–80% of the cases. Moreover, original and new NV variants are continuously emerging, concurrent with the recent global increase in NV infections. Hepatitis A virus (HAV) is another foodborne pathogen frequently implicated in acute gastroenteritis cases around the world. The virus is transmitted among humans via the fecal-oral route, and infection by HAV causes the most severe form of viral illness acquired from foods. In this study, we implemented primer sets to detect NV genotypes I and II. We also developed primer sets for the detection of HAV. The primers were used in a heminested reverse transcriptase PCR (hnRT-PCR) protocol that was rapid and sensitive for detecting NVG1, NVGII and HAV virus in food. The hnRT-PCR was applied successfully to strawberries and spinach obtained from a local fresh-food market, where we could see NVGI, NVGII and HAV.

Key words: Norovirus[1], Hepatitis A[2], gastroenteritis[3], genotypes[4], NVG1[5], NVGII[6], hnRT-PCR[7].

Introduction

Norovirus (NV), family Caliciviridae, is a major cause of acute viral gastroenteritis in humans[1]. Disease onset typically appears between 12 and 48 h after infection, and although symptoms are usually mild and self-limited, they can be severe in immunocompromised patients and the elderly[2]. NV disease is considered a foodborne illness, but person-to-person transmission and waterborne outbreaks are also important sources of infection[3]. The NV genome is composed of a single-stranded positive-sense RNA (+ssRNA), with approximately 7.7 kb and three open reading frames (ORFs): ORF1, ORF2, and ORF3[4]. ORF1 encodes six nonstructural proteins, including the RNA-dependent RNA polymerase (RdRp)[5]. ORF2 and ORF3 encode major (VP1) and minor (VP2) structural capsid proteins, respectively[6]. VP1 consists of a folded domain (S) and two prominent domains (P)[7]. The P1 domain, a central region of the flexible loop, is located between the S and P2 domains[5]. The P2 domain is a hypervariable region that binds to the host cell[8].

The stability of VP1 is increased by VP2, which prevents its degradation[5]. NV is classified into six groups, genogroups I to VI (GI to GVI), based on the amino acid sequences of the RdRp and VP1[9]. The genogroups GI, GII, and GIV, are found in humans[10], and outbreaks appear more frequently within these genogroups[11]. GII continuously evolved in an evolutionary pattern every 2 to 3 years[12]. This genotype is equivalent to 87% of the occurrence of noroviruses worldwide[13]. NV GII.4 Sydney type emerged in Korea between 2012 and 2013, where 60.4% of NV diagnoses showed GII[13]. The NV GII strain is difficult to identify the existing RT-PCR because of the continuous variation of the strain. In addition, the primer set does not always have sufficient specificity to detect NV and false positive detection frequently occurs[14].

Hepatitis A virus (HAV) is a hepatotropic virus that belongs to the family Picornaviridae[1,15]. The HAV has a single-stranded positive-sense RNA genome of 7.5-kilobase (kb). HAV genome is wrapped up by an icosahedral capsid, formed by up to 60 copies of three surface proteins, VP1, VP2, and VP3 (named 1D, 1B, and 1C), transcribed into one open reading frame (ORF)[16]. The single ORF of 2217 to 2280 amino acids of HAVs is divided into P1, P2, and P3 regions. The P1 part contains the capsid polypeptides VP1 to VP4, whereas P2 and P3 regions include the nonstructural polypeptides[1]. Flanking the HAV genome, there are regulatory 5' and 3'UTRs areas with a small poly-A tail[17]. HAV immunogenic neutralization sites are located on the structural surface of proteins[18].

Primates are the only natural host of HAV, and infection confers lifelong protection[19,20]. After ingestion, absorption from the gastrointestinal tract, and replication in the liver, HAV is excreted in the bile in high concentrations of viral particles that can be found in stool specimens. HAV transmission occurs by the fecal-oral through direct contact with

2

an HAV-infected person or by consuming HAV-contaminated food or water. The median latency period (i.e., time from exposure to onset of symptoms) is 28 days (range 15 to 50 days)[19] infectivity peaks two weeks before the onset of jaundice and declines one week after the start. Elevating serum alanine aminotransferase [ALT] levels can lead to maximal infectivity in people without jaundice. Viremia can be detected before ALT levels rise, and HAV RNA levels often remain detectable even after ALT levels normalize and symptoms resolve[21].

Hepatitis A begins with symptoms such as fever, loss of appetite, nausea, vomiting, diarrhea, muscle aches, and fatigue. Jaundice, dark-colored urine, or light-colored stools may be present initially or followed by systemic symptoms within a few days if the physical findings include abdominal tenderness, hepatomegaly or splenomegaly[22]. In most cases, hepatitis A lasts for several weeks. Recurrence of symptoms with new increases in serum aminotransferase levels occurs in 10% of patients, and relapses can last up to 6 months[12]. All-cause mortality is 0.3%, compared to 1.8% among people around age 50. People with underlying chronic liver disease are at increased risk of death[23].

HAV contamination of food can occur at any stage of growing, harvesting, processing, distribution, or preparation. Foodborne infections can be challenging to detect from routine surveillance data because case patients may have difficulty recalling their dietary history 2 to 6 weeks before illness[15,19], cases may accrue gradually or not be reported[24], a food item may be focally contaminated[21], some exposed persons may have unrecognized HAV infection[25], some susceptible persons may have preexisting immunity from a previous infection or vaccination[26], persons who acquire infection through contaminated food are not recognized amid an ongoing high incidence in the community. Cases are geographically scattered over several public health jurisdictions[27].

This study aimed to develop a rapid and sensitive detection method for Norovirus genotypes I and II and Hepatitis A in food matrices of high demand and consumption. The current problem in public health in Ecuador is that many diseases associated with gastrointestinal issues are associated with bacteria and not with viruses; in this context, the identification of Norovirus, specifically genogroup II, which is associated with high cases of foodborne infection, allows to identify the type of disease in relation to the infectious biological agent correctly. Concerning the Hepatitis A virus, many farmers in our country do not carry out good agricultural practices concerning the sanitary quality of the irrigation water used for fruit and vegetable crops, specifically strawberries and spinach, being a route of infection by cross-contamination. Since these foods are not heat-treated in most cases, the risk to public health is considerable.

Materials and methods

Analysis of HAV genomic sequences

The genomic sequences of NV GI, GII, and HAV strains were collected from the National Center for Biotechnical Information (NCBI) genetic sequence database and analyzed using Geneious Prime® 2021.0.3. The current study's sequences are listed in Tables 1, 2 and 3. Genetic sequences were aligned with Muscle to identify around 500 nucleotides as the target for RT-PCR diagnoses and positive controls. Selected sequences were cloned into a T7-driven vector for in vitro transcription of the favorable rules. Genetic sequences of the gene fragments and primers are shown in Tables 4 and 5.

Accession number (GenBank)	Genotype	Strain
FJ515294	GI.2	Leuven/2003/BEL
JN183159	GI.9	S48/2008/Lilla
JN603244	GI.3	S29/2008/Lilla Edet/Sweden
JQ388274	GI.6	Kingston/ACT160D/2010/AU
JQ911594	GI	10360/2010/VNM
KF039725	GI.1	CHA7A009/2010/USA
KF039726	GI.1	/CHA6A003 20091031/2009/USA
KF039727	GI.1	CHA2A014/2008/USA
KF039728	GI.1	CHA2A014/2008/USA
KF039729	GI.1	CHA6A007/2010/USA
KF306212	GI.2	Jingzhou/2013401/CHN
KF429761	GI.1	8MoIIIL/1972/USA
KF429765	GI.1	8W/1968/USA
KF429770	GI.1	8McIII/1973/USA
KF429773	GI.1	8CKIIIc/1974/USA
KF429774	GI.1	8UIIIf/1973/USA
KF429783	GI.1	8K/1979/USA
KF429789	GI.1	8MC/1978/USA
KM246914	GI.14	Nanning/2011/CHN
HQ637267	GI	Vancouver730/2004/CAN

Table 1. Description of NV GI sequences for genetic analysis.

Accession number (GenBank)	Genotype	Strain
AB447433	GII.4	Aormori/2006/JP
AB541321	GII.4	Osaka2/2007/JP
AB662873	GII.2	OC09104/2009/JP
AY485642	GII.4	Langen 1061/2002/GER
AY502023	GII.4	Farmington Hills/2002/USA
DQ658413	GII.4	MD-2004/2004USA
DQ078814	GII.4	Hunter504D/2004/AU
EF202588	GII.4	Toronto SK/2005/CAN
EU310927	GII.4	TCH186 2002 US
EU373815	GII	Luckenwalde591/2002/DE
EF684915	GII.4	Shellharbour NSW696T/2006/AUS
GQ845369	GII.4	Armidale NSW3901/2008/AU
GU134965	GII.7	1738/2009/USA
GU969058	GII.13	8679/Maizuru/2008 JPN
GU980585	GII.3	CBNU1/2006/KOR
HQ664990	GII.12	HS206/2010/USA
JN400623	GII.4	CGMH25/2010/TW
JN595867	GII.4	Ascension208/2010

Table 2. Description of NV GII sequences for genetic analysis.

Accession number (GenBank)	Genotype	Strain
JQ425480.1	HAV A	Hepatovirus A
KP879216.1	HAV A	Hepatovirus A
KP879217.1	HAV A	Hepatovirus A
KT891985.1	HAV A	Hepatovirus A
M16632.1	HAV A	Hepatovirus A
M59286.1	HAV A	Hepatovirus A
M59808.1	HAV A	Hepatovirus A
NC_001489	HAV A	Hepatovirus A
NC_008250.2	HAV A	Duck hepatitis A virus 1
NM_012206	HAV A	Homo sapiens

Table 3. Description of HAV sequences for genetic analysis.
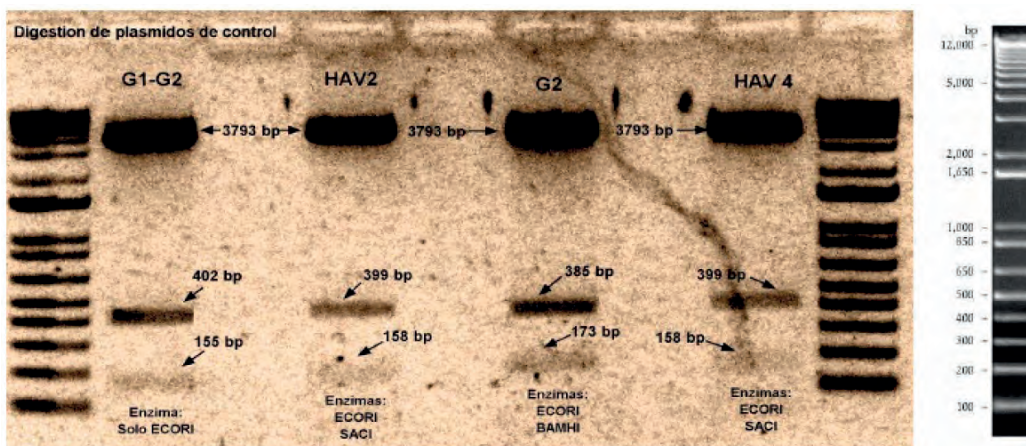
Figure 1. Digestion of plasmid pTop Blunt V2 with an inserted sequence of NVGI, NVGII, and HAV gene.

| Norovirus GII | TAATACGACTCACTATAGGGATTTCTGAGGATCTGGATGGTTTAACCTTTCTGCGGAGA ACTGTAACCCGTGATCCAGCTGGTTGGTTTGGTAAATTAGAACAGAGCTCAATACTTAG GCAGATGTACTGGACTAGGGGCCCCAACCATGAGGATCCATCTGAAACAATGATACCA CATTCCCAAAGGCCCATACAGTTGATGTCTCTGCTAGGTGAAGCTGCATTGCACGGTCC AGCATTCTACAGCAAAATCAGTAAACTAGTCATTGCAGAGTTGAAGGAAGGTGGCATG GACTTTTACGTGCCCAGGCAAGAGCCGATGTTCAGATGGATGAGATTCTCAGACCTGAG CACGTGGGAGGGCGATCGCAATCTGGCTCCCAGTTTTGTGAATGAAGATGGCGTCGAAT GACGCCGCCCATCTAATGATGGTGCAGCCGGTCTCGTACCAGAGGTCAACAACGAGAC GATGGCCCTCGAACCGGTGGCTGGGGCTTCTATAGCCGCCCCTCTAACCG | 521 |
| HAV_Hepatitis A | TAATACGACTCACTATAGGGAGATTCTACATTTGGATTGTTTCTATTCGAGATTGCAAAT TACAATCATTCTGATGAATATTTGTCCTTCAGTTGTTATTTGTCTGTCACAGAGCAATCA GAGTTCTATTTTCCTAGAGCTCCATTAAATTCAAATGCTATGTTGTCCACTGAATCCATG ATGAGTAGAATTGCAGCTGGAGACTTGGAGTCATCAGTGGATGATCCCAGATCAGAGG AGGATAGAAGATTTGAGAGTCATATAGAATGTAGGAAACCATACAAAGAATTGAGACT GGAGGTTGGGAAACAAAGACTCAAATATGCTCAGGAAGAGTTATCAAATGAAGTGCTT CCACCTCCTAGGAAAATGAAGGGGTTATTTTCACAAGCTAAAATTTCTCTTTTTTATACT GAGGAGCATGAAATAATGAAGTTTTCTTGGAGAGGAGTGACTGCTGATACTAGGGCTTT GAGAAGATTTGGATTCTCTCTGGCTGCTGGTAGAAGTGTGTGGACT | 520 |

Table 4. Sequence of genes synthesized for positive control and primer design Norovirus (GI And GII); Hepatitis A (HAV) obtained by alignment from strains the genetic sequence database at the National Center for Biotechnical Information (NCBI).

Verification of positive controls

Gene fragments were received in a pTop Blunt V2 vector and transformed in DH5alpha Escherichia coli competent cells. Gene fragments were verified by restriction digestion with the following sizes: NV GI 557bp; NV GII 558bp; and HAV 557 bp (Fig. 1).

Primer Design

Specific primers for NVand HAV were designed from conserved regions of ORF1 and ORF2. The expected size for NVGI in the first PCR is 288 bp, and using heminested PCR it is 213 bp, for NVGII the anticipated size of the initial amplification is 286 bp and using heminested PCR the predicted size is 215 bp while for HAV the anticipated length of the initial PCR is 395 bp and using the heminested PCR 160 bp.

Collection of food Samples

This study's test sample sizes were 25 g (fruit and vegetables like strawberry and spinach), 330 ml (bottled water) and 25 g of sausages. All samples were tested using the relevant matrix-specific test protocols[28]. All food samples were tested for NV GI and GII, and HAV. Samples were obtained at the wholesale food market of Mount Sinai, Guayaquil, during October and November of 2020.

Validation of hnRT-PCR

Thoroughly washed strawberries, spinach and sausages were inoculated with in vitro transcribed NV GI, GII and HAV RNA-positive controls. Food samples without inoculation were used as negative controls. The weight of strawberry, spinach and sausage was 25 grams and 300 ml for bottled water[28].

Food sample washed with water (except bottled water sample). It was established as a protocol to inoculate the food with NVGI (600 ng/ul), NVGII (500 ng/ul) and HAV (450 ng/ul), established as a positive control. Subsequently, a process was established by inoculating viral load without food NVGI (600 ng/ul), NVGII (500 ng/ul) and HAV (450 ng/ul) established as the positive control. Positive control was established within the process based on synthetic RNA obtained by reverse transcription of the PCR product of the plasmids.

Experimental protocol

Locally purchased strawberries, spinaches, sausages, and bottled water were used in this study. Food samples (25g) were mixed with 60 ml of elution buffer (50 mM glycine, 100 mM Tris, 1% [wt/vol] beef extract [pH 9.5]) for 15 min at room temperature with constantly shacking (Fig. 2). The elution buffer was then filtered through a 40-m pore size nylon cell strainer (BD Falcon, Basel, Switzerland). The recovered elution buffer was adjusted to pH 7.0 with 9.5 M HCl and centrifuged at 3,500 g for 15 min. The supernatant was transferred to a new tube, and the volume was brought up to 25 ml with phosphate buffer saline and left at 4C overnight. The next day the extract was centrifuged at 3,500 g for 15 min, and the supernatant was then transferred to a Centricon Plus-70 centrifugal filter device (100K NMWL; Millipore, Molsheim, France) and centrifuged at 3,500 g to concentrate viral particles into a volume of ca. 400 ul. The filter device was subsequently rinsed with 200 ul of elution buffer to improve virus recovery[29] (Fig. 2).

Viral RNA Extraction

Total RNA was extracted with TRI Reagent according to the manufacturer protocol (12). Total RNA was resuspended in 30 μL of elution buffer and stored at -80°C until use in the RT-hnPCR assay.

RT-PCR and Heminested PCR

Extracted RNA was reverse-transcribed and amplified using SuperScript III One-Step RT-PCR Kit (Thermo Fisher, USA) following the manufacturer's instructions. The reaction mixture consisted of 10 ul of reaction buffer, 0.4 ul of Triton x100, 0.2 μM of each primer (NVGI-F/R, NVGII-F/R, HAV-F/R), 0.5 ul of enzyme mix (SuperScript III One-Step RT PCR with Platinum Taq DNA Polymerase), 2 ul of the RNA template, and 11.1 ul and RNase-free water.

The thermocycling protocol was as follows

RT at 50 C for 30 min; initial denaturation at 94 C for 2 min; 40X cycles of 94 C for 30s, annealing at 60 C (NV GI), 55 C (NV GII), and 45 C (HAV), for 30 s, extension at 72 C for 40 s, and a final extension at 72 C for 5 min.

For the heminested PCR step, 1 ul of the RT-PCR reaction was mixed with 2 ul of 10X reaction buffer, 1 ul of 50mM

4

5

(a) NVGI	
NVGI primer set	
NVGI (forward)	
Primer	TGGACYCGHGGSCCCAAYCA
Promotor T7 + aligned sequence NVGI	C C G T
NVGI (reverse)	
Primer	GCGTCCTTAGACGCCATCATC
Promotor T7 + aligned sequence NVGI	TAAG
NVGI (reverse heminested)	
Primer	GAAVCGCATCCAGCGGAACATGG
Promotor T7 + aligned sequence NVGI	CC T A G

(b) NVGII	
NVGII primer set	
NVGII(forward)	
Primer	TGGACNAGRGGNCCYAAYCA
Promotor T7 + aligned sequence NVGII	T G C C C
NVGII (reverse)	
Primer	GTCATTCGACGCCATCTTCATTC
Promotor T7 + aligned sequence NVGII	T GC C G A
NVGII (reverse heminested)	
Primer	GARAAYCTCATCCAYCTRAAC
Promotor T7 + aligned sequence NVGII	GG T G T G A

(c) HAV	
HAV primer set	
HAV(forward)	
Primer	CTATTCAGATTGCAAATTAYAAT
Promotor T7 + aligned sequence NVGII	C
HAV (reverse)	
Primer	AAYTTCATYATTTCATGCTCCT
Promotor T7 + aligned sequence NVGII	A G A C
HAV (reverse heminested)	
Primer	CTCCAGCTGCAATTCTACTCATC
Promotor T7 + aligned sequence NVGII	T T T G T

Table 5. The sequence of genes synthesized of NV GI (a) NV GII (b) and HAV (c) obtained by alignment from strains in the genetic sequence database at the National Center for Biotechnical Information (NCBI) were compared to determine consensus identity with sequences of designed primer sets.

6
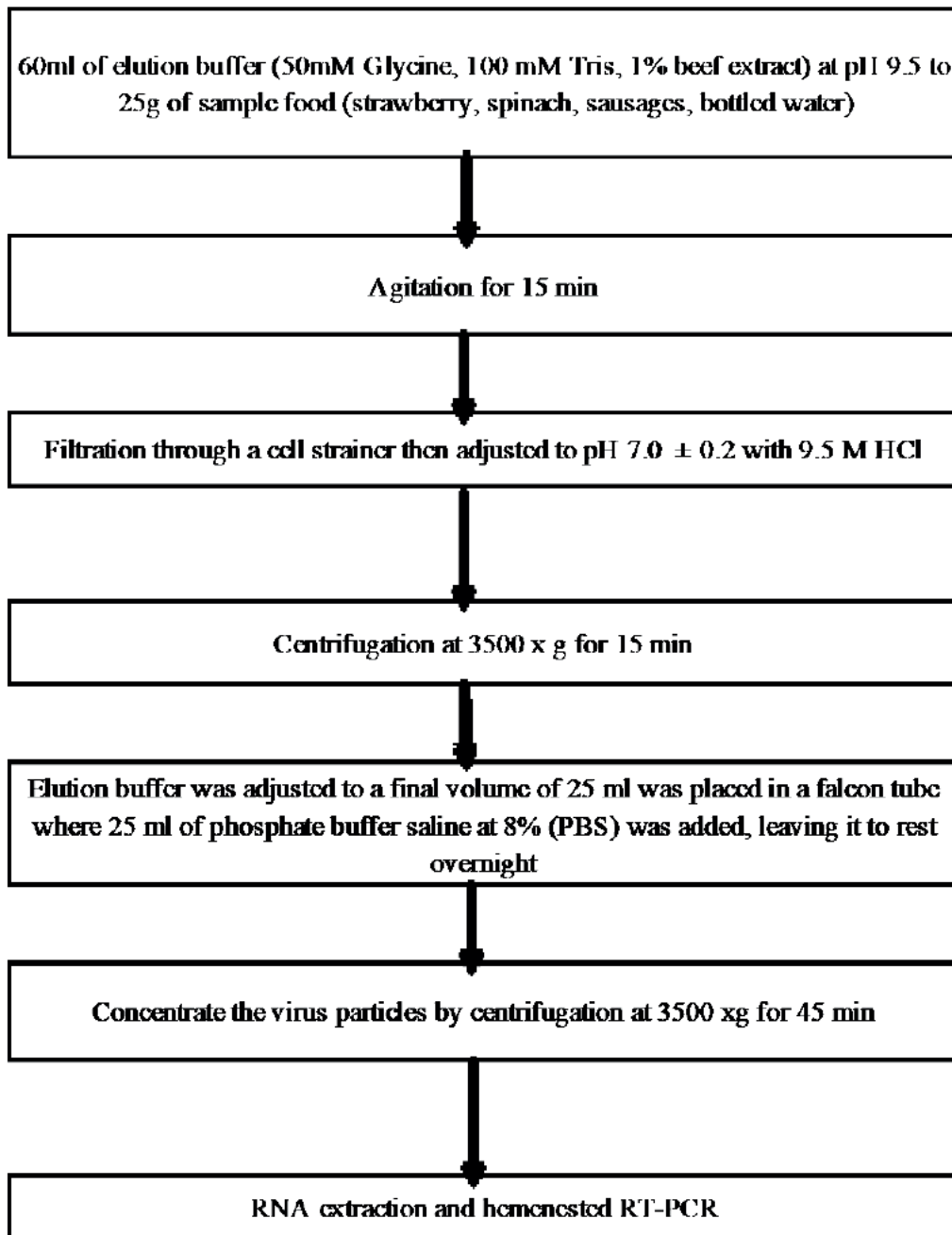
Figure 2. Flow chart of the method.

MgCl2, 0.4 ul of 10uM dNTPs, 1 ul of 0.2uM primers, 0.08 ul Platinum Taq DNA Polymerase (Invitrogen) and 14.52 ul of RNase-free water. PCR conditions were as follows: initial denaturation at 94°C for 2min, 40 cycles of denaturation at 94°C for 30s, annealing at each optimal annealing temperature (Tables 6, 7 and 8) for 30 s, extension at 72°C for 40 s, and a final extension at 72°C for 5min.

Analysis of PCR Products

The RT-PCR and heminested PCR products were analyzed using 2% agarose gel electrophoresis in TAE buffer. Bands were visualized with Sbyr Safe (Invitrogen, USA).

Results

To evaluate the efficiency of new primer sets (NV-GI-F/R, NVGII-F/R and HAV-F/R) to detect NV and HAV, we used RT-PCR followed by a heminested PCR to improve the sensitivity of the current diagnostic. To this end, four food samples were collected in the local wholesale food market to obtain contaminating viral RNA and diagnose for NV GI, GII and HAV. The presence of RT-PCR inhibitors was evaluated as previously described[29].

The RNA extraction method was also evaluated in conjunction with the food sample treatment process to avoid inhibiting viral RNA by substances present in them (phenols, vitamins, proteins, carbohydrates). This was evidenced since when amplifying the genetic material, amplification of the bands was observed in the food samples that were intentionally inoculated with the virus (NVGI / GII and HAV). The method of inhibiting substances inherent to the food[29] does not influence the extraction of genetic material; therefore, the process is validated concerning the results obtained.

NVGI was detected in the strawberry and spinaches

Primers	Sequence (5'- 3')[a]	Location[b]	Region	Annealing temperature (°C)	Polarity	Reference
NVGI-F	TGGACYCGHGGSCCCAAYCA	5092-5112	RdRP	60	(+)	this study
NVGI-R	GCGTCCTTAGACGCCATCATC	5359- 5380	Capsid	60	(-)	this study
NVGI-RH	GAAVCGCATCCAGCGGAACATGG	5282-5305	RdRP	60	(-)	this study
a. The means of alphabet sequence are the following: H= A, C, T; S = C, G; V=A, C, G; Y = C, T.						
b. Location is based on accession number M87661 (Norwalk virus).						

Table 6. Information of NV GI primer sets.

Primers	Sequence (5'- 3') a	Location[b]	Region	Annealing temperature (°C)	Polarity	Reference
NVGII-F	TGGACNAGRGGNCCYAAYCA	4820-4839	RdRP	55	(+)	this study
NVGII-R	GTCATTCGACGCCATCTTCATTC	5083-5106	Capsid	55	(-)	this study
NVGII-RH	GARAAYCTCATCCAYCTRAAC	5014-5035	RdRP	55	(-)	this study
a. The alphabet sequence means: N= A, C, G, T; R =A, G; Y = C, T.						
b. Location is based on accession number X86557 (Lordsdale virus).						

Table 7. Information of NV GII primer sets.

Primers	Sequence (5'- 3') a	Location[b]	Region	Annealing temperature (°C)	Polarity	Reference
HAV-F	CTATTCAGATTGCAAATTAYAAT	2896-2918	Capsid	45	(+)	this study
HAV-R	AAYTTCATYATTTCATGCTCCT	3269-3291	Capsid	45	(-)	this study
HAV-RH	CTCCAGCTGCAATTCTACTCATC	3033-3056	Capsid	45	(-)	this study
a. The means of alphabet sequence are the following: Y= C, T.						
b. Location is based on accession number M14707 (Hepatitis A virus).						

Table 8. Information of HAV primer sets.

samples. NVGII was detected in spinaches, while HAV was detected in bottled water. Each virus showed a clear amplification product at 213pb, 215 and 160pb, respectively (Fig 3, 4, 5, 6, 7, 8).

To evaluate the primers (NVGI-F/R, NVGII-F/R and HAV-F/R), 57 samples were amplified from the 4 samples selected in the Mount Sinai market and duplicated to the schematization of the proposed design. Of the 57 samples, 12 (21 %) were positive for the NVGI presence. In the case of NVGII, their presence was detected in 11 (19.3 %) of the analyzed samples. In 12 samples (21 %) HAV was detected with primers designed for HAV detection.

Except for the negative control, that is, they do not contain the genetic material; the rest were amplified, demonstrating the validation of the NV GI, NVGII, and HAV detection method through the design of the primers of the present study.

Discussion

In the USA, an estimated 570–800 people die annually from diseases associated with NV infection. Outbreaks of the virus occur regularly, and new variants are identified worldwide every 2 to 3 years[30].

The widespread use of RT-PCR and Heminested PCR for NV and HAV detection can be attributed to its superior sensitivity compared to other methods[31]. Virus detection is susceptible in food because, in most cases, the viral load is low; the virus does not infect food and therefore does not replicate its genetic material. Before extracting RNA from the food, we recommend inhibiting any substance that is part of the food such as phenols, vitamins, proteins, and carbohydrates, using the method described as an experimental protocol[29].

Norovirus GI was detected in strawberries and spinach, Norovirus GII in spinach, and HAV in bottled water. The virus's origin or source of contamination of the food is unknown. Contaminated water for plant irrigation or cross-contamination by sick food handlers can be a possible source of viral infection.

The food handler is an essential link in NV transmission, being epidemiologically involved in 80 % of the NV outbreaks in Belgium[32].

Contamination of food with HAV can occur anywhere in the food chain, from farm to fork. Contact with incorrectly treated sewage or sewage-polluted water, infected food handlers and, to a lesser extent, contaminated surfaces represent the most common routes of HAV contamination in food. Approximately 2–7% of all HAV outbreaks worldwide can be attributed to contaminated food.

In the present study, we developed specific primers to
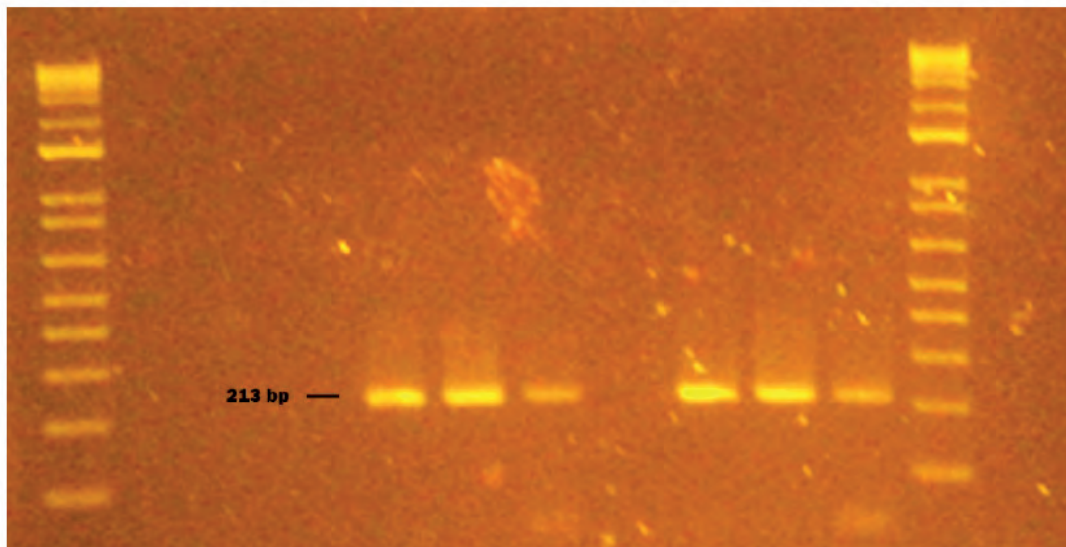
Figure 3. Genogroup GI NV obtained from naturally contaminated food during sampling from October to November 2020 in Monte Sinai, Guayaquil- Ecuador. Lanes 1 and 14: DNA ladder 12000 pb; lane 2 negative control PCR; lane 3 extraction control; lane 4 NVGI identified in strawberry (213pb); lane 5 washed strawberry sample; lane 6 strawberry inoculated with NVGI (Positive Control); lane 7 NVGI virus inoculated without strawberry (Positive Control); lane 8 sausage sample; lane 9 washed sausage sample; lane 10 sausages inoculated with NVGI (Positive Control); lane 11 NVGI virus inoculated without sausage (Positive Control); lane 12 bottled water sample; lane 13 NVGI Positive Control (Synthetic RNA). Samples were analyzed in 2 % agarose gels and stained with cyanine dye.
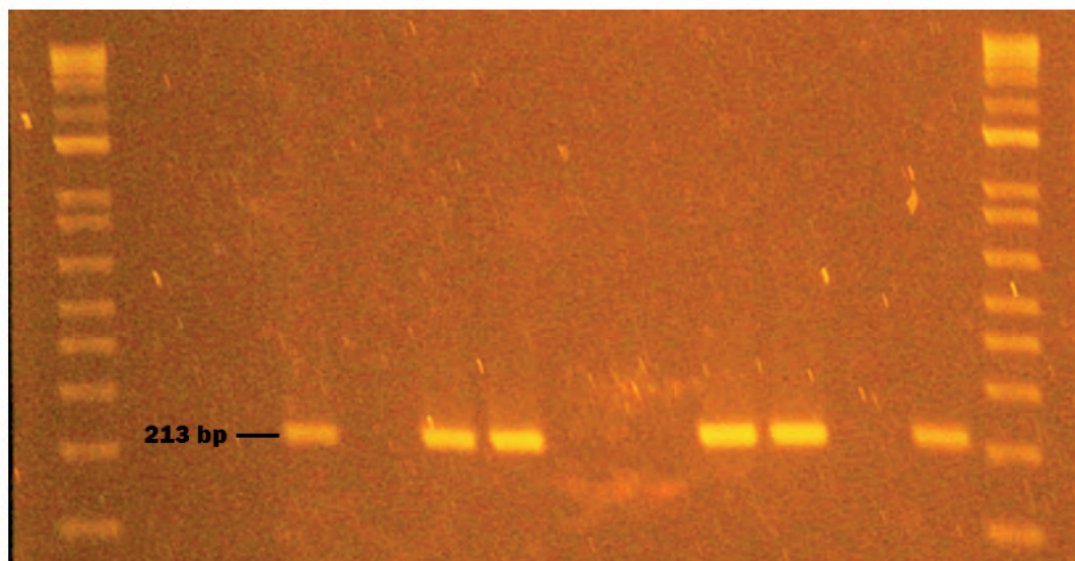
Figure 4. Genogroup GI NV obtained from naturally contaminated food during sampling from October to November 2020 in Monte Sinai, Guayaquil- Ecuador. Lanes 1 and 12: DNA ladder 12000 pb; lane 2 negative control PCR; lane 3 extraction control; lane 4 bottled water sample; lane 5 bottled water sample inoculated with NVGI (Positive Control); lane 6; NVGI virus inoculated without bottled water (Positive Control); lane 7 NVGI identified in spinach (213pb); lane 8 washed spinach; lane 9 spinach inoculated with NVGI (Positive Control); lane 10 NVGI virus inoculated without spinach(Positive Control); lane 11 NVGI Positive Control (Synthetic RNA). Samples were analyzed in 2 % agarose gels and stained with cyanine dye.

detect NV GI, GII and HAV, targeting ORF1, ORF2 and capsid genes, respectively. We used a one-step RT-PCR and heminested PCR protocol to enhance further our ability to detect human enteric food viruses. The study carried out is unprecedented in Ecuador because the presence of the virus has not been evaluated in food in our country. The results obtained in samples such as strawberries, spinach and bottled water in a popular sector of the city of Guayaquil suggest that gastrointestinal diseases in the city may have been crucial viral etiology besides bacterial contamination.

Our study showed that the NVGI-F/R, NVGII-F/R and HAV-F/R primer sets could be necessary for the epidemiological diagnosis of NVGI, NVGII and HAV considering the method of extraction and inhibition of food-specific substances that could inhibit or degrade viral RNA in food matrices.

The Biplot shows that only bottled water has a strong relationship with the presence of HA. Other relationships are observed, although not as strong, such as spinach with the presence of N.GI and N.GII. Sausages and strawberries show connections with the absence of pathogens.

The Biplot obtained through the multiple correspondence analysis (Fig.9) shows the significant relationship be-
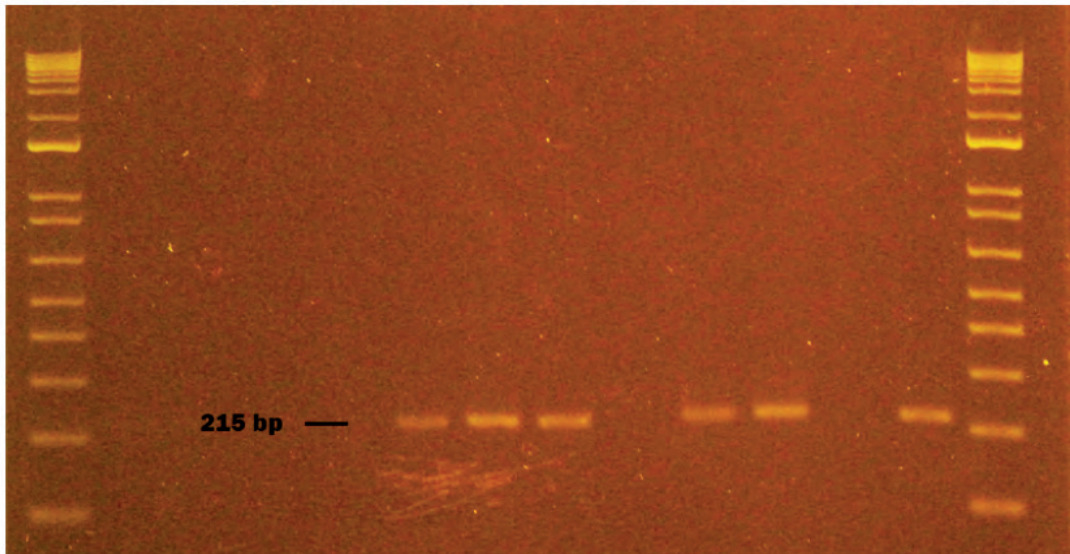
Figure 5. Genogroup GII NV obtained from naturally contaminated food during sampling from October to November 2020 in Monte Sinai, Guayaquil- Ecuador. Lanes 1 and 14: DNA ladder 12000 pb; lane 2 negative control PCR; lane 3 extraction control; lane 4 sausage sample; lane 5 washed sausage sample; lane 6 sausage inoculated with NVGII (Positive Control); lane 7 NVGII virus inoculated without sausage (Positive Control); lane 8 NVGII identified in spinach (215pb); lane 9 washed spinach sample; lane 10 spinach inoculated with NVGII (Positive Control); lane 11 NVGII virus inoculated without spinach (Positive Control); lane 12 strawberry sample; lane 13 NVGII Positive Control (Synthetic RNA). Samples were analyzed in 2 % agarose gels and stained with cyanine dye.
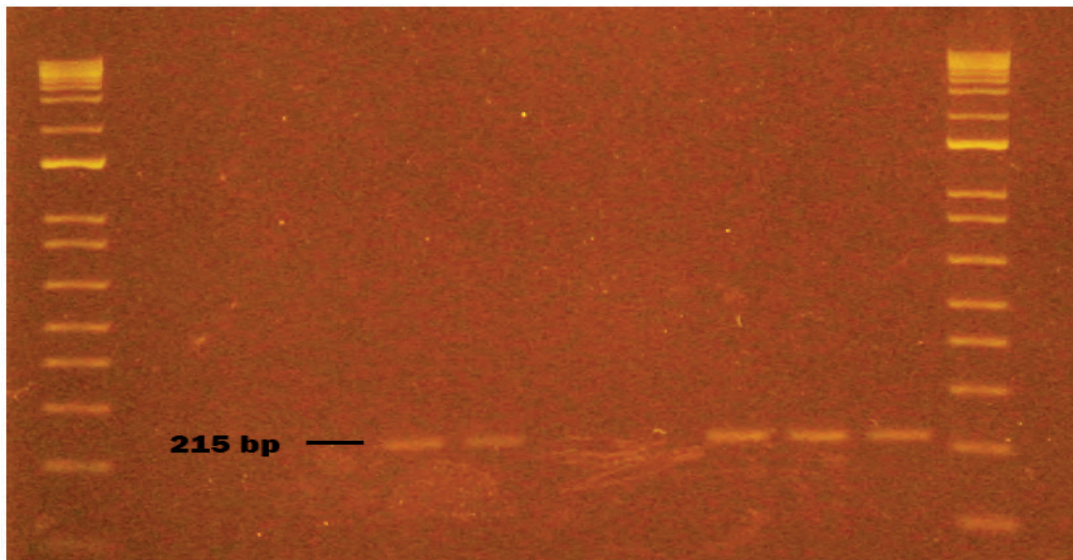
Figure 6. Genogroup GII NV obtained from naturally contaminated food during sampling from October to November 2020 in Monte Sinai, Guayaquil- Ecuador. Lanes 1 and 12: DNA ladder 12000 pb; lane 2 negative control PCR; lane 3 extraction control; lane 4 washed strawberry sample; lane 5 strawberry sample inoculated with NVGII (Positive Control); lane 6 NVGII virus inoculated without strawberry (Positive Control); lane 7 bottled water sample; lane 8 bottled water sample (duplicate); lane 9 bottled water inoculated with NVGII (Positive Control); lane 10 NVGII virus inoculated without bottled water (Positive Control); lane 11 NVGII Positive Control (Synthetic RNA). Samples were analyzed in 2 % agarose gels and stained with cyanine dye.

tween bottled water and the presence of Hepatitis A (Val-p = 0.004). It also shows a relationship (not significant) between spinach and the presence of Norovirus GI and GII (p-value > 0.05). Fisher's (Table 9) test was developed to determine the relationship between the presence of viruses and selected food matrices.

This study is very relevant in our country in the field of public health and food safety because the presence of these pathogens in food shows that the gastrointestinal problems associated with the population are not exclusively caused by bacteria, which a later study raises in determining in which other types of foods it is likely to detect viral load by Nv and HAV concerning a risk matrix.

In the case of viruses such as Hepatitis A and Norovirus present in spinach, strawberries and water samples, they show that many gastrointestinal problems that occur in Ecuador may not necessarily be caused by bacteria but also by viruses.
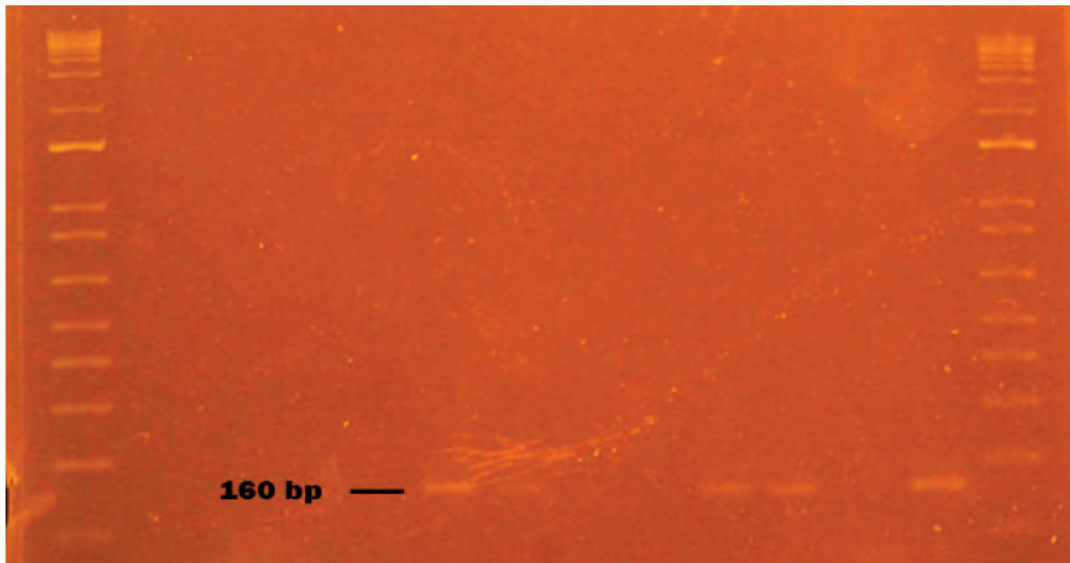
Figure 7. HAV virus obtained from naturally contaminated food during sampling from October to November 2020 in Monte Sinai, Guayaquil- Ecuador. Lanes 1 and 14: DNA ladder 12000 pb; lane 2 negative control PCR; lane 3 extraction control; lane 4 sausage sample; lane 5 washed sausage samp2le; lane 6 sausage inoculated with HAV (Positive Control); lane 7 HAV virus inoculated without sausage (Positive Control); lane 8 spinach sample; lane 9 washed spinach sample; lane 10 spinach inoculated with HAV (Positive Control); lane 11 HAV virus inoculated without spinach (Positive Control); lane 12 strawberry sample; lane 13 NVGII Positive Control (Synthetic RNA). Samples were analyzed in 2 % agarose gels and stained with cyanine dye.
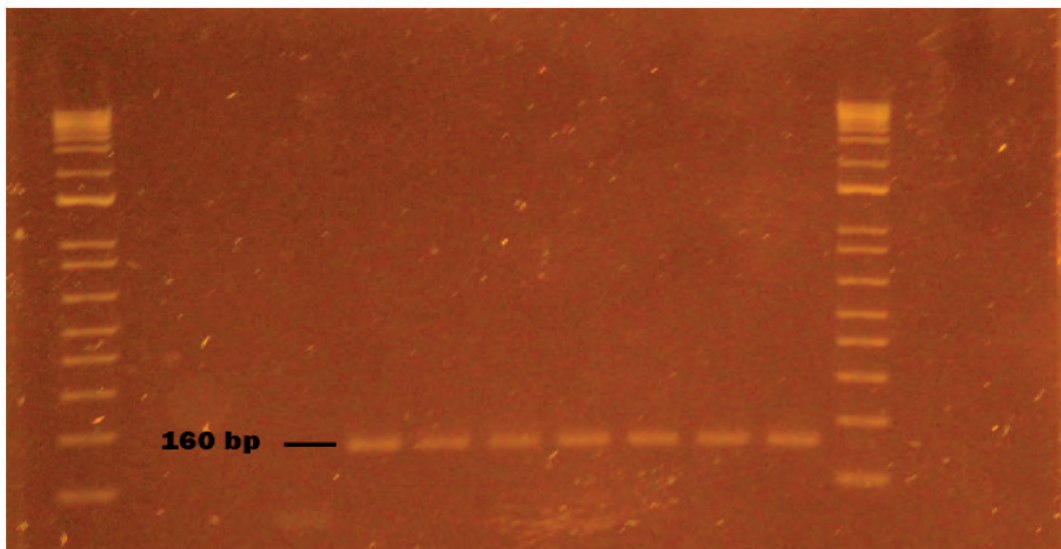
Figure 8. HAV virus obtained from naturally contaminated food during sampling from October to November 2020 in Monte Sinai, Guayaquil- Ecuador. Lanes 1 and 12: DNA ladder 12000 pb; lane 2 negative control PCR; lane 3 extraction control; lane 4 washed strawberry sample; lane 5 strawberry sample inoculated with HAV (Positive Control); lane 6 HAV virus inoculated without strawberry (Positive Control); lane 7 HAV identified in a bottled water sample (160pb); lane 8 HAV identified in bottled water sample duplicate (160pb); lane 9 bottled water inoculated with HAV (Positive Control); lane 10 HAV virus inoculated without bottled water (Positive Control); lane 11 HAV Positive Control (Synthetic RNA). Samples were analyzed in 2 % agarose gels and stained with cyanine dye.

Conclusions

Foodborne diseases are a public health problem worldwide. In the case of biological agents responsible for foodborne illnesses, it is common but largely underdiagnosed.

Norovirus and Hepatitis A are two classes of viruses that have been diagnosed within this group as the main ones responsible for foodborne illnesses, even according to reports documented by the United States Center for Disease Control and Prevention (CDC), 50% of Gastrointestinal disease in the American population is due to Norovirus, which can infect with a relatively low dose.

The great challenge of this research work was to develop a method that allows determining the presence of Norovirus and Hepatitis A in food, considering how complex it is to detect viruses in them because the food as such does not provide the requirements that the obligate intracellular parasite required to carry out the process of replication and increase in viral load.

To detect the viral load in food matrices such as strawberries, spinach, water and sausages, it was previously ne-
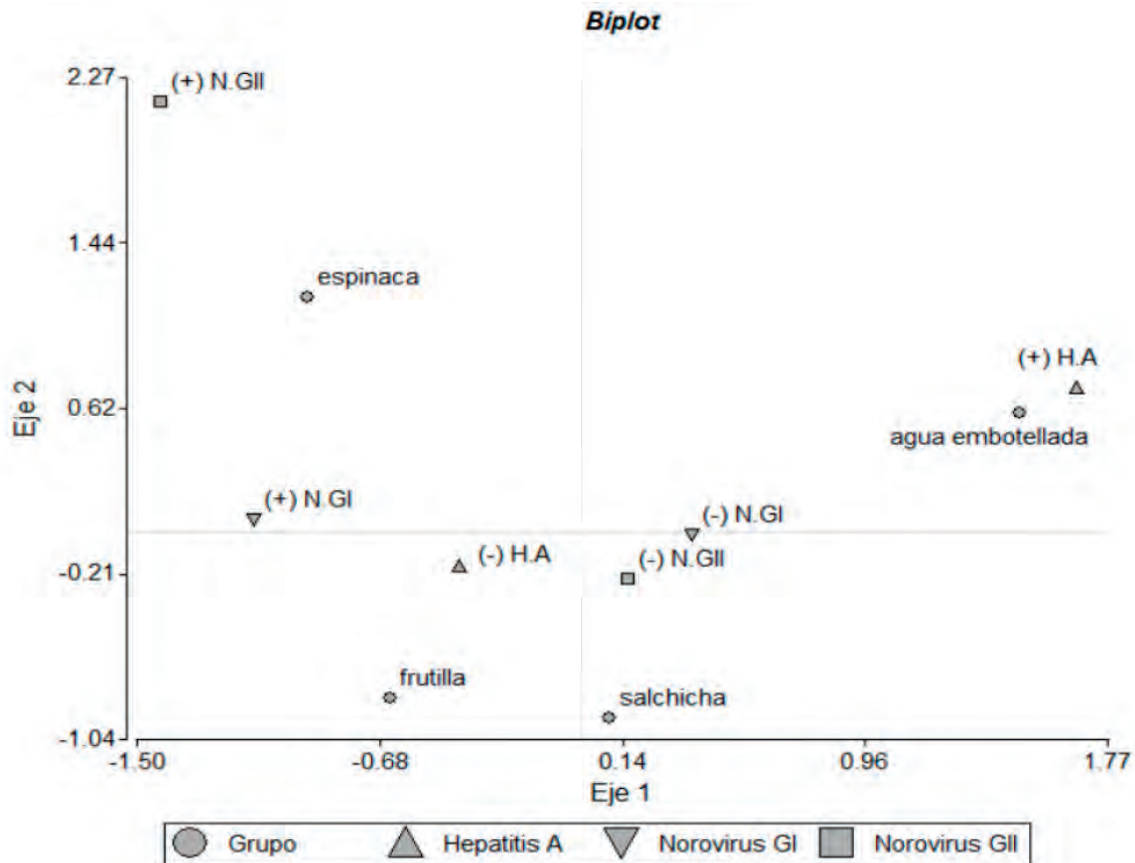
Figure 9. Biplot obtained through the A. Multiple Correspondence, which shows the relationships between pathogens and food groups.

cessary to inhibit compounds that are part of the chemical composition of the food, such as phenols, vitamins, proteins and carbohydrates, to avoid inhibition of the genetic material of the virus present. on the surface of the food.

The importance of this work was that through a good approach in developing the technique used to detect Hepatitis A and Norovirus in food matrices sampled in the city of Guayaquil, it has identified the presence of these infectious biological agents and probably the association of diseases. Significant foodborne infections associated with transmission by food handlers and sewage-contaminated food for these viruses. According to reports from the Ministry of Public Health in Ecuador, there are no reports related to gastrointestinal problems due to viral origin (Norovirus), which entails a greater challenge in properly identifying the origin of the disease and the palliative treatments applied to sick or dying people. recovery process. It is important to note that complex mixtures of human and animal viruses and other pathogens can be present in a single food, creating the potential for recombination or genetic rearrangement and thus further expansion of the diversity of these pathogens. Bringing together expertise from veterinary, food and clinical microbiology can help unravel these complexities and identify areas for intervention and prevention.

Author Contributions

"Conceptualization, E. J. Salazar and M.J. Guerrero.; methodology, E. J. Salazar.; software, M.J. Guerrero.; validation E. J Salazar, K.S. Suárez. and J.A. Villaquiran.; formal analysis M.J.Guerrero.; investigation, E.J. Salazar.; resources, J.M. Cevallos.; data curation M. J. Guerrero.; writing—original draft preparation, E.J. Salazar.; writing— review and editing, J.M. Cevallos.; visualization, E.J.Salazar.; supervision, J.M.Cevallos.; project administration, M.J. Guerrero.; funding acquisition, J.M.Cevallos.

Funding

Institutional Review Board Statement

Not applicable.

Informed Consent Statement

"Not applicable." for studies not involving humans.

Acknowledgments

Conflicts of Interest

There are no conflicts of interest.

Bibliographic references

1. Morillo, S. G., A. Cili, R.D.C.C Carmona and M.D.C.S.T Timenetsky. Investigation and molecular characterization of Norovirus in Sao Paulo State, Brazil. Braz. J. Microbiol 2008
2. Griffin SM, Brinkman NE, Hedrick EJ, Rhodes ER, Fout GS. Comparison of nucleic acid extraction and reverse transcription-qPCR approaches for detection of GI and GII noroviruses

11

Frequency table:

Hepatitis A

Group	Absence HA	Presence HA
bottled water	1	4
spinach	5	0
strawberry	5	0
sausage	5	0

Fisher's Exact Test for Count Data

p-value = 0.004128

alternative hypothesis: two. Sided

Frequency table:

Norovirus.GI

Group	Absence N.GI	Presence N.GI
bottled water	5	0
spinach	3	2
strawberry	2	3
sausage	5	0

Fisher's Exact Test for Count Data

p-value = 0.09701

alternative hypothesis: two. sided

Frequency table:

Norovirus.GII

Group	Absence N.GII	Presence N.GII
bottled water	5	0
spinach	3	2
strawberry	5	0
sausage	5	0

Fisher's Exact Test for Count Data

p-value = 0.2105

Alternative hypothesis: two. Sided

Table 9. Statistical support Fisher's exact test, for Annexes or complementary material.

in drinking water. J Virol Methods. 2014;199.

3. Barclay L, Park GW, Vega E, Hall A, Parashar U, Vinjé J, et al. Infection control for Norovirus. Vol. 20, Clinical Microbiology and Infection. 2014.

4. Green KY. Caliciviridae: The noroviruses. In: Fields Virology: Sixth Edition. 2013.

5. Bertolotti-Ciarlet   A, Crawford SE, Hutson AM, Estes MK. The 3′ End of Norwalk Virus mRNA Contains   Determinants That Regulate the Expression and Stability of the Viral Capsid Protein VP1: a Novel Function for the VP2 Protein. J Virol. 2003;77(21).

6. Hardy ME, Estes MK. Completion of the Norwalk virus genome sequence. Virus Genes. 1996;12(3).

7. Donaldson   EF, Lindesmith LC, Lobue AD, Baric RS. Viral shape-shifting: Norovirus evasion of the human immune system. Vol. 8, Nature Reviews Microbiology. 2010.

8. Bertolotti-Ciarlet   A, White LJ, Chen R, Prasad BVV, Estes MK. Structural Requirements for the Assembly of Norwalk Virus-Like Particles. J Virol. 2002;76(8).

9. Green KY, Ando T, Balayan MS, Berke T, Clarke IN, Estes MK, et al. Taxonomy of the caliciviruses. In: Journal of Infectious Diseases. 2000.

10. Zheng DP, Ando T, Fankhauser RL, Beard RS, Glass RI, Monroe SS. Norovirus classification and proposed strain nomenclature. Virology. 2006;346(2).

11. Fukuda S, Sasaki Y, Takao S, Seno M. Recombinant norovirus implicated in gastroenteritis outbreaks in Hiroshima Prefecture, Japan. J Med Virol. 2008;80(5).

12. Schiff ER. Atypical clinical manifestations of hepatitis A. Vaccine. 1992;10(SUPPL. 1).

13. Marshall   JA, Bruggink LD. The dynamics of norovirus outbreak epidemics: recent insights. Vol. 8, International journal of environmental research and public health. 2011.

14. Wollants E, van Ranst M. Detection of false positives with a commonly used Norovirus RT-PCR primer set. Vol. 56, Journal of Clinical Virology. 2013.

15. Fiore AE, Wasley A, Bell BP. Prevention of hepatitis A through active or passive immunization: recommendations of the Advisory Committee on Immunization Practices (ACIP). MMWR Recommendations and reports : Morbidity and mortality weekly report Recommendations and reports / Centers for Disease Control. 2006;55(RR-7).

16. Liu W, Zhai J, Liu J, Xie Y. Identification of recombination between subgenotypes IA and IB of hepatitis A virus. Vol. 40, Virus Genes. 2010.

17. Totsuka A, Moritsugu Y. Hepatitis A virus proteins. Vol. 42, Intervirology. 1999.

18. Pintó RM, Aragonès L, Costafreda MI, Ribes E, Bosch A. Codon usage and replicative strategies of hepatitis A virus. Virus Res. 2007;127(2).

19. Balayan MS.   Natural hosts of hepatitis A virus. Vaccine. 1992;10(SUPPL. 1).

20. Lemon SM, Jansen RW, Brown EA. Genetic, antigenic and biological differences between strains of hepatitis A virus. Vaccine. 1992;10(SUPPL. 1).

21. Bower WA,   Nainan O v., Han X, Margolis HS. Duration of viremia in hepatitis A virus infection. Journal of Infectious Diseases. 2000;182(1).

22. Koff RS.   Clinical manifestations and diagnosis of hepatitis A virus infection. Vaccine. 1992;10(SUPPL. 1).

23. Fiore AE.   Hepatitis A transmitted by food. Vol. 38, Clinical Infectious Diseases. 2004.

24. Krugman S,   Giles JP. Viral hepatitis: new light on an old disease. Trans Assoc Am Physicians. 1970;83.

25. Gingrich GA, Hadler SC, Elder HA, Ash KO. Serologic investigation of an outbreak of hepatitis A in a rural day-care center. Am J Public Health. 1983;73(10).

26. Lednar WM, Lemon SM, Kirkpatrick JW, Redfield RR, Fields ML, Kelley PW. Frequency of   illness associated with epidemic hepatitis a virus infection in adults. Am J   Epidemiol. 1985;122(2).

27. Yang NY, Yu PH, Mao ZX, Chen NL, Chai SA, Mao JS. Inapparent infection of hepatitis A virus. Am J Epidemiol. 1988;127.

28. Lowther JA,   Bosch A, Butot S, Ollivier J, Mäde D, Rutjes SA, et al. Validation of EN ISO method 15216 - Part 1 – Quantification of hepatitis A virus and Norovirus in food matrices. Int J Food Microbiol. 2019;288.

29. Butot S, Putallaz T, Sánchez G. Procedure for rapid concentration and detection of enteric viruses from berries and vegetables. Appl Environ Microbiol. 2007;73(1).

30. Patel MM, Hall AJ, Vinjé J, Parashar UD. Noroviruses: A comprehensive review. Vol. 44, Journal of Clinical Virology. 2009.

31. Kong BH, Lee SG, Han SH, Jin JY, Jheong WH, Paik SY. Development of enhanced primer sets for detection of Norovirus. Biomed Res Int. 2015;2015.

32. Baert L, Uyttendaele M, Stals A, van Coillie E, Dierick K, Debevere J, et al. Reported foodborne outbreaks due to noroviruses in Belgium: The link between food and patient investigations in an international context. Vol. 137, Epidemiology and Infection. 2009.

12

ARTICLE / INVESTIGACIÓN

Traditional agricultural knowledge of banana, cocoa and sugar cane crops as a basis for the sustainable development of the rural parish Mariscal Sucre

Alberto Yitzak Lozano Sacoto[1]*, Ítalo Edgar Mendoza Haro[2], Carlos Lazo Vento[3]

[1] Tecnológico Universitario ARGOS, Guayaquil, Ecuador.
[2] Universidad Estatal de Milagro Guayaquil, Ecuador.
[3] Universidad Estatal de Milagro Guayaquil, Ecuador.
Corresponding author: yitzaklozano121@gmail.com

Abstract: The research aimed to demonstrate the impact of traditional agricultural knowledge on the sustainable development of banana, cocoa and sugar cane crops in the rural parish of Mariscal Sucre. For this, it was necessary to investigate and adopt a methodology that would estimate the degree of sustainability of the productive systems, identify how it is related to the applied practices and propose an agro-ecological management strategy for these crops. The evaluation was carried out using the MESMIS method but modified through a 30-item form applied to 61 farmers, which collected information to diagnose the incidence of agro-ecological practices and the degree of sustainability of crops. The results were processed in Excel and SPSS and presented with tables and graphs. The agricultural systems showed poor performance, falling into the category of agro-ecological unsustainability. At the same time, the most frequent customary practices consisted of the application of Mulch, and knowledge about protective and antagonistic crops.
Consequently, it was determined that there is a moderately positive correlation between agro-ecological practices and sustainability with a Spearman's Rho coefficient of 0.48; therefore, the management proposal was aimed at reinforcing the productive component with agro-ecological practices. In conclusion, the customary practices contributed to the parish's sustainable development. Therefore, it is advisable to give technical training on the implementation of integrated farms and carry out campaigns to rescue traditional agricultural knowledge.

Key words: Agroecology, customary practices, sustainability assessment, agro-ecological management.

Introduction

The agroecosystems in a geographic area represent an indicator of great importance, which through the diversity of its components, allow the socioeconomic development of the population. Individuals, in turn, take advantage of the resources that nature provides them to obtain economic income; in exchange for these benefits, the required inputs are returned to the ecosystem so as not to destroy the ecosystem and maintain that harmonious balance between man and nature[1].

It is essential to incorporate various elements such as plants, animals and human beings to consider this ecosystem an agroecosystem. In other words, the richness of its components determines the level of development of the agroecosystem and, in turn, allows the establishment of the level of sustainability that it presents intrinsically for its constant evolution[2].

In contrast, conventional agriculture uses large chemical products, such as fertilizers and pesticides. Pesticides directly affect microfauna, endangering bees, the main insect of interest to agriculture worldwide. Fertilizers contribute to soil salinization and contamination of aquifers[2].

It is important to note that agroecology promotes the biodiversity of living microorganisms. Creating a suitable habitat for the optimal development of crops allows local production to be maximized. This contributes by generating

more excellent resistance to pests and diseases; In addition, the decrease in the use of agrochemicals will enable pests not to create resistance to the use of these products[4].

To support this research, the following question must be answered: Can traditional agricultural knowledge practices in agroecosystems be implemented in the rural parish of Mariscal Sucre, and what degree of incidence will they have based on previous scientific research?

As can be seen, it is urgent to answer this question as it is the best path to take to ensure food sovereignty and guarantee the balance of the ecosystem. Avoiding also the continuous deterioration of the environment is the main problem facing humanity today. This puts at risk the food resources of current and future generations and the existence of the human species on the face of the Earth.

The research aims to support the importance of traditional agricultural knowledge practices in the sustainable development of the banana, cocoa and sugar cane production systems of the Mariscal Sucre parish. Through the application of quantitative and statistical evaluation models, to diagnose the state of sustainability of crops, identify the main areas of intervention, and design proposals for agro-ecological management of these crops.

Much of the research focuses mainly on agro-ecological sustainability from a theoretical point of view, dealing

primarily with the production system, leaving a little aside from the social component and especially the knowledge of traditional agriculture. Therefore, the present investigation proposes to identify how these practices are related to the sustainable development of agricultural systems.

Ultimately, the research aims to design a proposal for the agro-ecological management of banana, cocoa and sugar cane crops in the Mariscal Sucre parish. For this, it is necessary to carry out a bibliographic review of sustainability assessment methodologies to choose the most appropriate methods and adapt them to local needs.

Materials and methods

This research has a mixed approach (quantitative and qualitative). The non-experimental - cross-sectional quantitative system will allow us to quantify-measure the frequency and percentage with which traditional agricultural knowledge practices are carried out. The qualitative approach will allow us to lay the scientific foundations through the analysis of scientific documents and the writing of ideas and concepts based on the subject of study. In addition, it will allow the use of an ethnographic design to evaluate the practices of traditional agricultural knowledge existing in the sector under study.

For the field exploration, the simple random sampling method was applied, which allows any member of the population to have the same probability of being chosen; however, because there is no exact record of the number of farmers in the sector. The study population was estimated based on data from the 2010 Population and Housing Census of the INEC, found in the Territorial Development and Planning Plan of the Autonomous Decentralized Parochial Government of Mariscal Sucre, where it is indicated that the Economically Active Population (PEA) employed that is dedicated to activities in the primary sector, corresponds to 67.48% of the PEA, which is equivalent to 1,359 people; distributed in 74.73% (1242) and 32.24% (117) male and female, respectively.

In addition, a mixed survey composed of 30 items was applied, structured in 4 sections, distributed in: classification data, economic dimension, the social dimension and environmental dimension. To evaluate the sustainability of the agricultural production systems of the parish, the MESMIS methodology was applied, which was adapted with the color classification criteria of REDAGRES, and other particular considerations of the present study; for its adequacy, a bibliographic review was carried out on the evaluation of the sustainability of agroecosystems in Latin American countries, obtaining a total of 20 indicators that correspond to the seven attributes (productivity, stability, resilience reliability, equity, adaptability and self-management) and the three dimension (economic, social and environmental) of agro-ecological development proposed in the MESMIS method[5].

Results

Agroecosystems are systems of production and self-sufficiency of agricultural and livestock products, which humans have designed with a biomimetic approach, which proposes to revolutionize conventional agriculture by combining it with ancestral agricultural practices that imitate the behavior of natural ecosystems, maintaining a high degree of biodiversity and recycling of nutrients, water and other materials[6].

The agro-ecological paradigm integrates the concepts of stability, resilience, adaptability and self-sufficiency of ecosystems to ensure farmers' livelihood and quality of life. According to Cevallos and his research, a holistic perspective should be considered regarding the biota, its productivity and the environment; In other words, production systems must be implemented that integrate the human, environmental and economic components with a sustainability approach[7].

Given the need for tools to quantitatively assess the sustainability of agroecosystems, experts have developed four methodological frameworks: Temporal trend, resilience and sensitivity, simulation and sustainability indicators. The latter is the most used due to its ease and versatility of operation and consists of using indicators to estimate the changes and trends of the variables, which intervene in the "improvement or degradation of economic, social and environmental conditions."[8].

Practices of traditional agricultural knowledge possessed by farmers of the Mariscal Sucre rural parish

The study of the demographic characteristics and traditional agricultural practices commonly applied in the Mariscal Sucre parish was carried out by applying a survey to a sample of 61 farmers. Next, the main findings are explained through frequency tables, cross tables and simple and grouped bar diagrams.

Category	Frequency	Percentage (%)
Male	59	96.7
Feminine	2	3.3
Total	61	100.0

Table 1. Frequency and percentages of gender (Source: Own elaboration).

Of the 61 respondents, 59, which corresponded to 96.7%, were male, while only 2, that is, 3.3%, were female. The findings were consistent with the assignment of tasks that rural families usually maintain. The coast, where the field activities are mainly carried out by men, while those of the home is assigned to women.

It was recorded that 75.4% of the farmers were adults aged 30 to 45 years, 19.7% of young people aged 18 to 29 years, and a small proportion of older people, whose percentage was 4.9%. In addition, most respondents recorded their schooling level as secondary, except for the elderly, where primary education was more frequent than secondary, with 3.28 and 1.64%, respectively.

Of the five ethnic groups that were raised in the form, the respondents only identified themselves as mestizos and montuvios, with 90.2 and 9.8%, respectively. Under this precedent, the categories of this variable could be reduced in the future.

The land is generally provided for services, and almost all of the respondents selected this option, in fact, only two people indicated that the land was their property.

95.1% of the respondents indicated that the farms they manage have an area between four to eight hectares, and 4.9% that their farms have a size of four hectares or less. Of the three types of crops established in the parish, the most widespread was banana, followed by cocoa and sugar cane, with percentages of 49.2; 41 and 9.8%, respectively.

The families of the Mariscal Sucre parish are 96.7% of

four to six people and 3.3% of seven to nine people.

The farms of the parish present intensive cultivation of bananas, cocoa and sugar cane, with percentages of 43.5; 36.2 and 8.7%; however, when dealing with family systems, other types of products can be found that are cultivated in a smaller proportion, or sometimes immersed in commercial crops, they are generally products for family consumption and represent 11.6% of the crops.

Of the 12 agro-ecological practices that were presen-

ted in the survey, all except one (crop rotation), had some degree of incidence in the agricultural production systems of the Mariscal Sucre parish. Therefore, this option is set aside for the analysis. The most frequent agro-ecological practices in the area consisted of the application of Mulch at 24.17%, then knowledge about the management of protective crops at 22.27%, followed by the administration of antagonistic crops at 16.11%.

Then, the practice of applying live barriers has a 10.43%

Categories			Education level		Total
			Primary	Secondary	
Age	Young (18 to 29 years old)	Count	3	9	12
		% of the total	4.9%	14.8%	19.7%
	Adult (30 to 45 years old)	Count	10	36	46
		% of the total	16.4%	59.0%	75.4%
	Older (46 to 60 years old)	Count	2	1	3
		% of the total	3.3%	1.6%	4.9%
Total		Count	15	46	61
		% of the total	24.6%	75.4%	100.0%

Table 2. Frequencies and percentages of the level of education compared to age (Source: Own elaboration)

Category	Frequency	Percentage (%)
Half-Blood	55	90.2
Montuvio	6	9.8
Total	61	100.0

Table 3. Frequency and percentages of the ethnic group (Source: Own elaboration).

Category	Frequency	Percentage (%)
Own	2	3.3
By services	59	96.7
Total	61	100.0

Table 4. Frequency and percentages of land ownership (Source: Own elaboration).

Categories			Farm size (ha)		Total
			4 or less	> 4 to 8	
Established crops	Banana	Count	1	29	30
		% of the total	1.6%	47.5%	49.2%
	Cocoa	Count	2	23	25
		% of the total	3.3%	37.7%	41.0%
	Sugar cane	Count	0	6	6
		% of the total	0.0%	9.8%	9.8%
Total		Count	3	58	61
		% of the total	4.9%	95.1%	100.0%

Table 5. Frequency and percentages of crops established by farm size (Source: Own elaboration).

Category	Frequency	Percentage (%)
4 – 6 people	59	96.7
7 – 9 people	2	3.3
Total	61	100.0

Table 6. Frequency and percentages of family size (Source: Own elaboration).

Categories	Frequency	Percentage (%)
Banana cultivation	30	43.5%
Cocoa cultivation	25	36.2%
Sugar cane cultivation	6	8.7%
Other crop	8	11.6%
Total	69	100.0%

Table 7. Frequency and percentages of the main crops (Source: Own elaboration)

4

Categories	Frequency	Percentage (%)
Antagonistic crops	3. 4	16.1%
Protective crops	47	22.3%
Agroforestry practices	6	2.8%
Live barriers	22	10.4%
Cover crops	6	2.8%
Mulch application	51	24.2%
Compost application	2	0.9%
Biol application	12	5.7%
Water recycling	1	0.5%
Seed recycling	11	5.2%
Agricultural production	19	9.0%
Total	211	100.0%

Table 8. Frequency and percentages of applied agro-ecological practices (Source: Own elaboration).

incidence. Lastly, agricultural production with 9.01%, application of Biol with 5.69% and recycling of seeds with 5.21%. These practices have a medium frequency. Finally, the least frequent were knowledge about agroforestry practices and cover crops, with 2.84% each and Compost and water recycling, with 0.95 and 0.47%, respectively.

Determine the level of correlation that exists between the practices of traditional agricultural knowledge and the development of the agroecosystems of the Mariscal Sucre rural parish.

Sustainability analysis of productive systems

To know the degree of sustainable development of the agricultural systems of the parish, a survey was applied to 61 farmers in the area; then the data was processed in an Excel matrix that can be viewed in the annexes to evaluate the degree of sustainability it was necessary to establish the average of the 61 respondents for each of the sustainability indicators that make up the three dimensions of agro-ecological development. The results are presented as radial graphs for each dimension.

From the economic dimension, the best score was that of economic solvency, since farmers rated their farms with an optimal value of 5, followed by profitability with a value of 4, then the productivity indicator with 3. The price indicators

of market and plant diversity are around medium sustainability, with values of 2.7 and 2.3, respectively. The indicators of sources of economic income, livestock diversity and integrated production tend to agro-ecological unsustainability since their values were 1.7, 1.7 and 1, respectively.

The best-scored indicator was technical training, with a value of 3.1, followed by the indicator of access to education since the parish has at least one educational institution and the indicator of belonging to local groups or associations. of farmers, both scored with a value of 3, that is to say that the three indicators are around a medium degree of sustainability. The indicators of knowledge of traditional or ancestral agricultural practices, the type of labor used in the work of the farm and the degree of participation that family members can have in decision-making, with values of 1.9, 1.8 and 1.1, respectively, that is, they have unsustainability.

The dimension of environmental sustainability is also made up of six indicators, of which the best score was the one that refers to the presence of weeds, with a value of 4.1 that tends to optimal sustainability, followed by the form of supply. of water, of the land cover practices applied, whose values were 3, and 2.9, that is, it is in a medium degree of sustainability, while the indicators referring to soil conservation practices, recycling of seedlings and seeds and fertilization practices presented values of 1.7; 1.6 and 1.5,
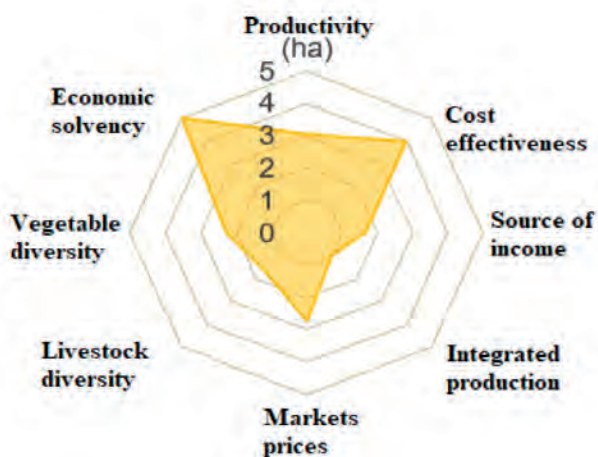
Figure 1. Economic Sustainability.
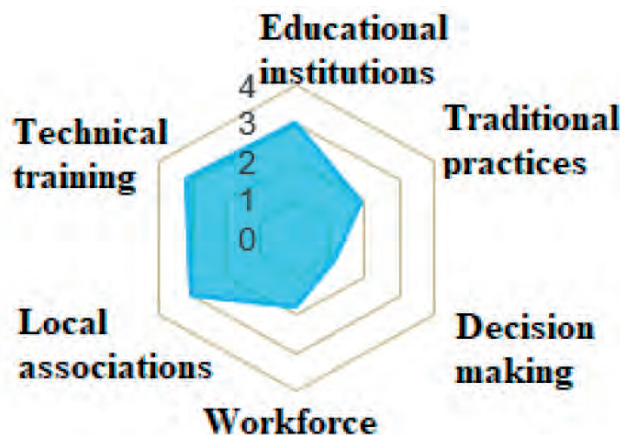
Figure 2. Social Sustainability.
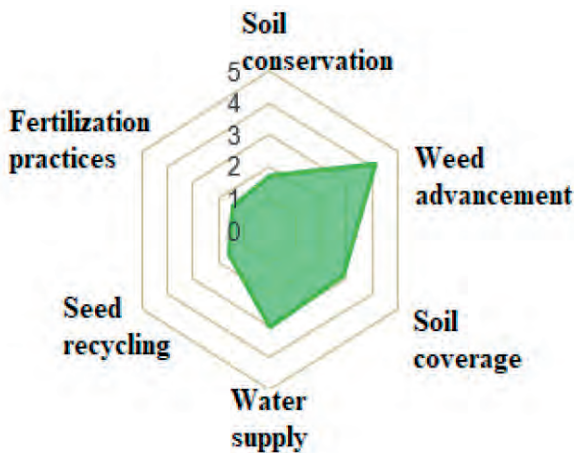
Figure 3. Environmental sustainability.

Figure 4. Performance for each dimension.

that is, the latter are close to the degree of environmental unsustainability of agricultural production systems.

The agricultural systems of the Mariscal Sucre parish presented a better development in the economic dimension, followed by the environmental size and the social dimension, with values of 2.7, 2.5 and 2.3, respectively; that is, they are close to average sustainability. However, the degree of total sustainability of the productive systems is estimated by adding the individual performance of each indicator, thus, the average sustainability of the agricultural systems of the parish was 50%, considered as agro-ecological unsustainability; however, 3 of the 61 agroecosystems presented values of 60 to 62 %, which would indicate a medium agro-ecological sustainability (see annexes).

Analysis of the instrument's reliability

The internal consistency statistic coefficient of Cronbach's Alpha was used to determine the reliability of the evaluation instrument (survey).

The index can take values from zero to one so that its assessment scale is distributed as: unreliable (<0.7), acceptable reliability (0.7 to 0.90) and redundancy or duplication (>0.90 to 1). Where a value of 0.80 would indicate the optimal reliability of the instrument.

The test was run in SPSS software, for which the database was exported from an Excel file; the data was normalized and refined, considering that it is a mixed form and the first section contains classification data. While of the sections corresponding to the dimensions: economic, social and environmental, Of the 20 evaluation items, 10 were excluded because their variables did not correspond to scalar or ordinal variables, and the particular cases were not discriminating enough, however. In the end, they were helpful in determining the degree of sustainability of agricultural systems.

Cronbach's alpha value of 0.72 indicated that the instrument was reliable enough to collect consistent information regarding the development of agricultural systems in the rural parish of Mariscal Sucre.

Before choosing the correlation statistic, the variables were analyzed to verify if they met the parametric or nonparametric statistics criteria.

The two variables come from independent samples; they are of the ratio scale type; however, only the variable: degree of sustainability, presented a significance > 0.05; complying with the normality criterion, so it is decided to use the statistic, Spearman's Rho[2] of nonparametric statistics.

The variables present a moderate positive correlation

	N	%	Cronbach's Alpha	Alpha based on standardized elements	No of elements
cases	Valid	61	100,0	,720	,717	10
	Excluded	0	.0			
	Total	61	100.0			

a. Elimination by list is based on all variables in the procedure. (Source: self-made)

Table 9. Reliability by Cronbach 's alpha.

	Kolmogorov–Smirnov [a]		
	Statistical	gl	Next.
No. of agro-ecological practices applied	.206	61	,000
Degree of sustainability	.088	61	.200 [*]

*. This is a lower bound of true significance.

a. Lilliefors significance correction (Source: Own elaboration)

Table 10. Normality tests.

5

index of 0.48 and a statistical significance of less than 0.05 (p-value < 0.05), so the null hypothesis is rejected, and the alternative is accepted, which maintains that the Traditional agricultural knowledge practices have a favorable impact on the sustainable development of agroecosystems in the rural parish of Mariscal Sucre.

Simple dispersion of the degree of sustainability by applied agro-ecological practices.

In the scattergram, it can be seen that the points have an increasing linear relationship.

Discussion

The research started from the need to know how agro-ecological sustainable the agricultural systems of the Mariscal Sucre parish, which belongs to the Milagro Canton.

A wide range of analysis methodologies was found, some that were developed more than two decades ago, and others more current, which are the result of the modification that the previous ones have suffered. For this reason, the document presented those that were applied. More frequently in Latin American countries. These methodologies were: IICA, SAFE, FESLM, MESMIS and REDAGRES; without a doubt, the one that presented the most significant number of cases was MESMIS. They promote these methodologies' ease of application; by sharing the same methodological framework, they assess the degree of sustainability through indicators[9].

The method chosen to evaluate the degree of sustainability of the agricultural systems in this study was MESMIS; there were a total of 20 indicators related to the indicators designed by Albarracín, although these were duly adapted to the local context[10]. Similarly, Fonseca's research was considered by including the REDAGRES traffic light classification in the presentation of the results[11]. The sustainability indices calculated for the 61 farmers yielded values from 40 to 62% with an average of 50%, being classified as unsustainable; on the other hand, the agroecosystems analyzed by Albarracín had indices of 62 to 76%, that is, they were classified as unsustainable. as moderately sustainable. In the parish, only three systems presented indexes of 60 to 62%, barely meeting the minimum values of average sustainability[12].

The most frequent agro-ecological practices corresponded to knowledge about the existence of protective, antagonistic crops and the application of Mulch as soil cover, the others were applied little, and even crop rotation was non-existent. The correlation between these practices and the degree of agro-ecological development was moderately positive, with a Spearman's Rho correlation index value of 0.48, which leads to the rejection of the null hypothesis and the acceptance of the alternative hypothesis, which indicates that the implementation of Traditional agricultural knowledge practices has a favorable impact on the sustainable development of agroecosystems in the rural parish of Mariscal Sucre. On the other hand, the farms' development

Spearman's rho		No. of agro-ecological practices applied	Degree of sustainability
No. of agro-ecological practices applied	Correlation coefficient	1,000	.475 **
	Next (2-sided)	.	,000
	N	61	61
Degree of sustainability	Correlation coefficient	.475 **	1,000
	Next (2-sided)	,000	.
	N	61	61

**. The correlation is significant at the 0.01 level (bilateral) (Source: Own elaboration)

Table 11. Nonparametric bivariate correlations.
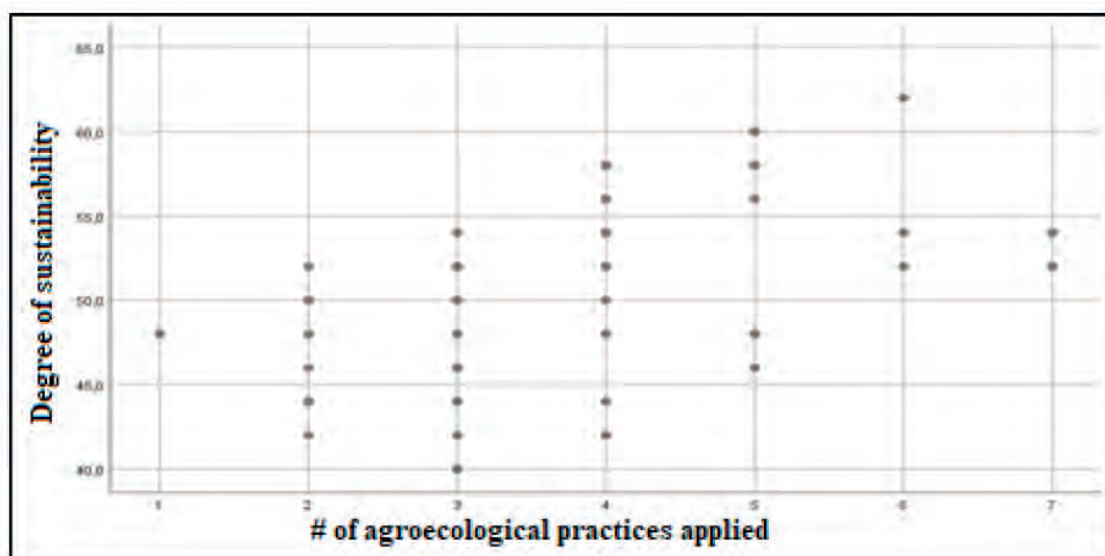
Figure 5. Correlation between agro-ecological practices.

is mostly influenced by the economic component; therefore, it cannot be assumed that there is direct causality between the variables.

Lodana experimental center of the Universidad Laica Eloy Alfaro de Manabí[13]; and the second, carried out in the Río Negro Sopladora National Park in Azuay, proposes the implementation of livestock production of minor species and the production of organic fertilizers from agricultural residues[14]. The authors state that these strategies can almost immediately affect farm productivity and therefore take another step toward the country's ecological transition. For these reasons, the agro-ecological management proposal was raised from the productive dimension, including some practices of traditional knowledge, both in the agricultural and livestock components.

Conclusions

It was determined that traditional agricultural knowledge practices favorably influence the development of banana, cocoa and sugar cane crops established in the rural parish of Mariscal Sucre, finding a value of 0.48 for the Spearman's Rho statistic, indicating that there is a moderate positive correlation between these variables.

An agro-ecological management proposal was established to promote the development of banana, cocoa and sugarcane crops through implementing practices for raising minor species, polycultures and the production of organic fertilizers from farm residues. To diversify the agricultural production system and boost the efficiency of the farms.

Conflicts of Interest

The authors declare no conflict of interest.

Bibliographic references

1. Food and Agriculture Organization of the United Nations. The State of Food and Agriculture. 38th ed. Rome: FAO Collection:; 2007.
2. Madrid A. Organic agriculture and traditional agriculture: an intercultural alternative.. Revista Flacso Andes. 2009; 844.
3. León X. Transgenics, agribusiness and food sovereignty. Revista Flacso Andes. 2014;(1235).
4. Tamayo A. Organic agriculture and traditional agriculture: an intercultural alternative. Revista Flacso Andes. 2013;(4).
5. Santamaría L, O. R. Evaluation of agroecosystems through sustainability indicators in san josé de las lajas, province of mayabeque, Cuba. SciELO Analytics. 2017;(44).
6. Cevallos M, Urdaneta F, Jaimes E. Development of agro-ecological production systems: Dimensions and indicators for their study.. Journal of Social Sciences (Ve). 2019;(3).
7. Cevallos M, Urdaneta Fátima , Jaimes E. Development of agro-ecological production systems: Dimensions and indicators for their study. Journal of Social Sciences (Ve). 2019;(3).
8. Saavedra M. Methodologies for obtaining indicators of agro-ecological sustainability in organic vineyards (Graduation work (Grade), UNIVERSIDAD DE CHILE). Universidad de Chile; 2015.
9. Saavedra M. Methodologies for obtaining indicators of agro-ecological sustainability in organic vineyards (Graduation work (Grade), UNIVERSIDAD DE CHILE).. [Online].; 2015. Available from: HYPERLINK "https://repositorio. uchile." https://repositorio.uchile.
10. Albarracín J, Fonseca N, López L. Agroecological practices as a contribution to the sustainability of agroecosystems. Science and Agriculture Magazine. 2019; 16(2).
11. Fonseca N, Vega Z. proposal of indicators to evaluate sustainability in agricultural and livestock agroecosystems in the sumapaz region.. Pensamiento Udecino. 2018; 2(1).
12. Albarracin J, Fonseca N, López L. Agroecological practices as a contribution to the sustainability of agroecosystems. Sumapaz province case. Science and Agriculture. 2019; 16(2).
13. Ávila E, Granda V. University Laica Eloy Alfaro de Manabi Faculty of Agricultural Sciences. [Online].; 2018. Available from: HYPERLINK "https://1library.co/document/ zw3lvmgy-universidad-laica-eloy-alfaro-manabi-facultad-ciencias-agropecuarias.html" https://1library.co/document/ zw3lvmgy-universidad-laica-eloy-alfaro-manabi-facultad-ciencias-agropecuarias.html .
14. Jadán A. Universidad Polytechnic Salesiana sede Cuenca. [Online].; 2020. Available from: HYPERLINK "https://dspace.ups. edu.ec/bitstream/123456789/18716/1/UPS-CT008760.pdf" https://dspace.ups.edu.ec/bitstream/123456789/18716/1/ UPS-CT008760.pdf .

Evaluation of hydroxymethylfurfural content in commercial and artisanal bee honey from Los Ríos-Babahoyo

Enrique José Salazar Llorente, Hugo Javier Alvarado Álvarez, Jamileth Marianela Castro Cano, Byanka Margarita Sosa Arias, Sonia Alexandra Puga Lascano

DOI. 10.21931/RB/2023.08.01.4

Facultad de Ciencias Agropecuarias, Universidad Técnica de Babahoyo, Km 7.5 Vía Babahoyo, Ecuador.
Corresponding author: ejsalazar@utb.edu.ec

Abstract: Hydroxymethylfurfural (HMF) is a compound that is produced after heat treatment of honey; that is, they are not present in the initial raw materials and can present a potential health hazard; they are known as chemical processing contaminants. This compound is an indicator parameter of the quality of honey produced spontaneously. Its concentration increases with time and other factors, such as improper heat treatment during processing, storage temperature and mode of transportation. The objective of this research is focused on evaluating the content of HMF present in 6 types of bee honey, 3 commercial brands and three artisanal brands; the honey was from eucalyptus and citrus flowering, and the place where the honey was acquired is in the Province of Los Ríos, since being a geographical area with abundant flora, the primary pollinators are bees (*Apis Mellifera*). In addition, the honey was heated at different temperatures and time intervals to evaluate whether Hydroxymethylfurfural increases when heat is added to the honey. The present work was carried out at the Technical University of Babahoyo; the commercial and artisanal bee honey were acquired between 1 and 5 days before the assay. For HMF analysis, a UV spectrophotometer was used, as specified in INEN 1637 standards, to determine the absorbance of the standard sample at 284 and 336 nm. The HMF values obtained for the three commercial brand honey and the artisanal brand honey are within limits allowed by INEN 1572 Technical Standard, which is 4_mg HMF/100_g of honey (40 mg HMF/kg of honey) as a maximum limit. The mean values ranged from 0.08 to 1.77 mg HMF-/g honey, while the honey subjected to heating had mean values ranging from 0.08 to 4.43 mg HMF/100_g honey. A high HMF content was determined, which exceeded the maximum limit, leading to the conclusion that commercial and artisanal honey does contain Hydroxymethylfurfural. Still, in small quantities, it is important to use good handling and preservation methods to prolong the product's shelf life.

Key words: spectrophotometer, *Apis Mellifera*, radiation.

Introduction

Beekeeping is an activity responsible for breeding and caring for bees, with the objective of obtaining products derived from the extraction of nectar that the bees make and that is later placed in their hives. The main products obtained from beekeeping are honey, propolis, wax and royal jelly; many of these products have been used for medicinal, nutritional and curative purposes for many years[1].

Beekeeping is an activity of great value because it stimulates the economy by being an additional source of income for thousands of rural Ecuadorian families. Its importance in agricultural production is also centered on the participation of bees in pollination, a process that guarantees harvests[2].

In Ecuador, one of the main activities that have been carried out for years is beekeeping, which has been characterized as being carried out on a small scale, in rural areas, by small and medium beekeepers. The boom of beekeeping in Ecuador occurred in 1993, with 38500 hives. According to the last National Cadastre of Beekeeping Operations published by the Ecuadorian Agency for Quality Assurance in Agriculture (Agrocalidad), Ecuador, by the end of 2014, presented a total of 12188 hives and 902 beekeepers; with a concentration of beekeepers in the provinces of Pichincha,

Loja, Imbabura and Manabí, these provinces together would represent 60% of beekeeping production in the Country[3].

The beekeeper and especially the beekeeping industry use thermal treatments to achieve fluidity and homogeneity for the honey packaging process or in the eventual blending of honey from different origins to achieve a pleasant honey to the consumer's sight and delay the crystallization process; these treatments and inadequate storage affect honey quality[4].

The beekeeper is in charge of beekeeping practices; his work depends on the time of the year since, during spring and summer, the bees are at their peak of activity. In winter, conditions must be prepared for the following season. When bees are foraging (during the flower pollination period), beekeepers must take care of population control and the subsequent extraction of honey[5].

Honey is considered a substance originated by bees from the transformation of the nectar they collect in nature to feed the members of the hive. However, since time immemorial, humans have benefited from it as part of their diet due to its innumerable nutritional and medicinal benefits[6].

Bee honey is the most represented product in Ecuadorian beekeeping with 85%; beeswax is produced in 5%,

Enrique José Salazar Llorente, Hugo Javier Alvarado Álvarez, Jamileth Marianela Castro Cano, Byanka Margarita Sosa Arias, Sonia Alexandra Puga Lascano

pollen in 3%, propolis in 6%, royal jelly in 1%, and Apitoxin in 0.1%. Approximately 90% of the bee farms in Ecuador are located in rural areas, and the remaining 10% are in urban areas[7].

The Codex Alimentarius defines bee honey as "a naturally sweet-tasting substance produced by Apis mellifera bees from the nectar of plants or the sweat of living parts of plants or from the excretions of plant-sucking insects." It further states that "honey sold shall not contain any additional ingredients, including food additives or additives other than honey"[8].

In bee honey and fruits, fructose is the primary sugar found naturally and in small amounts in some vegetables. Fructose is like glucose, a monosaccharide sugar and the sweetest of all-natural carbohydrates; one molecule of glucose and fructose together produce table sugar (sucrose) which is half[9].

Glucose is a monosaccharide, a simple sugar molecule, freely present in foods such as fruit and honey. This form of sugar is the primary source of energy that ensures the proper functioning of the organism[10].

The consumption of bee honey has excellent benefits for people's health; it has antioxidant and anti-anemic qualities. Products derived from bee honey are currently booming in the use of alternative medicine. Apitoxin (bee venom) has analgesic and anti-inflammatory properties, which are defined as apitherapy[11].

Pure or artisanal honey is the one that goes directly from the honeycomb to the jar, beekeepers sometimes temper it to a maximum of 30 degrees and filter it to remove traces of bees, flowers, etc., but it does not undergo any other process that may alter its nutrients. Processed or commercial honey is subjected to high temperatures and pressures that spoil its beneficial properties[12].

Commercial honey is processed with high-temperature heat followed by rapid cooling. Pasteurization of honey prolongs its shelf life in liquid form, improves its appearance and also kills yeast cells that could change the flavor of the honey. Store-bought commercial honey undergoes excessive processing, heated to about 70 degrees Celsius; due to this, commercial honey loses all its natural characteristics[13].

The melliferous bee or honey bee is an insect of the aphid family; the honey bee group consists of only five species of bees; this species is native to Europe, Africa and part of Asia; honey bees are vital for pollination and development of crops for agriculture, livestock and food. Bees pollinate eighty-four percent of food crops. At least five of every ten things we eat have had a direct relationship with bees by 75 to 80%[14].

The Apis mellifera bee, also known as the honey bee, is one of the most recognized bees among the bee species for its productive yields and honey storage. It has wax-producing glands located in the abdomen with which they make nests using poor-quality waxes or waxes that the workers of the hive[15] secrete.

The characteristics of honey are determined by various laboratory analyses such as physicochemical, sensory and pollen content. The latter is an indicator of the geographical and botanical origin of the honey, and helps determine whether it is multi-floral -when the honey is composed of various plant species- or monofloral[16].

HMF contains a hydroxyl group, an aldehyde and a furan ring, so its possible transformations include reactions such as oxidation, hydrogenation, hydration, decarbonylation or esterification[17].

HMF can be formed spontaneously by different processes, for example, by Maillard reactions, also called non-enzymatic browning or chemical browning reactions, caramelization reactions and acid-catalyzed dehydration of hexoses. In foods highly concentrated in sugars, such as honey, the most feasible reaction is caramelization, although when honey is subjected to processing, Maillard reactions may also be Maillard[18].

Hydroxymethylfurfural (HMF) is an indicator of honey freshness and invertase and diastase enzyme activities. HMF is a compound (aldehyde) formed by the dehydration of sugars, especially fructose. This formation of HMF occurs naturally over time and is accelerated if honey is subjected to high temperatures in the processes of extraction, homogenization, etc.[19].

Compounds generated after a thermal process, i.e., which were not present in the original raw material and may pose a potential health risk, are called processing chemical contaminants. Recently, two new chemical processing contaminants, acrylamide and Hydroxymethylfurfural, have aroused great interest in the scientific community due to their toxicological effects if found in the high range[20].

The spectrophotometer is an instrument used in chemical analysis to measure the radiation absorbed or transmitted by a solution containing an amount of the analyte. In spectroscopy, the term light applies not only to the visible form of electromagnetic radiation but also to the ultraviolet (UV) and infrared (IR) forms, which are invisible. In absorbance spectrophotometry, the ultraviolet and visible regions are used[20].

Materials and methods

The methodology was carried out in the Phytopathology Laboratory of the Technical University of Babahoyo in 6 types of honey, three commercial brands and three artisanal brands to determine the quality of the same, the honey of commercial bees and Artisanal honey acquired five days before. In contrast, artisanal honey was accepted the same day freshly harvested.

This methodology was carried out in two parts:

First: For the analysis of HMF, a UV wave spectrophotometer was used to measure the absorbed radiation; this study was based on the NTE INEN 1637 standards. To spectrophotometrically determine the content of Hydroxymethylfurfural (HMF), in which the absorbance varies depending on the content of Hydroxymethylfurfural (HMF). The product is caused by the overheating of honey from bees due to bad practices in its handling and inadequate storage.

Reagents

Potassium ferrocyanide solution: 15g of potassium ferrocyanide K4Fe (CN)6 was dissolved. $3H_2O$, in 100 cm^3 of distilled water.

Acetate solution of zinc: 30g of zinc acetate Zn $(OAc)^2$ was dissolved. $_2H_2O$, in 100 cm^3 of distilled water.

Sodium bisulfate solution (0.20%): 0.20 g of sodium bisulfate $NaHSO_3$ was dissolved in 100 cm^3 of distilled water.

Experimental procedure

The method used to determine HMF in honey is described below:

5 g of honey was weighed into a beaker and transferred to a 50 cm^3 volumetric flask with approximately 25 cm^3 of distilled water.

0.50 cm³ of potassium ferrocyanide solution was added with a pipette and mixed well; 0.50 cm³ of zinc acetate solution was added, brought to a volume of 50 cm³ with distilled water. The first 10 cm³ of the filtrate is discarded. Two test tubes (18 x 150 mm) were taken, and 5 cm³ of the filtrate was added to each.

In one tube, 5 cm³ of water (sample) was added, and to the other tube that will serve as a reference, 5 cm³ of NaHSO3 solution was added, mixing well.

The absorbance of the standard sample is determined against the absorbance of the reference sample at 284 and 336 nm in a 1 cm cell.

If the absorbance (A) is more significant than 0.6, the standard sample was diluted with water and also the reference sample with NaHS03 in the same proportion. The absorbance A was determined and, for the calculations, considered the dilution made.

Calculations

The content of Hydroxymethylfurfural in honey was determined as follows:
Being:
A1 = sample absorbance at 284 nm.

$$HMF = \left(\frac{mg}{100g}\right) = \frac{(A1-A2)\ x\ F\ x\ 5}{P} \qquad (I)$$

Factor 14.97 = (126/16.830) (1000/10) (100/5)
126 = mole molecular weight of HMF.
16,830 = molar an of HMF at 284 nm
a = molar absorbability for HMF.[21]

One commercial honey and one artisanal honey were used, which were subjected to thermal processes at different temperatures for different time intervals to determine at what temperature the HMF is increasing and if it exceeds the INEN standard's limits 4mg. HMF/100g of honey (40 mg HMF/Kg of honey), would not be suitable, and its quality would be affected; once the heating was done, the same methodology mentioned above in the first part was carried out to evaluate the HMF.

Experimental procedure

The thermal process to which the honey was subjected is detailed below:

100 g of commercial bee honey 1 was weighed and placed in a water bath at 25 °C for 1 h, at 40 °C for 3 hours, at 60 °C for 3 hours and at 80 °C for 3 hours.

100 g of Artisanal bee honey 1 was weighed and placed in a water bath at 25 °C for 1 h, at 40 °C for 3 hours, at 60 °C and at 80 °C for 3 hours.

Calculation of the standard deviation

The standard deviation is a numerical index of the spread of a data set (or population), that is, it is an average of the individual deviations of each observation from the mean. The greater the standard deviation, the greater the dispersion of the results obtained. The standard deviation is a parameter that accounts for the dispersion of the data obtained. For a sample it is calculated with the following formula:

$$S = \frac{\sqrt{\sum_{i=1}^{n}(xi-\bar{x})2}}{n-1} \qquad (II)$$

Pearson correlation

Pearson's correlation coefficient is a test that measures the statistical relationship between two continuous variables. If the association between the items is not linear, then the coefficient is not adequately represented. Pearson's correlation can take values from +1 to -1. A value of 0 shows no correlation between the two variables. A value greater than 0 indicates a positive correlation. As the value of one variable increases, the value of the other variable also increases. A value less than 0 indicates a negative correlation; as one variable's weight increases, the other's value decreases.

The Pearson correlation coefficient formula is as follows:

$$r_{xy} = \frac{\sum Z_X Z_y}{N} \qquad (III)$$

Where:
"x" is equal to variable number one, "y" belongs to variable number two, "zx" is the standard deviation of variable one, "zy" is the standard deviation of variable two, and "N" is the data number.
• If r = zero, there is no association or correlation between the two variables.
• If 0 < r < 0.25 = weak correlation.
• If 0.25 ≤ r < 0.75 = intermediate correlation.
• If 0.75 ≤ r < 1 = strong correlation.
• If r = ±1= perfect correlation.[22]

Results

The results obtained in the first part of the methodology to evaluate Hydroxymethylfurfural in commercial and artisanal honey were the following:

In this table, it is observed that the commercial honey brands underwent a study in triplicate to have more exact values, these values for Hydroxymethylfurfural are within the reference value (4 mg HMF/g of honey), established in the INEN 1572 standard, commercial-type honey has been purchased in a supermarket in the City of Babahoyo at a conservation temperature at room temperature.

This graph shows that commercial honey 1 has a high content of HMF, more than commercial honey 2 and 3, although it does not exceed the reference value (4 mgHMF/g of honey), established in the INEN standard. 1572, it can be determined that commercial honey does contain HMF in small amounts after processing.

In this table 2, it is observed that for the brands of artisanal honey, a study was carried out in triplicate to have more exact values; these values for Hydroxymethylfurfural are within the reference value (4 mg/g of honey), established in the INEN 1572 standard, while artisanal honey 3 does not register the presence of HMF, two of the artisanal honey were acquired in the Canton Ventanas, and the other in the City of Babahoyo at a temperature of environmental conservation.

This graph shows that artisanal honey 2 has a high content of HMF, more than artisanal honey 1. However, it does not exceed the reference value (4 mgHMF/g of honey), established in the INEN 1572 standard; while artisanal honey three did not present any level of HMF in its content, it can be determined that certain artisanal honey does contain HMF in small amounts, perhaps due to poor handling and the temperature at which it is stored, artisanal honey three

3

Enrique José Salazar Llorente, Hugo Javier Alvarado Álvarez, Jamileth Marianela Castro Cano, Byanka Margarita Sosa Arias, Sonia Alexandra Puga Lascano

4

BRANDS OF HONEY BEES	HMF content		CONCENTRATION HMF Technical Standard INEN 1637 Maximum limit allowed
	Unit Values	Average	
Commercial 1	1,76	1,77	4mg HMF/100g of honey
	1,77		
	1,77		
Commercial 2	0,45	0,45	4mg HMF/100g of honey
	0,45		
	0,46		
Commercial 3	0,76	0,76	4mg HMF/100g of honey
	0,76		
	0,77		
Each mark was made in triplicate.			

Table 1. HMF content is present in commercial honey.

Hydroxymethylfurfural maximum limit 4mg HMF/100g of honey
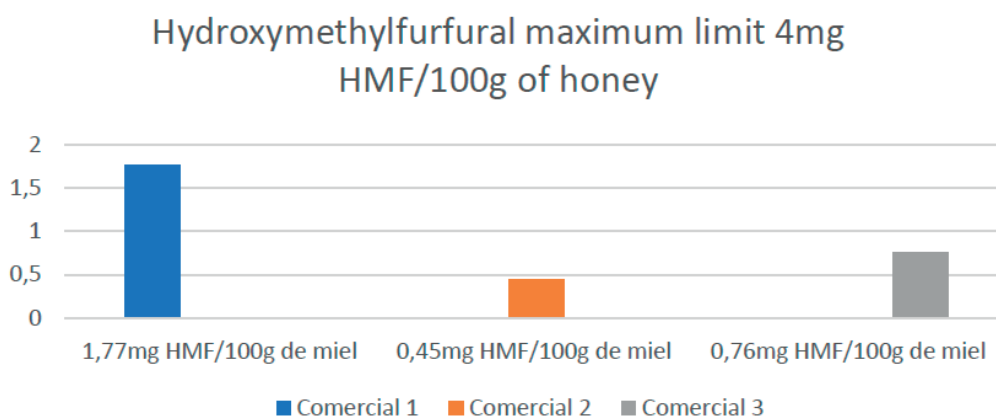
Figure 1. Statistical bars of HMF content in commercial honey.

BRANDS OF HONEY BEES	HMF content		CONCENTRATION HMF Technical Standard INEN 1637 Maximum limit allowed
	Unit Values	Average	
handmade 1	0,08	0,08	4mg HMF/100g of honey
	0,08		
	0,09		
handmade 2	0,11	0,11	4mg HMF/100g of honey
	0,11		
	0,12		
Handmade 3	0,00	0,00	4mg HMF/100g of honey
	0,00		
	0,00		
Each mark was made in triplicate.			

Table 2. HMF content is present in artisanal bee honey.

was newly harvested the day the experiment was going to take place.

The second part of the results was where two kinds of honey were heated in a water bath, applying different temperatures for different time intervals.

This table 3 shows that commercial honey 1 subjected to a temperature of 25 ºC for one hour is within the levels established in the standard, and no variation was obtained; at 40 ºC for three hours, the HMF increases; at 60ºC for three hours, the HMF continues to increase, and at 80ºC it exceeds the ranges established by the INEN standards of 4mg HMF/100g of honey.

This table 4 shows that artisanal honey 1 subjected to a temperature of 25 ºC for one hour is within the levels established in the standard, and no variation was obtained; at 40 ºC for three hours, the HMF increases, at 60ºC, the HMF continues to increase, and at 80ºC it exceeds the ranges established by the INEN standards of 4mg HMF/100g of honey.

X_i is the value obtained from each measurement, x is the arithmetic means of the measurements, and n is the number of measures made. In our case, the sizes of each

BRANDS OF HONEY BEES	TEMPERATURE (ºC)	WEATHER (h)	HMF CONCENTRATION 4mg HMF/100g of honey INEN 1637
Commercial 1	25 ºC	1	1,77
	40 ºC	3	2,03
	60 ºC	3	3,87
	80 ºC	3	4,43

Table 3. Data of the concentration of Hydroxymethylfurfural in the different thermal treatments.

Hydroxymethylfurfural maximum limit 4mg HMF/100g of honey

0,08mg HMF/100g de miel 0,11mg HMF/100g de miel 0,00mg HMF/100g de miel

■ Artesanal 1 ■ Artesanal 2 ■ Artesanal 3
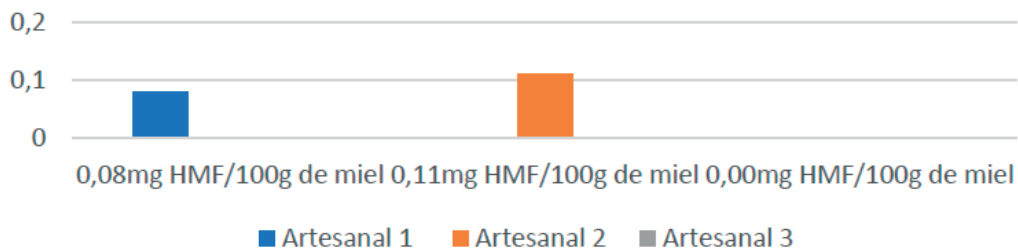
Figure 2. Statistical bars of HMF content in artisanal honeys.

BRANDS OF HONEY BEES	TEMPERATURE (ºC)	WEATHER (h)	HMF CONCENTRATION 4mg HMF/100g of honey INEN 1637
Handmade 1	25 ºC	1	0,08
	40 ºC	3	1,50
	60 ºC	3	3,04
	80 ºC	3	4,10

Table 4. Hydroxymethylfurfural concentration data in the different heat treatments.

of the analyzed honey have been carried out in triplicate. The standard deviation calculation was made in commercial samples 1 and artisan 2, in which the temperatures are varied (40 ºC, 60 ºC and 80 ºC), keeping the exposure time at a constant temperature for (3h).

For the analysis of results, according to the Pearson correlation coefficient = 0.9557, it can be said that the variables X and Y present a strong correlation. Since the value of r is positive, it indicates a positive relationship between the variables (growth in one variable is associated with development in the other variable).

For the analysis of results, according to the Pearson correlation coefficient = 0.9944, it can be said that the variables X and Y present a strong correlation. Since the value of r is positive, it indicates a positive relationship between the variables (growth in one variable is associated with development in the other variable).

Discussion

Once the research is completed, the non-presence of HMF for recently harvested artisanal honey 3 agrees with what is mentioned in various literature[23], indicating that HMF is not a standard component in honey. Fresh or just harvested.

The relatively low HMF values obtained in the three types of commercial honey and in the two types of artisanal

SAMPLES	HMF content	S	HMF (mg HMF/100g of honey)
Commercial 1	2,03		
	3,87	1,26	3,44 ± 1,26
	4,43		
Handmade 1	1,50		
	3,04	1,31	2,88 ± 1,31
	4,10		

Table 5. Calculation of the standard deviation (s) in the commercial 1 and artisanal 1 samples.

Variable Temperature X	Variable Hydroxymethylfurfural Y	X²	Y²	XY
40	2.03	1600	4.1209	81.2
60	3.87	3600	14.9769	232.2
80	4.43	6400	19.6249	354.4

Table 6. Data for Pearson's correlation coefficient in commercial honey 1.

$$r = \frac{n(\sum x_i y_i) - (\sum x_i)(\sum y_i)}{\sqrt{[n(\sum x_i^2) - (\sum x_i)^2][n(\sum y_i^2) - (\sum y_i)^2]}} \quad \text{(IV)}$$

$$r = \frac{3(667.8) - (180)(10.33)}{\sqrt{[3(11600) - (180)^2][3(38.7227) - (10.33)^2]}} = 0.9557$$
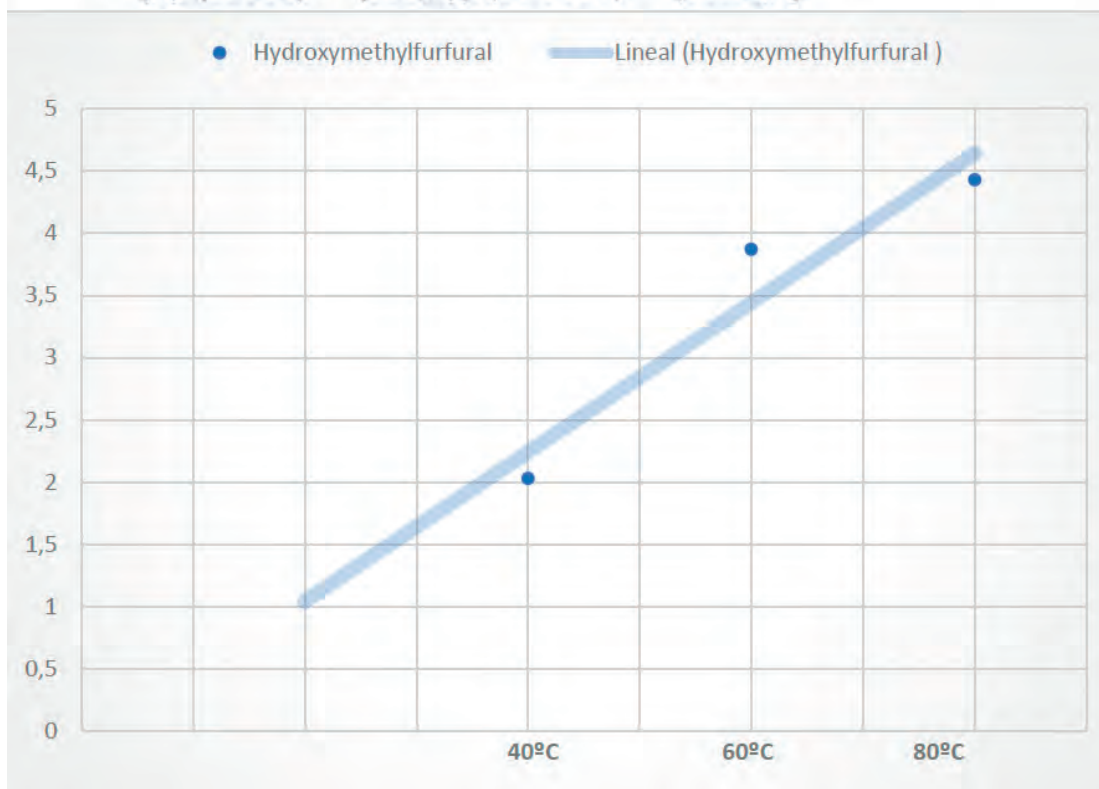
Figure 3. Dispersion diagram between variables.

Variable Temperatura X	Variable Hidroximetilfurfural Y	X²	Y²	XY
40	1.5	1600	2.25	60
60	3.04	3600	9.2416	182.4
80	4.1	6400	16.81	328

Table 7. Data for Pearson's correlation coefficient in commercial honey 1.

$$r = \frac{n(\sum x_i y_i) - (\sum x_i)(\sum y_i)}{\sqrt{[n(\sum x_i^2) - (\sum x_i)^2][n(\sum y_i^2) - (\sum y_i)^2]}} \quad \text{(V)}$$

$$\hat{r} = \frac{3(570.4) - (180)(8.64)}{\sqrt{[3(11600) - (180)^2][3(28.3016) - (8.64)^2]}} = 0.9944$$
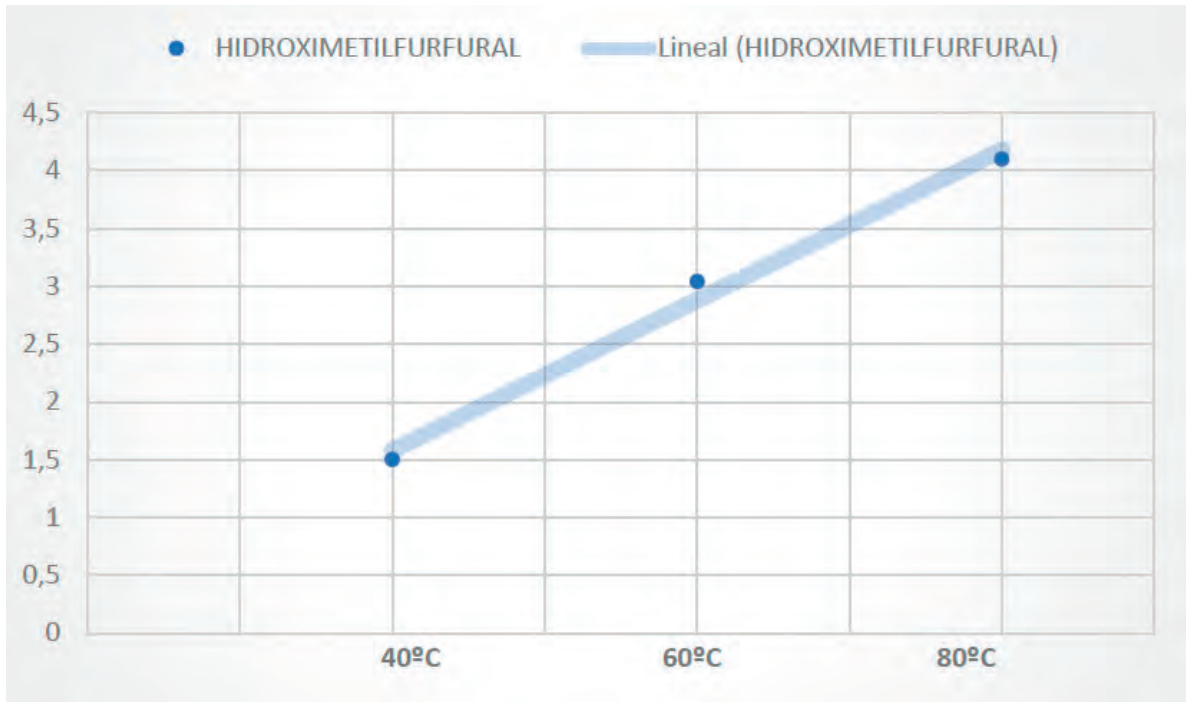
Figure 4. Dispersion diagram between variables.

honey also agree with their values, considering that HMF increases spontaneously with storage at high temperatures around 20°C to 25°C. It is these conditions that have not accelerated the increase in HMF[23].

According to (Villar *et al.*, 2019)[24], they agree with the results obtained when the honey was heated at different temperatures and time intervals when the honey samples were exposed to different temperatures; it was observed that the amount of HMF increased progressively as the temperature increased. In addition, if honey is exposed to very high temperatures for extended periods, it exceeds the legal limit of (4mg HMF/100g honey)[24]. The amount of Hydroxymethylfurfural formed in honey depends on the temperature to which it is exposed and the time of exposure[25].

Néstor Velásquez *et al.*[26] tell us that heating, such as temperature change, poor handling of packaging, transport and storage, are factors that affect the rate of formation of HMF (Hydroxymethylfurfural) in honey; the content increases spontaneously with time, a notable difference was also observed in the increase of HMF in the honey that was subjected to a prolonged heating time[26].

Conclusions

The honey that is sold commercially and artisanally, if they comply with the Ecuadorian Standard INEN 1 572 regarding the content of HMF, establishes a maximum limit of 4mg HMF / g of honey from bees.

According to the results obtained, the commercial honey presented a higher content of Hydroxymethylfurfural than the artisanal honey. However, they are within the limit of the norm. In contrast, one artisanal did not show any level of hydroxymethylfurfural content, for what is determined is that when the honey is freshly extracted from the honeycomb does not offer these levels. It is determined that hydroxymethylfurfural increases due to exposure to high temperatures for long periods in its processing, transportation and storage.

It was also determined that when honey is subjected to different temperatures, hydroxymethylfurfural increases, depending on the time and temperature to which the product is exposed. Therefore, it is considered that honey subjected to processing should not exceed 80 ºC for more than 3 hours because HMF increases and exceeds the permitted limits. In the statistical analysis, it was possible to determine that the temperature is strongly correlated with the rise of Hydroxymethylfurfural in the honey.

It should be considered that honey must be stored between 20-25 ºC so that the HMF remains within the range and its production is very slow.

and to Ing. Enrique Salazar for the advice and help to crystallize this research will be of significant contribution to the population in general.

Conflicts of Interest

There are no conflicts of interest.

Bibliographic references

1. Torres, A., Chimbo, J., & Vargas, J. (2022). Apicultura y bioeconomía: La miel de abeja como alternativa económica sostenible para pequeños productores. Revista Semilla del Este, pág. 3.
2. Vélez, P. (06 de 12 de 2019). Ministerio de Agricultura y Ganadería. Obtenido de https://www.agricultura.gob.ec/ii-foro-apicola-del-litoral-reunira-a-mas-de-200-productores-en-los-rios/
3. Granda, R. (19 de 12 de 2017). Análisis del potencial de la actividad apícola como desarrollado socioeconómico en sectores rurales. Quito, Ecuador. Obtenido de https://repositorio.usfq.edu.ec/bitstream/23000/7106/1/135301.pdf
4. Ruiz, D., Pilamunga, G. I., & Fonseca., E. (2020). Afectación térmica de la miel de abeja en una metodología alternativa, monitoreando hidroximetilfurfural, número de diastasa y vitamina C. Conciencia Digital, pág. 5.
5. Piedra, M. (22 de 02 de 2022). La Vanguardia. Obtenido de https://www.lavanguardia.com/comer/materia-prima/20211228/5027/limon-propiedades-beneficios-valor-nutricional.html-.
6. Carrillo, E., Rojas, L., & Noboa, T. (2021). Determinación de la demanda insatisfecha de miel de abeja en el cantón Morona, provincia de Morona Santiago. Conciencia Digital, pág. 3.
7. Toro, R., Hidalgo, V., Muñoz, R., & Robles, R. (2020). Análisis de las falencias del sector apicultor en la provincia del Guayas (Ecuador). Revista Espacios, pág. 3.
8. Velásquez, D., & Goetschel, L. (2019). Determinación de la calidad físico-química de la miel de abeja. Enfoque UTE, pág. 2.
9. Acurio, J. (14 de 01 de 2020). Food facts for healthy choices. Obtenido de https://www.eufic.org/es/que-contienen-los-alimentos/articulo/que-es-la-fructosa-y-es-mala-para-ti/ Apicultura y miel. (12 de 02 de 2018). Obtenido de https://apicultur-aymiel.com/miel/la-miel-componentes-y-tipos/
10. Barhum, L. (30 de 12 de 2021). Medical News Today. Obtenido de https://www.medicalnewstoday.com/articles/es/diabetes-tipo-2-y-miel
11. Vivanco, I., William, R., Blanca, V., & Verónica, M. (2020). El mercado de la producción de miel de abeja en la provincia del Guayas (Ecuador). Revista Espacios, pág. 2.
12. Martín, C. (16 de 07 de 2022). Clínicas Aleria. Obtenido de https://clinicasaleria.es/diferencias-entre-miel-pura-y-miel-procesada/
13. BEHONEY. (21 de 04 de 2019). Obtenido de https://behoney.es/miel-cruda-vs-miel-comercial/#:~:text=La%20Miel%20Comercial%20es%20la,el%20sabor%20de%20la%20miel.
14. Beevoo. (11 de 02 de 2021). Obtenido de https://beevoo.net/blog/abejas-meliferas-quienes-son-y-por-que-es-importante-saber-reconocerlas/
15. Arteaga, C. (2022). Problemas Sanitarios en Apis mellifera en la región Sierra del Ecuador. Riobamba, Ecuador. Obtenido de http://dspace.espoch.edu.ec/bitstream/123456789/16285/1/17T01700.pdf
16. Biodiversidad Mexicana. (11 de 04 de 2022). Obtenido de https://www.biodiversidad.gob.mx/diversidad/alimentos/mieles
17. Rodríguez, L. (2021). Oxidación de alcohol furfurílico, furfural y 5-hidroximetilfurfural con H2O2 y catalizadores. Ciencias Experimentales, pág. 9.
18. Martínez, J. (09 de 07 de 2018). Parámetros de la calidad de la miel. influencia de las condiciones del procesado. Valencia. Obtenido de https://riunet.upv.es/bitstream/handle/10251/107469/MART%C3%8DNEZ%20-%20PAR%C3%81METROS%20DE%20CALIDAD%20EN%20LA%20MIEL.%20INFLUENCIA%20DE%20LAS%20CONDICIONES%20DEL%20PROCESADO.pdf?sequence=1&isAllowed=y
19. Montiel, L. (2017). Recomendaciones para la calidad de miel: humedad, HMF y otros temas. Red para el desarrollo de la agricultura familiar de Latinoamérica y el Caribe, pág. 5. Piedra, M. (20 de 05 de 2022). Maes Honey. Obtenido de https://www.maeshoney.com/que-es-la-apicultura/
20. Jiménez, V. (2016). "Evaluación de Hidroximetilfurfural en diferentes marcas de miel de abeja, comercializadas en el supermercado de Guayaquil". Guayaquil, Ecuador. Obtenido de http://repositorio.ug.edu.ec/bitstream/redug/12966/1/VICTOR%20JIMENEZ.pdf
21. Vilaña, A. (2013). Miel de abejas. Determinación del contenido de Hidroximetilfurfural (HMF). Quito: Norma Técnica Ecuatoriana (NTE INEN).
22. Fiallos, G. (2021). La Correlación de Pearson y el proceso de regresión por el Método de Mínimos Cuadrados. Revista Científica Multidisciplinar, pág. 6-9.
23. Jiménez, V. (2016). "Evaluación de Hidroximetilfurfural en diferentes marcas de miel de abeja, comercializadas en el supermercado de Guayaquil". Guayaquil, Ecuador. Obtenido de http://repositorio.ug.edu.ec/bitstream/redug/12966/1/VICTOR%20JIMENEZ.pdf
24. Villar, M., Villar, P., Cobo, S., Rodríguez, D., & Serrano, M. (2015). Determinación de hidroximetilfurfural en mieles como parámetro indicador de la calidad de las mismas. Revista de Ciencias de la Universidad Pablo de Olavide, pág. 3.
25. Vargas, M. (2006). Efecto del tratamiento térmico temporal de la miel de abeja sobre la variación de su calidad. Ambato, Ecuador.
26. Velásquez, N. (2013). "Evaluación de diferentes tiempos de calentamiento de la miel de abeja (Apis mellifera) para retardar su cristalización y determinar los niveles de HMF (Hidroximetilfurfural), en la asociación de apicultores del sur Occidente de Guatemala". Guatemala. Obtenido de https://core.ac.uk/reader/35293030

In vitro inhibition of xanthine oxidase by hydroalcoholic extracts of *Corynaea crassa* Hook. F

Alexandra Jenny Lopez Barrera[1]*, Yamilet Irene Gutiérrez Gaitén[2]

[1] Faculty of Chemical Sciences "Salvador Allende", University of Guayaquil, Guayaquil, Ecuador.
[2] Department of Pharmacy, Institute of Pharmacy and Food, University of Havana, Havana, Cuba.
Corresponding author: alexandra.lopezb@ug.edu.ec

Abstract: *Corynaea crassa* is a hemiparasitic plant native to America, used for the treatment of erectile dysfunction and has been shown to have antimicrobial properties. However, it lacks other biological studies to justify its use in traditional medicine. The objective was to examine the *in vitro* inhibitory activity of xanthine oxidase in hydroalcoholic extracts of the species from Ecuador and Peru. The extracts obtained by maceration and the Allopurinol used as the reference drug, at concentrations of 10, 30, 40, 50 and 60 µg/mL, were tested to measure the degree of *in vitro* inhibition of xanthine oxidase employing spectrophotometric determination at 295nm, which is associated with the formation of uric acid. The two extracts showed significant inhibitory activity on xanthine oxidase in a concentration-dependent manner, with the highest percentages being observed at the highest concentrations, being higher for the extract from the Ecuadorian species with enzyme inhibition percentages comparable to Allopurinol. Median inhibitory concentration (IC_{50}) values of 15.35µg/mL and 17.42µg/mL were observed for the extracts from Ecuador and Peru, respectively, although the activity was more notable for the reference drug, which was shown to be an IC_{50} of 12.21 µg/mL. The results concluded the basis for the potential use of *C. crassa* in the treatment of hyperuricemia.

Key words: xanthine oxidase, hydroalcoholic extracts, Allopurinol.

Introduction

The species *Corynaea crassa* Hook. F (Balanophoraceae) is a hemiparasitic plant native to America, found in various countries, including Bolivia, Colombia, Costa Rica, Ecuador, Mexico, Panama, Peru and Venezuela. In Ecuador, it is located in the provinces of Azuay, Carchi, Chimborazo, Cotopaxi, Imbabura, Loja, Morona Santiago, Napo, Pichincha, Sucumbios, Tungurahua and Zamora Chinchipe[1].

In previous studies, the antioxidant activity of hydroalcoholic extracts of the species was evaluated, with similar or superior results to the tested reference substances (vitamin C and Trolox)[2]. Other studies demonstrated the anti-inflammatory effect of the aqueous and hydroalcoholic extracts of the plant from Ecuador and Peru[3] and the erectogenic effect on induced sexual dysfunction in rodents[4].

Phytochemical studies revealed by liquid chromatography-mass spectrometry the presence of catechin, quercetin, and a flavanone glycoside)[2]. Other investigations by gas chromatography-mass spectrometry allowed the detection of terpenoids and fatty acids as significant compounds[3]. On the other hand, Malca *et al.*[5], reported sterols, triterpenoids, flavonoids, tannins and anthocyanins.

In Ecuador, *C. crassa* is little used due to the population's ignorance. Because it develops in the Andean forests and lacks sufficient scientific studies to support said ancestral knowledge, the present investigation was carried out to examine the *in vitro* inhibitory activity of xanthine oxidase in hydroalcoholic extracts of the species from Ecuador and Peru.

Materials and methods

The species *Corynae crassa* was collected in August 2018, coming from Ecuador (Yanachoca reserve in the north of Pichincha Province (00° 05′S, 78° 33′E, 3700 m elevation)) and Peru (province of La Libertad, department of Santiago de Chuco, Agasmarca (08°07′53″S, 78°03′23″E, 2900 m elevation). One specimen from each collection was identified in the herbarium of the Faculty of Natural Sciences of the University of Guayaquil. It was deposited under the coupon specimen of 13,115 and 13,116, respectively. The whole plant was worked with. The hydroalcoholic extracts were obtained by maceration from 20 g of the dry drug in 100 mL of the hydroalcoholic mixture at 80%. Subsequently, they were concentrated to dryness in a rotary evaporator (Buchi REF 120) at a temperature of 50 °C and redissolved in dimethylsulfoxide (Sigma-Aldrich) for *in vitro* analysis.

Xanthine oxidase inhibition assay

The inhibitory activity of xanthine oxidase (XO) was assayed spectrophotometrically under aerobic conditions, according to the procedure described by Nguyen *et al.*[6]. The assay mixture consisted of 50 mL of test solution, 35 mL of 70 mM phosphate buffer (Sigma, Aldrich) (pH=7.5), and 30 mL of xanthine oxidase enzyme solution (Sigma, Aldrich) (0.01 units / mL in 70 mM phosphate buffer, pH=7.5), was prepared immediately before use. After preincubation at 25 °C for 15 min, the reaction was started by adding 60 mL of substrate solution (150 mM xanthine (Sigma, Aldrich) in the same buffer). The assay mix was incubated at 25°C for 30 min. The reaction was stopped by adding 25 mL of 1N HCL,

2

Figure 1. *Corynaea* is a monotypic genus of parasitic plants, belonging to the family Balanophoraceae. Its only species: *Corynaea crassa* Hook.f., is native to America.

and the absorbance at 290 nm was measured in a spectro-photometer (RAY LEIGH UV-1601 of Chinese origin). The enzyme solution was added to the assay mix after adding 1N HCL, and a blank was prepared in the same way. One XO unit is defined as the enzyme needed to produce 1 mol of uric acid/min at 25 °C.

XO inhibitory activity was expressed as the percentage inhibition of XO in the above assay system, calculated as $(1 - B/A)$ x 100, where A and B are the activities of the enzyme without and with test material, respectively. The extracts (from samples from Ecuador and Peru) and the Allopurinol (Sigma) used as a positive control were prepared at concentrations of 10, 30, 40, 50 and 60 μg/mL.

Statistical analysis

The results were expressed as mean/standard deviation (SD), and the experiments were carried out in triplicates. A one-way analysis of variance (ANOVA) was used to determine the differences between groups, followed by the Duncan test with $p \leq 0.05$. The mean inhibitory concentration (IC_{50}) of the reference drug and the extracts was calculated from the mean values of the data of three determinations. The Statgraphics statistical program Plus version 5.1 was used to process the experimental data.

Results

The inhibitory activity of xanthine oxidase (XO) was demonstrated by the hydroalcoholic extracts of C. crassa, with enzyme inhibition percentages more significant than 50% from a concentration of 30 μg/mL. The results of this study demonstrated that the active extracts inhibited XO in a dose-dependent manner. The results of the in vitro XO inhibitory activity of test samples and control are shown in table 1.

Discussion

Xanthine oxidase (XO) inhibitors are generally used for the treatment of gout and hyperuricemia since they can hinder the enzymatic reactions involved in the synthesis of uric acid, reduce the formation of uric acid and relieve the symptoms of said disease, a very painful medical condition caused by high levels of uric acid. Scientists have recently attempted to find new safe XO inhibitors from various plants[7,8].

In the Balanophoraceae family, especially in the *Balanophora* genus, many phytochemicals have been found with a hyperuricemic effect[7,9]. However, in the genus *Corynaea* ofthe same family, the inhibitory activity of the enzyme xanthine oxidase has not been studied, which allowed this research to be carried out on *C. crassa*.

Five concentrations of hydroalcoholic extracts of species from Ecuador and Peru were tested, and Allopurinol as a reference drug, which prevents the formation of uric acid and is the mainstay of prophylactic treatment for hyperuricemia in patients undergoing chemotherapy[10,11].

XO is an important enzyme that converts xanthine and hypoxanthine to uric acid; thus, an increased rate of XO activity leads to excessive uric acid production[11]. In the present investigation, the reference drug and the two tested extracts (Ecuador and Peru) were able to reduce the activity of the said enzyme with mean inhibitory concentration values of 12.21, 15.35 and 17.42 μg/mL, respectively. The extract from the Ecuadorian sample showed enzyme inhibition

Concentration (µg/mL)	XO inhibitory activity (%)		
	Allopurinol	Ecuador extract	Peru extract
10	43.01/2.11[a]	40.01/1.91[ab]	38.77/0.92[b]
30	71.35/0.70[a]	70.12/0.63[ab]	68.27/1.75[b]
40	79.93/1.39[a]	75.21/1.20[b]	71.44/0.68[c]
50	81.87/1.63[a]	78.66/1.01[a]	73.20/2.19[b]
60	88.31/0.96[a]	86.25/1.04[a]	83.36/2.04[b]
IC$_{50}$	12,21	15,35	17,42

Values represent Mean / Standard deviation (*n* =3)

Different letters in a row show significant differences (p <0.05) according to Duncan test

Table 1. *In vitro* xanthine oxidase inhibitory activity of *C. crassa* extract.

percentages comparable to Allopurinol at all concentrations tested (10, 30, 40, 50 and 60 µg/mL). An analysis of the results concerning the literature reports[9] demonstrated the excellent capacity of the extracts to inhibit xanthine oxidase, compared to the species *Balanophora laxiflora* (Balanophoraceae), where at a concentration of 10 µg/mL of the crude extract of the plant, an inhibition of 31.7% was obtained, lower than the experience carried out where the evaluated extracts registered values of 40.01% (Ecuador) and 38.77% (Peru). In addition, the IC$_{50}$ values(the concentration required to inhibit uric acid formation by 50%) of crude extract was 28.2 µg/mL, while for the extracts under study, the IC50 was 15.35 and 17.42 µg/mL.

Comparison with other investigations of the species *Balanophora subcupularis* P.C. Tam (IC50= 48.41 µg/mL), also confirms the high property of *C. crassa* extracts as inhibitors of the enzyme xanthine oxidase. In contrast, *Balanophora tobiracola Makino* (Balanophoraceae) showed higher activity (IC$_{50}$=11.87 µg/mL)[7].

Natural products have been taken as an ideal source of bioactive compounds with specific pharmacological activities. Inhibitors of xanthine oxidase have been identified and isolated in many plant extracts[12,13]. Several bioactive compounds, including polyphenols, saponins, terpenoids, phenylethane glycosides, and alkaloids, among other compounds, are effective inhibitors of XO[13,14].

Previous studies with hydroalcoholic extracts of *C. crassa* demonstrated the presence of a variety of metabolites, including catechin flavonoids, quercetin glycoside, and a flavanone glycoside[2], terpenoids (triterpenoids and sesquiterpenoids), saponins, tannins, among others compounds[3] that could contribute to the inhibition of xanthine oxidase.

Conclusions

The results of this research provide scientific evidence for the first time on the inhibitory capacity of *C. crassa* xanthine, and the species may be considered a potential resource in the treatment of hyperuricemia and gout.

Author Contributions

AJLB proposed the concept of this study and analyzed the results and wrote the initial draft; YIGG. Investigation, writing-review and editing.

Conflicts of Interest

The authors declare no conflict of interest.

Bibliographic references

1. Tropics. Flora Mesoamericans. Corynaea crassa Hook. f. [Online]. 2012. (Cited 2020 Dec 10. Available from: http://www.tropicos.org/name/03000026?projectid=3

2. Lopez, A.J.; Gutiérrez, G.Y.I.; Miranda, M.M.; Choez, G.I.A.; Ruiz, R.S.G.; Scull, L.R. Pharmacognostic, Phytochemical, and Anti-Inflammatory Effects of Corynaea crassa: A Comparative Study of Plants from Ecuador and Peru. Pharmacognosy Research 2021, 12, 394-402. Doi: 10.4103/pr.pr_42_20

3. Lopez, A.J.; Gutiérrez, Y.I.; Miranda, M.; Choez, I.A., Ruíz, S.G., Scull, R. Pharmacognostic, phytochemical, and anti-inflammatory effects of Corynaea crassa: A comparative study of plants from Ecuador and Peru. Pharmacogn. Res. 2020, 12, 394-402. https://dx.doi.org/10.4103/pr.pr_42_20

4. Acaro, F.; Arroyo, J. Efecto del extracto de Corynaea crassa y selenio en la disfunción sexual inducida en Rattus norvegicus albinus. Rev. Peru. Med. Integr. 2019, 4(3), 83-89.

5. Malca, G.R.; Hennig, L.; Sieler, J.; Bussmann, R.W. Constituents of Corynaea crassa Peruvian Viagra. Rev. Brasileira de Farmacognosia 2015, 25, 92-7.

6. Nguyen, M.T.T; Awale, S.; Tezuka, Y.; Tran, Q.L.; Watanabe, H; Kadota, S. Xanthine oxidase inhibitory activity of Vietnamese medicinal plants. Biol. Pharm. Bull. 2004, 27, 1414-1421.

7. Tung, N.T.; Quan, N.V.; Anh, N.P.; Phuong, N.V.; Hung, N.Q. Preliminary Phytochemical Evaluation and In Vitro Xanthine Oxidase Inhibitory Activity of Balanophora subcupularis P.C. Tam and Balanophora tobiracola Makino (Balanophoraceae). Trop J Nat Prod Res. 2019, 3(1), 6-9. Doi.org/10.26538/tjnpr/v3i1.2

3

4

8. Rodriguez, S.A.; Murray, A.P.; Leiro, J.M. Xanthine Oxidase Inhibition by Aqueous Extract of Limonium brasiliense (Plumbaginaceae). Chem. Proc. 2021, 3, 123. https://doi.org/10.3390/ecsoc-24-08410

9. Ho, S.T.; Tung, Y.T.; Huang, C.C.; Kuo, C.L.; Lin, C.C.; Yang, S.C.; et al. The Hypouricemic Effect of Balanophora laxiflora extracts and derived phytochemicals in hyperuricemic mice. Hindawi. Evidence-Based Complementary and Alternative Medicine 2012, 2012. Doi:10.1155/2012/910152

10. Bernardes, A.C.; Brandão, C.G.; Araújo, M.C.; Guimarães, D.A. In vivo anti-hyperuricemic activity of sesquiterpene lactones from Lychnophora species. Revista Brasileira de Farmacognosia 2019, 29, 241-245.

11. Cicero, A.F.G.; Fogacci, F.; Cincione, R.I.; Tocci, G.; Borghi, C. Clinical effects of xanthine oxidase inhibitors in hyperuricemic patients. Med Princ Pract 2021,, 30, 122-130. DOI:10.1159/000512178

12. Liu, Y.; Hou, Y., Si, Y.; Wang, W.; Zhang, S.; Sun, S.; et al. Isolation, characterization, and xanthine oxidase inhibitory activities of flavonoids from the leaves of Perilla frutescens. Natural Product Research. 2019. https://doi.org/10.1080/14786419.2018.1544981

13. Liu, L.; Zhang, L.; Ren, L.; Xie, Y. Advances in structures required of polyphenols for xanthine oxidase inhibition. Food Frontiers 2020, 1, 152-167. DOI: 10.1002/fft2.27

14. Mehmood, A.; Zhao, L.; Wang, C.; Nadeem, M.; Raza, A.; Ali, N.; et al. Management of hyperuricemia through dietary polyphenols as a natural medicament: A comprehensive review. Critical Reviews in Food Science and Nutrition. 2019, 59(9), 1433-1455. https://doi.org/10.1080/10408398.2017.1412939

ARTICLE / INVESTIGACIÓN

Trampeo masivo de *Plutella xylostella*: una alternativa ambiental y económicamente beneficiosa para su control en Costa Rica

Mass trapping of *Plutella xylostella*: an environmentally and economically beneficial alternative for its control in Costa Rica

Francisco González-Fuentes*, Steven Niño Narváez, Carlos Rodríguez-Chinchilla, Alejandro Vargas-Martínez, Allan Gonzalez-Herrera

DOI. 10.21931/RB/2023.08.01.6

Laboratorio de Entomología, Escuela de Ciencias Agrarias, Universidad Nacional de Costa Rica, Costa Rica.
Corresponding author: francisco_gonzalez@chemtica.com

1

Resumen: *Plutella xylostella* es globalmente la plaga más importante en Brassicaceae. Desgraciadamente, su manejo sigue enfocándose en insecticidas con poco efecto sobre la plaga y con altos costos económicos y ambientales. Esta investigación buscó confirmar reportes sobre su control basado en trampeo masivo con feromona y comparar el costo de esta técnica en contraposición con la aplicación calendarizada de insecticidas. Para esto, en el año 2020, se establecieron seis parcelas experimentales en fincas comerciales de repollo en la provincia de Cartago, Costa Rica. Trampas con feromona para monitoreo se colocaron en todas las parcelas, sin embargo, solamente tres parcelas recibieron el equivalente de 50 trampas/hectárea para establecer el trampeo masivo para control de la plaga, mientras que las otras tres parcelas no tuvieron trampas adicionales a las de monitoreo y el control se basó en la aplicación calendarizada de insecticidas. Para determinar el efecto del trampeo masivo y sus costos se determinaron las capturas en trampas semanalmente durante todo el ciclo, el daño de la plaga y los costos asociados al control de la misma. Los resultados demostraron que las aplicaciones calendarizadas de insecticidas no mantuvieron poblaciones significativamente menores que el trampeo masivo. No obstante, la diferencia más evidente a favor del uso de trampeo masivo como estrategia de control se observó en el porcentaje de daño en planta y los costos involucrados, los cuales fueron significativamente menores en el trampeo masivo que en las aplicaciones de insecticidas. Los resultados obtenidos corroboran reportes sobre la capacidad ecológica y el beneficio económico de la adopción de trampeo masivo como estrategia para el control de la polilla dorso diamante.

Palabras clave: Polilla dorsal del diamante, captura masiva, feromona, insecticidas, costes, insecticidas.

Abstract: *Plutella xylostella* is the most crucial pest in Brassicaceae globally. Unfortunately, its management focuses on insecticides with little effect on the problem and high economic and environmental costs. This research sought to confirm reports on its control based on pheromone mass trapping and compare the price of this technique as opposed to the scheduled application of insecticides. In 2020, six experimental plots were established in commercial cabbage farms in Cartago, Costa Rica. Pheromone traps for monitoring were placed in all plots. However, only three actions received the equivalent of 50 traps/hectare to establish mass trapping for pest control. At the same time, the other three plots did not have additional traps to those for monitoring and control based on the scheduled application of insecticides. To determine the effect of mass trapping and its costs, the captures in traps were chosen weekly throughout the cycle, as the damage of the past and the costs associated with its control. Results showed that scheduled insecticide applications did not maintain populations significantly lower than mass trapping. However, the most evident difference in favor of the use of mass trapping as a control strategy was observed in the percentage of plant damage and the costs involved, which were significantly lower with mass trapping than with insecticide applications. The results corroborate reports on the ecological capacity and the economic benefit of adopting mass trapping to control the diamondback moth.

Key words: Polilla dorso diamante, trampeo masivo, feromona, insecticidas, costos

Introducción

La polilla dorso diamante, *Plutella xylostella* Linnaeus, es la plaga más importante en la producción mundial de los cultivos de consumo humano de la familia Brassicacea, llámense brócoli, coliflor y repollo principalmente. Esta plaga es capaz de ocasionar pérdidas de hasta el 100% del cultivo, sea por daño directo o por afectación de la calidad del producto haciéndolo no comercializable[1]. Por tanto, como medida preventiva y correctiva del riesgo que esta plaga representa, los productores se han enfocado prácticamente de manera exclusiva en las aplicaciones calendarizadas de insecticidas sintéticos[2]. Desgraciadamente, la polilla dorso diamante dada su capacidad reproductiva (con más de 12

Francisco González-Fuentes, Steven Niño Narváez, Carlos Rodríguez-Chinchilla, Alejandro Vargas-Martínez, Allan Gonzalez-Herrera

generaciones por año) y su alta capacidad de adaptación ha desarrollado poblaciones con resistencia a la más diversa índole de productos fitosanitarios, incluyendo insecticidas orgánicos como *Bacillus thuringiensis* subs. kurstaki y más recientemente Spinosad[2-4]. Ante esto, los productores, recurren a aplicaciones aún más frecuentes de insecticidas, generando un círculo vicioso en su uso. En un estudio realizado en Costa Rica en 1999 se determinó que, en un ciclo de 3 meses, el número de aplicaciones de insecticidas en repollo para el control de la polilla del repollo iba de 9 a 16 veces por ciclo, lo cual representa 1 y hasta 2 aplicaciones químicas semanales[5]. Dos décadas más tarde, el panorama productivo no es muy diferente en la Región Centroamericana en donde el promedio de aplicaciones de insecticidas es diez, lo cual, consecuentemente, conlleva un efecto negativo importante en salud humana, en la presencia de enemigos naturales y finalmente en la inversión económica necesaria para producir estos cultivos.

Dado que el problema de *P. xylostella* no es nada nuevo, las alternativas para su control se han investigado por más de tres décadas. El control biológico y el control a través del uso de feromonas (monitoreo y trampeo masivo) son las alternativas con mayor potencial, incluso mostrándose como aliados perfectos con efectos sinergistas en programas de manejo integrado de plagas (MIP) que contemplen ambos métodos[1,6-8]. Una alternativa particularmente práctica y fácil de implementar por parte de los productores de brásicas es el uso de umbrales del número de machos de la polilla capturados por noche en trampas cebadas con la feromona como indicadores para la necesidad de realizar aplicaciones químicas. En un trabajo realizado en India, se determinó que la aplicación de insecticida 12 – 24 horas después de que las trampas con feromona capturaban 8, 12 y 16 machos por trampa por noche en repollo, coliflor y col silvestre respectivamente, eran capaces de disminuir más eficazmente la presencia de la plaga en campo, el daño en los vegetales y el rendimiento en comparación a aplicaciones calendarizadas a los 7, 9, 12 y 15 días después de transplante[6]. De manera similar, siempre en India, el trampeo masivo (colocación homogénea de múltiples trampas en alta densidad para capturar la mayor cantidad posible de adultos) se ha demostrado como una alternativa exitosa en múltiples ocasiones con aumentos significativos de producto comercializable, disminución de los gastos asociados al control de la plaga e incrementos en las ganancias brutas por hectárea[8-10].

Aunque las estrategias bio-racionales para el control de *P. xylostella* han sido demostradas en investigaciones académicas por al menos 20 años, la adopción de las mismas por parte de los productores ha sido pobre. Los factores que explican esta tendencia son varios. La prevalencia de insecticidas de amplio espectro imposibilita el establecimiento de enemigos naturales que mantengan a la plaga bajo control, mientras que productos de origen orgánico como Spinosad y *Bacillus thuringiensis* han sido víctimas de su propio éxito de manera tal que los productores hacen uso excesivo de los mismos hasta que pierden efecto y poco a poco regresan a los insecticidas de amplio espectro[7]. En el caso del uso de trampas cebadas con feromona la historia ha sido un poco diferente, dado que la baja adopción se relaciona con desconocimiento del uso y la percepción de que es una tecnología de mayor costo económico y que involucra mayor riesgo de pérdida del cultivo al atraer la plaga al cultivo, ambas razones completamente falsas debido al bajo costo de las feromonas y la imposibilidad de

la feromona de atraer hembras al cultivo las cuales son las únicas que pueden causar brotes de la plaga[5].

La presente investigación se llevó a cabo con el objetivo de determinar si el trampeo masivo con feromona y el uso de los umbrales reportados por investigadores en India eran capaces de ser una alternativa a la aplicación calendarizada de insecticidas ampliamente usada por productores comerciales de repollo en Costa Rica para el control de la polilla dorso diamante, *P. xylostella*.

Materiales y métodos

La investigación se llevó a cabo entre los meses de junio y octubre del 2020, en los distritos de Capellades y Pacayas, del Cantón de Alvarado de la provincia de Cartago, Costa Rica. Se escogieron seis parcelas comerciales de repollo pertenecientes a cinco productores independientes. La distancia entre fincas y por tanto entre parcelas fue variada, con un mínimo de 150 m y un máximo de 5 Km. De igual forma, el tamaño de la parcela en cada finca fue diferente con un mínimo de 2130 m² y un máximo de 7000 m².

Comparación trampeo masivo versus aplicación calendarizada de insecticidas

Las seis parcelas seleccionadas fueron divididas en dos grupos: un grupo control en el cual se colocaron de 3 a 6 trampas de galón plásticas con agua jabonosa cebadas con feromona (P054-lure, ChemTica, Costa Rica) para monitoreo de *Plutella xylostella* y en las cuales el productor siguió su protocolo tradicional de aplicación calendarizada de insecticidas al menos 1 vez por semana o cuando consideró necesario (ad libitum), y un segundo grupo en el cual se colocaron 6 trampas de monitoreo además de las correspondientes trampas de trampeo masivo cebadas también con la misma feromona comercial y siguiendo la proporción de 50 trampas/ha para trampeo masivo, y en las cuales se realizaron aplicaciones de insecticidas únicamente si las capturas superaron el umbral de 8 polillas por trampa por noche en las trampas de monitoreo. En todas las parcelas por igual se siguieron las prácticas agronómicas normales utilizadas en fincas comerciales (manejo de enfermedades, nutrición, hierbas, riego, etc).

Parámetros evaluados

Semanalmente, en cada parcela se realizaron visitas en las cuales se contabilizó el número total de individuos capturados por trampa de monitoreo, se dio renovación del agua jabonosa y mantenimiento en caso de que la trampa lo requiriese. De cada parcela se obtuvo el promedio de polillas capturadas por trampa por noche y se utilizó como parámetro para decidir si se necesitaban aplicaciones químicas en el caso de las parcelas bajo trampeo masivo. Con cada visita además se realizó un análisis del daño característico en planta debido a la larva de la polilla dorso diamante. Para esto en cada parcela se seleccionaron de manera completamente aleatoria 20 plantas semanalmente distribuidas lo más disperso y equidistante posible en la parcela. En cada planta se clasificó el tipo de daño según la escala reportada de Schuster, Workman y Chalfant[11]. A partir del número de plantas con algún tipo de daño se obtuvo el porcentaje de plantas dañadas por cada parcela y se promedió por tratamiento.

En el caso del análisis económico, se examinó el costo de cada tratamiento en relación a la inversión de los méto-

Trampeo masivo de *Plutella xylostella*: una alternativa ambiental y económicamente beneficiosa para su control en Costa Rica
Mass trapping of *Plutella xylostella*: an environmentally and economically beneficial alternative for its control in Costa Rica

3

dos utilizados para el manejo de la plaga, el mantenimiento, instalación, mano de obra, así como el beneficio económico de los rendimientos productivos encontrados. Los costos fueron separados según tratamiento; en el tratamiento de trampeo masivo se contemplaron las feromonas sexuales sintéticas utilizadas en cada parcela, el costo de los insecticidas, además de los objetos utilizados para su instalación y mantenimiento. En el caso del manejo convencional en parcelas control, se consideró el costo de los insecticidas aplicados y el número de aplicaciones, también se incluyó las trampas con feromonas de monitoreo utilizadas. En todas las parcelas los costos fueron ajustados al tamaño de cada parcela de manera que se obtuviera el costo por metro cuadrado de cada una de las alternativas. Para la estimación del beneficio económico, se consultó los rendimientos productivos de cuatro parcelas, dos de cada tratamiento, en las otras dos parcelas se dificultó la obtención de la información respectiva por parte de los productores. Con esto se compararon datos entre tratamientos según producción, el cual se contempló la diferencia de kilogramos cosechados por metro cuadrado entre tratamientos. Seguido a esto se procedió a establecer la diferencia de rendimientos a nivel de hectárea, dicha diferencia se tradujo al beneficio económico comercializando el producto a un precio promedio de referencia establecido a nivel nacional.

Análisis estadístico

Para determinar el efecto de los tratamientos sobre las variables de respuesta estudiada (adultos capturados por trampa por noche y porcentaje de daño), se realizó un análisis de varianza (ANOVA) con medidas repetidas en el tiempo bajo la teoría de los modelos lineales mixtos. El modelo lineal para el experimento bifactorial fue el siguiente:

Se utilizó el programa estadístico InfoStat para comprobar los supuestos del ANOVA con gráficos diagnósticos (cuantiles de los términos de error, gráficos de residuos y gráficos de residuos vs. predichos) y se escogió el mejor modelo en función de los criterios de Akaike (AIC) y de información Bayesiano (BIC). En las variables donde existieron diferencias estadísticas entre los tratamientos, se realizaron las comparaciones de medias por medio de la prueba de Prueba de Di Rienzo, Guzmán y Casanoves (DGC) (p ≤0.05) permitiendo la formación de grupos excluyentes y no transición entre tratamientos.

Resultados

Las capturas promedio de machos por trampa por noche fueron indicadores directos del nivel poblacional de la plaga en los dos tratamientos evaluados. El método de

aplicación calendarizada se mantuvo en el tratamiento control, mediante las constantes aspersiones de insecticidas como Spinosad, Emamectina benzoato y *B. thuringiensis*. No obstante, las poblaciones observadas en las trampas de monitoreo del tratamiento de trampeo masivo no fueron estadísticamente diferentes de las del control a pesar de que las aplicaciones químicas fueron casi nulas en este tratamiento (Figura 1). Es importante destacar que, si bien no se observaron diferencias estadísticamente significativas entre los dos tratamientos, la diferencia numérica es clara particularmente al observar los resultados de capturas por trampa por noche en cada semana de evaluación en cada parcela, mostrando poblaciones menores en las parcelas con trampeo masivo que en las de manejo convencional (Figura 2).

Al comparar el porcentaje promedio de plantas dañadas por la polilla dorso diamante durante la prueba, se constató que las parcelas control, es decir, con método de control químico únicamente, presentaron valores significativamente mayores a las parcelas con trampeo masivo (Figura 3).

En cuanto al análisis de costos asociados, la inversión en plaguicidas de cada productor en cada uno de los tratamientos fue adicionada al costo de mantener las trampas de monitoreo, así como las trampas de trampeo masivo en aquellas parcelas alternativas al control, y todos los costos fueron relativizados al tamaño de las parcelas evaluadas (Tabla 1). Los resultados mostraron que el costo total aproximado del manejo convencional es en promedio \$4200 por hectárea, el cual es mayor al costo del trampeo masivo el cual corresponde a aproximadamente \$3100, siendo esta diferencia estadísticamente significativa (P < 0.05).

Finalmente, al analizar el beneficio económico directamente reflejado en el rendimiento se observó que resultaron superiores los rendimientos de las parcelas con trampeo masivo comparado con el tratamiento control. En las parcelas con trampeo masivo se obtuvo 0.05 kilogramos más de repollo comercializable por cada metro cuadrado, resultando en 500 kilogramos más de repollo por hectárea para este tratamiento. A nivel comercial, dicho dato de 0.05 kilogramos más de repollo cosechado entre tratamientos, y a un precio de 0.28 dólares americanos/kg en el mercado se traduciría en 140 dólares más ganados por hectárea.

Discusión

El uso de feromonas sexuales sintéticas para la captura de adultos de la plaga *Plutella xylostella* en repollo en la provincia de Cartago, Costa Rica, resultaron ser positivos tanto para la captura como para la disminución del daño ob-

$$Y_{ijk} = \mu + \alpha_i + \gamma_j + \delta_{ij} + \varepsilon_{ijk} \text{ con: i = 1, 2. \quad j = 1\dots12. \quad k = 1\dots3} \qquad (1)$$

Y_{ijk}: variable de respuesta del i-ésimo tratamiento, j-ésimo semanas de conteo y la k-ésima repetición.

μ: media general

α_i: efecto de la i-ésimo tratamiento.

γ_j: efecto de la j-ésimo tiempo de evaluación

δ_{ij}: efecto adicional (interacción) para la combinación de los niveles i del tratamiento y j tiempo de evaluación.

ε_{ijk}: término de error que se distribuye normal independiente con media cero y varianza constante.

4

servado en el cultivo, además de un mayor ahorro de dinero e incluso un aumento ligero en los rendimientos productivos, por lo que en términos generales el tratamiento con trampeo masivo fue más satisfactorio para los productores. Las investigaciones realizadas en India a finales de los 90s y principios de la década del 2000 fueron claros ejemplos de la capacidad de conseguir un manejo adecuado de la polilla dorso diamante a través del uso de la feromona sexual de la misma en trampas diseñadas para su moni-

toreo y trampeo masivo[6,8-12]. No obstante, probablemente por poco acceso a la información y la percepción de mitos infundados sobre costos y riesgos del uso de feromonas, esta tecnología no ha sido ampliamente usada para controlar esta plaga en la región Centroamericana.

El hecho de que las poblaciones monitoreadas en parcelas con trampeo masivo no fueran significativamente menores que las parcelas control no es desalentador dado que lo que realmente demuestra es que aún sin aplicación
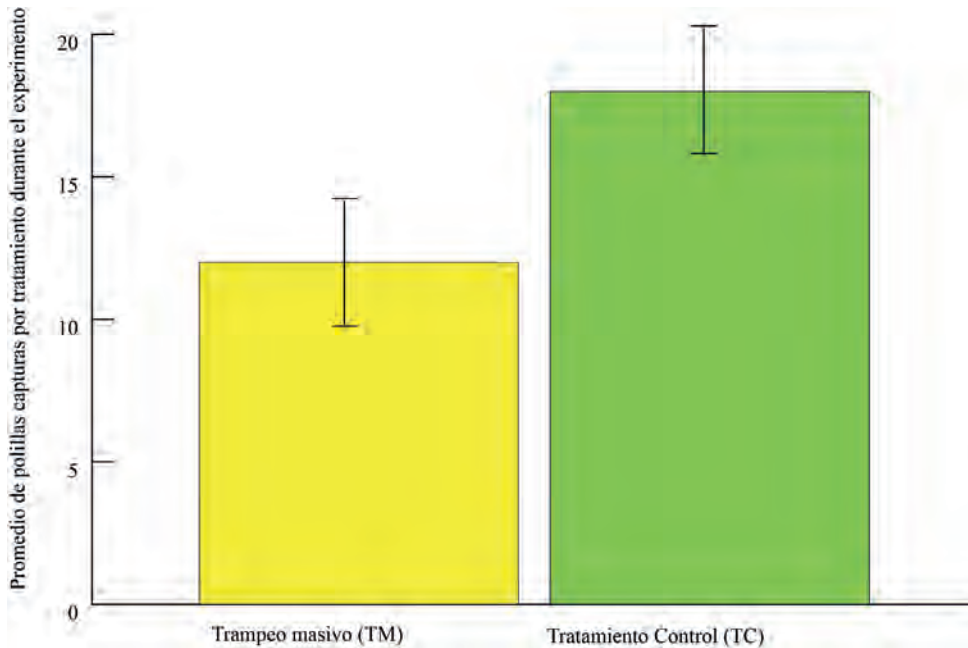
Figura 1. Promedio de capturas de machos de *P. xylostella* por tratamiento en trampas de monitoreo cebadas con feromona sexual de esta plaga. No se encontraron diferencias significativas entre los tratamientos (P > 0.05).
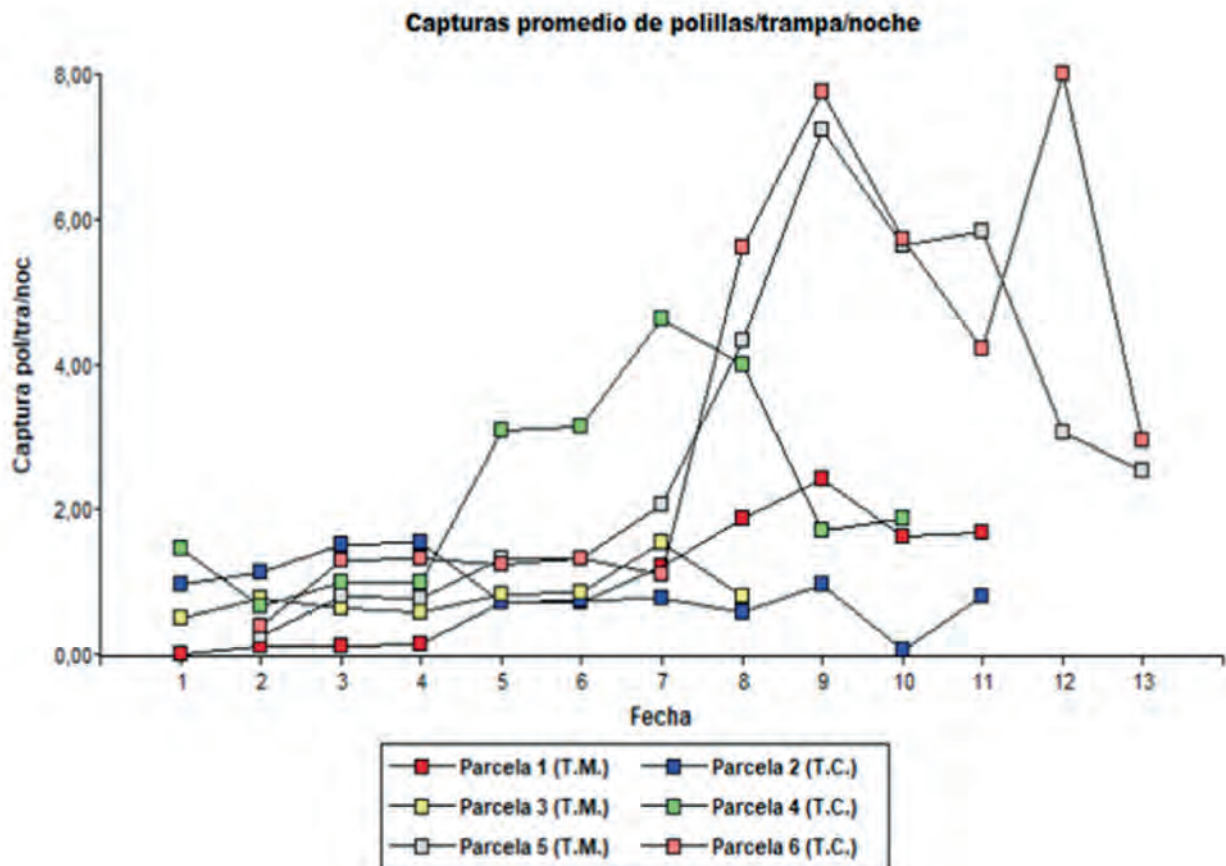
Figura 2. Promedio de captura de polillas/trampa/noche según parcela y semana de evaluación. TM: trampeo masivo; TC: tratamiento control.
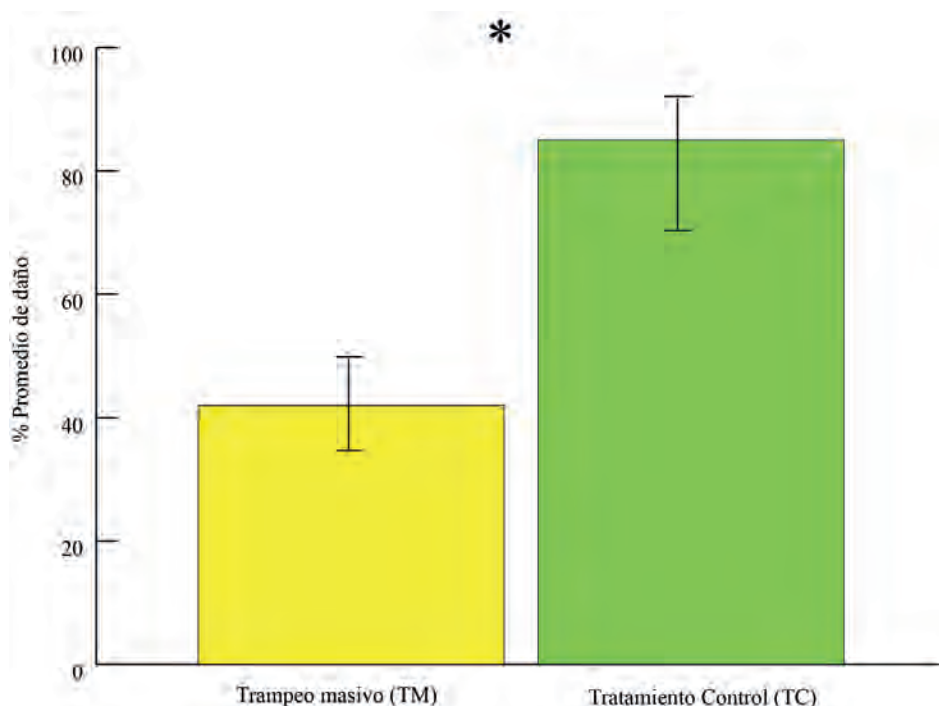
Figura 3. Promedio porcentual de plantas con daño de *P. xylostella* en parcelas control (TC) y parcelas con trampeo masivo (TM). Asterisco entre barras indica diferencias estadísticamente significativas entre los tratamientos (P < 0.05).

Parcela (Tratamiento)	Área (m²)	Inversión Total / m² (dólares americanos)
1 (Control)	7000	0.43
2 (Control)	3300	0.37
3 (Control)	2130	0.46
4 (Trampeo masivo)	3500	0.30
5 (Trampeo masivo)	7000	0.34
6 (Trampeo masivo)	3710	0.28

Tabla 1. Promedio de captura de polillas/trampa/noche según parcela y semana de evaluación. TM: trampeo masivo; TC: tratamiento control.

calendarizada de insecticidas el cultivo puede manejarse igual o incluso mejor (diferencias numéricas en capturas) que con el uso exclusivo de insecticidas. Esto se puede relacionar con la aparición de enemigos naturales de control biológico que se desencadena al disminuir la presión por el uso de insecticidas. Este aspecto es especialmente relevante puesto que se ha demostrado que incluso la eficacia misma de los insecticidas se ve beneficiada cuando otras medidas de control se combinan en programas MIP[13]. De manera similar, es esperable que la disminución en la dependencia en aplicaciones calendarizadas de agroquímicos represente un beneficio directo en la salud de los productores y finalmente en el consumidor final[14].

La disminución en el daño, la disminución en los costos para manejar la plaga y el aumento en rendimientos representan promesas sumamente atractivas para los productores. En una de las investigaciones citadas anteriormente en India se determinó que la diferencia en ganancia bruta por hectárea entre parcelas con MIP y parcelas con control convencional de la polilla dorso diamante eran de aproximadamente 330 dólares americanos por hectárea[6]. Nuestro estudio evidencia que desde el punto de vista económico y comparado con los resultados en la India, nuestros resultados son explícitamente más exitosos: aún incluyendo los costos (feromona y trampas, su instalación y mantenimiento y el costo de mano de obra e insecticidas usados cuan-

do fue necesario) la diferencia promedio por hectárea de ahorro en insecticidas es de 1100 dólares americanos por hectárea a lo cual debe sumarse un extra estimado de 140 dólares por incremento en rendimiento, lo cual hace un total de 1240 dólares americanos por hectárea de diferencia. Respecto al rendimiento, es interesante que una disminución en el uso de insecticidas tenga efectos probables en la producción. Algunos autores se han referido a este tema y como algunas interacciones planta-insecto puede terminar siendo beneficiosas en el rendimiento[15].

Es importante considerar que si bien los resultados fueron en general positivos, existen una serie de factores que también pueden ser decisivos en el éxito del programa de manejo de la plaga. El tipo de suelo, la diversidad de las plantas asociadas, la amplitud de la dieta de los insectos plaga, la composición química y física de las plantas huésped, la abundancia de enemigos naturales, y los micro y macro climas presentes en cada área que influyen en la abundancia de la polilla en cada ciclo de cultivo y que se deben considerar para el control biorracional de la plaga[16–18].

Conclusiones

La investigación realizada permitió corroborar reportes

6

sobre la capacidad del monitoreo y trampeo masivo de la polilla dorso diamante, *Plutella xylostella*, para controlar la plaga con beneficios económicos tangibles para el productor. En lo que se conoce de la literatura científica hasta el momento esta es la primera vez que se da a cabo esta demostración en Centroamérica y abre la puerta para la adopción de esta tecnología por parte de los productores de brásicas en la región.

Contribuciones de los autores

Financiamiento

Agradecimientos

Conflictos de Interés

Los autores declaran no conflicto de interés.

Referencias bibliográficas

1. Macharia I, Löhr B, de Groote H. Assessing the potential impact of biological control of Plutella xylostella (diamondback moth) in cabbage production in Kenya. J. Crop Pro. 2005, 24(11):981–9.
2. Perez CJ, Shelton AM. Resistance of Plutella xylostella (Lepidoptera: Plutellidae) to Bacillus thuringiensis Berliner in Central America., J. Econ. Entomol.1997, 90(1): 87–93.
3. Agboyi LK, Ketoh GK, Martin T, Glitho IA, Tamó M. Pesticide resistance in Plutella xylostella (Lepidoptera: Plutellidae) populations from Togo and Benin. Int J Trop Insect Sci. 2016, 36(4):204–10..
4. Sarfraz M, Keddie BA. Conserving the efficacy of insecticides against Plutella xylostella (L.) (Lep., Plutellidae). J Entomol Nematol. 2005, 129(3):149–157.
5. Araya L, Monge L, Carazo E, Cartín V. Diagnóstico del uso de insecticidas para el combate de Plutella xylostella en Costa Rica. Manejo Integrado de Plagas 1999, 52:49–61.
6. Reddy GVP, Guerrero A. Optimum timing of insecticide applications against diamondback moth Plutella xylostella in cole crops using threshold catches in sex pheromone traps. Pest Manag Sci. 2001, 57(1):90–4.
7. Furlong MJ, Wright DJ, Dosdall LM. Diamondback moth ecology and management: Problems, progress, and prospects. Annu Rev Entomol. 2013, 58(1):517–41.
8. Reddy GV. Comparative effect of integrated pest management and farmers' standard pest control practice for managing insect pests on cabbage (Brassica spp.). Pest Manag Sci. 2011, 67(8):980–985.
9. Reddy GVP, Guerrero A. Pheromone-based integrated pest management to control the diamondback moth Plutella xylostella in cabbage fields. Pest Manag Sci. 2000, 56:882–8.
10. Reddy G, Urs K. Mass trapping of diamondback moth Plutella xylostella in cabbage fields using synthetic pheromones. Int. Pest Control 1997, 39(4):125–6.
11. Schuster DJ, Workman RB, Chalfant RB. Evaluation of a visual damage threshold for management of lepidopterous larvae on cabbage with pyrethroid insecticides. J. Agric. Entomol. 1984, 1:318 – 322.
12. Reddy GV. Comparative effect of integrated pest management and farmers' standard pest control practice for managing insect pests on cabbage (Brassica spp.). Pest Manag Sci. 2011, 67(8):980–985.
13. Anjum F, Wright D. Relative toxicity of insecticides to the crucifer pests Plutella xylostella and Myzus persicae and their natural enemies. J. Crop Prot. 2016, 88:131–6.
14. Shakeel M, Farooq M, Nasim W, Akram W, Khan FZA, Jaleel W, et al. Environment polluting conventional chemical control compared to an environmentally friendly IPM approach for control of diamondback moth, Plutella xylostella (L.), in China: a review. Environ. Sci. Pollut. 2017, 24(17):14537–14550.
15. Poveda K, Díaz MF, Ramirez A. Can overcompensation increase crop production? Ecol. 2018, 9(2):270–280.
16. Baur ME, Kaya HK, Thurston GS. Factors affecting entomopathogenic nematode infection of Plutella xylostella on a leaf surface. Entomol Exp Appl. 1995, 77(3):239–250.
17. Badenes-Perez FR, Shelton AM, Nault BA. Evaluating Trap Crops for Diamondback Moth, Plutella xylostella (Lepidoptera: Plutellidae). J. Econ. Entomol. 2004, 97(4):1365–72.
18. Braga L, Diniz IR. The Abundance of Specialist and Generalist Lepidopteran Larvae on a Single Host Plant Species: Does Spatial Scale Matter? Fla Entomol. 2015, 98(3):954–61.

Biotechnological plant breeding applied to purple blackberries

Juan Marcelo Morales and Patricia Marcela Andrade

DOI. 10.21931/RB/2023.08.01.7

Universidad Técnica de Cotopaxi (UTC), Facultad de Ciencias Agropecuarias y Recursos Naturales (CAREN), Carrera de Agronomía, Latacunga, Ecuador.
Corresponding author: juan.morales3796@utc.edu.ec

Abstract: The current project addresses the great potential of *S. caripense* Dunal (Tzimbalo) for intraspecific breeding and interspecific gene flow towards the related commercial crop *S. muricatum* Aiton (Pepino) to develop fruits with improved antioxidants, flavor, and fruit weight. This study aims to determine the interaction between genotype x altitude and identify significant differences between treatments according to fruit weight. Tzimbalo varieties GenPurpura, Gennbiotz, and GenDulce, were used. Fruit weight was analyzed using a factorial experiment under a completely randomized design (CRD). The interaction Var. x m.a.s.l. was significant (mean ± SE), Gennbiotz:a1 (4.88 g ± 0.44; C) and GenDulce:a2 (4.38 g ± 0.25; BC), followed by GenPurpura:a1 (3.33 g ± 0.36; AB); also the principal effect Var. was significant, Gennbiotz (3.93 g ± 0.23; B) and GenDulce (3.64 g ± 0.25; B), followed by GenPurpura (2.90 g ± 0.19; A). These results demonstrate distinctness, uniformity, and stability (DUS) of at least one tzimbalo variety. Fruit weight and other characteristics are relevant to improve quality and commercial potential. They are used to develop biofortified beer, jam, ice cream, and plant tissue culture media with sucrose and vitamins to strengthen biotechnological production in Cotopaxi-Ecuador.

Key words: Factorial experiment, tzimbalo varieties, fruit quality, genotype, agri-biotechnology.

Introduction

The tzimbalo plant is phylogenetically complex[1], mostly wild, and native to the Andean region[2,3]. This species is the ancestor of cucumber due to chromosomal similarities and the generation of interspecific hybrids[4-6]. The fruit of tzimbalo contains significantly more sucrose, vitamin C[7], and minerals compared to modern varieties of Pepino[8]. Even some developed materials of these fruits are suitable for diabetic people. The great potential of S. caripense for interspecific gene flow to related commercial Solanum crops includes genomic studies of these species[9,10], applied biotechnological tools[11,12] and plant breeding methods[13,14] as discussed in this article, which help to overcome production, marketing and export constraints.

In Ecuador, cucumber fruit is included as one of the sixteen non-traditional products (mango, pineapple, abaca, eddo, dragon fruit, papaya, passion flower, golden berry, cucumber, asparagus, soursop, tree tomato, passion fruit, lemons, avocado and orange), with international demand and added value promoted by an export model[15]. In addition, the National Finance Corporation (CFN) mentions that 269.5 million dollars (USD) were export credits, and 25% of that amount to agribusiness[16], Approximately 67375,000 USD, or 3396.77 ha in sweet cucumber production. The estimated agricultural extension for permanent and transitory crops and cultivated pastures were 4872049.88 ha, 19% of national territory[17]. The high nutritional value and exotic fruity aroma of cucumber and tzimbalo[6] fruits, their high commercial value for local and international markets and the possibility of developing industrial products[18] encourage the improvement of these natural resources. The information about the extension (ha) of the Pepino crop is limited; nevertheless, the opportunity to introduce non-tra-

ditional products to the market is feasible. Therefore, some projects support cucumber export to Bolivia[19], Germany[20] and Japan[21]. Cucumber fruit traditionally produced in Carchi is being exported to the United States[22]. Plant breeding with tzimbalo and Pepino is carried out through backcrosses. It contributes to estimating sucrose and ascorbic acid concentrations[23], antioxidants, chlorogenic acid quantification[12], and, subsequently, heritability parameters. Additionally, fruit flavor, seed diameter, corolla color, fruit stripes, fruit length, inner placental area length, and inner placental area breadth contribute more to the variability; they are agronomically essential to increase the commercial potential[12].

The yield of the selected interspecific hybrids *S. muricatum* x *S. caripense* and *S. muricatum* x *S. tabanoense* (30-40 t*ha^{-1}) is comparatively higher than their corresponding wild parents. Fruit weight is intermediate (40-60 g) and considerably higher than their connected wild progenitors. The *S. caripense* (tzimbalo) and *S. tabanoense* show high soluble solid content (SSC) (10-14 %; at least 8 % to be acceptable). Export-oriented exploitations of Pepino fruit exist in Ecuador, Peru, Colombia, New Zealand and Australia, and it is mentioned that innovative and entrepreneurial farmers from Brazil, Europe and USA are interested in scaling the production and consumption of this crop. The availability of new cultivars improved for fruit quality is critical for expanding commercial exploitation[6,23]. According to analytical methods, from *S. muricatum* × *S. caripense* and *S. muricatum* × *S. tabanoense* materials, several individuals of the first backcross towards *S. muricatum* (BC1) are selected for high SSC (9.2–11.7 %), yield (23–121 t*ha^{-1}), and fruit weight (65–262 g). These BC1 selected individuals are selfed to accumulate favorable alleles from the wild species for

Publisher's Note: Bionatura stays neutral with regard to jurisdictional claims in published maps and institutional affiliations.

SSC in homozygosis in the segregating offspring (BC1Ø). Then a preliminary clonal selection is performed in BC1Ø populations; clones are propagated and evaluated. The best BC1Ø clones are selected and utilized for a second backcross toward *S. muricatum* (P1×BC1Ø). Clonal propagation and evaluation are performed, and varieties are chosen for high yield (38–82 t*ha^{-1}), commercial fruit weight (200–300 g), and high SSC (8.4–11.2 %)[7].

The expression levels of candidate genes identified and quantified through RT-PCR and RT-qPCR[12] and the selection of genotypes that demonstrate exemplary performance in front of different crop conditions represent a solution for introducing new varieties into agro-markets, focused on the conservation and utilization of Andean resources (Figure 1). In Ecuador, there is a community of traditional producers of S. muricatum (Pepino) in Chimborazo. Each bag of fruit is marketed between Alausí, Riobamba and Cañar; Cucumber production in Ibarra, Checa, Patate, Píllaro, and Vilcabamba. In other growing environments, the monthly yield of cucumber above 2000 m.a.s.l. (14-18 ºC) after five months of sowing is equivalent to 6000 kg[24]. In contrast, in Imbabura, the yield of Pepino (Sweet round) is 72.80 t/ha[25]; the production zone is Pimampiro and part of Chota valley, where the Pepino fruit has a high commercial value at local markets; traditional production also exists in Pichincha and Loja[26].

In Ecuador, the tzimbalo fruit is used to quench thirst and eliminate skin blemishes and freckles[27]. It is also used to treat sore throats, flu and diarrhea in children[28]. The natives make necklaces with the fruits of the tzimbalo for their children to use in healing ceremonies[29] and as a curdling agent to make soft cheese[30]. There are poems related to the tzimbalo[31]. Finally, the Pepino fruit was significant during pre-Columbian times; in its region of origin exists pottery representations and depictions from the Mochica (approximately 500 AD)[32,33], and Nazca cultures in Peru[34], and many references by the first Spanish chroniclers[35]. There was a rediscovery of the Pepino for commercial exploitation in the 1970s–80s, stimulated by the attempts to introduce exotic fruits[36-38], and several cultivars were released at that time[36,39,40].

The biological wealth of third-world countries is 91.1% of germplasm of the International Plant Genetic Resources Bank and 23% from Latin America[41]; this explains the significant input of Andean countries to food and agriculture[30]. The remarkable climatological and orographic configuration of Ecuador originates a wide range of resources in its four natural regions (Coast, Highlands, Amazon, and Galapagos); the environmental conditions generate an impressive diversity of habitats and types of vegetation; flora comprises almost 25000 species of vascular plants, with an endemism of 32.25%[42].

Native edible species are essential for the food security of the Andean countries and the entire world due to their nutritional potential and medicinal and economic values. The genus *Solanum L.* with about 1500 species, is one of the largest among flowering plants[43]. Includes cultivated species such as tomato (*S. Lycopersicum* L.), potato (*S. tuberosum* L.), and others of importance in South America, such as Pepino (*S. muricatum* Aiton) and naranjilla (*S. quitoense* Lam.)[44].

Factorial experiments are treatment orderings to be analyzed into experimental designs such as completely randomized design (CRD), randomized complete block design (RCBD), Latin square design (LSD), and others. Factorial arrangements provide simultaneous studies of two or more factors, with two or more levels for each; they are also used in agricultural, biological and sociological research. Using factorial arrangements makes it possible to obtain information on the factors independently and with interaction[45]. The advantages of applying factorial structures are the more efficient use of the available resources, studied factors are under conditions closer to reality, and these are analyzed under many experimental designs. The number of degrees of freedom for the error is high and contributes to decreasing the experimental error and increasing the accuracy of the experiment.

Materials and methods

Plant material

Selected material of *S. caripense* GenPurpura (5.67-10.33 °Brix), Gennbiotz (8.33-10.50 °Brix), and GenDulce (8.83-11.0 °Brix) were used, provided by the company GENNBIO (Quito, Ecuador); a total of sixty-four (n=64) plants of the registered genotypes were biotechnological cultivated at different altitudes (m.a.s.l.).

Growing conditions

In vitro plantlets were acclimatized in Cotopaxi-Ecuador after laboratory propagation at 15-28 °C throughout the

Figure 1. (a) Genetic variability of the Pepino (*Solanum muricatum* Aiton), and varieties of its ancestor tzimbalo *(Solanum caripense* Dunal) with high soluble solid content. (b) The cross-section of Pepino fruit. (c) Derived agri-industrial natural products. Source: GENNBIO

field experiment. Plants were spaced 0.3 m within the row and 1.0 m between rows. Plants were trained with vertical strings. Mechanically irrigation was used, and nutrients were provided through doses of commercial fertilizer plus micronutrients. Due to the significant self-incompatibility of these species, some materials were hand-pollinated to set fruits.

Data analysis

The agronomic traits, fruit weight (g), and other traits were recorded. Analytical measurements of fruit weight were randomly repeated for each variety of *S. caripense* (1000 fruits). The data were disposed under CRD in a factorial experiment 3 x 2 with three genotypes (Var.) and two altitudes (m.a.s.l.) for analysis with the mean values into a linear additive statistic model[47,48]. Thus, there are three effects of interest without considering decomposition and three null hypotheses raised with their corresponding alternative hypothesis. The level of corruption or detail of the study depends on the number of groups utilized in each factor. Statistic packages InfoStat 2018, Minitab 16, and RStudio 4.1.2. were used.

Where u is the general mean; a_i is the effect of the level $i=1,2$ of factor A; b_j is the effect of the level $j=1,2$ of factor B; $(ab)_{ij}$ represents effects of double interaction on the levels ij, respectively; E_{ijk} represents the random error in the combination ijk, and k are replicated.

The mathematical model on the factorial experiments is linked to the experimental design model in which the data is analyzed, except that in these cases, the effect of treatments (Ti) is decomposed in as many effects as factors and interactions are studied in factorial arrangements[45,49].

Results

GenPurpura is a population of selected clones from a segregating progeny, cross-pollinated with Gennbiotz to set fruits; Gennbiotz is a population of selected clones from F_1 progeny after mass selection on the previous generation, cross-pollinated with GenPurpura; and GenDulce is a self-compatible progeny from previous breeding proceedings, too[13,46].

Interaction genotype x altitude

It was observed that fruit weight is statistically differentiated by genotype (Var.) and altitude (m.a.s.l.); the fruit weight (mean ± SE) was higher in the experimental points corresponding to Gennbiotz:a1 (4.88 g ± 0.44) and GenDulce:a2 (4.38 g ± 0.25), followed by GenPurpura:a1 (3.33 g ± 0.36), Gennbiotz:a2 (2.98 g ± 0.11), GenDulce:a1 (2.91 ± 0.44), and GenPurpura:a2 (2.46 ± 0.13) (Figure 2). The null hypothesis is accepted with p-value = 0.4528 (W = 0.98155). Therefore, the errors have a normal distribution.

The interaction effect Var. x m.a.s.l. demonstrates significant differences in the mean fruit weight (Table 1) between the genotype of tzimbalo varieties and levels of altitude in meters above sea level, p-value < 0.0001. The principal effects of Var. are significant also, suggesting that the effect of genotype contributes more to the differences in fruit weight due to its F-value = 6.72, followed by the principal effects of m.a.s.l. which F-value = 2.75, and no significant p-value = 0.1027. The CV = 20.56 %.

The mean of fruit weight in the level $i=2$ (Var.=Gennbiotz) of factor A and level $j=1$ of factor B (m.a.s.l. = a1) is significantly different from the mean in the level I =3 (Var. = GenPurpura) of the factor A and level $j=1$ of the factor B (m.a.s.l. = a1), with alpha = 0.05; the null hypothesis (H$_0$: $u_{21} = u_{31}$) is rejected and the alternative hypothesis (H$_1$: $u_{21} \neq u_{31}$) is accepted. This means that the mean fruit weight in Gennbiotz at the first altitude (a1) is significantly different from that of GenPurpura at the first altitude (a1).

On the other hand, the mean of fruit weight in the level $i=1$ (Var.=GenDulce) of factor A and level $j=2$ of factor B (m.a.s.l. = a2), is significantly different from the mean in level i=3 (Var. = GenPurpura) of the factor A and level $j=2$ of factor B (m.a.s.l. = a2), with alpha = 0.05; the null hypothesis (H$_0$: $u_{12} = u_{32}$) is rejected and the alternative hypothesis (H$_1$: $u_{12} \neq u_{32}$) is accepted. This means that the mean fruit weight in GenDulce at the second altitude (a2) is significantly different from that of GenPurpura at the second altitude (a2) (Figure 3).

Principal effects

The mean of principal effects on genotype, according to the Tukey test with alpha = 0.05 (Table 2), is statistically similar for both Gennbiotz (3.93 g) and GenDulce (3.64

H$_0$: $(a)_i = 0$ $i=1,2,3$
All levels of factor A have the same effect on the fruit weight.
H$_1$: $(a)_i \neq 0$ $i=1,2,3$
Not all levels of factor A have the same effect on the fruit weight.

H$_0$: $(b)_j = 0$ $j=1,2$
All levels of factor B have the same effect on the fruit weight.
H$_1$: $(b)_j \neq 0$ $j=1,2$
Not all levels of factor B have the same effect on the fruit weight.

H$_0$: $(ab)_{ij} = 0$ $i=1,2,3; j=1,2$
Interaction between factor A and factor B exists.
H$_1$: $(ab)_{ij} \neq 0$ $i=1,2,3; j=1,2$
No interaction between factor A and factor B exists.
In factorial arrangements axb, the response variable (Y) is described through the model of effects given by:

$$Y_{ij} = u + a_i + b_j + ab_{ij} + E_{ijk} \qquad (1)$$

$$i=1,2..., a; j=1,2..., b; k=1,2..., n$$

4
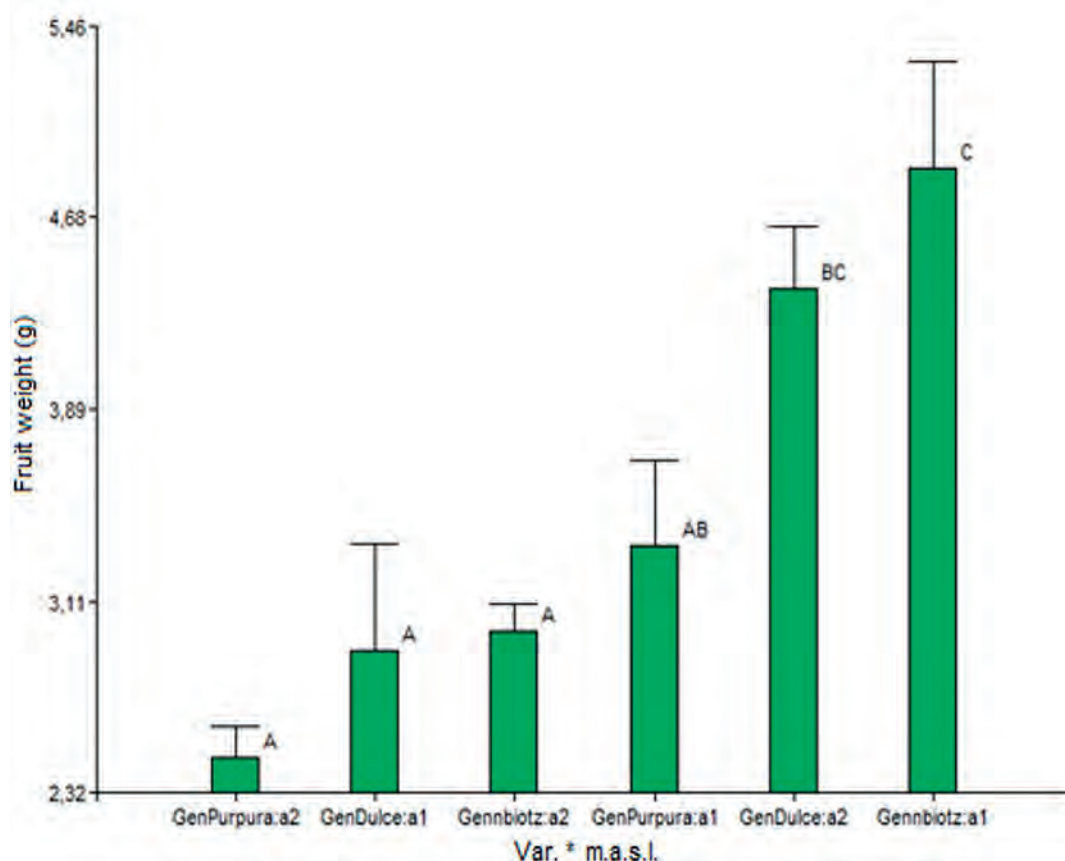
Figure 2. Fruit weight (mean ± S. E.) of tzimbalo varieties GenPurpura, Gennbiotz, and GenDulce at different altitudes in meters above sea level. Factorial experiment 3 x 2. Other letters demonstrate significant differences according to the Tukey test (p-value < 0.05).

Source of variation	D. F.	M. S.	F	P-value
Model	5	5.05	13.21	< 0.0001
Var.	2	2.57	6.72	0.0024
m.a.s.l.	1	1.05	2.75	0.1027
Var. x m.a.s.l.	2	4.91	12.86	< 0.001
Error	58	0.38		
Total	63			

Table 1. ANOVA of fruit weight in tzimbalo varieties GenPurpura, Gennbiotz, and GenDulce.

g), whereas, GenPurpura (2.90 g; A) is statistically different from Gennbiotz and GenDulce. As the mean of principal effects on altitude, a1 and a2 are both statistically similar, and no significant differences were found (Table 3).

Discussion

Gennbiotz generated the higher fruit weight:a1 (4.88 g; C) and GenDulce:a2 (4.38 g; BC); in previous studies, the fruit weight for tzimbalo EC-40 is 8.8 g[7], ranging from 1.9-9.7 g[50]. Nevertheless, the F_1 from Gennbiotz x GenPurpura, and GenPurpura x Gennbiotz cultivated at altitude a1 in our breeding program have higher yield than EC-40 (66 g/plant) due to gene flow of yield and stability traits. It is mentioned that when a variety shows uniform, it can also be considered stable[51]. In contrast, these results demonstrate the stability of GenPurpura at different altitudes.

In the Andean region, it is mentioned that for exotic fruits such as uchuva (*Physalis peruviana* L.), the fruit weight (± SD) of a heterogeneous collection is 5.62 g ± 0.92[52], and for the genotype Regional Nariño the fruit weight is 4.8 g[53]. In other studies, the fruit weight of golden berry is 2.77 g ± 0.67[54]; for the ecotype, Colombia is 6.79 g[55]; and for the American Southern variety, the fruit weight is 6.95 g ± 1.49[56]. This suggests that the fruit weight (± SE) of the tzimbalo variety Gennbiotz:a1 (4.88 g ± 0.44) is similar to that of Regional Nariño, with high SSC.

This current work through intraspecific gene flow between tzimbalo varieties leads to the development of hybrids by introducing relevant genes, which are utilized to improve stability, uniformity, and nutritional values, to generate simultaneously original varieties of Pepino. A difference between the two varieties is clear depending on many factors, considering the type of expression of the measurements analysed[12,13]. Visual measurements refer to sensory
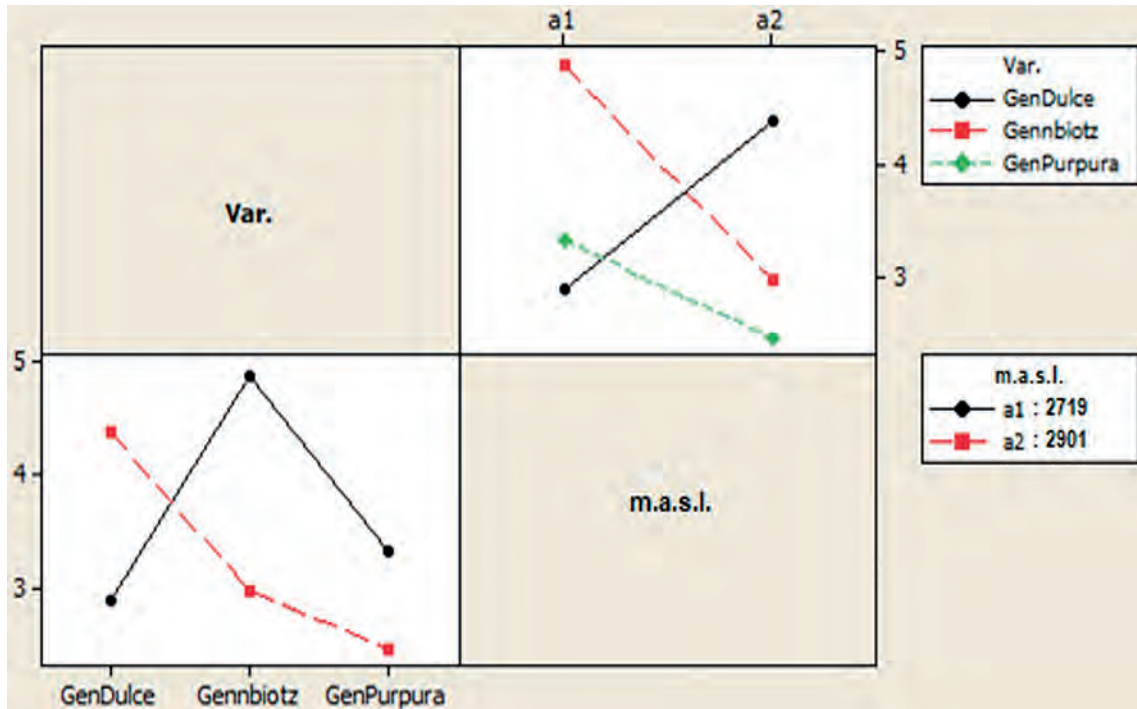
Figure 3. Interaction for fruit weight in tzimbalo varieties GenPurpura, Gennbiotz, and GenDulce at different altitudes in meters above sea level.

Var.	Mean	N	SE.	
GenPurpura	2.90	25	0.19	A
GenDulce	3.64	8	0.25	B
Gennbiotz	3.93	31	0.23	B

Table 2. Fruit weight (mean ± S. E.) of tzimbalo varieties GenPurpura, Gennbiotz, and GenDulce.

m.a.s.l.	Mean	SE.	
a2	3.28	0.10	A
a1	3.71	0.24	A

Table 3. Fruit weight (mean ± S. E.) of tzimbalo varieties at different altitudes.

observations of experts, including smell, taste, and touch, as well as statements with reference points as diagrams, examples of varieties, and others[51].

Conclusions

Gennbiotz generated the higher fruit weight:a1 (4.88 g ± 0.44) and GenDulce:a2 (4.38 g ± 0.25), which increase over generations through compatible crosses between tzimbalo varieties. The tzimbalo variety GenPurpura (2.90 g ± 0.19) was stable at different altitudes; it demonstrates these species' stability through biotechnological plant breeding. Our distinct varieties of tzimbalo are the base for improving the Pepino crop to increase the nutritional quality and healthy food in the highlands region of Cotopaxi-Ecuador.

Conflicts of Interest

The authors declare no conflict of interest.

Bibliographic references

1. Zuriaga, E. Análisis de la variabilidad en poblaciones naturales de Solanum, secciones Lycopersicon y Basarthrum. Doctoral thesis, Univ. Politécnica de Valencia, Valencia, Spain, 2009.
2. Correll, D.S. Flora of Perú, Volume VIII, Parte V-B, Number 2; Field Museum of Natural History, United States, 1967; pp. 281-290.
3. Jorgensen, P.M.; Leon-Yanez, S. Catalogue of the Vascular Plants of Ecuador; Missouri Botanical Garden Press, Saint Louis, 1999; the internet version (W3CEC).
4. Heiser, C.B. Origin and variability of the Pepino (Solanum muricatum): A preliminary report. Baileya 1964; 12:151-158.
5. Murray, B.C.; Hammett, K.R.; Grigg, F.D. Seed set and breed-

5

6

ing system in the Pepino Solanum muricatum, Ait., Solanaceae. Sci. Hortic. 1992; 49(1-2):83-92.

6. Rodríguez-Burruezo, A.; Prohens, J.; Fita, A. Breeding strategies for improving the performance and fruit quality of the Pepino (Solanum muricatum): A model for the enhancement of underutilized exotic fruits. Food Res. Int. 2011; 44:1927–1935.

7. Prohens, J., et al. Morphological and physico-chemical characteristics of fruits of Pepino (Solanum muricatum), wild relatives (S. caripense and S. tabanoense) and interspecific hybrids: Implications in Pepino breeding. Eur. J. Hortic. Sci. 7 2005; 224-230.

8. Prohens, J., et al. Fruit composition diversity in land races and modern Pepino (Solanum muricatum) varieties and wild related species. Food Chem. 2016; 15:49-58.

9. Herraiz, F., et al. Morphological and molecular characterization of local varieties, modern cultivars and wild relatives of an emerging vegetable crop, the Pepino (Solanum muricatum), provides insight into its diversity, relationships and breeding history. Euphytica 2015; 206:301-318.

10. Herraiz, F., et al. The first de novo transcriptome of Pepino (Solanum muricatum): assembly, comprehensive analysis and comparison with the closely related species S. caripense, potato and tomato. BMC Genomics 2016; 321:1-17.

11. Morales, J.; Vaca, I. Propagación in vitro de tzímbalo (Solanum caripense Dunal). RTE 2016; 29:89-104.

12. Morales, J., et al. Gene expression of flavanone 3-hydroxylase (F3H), anthocyanidin synthase (ANS), and p-coumaroyl ester 3-hydroxilase (C3H) in tzimbalo fruit. IJASEIT 2021; 11(2):805-813.

13. Morales, J. Purple Black Berries. II International Agrobiodiversity Congress, Innovation Space, Rome, Italy, Nov. 15-18, 2021.

14. Morales, J.; Chiluisa-Utreras, V. Mejoramiento biotecnológico de plantas y modificación genética. Editorial Grupo Compás, Guayaquil, Ecuador, 2022. pp. 104-179.

15. La República (2019) Ecuador impulsa línea financiera para que agricultura abra nuevos mercados. Available online: https://www.larepublica.ec/blog/economia/2019/02/19/ecuador-impulsa-linea-financiera-para-que-agricultura-abra-nuevos-mercados/.

16. El Comercio (2019) 16 productos agrícolas tendrán acceso a crédito para diversificar exportaciones. Available online: https://www.elcomercio.com/actualidad/productos-agricolas-creditos-cfn-exportaciones.html.

17. INEC (Instituto Nacional de Estadística y Censos) (2016). Módulo ambiental de la encuesta de superficie y producción agropecuaria continua. ESPAC 2016. Available online: https://www.ecuadorencifras.gob.ec/documentos/web-inec/Encuestas_Ambientales/Informacion_ambiental_en_la_agricultura/2016/informe_ejecutivo_ESPAC_2016.pdf

18. García-García, M.C., et al. Pepino dulce, una solanácea por descubrir (Solanum muricatum). XL Foro Colab. Público-Privada, Nuevas materias primas sostenibles en alimentación, Madrid, Spain, Jun. 14, 2017.

19. Fernandez A. Plan de exportación de Pepino dulce desde San Antonio de Pichincha – Ecuador hasta Santra Cruz – Bolivia. Graduate thesis, Univ. De las Américas, Quito, Ecuador, 2013.

20. Erazo, G. Proyecto de pre-factibilidad para la exportación de Pepino dulce de origen ecuatoriano al mercado alemán. Graduate thesis, Univ. Tecnológica Equinoccial, Quito, Ecuador, 2014.

21. Pacheco, J. Formulación de un plan de negocios para la exportación de Pepino dulce al mercado asiático. Graduate thesis, Univ. Internacional del Ecuador, Loja, Ecuador, 2015.

22. Revista Líderes (2021) El Pepino dulce que se produce en el Carchi rebasó las fronteras. Available online: https://www.revistalideres.ec/lideres/Pepino-dulce-produccion-carchi-exportacion.html.

23. Rodríguez-Burruezo, A.; Prohens, J.; Nuez, F. Wild relatives can contribute to the improvement of fruit quality in Pepino (Solanum muricatum). Euphytica 2003; 129:311–318.

24. Revista Líderes (2012) El Pepino dulce se cultiva al calor de los valles ecuatorianos. Available online: https://www.revistalideres.ec/lideres/Pepino-dulce-cultiva-calor-valles.html.

25. España, E. Respuesta del cultivo de Pepino dulce (Solanum muricatum Ait) a la fertilización química mediante el sistema de parcelas de omisión en el cantón Ibarra, provincia de Imbabura. Graduate thesis. Univ. Técnica de Babahoyo, Carchi, Ecuador, 2015.

26. Andrango, J. Determinar el rendimiento a la aplicación de tres niveles de fertilización con dos bioestimulantes enraizadores en el cultivo de Pepino dulce (solanum muricatum aiton) en la zona de Ibarra, provincia de Imbabura. Graduate tesis, Univ. Técnica de Babahoyo, Carchi, Ecuador, 2015.

27. Peñafiel, M. Flora y vegetación de Cuicocha. Abya-Yala, Universidad Politécnica Salesiana, Quito, Ecuador, 2003; pp. 44.

28. Quilo, M. Estudio de plantas medicinales en los sectores Rumiñahui y Atahualpa e implementación de un huerto demostrativo, Pijal-Imbabura. Graduated thesis, Univ. Politécnica Salesiana, Quito, Ecuador, 2012.

29. de la Torre, L., et al. (Eds.) Enciclopedia de las plantas útiles del Ecuador. Quito & Aarhus: Herbario QCA de la Escuela de Ciencias Biológicas de la Pontificia Universidad Católica del Ecuador & Herbario AAU del Departamento de Ciencias Biológicas de la Universidad de Aarhus, 2008; pp 590.

30. INIAP (Instituto Nacional de Investigaciones Agropecuarias). Diversidad de frutales nativos comestibles Caricaceae - Solanaceae, fenología, usos y recolección de germoplasma en el Sur del Ecuador. Estación Experimental Chuquipata, Granja Experimental Bullcay, 2003.

31. Jara, F.; Moya, R. "Taruca" Próxima aparición. En Instituto Andino de Artes Populares, Poesía Popular Andina. Ecuador, Perú, Bolivia, Chile. Tomo 2, Quito-Ecuador, 1983; pp. 143-144.

32. Vargas, C. Phytomorphic representations of the Ancient Peruvians. Economic Botany 1962; 16(2):106–115.

33. National Gallery of Australia. (2021) Gold and the Incas: Lost worlds of Peru, Moche culture, Stirrup vessel in the form of Pepinos. Available online: https://nga.gov.au/exhibition/incas/default.cfm?IRN=231329&BioArtistIRN=91411&MnuID=3&GalID=0&ViewID=2.

34. Leiva, S.; Gayoso, G.; Chang, L. Solanum lycopersicum L. "tomate" y Solanum muricatum Aiton "Pepino" (Solanaceae) dos frutas utilizadas en el Perú Prehispánico. Arnaldoa 2015; 22:201-224.

35. Prohens, J.; Ruiz, J.; Nuez, F. The Pepino (Solanum muricatum, Solanaceae): A "new" crop with a history. Economic Botany 1996; 50:355−368.

36. Dawes, S.N.; Pringle, G.J. Subtropical fruits from South and Central America. In G. Wratt, and H. C. Smith (Eds.), Plant breeding in New Zealand (pp. 33−35). Wellington, New Zealand: Butterworths, 1983.

37. Morley-Bunker, M. A new commercial crop, the Pepino (Solanum muricatum Ait) and suggestion for further development. RNZIH 1983; 11:8-19.

38. National Research Council. Lost crops of the Incas: Little-known plants of the Andes with promise for worldwide cultivation. Washington, DC: National Academy Press, 1989; pp. 296-305.

39. Cavusoglu, A.; Erkel, E.I.; Sulusoglu, M. The effect of climatic factors at different growth periods on Pepino (Solanum muricatum Aiton) fruit quality and yield. J. Food Agric. Environ. 2009; 7:551−554.

40. Nemati, S.H., et al. Investigation of some effective factors on yield traits of Pepino (Solanum muricatum) as a new vegetable in Iran. PJBS 2009; 12:492−497.

41. Bravo, E. La problemática mundial de los recursos fitogenéticos. En: Memorias de la 11 reunión nacional sobre recursos fitogenéticos. R. Castillo; C. Tapia; J. Estrella (Eds.), Quito, Ecuador, 1991.

42. INIAP (Instituto Nacional de Investigaciones Agropecuarias). Informe Nacional sobre el Estado de los Recursos Fitogenéti-

cos para la Agricultura y la Alimentación. Quito, Ecuador, 2008.

43. Frodin, D.G. History and concepts of big plant genera. Taxon 2004; 53:753-776.

44. Särkinen T., et al. Listado anotado de Solanum L. (Solanaceae) en el Perú. Rev. peru. biol. 2015; 22(1):003-062. http://dx.doi.org/10.15381/ rpb.v22i1.11121

45. Sánchez-Otero, J. Introducción al diseño experimental. Escuela de Ciencias Biológicas de la Pontificia Universidad Católica del Ecuador, Quito, Ecuador, 2013; pp. 74-77.

46. Morales, J., et al. Gene expression of flavanone 3-hydroxylase (F3H), anthocyanidin synthase (ANS), and p-coumaroyl ester 3-hydroxilase (C3H) in tzimbalo fruit. Proc. CIT 2020 - ESPE, Sangolquí, Ecuador, paper 211, p. 10, Oct. 26-30, 2020.

47. Montgomery, D. Diseño y análisis de experimentos. Editorial Limusa Wiley, Univ. Estatal de Arizona, United States, 2004; pp. 175-184.

48. Gutiérrez, H.; de la Vara, R. Análisis y diseño de experimentos, 3rd ed; McGraw-Hill/Interamericana Editores, S.A. de C.V., 2012; pp 116-128.

49. Federer, W. Experimental design. Theory and application. The Macmillan Company, New York, United States, 1955; pp. 166-181.

50. Prohens, J., et al. Bulletin UASVM Horticulture 2010; 67(1):264-269.

51. UPOV (International Union for The Protection of New Varieties of Plants). Guidelines for the conduct of tests for distinctness, uniformity, and stability. TG/326/1, 2018.

52. Herrera, A.; Fischer, G.; Chacón, M. Agronomical evaluation of cape gooseberries (Physalis peruviana L.) from central and north-eastern Colombia. Agron. Colomb. 2012; 30(1):15-24.

53. Álvarez-Herrera, J.; Fischer, G.; Vélez, J. Analysis of the production of Cape gooseberry (Physalis peruviana L.) in the greenhouse with different irrigation levels during the harvest cycle. Rev. Acad. Colomb. Cienc. Ex. Fis. Nat. 2021; 45(174):109-121.

54. Olievira, S., et al. Physical properties of Physalis Peruviana L. International Conference on Engineering, ICEUBI 2015, University of Beira Interior, Faculty of Engineering, Portugal, 2015.

55. Aguilar-Carpio, C., et al. analysis of growth and yield of cape gooseberry (Physalis peruviana L.) grown hydroponically under greenhouse conditions. Rev. Chapingo 2018; Serie horticultura XXIV(3).

56. Thuy, N.M., et al. Physical and chemical characteristics of goldenberry (Physalis peruviana) grown in Lam Dong province, Vietnam. Food Research 2020; 4(4):1217–1225.

ARTICLE / INVESTIGACIÓN

Indicator framework for large-scale cacao (*Theobroma cacao* L.) *in vitro* plant production planning and controlling

Ana María Henao Ramírez[1]*, David Hernando Palacio Hajduk[1], Diana Maria Cano Martínez[1], Aura Inés Urrea Trujillo[2]

[1] Center of Agrobiotechnological Development and Innovation – CEDAIT, Universidad de Antioquia, Colombia.
[2] Biology Institute, Universidad de Antioquia, Colombia.
Corresponding author: amaria.henao@udea.edu.co

Abstract: Somatic embryogenesis (SE) is considered the most suitable and integrated biotechnology for the large-scale production of clonal cacao plants compared to conventional methods. Hence, the scale-up of relevant technologies must be interfaced with effective and efficient management of productive processes at an industrial scale like biofactories. Production facilities like biofactories serve to transform plant resources into products like plantlets. This technology constitutes an essential innovative variant since it allows obtaining high multiplication coefficients in short periods. Currently, there is no reference to carrying out adequate planning of the entire production process; for this reason, it is not used for the maximum production capacity of the facilities, and there is a high level of uncertainty. With the aid of production planning and controlling (PPC) systems, inputs can be planned to achieve a determined output of products. Therefore, this work proposes a production planning and controlling (PPC) system for SE cacao plantlet multiplication through the pilot large-scale. This paper presents input and output information considering the leading indicators of the production process, like materials, labor, quality, and performance. Emphasis is placed on technical details on the production process of 100.000 plantlets in batches from the *CCN51* genotype. Through the model analysis, challenges and requirements for PPC system have been defined as a basis for future works and will have successfully managed the production process.

Key words: Commercial-scale propagation, cost of production, indicators, somatic embryo, vegetative propagation.

Introduction

The production program's central nervous system, production planning and control (PPC) oversee making sure that all materials and components of the assembly are available at the appropriate times, locations, and in the proper quantities to allow operations to proceed following the predetermined schedules while incurring the least amount of costs[1]. However, in the construction of the production system is essential to understand the production system. PPC collaborates with procurement, manufacturing, and program management to create strategies to meet client needs. Production planning is dynamic by nature and always remains in flux since plans may need to be modified in response to situation[2].

Input-output models are usually used to simplify natural systems[3]. The models can be used to answer a research question and explore how the system behaves in particular circumstances[4]. There are no broad principles for creating an input-output system[5]. Günther and Velten (2014)[4] outlined the four general phases that must be followed to describe and analyze the behavior of a system:

(1) System analysis;
(2) Modeling;
(3) Simulation;
(4) Validation.

System analysis's first step involves gathering all the data needed to explain the system's behavior under consideration. In step two, a model is created, for example,

analytically, numerically, or probabilistically based on the data that was gathered in step one. The model describes the relationship between the system's input and output information. The model is converted into a simulation in step three. The initial experiments are conducted to display the simple design based on the data gathered in step one. The simulation results are validated in step four to address the research issues in a natural system.

In step one of system analysis is essential the selection of indicators. An indicator monitors an issue or condition and demonstrates a desired outcome. Hands are varied and depend on the type of systems they watch, with different levels of complexity[6]. A system's status 3zcan be described via indicators. Choosing the appropriate indicators requires a scientific and technical understanding of how the system functions and what data are needed[7].

An indicator does not mean the same as an indication or goal; an arrow is generally quantifiable by aggregating different and multiple data. The resulting information is synthesized and used to measure goal achievement. Indicators should be based on criteria and present some characteristics, such as specific, measurable, understandable, relevant, realistic, reliable, etc.[8].

In the Input-output model for conventional PPC systems, production facilities transform raw materials into products, typically producing a predetermined output in quantity and quality at the lowest possible cost[9]. For this transfor-

2

mation process, PPC systems serve two primary purposes. First, with the help of PPC systems, labor, costs, and raw material input are planned to produce specific items. Second, PPC systems manage orders through product delivery. The data bill of materials (BOM) and manufacturing plans are required for both functions[10]. A BOM is a formal list of raw materials that specifies the components needed to make a particular product. Work plans outline the procedures that must be taken to generate a specific product. The description includes details on the requirements for workstations, the interval between two subsequent processes, the production times, which are broken down into waiting time, setup time, processing time, and clearing time, as well as the raw materials that must be used[11].

In plant production through ES, we must solve the research question aimed at identifying the anticipated real cost of production in the biofactory facilities. The first step is to develop a system analysis, which uses the input and output model and describes the behavior of the system's production from a PCC perspective in a biofactory. A search for biofactory indicators is carried out, where an overview of relevant indicators for choosing appropriate indicators for PPC processes in plant biotechnology is not presented. To fill this gap, this paper presents information for current PPC systems in plant production by SE. An input-output model has been created, and PPC systems have been defined as a platform for further research and study through the analysis of plant biotechnology requirements and challenges.

Materials and methods

In the analysis system, each part of the ES cacao plant production at the biofactory was detailed. The required input and output information to describe the behavior of the considered procedure was collected with the direction of staff belonging to the biofactory of Universidad de Antioquia and researchers with significant experience in ES cacao production[12–17]. Production plans and data bill of materials (BOM) for 100.000 batch plant production were realized according to Gronau, (2014)[10] (Supplemental 1 and 2). From BOM and production plan following Joung et al. (2013)[8] conceptual proposals have selected the indicators based on the following criteria and characteristics:

(1) Specific: An indicator should be detailed and transparent as possible, precisely formulated to measure only the desired output;

(2) Measurable: Clearly and concretely, the indicator defines the measurement type, allowing data collection to be consistent and comparable. It can be easily measured by quantitative or qualitative means;

(3) Understandable: An indicator should be easily interpreted, and one should know exactly what the output of an indicator demonstrates to act accordingly to the needs;

(4) Relevant and realistic: An indicator must be appropriate, fitting the measuring purpose and underlying the pointed issue, directly related to meaningful and purposeful aspects, and realistic considering that the needed data to calculate the indicators should be collected only through available resources, not being the collection too tricky or too expensive.

(5) Reliable: It must give an accurate picture of what is measured, which does not mean the same as being precise, but instead that it contains trusted and accurate information.

(6) Timely manner: The data collection, calculation,

and evaluation must be done promptly, providing a structure that allows meaningful progress monitoring. In other words, it should be perfectly stated the desired frequency for calculating the indicator to track the outcome results better;

(7) Long-term-oriented: It must ensure their future use and reflect the development and adoption of organizational, process or product changes.

Results and discussion

It is the result of more than ten years of research, development of knowledge and experience in the production of elite plants from biotechnological techniques to improve the agro-industrial output similar to other biotechnologies in South America[18]. Different production stages were identified in the analysis system of the SE cacao plant production. SE as a productive approach is a complex process involving other biological mechanisms in each one of its stages: initiation, multiplication, maturation, and germination, as reported by Egertsdotter et al. (2019)[19]. The initiation stage includes the introduction to in vitro conditions (laboratory) and the induction phase. In the introduction phase, the plant material from the donor or parental plants is taken from field conditions to the laboratory for a disinfection process and obtaining sterile material. In the induction phase, the plant material in controlled conditions is required a culture medium that promotes cellular differentiation and the formation of embryogenic cells[20]. Once the embryogenic potential is induced, indirectly pro, embryonic masses (PEM) are formed[21]. At this point, the SE allows unlimited multiplication of the original plant material[22]. Cacao SE could be developed directly on previously somatic embryos in a process called secondary or recurrent somatic embryogenesis producing more embryos in multiplication stage[15]. The change of culture conditions in embryogenic tissues allows the somatic embryo development through the maturation and germination stages[23–25]. In the conversion phase, the embryo transitions to a plantlet with the extension of the first leaves, elongating the stem and forming primary and secondary roots. Then, the plantlets continue developing until they form at least -14 leaves, a stem, and roots with a length greater than 3-10 cm. Subsequently, the obtained plantlets can be transferred to ex vitro conditions for hardening or acclimatization. The seedlings adapt to the new environmental needs in the greenhouse with a specific substrate, lighting, and adequate irrigation. Later, seedlings are transferred to a new substrate, and when they reach sufficient growth, they are taken to the nursery for their subsequent transfer to the field (Figure 3-1.). The productive approach is like another successful process of plant in vitro propagation like Al-Aizari et al. (2020)[2]; Dhiman et al. (2021)[2]; Sriskanda (2021)[2]; Vyas et al. (2021)[2].

Different informational elements on controls are considered for the productive process of cacao plantlets. This allows measuring the degree of objective attainment desired to be achieved in each stage of the process. The following has been taken into account when creating indicators in each stage: (1) Plant production requires a close relationship between the stages of SE and labor operations; (2) Labour operations must be executed in an inviolable sequential manner from the initiation stage to acclimation (3) The type of tissue obtained at the end of a phase of the initial material for the subsequent phase; (4) Labour operations are entirely manual and are the basis for calculating
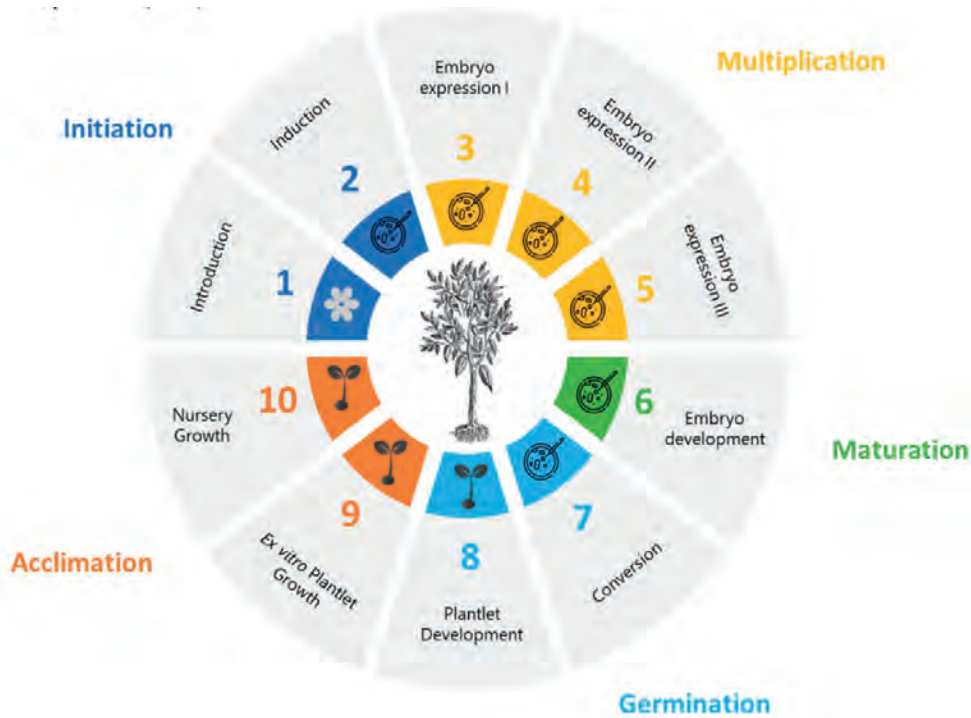
Figure 1. Flow chart of the plantlets production stages via somatic embryogenesis for different cacao genotypes.

the work (amount of plant material by the vessel being processed by workday per person).

Based on BOM (Supplemental 1) and production plan description (Supplemental 2) for each stage: initiation, development, maturation, germination, and acclimation of ES cacao plant production and the needed requirements to create useful input-output model, figure 3-2 shows an overview of a basic model for PPC systems. The indicators for PPC systems for ES plant production were categorized into five groups: materials, costs, labor, quality, and performance (Figure 3-3), similar to Chen, (2016)[30].

Materials

The total materials used to produce and package the plantlets are detailed in BOM (Supplemental 1). This includes raw materials and items required for manufacturing but is not part of the finished product. The group of indicators materials considers the predictable material consumption from production, in particular, the materials needed to prepare culture media and the consumables used in the process operation such as chemical products, gelling agents, culture vessels, glassware, culture tools, laboratory tools and other various items that are necessary for the process[31].

Labour

The group of labour indicators considers the production facility's workers' predictable work schedules. The total number of workers in production determines how many people are employed. For Colombia, a potential working time per month of 166 hours was obtained (Supplemental 2). Labour was defined in two ways, direct and indirect labor, indirect labour there are considered functions in the laminar flow chamber in all production stages like disinfection of explants, disinfection of tools and containers, bowl protection removal, vessels opening, cutting of the explants, culture medium replacement, selection of keys with embryos, cut to separate the embryos, selection by the size of embryos, material discard, closing of the reseeded container, container labeling, fill tracking lists, etc. In indirect labor, some people perform operational and technical functions and work individually in the purchase of reagents, preparation of transport boxes for plant material from the field, repackaging reagents, storage, weighing of reagents, preparation of culture medium, autoclaving of culture media and materials, dispensing of culture media, washing of glassware and tools, etc.

Following Cervelli and Senaratna (1995)[32] supervisory positions must also be considered, including those in charge of supervising direct work. For example, a supervisor must calculate the number of vessels and culture media required daily and weekly and manage chemical products, media stock, equipment, and the maintenance of the respective laboratory stations for working. They ensure all explants start producing on schedule, in the correct quantities, and without contamination. Besides, they are responsible for maintaining productivity and, most importantly, mana-
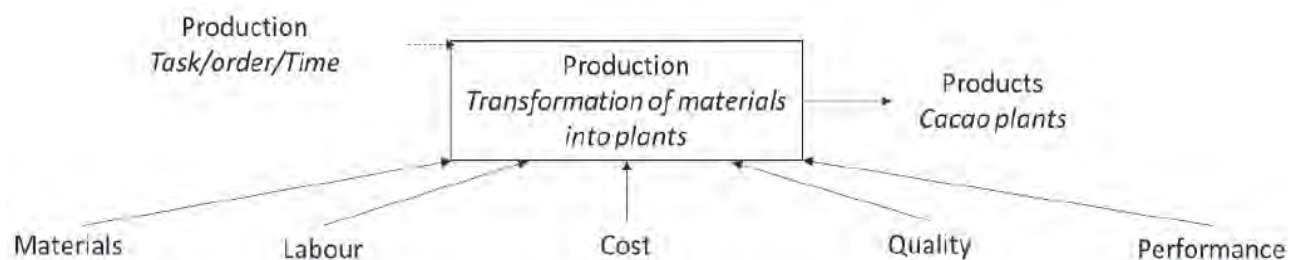
Figure 2. Input-output model for somatic embryogenesis (SE) cacao plant production planning and controlling (PPC) system.

Figure 3. The indicator categorization structure contains five main groups: materials, costs, labor, quality, and performance for ES plant PPC system.

ging the group of direct workers and deciding whether crop production must be continued, harvested, or discarded at their discretion.

The strategy implemented to monitor the work carried out by an operator is using productivity norms or standards (W), which are obtained from the average time it takes for the personnel to carry out a particular activity. The staff is expected to develop a volume of processes at each time. The following table presents an abstract of the action and the unit of measure (Supplemental 2).

Cost

The group of indicators costs reflects the actual and anticipated expenses of production. The total economic value is the sum of material of culture medium materials, direct and indirect labor of employees including wages, benefits, indirect cost of manufacturing like transportation and laboratory tools and operation expenses. Operation expenses are cash payments for facilities, energy, services purchased, depreciation of construction, installations, and equipment (refrigerator, oven, autoclave, scale, pH meter, magnetic stirrer, stereomicroscope, water distillation unit, lighted shelves, timers, air conditioning, orbital shakers, etc.) and administration[33]. Payments for the services received include those to independent contractors, staffing firms, and other service providers (e.g., maintaining a machine). Employee salary, employee taxes, levies, unemployment funds, and total benefits, including pensions, insurance, health, and safety, make up the entire payroll[34].

Quality

Quality indicators are tangible and quantifiable measurement instruments that evaluate the quality of each process's stages, considering both input and output factors. The ideal morphological characteristics of flower buds, primary embryogenic callus, globular embryos, repetitive so-matic embryos and plantlets are specified for each stage. In addition, indicators such as microbial contamination, necrosis and abnormality are also specified (Table 3-1).

Performance

Performance indicators allow qualitatively and quantitatively demonstrating progress in each stage expressed as percentages defined following the productive biofactory-scale works[35,36] and practical experience (Table 3-2). Three leading indicators were defined: disinfection, biological response and multiplication coefficients.

Percentages of disinfection: The production process requires a high level of safety, which can be jeopardized by involving contaminated material, contamination of the culture medium, or contamination caused by poor washing of containers. Contamination processes are too risky since they can lead to the complete loss of a production batch.

Percentage of biological response: It is estimated that only a portion of the plant material introduced in the process generates a callus, which develops embryos, and these develop into seedlings without malformations. According to quality indicators (Table 3-1).

Multiplication coefficients: In the multiplication stages of the production process, there are three phases in which several embryos are obtained from one callus and previous sources. This process is strategic since it exponentially increases the formation of embryos that become seedlings.

For each stage defined, percentages of disinfection, survival, microbial contamination, callogenesis, callus-forming embryos, primary globular somatic embryos, primary cotyledonary somatic embryos, callus with recurrent embryogenesis, different types and amounts of existing abnormalities, cotyledonary embryos with secondary roots, photosynthetically active cotyledonary embryos, typically developed in vitro plantlets, normally produced ex vitro plantlets, etc. (Table 3-2).

Stage	Input	Output
Initiation	**Flower Buds**	**Callus**
	Morphological characteristics of flower buds: Flower buds in intermediate development stages, closed, at least 0.3 – 0.5 cm of length between the base of the peduncle and the apex. Flower buds with mechanical damage or necrosis and those that open during the disinfection process are excluded.	Morphological characteristics of callus: Undifferentiated growth on the filamentous, cream-white staminode in a proportion greater than 70% of the explant.
Multiplication	**Callus**	**Immature Embryos**
	Morphological characteristics of callus: Undifferentiated growth on the filamentous, cream-white staminode in a proportion greater than 70% of the explant.	Morphological characteristics of embryos from repetitive embryogenesis: Somatic embryos in an immature cotyledonary state, with differentiation of the epicotyl and hypocotyl, of at least 2 mm - 5 mm from the base of the radicular pole to the cotyledons, radicular axis with an off-white color.
	INDexp-CM2 transition. Morphological characteristics of embryogenic callus with primary embryos: Aggregates of waxy light to dark brown callus with somatic embryos in a globular state of at least 0.5 mm – 3 mm, without walls defined between them and a translucent to off-white color, mostly in a cluster.	
	Transition between CM2-EM2. Morphological characteristics of embryos from repetitive embryogenesis: Somatic embryos is an immature cotyledonary state, with differentiation of the epicotyl and hypocotyl, of at least 2 mm – 5 mm from the base of the radicular pole to the cotyledons, radicular axis with an off-white color.	Embryos with abnormalities: monocotyledonous embryos, multicotyledonous embryos, embryonic axis fusion, embryos without apical or radicular development, number of contaminated embryos, number of necrotic embryos.
	Embryos with abnormalities: monocotyledonous embryos, multicotyledonous embryos, embryonic axis fusion, embryos with numerous trichomes on their axes, embryos without apical or radicular development.	
Maturation	**Immature Embryos**	**Mature Embryos**
	Morphological characteristics of cotyledonary embryos from repetitive embryogenesis: Somatic embryos with a defined polarity, differentiation between the epicotyl and hypocotyl,	Morphological characteristics of mature cotyledonary embryos from repetitive embryogenesis: Somatic embryos
	with an axis of at least 5 mm – 10 mm from the base of the radicular pole to the apex, an off-white axis, radicular axis with brown basal grooves and different shades in the cotyledons (transparent, ivory, pink and greenish).	with a defined polarity, differentiation between the epicotyl and hypocotyl, with an axis of at least 5 mm – 10 mm from the base of the radicular pole to the apex, an off-white axis and different shades in the cotyledons (transparent, ivory, pink and greenish).
	Embryos with abnormalities: monocotyledonous embryos, multicotyledonous embryos, embryonic axis fusion, embryos with curved or coiled hypocotyls, embryos with numerous trichomes on their axes, embryos without apical or radicular development.	Embryos with abnormalities: monocotyledonous embryos, multicotyledonous embryos, embryonic axis fusion, embryos with curved or coiled hypocotyls, embryos without apical or radicular development.
Germination	**Mature Embryos**	**Plantlets**
	Morphological characteristics of mature cotyledonary embryos from repetitive embryogenesis: Somatic embryos with a defined polarity, differentiation between the epicotyl and hypocotyl, with an axis of at least 10 mm - 15 mm from the base of the radicular pole to the apex, an off-white axis and different shades in the cotyledons (transparent, ivory, pink and greenish).	Morphological characteristics of complete plantlets: with a stem length of at least 3 cm, at least 1 distinguishable internode, prominent radical development of at least 5 – 10 cm, and at least 1 – 4 true leaves.
	Embryos with abnormalities: monocotyledonous embryos, multicotyledonous embryos, embryonic axis fusion, embryos with curved or coiled hypocotyls and embryos without apical or radicular development.	Plantlets with abnormalities: tuberous roots, roots without the presence of pivotal roots, bifurcated stems, curved or twisted roots, and necrotic roots.
	MM6-MM6 transition: Morphological characteristics of plantlets: a height of between 0,8 cm – 1,2 cm, radical development of at least 1 – 2 cm with primary roots, photosynthetically active cotyledons, and the formation of 1 - 2 true leaves.	
	Mature embryos with abnormalities: monocotyledonous embryos, multicotyledonous embryos, embryonic axis fusion, embryos with curved or coiled hypocotyls, embryos with numerous trichomes on their axes, embryos without apical or radicular development.	
Acclimation	**Plantlets**	**Hardened Plantlets**
	Morphological characteristics of complete plantlets: with a stem length of at least 3 cm, at least 1 distinguishable internode, prominent radical development of at least 5 - 10 cm, and at least 1 – 4 true leaves.	Morphological characteristics of complete plantlets: with a stem length of at least 8 cm, at least 2 - 3 distinguishable internodes, prominent radical development of at least 20 cm, and at least 6 – 10 true leaves.

Table 1. Quality indicators for producing cacao plantlets in a biofactory (initiation, multiplication, maturation, germination, and acclimation stages).

Initiation		Multiplication			Maturation	Germination		Acclimatization
Introduction	Induction	Expression I	Expression II	Expression III	Embryo development	Conversion	Plantlet development	
≥ 90% disinfection	≥ 95% callogenesis	5 embryos per explant	5 embryos per explant	10 embryos per explant	10 embryos per explant	≥ 70% mature cotyledonary embryos with normal steam	≥ 50% vitroplantlets with normal steam	≥ 60% plantlets with normal steam
≥ 90% survival	≤ 5% contamination	≤ 5% contamination	≤ 5% contamination	≤ 5% contamination	≥ 70% cotyledonary embryos	≥ 70% cotyledonary mature embryos with secondary roots	≥ 50% plantlets with secondary roots	≥ 80% plantlets with secondary roots
	≤ 50% embriogenic callus	≤ 10% primary somatic embryos (globular and cotyledonary)	≥ 90% repetitive embryogenesis	≥ 90% repetitive embryogenesis	≥ 70% cotyledonary embryos with secondary roots	≥ 70% photosynthetic mature cotyledonary embryos	≥ 70% vitroplantlets with true leaves	≥ 80% plantlets with true leaves
			≥ 70% globular and cotyledonary secundary somatic embryos	≥ 70% globular and cotyledonary secundary somatic embryos	≥ 70% photosynthetic cotyledonary embryos	≤ 5% contamination	≤ 5% contamination	≤ 60% survival
			≤ 30% abnormalities	≤ 30% abnormalities	≤ 30% abnormalities	≤ 30% abnormalities		

Table 2. Performance indicators for producing cacao plantlets in a biofactory (initiation, multiplication, maturation, germination, and acclimatization stages).

Figure 3-2 also shows the information stream production Task/Order/Time and the indications. It is feasible to normalize the indicators using this information. The input indicators for "Expenses" and "Materials" can be expressed as time, production tasks, material consumption, or costs per production order[37]. The normalized indicator can be used to improve production efficiency by, among other things, benchmarking procedures, comparing equal production orders, and monitoring production[38]. The set of product indicators also reflects the output of the production process. The outcome of products generated in production using input materials is the weight or volume of such products.

In this sense, the Task/Order/Time refers to the efficiency of the production process; it is the flower ratio that enters the process concerning the seedlings that leave it. In the efficiency of the production process, it is sought to reduce the number of explants such as cacao flowers that enter the production process and that the number of plants that leave it is more significant.

Conclusions

PPC plays an essential role in modern production enterprises. Current production management systems consider resources such as material, labor and production capacity and their respective costs but sometimes neglect the quality and performance for cost savings. The PPC system has been identified, and analytical modeling of the operation of the productive propagation was carried out through ES plant cacao production, in which the primary and support activities were identified, with the respective consumption, until the final product was obtained. With the data from the model, the simulation was carried out, in which the indicators considered of greater relevance are monitored, which tells us about the production process. This work constitutes the first step toward approximating costs closer to reality.

Supplementary Materials

The following are available online at www.revistabionatura.com/xxx/s1, Table Supplemental 1: Data bill of materials, Sheet 1 Inventory Sheet. Supplemental 2 Production Plan Sheet 1 Batch Plants to be obtained, Sheet 2 Stages of production, Sheet 3 Direct and indirect labor, Sheet 4 Culture medium and tools, Sheet 5 Assumptions.

Author Contributions

Conceptualization, Ana María Henao Ramírez and Aura Inés Urrea Trujillo; methodology Hernando David Palacio Hajduck and Diana Maria Cano Martinez; validation and formal analysis, Ana María Henao Ramírez and Diana Maria Cano Martinez; investigation, resources, data curation, writing—original draft preparation, Ana María Henao Ramírez; writing—review and editing and supervision, Aura Inés Urrea Trujillo. All authors have read and agreed to the published version of the manuscript.

Conflicts of Interest

The authors declare no conflict of interest.

Bibliographic references

1. Akmal A, Podgorodnichenko N, Greatbanks R, Everett AM. Bibliometric analysis of production planning and control (1990–2016). Production Planning & Control. 2018;29(4):333-351.

7

2. Belhadi A, Touriki FE, El Fezazi S. Benefits of adopting lean production on green performance of SMEs: a case study. Production Planning & Control. 2018;29(11):873-894.

3. Bonney M. Reflections on production planning and control (PPC). Gestao & Producao. 2000;7(3):181-207.

4. Günther M, Velten K. Mathematische Modellbildung Und Simulation: Eine Einführung Für Wissenschaftler, Ingenieure Und Ökonomen. Wiley-VCH GmbH; 2014. https://books.google.com.co/books?id=ekyCoAEACAAJ

5. Moreau V, Massard G. Material and Energy Flow Analysis. Published online 2017. doi:10.1093/acrefore/9780199389414.013.109

6. Schreiber M, Schutte CSL, Braunreuther S, Reinhart G. A performance measurement system for integrated production and maintenance planning. Procedia CIRP. 2020;93:1037-1042. doi:https://doi.org/10.1016/j.procir.2020.03.041

7. Bila M. Developing an Input-Output Model for Benchmarking Company Resource Usage. Universidade Nova de Lisboa; 2016.

8. Joung CB, Carrell J, Sarkar P, Feng SC. Categorization of indicators for sustainable manufacturing. Ecol Indic. 2013;24:148-157. doi:10.1016/j.ecolind.2012.05.030

9. Stark R, Seliger G, Bonvoisin J. Sustainable Manufacturing: Challenges, Solutions and Implementation Perspectives. Springer Nature; 2017.

10. Gronau N. Enterprise resource planning. Architektur, Funktionen und Management von ERP-Systemen. 2014;2.

11. Trost M, Claus T, Herrmann F. Master Production Scheduling and the relevance of included social criteria. ACC Journal. Published online 2017.

12. Gallego A, Henao A, Urrea A, Atehortúa L. Polyphenols distribution and reserve substances analysis in cocoa somatic embryogenesis. Acta Biolo Colomb. 2016;21(2):335-345. doi:http://dx.doi.org/10.15446/abc.v21n2.50196

13. Henao A, Salazar H, Urrea A. Quality of cocoa (Theobroma cacao L.) DNA from foliar tissue at different stages of development. Acta Agron. 2018;67(2):1-10. doi:10.15446/acag.v67n2.63046

14. Henao A, De-La-Hoz T, Ospina T, Garcés L, Urrea A. Evaluation of the potential of regeneration of different Colombian and commercial genotypes of cocoa (Theobroma cacao L.) via somatic embryogenesis. Sci Hortic. 2018;229:148–156. doi:10.1016/j.scienta.2017.10.040

15. Henao-Ramírez A, Urrea-Trujillo A. Somatic Embryogenesis for Clonal Propagation and Associated Molecular Studies in Cacao (Theobroma cacao L.). In: Chong P, Newman D, eds. Agricultural, Forestry and Bioindustry Biotechnology and Biodiscovery. Springer, Cham; 2020:63-102. doi:https://doi.org/10.1007/978-3-030-51358-0_5

16. Henao A, Jaime H, Duque S, Calle A, Urrea A. Determination of Genetic Stability in Cacao Plants (Theobroma Cacao L.) Derived from Somatic Embryogenesis Using Microsatellite Molecular Markers (SSR). International Journal of Fruit Science. 2021;00(00):1-15. doi:10.1080/15538362.2021.1873219

17. Osorio T, Henao A, de la Hoz T, Urrea A. Propagation of IMC67 Plants, Universal Cacao (Theobroma Cacao L.) Rootstock via Somatic Embryogenesis. International Journal of Fruit Science. 2022;22(1):78-94. doi:10.1080/15538362.2021.2023067

18. Galian CE, Cabral J, Jacobo LA, Suárez M. Industrial biotechnological laboratory with adjustable scale of the model of biofabricas-Phytolab. Brazilian Journal of Development. 2019;5(6):4513-4524.

19. Egertsdotter U, Ahmad I, Clapham D. Automation and scale up of somatic embryogenesis for commercial plant production, with emphasis on conifers. Front Plant Sci. 2019;10(February):1-13. doi:10.3389/fpls.2019.00109

20. Kouassi MK, Kahia J, Kouame CN, Tahi MG, Koffi EK. Comparing the effect of plant growth regulators on callus and somatic embryogenesis induction in four elite Theobroma cacao L. genotypes. HortScience. 2017;52(1):142-145. doi:10.21273/HORTSCI11092-16

21. Daouda K, Kan K, Alla N, Kouablan K. Induction of somatic embryos of recalcitrant genotypes of Theobroma cacao L. J Appl Biosci. 2019;133(1):13552. doi:10.4314/jab.v133i1.7

22. Fehér A. Callus, dedifferentiation, totipotency, somatic embryogenesis: What these terms mean in the era of molecular plant biology? Front Plant Sci. 2019;10(April):1-11. doi:10.3389/fpls.2019.00536

23. Garcia C, Marelli J, Motamayor J, Villela C. Somatic Embryogenesis in Theobroma cacao L. In: Loyola-Vargas V, Ochoa-Alejo N, eds. Plant Cell Culture Protocols, Methods in Molecular Biology. Vol 1815. Springer Science; 2018:227-245. doi:https://doi.org/10.1007/978-1-4939-8594-4_15

24. Ajijah N, Hartati R, Rubiyo R, Sukma D, Sudarsono D. Effective cacao somatic embryo regeneration on kinetin supplemented DKW medium and somaclonal variation assessment using SSRs markers. Agrivita. 2016;38(1):80-92. doi:10.17503/agrivita.v38i1.619

25. Bustami M, Werbrouck S. Somatic Embryogenesis in Elite Indonesian cacao Theobroma cacao L. In: Jain SM, Gupta P, eds. Step Wise Protocols for Somatic Embryogenesis of Important Woody Plants. Springer International Publishing AG; 2018:73-81. doi:10.1007/978-1-4939-8594-4_15

26. Sriskanda D, Liew YX, Khor SP, Merican F, Subramaniam S, Chew BL. An efficient micropropagation protocol for Ficus carica cv. Golden Orphan suitable for mass propagation. Biocatal Agric Biotechnol. 2021;38:102225. doi:https://doi.org/10.1016/j.bcab.2021.102225

27. Vyas KD, Ranawat B, Singh A. Development of high frequency cost-effective micropropagation protocol for Juncus rigidus using liquid culture medium and extraction of cellulose from their in vitro shoots - An important rush. Biocatal Agric Biotechnol. 2021;35:102099. doi:https://doi.org/10.1016/j.bcab.2021.102099

28. Al-Aizari AA, Al-Obeed RS, Mohamed MAH. Improving micropropagation of some grape cultivars via boron, calcium and phosphate. Electronic Journal of Biotechnology. 2020;48:95-100. doi:https://doi.org/10.1016/j.ejbt.2020.10.001

29. Dhiman N, Devi K, Bhattacharya A. Development of low cost micropropagation protocol for Nardostachys jatamansi: A critically endangered medicinal herb of Himalayas. South African Journal of Botany. 2021;140:468-477. doi:https://doi.org/10.1016/j.sajb.2021.04.002

30. Chen C. Cost analysis of plant micropropagation of Phalaenopsis. Plant Cell Tissue Organ Cult. 2016;126(1):167-175. doi:10.1007/s11240-016-0987-4

31. Prakash S, Hoque M, Brinks T. Culture media and containers. In: Low Cost Options for Tissue Culture Technology in Developing Countries. FAO/IAEA Division of Nuclear Techniques in Food and Agriculture; 2004:29-40.

32. Cervelli R, Senaratna T. Economic aspects of somatic embryogenesis. In: Aitken J, Kozai T, Lila M, eds. Automation and Environmental Control in Plant Tissue Culture. Springer Science; 1995:29-64. doi:10.1007/978-94-015-8461-6_3

33. Tomar UK, Negi U, Sinha AK, Danatu PK. An overview of the economic factors influencing micropropagation. In: Parihar P, Parihar L, eds. Advances in Applied Biotechnology. Agrobios. ; 2010:1-12.

34. Henao A, Palacio D, Urrea A. Cost Analysis of Cacao (Theobroma cacao L.) Plant Propagation through the Somatic Embryogenesis Method. Bionatura. 2022;7(2):1-13. doi:10.21931/rb/2022.07.02.2

35. Alvarez N. Desarrollo de Ecuaciones Funcionales Para El Apoyo a La Toma de Decisiones En La Planificación de La Producción Masiva de Plantas in Vitro Por Embriogénesis Somática En El IBP. Universidad Central" Marta Abreu" de Las Villas; 2014.

36. Sánchez C. Alternativas Para El Control de Malezas En El Cultivo de Cacao (Theobroma Cacao) En El Cantón Montalvo. Universidad Técnica de Babahoyo - Ecuador; 2018.

37. Stevenson M, Hendry LC, Kingsman BG. A review of production planning and control: The applicability of key concepts to the make-to-order industry. Int J Prod Res. 2005;43(5):869-898. doi:10.1080/0020754042000298520

38. Pechmann A, Zarte M. Procedure for Generating a Basis for PPC Systems to Schedule the Production Considering Energy Demand and Available Renewable Energy. Procedia CIRP. 2017;64:393-398. doi:https://doi.org/10.1016/j.procir.2017.03.033

Protocol for histological analysis of the interaction *Vanilla planifolia* - *Fusarium oxysporum* f. sp. *vanillae*

Quirino Villarreal Alejandro[1], Ramírez Vázquez Mónica[2], Velázquez López Olinda Elizabeth[3], Rivera-Fernández Andrés[1], Luna-Rodríguez Mauricio[1]*

DOI. 10.21931/RB/2023.08.01.9

[1] Laboratorio de Genética e Interacciones Planta Microorganismos, Facultad de Ciencias Agrícolas, Universidad Veracruzana, México.
[2] Facultad de Ciencias, Universidad Nacional Autónoma de México (UNAM), México.
[3] Instituto de Ecología A.C. El Haya, Xalapa, Veracruz, México.
Corresponding author: mluna@uv.mx.

Abstract: *Fusarium oxysporum* f. sp. *vanillae* (Fov) is the main phytosanitary problem of Vanilla planifolia, invading the root and causing the rotting of up to 80% of the plants. The histological process is used to study the morphological characteristics of the tissues of interest and published a protocol to check *Fov-V. planifolia* interaction that was not reproducible under our conditions, so the study aimed to adapt a procedure that allows differential analysis of the mechanism of Fov invasion in *V. planifolia* by confocal microscopy. The bioassays consisted of analyzing Fov-infected roots. The experimental design consisted of three replicates evaluated at 12, 24, 36, 48, 60 and 72 hours post-inoculation. Roots without inoculum were used as controls. The samples were fixed in paraformaldehyde and 4% sucrose (PBS). Subsequently, the tissues were dehydrated by a combination of alcohols at different concentrations. The cuts were made with a microtome. The sections were observed under a Leica confocal microscope with a 63X objective with ap. No. 1.4, plus immersion oil; excitation lines: 405, 488, 532. The FAA + kerosene method was the procedure that allowed complete tissue sections.

Key words: Fusariosis, Vanilla, interaction.

Introduction

Vanilla planifolia Jacks. is one of the few orchids in widespread commercial use. Its pods are essential for the manufacture of vanilla flavoring. Because of its clonal propagation, *V. planifolia* has been reported to have low genetic diversity, which makes it susceptible to diseases. In particular, root and stem rot caused by *Fusarium oxysporum* f. sp. *vanillae*, is the result of the penetration of hyphae into the root tissues, which in severe cases causes tissue death and, consequently, the death of the plant[1]. Fusarium has caused the loss of entire crops and represents a critical point for current production systems.

Studies of the *V. planifolia - F. oxysporum* interaction are still limited. Most of them focus on the evaluation of physiological aspects of the stem, leaves and fruits, giving less importance to the interaction with the roots[1-4]. Vascular symptoms, such as colonization and dissemination of the causal agent in root tissues, have been ambiguously described[5].

Improving methods that help to understand the basis of this interaction is of utmost relevance for developing disease control strategies. The histological process is a series of methods and techniques used to study the morphological and molecular characteristics of the tissues of interest, depending on what is to be observed and the type of microscopy to be used. Since the technical requirements of the proposed methods for the study of this interaction were not available, it was proposed to establish an alternative histological procedure that allows differential analysis of the mechanism of invasion of *F. oxysporum* f. sp. *vanillae* in the cellular structures of the root tissue of *V. planifolia* using confocal microscopy.

Materials and methods

Bioassays

The *V. planifolia* material was collected in an orchard established in the town of Aparicio in the municipality of Vega de Alatorre, Veracruz. According to Solano-de la Cruz *et al.* (2019)[5], root generation was induced in vanilla cuttings. To promote the invasion of *Fusarium oxysporum* f. sp. *vanillae* (Fov) in *V. planifolia* tissues, aqueous suspensions of spores of strain HG3C1 inoculated in the zone of absorbent root hairs were used. Previously, the fungus was activated on potato dextrose agar (PDA) medium for ten days. After inoculation, the roots were incubated at 28 2 ºC in a humid chamber for 72 hours, with observations every 12 hours, until the appearance of the initial symptoms of the disease was detected.

Prefixation of the samples

After detecting the initial symptoms of the disease, the roots were cut and prefixed in paraformaldehyde and 4% sucrose solution (PBS) in a 1:10 ratio (weight/volume)[6]. Subsequently, three washes were performed by immersion in sterile distilled water at one-hour intervals, changing the water at each immersion. To ensure PBS removal, the samples were observed under a light microscope. Once the PBS was removed, the samples were immersed in FAA fixative solution (90 mL of 70% ethyl alcohol, 5 mL of formaldehyde and 5 mL of acetic acid) for 24 h. The samples were then immersed in the FAA fixative solution (90 mL of 70% ethyl alcohol, 5 mL of formaldehyde and 5 mL of acetic acid) for 24 h. The fixative solution was then removed by immersing

the samples in sterile distilled water, with changes every 30 min[7,8]. The examples were dehydrated by immersion in alcoholic solutions (ABT) (Table 1). In the first instance, solutions ABT1 to ABT5 were used, with immersion times of 30 min. Subsequently, they were immersed in the ABT6 solution for at least 2 hours if the sample was used immediately for mounting and cutting; otherwise, it was left engaged in ABT6 until it was used for climbing, not exceeding 24 hours.

Mounting of the samples

The following methods were tested for the mounting stage: a) Mounting in kerosene. The samples were dried in a heating oven at 60 °C. Histological kerosene was heated to the liquid phase and poured into 1.5 cm³ cubic cardboard molds. While filling the molds, the root was placed in a horizontal orientation and kerosene was added until the tissue was covered entirely. It was left to solidify at room temperature for one hour; b) Mounting in freezing with paraplast. The roots were placed horizontally in a plastic mold, and liquid paraplast was added. The mold was placed in a cryostat for freezing; c) Mounting with paraplast. The sample was placed horizontally in a plastic mold, and liquid paraplast was added. It was left to solidify at room temperature for one hour; d) Mounting with polyethylene glycol. Cubic cardboard molds were filled with liquid polyethylene glycol. Root samples were placed horizontally and allowed to stand at room temperature for one hour; e) Mounting with FAA + kerosene. The samples were placed horizontally in plastic molds and dried in an oven at 60 °C until complete evaporation of the FAA; then, liquid kerosene was added and allowed to stand at room temperature for 30 minutes until solidification.

Cutting

Two techniques, microtome and cryostat, were used to obtain root tissue sections. For this, a Leica slide microtome (Mod. SM2010 R) with thickness settings at 10, 20, 40 and 60 µm[1] was used; for cryostat cuts, a Leica Biosystems (Mod. CM 1860 UV) with thickness settings at 10, 20, 40 and 60 µm, and temperature settings at -13, -15 and -21 °C was used.

Sample recovery and staining

Tissue sections obtained with cryostat were placed directly on the slides for staining. For the separation of kerosene, PEG and paraplast from tissue sections obtained with a microtome, these were immersed in an aqueous solution of 1 g/L porcine skin gelatin type A at 60 °C. A Barnant flotation bath (Mod. MH8517) was used to maintain a constant temperature. After separation, the sections were placed on slides. Tissue integrity was checked under a compound microscope at 40X.

In all cases, staining was carried out with fluoride tracing white (5 min) and then propidium iodide (5 min)[9]. After adding the dyes, the slides were placed at 60 °C, two to three drops of ethanolic solutions from 96, 70, 50 and 30 % were gradually administered, and finally, sterilized distilled water for tissue rehydration[1].

Microscopic observation

A Leica confocal microscope (SP8 STED) with 63X objective. ap. no. 1.4 + immersion oil and 405, 488, and 532 nm excitation lines were used.

Results

Cryostat slices

Samples 40 and 60 µm thick from all mounting methods (kerosene, paraplast, paraplast freezing, PEG and FAA+paraffin) were inadequate to differentiate Vanilla root and fungal structures (Figure 1 A, a). Samples 10 and 20 µm thick did not show tissue integrity (Figure 1 B, b and C, c).

Microtome slices

Only the 10 and 20 µm thick samples from the FAA + kerosene mounting method were intact and of good quality for microscopic observation (Figure 2a). The internal tissues of vanilla root were differentially recognized by the blue coloration, produced by the reaction of the white reagent fluorine chalcogenate with the plant cell walls, and the red coloration produced by the interaction of propidium iodide with the fungal hyphae (Figure 2b).

Discussion

The use of histological techniques makes it possible to observe structures, in a general or detailed manner, of the different components of a sample; therefore, they have been useful for studying the behavior of pathogens at the tissue and cellular level, which has made it possible to make timely diagnoses[10-12]. A complementary tool to histological techniques is confocal scanning optical microscopy, where the operation of such a microscope is similar to that of an epifluorescence microscope since both are based on the

Serie	Alcohol etílico al 96%	Alcohol etílico absoluto	Alcohol butílico terciario	Agua
ABT1	50 %	-	10 %	40 %
ABT2	50 %	-	20 %	30 %
ABT3	50 %	-	35 %	15 %
ABT4	50 %	-	50 %	-
ABT5	-	25 %	75 %	-
ABT6	Alcohol absoluto			

Table 1. Concentration of alcohols used for dehydration of V. planifolia Jacks. root samples.
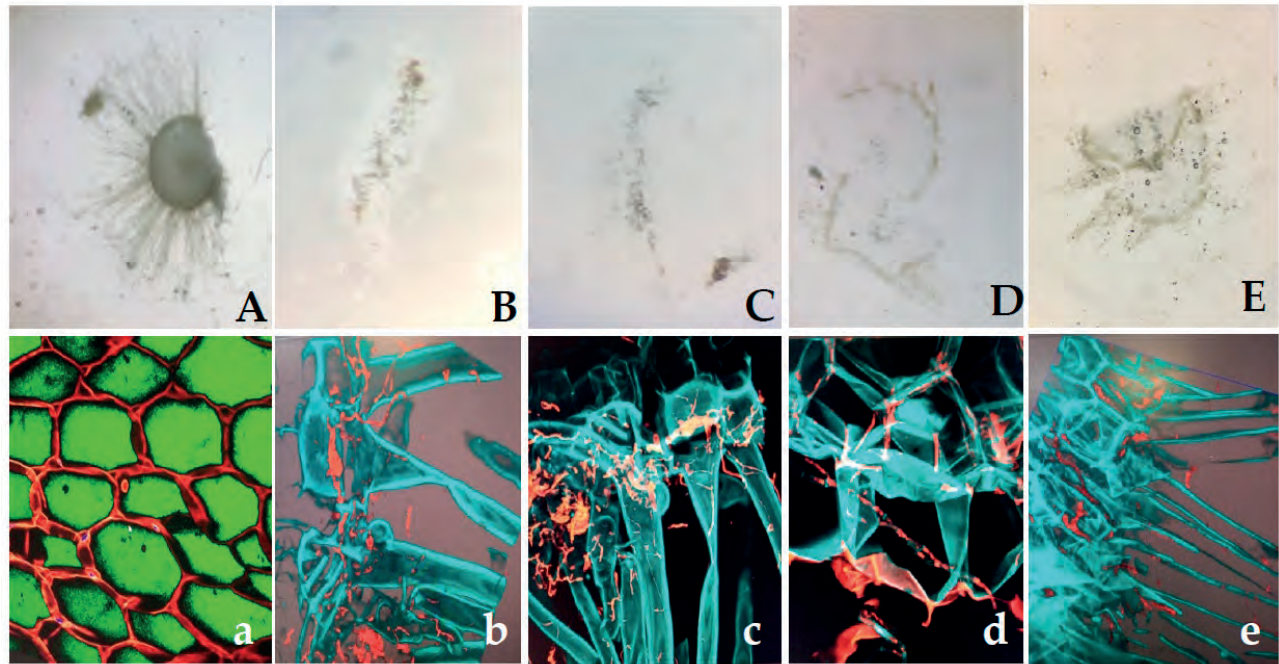
Figure 1. Appearance of images from histological sections of *F. oxysporum* f. sp. *vanillae*-infected *V. planifolia* roots processed by the different mounting and cutting techniques tested. A, thick aspect slice; B and C, fragmented slices obtained with cryostat; D and E, fragmented slices obtained with a microtome. a, b, c, d and e, confocal microscopy images of the pieces referred to in A, B, C, D and F, obtained with 63X objective. ap. no. 1.4, immersion oil and excitation lines 405, 488 and 532. Photos: Quirino, V. A., 2021.
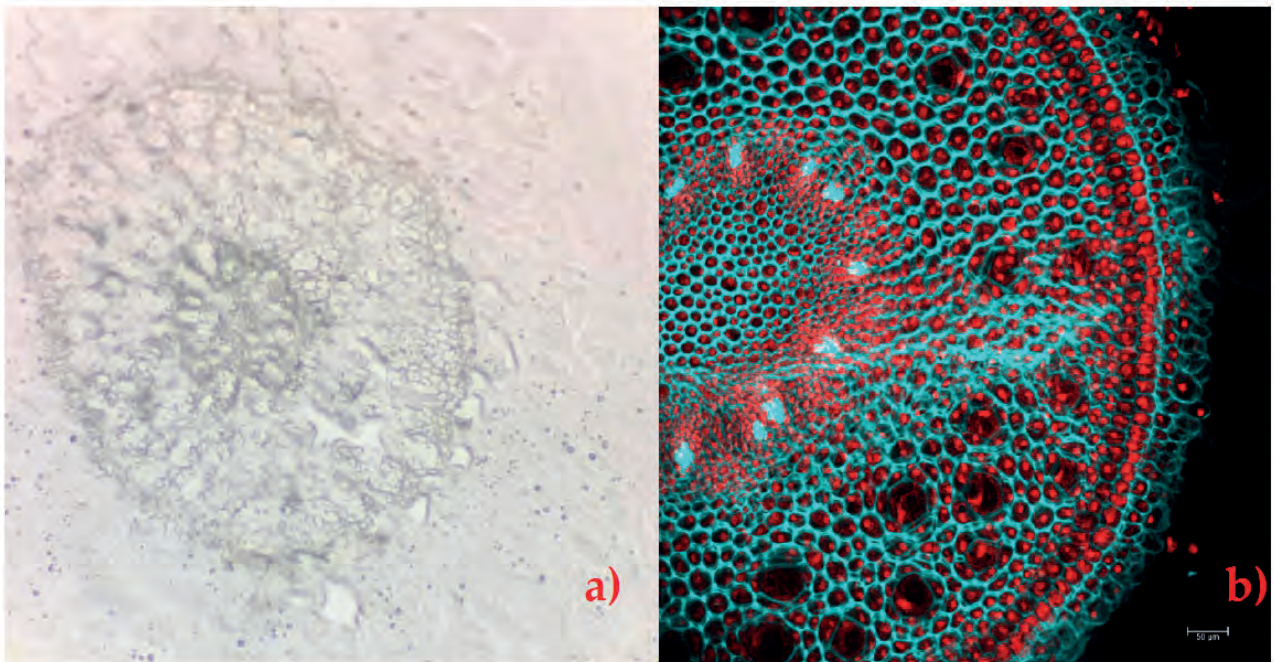
Figure 2. Appearance of *V. planifolia* root sections with FAA+ paraffin mounting made with microtome at 10 µm thickness. a) verification of tissue integrity with compound microscopy; b) root stained and visualized in confocal microscopy with 63X objective. ap. no. 1.4, immersion oil and excitation lines 405, 488 and 532. Plant cells are shown in blue, and *F. oxysporum* f. sp. *vanillae* colonization is in red. Photos: Quirino V.A., 2021

phenomenon of fluorescence; however, the latter provides images of poorer quality. This is because epifluorescence microscopes show information from all planes of the sample, focused or not, because they lack the confocal detection diaphragm and use a mercury lamp as an illumination source, which has a very irregular power, with different intensity peaks[13].

Although, for the study of the pathosystem *V. planifolia* - *F. oxysporum*, they reported an investigation where they used epifluorescence microscopy and multiphoton microscopy with different techniques of mounting and staining of the samples; however, some images are far from being quick decipherable[1]. In addition, not all laboratories have the technical and instrumental elements necessary to reproduce the method, hence the importance of adapting alternative ways that do not limit the research.

4

In the case in question, the confocal microscopy and the histological techniques used allowed for obtaining clear images, which facilitated the differentiation of the cellular structures corresponding to each organism; by staining the cells of the vanilla root in blue color due to the affinity of the white fluoride tracing reagent with the lignin and the fungus cells in red color due to the affinity of the propidium iodide reagent with the chitin[9]. Additionally, it was observed that only mounting with FAA + kerosene maintained the integrity of vanilla root tissue upon sectioning. FAA is a widely used fixative for soft plant tissues, such as vanilla root, whose advantages include rapid and complete penetration of formaldehyde into the tissue, prolonged storage possibilities, and a balance of alcohol and acid shrinkage/expansion. In addition, formaldehyde is a non-coagulation fixative that chemically binds cellular components to preserve the structure[14]. For its part, polyethylene glycol acts as a barrier by blocking the entry of other substances into the tissue[15], which could have caused the lack of rigidity of the vanilla root to remain intact at the time of cutting.

Conclusions

A histological method based on FAA + kerosene for sample mounting and confocal microscopy was adapted to differentiate the cellular structures of Vanilla planifolia root and those of *Fusarium oxysporum* f. sp. *vanillae* during their interaction in the development of the disease known as Vanilla root and stem rot.

Author Contributions

Generation of the idea and resources: Mauricio Luna Rodríguez, Alejandro Quirino Villarreal and Mónica Ramírez Vázquez. Methodology: Alejandro Quirino Villarreal, Mónica Ramírez Vázquez, Olinda Elizabeth Velázquez López and Mauricio Luna Rodríguez. Concepts: Mauricio Luna Rodríguez, Andrés Rivera Fernández and Mónica Ramírez Vázquez. Preparation of the original draft: All authors.

Funding

Acknowledgments

Conflicts of Interest

The authors declare no conflict of interest.

Bibliographic references

1. Koyyappurath S, Atuahiva T, Le Guen R, Batina H, Le Squin S, Gautheron N, et al. Fusarium oxysporum f. sp. radicis-vanillae is the causal agent of root and stem rot of Vanilla. Plant Pathol. 2016;65(4):612–25.
2. Michielse CB, Rep M. Pathogen profile update: Fusarium oxysporum. Vol. 10, Molecular Plant Pathology. 2009. p. 311–24.
3. Cardona SC, Montoya MM, Diez CM. Identificacion del agente causal de la pudrición basal del tallo de vainilla en cultivos bajo covertizos en Colombia. Rev Mex Micol [Internet]. 2012;35:23–34. Available from: http://www.redalyc.org/articulo.oa?id=88325120005
4. Adame-García J, Rodríguez-Guerra R, Iglesias-Andreu LG, Ramos-Prado JM, Luna-Rodríguez M. Molecular Identification and Pathogenic Variation of. Bot Sci. 2015;93(3):669–78.
5. Solano-De La Cruz MT, Adame-García J, Gregorio-Jorge J, Jiménez-Jacinto V, Vega-Alvarado L, Iglesias-Andreu LG, et al. Functional categorization of de novo transcriptome assembly of Vanilla planifolia Jacks. potentially points to a translational regulation during early stages of infection by Fusarium oxysporum f. sp. vanillae. BMC Genomics. 2019;20(1):1–15.
6. Gonzalez, A. M. El uso de la Histología en los sistemas de Cultivo in Vitro de tejidos. Curso Posgrado: Cultivo in Vitro de Tejidos. 2006. 1–7.
7. Johansen, D.A. Plant Microtechinique. McGraw Hill Book Co. New York. 1940. 511 págs. Disponible en: https://archive.org/details/in.ernet.dli.2015.271824/page/n11/mode/2up
8. González A.M. y Cristóbal C.L Anatomía y ontogenia de semillas de Helicteres Lhotzkyana (Sterculiaceae). Bonplandia. 1997. 9:287-294.
9. Redkar A, Jaeger E, Doehlemann G. Visualization of Growth and Morphology of Fungal Hyphae in planta Using WGA-AF488 and Propidium Iodide Co-staining. Bio- Protocol. 2018;8(14):1–7.
10. Walwyn Salas Verónica, Iglesias Duquesne C. Magaly, Almarales María Rosa, Acosta Tieles Néstor, Mera Fernández Ana, Cabrejas Acuña María Ofelia. Utilidad de técnicas histológicas para el diagnóstico de infección en piezas anatómicas. Rev Cub Med Mil [Internet]. 2004 Jun [citado 2022 Oct 06] ; 33(2). Disponible en: http://scielo.sld.cu/scielo.php?script=sci_arttext&pid=S0138-65572004000200006&lng=es.
11. Doehlemann G, Reissmann S, Aßmann D, Fleckenstein M, Kahmann R. Two linked genes encoding a secreted effector and a membrane protein are essential for Ustilago maydis-induced tumour formation. Vol. 81, Molecular Microbiology. 2011. p. 751–66.
12. Megías M, Molist P, Pombal MA. Atlas de histología vegetal y animal. España. Depto. de Biología Funcional y Ciencias de la Salud, Facultad de Biología. Disponible en: http://mmegias.webs.uvigo.es/inicio.html. Consultado: 06 de octubre de 2022.
13. Morales García MD. Uso de la fluorescencia y la microscopía confocal en la investigación científica. Soc Española bioquímica y Biol Mol. 2012;2.
14. Penn State collage of agricultural sciencies, Department of Plant Science. The Pennsylvania State University. Consejos para preservar tejidos. 2022. Recuperado a partir de: https://plantscience.psu.edu/research/labs/roots/methods/metodologia-de-investigacion/examinando-la-anatomia-fina-de-la-raiz/consejos-para-preservar-tejidos
15. Thakkar H, Murthy RSR. El polietilenglicol como agente antiagregante en la preparación de microesferas de gelatina con celecoxib. Ars Pharm. 2005;46(1):19–34.

ARTICLE / INVESTIGACIÓN

Regeneration of cocoa (*Theobroma cacao* L.) via somatic embryogenesis: Key aspects in the *in vitro* conversion stage and in the *ex vitro* adaptation of plantlets

Ana María Henao Ramírez[1]*, Julián David Morales Muñoz[1], Diana Marcela Vanegas Villa[1], Ruth Tatiana Hernández Hernández[2], Aura Inés Urrea-Trujillo[3]

[1] Center of Agrobiotechnological Development and Innovation – CEDAIT, Universidad de Antioquia, Colombia.
[2] Microbiology Institute, Universidad de Antioquia, Medellín, Colombia.
[3] Biology Institute, Universidad de Antioquia, Medellín, Colombia.
Corresponding author: amaria.henao@udea.edu.co

1

Abstract: Adapting plantlets to *ex vitro* conditions is a decisive step in the micropropagation process via organogenesis or somatic embryogenesis (ES). The percentage of success in this stage determines the quality of the product, an example of which is found in cocoa plantlets regenerated by ES, which require specific conditions to overcome the stress of the new environment. Considering the quality of the *in vitro* plantlets largely determines the survival and growth in *ex vitro* conditions, the effect of two culture media between the embryo maturation stage and the initial stage of conversion to plantlet was evaluated (EM2 - MM6 and EM2 – MF medium), achieving with the latter greater stem height, root length and the number of true leaves. In the final stage of the conversion and growth of the plantlet, the effect of five culture media was evaluated (ENR6, MF, ENR8, EDL, PR), achieving better results in stem height, root length, and the number of true leaves on MF medium. In addition, it was found that the transition of the EM2-MF had a significant development in the presence of the desired pivoting root and fibrous roots. Under nursery conditions, the growth and development of the plantlets was tested through the inoculation of beneficial microorganisms to promote survival. The plantlets that met the minimum morphological parameters for acclimation were planted in a substrate of coconut palm and sand (3:1 v/v) previously selected in the laboratory (BS). The effect of *Pseudomonas* ACC deaminase (PAACd), *Trichoderma asperellum* (Ta) and arbuscular mycorrhiza forming fungus (AMF) and different concentrations of phosphorus (PC) (0%, 50% and 100%) in the Hoagland nutrient solution (1:10) was evaluated. First, for CCN5, 62.5% of survival was obtained with PAACd + AMF. Second, the largest leaf size and survival were obtained with PAACd + Ta for *CNCh12* and *CCN51*; likewise, for *CNCh13*, the best result was obtained with PAACd.

Key words: Cacao, Clonal propagation, Mycorrhiza, Pseudomonas, Trichoderma.

Introduction

Cocoa (*Theobroma cacao* L.) is an economically important crop and the most valuable agricultural product worldwide[1]. It has been grown in the lowlands of tropical regions, South and Central America, West Africa, and Southeast Asia, with social and economic importance. Cocoa powder and cocoa butter are the major cocoa seed products with several common usages, especially in high-demand food industries[2]. Cocoa seeds are rich in phenolic compounds and flavonoids and contain several bioactive compounds, such as procyanidins, anthocyanins, flavone and flavonol glycosides, epicatechin, gallocatechin, epigallocatechin, etc.[3,4]. Cocoa polyphenols have anti-inflammatory, anticarcinogenic, antimicrobial, antiulcer, and immune-modulating properties, and antioxidants with a protective effect against cardiovascular diseases[5–8]. Thus, producing high-quality and uniform cocoa planting materials is crucial to supply industrial demands. This could be achieved through plant tissue culture techniques such as somatic embryogenesis (SE) since conventional methods do not complete the quantities required by the market. In SE a single somatic cell ob-

tained from leaf, flower, or stem explants undergoes several differentiation processes before developing into the whole plant after culture[9]. For cocoa, the protocols for somatic embryogenesis culture have been developed by several researchers[10–12]. However, low acclimation percentages of around 8.3% to 54.57% with different genotypes were reported[13–15].

The acclimation is a transitory phase between the laboratory and the field, whose objective is to take the plantlet from an *in vitro* culture to *ex vitro* conditions[16]. The *ex vitro* adaptation of Vitro plantlets requires time and conditions for the plantlets to acquire the necessary vigor to survive. They usually need several weeks under shade and gradually decreasing air humidity to acclimate to the new requirements and correct some changes in their anatomy and physiology induced by in vitro culture conditions. For plant survival, the most important changes include the development of cuticles, epicuticular waxes, and effective stomatal regulation of transpiration leading to stabilization of water status[17]. From Aguilar *et al*. (1992) and Figueira & Janick, (1995)[1], to

Ana María Henao Ramírez, Julián David Morales Muñoz, Diana Marcela Vanegas Villa, Ruth Tatiana Hernández Hernández, Aura Inés Urrea-Trujillo

Jones *et al.* (2022)[20] and Manlé *et al.* (2021)[1], the acclimation of cocoa vitro-plants is a difficult and crucial stage as it happens in most plantlets produced by *in vitro* tissue cultures[21]. Therefore, knowing the factors that affect the survival of vitroplantlets is essential when implementing the production of plant material on a large scale, whose main contribution is the development of an optimal propagation protocol.

On the other hand, it is necessary to have plantlets produced in laboratory commercials that ensure plant material is in good physiological condition to survive the definitive transplant without affecting their establishment and optimal development in the field. In this sense, crucial developmental phases such as the maturation of the somatic embryo, the conversion of the embryos to plantlet, and the acclimation of plants to nursery conditions are essential to ensure physiological vigor characteristics. This last step can be favored using microorganisms as nursery substrate improvers, which are recognized as promoters of root development in cocoa seedlings and their effect on the increase and nutrient absorption capacity[22–26].

Many plants' growth-promoting microorganisms (PGPM) can help in rooting and shoot elongation and can be useful in the acclimation phase. They can protect against the biotic and abiotic stress that occurs *in vitro* propagation, mainly in the acclimation phase, a crucial step for the success of micropropagation[27]. Within these microorganisms, the Trichoderma fungus is considered a soil organism associated with plant roots and is commonly viewed for its potential to control plant diseases in what may be a close association with many typical aspects of endophytic associations with cocoa[28], in addition to being able to behave as a plant growth stimulator[29,30]. Other beneficial microorganisms are mycorrhizal fungi, which are the mutualistic symbiosis between the fungi of the Glomeromycota phylum and the roots of most vascular plants, which are supposed to play a key role in the nutrient cycle of agroforestry systems[31]. In the case of crops with thick roots and few root hairs, such as cocoa, coffee, timber trees, and citrus, they tend to be highly dependent on mycorrhizae[32]. Specifically in cocoa, due to its mycorrhizal dependency, the fertilization practice, mainly nitrogenous and phosphate, must be fully evaluated, considering not only the yield of the crop and the availability of nutrients in the soil but also the composition and behavior of the biota, in order not to inhibit these biological processes or stimulate dependence on external inputs in these systems[33].

Other microorganisms are the bacterias that produce the enzyme ACC (1-aminocyclopropane-1-carboxylate) deaminase, being a critical bacterial trait to facilitate plant growth. This enzyme is responsible for the cleavage the plant ethylene precursor, ACC, into ammonia and ketobutyrate. Ethylene is an essential plant hormone, also known as a stress hormone because the induction of a variety of biotic and abiotic stress accelerates its synthesis by lowering ACC levels in plants, ACC deaminase-producing organisms lower ethylene levels, which, when present in high concentrations, can lead to plant growth inhibition or even death[33]. These bacteria are relatively common in soil, having been found in a wide range of environments around the world[33].

According to the above, the objective of this work was to evaluate from the stage of maturation and conversion to plantlet *in vitro* the effect of culture media composition and, in the acclimation phase, the effect of beneficial microorganisms such as Pseudomonas ACC deaminase, the fungus *Trichoderma asperellum* and mycorrhizal fungi on characteristics physiological vigour in plantlets to establish a complete process in the production of plant material on an industrial scale.

Materials and methods

Plant materials and culture conditions

For this research, the experiments included *CCN51*, *CNCh12*, and *CNCh13* genotypes, the primary genotype used in the experiments was *CCN51*, a universal genotype from Ecuador[34]. *CNCh12* and *CNCh13* are Colombian genotypes from the certified clonal garden of the Colombian National Chocolate Company (CNCH). The immature closed flower buds were collected from La Nacional Farm field-grown plants (Támesis, Antioquia-Colombia) and Yariguíes farm (Barrancabermeja, Santander-Colombia). The flower bud's collection and disinfection process were performed following the methodology described by Henao *et al.* (2018)[3]. The explants consisted of staminodes (sterile stamens) for *CCN51*, *CNCh13*, and *CNCh12*. Staminodes were extracted from the basal portion of the flower bud using sterile scalpels and placed on the culture media on the Petri dish. For *CNCh12* was used, the following culture media was according to the stages of the embryogenic process: PCG-SCG-ED-CM2-EM2-MM6, for *CNCh13*, was INDI-INDexp-CM2-EM2-MM6 and for *CCN51* was INDI-INDexp-CM2-EM2-MM6 (Table 1).

All the cultures were randomly placed in a growth chamber in continuous darkness for callogenesis, induction of primary embryo, and induction of secondary embryo stages, at an average temperature of 26°C ± 2°C and 70% relative humidity. The mature embryos were cultured in a Petri dish, and later plantlets were cultured in 500 ml vessels. The cultures were placed in a growth chamber under light with a 16-hour photoperiod and a photosynthetic photon flux density (PPFD) of 50 µmol per second, at an average temperature of 26°C ± 2°C and 70% relative humidity.

In vitro growth

Embryo maturation

Once the secondary somatic embryos of *CCN51* had been developed, they were transferred for maturating and growth. In this stage, the effect of two different culture media transitions between embryo maturation - plantlet development stage (EM2 – MF and EM2 – MM6) (Table 2) and culture time (30, 60, and 90 days) were evaluated on stem height (cm), root length (cm) and the number of true leaves per plantlet (n). The experiment was laid out in a Completely Randomized Design (CRD) with two factors: culture media (2 levels) and culture time (3 levels). Each treatment with at least 30 experimental units, for a total of n = 524.

Plantlet development

For *CCN51*, the effect of five different plantlet development culture media (ENR6, MF, ENR8, EDL, PR) (Table 2) was evaluated on stem length (cm), root length (cm), number of true leaves (n) after 30 days from the plant out. The experiment was laid out in a CRD with one factor, culture media, with five levels. Each treatment with at least 10 experimental units, for a total of n = 43.

2

Composition	CNCh13 and CCN51					CNCh12		
	Calli Induction	Primary somatic embryo induction	Secondary somatic embryo induction	Embryo maturation	Plantlet development	Calli Induction		Primary somatic embryo induction
	INDI[1]	INDexp[2]	CM2[3]	EM2[4]	MM6[5]	PGC[10]	SCG[11]	ED[12]
Macronutrients	DKW[6]	DKW	MS[14]	MS	½ MS	DKW	Lloyd & McCown[15]	DKW
Micronutrients			DKW	DKW	DKW			
Myoinositol	100	100	100	100	100	100	100	
Nicotinic acid Vit B3	1	1	1	1	1	1	1	
Thiamine Vit B1	2	2	2	2	2	2	10	
Pyridoxine							1	
Glutamine						250		
Glycine	2.18	2.18	2.18					
L-lysine	0.45	0.45	0.45					
L-leucine	0.32	0.32	0.32					
L-arginine	0.43	0.43	0.43					
L-tryptophan	0.51	0.51	0.51					
2,4,5-Trichlorophenoxyacetic acid (2,4,5-T)			1					
2,4-dichlorophenoxyacetic acid (2,4-D)	1					1.98	1.98	
1-Naphthaleneacetic acid (NAA)					0.1			
Kinetin (KIN)	0.25						0.3	
Adenine			0.25					
Gibberellic acid (GA$_3$)					0.02			
Thidiazuron						0.005		
Activated charcoal					1			
Glucose	30	30	30		40	20	20	1
Saccharose				40				20
Gelling	3	3	3	3	4	2.9	2.9	2.9

35, 4, 6 36, 10, 11, 12 37, 13 38, 14 39, 15 40

Table 1. Culture media for primary and secondary somatic embryogenesis with CCN51, CNCh13, and CNCh12 genotypes of cacao (T. cacao L.). 1,2,3,5

Ex vitro adaptation

Plantlets of different genotypes with 60 days in MF culture medium were used for the different experiments; these plantlets had stem and root development. The plantlets were removed from culture vessels and washed with running water to eliminate excess gelled culture medium. The plantlets were subsequently transferred to 50 germination trays with 10 cm deep cavities, with a capacity between 67 - 70 g of basal substrate. The tray was covered with a transparent dome for one day, and holes are subsequently made to allow exchanges until 15 days were completed, keeping the substrate hydrated with water as required and a nutrient solution of Hoagland (1:10) every 15 days. After 50 days, the plants were transplanted into 45cm deep bags. Plantlets were kept in growth conditions at the mesh house, relative moisture major to 40%, temperature between 24 - 30°C at day and 16-18 °C at night, 16:8 natural sun photoperiod, and shade of 50%.

Basal substrate (BS)

The basal substrate consisted of a 1:3 (w/w) proportion of washed river sand and ground coconut fiber without enrichment. Once the substrate is prepared, the electrical conductivity of the soil (EC) must be verified since; for cocoa, it must be kept at an optimal level of <1 mS/cm. Likewise, the pH must be verified, which must be within the optimal range of 5.8 to 7.0[42,43].

Minimum quality characteristics for in vitro plantlets

Plantlets from *in vitro* conditions were classified according to quality characteristics. The minimum quality characteristics of plantlets were evaluated in terms of stem height (cm), root length (cm), number of true leaves (n), length leaf (cm), and width of the leaf (cm) on the survival of the plantlets in the BS.

Beneficial microorganisms' preparation

Pseudomonas ACC desaminasa (PAACd) inoculum

To prepare the inoculum of PAACd, the strains of 5 bacteria preserved in the deep freezer were placed in the TSA (trypticase soy agar) culture medium. They were then grown under stirring for 72 hours in a 50% TSB (trypticase soy broth) liquid medium. After this time, the bacteria were mixed and centrifuged at 3,500 rpm for 50 minutes to eliminate the culture medium. The pellet was resuspended in a 0.03M magnesium sulfate solution with the help of a vortex. Subsequently, this solution was brought to an OD of 0.1-0.15 at 600 nm, which indicates an approximate concentration of 1x108 CFU/mL. 10mL of the bacterial inoculum near the plantlet was added to each well with 69 - 70g.

Mycorrhizal fungi (AMF) inoculum

For the preparation of the inoculum of AMF, the commercial product Mycorfos® (contained a minimum concentration of 230 spores/gram with *Glomus sp.*, *Acaulospora sp.*, *Scutellospora sp.* and *Entrophospora sp.*) was taken. The product was sieved to 1mm to remove large particles. Between 7-8 g of this product was added to each well and mixed with the substrate.

Trichoderma asperellum (Ta) inoculum

The fungus was grown in PDA medium (potato dex-

Ana María Henao Ramírez, Julián David Morales Muñoz, Diana Marcela Vanegas Villa, Ruth Tatiana Hernández Hernández, Aura Inés Urrea-Trujillo

Composition	Embryo maturation experiment			Plantlet development experiment			
	EM2[4]	MF[4]	MM6[5]	ENR6[6]	ENR8[7]	EDL[8]	PR[9]
Macronutrients	MS	½ MS	½ MS	½ MS	MS	DKW	DKW
Micronutrients	DKW	DKW	DKW	DKW	DKW		
Myoinositol	100	100	100	100	100	100	50
Nicotinic acid Vit B3	1	1	1	1	1	1	0.5
Thiamine Vit B1	2	2	2	2	2	2	1
Glycine					0.4	0.45	0.45
L-lysine					0.4	0.33	0.33
L-leucine					0.4	0.51	0.51
L-arginine					0.4	0.43	0.43
L-tryptophan					0.2	0.19	0.19
1-Naphtha-leneacetic acid (NAA)		0.01	0.1				
Gibberellic acid (GA3)		0.02	0.02				
Potassium nitrate (KNO3)					0.3	0.3	
Activated charcoal		1	1				
Glucose		40	40	10	30	20	20
Saccharose	40			5			
Gelling	3	3.8	4	3	3.2	1.8	2

Table 2. Culture media for primary and secondary somatic embryogenesis with CCN51 genotype of cacao (T. cacao L.) in embryo maturation and plantlet development experiments.

[5] (Henao et al., 2018) [35], [4, 6] (Fontal et al., 2002)[36], [7] (Guillou et al., 2018) [41], [8, 9] (Garcia et al., 2018) [11]

trose agar) for five days. Then a spore solution was made in sterile distilled water and inoculated into a bag with rice as substrate. It was incubated at in room temperature with photoperiod 12:12 for 14 days. After this, sterile distilled water was added, it was mixed very well with the rice to obtain the spore suspension, and the solution was filtered in a clean beaker passing through gauze. Then serial dilutions were made, and a spore count was performed in a Neubauer chamber to find the concentration. With this data, the fungus solution to be used was prepared at a concentration of 1×10^8 spores/mL. 5 mL of the spore suspension of the fungus *T. asperellum* was inoculated per well.

The Agricultural and Environmental Bacteriology Research Group of the Universidad de Antioquia donated all the microorganisms used.

Beneficial microorganisms' experiments

Effects of PAACd and AMF

The genotype used in this experiment was *CCN51* for two months. The effect of PAACd, AMF, and the mixture of both microorganisms and control were evaluated on survival percentage. The experiment was laid out in CRD, the factor type of substrate, with four treatments. Each treatment had 10 experimental units for a total of 40 plantlets.

Effects of PAACd and Ta

The genotypes used in the experiment were *CCN51*, *CNCh12*, and *CNCh13*. The effect of PAACd and *Ta*, the mixture of microorganisms and control, was evaluated on survival percentage and leaf area (cm²). The experiment was laid out in a CRD with the factor type of substrate with four treatments. Each treatment had 10 experimental units for a total of 40 plantlets.

Effects of AMF and phosphor (P) concentrations

Since a negative effect on mycorrhizal fungi colonization has been described when phosphorus concentrations are greater than 0.02 mg/L., the amount of phosphorus present in BS was quantified. For this, the methodology described by Osorio (2017) was followed, which consists of taking 3 g of an essential dry substrate and transferring them to centrifuge tubes, subsequently adding 30 mL of CaCl2 0.01 M and two drops of toluene for inhibition of microbial activity. The tubes were shaken horizontally for 1 hour, centrifuged at 5000 rpm for 15 minutes, and the supernatant passed through Whatman No. 1 filter paper. The concentration of P was determined by the molybdate blue method by making measurements in a spectrophotometer at a wavelength of 890 nm.

Different concentrations of P in the irrigation solution and AMF quantity (g) were evaluated. In the fertilization process, the Hoagland solution was prepared at 1:10 by modifying the amount of phosphorus as K_2HPO_4 salt at 0%, 50% and 100%. The fertilization was carried out biweekly, adding 5mL per plant for up to 60 days. The plantlets received irrigation with water as needed. The AMF inoculation consisted of applying the commercial formula in different quantities of 0g, 2g, and 3g, which were sieved and mixed with the BS. The effect of AMF quantity (0g, 2g, 3g) and

phosphor concentrations (P) (0%, 50% and 100%) were evaluated on the percentage of mycorrhizal infection and survival percentage. The experiment was laid out in a CRD with nine treatments. Each treatment had 10 experimental units for a total of 90 plantlets.

Statistical analysis

Results were subjected to an analysis of variance (ANOVA), and a comparison test was performed based on residuals to test normality (Shapiro-Wilk test). Additionally, the variance homogeneity test (Levene's test) was performed. Likewise, the comparison of means was carried out through Tukey or Dunnet's test. If they were not normal, the Kruskal-Wallis and Mann-Whitney tests were used. On the other hand, for comparisons between 2 treatments, the t-test was used for parametric data and the Wilcoxon test for non-parametric data. For unequal numbers, an analysis of variance across the generalized linear model (GLM) was performed for some stages with a Poisson variable response distribution. The Pearson Chi-square ($\chi 2$) test was carried out regarding the qualitative data. Dispersion, box, and whisker diagrams were used. A significance of 95% was determined for all comparisons using the R project v3.6.1 software.

Results

In vitro growth

Effects of culture media on embryo maturation

In this experiment, there was a higher average in the number of true leaves per plantlet in the EM2-MF transition. An average of 3.12, 3.12, and 4.10 was obtained at 30, 60, and 90 days, respectively, with significant differences concerning EM2-MM6 (Figure 1 A). For the stem height in the EM2-MF medium, an average of 3.64 cm was obtained at 60 days of cultivation with differences with respect to 2.91 with EM2-MM6 (Figure 1 B). For root length, 4.07 cm was obtained for EM2-MF and 4.4 cm for EM2-MM6, without a difference (Figure 1 C). Consequently, the appropriate medium for somatic embryo maturation was the transition between EM2 and MF medium for the CCN51 genotype with sufficient fibrous and tap root development (Figure 1 S1).

Effects of culture media on the development of plantlet

At this stage, the average number of leaves per plantlet was 4.77 obtained in the ENR8 medium, 4.55 in the MF medium, and 4,26 in the ENR6 medium without a difference (Figure 2 A). Likewise, the highest values of height stem were 4.42 cm in the MF medium and 4.03 cm in the ENR8 medium (Figure 2 B), and finally, the most excellent root length of 5.67 cm was obtained in the MF medium, followed by 4.31 cm in ENR8 (Figure 2 C). Therefore, the adequate development of the plantlets was achieved in general in the MF medium, with results consistent with the experiment detailed in the maturation assay.

Ex vitro adaptation

BS on survival plantlets

During the evaluation of the BS substrate's effect on the *ex vitro* adaptation process, it was possible to verify that

the conductivity of the substrate is critical in the process since only the addition of organic matter (MO) can significantly alter this parameter. In previous experiments, using irrigation solutions such as full and half concentration MS and DKW salts or including MO in the essential substrate, it was found that the electrical conductivity increased more than twice the ideal for cocoa (Table 3). Due to this condition, the plants stopped their growth and development; on the contrary, the mortality was 100%. Likewise, in previous trials, it was found that the corrections in the conductivity of the BS substrate supplemented with different plant growth-promoting components like AMF and OM had a positive effect on survival. In addition, the formation of the white root is observed, like a characteristic of healthy roots for cacao (Table 1 S1, Figure 2 S1).

Minimum morphological quality characteristics

Identifying the plantlet's minimum morphological quality characteristics for survival during the adaptation process was possible. *CCN51* plantlets must have at least: 3.98 cm of height stem, five true leaves with 3.58 cm of length and 1.76 of width, and prominent radical development of 6.71 cm root length with both primary pivotal roots and secondary roots (Table 4).

Effect of PAACd and AMF mix on plantlet's survival

In the effects of PAACd and AMF on the survival of plantlets, no association was found between the different treatments evaluated and the survival. The highest survival percentage of 62.5% was obtained with the substrate supplemented with PAACd + AMF, the same result was obtained with only PAACd (Figure 3B).

Effects of PAACd and Ta on plant survival and leaf area

For the leaf area, an average of 20.41 cm^2 was obtained in the substrate supplement with PAACd + Ta for the *CNCh12* genotype, with a significative difference from the control. The same result was for *CCN51*, with an average of 37.65 with PAACd + Ta but without significant differences between PAACd and control. For the *CNCh13* genotype, an average of 14.64 was obtained with PAACd, with a significative difference from the control (Table 5). In the survival percentage, 83% was obtained with PAACd + Ta for *CNCh12*, 67% was obtained with PAACd for *CNCh13*, and 67% was obtained with PAACd and Ta for *CCN51* but without significative differences (Figure 3 S1).

Effects of AMF and P concentrations on survival and mycorrhizal infection

The phosphorus absorbance measurements recorded from known concentrations allowed the drawing of a standard calibration curve (Figure 4 S1), on which the phosphorus concentration in the substrate was determined. For the BS sample, an absorbance of 0.1139 was obtained, which corresponds to a concentration of 0.2651 mg/L of P.

The percentage of mycorrhizal infection in the treatments with 2g and 3g was significantly different from to control, with an average of 74% of condition for three phosphor concentrations (Figure 5). Survival of 100% of the plantlets was observed in the treatments of 2g AMF + 50% P and 3g AMF + 50% P, results that reveal the importance of phosphorus for the process of adaptation of cocoa plantlets to the *CCN51* genotype (Figure 5 S1).

Ana María Henao Ramírez, Julián David Morales Muñoz, Diana Marcela Vanegas Villa, Ruth Tatiana Hernández Hernández, Aura Inés Urrea-Trujillo
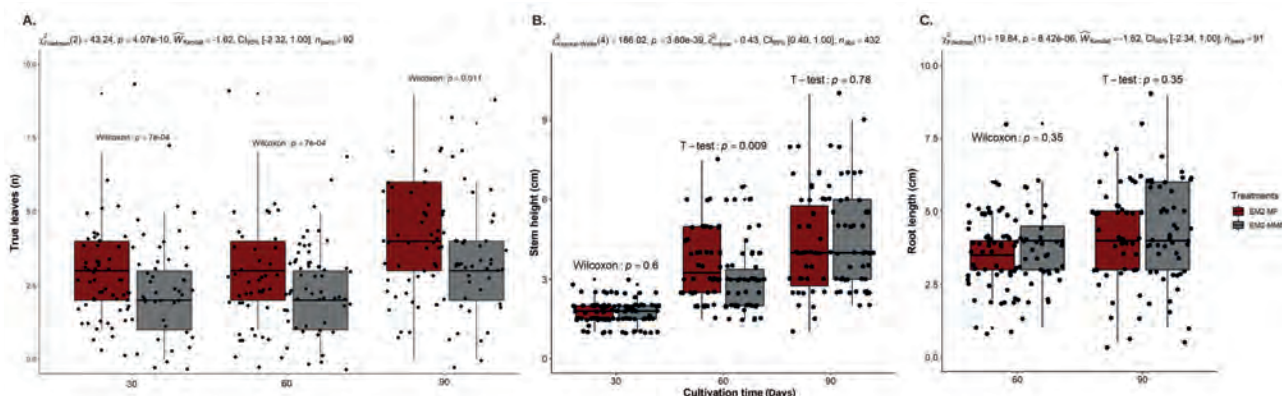
Figure 1. In the maturation stage of somatic embryogenesis development for the CCN51 genotype. Effects of culture media transition EM2-AMF and EM2-MM6 on (A) number of leaves (n) per plantlet at 30, 60, and 90 days of time cultivation, (B) height of stem (cm) at 30, 60 and 90 days of time cultivation and (C) root length (cm) at 60, and 90 days of time cultivation.
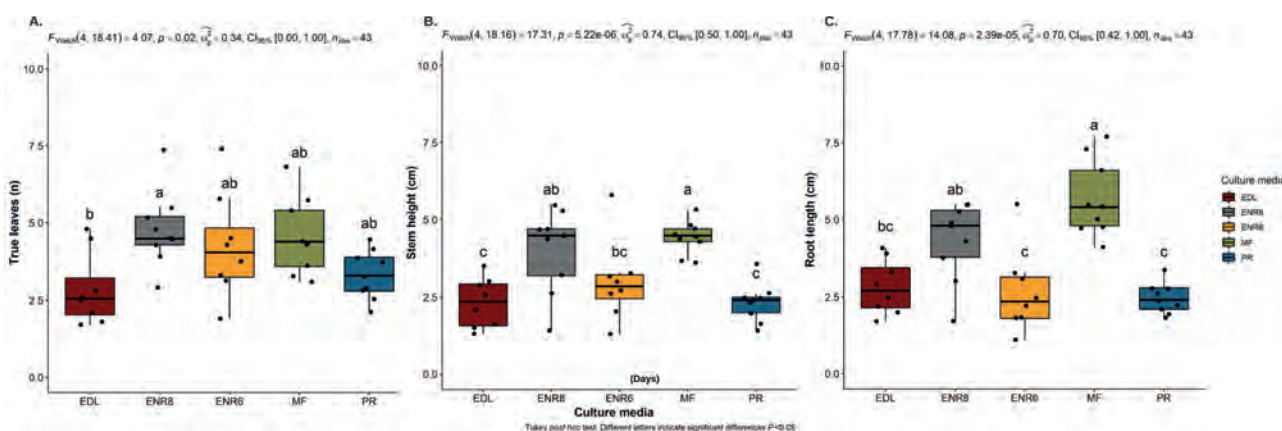
Figure 2. In the germination stage of somatic embryogenesis development for CCN51 genotype. Effects of culture media (ENR6, AMF, ENR8, EDL, PR) on (A) number of true leaves (n), (B) height stem (cm), (C) root length (cm).

Substrate	EC (mS/cm).	pH	EC (Tap water)	pH (Tap water)
BS in sowing	0.44	6.21	0.12	6.97
BS 30 days after sowing	0.27	6.35	0.14	6.33
BS + MO in sowing	2.13	6.01	0.09	6.67
BS + MO 30 days after sowing	2.34	5.95	0.08	6.28
BS + ½ MS	2.89	4.31		
BS + ½ DKW	3.28	4.21		

Table 3. Conductivity and pH results in basal substrate supplemented with organic matter and irrigation with ½ de MS and DKW macronutrients and micronutrients.

Discussion

Cacao somatic embryogenesis process is divided into six well-defined steps induction, expression, multiplication, maturation, germination, and plant conversion[44]. All these steps are mediated by a complex regulatory network where genetic and epigenetic mechanisms regulate different genes at the transcriptional level[45]. In this work, the acclimation process is addressed from the stage of embryo maturation. Conceptually, the developmental stages of the somatic and zygotic embryo are divided into two main metabolic stages; the first is a morphogenetic stage that is characterized by cell division and the onset of cell differentiation; the second is a metabolic stage or maturation phase that is characterized by biochemical activities, which involves the accumulation of significant storage products and the preparation for desiccation, dormancy, and germination/conversion[46,47]. In this last phase, somatic embryos achieve both morphological and physiological maturity, guaranteeing satisfactory post-embryonic performance. Therefore, the conversion potential is programmed during embryo maturation[48].

Embryo maturation

Better characteristics were obtained in the plants from embryo maturation in the transition between EM2-MF medium. The EM2 medium first reported by Fontanel *et al.* (2002)[36] has been effective for the maturation different researchers have often modified it according to the genotype of interest. On the other hand, the MF medium is a modification of the MM6 medium that was first reported by Fontanel *et al.* (2002)[36] and later modified by Henao *et al.* (2018)[35]. However, the MF medium has not been as widely used as the ED medium initially reported by (37), a medium without growth regulators for the maturation process. Both MF and MM6 medium have NAA and GA_3, a combination of growth

Stem height (cm)

Survival	Length	Min	Max	Median	Mean	ipr	Mad	sd	se	ci	range	cv	Var
Survive	33	1,7	6,0	4	3,98	2,6	2,07	1,42	0,24	0,50	4,3	0,35	2,03
Demise	101	1,0	8,5	3	3,34	2,0	1,48	1,66	0,16	0,32	7,5	0,49	2,73

Root length (cm)

Survival	Length	Min	Max	Median	Mean	ipr	Mad	sd	se	ci	range	cv	Var
Survive	33	1,5	14,0	6,2	6,71	3,0	1,77	2,79	0,48	0,99	12,5	0,41	7,82
Demise	101	0,3	15,2	4,5	5,02	3,2	2,22	2,53	0,25	0,50	14,9	0,50	6,44

Number of true leaves (n)

Survival	Length	Min	Max	Median	Mean	ipr	Mad	sd	se	ci	range	cv	Var
Survive	33	1	12	5	5,57	3	1,48	2,46	0,42	0,87	11	0,44	6,06
Demise	101	1	8	3	2,87	2	1,48	1,45	0,45	0,28	7	0,50	2,12

Length leaf (cm)

Survival	Length	Min	Max	Median	Mean	ipr	Mad	sd	se	ci	range	cv	Var
Survive	33	1,3	5,2	3,5	3,58	1,4	0,74	0,95	0,16	0,33	3,9	0,26	0,90
Demise	101	0,4	5,0	2,3	2,50	1,0	0,88	0,86	0,08	0,17	4,6	0,34	0,75

Width leaf (cm)

Survival	Length	Min	Max	Median	Mean	ipr	Mad	sd	se	ci	range	cv	Var
Survive	33	0,4	8	1,6	1,76	0,6	0,44	1,20	0,20	0,42	7,6	0,68	1,44
Demise	101	0,2	7	1,0	1,03	0,5	0,44	0,71	0,07	0,14	6,8	0,69	0,51

Table 4. Central tendency measures for minimum morphological quality characteristics of CCN51 in vitro-plantlets to continue ex vitro adaptation.
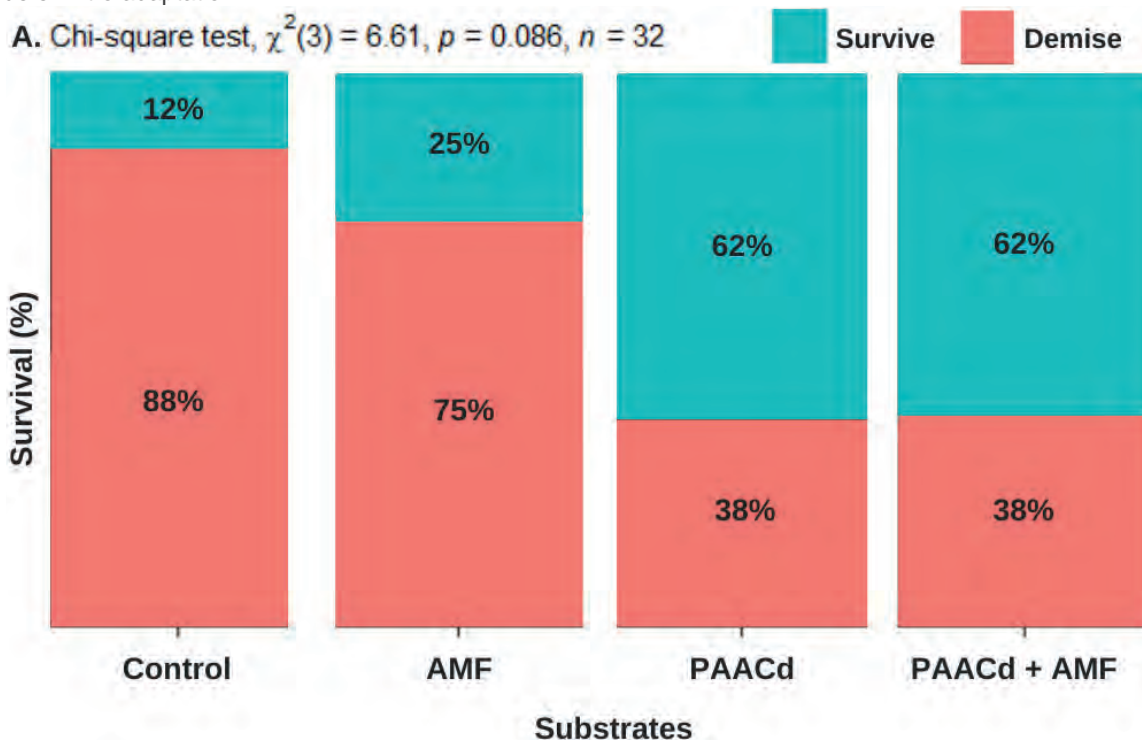
Figure 3. Effects of Pseudomonas ACC desaminase (PAACd), mycorrhizal fungi (AMF), and mix of Pseudomonas ACC desaminase (PAACd), mycorrhizal fungi (AMF) and control.

regulators suitable for different cocoa genotypes, such as *CCN51*.

Plantlet development

In the maturation of the embryo and the conversion to plantlet, the MF medium had the best results in the number of leaves and length of stem and root. The results obtained with the MF medium were like the results with the ENR8 medium. The ENR8 medium does not have the growth re-gulators NAA-GA$_3$; instead amino acids. The continuation of embryo development and conversion in the MF medium result from the effect of the NAA and GA3, activated carbon and other culture medium components, such as high concentrations of macroelements, especially nitrogen as NH$_4$NO$_3$ and high carbon concentrations like glucose. NAA and GA$_3$ have also been used by Iracheta *et al.* (2019)[50] to facilitate cotyledonary embryo development plus 3.7 µM of abscisic acid. Various authors have developed somatic

Ana María Henao Ramírez, Julián David Morales Muñoz, Diana Marcela Vanegas Villa, Ruth Tatiana Hernández Hernández, Aura Inés Urrea-Trujillo

Substrate	Leaf area (cm^2)		
	CNCh12	*CNCh13*	*CCN51*
PAACd + Ta	20,41 a	7,45 ab	37,65 a
Ta	10,90 ab	9,45 ab	9,88 b
PAACd	10,88 ab	14,64 a	14,70 ab
Control	6,16 b	4,87 b	14,92 ab

Tukey post hoc test. The values followed by the same letter within a column indicate that they are not significantly different ($p < 0.05$).

Table 5. Effects of Pseudomonas ACC deaminase (PAACd) and Trichoderma asperellum (Ta) on leaf area of regenerated plantlets for CNCh12, CNCh13, and CCN51 genotype.

Figure 4. In vitro plantlets of CCN51 in (A) EM2-AMF transition media during maturation stage; (B) Conversion to plantlet in MF culture media; (C) Transparent dome used for the first day of ex vitro adaptation process and holes for 15 days; (D) Experiment of beneficial microorganism Pseudomonas ACC desaminase (PAACd), mycorrhizal fungi (AMF) and Trichoderma asperellum (Ta) on survival and leaf area; Plantlets with pivotal and fibrous roots of (E) CNCh12 and (F) CNCh13; Cocoa seedling with adequate state of development and vigor with at least one month of ex vitro adaptation process ready to be transplanted from the bag (40cm h x 15 cm d).
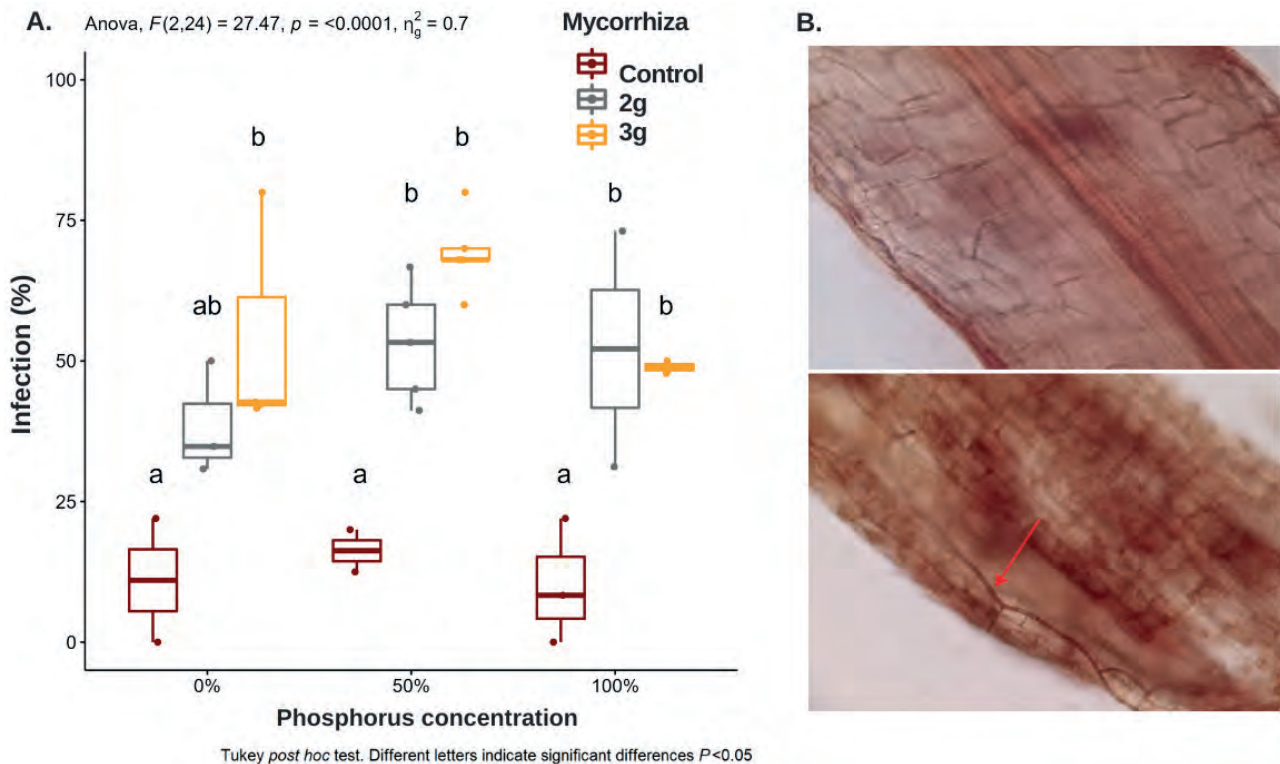
Tukey *post hoc* test. Different letters indicate significant differences $P < 0.05$

Figure 5. Effects of AMF (0g, 2g y 3g) and different concentrations of phosphorus (0%, 50% and 100%) in the Hoagland nutrient solution (1:10) on the percentage of infection. B. Above: the root of control plant without structures of mycorrhizal fungi. Under: plant root treated with 2g of AMF and Hoagland's solution with 50% P with hyphae traversing the root.

embryos in the culture medium with MS salts supplemented with NAA and GA$_3$[51]. In addition, GA$_3$ has also been used to elongate and produce embryos and plantlets in other species[52]. Furthermore, activated carbon can significantly affect embryo development because it can absorb substances, such as toxic metabolites and phenolic exudates, which inhibit the process, preventing correct maturation[53].

The biggest bottleneck in the embryogenic process is presented in the maturation and germination stage. Genotype plays a dominant role in somatic embryogenesis response and in the conversion rate of embryos 54. The embryo-to-plant conversion rate reached 20 to 40% with a very strong genotype dependency and high batch-to-batch variability[10,44,55].

Beneficial microorganisms

The inoculation with beneficial microorganisms improves the characteristics of the SE cocoa plants in the evaluated genotypes. With mycorrhizal fungi, better physiological characteristics were observed in the roots of the plantlets of the *CCN51*, *CNCh12* and *CNCh13* genotypes. Respect mycorrhizal fungi; they are known as a biostimulant and are anchored on their potential to increase plant nutrient uptake, improve plant resilience to drought, and reduce pesticides and inorganic fertilizers[33]. For abiotic stresses, the mechanisms of adaptation of mycorrhizal fungi to these stresses are generally linked to increased hydromineral nutrition, ion selectivity, gene regulation, production of osmolytes, an extension of the root absorbing area, and the synthesis of phytohormones and antioxidants. These benefits are influenced by its ability to colonize its host plant, a phenomenon that depends on the fungal genotype, the soil characteristics and the plant genotype[30].

For the *CCN51* genotype, using mycorrhizal fungi allows a better characteristic in root development was observed. This has been evidenced in other plants but directly in seeds with four selected microorganisms (*Pseudomonas chlororaphis* MA342, *P. fluorescens* CHA0, *Clonostachys pityriasis* IK726d11 and *Trichoderma harzianum* T22), generating a decrease in seedling mortality and stimulation of establishment[56]. Directly in cocoa plants at the greenhouse level, it was shown that inoculation with a mixture of microorganisms such as *Trichoderma sp.*, *Candida utilis* and *Pseudomonas putida* had better behavior in these plants compared to the control[57]. Also, in cocoa with *Trichoderma spp.* was possible to obtain a beneficial association, and the association could be a first step in developing of biocontrol strategies against diseases[58]. In another study, colonization of cocoa seedlings by the *Trichoderma hamatum* isolate DIS 219b was shown to enhance seedling growth, alter gene expression, and delay the onset of cocoa drought response in leaves at the molecular physiological and phenotypic level[58]. With the *Pseudomonas* ACC deaminase promoting plant growth from seed has been observed, specifically in the production of tomato roots[59]. Likewise, in cocoa, *Pseudomonas* ACC deaminase significantly affected on plant height, number of leaves, stem diameter, wet weight and dry weight of roots, number of roots, and root volume[60]. In the present study, different responses with each genotype were obtained; however, an improvement in survival was observed in the acclimation process for *CNCh12* y *CNCh13*, as well as in the *CCN51* genotype.

Furthermore, an improvement in plant height, number of leaves, and root length were observed. The results obtained for *CCN51* agree with other reports[61–63]. Chavez-Jalk *et al.* (2022)[62] used *T. harzianum* with a 100% colonization of the root hairs and trichomes on stems, and (65) used strains of Trichoderma and arbuscular mycorrhizal fungi ob-

Ana María Henao Ramírez, Julián David Morales Muñoz, Diana Marcela Vanegas Villa, Ruth Tatiana Hernández Hernández, Aura Inés Urrea-Trujillo

taining a higher yield of cocoa beans. This could be because Trichoderma has different auxin production mechanisms that, when entering into symbiosis with the root, improve the agronomic characteristics of the cocoa plant in such a way that when developing a greater amount of root, this has greater ease of absorption of the nutrients available in the soil; in addition, Trichoderma together with the microorganisms creates associations that help increase the rhizosphere of the soil, degrading the organic matter in less time and allowing the plants to extract the nutrients with a greater degree of assimilation[66,67]. On the other hand, the positive effects on plantlet development occur through the reduction of ethylene, a hormone that negatively affects root growth under biotic and abiotic stress[68,69].

Phosphate is the second essential nutrient required by plants, and its bioavailability is associated with increased plant growth[70]. Only a low percentage of this amount of P (15–30%) can be taken by plants, while the remaining part is converted into insoluble complexes[71]. Therefore, increasing P-use efficiency is a major challenge in intensive agricultural production systems. In this regard, using rock phosphate as substrates in P solubilization by microorganisms is a promising strategy[72]. This strategy aims to reduce P adsorption and precipitation by promoting P sources with a low solubility instead of soluble P sources[73]. The result showed that the survival of plantlets was more significant in the treatments with 2g and 3g of mycorrhiza and 50% phosphorus. Therefore, for the *CCN51* genotype, AMF can make an alternative to reduce phosphorus loss by improving P-use efficiency, plant health, and growth[74].

The concentration of P in the basal substrate was 0.2651 mg/L, and the concentration of P in the Hoagland solution negatively affected the plantlets' survival (Data not shown). However, when the concentration of P in the Hoagland solution was modified to half of KH_2PO_4 and the substrate was supplemented with mycorrhizae, the effect on plant growth and survival was positive. As described by Osorio (2012)[75], for correct AMF colonization in plant roots, the substrate must have a phosphorus (P) concentration of 0.02 mg/L, and low concentrations of 0.001-0.005 mg/L do not allow a response to the inoculation of AMF, while very high concentrations above 0.2 mg/L inhibit the effectiveness of the fungus. According to Quiñones *et al.* (2012)[76], the mechanism of the dose-effect on mycorrhizae is not precise. Still, it seems to depend on the interaction of the fungus and the plant species since different species of mycorrhizae are tolerant to high concentrations. The results of this study show that cocoa seedlings obtained by somatic embryogenesis inoculated with mycorrhizae were favored in terms of survival by phosphorus concentrations higher than 0.02 mg/L in the substrate, even requiring an additional supply of phosphorus in irrigation.

Based on the results obtained, it is proposed one possibility for the future is to carry out tests where plant defenses are reinforced by inoculating competent plant growth-promoting microorganisms from the *in vitro* phase to the *ex vitro* phase through a process called digitization[77]. These could act as biostimulants or biocontrol agents and help deal with biotic and abiotic stressors[78–80]. Finally, work on rhizosphere bacteria and fungi has already shown potential in managing various agricultural problems. Their use in the form of biofertilizers and biopesticides has resulted in a lesser reliance on synthetic agrochemicals[81].

Conclusions

In *ex vitro* adaptation processes of cocoa plantlets obtained by SE, the adequate physiological development of plantlets is essential in embryo maturation and conversion to plantlet. In the present work, it was possible to address critical factors affecting the growth of cocoa plantlets from ES *in vitro* to *ex vitro* transition. It was possible to establish efficient culture media for embryo maturation, plantlet conversion and development, as well as some parameters that affect development in *ex vitro* conditions. The culture of the embryos in the cotyledonary state in the EM2 and MF media, and with subsequent subculture in the MF medium, allows plants with prominent root development, stem elongation and leaf formation to continue to the greenhouse adaptation phase. The use of mycorrhizae in the *ex vitro* adaptation stage significantly improved the survival percentages, thus advancing the production process. It was found that, although the concentrations in the substrate were greater than 0.2 mg/L, a concentration reported as high and that can affect mycorrhizal infection, in the case of cocoa plantlets and the mycorrhizae used, there was no affectation in the infection for the mycorrhizae.

For this reason, it is recommended that for each genotype, it should be established how much phosphorus in the substrate and the irrigation solution affect mycorrhizal infection and plant growth. These results will help optimize beneficial microorganisms' use in SE plantlets production and the subsequent physiological performance of plants under nursery and open field conditions. Also, it is a significant starting point to carry out in other cacao genotypes, achieving increasing survival and contributing to the establishment of complete production protocols via ES.

Supplementary Materials

The following are available online at www.revistabionatura.com/xxx/s1, Figure 1 S1. Association of culture media transition EM2-AMF and EM2-MM6 (Secondary embryogenesis-maturation) and the fibrous root and tap root percentage in *CCN51* genotype plantlets, Table 1 S1 Effect of BS (Basal substrate) supplemented with MZ and OM on plant survival of *CCN51* genotype, Figure 2 S1. Effects of mycorrhizae (MZ) and organic matter (MO) increased in the percentage of BS substrate on white roots in *CCN51* genotype. Green: Survival, Pink: Demise. Figure 3 S1. Effects of Pseudomonas ACC deaminase (PAACd) and *Trichoderma asperellum* (Ta) supplemented in the substrate on survival (%). A. Effects on CNCh12 genotype. B. Effects CNCh13 genotype. C. Effects CCN51 genotype. Figure 4 S1. Figure 4. Standard calibration curve of phosphorus (P) measurement in the basal substrate (BS). Figure 5 S1. Figure 5. Effects of AMF (0g, 2g y 3g) and different concentrations of phosphorus (0%, 50% and 100%) in the Hoagland nutrient solution (1:10) on the percentage of survival.

Author Contributions

Conceptualization, Ana María Henao Ramírez and Aura Inés Urrea Trujillo; methodology and software, Julian David Morales Muñoz, Ruth Tatiana Hernández Hernández; validation and formal analysis, Juliam David Morales Muñoz, Ana María Henao Ramírez; investigation, resources, data curation, writing—original draft preparation, Ana María Henao Ramírez; writing—review and editing and supervision, Aura Inés Urrea Trujillo. All authors have read and agreed

to the published version of the manuscript.

Conflicts of Interest

The authors declare no conflict of interest.

Bibliographic references

1. Patalinghug M. Status of Cacao (Theobroma cacao L.) production on its challenges and prospect in Zamboanga del Norte Province in the Philippines. International Journal of Agricultural Technology. 2022;18(3).

2. Nair K. Cocoa (Theobroma cacao L.). In: Nair KP, ed. Tree Crops . Springer International Publishing; 2021:153-213. doi:10.1007/978-3-030-62140-7_5

3. Sayago-Ayerdi S, García-Martínez D, Ramírez-Castillo A, Ramírez-Concepción, H. Viuda-Martos M. Tropical Fruits and Their Co-Products as Bioactive Compounds and Their Health Effects: A Review. Foods. 2021;10(8). doi:10.3390/foods10081952

4. Cádiz-Gurrea M, Fernández-Ochoa A, Leyva-Jiménez F, et al. LC-MS and Spectrophotometric Approaches for Evaluation of Bioactive Compounds from Peru Cocoa By-Products for Commercial Applications. Molecules. 2020;25(14). doi:10.3390/molecules25143177

5. Ebuehi OAT, Anams C, Gbenle OD, Ajagun-Ogunleye MO. Hydro-ethanol seed extract of Theobroma cacao exhibits antioxidant activities and potential anticancer property. J Food Biochem. 2019;43(4):e12767. doi:https://doi.org/10.1111/jfbc.12767

6. Singh M, Agarwal S, Agarwal M, Rachana. Benefits of Theobroma cacao and Its Phytocompounds as Cosmeceuticals. In: Swamy MK, ed. Plant-Derived Bioactives. Springer Singapore; 2020:509-521. doi:10.1007/978-981-15-1761-7_21

7. Liaqat H, Parveen A, Kim SY. Neuroprotective Natural Products' Regulatory Effects on Depression via Gut–Brain Axis Targeting Tryptophan. Nutrients. 2022;14(16). doi:10.3390/nu14163270

8. Boriollo MFG, Alves VE, Silva TA, et al. Decrease of the DXR-induced genotoxicity and nongenotoxic effects of Theobroma cacao revealed by micronucleus assay. Brazilian Journal of Biology. 2021;81(2):268-277. doi:10.1590/1519-6984.223687

9. Méndez-Hernández HA, Ledezma-Rodríguez M, Avilez-Montalvo RN, et al. Signaling Overview of Plant Somatic Embryogenesis. Front Plant Sci. 2019;10. doi:10.3389/fpls.2019.00077

10. Guillou C. Theobroma cacao: Somatic Embryogenesis. In: Guillou C, Verdier D, eds. Somatic Embryogenesis. Vol 2527. ; 2022:69-81.

11. Garcia C, Marelli J, Motamayor J, Villela C. Somatic Embryogenesis in Theobroma cacao L. In: Loyola-Vargas V, Ochoa-Alejo N, eds. Plant Cell Culture Protocols, Methods in Molecular Biology. Vol 1815. Springer Science; 2018:227-245. doi:https://doi.org/10.1007/978-1-4939-8594-4_15

12. Henao-Ramírez A, Urrea-Trujillo A. Somatic Embryogenesis for Clonal Propagation and Associated Molecular Studies in Cacao (Theobroma cacao L.). In: Chong P, Newman D, eds. Agricultural, Forestry and Bioindustry Biotechnology and Biodiscovery. Springer, Cham; 2020:63-102. doi:https://doi.org/10.1007/978-3-030-51358-0_5

13. Garcia C, Corrêa F, Seth F, et al. Optimization of somatic embryogenesis procedure for commercial clones of Theobroma cacao L . Afr J Biotechnol. 2016;15(36):1936-1951. doi:10.5897/AJB2016.15513

14. Traore A. Somatic Embryogenesis, Embryo Conversion, Micropropagation and Factors Affecting Genetic Transformation. Pdf. Pennsylvania State University; 2000.

15. Manlé TE, Kouassi KM, Soumahoro BA, Koné T, Koffi KE, Koné M. Effect of water stress induced by polyethylene glycol 6000 on the somatic embryos conversion into whole plantlets in cocoa (Theobroma cacao L.). Int J Biol Chem Sci. 2021;15(1):12-25. doi:10.4314/ijbcs.v15i1.2

16. Goenaga R, Guiltinan M, Maximova S, Seguine E, Irizarry H. Yield performance and bean quality traits of cacao propagated by grafting and somatic embryo-derived cuttings. HortScience. 2015;50(3):358-362. doi:10.21273/hortsci.50.3.358

17. Pospisilova J, Synkova H, Haisel D, Semoradova S. Acclimation of plantlets to ex vitro conditions: effects of air humidity, irradiance, co2 concentration and abscisic acid. In: Acta Horticulturae. International Society for Horticultural Science (ISHS), Leuven, Belgium; 2007:29-38. doi:10.17660/ActaHortic.2007.748.2

18. Figueira A, Janick J. Somatic embryogenesis in cacao (Theobroma cacao L.). 1995;2:291-310.

19. Aguilar ME, Villalobos VM, Vasquez N. Production of cocoa plants (Theobroma cacao L.) via micrografting of somatic embryos. In Vitro Cellular & Developmental Biology - Plant. 1992;28(1):15-19. doi:10.1007/BF02632186

20. Jones J, Zhang E, Tucker D, et al. Screening of cultivars for tissue culture response and establishment of genetic transformation in a high-yielding and disease-resistant cultivar of Theobroma cacao. In Vitro Cellular and Developmental Biology - Plant. 2022;58(1):133-145. doi:10.1007/s11627-021-10205-0

21. Hazarika BN. Acclimatization of tissue-cultured plants. Curr Sci. Published online 2003:1704-1712.

22. Tarigan D, Siregar H, Utami S, Basyuni M, Novita A. Seedling Growth in Response to Cocoa (Theobroma cacao L.) for The Provision of Guano Fertilizer and Mycorrhizal Organic Fertilizer in the Nursery. Proceedings of the International Conference on Sustainable Agriculture and Natural Resources Management. 2018;(January):47-50.

23. Aggangan NS, Cortes AD, Reaño CE. Growth response of cacao (Theobroma cacao L.) plant as affected by bamboo biochar and arbuscular mycorrhizal fungi in sterilized and unsterilized soil. Biocatal Agric Biotechnol. 2019;22:101347. doi:https://doi.org/10.1016/j.bcab.2019.101347

24. Groppa MD, Benavides MP, Zawoznik MS. Root hydraulic conductance, aquaporins and plant growth promoting microorganisms: A revision. Applied Soil Ecology. 2012;61:247-254. doi:https://doi.org/10.1016/j.apsoil.2011.11.013

25. Balkrishna A, Sharma IP, Arya V, Sharma AK. Biologicals and their plant stress tolerance ability. Symbiosis. 2022;86(3):243-259. doi:10.1007/s13199-022-00842-3

26. Schmidt JE, DuVal A, Isaac ME, Hohmann P. At the roots of chocolate: understanding and optimizing the cacao root-associated microbiome for ecosystem services. A review. Agron Sustain Dev. 2022;42(2):14. doi:10.1007/s13593-021-00748-2

27. Mahendra R, Chauhan N, Sharma JB, Rana K, Bakshi M. Ex-vitro Establishment of Tissue Cultured plants in Fruit Crops-A Review. Int J Curr Microbiol Appl Sci. 2020;9(11):3321-3329. doi:10.20546/ijcmas.2020.911.397

28. Bailey BA, Strem MD, Wood D. Trichoderma species form endophytic associations within Theobroma cacao trichomes. Mycol Res. 2009;113(12):1365-1376. doi:https://doi.org/10.1016/j.mycres.2009.09.004

11

29. Song Z, Bi Y, Zhang J, Gong Y, Yang H. Arbuscular mycorrhizal fungi promote the growth of plants in the mining associated clay. Sci Rep. 2020;10(1):2663. doi:10.1038/s41598-020-59447-9

30. Diagne N, Ngom M, Djighaly PI, Fall D, Hocher V, Svistoonoff S. Roles of Arbuscular Mycorrhizal Fungi on Plant Growth and Performance: Importance in Biotic and Abiotic Stressed Regulation. Diversity (Basel). 2020;12(10). doi:10.3390/d12100370

31. Boubekri K, Soumare A, Mardad I, et al. The Screening of Potassium- and Phosphate-Solubilizing Actinobacteria and the Assessment of Their Ability to Promote Wheat Growth Parameters. Microorganisms. 2021;9(3). doi:10.3390/microorganisms9030470

32. Borden KA, Thomas SC, Isaac ME. Variation in fine root traits reveals nutrient-specific acquisition strategies in agroforestry systems. Plant Soil. 2020;453(1):139-151. doi:10.1007/s11104-019-04003-2

33. Snoeck D, Koko L, Joffre J, Bastide P, Jagoret P. Cacao Nutrition and Fertilization BT. In: Lichtfouse E, ed. Sustainable Agriculture Reviews. Springer International Publishing; 2016:155-202. doi:10.1007/978-3-319-26777-7_4

34. Jaimez RE, Barragan L, Fernández-Niño M, et al. Theobroma cacao L. cultivar CCN 51: a comprehensive review on origin, genetics, sensory properties, production dynamics, and physiological aspects. PeerJ. 2022;9:1-23. doi:10.7717/peerj.12676

35. Henao A, De-La-Hoz T, Ospina T, Atehortúa L, Urrea A. Evaluation of the potential of regeneration of different Colombian and commercial genotypes of cocoa (Theobroma cacao L .) via somatic embryogenesis. Sci Hortic. 2018;229:148-156. doi:10.1016/j.scienta.2017.10.040

36. Fontanel A, Gire S, Labbe G, et al. In vitro multiplication and plant regeneration of Theobroma cacao L. via stable embryogenic calli. IAPTC Congress, Plant Biotechnology 2002 and beyond. Published online 2002:23-28.

37. Li Z, Traore A, Maximova S, Guiltinan M. Somatic embryogenesis and plant regeneration from floral explants of cacao (Theobroma cacao L.) using thidiazuron. In vitro Cell Dev Biol. 1998;34:293-299. doi:https://doi.org/10.1007/BF02822737

38. McGranahan GH, Driver JA, Tulecke W. Tissue Culture of Juglans. In: J.M B, D.J. D, eds. Cell and Tissue Culture in Forestry. Springer, Dordrecht; 1987:232-248. doi:10.1007/978-94-017-0992-7

39. Murashige T, Skoog F. A revised medium for rapid growth and bio assays with tobacco tissue cultures. Physiol Plant. 1962;15(3):473-497.

40. Lloyd G, McCown B. Commercially-feasible micropropagation of mountain laurel, Kalmia latifolia, by use of shoot-tip culture. Commercially-feasible micropropagation of mountain laurel, Kalmia latifolia, by use of shoot-tip culture. 1980;30:421-427.

41. Guillou C, Fillodeau A, Brulard E, et al. Indirect somatic embryogenesis of Theobroma cacao L. in liquid medium and improvement of embryo-to-plantlet conversion rate. In Vitro Cellular and Developmental Biology - Plant. 2018;54(4):377-391. doi:10.1007/s11627-018-9909-y

42. Vargas JRN, Solis EC, Salgado MDO. Diagnóstico de la calidad del suelo y el agua en una parcela de cacao en Huehuetan, Chiapas, Mexico. In: Quinto Congreso Nacional de Riego y Drenaje. COMEII; 2019:1-12.

43. Barrezueta S. Construcción de Indicadores Agrarios Para Medir La Sostenibilidad de La Producción de Cacao En El Oro, Ecuador. Universidade Da Coruña; 2018.

44. Henao A, Palacio D, Urrea A. Cost Analysis of Cacao (Theobroma cacao L.) Plant Propagation through the Somatic Embryogenesis Method. Bionatura. 2022;7(2):1-13. doi:10.21931/rb/2022.07.02.2

45. Garcia C, Furtado de Almeida AA, Costa M, et al. Single-base resolution methylomes of somatic embryogenesis in Theobroma cacao L. reveal epigenome modifications associated with somatic embryo abnormalities. Sci Rep. 2022;12(1):15097. doi:10.1038/s41598-022-18035-9

46. Noah AM, Niemenak N, Sunderhaus S, et al. Comparative proteomic analysis of early somatic and zygotic embryogenesis in Theobroma cacao L. J Proteomics. 2013;78:123-133. doi:https://doi.org/10.1016/j.jprot.2012.11.007

47. Winkelmann T. Somatic Versus Zygotic Embryogenesis: Learning from Seeds BT - In Vitro Embryogenesis in Higher Plants. In: Germana MA, Lambardi M, eds. Springer New York; 2016:25-46. doi:10.1007/978-1-4939-3061-6_2

48. Juarez-Escobar J, Bojórquez-Velázquez E, Elizalde-Contreras, JM. Guerrero-Analco JA, Loyola-Vargas VM, Mata-Rosas M, Ruiz-May E. Current Proteomic and Metabolomic Knowledge of Zygotic and Somatic Embryogenesis in Plants. Int J Mol Sci. 2021;22(21). doi:10.3390/ijms222111807

49. Henao A, De-La-Hoz T, Ospina T, Garcés L, Urrea A. Evaluation of the potential of regeneration of different Colombian and commercial genotypes of cocoa (Theobroma cacao L.) via somatic embryogenesis. Sci Hortic. 2018;229:148–156. doi:10.1016/j.scienta.2017.10.040

50. Iracheta L, Cruz L, Lopez P, Avendaño C, Ortiz S. 2iP and brasinosteroids promote somatic embryogenesis induction in Theobroma cacao L. Agroproductividad. 2019;12(1):65-70. doi:https://doi.org/1010.32854/agrop.v0i0.1340

51. Urbanek A, Zechmann B, Müller M. Plant regeneration via somatic embryogenesis in Styrian pumpkin: Cytological and biochemical investigations. Plant Cell Tissue Organ Cult. 2004;79(3):329-340. doi:10.1007/s11240-004-5177-0

52. Kordestani G, Karami O. Picloram-induced somatic embryogenesis in leaves of strawberry (fragaria ananassa l.). Acta Biol Crac Ser Bot. 2008;50(1):69-72.

53. López A, Carreño J, Martínez A, Dabauza M. High embryogenic ability and plant regeneration of table grapevine cultivars (Vitis vinifera L.) induced by activated charcoal. Vitis - Journal of Grapevine Research. 2005;44(2):79-85.

54. Guillou C, Fillodeau A, Brulard E, et al. Nestlé Cocoa plan: Cocoa propagation by somatic embryogenesis. In: Park YS, Bonga JM, eds. Proceedings of the Third International Conference of the IUFRO on "Woody Plant Production Integrating Genetic and Vegetative Propagation Technologies ". Vol 1. IUFRO; 2015:75-80.

55. Osorio T, Henao A, de la Hoz T, Urrea A. Propagation of IMC67 Plants, Universal Cacao (Theobroma cacao L.) Rootstock via Somatic Embryogenesis. International Journal of Fruit Science. 2022;22(1):78-94. doi:10.1080/15538362.2021.2023067

56. Bennett AJ, Whipps JM. Beneficial microorganism survival on seed, roots and in rhizosphere soil following application to seed during drum priming. Biological control. 2008;44(3):349-361.

57. Cortes-Patiño S, Vesga-Ayala N, Sigarroa-Rieche A, Moreno-Rozo L, Cardenas-Caro D. Substrates inoculated with microorganisms for cocoa plants development (Theobroma cacao L.) during nursery stage. Bioagro. 2015;27:151-158.

58. Cortes-Patiño S, Vesga-Ayala N, Sigarroa-Rieche A, Moreno-Rozo L, Cardenas-Caro D. Substrates inoculated with microorganisms for cocoa plants development (Theobroma cacao L.) during nursery stage. Bioagro. 2015;27:151-158.

59. Orozco-Mosqueda Ma del C, Duan J, DiBernardo M, et al. The Production of ACC Deaminase and Trehalose by the Plant Growth Promoting Bacterium Pseudomonas sp. UW4 Synergistically Protect Tomato Plants Against Salt Stress. Front Microbiol. 2019;10. doi:10.3389/fmicb.2019.01392

60. Irawan T, Soelaksini L, Nuraisyah A. The growth response of cocoa (Theobroma cacao L.) growth with various concentrations of PGPR (Plant Growth Promoting Rhizobacteria) cocoa roots. Jurnal Ilmiah Hijau Cendekia. 2022;7(1):7-17. doi:10.32503/hijau.v7i1.2205

61. Cargua J, Echeverria C, Cedeño G. Effectiveness of biochar and biofertilizers in the growth and quality of cocoa seedlings. Revista ESPAMCIENCIA. 2020;11:95-100.

62. Chavez-Jalk A, Leiva S, Bobadilla LG, Vigo CN, Arce M, Oliva-Cruz M. Effect of Endophytic Trichoderma sp. Strains on the Agronomic Characteristics of Ecotypes of Theobroma cacao L. under Nursery Conditions in Peru. Gahlaut V, ed. International Journal of Agronomy. 2022;2022:5297706. doi:10.1155/2022/5297706

63. Irawan T, Soelaksini L, Nuraisyah A. The growth response of cocoa (Theobroma cacao L.) growth with various concentrations of PGPR (Plant Growth Promoting Rhizobacteria) cocoa roots. Jurnal Ilmiah Hijau Cendekia. 2022;7(1):7-17. doi:10.32503/hijau.v7i1.2205

64. Chavez-Jalk A, Leiva S, Bobadilla LG, Vigo CN, Arce M, Oliva-Cruz M. Effect of Endophytic Trichoderma sp. Strains on the Agronomic Characteristics of Ecotypes of Theobroma cacao L. under Nursery Conditions in Peru. Gahlaut V, ed. International Journal of Agronomy. 2022;2022:5297706. doi:10.1155/2022/5297706

65. Tuesta-Pinedo A, Trigozo-Bartra E, Cayotopa-Torres J, et al. Optimization of organic and inorganic fertilization cocoa (Theobroma cacao L.) with the inclusion of Trichoderma endophyte and arbuscular mycorrhizae. Revista Tecnologia en Marcha. 2017;30:67-78.

66. Naik K, Mishra S, Srichandan H, Singh PK, Sarangi PK. Plant growth promoting microbes: Potential link to sustainable agriculture and environment. Biocatal Agric Biotechnol. 2019;21:101326. doi:https://doi.org/10.1016/j.bcab.2019.101326

67. Hipólito-Romero E, Carcaño-Montiel MG, Ramos-Prado JM, Vázquez-Cabañas EA, López-Reyes L, Ricaño-Rodríguez J. [Effect of mixed edaphic bacterial inoculants in the early development of improved cocoa cultivars (Theobroma cacao L.) in a traditional agroforestry system of Oaxaca, Mexico]. Rev Argent Microbiol. 2017;49(4):356-365. doi:10.1016/j.ram.2017.04.003

68. Soumare A, Diédhiou AG, Arora NK, et al. Potential Role and Utilization of Plant Growth Promoting Microbes in Plant Tissue Culture. Front Microbiol. 2021;12. doi:10.3389/fmicb.2021.649878

69. Cortes AD, Opulencia RB, Aggangan NS. Characterization of plant growth promoting diazotrophic bacteria isolated from cacao (Theobroma cacao l.) rhizosphere treated with bamboo biochar and arbuscular mycorrhizal fungi. Philipp J Sci. 2020;149(4):1063-1070.

70. Fonseca AA, Santos DA, Passos RR, Andrade FV, Rangel OJP. Phosphorus availability and grass growth in biochar-modified acid soil: A study excluding the effects of soil pH. Soil Use Manag. 2020;36(4):714-725. doi:https://doi.org/10.1111/sum.12609

71. Singh H, Reddy MS. Effect of inoculation with phosphate solubilizing fungus on growth and nutrient uptake of wheat and maize plants fertilized with rock phosphate in alkaline soils. Eur J Soil Biol. 2011;47(1):30-34. doi:https://doi.org/10.1016/j.ejsobi.2010.10.005

72. Soumare A, Boubekri K, Lyamlouli K, Hafidi M, Ouhdouch Y, Kouisni L. From Isolation of Phosphate Solubilizing Microbes to Their Formulation and Use as Biofertilizers: Status and Needs. Front Bioeng Biotechnol. 2020;7. doi:10.3389/fbioe.2019.00425

73. Soltangheisi A, Santos VR dos, Franco HCJ, et al. Phosphate Sources and Filter Cake Amendment Affecting Sugarcane Yield and Soil Phosphorus Fractions. Rev Bras Cienc Solo. 2019;43. doi:10.1590/18069657rbcs20180227

74. Soumare A, Boubekri K, Lyamlouli K, Hafidi M, Ouhdouch Y, Kouisni L. Efficacy of phosphate solubilizing Actinobacteria to improve rock phosphate agronomic effectiveness and plant growth promotion. Rhizosphere. 2021;17:100284. doi:https://doi.org/10.1016/j.rhisph.2020.100284

75. Osorio W. Use of mycorrhiza-forming fungi as a biotechnological alternative to promote seedling nutrition and growth. Manejo Integral Suelo Nutr Veg. 2012;1(2):1-4.

76. Quiñones E, Hernández E, Rincon G, Ferrera R. Interaction of arbuscular mycorrhizal fungi and phosphate fertilization in papaya. Terra Latinoam . 2012;30(2).

77. Kanani P, Modi A, Kumar A. Biotization of endophytes in micropropagation: A helpful enemy. In: Kumar A, Singh VKBTME, eds. Woodhead Publishing Series in Food Science, Technology and Nutrition. Woodhead Publishing; 2020:357-379. doi:https://doi.org/10.1016/B978-0-12-818734-0.00015-2

78. Hamid B, Zaman M, Farooq S, et al. Bacterial Plant Biostimulants: A Sustainable Way towards Improving Growth, Productivity, and Health of Crops. Sustainability. 2021;13(5). doi:10.3390/su13052856

79. Cataldo E, Fucile M, Mattii GB. Biostimulants in Viticulture: A Sustainable Approach against Biotic and Abiotic Stresses. Plants. 2022;11(2). doi:10.3390/plants11020162

80. Dubey A, Kumar A, Khan ML. Role of Biostimulants for Enhancing Abiotic Stress Tolerance in Fabaceae Plants BT - The Plant Family Fabaceae: Biology and Physiological Responses to Environmental Stresses. In: Hasanuzzaman M, Araújo S, Gill SS, eds. Springer Singapore; 2020:223-236. doi:10.1007/978-981-15-4752-2_8

81. Mishra J, Singh R, Arora NK. Plant Growth-Promoting Microbes: Diverse Roles in Agriculture and Environmental Sustainability BT - Probiotics and Plant Health. In: Kumar V, Kumar M, Sharma S, Prasad R, eds. Springer Singapore; 2017:71-111. doi:10.1007/978-981-10-3473-2_4

ARTICLE / INVESTIGACIÓN

Condiciones óptimas de extracción de compuestos antioxidante del alga roja *Acanthophora spicifera*

Optimal conditions for the extraction of antioxidant compounds from the red alga *Acanthophora spicifera*

Arianna Valdez N[1]*, Iván Choez[2], Sofie Van Der Hende[3], Omar Ruìz[4], Patricia Manzano[2]

[1] ESPOL Polytechnic University, Facultad de Ciencias de la Vida (FCV), Campus Gustavo Galindo, Guayaquil, Ecuador.
[2] ESPOL Polytechnic University, Centro de Investigaciones Biotecnológicas del Ecuador (CIBE), Campus Gustavo Galindo, Guayaquil, Ecuador.
[3] ESPOL Polytechnic University, Centro Nacional de Acuicultura e Investigaciones Marinas (CENAIM), Campus Gustavo Galindo, Guayaquil, Ecuador.
[4] ESPOL Polytechnic University, Facultad de Ciencias Naturales y Matemáticas (FCNM), Campus Gustavo Galindo, Guayaquil, Ecuador.
Corresponding author: alvaldez@espol.edu.ec

1

Resumen: La *Acanthophora spicifera* un alga roja de fácil adaptación a diferentes condiciones ambientales, por su capacidad de regenerarse por fragmentación, convirtiéndola en una especie invasora en áreas tropicales y subtropicales. Además, es conocida por sus componentes bioactivos (antioxidantes, fitohormonas, fitopigmentos). En este estudio se plantea determinar las condiciones óptimas de extracción de compuestos antioxidantes de la macroalga que crece en la zona intermareal de la playa de San Pedro de la provincia de Santa Elena, en dos procesos de secado (horno y liofilización) y extracción etanólica (digestión y ultrasonido) a diferentes concentraciones de etanol (50% y 70%) en rangos de tiempo y temperatura para su posterior determinación de actividad antioxidante por los métodos DPPH, ABTS, fenoles, flavonoides y auxinas totales en microplacas. Los datos se analizaron mediante análisis de varianza (ANOVA) usando el software estadístico R.4.2.0 e InfoStat, observan que los mejores resultados se dieron por digestión con una concentración de etanol al 50% y se obtuvieron valores para: la actividad captadora de radicales DPPH 3.65±0.011 μmol ET/g ps, mayor actividad inhibidora del radical catiónico ABTS 14.06±0.03 μmol ET/g ps, para flavonoides 1278.58±2.94 μg EQ/g ps, para fenoles 900±0.129 μg GEA/g ps. Las condiciones óptimas para la extracción etanolica de la macroalga *A. spicifera*., fueron 47 °C y 47 minutos para la actividad captadora de radicales DPPH y 47 °C y 39 minutos para la actividad inhibidora del radical catiónico ABTS, 45 °C y 37 minutos para Fenoles totales y 43 °C y 38 minutos para Flavonoides totales.

Palabras clave: Actividad antioxidante, *Acanthophora spicifera*, optimización.

Abstract: *Acanthophora spicifera* is a red seaweed that is easily adapted to different environmental conditions due to its ability to regenerate by fragmentation, making it an invasive species in tropical and subtropical areas. In addition, it is known for its bioactive components (antioxidants, phytohormones, and phytopigments). This study proposes to determine the optimal conditions for extracting antioxidant compounds from the macroalgae that grow in the intertidal zone of San Pedro beach in the province of Santa Elena, in two drying processes (oven and freeze-drying) and ethanolic extraction (digestion and ultrasound) at different ethanol concentrations (50% and 70%) in time and temperature ranges for subsequent determination of antioxidant activity by the DPPH, ABTS, phenols, flavonoids, and total auxin methods in microplates. . The data were analyzed by analysis of variance (ANOVA) using the statistical software R.4.2.0 and InfoStat, they observe that the best results were given by digestion with a 50% ethanol concentration and values were obtained for: activity radical scavenger DPPH 3.65±0.011 μmol ET/g d.w., higher cationic radical inhibitory activity ABTS 14.06±0.03 μmol ET/g d.w., for flavonoids 1278.58±2.94 μg EQ/g d.w., for phenols 900±0.129 μg GEA/g d.w. The optimal conditions for the ethanolic extraction of the macroalga *A. spicifera* were 47 °C and 47 minutes for the DPPH radical scavenging activity and 47 °C and 39 minutes for the ABTS cationic radical inhibitor activity, 45 °C and 37 minutes for total phenols and 43 °C and 38 minutes for total flavonoids.

Key words: Antioxidant activity, *Acanthophora spicifera*, optimization.

Introducción

La *Acanthophora spicifera* es un alga roja ampliamente distribuida en mares subtropicales y tropicales y se encuentra en muchos hábitats intermareales y submareales. Está distribuida desde los arrecifes poco profundos hasta profundidades de hasta 17m reportado en Puerto Rico y 22m en las Islas Vírgenes[1], esta macroalga se la considera como una especie invasora en las islas del Pacífico central y en lugares como Hawaii es la principal invasora[2], esto se debe a su estrategia reproductiva sexual como asexual, la capacidad de regenerarse por fragmentación y que se adapta fácilmente a diversas condiciones ambientales por lo que representa una amenaza para su nuevo ecosistema[3,4]. A lo largo de diversos estudios se ha encontrados que posee diversas propiedades en como bioindicador de

Publisher's Note: Bionatura stays neutral with regard to jurisdictional claims in published maps and institutional affiliations.

enriquecimiento de nutrientes, también se ha documentado que es un buen productor de oxígenos y como materia prima para la producción de biocombustible por su alto contenido en lignina[2].

Los principales antioxidantes encontrados en las algas marinas son compuestos fenólicos y pigmentos fotosintéticos (clorofilas, carotenoides y ficobiliproteínas), que también son conocidos por sus actividades biológicas (anticancerígenas, antiinflamatorias, antiobesidad y antiangiogénicas)[5]. Sin embargo, tanto los compuestos fenólicos como los pigmentos son susceptibles a la oxidación, especialmente a altas temperaturas[6]. Además, las algas marinas se consideran una fuente alternativa de proteínas, carbohidratos, ácidos grasos y minerales, que pueden sufrir degradación a temperaturas elevadas y pérdida de agua, el uso de algas marinas como ingrediente en la industria alimentaria a menudo requiere que se deshidrate antes de su uso[7], ya que el secado inhibe la actividad microbiológica y ralentiza o detiene las reacciones químicas que causan el deterioro de los alimentos (es decir, oxidación o reducción), prolongando así la vida útil[7,8] y ayuda a la extracción de ciertos componentes químicos[9].

Los procesos de secado más comunes utilizados para las algas marinas son: el secado al sol, el secado al horno y la liofilización[10], el procesamiento de cada método puede cambiar la composición química y las propiedades antioxidantes de las algas destinadas a ser utilizadas como bioproductos funcionales para alimentos y piensos (alimento para el ganado), aplicaciones cosméticas, farmacéuticas e industriales[11,12]. Si bien existen diferentes técnicas de secado disponibles, varios factores como el costo, el consumo de energía, la efectividad y el impacto en la calidad de los alimentos deben tenerse en cuenta al seleccionar el método más apropiado[13,14].

Sin embargo, cuando se seca al sol, las algas marinas se exponen al aire libre a la luz solar directa, donde hay una gran oportunidad de contaminación en el aire (es decir, con partículas, microbios, etc.) que luego pueden afectar la calidad e higiene del producto final[15]. Diferentes estudios han demostrado el valor de selección de tratamientos de secado apropiados para preservar compuestos bioactivos importantes de las algas destinadas a diferentes procesos[16], aunque existen pocos estudios que describan los efectos de los procesos de secado en los extractos de algas marinas[17], el interés en este tema ha aumentado en los últimos años[18,19].

El objetivo de este estudio fue determinar las condiciones óptimas de extracción de compuestos antioxidantes del alga roja *A. spicifera* empleando diferentes métodos de secado para preservar la calidad de los biocomponentes del producto final, Las muestras secas se extrajeron mediante dos métodos diferentes (digestión y extracción asistida por ultrasonido) utilizando etanol a diferentes concentraciones.

Materiales y métodos

Los productos químios que se utilizaron eran de grado analítico y se obtuvieron de Sigma-Aldrich.

Material de alga y metodos de secado

La macroalga *A. spicifera*, se cosecho en la playa de San Pecdro de Manglralto de la provincia de Santa Elena en el mes de enero del 2021. Las algas cosechadas se lavaron con agua potable para eliminar las epifitas y luego se las dividieron en grupos para probar el efecto de diferentes métodos de secado sobre la actividad antioxidante, los compuestos fenolicos y polifenoles.

Las algas se secaron de la suiguiente manera: se secaron al horno de estufa ventilada por 36 h a 45°C y secado por liofilización por durante 60 h, despues todas las muestras se molieron durante 1 minuto en un molino de alta velocidad.

Extracciones

Las muestras de algas se extrajeron con etanol al 50% y etanol al 70% utilizando dos métodos de extracción, colocando la muestra de alga seca y el solvente en una relación 1:15, se aplico los siguientes metodos de extracción: digestión a 40, 45 y 50 °C durante 30, 40 y 50 minutos; y extracción asistida por ultrasonido (UEA) a 40kHz de frecuencia a temperatura ambiente durante 10,20 y 30 minutos. Despues de las extracciones, la muestras se centrifugaron a 12000 rpm durante 10 min a 4 °C. Todos los extractos se mantuvieron en congelación a -4°C antes de los análisis. Cada extracción se lo realizó por duplicado.

Actividad antiódiante

La actividad antioxidante de los extractos de *A. spicifera* se evaluo mediante dos métodos diferentes: DPPH (1,1-difenil-2-picrilhidrazilo) y ABTS (Ácido 2, 2'-azino-bis(3-etilbenzotiazolín)-6-sulfónico).

Se midió la capacidad de captación de radicales libres DPPH de los extractos descrita por Viteri *et al.*,2021[20] en una placa de 96 posillos, después de 30 minutos de incubación en oscuridad se midió la absorbancia a 517 ŋm usando un Lector multi-modal Synergy HTX con detector UV-VIS (Biotek).

Se midio la actividad inhibidora del radical catiónico ABTS de los extractos descrita por Viteri *et al.*,2021[20] en una placa de 96 posillos, se incubo durante 30 min y se midió la absorbancia en una longitud de onda de 732 ŋm. Los resultados de la actividad antioxidante fueron expresados como µmol equivalentes de Trolox por gramo de peso seco (µmol TE). Se utilizaron concentraciones de Trolox entre (10 - 200 µmol/L) para DPPH y ABTS.

Composición fenólica

Los extractos obtenidos se analizaron para contenido fenólico total (TPC) y contenido total de flavonoides (TFC)

Para el TPC de los extractos de *A. spicifera* se realizó el método colorimétrico Folin-Ciocalteu empleado por Zhong *et al.*,2020[21]. Se agregó 25 µL de muestra, 25 µL de solución folin al 25% (v/v) y 200 µL de agua destilada en los pocillos de una placa de 96 pocillos y se incubaron durante 5 min a 25°C. Posteriormente se agregó 25 µL de carbonato de sodio al 10% (p/p) y dejando incubar durante 1 hora a 25°C. La absorbancia se midió a 765 ŋm en un espectrofotómetro UV-160A (Shimadzu). En la curva de calibración estándar (10 - 250 µmol/L) se utilizó ácido gálico (y = 0,0041x + 0,029,R² = 0,9952) y los resultados se presentaron en mg equivalentes de ácido gálico (GAE) por gramo de extracto seco (mg GAE/g).

Los TFC de los extractos de *A. spicifera* se realizó el método colorimétrico del cloruro de aluminio como lo describe Avramova *et al.*,2017[22]. En una placa de 96 pocillos se reaccionó 20 µL de muestra y 200 µL de una mezcla de reactivos en donde se utilizó 60 µL de etanol, 10 µL de cloruro de aluminio al 10% (w/v), 10 µL de acetato de potasio al 1M y 120 µL de agua destilada, dejando incubar

a temperatura ambiente durante 30 min para su posterior lectura a una absorbancia de 415 ηm usando un Lector multi-modal Synergy HTX con detector UV-VIS (Biotek). La medición se comparó con una curva de calibración (10 - 100 µmol/L) preparada con soluciones de catequina (y = 0,006x - 0,0249, R² = 0,9979) y el resultado se expresó en µg equivalentes de catequina (CE) por gramo de extracto seco[23].

Análisis estadistico

Las diferencias significativas entre los tratamientos fueron determinados estadísticamente utilizado, un análisis de desviación estándar y un análisis de matriz de dispersión para tipo de secado (X_1), concentración de Etanol (X_2), tipo de extracción (X_3), con estas nuevas condiciones se realizó el análisis de superficie de respuesta analizando el efecto de las variables de temperatura (X_4) y tiempo (X_5) de extracción sobre las variables de la actividad captadora de radicales DPPH (Y_1), la actividad inhibidora del radical catiónico ABTS (Y_2), de los y el contenido de fenoles totales (Y_3), el contenido de flavonoides totales (Y_4) respectivamente para todo el proceso estadístico se emplearon los softwares estadísticos Rstudio e InfoStat obteniendo el los modelos matemáticos, gráficas y la verificación de los valores óptimos.

Resultados

Actividad Antioxidante

La actividad antioxidante se determinó utilizando los ensayos DPPH y ABTS y los resultados se muestra en las figuras 1 y 2 Los valores de DPPH en los extractos de *A. spicifera* oscilaron entre 0,171±0,06 y 3,651±0,61 µmol TE. Las muestras secadas al horno con etanol al 50% tubieron valores mas altos para todos los métodos de extracción. Al utilizar etanol al 70% en muestras liofilizadas se tubieron un DPPH mas bajo que en las muestras secadas al horno. El secado al horno muestra ser un mejor metodo de secado para obtener extractos con alta actividad captadora de radicales libres.

Al comparar los metodos de extracción una mayor actividad captadora de radicales libres se obtuvo en el método de digestión teniendo valores altos entre 3,240±0.01 y 3,651±0,61 µmol TE, en cuanto al metodo UEA se obtuvo dos valores altos; 3,151±0.12 y 3,478±0,01 µmol TE con un tiempo de 20 y 30 min respectivamente.

Los extractos de *A. spicifera* mostraron una actividad inhibidora de radical cationico, ABTS, entre 4,645±0,08 y 14,033±0,04 µmol TE. Al igual que en el ensayo de DPPH las muestras secadas al horno tratadas con etanol al 50% se evidenció valores altos en todos los métodos de extracción, los valores mas altos se obtuvieron con el metodo de digestión a 45°C y 30 min. Con el método UEA tambien se obtivieron valores altos en la muestra liofilizada durante 10 min (11,445±0,05 µmol TE) y secada al horno durante 30 min (13,845±0,11 µmol TE).

Composición fenólica

Los resultados de TPC y TFC para extractos de *A. spicifera* se muestran en la tabla 2. El TPC de A. specifera osciló entre 0,109±0.01 y 0,941±0.01 mg GAE /g p.s., los extractos liofilizados tuvieron un TPC mas altos en comparación con secado al horno, en algunos casos las muestra liofilizadas eran dos veces mas TPC que las muestras secadas al horno. Los resultados mostrano que el metodo de secado por liofilización fue el mejor metodo para conservar TPC en materia de algas.

Comparando los solventes en extracción en muestras liofilizadas, las que se extrajeron con etanol al 50% se obtuvo TPC mas altos que las extraidas con etanol al 70%. El TPC mas alto se encontró en la muestra extraida por digestión con temperatura de 40°C y 40 minutos en etanol al 50% (0,941±0,01 mg GAE /g p.s). Las muestras liofilizadas extraidas con etanol al 70% tubieron los resultados mas bajos para todos los métodos de extracción. El TPC mas alto entre las muestras secadas al horno fueron los extractos preparados con etanol al 50% utilizando EAU durante 30 minutos (0,834±0,05 mg GAE /g p.s).

El TFC de *A. specifera* osciló entre 73,778±5,67 y 1281,083±3,53 ug QE/g p.s., los extractos liofilizados tuvieron un TFC mas altos en comparación con secado al
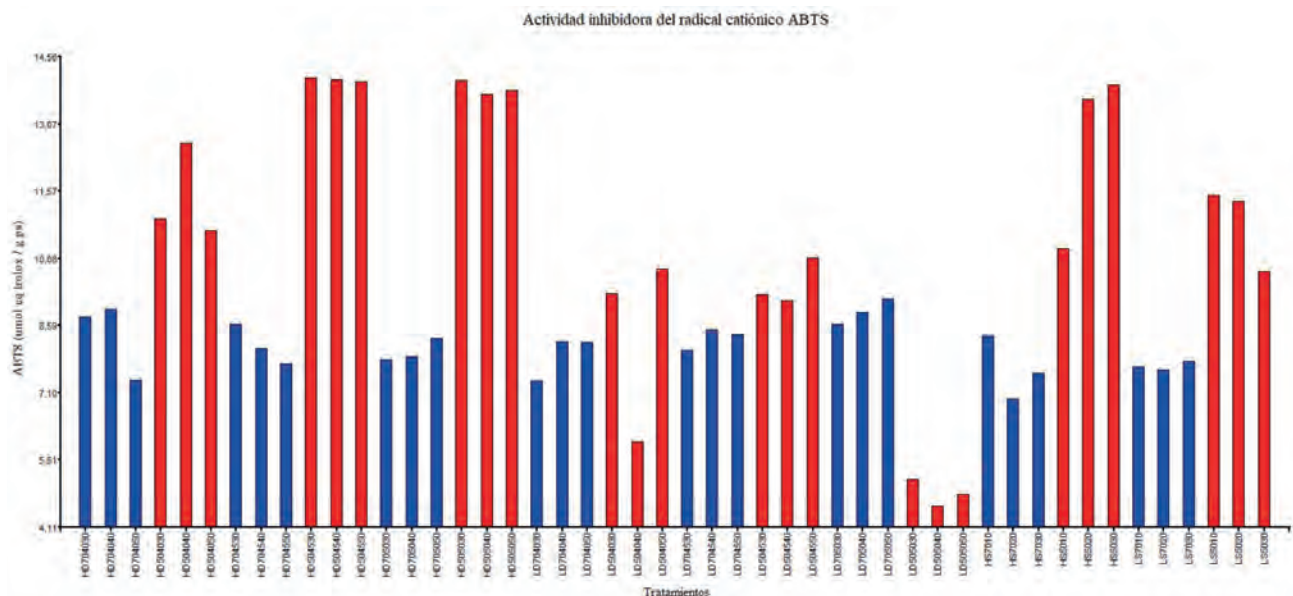
Figura 1. Actividad captadora de radicales libres - DPPH de los extractos de *A. spicifera*: tipo de secado: secado al horno (H), lifilizado (L); extracción: digestión (D), extracción asistida por ultrasonido (S); solvente: etanol 70% (70-azul), etanol 50% (50-rojo); temperatura: 40, 45 y 50; tiempo: 10, 20, 30, 40, 50.

Arianna Valdez N, Iván Choez, Sofie Van Der Hende, Omar Ruìz, Patricia Manzano
Volume 8 / Issue 1 / 11   •   http://www.revistabionatura.com
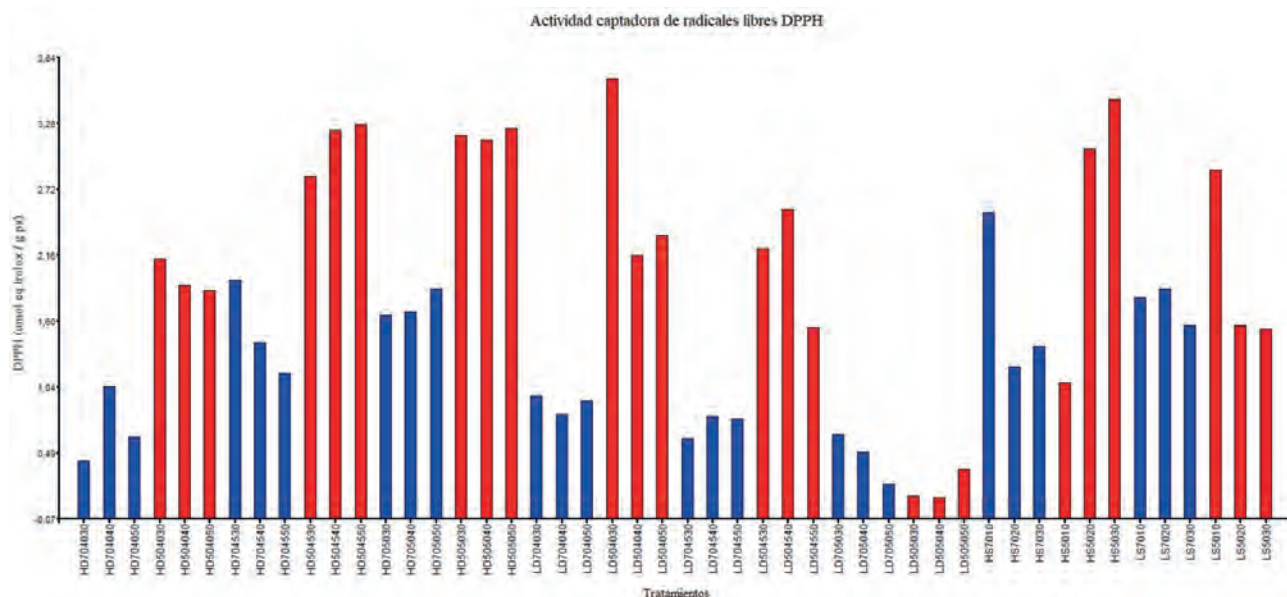
Figura 2. Actividad inhibidora del radical cationico - ABTS de los extractos de *A. spicifera*: tipo de secado: secado al horno (H), lifilizado (L); extracción: digestión (D), extracción asistida por ultrasonido (S); solvente: etanol 70% (70-azul), etanol 50% (50-rojo); temperatura: 40, 45 y 50; tiempo: 10, 20, 30, 40, 50.

horno, en algunos casos las muestra liofilizadas era entre tres y seis veces mas que las muestras secadas al horno. Los resultados obtenidos en el secado por liofilización fue el mejor metodo para conservar TFC en materia de algas.

Se pudo observar una diferencia significativa en la extracción en muestras liofilizadas, las que se extrajeron con etanol al 50% se obtuvo TFC mas altos que las extraidas con etanol al 70%. El valor mas alto de TFC se obtivo en la muestra extraida por digestión con temperatura de 50°C y 30 minutos en etanol al 50% (1281,083±3,53 ug QE /g p.s). Las muestras liofilizadas extraidas con etanol al 70% tubieron los resultados mas bajos para todos los métodos de extracción. El TFC mas alto entre las muestras secadas al horno fue el extracto preparados con etanol al 70% utilizando digestión a una temperatura de 40°C y 40 minutos (504,577±5,75 mg GAE /g p.s).

Encuanto al metodo EAU los valores mas altos fueron con secado por liofilización durante 30 minutos con etanol al 70% (307,994±1,57 ug QE /g p.s.), mientras que el mas bajo se obtuvo con etanol al 70% durante 20 minutos.

Optimización

El análisis de superficie de respuesta se ha obtenido de los datos experimentales donde el análisis con la matriz de dispersión indica que el tiempo y temperatura de extracción tuvieron un efecto cuadrático sobre la actividad captadora de radicales DPPH y su influencia la vemos reflejada en la ecuación (1).

El análisis de superficie de respuesta de los contenido de fenoles totales (TPC) y contenido de flavonoides totales (TFC) de los extractos de *A. spicifera* obtenido de los datos experimentales que se muestran en la Tabla 1, demostró que los parámetros de extracción ejercieron un efecto cuadrático sobre el contenido de fenoles totales. El efecto de la temperatura y el tiempo de extracción sobre el contenido

de fenoles totales se muestra en la ecuación (3) a continuación:

Para el contenido flavonoides totales se demostró que los parámetros de extracción ejercieron un efecto cuadrático, el efecto de la temperatura y el tiempo de extracción sobre el contenido de fenoles totales se muestra en la ecuación (4).

Discusión

Los resultados obtenidos al compáralo con otros estudios con diferentes métodos de extracción con la misma alga *A. spicifera* podemos observar que existe una diferencia entre el alga que crece en Ecuador con la que crece en la India en el caso del % DPPH se obtuvo un 19.29±0.011 en comparación con 6.91±0.42 que tiene un proceso de extracción por maceración por 24 h con metanol al 98%[25]. En cuanto a fenoles totales se extrajo 60.24±0.129 µg GAE /mL mientras que en estudio de Murugan *et al.* 2014 nos indica que obtuvo 0.87±0.10 µg GAE /mL con una extracción con metanol al 98% y 0.24±0,08 µg/mL GAE con una extracción con agua, así mismo se reporta que obtuvieron 25.7±0.6 µg QE /mL en extracción con metanol al 98% mientras que en la extracción con agua reportaron 8,5±0,4 µg QE /mL en la extracción de flavonoides totales[24], comparado con la extracción que se realizó con etanol al 50% que fue de 85.41±3.53 µg QE /mL.

Conclusiones

Los resultados de este estudio contribuyen a la caracterización del alga roja *A. spicifera* como una matriz que puede producir componentes con potencial antioxidantes.

$$Y_1 = -34.3818 + 1.4821X_4 + 0.1038X_5 - 0.0159X_4^2 - 0.00141X_5^2 + 0.00064X_4X_5 \qquad (1)$$

$$Y_2 = -1.1114e^2 + 4.9559X_4 + 4.6452e^{-1}X_5 - 5.2545e^{-2}X_4^2 - 5.8668e^{-3}X_5^2 - 1.3868e^{-4}X_4X_5 \qquad (2)$$

$$Y_3 = 25.18 - 1.2203X_4 + 0.13414X_5 + 0.01362X_4^2 - 0.00191X_5^2 + 0.00021X_4X_5 \qquad (3)$$

$$Y_4 = 41444.13 - 1959.31X_4 + 52.7118X_5 + 22.3916X_4^2 - 1.1625X_5^2 + 0.8104X_4X_5 \qquad (4)$$

Con el análisis de superficie de respuesta se obtuvo las condiciones temperatura y tiempo óptimo de extracción a 47 °C y 47 minutos para la actividad captadora de radicales libres DPPH, para la actividad inhibidora del radical catiónico ABTS 47 °C y 39 minutos, para fenoles totales 45 °C y 37 minutos y en flavonoides totales 43 °C y 38 minutos en los extractos etanolicos al 50%.

La Acanthophora spicifera que crece en Ecuador se extrajo una mayor cantidad de fenoles y flavonoides (60.24±0.129 µg GAE /mL y 85.41±3.53 µg QE /mL) en comparación con la que crece en India (0.87±0.10 µg GAE /mL y 25.7±0.6 µg QE /mL).

Los resultados obtenidos de este estudio muestran que *A. spicifera* debería tener una buena actividad antioxidante a pesar de un TPC relativamente bajo, pero se deben realizar más análisis para identificar el perfil fenólico de los extractos, el efecto estacional sobre el contenido fitoquímico, así como su potencial biológico.

Contribuciones de los autores

Conceptualización, Patricia Manzano, PhD; metodología, Ing. Qco Arianna Valdez, e Ing. Qco Ivan Choez; software, Omar Ruiz, PhD ; validación, Ing. Qco Ivan Choez; investigación, Ing. Qco Arianna Valdez; recursos, Sofie Van

5
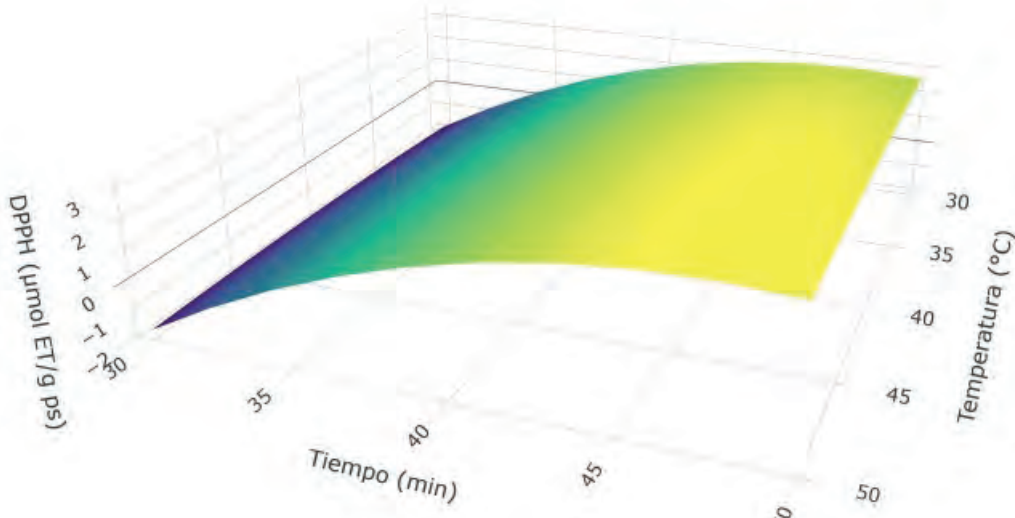
Figura 3. Efecto de la temperatura y el tiempo de extracción sobre la actividad captadora de radicales DPPH.
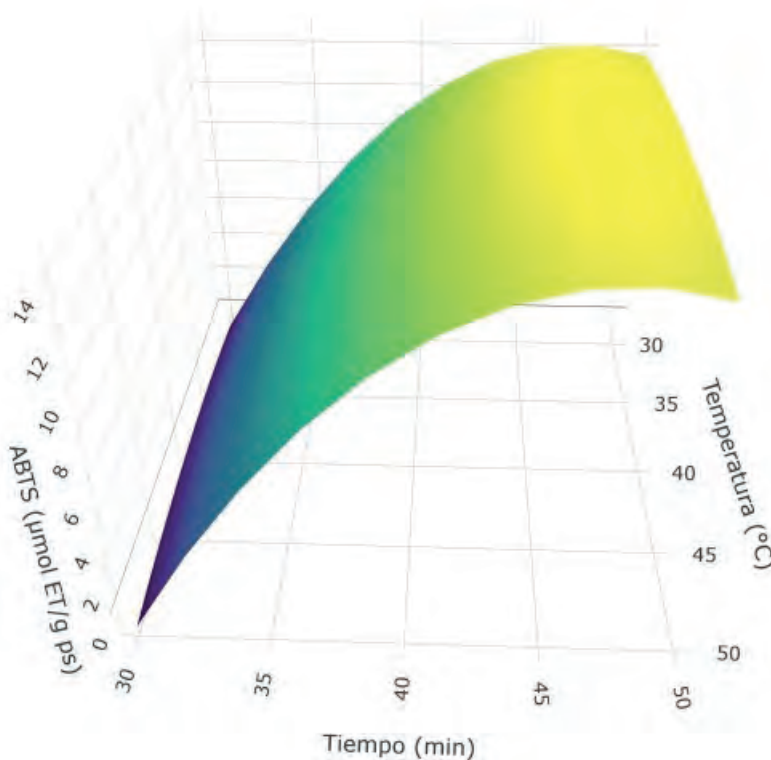
Figura 4. Efecto de la temperatura y el tiempo de extracción sobre la actividad inhibidora del radical catiónico ABTS.

Arianna Valdez N, Iván Choez, Sofie Van Der Hende, Omar Ruìz, Patricia Manzano
Volume 8 / Issue 1 / 11 • http://www.revistabionatura.com

6

Superficie de respuesta para Fenoles Totales
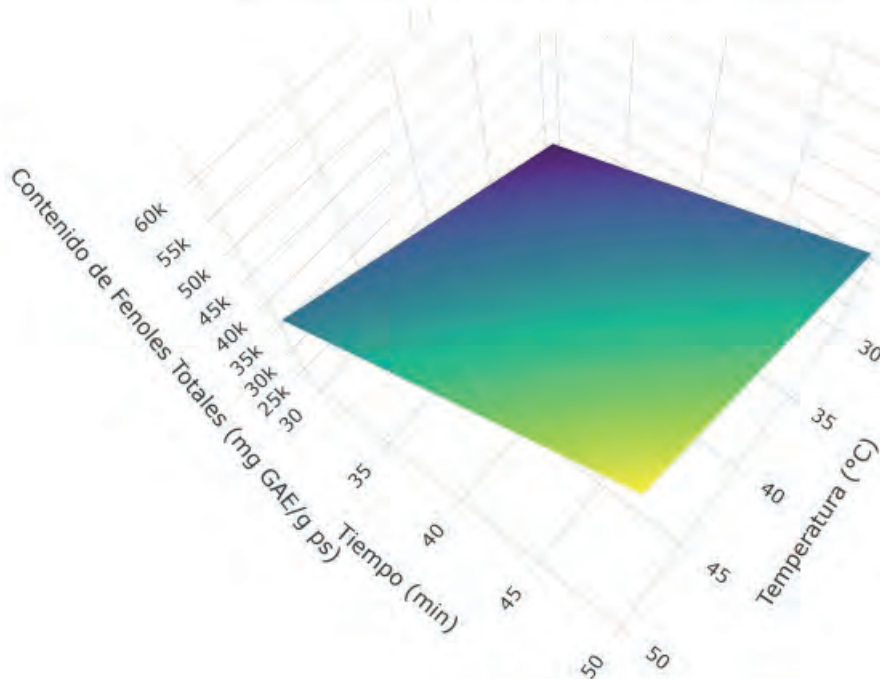
Figura 5. Efecto de la temperatura y el tiempo de extracción sobre el contenido de fenoles.

Superficie de respuesta para Flavonoides Totales
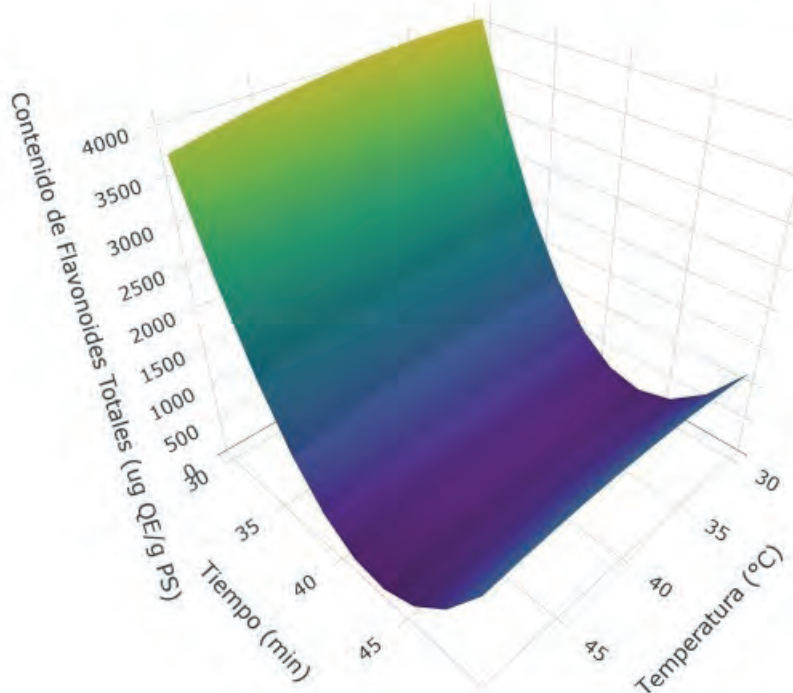
Figura 6. Efecto de la temperatura y el tiempo de extracción sobre el contenido de flavonoides totales.

Der Hende; curación de datos, Omar Ruiz, PhD; redacción—preparación del borrador original, Ing. Qco Arianna Valdez; "Todos los autores han leído y aceptado la versión publicada del manuscrito.

Declaración de la Junta de Revisión Institucional

No aplicable.

Declaración de consentimiento informado

No aplicable.

Declaración de disponibilidad de datos

Disponibilidad de datos previa solicitud.

Condiciones óptimas de extracción de compuestos antioxidante del alga roja *Acanthophora spicifera*
Optimal conditions for the extraction of antioxidant compounds from the red alga *Acanthophora spicifera*

7

Método de extracción	Solvente	Temperatura (°C)	Tiempo (min)	FD	OD	FD	OD
				TPC (mg GAE /g p.s)		TFC (µg CE /g p.s)	
Digestión	EtOH 50%	40	30	0,699±0,03	0,330±0,04	391,917±0,01	106,851±5,36
			40	0,941±0,01	0,312±0,01	545,667±0,58	106,095±1,12
			50	0,360±0,01	0,374±0,05	159,417±0,01	126,092±1,88
		45	30	0,673±0,03	0,374±0,04	187,750±2,35	194,142±3,48
			40	0,656±0,04	0,414±0,01	293,583±2,35	216,192±0,69
			50	0,640±0,05	0,406±0,01	261,500±0,58	277,750±5,07
		50	30	0,913±0,09	0,619±0,05	1281,083±3,53	238,583±2,35
			40	0,904±0,01	0,622±0,01	1255,667±2,94	249,833±1,76
			50	0,615±0,04	0,631±0,02	1210,667±2,94	307,750±5,62
	EtOH 70%	40	30	0,285±0,03	0,315±0,02	328,222±4,32	409,977±5,67
			40	0,276±0,03	0,350±0,02	423,501±2,35	504,577±5,75
			50	0,252±0,02	0,323±0,01	461,278±3,14	395,023±0,14
		45	30	0,286±0,02	0,403±0,06	532,667±0,39	181,413±5,58
			40	0,305±0,01	0,305±0,02	501,278±0,78	349,806±2,39
			50	0,286±0,01	0,387±0,01	538,778±0,39	318,796±5,85
		50	30	0,316±0,01	0,198±0,01	492,389±3,14	132,389±5,34
			40	0,331±0,01	0,190±0,01	558,778±2,75	133,504±0,78
			50	0,382±0,01	0,224±0,01	701,006±0,39	156,556±2,75
EAU	EtOH 50%	ambiente	10	0,398±0,03	0,406±0,01	136,917±3,53	261,917±2,35
			20	0,359±0,01	0,785±0,02	181,083±2,35	234,833±2,94
			30	0,301±0,04	0,834±0,05	147,333±2,94	176,083±2,35
	EtOH 70%	ambiente	10	0,227±0,02	0,298±0,02	248,502±1,57	194,278±3,92
			20	0,220±0,01	0,109±0,01	243,778±3,53	73,778±5,67
			30	0,292±0,01	0,149±0,01	307,944±1,57	105,167±5,42

EUA, extracción asistida por ultrasonido; **FD**, Liofilizado; **OD**, Secado al horno; **GAE**, ácido gálico; **CE**, catequina; **p.s**, peso seco

Tabla 1. Contenido de fenoles totales (TPC) y contenido de flavonoides totales (TFC) de los extractos de *A. spicifera*.

Conflictos de Interés

Los autores declaran no tener conflicto de interés.

Referencias bibliográficas

1. Ceramiales R. A taxonomic , of species relationships Acanthophora study phylogenetic general and biogeographical biogeographical phologically distinguishable species , Jong Rhodophyta), phylogenetic biogeographical analysis , monophyletic algae (Falkenberg ,. 1999;44:217-249.

2. CONABIO. Método de Evaluación Rápida de Invasividad (MERI) para especies exóticas en México. Published 2017. Accessed October 19, 2022. https://enciclovida.mx/pdfs/exoticas_invasoras/Acanthophora%20spicifera.pdf

3. Schnöller VCG. Caracterización química del alga roja Acanthophora spicifera (M . Vahl) Børgesen (Ceramiales: Rhodophyta) en La Bahía De La Paz, Baja California Sur, México. Published online 2016:64.

4. Budiyanto F, Ghandourah MA, Bawakid NO, Alorfi HS, Abdel-Lateff A, Alarif WM. Threat and gain: The metabolites of the red algae genus Acanthophora. Algal Res. 2022;65:102751. doi:10.1016/J.ALGAL.2022.102751

5. Pangestuti R, Kim SK. Biological activities and health benefit effects of natural pigments derived from marine algae. J Funct Foods. 2011;3(4):255-266. doi:10.1016/j.jff.2011.07.001

6. Humphrey AM. Chlorophyll as a Color and Functional Ingredient. J Food Sci. 2006;69(5):C422-C425. doi:10.1111/j.1365-2621.2004.tb10710.x

7. Gupta S, Cox S, Abu-Ghannam N. Effect of Different Drying Temperatures on the Moisture and Phytochemical Constituents of Edible Irish Brown Seaweed Recommended Citation Effect of different drying temperatures on the moisture and phytochemical constituents of edible Irish brown seaweed. LWT-Food Science and Technology. Published online 2011. doi:10.1016/j.lwt.2010.12.022

8. Gupta S, Abu-Ghannam N. Recent developments in the application of seaweeds or seaweed extracts as a means for enhancing the safety and quality attributes of foods. Innovative Food Science and Emerging Technologies. 2011;12(4):600-609. doi:10.1016/j.ifset.2011.07.004

9. Ito K, Hori K. Seaweed: Chemical composmon and potential food uses. Food Reviews International. 1989;5(1):101-144. doi:10.1080/87559128909540845

10. Ling ALM, Yasir S, Matanjun P, Abu Bakar MF. Effect of different drying techniques on the phytochemical content and antioxidant activity of Kappaphycus alvarezii. J Appl Phycol. 2015;27(4):1717-1723. doi:10.1007/s10811-014-0467-3

11. Jiménez-Escrig A, Jiménez-Jiménez I, Pulido R, Saura-Calixto F. Antioxidant activity of fresh and processed edible seaweeds. J Sci Food Agric. 2001;81(5):530-534. doi:10.1002/jsfa.842

12. le Lann K, Jégou C, Stiger-Pouvreau V. Effect of different conditioning treatments on total phenolic content and antioxidant activities in two Sargassacean species: Comparison of the frondose Sargassum muticum (Yendo) Fensholt and the cylindrical Bifurcaria bifurcata R. Ross. Phycological Res. 2008;56(4):238-245. doi:10.1111/j.1440-1835.2008.00505.x

13. Chen J, Li M, Yang R, Luo Q, Xu J, Ye Y. Profiling lipidome changes of Pyropia haitanensis in short-term response to high-temperature stress. Published online 2015. doi:10.1007/s10811-015-0733-z

14. Stramarkou M, Papadaki S, Kyriakopoulou K. Effect of drying and extraction conditions on the recovery of bioactive compounds from Chlorella vulgaris. Published online 2017. doi:10.1007/s10811-017-1181-8

15. Wong K, Chikeung Cheung P. Influence of drying treatment on three Sargassum species 2. Protein extractability, in vitro protein digestibility and amino acid profile of protein concentrates. J Appl Phycol. 2001;13(1):51-58. doi:10.1023/A:1008188830177

16. Kadam SU, Álvarez C, Tiwari BK, O'Donnell CP. Processing of seaweeds. In: Seaweed Sustainability: Food and Non-Food Applications. Elsevier Inc.; 2015:61-78. doi:10.1016/B978-0-12-418697-2.00004-0

17. Rioux LE, Beaulieu L, Turgeon SL. Seaweeds: A traditional ingredients for new gastronomic sensation. Food Hydrocoll. 2017;68:255-265. doi:10.1016/j.foodhyd.2017.02.005

18. Chenlo F, Arufe S, Díaz D, Torres MD, Sineiro J, Moreira R. Air-drying and rehydration characteristics of the brown seaweeds, Ascophylum nodosum and Undaria pinnatifida. J Appl Phycol. 2018;30(2):1259-1270.   doi:10.1007/s10811-017-1300-6

19. Badmus UO, Taggart MA, Boyd KG. The effect of different drying methods on certain   nutritionally important chemical constituents in edible brown seaweeds. J Appl Phycol. 2019;31(6):3883-3897. doi:10.1007/s10811-019-01846-1

20. Viteri R, Giordano A, Montenegro G, Zacconi F. Eucryphia cordifolia extracts: Phytochemical screening, antibacterial and antioxidant activities. https://doi.org/101080/1478641920 211960525. 2021;36(16):4177-4181. doi:10.1080/14786419.2021.1960525

21. Zhong B, Robinson NA, Warner RD, Barrow CJ, Dunshea FR, Suleria HAR. LC-ESI-QTOF-MS/MS Characterization of Seaweed Phenolics and Their Antioxidant Potential. Mar Drugs. 2020;18(6). doi:10.3390/MD18060331

22. Avramova V, Abdelgawad H, Vasileva I, et al. High antioxidant activity facilitates maintenance of cell division in leaves of drought tolerant maize hybrids. Front Plant Sci. 2017;8(FEBRUARY):84. doi:10.3389/FPLS.2017.00084/BIBTEX

23. Chang   CC, Yang MH, Wen HM, Chern JC. Estimation of Total Flavonoid Content in   Propolis by Two Complementary Colorimetric Methods. J Food Drug Anal.   2002;10(3):178-182. Accessed September 17, 2022.   https://scholar.google.com/scholar_lookup?author=C.+C.+Chang&author=M.+H.+Yang&author=H.+M.+Wen&author=J.+C.+Chern+&publication_year=2002&title=Estimation+of+total+flavonoid+content+in+propolis+by+two+-complementary+colorimetric+methods&journal=J.+-Food+Drug+Anal.&volume=10&pages=178-182

24. Murugan K, Iyer VV. Antioxidant and antiproliferative activities of extracts of selected red and brown seaweeds from the Mandapam Coast of Tamil Nadu. J Food Biochem. 2014;38(1):92-101. doi:10.1111/jfbc.12029

25. Ganesan P, Kumar CS, Bhaskar N. Antioxidant properties of methanol extract and its solvent fractions obtained from selected Indian red seaweeds. Bioresour Technol. 2008;99(8):2717-2723. doi:10.1016/J.BIORTECH.2007.07.005

8

Characterization of the microbial community associated with the roots of joyapa (*Macleania rupestris*) and the effect of fungal isolates on seedling development

Diana Curillo[1]*, Juan Manuel Cevallos-Cevallos[2], Eduardo Chica[1] and Denisse Peña[1]

[1] Facultad de Ciencias Agropecuarias, Universidad de Cuenca, Cuenca, Ecuador.
[2] Centro de Investigaciones Biotecnológicas del Ecuador (CIBE), Escuela Superior Politécnica del Litoral, ESPOL, Guayaquil, Ecuador.
Corresponding author: diana.curillos@ucuenca.edu.ec

Abstract: *Macleania rupestris* is a native Ericaceae with high potential benefits for health and the environment. Characterizing the interactions between *M. rupestris* and associated fungi is vital to supporting the plant's conservation and future domestication. However, little is known about the relationship between plant growth-promoting endophytes and *M. rupestris*. To learn more about the soil-associated microbiota of *M. rupestris*, we analyzed endophyte communities associated with the plant's rhizosphere and surrounding soil using nanopore sequencing. Additionally, fungal endophyte cultivable strains were isolated from the roots of *M. rupestris* to evaluate their growth-promoting activity on seedlings by applying a strain inoculation bioassay. Over 1000 genera were identified using nanopore sequencing, *Bradyrhizobium* and *Mesorhizobium* the most abundant in all samples analyzed. Similarly, six cultivable fungi were characterized by the molecular markers ITS (internal transcribed spacer) and LSU (large subunit). Amongst all isolates, *Clonostachys rosea* and *Trichoderma paravidescens* positively impacted seedlings' development. This study shows the potential of fungal strains as inoculants for the potential domestication of *Macleania rupestris*.

Key words: Endophyte, growth promoter, *Macleania rupestris*, microbial communities.

Introduction

Ericaceae is considered one of the most prominent families of angiosperm, plants that include herbs, dwarf shrubs, shrubs, and trees commonly found in acidic and infertile growing conditions[1]. In the Andean region of Ecuador, there is an excellent variety of Ericaceae used by rural and indigenous communities. Among them, *Macleania rupestris*, known locally as "joyapa" is a species of Ericaceae that provides fruits for human consumption in communities of the Andean region[2,3]. The Ericaceae family is one of the most representatives of the Ecuadorian Andean forests, mainly in the montane cloud forests, as well as in the paramo and sub-paramo regions[4], where these plants play critical ecological roles such as a water regulator, a food source for several birds species and other animals such as the Andean bear; and, in some cases, a source of income for the inhabitants of the region[2]. Additionally, *M. rupestris* have the potential to be used in recovery projects for degraded areas[5]. Even though the importance of *M. rupestris* to its habitat, very little is known about the conservation and propagation of this species.

Mycorrhizal endophytic associations are complex fungal-derived traits that help develop plant physiology[6,7]. In other Ericaceae species, various endophytes have been examined for their ability to produce growth-promoting metabolites like those made by their hosts, but in more significant quantities[8,9]. However, the information regarding these symbiotic associations in *M. rupestris* is minimal[10], so a complete characterization of these fungal communities is required to know more about the conservation of *M. rupestris*.

This study contributes to the knowledge of the complex associations established by *M. rupestris* in the Andes of southern Ecuador. We set out to characterize the endophytic communities of rhizospheric soil and soil surrounding *M. rupestris* seedlings in specimens collected in three locations in the southern highlands of Ecuador province Azuay. To better understand the effect of endophyte fungi, we isolated and identified cultivable fungal strains from *M. rupestris* roots to later evaluate their effect on the initial development of *M. rupestris* seedlings germinated under laboratory conditions.

Materials and methods

Location and sampling

Three sampling points were established within the province of Azuay, Ecuador, in the parishes of Baños (2°57'25.1"S 79°05'46.8"W), Sayausí (2°51'12.5"S 79°06'10.4"W) and Sigsig (3°00'51.7"S 78°46'48.0"W), located at altitudes between 2900 and 3100 masl. The collected samples were processed in March 2021 at the Faculty of Agricultural Sciences of the University of Cuenca as described below.

1

2

Soil sample collection

The soil samples were collected from the roots of *M. rupestris*, in the seedling stage, using the protocol described by Barrilot *et al.*[11], which consists of digging an approximate depth of 30 cm to obtain the samples; approximately 200 g of soil was collected. To get surrounding soil samples, part of the roots of the joyapa seedlings selected in the field were extracted and shaken vigorously for 10 min to collect the soil. Additionally, the rhizospheric soil samples were obtained manually by removing the soil that remained attached to the roots of the seedlings. Separately collected soil samples from the surrounding soil were sieved and stored in plastic bags in the dark at approximately 4°C, using ice. All samples were transported to the laboratory and stored at -20 °C until analysis.

DNA extraction from soils and metagenomic sequencing

To characterize the microbial community associated with the surrounding soil and rhizosphere of *M. rupestris*, Nanopore MinION Oxford sequencing was carried out[12]. DNA extraction was performed using 250 mg of soil, previously stored at -20 °C. The extraction was performed using the DNeasy PowerSoil Pro Kit (Qiagen, Hilden, Germany), according to the manufacturer's instructions. The quality and concentration of the DNA were evaluated using the QubitTM 4.0 fluorometer (Thermo Fisher Scientific, 2018).

Libraries for MinION sequencing were prepared using the 1D Ligation Sequencing Kit (SQK-LSK109), and the DNA from each sample was barcoded using the Native Barcode Expansion Kit (EXP-NBD103) (Oxford Nanopore Technologies, Oxford, UK)[13,14]. All kits were used following the manufacturer's instructions. The libraries were then sequenced in a MinION Mk1B for 6 hours using an R9 flow cell. Data was processed using the Oxford Nanopore Technology (ONT) cloud-based pipeline EPI2ME (WIMP rev. 3.2.3) workflow for WIMP (what is in my pot) analysis to obtain the microbial community information down to the genus level as well as some species.

Statistical analysis

The α diversity of the community was estimated using the indices of Shannon, Simpson and Chao1. Beta diversity was estimated using Bray-Curtis dissimilarity, employing the verdict function of the vegan package in R. Then, permutational multivariate analysis of variance (PERMANOVA) was used to compare the microbial community structure between surrounding and rhizospheric soil; this was done with 999 permutations using the adonis function from the vegan package in R.

Isolation of endophytic fungi

M. rupestris roots previously collected and stored at 4 °C were disinfected by washing with running water, then immersed in a 70 % (v/v) ethanol solution for 1 min, followed by a 1.5% sodium hypochlorite solution for 5 minutes. Finally, the roots were rinsed three times with sterile distilled water[10]. Then, a fragment of approximately 3 cm of the disinfected root was placed in a sterile Petri dish and cut into small pieces with the help of tweezers and a scalpel. Sterile FIM culture medium (Fungi Isolation Medium) was added to the fragments obtained. The Petri dishes were then closed and kept at room temperature (around 20 °C) for 96 hours, observing the emergence of hyphae daily and transferring them to PDA medium (potato dextrose agar) for further de-

velopment; PDA petri dishes were incubated at room temperature for 5 days. Fully grown fungi were classified according to color and appearance[10,15].

DNA extraction from isolated fungal strains

Genomic DNA extraction was performed by adding 500 μl of TE buffer pH 8.0 to 50 mg of mycelium collected from the PDA culture dishes, then centrifuging at 15,000 rpm for 5 min and removing the TE buffer, adding 300 μl of extraction solution (200 mM Tris HCl pH 8.5, 250 mM NaCl, 25 mM EDTA 0.5% SDS). The mycelium was then ground in a TissueLyser II (Qiagen) with metal beads for 3 minutes, and 150 μl of 3 M sodium acetate, pH 5.2, was added. The suspension was then incubated at -80°C for 10 minutes, thawed and centrifuged (Eppendorf Centrifuge 5430 R) at 15,900 x g for 5 min. The supernatant was transferred to another test tube, and an equal amount of isopropanol was added. After 5 min of incubation at room temperature, the supernatant was combined with 300 μl of 70% ethanol and centrifuged at 15,900 x g for 15 min to perform a wash[16]. Electrophoresis was performed on a 1.5% agarose gel using ethidium bromide to visualize the extracted DNA. To analyze DNA, 2μl of the sample was read through a spectrophotometer (Epoch Biotek Instruments) to determine DNA quantity and quality.

Identification of isolated fungal strains

From the extracted DNA, a fragment of the ITS region was amplified using the primers ITS1 (5'-TCCGTAGGT-GAACCTGCGG-3') and ITS4 (5'-TCCTCCGCTTA TT-GATATGC-3')[17] as well as the large subunit (LSU) region using the primers LR0R (5'-ACCCGCTGAACTTAAGC-3') and LR3 (5'-CCGTGTTTCAAGACGGG-3')[18]. The amplified fragments were sequenced by an external service provider (Macrogen Inc., South Korea) and then compared to the NCBI (National Center for Biotechnology Information) GenBank database using BLAST[19]. The identity of each isolate was assigned based on the percentage of similarity with the sequences found in the GenBank database.

Germination of seeds and obtaining seedlings

Ripe fruits of *M. rupestris* were collected between the months of January - March. Fruit disinfection was carried out in a laminar flow hood, for which the fruits were immersed in a 70% (v/v) ethanol solution for 1 min and then in a sodium hypochlorite solution (3.5%) for 10 min. Finally, the fruits were rinsed three times with sterilized distilled water[20]. The seeds were then extracted with the help of a syringe needle and placed in a 2000 ppm AG3 (gibberellic acid) solution for 24 h at 20 ºC.

Subsequently, the seeds were placed in a 9-cm diameter Petri dish with filter paper and sterile distilled water for 8 weeks to germinate and obtain seedlings. The seedlings were placed in sterile peat for the inoculation tests using the fungi previously isolated from the roots of *M.rupestris*.

Inoculation of fungal strains in *M. rupestris* seedlings

A total of six isolated fungi were selected to evaluate their effect on the initial development of *M. rupestris* seedlings. After two weeks of adaptation of the seedlings in the sterile peat, the inoculation of the different strains of isolated fungi was carried out, for which a solution prepared with half a Petri dish of mycelium diluted in 250 ml of sterile distilled water was applied[21].The seedling growth assay was carried out under controlled conditions in a growth room for

90 days under a photoperiod of 16 hours of light and 8 hours of darkness at 25 ± 2ºC with 10 individual seedlings for each isolated endophytic fungus and the non-inoculated control group. All seedlings were treated with conventional organic fertilizer with nutrient solution and then inoculated with fungi isolates except for the control group. The number of roots and the height of the seedlings were recorded 90 days after inoculations. Plant height was measured from the soil surface to the tip of the stem. Plant growth data were subjected to one-way ANOVA (α = 0.05)[22].

Results

Microbial communities present in the surrounding and rhizospheric soil of *M. rupestris*

From the two samples collected (1 surrounding and one rhizospheric), for each of the 3 sampling points, community compositions indicated the presence of 4 kingdoms, 40 phyla, 83 classes, 175 orders, 366 families, 1090 genera and 3151 species in the rhizospheric soil samples and for the surrounding soil, 4 kingdoms, 36 phyla, 72 classes, 156 orders, 330 families, 894 genera and 2432 species were found. It was observed that a total of 15 phyla belonging to the bacteria kingdom presented a relatively high abundance, greater than 1%, in the rhizospheric and surrounding soil samples. According to the data obtained, the Bacteria kingdom was the most abundant, constituting 96% of the total readings. The Fungi kingdom only included 4%, of which none was categorized as an endophyte.

When analyzing the diversity index (Shannon), dominance index (Simpson) and richness index (Chao1) for the bacterial communities in the surrounding and rhizospheric soil, it's evident that there is greater diversity in the rhizospheric soil of *M. rupestris* compared to the surrounding soil samples (Figure 1). It was also found that the structure of the microbial community differed from the type of soil sampled (rhizospheric/surrounding), observing an increase in the distance (Bray – Curtis, *p* = 0.03) between the rhizospheric and surrounding soil samples. (PERMANOVA Shannon, *p* = 0.05, PERMANOVA Simpson, *p* = 0.02, PERMANOVA Chao1, *p* = 0.01).

Comparing the rhizospheric soil samples with the surrounding soil samples, the dominant genera (average relative abundance > 1%) in all samples were *Bradyrhizobium* (16%), *Pseudomonas* (4.7%), *Sphingomonas* (3.3%), *Mesorhizobium* (3 %), *Burkholderia* (2.8%), *Variovorax* (2.5%), *Paraburkholderia* (2.7%),) and *Rhodopseudomonas* (1.4%). The relative abundance of *Bradyrhizobium* and *Burkholderia* in the rhizosphere soil was like the composition of the surrounding soil (Figure 2).

Isolation of cultivable fungi

A total of 12 fungal strains were isolated from the roots of *M. rupestris*. Fungal strains with similar morphotypes were present in most of the cultivated roots, which is why they were grouped according to their morphology (color, shape, and growth time) in a total of six morphotypes, which were used in the subsequent identification and molecular analysis (Figure 3).
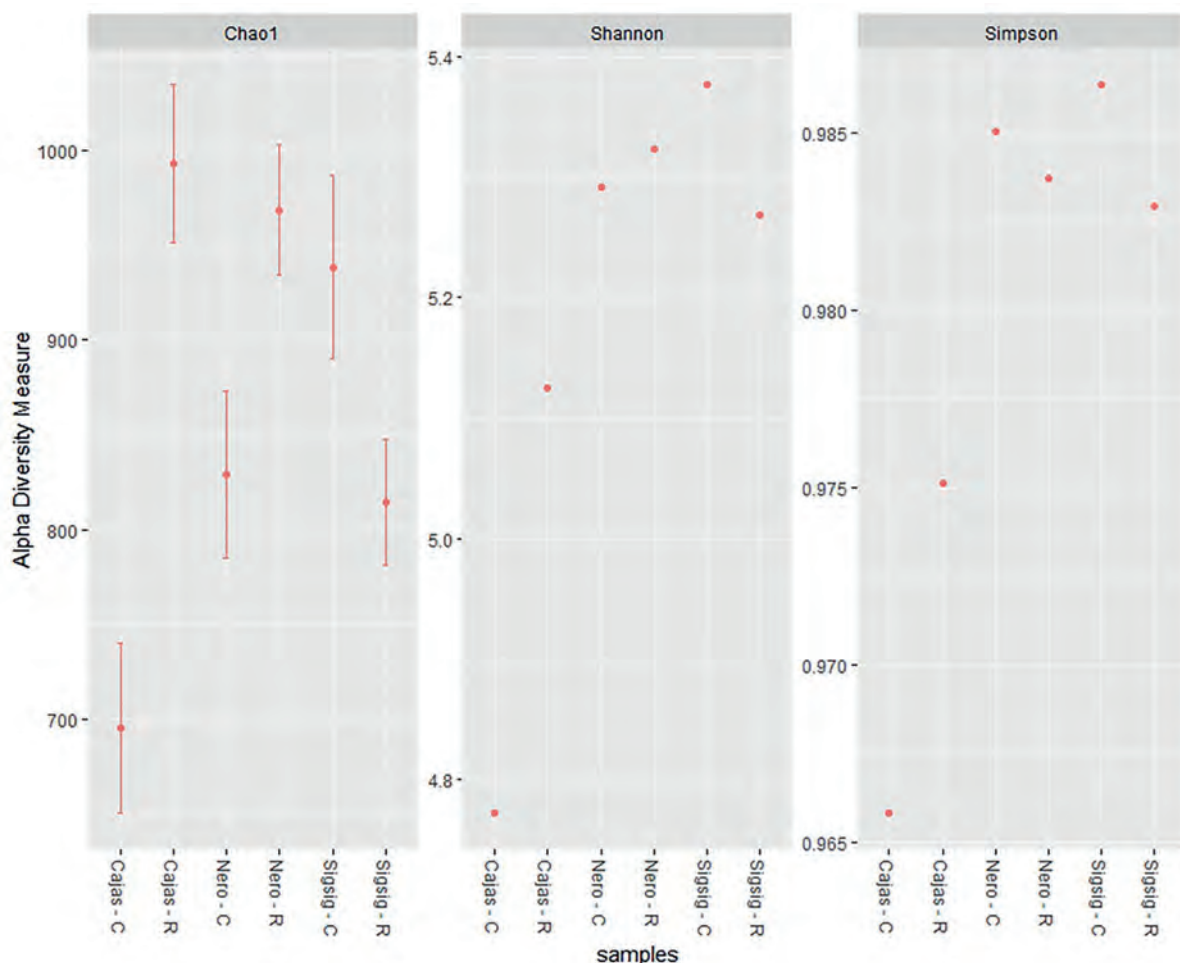
Figure 1. Alpha diversity indices (Chao1, Shannon and Simpson). R = rhizospheric soil C = surrounding soil.
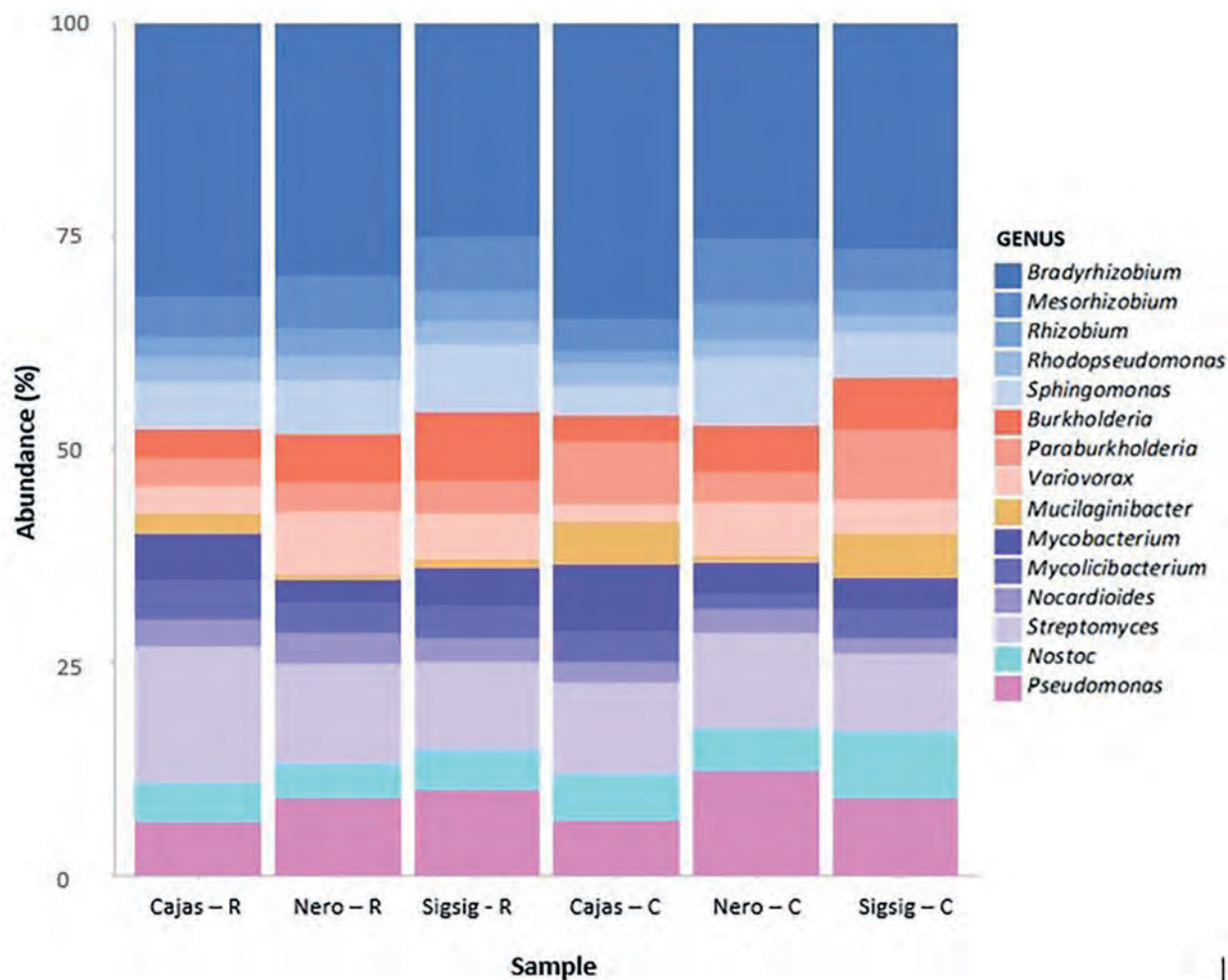
Figure 2. Relative abundance of identified genera for each soil sample. The EPI2ME WIMP workflow analyzed reads. Bacterial genera contributing more than 0.5% of the classified reads are shown. R = rhizospheric soil C = surrounding soil.

Of the six strains of isolated fungi, 3 belonged to the genus *Trichoderma*, and included *T. paraviridescens*, *T. viridescens*, and *T. atroviridae*. Additionally, two strains were within the *Fusarium genus*, and included *F. asiaticum* and *F. graminearum*, and finally, a *Clonostachys rosea* isolate was obtained. All species shared a 99% similarity to those from Genebank (Table 1).

Inoculation of cultivable endophytic fungi in *M. rupestris* seedlings

After 90 days, plants inoculated with *Clonostachys rosea* presented the best results in their development, evaluated by the number of leaves and the height of the seedlings. The seedlings exhibited better development than the control group seedlings (Figure 4a). As for the number of leaves, the average was of 8 per seedling and 6.5 cm in height, unlike the control group, which presented standards of 5 leaves per seedling and 2 cm in height (Figure 4b,c). The results were similar to the seedlings inoculated with *T. paraviridescens*, which registered 7 leaves and an average size of 5 cm (Figure 4b,c). Except for *T. viridescens*, all the fungal strains influenced the development of the seedlings, surpassing the control treatment in height, however concerning the number of leaves, in addition to *C. Rosea* and *T. paraviridescens*, only *T. viridescens*, slightly outperformed the control group.

Discussion

Microbial diversity present in rhizospheric and surrounding soils of *M. rupestris*

Soil microorganisms play a critical role in regulating soil fertility and plant health[30]. We are beginning to understand how soil microbial diversity varies worldwide and how this diversity is related to the physical, chemical, and biological characteristics of ecosystems[31]. The study carried out in the surrounding and rhizospheric soil of *M. rupestris* showed that the diversity of microbial communities could vary significantly concerning the proximity to the root. The metagenomic analysis of the surrounding and rhizosphere soil samples obtained a higher abundance of bacterial communities than fungal communities. This can happen due to several factors, such as changes in the types and amounts of organic carbon in the soil[32,33]. Although fungi and other eukaryotes may represent a large part of the soil microbial biomass, their representation in the metagenomic data obtained was low. A similar pattern has been observed in comparable shotgun metagenomic datasets obtained from other soils[34,35] and is most likely a product of many eukaryotic taxa (including fungi), which have a much lower ratio of rRNA gene copies per unit biomass than bacterial cells[35].

Analyzing the bacterial communities obtained, we find that bacteria belonging to the genera *Bradyrhizobium*, *Pseu-*
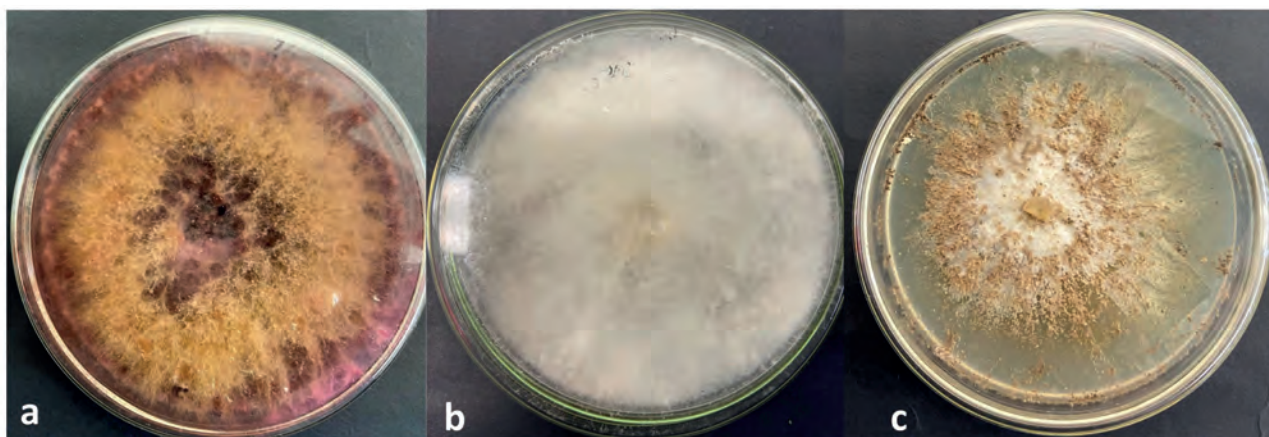
Figure 3. Fungal strains isolated from *M. rupestris* roots. a.) *Fusarium asiaticum* b.) *Trichoderma paraviridescens* c.) *Clonostachys rosea*.

ID Fungi	Isolate closest match	Similarity (%)
MS1	*Fusarium asiaticum*	99
MC2	*Clonostachys rosea*	99
MC1	*Fusarium graminearum*	99
JF	*Trichoderma viridescens*	99
JM	*Trichoderma atroviridae*	99
JC2	*Trichoderma paraviridescens*	99

Table 1. Search closest matches of fungal isolates against NCBI Genbank databases.

domonas, *Sphingomonas*, have been previously shown to be the most abundant taxa in the rhizosphere and endosphere of plants[24,36]. Therefore, the same taxa are expected to be the most productive in the analyzed samples.

Actinobacteria are a species and class of Gram-positive bacteria and are the group with the highest representation in surrounding soils and the second most represented in rhizospheric soils. This taxon is particularly interesting for its wide biotechnological potential[37]. *Actinobacteria* in soils have capacities for mutualism, symbiosis and pathogenesis[38].

The most abundant genera within the samples are *Bradyrhizobium*, *Pseudomonas*, and *Sphingomonas*. *Bradyrhizobium spp.* is an agronomically crucial gram-negative bacterium capable of forming root nodules and fixing atmospheric nitrogen[39]. *Bradyrhizobium* species produce auxins, cytokinins, abscisic acid, vitamins and riboflavin, which stimulate plant growth[40]. *Pseudomonas* are important bacteria in agriculture and have been shown to promote growth and protect plants from pathogens[41] and are part of the core microbiome of many plants[42]. These genera present in the soil samples are essential because they are involved in plant growth, which is of utmost importance for the propagation of *M. rupestris*.

Inoculation of plants with isolated fungi

Endophytic interactions are a complex matrix of symbiotic functions between the host plant and its microbiome.

For several years, many endophytic communities and their vital role in the development and growth of Ericaceae have been studied[23,24]. In the inoculation test of endophytic fungi in *M. rupestris* plants, *C. rosea* presented favorable results in terms of seedling development. *C. rosea* is reported as an endophytic fungus for various plants such as corn[25], wheat[26] and blueberry[27]. It has been reported as a promoter of seed germination and helps plants such as blueberry plants to resist extreme environmental factors like major droughts[27]. *C. rosea* has also been reported as a biological controller of *Botrytis cinerea* in tomato plants[28].

Among the isolated fungi, 3 species of *Trichoderma* were also found, which also presented favorable results in terms of the number of leaves per plant and plant height; this can be attributed to the fact that fungi of the genus *Trichoderma* produce glucanases, chitinases and proteases, enzymes that break down the components of the cell wall chitin, polysaccharides and β-glucans, facilitating the obtaining of nutrients for plants[28]. *Trichoderma paraviridescens* is also used in crops as growth promoters or for seed germination[29].

The results obtained show that the fungi isolated from the roots of *M. rupestris* did help the leaf development and height of seedlings. *C. rosea* was one of the fungi with the greatest potential to be used in future studies, with *M. rupestris* as a growth promoter.

Further research is needed to assess the role of bacteria isolates in seedlings and plants of *M. rupestris*.

Conclusions

This study is the first to analyze the diversity of microbial communities present in the surrounding and rhizospheric soil of *M. rupestris* using metagenomic analysis. The data obtained provide information on the microbial distribution in *M. rupestris* plants and the dominant genera present in the development of the plants, the most prominent groups being *Bradyrhizobium*, *Proteobacteria* and *Actinobacteria*. In conclusion, the rhizospheric soil of *M. rupestris* has greater microbial diversity than the surrounding soil and a large part of the microbial community is recurrent for these plants, even though they come from different sites, which could indicate a close interrelationship and/or dependence between these plants and some of the microorganisms with which it is associated.

The treatments that were inoculated with fungal strains isolated from the roots of plants of the same species showed more significant growth than the control treatment, and even though the effect regarding the number of leaves was not higher in all cases than the control treatment, it can be evidenced the importance of microbial associations in the development of *M. Rupestris* seedlings, highlighting the effect of *C. rosea* and *T. paraviridescens*.

Acknowledgments

Bibliographic references

1. Ștefănescu BE, Szabo K, Mocan A, Crişan G. Phenolic Compounds from Five Ericaceae Species Leaves and Their Related Bioavailability and Health Benefits. Molecules 2019; 24: 2046.
2. Durán-Casas S, Veloza-Suan C, Magnitskiy S, Lancheros HO. Evaluation of uva camarona (Macleania rupestris Kunth A.C. Smith) propagation with air layering. 2013; : 9.
3. Veloza C, Durán S, Magnitskiy S, Lancheros H. Rooting Ability of Stem Cuttings of Macleania rupestris Kunth A.C. Sm., a South American Fruit Species. International Journal of Fruit Science 2014; 14: 343–361.
4. Luteyn JL, Wilbur RL. FLORA COSTARICENSIS Family #172 Ericaceae. 2005; : 105.
5. Ortiz S, Consuegra C, van der Hammen MC, Pérez D. Perspectivas urbano-rurales sobre la circulación de dos frutos silvestres del Bosque Altoandino en sistemas agroalimentarios de Bogotá, Colombia. Revista Etnobiología 2021; 19: 81–95.
6. Hawksworth DL. Fungal diversity and its implications for genetic resource collections. 2004www.indexfungorum.org/names.
7. Wang Z, Li T, Wen X, Liu Y, Han J, Liao Y et al. Fungal Communities in Rhizosphere Soil under Conservation Tillage Shift in Response to Plant Growth. Front Microbiol 2017; 8. doi:10.3389/fmicb.2017.01301.
8. Zhao J, Zhou L, Wang J, Shan T, Zhao J, Zhou L et al. Endophytic fungi for producing bioactive compounds originally from their host plants Spin-wave resonance in (Ga,Mn)As thin films View project Gamma-ray burst polarimeter POLAR View project Endophytic fungi for producing bioactive compounds originally from their host plants. https://www.researchgate.net/publication/229024535.
9. Alurappa R, Chowdappa S, Narayanaswamy R, Sinniah UR, Mohanty SK, Swamy MK. Endophytic Fungi and Bioactive Metabolites Production: An Update. In: Microbial Biotechnology. Springer Singapore: Singapore, 2018, pp 455–482.
10. Hamim A, Miché L, Douaik A, Mrabet R, Ouhammou A, Duponnois R et al. Diversity of fungal assemblages in roots of Ericaceae in two Mediterranean contrasting ecosystems. C R Biol 2017; 340: 226–237.
11. Barillot CDC, Sarde C-O, Bert V, Tarnaud E, Cochet N. A standardized method for the sampling of rhizosphere and rhizoplan soil bacteria associated to a herbaceous root system. Ann Microbiol 2013; 63: 471–476.
12. Leggett RM, Clark MD. A world of opportunities with nanopore sequencing. J Exp Bot 2017; 68: 5419–5429.
13. Huang Z, Liu B, Yin Y, Liang F, Xie D, Han T et al. Impact of biocontrol microbes on soil microbial diversity in ginger (Zingiber officinale <scp>Roscoe</scp>). Pest Manag Sci 2021; 77: 5537–5546.
14. Srivastava R, Srivastava AK, Ramteke PW, Gupta VK, Srivastava AK. Metagenome dataset of wheat rhizosphere from Ghazipur region of Eastern Uttar Pradesh. Data Brief 2020; 28: 105094.
15. Declerck S, Séguin S, Dalpé Y. The Monoxenic Culture of Arbuscular Mycorrhizal Fungi as a Tool for Germplasm Collections. In: In Vitro Culture of Mycorrhizas. Springer-Verlag: Berlin/Heidelberg, pp 17–30.
16. Moťková P, Vytřasová J. Comparison of Methods for Isolating Fungal DNA. Czech J Food Sci 2011; 29: 10.
17. Bruns TD, Lee SB, Taylor JW. Amplification and Direct Sequencing of Fungal Ribosomal RNA Genes for Phylogenetics Evolution of Gene Expression View project. https://www.researchgate.net/publication/262687766.
18. Vilgalys R, Hester M. Rapid genetic identification and mapping of enzymatically amplified ribosomal DNA from several Cryptococcus species. J Bacteriol 1990; 172: 4238–4246.
19. Altschul S. Gapped BLAST and PSI-BLAST: a new generation of protein database search programs. Nucleic Acids Res 1997; 25: 3389–3402.
20. TURNER SR, COMMANDER LE, BASKIN JM, BASKIN CC, DIXON KW. Germination behaviour of Astroloma xerophyllum (Ericaceae), a species with woody indehiscent endocarps. Botanical Journal of the Linnean Society 2009; 160: 299–311.
21. Repáč I. Ectomycorrhizal Inoculum and Inoculation Techniques. 2011, pp 43–63.
22. Prasad R. Plant promoting activities of fungal endophytes associated with tomato roots from Central Himalaya, India and their interaction with Piriformospora indica Improvement of water quality of Sitalakhaya River by using hydrodynamic model View project Molecular characterization of bacteria isolated from different environment View project. 2015www.ijpbs.net.
23. Vano I, Sakamoto K, Inubushi K. Selection of dark septate endophytes from Ericaceae plants to enhance blueberry (Vaccinium corymbosum L.) seedling growth. 2010.
24. Yurgel SN, Douglas GM, Dusault A, Percival D, Langille MGI. Dissecting Community Structure in Wild Blueberry Root and Soil Microbiome. Front Microbiol 2018; 9. doi:10.3389/fmicb.2018.01187.
25. Goh YK, Marzuki NF, Tuan Pa TNF, Goh T-K, Kee ZS, Goh YK et al. Biocontrol and Plant-Growth-Promoting Traits of Talaromyces apiculatus and Clonostachys rosea Consortium against Ganoderma Basal Stem Rot Disease of Oil Palm. Microorganisms 2020; 8: 1138.
26. Nagasawa AElise. Evaluation of Clonostachys rosea for growth enhancement and suppression of fusarium seedling blight in wheat. Library and Archives Canada = Bibliothèque et Archives Canada, 2010.
27. Sutton JC, Liu W, Ma J, Brown WG, Stewart JF, Walker GD. EVALUATION OF THE FUNGAL ENDOPHYTE CLONOSTACHYS ROSEA AS AN INOCULANT TO ENHANCE GROWTH, FITNESS AND PRODUCTIVITY OF CROP PLANTS. Acta Hortic 2008; : 279–286.
28. Nordström SA. Endophytic growth of Clonostachys rosea in tomato and Arabidopsis thaliana. http://stud.epsilon.slu.se.
29. Zheng H, Qiao M, Lv Y, Du X, Zhang K-Q, Yu Z. New Species

of Trichoderma Isolated as Endophytes and Saprobes from Southwest China. Journal of Fungi 2021; 7: 467.

30. Jacoby R, Peukert M, Succurro A, Koprivova A, Kopriva S. The Role of Soil Microorganisms in Plant Mineral Nutrition—Current Knowledge and Future Directions. Front Plant Sci 2017; 8. doi:10.3389/fpls.2017.01617.

31. Dasgupta D, Brahmaprakash GP. Soil Microbes are Shaped by Soil Physico-chemical Properties: A Brief Review of Existing Literature. Int J Plant Soil Sci 2021; : 59–71.

32. Fierer N, Bradford MA, Jackson RB. TOWARD AN ECOLOGICAL CLASSIFICATION OF SOIL BACTERIA. Ecology 2007; 88: 1354–1364.

33. Goldfarb KC, Karaoz U, Hanson CA, Santee CA, Bradford MA, Treseder KK et al. Differential Growth Responses of Soil Bacterial Taxa to Carbon Substrates of Varying Chemical Recalcitrance. Front Microbiol 2011; 2. doi:10.3389/fmicb.2011.00094.

34. Delmont TO, Prestat E, Keegan KP, Faubladier M, Robe P, Clark IM et al. Structure, fluctuation and magnitude of a natural grassland soil metagenome. ISME J 2012; 6: 1677–1687.

35. Fierer N, Lauber CL, Ramirez KS, Zaneveld J, Bradford MA, Knight R. Comparative metagenomic, phylogenetic and physiological analyses of soil microbial communities across nitrogen gradients. ISME J 2012; 6: 1007–1017.

36. Hacquard S, Garrido-Oter R, González A, Spaepen S, Ackermann G, Lebeis S et al. Microbiota and Host Nutrition across Plant and Animal Kingdoms. Cell Host Microbe 2015; 17: 603–616.

37. Worthen DB. Streptomyces in Nature and Medicine: The Antibiotic Makers. J Hist Med Allied Sci 2007; 63: 273–274.

38. Schrempf H. Actinobacteria within soils: capacities for mutualism, symbiosis and pathogenesis. FEMS Microbiol Lett 2013; 342: 77–78.

39. Li C, Li X, Kong W, Wu Y, Wang J. Effect of monoculture soybean on soil microbial community in the Northeast China. Plant Soil 2010; 330: 423–433.

40. Parihar J, Parihar SP, Suravajhala P, Bagaria A. Spatial Metagenomic Analysis in Understanding the Microbial Diversity of Thar Desert. Biology (Basel) 2022; 11: 461.

41. Adesemoye AO, Kloepper JW. Plant–microbes interactions in enhanced fertilizer-use efficiency. Appl Microbiol Biotechnol 2009; 85: 1–12.

42. Lally RD, Galbally P, Moreira AS, Spink J, Ryan D, Germaine KJ et al. Application of Endophytic Pseudomonas fluorescens and a Bacterial Consortium to Brassica napus Can Increase Plant Height and Biomass under Greenhouse and Field Conditions. Front Plant Sci 2017; 8. doi:10.3389/fpls.2017.02193.

7

ARTICLE / INVESTIGACIÓN

Antibacterial effect of Cannabidiol oil against *Propionibacterium acnes*, *Staphylococcus aureus*, *Staphylococcus epidermidis* and level of toxicity against *Artemia salina*

Grace Pila*, Danny Segarra and Marco Cerna
Universidad Politécnica Salesiana, Ecuador.
Corresponding author: grace.pila@outlook.com

Abstract: Acne is one of the most common skin pathologies; one of the causes is *Propionibacterium acnes*, an anaerobic and gram-positive microorganism that lives in the hair follicles of the skin and currently presents resistance to antibiotic-based treatments; this research topic has the purpose of evaluating the antibiotic activity of *Cannabidiol* oil against *Propionibacterium acnes*, *Staphylococcus aureus* and *Staphylococcus epidermidis* and the level of toxicity against *Artemia salina*. For the methodology, antibiograms were used by the Kirby-Bauer method, where the concentrations were evaluated: 0,8 %; 0,6 %; 0,4 %; 0,3 % and 0,1 %; Amoxicillin for positive control and Dimethyl sulfoxide (DMSO) for negative control; the percentage of inhibition against *Propionibacterium acnes* and two control bacteria were calculated: *Staphylococcus aureus* and *Staphylococcus epidermidis*. Once the percentage of inhibition was tested, a toxicity study was carried out against Artemia salina to determine its LD50. The *Cannabidiol* oil obtained from the Ecuadorian company was used as the antibiotic agent to be evaluated, and it was found that at a concentration of 0,8%, it presented a percentage of inhibition of 91,2 %; 98,7 % and 93,6 % against *Propionibacterium acnes*, *Staphylococcus aureus* and *Staphylococcus epidermidis*, respectively, data that do not present a significant difference against Amoxicillin; for the Artemia salina test, an LD50 of 4,8 % was obtained; taking into account that the commercial oil has a presentation of 1,6 % (500 mg/30 mL), it results in a relatively innocuous product. Thus concluding that *Cannabidiol* oil is a very promising antibiotic due to the inhibition percentages presented and low toxicity.

Key words: CBD, antibiograms, bioassay, LD50.

Introduction

The use and abuse of antibiotics, not only in Ecuador but worldwide, is a fashionable and controversial topic; due to the efforts made by professionals, this is a practice that continues to leave in its wake several severe and irreversible consequences. one of them is the bacterial resistance acquired by microorganisms to antibiotics. Several resistances of *Propionibacterium acnes* have been reported over the years, as is the case of Clindamycin and Erythromycin, which were reported in 1979, and later in 1983 the first resistance to tetracycline was reported[10].

It has been reported in patients with severe acne that 70% of them present high biofilm formation and multi-resistance of *Propionibacterium acnes* to various antibiotics. For this reason, it is interesting to use new alternatives. It has been reported in patients with severe acne that 70% of them present high biofilm formation and multi-resistance of *Propionibacterium acnes* to various antibiotics. For this reason, it is interesting to use new alternatives against Propionibacterium acnes; it has been reported in studies[5,11] that *Cannabidiol* works excellent with biofilms of gram-positive microorganisms; therefore, studying the effect of *Cannabidiol* against *Propionibacterium acnes* is promising.

Materials and methods

Cannabidiol oil was obtained from an Ecuadorian company in a 500 mg/30mL presentation. The bacterial strain of *Propionibacterium acnes* ATCC 11827, *Staphylococcus aureus* ATCC 29213, and *Staphylococcus epidermidis* ATCC 14990 were obtained from the Cryobank of the Life Sciences Laboratories of the Salesian Polytechnic University. The manual described by (20) was used as a reference, and the tubes containing the bacterial beads were thawed with a punch to perform the striation in triplicate throughout the petri dish.

The recommendations of (7) were followed to prepare dilutions with oils and dimethyl sulfoxide. Five oil-based dilutions were prepared at concentrations of 0.1 %; 0.3 %; 0.4 %; 0.6 %, and 0.8 %, whose solvent was DMSO; the final volume for each dilution was 5 mL in every amber bottle.

A commercial antibiotic (Amoxicillin) was taken as a positive control, a beta-lactam antibiotic used for both gram-positive and gram-negative bacteria, due to its broad spectrum of bacterial activity[1]. This antibiotic is used for antibiotic testing in the *Staphylococcus* and *Propionibacterium* families because of their sensitivity to its compounds[8,10].

2

P. acnes was incubated in TSB medium under anaerobic conditions at 35 °C for 16 hours, for *S. aureus* and *S. epidermidis* were incubated in TSB medium at 37 °C in an incubator.

After the established time passed, it was centrifuged at 350 rpm for 20 minutes, the supernatant was discarded in a beaker with alcohol, the bottom of the bacterial biomass was conserved, sterile saline was added to each tube, and vortexed for 2 minutes until reaching the 0,5 McFarland scale and read in the JASCO V-730 spectrophotometer with the spectra manager TM software until reaching an absorbance of 0,200 at 655 nm, obtaining an inoculum of 106 CFU/mL.

500 μL of bacterial inoculum was taken and dropped in the center of the Petri dish with Muller Hinton[15]. One disc of antibiotic Amoxicillin was placed as the positive control, one blank disk with DMSO as the negative control and 5 blank discs with the respective dilutions from *Cannabidiol* oil, which would be at concentrations of 0,1 %; 0,3 %, 0,4 % 0,6 % and 0,8 % in a volume of 20 μL. Petro dishes with *S. aureus* and *S. epidermidis* were placed in an incubator at 37°C for 24 hours; *P. Acnes* was incubated in anaerobiosis at 35 °C.

When the time of 24 hours in the incubator for *S. aureus*, *S. epidermidis* and *P. acnes* had passed, each Petri dish was checked with a caliper ruler.

The percentage of inhibition of each bacterium concerning each concentration was calculated using the following reference formula (1) from[9].

7 grams of *A. salina* eggs were obtained from a commercial house, 2 g of egg were weighed, hydrated for 30 min with distilled water, then 25 mL of sodium hypochlorite were added (4 replicates); the eggs were recovered and rinsed with distilled water. For the incubation, a 3-liter bottle was used, 1500 mL of 2 % saline water was added, pH 8, temperature 24 °C and constant aeration for 48 hours[22].

To make the emulsions with *Cannabidiol* (CBD) oil, a 1:1 ratio of oil and tween 80 was used as a co-emulsifier used in the cosmetic and food area due to its low toxicity level and according to work carried out by (15) it is considered innocuous with *Artemia*. *Cannabidiol* oil was used to obtain emulsion at 3.2 %; 1.6 %; 0.8 %; 0.4 %, and 0.2 %, with which we worked in test tubes with *A. salina* to determine the LD50.

After 24 hours of incubation, dead nauplii were counted using a NIKON SMZ745 stereoscope, where those that did not show any seconds were considered dead

Results

The percentage of inhibition for *P. acnes* is 91.2% at a concentration of 0.8% of *Cannabidiol* oil, which gives a high percentage of inhibition compared to a commercial antibiotic, Amoxicillin, supporting inhibition compared with a commercial antibiotic, Amoxicillin, supporting the alternative hypothesis showing that *Cannabidiol* oil inhibits *P. acnes*.

A Tukey study showed an essential group of data, in which their averages are not significantly different; the group is formed by the positive control (commercial antibiotic), CBD5 (0.8% *Cannabidiol* oil).

The concentration of *Cannabidiol* oil at 0.8 % has an inhibition percentage of 98.7 %, a value very close to the positive control, which was the commercial antibiotic Amoxicillin.

A Tukey test proved that there is a group of interest where their averages are not significantly different; the group is formed by the control + (antibiotic Amoxicillin) and CBD5 (0.8% *Cannabidiol* oil).

The results show that the percentage of inhibition for S. epidermidis with 0.8 % oil was 93.6 %, affirming the alternative hypothesis on the inhibition of *Cannabidiol* oil against *S. epidermidis*.

The Tukey test shows a critical group where the positive control (Amoxicillin) and CBD5 (0.8 % *Cannabidiol* oil) are grouped. As a result, we would obtain that the 0.8 % *Cannabidiol* oil is similar in inhibition to the positive control (Amoxicillin), supporting the alternative hypothesis that there is at least one concentration that inhibits *S. epidermidis*.

Toxicity test

Dilutions of cannabidiol oil were made at intervals of: 3.2 %; 2.8 %; 2.4 % 2.0 %. In order to determine the lethal dose, a linear regression was performed, and an LD50 of 4.86 % (48 mg/mL) was obtained.

Formatting of Mathematical Components

$$Inhibitory\ effect = \frac{Inhibition\ halo\ diameter}{Positive\ control\ halo\ diameter} * 100 \qquad (1)$$

Bacteria	Concentration	X	% inhibition
P. acnes	0,8	1,9	91,2
	Control +	2,0	100

[1] Average halo and percentage inhibition of cannabidiol oil against *P. acnes*

Table 1. Determination of the antibiotic activity of *Cannabidiol* oil against *P. acnes*.

Bacteria	Concentration	X	% inhibition
S. aureus	0,8	1.7	98.7
	Control +	1.8	100

[2] Average halo and percentage inhibition of cannabidiol oil against S. aureus.

Table 2. Determination of the antibiotic activity of *cannabidiol* oil against *S. aureus*.

Bacteria	Concentration	X	% inhibition
S. epidermidis	0,8	1.8	93.6
	Control +	1.9	100

[3] Average halo and percentage inhibition of cannabidiol oil against S. epidermidis

Table 3. Determination of the antibiotic activity of *cannabidiol* oil against *S. epidermidis*.

Discussion

Following the studies of (18) where he mentions that *Cannabidiol* has a potential antimicrobial activity against gram-positive bacteria, such as *P. acnes*, with which using it could be beneficial for the treatment of acne vulgaris. *Cannabidiol* has a potential role as an antimicrobial agent[22]; it was demonstrated through clinical studies that *Cannabidiol* oil acts on sebocytes, thus having an anti-acne function, controlling sebum production, mitigating the inflammatory process and functioning as a bactericidal agent by reducing bacterial proliferation[4,21].

Cannabidiol oil inhibits *S. aureus*; the results obtained by (2) can be compared with those of this work since Cannabidiol, one of the main cannabinoids of the plant, showed potent activity against the strain *S. aureus*.

The results obtained from the test with *S. epidermidis* can be compared with the study conducted by (19), where the mechanism of action of *Cannabidiol* in causing the death of gram-positive bacteria was evaluated due to the ability of this compound to inhibit the release of vesicles from the bacterial membrane; these vesicles are extremely important for cell communication and pathogen-host interaction.

In the negative control of the toxicity test with Artemia salina, saline water was used, and there was no dead individual, so the test is validated as there are no natural factors that can kill the study individuals, as indicated by (13,24); the percentage of mortality in the negative controls did not exceed 10 %. In the positive control, where 96% alcohol was used, it was confirmed as an adequate positive control since the death of the individuals in the study was approved, as indicated by the study of (23).

The use of *Cannabidiol* oil at concentrations from 2 % onwards gradually increases the number of dead *A. salina*[14]. A plant oil, when exceeding an LC50 of 1000 ppm in bioassays with A. salina does not have a high degree of toxicity due to the ability of the nauplii to present a very thin cuticle, which makes them sensitive to toxicants in the medium, which penetrate through the physiological barriers and are rapidly absorbed[6,25].

Conclusions

The valued *Cannabidiol* oil was obtained from an Ecuadorian company, which presents a concentration of 500 mg/30mL. Evaluation by means of the HPLC technique.

Cannabidiol oil showed antibacterial activity with halo averages of 1.8 cm, 1.7 cm and 1.8 cm for *Propionibacterium acnes*, *Staphylococcus aureus* and *Staphylococcus epidermidis*, respectively, at a concentration of 0.8 %, compared to the control antibiotic (Amoxicillin) with 2 cm of halo, using the statistical analysis it was possible to reject the null hypothesis and accept the alternative since *Cannabidiol* oil inhibits *Propionibacterium acnes*, *Staphylococcus aureus* and *Staphylococcus epidermidis* with the proposed concentrations. Likewise, the alternative ideas for the analysis of variance and Tukey are accepted; at least one degree of concentration of *Cannabidiol* oil inhibits the 3 bacteria with a similar effect to Amoxicillin. At the end of the experimental work, it was concluded that the results obtained under the laboratory test show that the use of *Cannabidiol* oil is effective for the control of the mentioned bacteria, and it is a promising field for the possible elaboration of phytoproducts for human use in order to improve and provide all the benefits offered by *Cannabidiol* oil.

For the toxicity bioassay where *Artemia salina* was used, an LD50 value of 4.8 % was obtained, which showed that the commercial *Cannabidiol* oil in a 500 mg/30mL presentation, equivalent to 1.6 %, is a relatively innocuous product at the highest concentration and non-toxic at deficient concentrations. Although at higher concentrations, survival may be negatively affected by swimming problems, the results confirmed the alternative hypothesis that the concentration of *Cannabidiol* oil is directly proportional to the percentage of mortality of *Artemia salina*.

Author Contributions

Funding

Informed Consent Statement

Not applicable.

Data Availability Statement

https://docs.google.com/spreadsheets/d/1mGvmA-Ht5Q6ZsTLvIysinZDh_uoFFovcHAcjse0yb7ug/edit#-gid=816728436

Acknowledgments

Conflicts of Interest

The authors declare no conflict of interest.

Bibliographic references

1. Adm R, María J, Ramos F, Guadalupe M, Zaragoza O, Lorena López Rodríguez L, et al. www.medigraphic.org.mx [Internet]. Medigraphic.com. Disponible en: https://www.medigraphic.com/pdfs/adm/od-2016/od165c.pdf

2. Appendino G, Gibbons S, Giana A, Pagani A, Grassi G, Stavri M, et al. Antibacterial cannabinoids from Cannabis sativa: a structure-activity study. J Nat Prod [Internet]. 2008;71(8):1427–30. Disponible en: http://dx.doi.org/10.1021/np8002673

3. Arima H, Danno G-I. Isolation of antimicrobial compounds from guava (Psidium guajava L.) and their structural elucidation. Biosci Biotechnol Biochem [Internet]. 2002;66(8):1727–30. Disponible en: http://dx.doi.org/10.1271/bbb.66.1727

4. Baswan SM, Klosner AE, Glynn K, Rajgopal A, Malik K, Yim S, et al. Therapeutic potential of Cannabidiol (CBD) for skin health and disorders. Clin Cosmet Investig Dermatol [Internet]. 2020;13:927–42. Disponible en: http://dx.doi.org/10.2147/CCID.S286411

5. Blaskovich MAT, Kavanagh AM, Elliott AG, Zhang B, Ramu S, Amado M, et al. The antimicrobial potential of Cannabidiol. Commun Biol [Internet]. 2021;4(1):7. Disponible en: http://dx.doi.org/10.1038/s42003-020-01530-y

6. Berame JS, Cuenca SME, Cabilin DRP, Manaban ML. Preliminary phytochemical screening and toxicity test of leaf and root parts of the snake plant (Sansevieria trifasciata). J Phylogenetics Evol Biol [Internet]. 2017;05(03). Disponible en: http://dx.doi.org/10.4172/2329-9002.1000187

3

4

7. Bermúdez-Vásquez MJ, Granados-Chinchilla F, Molina A. Composición química y actividad antimicrobiana del aceite esencial de Psidium guajava y Cymbopogon citratus. Agron Mesoam [Internet]. 2019 30(1):147–63. Disponible en: https://www.scielo.sa.cr/scielo.php?pid=S1659-1321201900010001 0&script=sci_abstract&tlng=es

8. Castro Orozco R, Villafañe Ferrer L, Rocha Jiménez J, Alvis Guzmán N. Resistencia antimicrobiana en staphylococcus aureus y staphylococcus epidermidis : tendencia temporal (2010-2016) y fenotipos de multirresistencia, Cartagena (Colombia). Biosalud [Internet]. 2018;17(2):25–36. Disponible en: http://dx.doi.org/10.17151/biosa.2018.17.2.2

9. Corzo Barragán DC, Botánico J, Celestino J, Resumen M. Evaluación de la actividad antimicrobiana del extracto etanólico Evaluation of antimicrobial activity of ethanol extract of Cestrum buxifolium Kunth [Internet]. Org.mx. Disponible en: https://www.scielo.org.mx/pdf/rmcf/v43n3/v43n3a9.pdf

10. Dréno B, Pécastaings S, Corvec S, Veraldi S, Khammari A, Roques C. Cutibacterium acnes(Propionibacterium acnes) and acne vulgaris: a brief look at the latest updates. J Eur Acad Dermatol Venereol [Internet]. 2018;32:5–14. Disponible en: http://dx.doi.org/10.1111/jdv.15043

11. Dessinioti C, Katsambas A. Propionibacterium acnes and antimicrobial resistance in acne. Clin Dermatol [Internet]. 2017;35(2):163–7. Disponible en: http://dx.doi.org/10.1016/j.clindermatol.2016.10.008

12. Feldman M, Sionov RV, Mechoulam R, Steinberg D. Anti-Biofilm Activity of Cannabidiol against Candida albicans. Microorganisms [Internet]. 2021;9(2):441. Disponible en: http://dx.doi.org/10.3390/microorganisms9020441

13. Fernández A, Mendiola J, Monzote L, García M, Sariego I, Acuña D, et al. Evaluación de la toxicidad de extractos de plantas cubanas con posible acción antiparasitaria utilizando larvas de Artemia salina L. rEVISTA cUBANA MEDICINA TROPICAL [Internet]. 2009 [citado el 2 de febrero de 2023]; Disponible en: http://scielo.sld.cu/pdf/mtr/v61n3/mtr09309.pdf

14. Ferrante C, Chiavaroli A, Angelini P, Venanzoni R, Angeles Flores G, Brunetti L, et al. Phenolic Content and Antimicrobial and Anti-Inflammatory Effects of Solidago virga-aurea, Phyllanthus niruri, Epilobium angustifolium, Peumus boldus, and Ononis spinosa Extracts. Antibiotics (Basel) [Internet]. 2020;9(11):783. Disponible en: http://dx.doi.org/10.3390/antibiotics9110783

15. Hernández A, Cruz M, Guerra D, Guerra P, Rivera F, Ramírez-Marroquín O, et al. Estudio de la actividad antioxidante, antimicrobiana y toxicidad de tres extractos de heliocarpus appendiculatus turcz (malvaceae) [Internet]. [Cuernavaca, Morelos, México]: Universidad Autónoma del Estado de Morelos; 2021. Disponible en: http://aap.uaem.mx/index.php/aap/article/view/78/71

16. Ibarra M, Paredes E. Eficacia antibacteriana in vitro de marco (Ambrosia arborescens Mill.) y paico (Chenopodium ambrosioides L.) en una formulación cosmética [Internet]. [Quito, Ecuador]: Universidad Politécnica Salesiana; 2013. Disponible en: https://dspace.ups.edu.ec/bitstream/123456789/6007/1/UPS-QT03776.pdf

17. Juana MAC, Aguilera R, Yolanda ME, Romero M. MANUAL DE LABORATORIO DE MICROBIOLOGIA [Internet]. Www.uv.mx. Disponible en: https://www.uv.mx/qfb/files/2020/09/Guia-de-Microbiologia.pdf

18. Kircik LH. What's new in the management of acne vulgaris. Cutis [Internet]. 2019;104(1):48–52. Disponible en: https://cdn.mdedge.com/files/s3fs-public/KircikCT104001048.PDF

19. Kosgodage US, Matewele P, Awamaria B, Kraev I, Warde P, Mastroianni G, et al. Cannabidiol is a novel modulator of bacterial membrane vesicles. Front Cell Infect Microbiol [Internet]. 2019;9:324. Disponible en: http://dx.doi.org/10.3389/fcimb.2019.00324

20. Moon SH, Roh HS, Kim YH, Kim JE, Ko JY, Ro YS. Antibiotic resistance of microbial strains isolated from Korean acne patients: Antibiotic resistance of microbial strains. J Dermatol [Internet]. 2012;39(10):833–7. Disponible en: http://dx.doi.org/10.1111/j.1346-8138.2012.01626.x

21. Oláh A, Markovics A, Szabó-Papp J, Szabó PT, Stott C, Zouboulis CC, et al. Differential effectiveness of selected non-psychotropic phytocannabinoids on human sebocyte functions implicates their introduction in dry/seborrhoeic skin and acne treatment. Exp Dermatol [Internet]. 2016;25(9):701–7. Disponible en: http://dx.doi.org/10.1111/exd.13042

22. Palmieri S, Maggio F, Pellegrini M, Ricci A, Serio A, Paparella A, et al. Effect of the distillation time on the chemical composition, antioxidant potential and antimicrobial activity of essential oils from different Cannabis sativa L. cultivars. Molecules [Internet]. 2021;26(16):4770. Disponible en: http://dx.doi.org/10.3390/molecules26164770

23. Quinchuela Barahona CD, Vaca Estrella IA. Estudio de las propiedades antibacterianas, antioxidantes y toxicidad de cuatro especies del género Huntleya (Orchidaceae) del Ecuador. 2020.

24. Saetama V, L. V, Vanegas ME, Cruzat C, D. B. Evaluación toxicológica de soluciones acuosas de ibuprofeno mediante bioensayos con Artemia salina, Allium schoenoprasum L y Lactuca sativa. Revista toxicológica [Internet]. 2018 [citado el 2 de febrero de 2023]; Disponible en: http://rev.aetox.es/wp-content/uploads/2018/12/Revista-de-Toxicologia-35.2-34-40.pdf

25. Sarah QS, Anny FC, Misbahuddin M. Brine shrimp lethality assay. Bangladesh J Pharmacol [Internet]. 2017;12(2):5. Disponible en: http://dx.doi.org/10.3329/bjp.v12i2.32796

26. Valdés AF-C, Martínez JM, Fidalgo LM, Parra MG, Ramos IS, Rodríguez DA, et al. Evaluación de la toxicidad de extractos de plantas cubanas con posible acción antiparasitaria utilizando larvas de Artemia salina L. Revista Cubana de Medicina Tropical [Internet]. c 2009; Disponible en: http://scielo.sld.cu/scielo.php?script=sci_arttext&pid=S0375-07602009000300009

Fermentation of *Agave americana* L. sap produced in Cayambe – Ecuador

Francisco Munive, María Páez, Cristina Romero Granja, Neyda Espín, Mary Casa-Villegas*   DOI. 10.21931/RB/2023.08.01.15

Department of Food Science and Biotechnology, Escuela Politécnica Nacional, Quito, Ecuador.
Corresponding author: mary.casa@epn.edu.ec

Abstract: Fermentation of agave sap, also known as exudate, has become an ancestral practice throughout Ecuadorian Andean. In Cayambe, located in this region, grows Agave americana L., which is recollected, and its sap is fermented. The agave-based fermented beverage, locally named "tzawar mishki", exhibits variable features, mainly ethanol concentration. In this work, fermentation conditions of agave sap were studied to enhance ethanol yield. Two thermal treatments for raw exudate were evaluated, pasteurization at boiling point for 30 minutes and sterilization at 121°C for 15 minutes; fermentation temperature, 30°C and room (around 18°C); and two yeast strains. Thermal pretreatments have a positive impact on reducing sugars and sucrose concentration. In the first case, an increase of 76 % and 30 % has been reported, while sucrose concentration quadrupled and doubled in pasteurized and sterilized samples, respectively. The highest ethanol concentration (63,31 g/L) and the best yield (66,21 %) were accomplished through agave sap pasteurized and fermented for 96 hours at 30°C. Negligible differences have been evidenced in ethanol and other volatile compounds content between the two yeast strains evaluated.

Key words: Agave sap, ethanol, fermentation, fermentable sugars, yeast.

Introduction

Agave (*Agave americana* L.), also known as Penco, Cabuya or Tzawar, is an endemic multipurpose vegetable specie that likely grows in arid lands of low fertility[1,2]. One of its primary uses relies on the agave sap called "tzawar mishki", here in after also called exudate, produced at the plant's optimum ripening point. Cutting the flower buds and drilling a bore in the central stem of the agave promotes exudate generation[3,4]. The composition of agave sap includes water, sucrose, fructose, glucose, proteins, and mineral salts. Sugars represent 75% of dry matter, within which 10% are fructooligosaccharides (FOS)[5]. Therefore, this sap becomes a suitable raw material for fermented beverages such as Guarango in Ecuador, Pulque in Mexico, and other distilled spirits[6,7]. Fermentation of agave sap from Mexico has been widely investigated even for optimizing operating conditions[8,9].

Although fermentation practices have spread across the Ecuadorian Andean region, few studies approach the technical aspects of Guarango production[6]. Agave sap fermentation carried out under non-controlled and non-aseptic conditions leads to the rise of the microbial population throughout the collection, transport, and treatment stages. Frequently, as the original microbiota of gathered exudate turns into the inoculum, it results in 24 to 96 hours of spontaneous fermentation[10]. Low replicability due to significant variations is reflected in ethanol concentration, volatile compounds occurrence, and ultimately different sensory attributes for the beverage. Hence, a standardized product requires controlled operating conditions highlighting temperature and yeast strain[11,12].

Temperature directly influences yeast growth and, thus, the satisfactory performance of the fermentation process. Below 18°C lag phase extends, and the specific growth rate decreases. The election of a commercial yeast averts fermented product alterations and reduces the antagonistic interaction between endemic microorganisms in raw agave sap[11,12]. Likewise, thermal pretreatment promotes modifications in the chemical composition of agave sap, referring to sugar composition, where higher sucrose concentration is evidenced after the sterilization process[13]. This study aims to determine operating conditions for agave sap fermentation related to thermal pretreatment, yeast strains and temperature to achieve a standardized beverage at an optimum ethanol yield.

Materials and methods

Sample collection and treatment

The exudate from Agave americana L. was collected in Cayambe city, located northeast of Pichincha province, Ecuador. Samples were filtered through a strainer, stored at 4°C and transported in sterile containers before a complementary filtration with a baghouse filter. Then, two thermal treatments were conducted, sterilization at 121°C for 15 minutes and pasteurization at boiling point for 30 minutes. Raw agave sap and treated samples were frozen at -14°C for physicochemical characterization..

Physicochemical analysis

For untreated and thermally treated agave sap and fermented samples drawn every 24 hours, the concentration of

2

total sugars, reducing sugars, soluble solids, glucose, fructose, sucrose, ethanol, and optical density (600 nm) was determined. In the fermentation case, the concentration of glucose, fructose, sucrose, and pH was measured only in the final product.

For total sugars, 10 µL of 80% wt. The phenolic solution was blended with 200 µL of the sample, then 1000 µL of sulphuric acid 96% was added with agitation and left for 10 minutes at room temperature. Later, the temperature rise to 25 °C for 10 minutes and absorbance was measured at 490 nm[14]. For reducing sugars, 250 µL of 3,5-dinitrosalicylic acid (DNS) was blended with 500 µL of sample and placed in a water bath at boiling point for 15 minutes. Then, 900 µL of distilled water was added to 100 µL of the solution to cool down, and absorbance was measured at 540 nm[15].

Soluble solids content and pH were determined by AOAC 932.14 (C) and AOAC 981.12, respectively. Glucose, fructose, and sucrose concentration were quantified through a commercial enzymatic kit (Sucrose/D-Fructose/D-Glucose Assay Kit–Megazyme). Likely, ethanol concentration by means of a commercial enzymatic kit (Ethanol Assay Kit – Megazyme, AOAC Method 2017.07).

Yeast strains

Two Saccharomyces cerevisiae strains were used. A commercial fructophilic yeast for agave fermentation (DistillaMax® TQ – LALLEMAND), and a commercial baker's yeast (LEVAPAN).

Fermentation

Laboratory fermentations were performed in tubes holding 40 mL of agave exudate thermally treated, which were inoculated with pre-activated yeast, as specified by providers, at an initial OD_{600nm} of 0,5. Fermentation tubes were covered with a cork stopper coupled with an air trap. Experiments were performed at 30 °C and room temperature (approximately 18 °C) without agitation. A total of eight treatments were conducted and identified, as shown in Table 1.

Yeast strain	Fermentation temperature	Thermal treatment	
		Pasteurized	Sterilized
BY	Room	T1	T2
	30 °C	T3	T4
AY	Room	T5	T6
	30 °C	T7	T8

Table 1. Experimental design for laboratory fermentations.

Volatile compounds determination

Methanol, n-propanol, ethyl acetate, and furfural were determined by GC using Agilent 7890A equipment fit in with a flame ionization detector (FID), Elite-volatiles column of 30 m length, 0,32 mm inner diameter, and 1,8 µm film thickness. Automatic injections of 0,5 µL were conducted with a 75:1 split at 220 °C. The column temperature was kept at 45 °C for 14 minutes. Helium was managed as the carrier gas at 6,5 mL/min. The FID detector was operated at 260 °C.

Statistical analysis

Analysis of variance (ANOVA) was managed by the software Statgraphics Centurion 19. Multiple range Fisher test was conducted for comparisons within individual assays. Mean differences were considered significant at p ≤ 0,05.

Results and discussion

Thermal pretreatment effect

The physicochemical evaluation of raw and thermally treated agave sap is shown in Table 2. Measured and theoretical ethanol concentration and the final to initial volume ratio after thermal treatment are also displayed.

After thermal treatments, results reveal a modification in sugar concentration, particularly in reducing sugars and sucrose. Figure 1 and Table 2 exhibited a slight variation in glucose concentration and a non-significant difference in fructose concentration when applied thermal treatments were. On the other hand, pasteurization increases sucrose concentration four times, while sterilization doubles it. This trend is primarily due to a high concentration of inulin and another fructooligosaccharide (FOS), usually part of raw agave sap. As thermal treatments are implemented, these carbohydrates could hydrolyze to monosaccharide or another oligosaccharide of lesser polymerization degree[4,16,17].

A noted increase in sucrose concentration from 1,66 g/L to 41,39 g/L was demonstrated when Agave salmiana exudate was heated up at 121°C for 15 minutes. The hydrolysis of fructans such as inulin with β- (2-1) bonds and levan with β- (2-6) is a likely cause[13]. Nevertheless, since the wide variety of oligosaccharides form different agave species, it is not feasible to grant inulin as the main hydrolyzable polysaccharide in agave[18]. Likewise, an increment of reducing sugars up to 46% has been reported after thermal treatments[13], which exceeds the increase of 30% reached in this work by means of sterilization. This variation could respond to the polymerization degree in sugars forming the samples. Moreover, fructans' structure and concentration are shifting since they mainly depend on environmental conditions and the plant's age[4,17].

A higher increase in total sugar concentration is evidenced after pasteurization due to the thermal hydrolysis of fructans and FOS forming agave sap. Also, water evaporation produced over 30 minutes of thermal treatment raises soluble solids in the sample. An increment of reducing sugars up to 63% has been stated when Agave americana L. sap is pasteurized at 80 °C for 30 minutes[19]. Primary outcomes are considerably lower than the 76% achieved in the present work.

The physicochemical composition of agave sap is also influenced by environmental factors as well as earlier fermentation processes in plant hollows as a result of multiple recollections throughout the day as common practice[13]. This statement has been validated since sugar composition strongly changes throughout the day; thus, fructan content at first recollection is significantly higher than 7 hours later[20]. Such variability in the initial composition of agave sap encourages standardization and industrialization employing dilution or concentration after thermal pretreatment.

The relevance of thermal pretreatments relies on fructans hydrolysis to get free sugars and initial microbiota reduction. Therefore, inoculation with commercial yeast strains is feasible after pasteurization or sterilization of agave sap. Native microbiota of Agave americana sap mainly comprises yeast (particularly Saccharomyces and Kluyveromyces species), lactic acid bacteria (LAB), and exopolysaccharides (EPS) producer bacteria[14,21]. This microbiota combination advocates much more complex fermented products with significant variability within batches referred to

Parameter	Raw	Pasteurized	Esterilized
Total sugars [mM]	555,92 ± 13,48[b]	906,38 ± 8,99[a]	550,10 ±9,74[b]
Reducing sugars [mM]	111,94 ± 4,25[a]	197,28 ± 2,13[c]	145,00 ± 0,94[b]
Glucose [g/L]	10,38 ± 0,98[b]	18,69 ± 2,94[a]	6,92 ± 1,96[b]
Fructose [g/L]	10,47 ± 0,99[a]	14,65 ± 2,96[a]	12,56 ± 1,97[a]
Sucrose [g/L]	35,50 ± 1,86[c]	145,95 ± 5,58[a]	86,78 ± 3,72[b]
Ethanol [g/L]	0,68 ± 0,03[a]	0,06 ± 0,01[c]	0,56 ± 0,01[b]
Soluble solids [°Brix]	11,50 ± 0,00[b]	19,05 ± 0,07[a]	11,50 ± 0,00[b]
OD	0,44 ± 0,00[b]	0,39 ± 0,00[c]	0,51 ± 0,00[a]
pH	6,34 ± 0,01[c]	8,74 ± 0,01[a]	7,29 ±0,01[b]
V_f/V_i	-	0,56	1,00
Theoretical ethanol [g/L]	29,77	95,62	56,68

Table 2. Physicochemical composition of raw and thermally treated agave sap.

3

*Values are expressed as mean ± standard deviation
†Values in the rows with different letters are significantly different at $p < 0,05$
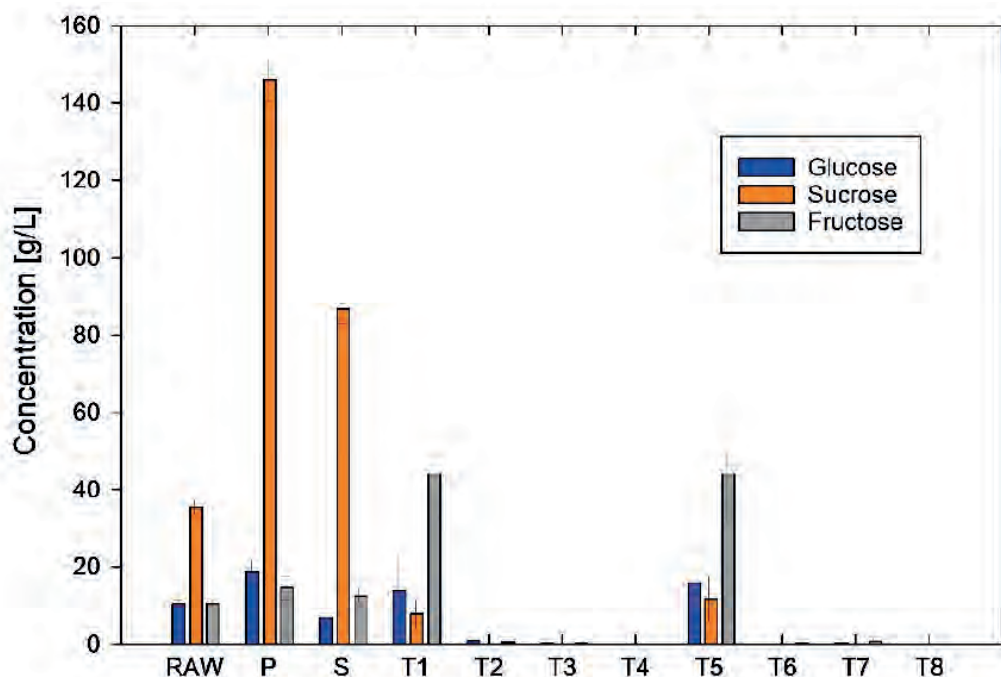
Figure 1. Glucose, fructose, and sucrose concentration for raw, pasteurized (P), sterilized (S) agave sap and for final fermented products (T1 – T8).

as ethanol concentration and organoleptic features. In this context, thermal treatments likely reduce heterogeneity in the final outcome of fermentation.

Fermentation

For each set of fermentation conditions, pH decreases to approximately 5 despite temperature and yeast strain. Concerning fermentation kinetics, Figure 2A reveals that at 30 °C stationary phase was achieved after about 48 hours, while maximum OD was evidenced after 96 hours at room temperature. At 18 °C fermentation process slows down regardless of yeast strain whenever it is a commercial one[22].

Despite the fact that more than 90% of total sugars were consumed in all treatments (except T1 and T5), the consumption rate was significantly different. Figure 2B denotes a maximum reduction of soluble solids at 30 °C after 48 hours and 96 hours for sterilized and pasteurized agave sap, respectively. Contrastingly, at room temperature, the maximum reduction was accomplished after 96 hours for sterilized agave sap; instead, uncompleted sugars consumption was registered after 144 hours for pasteurized agave sap.

According to Figure 2C, similar profiles can be distinguished for all treatments, excluding T5. In the early stages reducing sugars were accumulated until a maximum concentration due to invertase (β – D -fructosidase) action, which is released by yeast in peri plasmatic space and ultimately hydrolyses sucrose into glucose and fructose[23]. This is consistent with results in Figure 1, where pasteurized and sterilized agave sap exhibit higher sucrose concentrations than glucose and fructose before fermentation. At high sucrose concentrations, a significant increase of invertase activity is registered along with a temporary rise of reducing sugar concentration until yeast[24,25] metabolizes monosaccharides. Such behavior is also depicted in Figure 2C, where a maximum peak is evidenced. Then, decreasing sugars

4
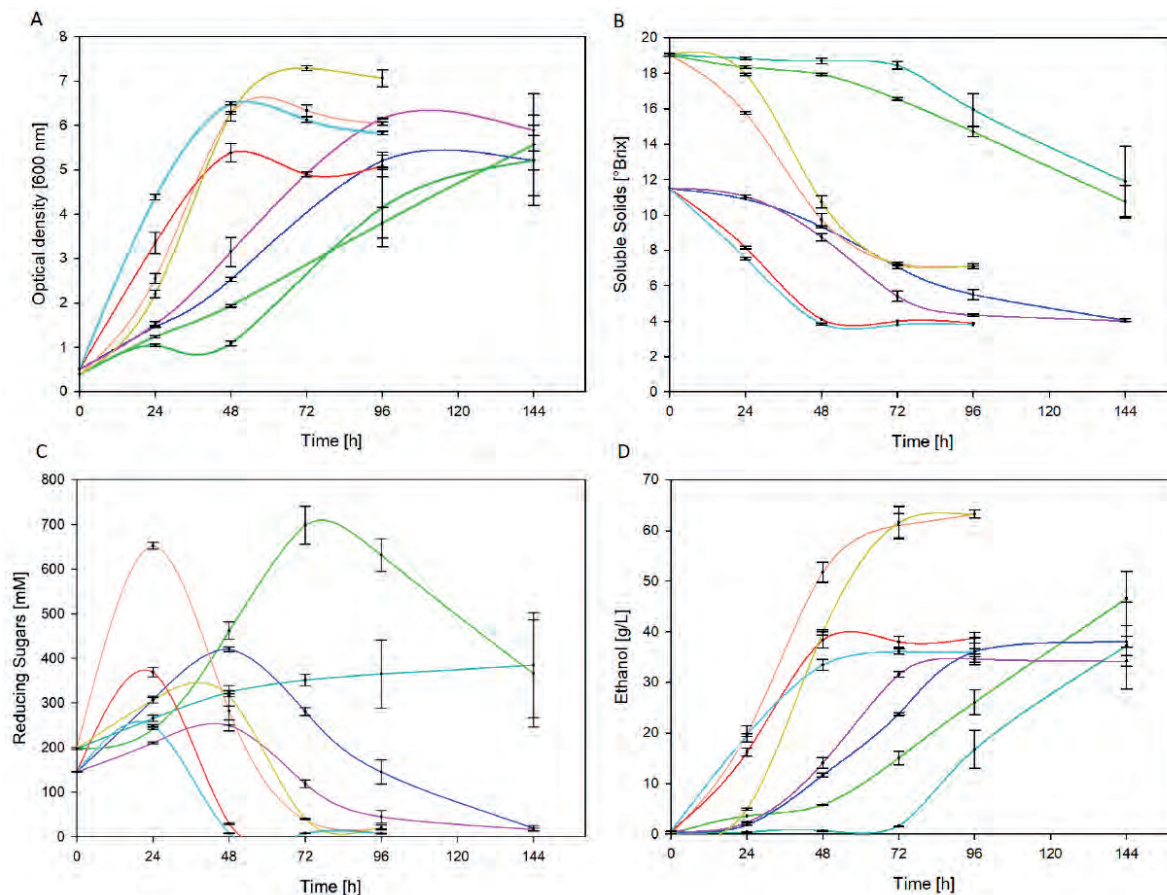
Figure 2. Fermentation kinetics of thermally treated agave sap at 30°C and room temperature related to optical density (A), soluble sugars (B), reducing sugars (C) and ethanol (D).

are metabolized in the cell interior through glycolysis and pyruvate converts to ethanol under anaerobic conditions[26].

The highest ethanol concentration reached was 63,31 g/L at 30°C with pasteurized agave sap through treatments T3 and T7 with yeast strain BY and AY, respectively. ANOVA analysis reveals that thermal pretreatment, fermentation temperature and interaction among them significantly influence (p ≤ 0,05) ethanol concentration, similar to yeast strain (p > 0,05). In turn, ethanol concentration achieved in fermentations from sterilized agave sap is not significantly different.

Figure 2D shows that fermentations conducted at 30 °C (T4 and T8) reached maximum ethanol concentration after 48 hours, while a similar concentration is attained at room temperature (T2 and T6) in twice as long. Furthermore, in treatments T1 and T5, sugars are partially metabolized as depicted in Figure 1, which advocates longer fermentations to achieve comparable ethanol concentration. Likewise, outcomes at present work overcome the final ethanol concentration of 28,67 g/L achieved after 72 hours by *Kluveromyces marxianus* strain fermentation of a 22 °Brix (60 % *Agave americana* sap and 40 % panela) must[27]. Similarly, ethanol concentration by fermentation of sterilized agave sap corresponds to that achieved afterward in the optimization of the fermentation process of *Agave salmiana* sap. At 28 °C and 105 g/L initial sugar concentration, a maximum ethanol concentration of 36,63 g/L was attained[8].

Ethanol yield and volatile compounds

Final ethanol concentration and yield for each set of conditions throughout fermentation are indicated in Table 3.

Ethanol yields in different treatments are equivalent

to 65 % and 66% achieved through the evaluation of two *Saccharomyces cerevisiae* strains for agave sap fermentation with an initial sugar concentration of 220 g/L. Superior ethanol yields, up to 81%, are reported by *Kluveromyces marxianus*; thus, this yeast seems more suitable than *Saccharomyces cerevisiae* for agave sap fermentation[28].

ANOVA analysis denotes that yeast strain, thermal pretreatment, fermentation temperature, and the interaction among two last significantly affect (p ≤ 0,05) ethanol yield. Even though no significant differences are identified between treatments (except T1 and T5), fermentations conducted at 30 °C fulfilled the maximum concentration in half of the time of analogous fermentations carried out at room temperature.

According to ethanol concentration in the final fermented product, treatments T3 and T7 have been selected as the optimum ones. In this sense, to accomplish superior productivity, it is proposed to pasteurize agave sap at boiling point for 30 minutes to implement a fermentation process at 30 °C employing any commercial yeast strain evaluated in this work. Table 4 depicts the concentration of volatile compounds identified in fermented products from optimum treatments.

Slight differences are evidenced in the volatile compounds profile when commercial *Saccharomyces cerevisiae* strains are employed. One of the major volatile compounds appearing in agave beverages is ethyl acetate, which builds up throughout fermentation by the esterification of acetyl CoA[29]. The concentration reached goes with 5 mg/L achieved in tequila must fermentation at 35 °C with *Saccharomyces cerevisiae* isolated strains[29] but differs significantly from 270 mg/L reported for commercial pulque[30]. Such divergence responds to the fermentation process,

	Ethanol [g/L]	Yield %	Total time [h]
T1	46,58 ± 5,38[b]	48,71 ± 5,62[b]	144
T2	38,03 ± 1,08[c]	67,09 ± 1,90[a]	144
T3	63,31 ± 0,81[a]	66,21 ± 0,84[a]	96
T4	38,79 ± 1,08[bc]	68,43 ± 1,90[a]	96
T5	37,27 ± 8,60[c]	38,97 ± 9,00[c]	144
T6	34,22 ± 1,08[c]	60,38 ± 1,90[a]	144
T7	63,31 ± 0,81[a]	66,21 ± 0,84[a]	96
T8	36,12 ± 0,54[c]	63,73 ± 0,95[a]	96

*Values are expressed as mean ± standard deviation
†Values in the column with different letters are significantly different (LSD; $p \leq 0,05$)

Table 3. Ethanol yields and concentration in the final fermented product.

Volatile [mg/L]	T3	T7
Ethyl acetate	4,154 ± 0,446	3,899 ± 1,09
1-Propanol	3,361 ± 0,301	2,312 ± 0,202
Methanol	< 0,105	< 0,105
Furfural	< 0,002	< 0,002

Table 4. Concentration of volatile compounds in the final fermented product.

which is mainly spontaneous for non-thermal treated agave sap[12]. The generation of ethyl acetate strongly depends on microbiota variety and density, where non-*Saccharomyces* strains exhibit an excessive production that negatively impacts the aroma profile of the beverage[12,31].

1-Propanol, as higher alcohol, promotes floral and fruity aromas as well as flavor release in the beverage[31]. The concentration of this alcohol in commercial pulque has been detected to be lower than 10 mg/L30 while could be up to 15 mg/L for agave must fermentation[29]. 1-Propanol can be generated through the α-ketobutyrate and subsequent decarboxylation or amino acid synthesis from sugars enzymatically managed[29,32]. The first is likely the pathway since significant reducing sugar consumption has been reported during fermentation, even though the path conducted by *Saccharomyces* strains is unspecified.

Methanol is the product of pectin demethylation at high temperatures and low pH during agave pineapple cooking[33]. As thermally treated agave sap has been fermented, like in commercial pulque, very low methanol concentration has been detected. Referring to furfural, it is part of all agave-based beverages since agave heads and sap are rich in inulin and FOS, which thermally hydrolyzed produce this aromatic aldehyde[34]. Agave sap recollected from 8 to 10 years old species heating up to boiling point under moderate monitoring of pH, and soluble solids content exhibits 0,051 mg/L furfural concentration[35]. In contrast, sap from 4 to 5 old *Agave salmiana* boiled and stored for two weeks at 25°C and 85 % of relative humidity evinces 0,004 mg/L[34]. In this sense, undetected concentration has been found in the fermented product, most probably because of *Agave americana* L. age during harvest.

Conclusions

Thermal pretreatments in agave sap positively impact reducing sugar concentration involving glucose, fructose, and sucrose.

The fermentation of thermally treated agave sap conducted at 30°C speeds up sugars to ethanol conversion compared to the fermentation process at room temperature.

Fermentation of pasteurized agave sap at 30°C (T3 and T7) achieved an ethanol concentration of 63,31 g/L, which significantly differs from the maximum concentration reported for sterilized agave sap at the same fermentation conditions.

Similar ethanol concentration was measured in sterilized agave sap samples. However, fermentation of these samples at 30°C reached the maximum ethanol concentration in half the time (48 hours) of those fermented at room temperature (96 hours).

Author Contributions

Francisco Munive: laboratory experiments performance and original draft writing. María Páez: writing review and editing. Cristina Romero Granja: funding acquisition and project administration. Neyda Espín: language review. Mary Casa-Villegas: experiments design and data analysis and interpretation.

Conflicts of Interest

The authors declare no conflict of interest.

Bibliographic references

1. Chen, Y., Chen, X., Hu, F., Yang, H., Yue, L., Trigiano, R., y Cheng, Z. Micropropagation of Agave Americana. HortScience, 2014, 49(3), 320–327.
2. Santos-Zea, L., Leal-Díaz, A., Cortés-Ceballos, E., y Gutiérrez- Uribe, J. Agave (Agave spp.) and its Traditional Products as a Source of Bioactive Compounds. Current Bioactive Compounds, 2012, 8(3), 218–231.
3. Molina-Guerrero, J. A., Botello-Álvarez, J. E., Estrada-Baltazar, A., Navarrete-Bolaños, J. L., Jiménez-Islas, H., Cárdenas-Manríquez, M., & Rico-Martínez, R. Compuestos volátiles en el mezcal. Revista Mexicana de Ingeniería Química, 2007, 6(1), 41-50.

5

6

4. Velázquez-Martínez, J., González-Cervantes, R., Hernández-Gallegos, M., Campos, R., Jiménez, A., y Arenas, M. Prebiotic potential of Agave angustifolia haw fructans with different degrees of polymerization. Molecules, 2014, 19(8), 12660–12675.

5. Ortiz, R., Pourcelly, G., Doco, T., Williams, P., Dormer, M., y Belleville, M. Analysis of the Main Components of the Aguamiel Produced by the Maguey-Pulquero (Agave mapisaga) throughout the Harvest Period. Journal of Agricultural and Food Chemistry, 2008, 56(10), 3682–3687.

6. De La Torre, L., Cummins, I., y Logan-Hines, E. Agave americana and Furcraea andina: Key Species to Andean Cultures in Ecuador. Botanical Sciences, 2018, 96(2), 246–266.

7. Paniagua-Zambrana, N., Bussmann, R., y Romero, C. Agave americana L. Agavaceae. Ethnobotany of the Andes. Ethnobotany of Mountain Regions. Springer, Cham. 2020, 1–6.

8. De León-Rodríguez, A., Escalante-Minakata, P., Barba de la Rosa, A., y Blaschek, H. Optimization of fermentation conditions for the production of the mezcal from Agave salmiana using response surface methodology. Chemical Engineering and Processing: Process Intensification, 2008, 47(1), 76–82.

9. Flores, J., Gschaedler, A., Amaya-Delgado, L., Herrera-López, E., Arellano, M., y Arrizon, J. Simultaneous saccharification and fermentation of Agave tequilana fructans by Kluyveromyces marxianus yeasts for bioethanol and tequila production. Bioresource Technology, 2013, 146, 267–273.

10. Valadez-Blanco, R., Bravo-Villa, G., Santos-Sánchez, N., Velasco-Almendarez, S., y Montville, T. The Artisanal Production of Pulque, a Traditional Beverage of the Mexican Highlands. Probiotics and Antimicrobial Proteins, 2012, 4(2), 140–144.

11. Escalante, A., López-Soto, D., Velázquez-Gutiérrez, J., Giles-Gómez, M., Bolívar, F., y López-Munguía, A. Pulque, a Traditional Mexican Alcoholic Fermented Beverage: Historical, Microbiological, and Technical Aspects. Frontiers in Microbiology, 2016, 7, 1026.

12. Lappe-Oliveras, P., Moreno-Terrazas, R., Arrizón-Gaviño, J., Herrera-Suárez, T., García-Mendoza, A., & Gschaedler-Mathis, A. Yeasts associated with the production of Mexican alcoholic nondistilled and distilled Agave beverages. FEMS yeast research, 2008, 8(7), 1037-1052.

13. Muñiz-Márquez, D., Contreras, J., Rodríguez, R., Mussatto, S., Wong-Paz, J., Teixeira, J., y Aguilar, C. Influence of thermal effect on sugars composition of Mexican Agave syrup. CyTA - Journal of Food, 2015, 13(4), 1–6.

14. Albalasmeh, A. A., Berhe, A. A., & Ghezzehei, T. A. A new method for rapid determination of carbohydrate and total carbon concentrations using UV spectrophotometry. Carbohydrate polymers, 2013, 97(2), 253–261.

15. Zhang, P., Hong, J., y Ye, X. Cellulase assays. Methods in molecular biology, 2009, 581, 213–231.

16. Garcia-Soto, M., Jiménez-Islas, H., Navarrete-Bolaños, J., Rico-Martinez, R., Miranda-López, R., y Botello-Álvarez, J. Kinetic study of the thermal hydrolysis of Agave salmiana for mezcal production. Journal of Agricultural and Food Chemistry, 2011, 59(13), 7333–7340.

17. Michel, C., Gallegos, G., Maldonado, E., y Aguilar, N. Effect of temperature and pH environment on the hydrolysis of maguey fructans to obtain fructose syrup. Revista Mexicana de Ingeniería Química, 2015, 20(3), 615–622.

18. Waleckx, E., Gschaedler, A., Colonna-Ceccaldi, B., y Monsan, P. Hydrolysis of fructans from Agave tequilana Weber var. azul during the cooking step in a traditional tequila elaboration process. Food Chemistry, 2008, 108(1), 40–48.

19. Chagua, P., Malpartida, R., y Ruíz, A. Tiempo de pasteurización y su respuesta en las características químicas y de capacidad antioxidante de aguamiel de Agave americana L. Revista de Investigaciones Altoandinas - Journal of High Andean Research, 2020, 22(1), 45–57.

20. Peralta-García, I., González-Muñoz, F., Rodríguez-Alegría, E., Sánchez-Flores, A., y López-Munguía, A. Evolution of Fructans in Aguamiel (Agave Sap) During the Plant Production Lifetime. Frontiers in Nutrition, 2020, 7, 175.

21. Villarreal-Morales, S., Montañez-Saenz, J., Aguilar-González, C., y Rodriguez-Herrera, R. Metagenomics of Traditional Beverages. Advances in Biotechnology for Food Industry, 2018, 14, 301–326.

22. Nuñez, M., Salazar, E., Páez, J., Rodríguez, R., y Soto, N. Caracterización fisiológica de dos levaduras nativas en cultivo puro y mixto usando fermentaciones de jugo de agave. Ciencia e Investigación Agraria, 2019, 46(1), 1–11.

23. Walker, G., y Stewart, G. Saccharomyces cerevisiae in the Production of Fermented Beverages. Beverages, 2016, 2(4), 30.

24. Islam, M., y Lampen, J. Invertase secretion and sucrose fermentation by Saccharomyces cerevisiae protoplasts. Biochimica et Biophysica Acta, 1962, 58(2), 294–302.

25. Marques, W., Raghavendran, V., Stambuk, B., y Gombert, A. Sucrose and Saccharomyces cerevisiae: a relationship most sweet. FEMS Yeast Research, 2016, 16(1), 107.

26. Batista, A., Miletti, L., y Stambuk, B. Sucrose fermentation by Saccharomyces cerevisiae lacking hexose transport. Journal of Molecular Microbiology and Biotechnology, 2004, 8(1), 26–33.

27. Archila, M. A., Ventura-Canseco, C., Ruiz-Valdiviezo, V. M., Gutiérrez-Miceli, F. A., Ruiz-Cabrera, M. A., Lara-Hidalgo, C., & Grajales-Lagunes, A. Agave americana honey fermentation by Kluyveromyces marxianus strain for "comiteco" production, a spirit from Mexican southeast. Revista Mexicana de Ingeniería Química, 2017, 16(3), 771-779.

28. López-Alvarez, A., Díaz-Pérez, A., Sosa-Aguirre, C., Macías-Rodríguez, L., y Campos-García, J. Ethanol yield and volatile compound content in fermentation of agave must by Kluyveromyces marxianus UMPe-1 comparing with Saccharomyces cerevisiae baker's yeast used in tequila production. Journal of Bioscience and Bioengineering, 2012, 113(5), 614–618.

29. Arellano, M., Pelayo, C., Ramírez, J., y Rodriguez, I. Characterization of kinetic parameters and the formation of volatile compounds during the tequila fermentation by wild yeasts isolated from agave juice. Journal of Industrial Microbiology and Biotechnology, 2008, 35(8), 835-841.

30. Léon-Rodríguez, D., Escalante-Minakata, P., Jiménez-García, M. I., Ordoñez-Acevedo, L. G., Flores Flores, J. L., y Barba de la Rosa, A. P. Characterization of volatile compounds from ethnic agave alcoholic beverages by gas chromatography-mass spectrometry. Food Technology and Biotechnology, 2008, 46(4), 448-455.

31. Gamero, A., Dijkstra, A., Smit, B., y de Jong, C. Aromatic potential of diverse non-conventional yeast species for winemaking and brewing. Fermentation, 2020, 6(2), 50.

32. Guzmán, A. M. V., López, M. G., y Chávez-Servia, J. L. Chemical composition and volatile compounds in the artisanal fermentation of mezcal in Oaxaca, Mexico. African Journal of Biotechnology, 2012, 11(78), 14344-14353.

33. Díaz-Montaño, D. M., Délia, M. L., Estarrón-Espinosa, M., y Strehaiano, P. Fermentative capability and aroma compound production by yeast strains isolated from Agave tequilana Weber juice. Enzyme and Microbial Technology, 2008, 42(7), 608-616.

34. Santos-Zea, L., Leal-Díaz, A. M., Jacobo-Velázquez, D. A., Rodríguez-Rodríguez, J., García-Lara, S., y Gutiérrez-Uribe, J. A. (2016). Characterization of concentrated agave saps and storage effects on browning, antioxidant capacity and amino acid content. Journal of Food Composition and Analysis, 45, 113-120.

35. Maldonado-Guevara, B. I., Martín del Campo, S. T., y Cardador-Martínez, A. (2018). Production process effect on Mexican agave syrups quality: A preliminary study. Journal of Food Research, 7(3), 50-57.

ARTICLE / INVESTIGACIÓN

Propagation of the Colombian genotype of cacao (*Theobroma cacao* L.) CNCh-12 by somatic embryogenesis

Sandra Marcela Macias Naranjo[1]*, Ana María Henao Ramírez[1], Aura Inés Urrea Trujillo[2]

[1] Agrobiotechnological Development Center for Innovation – CEDAIT, Universidad de Antioquia, Colombia.
[2] Biology Institute, Universidad de Antioquia, Colombia.
Corresponding author: smarcela.macias@udea.edu.co

Abstract: Cocoa production (*Theobroma cacao* L.) is essential globally and constitutes one of the leading export products for Colombia. Understanding the limitations faced by this crop in Latin American countries, it is required, among other aspects, to contribute to strengthening the first link in the production chain through efficient propagation methods and genetic improvement. Knowing that somatic embryogenesis is an alternative to conventional propagation and constitutes an obligatory step in a breeding platform, the objective of this work was to establish a somatic embryogenesis protocol until the plantlet acclimatization in the nursery for the regional genotype *CNCh-12*, a promising material with productivities higher than 2,000 kg/ha. Different protocols were evaluated, from callogenesis induction, through the expression of primary somatic embryos (PSE) followed by maturation and subsequent conversion to plantlet two types of explants (petal and staminode) and culture time (according to the stage). Additionally, the induction of secondary somatic embryos (SSE) was evaluated in two culture media (L and F). For *CNCh-12*, the petal was found as an appropriate explant, with a minimum time of 15 days in induction for PSE formation, without difference between the culture media F and L (22 average embryos). Embryo maturation was achieved in medium F after 30 days, followed by an additional 30 days for conversion to plantlet (52.83%). The concentration of salts to increase the conversion and development of the embryos was 1/5 of that used in F. The highest number of SSE was in the L medium. Finally, the *ex-vitro* adaptation was achieved when the plants were planted in 50:50 sand-coconut fiber and moistened weekly with Hoagland's solution (1:10).

Key words: Cacao, petals, *in vitro* propagation, plant growth regulators, somatic embryogenesis.

Introduction

The *Theobroma cacao* L. is a diploid tree species (2N), native to South America and domesticated approximately 3000 years ago in Central America[1]; it belongs to the class Magnoliopsida, order Malvales and family Malvaceae[2]. The genus Theobroma has 22 species; the only ones that represent high commercial value are *T. Grandiflorum* and mainly *T. cacao*[3].

Cocoa cultivation is essential as it is a fundamental part of the economy of many underdeveloped countries[4]. According to The International Cocoa Organization (ICCO), most of the production is concentrated on the African continent in countries such as Côte d'Ivoire and Ghana[5]. Although traditional cocoa production figure at worldwide, in average the yield is low, per example, world production of fine cocoa is less than 5%. In general, low productivity is due to the incidence of diseases, poor technological infrastructure, lack of training of farmers, etc. that affect the production of the crop and obtain fine flavor cocoa[1]. In Colombia, cocoa is grown in 29 of the 32 departments of the country; for the year 2020, 188 thousand hectares of planted areas were registered, distributed in the departments of Santander (41%), Antioquia (9%), Arauca and Huila (8%), Tolima (7%) and Nariño (5%)[6]. The national average production in the last ten years was 46 thousand tons. However, for the year 2020, it was close to 63 thousand, distributed mainly in the departments of Santander (26 thousand tons), Antioquia (5 thousand tons), and Arauca (5 thousand tons), which on average register annual productivity of 500 kg/ha/year[6].

Currently, the Colombian market is seeking to increase the areas of cocoa crops and the efficient production of cocoa since there are many unproductive trees, mainly due to inadequate crop management, deterioration, old age and sexual incompatibility[7]. Some of the methods used for the propagation of *T. cacao*, such as planting from seeds, have as a disadvantage the germination times, the rapid loss of viability of the seed after being extracted and the high genetic variability characteristic of the crop, so it has been necessary to implement asexual propagation methods such as grafting (conventional procedure) and somatic embryogenesis (biotechnological method). The induction of embryogenic structures in somatic tissue permits us to keep the same genetic information as the parental plant from which the explant was taken[8]. To this end, effective propagation protocols have been developed following the guidelines of somatic embryogenesis in different cocoa genotypes[9–13].

Traditionally, new cocoa genotypes have been developed that can improve crop yields or add value due to their chemical, organoleptic and aroma characteristics, among others. Currently, despite having these new genotypes, they are not having a sufficient impact on the country's production chain due, among other causes to the lack of sufficient production of plant material[7]. An example of these genotypes is the regional elite genotype *CNCh-12*. This genotype has high polyphenol content, with approximately

76.23 mg GAE g-1[14] and high productivity of 2.000kg/ha; these characteristics make it a candidate for mass propagation by somatic embryogenesis. There is only one research work about somatic embryogenesis with *CNCh-12*, in which it was possible to induce the formation of embryos until the globular stage. Still, the somatic embryos did not continue their development until the complete plant[15]. Considering the importance of *CNCh-12* and intending to contribute to strengthening the cocoa production chain, the objective of this research was to establish a protocol for propagation by somatic embryogenesis of this regional genotype.

For this purpose, we studied the embryogenic response of *CNCh-12* to different culture protocols that vary in growth regulators and nutrient concentrations in the different stages of the embryogenic process: induction, expression, multiplication, maturation, and germination to plantlet.

Materials and methods

Plant material

For the explant type, the response of petals and staminodes to the embryogenic process was studied. Unopened flower buds of the cocoa genotype *CNCh-12* were provided by the Compañía Nacional de Chocolates (CNCh) at the Yariguies farm, located in the department of Santander, Colombia; the flower buds were collected and duly stored in Falcon™ tubes containing a solution of DKW salts[16,17] at half concentration. Shipment was carried out in thermal coolers with cold gel packs.

For the disinfection of plant material, the protocol proposed by Henao *et al.* (2018)[15] was followed with some modifications. Initially, flower buds are immersed in a solution of Belico® fungicide; the active ingredient is carbendazim at a concentration of 2 g/l for 40 minutes, followed by washing with sterile distilled water. Subsequently, they are immersed in a 0.5% hypochlorite solution for 5 minutes. They were washed with sterile distilled water, and finally, they were engaged in a streptomycin solution at 250 ppm for 20 minutes, renewing the solution after 10 minutes. Finish then with rinses in sterile water. All steps are performed in sterile Falcon™ tubes and constant agitation in a rotator. After the disinfection process, the flower buds were transferred to sterile Petri dishes, where they were dissected to extract the petals and staminodes to be sown in the respective culture media. The disinfection process and all stages of culture and subculture were carried out in a laminar flow chamber to maintain the required sterile conditions.

Protocols

To address the embryogenic process, the developmental stages of somatic embryogenesis were taken as a reference: induction, expression, multiplication, maturation, germination, and plant development. The induction stage comprises the induction of callogenesis and embryogenic callus formation; in the expression stage, the formation of primary somatic embryos occurs; in multiplication, the formation of secondary embryos or repetitive embryogenesis is induced; in maturation, the embryo continues with the development of its apical and root poles with the extension of the hypocotyl; in germination, the conversion to a plantlet with photosynthetically active tissues is achieved.

To induce the embryogenic process and evaluate the development of the different stages, the protocols selected were those proposed by Li, Traore, Maximova, & Guiltinan (1998)[18] (Protocol L), Maximova *et al.* (2002)[19] (Protocol M), Fontanel *et al.* (2002)[20] (Protocol F) and Henao *et al.* (2018)[15] (Protocol H).

Induction stage

In the induction stage, the effect of the culture media (protocols) was evaluated during a culture time of 15 days in each medium for protocols L and M and 15, 30, 45 and 60 days for protocols F and H, on callogenesis like the number of explants with granular, filamentous, friable, and nodular callus. The culture media used were as follows: PCG [micronutrients, macronutrients and vitamins DKW, 2,4-D (1.98 mg/L), TDZ (0.005 mg/L), L-glutamine (250 mg/L), glucose (20000 mg/L) and Gellex (2700 mg/L)], SCG-1 [Gamborg Vitamins, 2,4-D (1.98 mg/L), kinetin (0.3 mg/L), coconut water (5%), Mc Cowns salts, glucose (20000 mg/L) and Gellex (2700 mg/L)], SCG-2 [Gamborg vitamins, 2,4-D (1.98 mg/L), BA (0, 3 mg/L), Mc Cowns salts, glucose (20000 mg/L) and Gellex (2700 mg/L)], INDI [micronutrients, macronutrients and vitamins DKW, 2,4-D (1 mg/L), kinetin (0.25 mg/L), glucose (30000 mg/L) and Gellex (3000 mg/L)] and INDILab [same as INDI with the addition of arginine (0.4355 g/L), glycine (0.1876 g/L), leucine (0.328g/L), lysine (0.4565 g/L), tryptophan (0.5105 g/L)].

Expression stage

In the expression stage, the culture medium, explant type and time in the induction medium were evaluated on (1) the total number of somatic embryos; (2) the number of embryos between globular and torpedo and the number of cotyledonary embryos; (3) the number of roots and (4) the number of necrotic explants at 15, 30, 45 and 60 days of culture. The following culture media were used: ED [micronutrients, macronutrients and vitamins DKW, sucrose (30000 mg/L), glucose (20000 mg/L), Gellex (2700 mg/L)] and INDIExp [micronutrients, macronutrients and vitamins DKW, glucose (30000 mg/L), Gellex (3000 mg/L)]. For the evaluation of repetitive embryogenesis at the expression stage, EM2 medium [MS macronutrients, DKW micronutrients and vitamins, sucrose (40000 mg/L) and Gellex (3000 mg/L)] was used.

Multiplication stage

The repetitive embryogenic response of the *CNCh-12* genotype was evaluated based on the protocols of Fontanel *et al.* (2002)[20] and Li *et al.* (1998)[18], which presented the best significant results after statistical analysis in primary embryogenesis in terms of embryos formed number. Regarding repetitive embryogenesis, a stage where a greater number of embryos per explant is obtained, primary embryos in the early cotyledonary stage were taken from culture media at the expression stage, ED and INDIexp media for the L and F protocols, respectively. The embryos were cut transversely into fragments and placed in CM2 repetitive embryogenesis induction medium in the case of protocol F. They were subsequently transferred to EM2 maturation medium and MM6 germination medium. In the case of protocol L, the embryo fragments are placed in a PCG induction medium for the induction of repetitive embryogenesis. They subsequently follow the process and media used in primary embryogenesis to finish MM6 maturation and germination medium.

For the induction of repetitive embryogenesis, CM2 medium [MS macronutrients, micronutrients and DKW vi-

tamins, 2,4,5-T (1 mg/L), adenine (0.25 mg/L), glucose (30000 mg/L) and Gellex (3000 mg/L)] was used.

Maturation and germination stage

In the embryo maturation and germination stage, the culture media PR and MM6 of protocols L and F were first evaluated on embryos with the renewal of the culture media every 30 days. In the second step, the response of embryos as stem height and root length to different concentrations of macronutrients was studied. Three different concentrations of macro MS salts were evaluated, ½ of concentration (½ C) = 2.115 g/l (Fontanel et al., 2002), ¼ of concentration (¼ C) = 1.0575 g/l and 1/5 of concentration (1/5 C) = 0.846 g/l. To continue with the conversion of embryos to plantlets, the effect of macronutrient concentration on stem and root length and the number of leaves formed on plantlets at 45 days was evaluated in embryos from EM2-MM6 (after remaining 15 days in MM6 medium).

The culture media used were: MM6Lab [equal to MM6 with different concentrations of NAA (0.1 mg/L)], MM6-1 (1) [MS macronutrients at 1/5 concentration, micronutrients and DKW vitamins, NAA (0.01 mg/L), GA3 (0.02 mg/L), activated carbon (1000 mg/L), glucose (40000 mg/L) and Gellex (3000 mg/L)], MM6-2 (2) [DM macronutrients at 1/4 concentration, DKW micronutrients and vitamins, NAA (0.01 mg/L), GA3 (0.02 mg/L), GA3 (0.02 mg/L), activated carbon (1000 mg/L), glucose (40000 mg/L) and Gellex (3000 mg/L)], MM6-3 (3) [DM macronutrients at 1/2 concentration, DKW micronutrients and vitamins, NAA (0.01 mg/L), GA3 (0.02 mg/L), GA3 (0.02 mg/L), activated carbon (1000 mg/L), glucose (40000 mg/L) and Gellex (3000 mg/L)] and PR [micronutrients, macronutrients and vitamins DKW, KNO3 (200 mg/L), sucrose (5000 mg/L), glucose (10000 mg/L), Gellex (2700 mg/L)].

For all experiments performed, the culture media were pH adjusted to 5.8 and autoclaved for 20 minutes at 121ºC.

Culture conditions

All the cultures were randomly placed in a growth chamber at an average temperature of 28°C ± 2°C and 70% relative humidity and continuous darkness in induction, expression, and multiplication stages. In the maturation stage and germination, the early cotyledonary embryos and plantlets were cultured in 500 ml vessels and placed in a growth

chamber under light with a 12-hour photoperiod and a photosynthetic photon flux density (PPFD) of 50 µmol m − 2 per second, at an average temperature of 28°C ± 2°C and 70% relative humidity.

Statistical analysis

For each of the protocols (treatments) evaluated, 5 replicates per explant (petal and staminode) were considered; the experimental unit is a Petri dish, in each of which 25 explants were sown. There were 10 Petri dishes per treatment, 1000 explants were planted per replicate, 8 replicates were performed for induction and expression, and 3 replicates to evaluate multiplication. In maturation, there were 3 replicates to assess the incidence of macronutrient concentration conversion with 5 replicates, each with 5 plants.

The data obtained from the experiments carried out to determine the effect of culture medium, explant type and culture time on the formation of embryogenic structures (factors) were analyzed using the R project statistical software. Compliance with the assumptions of normality and homoscedasticity of variance was verified; in cases where this was not achieved, nonparametric tests, Friedman's test, Wilcoxon's test and Welch's test were applied as appropriate. All tests were tested with 95% confidence intervals and a significance value of 0.05.

Results

Induction stage

In this initial phase of the culture, it was found that the explants began to increase in size after one week, mainly the staminodes. From day 15 of the culture, callus growth was observed on the surface of the explants in all the protocols evaluated. The 4 most common callus types of the embryogenic process in cocoa were recorded: granular (GC), nodular (NC), filamentous (FC) and friable (FR), described by Henao et al. (2018) (Fig. 1A-1D).

Between INDI (Protocol F) and INDILab (Protocol H) culture media, there were no significant differences in callus formation. However, for the type of explants, callus formation was achieved in the staminodes at 15 days (p=0.030, p=0.006 and p=0.831) (Fig.S1). On the other hand, for

STAGE	Somatic Embryogenesis Protocols							
	Li et al. (1998)		Maximova et al. (2002)		Fontanel et al. (2002)		Henao et al. (2018)	
	Culture media	Days	Culture media	Days	Culture media	Days	Culture media	Days
Induction	PCG	15	PCG	15	INDI	15, 30, 45, 60	INDILab	15, 30, 45, 60
	SCG-1	15	SCG-2	15				
Expression	ED	60	ED	60	INDIExp	45	INDIExp	45
Multiplication	PCG	15	N/A		CM2	60	N/A	
	SCG-1	15			EM2	45		
Maturation and germination	PR	150	PR	150	MM6	150	MM6Lab	150

Table 1. Different culture media are used in each stage of the somatic embryogenesis process and the permanence of explants.

3

4
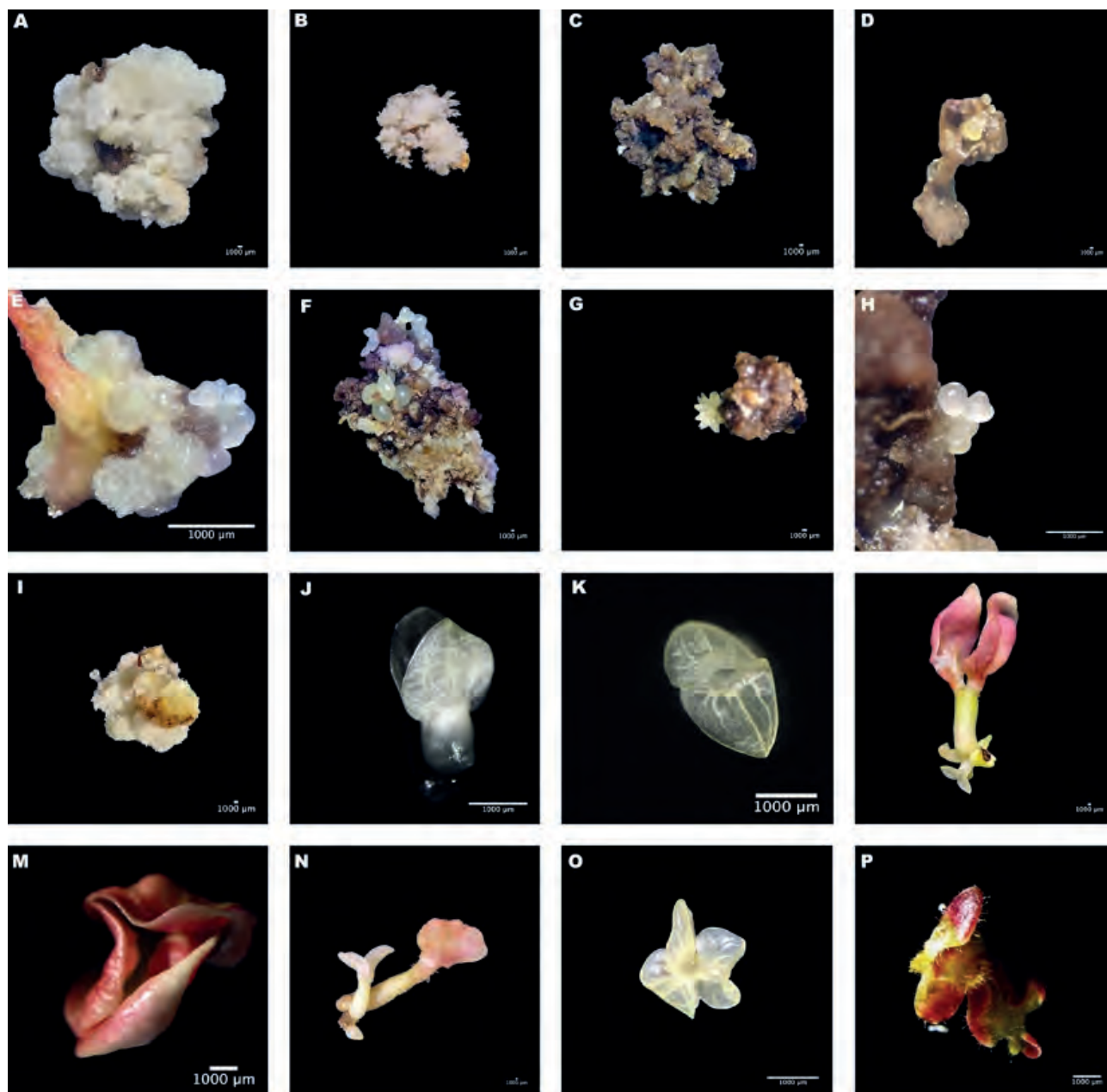
Figure 1. Different callus types and embryonic stages were observed in the process of somatic embryogenesis for the *CHCh-12* genotype. Granular callus (A), filamentous callus (B), friable callus (C), and nodular callus (D). Clusters of embryos in different callus types, granular from staminode, mixed and friable from petals (E-G). Different stages of embryo development globular and heart (H), torpedo (I), and early cotyledonary (J-K). Growth of somatic embryos on embryos with mature cotyledons (L). Abnormalities are presented by some somatic embryos, tricotyledonary (M), monocotyledonary (N), and multicotyledonary (O). Abnormal cotyledons with overgrowth and abundant trichomes in their structure (P).

SCG-1 (Protocol L) and SCG-2 (Protocol M) culture media, the result was similar; there were no significant differences between media, but important differences between explants (p<0.001), being higher callus formation in staminodes (Fig. S2).

Regarding the type of callus developed, in all protocols and in both explants, the formation of granular callus was similar between culture media and days of evaluation. Staminodes in INDI (Protocol F) and INDILab (Protocol H) media showed higher granular callus development concerning petals at days 30 and 45 (p=0.002 and p=0.001) (Fig.S3).

In the induction media of protocols L and M, the amount of nodular callus was not higher than 10%, no significant differences were found between them, but between ex-

plants, favoring the production of this type of callus in petals (p<0.001) (Fig.S4). The percentage obtained of filamentous and friable callus in protocols F and H did not exceed 0.5% and 5.3%, respectively; for protocols L and M it was no more than 0.07% and 0.22%, respectively. With these values, in some cases, it was not possible to perform an analysis of variance.

Expression stage

In the culture media used in the expression stage, normal and abnormal embryos were obtained. The external appearance of normal embryos agrees with that described by Li *et al.* (1998)[18] and Henao *et al.* (2018)[15] for other genotypes, with characteristics such as yellowish, matte white

and translucent white color, with pink or white cotyledons and with defined embryonic axis, sometimes, the growth of embryos occurred in groupings or clusters (Fig. 1E-1G). Among the abnormalities found, trichotyledonary embryos were the most abundant, followed by multi-cotyledonary, mono-cotyledonary embryos (Fig. 1M-1O), without hypocotyl and without a defined embryonic axis. Trichome-like structures were also present on the cotyledons, as described by Maximova *et al.* (2002)[19] (Fig. 1P). It should be emphasized that all embryos, normal and abnormal, were transferred to maturation media. In addition, the number of embryos obtained in the expression media of protocols F and H was analyzed considering the time the explants remained in the induction media.

For explants with 15 days in the induction medium and subculture in expression media, the medium of protocol F (p=0.016) has the highest production, an average of 22 embryos per explant compared to an average of 2 embryos obtained with protocol H. The difference between petals and staminodes was significant (p=0.005), obtaining with petals a higher formation of embryos (22 on average per explant), 11 times more than in staminodes (Fig. 2A). For the explants maintained for 30 days in the induction medium, the difference in total embryos formation was not significant. However, in the explant type, staminodes have a higher average number of embryos. 35 embryos (p=0.009) (Fig. S5A-B). This indicates that both petal and staminode are suitable explants for embryo expression in this genotype.

In explants maintained for 45 days in the induction medium, total embryo production did not show significant differences between culture media or explants (Fig.S5C). The explants maintained for 60 days in induction did not show substantial differences in the total number of embryos formed in the expression media. Regarding the type of explant, callus from petals formed an average of 22 somatic embryos, with significant differences compared to those

obtained from staminodes, with an average of one embryo (p=0.0024) (Fig. 2B).

Multiplication stage

The embryogenic response of the *CNCh-12* genotype to repetitive embryogenesis was positive for both the F and L protocols, being statistically significant in embryo production (p-value = 0.011 and 0.002, respectively). A higher embryo production was obtained in repetitive embryogenesis concerning primary embryogenesis. In the case of repetitive embryogenesis, 4.7 embryos were obtained using protocol L, compared to 6.4 obtained with protocol F. Also, with protocol L the embryo formation was uniform per explant, while with protocol F embryo production was discontinuous over time (Fig. 3).

Maturation and germination stage

Initially, after one month of being transferred to the maturation media, MM6 (Protocol F) and MM6Lab (Protocol H), the embryos continued with the development of the cotyledons and elongated, some reaching 1 cm in height. By the second month, the formation of the main root, the consolidation of the cotyledons and the growth in the height of the embryos were evident. In the third month, for both protocols, the development of leaf primordia and cotyledon fell, defined apices, and developed root systems were observed in some embryos (Fig. 4B), with secondary roots and root hairs. By the fourth month, true leaves were present, with plantlets up to 6 cm in protocol F (Fig. 4A) and 2 cm in protocol H. In both protocols, the persistence of cotyledons was present in some plantlets.

Complete plants were obtained *in vitro* in protocols F (Fig. 4A-C) and H with a germination percentage in the fifth month of 52.83% and 40.42%, respectively. Regarding explant type, both petal and staminode complete plants were obtained with a conversion percentage of up to 54% and
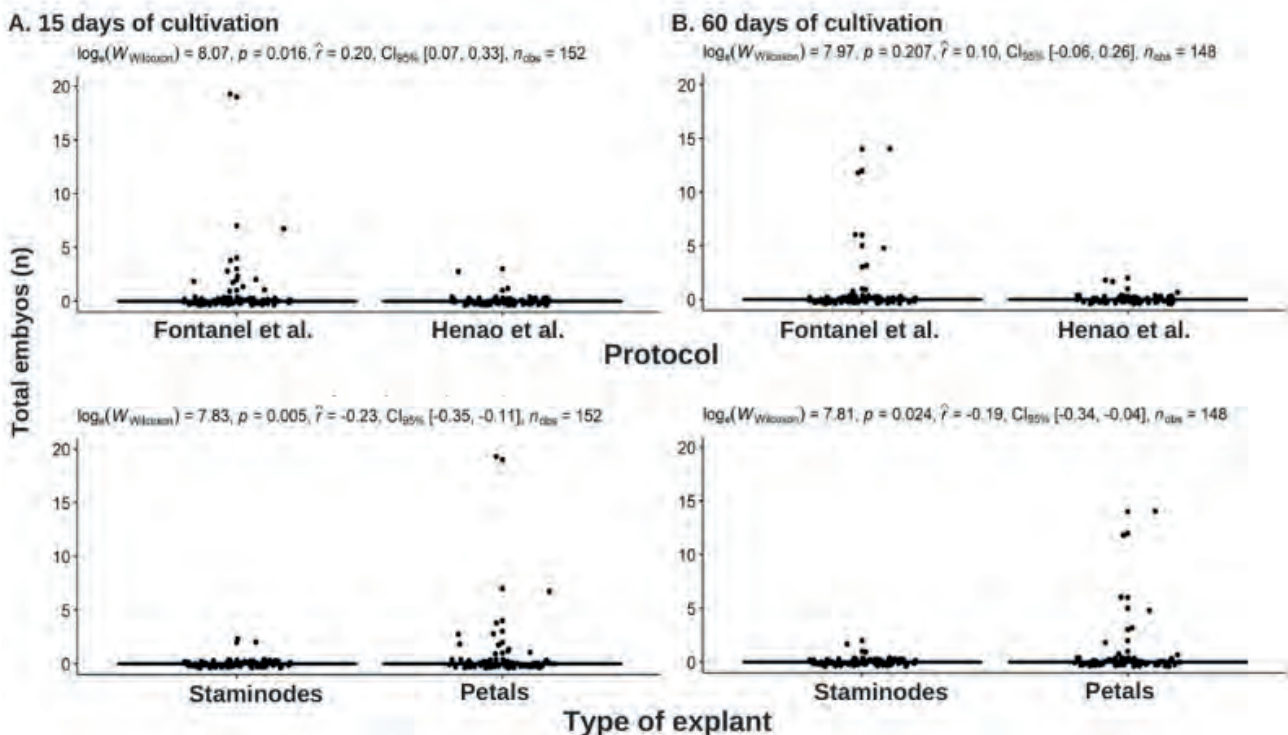
Figure 2. Effect of culture medium expression stage, explant type and time in induction medium on the total number of somatic embryos obtained in the Fontanel *et al.* (2002) (F) and Henao *et al.* (2018) (H) protocols. (A) 15 days of culture, (B) 60 days of culture.

5

6
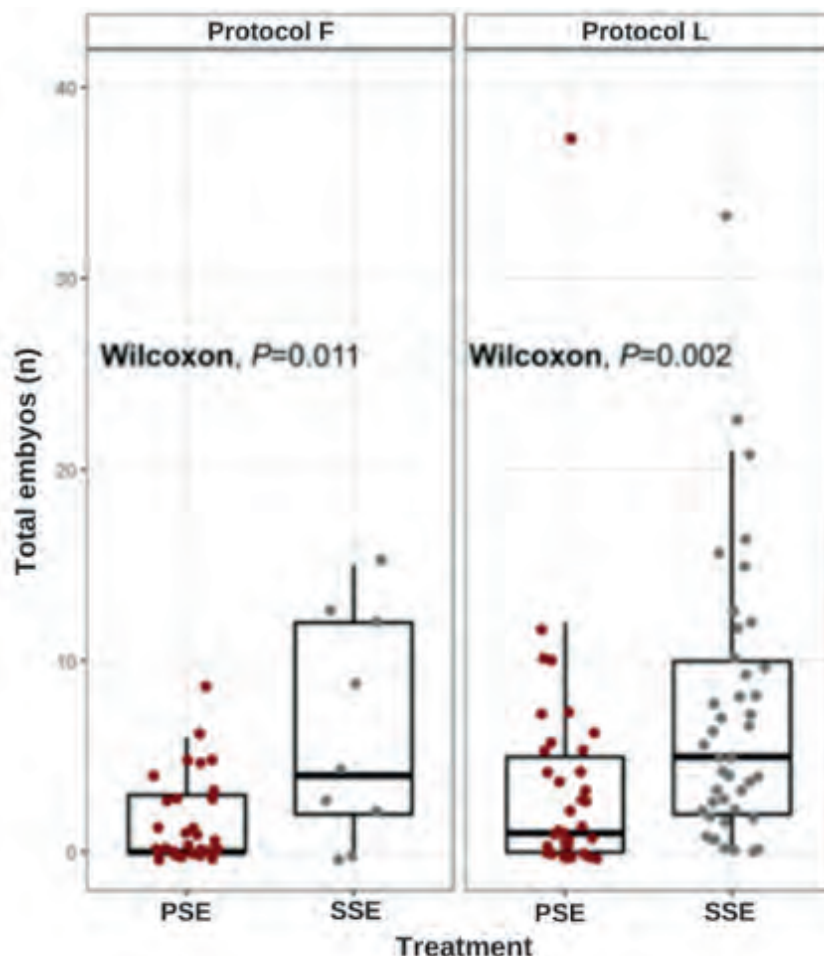
Figure 3. Effect of culture protocol F (Fontanel *et al.* (2002)) and protocol L (Li *et al.* (1998) on the induction of primary and repeat or secondary embryogenesis measured as a total number of somatic embryos.

21%, respectively. Between protocols and between explant types, no significant differences were found in the number of embryos advancing in their development. Some of the embryos with abnormalities continued to develop to full plant, and abnormal germinated embryos were also obtained with characteristics such as overgrowth of the cotyledons, atrophied apices, or absence of roots (data not shown).

Embryos at the maturation stage on PR medium (Protocols L and M), did not show root development or true leaves and cotyledon growth was slow. By the fourth month on maturing medium, embryos had not exceeded 1 - 3 cm in height (Fig. 4E) and some with true leaves (Fig. 4D). Embryos from both protocols were completely necrotic (Fig. 4F).

On the other hand, for the growth and development of the plantlets, two types of embryos were considered, embryos coming from the EM2 medium and embryos coming from the transition of the EM2-MM6 medium. In embryos from EM2 medium, the effect of the salt concentration of the MS medium on embryo development was found to be significant after 45 days of culture (p<0.0001) (Fig.S6). The highest growth 2.33 cm in length, was obtained in the culture medium 1/5 C salts. When the culture medium contained ¼ C the length was 1.64 cm and with ½ C was 1.43 cm. Regarding root length, significant differences were found in growth after 45 days (p<0.0001) (Fig.S7), 3.64 cm of root length was the highest root growth with ¼ C, with 1/5 C was 2.87 cm and 1.40 cm with ½ C was.

In treatment 2, embryos from the transition between EM2-MM6 media, there was no significant difference in elongation between the 3 concentrations evaluated after 45 days of culture (p=0.75) (Fig.S8). The average measurements for 1/5 C, ¼ C and ½ C were 1.86 cm, 2.27 cm and 1.91 cm, respectively. Root growth was evident in the three treatments at this stage, having significant differences among them (p<0.0001) (Fig.S9), with ½ C having the highest growth with an average of 3.77 cm, followed by 3.71 cm for ¼ C and 3.49 cm for the ½ C. For the number of true leaves, there were significant differences between treatments after 45 days (p=0.00058) (Fig.S10)., having plants with an average of 2.34 leaves in 1/5 C, 1.69 in ¼ C and 1.57 in ½ C. Therefore, embryo growth is favored in the mentioned parameters in the MS medium at 1/5 C.

Plantlets with ≥2 cm of height with the root system (primary and secondary roots) and more than one true leaf were adapted to *ex vitro* conditions (Fig. 5A). They were initially sown in magentas containing a 1:3 sand: coconut fiber mixture, moistened with Hoagland solution 1:10 and with the addition of 1 g of mycorrhiza per planting well (Fig. 5B). Subsequently, they were covered and placed in a climatic chamber (conditions previously mentioned) for 40 days, with irrigation every 2 days and fertilization once a week (Fig. 5C) and were uncovered after 20 days. The plants were then transferred to the Yariguies farm in Barrancabermeja, Santander, where the adaptation process continued (Fig. 5D-E). After 1 month of adaptation, the survival rate was 89.4%, and after 2 months, it was 71.2%.

Discussion

Staminodes excelled in their response to callus formation, mainly because of the short time they took to form. This behavior was observed in all the protocols studied and
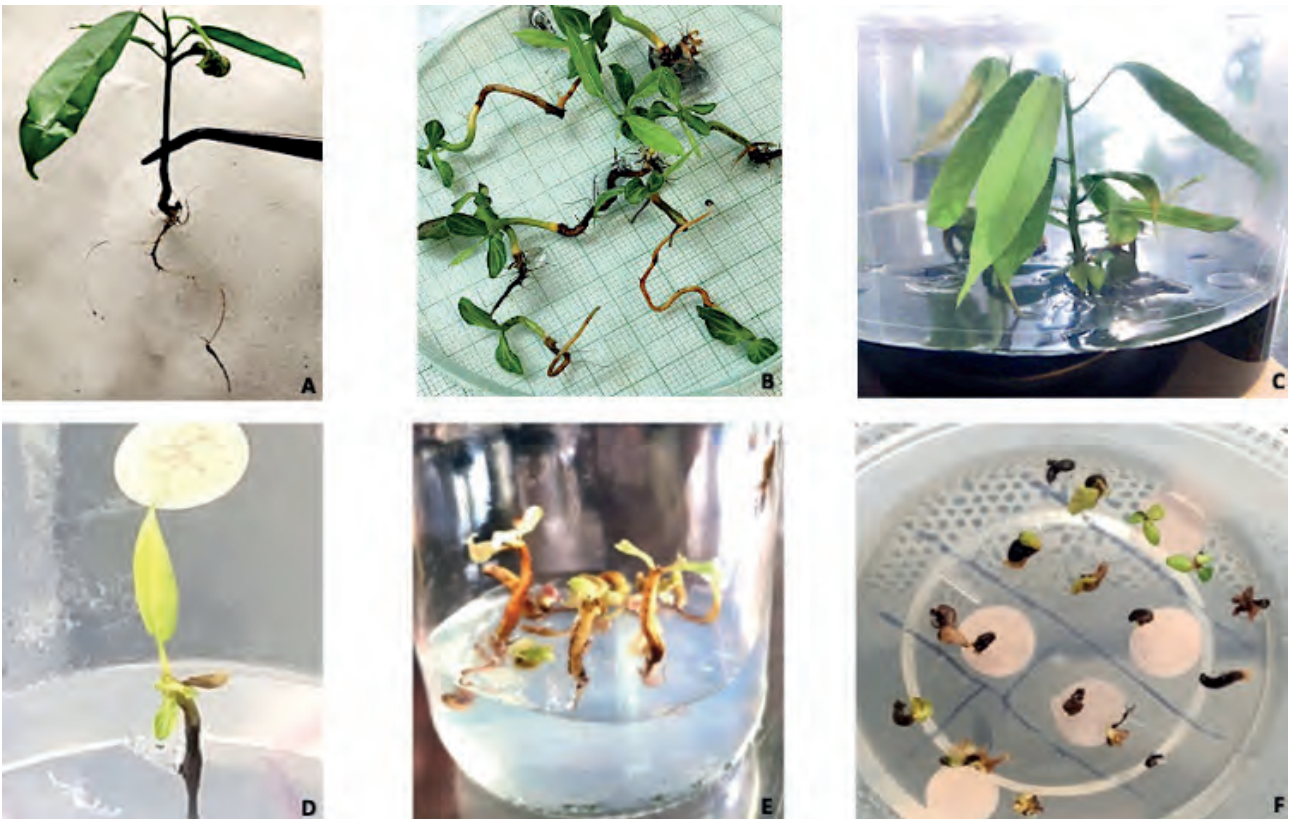
Figure 4. Maturation stage. Plants on MM6 maturation medium (A-C) from protocol F (Fontanel *et al.* (2002)). Single embryo with true leaf growth on PR maturation medium belonging to protocol M (Maximova *et al.* (2002)) (D). Growing embryos in PR medium from protocol L (Li *et al.* (1998) (E). Necrosis of explants from protocols M (Maximova *et al.* (2002)) and L (Li *et al.* (1998)) in PR medium after four months (F).

Concentration of MS salts	Embryos from EM2 medium		Embryos from the transition between EM2-MM6 medium		
	Stem height (cm)	Root length (cm)	Stem height (cm)	Root length (cm)	Number of true leaves (n)
1/5 C	1,4	2,64	1,88	3,72	3,4
¼ C	1,3	3,57	0,72	1,56	2,1
½ C	0,8	2,00	1,28	4,48	2,0

Table 2. Effect of salt concentration of MS medium (1/5 C, ¼ C, ½ C) on plantlet development after 45 days of culture.

was repetitive for the culture times. This result agrees with that described by Díaz, Sánchez, Valera-Leal, & García (2015)[21], where more excellent callus formation is reported in staminodes in Venezuelan cocoa genotypes. It is possible that the structure of the petals, being concave, does not allow total contact with the culture medium, and this undoubtedly influences the response to the callusing process, initiating the development on the surfaces in direct interaction with the culture medium, taking longer to develop completely, the opposite happens in the staminodes, where most of it is in contact with the medium. This result in the callogenesis stage could lead to suggest the exclusive use of cocoa staminodes as described by Guillou *et al.* (2018)[10], Li *et al.* (1998)[18] and Maximova *et al.* (2002)[19]; however, the embryogenic response of explants with slow callus growth, such as petals, should not be ruled out, as some genotypes have developed a greater number of embryos in petals with respect to staminodes[22].

In protocols, F and H, contrary to what was described by Henao *et al.* (2018)[15], complete regeneration of embryos of the *CNCh-12* genotype was achieved, and the average number of embryos at 15 days exceeded those reported at 30 days of evaluation. The embryogenic tissues in the present study were not dedifferentiated like the previously reported ones. This response is because cocoa crops are subject to changing climatic conditions, and some variables, such as the stages of development of flower buds, tree age, and environmental factors, among others, were not evaluated in this study. It is not excluded that these variables had a different incidence on the results of both studies, even if they were of the same genotype.

The protocol developed by Li *et al.* (1998)[18] and the modifications made by Maximova *et al.* (2002)[19] have been widely used in the primary and secondary somatic embryogenesis of different cocoa genotypes. With these protocols, it has been possible to evaluate parameters such as *in vi-*

Figure 5. *Ex vitro* adaptation process. Plants in MM6 medium with desirable characteristics initiate the adaptation process (A). Newly planted plants of the *CNCh-12* genotype after remaining in ideal conditions in the climatic chamber and maturation medium (B-C). Plants recently transferred to the Yariguies farm and were fully exposed to the environment (D) and two months after the transfer (E).

tro culture efficiency, response to other exogenous agents such as antioxidants, optimal concentrations of growth regulators and their effects, among others. *CNCh-12* genotype with the L and M protocols formed somatic embryos on the second week in the expression medium, a result that does not coincide with that described by Li *et al.* (1998)[18] and Maximova *et al.* (2002)[19]. Most embryos originated from white granular callus, against the results described by Boutchouang *et al.* (2016)[23] and Kone *et al.* (2019)[24], who found that most embryogenic structures came from friable callus. The difference obtained in embryo formation between these two protocols has as a possible explanation for the use of kinetin in the SCG-1 medium; this is supported by the results of Kouassi, Kahia, Kouame, Tahi, and Koffi (2017)[25], who evaluated four elite genotypes of Ivory Coast and found that in culture media enriched with kinetin, more embryogenic callus formation was presented than in those supplemented with 6-Benzylaminopurine (BAP). In this same sense, García *et al.* (2016)[26] suggest that depending on the genotype evaluated, kinetin or BAP can be used in this stage of the embryogenic process.

The abnormalities presented by some of the embryos can be attributed to the presence in the induction media of the auxin 2,4-dichloro phenoxy acetic acid (2,4D) and the thidiazuron (TDZ). These have been considered to cause increased proportions of abnormal embryos in different species[27,28], particularly in cocoa, Garcia *et al.* (2016) describe that depending on the genotype evaluated and the concentration of 9.05 uM of 2,4D it is possible to induce the formation of abnormal embryos.

Endogenous signals, such as phytohormones present in the tissue, and exogenous signals, such as added growth regulators, stress (temperature, light, mechanical damage), explant type-dependent tissue sensitivity or combinations of several of these factors, can result in tissue dedifferentiation and callus formation, root formation or somatic embryo development. In this study, the root was obtained on the explant, and a similar result was described by Botero *et al.* (2015)[29], who obtained root formation in embryogenic callus induced under dark conditions for the species *Psychotria ipecacuana*. These responses may obey the same principle explained by Fehér (2014)[30], who, in his compilation of several studies using Arabidopsis tissues, demonstrated that auxin and cytokinin-enriched media induce the formation of a particular callus characterized by a gene expression pattern similar to root meristems and also that the early stages of callus development are similar to those of lateral root development even when the process are induced in explants from aerial organs.

A problem *in vitro* cocoa culture is the browning of callus and embryos by exudation of phenolic compounds, and autocatalytic and light-driven processes[31]. Activated char-

coal has been widely used in somatic embryo production and germination processes by various researchers for its ability to adsorb growth inhibitory substances in culture media, it has been shown that in liquid or semi-solid media, it decreases the concentration of phenolic compounds and oxidants[32]. Phenolic compounds are abundant in the genotype studied, *CNCh-12*; taking this into account, the results obtained lead us to think that at this stage of development, phenolic substances accumulate in greater proportion, inhibiting or weakening the normal development of the embryos.

Furthermore, sucrose is used as a carbon source in the PR medium; Thomas (2008)[32] also states that the autoclaving of this carbohydrate results in a growth inhibitor compound called 5-hydroxymethyl-furfural, which is eliminated by absorption thanks to the activated carbon. Due to the above, apart from the concentrations of phenolic compounds in the PR medium, there could be the formation of other inhibitory compounds in the medium that do not allow the development of somatic embryos. On the other hand, the MM6 and MM6Lab media have GA3 (gibberellic acid) in their composition, which in species such as *Sesamum indicum* and *Panax ginseng*, favors the conversion of somatic embryos to plantlets (Gaj 2004)[33]. The slow growth observed in the cotyledons in the PR medium could be the effect of the lack of growth regulators in the culture medium.

Embryos with high presence of trichomes on mature cotyledons (Fig. 1P) did not develop complete plants, similar to that reported by Iracheta-Donjuan *et al.* (2019)[34], who describes that globular embryos with the presence of trichomes did not continue development to the cotyledonary stage. In the present study, the formation of embryos from other embryos (Fig. 1L and 1N) in the maturation medium reflects repetitive embryogenesis, as described by Maximova *et al.* (2002)[19].

The most plausible causes of the difference between our results with those of other researchers may lie first in the contrast of the genotypes evaluated, reiterating that the genetic information of each one of them is decisive in the embryogenic response[26,35]. Second, not all explants nor all culture media are suitable to induce embryo formation; for this to happen, each genotype has different requirements of carbon sources, growth regulators, vitamins, and minerals, among others and differential sensitivity of their tissues[25,36–38].

Conclusions

This study describes for the first time the induction of primary and repetitive embryogenesis up to the production of nursery-adapted plantlets of the Colombian regional elite genotype *CNCh-12*. To produce *CNCh-12* plantlets, the protocol of Li *et al.* (1998)[18] is effective up to the germination stage, where the culture media of the protocol of Fontanel *et al.* (2002)[20] allows obtaining plantlets with better characteristics for the subsequent process of growth in nursery and planting in the field. It was validated that the optimal explant for the embryogenic process is the staminodium for shorter response time and the complete culture cycle until obtaining plantlets is at least 4 months, and it was found that, for this genotype, as in other cases, the total number of somatic embryos obtained in the process of secondary or repetitive embryogenesis is greater than that obtained in primary embryogenesis. In addition, the *ex vitro* adaptation process is successfully carried out with high survival percentages for plants with desirable characteristics.

Supplementary Materials

The following are available online, Figure S1: Effect on induction stage of culture medium, explant type and time in induction medium on the total number of callus obtained in Fontanel *et al.* (2002) (F) and Henao *et al.* (2018) (H) protocols at 15, 30 and 45 days of culture, Figure S2: Effect on induction stage of culture medium, explant type and time in induction medium on the total number of callus obtained in Maximova et al. (2002) (M) and Li et al. (1998) (L) protocols at 15, 20, 25 and 30 days of culture, Figure S3: Effect on induction stage of culture medium, explant type and time in induction medium on the total number of granular callus obtained in Fontanel *et al.* (2002) (F) and Henao *et al.* (2018) (H) protocols at 15, 30, 25 and 45 days of culture, Figure S4: Effect on induction stage of culture medium and explant type on the total number of nodular callus obtained in Maximova *et al.* (2002) (M) and Li *et al.* (1998) (L) protocols, Figure S5: Effect on the stage of expression of the culture medium, type of explant and time spent in the induction medium on the total number of somatic embryos obtained in treatments F and H. Where S4-S8 corresponds to 15 days (A), S6-S7 corresponds to 30 days (B), S2-S5 corresponds to 45 days (C) and S1-S3 to 60 days (D), Figure S6: Stage I for genotype *CNCh-12*. Embryo length from EM2 medium in the different treatments. T1: 1/5 MS salts, T2: ¼ MS salts, T3: ½ MS salts, after 45 days of culture on MM6 medium, Figure S7: Stage I for genotype *CNCh-12*. Root length of embryo from EM2 medium in the different treatments. T1: 1/5 MS salts, T2: ¼ MS salts, T3: ½ MS salts, after 45 days of culture on MM6 medium, Figure S8: Stage II for genotype CNCh-12. Embryo length from EM2-MM6 medium in the different treatments. T1: 1/5 MS salts, T2: ¼ MS salts, T3: ½ MS salts, after 45 days of culture on MM6 medium., Figure S9: Stage II for genotype *CNCh-12*. Root length of embryo from EM2-MM6 medium in the different treatments. T1: 1/5 MS salts, T2: ¼ MS salts, T3: ½ MS salts, after 45 days of culture on MM6 medium, Figure S10: Stage II for genotype *CNCh-12*. Number of true leaves of the embryo from EM2-MM6 medium in the different treatments. T1: 1/5 MS salts, T2: ¼ MS salts, T3: ½ MS salts, after 45 days of culture on MM6 medium.

Author Contributions

Conceptualization, Sandra Marcela Macias Naranjo; formal analysis, Sandra Marcela Macias Naranjo, Ana Maria Henao Ramirez; methodology, software, investigation, resources, data curation, writing—original draft preparation, Sandra Marcela Macias Naranjo; writing—review, editing, and supervition, Ana Maria Henao Ramirez, Aura Inés Urrea Trujillo. All authors have read and agreed to the published version of the manuscript.

Conflicts of Interest

The authors declare no conflict of interest.

Bibliographic references

1. Argout X, Salse J, Aury JM, et al. The genome of Theobroma cacao. Nature Genetics. 2011;43(2):101-108. doi:10.1038/ng.736
2. Nair KPP. Cocoa (Theobroma Cacao L.).; 2010. doi:10.1016/b978-0-12-384677-8.00005-9
3. Diby L, Kahia J, Kouamé C, Aynekulu E. Tea, Coffee, and Cocoa. Encyclopedia of Applied Plant Sciences. 2016;3:420-425. doi:10.1016/B978-0-12-394807-6.00179-9
4. Rizzuto L, Díaz K. El mercado mundial de cacao. Revista agroalimentaria, ISSN 1316-0354, No 18, 2004, pags 48-60. 2004;10.
5. ICCO. Quarterly Bulletin of Cocoa Statistics, Vol. XLIV, No. 3, Cocoa Year 2017/18.; 2018.
6. Ministerio de Agricultura y Desarrollo Rural (MADR) -Dirección de Cadenas Agrícolas y Forestales. Cadena de Cacao.; 2021. Accessed September 30, 2022. https://sioc.minagricultura.gov.co/Cacao/Documentos/2020-03-31 Cifras Sectoriales.pdf
7. Abbott P, Benjamin T, Burniske G, et al. Análisis de La Cadena Productiva Del Cacao En Colombia.; 2019. doi:10.13140/RG.2.2.10934.14400
8. Winkelmann T. Somatic Versus Zygotic Embryogenesis: Learning from Seeds BT - In Vitro Embryogenesis in Higher Plants. In: Germana MA, Lambardi M, eds. Springer New York; 2016:25-46. doi:10.1007/978-1-4939-3061-6_2
9. Ajijah N, Syafaruddin, Inoue E. Cacao (Theobroma cacao L.) somatic embryos development under heat stress condition. IOP Conference Series: Earth and Environmental Science. 2020;418:12012. doi:10.1088/1755-1315/418/1/012012
10. Guillou C, Fillodeau A, Brulard E, et al. Indirect somatic embryogenesis of Theobroma cacao L. in liquid medium and improvement of embryo-to-plantlet conversion rate. In Vitro Cellular & Developmental Biology - Plant. 2018;54(4):377-391. doi:10.1007/s11627-018-9909-y
11. Henao-Ramírez AM, Urrea-Trujillo AI. Somatic Embryogenesis for Clonal Propagation and Associated Molecular Studies in Cacao (Theobroma cacao L.). Agricultural, Forestry and Bioindustry Biotechnology and Biodiscovery. Published online 2020:63-102. doi:10.1007/978-3-030-51358-0_5
12. Urrea Trujillo AI, Atehortúa Garcés L, Gallego Rúa AM. Regeneración vía embriogénesis somática de una variedad colombiana élite de Theobroma cacao L. Revista Colombiana de Biotecnología; Vol 13, Núm 2 (2011). Published online 2011. https://revistas.unal.edu.co/index.php/biotecnologia/article/view/27916
13. Garcia C, Marelli JP, Motamayor JC, Villela C. Somatic Embryogenesis in Theobroma cacao L. Methods in Molecular Biology. 2018;1815:227-245. doi:10.1007/978-1-4939-8594-4_15
14. Rojas L, Rúa A, Gil A, Londoño J, Atehortúa L. Monitoring accumulation of bioactive compounds in seeds and cell culture of Theobroma cacao at different stages of development. In Vitro Cellular & Developmental Biology - Plant. 2015;51:174-184. doi:10.1007/s11627-015-9684-y
15. Henao Ramírez AM, de la Hoz Vasquez T, Ospina Osorio TM, Garcés LA, Urrea Trujillo AI. Evaluation of the potential of regeneration of different Colombian and commercial genotypes of cocoa (Theobroma cacao L.) via somatic embryogenesis. Scientia Horticulturae. 2018;229(October):148-156. doi:10.1016/j.scienta.2017.10.040
16. Driver J, Kuniyuki AH. In vitro propagation of Paradox Walnut root stock. HortScience: a publication of the American Society for Horticultural Science. 1984;18:506-509.
17. Mcgranahan G, Driver J, W T. Tissue Culture of Juglans. In: Vol 26. ; 1987:261-271. doi:10.1007/978-94-017-0992-7_19
18. Li Z, Traore A, Maximova S, Guiltinan MJ. Somatic embryogenesis and plant regeneration from floral explants of cacao (Theobroma cacao L.) using thidiazuron. In Vitro Cellular & Developmental Biology - Plant. 1998;34(4):293-299. doi:10.1007/BF02822737
19. Maximova S, Alemanno L, Young A, Ferriere N, Traore A, Guiltinan M. Efficiency, genotypic variability, and cellular origin of primary and secondary somatic embryogenesis of Theobroma Cacao L. In Vitro Cellular & Developmental Biology - Plant. 2002;38:252-259. doi:10.1079/IVP2001257
20. Fontanel A, Gire-Bobin S, Labbé G, et al. In vitro multiplication and plant regeneration of Theobroma cacao L. via stable embryogenic calli. 10 IAPTC Congress. Plant Biotechnology. Published online 2002:23-28.
21. Díaz A, Sánchez D, Valera-Leal J, García A. Formación de embriones somáticos en cinco cultivares de Theobroma cacao L. cultivados en Venezuela. Biotecnología Vegetal. 2015;15:27-34.
22. Kouassi M, Koffi K, Oumar S, Tahi M, Toure M, Konan E. Comparison of systems combining auxins with thidiazuron or kinetin supplemented with polyvinylpirrolidone during embryogenic callus induction in three Theobroma cacao L. genotypes. International Journal of Biological and Chemical Sciences. 2018;12:804. doi:10.4314/ijbcs.v12i2.15
23. Boutchouang R, Olive F, Tchouatcheu GA, Niemenak N. Influence of the position of flowers buds on the tree on somatic embryogenesis of cocoa (Theobroma cacao L.). International Journal of Plant Physiology and Biochemistry. 2016;8:7-16. doi:10.5897/IJGMB2016.0247
24. Kone D, Kouassi M, N'Nan-Alla O. Induction of somatic embryos of recalcitrant genotypes of Theobroma cacao L. Journal of Applied Biosciences. 2019;133:13552. doi:10.4314/jab.v133i1.7
25. Kouassi M, Kahia J, Kouame C, Tahi M, Koffi K. Comparing the Effect of Plant Growth Regulators on Callus and Somatic Embryogenesis Induction in Four Elite Theobroma cacao L. Genotypes. HortScience. 2017;52:142-145. doi:10.21273/HORTSCI11092-16
26. Garcia C, Corrêa F, Findley S, et al. Optimization of somatic embryogenesis procedure for commercial clones of Theobroma cacao L. African Journal of Biotechnology. 2016;15(36):1936-1951. doi:10.5897/ajb2016.15513
27. Dewir YH, Nurmansyah, Naidoo Y, Teixeira da Silva JA. Thidiazuron-induced abnormalities in plant tissue cultures. Plant Cell Reports. 2018;37(11):1451-1470. doi:10.1007/s00299-018-2326-1
28. Garcia C, Furtado de Almeida AA, Costa M, et al. Abnormalities in somatic embryogenesis caused by 2,4-D: an overview. Plant Cell, Tissue and Organ Culture. 2019;137(2):193-212. doi:10.1007/s11240-019-01569-8
29. Botero Giraldo C, Urrea Trujillo AI, Naranjo Gómez EJ. Potencial de regeneración de Psychotria ipecacuanha (Rubiaceae) a partir de capas delgadas de células. Acta Biológica Colombiana. 2015;20:181-192.
30. Fehér A. Somatic embryogenesis — Stress-induced remodeling of plant cell fate. Biochimica et Biophysica Acta (BBA) - Gene Regulatory Mechanisms. 2014;1849. doi:10.1016/j.bbagrm.2014.07.005
31. Pancaningtyas S. Study on the presence and influence of phenolic compounds in callogenesis and somatic embryo development of cocoa (Theobroma cacao L.). Pelita Perkebunan (a Coffee and Cocoa Research Journal). 2015;31:14-20. doi:10.22302/iccri.jur.pelitaperkebunan.v31i1.81
32. Thomas TD. The role of activated charcoal in plant tissue culture. Biotechnology advances. 2008;26(6):618-631. doi:10.1016/j.biotechadv.2008.08.003

33. Gaj MD. Factors Influencing Somatic Embryogenesis Induction and Plant Regeneration with Particular Reference to Arabidopsis thaliana (L.) Heynh. Plant Growth Regulation. 2004;43(1):27-47. doi:10.1023/B:GROW.0000038275.29262.fb

34. Iracheta-Donjuan L, Cruz-López LA, López-Gómez P, Avendaño-Arrazate CH, Ortíz-Curiel S. 2iP Y BRASINOSTEROIDES PROMUEVEN LA INDUCCIÓN DE LA EMBRIOGÉNESIS SOMÁTICA EN Theobroma cacao L. AGROProductividad. 2019;12:65+.

35. Ajijah N, Hartati RS, Rubiyo R, Sukma D, Sudarsono S. EFFECTIVE CACAO SOMATIC EMBRYO REGENERATION ON KINETIN SUPPLEMENTED DKW MEDIUM AND SOMACLONAL VARIATION ASSESSMENT USING SSRs MARKERS. AGRIVITA, Journal of Agricultural Science; Vol 38, No 1 (2016): FEBRUARYDO - 1017503/agrivita.v38i1619 . Published online January 8, 2016. http://agrivita.ub.ac.id/index.php/agrivita/article/view/619

36. Ajijah N, Hartati R. PRIMARY AND SECONDARY SOMATIC EMBRYOGENESIS OF CACAO: THE EFFECT OF EXPLANT TYPES AND PLANT GROWTH REGULATORS. Indonesian Journal of Agricultural Science. 2020;20:69. doi:10.21082/ijas.v20n2.2019.p69-76

37. Issali A, Abdoulaye T, Koffi K, N'goran J, Sangaré A. Characterization of Callogenic and Embryogenic Abilities of Some Genotypes of Cocoa (Theobroma cocoa L.) Under Selection in Cote d`Ivoire. Biotechnology. 2008;7. doi:10.3923/biotech.2008.51.58

38. Quainoo A, Dwomo A. The Effect of TDZ and 2, 4-D Concentrations on the Induction of Somatic Embryo and Embryogenesis in Different Cocoa Genotypes. Journal of Plant Studies. 2012;1. doi:10.5539/jps.v1n1p72

11

ARTICLE / INVESTIGACIÓN

Effect of different drying airflows and harvest periods on the quality of specialty coffee (*Coffea arabica* L.)

Valeria Arévalo[1], William Mejía[1], Juan Manuel Cevallos-Cevallos[2], Johana Ortiz-Ulloa[1]*

[1] University of Cuenca, Faculty of Chemical Sciences, Department of Biosciences, Cuenca, Ecuador.
[2] Escuela Superior Politécnica del Litoral (ESPOL), Centro de Investigaciones Biotecnológicas del Ecuador (CIBE), Guayaquil, Ecuador.
Corresponding author: johana.ortiz@ucuenca.edu.ec

Abstract: Coffee is one of the most consumed commercial beverages worldwide, and coffee growers are constantly seeking innovative processing techniques to improve the quality of the final product. This study evaluated the influence of four drying airflows and three harvest periods on the chemical composition of green and roasted specialty coffee beans. The samples were obtained from the Hacienda La Papaya in Loja, Ecuador. Liquid and gas chromatographic techniques characterized the chemical profile of coffee beans, and sensory analysis was performed using the Specialty Coffee Association of America methodology. In total, 49 compounds were described, 29 in green beans and 20 in roasted beans. A significant ($p<0.05$) effect of the harvest period was observed in all phenolic compounds except for chlorogenic acid. The drying type significantly affected the levels of rutin and trigonelline. In addition, samples from different harvest periods observed significant differences in the levels of the amino acids serine, arginine, phenylalanine and leucine. Similarly, the drying type significantly influenced glycine, alanine, valine and isoleucine levels. For all drying-harvest combinations, the final cupping score was higher than 85/100, as the different drying processes slightly influenced the cupping attributes. Drying with minimal airflow was characterized by a low balance and intense flavor while drying with medium airflow presented a high ratio and soft body. The harvest period and drying type cannot be used as cupping predictors since no clear trends were observed to classify specialty coffee organoleptic attributes. Therefore, other variables involved in specialty coffee processing should be explored to evaluate higher sensitivity toward flavor prediction and innovation.

Key words: Chromatographic analysis, *Coffea arabica* L., sensory analysis, specialty coffee.

Introduction

Worldwide, coffee is the second most traded commodity after oil[1], and drinkable coffee is one of the most significantly consumed foods[2,3]. Coffee aroma is the determining attribute factor that defines the quality and coffee acceptance by the consumer[2-4], and it is crucial for the specialty coffee market (Arabic variety), which is very elitist[5,6].

The chemical composition of green beans is very complex and plays a significant role in aroma formation[7]. Organic acids and certain bioactive compounds have been identified as possible coffee sensory quality descriptors[8,9]. Trigonelline and chlorogenic acids are precursors to other volatile compounds produced during coffee roasting and contribute directly to the coffee aroma[10]. Trigonelline is an alkaloid in green coffee beans that is degraded considerably into pyridines and pyrroles[11]. Caffeine is associated with an undesirable bitterness that, depending on its concentration, can make the drink worthless[8]. Other aroma precursors in green coffee beans are sugars, proteins and free amino acids[12]. The protein content of dry green coffee beans is about 8-12%, and it is mainly degraded to amino acids during maturation, which is accelerated by chlorogenic acids and their derivatives[13]. Coffee beans contain several free amino acids such as alanine, arginine, asparagine, cysteine, glutamic acid, histidine, glycine, isoleucine, leucine, lysine, methionine, phenylalanine, proline, serine, tyrosine, threonine, and valine[14]. Those compounds could contribute to the character and even the acceptability of the beverage since it has been suggested that the amino acid profile influences the yield of specific volatiles during roasting[15].

Coffee bean processing is essential to obtain a high-quality product[16]. Roasting, washing and drying processes are the major stages that may influence coffee's chemical composition and, consequently, its aroma[17,18]. Drying is one of the post-harvest steps with the most significant influence on coffee quality[19,20]. The coffee drying process reduces the bean's moisture content and prevents the microbial action responsible for spoilage during storage[21]. The drying process of green coffee beans may be accompanied by changes in the physical, chemical, and organoleptic properties of heat-sensitive components[20]. Thus, the quality of the beverage could be defined while controlling the drying process[22]. The need for lower production costs and mitigating environmental damage has led to the development and research new drying techniques[21].

Coffee aroma generation occurs predominantly during roasting through a complex series of Maillard reactions, in which nitrogenous heterocyclic compounds (pyridines, pyrazines and pyrroles) are formed. In addition, caramelization products generated by the thermal degradation of polysaccharides and simple sugars present in green coffee beans contribute to the development of roasting characteristics[4,23,24].

2

Besides pre and post-harvest practices, the sensory attributes can be influenced by the coffee variety and environmental/climatic factors (soil, altitude, sun exposure, rainfall, temperature)[25-27]. According to the Specialty Coffee Association of America (SCAA), the sensorial attributes evaluated in coffee cupping are fragrance/aroma, flavor, aftertaste, acidity, body, balance, sweetness, uniformity, clean cup and overall cupping[28]. Limited literature relates the composition of green coffee beans to the coffee cup quality[22,29]. Thus, more studies are required to support coffee to identify quality parameters at the green coffee bean stage, which is the most widely used maturity stage for purchasing and trading[30].

The objective of this study was to evaluate the influence of the combination of different drying processes and harvest periods in aroma related-compounds and its relation with the sensory quality of the final product in green beans of an Ecuadorian specialty coffee.

Materials and methods

Coffee samples

Green coffee beans samples of *Coffea arabica* L. typica variety were obtained from the Hacienda La Papaya, located in Saraguro, Loja province, Ecuador, at 1700 m.a.s.l. This farm produces specialty coffee, and all process parameters are controlled until parchment coffee is obtained. Coffee beans were manually collected as mature fruits (17 - 22 °Brix). Ripe coffee beans were subjected to wet fermentation for 15 hours, followed by drying for 7 - 10 days in greenhouse-type experimental rooms, where temperature, relative humidity and aeration were controlled. Grains were homogenized four times a day using a wooden paddle. Grains were dried until reaching a humidity level between 10 - 12% to prevent fungal contamination. After drying, the samples were stored in a controlled temperature chamber at 10°C and 60% relative humidity for 30 days. Experimental models of 250 g of dried green grains were collected and processed in July-August 2019. Samples were packed in hermetic metalized bags until analysis.

Experimental design

The study was based on an unbalanced 3x4 factorial design. Experimental variables were the harvest period (mid-July, early August and mid-August) and drying airflow: i) minimum (internal air movement produced by forced air from fans); ii) medium (high and low windows closed 50%, doors closed during the day and night); iii) zero airflow (high and low windows closed at 100%, doors closed during the day and night) and iv) maximum airflow (high and low windows open 100%, doors open during the day and closed at night). The experimental drying rooms were of the greenhouse type, built with wood and plastic. The drying rooms were rectangular, approximately 7 x 3.5 m²; the front and back parts correspond to the windows, and these were divided in half so that when the upper windows were opened, the lower ones could remain closed and vice versa. The lateral sides correspond to the doors of the greenhouses. In total, 36 samples were collected (12 conditions in triplicate). The response variables were the contents of some polyphenols, amino acids and volatile compounds involved in coffee aroma development.

Chemical analysis

Materials and reagents

Methanol and acetonitrile HPLC grade, fluorenyl-methoxycarbonyl chloride (FMOC; > 99%), and ortho-phthalaldehyde (OPA; > 99%) were supplied by Sigma Aldrich (St. Louis, MO, USA). Dibasic sodium phosphate is anhydrous by Mallincroudt AR (Phillipsburg, USA), glacial acetic acid and fuming hydrochloric acid by Merck KGaA (Darmstadt, Germany). Borate buffer and 3-mercaptopropionic acid, and ultrapure water were obtained from a NANOpure Diamond system (Barnstead, USA). Standards 3-O-caffeoylquinic acid, 4-O-caffeoylquinic acid, 5-O-caffeoylquinic acid, caffeine, trigonelline, caffeic acid, gallic acid, ferulic acid, apigenin, epicatechin, luteolin, rutin, DL-norvaline supplied by Sigma Aldrich (St. Louis, MO, USA) and quercetin by ROTH Carl (Karlsruhe, Germany). A stock solution of the amino acid standards (L-alanine, ammonium chloride, L-arginine, L-aspartic acid, L-cysteine, L-glutamic acid, L-leucine, L-lysine, L-serine, L-threonine, L-tyrosine, L-valine, L-histidine, L-isoleucine, L-methionine, L-phenylalanine, L-proline and glycine) were provided as a mixed solution at a concentration of 2500 pmol/μl was supplied by Sigma Aldrich (St. Louis, MO, USA).

Instrumentation

For the analysis of phenolic compounds and derivatives, as well as amino acids, a high-performance liquid chromatography (HPLC) equipment (Agilent 1200 series) equipped with a quaternary pump, diode array (DAD) and fluorescence (FLD) detectors (Agilent Technologies, USA) was used. For volatile compounds, a gas chromatograph (GC) (7890A series) coupled to a mass spectrometer (MS) (5975C series) (Agilent Technologies, Santa Clara, CA) was used.

Analysis of phenolic compounds and alkaloids

The extraction was carried out from 250 mg of dry and ground green coffee beans with 10 mL of an aqueous solution of 70% methanol. The solution was stirred for 1 minute with a vortex homogenizer, followed by sonication (BRANSONIC 3510, Mexico) for 1 hour with vigorous shaking every 10 minutes. Then, it was centrifuged at 6000 rpm for 10 minutes (Hettich MIRKO 220R, Germany). One mL of the supernatant was diluted with 9 mL of ultrapure water. The extract was filtered through 0.45 μm PVDF membrane filters before analysis.

Chromatographic separation of chlorogenic acids (5-CQA, 3-CQA and 4-CQA), caffeine, caffeic acid, gallic acid, ferulic acid, apigenin, epicatechin, luteolin, quercetin, rutin and trigonelline was performed by HPLC-DAD based on the method described in Saquicela (2018)[31] with some adaptations to include alkaloids. Separation was achieved with a Zorbax Eclipse C18 column (250 x 4.6 mm; 5 μm) (Agilent Technologies, USA), set at 30 °C and using a gradient elution at 1 mL/min of flow rate. The mobile phases were A: water acidified at 0.3% with acetic acid, B: acetonitrile: water/mobile phase A, 50:50 v/v, and C: acetonitrile 100%. Elution started with 10% B for 2 min, then increased to 55% B until 27 min and remained until 37 min. At 39 min, 100% C was reached and kept until 42 min (to wash the column). Finally, the column was re-equilibrated until 43.5 min. The injection volume was 10 μl. Detection was performed at 254 nm (trigonelline, rutin, luteolin and quercetin), 280 nm

Effect of different drying airflows and harvest periods on the quality of specialty coffee (*Coffea arabica* L.)

3

(gallic acid, caffeine and epicatechin), and 320 nm (5-CQA, 3-CQA, 4-CQA, caffeic acid, ferulic acid and apigenin). The analytical parameters of the HPLC method are shown in Supplementary material (S1).

Analysis of amino acid

The extraction was performed according to the method described in Murkovic & Derler (2006)[32]. Briefly, 200 mg of dry and ground green coffee beans were mixed with 10 mL of 0.1 N HCl solution. The solution was shaken for 1 min with a vortex homogenizer and sonicated for 15 min. Finally, the extract was filtered with a 0.45 µm PVDF membrane filter prior to analysis.

The extracts were subjected to programmed pre-column derivatization in the HPLC autoinjector. Primary amino acids were derivatized with OPA (5.12 mg in 1 mL methanol, adding 4 mL 0.4 M borate buffer) and 10 µl 3-MPA. Secondary amino acids (particularly proline) derivatization was performed with FMOC (2.5 mg/mL in acetonitrile)[33].

Derivatized amino acids were separated with a Zorbax Eclipse AAA column (4.6 x 150 mm; 5 µm) (Agilent Technologies, USA), set at 40 °C. A flow rate of 2 mL/min was applied. Mobiles phases were A) 40 mM Na2HPO4, pH 7.8, and B) methanol/acetonitrile/water 45:45:10 v/v/v. Elution started with 100% A from 0 to 1.9 min, followed by an increase in B from 0-57% until 18.1 min and then increased to 100% at 18.6 min, maintained until 22.3 min, to finally re-equilibrate until 26 min. Compounds eluted up to 10 min were detected at 340 nm excitation and 450 nm emission, while eluates up to 15 min were detected at 266 nm excitation and 305 nm emission[34]. The analytical parameters of the HPLC method are shown in S1.

Analysis of volatile compounds

Volatile compounds were evaluated in the experimental coffee samples after a standardized roasting process carried out in 50 g-roaster (Ikawa V2 model, London). The roasting process begins with a preheating phase of the Ikawa toaster until it reaches a temperature of 159.8 °C. In the meantime, 50 grams of green coffee beans were weighed and introduced into a doser of the roasting equipment. When the Ikawa equipment was preheated, the doser was opened, and the coffee beans fell through the hole into the roasting chamber. Then the roasting process begins at minute zero at 158.2 °C; this process lasts approximately 5 minutes and reaches a temperature of 205 °C. After roasting, Ikawa entered a cooling phase. Coffee was cool down inside of Ikawa, this took about 2 minutes more, and the roasted coffee was obtained ready for analysis in GC-MS.

Roasted grains were ground and kept in liquid nitrogen. Volatile compounds were extracted by solid phase headspace microextraction (SPME). Approximately 1 g of ground material was transferred to 50 mL vials of SPME. The samples were equilibrated at 50 °C for 30 minutes in a water bath. Finally, they were placed on a 50/30 ☐m SPME fiber of Divinylbenzene / Carboxen / Polydimethylsiloxane (DVB/CAR/PDMS) (Supelco, Bellefonte, PA, USA) in the headspace of each sample vial for 30 min at 50°C. SPME fiber received initial conditioning at 270°C for 1 hour and daily maintenance conditioning at 240°C for 10 min.

The SPME fiber was removed from the vial and injected in Split mode at 240°C into the GC-MS. Chromatographic separation was performed with a DB5-MS column (30m x 250☐m x 0.25☐m). The oven temperature ramp started at 70°C and rose to 310°C at a rate of increase of 7°C/min.

Helium was used as carrier gas at a flow rate of 0.8 mL/min. The MS was set to maximum sensitivity in electron impact mode, positive polarity, and the total ion current was recorded for a mass range of 50 to 550 amu.

For the identification of metabolites, the MZmine 2 software was used. First, the data from the analysis of aromatic compounds obtained from the chromatography equipment were imported. The presence of peaks (metabolites) in each sample was then checked, and low-quality samples (chromatograms with few peaks) were discarded. The aromatic compounds that are present in coffee were searched in the literature according to the peaks found in each sample obtained after discarding the low-quality samples. The baseline height and the height of the smallest peak in each sample were defined. The following parameters were determined: the average baseline, the average value of the small peaks and the minimum value of the peaks. Parameters that were later used for mass detection and construction of chromatograms. Then deconvolution, normalization and alignment of the peaks were performed. Subsequently, the process known as gap filling was carried out, making it possible to search for peaks that could have been erroneously eliminated in the previous steps. The data obtained in the MZmine 2 software was exported to an Excel file to identify the metabolites. The metabolites were defined by comparing the retention times obtained in the MZmine 2 software and the retention times of the data obtained from the chromatography equipment, as well as with the metabolites described in the literature and the probability percentage for each compound that was obtained from the chromatograph data.

Sensory analysis

The coffee sample cupping process was performed per the SCAA standards with the support of trained tasters. Initially, the samples were roasted (Ikawa V2, London) with a roasting profile adapted to 2500 m.a.s.l. and then ground (Coffee mill Mahlkonig Guatemalan, Germany). A sample of 12.5 g of ground coffee was weighed and placed in a 200 ml glass beaker. To reduce the subjectivity, coffee samples were coded. Aroma and fragrance were the first evaluated parameters. For this, the glass cup with the coffee was shaken and sucked by the tasters as many times as necessary to score it. Then, hot purified water was added to the coffee in the glass until it was almost complete. After 4 minutes, the foam was removed from the upper part of the glass, and the odor emanating from it was inhaled (a process known as "break cup"). The tasting was done 12 min after the contact of the coffee with the water. Coffee was absorbed with a spoon, and after a few seconds, the coffee was expectorated. With this, flavor, acidity, body, aftertaste and balance were determined. The absorption process was repeated as many times as necessary to evaluate each parameter. At the end of the tasting, a discussion and exchange of opinions on the scores were held to know each taster's points of view and observations regarding the samples evaluated without this influencing the already established scores. The samples were classified according to the scores within the following scale: 65-74.99, 75-79, 99, 80-84.99, 85-94.99 and 95-100, which corresponds to a cup quality of good, very good, specialty, excellent and exceptional, respectively.

Statistical analysis

Chromatographic data obtained on HPLC were pro-

Valeria Arévalo, William Mejía, Juan Manuel Cevallos-Cevallos, Johana Ortiz-Ulloa
Volume 8 / Issue 1 / 17   •   http://www.revistabionatura.com

cessed using Chemstation software (Agilent Technologies, USA). Compounds were identified by comparison with the retention times of analytical standards. Each compound's concentration was calculated by interpolating the area values in the corresponding calibration curves.

To evaluate possible differences in the chemical coffee composition with respect to drying methods and harvest times, data was pre-processed. For the coffee samples subjected to the minimum airflow drying method, no experimental results were obtained for any of the analyzed samples. In the case of medium, zero and maximum airflow, results were obtained in some of the replicates. Considering the experimental design, data imputation before principal component analysis was performed specifically for those missing GC-MS results.

Then a normalization of the data was performed using two scaling methods: 1) the Min-max scaling method, used to scale the data in a 0-1 range, and 2) the Standard scaler method, in which the mean of the values becomes zero, and the standard deviation became one. Subsequent analyzes were performed with the values of all repetitions. Ordinary Least Squares performed linear regression to identify the compounds influenced by drying and harvest time and/or the interaction between them. Then, a principal component analysis (PCA) and heat map was constructed with the compounds that were sensitive to the study variables. The individual influence of the drying type and harvest time on the chemical composition of experimental coffee samples was evaluated by two-way ANOVA. To determine the different experimental conditions, the posthoc Tukey's test was applied. For the evaluation of cupping data and its relation with the type of drying, the Random Forest method and Shap plots were used. In addition, a heat map was built with the significant variables. Statistical analyzes were performed with a 95% confidence level using Python software version 3.9.0 and R version 4.1.2.

Results and discussion

Chemical composition of specialty coffee beans (*Coffea arabica* L.)

In this study, several compounds related directly or indirectly to the organoleptic characteristics of specialty coffee were evaluated.

The quantified alkaloids and phenolic compounds in green beans of specialty coffee are presented in Table 1. Caffeine concentration ranged between 7580.04 - 9482.43 µg/g, and trigonelline ranged between 8653.24 – 10322.03 µg/g. The composition of trigonelline was comparable with other studies where concentrations ranged between 7100 - 13200 µg/g; meanwhile, caffeine composition was within a broad range of 500 - 44420 for Arabica varieties from different geographical origins, µg/g previously reported[4,25,35–39]. For most bio compounds, the highest concentrations were

Compound	Drying type				Harvest time
	Minimum airflow	**Medium airflow**	**Zero airflow**	**Maximum airflow**	
Rutin [a]	71.71 ± 15.37 [A]	33.79 ± 6.31 [A]	64.33 ± 10.85 [A]	54.60 ± 17.82 [A]	Mid-July
	35.28 ± 5.78 [B]	21.62 ± 19.02 [B]	29.41 ± 27.71 [B]	N.D	Early Aug
	35.50 ± 35.06 [AB]	38.64 ± 33.72 [AB]	26.94 ± 25.84 [AB]	N.D	Mid-Aug
Epicatechin	304.43 ± 8.69	288.94 ± 15.88	289.61 ± 16.24	318.96 ± 29.34	Mid-July
	333.81 ± 21.14	315.51 ± 11.79	327.24 ± 8.45	307.63 ± 14.59	Early Aug
	317.97 ± 8.85	328.48 ± 2.29	314.91 ± 24.32	331.39 ± 15.94	Mid-Aug
Apigenin [a]	122.36 ± 8.95 [B]	121.14 ± 2.88 [B]	121.71 ± 6.92 [B]	124.47 ± 2.21 [B]	Mid-July
	142.32 ± 6.38 [AB]	126.89 ± 6.77 [AB]	131.17 ± 10.09 [AB]	121.84 ± 6.74 [AB]	Early Aug
	122.13 ± 2.11 [A]	168.32 ± 20.40 [A]	186.35 ± 49.85 [A]	156.01 ± 84.02 [A]	Mid-Aug
Caffeic Acid	88.45 ± 0.97	86.81 ± 0.94	87.15 ± 0.18	90.90 ± 2.14	Mid-July
	92.89 ± 2.52	89.25 ± 0.46	89.60 ± 2.15	88.15 ± 1.03	Early Aug
	89.66 ± 0.88	91.35 ± 2.09	90.17 ± 0.95	92.22 ± 0.64	Mid-Aug
3-CQA	29120.97 ± 665.39	27264.53 ± 963.99	28421 ± 1287.98	29758.10 ± 1886.41	Mid-July
	29328.68 ± 1595.36	28287.42 ± 776.69	28758.13 ± 1531.08	27531.08 ± 1172.34	Early Aug
	28101.59 ± 514.63	28749.34 ± 1559.64	27483.01 ± 950.50	28989.20 ± 786.07	Mid-Aug
4-CQA [a]	4387.57 ± 89.23 [AB]	4093.97 ± 127.21 [AB]	4300.40 ± 259 [AB]	4480.51 ± 303.92 [AB]	Mid-July
	4180.95 ± 294.43 [B]	4006.46 ± 39.96 [B]	4267.59 ± 116.20 [B]	3946.99 ± 119.08 [B]	Early Aug
	4376.07 ± 38.91 [A]	4578.96 ± 430.39 [A]	4285.95 ± 39.21 [A]	4718.85 ± 65.98 [A]	Mid-Aug
5-CQA [a]	3429.42 ± 31.80 [AB]	3186.77 ± 113.90 [AB]	3342.41 ± 263.09 [AB]	3490.28 ± 320.91 [AB]	Mid-July
	3014.71 ± 239.02 [B]	3107.93 ± 54.25 [B]	3195.23 ± 80.47 [B]	3102.44 ± 66.32 [B]	Early Aug
	3413.60 ± 68.98 [A]	3697.03 ± 365.50 [A]	3350.75 ± 38.48 [A]	3713.19 ± 88.32 [A]	Mid-Aug
Trigonelline	9655. 50 ± 384.06	9099.89 ± 211.46	9131.70 ± 422.03	9337.50 ± 354.15	Mid-July
	9682.93 ± 424.77	9096.21 ± 386.49	9674.59 ± 646.21	8931.38 ± 215.79	Early Aug
	9982.94 ± 311.38	9868.87 ± 310.29	9678.77 ± 173.28	9580.68 ± 247.72	Mid-Aug
Caffeine [a]	8070.70 ± 201.25 [B]	8127.50 ± 207.23 [B]	7806.27 ± 137.73 [B]	8165.46 ± 471.50 [B]	Mid-July
	8429.77 ± 308.93 [B]	7997.64 ± 382.23 [B]	8317.77 ± 642.36 [B]	7867.57 ± 277.76 [B]	Early Aug
	8986.72 ± 185.59 [A]	9006.92 ± 376.16 [A]	8799.83 ± 200.08 [A]	8984.66 ± 436.55 [A]	Mid-Aug

[A, B] Values with different capital letters in superscript indicate which treatment was different for each compound analyzed ($p < 0.05$).

[a] Compound with significant differences due to the harvest time

[b] compound with significant differences due to the drying type

Table 1. Alkaloids and phenolic compounds composition in green coffee beans (µg/g).

Effect of different drying airflows and harvest periods on the quality of specialty coffee (*Coffea arabica* L.)

5

obtained at zero and maximum airflow and in samples of the last harvest (mid-August).

Chlorogenic acids are the most abundant phenolic compounds in coffee samples[40–42]. In general, the contents of 3-CQA (26250.39 - 31912.57 µg/g), 4-CQA (3861.64 - 5044.66 µg/g) and 5-CQA (2744.60 - 4054.43 µg/g) did not differ considerably among experimental samples. The results for 3-CQA and 4-CQA were within the broad ranges reported in another stud (4930 - 149200 µg/g and 7020 - 101900 µg/g, respectively), while our results for 5-CQA were markedly lower than previous reports (57330 - 263600 µg/g)[4,39,43–45]. The significant variations among the concentrations of chlorogenic acids in coffee beans have been attributed to the application of different post-harvest processing[46], environmental factors and genetic variability between coffee species[45]. Consequently, it has been suggested that more studies are required to elucidate the correlation between these factors and grain chemistry[46].

The highest concentrations for alkaloids and phenolic compounds quantified corresponded to the last harvest time (mid-Aug), except for rutin and acid 3-CQA whose highest concentrations were for the first harvest time (mid-July). Concerning the drying method, the highest concentrations of compounds were obtained in samples dried at zero and maximum airflow.

The concentration of amino acids in green coffee samples is shown in Table 2. In total, 14 amino acids were quantified, from which proline was the most abundant (4931.48 - 8704.18 µg/g), followed by glutamic acid (852.10 - 2377.78 µg/g) and aspartic acid (274.22 - 1279.43 µg/g). The highest concentrations quantified for the amino acids corresponded to the samples harvested during mid-July and early August; meanwhile, the highest concentrations were obtained when samples were dried at zero airflows, except for glycine, phenylalanine, lysine and proline, whose highest concentrations corresponded to the drying at maximum airflow.

Different amino acid profiles have been previously reported. Wei & Tanokura, (2015)[47] reported 29 types of free amino acids in green coffee bean extracts, where aspartic acid, glutamic acid, serine, glycine, valine, phenylalanine and lysine were similar to our results. In contrast, the concentrations of histidine, threonine and alanine were higher, while arginine, isoleucine, leucine and proline were lower to those determined in the present study. In Casal *et al.*, (2003)[48], the concentrations of glycine and proline were lower, whereas leucine concentrations were higher than our results. In Lee *et al.* (2017)[49], lower concentrations of glutamic acid, glycine and proline, and high amounts of serine and valine were reported. Other studies reported similar proline, aspartic acid and glutamic acid concentrations but higher concentrations for the other amino acids[19,50]. Dong *et al.* (2017)[20] suggest that composition variations in coffee can be attributed to factors such as coffee variety[50,51], geographical origin[51] or analytical methods[52] used. Regarding drying methods, Kulapichitr *et al.*, (2019)[19] evaluated different drying methods in Thai coffee beans. Samples subjected to heat pump drying presented slightly higher levels of most amino acids and no differences at higher temperatures. Tray drying showed a moderate effect on amino acids compared to sun drying, possibly due to shorter drying times.

The volatile compounds identified in the coffee beans after standardized roasting are presented in Table 3. A total of 20 volatile compounds, including pyridines, pyrazines, alcohols, pyrroles, cyclohexanes, aldehydes, furans, and ketones, were identified, similarly as reported elsewhere[24,53]. The highest concentrations of volatile compounds were obtained for samples harvested during mid-August and dried under zero airflow. No significant differences among experimental treatments were determined for the aromatic compounds.

Volatile compounds profile depends on a series of factors such as the species and variety grain, geographical origin, soil conditions and grains storage, as well as the time and temperature of the roasting process, among others[20,54]. Cheong *et al.* (2013)[53] determined volatile sulfur compounds in roasted coffee, which impacted the sensory evaluation. Additionally, furans, pyrazines, pyridines, pyrroles and furanone were the main contributors to the roasted coffee aroma. Amanpour & Selli (2016)[54], mainly furans and lactones, followed by pyrazines, pyridines, acids, cyclopentane, pyrroles, furanone, ketones, thiols, alcohols, aldehydes, among others, were identified. Lee *et al.* (2017)[49] evaluated the effect of the reverse process of grinding and roasting coffee on volatile compounds profiles, identifying 50 compounds in coffee roasted with the conventional method and 39 using the reverse method of grinding and roasting. To Laukaleja *et al.* (2019)[55], main volatile compounds were furans, pyrazines, aldehydes and ketones, attributing to the last three an association with a pleasant aroma and flavor in specialty coffees. Heo *et al.* (2020)[56] identified 36 volatile compounds, highlighting that the extraction method and temperature could influence the volatile compound profiles.

Influence of drying processes and harvest time on coffee beans chemical composition

In this study, the content of several aroma-related compounds from specialty coffee samples harvested in different periods and subjected to other drying processes was assessed (Table 4). The harvest time significantly influenced all phenolic compounds' composition ($p<0.05$), except chlorogenic acid (3 CQA). Harvest time also influenced on the content of the amino acids serine ($p=0.003$), arginine ($p=0.009$), phenylalanine ($p=0.0004$) and leucine ($p=0.00006$) and the only one aromatic compound cyclohexane ($p=0.04$). Drying type significantly influenced on the concentration of rutin ($p=0.03$), trigonelline ($p=0.04$) and the amino acids glycine ($p=0.04$), alanine ($p=0.01$), valine ($p=0.02$) and isoleucine ($p=0.01$).

Experimental treatments that significantly differed were identified (Tables 1 & 2). For polyphenols, the quantified concentrations of rutin, 4-CQA and 5-CQA of the coffee beans collected in early August were statistically lower than the other harvest periods. For apigenin and caffeine, concentrations in the coffee beans collected in mid-August were significantly higher than in the other harvest periods. For amino acids, concentrations of aspartic acid were quite different among all harvest periods, obtaining the highest concentration in samples collected mid-July. Serine and arginine concentrations in samples collected in early August were significantly lower than those obtained from other harvest periods. For phenylalanine, statistically lower concentrations were observed in samples collected in mid-August. For histidine and threonine, significantly lower concentrations were obtained in coffee samples subjected to minimal aeration.

The combined influence of the experimental variables was explored by constructing a PCA based on the biocompounds whose simple linear regressions were statistically significant. Those compounds were one polyphenol (apige-

6

Compound	Drying Type				Harvest time
	Minimum airflow	Medium airflow	Zero airflow	Maximum airflow	
Aspartic acid [a]	773.34 ± 81.96 [A]	727.73 ± 27.38 [A]	885.46 ± 341.29 [A]	691.61 ± 46.64 [A]	Mid-July
	432.16 ± 137.59 [C]	472.54 ± 20.74 [C]	463.04 ± 28.64 [C]	510.59 ± 54.87 [C]	Early Aug
	563.79 ± 113.41 [B]	595.94 ± 51.10 [B]	661.28 ± 40.21 [B]	623.46 ± 41.47 [B]	Mid-Aug
Glutamic acid	1468.28 ± 153.40	1441.29 ± 17.25	1773.14 ± 525.93	1509.35 ± 68.51	Mid-July
	1314.31 ± 402.06	1315.07 ± 27.40	1475.98 ± 63.29	1261.42 ± 102.67	Early Aug
	1478.32 ± 228.86	1494.14 ± 104.87	1458.12 ± 138.63	1571.22 ± 77.67	Mid-Aug
Serine [a]	199.35 ± 16.79 [A]	201.47 ± 8.39 [A]	252.17 ± 72.90 [A]	202.10 ± 13.80 [A]	Mid-July
	153.29 ± 41.44 [B]	171.99 ± 5.81 [B]	187.21 ± 2.57 [B]	172.79 ± 14.35 [B]	Early Aug
	184.89 ± 35.56 [AB]	214.72 ± 11.23 [AB]	205.70 ± 15.59 [AB]	223.15 ± 22.17 [AB]	Mid-Aug
Histidine [b]	53.64 ± 1.68 [B]	58.78 ± 5.71 [AB]	71.18 ± 24.51 [A]	55.22 ± 6.29 [A]	Mid-July
	39.37 ± 34.54 [B]	58 ± 3.53 [AB]	65.61 ± 9.41 [A]	65.23 ± 6.43 [A]	Early Aug
	42.13 ± 36.69 [B]	63.85 ± 3.42 [AB]	60.30 ± 3.83 [A]	71.10 ± 11.56 [A]	Mid-Aug
Glycine	831.82 ± 79.48	981.23 ± 19.45	921.54 ± 81.50	918.38 ± 11.68	Mid-July
	829.50 ± 282.14	898.31 ± 130.54	1067.46 ± 117.47	1008.13 ± 75.54	Early Aug
	566.69 ± 494.58	963.98 ± 146.08	946.59 ± 37.51	1034.10 ± 174.27	Mid-Aug
Threonine [b]	12.34 ± 10.76 [B]	16.93 ± 1.44 [AB]	26.77 ± 6.99 [A]	20.27 ± 1.84 [AB]	Mid-July
	12.94 ± 11.23 [B]	23.08 ± 1.26 [AB]	24.77 ± 2.33 [A]	23.26 ± 2.04 [AB]	Early Aug
	2.017 ± 21.63 [B]	12.95 ± 11.24 [AB]	16.68 ± 1.12 [A]	17.06 ± 1.03 [AB]	Mid-Aug
Arginine [a]	182.24 ± 17.72 [AB]	242.87 ± 5.10 [AB]	294.33 ± 117.60 [AB]	227.13 ± 20.16 [AB]	Mid-July
	229.43 ± 85.08 [B]	221.62 ± 29.74 [B]	244.66 ± 29.88 [B]	207.65 ± 37.31 [B]	Early Aug
	265.73 ± 35.24 [A]	308.85 ± 21.06 [A]	278.13 ± 72.15 [A]	345.76 ± 85.97 [A]	Mid-Aug
Alanine	206.91 ± 14.22	227.48 ± 3.28	296.57 ± 95.80	222.55 ± 5.71	Mid-July
	203.93 ± 54.86	276.76 ± 15.05	304.15 ± 10.96	272.08 ± 19.45	Early Aug
	240.20 ± 40.45	277.48 ± 10.32	239.69 ± 16.90	288.61 ± 38.15	Mid-Aug
Valine	54.28 ± 3.09	60.25 ± 0.50	72.07 ± 24.75	57.21 ± 2.87	Mid-July
	52.67 ± 14.36	67.81 ± 2.65	77.95 ± 1.66	69.64 ± 2.45	Early Aug
	61.17 ± 7.68	68.37 ± 3.20	61.28 ± 2.73	70.40 ± 7.72	Mid-Aug
Phenylalanine [a]	143.56 ± 14.19 [A]	141.12 ± 21.42 [A]	172.20 ± 69.90 [A]	153.59 ±6.12 [A]	Mid-July
	138.05 ± 43.99 [A]	172.39 ± 20.13 [A]	170.91 ± 5.20 [A]	185.80 ± 4.60 [A]	Early Aug
	116.97 ± 23.80 [B]	124.41 ± 17.17 [B]	106.39 ± 6.80 [B]	116.88 ± 7.11 [B]	Mid-Aug
Isoleucine	43.21 ± 2.08	47.44 ± 0.94	57.58 ± 19.34	45.31 ± 2.23	Mid-July
	42.39 ± 12.04	55.67 ± 2.51	64.18 ± 2.45	58.42 ± 1.57	Early Aug
	48.56 ± 6.79	55.50 ± 2.74	49.60 ± 1.54	55.28 ± 5.51	Mid-Aug
Leucine	29.55 ± 0.77	35.70 ± 0.43	41.74 ± 12.91	34.29 ± 3.22	Mid-July
	34.92 ± 10.12	47.00 ± 2.50	57.50 ± 2.79	49.10 ± 2.32	Early Aug
	39.10 ± 3.25	44.28 ± 2.33	37.15 ± 2.18	44.51 ± 4.78	Mid-Aug
Lysine	27.41 ± 47.47	80.89 ± 6.72	26.77 ± 46.37	87.96 ± 6.85	Mid-July
	67.77 ± 59.43	67.07 ± 58.09	105.28 ± 8.20	91.27 ± 5.22	Early Aug
	32.41 ± 56.13	68.65 ± 59.52	89.11 ± 13.64	96.64 ± 11.34	Mid-Aug
Proline	7510.47 ± 1035.40	7169.54 ± 416.42	7248.46 ± 1090.10	6838.75 ± 1452.58	Mid-July
	6393.97 ± 1295.46	6652.94 ± 427.68	6717.53 ± 1031.98	6540.74 ± 1053.70	Early Aug
	5675.32 ± 735.74	7079.78 ± 583.75	6874.80 ± 1289.95	7847.51 ± 848.53	Mid-Aug

[A,B,C] Values with different capital letters in superscript indicate which treatment was different for each compound analyzed (p < 0.05).

[a] Compound with significant differences due to the harvest time

[b] compound with significant differences due to the drying type

Table 2. Amino acid composition in green coffee beans (μg/g).

nin), five amino acids (arginine, alanine, valine, isoleucine, and leucine), and 10 aromatics (2,3-pentanedione, carbon monoxide, butane, dihydro-2-methyl 3(2H)-furanone, 2-methylpyrazine, 2-furancarboxaldehyde, 2,6-dimethylpyrazine, 2-ethylpyrazine, 2-ethyl-6-methylpyrazine, and 2-ethyl-3-methylpyrazine). Three main components were defined and explained 73% of the variation of the data based on the harvest time (PCA1 39% and PCA2 24%).

Figure 1 shows a heat map of the variation of coffee bean composition according to the drying type and harvest time. Two groups were distinguished, one for amino acids and another for aromatic compounds, except for butane and

carbon monoxide. This suggested assembling early formed precursors and roasting products, discarding intermediate processes, such as ripening and drying, that were not significant when constructing the PCA model. These results may support the observed more considerable influence of the harvest period compared to the evaluated drying processes.

Several studies refer to the interaction of the chemical composition of coffee with genotype[10], environment[10], geographical origin[57], climatic factors[58], and processing[10], among others. Kulapichitr et al. (2019)[19] evaluated the influence of heat pump drying, tray drying and sun drying on

Compound	Functional Group	Drying type			Harvest time
		Medium airflow	Zero airflow	Maximum airflow	
2,3-Pentanedione	Ketone	19.49 ± 16.65	18.39 ± 21.64	2.78 ± 0.12	Mid-July
		28.22 ± 5.93	2.53 ± 0.18	13.23 ± 12.94	Early Aug
		8.91 ± 6.20	2.01 ± 0.96	17.70 ± 20.83	Mid-Aug
Carbon monoxide	Carbonyl	10.41 ± 7.85	35.41 ± 39.48	63.82 ± 5.41	Mid-July
		5.80 ± 0.24	59.17 ± 7.37	15.80 ± 20.17	Early Aug
		26.36 ± 27.23	68.22 ± 1.74	13.96 ± 14.70	Mid-Aug
Butane	Ketone	17.97 ± 15.65	5.62 ± 3.54	1.21 ± 0.61	Mid-July
		4.34 ± 2.99	1.96 ± 0.87	7.49 ± 7.41	Early Aug
		3.68 ± 2.18	1.50 ± 0.82	3.86 ± 2.25	Mid-Aug
Pyridine	Pyridine	0.71 ± 0.19	1.16 ± 0.66	0.44 ± 0.03	Mid-July
		1.42 ± 0.29	0.54 ± 0.11	1.14 ± 1.39	Early Aug
		0.85 ± 0.03	0.45 ± 0.22	0.96 ± 0.38	Mid-Aug
Dihydro-2-methyl 3(2H)-Furanone	Furanone	0.64 ± 0.44	1.31 ± 0.82	0.62 ± 0.06	Mid-July
		1.70 ± 0.32	0.64 ± 0.04	0.67 ± 0.13	Early Aug
		1.42 ± 0.24	0.54 ± 0.23	1.00 ± 0.30	Mid-Aug
2-methyl pyrazine	Pyrazine	4.54 ± 0.27	4.57 ± 2.82	2.56 ± 0.48	Mid-July
		7.60 ± 0.19	2.26 ± 1.10	6.23 ± 3.20	Early Aug
		2.84 ± 0.38	1.75 ± 0.31	4.04 ± 0.97	Mid-Aug
2-Furancarboxaldehyde	Pyrazine	23.01 ± 23.43	7.72 ± 1.51	11.60 ± 6.70	Mid-July
		12.33 ± 10.82	15.07 ± 7.99	20.55 ± 5.66	Early Aug
		24.96 ± 13.28	10.43 ± 5.94	33.25 ± 14.71	Mid-Aug
Methylpyrazine	Furanone	0.33 ± 0.23	0.55 ± 0.32	0.17 ± 0.01	Mid-July
		0.83 ± 0.05	0.23 ± 0.09	0.90 ± 0.75	Early Aug
		0.48 ± 0.04	0.24 ± 0.08	0.44 ± 0.24	Mid-Aug
2-Furamethanol	Alcohol	1.81 ± 0.10	2.62 ± 1.26	1.59 ± 0.048	Mid-July
		3.93 ± 0.46	1.59 ± 0.03	2.36 ± 0.50	Early Aug
		2.60 ± 1.09	1.49 ± 0.40	2.83 ± 0.79	Mid-Aug
2-Propanone, 1-(acetyloxy)	Ketone	4.51 ± 0.91	4.02 ± 1.24	3.08 ± 0.69	Mid-July
		7.01 ± 2.29	4.49 ± 0.03	7.84 ± 3.87	Early Aug
		7.89 ± 7.71	3.01 ± 0.80	4.41 ± 2.10	Mid-Aug
2,6-Dimethyl pyrazine	Furan	4.12 ± 0.17	5.70 ± 2.92	2.62 ± 1.25	Mid-July
		7.14 ± 0.80	2.84 ± 0.95	3.17 ± 1.27	Early Aug
		5.13 ± 0.14	2.02 ± 0.09	4.50 ± 1.74	Mid-Aug
1-(2-furanyl)-ethanone	Pyrazine	4.82 ± 1.26	1.13 ± 0.37	1.58 ± 1.14	Mid-July
		5.07 ± 5.39	0.92 ± 0.003	6.93 ± 7.22	Early Aug
		3.18 ± 3.17	1.84 ± 1.55	1.33 ± 0.17	Mid-Aug
2-Ethylpyrazine	Pyrazine	0.49 ± 0.51	1.12 ± 0.87	1.48 ± 1.50	Mid-July
		0.76 ± 0.85	0.58 ± 0.12	3.19 ± 0.90	Early Aug
		0.73 ± 0.19	0.41 ± 0.01	0.65 ± 0.77	Mid-Aug
5-Methyl 2-Furancarboxaldehyde	Aldehyde	3.35 ± 0.35	5.14 ± 2.01	3.22 ± 0.87	Mid-July
		6.61 ± 0.72	3.45 ± 0.33	5.00 ± 2.59	Early Aug
		5.15 ± 0.37	2.81 ± 0.75	5.32 ± 0.97	Mid-Aug
2-Furamethanol, acetate	Alcohol	1.77 ± 0.36	2.93 ± 0.83	1.80 ± 0.32	Mid-July
		3.86 ± 0.99	1.94 ± 0.16	2.52 ± 0.86	Early Aug
		2.94 ± 0.25	1.75 ± 0.31	2.83 ± 0.98	Mid-Aug
2-Ethyl-6-methylpyrazine	Pyrazine	0.34 ± 0.07	0.39 ± 0.19	0.16 ± 0.10	Mid-July
		0.51 ± 0.09	0.27 ± 0.02	0.39 ± 0.06	Early Aug
		0.40 ± 0.03	0.23 ± 0.03	0.48 ± 0.06	Mid-Aug
2-Ethyl-3-methylpyrazine	Pyrazine	1.16 ± 0.12	1.54 ± 0.85	0.76 ± 0.09	Mid-July
		1.80 ± 0.52	0.99 ± 0.06	1.67 ± 0.78	Early Aug
		1.63 ± 0.18	0.89 ± 0.03	1.59 ± 0.81	Mid-Aug
1-methyl-4-(1-methylethenyl)-cyclohexane	Cyclohexane	0.11 ± 0.03	0.16 ± 0.05	0.12 ± 0.02	Mid-July
		0.26 ± 0.10	0.08 ± 0.02	0.19 ± 0.03	Early Aug
		0.17 ± 0.07	0.05 ± 0.04	0.20 ± 0.04	Mid-Aug
2-Ethyl-3,5-dimethylpyrazine	Pyrazine	0.25 ± 0.03	0.39 ± 0.15	0.21 ± 0.03	Mid-July
		0.45 ± 0.12	0.29 ± 0.03	0.43 ± 0.22	Early Aug
		0.40 ± 0.07	0.21 ± 0.01	0.44 ± 0.16	Mid-Aug
Pyrrole N-furfuryl	Pyrrole	0.19 ± 0.01	0.13 ± 0.09	0.18 ± 0.01	Mid-July
		0.37 ± 0.09	0.17 ± 0.01	0.30 ± 0.18	Early Aug
		0.27 ± 0.01	0.15 ± 0.001	0.21 ± 0.06	Mid-Aug

Table 3. Volatile compounds identified in roasted coffee beans (%).

8

Response Variables	p-values		
	Harvest period	Drying type	Interaction
Polyphenols			
Rutin	0.001*	0.031*	0.319
Epicatechin	0.004*	0.530	0.130
Apigenin	0.016*	0.637	0.377
Caffeic Acid	0.001*	0.081	0.002*
5 CQA	0.019*	0.3125	0.909
3 CQA	0.820	0.463	0.138
4 CQA	0.0004*	0.446	0.035*
Trigonelline	0.007*	0.041*	0.316
Caffeine	0.002*	0.539	0.451
Amino acids			
Aspartic acid	0.905	0.207	0.142
Glutamic acid	0.072	0.421	0.729
Serine	0.003*	0.098	0.542
Histidine	0.919	0.068	0.786
Glycine	0.643	0.035*	0.558
Threonine	0.489	0.306	0.539
Arginine	0.009*	0.374	0.375
Alanine	0.196	0.011*	0.098
Valine	0.260	0.020*	0.203
Phenylalanine	0.0004*	0.4584	0.5138
Isoleucine	0.092	0.011*	0.174
Leucine	0.00006*	0.244	0.227
Lysine	0.256	0.089	0.450
Proline	0.333	0.664	0.386
Aromatic compounds			
2,3-Pentanedione	0.765	0.332	0.317
Carbon monoxide	0.014*	0.610	0.065
Butane	0.287	0.351	0.262
Pyridine	0.295	0.366	0.058
3(2H)-Furanone, dihydro-2-methyl-	0.092	0.749	0.045
2-methyl pyrazine	0.099	0.056	0.083
2-Furancarboxaldehyde	0.284	0.429	0.537
Methylpyrazine	0.481	0.210	0.229
2-Furamethanol	0.139	0.343	0.056
2-Propanone, 1-(acetyloxy)	0.384	0.398	0.748
2,6-dimethyl pyrazine	0.816	0.047	0.046
Ethanone	0.307	0.495	0.629
2-Ethylpyrazine	0.059	0.182	0.178
2-Furancarboxaldehyde, 5-methyl	0.274	0.341	0.086
2-Furamethanol, acetate	0.250	0.311	0.051
2-Ethyl-6-methylpyrazine	0.095	0.201	0.029
2-Ethyl-3-methylpyrazine	0.437	0.542	0.262
Cyclohexane	0.040*	0.292	0.063
2-Ethyl-3,5-dimethylpyrazine	0.512	0.321	0.181
Pyrrole N-Furfuryl	0.079	0.058	0.755

*Significant different ($p > 0.05$) by two-way ANOVA

Table 4. Individual influence of the drying type and harvest time on the chemical composition of green coffee beans, evaluated by analysis of variance.
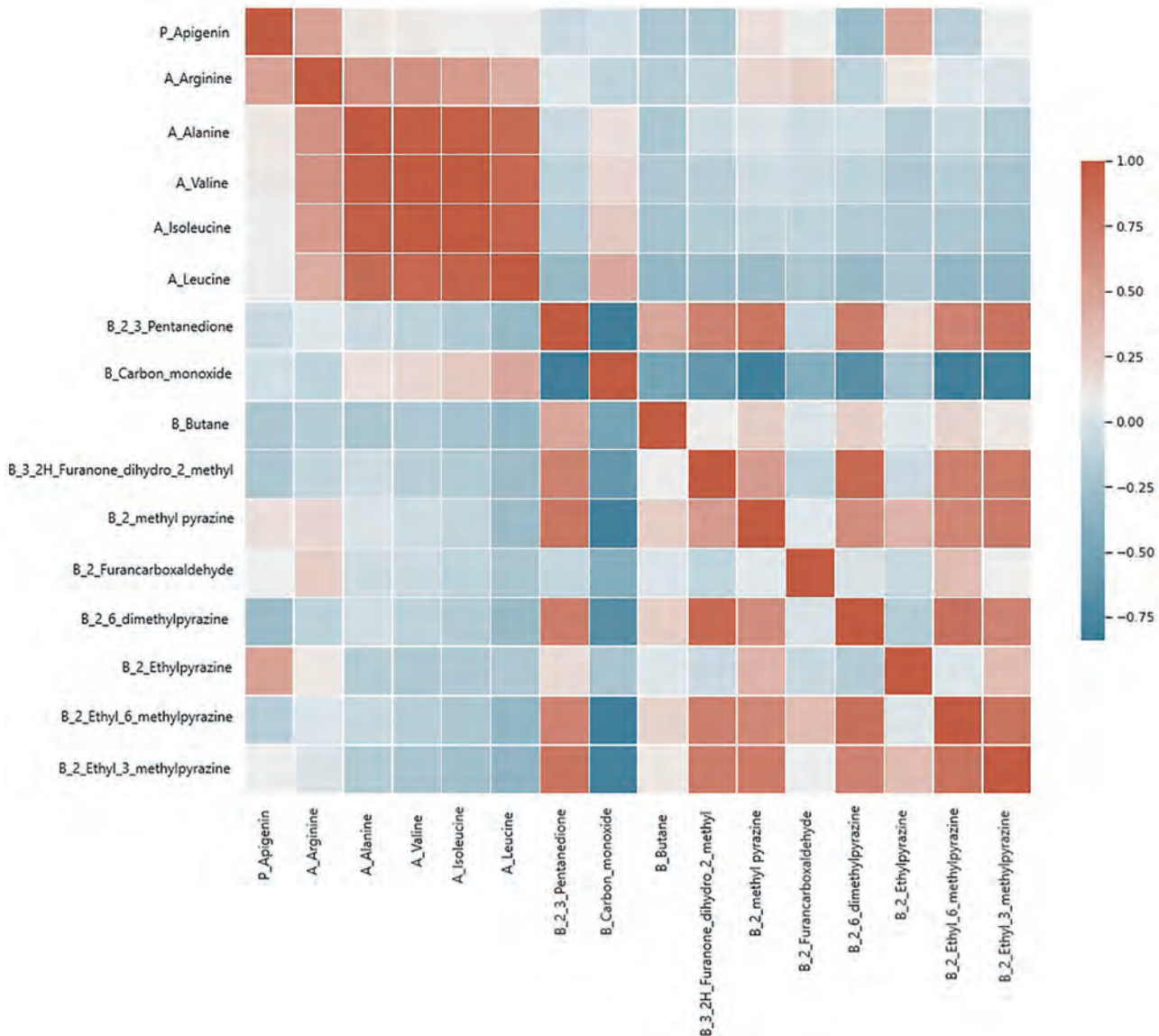
Figure 1. Heat map for coffee samples subjected to different drying airflow types and different harvest times.

coffee's chemical composition. The drying process did not affect the caffeine content, but it influenced the concentration of histidine, as in the present study. In addition, significant differences were observed for aspartic acid and phenylalanine. Significant differences among drying methods in several compounds were described for the aromatic compounds. Green coffee beans subjected to heat pump drying presented slightly higher levels of most amino acids[19]. Heat pump and tray drying shared the same profile and compound content, while both differed from the composition of sun-dried coffee samples[19]. Tolessa *et al.*, (2017)[59] evaluated the influence of growing altitude, shade and harvest period on Ethiopian specialty coffee's quality and biochemical design.

It was determined that beans harvested at early and middle harvest periods were generally higher in cup quality compared to late-harvested beans. Interactions among altitude, shade and harvest periods were significant for caffeine content. The highest caffeine content (17.9 g Kg⁻¹) was obtained in early harvested beans at middle altitude with dense shade. In comparison, the lowest range (14.5 g Kg⁻¹) was observed in middle-harvested beans from high altitudes with the medium shade. No interactions were found for

the total chlorogenic acids content of coffee beans. Laderach *et al.* (2011)[60] evaluated two harvest times and their correlation with the sensory properties of coffee harvested in two Colombian states and two Mexican farms. They found significant differences in the sensory attributes of the coffee and determined that for an early harvest, most characteristics score higher except for aroma/fragrance, body and sweetness. Final cupping scores for early and late harvest coffees were 77.8 points and 72.6 pints, respectively. Jeszka-Skowron *et al.*, (2016)[43], evaluated the concentration of chlorogenic acids and caffeine in coffee beans from different geographical origins of the Arabica and Robusta varieties. They determined that there were no significant differences between the contents of caffeine and chlorogenic acids (3-CQA, 4-CQA and 5-CQA) of the coffee collected from different geographical origins for the Arabica variety. However, for the Robusta variety, there were significant differences in the contents of these compounds. Scarce information about associations between green coffee beans' chemical compositions and the harvest period has been published.

Other studies have evaluated the relationship between coffee chemical composition and drying conditions. In Dong

et al. (2017)[20], five drying conditions were assessed, and, by PCA, it was determined that both hot air-dried and cold-dried samples were located in the positive direction of PC1. In contrast, the models treated with the heat pump drying, solar drying, and room temperature drying methods were close to each other and in the negative PC1 direction, indicating that the different drying methods influence coffee chemical compounds' content. In addition, solar drying significantly influenced caffeine and trigonelline content; meanwhile, freeze-drying and heat-pump drying significantly influenced the concentration of amino acids and volatile compounds, respectively[20].

Other factors before harvest, such as the species, cultural practices, fertilization, temperature and altitude, can influence the quality of the coffee cup. According to Bastian et al., (2021)[61], the quality of coffee beverages is affected by the ripening time of the fruit, which is also related to geographic and climate conditions[62]. Velásquez & Banchón, (2022)[63] mentioned that climatic changes where there are heat waves and droughts directly affect the production of Arabica coffee due to its greater sensitivity to climatic changes. Overall, the association of different variables throughout the pre-and post-harvest coffee processing should continue being explored towards defining predictor variables for coffee classification, particularly for high-quality coffee due to its sensitiveness.

Sensory analysis results

The drink quality, given by its sensory attributes, is the main characteristic that differentiates specialty coffee from regular coffee[46,64]. In this study, drink quality was subjected to sensorial panels only considering the drying type since it was the less sensitive variable related to the coffee chemical composition. The sensory scores given by professional tasters are shown in Table 5. According to the SCAA, specialty coffee must present a final sensory score greater than or equal to 80 out of 100[65]. This narrow scoring is scale-based, which reduces the possibility of quantitative analysis. A proposal to match sensory attributes with the drying type was modeled by Random Forest analysis, through which the drying type could be predictable only within a cupping range between 8 and 9.5.

The primary tasting descriptors were the balance and the general tasting value—figure 2. A shows the results obtained for samples dried under minimum airflow, in which the most representative descriptors were balance, flavor and final score. A low balance and high flavor values characterized drying at minimum airflow. Figure 2.B presents the model for drying at medium airflow. This drying type was defined as a tasting result with low body values, high balance and high general tasting values. For drying at zero airflows, balance, available tasting value and body were the most relevant descriptors without defining any trend since the medium and low values were mixed (Figure 2.C). This drying type could only be defined with high aroma values. Similarly, for drying at maximum airflow, no clear trend of cupping descriptors was observed (Figure 2.D).

These results suggested an association between the drying at a minimum and medium airflow with the final tasting. In contrast, extreme drying conditions, i.e., zero and maximum airflow, could trigger diverse metabolic processes that result in a mixture of tasting characteristics.

Previous studies evaluate the sensory analysis relationship of coffee with the processing type. Wet processing requires large amounts of water[66] and involves the mechanical depulping of coffee cherries, which removes most of the bean flesh[61]. What is obtained is parchment coffee surrounded by mucilaginous residues, which are degraded through fermentation in water pools that cover the coffee beans entirely for a certain period; the final product is a "washed" or "parchment" coffee[67]. This method is widely used in Arabica coffee[61]. Pinto et al., (2013)[68] established that for the sensory attributes evaluated in their study (drink clarity, acidity, body, flavor, aftertaste, balance, general value and final score) there was a significant difference between the treatments, being the wet superior to dry processing coffees with final scores between 82.93-82.95 and 78.12-75.65, respectively. Rodriguez et al. (2020)[69] determined that post-harvest coffee processing did not affect the total cup score, obtaining a mean value for the semi-dry processing method of 85.94 ± 0.57, while for wet processing, it was 84.13 ± 0.42. In addition, none of the attributes analyzed individually for final tasting was significantly different between both processes; however, they noted slightly better values for fragrance/aroma, aftertaste, acidity, and body attributes for the wet processing. They also observed that uniformity, balance, clean cup, and sweetness parameters increased the overall rating. Ribeiro et al. (2016)[10] obtained results contrary to the studies mentioned above, where the significantly highest average values final score were observed in dry-processed coffee, with a value of 85.57 vs. 84.61 obtained with the wet method.

Attributes	Drying Method (Mean ± SD)			
	Minimum airflow	Medium airflow	Zero airflow	Maximum airflow
Fragrance/Flavor	8.04 ± 0.17	7.96 ± 0.17	8.00 ± 0.20	8.04 ± 0.17
Taste	8.00 ± 0.20	7.96 ± 0.09	8.04 ± 0.09	8.00 ± 0.14
Aftertaste	8.00 ± 0.14	7.96 ± 0.09	8.04 ± 0.17	8.00 ± 0.14
Acidity	7.86 ± 0.13	7.96 ± 0.17	7.96 ± 0.17	8.04 ± 0.22
Body	7.93 ± 0.12	7.89 ± 0.13	8.00 ± 0.20	8.00 ± 0.14
Balance	7.86 ± 0.24	8.07 ± 0.19	8.00 ± 0.14	8.14 ± 0.20
General	7.89 ± 0.24	8.07 ± 0.19	7.96 ± 0.17	8.07 ± 0.19
Final Score	85.54 ± 0.99	85.89 ± 0.66	86.07 ± 0.28	86.11 ± 0.24

Table 5. Sensory analysis scores of coffee samples by type of drying.
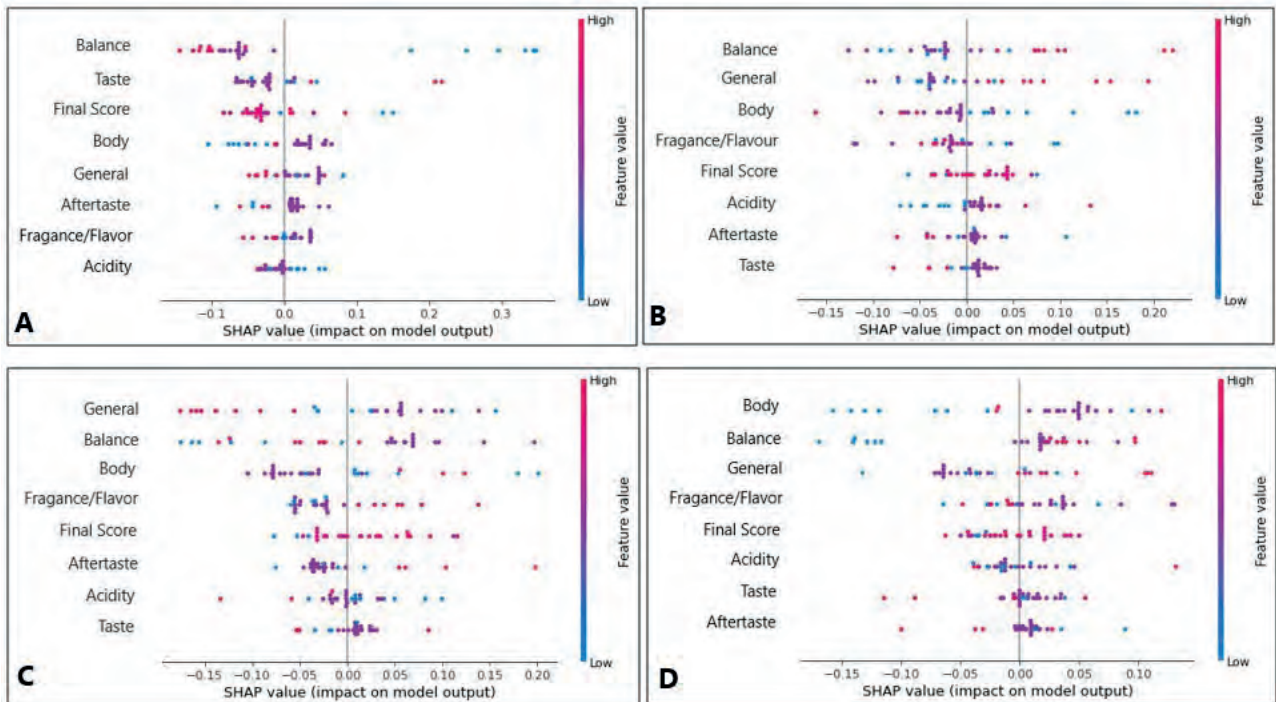
Figure 2. (A) Tasting parameters with the greatest influence on samples subjected at minimum airflow drying, (B) Tasting parameters with the greatest influence on samples subjected at medium airflow drying, (C) Tasting parameters with the greatest influence on samples dried without airflow, and (D) Tasting parameters with the greatest influence on samples subjected at maximum airflow drying.

Conclusions

In this study, the influence of the different drying processes and harvest periods on the quality of specialty green bean coffee was evaluated through the characterization of aroma-responsible compounds and their relationship with the tasting attributes of coffee drinks. Four drying types and three harvest times were considered for 36 coffee bean samples. The techniques for extracting and analyzing chemical compounds from coffee were optimized. The concentrations of polyphenols, amino acids and aromatic compounds were quantified and some differed from those reported in the literature, attributing to a series of factors such as geographical origin, environmental factors, agricultural practices, grain species and variety, post-harvest treatments, type of roasting, among others. Slight differences were established in chemical compound content concerning harvest periods, but these differences were not significant. The drying type did not significantly influence the bio compounds concentration determined in specialty coffee. Therefore, both the harvest period and the drying type alone cannot be considered predictive scale variables that explain the sensory differences of specialty coffee. It is suggested to analyze the entire production process of specialty coffee to define other variables that adequately explain these differences in composition for the chemical compounds of coffee. Tasting according to drying type allowed to establish a predictive model, particularly for drying types with minimum and medium airflow, as long as the tasting values are within a range of 8-9.5. Considering that cupping scores for specialty coffee should be high, it is suggested to create an internal cupping scale to obtain a broader cupping range, allowing a more sensitive evaluation of processing variables and even chemical coffee composition.

Conflicts of Interest

The author(s) declare that they have no competing interests.

Bibliographic references

1. Rodrigues N, Bragagnolo N. Identification and quantification of bioactive compounds in coffee brews by HPLC-DAD-MS. J Food Compos Anal 2013; 32: 105–115.
2. Borrella I, Mataix C, Carrasco-Gallego R. Smallholder Farmers in the Speciality Coffee Industry: Opportunities, Constraints and the Businesses that are Making it Possible. IDS Bull 2015; 46: 29–44.
3. González Sánchez H, Gonzales Palomares S, Rosales Reyes T. Café (Coffea arabica L.): Compuestos volátiles relacionados con el aroma y el sabor. Unacar Tecnociencia 2011; 5: 35–45.
4. Lee LW, Cheong MW, Curran P, Yu B, Liu SQ. Coffee fermentation and flavor--An intricate and delicate relationship. Food Chem 2015; 185: 182–191.
5. Anthony J. Top 10 Most Expensive Coffee In The World: Luwak Coffee Is Not The No. 1. Financesonline.com. 2014.https://financesonline.com/top-10-most-expensive-coffee-in-the-world-luwak-coffee-is-not-the-no-1/ (accessed 25 Jul2021).
6. Transparent Trade Coffee. SCRPI. Transparent Trade Coffee. 2020. https://www.transparenttradecoffee.org/scrpi (accessed 25 Jul2021).
7. Fisk ID, Kettle A, Hofmeister S, Virdie A, Kenny JS. Discrimination of roast and ground coffee aroma. Flavour 2012; 1: 14.
8. Borém FM, Figueiredo LP, Ribeiro FC, Taveira JHS, Giomo GS, Salva TJG. The relationship between organic acids, sucrose and the quality of specialty coffees. Afr J Agric Res 2016; 11: 709–717.

9. Farah A, Marino Donangelo C. Phenolic compounds in coffee. Braz J Plant Physiol 2006; 18: 23–36.

10. Ribeiro DE, Meira Borém F, Cirillo M, Bernardes MV, Ferraz V, Ramos Alves H et al. Interaction of genotype, environment and processing in the chemical composition expression and sensorial quality of Arabica coffee. Afr J Agric Res 2016; 11: 2412–2422.

11. Arruda NP, Hovell AMC, Rezende CM, Freitas SP, Couri S, Bizzo HR. Correlação entre precursores e voláteis em café arábica brasileiro processado pelas vias seca, semiúmida e úmida e discriminação através da análise por componentes principais. Quím Nova 2012; 35: 2044–2051.

12. Poisson L, Blank I, Dunkel A, Hofmann T. Chapter 12 - The Chemistry of Roasting—Decoding Flavor Formation. In: Folmer B (ed). The Craft and Science of Coffee. Academic Press, 2017, pp 273–309.

13. Chu Y-F. Coffee: Emerging Health Effects and Disease Prevention. John Wiley & Sons, 2012.

14. Grembecka M, Malinowska E, Szefer P. Differentiation of market coffee and its infusions in view of their mineral composition. Sci Total Environ 2007; 383: 59–69.

15. Arya M, Rao LJM. An impression of coffee carbohydrates. Crit Rev Food Sci Nutr 2007; 47: 51–67.

16. Bressanello D, Liberto E, Cordero C, Rubiolo P, Pellegrino G, Ruosi MR et al. Coffee aroma: Chemometric comparison of the chemical information provided by three different samplings combined with GC-MS to describe the sensory properties in cup. Food Chem 2017; 214: 218–226.

17. Gonzalez-Rios O, Suarez- Quiroz M, Renaud B, Barel M, Guyot B, Guiraud J-P et al. Impact of "ecological" post-harvest processing on coffee aroma: II. Roasted coffee. J Food Compos Anal - J FOOD COMPOS ANAL 2007; 20: 297–307.

18. Puerta G, Echeverry J. Fermentación controlada del café: Tecnología para agregar valor a la calidad. 2015.https://biblioteca.cenicafe.org/bitstream/10778/558/1/avt0454.pdf.

19. Kulapichitr F, Borompichaichartkul C, Suppavorasatit I, Cadwallader KR. Impact of drying process on chemical composition and key aroma components of Arabica coffee. Food Chem 2019; 291: 49–58.

20. Dong W, Hu R, Chu Z, Zhao J, Tan L. Effect of different drying techniques on bioactive components, fatty acid composition, and volatile profile of robusta coffee beans. Food Chem 2017; 234: 121–130.

21. Firdissa E, Mohammed A, Berecha G, Garedew W. Coffee Drying and Processing Method Influence Quality of Arabica Coffee Varieties (Coffee arabica L.) at Gomma I and Limmu Kossa, Southwest Ethiopia. J Food Qual 2022; 2022: e9184374.

22. Coradi PC, Borém FM, Saath R, Marques ER. Effect of drying and storage conditions on the quality of natural and washed coffee. Coffee Sci 2007; 2: 10.

23. Lee LW, Cheong MW, Curran P, Yu B, Liu SQ. Modulation of coffee aroma via the fermentation of green coffee beans with Rhizopus oligosporus: I. Green coffee. Food Chem 2016; 211: 916–924.

24. Petisca C, Pérez-Palacios T, Farah A, Pinho O, Ferreira IM-PLVO. Furans and other volatile compounds in ground roasted and espresso coffee using headspace solid-phase microextraction: Effect of roasting speed. Food Bioprod Process 2013; 91: 233–241.

25. Yisak H, Redi-Abshiro M, Chandravanshi BS. Selective determination of caffeine and trigonelline in aqueous extract of green coffee beans by FT-MIR-ATR spectroscopy. Vib Spectrosc 2018; 97: 33–38.

26. Kitzberger CSG, Scholz MB dos S, Benassi M de T. Bioactive compounds content in roasted coffee from traditional and modern Coffea arabica cultivars grown under the same edapho-climatic conditions. Food Res Int 2014; 61: 61–66.

27. Cheng B, Furtado A, Smyth HE, Henry RJ. Influence of genotype and environment on coffee quality. Trends Food Sci Technol 2016; 57: 20–30.

28. Specialty Coffee Association of America. SCAA. Coffee Standards. 2018.https://static1.squarespace.com/static/584f6bbef5e23149e5522201/t/5d936fa1e29d4d5342049d74/1569943487417/Coffee+Standards-compressed.pdf (accessed 27 Jul2021).

29. Farah A, Monteiro MC, Calado V, Franca AS, Trugo LC. Correlation between cup quality and chemical attributes of Brazilian coffee. Food Chem 2006; 98: 373–380.

30. Barbosa M de SG, Scholz MB dos S, Kitzberger CSG, Benassi M de T. Correlation between the composition of green Arabica coffee beans and the sensory quality of coffee brews. Food Chem 2019; 292: 275–280.

31. Saquicela JE. "Optimización experimental de un método cromatográfico HPLC-DAD para el análisis de polifenoles en frutas." 2018.http://dspace.ucuenca.edu.ec/bitstream/123456789/30853/1/TRABAJO%20DE%20TITULACI%c3%93N.pdf.

32. Murkovic M, Derler K. Analysis of amino acids and carbohydrates in green coffee. J Biochem Biophys Methods 2006; : 8.

33. Kerkaert B, Mestdagh F, Cucu T, Aedo PR, Ling SY, De Meulenaer B. Hypochlorous and peracetic acid induced oxidation of dairy proteins. J Agric Food Chem 2011; 59: 907–914.

34. Henderson JW, Ricker RD, Bidlingmeyer BA, Woodward C. Rapid, accurate, sensitive, and reproducible HPLC analysis of amino acids. Amino acid analysis using Zorbax Eclipse-AAA columns and the Agilent, 1100. Agil Technol 2000; : 1–10.

35. Mehari B, Redi-Abshiro M, Chandravanshi BS, Atlabachew M, Combrinck S, McCrindle R. Simultaneous Determination of Alkaloids in Green Coffee Beans from Ethiopia: Chemometric Evaluation of Geographical Origin. Food Anal Methods 2016; 9: 1627–1637.

36. Atlabachew M, Abebe A, Alemneh Wubieneh T, Tefera Habtemariam Y. Rapid and simultaneous determination of trigonelline, caffeine, and chlorogenic acid in green coffee bean extract. Food Sci Nutr 2021; 9: 5028–5035.

37. Macheiner L, Schmidt A, Schreiner M, Mayer HK. Green coffee infusion as a source of caffeine and chlorogenic acid. J Food Compos Anal 2019; 84: 103307.

38. Demissie EG, Woyessa GW, Abebe A. Uv/Vis spectrometer determination of caffeine in green coffee beans from Hararghe, Ethiopia, using beer-lambert's law and integrated absorption coefficient techniques. 2016; : 16.

39. De Luca S, Ciotoli E, Biancolillo A, Bucci R, Magrì AD, Marini F. Simultaneous quantification of caffeine and chlorogenic acid in coffee green beans and varietal classification of the samples by HPLC-DAD coupled with chemometrics. Environ Sci Pollut Res 2018; 25: 28748–28759.

40. Perrone D, Farah A, Donangelo C, Paulis T, Martin P. Comprehensive analysis of major and minor chlorogenic acids and lactones in economically relevant Brazilian coffee cultivars. Food Chem 2008; 106: 859–867.

41. Król K, Gantner M, Tatarak A, Hallmann E. The content of polyphenols in coffee beans as roasting, origin and storage effect. Eur Food Res Technol 2020; 246: 33–39.

42. Rostagno MA, Celeghini RMS, Debien ICN, Nogueira GC, Meireles MAA. Chapter 15 - Phenolic Compounds in Coffee Compared to Other Beverages. In: Preedy VR (ed). Coffee in Health and Disease Prevention. Academic Press: San Diego, 2015, pp 137–142.

43. Jeszka-Skowron M, Sentkowska A, Pyrzyńska K, De Peña MP. Chlorogenic acids, caffeine content and antioxidant properties of green coffee extracts: influence of green coffee bean preparation. Eur Food Res Technol 2016; 242: 1403–1409.

44. Craig AP, Fields C, Liang N, Kitts D, Erickson A. Performance review of a fast HPLC-UV method for the quantification of chlorogenic acids in green coffee bean extracts. Talanta 2016; 154: 481–485.

45. Ribeiro DE, Borém FM, Nunes CA, Alves AP de C, Santos CM dos, Taveira JH da S et al. Profile of organic acids and bioactive compounds in the sensory quality discrimination of arabica coffee. Coffee Sci - ISSN 1984-3909 2018; 13: 187–197.

46. Ribeiro DE, Borém FM, Nunes CA. Sensory quality discrimination of Coffea arabica. Coffee Sci 2018; 13: 11.
47. Wei F, Tanokura M. Organic Compounds in Green Coffee Beans. In: Coffee in Health and Disease Prevention. Elsevier, 2015, pp 149–162.
48. Casal S, Alves MR, Mendes E, Oliveira MBPP, Ferreira MA. Discrimination between Arabica and Robusta Coffee Species on the Basis of Their Amino Acid Enantiomers. J Agric Food Chem 2003; 51: 6495–6501.
49. Lee LW, Tay GY, Cheong MW, Curran P, Yu B, Liu SQ. Modulation of the volatile and non-volatile profiles of coffee fermented with Yarrowia lipolytica: I. Green coffee. LWT 2017; 77: 225–232.
50. Dong W, Tan L, Zhao J, Hu R, Lu M. Characterization of Fatty Acid, Amino Acid and Volatile Compound Compositions and Bioactive Components of Seven Coffee (Coffea robusta) Cultivars Grown in Hainan Province, China. Molecules 2015; 20: 16687–16708.
51. Wei F, Furihata K, Koda M, Hu F, Kato R, Miyakawa T et al. 13C NMR-Based Metabolomics for the Classification of Green Coffee Beans According to Variety and Origin. J Agric Food Chem 2012; 60: 10118–10125.
52. Ramón-Gonçalves M, Gómez-Mejía E, Rosales-Conrado N, León-González ME, Madrid Y. Extraction, identification and quantification of polyphenols from spent coffee grounds by chromatographic methods and chemometric analyses. Waste Manag 2019; 96: 15–24.
53. Cheong MW, Tong KH, Ong JJM, Liu SQ, Curran P, Yu B. Volatile composition and antioxidant capacity of Arabica coffee. Food Res Int 2013; 51: 388–396.
54. Amanpour A, Selli S. Differentiation of Volatile Profiles and Odor Activity Values of Turkish Coffee and French Press Coffee: Turkish Coffee and French Press Coffee Volatiles. J Food Process Preserv 2016; 40: 1116–1124.
55. Laukaleja I, Kruma Z. Phenolic and volatile compound composition influence to specialty coffee cup quality. 2019; : 441.8Kb.
56. Heo J, Adhikari K, Choi KS, Lee J. Analysis of Caffeine, Chlorogenic Acid, Trigonelline, and Volatile Compounds in Cold Brew Coffee Using High-Performance Liquid Chromatography and Solid-Phase Microextraction—Gas Chromatography-Mass Spectrometry. Foods 2020; 9: 1746.
57. Mehari B, Redi M, Chandravanshi B, Combrinck S, Atlabachew M, Mccrindle R. Profiling of Phenolic Compounds Using UPLC-MS for Determining the Geographical Origin of Green Coffee Beans from Ethiopia. J Food Compos Anal 2016; 45: 16–25.
58. Bertrand B, Renaud B, Dussert S, Laffargue A, Ribeyre F, Berthiot L et al. Climatic factors directly impact the biochemical composition and the volatile organic compounds fingerprint in green Arabica coffee bean as well coffee beverage quality. 2012.
59. Tolessa K, D'heer J, Duchateau L, Boeckx P. Influence of growing altitude, shade and harvest period on quality and biochemical composition of Ethiopian specialty coffee. J Sci Food Agric 2017; 97: 2849–2857.
60. Läderach P, Oberthür T, Cook S, Estrada Iza M, Pohlan JA, Fisher M et al. Systematic agronomic farm management for improved coffee quality. Field Crops Res 2011; 120: 321–329.
61. Bastian F, Hutabarat OS, Dirpan A, Nainu F, Harapan H, Emran TB et al. From Plantation to Cup: Changes in Bioactive Compounds during Coffee Processing. Foods 2021; 10: 2827.
62. Wintgens JN. Factors Influencing the Quality of Green Coffee. In: Coffee: Growing, Processing, Sustainable Production. John Wiley & Sons, Ltd, 2004, pp 789–809.
63. Velásquez S, Banchón C. Influence of pre-and post-harvest factors on the organoleptic and physicochemical quality of coffee: a short review. J Food Sci Technol 2022. doi:10.1007/s13197-022-05569-z.
64. Silveira A de S, Pinheiro ACT, Ferreira WPM, Silva LJ da, Rufino JL dos S, Sakiyama NS. ' Sensory analysis of specialty coffee from different environmental conditions in the region of Matas de Minas, Minas Gerais, Brazil. Rev Ceres 2016; 63: 436–443.
65. Santos DF, Franco Junior KS, da Silva CH, Da Silva Neto JF, Paiva LC, Brigante GP. Efect of lnf (cna - cnb) enzyme complex in the drying process and the coffee quality. 2020. doi:10.25186/.v15i.1677.
66. Haile M, Hee Kang W. The Harvest and Post-Harvest Management Practices' Impact on Coffee Quality. In: Toledo Castanheira D (ed). Coffee - Production and Research. IntechOpen, 2020 doi:10.5772/intechopen.89224.
67. Duarte GS, Pereira AA, Farah A. Chlorogenic acids and other relevant compounds in Brazilian coffees processed by semi-dry and wet post-harvesting methods. Food Chem 2010; 118: 851–855.
68. Pinto G, Silva Q, Ribeiro M, De Souza S. Quality of coffee produced in the Southwest region of Bahia, Brazil subjected to different forms of processing and drying. Afr J Agric Res 2013; 8: 2334–2339.
69. Rodriguez YFB, Guzman NG, Hernandez JG. Effect of the post-harvest processing method on the biochemical composition and sensory analysis of Arabica coffee. Eng Agríc 2020; 40: 177–183.

13

ARTICLE / INVESTIGACIÓN

Fitorremediación de cinco productos farmaceúticos registrados como contaminantes emergentes en medio acuoso empleando la especie Jacinto de Agua (*Eichhornia crassipes*)

Phytoremediation of five pharmaceutical products registered as emerging contaminants in an aqueous medium using the species Water Hyacinth (*Eichhornia crassipes*)

Checa-Artos Miriam[1,2]*, Barcos-Arias Milton[1,3], Sosa-Del Castillo Daynet[1], Vanegas María Eulalia[5], Ruiz-Barzola Omar[1,4]

DOI. 10.21931/RB/2023.08.01.18

[1] Escuela Superior Politécnica del Litoral, Facultad de Ciencias de la Vida, Centro de Investigaciones Biotecnológicas del Ecuador, Guayaquil, Ecuador.
[2] Universidad de las Fuerzas Armadas ESPE, Sangolquí, Ecuador.
[3] Facultad de Ingenierías. Universidad Espíritu Santo. Samborondón, Ecuador.
[4] Departamento de Estadística, Universidad de Salamanca, USal, Salamanca, España.
[5] Centro de Estudios Ambientales, Departamento de Química Aplicada y Sistemas de Producción, Facultad de Ciencias Químicas, Universidad de Cuenca, Cuenca, Ecuador.
Corresponding author: mcheca@espol.edu.ec

Resumen: La contaminación de los sistemas acuáticos de agua dulce constituye un problema ambiental recurrente en el ámbito mundial, que se agudiza cada vez más con la presencia frecuente de nuevos compuestos químicos, tal es el caso de los contaminantes emergentes, dentro de los cuales se incluyen los productos farmacéuticos. El objetivo de esta investigación fue estimar la capacidad de la especie jacinto de agua (*Eichhornia crassipes*) para remover del medio acuoso cinco fármacos altamente recetados y de venta libre como ciprofloxacina, ibuprofeno, sulfametaxazol, diclofenaco y acetaminofén. El trabajo se llevó a cabo en condiciones de invernadero a una temperatura de 25 0C y a un pH de 6,5; con una toma de muestras cada 24 h a diferentes concentraciones (3, 6, 9,12) mg/L. Para el análisis de las muestras se utilizó Espectrofotometría UV-VIS con lectura directa de las absorbancias de cada uno de los fármacos. Se empleó la metodología de superficies de respuesta para el análisis estadístico de los datos, lo que permitió determinar los modelos para establecer tiempos y concentraciones óptimas maximizando la absorción de cada producto farmacéutico, así como obtener las pendientes de crecimiento para definir hacia donde se puede proyectar el óptimo. Los principales resultados en este estudio indican que *E. crassipes* removió 95% de diclofenaco en soluciones acuosas con una concentración de 3 mg/L en un tiempo de 24 h, seguido de ciprofloxacina y acetaminofén con una remoción máxima de 91,18% y 71% a las 96 h, respectivamente. Mientras que los más bajos porcentajes de remoción se obtuvo para ibuprofeno y sulfametaxazol con 57,56% y 36%, respectivamente. En el presente estudio, se comprobó la alta capacidad de remoción *E. crassipes* de los cinco productos farmacéuticos en condiciones controladas, evidenciando una gran posibilidad de aplicación en el campo de la fitorremediación de contaminantes emergentes en medio acuoso, lo cual constituye un importante aporte en este ámbito de la investigación.

Palabras clave: Fitorremediación, contaminantes emergentes, jacinto de agua (*Eichhornia crassipes*), superficie de respuesta.

Abstract: Contamination of freshwater aquatic systems is a recurring environmental problem worldwide, which is becoming increasingly acute with the frequent presence of new chemical compounds, such as emerging pollutants, including pharmaceutical products. The objective of this research was to estimate the ability of the water hyacinth species (*Eichhornia crassipes*) to remove from the aqueous environment five highly prescribed and over-the-counter drugs such as ciprofloxacin, ibuprofen, sulfamethoxazole, diclofenac, and acetaminophen. The work was carried out under greenhouse conditions at a temperature of 25 0C and a pH of 6.5; with a sampling every 24 h at different concentrations (3, 6, 9.12) mg/L. For the analysis of the samples, UV-VIS Spectrophotometry was used with direct reading of the absorbances of each one of the drugs. The response surface methodology was used for the statistical analysis of the data, which allowed determining the models to establish optimal times and concentrations maximizing the absorption of each pharmaceutical product, as well as obtaining the growth slopes to define where it can be projected the optimum. The main results in this work indicate that *E. crassipes* removed 95% of diclofenac in aqueous solutions with a concentration of 3 mg/L in 24 h, followed by ciprofloxacin and acetaminophen with a maximum removal of 91.18% and 71% at 96 h, respectively. At the same time, the lowest removal percentages were obtained for ibuprofen and sulfamethoxazole at 57.56% and 36%, respectively. In the present study, the high *Eichchornia crassipes* removal capacity of the five pharmaceutical products under controlled conditions was verified, evidencing a great possibility of application in the phytoremediation of emerging contaminants in an aqueous medium.

Key words: Phytoremediation, emerging contaminants, water hyacinth (*Eichhornia crassipes*), response surface.

2

Introducción

Los contaminantes emergentes (CE) tales como los productos farmacéuticos (PFs) y sus metabolitos, productos de cuidado personal (PCP), compuestos disruptores endocrinos (CDE) entre otros, son motivo de preocupación debido a su incidencia en la salud humana y en los ecosistemas acuáticos, cuya presencia se ha detectado en niveles traza en aguas residuales, aguas superficiales y subterráneas e inclusive en agua potable[1-4].

Las principales fuentes de CE del agua dulce generalmente se originan en las descargas de aguas residuales municipales, de la industria, de las prácticas domésticas, de la agricultura y la ganadería[5-7].

Es importante señalar que, a pesar de los avances tecnológicos, los sistemas actuales de tratamiento de aguas residuales no son eficientes para eliminar estos CE[8]. Asimismo, aun no existen suficientes regulaciones que brinden pautas en el tratamiento de CE en el ámbito local y mundial[9,10].

En los últimos 20 años, se han llevado a cabo diferentes investigaciones en la mayoría de países del mundo, en las cuales se establece la presencia frecuente de PFs y de demás CE[4,11,12]. En este contexto, un estudio realizado en Ecuador en el año 2013 por (13), determinó la presencia de algunos PFs como venlafaxina, carbamazepina, sulfametoxazol y benzoilcgonina, en los ríos San Pedro-Guayllabamba-Esmeraldas.

Cabe destacar que, los productos farmacéuticos incluidos en la presente investigación, figuran como los más altamente recetados y de venta libre en todos los continentes, excepto Oceanía[12,14-17]. Lo que encuentra relación con su aparición frecuente en aguas superficiales, subterráneas, aguas residuales y agua potable[1,18-26].

La presencia de fármacos en los ambientes acuáticos y sus riesgos consecuentes, son cada vez más evidentes porque las tecnologías de identificación de estos contaminantes han mejorado sustancialmente[19,27-30]. Asimismo, el riesgo ambiental como es la resistencia a antibióticos, alteración endócrina y carcinogenicidad, se ha incrementado debido a que las industrias relacionadas con la salud humana y veterinarias han incrementado la producción de PFs, lo que implica un mayor consumo y por tanto mayores descargas a los ecosistemas acuáticos[2,22,23,27,31-36].

El derecho de los seres humanos al acceso y consumo de agua segura es un precepto sine qua non para la convivencia en nuestro planeta, esto significa que el suministro de agua potable debe estar garantizado, así como también, la eliminación de aguas residuales a través de la implementación de sistemas eficientes de tratamiento de CE previo a su descarga a las fuentes hídricas, o al uso posterior que se destine como para el riego de cultivos o de áreas verdes[20,22,37].

En este sentido, los ecosistemas acuáticos se enfrentan a un alto nivel de estrés y agotamiento, debido a la frecuente y creciente entrada de diversos tipos de contaminantes incluidos los CE[38],, por lo que se vuelve imprescindible la investigación de sistemas alternativos para prevenir y mitigar la contaminación de las fuentes hídricas.

Los métodos actuales más adoptados para la eliminación de PFs del agua como los antibióticos, incluyen la adsorción avanzada de carbono, la oxidación avanzada, la tecnología de membranas y la degradación fotocatalítica[39-42]. Sin embargo, la fitorremediación está siendo empleada como método alternativo principal para reducir los antibióticos de las fuentes de agua debido a su bajo costo, amplio espectro, manejo simple y libre de subproductos contaminantes[36,40].

La especie *Eichhornia crassipes* es una planta acuática flotante cuyas raíces intervienen en la absorción de todo tipo de contaminantes del agua como metales pesados, compuestos orgánicos, pesticidas, PFs, entre otros[43-45]. Estas características de la especie han permitido que se instalen sistemas de tratamiento de aguas residuales en varios países como en la India y otros países asiáticos[38]. Asimismo, la combinación adecuada de *Eichhornia crassipes* con otras plantas acuáticas como la alga de pato y las algas verde azules produce una reducción de contaminantes superior a la *E. crassipes* por sí sola[46].

Con estos antecedentes, se seleccionó la especie jacinto de agua (*Eichhornia crassipes*), debido a sus características morfológicas y fisiológicas, así como también por la versatilidad de la especie para remover del medio acuoso diferentes tipos de contaminantes orgánicos, inorgánicos e inclusive algunos CE como los PFs[43,44,47-50].

En este contexto, la presente investigación tuvo como objetivo principal contribuir con una técnica probada bajo condiciones controladas para la fitorremediación de acetaminofén, ciprofloxacina, diclofenaco, sulfametoxazol e ibuprofeno, utilizando jacinto de agua (*Eichhornia crassipes*).

Materiales y métodos

Recolección y acondicionamiento de la especie jacinto de agua (*Eichhornia crassipes*)

El experimento se realizó en el Centro de Investigaciones Biotecnológicas del Ecuador (CIBE) de la Escuela Superior Politécnica del Litoral (ESPOL), las plántulas de *E. crassipes* se recolectó de un estero ubicado en la vía Durán – Tambo a 14 msnm, luego de lo cual se lavó a fondo sus raíces con agua de grifo y se acondicionó su permanencia en un pozo artificial durante 30 días. Posteriormente, las plántulas fueron trasladadas al invernadero para la experimentación bajo condiciones controladas. Este es un procedimiento basado en lo desarrollado por (43).

Diseño del experimento

Para el estudio se obtuvo cinco PFs (sulfametoxazol, ciprofloxacina, acetaminofén, ibuprofeno y diclofenaco) de la marca SIGMA-ALDRICH al 99,9% de pureza. De cada PFs se preparó soluciones acuosas por triplicado, utilizando metanol ultrapuro de la marca Merck a cuatro concentraciones diferentes (3, 6, 9 y 12) mg/L, manteniendo la temperatura de 25oC y un pH de 6,5 durante todo el experimento. Se estableció cuatro tiempos de muestreo (24, 48, 72 y 96) h. Se trabajó con un volumen de 2 litros de solución de cada concentración del fármaco, luego se introdujo las plántulas de *E. crassipes* de un peso aproximado de 60 g. Concluido el tiempo de exposición, se tomó alícuotas de cada unidad experimental para su posterior análisis, para lo cual se utilizó la técnica de espectrofotometría de luz UV visible para medir la absorbancia de cada uno de los fármacos.

Se utilizó el diseño factorial, con , con dos puntos internos donde los factores fueron concentración ( ) y tiempo (; los niveles considerados se indican en la figura 1.

En la determinación del porcentaje de remoción (%) de
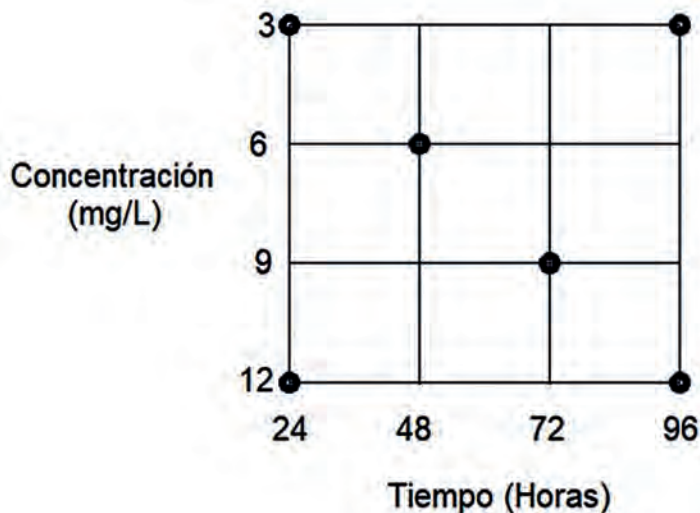
Figura 1. Esquema del diseño experimental con *Eichhornia crassipes.*

los PFs de estudio, que constituye la variable de respuesta se aplicó la fórmula 1:

$$\% = \frac{Concentración\ inicial - Concentración\ final}{Concentración\ inicial} \ X \ 100 \quad (1)$$

Análisis de datos

Para el análisis estadístico de los datos se utilizó el software estadístico R versión 3.6.0 y RStudio versión 1.1.453 y se empleó la técnica de superficies de respuesta para encontrar los modelos que ayuden a determinar tiempos y concentraciones óptimas donde se maximizó la absorción de cada fármaco, así como la obtención de las pendientes de crecimiento para determinar hacia donde se deberá buscar el óptimo, en los casos donde no se los encontró.

Resultados

Modelo General

El modelo general de la superficie de respuesta está representado en la ecuación (1).

$$Y = b_0 + b_1C + b_2T + b_3C^2 + b_4T^2 + b_6C*T \quad (1)$$

La matriz resultante no permitió obtener un modelo polinómico de grado 2 para ambos factores en forma simultánea, por lo que se desarrolló un modelo con forma cuadrática para un factor, mientras se mantuvo la linealidad en el otro factor, conforme a las ecuaciones (2), (3). El modelo general de la superficie de respuesta está representado por la ecuación:

Donde,
= porcentaje de remoción
= intercepto
= coeficientes del modelo
= Concentración
= Tiempo

Con la finalidad de describir gráficamente de mejor forma el fenómeno, en todas las ecuaciones se mantuvo los coeficientes de los efectos simples o de orden uno, los efectos cuadráticos y la interacción, aun cuando en algunas ocasiones no hayan resultado significativos.

En el modelo obtenido para sulfametaxazol (Figura 2A), los coeficientes de las variables C, T, T2 no fueron significativos, ver la ecuación (4).

Si se examina el modelo considerando al tiempo como un factor cuadrático que le da curvatura al modelo, se presenta que el coeficiente de la interacción entre los factores de tiempo y concentración no es significativo, en comparación a los otros coeficientes.

Eichhornia crassipes fue menos eficiente removiendo sulfametaxazol en comparación con el resto de fármacos en estudio, dado que se evidencia porcentajes bajos de remoción de este fármaco a medida que se aumenta la concentración y el tiempo (48 y 72 h). Asimismo, se observa que el mayor porcentaje de remoción de 36,05% se da con la concentración más baja de 3 mg/L a las 24 h, este porcentaje de remoción es el más bajo en comparación con los restantes cuatro fármacos de estudio.

En el caso de la ciprofloxacina (Figura 2B), se visualiza que el modelo no presenta concavidad, dado que el coeficiente del término cuadrático es pequeño, de acuerdo con la ecuación (5).

El valor óptimo de remoción al 91,18% se da con una concentración de 3 mg/L y un tiempo de 96 h, lo que demuestra la eficiencia de *Eichhornia crassipes* en la remoción de este fármaco en medio acuoso. Se puede observar que el porcentaje de remoción disminuye en relación con el aumento de la concentración.

En el modelo estudiado para el ibuprofeno (Figura 2C), se presenta un modelo que obtiene la mayor información, acorde a la ecuación (6).

En este caso, se evidencia que el valor óptimo de porcentaje de remoción 65,04% se ha obtenido con una concentración de 12 mg/L en un tiempo de 60 h, estos resultados indican una eficiencia aceptable de *Eichhornia crassipes* en la remoción de este PF. A su vez, se observa que a mayor tiempo y a menor concentración se obtienen porcentajes de remoción bajos. Es decir, en el nivel de concentración más bajo se obtiene el porcentaje de remoción mínimo.

C^2	T^2
$Y = b_0 + b_1C + b_2T + b_3C^2 + b_4T*C \quad (2)$	$Y = b_0 + b_1C + b_2T + b_3T^2 + b_4C*T \quad (3)$

En el modelo estudiado para el diclofenaco (Figura 2D), los valores de la variable T, T2 y C T son significativos, ver la ecuación (7).

En este rango de estudio, se observa que el diclofenaco inicia con un porcentaje de remoción de 95,01%, con una concentración de 3 mg/L en un tiempo de 24 h, lo que señala una alta eficiencia de Eichhornia crassipes en la remoción de diclofenaco. Como se visualiza en la figura 2D, dicho porcentaje presenta un descenso pronunciado, es decir, a medida que aumenta el tiempo se produce el proceso inverso y el porcentaje de remoción comienza a reducirse. Mientras que, por el contrario, con una concentración de 12 mg/L, el porcentaje de remoción inicia de 23,32% y a medida que se aumenta el tiempo, el porcentaje de remoción va aumentando.

En las condiciones estudiadas para el acetaminofén (Figura 2E), los valores de las variables de la concentración y la interacción de esta con el tiempo no son significativos para el estudio, ver la ecuación (8).

En el rango estudiado para el acetaminofén, se observa que existen dos casos, el primero muestra que con una concentración de 3 mg/L y a medida que aumenta el tiempo, se alcanza un porcentaje máximo de remoción de 71,09%. Para el segundo caso con una concentración de 12 mg/L y a medida que aumenta el tiempo se alcanza un máximo de remoción de 70,57%. Estos resultados indican una buena capacidad removedora de este fármaco por parte de Eichhornia crassipes a diferentes concentraciones. Adicionalmente, se observa que para alcanzar el valor óptimo es necesario usar una concentración baja (3 mg/L) y aumentar el tiempo.

Discusión

Los resultados obtenidos demostraron la capacidad de Eichhornia crassipes para remover los cinco fármacos estudiados en medio acuoso, en un periodo experimental de 96 h a diferentes concentraciones consideradas en esta investigación (3, 6, 9 y 12 mg/L).

La especie E. crassipes presentó un porcentaje de remoción relativamente bajo de sulfametaxazol de 36,05% en soluciones del fármaco con una concentración de 3 mg/L a las 24 h (Figura 2A). En el estudio realizado por (51), se obtuvo del 70% al 90% de remoción de sulfametoxazol, a las 96 h de exposición con Typha latifolia, lo que indica que dicha especie es más eficiente en la remoción de este fármaco que E. crassipes.

En la Figura 2B, se observa que el valor óptimo de remoción de ciprofloxacina de 91,18%, se obtuvo con una concentración de 3 mg/L a las 96 h de exposición. En el estudio llevado a cabo por (40), se encontró que la absorción de ciprofloxacina de E. crassipes fue de hasta 84,38% y la raíz fue el principal tejido de absorción.

Asimismo, en el caso del ibuprofeno, E. crassipes presentó un valor óptimo en el porcentaje de remoción 65,04% con una concentración de 12 mg/L en un tiempo de 60 h (Figura 2C). Estos resultados son comparables con la investigación de (49), que reportó que Typha eliminó casi el 60% de ibuprofeno en las primeras 24 h, logrando una re-

$$\% \text{ de remoción } = 44.24 - 0.7534\,C - 0.3033\,T + 0.0024\,T^2 - 0.0005\,C*T \qquad (4)$$

$$\% \textit{ de remoción } = 94.35 - 0.9461C - 0.0398\,T + 0.0004\,T^2 + 0.0007\,C*T \qquad (5)$$

$$\% \textit{ de remoción } = -39.86 + 1.0694\,C + 2.8956\,T - 0.0249\,T^2 + 0.0110\,C*T \qquad (6)$$

$$\% \textbf{ de remoción } = 172.26 - 12.74\,C - 2.1989\,T - 0.0010\,T^2 + 0.1987\,C*T \qquad (7)$$

$$\% \text{ de remoción } = 83.06 + 0.9396\,C - 1.1035\,T + 0.0102\,T^2 - 0.0104\,C*T \qquad (8)$$

FÁRMACO	C^2	T^2
SULFAMETOXAZOLE (SMX)	$Y = 44.24 - 3.07\,C - 0.0142\,T + 0.1542\,C^2 - 0.0005\,C*T$	$Y = 44.24 - 0.7534\,C - 0.3033\,T + 0.0024\,T^2 - 0.0005\,C*T$
CIPROFLOXACINA (Cx)	$Y = 94.35 - 1.2874\,C + 0.0029\,T + 0.0228\,C^2 + 0.0007\,C*T$	$Y = 94.35 - 0.9461C - 0.0398\,T + 0.0004\,T^2 + 0.0007\,C*T$
ACETAMINOFEN (AC)	$Y = 83.06 - 8.8664\,C + 0.1223\,T + 0.6537\,C^2 - 0.0104\,C*T$	$Y = 83.06 + 0.9396\,C - 1.1035\,T + 0.0102\,T^2 - 0.0104\,C*T$
IBUPROFENO (IB)	$Y = -39.86 + 24.97\,C - 0.0917\,T - 1.59\,C^2 + 0.0111\,C*T$	$Y = -39.86 + 1.0694\,C + 2.8956\,T - 0.0249\,T^2 + 0.0110\,C*T$
DICLOFENACO (DF)	$Y = 172.26 - 11.78\,C - 2.3189\,T - 0.0640\,C^2 + 0.1987\,C*T$	$Y = 172.26 - 12.74\,C - 2.1989\,T - 0.0010\,T^2 + 0.1987\,C*T$

Tabla 1. Modelo de superficie de respuesta, obtenidos para cada uno de los fármacos de estudio con Eichhornia crassipes. Este es un modelo con forma cuadrática para un factor, mientras se mantuvo la linealidad en el otro factor.

5
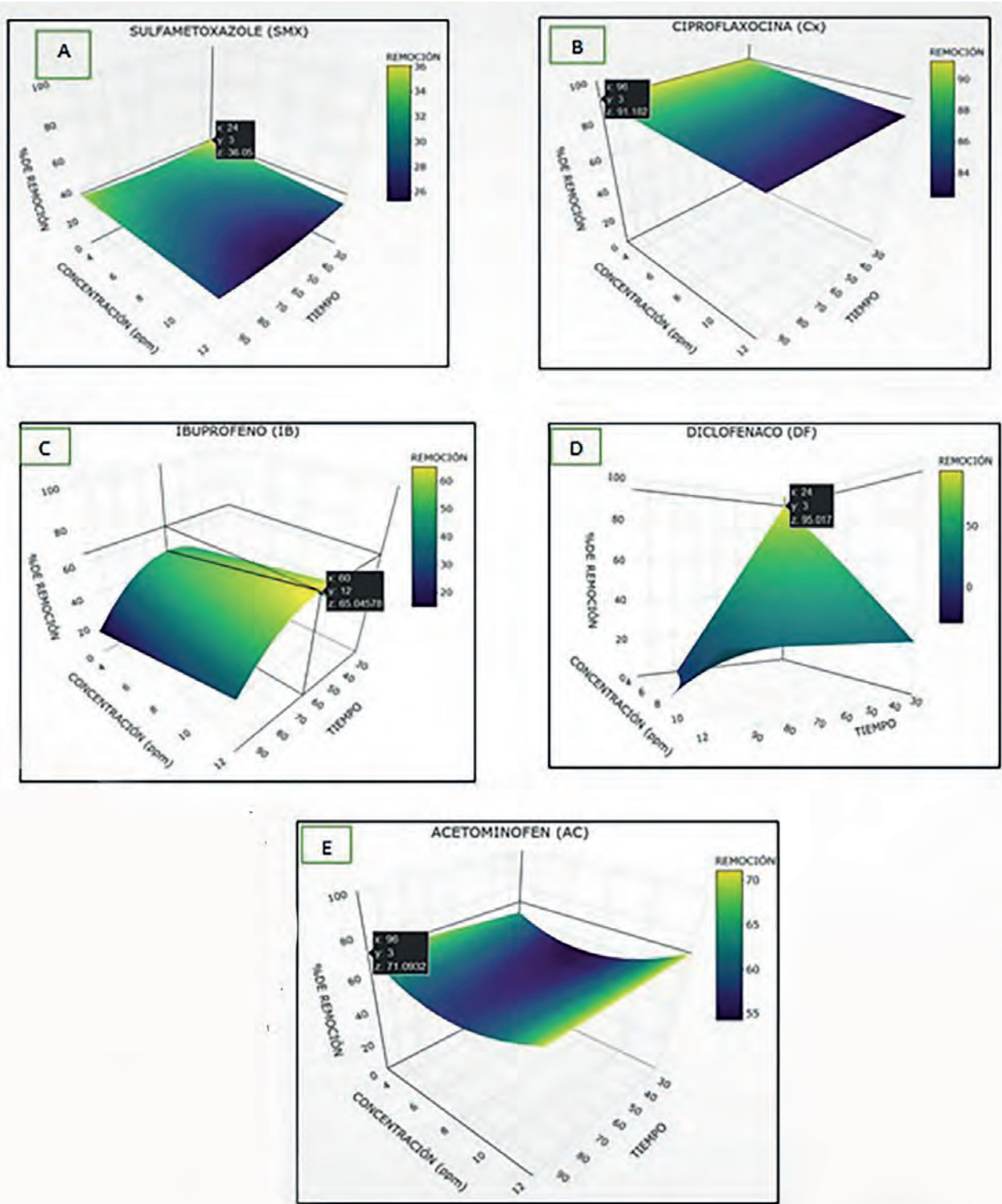
Figura 2. Resultados obtenidos con la técnica superficie de respuesta para la remoción con *Eichhornia crassipes* de los fármacos A) sulfametoxazol (SMX), B) ciprofloxacina (CX), C) ibuprofeno (IBU), D) diclofenaco (DF) y E) acetaminofén (AC) en medio acuoso.

moción superior al 99%, en una solución de ibuprofeno con una concentración inicial de 20 mg/L, en un periodo de 21 días. Asimismo, un estudio realizado por (52), reportó que *Phragmites australis* eliminó completamente el ibuprofeno del medio líquido después de 21 días.

Por un lado, se observa que se alcanzó un porcentaje de remoción de 95.01% de diclofenaco, a una concentración de 3mg/L en un tiempo de 24 h (Figura 2D), mientras

que, con una concentración alta de 12mg/L, el porcentaje de remoción inicia con 23,32% y a medida que aumenta el tiempo, el porcentaje de remoción se incrementa. Según (52), *Phragmites autralis* removió 18% de diclofenaco en soluciones con concentraciones de 30 mg/L, en un periodo de 14 días, lo que demuestra que *E.crassipes* se comporta de forma más eficiente en la remoción del fármaco en mención.

Se presentan dos casos en cuanto al acetaminofén (Figura 2E), el primero muestra que *E.crassipes* con una concentración de 3 mg/L y a medida que aumenta el tiempo se obtuvo un porcentaje máximo de remoción de 71,09%. Para el segundo caso, con una concentración de 12 mg/L y a medida que aumenta el tiempo se estableció un máximo de remoción de 70,57%.

En este escenario, es importante señalar que *Eichhornia crassipes*, tiene un comportamiento similar a algunas especies de plantas acuáticas, *Ipomoea aquatica, Azolla caroliniana, Lemna minor, Phragmites australis, Typha latifolia, Salix atrocinerea* y *Scirpus validushan*, que han demostrado capacidad para remover ciprofloxacina, ibuprofeno, diclofenaco, sulfametaxazol y acetaminofén de las aguas residuales, que han logrado una alta eficacia de remoción de entre el 70% y 90%[44,53-55].

Los resultados obtenidos en esta investigación permiten establecer que *E. crassipes* presentó un comportamiento eficiente en la remoción de los cinco fármacos de estudio, lo que demuestra que esta técnica de fitorremediación probada a nivel laboratorio puede ser prometedora a mayor escala, lo cual guarda coherencia con lo reportado por la literatura científica.

Conclusiones

En esta investigación, se comprobó la eficiencia de la especie *Eichhornia crassipes* con un importante porcentaje de remoción de los cinco PFs estudiados bajo condiciones controladas en medio acuoso.

Los mejores resultados se registraron cuando *Eichhornia crassipes* removió DF en un 95% de una solución con una concentración de 3 mg/L en un tiempo de 24 h. De la misma manera, el porcentaje de remoción máxima de 91,18% y 71% respectivamente de CX y AC, se obtuvo en soluciones con una concentración de 3 mg/L y a las 96 h de exposición, así como el IB, que alcanzó una remoción máxima del 57.56% en soluciones con una concentración de 7.5 mg/L en el tiempo de 24 h.

Por otro lado, el SMX reportó un porcentaje menor de remoción alcanzando un 36 % que se estableció en soluciones con una concentración de 3 mg/L, a las 24 h de exposición. Este resultado tiene relevancia al comparar con otras especies reportadas en la literatura, que en similares condiciones de experimentación alcanzaron menores porcentajes de remoción de este fármaco.

Como se puede evidenciar en esta investigación, a través de la metodología superficie de respuesta se estableció los máximos porcentajes de remoción de los cinco PFs en condiciones controladas. Asimismo, con esta base, se puede proyectar futuras investigaciones para buscar los tiempos y concentraciones óptimos.

Esto, a su vez, dará un impulso para la transferencia de tecnología, de tal forma que las plantas de tratamiento de aguas residuales existentes pueden volverse más eficientes desde el punto de vista tecnológico y económico, al contar con una alternativa sostenible como es la fitorremediación de PFs en medio acuoso, potenciando las instalaciones con un enfoque de economía circular.

Referencias bibliográficas

1. Fekadu, S., Alemayehu, E., Dewil, R. & Van der Bruggen, B. Pharmaceuticals in freshwater aquatic environments: A comparison of the African and European challenge. Sci. Total Environ. 654, 324–337 (2019).

2. Bagnis, S. et al. Characterization of the Nairobi River catchment impact zone and occurrence of pharmaceuticals: Implications for an impact zone inclusive environmental risk assessment. Sci. Total Environ. 703, 134925 (2020).

3. Desbiolles, F., Malleret, L., Tiliacos, C., Wong-Wah-Chung, P. & Laffont-Schwob, I. Occurrence and ecotoxicological assessment of pharmaceuticals: Is there a risk for the Mediterranean aquatic environment? Sci. Total Environ. 639, 1334–1348 (2018).

4. Sharma, B. M. et al. Health and ecological risk assessment of emerging contaminants (pharmaceuticals, personal care products, and artificial sweeteners) in surface and groundwater (drinking water) in the Ganges River Basin, India. Sci. Total Environ. 646, 1459–1467 (2019).

5. Archer, E., Wolfaardt, G. M. & van Wyk, J. H. Pharmaceutical and personal care products (PPCPs) as endocrine disrupting contaminants (EDCs) in South African surface waters. Water SA 43, 684–706 (2017).

6. Quesada, H. B. et al. Surface water pollution by pharmaceuticals and an alternative of removal by low-cost adsorbents: A review. Chemosphere 222, 766–780 (2019).

7. Ravikumar, Y., Yun, J., Zhang, G., Zabed, H. M. & Qi, X. A review on constructed wetlands-based removal of pharmaceutical contaminants derived from non-point source pollution. Environ. Technol. Innov. 26, 102504 (2022).

8. Yang, Y., Ok, Y. S., Kim, K. H., Kwon, E. E. & Tsang, Y. F. Occurrences and removal of pharmaceuticals and personal care products (PPCPs) in drinking water and water/sewage treatment plants: A review. Sci. Total Environ. 596–597, 303–320 (2017).

9. Küster, A. & Adler, N. Pharmaceuticals in the environment: Scientific evidence of risks and its regulation. Philos. Trans. R. Soc. B Biol. Sci. 369, (2014).

10. Caviedes, Diego., Delgado, D. Environmental normativity to regulate the presence of residual pharmaceutical products in aquatic environments. Rev. Jurídica 16, 121–130 (2017).

11. Kermia, A. E. B., Fouial-Djebbar, D. & Trari, M. Occurrence, fate and removal efficiencies of pharmaceuticals in wastewater treatment plants (WWTPs) discharging in the coastal environment of Algiers. Comptes Rendus Chim. 19, 963–970 (2016).

12. Klein, E. Y. et al. Global increase and geographic convergence in antibiotic consumption between 2000 and 2015. Proc. Natl. Acad. Sci. 115, E3463–E3470 (2018).

13. Voloshenko-Rossin, A. et al. Emerging pollutants in the Esmeraldas watershed in Ecuador: Discharge and attenuation of emerging organic pollutants along the San Pedro-Guayllabamba-Esmeraldas rivers. Environ. Sci. Process. Impacts 17, 41–53 (2015).

14. Ebele, A. J., Abou-Elwafa Abdallah, M. & Harrad, S. Pharmaceuticals and personal care products (PPCPs) in the freshwater aquatic environment. Emerg. Contam. 3, 1–16 (2017).

15. Gogoi, A. et al. Occurrence and fate of emerging contaminants in water environment: A review. Groundw. Sustain. Dev. 6, 169–180 (2018).

16. Kalia, V. C. Pharmaceutical and personal care product contamination: a global scenario. Pharmaceuticals and Personal Care Products: Waste Management and Treatment Technology (Elsevier Inc., 2019). doi:10.1016/b978-0-12-816189-0.00002-0

17. Kwarciak-Kozłowska, A. Removal of pharmaceuticals and personal care products by ozonation, advance oxidation processes, and membrane separation. Pharmaceuticals and Personal Care Products: Waste Management and Treatment Technology (Elsevier Inc., 2019). doi:10.1016/b978-0-12-816189-0.00007-x

6

18. Kibuye, F. A. et al. Fate of pharmaceuticals in a spray-irrigation system: From wastewater to groundwater. Sci. Total Environ. 654, 197–208 (2019).
19. Miller, T. H., Bury, N. R., Owen, S. F., MacRae, J. I. & Barron, L. P. A review of the pharmaceutical exposome in aquatic fauna. Environ. Pollut. 239, 129–146 (2018).
20. Shraim, A. et al. Analysis of some pharmaceuticals in municipal wastewater of Almadinah Almunawarah. Arab. J. Chem. 10, S719–S729 (2017).
21. Guerra, P., Kim, M., Shah, A., Alaee, M. & Smyth, S. A. Occurrence and fate of antibiotic, analgesic/anti-inflammatory, and antifungal compounds in five wastewater treatment processes. Sci. Total Environ. 473–474, 235–243 (2014).
22. Semerjian, L., Shanableh, A., Semreen, M. H. & Samarai, M. Human health risk assessment of pharmaceuticals in treated wastewater reused for non-potable applications in Sharjah, United Arab Emirates. Environ. Int. 121, 325–331 (2018).
23. Zhang, Y. et al. Wastewater-based epidemiology in Beijing, China: Prevalence of antibiotic use in flu season and association of pharmaceuticals and personal care products with socioeconomic characteristics. Environ. Int. 125, 152–160 (2019).
24. Yang, Y., Ok, Y. S., Kim, K.-H., Kwon, E. E. & Tsang, Y. F. Occurrences and removal of pharmaceuticals and personal care products (PPCPs) in drinking water and water/sewage treatment plants: A review. Sci. Total Environ. 596–597, 303–320 (2017).
25. Sui, Q. et al. Occurrence, sources and fate of pharmaceuticals and personal care products in the groundwater: A review. Emerg. Contam. 1, 14–24 (2015).
26. Peña-Álvarez, A. & Castillo-Alanís, A. Identificación y cuantificación de contaminantes emergentes en aguas residuales por microextracción en fase sólida-cromatografía de gases-espectrometría de masas (MEFS-CG-EM). TIP 18, 29–42 (2015).
27. Szekeres, E. et al. Investigating antibiotics, antibiotic resistance genes, and microbial contaminants in groundwater in relation to the proximity of urban areas. Environ. Pollut. 236, 734–744 (2018).
28. Guo, Y., Qi, P. S. & Liu, Y. Z. A Review on Advanced Treatment of Pharmaceutical Wastewater. IOP Conf. Ser. Earth Environ. Sci. 63, (2017).
29. Buonocore, E., Mellino, S., De Angelis, G., Liu, G. & Ulgiati, S. Life cycle assessment indicators of urban wastewater and sewage sludge treatment. Ecol. Indic. 94, 13–23 (2018).
30. Rasheed, T., Bilal, M., Nabeel, F., Adeel, M. & Iqbal, H. M. N. Environmentally-related contaminants of high concern: Potential sources and analytical modalities for detection, quantification, and treatment. Environ. Int. 122, 52–66 (2019).
31. Riva, F., Zuccato, E., Davoli, E., Fattore, E. & Castiglioni, S. Risk assessment of a mixture of emerging contaminants in surface water in a highly urbanized area in Italy. J. Hazard. Mater. 361, 103–110 (2019).
32. Wang, J. & Wang, S. Removal of pharmaceuticals and personal care products (PPCPs) from wastewater: A review. J. Environ. Manage. 182, 620–640 (2016).
33. Rivera-Jaimes, J. A. et al. Study of pharmaceuticals in surface and wastewater from Cuernavaca, Morelos, Mexico: Occurrence and environmental risk assessment. Sci. Total Environ. 613–614, 1263–1274 (2018).
34. Hossain, A. et al. Occurrence and ecological risk of pharmaceuticals in river surface water of Bangladesh. Environ. Res. 165, 258–266 (2018).
35. Wilkinson, J. L., Hooda, P. S., Barker, J., Barton, S. & Swinden, J. Ecotoxic pharmaceuticals, personal care products, and other emerging contaminants: A review of environmental, receptor-mediated, developmental, and epigenetic toxicity with discussion of proposed toxicity to humans. Critical Reviews in Environmental Science and Technology 46, (2016).
36. Liu, C., Tan, L., Zhang, L., Tian, W. & Ma, L. A Review of the Distribution of Antibiotics in Water in Different Regions of China and Current Antibiotic Degradation Pathways. Front. Environ. Sci. 9, 1–24 (2021).
37. Liu, Y. et al. Toxic effects of diclofenac on life history parameters and the expression of detoxification-related genes in Daphnia magna. Aquat. Toxicol. 183, (2017).
38. Ali, A., Naeem, M., Singh, S. & Alzuaibr, F. M. Phytoremediation of contaminated waters : An eco-friendly technology based on aquatic macrophytes application. Egypt. J. Aquat. Res. (2020). doi:10.1016/j.ejar.2020.03.002
39. Patel, M. et al. Pharmaceuticals of emerging concern in aquatic systems: Chemistry, occurrence, effects, and removal methods. Chemical Reviews 119, (2019).
40. Yan, Y. et al. Phytoremediation of antibiotic-contaminated wastewater: Insight into the comparison of ciprofloxacin absorption, migration, and transformation process at different growth stages of E. crassipes. Chemosphere 283, 131192 (2021).
41. Chen, Q. et al. Optimization of photocatalytic degradation conditions and toxicity assessment of norfloxacin under visible light by new lamellar structure magnetic ZnO/g-C3N4. Ecotoxicol. Environ. Saf. 225, 112742 (2021).
42. He, Y. et al. Evaluation of attenuation of pharmaceuticals, toxic potency, and antibiotic resistance genes in constructed wetlands treating wastewater effluents. Sci. Total Environ. 631–632, 1572–1581 (2018).
43. Khare, A. & P. Lal, E. Waste Water Purification Potential of Eichhornia crassipes (Water Hyacinth). Int. J. Curr. Microbiol. Appl. Sci. 6, 3723–3731 (2017).
44. Lin, Y. L. & Li, B. K. Removal of pharmaceuticals and personal care products by Eichhornia crassipe and Pistia stratiotes. J. Taiwan Inst. Chem. Eng. 58, 318–323 (2016).
45. Mahbub, M. et al. Chemosphere Highly effective water hyacinth (Eichhornia crassipes) waste-based functionalized sustainable green adsorbents for antibiotic remediation from wastewater. Chemosphere 304, 135293 (2022).
46. Ansari, A. A., Naeem, M., Gill, S. S. & AlZuaibr, F. M. Phytoremediation of contaminated waters: An eco-friendly technology based on aquatic macrophytes application. Egypt. J. Aquat. Res. (2020). doi:10.1016/j.ejar.2020.03.002
47. Carlini, M., Castellucci, S. & Mennuni, A. Water hyacinth biomass: Chemical and thermal pre-treatment for energetic utilization in anaerobic digestion process. Energy Procedia 148, 431–438 (2018).
48. Bote, M. A., Naik, V. R. & Jagadeeshgouda, K. B. Review on water hyacinth weed as a potential bio fuel crop to meet collective energy needs. Mater. Sci. Energy Technol. 3, 397–406 (2020).
49. Madikizela, L. M., Ncube, S. & Chimuka, L. Uptake of pharmaceuticals by plants grown under hydroponic conditions and natural occurring plant species: A review. Sci. Total Environ. 636, 477–486 (2018).
50. Saha, P., Shinde, O. & Sarkar, S. Phytoremediation of industrial mines wastewater using water hyacinth. Int. J. Phytoremediation 19, 87–96 (2017).
51. Cui, H. Options for the Phytoremediation of Polar Pharmaceuticals: Uptake and Removal of Metformin and Iopromide by Typha latifolia L. (2016).
52. He, Y. et al. Metabolism of Ibuprofen by Phragmites australis: Uptake and Phytodegradation. Environ. Sci. Technol. 51, 4576–4584 (2017).
53. Cardinal, P. et al. Macrophytes may not contribute significantly to removal of nutrients, pharmaceuticals, and antibiotic resistance in model surface constructed wetlands. Sci. Total Environ. 482, 294–304 (2014).
54. Yan, Y. et al. Migration of antibiotic ciprofloxacin during phytoremediation of contaminated water and identification of transformation products. Aquat. Toxicol. 219, 105374 (2020).
55. He, Y. et al. Improving removal of antibiotics in constructed wetland treatment systems based on key design and operational parameters: A review. J. Hazard. Mater. 407, 124386 (2021).

Microorganisms isolated from seabirds feathers for mercury bioremediation

Lorena Monserrate-Maggi[1], Lizette Serrano-Mena[1], Louise Delahaye[2], Paola Calle[3], Omar Alvarado-Cadena[3], Omar Ruiz-Barzola[3,4], Juan Manuel Cevallos-Cevallos[1,3]*

DOI. 10.21931/RB/2023.08.01.19

[1] Escuela Superior Politécnica del Litoral, ESPOL, Centro de Investigaciones Biotecnológicas del Ecuador, CIBE, Guayaquil, Ecuador.
[2] VIVES University CollegePost-graduate International Cooperation North-South, Kortrijk, Belgium.
[3] Escuela Superior Politécnica del Litoral, ESPOL, Facultad de Ciencias de la Vida, FCV, Guayaquil, Ecuador.
[4] Universidad de Salamanca, Departamento de Estadística; Campus Miguel de Unamuno, Salamanca, España.
Corresponding author: pcalle@espol.edu.ec

Abstract: Environmental pollution caused by mercury has received increasing attention in recent years. Several studies have warned of the high rates of biomagnification in superior levels of marine food networks affecting seabirds. Although seabird feathers are reported as bioindicators of mercury, the possibility of using the microbiota associated with them for the bioremediation of this metal has not been considered. Despite the potential of the seabird feather microbiota, the cultivable microorganisms from this sample matrix have not been identified. In this study, we isolated and identified the organisms in the feathers from three types of seabirds, two species of penguins (*Pygoscelis antartica* and *Pygoscelis papua*) and the brown skua bird (*Catharacta lonnbergi*) through poisoned media a final concentration of 10 mg / L Hg2+ in the culture medium for the microbial consortia. Yeast isolates belonged to the genus *Debaryomyces*, *Meyerozyma*, *Papiliotrema*, and *Rhodotorula*, and fungi genera *Leiotrametes*, *Penicillium*, *Pseudogymnoascus*, and *Cladosporium* were identified. Adult bird feathers with high mercury concentrations can serve as a matrix to isolate microorganisms capable of removing mercury.

Key words: Antarctica, bioremediation, feathers, mercury, microorganisms.

Introduction

Mercury (Hg) is among the most severe pollutants due to its accumulation in food chains, resulting in risks to human, animal, and environmental health[1–4]. The atmospheric transport of this metal affects the most remote and cleanest areas of the planet, such as the polar zones, reaching even higher levels of deposition than in other parts of the world[5–8], thus affecting the aquatic ecosystems of Antarctica[9,10].

The elemental mercury (Hg0) and ionic mercury (Hg2+) that reach Antarctica fall on sediment and water bodies, while some elemental mercury remains dissolved in the water column. Another part of mercury is transformed by microorganisms, through the biomethylation process, to a more toxic organometallic compound, the methylmercury (CH3Hg+), which will be bioaccumulated and biomagnified along the marine trophic chain[11]. With a trophic magnification factor (TMF) of 4 to 8 for each step of the trophic level[12,13], the amount of CH3Hg+ in predatory species can be up to 100 times higher than their primary food source so that birds, among other species, are the most exposed in the marine ecosystems of Antarctica[9]. In addition to its high position in the food chain, the bioaccumulation of Hg in birds is favored by factors such as its wide distribution, population variety, long life cycles, and its type of diet[14,15].

Although in Antarctica there is no industrial development that contributes to mercury emissions[4,6,16], its proximity to the southern hemispheres, the tourism, the pollution from logistics activities of scientific stations[17–20] as well as contamination of natural origin from volcanic activity[10,21] contribute to the increase of Hg in predatory seabirds from different locations in this continent[14,22].

Complex communities of microorganisms are found in birds' feathers whose composition can be influenced by exposure to heavy metals[23]. It is well known that organisms living in contaminated or toxic conditions have developed different mechanisms to adapt to high levels of various forms of mercury present in the environment and can be used for bioremediation or mitigation of the contaminant[24–26]. Bioremediation is an option that uses those strategies that microorganisms have developed to deal with Hg, with exceptional advantages that include high efficiency, low cost and environmentally friendly[27]. Therefore, it is essential to identify the microorganisms living in high-mercury environments[28–30].

Current research primarily focuses on the ability of Antarctic seabird feathers to act as bioindicators of Hg[31–33] or in the isolation of microorganisms from soils and water contaminated with Hg[24,25,27–30]. However, the microbiota associated with bird feathers having high mercury levels has not been fully described.

Therefore, the objective of this study was to identify the culturable microorganisms from the feathers of three Antarctic seabirds known to biomagnify mercury, including the geentoo penguins *Pygoscelis papua* and chinstrap *Pygoscelis antartica* and the skuas brown *Catharacta lonnbergi*, which inhabit the surroundings of the Pedro Vicente Maldonado Scientific Station in Antarctica, as a first step that can aid further mercury bioremediation studies.

Lorena Monserrate-Maggi, Lizette Serrano-Mena, Louise Delahaye, Paola Calle, Omar Alvarado-Cadena, Omar Ruiz-Barzola, Juan Manuel Cevallos-Cevallos

Materials and methods

Sample collection

The present investigation corresponds to an exploratory study using a purposive (judgmental) sampling method. The seabird feather samples were collected during the scientific expeditions to Antarctica carried out by the Instituto Antártico Ecuatoriano (INAE) during the summer of 2013 and 2014. The sampling was carried out in the surrounding areas of the Ecuadorian Scientific Station Pedro Vicente Maldonado (PEVIMA), located in the South Shetland archipelago of the Antarctic Peninsula. The islands evaluated were Barrientos (n = 2 sites), Dee (n = 1 site) and Greenwich (n = 2 sites). Figure 1 shows the sampling sites.

The molting feathers were collected using a non-invasive method and following the guidelines of the Antarctic Treaty (1959), in which animal welfare is preserved and the capture of living individuals is avoided (34). Therefore, fallen feathers were randomly collected in nests and colonies of three bird species: *P. antarctica* and *P. papua*, corresponding to chicks and adults with feathers lengths measured between 3-6 cm, while *C. lonnbergi,* compared to juveniles and adults with feathers lengths measured between 15-30 cm. The description of the samples is shown in table 1.

Year	Bird feathers isolation	Island	Sample
2013	*Pygocelys antarctica*	Barrientos	1
	Pygocelys papua	Barrientos	2
	Chataracta lonnbergi	Greenwich	3
	Chataracta lonnbergi	Barrientos	4
2014	*Chataracta lonnbergi* data	Dee	5
	Chataracta lonnbergi data	Greenwich	6
	Pygocelys antarctica	Barrientos	7
	Pygocelys papua	Barrientos	8

Table 2. Origin of the collection of feathers by years.

The samples were collected in Ziploc bags and delivered to the PEVIMA station laboratory, where they were rinsed with deionized water, dried at room temperature, wrapped in aluminum foil, and kept in the freezer (-20oC) until they were analyzed at the Centro de Investigaciones Biotecnológicas del Ecuador (CIBE-ESPOL) in Guayaquil, Ecuador.

Isolation of microorganisms from feathers

The feathers were subjected to an individual cleaning process in which the barbs exposed to external conditions and/or feather age, which could influence the interpretation of the results, were removed[35,36]. The rachis was cleaned with hypochlorite solution (30%) for 30 seconds and immersed in 99% and 70% ethanol for 30 seconds each. Finally, they were rinsed with plenty of ultrapure water. The rachis of the feathers was then ground under liquid nitrogen (LN2) in a porcelain mortar and collected in 15-ml falcon tubes to enrich microorganisms in the feathers.

For the enrichment process of the samples, 1 gr of the crushed sample was weighed and placed in a 15ml falcon tube with 9ml of liquid culture medium. The culture media used were Peptone water (AP, Oxoid, Thermo Scientific, USA), Luria Bertani (LB, Oxoid, Thermo Scientific, USA), and Potato Dextrose Broth (PDB, Oxoid, Thermo Scientific, USA) that were previously autoclaved at 121 °C for 25 minutes. Then, the samples were incubated at 10 °C for seven days with constant shaking at 110 rpm (Innova 44R, New Brunswick, USA).

Then, to determine the tolerance of microorganisms to Hg, the reference standard of inorganic mercury, Hg_2+ (HACH, Germany), was added, using aseptic techniques, at a concentration 10 times higher than that reported in certain feathers of Antarctic birds[31] and taking into account the toxicity threshold for adverse effects in seabird feathers of between 5-30 mg / L as reported by some authors[14,37]. For this reason, a final concentration of 10 mg / L Hg_2+ in the culture
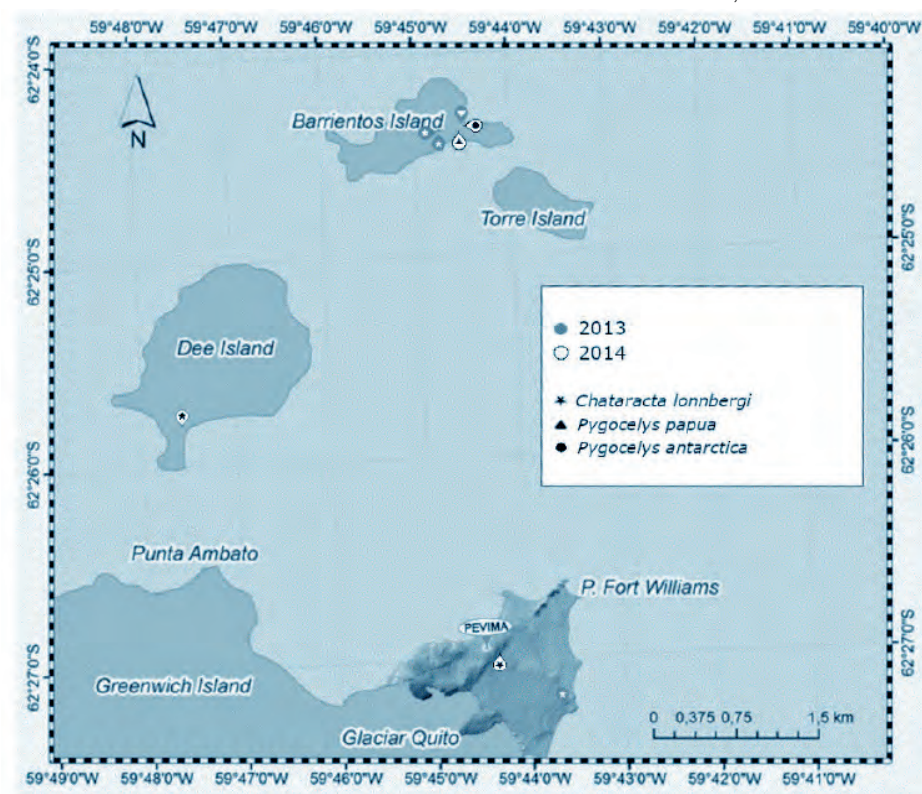
Figure 1. The geographical location of the sampling sites.

medium was used for the microbial consortia and 5mg / L Hg2+ for the isolates cultured from the microbial consortia. The three poisoned media without samples were used as a blank, and each treatment was performed in duplicate.

Isolation and molecular identification of microorganisms present in the consortia feathers

Seven days after adding Hg to the microbial cultures of bird feather consortia, 100ul of the culture were taken and dispersed in Petri dishes previously prepared with 57.5 g / L of Potato Dextrose Agar medium (PDA, Oxoid, Thermo Scientific, USA) plus 10 mg / L Hg2+, and incubated at 10°C for isolation of cultivable microorganisms. After this, the obtained strains were separated into yeasts and fungi according to their macro and micromorphology.

The DNA extraction from isolates was carried out using a rapid fungal DNA extraction protocol according to Cenis (1992)[38]. Molecular identification was performed by PCR amplification and sequencing of the internal transcribed spacer regions (ITS1, 5.8S, and ITS2) using ITS1 (TCCGTAGGTGAACCTGCGG) and ITS4 (TCCTCCGCTTATTGATATGC) primers, the samples that did not amplify, a PCR of nesting using primers ITS3 (GCTTCGATGAAGAACGCAGC) and ITS4. The master mix for both PCRs was: 1X PCR buffer, 0.2 mM dNTP, 1.5 mM MgCl2, 5 U / µL Taq polymerase (ThermoFisher, USA), 0.4 µM of each primer, and the DNA concentration comprised 15-20ng / ul. The program in the thermal cycler (Eppendorf, Mastercycler Nexus GSX1-6345, Germany) for the first set of primers consisted of initial heating of 1 minute at 94 °C, followed by 30 cycles of 1 minute at 94 °C, 1 min at 55 °C, 1 min at 68 °C, and a final extension for 3 min at 68 °C. For the second set of primers, the PCR conditions were: 6 min at 95 ° C, 30 cycles from 0:30 min to 95 ° C, 0:30 min to 55 ° C, 0:30 min to 70 ° C, followed by a final extension of 0:30 min at 72 ° C. Amplification was verified by electrophoresis of a 1.5% agarose gel in 1X TAE solution (Tris base, boric acid, and 0.5M EDTA, pH 8.0), loading 5 µL of PCR product with 1 µL of loading dye (Loading dye, Promega, USA) at 100 volts for 30 minutes. The size of each DNA fragment was estimated using a 100 bp DNA marker (cat. 15628050, Invitrogen ™). Gel images were analyzed using the Gel Doc XR Imager program (Bio-Rad, Philadelphia, PA).

The obtained PCR products were sequenced by Sanger at Macrogen, Inc., an external laboratory in South Korea, according to Genetic Resource Access Contract No MAE-DNB-CM-2017-0059, material transfer agreement MAE-DNB-CM-2017-0059-000-ATM-0001, and sample export authorization No 074-17-EXP-IC-FAU-DNB/MA granted by the Ministry of the Environment of Ecuador.

The chromatograms of the DNA sequences of the different isolates were visualized and edited manually using the program Finch TV version 1.4.0 (Geospiza Inc.) and then compared with the database of the National Center for Biotechnological Information (NCBI) using BLAST. The sequences were deposited in the GenBank public database (http://www.ncbi.nlm.nih.gov/GenBank), and the isolates collection resides in the Microorganism Culture Collection of CIBE at Escuela Superior Politécnica del Litoral (http://www.wfcc.info/ccinfo/index.php/collection/by_id/1151/).

Results and discussion

Seabirds' bioaccumulation mercury has been repor-

ted from different locations in the Antarctic and including in petrel feathers *Pagodroma nivea* 0.54 ± 0.18 µg g−1 dry wt[18], antarctic petrel *Thalassoica antarctica* 2.71 ± 0.25 mg g-1 dw[39]; Gentoo penguins *Pygoscelis papua* 1.83 ± 0.80 ug g−1 dw[31,40–42], Chinstrap penguins *Pygoscelis antarctica* 1.53 ± 0.08 ug g−1 dw[31,40,41], *Pygoscelis adeliae* 0.82 to 1.40 ± 0.13 µg g−1 dw[18,40,41], *Aptenodytes forsten* 0.98 ± 0.2 µg g−1 dw; skuas *Catharacta maccormicki* 2.91 ± 1.93 µg g -1 dw[18], *Catharacta lonnbergi* 2.86 ± 2.60 ug g−1 dw[31] and gull *Larus dominicanus* 426.6 ng g−1[9].

In this study, isolated species of seabirds used in this study corresponding to the following yeast genera were identified: *Debaryomyces, Meyerozyma, Papiliotrema*, and *Rhodotorula* also fungi genera: *Leiotrametes, Penicillium, Pseudogymnoascus*, and *Cladosporium*. The most abundant species in the bird consortiums correspond to yeasts of the genus *Debaromyces* followed by the fungi genus *Pseudogymnoascus* and *Penicillum*. Table 2 and table S1. Some of the yeasts belonging to the *Rhodotorula* and family *Saccharomycetaceae* and fungi between these *Cladosporium* and *Penicillium* have been reported with efficient accumulation strategies and biovolatilization of mercury regardless of their origin. They are considered suitable for application in remedial technology[43–45].

Regarding the efficiency of the culture media for metal removal, they were AP and PDB, and the fact that only yeasts and fungi have been isolated may be due to these culture media being a broad spectrum range favoring the growth of these groups[46].

On the other hand, the differences in the level of resistance to metals among genera and strains depend on different growth requirements (such as temperature, pH, and nutrients), biological function[47], or pressure origin[43].

One of the mechanisms responsible for removing mercury in the medium from cultivable isolated may be due to the biosorption capacity of the fungal cell wall, which contains polysaccharides with reactive functional groups, amino, carboxyl, and phosphate. Of these, it is known that the carboxyl and phosphate groups carry negative charges that allow fungal cell wall components to be highly metal ion-retaining[48]. The peptide links of nitrogen and oxygen could be accompanied by the displacement of protons, depending on the pH, which also favors the removal of the metal[49,50]. The number of available binding sites determines metal biosorption[51]. On the other hand, fungal mycelium secretes many extracellular enzymes and acids that decompose metals and has a huge potential for degrading contaminants[45,52,53].

Urík *et al.* (2014)[43] indicated fungal mercury uptake increases linearly with increased initial media mercury concentration until a threshold concentration near 8.2 mg L−1. When the amount of mercury remaining in media with higher than threshold concentration decreased by 75 % or more, sorption via mercury immobilization on the fungal cell wall and bioaccumulation in the intracellular compartments play insignificant roles in mercury resistance strategy; hence the fungal necessity to trigger other detoxification mechanisms confirm that biovolatilization is the main mechanism of detoxification of mercury by fungal strains. Also, some authors confirm that biovolatilization is the primary mechanism of the detoxification of mercury by fungal strains[43].

Other fungi strains isolated from soil samples like Aspergillus niger removed more than 90% and proved an excellent mercury absorber. *Aspergillus flavus* strain and *Cladosporium* can eliminate more than 90% of 10 mg L−1 of initial mercury concentration in static culture for 7 days

Lorena Monserrate-Maggi, Lizette Serrano-Mena, Louise Delahaye, Paola Calle, Omar Alvarado-Cadena, Omar Ruiz-Barzola, Juan Manuel Cevallos-Cevallos

4

Samples	Closest related taxon (blast search)	Similarity (%)	Source
1AP3, 1PDB3 2LB3, 2PDB3 3LB3, 3PDB3 4AP3 5PDB4 6PDB4 7PDB4 8AP4, 8LB4	*Debaryomyces hansenii* (MK394104.1)	100	1: *P.antartica*- I. Barrientos 2013 2: *P.papua*- I. Barrientos 2013 3: *C.lonnbergi*-I.Barrientos 2013 4: *C.lonnbergi*-I.Greenwich 2013 5: *C.lonnbergi*-I. Dee 2014 6: *C.lonnbergi*-I. Greenwich 2014 7: *P.antartica*- I. Barrientos 2014 8: *P.papua*- I. Barrientos 2014
2AP3	*Meyerozyma guilliermondii* (MH986817.1)	100	2: *P.papua*- I. Barrientos 2013
5RAP4 6PDB4	*Papiliotrema flavescens* (FN428902.1)	100	5: *C.lonnbergi*-I.Dee 2014 6: *C.lonnbergi*-I. Greenwich 2014
6PDBP4	*Papiliotrema terrestris* (NG_062961.1)	100	6: *C.lonnbergi*-I. Greenwich 2014
4APR4	*Rhodotorula mucilaginosa* (KY104874.1)	100	4: *C.lonnbergi*-I.Greenwich 2013
5RLB4	*Cladosporium cycadicola* (NR_156279.1)	100	5: *C.lonnbergi*-I.Dee 2014
2LB3 4LB3, 4PDB4 5PDB4 7RAP4 8AP4, 8PDB4, 8RPDB4	*Pseudogymnoascus pannorum* (MH864459.1 y MH864756.1)	100	2: *P.papua*- I. Barrientos 2013 4: *C.lonnbergi*-I.Greenwich 2013 5: *C.lonnbergi*-I.Dee 2014 7: *P.antartica*- I. Barrientos 2014 8: *P.papua*- I. Barrientos 2014
1RPDB3	*Leiotrametes flavida* (KC589130.1)	100	1: *P.antartica*- I. Barrientos 2013
1RPDB3 6AP, 6PDB4 8PDB4	*Penicillium adametzioides* (LT558904.1, KT279815.1, NR_103660.1 y AF033403.1)	100	1: *P.antartica*- I. Barrientos 2013 6: *C.lonnbergi*-I. Greenwich 2014 8: *P.papua*- I. Barrientos 2014
1PDB3	*Penicillium bialowiezense* (MH854996.1)	100	1: *P.antartica*- I. Barrientos 2013
2LB3 3PDB3 5RPDB4	*Penicillium brevicompactum* (KF465776.1)	100	2: *P.papua*- I. Barrientos 2013 3: *C.lonnbergi*-I.Barrientos 2013 5: *C.lonnbergi*-I.Dee 2014
4AP_75 5RAP_55	*Penicillium sp.* (MW018928.1)	100	4: *C.lonnbergi*-I.Greenwich 2013 5: *C.lonnbergi*-I.Dee 2014

Table 2. Formulas and variables for calculating the components of the productive process' cost.

and have been reported with biovolatilization rendering them the most suitable for application in remedial technology[43,54,55].

The precise fungal mercury volatilization mechanism is not currently elucidated, but it most likely involves some intra or extracellular reducing factor and/or methylation agent when considering mercury volatilization in dimethyl form[56,57]. However, it should not be ruled out that another mechanism of action of the cultivable isolates proposed by Kelly *et al.* (2006) where mercury deposition as HgS in microfungi dominates at low mercury concentrations[58].

Findings focused on bioremediation, comparing the use of consortia (multiple or heterogeneous systems) with pure isolates (homogeneous systems), describe the advantages of living in the community. Many factors can influence passive and active mechanisms in the removal of metals, as well as considering the relationship with the use of carbon sources and biodegradation processes[59], and they can withstand higher concentrations of heavy metals. The use of these represents a closer approximation to what occurs in nature. This also allows the development of experimental model systems, which can explain the lag between the boiadsorption of pure cultures *in situ*[60]. While pure isolates can resist lower concentrations of mercury compared to consortia, and few mechanisms of action on metal could be focused on, like bioaccumulation, biosorption, biopreciping, and/ or biovolitizion[45,52,59].

Conclusions

Microorganisms isolated from bird feathers that biomagnify Hg in Antarctica are yeast genera identified: *Debaryomyces, Meyerozyma, Papiliotrema*, and *Rhodotorula*

also, fungi genus: *Leiotrametes, Penicillium, Pseudogymnoascus*, and *Cladosporium*. Of these, yeasts belonging to the genus *Rhodotorula* and family *Saccharomycetaceae* and fungi between these *Cladosporium* and *Penicillium* have been reported with efficient strategies of accumulation and biovolatilization of mercury and are considered suitable for application in remedial technology according to the reported bibliography.

This study opens the opportunity for bioprospecting microorganisms isolated from other matrices, not mercury-contaminated water and soil, but bird feathers that biomagnified this metal. However, is a need to evaluate in time and elucidate the mechanisms used for these microorganisms in mercury removal and include other factors such as growth requirements between these pH and temperature, tolerance indices to major concentrations, and evaluation of their potential as adsorbents a low-cost and environmentally friendly. Therefore, the bioremediation of mercury from microorganisms isolated from bird feathers is still a developing technology.

Supplementary Materials

Table S1. Cultivable isolates with source and Genbank accession number.

Author Contributions

Conceptualization, Cevallos-Cevallos.J., Calle.P. and Monserrate-Maggi.L.; methodology, Cevallos-Cevallos.J., Monserrate-Maggi.L.,Delahaye.L., Alvarado-Cadena. O. and Ruiz-Barzola.O.; formal analysis, Ruiz-Barzola.O. and Serrano-Mena. L.; investigation, Cevallos-Cevallos.J., Calle.P., Monserrate-Maggi.L., Delahaye.L.; resources, Calle.P., Alvarado-Cadena. O., Ruiz-Barzola.O. and Serrano-Mena. L.; data curation, Serrano-Mena. L.; writing—original draft preparation, Cevallos-Cellos. J., Monserrate-Maggi.L. and Serrano-Mena. L.; writing—review and editing, Monserrate-Maggi.L., Cevallos-Cevallos.J. and Calle.P.; visualization, Monserrate-Maggi.L., Cevallos-Cevallos.J. and Calle.P.; supervision, Calle.P. and Cevallos-Cevallos.J.; project administration, Cevallos-Cevallos.J. All authors have read and agreed to the published version of the manuscript.

Funding

Data Availability Statement

The partial DNA sequences obtained in this study were deposited in the GenBank database. Accession numbers for each of the isolates are given in Table S1.

Conflicts of Interest

The authors declare no conflict of interest.

Bibliographic references

1. Macdonald RW, Harner T, Fyfe J. Recent climate change in the Arctic and its impact on contaminant pathways and interpretation of temporal trend data. Sci Total Environ. 2005;342(1–3):5–86.

2. Mason RP, Choi AL, Fitzgerald WF, Hammerschmidt CR, Lamborg CH, Soerensen AL, et al. Mercury biogeochemical cycling in the ocean and policy implications. Environ Res [Internet]. 2012;119:101–17. Available from: http://dx.doi.org/10.1016/j.envres.2012.03.013

3. Scheuhammer AM, Meyer MW, Sandheinrich MB, Murray MW. Effects of environmental methylmercury on the health of wild birds, mammals, and fish. Ambio. 2007;36(1):12–8.

4. Weinberg J. Introducción a la contaminación por Mercurio para las ONG [Internet]. Red Internacional de Eliminación de los Contaminantes Orgánicos Persistentes, (IPEN), editors. 2014. Available from: https://ipen.org/sites/default/files/documents/ipen_mercury_booklet-es.pdf

5. Ebinghaus R, Kock HH, Temme C, Einax JW, Löwe AG, Richter A, et al. Antarctic springtime depletion of atmospheric mercury. Environ Sci Technol. 2002;36(6):1238–44.

6. Gilmour C, Riedel G. Biogeochemistry of Trace Metals and Metalloids. In: INORGANIC CHEMICALS: CYCLES AND DYNAMICS. Elsevier Inc.; 2009. p. 1–6.

7. Hylander LD, Goodsite ME. Environmental costs of mercury pollution. Sci Total Environ. 2006;368(1):352–70.

8. Nerentorp Mastromonaco M, Gårdfeldt K, Jourdain B, Abrahamsson K, Granfors A, Ahnoff M, et al. Antarctic winter mercury and ozone depletion events over sea ice. Atmos Environ. 2016;129:125–32.

9. Dos Santos IR, Silva-Filho EV, Schaefer C, Maria Sella S, Silva CA, Gomes V, et al. Baseline mercury and zinc concentrations in terrestrial and coastal organisms of Admiralty Bay, Antarctica. Environ Pollut. 2006;140(2):304–11.

10. Mão de Ferro A, Mota AM, Canário J. Pathways and speciation of mercury in the environmental compartments of Deception Island, Antarctica. Chemosphere. 2014;95:227–33.

11. Barkay T, Poulain AJ. Mercury (micro)biogeochemistry in polar environments. FEMS Microbiol Ecol. 2007;59(2):232–41.

12. Kidd K, Clayden M, Jardine T. Part Iv Bioaccumulation , Toxicity , and Metallomics Chapter 14 Bioaccumulation and Biomagnification of Mercury Through Food Webs. Environ Chem Toxicol Mercur. 2012;

13. Lavoie R, Jardine TD, Chumchall MM, Kidd KA, Campbell LM. Biomagnification rate of mercury in aquatic food webs: a world-wide meta-analysis. 2013;

14. Burger J, Gochfeld M. Marine Birds as Sentinels of Environmental Pollution. Ecohealth. 2004;263–74.

15. Taniguchi S, Montone RC, Bícego MC, Colabuono FI, Weber RR, Sericano JL. Chlorinated pesticides, polychlorinated biphenyls and polycyclic aromatic hydrocarbons in the fat tissue of seabirds from King George Island, Antarctica. Mar Pollut Bull [Internet]. 2009;58(1):129–33. Available from: http://dx.doi.org/10.1016/j.marpolbul.2008.09.026

16. Krabbenhoft DP, Sunderland EM. Global change and mercury. Science (80-). 2013;341(6153):1457–8.

17. Amaro E, Padeiro A, Mão de Ferro A, Mota AM, Leppe M, Verkulich S, et al. Assessing trace element contamination in Fildes Peninsula (King George Island) and Ardley Island, Antarctic. Mar Pollut Bull [Internet]. 2015;97(1–2):523–7. Available from: http://dx.doi.org/10.1016/j.marpolbul.2015.05.018

18. Bargagli R, Monaci F, Sanchez-Hernandez JC, Cateni D. Biomagnification of mercury in an Antarctic marine coastal food web. Mar Ecol Prog Ser. 1998;169(June 2014):65–76.

19. Jerez S, Motas M, José M, Valera F, Javier J, Barbosa A. Concentration of trace elements in feathers of three Antarctic penguins : Geographical and interspeci fi c differences. Environ Pollut [Internet]. 2011;159(10):2412–9. Available from: http://dx.doi.org/10.1016/j.envpol.2011.06.036

20. Santos IR, Silva-Filho E V., Schaefer CEGR, Albuquerque-Filho MR, Campos LS. Heavy metal contamination in coastal sediments and soils near the Brazilian Antarctic Station, King George Island. Mar Pollut Bull. 2005;50(2):185–94.

21. Rey J, Somoza L, Martínez-Frías J. Tectonic, volcanic, and hydrothermal event sequence on Deception Island (Antarctica). Geo-Marine Lett. 1995;15(1):1–8.

6

22. Blévin P, Carravieri A, Jaeger A, Chastel O, Bustamante P, Cherel Y. Wide Range of Mercury Contamination in Chicks of Southern Ocean Seabirds. PLoS One. 2013;8(1).

23. Chatelain M, Frantz A, Gasparini J, Leclaire S. Experimental exposure to trace metals affects plumage bacterial community in the feral pigeon. J Avian Biol. 2016;47(4):521–9.

24. García-Sánchez M, Száková J. Biological Remediation of Mercury-Polluted Environments. Plant Met Interact Emerg Remediat Tech. 2015;311–34.

25. Gururajan K, Belur PD. Screening and selection of indigenous metal tolerant fungal isolates for heavy metal removal. Environ Technol Innov [Internet]. 2018;9:91–9. Available from: https://doi.org/10.1016/j.eti.2017.11.001

26. Matsui K, Endo G. Mercury bioremediation by mercury resistance transposon-mediated in situ molecular breeding. Appl Microbiol Biotechnol. 2018;102(7):3037–48.

27. Yin K, Wang Q, Lv M, Chen L. Microorganism remediation strategies towards heavy metals. Chem Eng J [Internet]. 2019;360(August 2018):1553–63. Available from: https://doi.org/10.1016/j.cej.2018.10.226

28. Liang X, Gadd GM. Metal and metalloid biorecovery using fungi. Microb Biotechnol. 2017;10(5):1199–205.

29. McCarthy D, Edwards GC, Gustin MS, Care A, Miller MB, Sunna A. An innovative approach to bioremediation of mercury contaminated soils from industrial mining operations. Chemosphere. 2017;184(December 2018):694–9.

30. Mishra A, Malik A. Recent advances in microbial metal bioaccumulation. Crit Rev Environ Sci Technol. 2013;43(11):1162–222.

31. Calle P, Alvarado O, Monserrate L, Cevallos J et al. Mercury accumulation in sediments and seabird feathers from the Antarctic Peninsula. Mar Pollut Bull [Internet]. 2015;91(2):410–7. Available from: http://dx.doi.org/10.1016/j.marpolbul.2014.10.009

32. Becker PH, Goutner V, Ryan PG, González-Solís J. Feather mercury concentrations in Southern Ocean seabirds: Variation by species, site and time. Environ Pollut. 2016;216:253–63.

33. Carravieri A, Cherel Y, Blévin P, Brault-Favrou M, Chastel O, Bustamante P. Mercury exposure in a large subantarctic avian community. Environ Pollut [Internet]. 2014;190:51–7. Available from: http://dx.doi.org/10.1016/j.envpol.2014.03.017

34. Metcheva R, Yurukova L, Teodorova S, Nikolova E. The penguin feathers as bioindicator of Antarctica environmental state. Sci Total Environ. 2006;362(1–3):259–65.

35. Dauwe T, Bervoets L, Pinxten R, Blust R, Eens M. Variation of heavy metals within and among feathers of birds of prey: Effects of molt and external contamination. Environ Pollut. 2003;124(3):429–36.

36. Goede AA, de Bruin M. The use of bird feather parts as a monitor for metal pollution. Environ Pollution Ser B, Chem Phys. 1984;8(4):281–98.

37. Polito MJ, Brasso RL, Trivelpiece WZ, Karnovsky N, Patterson WP, Emslie SD. Differing foraging strategies influence mercury (Hg) exposure in an Antarctic penguin community. Environ Pollut. 2016;218:196–206.

38. Cenis JL. Rapid extraction of fungal DNA for PCR amplification. Nucleic Acids Res. 1992;20(9):2380.

39. Carravieri A, Fort J, Tarroux A, Cherel Y, Love OP, Prieur S, et al. Mercury exposure and short-term consequences on physiology and reproduction in Antarctic petrels. Environ Pollut. 2018;237:824–31.

40. Álvarez-Varas R, Morales-Moraga D, González-Acuña D, Klarian SA, Vianna JA. Mercury Exposure in Humboldt (Spheniscus humboldti) and Chinstrap (Pygoscelis antarcticus) Penguins Throughout the Chilean Coast and Antarctica. Arch Environ Contam Toxicol [Internet]. 2018;75(1):75–86. Available from: https://doi.org/10.1007/s00244-018-0529-7

41. Brasso RL, Chiaradia A, Polito MJ, Raya Rey A, Emslie SD. A comprehensive assessment of mercury exposure in penguin populations throughout the Southern Hemisphere: Using trophic calculations to identify sources of population-level variation. Mar Pollut Bull [Internet]. 2015;97(1–2):408–18. Available from: http://dx.doi.org/10.1016/j.marpolbul.2015.05.059

42. Chiang G, Kidd KA, Díaz-Jaramillo M, Espejo W, Bahamonde P, O'Driscoll NJ, et al. Methylmercury biomagnification in coastal aquatic food webs from western Patagonia and western Antarctic Peninsula. Chemosphere [Internet]. 2021;262(128360). Available from: https://doi.org/10.1016/j.chemosphere.2020.128360

43. Urík M, Hlodák M, Mikušová P, Matúš P. Potential of microscopic fungi isolated from mercury contaminated soils to accumulate and volatilize mercury(II). Water Air Soil Pollut. 2014;225(2219).

44. Kordialik-Bogacka E. Surface properties of yeast cells during heavy metal biosorption. Cent Eur J Chem. 2011;9(2):348–51.

45. Mustapha MU, Halimoon N. Microorganisms and Biosorption of Heavy Metals in the Environment: A Review Paper. J Microb Biochem Technol [Internet]. 2015;07(05):253–6. Available from: https://www.omicsonline.org/open-access/microorganisms-and-biosorption-of-heavy-metals-in-the-environment-a-review-paper-1948-5948-1000219.php?aid=60592

46. American Type Culture Collection A. Mycology Culture Guide Table of Contents [Internet]. Manassas; 2013. 33 p. Available from: www.atcc.org

47. Ezzouhri L, Castro E, Moya M, Espinola F, Lairini K. Heavy metal tolerance of filamentous fungi isolated from polluted sites in Tangier, Morocco. African J Microbiol Res. 2009;3(2):35–48.

48. Say R, Yilmaz N, Denizli A. Biosorption of cadmium, lead, mercury, and arsenic ions by the fungus Penicillium purpurogenum. Sep Sci Technol. 2003;38(9):2039–53.

49. Gow NAR, Latge J, Munro CA, De Groot PWJ, Hellingwerf KJ, Klis FM, et al. Cell Wall Architecture in Yeast : New Structure and New Challenges MINIREVIEW Cell Wall Architecture in Yeast : New Structure and New Challenges †. Yeast. 2003;9(3):3341–54.

50. Ozsoy HD. Biosorptive removal of Hg(II) ions by Rhizopus oligosporus produced from corn-processing wastewater. African J Biotechnol. 2010;9(51):8791–9.

51. Rezaee A, Derayat J, Mortazavi SB, Yamini Y, Jafarzadeh MT. Removal of Mercury from chlor-alkali Industry Wastewater using Acetobacter xylinum Cellulose. Am J Environ Sci. 2005;1(2):102–5.

52. Gupta A, Joia J. Microbes as Potential Tool for Remediation of Heavy Metals: A Review. J Microb Biochem Technol. 2016;8(4):364–72.

53. Veglio F, Beolchini F. Removal of metals by biosorption: A review. Hydrometallurgy. 1997;44(3):301–16.

54. Joo J-H, Hussein KA. Heavy Metal Tolerance of Fungi Isolated from Contaminated Soil. Korean J Soil Sci Fertil. 2012;45(4):565–71.

55. Oladipo OG, Awotoye OO, Olayinka A, Bezuidenhout CC, Maboeta MS. Heavy metal tolerance traits of filamentous fungi isolated from gold and gemstone mining sites. Brazilian J Microbiol [Internet]. 2018;49(1):29–37. Available from: http://dx.doi.org/10.1016/j.bjm.2017.06.003

56. Jiménez-Moreno M, Perrot V, Epov VN, Monperrus M, Amouroux D. Chemical kinetic isotope fractionation of mercury during abiotic methylation of Hg(II) by methylcobalamin in aqueous chloride media. Chem Geol [Internet]. 2013;336:26–36. Available from: http://dx.doi.org/10.1016/j.chemgeo.2012.08.029

57. Yannai S, Berdicevsky I, Duek L. Transformations of inorganic mercury by Candida albicans and Saccharomyces cerevisiae. Appl Environ Microbiol. 1991;57(1):245–7.

58. Kelly DJA, Budd K, Lefebvre DD. The biotransformation of mercury in pH-stat cultures of microfungi. Can J Bot. 2006;84(2):254–60.

59. Sprocati AR, Alisi C, Segre L, Tasso F, Galletti M, Cremisini C. Investigating heavy metal resistance, bioaccumulation and metabolic profile of a metallophile microbial consortium native to an abandoned mine. Sci Total Environ. 2006;366(2–3):649–58.

60. Ledin M. Accumulation of metals by microorganisms - processes and importance for soil systems. Earth Sci Rev. 2000;51(1–4):1–31.

Genetic improvement in *Musa* through modern biotechnological methods

Villao, L.[1], Chávez, T.[1], Pacheco, R.[1], Sánchez, E.[1,2], Bonilla J.[1,2], Santos, E.[1,2]

DOI. 10.21931/RB/2023.08.01.20

[1] Escuela Superior Politécnica del Litoral, ESPOL, Biotechnological Research Center of Ecuador, Guayaquil, Ecuador.
[2] Escuela Superior Politécnica del Litoral, ESPOL, Faculty of Life Sciences, Guayaquil, Ecuador.
Corresponding author: gsantos@espol.edu.ec

Abstract: Bananas, one of the most valued fruits worldwide, are produced in more than 135 countries in the tropics and subtropics for local consumption and export due to their tremendous nutritional value and ease of access. The genetic improvement of commercial crops is a crucial strategy for managing pests or other diseases and abiotic stress factors. Although conventional breeding has developed new hybrids with highly productive or agronomic performance characteristics, in some banana cultivars, due to the high level of sterility, the traditional breeding strategy is hampered. Therefore, modern biotechniques have been developed in a banana for genetic improvement. *In vitro*, culture techniques have been a basis for crop micropropagation for elite banana varieties and the generation of methods for genetic modification. This review includes topics of great interest for improving bananas and their products worldwide, from their origins to the different improvement alternatives.

Key words: Banana, genetic improvement, pest management, diseases, abiotic stress factors.

Introduction

Origin of bananas and plantains

Bananas and plantains belong to the genus *Musa* and are native to Southeast Asia, including the Indo-Malaysia region and the Australian tropics[1]. Therefore, Southeast Asia is the first center of diversity for diploid bananas and plantains[2]. Following the introduction of triploid bananas in West Africa and cooking and beer bananas in East Africa, the second center of diversification occurred on this continent, based primarily on mutations[3,4]. Thus, the most significant variability of banana cultivars is found in India and Southeast Asia, followed by plantains in Central and West Africa[1].

Botany of bananas and plantains

Bananas and plantains are perennial herbs consisting of an underground stem called a rhizome (commonly called a corm), with roots and vegetative shoots, from which a pseudostem composed of clustered leaf bases protrudes from the ground[5]. From the apical meristem, the primordia of the different leaves are distinguished, which grow vertically and differentiate into a leaf base, a petiole, and a blade.

The cultivation cycle varies between 8-12 months, while propagation occurs vegetatively due to the generation of shoots from the corm of the plants. Bananas and plantains are grown in Ecuador, of which many producing countries are parthenocarpy and do not have seeds in the fruit. However, wild species have roots and are essential components in germplasm banks as sources of genes of agricultural importance in conventional and biotechnological breeding programs.

An example is the 'species Calcutta 4' (genotype AA, *Musa acuminata* ssp. burmaniccoides), recommended for field trials as a highly resistant reference to black sigatoka[5-7], used as a parent in conventional breeding programs[8,9], used in molecular studies on plant-pathogen interaction and the discovery of resistance genes to fungal diseases such as black Sigatoka (caused by *Pseudocercospora fijiensis*[10-14] and Panama disease (*Fusarium oxysporum* f sp. cubense[15,16]).

Inflorescence

At a physiological stage of plant development, after 25 to 50 leaves have been produced, the apical growing point stops producing leaves and becomes an inflorescence. The peduncle grows through the pseudo stem and out the top of the plant. The bracts cover double rows of female nodes with grouped fruits called hands. Each fruit that stands out from each flower is called a finger; later, the bracts will dry up and fall.

The hermaphroditic flowers, usually drooping, are found next to the developing fruit. At the end of the peduncle, the male flowers stand out, full of bracts. This terminal part is called the acorn or male inflorescence[5]. Each plant flowers only once, at the end of its life cycle and pollen production. The fertility of cultivated bananas and plantains depends mainly on genetic factors, although environmental factors may also play a role.

Lowering and fruit production, the mother plant dies, which will be replaced by the offspring that develops from the corm, which emerges during the vegetative development of the mother plant.

2

Origin of edible bananas and plantains

Wild Musa species produce seeds and generally grow wild in forest clearings and along streams. In the past, farmers selected plants with a high level of parthenocarpy (fruit formation without fertilization) because the fruits had fewer seeds due to selection for female sterility, which also helped increase the edibility of this fruit.

These selected plants probably propagated vegetatively by removing suckers from the mother plant. Population movement allowed the dispersal of bananas and plantains to other parts of the world[5]. Wild banana species are diploid *M. acuminata* (AAw) or *M. balbisiana* (BBw); hybridization between the two wild species occurred in peripheral dry areas of Southeast Asia, where *M. balbisiana* was endemic when cultivation from *M. acuminata* started. In addition, triploidy, an essential feature in the evolution of bananas and plantains, was due to the fertilization of a viable diploid ovule formed in interrupted meiosis in the second division with haploid pollen[17].

Most cultivable bananas are triploid (2n= 3X = 33 chromosomes) and are responsible for the world's largest producer of bananas. For example, banana varieties of the Cavendish subgroup (AAA genotypes) are grown in Ecuador, including 'Williams,' 'Gran Enano,' and 'Valery.' On the other hand, there are also diploids (2n = 2X = 22 chromosomes) and tetraploid bananas (2n = 4X = 44 chromosomes), while all wild species of the genus Musa are diploid. Jones (2000) describes a compendium of cultivars divided into genomic groups and ploidy levels[5].

Pollen dispersal and viability

Pollen viability is high in diploid species (88%) and higher in tetraploid species (29%), being nine times lower in cultivable triploids (6%-10%). On the other hand, the triploid cultivar' Gros Michel' (AAA) has 13% viable pollen[18].

Different studies of the cultivar' Valery''[19] reported apparent sterility of cultivars of the Cavendish subgroup. However, despite the various difficulties, it has been possible to generate crosses between Cavendish cultivars, obtaining 40 viable embryos from 200 seeds. Then 20,000 pollinated seeds, revealing that the Cavendish cultivars ('Grand Naine' and 'Williams') have low fertility[19].

Sexual and asexual reproduction

Most cultivable bananas and plantains are partially or wholly sterile. Some edible diploids may have female and male sterility due to structural heterozygosity (translocations, inversions), lack of homology between A and B chromosomes, or genetic effects[1]. Triploid cultivars have reproductive cells with one or three sets of chromosomes. The plants produce little or no pollen and are partially sterile. They develop fruits without pollination (parthenocarpic); they are seedless and propagate vegetatively. Crossing a triploid (as a female parent) with a diploid (as a male parent) can produce offspring with two, three, or four sets of chromosomes. In those offspring that maintain a uniform set of chromosomes, fertility is re-established; they can produce fruits with seeds when the flowers are pollinated[1]. The commercialization of the triploids was possible due to their reduced seed production capacity due to: i) the sterility of the gametes caused by the combination problems generated by the triploid germinative tissue, ii) the irregular or late growth of the pollen tubes in the styles of the female flowers, iii) absence of fertilization even with the development of the

tube due to unknown causes; and iv) nectary necrosis at flowering[20].

Conventional breeding programs use the fertility of wild diploid species, but the seeds produced have a low germination rate. At the same time, male infertility and parthenocarpy are closely related, with few exceptions.

Propagation of banana and plantain cultivars is by basal shoots or corms, which develop underground. Each bud is genetically identical to the mother (a clone). Furthermore, although wild banana species are fertile, they propagate vegetatively through shoot production

Seed dispersal, dormancy, volunteers, invasion, and potential as weeds

Bats perform seed dispersal, as do rodents, squirrels, and monkeys[1,21]. In addition, the dormant seeds of some wild bananas are believed to remain viable in the soil for years and can germinate when light passes through the plant bark.

Established populations can be very persistent due to their ability to propagate vegetatively. However, the probability of spontaneously established volunteers is relatively low due to the lack of seeds in cultivars. Edible bananas are not considered invasive and do not compete well with forest species under natural conditions[1]. Despite the vegetative reproduction of bananas, suckers may emerge from the remaining corms; however, if insufficient watering and fertilization, the offspring can become stressed and die.

Bananas and plantains are one of the most important crops in the world and are among the top 10 crops for food production. Musaceae are widely distributed in tropical areas and form an essential component in the diet of millions of consumers worldwide. In several countries, bananas and plantains are a staple and leading food; thus, in countries such as Uganda, the average consumption level is 0.5 kg per person per day, rising in some regions to around 1 kg per person per day[22,23].

Bananas and plantain crops represent a sizeable economic export item for Ecuador that reached USD 3,682 million in 2021 (CFN 2022) and, in turn, is a product of high nutritional interest.

These crops grow in humid tropical and subtropical regions, favoring Musaceae to be strongly threatened by pests and diseases. Given rise to the growth of pathogens such as the causal agent of black sigatoka (*Pseudocercospora fijiensis*), Fusarium (*Fusarium oxysporum* f. sp. cubense, Foc.), banana bacterial wilt (*Xanthomonas campestris* pv. musacearum), virus (Banana Bungee Top, Banana Streak Virus), nematodes (*Radopholus similis* and *Pratylenchus coffeae*) and insects (*Cosmopolites sordidus*) which cause significant economic losses worldwide.

All these problems have created a growing demand for new and improved varieties of these crops that respond to the high demand worldwide. This increased consumption highlights the scientific interest in developing and improving this fruit and the constant search for improvements in programs based on yield, quality, and the ability to resist such devastating diseases caused by fungi or other vectors.

There are extensive works published on bananas and plantains, where they deal with issues on the application of genetic engineering to improve characters that confer tolerance to biotic and abiotic stresses and for their biofortification.

The improvement of bananas through conventional crossing techniques continues today to be a process with

great difficulties due to the time of the crop cycle between generations, the ploidy levels, the sterility of the edible cultivars, the requirement of physical space, and the limited genetic variation of the species. It is estimated that more than 1000 manual pollinations from 200 plants are needed to obtain around 1000 seeds/year of a selected tetraploid plantain-banana hybrid[24]. This estimate makes evident the high degree of labor involved in continuing to depend on traditional techniques for crops such as bananas and plantains without even considering the economic and human cost that is required. It is essential to highlight that, despite these difficulties, it has been possible to obtain hybrids that present genetic resistance to diseases such as black sigatoka and, at the same time, agronomic characteristics of interest.

In 1992, the widespread involvement of important banana plantations by diseases, particularly the fungus *Fusarium oxysporum* f. sp. cubense called Mal de Panama, and the little research in the search for improved plant material led to the beginning of breeding programs for this crop to obtain resistance to the said pathogen[25]. Due to the lack of controls and the threat created by this disease, added to the outbreak of black sigatoka in the early 1970s, genetic techniques began in plant breeding programs to search for varieties with resistance to these diseases. One of the oldest *Musa* genetic improvement programs still in force is that of the Honduran Foundation for Agricultural Research (FHIA). The United Fruit Company initially established this program for sweet bananas but later included plantains and bananas. Other institutions working actively since the late 1980s and early 1990s on breeding programs are the Center de Coopération Internationale en Recherche Agronomique pour le Développement (CIRAD, France), Center Africain de Recherches Sur Les Bananiers et Plantains (CARBAP, Cameroon), the Internationale Institute of Tropical Agriculture (IITA, Africa), Empresa Brasileira de Pesquisa Agropecuaria (EMBRAPA, Brazil), Center National de Recherches Agronomiques (CNRA, Ivory Coast), the National Center for Research on Banana (NCRB, India), among others[3].

The challenges described above allowed directing the research on *Musa* spp. towards the field of cell and molecular biology for the improvement of bananas. Plant tissue culture techniques have facilitated germplasm exchange, rapid multiplication, and conservation. Molecular techniques began to be useful for banana breeding due to the use of molecular markers to help in the germplasm management process, select genes and characteristics of interest from a wild population for genetic introgression, and even detect and determine pathogens in banana plants[26].

Traditional banana cultivation and improvement techniques require years of study to evaluate everything from pollination to the generation of the first bunches. These analyses are preliminary tests to determine resistance to pathogens, which may require several crop cycles. Currently, the decreasing costs of molecular assays make these techniques cheaper than the formal study by phenotypes, not to mention the precision and speed when handling many individuals. The development of bioinformatic tools and nucleic acid sequencing technologies for the analysis of genomes of species of agronomic interest is on the rise, facilitating access and understanding of their genetic information, not only to understand and predict the functions of the genes but also to detect regions in the genome that present associations with agronomic characteristics of interest.

Alternative to conventional improvement in *Musa*

Due to the rapid adaptation of pathogenic organisms to control methods in the field (fungicides, antibiotics, etc.) and the environmental conditions that affect different crops, genetic engineering has become an indispensable tool in various genetic improvements. The ability to modify crops to improve their production, tolerance to environmental changes, and ecological adaptations, among others, are reasons why targeted genetic modification of crops proves to be an essential tool.

Genetic engineering has made it possible to generate genetically modified plants resistant to the burrowing nematode[27] to the bacterial wilt of bananas caused by the pathogen *Xanthomonas campestris* pv. musacearum[28], fusariosis caused by Foc race 4[29], among others. Resistance to pathogens and adverse environmental conditions that affect crop development has not been the only approach in which genetic engineering has participated. The biofortification or growth of plants with improved nutritional content has also attracted the attention of researchers. In this area, using a genetic modification of plants has served to obtain a higher provitamin A, known as golden bananas[30] Researchers in India and Australia are working on developing banana plants with enriched iron content to alleviate iron deficiency anemia[31]. In Ecuador and Belgium, a team of researchers from CIBE-ESPOL and the University of Ghent is developing a biofortified banana plant to increase folate in the fruit (Efrén Santos, personal communication).

Biosafety and the improvement of human health is scientists' primary interest, for which molecular tools have significantly impacted the development of banana plants with resistance to diseases or adaptation to environmental conditions such as drought, high salinity, and high temperatures. In addition, genetic engineering allows us to develop edible vaccines. For this, the banana is an excellent candidate due to the size of its fruit, edible pulp, adequate postharvest handling, great demand worldwide, low production cost, not require cooking for consumption, and proteins maintain their integrity even when cooked at high temperatures, widely planted and harvested in different countries, especially in developing countries. In this sense, in 1992, Charles Arntzen and his colleague Hugh Mason and Colonel Lam of the United States Armed Forces published the first work that began what is now known as edible vaccines. This group of scientists recovered an antigenic molecule (HBsAg, hepatitis B surface antigen) similar to a viral particle from a transgenic tobacco plant[32]. This finding could combine genetic engineering and plant molecular biology to create low-cost vaccine production systems. This discovery opened the doors to new research in food crops for synthesizing antigens for various diseases that affect humans and animals. Among these crops, using the fruit of banana plants as a store for edible vaccines seemed to be a great option. However, this crop has problems such as low expression and accumulation of antigens in the fruit, so it must be investigated and optimized[33].

Methods of genetic transformation

The continuous evolution and appearance of new races of pathogens have created the need to accelerate the genetic improvement process to obtain new resistant banana varieties in the short term. To solve the problems that come from having limited genetic variability, low or null fertility, and polyploidy, among others[34], biotechnology has been the tool

3

4
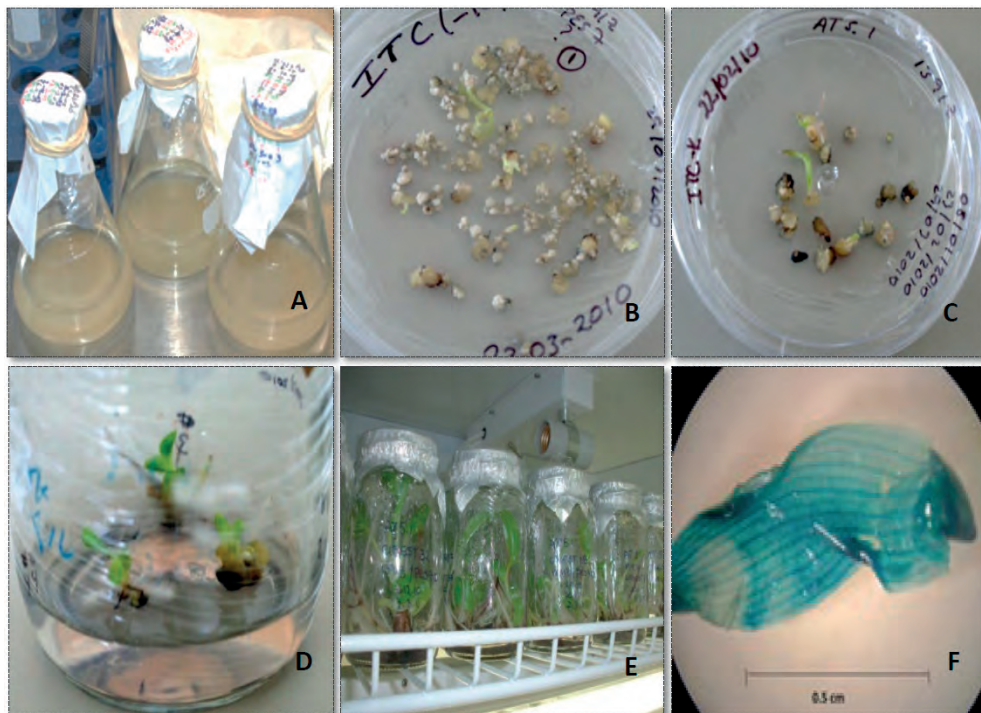
Figure 1. Scheme of the genetic transformation process using *Agrobacterium tumefaciens*, A) banana cell suspensions (cultivar 'Williams' AAA), B) and C) regeneration of banana embryogenic cells and calluses in ITC-K selection medium after genetic transformation, D) and E) maintenance and cocultivation under controlled light and temperature conditions of genetically transformed banana seedlings, F) GUS histochemical assay on the leaf. (Photo from Santos *et. al.*)[35].

of choice to deal with this complex situation.

In the case of genetic engineering, there are several methods to insert new genes into banana plants to obtain new plants resistant to different types of stress or even to create biofortified fruits[36] without altering the characteristics of plant sales. One of the first methodologies used to generate genetically modified banana plants was particle bombardment, a technique that introduces DNA into a living cell by shooting gold or tungsten particles (1-4 µm in diameter), penetrating the cell wall and membranes without being lethal[37]. The plant material used are embryogenic calli and embryogenic cell suspensions (ECS) and young tissues to regenerate stably transformed plants. Despite being an efficient method to generate transformed banana plants, this methodology tends to insert multiple copies of DNA into cells, and plants composed of genetically distinct tissues, called chimeras, are also often produced[3].

Using tissues such as embryogenic cells and protoplasts is ideal when avoiding the appearance of possible chimeras. In protoplasts, gene transfer to the cell nucleus is by electroporation, a technique that requires a prior standardization of parameters adjusted to the cultivar with which it will work. The most significant problem in the generation of protoplasts occurs in monocot species[38].

Another methodology for plant modification is by the soil bacterium *Agrobacterium tumefaciens*, known to cause tumors in dicotyledonous plants through the transfer of genes located in plasmids present in the *Agrobacterium*, which are modified to be able to transform plant cells using genes of interest[39]. For this same reason, it was not initially used in bananas because, as a monocotyledonous plant, it was not within the host range of the bacterium.

However, May *et al.* (1995) showed that using a co-culture system of the bacteria and meristematic tissue, they could transform and regenerate genetically modified banana plants, then verify the transformation using the GUS reporter gene and the Southern blot technique[40]. A variation of this method is the infiltration of *A. tumefaciens* employing a vacuum, which was tested by (41) in meristematic banana

tissue, using the gene encoding neomycin phosphotransferase II (nptII), which generates resistance to the antibiotic kanamycin as a selection tool. Although this variant managed to reduce the mortality rate of the transformed tissue and regenerated a more significant number of plants, it was prone to the generation of chimeras, which it tried to solve (unsuccessfully) by increasing the concentration of antibiotics.

This *Agrobacterium*-mediated genetic transformation methodology was standardized and is routinely applied at CIBE-ESPOL to transform Ecuadorian banana and plantain cultivars[42]. For which SCE from the cultivar 'Williams' were used in co-culture with the EHA105 strain of A. tumefaciens, the reporter gene uidA was introduced together with the selection gene hpt, which gives resistance to hygromycin (Fig. 3). Green fluorescent protein (GFP) and luciferase (LUC) is also highly used as plant reporter genes[43-46].

Commonly, a transgenic organism is associated with environmental biosafety and health risks due to the insertion of foreign DNA. According to Schouten *et al.* (2006)[48], cisgenesis is very similar to traditional plant breeding because a complete copy of one or more genes of interest, including introns, exons, and promoters, is transferred from sexually compatible organisms. Without altering the recipient species' gene pool and giving them unwanted traits[48].

On the other hand, intragenesis transfers one or several genes. However, these can have genetic elements from different genes and loci, allowing new genetic combinations that can give unique characteristics or desired traits to the modified organism, and which, in turn, like cisgenesis, these genes are from organisms of the same species or family. Due to international regulations on genetically modified organisms that do not discriminate whether an organism is transgenic or cisgenic and the lack of regulatory bodies in this study, future research to improve crop varieties could be delayed[48].

Precision tools for genome editing

The development of reliable and efficient tools that

Figure 2. A) In vitro banana plants from the 'Williams' cultivar was used for transformation. B) Meristematic tissue section. C) Cocultivation of the explants in MS medium supplemented with acetosyringone (200 μM) and *Agrobacterium tumefacien.*s D) Growth of putative transgenic plants two months after the meristematic transformation process.
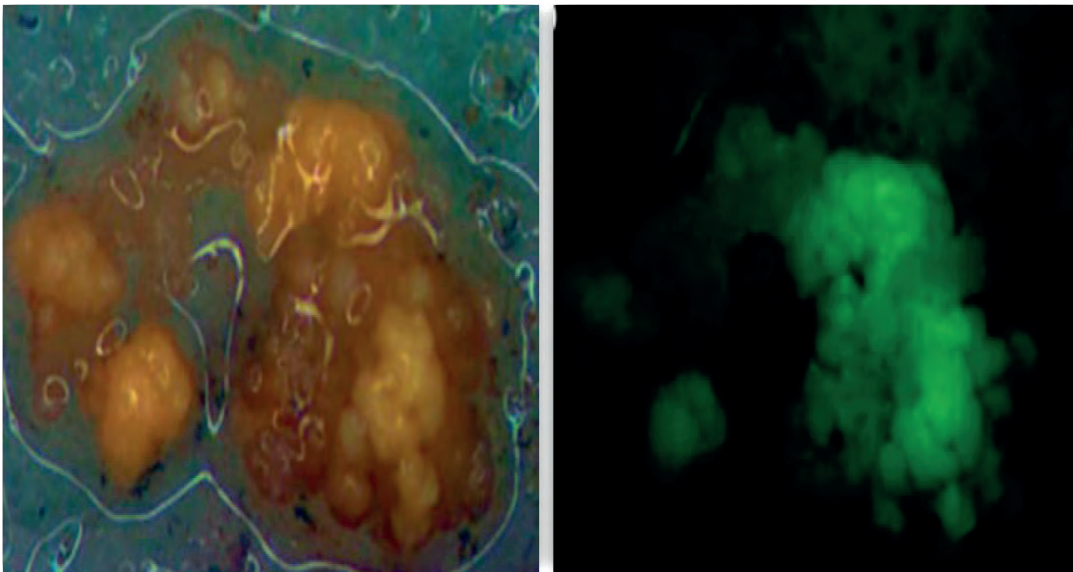
Figure 3. Banana colonies after three months of transformation with the pCAMBIA 1304 and the detection of the GFP reporter gene. (Photo from Santos *et.*, *al*)[47].

allow making precise changes in the genome of living cells has been a long-awaited desire for researchers involved in life sciences. The controversy generated by using and applying genetically modified crops impacts the favorable development of these technologies for developing cultivars better adapted to biotic and abiotic conditions.

These complications, mainly political and ethical, added to the accelerated growth of biotechnology in recent decades and have allowed the identification and creation of molecular techniques. These new technologies are known as precision genetic engineering technologies, where it is theoretically possible to make changes or edits to the genome of any organism without adding any foreign sequences. Other techniques for editing genetic material incur the problem of being imprecise, and in several cases, it is impossible to determine the insertion site in the genomic sequence.

Additionally, the time it takes to develop new varieties using conventional genetic engineering technologies is considerably high.

Nucleases are a group of enzymes capable of breaking the phosphodiester bond that exists between the monomers of nucleic acids. These enzymes have a standard function during the repair of the genetic material of living beings, having the ability to make breaks in one or both DNA strands. The study of these enzymes has made possible their application in molecular biology for the modification of the genetic material of different organisms. The extensive research and characterization of these enzymatic mechanisms in

6

molecular biology, molecular genetics, and biochemistry have allowed the development of novel tools for their application in genetic improvement and biotechnology, not only in bacteria but also in more complex organisms such as animals and plants. These "new" molecular tools differ from their predecessors, i.e., A. tumefaciens mediated transformation, due to the degree of precision with which they can recognize and manipulate the genetic material of the host organism. These editing tools allow the cutting and joining of DNA molecules at specific sites, creating insertions, deletions, or changes in the host cell's genetic material.

One of the first tools available to scientists was published by Kim et al. (1996), describing the creation of endonucleases capable of recognizing specific sites in the genetic material[49]. This group of scientists fused two structural motifs of proteins called zinc fingers to the cutting domain of the endonuclease enzyme Flavobacterium okeanokoites (FokI). The specificity of zinc-finger nucleases (ZFNs) is due to recognizing a set of three nucleotides (triplet) by zinc fingers. Zinc finger proteins (ZFs) of the Cys2-Hys2 type are among eukaryotes' most common DNA-binding motifs and represent the second most encoded protein domain in the human genome[50].

Each Cys2-His2 ZF domain consists of 30 amino acids in a conserved ββα configuration and binds three base pairs of a double-stranded DNA sequence (Liu et al. 1997)[51].

The ability to confer specificity to a protein that binds to DNA at a specific site in a universe of 3.5 million base pairs, as is the case of the human genome, requires at least the recognition of 16-18 base pairs[51]. Being able achieved if a protein containing at least 6 ZFs domains is used, and this type of structure was constructed thanks to the discovery of binding sequences, which allow the construction of synthetic ZFs proteins[50].

A ZFNs monomer is composed of 2 distinct functional domains: Cys2-Hys2 ZFs artificial domains at the N-terminus and the FokI non-specific cleavage domain at the C-terminus of the chimeric protein[52]. Due to the nature of the FokI endonuclease, it works as a dimer. For this, it needs two binding sites for the ZFs separated by 5-7 bp, which will be the recognition sequence for the cut by the FokI domain.

Each ZFs binding site must be found on one of the targeted DNA strands[49], forming a FokI dimer for cutting both DNA strands. ZFNs have been engineered for gene activation and repression in plants when fused to transcriptional activation or repression domains. Cutting both DNA strands makes it possible to exploit the natural DNA repair mechanisms such as homologous and nonhomologous recombination, allowing the disruption of genes through insertions or deletions typical of repair mechanisms, even achieving the insertion of sequences or processes of complete coding with the help of donor plasmids[53]. Since the first report in 1996, ZFNs have been used to manipulate the genome of plants such as Arabidopsis[54], tobacco[55], soybean[56], corn[57], rice[58], and tomato[59]. Despite the utility of ZFNs in various crops and organisms, the efficiency of this technology to make specific changes in DNA is usually less than 5%[60].

Another new technology that seeks to identify and localize specific sequences in an organism's genome is transcription activator-like effector-coupled nucleases or TALENs. This precise genome-editing tool works in pairs to search for and cut specific DNA sequences in the same way that ZFNs technology does. Transcription activator-like effector proteins recognize and activate specific plant promoters through tandem repeats. In 2007, Römer et al.

reported the ability to identify DNA sequences by proteins secreted by the phytopathogenic bacterium Xanthomonas campestris pv[61].

Bosch et al., in 2009, discovered how proteins related to the activation of promoters in host cells could recognize the target sequence in DNA[62]. The effector or activator proteins of transcription are found naturally in the genus Xanthomonas bacteria. The domain in charge of recognition is formed by a series of 33-35 amino acids repeated between 15 and 19 times in identical tandems. Each sequence of 33-35 amino acids is responsible for recognizing a nucleotide, where the residues located at positions 12 and 13 of each series confer the specificity of the recognition. This position of high variability is known as the diresidual variable repeat (DVR)[52]. The most common diresidual combinations are NI, NG, HD, and NN at the two specific positions mentioned above, which bind to nucleotides A, T, C, and G, respectively[53]. These molecules can change the target organism's DNA when these transcriptional activating effectors fuse with a nuclease domain. The functionality of this technology has been tested in model plants such as Arabidopsis thaliana and Nicotiana benthamiana[63-66].

One of the most current and novel tools that have quickly become popular in the field of genome editing is the so-called clustered regularly interspaced short palindromic repeats associated with the Cas protein or, in other words, CRISPR/Cas9 (based on the Cas9 protein) for its acronym in English. This new technology has emerged as a faster, cheaper, more accurate, and more efficient option than other precision technologies, such as those mentioned earlier in this chapter.

These palindromic repeats were first found in Escherichia coli by a group of Japanese scientists[67], Although the researchers did not understand their biological role at the time. In 1993, at the University of Alicante, the Spanish researcher Francisco Mojica described palindromic repeats in the halophilic archaea Haloferax mediterranei[88]. Mojica himself, together with Janssen in 2002, agreed to coin the term CRISPR to reduce the confusion generated by various acronyms in the scientific community. Several years later, specifically in 2007, Barrangou and colleagues (2007)[69] determined that this series of repetitions corresponded to a bacterial immunity system against bacteriophages based on sequences of the pathogen's genetic material. Three types of CRISPR mechanisms and 12 subtypes have been identified so far, which depend on their genetic content structural and content differences[70].

Seen from genetics, cas1 and cas2 are found in all types and subtypes; in Type I, there is cas3; in type II the cas9 gene and in Type III, cas10[70,71]. The CRISPR-Cas Type II system is the most studied. This defense system works in such a way that the bacterium integrates into the CRISPR locus of its genome, a small fragment of the infectious virus, called a protospacer, with a length of between 32-38 nucleotides usually. This fragment of the virus's genetic material is incorporated into a new interspaced region after a palindromic repeat at one end of the CRISPR locus and is used by the bacterium to recognize and defend itself from the virus or plasmid in a subsequent attack. The CRISPR locus (the protospacer and part of the CRISPR repeat) is transcribed, and these small RNA fragments generate a CRISPR RNA or crRNA, which is used to guide endonucleases, Cas to the target DNA of the invader based on the complementarity of the spacer sequence[72]. The crRNA hybridizes with a second RNA, called a transactivating

crRNA (tracrRNA), to form a new complex with the nuclease Cas9. This now mature crRNA, in conjunction with the Cas9 protein, can "seek and recognize" a specific sequence in the host's DNA, thanks to the protospacer sequence, to cut the genetic material of the target organism. The cut in the specified region results from the binding between the crRNA and the protospacer target sequence and a small region called the Protospacer Adjacent Motif (PAM)[73]. PAM is a conserved region of between 2-5 nucleotides followed by the 3'-end of the complementary sequence of the crRNA, so important for the nuclease activity of Cas9 that if it is not present, the Cas9:crRNA:tracrRNA complex is not presently capable of recognizing the target sequence.

As described before, the Cas9 enzyme has a molecular scissors-like function capable of cutting both strands of DNA at a specific site in the genome, thanks to the guidance of the crRNA:tracrRNA complex. The Cas9 protein most commonly used for gene editing has been adapted from the Type II CRISPR system of the bacterium *Streptococcus pyogenes* (Sp)[74]. Ongoing studies of the Cas9 enzyme have succeeded in creating three variants for genome editing. The first, the wild-type enzyme Cas9, is capable of cutting double-stranded DNA, resulting in the activation of the cellular repair system for double-stranded damage. There are two mechanisms for repairing these cuts: Nonhomologous DNA End Joining (NHEJ) and Homologous Recombination Repair (HDR)[75]. The second variant is mutant versions of Cas9 that have been modified so that they cut a single strand of the target DNA[76]. This second variant allows DNA repair by HDR alone because cutting a DNA strand does not activate the NHEJ mechanism. This option allows the design of experiments that use a pair of these mutant complexes to generate two simultaneous cuts at adjacent DNA sites[77]. A third variant is called a nuclease deficient Cas9 (dCas9), which has mutations in both the RuvC1 and HNH domains, which inactivate the nuclease activity of the enzyme but do not prevent its ability to bind to target DNA[77,78]. This ability to bind uncut DNA has been used to repress or express genes, and if this mutant complex is fused with effector domains, dCas9 can be used to silence or activate gene expression[71,73,77,79-82].

The gene editing process of the CRISPR-Cas9 system occurs in two steps. The first step is recognizing the specific sequence in the target DNA and cutting the DNA chain, which can be cut in both strands or just one. The second step is DNA repair which follows the action described above. The two repair mechanisms mentioned are the NHEJ and the HDR. The NHEJ repair mechanism causes mutations such as insertions and deletions at the double-strand cleavage site, leading to the silencing of the gene involved. This silencing may be due to a shift in the gene's reading frame or a significant change in the protein-coding region. On the other hand, the HDR repair system can be used to replace a particular sequence at the double-strand break site. This replacement is achieved thanks to homologous recombination guided by a DNA template that performs an insertion, deletion, mutation, correction, or complete replacement of a sequence or gene[58].

The application of the CRISPR-Cas9 gene editing system in plants has been growing in recent years. As mentioned throughout this chapter, the banana is a plant that presents multiple difficulties for its genetic improvement using conventional methodologies. Establishing this molecular tool in bananas allows a step toward applying innovative biotechnological techniques that can be considered in bre-

eding programs. Kaur *et al.* (2018) presented evidence of phytoene desaturase (PDS) gene editing in the genome of banana cv. 'Rasthali.' They demonstrated the capacity and efficiency of gene editing using the CRISPR-Cas9 system in this plant material, revealing its usefulness for the functional study of genes and use in breeding programs for this crop[83].

Since 2012, the CRISPR-Cas9 system has proven to be a powerful tool that allows the genetic information of various cell types and organisms to be modified. Until now, the versatility and considerable ease of use of the CRISPR-Cas9 system have allowed this tool to be used to modify the genome of organisms such as *Streptococcus pneumoniae*[84], *Escherichia coli*[84,85], *Lactobacillus reuteri*[86], *Mycobacterium tuberculosis*[87], *Saccharomyces cerevisae*[88], *Aspergillus nidulans*[89], *Trichoderma reesi*[90], *Nicotiana benthamiana*[91], *Arabidopsis thaliana*[92], *Oryza sativa*[93], *Solanum lycopersicum*[94], *Gossypium hirsutum*[95], *Musa* spp.[83], *Mus musculus*[96], *Xenopus laevis*[97], *Drosophila melanogaster*[98], *Caenorhabditis elegans*[99], among others.

Genetic manipulation applied to banana breeding

Different factors can severely impact banana production since it is a stress-sensitive crop. Banana cultivation can be affected by many biotic factors, such as bacterial, fungal, and viral infections and nematode attacks. *Xanthomonas campestris pv. musacearum* is a bacterium that threatens production in fields planted with susceptible varieties, specifically in the African continent. Infected plants show rapid yellowing and subsequent wilting of the leaves, affecting the inflorescence and pseudostem, which causes premature fruit ripening[100]. This disease is considered of quarantine importance for Latin America, where the best control is not to let the disease enter[101], for which molecular tools have been developed for efficient and specific detection of this bacterium[102]. Due to the lack of resistant varieties to this disease, genetic engineering has been considered a strategy for developing resistant varieties[103]. Banana plants genetically modified with the ferredoxin-like protein (Pflp) gene from *Capsicum annuum*, and regulated by the constitutive promoter CaMV35S, have been shown to have up to 100% resistance to the disease compared to infected controls. They develop the typical symptoms of the same due to the existence of a hypersensitivity response, which through programmed cell death (apoptosis), isolates the pathogen, stopping the progress of the infection[104].

The most important fungi in banana are i) *Pseudocercospora fijiensis* and ii) *Fusarium oxysporum* f. sp. cubense (Foc). *P. fijiensis*, the causal agent of black Sigatoka, spread throughout America in the 1980s. This disease produces a progressive yellowing of the leaves and wilting in a few weeks, affecting the fruit's filling and its ripening, causing the cluster to fall[105]. In the control of this disease, applications are made with fungicides such as benzimidazoles, triazoles, and others, representing an increase in the selective pressure of the pathogen, increasing resistance to them, leading producers to spray in different cases every 10 to 12 days.

On the other hand, *F. oxysporum* (with more than 150 unique forms), tropical race 4, represents a severe problem due to its high virulence, almost impossible control, and lack of resistant varieties. This disease is mainly localized in Asia and northern Australia4, recently reported in Colombia and Peru[1]. This pathogen produces yellowing and wilting of the leaves, penetrating through the roots and moving through the xylem until it colonizes the pseudostem, blocking it and causing the death of the plant. There is no effective con-

trol of this fungus since it can develop survival structures (chlamydospores) that can remain in the soil for more than 20 years. The best rule is to use resistant/tolerant varieties of the disease. However, there is a shortage of varieties resistant to the new races, and conventional breeding is too slow to deal with it quickly enough.

In both cases, genetic engineering has been considered an effective tool to obtain resistant banana varieties in the short term. Chitinases are a family of proteins that can degrade the chitin present in the cell wall of fungi. Kovács *et al.* (2013) experimented with overexpression of two chitinases from rice (*Oryza sativa*) in banana, rcc2, and rcg3, to analyze the resistance of modified plants against *P. fijiensis*, being the first report of stable transformation in the cultivar' Gros Michel' (AAA)[106]. The experiment compared the GM lines produced against a susceptible control,' Gros Michel' (untransformed), and a resistant wild species, 'Calcutta 4' (AA), where most of the GM lines showed a marked average area reduction infected compared to the susceptible variety. A similar approach to finding Foc-resistant varieties is known, where Hu *et al.* (2013) tested an endo-chitinase gene (chit42) from *Trichoderma harzianum* in the cultivar 'Furenzhi' (AA) in vitro resistance tests, the genetically modified plants showed a higher level of tolerance compared to non-controls transformed.

Pei and colleagues (2005) transformed banana plants with the gene for a human lysozyme (HL)[107]. This enzyme can count on the β-(1,4) glycosidic bond of the peptidoglycan, present in the bacterial cell wall, as well as in the chitin of the fungal cell wall, to obtain plants resistant to FocR4 and bacterial infections. Fifty-one transformed plants were received for greenhouse tests, of which 24 showed tolerance to pathogen infection. Then they were taken to field conditions, where they were infected with the pathogen. Only two of them did not present symptoms, these two being the ones with the highest expression of HL, demonstrating the correlation between the expression of human lysozyme and resistance to FocR4. Currently, there are genetically modified plants of the Cavendish variety that express the genes RGA2 (NB-LRR of *Musa acuminata* ssp.) and Ced9 (of the nematode *Caenorhabditis elegans*), which in their majority present resistance to *Fusarium oxysporum*, even some lines never showed symptoms of *Fusarium oxysporum*. infection[29].

Genetic engineering for improvement against abiotic stress

The climate change we have experienced in recent years requires obtaining banana varieties that are tolerant to different types of abiotic stress (drought, salinity, low temperatures). Banana is a crop that needs large amounts of water, is susceptible to abiotic factors, and has problems finding varieties resistant to pathogens. For this reason, genetic engineering serves as an instrument to speed up the process of obtaining new types which can cope with possible climate changes and meet food needs.

Shekhawat and collaborators (2011) reported the first study of the generation of transgenic banana plants tolerant to drought and salinity. In this study, they expressed a banana dehydrin (MusaDHN-1), regulating its expression under different types of stress[108]. The transformed events showed an increase in the production of proline in plants (necessary for cellular osmotic adjustment) under abiotic stress conditions, as well as a reduction in the accumulation of malondialdehyde, a marker of oxidative stress, a relative

percentage of water in the leaves, which explains in part the correlation of expression of this gene during pressure and the function of dehydrins to protect the lipid membrane. Another gene showing promising results concerning tolerance to abiotic stress is the one belonging to class-10 with pathogenesis (Pathogenesis-Related Class 10; PR10), a group with RNase activity. This gene was isolated from peanut (*Arachis hypogaea*) and PR10-transformed events also showed increased tolerance to salt stress, with increases in proline production and cell membrane stability compared to control[109].

Aquaporins are a family of proteins that maintain homeostasis and water balance in plant cells. The overexpression of the aquaporin MusaPIP1;2 of the banana cultivar Karibale Monthan', generated an increase in the tolerance to different types of abiotic stress, for they subjected transgenic banana plants to low temperatures (8°C) for two weeks, drought for another two weeks, and high salinity (250 mM NaCl) for ten days. The physiological parameters for all the tests were photosynthetic capacity, relative water content, and proline production, among others, to measure the behavior and response of all events against stress factors. In all the analyses, the genetically modified plants showed a higher tolerance than the non-transformed control, demonstrating the relationship of these aquaporins with the ability of plants to respond favorably under stress conditions. There are similar experiments overexpressing the aquaporin Musa COP26, which improves the tolerance of transgenic bananas to salinity stress[110,111].

The genetic transformation from 'Williams' banana embryogenic suspensions at CIBE used genes such as ADP 1 (SaARF1) from *Spartina alterniflora*, a grass that grows in coastal areas and is known to prevent soil erosion in areas with high salinity[112]. This gene has proven effective in rice cultivation, conferring tolerance to saline and drought stress to the events that express it[113]. The regenerated plants are currently in the *in vitro* multiplication phase to perform the respective tests (Fig. 4).

Genetic engineering for biofortification

Finally, a marked trend in recent years is the biofortification of crops, and bananas are no exception, given the need in countries where micronutrient deficiencies result from unbalanced diets[114]. Plantains from the Cavendish group are genetically modified using the MtPsy2a and ZmPsy1 genes (used in Golden rice) to produce a minimum β-carotenoid concentration of 20 μg/g dry matter, rising to 55 μg/g. g in one of the transgenic events expressing MtPsy2a. However, plants that overexpressed ZmPsyI showed undesirable phenotypes, such as the presence of "golden" young leaves (they returned to their greenish color over time), "golden" clusters (with the ripening of the fruit, the color changed to a mixture between green and orange) and fruit pulp with a coloration that went from intense yellow to orange.

The production of β-carotenoids proved stable in different generations of transgenic lines[30]. Human studies are underway with the "golden" banana in the United States of America, a project funded by the Bill and Melinda Gates Foundation[36].

Recently, at CIBE-ESPOL, a research project is being carried out using the GTPCHI genes of bananas and the ADCS of *Arabidopsis thaliana* in collaboration with the Laboratory of Functional Biology in Plants of the University of Ghent, led by Professor Dominique Van Der Straeten. The genes were fused with the promoter of the expansin gene in

Figure 4. Banana plants (cultivar 'Williams', AAA) genetically modified by *Agrobacterium tumefaciens* in the *in vitro* multiplication phase.

bananas, active in fruit tissues (Efrén Santos personal communication). Table 1 summarizes different works published on genetic engineering in *Musa* species.

Conclusions

Genetic engineering is a tool used worldwide for the improvement of crops. In species of the Musa genus, there are many studies carried out for genetic modification for disease resistance and biofortification. Recently, genome editing has been used massively in crop improvement, and bananas are no exception. Although there are few studies published to date, it is expected to increase in the coming years. Among the pending challenges is allowing the cultivation of genetically modified bananas and plantains for food security and commercial purposes.

Bibliographic references

1. Nuez, F. M.S. Andersson and MC de Vicente: Gene flow between crops and their wild relatives. Genetic Resources and Crop Evolution 2011 58:4 58, 619–619 (2011).
2. Daniells, J. W., Jenny, C., Karamura, D. A. & Tomekpe, K. Musalogue: a catalogue of Musa germplasm. Diversity in the genus Musa. Cirad 213 (2001) doi:10.3/JQUERY-UI.JS.
3. Pillay, M., Tenkouano, A., Ude, G. & Ortiz, R. Molecular characterization of genomes in Musa and its applications. Banana improvement: cellular, molecular biology, and induced mutations. Proceedings of a meeting held in Leuven, Belgium, 24-28 September 2001 271–286 (2004).
4. Nelson, S., Ploetz, R. & Kepler, A. Musa species (banana and plantain). Species profiles for pacific island agro forestry 2006, (2006).
5. Muirhead, I.F. y Jones, D. R. Diseases of Banana, Abacá and Enset. Postharvest disease 50, 190–206 (2000).
6. Orjeda, G. Evaluating bananas: a global partnership. Results of IMTP Phase II. International Network for the Improvement of Banana and Plantain, Montpellier, France. ISBN.
7. Carlier, J. (Jean) & International Network for Improvement of Banana and Plantain. Global evaluation of Musa germplasm for resistance to Fusarium wilt, Mycosphaerella leaf spot diseases, and nematodes : in-dept evaluation. 63 (2002).
8. Rosales, F. E. & Pocasangre, L. E. Mejoramiento convencional de banano y plátano: estrategias y logros [Conventional banana and plantain breeding: strategies and achievements]. (2002).
9. Menon, R. Banana breeding. Banana: Genomics and Transgenic Approaches for Genetic Improvement 13–34 (2016) doi:10.1007/978-981-10-1585-4_2.
10. Zandjanakou-Tachin, M. et al. Identification and genetic diversity of Mycosphaerella species on banana and plantain in Nigeria. Plant Pathol 58, 536–546 (2009).
11. Azhar, M. & Heslop-Harrison, J. S. Genomes, diversity and resistance gene analogues in Musa species. Cytogenet Genome Res 121, 59–66 (2008).
12. Miller, R. N. G. et al. Analysis of non-TIR NBS-LRR resistance gene analogs in Musa acuminata Colla: Isolation, RFLP marker development, and physical mapping. BMC Plant Biol 8, 15 (2008).
13. N Passos, M. A. et al. Development of expressed sequence tag and expressed sequence tag–simple sequence repeat marker resources for Musa acuminata. AoB Plants 2012, 30 (2012).
14. Sánchez Timm, E. et al. Identification of Differentially-Expressed Genes in Response to Mycosphaerella fijiensis in the Resistant Musa Accession 'Calcutta-4' Using Suppression Subtractive Hybridization. PLoS One 11, (2016).
15. Swarupa, V., Ravishankar, K. v. & Rekha, A. Plant defense response against Fusarium oxysporum and strategies to develop tolerant genotypes in banana. Planta 239, 735–751 (2014).
16. Ravishankar, K. v. et al. Genetic diversity and population structure analysis of mango (Mangifera indica) cultivars assessed by microsatellite markers. Trees - Structure and Function 29, 775–783 (2015).
17. Simmonds, N.W. 1962. The evolution of the bananas. Tropical Science Series. Longmans, London (GBR). 170p.
18. Fortescue, J. A. & Turner, D. W. Pollen fertility in Musa: Viability in cultivars grown in Southern Australia. Aust J Agric Res 55, 1085–1091 (2004).
19. Aguilar Morán, J. F. Improvement of cavendish banana cultivars through conventional breeding. Acta Hortic 986, 205–208 (2013).
20. Citogenética y mejoramiento genético del banano (Musa spp.). - Portal Embrapa. https://www.embrapa.br/busca-de-publicacoes/-/publicacao/641469/citogenetica-e-melhoramento-genetico-da-bananeira-musa-spp.

10

Cultivar	Gene	Source of gene	Character	Transformation Method	Reference
Cavendish, 'Gran Enano' (AAA)	RGA2	Musa acuminata ssp. Malaccensis	Resistencia a Fusarium oxysporum f. sp. cubense raza 4	A. tumefaciens	29
'Furenzhi' (AA)	chit42	Trichoderma harzianum	Resistencia a Fusarium oxysporum f. sp. cubense	A. tumefaciens	109
'Sukali ndiizi' (AAB)	Pflp	Capsicum annuum	Resistencia a Xanthomonas campestris pv. musacearum	A. tumefaciens	104
'Nakinyika' (AAA)	Hrap	Capsicum annuum	Resistencia a Xanthomonas campestris pv. musacearum	A. tumefaciens	28
Cavendish, 'Gran Enano' (AAA)	MtPsy2a	Musa spp.	Producción de β-Caroteno	A. tumefaciens	30
Cavendish, 'Gran Enano' (AAA)	ZmPsy1	Zea maize	Producción de β-Caroteno	A. tumefaciens	30
'Rasthali' (AAB)	MSI-99	Análogo sintético (modificado) del Magainin de Xenopus laevis	Resistencia a Fusarium oxysporum f. sp. cubense (Foc)	A. tumefaciens	115
Cavendish, 'Gran Enano' (AAA)	OclΔD86	Oryza sativa	Resistencia a nemátodos	A. tumefaciens	27
'Rasthali' (AAB)	HBsAG	Antígeno de Hepatitis B	Producción de vacuna en el fruto	A. tumefaciens	109
'Rasthali'(AAB)	β-1, 3-glucanasa	Glycine max	Resistencia a Fusarium oxysporum f. sp. cubense raza 1	A. tumefaciens	116
'Rasthali' (AAB)	MusaPIP1;2	Musa spp.	Tolerancia a sequía, salinidad y bajas temperaturas.	A. tumefaciens	110
'Rasthali' (AAB)	MusaPIP1;6	Musa spp.	Tolerancia al estrés por salinidad	A. tumefaciens	111
'Rasthali' (AAB)	MusaDHN-1	Musa spp.	Tolerancia a sequía y salinidad	A. tumefaciens	117
Musa acuminata cv. 'Matti' (AA)	PR-10	Arachis hypogaea	Tolerancia a sequía y salinidad	A. tumefaciens	109
Musa acuminatacv. 'Gros Michel' (AAA)	rcc2, rcg3	Oriza sativa	Resistencia a Pseudocercospora fijiensis	A. tumefaciens	106

Table 2. Formulas and variables for calculating the components of the productive process' cost.

21. Meng, L., Gao, X., Chen, J. & Martin, K. Spatial and temporal effects on seed dispersal and seed predation of Musa acuminata in southern Yunnan, China. Integr Zool 7, 30–40 (2012).

22. Komarek, A. The determinants of banana market commercialization in Western Uganda. Afr J Agric Res 5, 775–784 (2010).

23. Smale, M. et al. An Economic Assessment of Banana Genetic Improvement and Innovation in the Lake Victoria Region of Uganda and Tanzania. doi:10.2499/9780896291645RR155.

24. Ortiz, R, Vuylsteke D (1993) The genetics of black sigatoka resistance, growth and yield parameters in 4x and 2x plantain-banana hybrids En: Ganry J (ed.) breeding banana and plantain for resistance to diseases and pests, p. 379. CIRAD-INIBAP. Montpellier.

25. Kumar, J., Chaube, H., Singh, U. & Mukhopadhyay, A. Plant diseases of international importance. Volume III. Diseases of fruit crops. Undefined (1992).

26. Ortiz, R. (2013). Conventional banana and plantain breeding. Acta Hortic. 986, 177-194 DOI:10.17660/ActaHortic.2013.986.19.

27. Atkinson, H. J., Grimwood, S., Johnston, K. & Green, J. Prototype demonstration of transgenic resistance to the nematode Radopholus similis conferred on a banana by a cystatin. Transgenic Res 13, 135–142 (2004).

28. Tripathi, L., Mwaka, H., Tripathi, J. N. & Tushemereirwe, W. K. Expression of sweet pepper Hrap gene in banana enhances resistance to Xanthomonas campestris pv. musacearum. Mol Plant Pathol 11, 721–731 (2010).

29. Dale, J. et al. Transgenic Cavendish bananas with resistance to Fusarium wilt tropical race 4. Nat Commun (2017) doi:10.1038/s41467-017-01670-6.

30. Paul, J. Y. et al. Golden bananas in the field: elevated fruit pro-vitamin A from the expression of a single banana transgene. Plant Biotechnol J 15, 520–532 (2017).

31. Patel, P., Yadav, K. & Ganapathi, T. R. Biofortification for alleviating iron deficiency anemia. Banana: Genomics and Transgenic Approaches for Genetic Improvement 301–337 (2016) doi:10.1007/978-981-10-1585-4_20.

32. McQueen-Mason, S., Durachko, D. M. & Cosgrove, D. J. Two Endogenous Proteins That Induce Cell Wall Extension in Plants. Plant Cell (1992) doi:10.2307/3869513.

33. Arntzen, C. Plant☐made pharmaceuticals: from 'Edible Vaccines' to Ebola therapeutics. Plant Biotechnol J 13, 1013 (2015).

34. Genetic Transformation of Perennial Tropical Fruits on JSTOR. https://www.jstor.org/stable/4293771.

35. Santos, E. et al. Advances in banana transformation through Agrobacterium tumefaciens in Ecuador: Progress, challenges, and perspectives. in Acta Horticulturae vol. 1114 197–202 (International Society for Horticultural Science, 2016).

36. Waltz, E. Vitamin A Super Banana in human trials. Nat Biotechnol 32, 857 (2014). https://doi.org/10.1038/nbt0914-857.

37. Sanford, J. C., Klein, T. M., Wolf, E. D. & Allen, N. Delivery of substances into cells and tissues using a particle bombardment process. http://dx.doi.org/10.1080/02726358708904533 5, 27–37 (2007).

38. Roderick, H., Tripathi, L. & Poovarasan, S. Transgenic Approaches to Improve Resistance to Nematodes and Weevils. Undefined 247–260 (2016) doi:10.1007/978-981-10-1585-4_17.

39. Hoekema, A., Hirsch, P. R., Hooykaas, P. J. J. & Schilperoort, R. A. A binary plant vector strategy based on separation of vir- and T-region of the Agrobacterium tumefaciens Ti-plasmid. Nature vol. 303 179–180 Preprint at https://doi.org/10.1038/303179a0 (1983).

40. Hard, T., Barnes, H., Larsson, C., Gustafsson., Lund, J. © 199 5 Nature Publishing Group http://www.nature.com/nsmb. Nature 2, 983–989 (1995).

41. Acereto-Escoffié, P. O. M. et al. Agrobacterium-mediated transformation of Musa acuminata cv. 'Grand Nain' scalps by vacuum infiltration. Sci Hortic 105, (2005).

42. Luis Eduardo Sánchez & Ordoñez, E. G. S. Estandarización del protocolo de transformación genética de células embriogénicas de banano de la variedad 'Williams' (AAA) mediada por Agrobacterium tumefaciens. Revista Tecnológica - ESPOL 23, (2010).

43. Santos, E. et al. Tagging novel promoters in banana using the luciferase reporter gene. in Acta Horticulturae vol. 763 99–105 (2007).

44. Santos Ordóñez EG. Characterization and isolation of T-DNA tagged banana promoters active during in vitro regeneration and low temperature stress. (Katholieke Universiteit Leuven, 2008).

45. Santos, E. et al. Characterization and isolation of a T-DNA tagged banana promoter active during in vitro culture and low temperature stress. BMC Plant Biol 9, 77 (2009).

46. Villao, L. et al. Activity characterization of the plantain promoter from the heavy metal-associated isoprenylated plant gene (MabHIPP) using the luciferase reporter gene. Plant Gene 19, (2019).

47. Santos, E. et al. Promoter Analysis in Banana BT - Banana: Genomics and Transgenic Approaches for Genetic Improvement. in (eds. Mohandas, S. & Ravishankar, K. v) 157–179 (Springer Singapore, 2016). doi:10.1007/978-981-10-1585-4_11.

48. Schouten, H. J., Krens, F. A. & Jacobsen, E. Cisgenic plants are similar to traditionally bred plants: International regulations for genetically modified organisms should be altered to exempt cisgenesis. EMBO Rep 7, 750–753 (2006).

49. Kim, Y. G., Cha, J. & Chandrasegaran, S. Hybrid restriction enzymes: Zinc finger fusions to Fok I cleavage domain. Proc Natl Acad Sci U S A 93, (1996).

50. Gaj, T., Gersbach, C. A. & Barbas Iii, C. F. ZFN, TALEN, and CRISPR/Cas-based methods for genome engineering. Trends Biotechnol 31, 397–405 (2013).

51. Liu, Q., Segal, D. J., Ghiara, J. B. & Barbas, C. F. Design of polydactyl zinc-finger proteins for unique addressing within complex genomes. Proc Natl Acad Sci U S A 94, (1997).

52. Kamburova, V. S. et al. Genome Editing in Plants: An Overview of Tools and Applications. International Journal of Agronomy vol. 2017 Preprint at https://doi.org/10.1155/2017/7315351 (2017).

53. Liu, W. & Stewart, C. N. Plant synthetic promoters and transcription factors. Curr Opin Biotechnol 37, 36–44 (2016).

54. Zhang, F. et al. High frequency targeted mutagenesis in Arabidopsis thaliana using zinc finger nucleases. Proc Natl Acad Sci U S A 107, (2010).

55. Townsend, J. A. et al. High-frequency modification of plant genes using engineered zinc-finger nucleases. Nature 459, (2009).

56. Curtin, S. J. et al. Targeted mutagenesis of duplicated genes in soybean with zinc-finger nucleases. Plant Physiol 156, (2011).

57. Shukla, V. K. et al. Precise genome modification in the crop species Zea mays using zinc-finger nucleases. Nature 459, (2009).

58. Zhang, Y. et al. An A20/AN1-type zinc finger protein modulates gibberellins and abscisic acid contents and increases sensitivity to abiotic stress in rice (Oryza sativa). J Exp Bot 67, (2016).

59. Hilioti, Z., Ganopoulos, I., Ajith, S., Bossis, I. & Tsaftaris, A. A novel arrangement of zinc finger nuclease system for in vivo targeted genome engineering: the tomato LEC1-LIKE4 gene case. Plant Cell Rep 35, (2016).

60. Ainley, W. M. et al. Trait stacking via targeted genome editing. Plant Biotechnol J 11, (2013).

61. Römer, P. et al. Plant pathogen recognition mediated by promoter activation of the pepper Bs3 resistance gene. Science (1979) 318, (2007).

62. Boch, J. et al. Breaking the code of DNA binding specificity of TAL-type III effectors. Science (1979) 326, (2009).

63. Zhang, Y. et al. Transcription activator-like effector nucleases enable efficient plant genome engineering. Plant Physiol 161, (2013).

64. Mahfouz, M. M. & Li, L. TALE nucleases and next generation GM crops. GM Crops 2, (2011).

65. Christian, M., Qi, Y., Zhang, Y. & Voytas, D. F. Targeted Mutagenesis of Arabidopsis thaliana Using Engineered TAL Effector Nucleases. G3: Genes, Genomes, Genetics 3, (2013).

66. Cermak, T. et al. Erratum: Efficient design and assembly of custom TALEN and other TAL effector-based constructs for DNA targeting (Nucleic Acids Research (2011) 39 (e82) DOI: 10.1093/nar/gkr218). Nucleic Acids Research vol. 39 Preprint at https://doi.org/10.1093/nar/gkr739 (2011).

67. Ishino, Y., Shinagawa, H., Makino, K., Amemura, M. & Nakatura, A. Nucleotide sequence of the iap gene, responsible for alkaline phosphatase isoenzyme conversion in Escherichia coli, and identification of the gene product. J Bacteriol 169, (1987).

68. Mojica, F. J. M., Juez, G. & Rodriguez☐Valera, F. Transcription at different salinities of Haloferax mediterranei sequences adjacent to partially modified PstI sites. Mol Microbiol 9, (1993).

12

69. Barrangou, R. et al. CRISPR provides acquired resistance against viruses in prokaryotes. Science (1979) 315, (2007).

70. Barrangou, R. & Marraffini, L. A. CRISPR-cas systems: Prokaryotes upgrade to adaptive immunity. Molecular Cell vol. 54 Preprint at https://doi.org/10.1016/j.molcel.2014.03.011 (2014).

71. Fichtner, F., Urrea Castellanos, R. & Ülker, B. Precision genetic modifications: A new era in molecular biology and crop improvement. Planta vol. 239 Preprint at https://doi.org/10.1007/s00425-014-2029-y (2014).

72. Brouns, S. J. J. et al. Small CRISPR RNAs guide antiviral defense in prokaryotes. Science (1979) 321, (2008).

73. Jinek, M. et al. A programmable dual-RNA-guided DNA endonuclease in adaptive bacterial immunity. Science (1979) 337, 816–821 (2012).

74. Hsu, P. D. et al. DNA targeting specificity of RNA-guided Cas9 nucleases. Nat Biotechnol 31, (2013).

75. Sander, J. D. & Joung, J. K. CRISPR-Cas systems for editing, regulating and targeting genomes. Nature Biotechnology vol. 32 Preprint at https://doi.org/10.1038/nbt.2842 (2014).

76. Nishimasu, H. et al. Crystal structure of Cas9 in complex with guide RNA and target DNA. Cell 156, (2014).

77. Chen, X. et al. In trans paired nicking triggers seamless genome editing without double-stranded DNA cutting. Nat Commun 8, (2017).

78. Gasiunas, G., Barrangou, R., Horvath, P. & Siksnys, V. Cas9-crRNA ribonucleoprotein complex mediates specific DNA cleavage for adaptive immunity in bacteria. Proc Natl Acad Sci U S A 109, (2012).

79. Gilbert Luke A et al. CRISPR-mediated modular RNA-guided regulation of transcription in eukaryotes. Cell 154, (2013).

80. Lowder, L. G., Malzahn, A. & Qi, Y. Plant gene regulation using multiplex CRISPR-dCas9 artificial transcription factors. in Methods in Molecular Biology vol. 1676 (2018).

81. Perez-Pinera, P. et al. RNA-guided gene activation by CRISPR-Cas9-based transcription factors. Nat Methods 10, (2013).

82. LS, Q. et al. Repurposing CRISPR as an RNA-guided platform for sequence-specific control of gene expression. Cell 184, (2021).

83. Kaur, N. et al. CRISPR/Cas9-mediated efficient editing in phytoene desaturase (PDS) demonstrates precise manipulation in banana cv. Rasthali genome. Funct Integr Genomics 18, (2018).

84. Jiang, W., Bikard, D., Cox, D., Zhang, F. & Marraffini, L. A. RNA-guided editing of bacterial genomes using CRISPR-Cas systems. Nat Biotechnol 31, (2013).

85. Cong, L. et al. Multiplex genome engineering using CRISPR/Cas systems. Science (1979) 339, (2013).

86. Oh, J. H. & van Pijkeren, J. P. CRISPR-Cas9-assisted recombineering in Lactobacillus reuteri. Nucleic Acids Res 42, (2014).

87. Choudhary, E., Thakur, P., Pareek, M. & Agarwal, N. Gene silencing by CRISPR interference in mycobacteria. Nat Commun 6, (2015).

88. Ronda, C. et al. CrEdit: CRISPR mediated multi-loci gene integration in Saccharomyces cerevisiae. Microb Cell Fact 14, (2015).

89. Nødvig, C. S., Nielsen, J. B., Kogle, M. E. & Mortensen, U. H. A CRISPR-Cas9 system for genetic engineering of filamentous fungi. PLoS One 10, (2015).

90. Liu, R., Chen, L., Jiang, Y., Zhou, Z. & Zou, G. Efficient genome editing in filamentous fungus Trichoderma reesei using the CRISPR/Cas9 system. Cell Discov 1, (2015).

91. Nekrasov, V., Staskawicz, B., Weigel, D., Jones, J. D. G. & Kamoun, S. Targeted mutagenesis in the model plant Nicotiana benthamiana using Cas9 RNA-guided endonuclease. Nature Biotechnology vol. 31 Preprint at https://doi.org/10.1038/nbt.2655 (2013).

92. Li, J. F. et al. Multiplex and homologous recombination-mediated genome editing in Arabidopsis and Nicotiana benthamiana using guide RNA and Cas9. Nature Biotechnology vol. 31 Preprint at https://doi.org/10.1038/nbt.2654 (2013).

93. Belhaj, K., Chaparro-Garcia, A., Kamoun, S. & Nekrasov, V. Plant genome editing made easy: Targeted mutagenesis in model and crop plants using the CRISPR/Cas system. Plant Methods vol. 9 Preprint at https://doi.org/10.1186/1746-4811-9-39 (2013).

94. Shimatani, Z. et al. Targeted base editing in rice and tomato using a CRISPR-Cas9 cytidine deaminase fusion. Nat Biotechnol 35, (2017).

95. Li, C., Unver, T. & Zhang, B. A high-efficiency CRISPR/Cas9 system for targeted mutagenesis in Cotton (Gossypium hirsutum L.). Sci Rep 7, (2017).

96. Hirose, M. et al. CRISPR/Cas9-mediated genome editing in wild-derived mice: Generation of tamed wild-derived strains by mutation of the a (nonagouti) gene. Sci Rep 7, (2017).

97. Wang, F. et al. Targeted gene disruption in Xenopus laevis using CRISPR/Cas9. Cell and Bioscience vol. 5 Preprint at https://doi.org/10.1186/s13578-015-0006-1 (2015).

98. Bassett, A. R., Tibbit, C., Ponting, C. P. & Liu, J. L. Highly Efficient Targeted Mutagenesis of Drosophila with the CRISPR/Cas9 System. Cell Rep 4, (2013).

99. Waaijers, S. et al. CRISPR/Cas9-targeted mutagenesis in Caenorhabditis elegans. Genetics vol. 195 Preprint at https://doi.org/10.1534/genetics.113.156299 (2013).

100. Tripathi, L. et al. Xanthomonas wilt: A threat to banana production in East and Central Africa. Plant Dis 93, (2009).

101. Manzo-sánchez, G., Ciencias, F. de & Colima, U. de. Diseases of quarantine and economic importance in banana tree (Musa sp.) in México. Revista Mexicana de Fitopatología 32, 89–107 (2014).

102. Adikini, S. et al. Development of a specific molecular tool for detecting Xanthomonas campestris pv. musacearum. Plant Pathol 60, (2011).

103. Tripathi, L., Tripathi, J. N. & Tushemereirwe, W. K. Strategies for resistance to bacterial wilt disease of bananas through genetic engineering. African Journal of Biotechnology vol. 3 Preprint at (2004).

104. Namukwaya, B. et al. Transgenic banana expressing Pflp gene confers enhanced resistance to Xanthomonas wilt disease. Transgenic Res 21, (2012).

105. F., G. [Epidemiology and ecology of the Sigatoka negra (Mycosphaerella fijiensis, Morelet) in bananas (Musa sp.), in Costa Rica]. [Spanish]. (1990) doi:10.3/JQUERY-UI.JS.

106. Kovács, G. et al. Expression of a rice chitinase gene in transgenic banana ('Gros Michel', AAA genome group) confers resistance to black leaf streak disease. Transgenic Res 22, 117–130 (2013).

107. Pei, X. W. et al. Creation of transgenic bananas expressing human lysozyme gene for Panama wilt resistance. J Integr Plant Biol 47, (2005).

108. Shekhawat, U. K. S., Srinivas, L. & Ganapathi, T. R. MusaDHN-1, a novel multiple stress-inducible SK(3)-type dehydrin gene, contributes affirmatively to drought- and salt-stress tolerance in banana. Planta 234, 915–932 (2011).

109. Rustagi, A. et al. High Efficiency Transformation of Banana [Musa acuminata L. cv. Matti (AA)] for Enhanced Tolerance to Salt and Drought Stress Through Overexpression of a Peanut Salinity-Induced Pathogenesis-Related Class 10 Protein. Mol Biotechnol (2014) doi:10.1007/s12033-014-9798-1.

110. Sreedharan, S., Shekhawat, U. K. S. & Ganapathi, T. R. Transgenic banana plants overexpressing a native plasma membrane aquaporin MusaPIP1;2 display high tolerance levels to different abiotic stresses. Plant Biotechnol J 11, 942–952 (2013).

111. Sreedharan, S., Shekhawat, U. K. S. & Ganapathi, T. R. Constitutive and stress-inducible overexpression of a native aquaporin gene (MusaPIP2;6) in transgenic banana plants signals its pivotal role in salt tolerance. Plant Mol Biol 88, 41–52 (2015).

112. Joshi, R. et al. Salt adaptation mechanisms of halophytes: Improvement of salt tolerance in crop plants. in Elucidation of Abiotic Stress Signaling in Plants: Functional Genomics Perspectives, Volume 2 (2015). doi:10.1007/978-1-4939-2540-7_9.

113.   Joshi, R., Ramanarao, M. V., Lee, S., Kato, N. & Baisakh, N. Ectopic expression of ADP ribosylation factor 1 (SaARF1) from smooth cordgrass (Spartina alterniflora Loisel) confers drought and salt tolerance in transgenic rice and Arabidopsis. Plant Cell Tissue Organ Cult 117, (2014).

114.   de Valença, A. W., Bake, A., Brouwer, I. D. & Giller, K. E. Agronomic biofortification of crops to fight hidden hunger in sub-Saharan Africa. Global Food Security vol. 12 Preprint at https://doi.org/10.1016/j.gfs.2016.12.001 (2017).

115.   Chakrabarti, A., Ganapathi, T. R., Mukherjee, P. K. & Bapat, V. A. MSI-99, a magainin analogue, imparts enhanced disease resistance in transgenic tobacco and banana. Planta 216, (2003).

116.   Maziah, M., Sariah, M. & Sreeramanan, S. Transgenic banana Rastali (AAB) with β-1, 3-glucanase gene for tolerance to fusarium wilt race 1 disease via Agrobacterium-mediated transformation system. Plant Pathol J (Faisalabad) 6, (2007).

117.   Shekhawat, U. K. S., Srinivas, L. & Ganapathi, T. R. MusaDHN-1, a novel multiple stress-inducible SK(3)-type dehydrin gene, contributes affirmatively to drought- and salt-stress tolerance in banana. Planta 234, 915–932 (201

13

Physicochemical characteristics and antioxidant capacity of Ecuadorian paramo flowers

Elena Coyago-Cruz[1]*, Aida Guachamin[1], Edwin Vera[2], Melany Moya[3], Jorge Heredia-Moya[4], Elena Beltrán[5]

DOI. 10.21931/RB/2023.08.01.21

[1] Universidad Politécnica Salesiana, Carrera de Ingeniería en Biotecnología de los Recursos Naturales, Grupo de Investigación y Desarrollo en Ciencias Aplicadas a los Recursos Biológicos, Quito, Ecuador.
[2] Escuela Politécnica Nacional, Departamento de Ciencias de los Alimentos y Biotecnología, Facultad de Ingeniería Química, Quito, Ecuador.
[3] Universidad Central del Ecuador, Facultad de Ciencias Médicas, Carrera de Obstetricia, Iquique, Quito, Ecuador.
[4] Universidad UTE, Facultad de Ciencias de la Salud Eugenio Espejo, Centro de Investigación Biomédica (CENBIO), Quito, Ecuador.
[5] Investigación de Alimentos (CIAL), Facultad de Ciencias de la Ingeniería e Industrias, Ingeniería de Alimentos, Quito, Ecuador.
Corresponding author: ecoyagoc@ups.edu.ec

Abstract: Ecuador is a megadiverse country with a wide variety of floral species that have been little studied. In this context, the study's objective was to evaluate the physicochemical characteristics and the antioxidant activity of several floral species of paramo of Pichincha Province in Ecuador. Thus, the weight, size, color, pH, soluble solids, moisture and ash of fresh flower was quantified. In addition, carotenoids, phenolic compounds and antioxidant activity were quantified in lyophilized powder. The results obtained showed that the flowers of *Werneria nubigena* were the longest (43,80 cm); *Brugmansia x candida* the widest (9,88cm) and heaviest (9,22g); *Tristerix longebracteatus* presented high soluble solids content (21,5 °Brix), *Lupinus microphyllus* high pH (14,00), *Ceanothus maritimus* high titratable acidity (0,26%), *Castilleja integrifolia* high ash content (6,42%) and *Bidens ferulifolia* high moisture content (95,73%). In addition, the highest ranges of total carotenoids and total phenolics were presented by yellow *Bidens ferulifolia* (24,81 µg β-carotene/g PS) and *Fuchsia vulcania* (531,77 mg EAG /g PS), respectively. Finally, it was found in *Bomarea multiflora* high values of antioxidant capacity (182,08 trolox eq. µmol/ g PS). These results suggest that the paramo flowers contain essential bioactive compounds that could be used for food, medicinal and cosmetic purposes.

Key words: Bioactive compounds, carotenoids, phenolic compounds, Andean flowers.

Introduction

Ecuador is divided into four regions: the coast, which the Pacific Ocean borders, the Andean highlands, which is hilly and volcanic; the Amazonian region, which is home to the Amazon Rainforest; and the insular region, which is made up of islands and archipelagos in the Pacific Ocean.

Due to its unique geography, it is a megadiverse country with a wide variety of habitats, enabling it to support a diversity of plant and animal species. Evolutionary processes have conferred characteristics on a continental and regional scale, geomorphology, soil type, fluctuating precipitation patterns, habitat fragmentation and temperature gradient. Thus, the paramo is a high mountain ecosystem located at an altitude of more than 2800 meters above sea level (masl) with cold and humid climates, frequent rainfall, strong winds and nearly constant cloud cover; however, above 4200 masl the vegetation is scarce, and the paramo is desert or has large sandbanks[1].

The paramos are biologically crucial due to the diversity and singularity of its flora and fauna species, which are endemic to the region. As a result, species diversity increases between 3000 and 3400 masl and diminishes as altitude increases[2]. *Asteraceae, Orchidaceae, Melastomataceae, Campanulaceae, Poaceae, Bromeliaceae, Gentianaceae, Cyperaceae, Ericaceae* and *Solanaceae*, are the most abundant families of plants in Ecuador's paramo; the first seven of these have endemic species. The genera with the most significant number of species are *Miconia, Stelis, Epidendrum, Baccharis, Calceolaria, Pleurothalis, Pentacalia* and *Tillandsia*[3]. Many of these plants have showy flowers mainly used for decoration and have not received much attention from researchers looking into bioactive compounds. However, certain flowers contain carotenoids, phenols, and alkaloids, among other organic molecules. This characteristic has contributed to the use of floral species in food and traditional medicine[4].

On the other hand, an antioxidant is any substance that delays or prevents the oxidation of oxidable substrates such as lipids, proteins, carbohydrates, and DNA[5]. Some carotenoids and phenolic compounds are antioxidants, which can help to prevent disease[6]. Table 1 shows the edible uses, analyzed parts, phenolic compounds, carotenoids and antioxidant activity by ABTs and DPPH method of some paramos floral species. Thus, it is shown that most of the paramo species were used in food as an infusion using flowers. In addition, in most cases, the concentration of total phenolic compounds was evaluated, except in *Diplostephium hartwegii* and *Bidens ferulifolia*. Only 5 of the 13 species studied bibliographically (*Hypochaeris radicata, Taraxacum officinale, Fuchsia vulcania, Tropaeolum majus* and *Chuquiraga jussieuri*) presented carotenoids studies, and antioxi-

Elena Coyago-Cruz, Aida Guachamin, Edwin Vera, Melany Moya, Jorge Heredia-Moya, Elena Beltrán

dant activity was measured in the majority of cases using the ABTS or DPPH assay. In this context, the objetive of this study was to evaluate the physicochemical characteristics and antioxidant activity of paramo flowers.

Materials and methods

Reagents and Standards

Ethanol HPLC grade and reagents of analytical quality such as hydrochloric acid, sodium hydroxide, dichloromethane, acetone, and sodium carbonate were purchased from Merck (Merck, Germany), while methanol HPLC grade from Pharmco (PHARMCO by Greenfield Global, California). Folin Ciocalteu reagent and all standard (β-Carotene, gallic acid, and Trolox) were obtained from Sigma-Aldrich (Merck, Germany).

Plant Materials

The experimentation was authorized by the Ministerio del Ambiente of Ecuador under the framework contract MAE-DNB-CM-2017-0080-UTE, Project MAE-DNB-2019-0911-O. The collection used the International Code of Conduct for the collection and transfer of plant germplasm of the FAO[21], and the publications of Biodiversity International[22] were utilized in sampling 30 species of paramos in the Pichincha province (Table 2). The collection was carried out between February and July 2020.

Determination of physicochemical characteristics

The weight (g) of fresh flower petals was determined using a Mettler Toledo scale (Mettler Toledo, United States), as well as the equatorial diameter and longitudinal diameter (mm)[11]. Additionally, the soluble solids (°Brix) using a Hitech hand-held refractometer (Hitech RHB-32 ATC, United States)[23], % total titratable acidity[24], pH using a SevenMulti S47 automatic pH meter (Mettler Toledo, United States)[25], % humidity in a Memmert Be 20 oven (Memmert GmbH+Co. KG, Spain)[26,27], and % ash in a Thermolyne muffle (Thermo Fisher Scientific, United States)[28] were quantified. The other fresh flowers were frozen at -80 °C and freeze-dried in a Christ Alpha 1-4 LDplus equipment (Martin Gwfriertrocknungsanlagen GmbH, Germany). The freeze-dried samples were ground and stored in amber bottles until analysis.

Determination of bioactive compounds and antioxidant activity

Quantification of total carotenoids

Approximately 10 mg of lyophilized material and 300 µL of acetone:methanol: dichloromethane (1:1:2) were used for the microextraction of carotenoids. The mixture was stirred for one minute in an ultrasound model VWR (VWR International, EE.UU.), and the supernatant was recovered after centrifugation at 14000 rpm for 4 min in a MiniSpin microcentrifuge (Eppendorf, EE.UU.). This process was repeated until the solids showed no color. Finally, the combined extracts were dried in a rotary evaporator, re-dissolved in ethanol HPLC, and quantified in a Jasco V-730 spectrophotometer (Mettler Toledo, Ecuador), at a wavelength of 450 nm. The total carotenoids were expressed as µg equivalent of β-carotene / g of dry weight (DW)[4].

Family	Species	Edible use	Analyzed part	Phenolic compounds	Carotenoids	Antioxidant activity		References
						ABTS	DPPH	
Compositae	*Diplostephium* hartwegii Hieron	Infusion	Leaf	na	na	IC$_{50}$ 10.1 mg/L MeOH	IC$_{50}$ 13.8 mg/L MeOH	7
Compositae	*Hypochaeris radicata* L.	Flavoring	Flower	50.8 mg GAE/g	3.9 mg/g	97 % inhibition	82 % inhibition	8
Compositae	*Taraxacum officinale* (L.) Weber ex F. H. Wigg.	Infusion	Flower	0.4 mg GAE/g DW	41.9 mg/kg	na	0.9 mg TE/g	9
				11.9 mg GAE/kg			71.6 g AAE/kg	10
Onagraceae	*Fuchsia vulcania* Lam.	Infusion	Flower	42.5 mg GAE/100 g DW	11.8 µg/g	na	na	11
Tropaeolaceae	*Tropaeolum majus* L.	Salad	Flower	406 mg GAE/100 g DW	7643.2 µg/g	458 µm TE/ g	na	12
Orobanchaceae	*Castilleja fissifolia* L.f.	Infusion	Whole plant	61.9 mg GAE/g DW	na	na	0.6 g/ mmol DPPH	13,14
Oxalidaceae	*Oxalis pes-caprae* L.	Salad	Flower				110.7 % inhibition	15
			Leaf	121.7 µmol GAE/g	na	88.5 µmol TE/g	na	16
Fabaceae	*Dalea coerulea* (L.f.) Schinz & Thell	Infusion	Flower	15.6 mg GAE/100 g DW	na	IC$_{50}$ 130.6 µg/mL	na	17
Fabaceae	*Lupinus mutabilis* Sweet	Drink	Seed	12.1 mg GAE/g DW	na	202.7 µmol TE/g DW	277.5 µmol TE/g DW	18
Xanthorrhoeaceae	*Hemerocallis citrina* Baroni	Infusion	Flower	102.9 mg GAE/100 g DW	na	IC50 7.2 µg/mL	IC$_{50}$ 20.8 µg/mL	6
Asteraceae	*Chuquiraga jussieui* J.F.Gmel.	Infusion	Flower	13 mg GAE/g DW	1 mg/100 g DW	na	6 µmol TE/g DW	19
Compositae	*Bidens ferulifolia* (Jacq.) Sweet	na	Flower	na	na	na	85 % inhibition	20
Asparagaceae	*Agave americana* L.	Infusion and salad	Leaf	9.9 mg GAE/g DW	na	126.5 µmol TE/g DW	35.0 µmol TE/g DW	18

na: not available; GAE: gallic acid equivalent; TE: Trolox equivalent; AAE: Ascorbic acid equivalent; DW. dry weight;

Table 1. Content of phenolic compounds, carotenoids and antioxidant activity of some paramo flowers.

2

N°	Family	Species	Sampling location		Altitude (masl)	Image
1	Scrophulariaceae	*Buddleja incana* Ruiz & Pav	N0.0°7.0'3.4"	W78.0°14.0'58.8"	3997	
2	Compositae	*Diplostephium hartwegii* Hieron	N0.0°7.0'15.0"	W78.0°15.0'16.0"	4020	
3	Compositae	*Senecio formosoides* Cuatrec.	N0.0°7.0'4.6"	W78.0°15.0'58.8"	4014	
4	Asteraceae	*Pentacalia peruviana* (Pers.) Cuatrec.	N0.0°7.0'0.9"	W78.0°14.0'59.9"	4027	
5	Hypericaceae	*Hypericum laricifolium* Juss.	N0.0°5.0'2.8"	W78.0°13.0'59.1"	3598	
6	Gentianaceae	*Gentianella cerastioides* (Kunth) Fabris	N0.0°4.0'58.9"	W78.0°13.0'59.7"	3598	
7	Calceolariaceae	*Calceolaria colombiana* Pennell.	N0.0°4.0'59.2"	W78.0°13.0'59.9"	3610	
8	Compositae	*Hypochaeris radicata* L.*	N0.0°4.0'59.2"	W78.0°13.0'59.8"	3610	
9	Compositae	*Taraxacum campylodes* G.E. Haglund	N0.0°4.0'59.4"	W78.0°13.0'59.9"	3445	
10	Onagraceae	*Fuchsia vulcanica* André	S0.0°6.0'10.2"	W78.0°32.0'38.8"	3337	
11	Tropaeolaceae	*Tropaeolum majus* L.	S0.0° 21.0'43.2"	W78.0°32.0'51.0"	3200	
12	Asteraceae	*Hypochaeris robertia* (Sch.Bip.) Fiori	N0.0°7.0'15.0"	W78.0°15.0'15.0"	4020	
13	Compositae	*Ageratina pichinchensis* (Kunth) RMKing & H.Rob.	N0.0°4.0'59.5"	W78.0°13.0'59.7"	3598	
14	Lamiaceae	*Salvia carnea* Kunth	N0.0°4.0'58.9"	W78.0°13.0'59.9"	3598	
15	Loranthaceae	*Tristerix longebracteatus* (Desr.) Barlow & Wiens	N0.0°4.0'59.3"	W78.0°13.0'59.8"	3610	
16	Orobanchaceae	*Castilleja integrifolia* L.f.	N0.0°6.0'59.2"	W78.0°14.0'59.6"	4014	
17	Alstroemeriaceae	*Bomarea glaucescens* (Kunth) Baker	N0.0°4.0'59.2"	W78.0°13.0'59.9"	3610	
18	Asteraceae	*Werneria nubigena* Kunth	N0.0°5.0'22.0"	W78.0°14.0'41.0"	3550	
19	Oxalidaceae	*Oxalis lotoides* Kunth	S0.0°26.0'59.3"	W78.0° 36.0'59.7"	3165	
20	Alstroemeriaceae	*Bomarea multiflora* (L.f.) Mirb.	S0.0°26.0'59.2"	W78.0°36.0'59.5"	3106	
21	Micondaceae	*Miconia theaezans* (Bonpl.) Cogn	S0.0°21.0'58.9"	W78.0°22.0'59.5"	3207	
22	Micondaceae	*Miconia argentea* (Sw.) DC.	S0.0°17.0'59.5"	W78.0°27.0'59.6"	3246	
23	Rhamnaceae	*Duranta triacantha* Juss	S0.0°13.0'59.2"	W78.0°27.0'59.8"	3030	
24	Fabaceae	*Dalea coerulea* (L.f.) Schinz & Thell.	S0.0°17.0'59.5"	W78.0°27.0'59.6"	3246	
25	Fabaceae	*Lupinus microphyllus* Desr.	S0.0°22.0'46.7"	W78.0°33.0'6.2"	3031	
26	Xanthorrhoeaceae	*Hemerocallis citrina* Baroni	S0.0°22.0'46.7"	W78.0°33.0'6.2"	3031	
27	Asteraceae	*Chuquiraga jussieui* J.F.Gmel.	S0.0°22.0'46.7"	W78.0°33.0'6.2"	3031	
28	Compositae	*Bidens ferulifolia* (Jacq.) Sweet	S0.0°22.0'46.7"	W78.0°33.0'6.2"	3031	
29	Asparagaceae	*Agave americana* L.	N0.0°8.0'37.9"	W78.0°4.0'32.1"	3157	
30	Brugmdaceae	*Brugmansia x candida* Pers.	S0.0°27.0'4.6"	W78.0° 36.0'59.9"	3165	

Note: masl: meters above sea level: *. Is an unresolved name

Table 2. Family, species, sampling location, altitude and flower image in the studio.

Quantification of total phenolic compounds

About 10 mg of lyophilized samples were extracted with 500 µL of an 80 % methanol solution that had been acidified with 0.1% hydrochloric acid. The mixture was homogenized in a Vortex Mixer VM 300 (Interbiolab Inc., Florida), shaken in a Fisher Scientific FS60 ultrasonic bath (Fisher Scientific, USA) for 3 min, centrifuged at 1400 rpm for 5 min at 4 °C in a MiniSpin series microcentrifuge (Eppendorf, Germany), and the supernatant was collected The extraction procedure was carried out in triplicate[11,29]. The recovered supernatant was filtered through a 0.45 µm PVDF filter to quantify phenolic compounds. In a 96-well plate, 20 µL of the methanolic extract was mixed with 100 µL of a 1:4 Folin-Cioacalteu solution, shaken, and allowed to standard for 4 min. Then, 75 µL of a sodium carbonate solution (100 g/L) was added to the mixture and shaken for 1 min. After two hours at room temperature, absorbance was measured at 750 nm using a BioTek Symergy H1 microplate reader (Agilent, United States). In addition, a solution of gallic acid between 10 to 200 mg/L was employed as a calibration curve. The results were reported as mg of gallic acid equivalent / g of dry weight (DW)[30].

Determination of antioxidant activity by ABTS

Approximately 20 mg of lyophilized powder were weighed and combined with 400 µL of Pharmco HPLC-grade methanol (Greenfield Global, California) and 400 µL of distilled water. The mixture was homogenized in a vortex, shaken in an ultrasonic bath for 3 min, and the supernatant was separated by microcentrifugation at 14000 rpm for 5 min at 4 °C. The resulting solid was dissolved in 560 µL acetone and 240 µL distilled water. The procedure was repeated to recover the supernatant that had been combined with the previous supernatant. The resulting combination was refrigerated until it was quantified[30].

The ABTS•+ radical was prepared by mixing a 1:1 solution of 7 mM ABTS Sigma-Aldrich (Merck, Germany) with 2.45 mM potassium persulfate Sigma-Aldrich (Merck, Germany) and letting itstand for 16 hours in the dark. After that, the ABTS•+ radical solution was diluted with absolute ethanol by a factor of about 1 to 10, or until an absorbance of 0.7 at 754 nm was obtained. On the other hand, a stock solution of 2.5 nM Trolox Sigma-Aldrich (Merck, Germany) was used to prepare the calibration curve, which was diluted by 75, 50, 25, and 12.5 %. For sample quantification, 20 µL of ABTS•+ radical solutions were added to a 96-well VWR Tissue culture plate (Novachen, USA) together with 10 µL of the final or standard supernatant. The measurement was taken at 270 nm using a spectrophotometer with a Thermo Scientific Multiskan GO microplate reader (Agilent Scientific Instruments, California)[31,32]. Antioxidant activity was expressed as mmol trolox equivalent per gram dry weight (mmol TE/g PS).

Results and discussion

Physicochemical properties (weight, flower height, flower width, pH, soluble solids, total titratable acidity, ash, and humidity)

The weight (Figure 1-A), color (Figure 1-B), height (Figure 1-C) and width (Figure 1-D) of the flowers under study are shown in Figure 1. Thus, the weight of the flowers ranged from 0.01 (Ageratina pichinchensis) to 9.22 g (Brugmansia x candida). Thus, this study's weight of Tropaeolum

majus (0.61 g) was lower than the same species reported by other authors (0.72 g)[33]. In addition, as shown in Figure 1-B, most flowers are concentrated in the first quadrant with yellow to red colorations, followed by the fourth quadrant with violet to blue flowers.

The height of the flowers under study varied from 0.17 cm (Hypochaeris robertia) to 43.80 cm (Werneria nubigena), and the width from 0.14 cm (Miconia argentea) to 9.88 cm (Brugmansia x candida). Thus, the length and width of Buddleja globosa (2.00 and 1.24 cm, respectively), Diplostephium hartwegii (2.47 and 1.05 cm, respectively), Fuchsia vulcania (1.88 and 1.95 cm, respectively), and Agave americano (8.16 and 1.75 cm, respectively) showed comparable values with other studies, which presented values of 0.50 to 0.60 cm height and 0.30 to 0.40 cm width[34]; 1.40 to 1.50 cm height and 0.12 to 0.16 cm width[35]; 2.94 cm height and 0.50 cm width[36]; and 11 cm height and 6.00 cm width[37], respectively. In addition, the length of Brugmansia x candida (27.84 cm) in this study showed comparable results with other authors[38].

The pH (Figure 2-A), soluble solids (Figure 2-B), titratable acidity (Figure 2-C), ash (Figure 2-D), and humidity (Figure 2-E) of the flowers under study are shown in Figure 2. Thus, the pH varied from 2.20 (Oxalis lotoides and Miconia theazans) to 9.7 (Salvia carnea); the soluble solids ranged from 1.00 (Hypericum laricifolium and Gentianella cerastioides) to 21.5 °Brix (Tristerix longebracteatus), while the total titratable acidity expressed as percentage of citric acid varied from 0.10 (Salvia carnea) to 0.26 (Duranta triacantha). The values of soluble solids (6.30 °Brix), pH (4.3), and total titratable acidity (0.04 %) in this study for Tropaeolum majus were similar to those reported by other authors (7.53 °Brix, 4.97 of pH, and 0.32 % of total titratable acidity, respectively) 39. In addition, edible flowers such as Diplostephium hartwegii, Taraxacum campylodes, Fuchsia vulcanica, Tropaelum majus, Dalea coerulea, Hemerocallis citrina, Chuquiraga jussieui, and Agave amaricana showed pH values between 4.3 and 7, indicating that the petals of these flowers may be susceptible to attack by microorganisms, causing organoleptic alterations, as suggested by otrer authors[40].

In this study, the ranges for ash and moisture were 0.33 % (Brugmansia x candida) to 6.42 % (Castilleja integrifolia) and 42.24 % (Buddleja globosa) to 95.73 % (Bidens ferulifolia), respectively. As a result, the humidity of Fuchsia vulcania (81.26 %) was comparable to values reported by other authors[11]. In contrast, the values of ash and humidity of Troapaeolum majus (21.5 % and 91.81 %, respectively) were similar to other studies (0.63 % and 89.93 %, respectively)[41]. While the humidity of the Agave americana flowers in this study (61.73 %) was lower than that reported by other authors (86.62 %)[37]. In turn, the ash and moisture values (0.66 % and 93.3 %, respectively) of the Chuquiraga jussieui flowers in this study differed from those found by other authors (5.08 % and 9.77 %, respectively)[42]. In contrast, these values for Taraxacum campylodes (1.34 % and 69.31 %%, respectively) had a certain relationship with those reported by other authors (2.00 % and 5.9 %, respectively)[43].

Bioactive compounds and antioxidant activity quantification

Total carotenoids of the flowers under study are shown in Figure 3. Thus, the total carotenoids content ranged from 0.32 (Senecio formosoides) to 24.81 µg β-carotene/ g dried weight (DW) (Bidens ferulifolia). These results indicated that yellow and orange flowers, such as Bidens ferulifolia
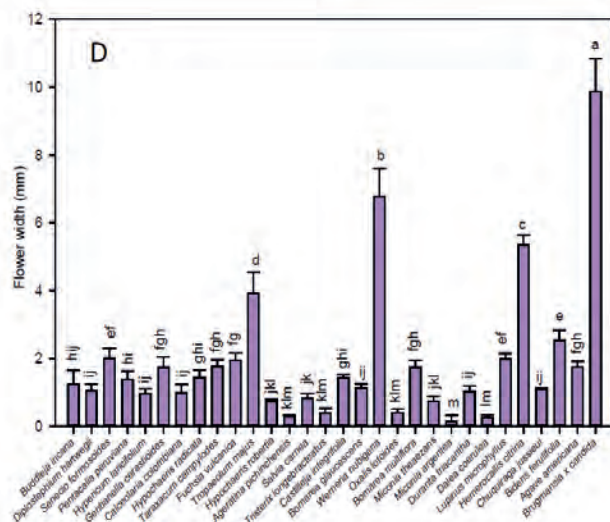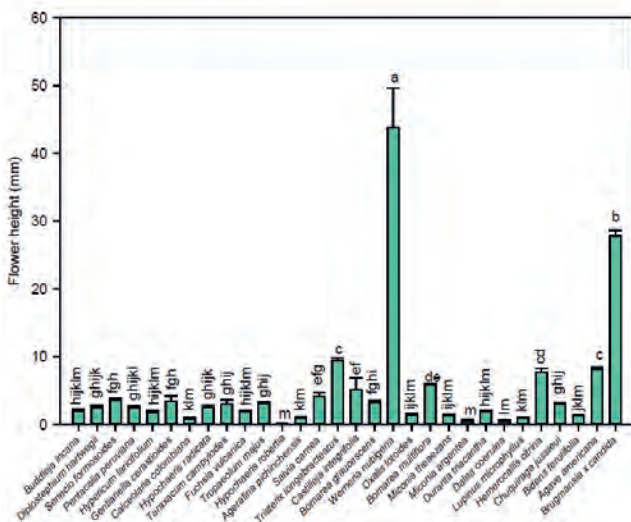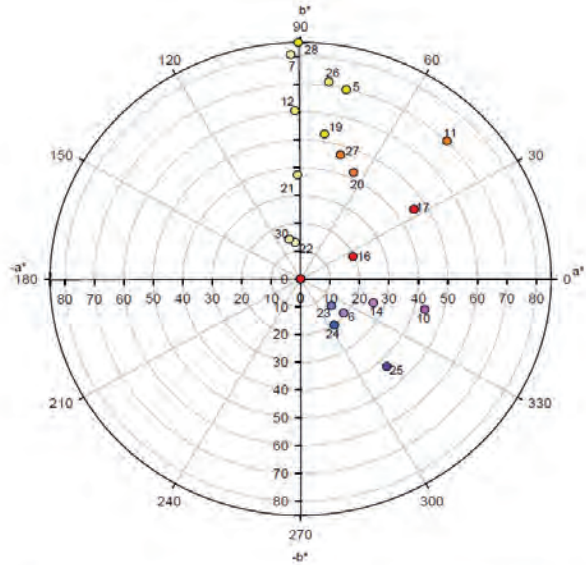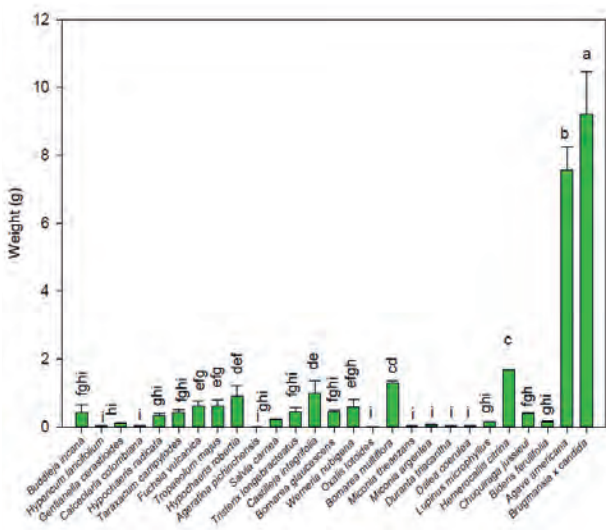
Figure 1. Average values of weight, color, height and width of the flowers under study.
Note: Vertical bars indicate the standard error. Different lowercase letters indicate homogeneous groups with Tukey, p < 0.05. *1, Buddleja incana; 2, Diplostephium hartwegii; 3, Senecio formosides; 4, Pentacalia peruviana; 5, Hypericum laricifolium; 6, Gentianella cerastioides; 7, Calceolaria colombiana; 8, Hypochaeris radicata; 9, Taraxacum campylodes; 10, Fuchsia vulcanica; 11, Tropaeolum majus; 12, Hypochaeris robertia; 13, Ageratina pichinchensis; 14, Salvia carnea; 15, Tristerix longebracteatus; 16, Castilleja integrifolia; 17, Bomarea glaucescens; 18, Werneria nubigena; 19, Oxalis lotoides; 20, Bomarea multiflora; 21, Miconia theaezans; 22, Miconia argentea; 23, Durantha triacantha; 24, Dalea coerulea; 25, Lupinus microphyllus; 26, Hemerocallis citrina; 27, Chuquiraga jussieui; 28, Bidens ferulifolia; 29, Agave americana; 30, Brugmansia x candida.*

(24,81 µg β-carotene/ g DW), *Hypericum laricifolium* (22,18 µg β-carotene/ g DW), *Oxalis lotoides* (21,66 µg β-carotene/ g DW), and *Buddleja globose* (15,74 µg β-carotene/ g DW) showed the highest concentrations of total carotenoids, a result that was also reported by other authors[11,44,45].

Total phenolics of the flowers under study are shown in Figure 4. Total phenolic compounds of the flowers under study varied from 72.13 (*Agave americana*) to 531.77 mg gallic acid equivalents (GAE)/g DW (*Fuchsia vulcania*). In this study, the highest phenolic compound concentrations were found in *Fuchsia vulcania* (531.77 mg GAE/g DW), *Lupinus microphyllus* (498.58 mg GAE/g DW), *Miconica theaezans* (469.27 mg GAE/g DW), *Gentianella cerastioides* (350.63 mg GAE/g DW), and *Senecio formosoides* (346.58 mg GAE/g DW). In contrast, *F. magellanica* in this study showed lower values than those reported by other authors (42.49 mg GAE/100 g DW)[11]. Despite using the same extraction metho-

dology, this difference may be due to the fact that this study sampled paramo species at altitudes higher than 3000 meters above sea level, whereas the comparison species were cultivated in four seasons and at sea level, conditions that modify the content of phenolic compounds[4].

Figure 5 depicts the antioxidant activity of the flowers under investigation. Thus varied from 43.13 trolox equivalent µmol / g DW (*Hypochaeris radicata*) to 182.08 trolox equivalent µmol / g DW (*Bomarea multiflora*). The highest antioxidant activity values were found in *Bomarea multiflora* (182.08 trolox equivalent µmol / g DW), *Miconia theaezans* (165.14 trolox equivalent µmol / g DW), *Bomarea glaucescens* (164.10 trolox equivalent µmol / g DW), and *Fuchsia vulcania* (161.08 trolox equivalent µmol / g DW). As a result, the inhibitory activity of *Hypochaeris radicata* in this study (26.39 % inhibition) was lower than the values reported by other authors (97.00 % inhibition)[46]. Several studies have

6
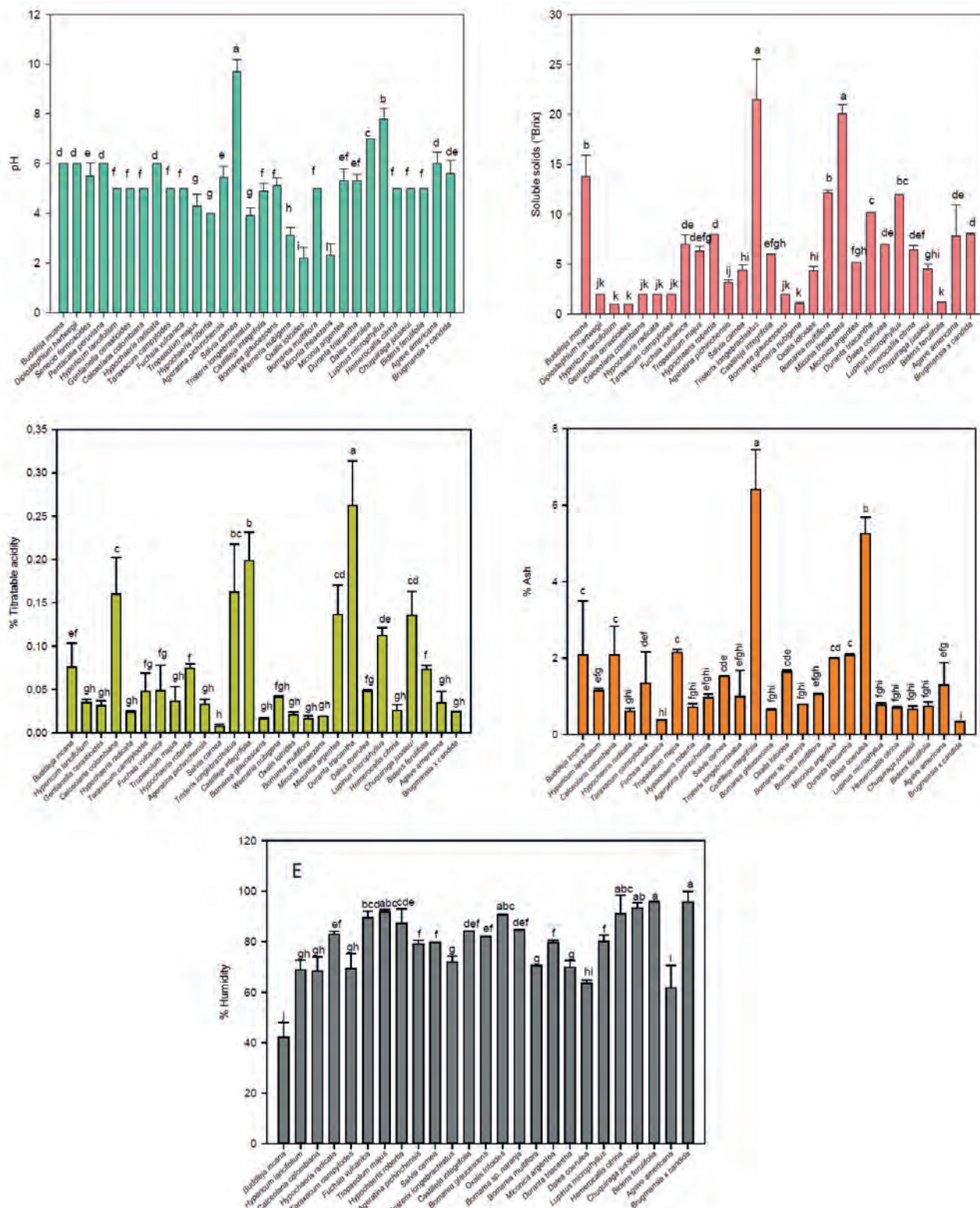
Figure 2. Average values of pH, soluble solids, titratable acidity, ash, and humidity of the flowers under study.Note: Vertical bars indicate the standard error. Different lowercase letters indicate homogeneous groups with Tukey, p < 0.05

shown that this variation could be attributable to the method used for quantification[47].

Conclusions

Ecuador, due to its great biodiversity, hosts a great variety of floral species with potential medicinal and nutritional properties. As a result, different species had high values of weight (9.22 g *Brugmansia x candida*), height (43.80 cm *Werneria nubigenea*), width (9.88 *Brugmansia x candida*), pH (9.7 *Salvia carnea*), soluble solids (21.5 °Brix *Tristerix longebracteatus*), titratable acidity (0.26 % *Ceanothus maritimus*), ash (6.42 % *Castilleja integrifolia*, moisture (95.73 % *Bidens ferulifolia*), total carotenoids (24.81 µg of β-carotene / g of DW *Bidens ferulifolia*), total phenolic compounds
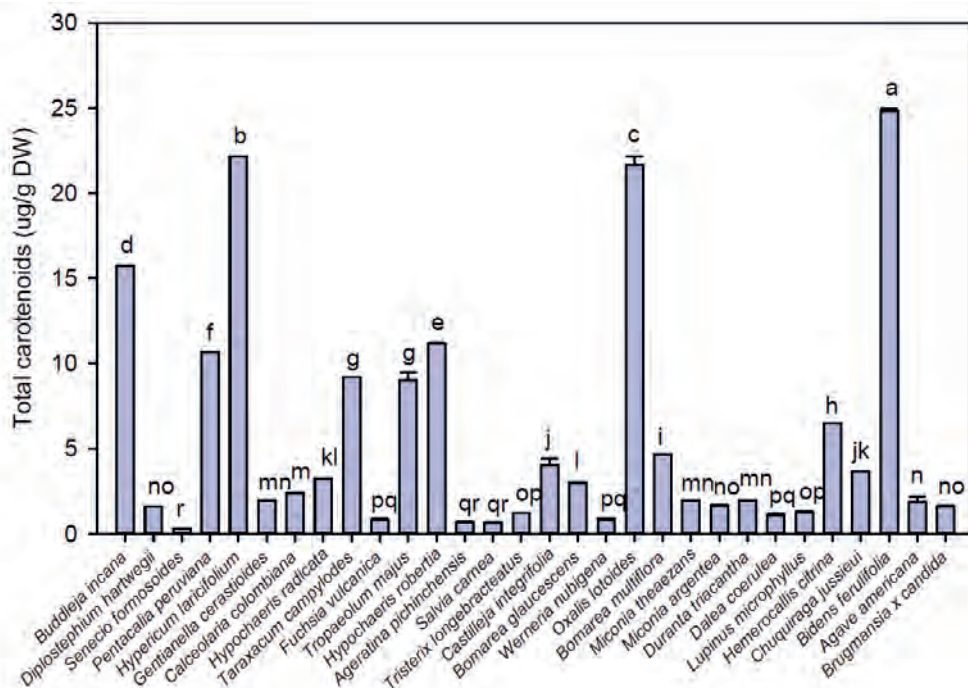
Figure 3. Average values of total carotenoids of the flowers under study
Note: Vertical bars indicate the standard error. Different lowercase letters indicate homogeneous groups with Tukey, p < 0.05.
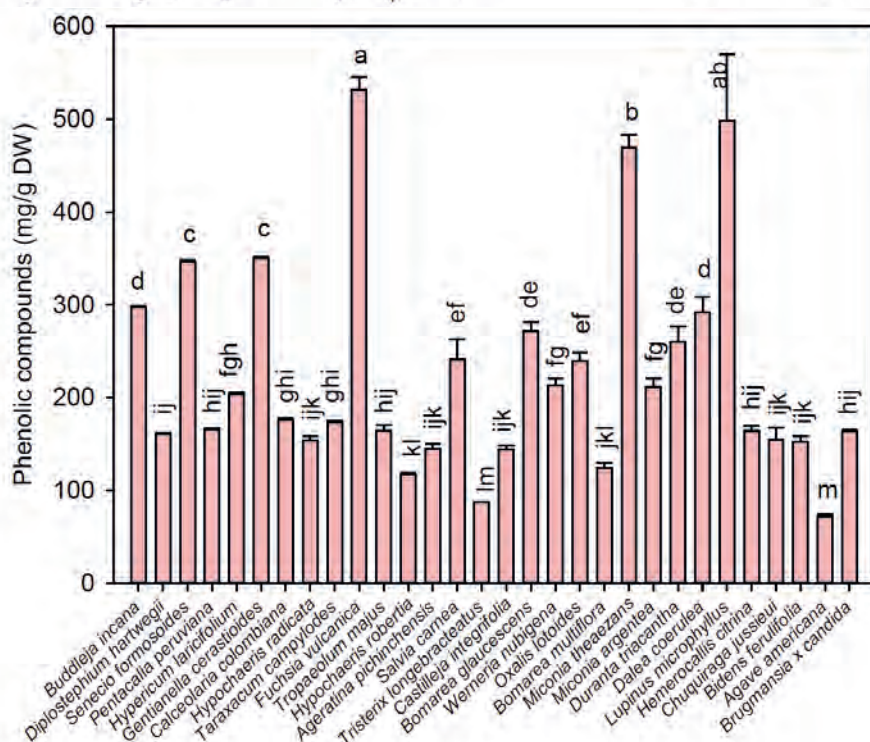
Figure 4. Average values of total phenolic compounds of the flowers under study
Note: Vertical bars indicate the standard error. Different lowercase letters indicate homogeneous groups with Tukey, p < 0.05.

(531.77 mg of GAE / g of DW *Fuchsia vulcania*), and antioxidant activity (182.08 µmol Eq trolox / g of DW *Bomarea multiflora*). Present results could contribute to the development of new products in the field of medicine, cosmetics and food.

Author Contributions

Formal analysis, Coyago Elena; investigation, Coyago Elena.; resources, Coyago Elena.;writing—original draft preparation, Aida Guachamin, Coyago Elena, Michael Villacís; writing—review and editing, Coyago Elena, Vera Edwin, Moya Melany, Jorge Heredia-Moya; project administration, Coyago Elena.; funding acquisition, Coyago Elena. All authors have read and agreed to the published version of the manuscript.

Funding

Conflicts of Interest

The authors declare no conflict of interest.

8
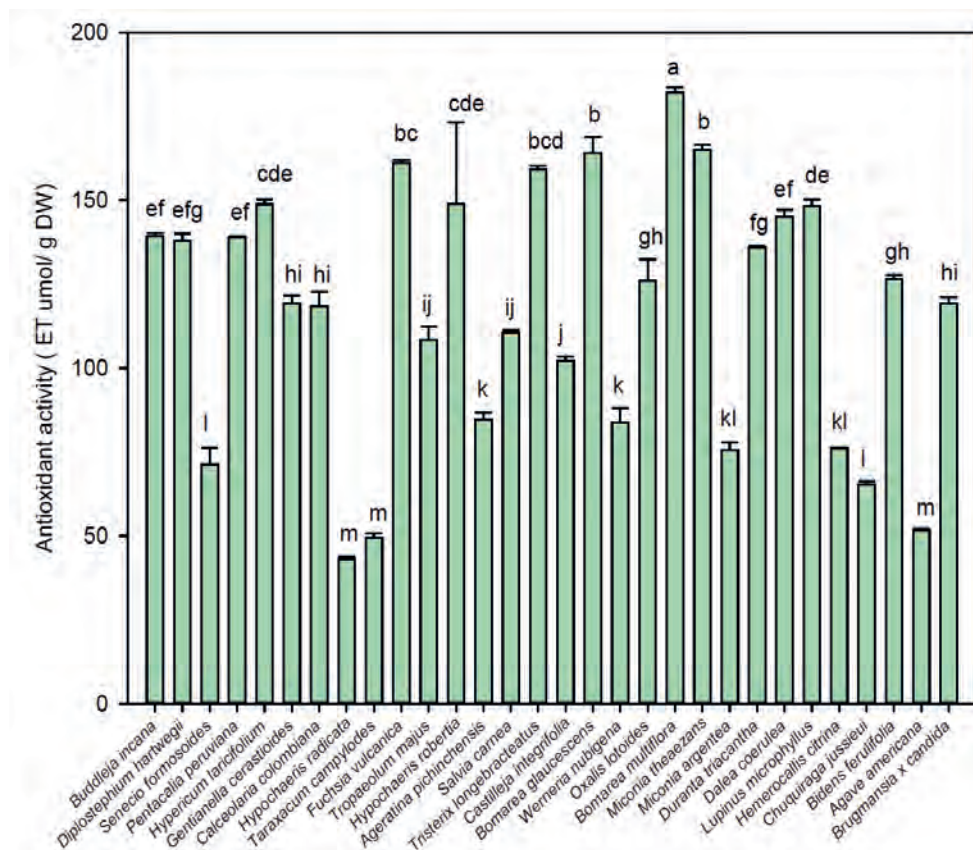
Figure 5. Average values of antioxidant activity of the flowers under study
Note: Vertical bars indicate the standard error. Different lowercase letters indicate homogeneous groups with Tukey, $p < 0.05$.

Bibliographic references

1. MAE. Sistema de clasificación de los ecosistemas del Ecuador continental. Subsecretaría de Patrimonio Natural https://www.ambiente.gob.ec/wp-content/uploads/downloads/2012/09/LEYENDA-ECOSISTEMAS_ECUADOR_2.pdf (2012).

2. Hofstede, R. Los páramos andinos ¿Qué sabemos? Estado de conocimiento sobre el impacto del cambio climático en el ecosistema páramo. Tiempos de Crisis sistémica (UICN, Quito, Ecuador, 2014). doi:10.2307/j.ctvpv50bh.8.

3. Rangel-Ch., J. R. Colombia diversidad biótica XVI Patrones de riqueza y de diversidad de las plantas con flores en el bioma de páramo. (Universidad Nacional de Colombia. Facultad de Ciencias, Instituto de Ciencias Naturales, 2018).

4. Coyago-Cruz, E., Corell, M. & Meléndez-Martínez, A. Estudio sobre el contenido en carotenoides y compuestos fenólicos de tomates y flores en el contexto de la alimentación funcional. (Punto Rojo Libros, S.L., 2017).

5. Venereo, J. Daño oxidativo, radicales libres y antioxidantes. Rev. Cuba. Med. Mil. 31, 126–159 (2002).

6. Wang, J. et al. Ethyl acetate fraction of Hemerocallis citrina Baroni decreases tert-butyl hydroperoxide-induced oxidative stress samage in BRL-3A cells. Oxid. Med. Cell. Longev. 2018, 1–13 (2018).

7. Rodriguez, O. & Torrenegra, R. Flavonoids, terpenes and the anti-Oxidant activity of Diplostephium phylicoides (HBK.) Wedd. Indian J. Sci. Technol. 11, 1–7 (2018).

8. Senguttuvan, J. & Subramanium, P. Micropropagation of medicinal herb, Hypochaeris radicata L. via indirect organogenesis. Res. Biotechnol. 5, 1–9 (2014).

9. Pădureţ, S., Amariei, S., Gutt, G. & Piscuc, B. The evaluation of dandelion (Taraxacum officinale) properties as a valuable food ingredient. Rom. Biotechnol. Lett. 21, 11569–11575 (2016).

10. Kucekova, Z., Mlcek, J., Humpolicek, P. & Rop, O. Edible flowers - antioxidant activity and impact on cell viability. Cent. Eur. J. Biol. 8, 1023–1031 (2013).

11. Meléndez-Martínez, A. et al. Screening for innovative sources of carotenoids and phenolic antioxidants among flowers. Foods 10, 1–23 (2021).

12. Garzón, G. A. & Wrolstad, R. E. Major anthocyanins and antioxidant activity of Nasturtium flowers (Tropaeolum majus). Food Chem. 114, 44–49 (2009).

13. Ulloa, C., Álvarez, S., Jørgensen, P. & Minga, D. Guía de 100 Plantas silvestres del páramo del Parque Nacional Cajas. Guia de 100 plantas silvestres del paramodel Parque Nacional de Cajas (Ministerio del Ambiente, 2008).

14. Mejía-Giraldo, J., Henao-Zuluaga, K., Gallardo, C., Atehortúa, L. & Puertas-Mejía, M. Novel in vitro antioxidant and photoprotection capacity of plants from high altitude ecosystems of Colombia. Photochem. Photobiol. 92, 150–157 (2016).

15. Purohit, S., Rana, S., Idrishi, R., Sharma, V. & Ghosh, P. A review on nutritional, bioactive, toxicological properties and preservation of edible flowers. Futur. Foods 4, 1–14 (2021).

16. Gonçalves, J., Oliveira, G. & Almeida, L. Compostos bioativos em flores comestíveis. Biológicas & Saúde 9, 11–20 (2019).

17. De la Cruz, M. A. et al. Compuesto fenólicos y actividad antioxidante de extractos hidroalcohólicos provenientes de la flores de Dalea Coerulea (L.F.) Schinz & Thell. in VII Congreso latinoamericano de plantas medicinales 'Plutarco Naranjo' 207 (2019).

18. Chirinos, R., Pedreschi, R., Rogez, H., Larondelle, Y. & Campos, D. Phenolic compound contents and antioxidant activity in plants with nutritional and/or medicinal properties from the Peruvian Andean region. Ind. Crops Prod. 47, 145–152 (2013).

19. Guerrero Bonilla, D. et al. Bioactive compounds and antioxidant capacity of Chuquiraga jussieui J.F.Gmel from the highlands of Ecuador. Nat. Prod. Res. 34, 2652–2655 (2019).

20. Shymanska, O., Vergun, O., Fishchenko, V. & Rakhmetov, D. Antioxidant potential of some Asteraceae Bercht. & J. Presl. representatives. Agrobiodiversity Improv. Nutr. Heal. Life Qual. 70–77 (2020) doi:10.15414/agrobiodiversity.2020.2585-8246.070-77.

21. FAO. Texto concertado del proyecto de código internacional de conducta para la recolección y transferencia de germoplasma vegetal. (1993).

22. Guarino, L., Ramanatha Rao, V. & Goldberg, E. Collecting plant genetic diversity: technical guidelines. 2011 update. (2011).

23. US-ISO-2173:2003. Fruit and vegetable products. Determination of soluble solids. Refractometric method. Int. Organ. Stand. 1, 17 (2009).

24. US-ISO750:1998. Fruit and vegetable products — Determination of titratable acidity. Int. Organ. Stand. 1, 4 (2009).

25. ISO1842:1991. Fruits, vegetables and derived products-Sampling and methods of test. Part 5: Determination of pH. East African Stand. 5, (2000).

26. Garcia-Mogollon, C., Alvis-Bermudez, A. & Dussán-Sarria, S. Validación del método de microondas para determinar humedad en ñame espino (Dioscorea Rotundata Poir). Inf. Tecnol. 28, 87–94 (2017).

27. INEN1953. Gelatina pura comestible. Determinación de la pérdida por calentamiento. Instituto Ecuatoriano De Normalización vol. 1 4 (2012).

28. ISO-5520. Fruits, vegetables and derived products - Determination of alkalinity of total ash and of water-soluble ash. Int. Stand. ISO 1, 13 (1981).

29. Periago, M. J., Martínez-Valverde, I., Chesson, A. & Provan, G. Phenolic compounds, lycopene and antioxidant activity in commercial varieties of tomato (Lycopersicum esculentum). J. Sci. Food Agric. 82, 323–330 (2002).

30. Bobo-García, G., Davidov-Pardo, G., Arroqui, C. & Marín-Arroyo, M. Intra-laboratory validation of microplate methods for total phenolic content and antioxidant activity on polyphenolic extracts, and comparison with conventional spectrophotometric methods. SCI 46, 29–33 (2014).

31. Kuskoski, E. M., Asuero, A. G., Troncoso, A. M., Mancini-Filho, J. & Fett, R. Aplicación de diversos métodos químicos para determinar actividad antioxidante en pulpa de frutos. Food Sci. Technol. 25, 726–732 (2005).

32. Rivero-Pérez, M. D., Muñiz, P. & González-Sanjosé, M. L. Antioxidant profile of red wines evaluated by total antioxidant capacity, scavenger activity, and biomarkers of oxidative stress methodologies. J. Agric. Food Chem. 55, 5476–5483 (2007).

33. Nunes, E. et al. Determinação do ponto de colheita de flores de Tropaeolum majus L. Rev. Bras. Agropecuária Sustentável 8, 37–43 (2018).

34. Navas, L. Flora de la cuenca de Santiago de Chile, Tomo III. (Ediciones de la Universidad de Chile, 1979).

35. Bohorquez, R. Determinación de actividad antioxidante de extractos de hojas de Diplostephium phylicoides (Kunth) Wedd. (Universidad de Ciencias Aplicadas y Ambietales, 2016).

36. Smith-Ramirez, C. Los picaflores y su recurso floral en el bosque templado de la isla de Chiloé, Chile. Rev. Chil. Hist. Nat. 66, 65–13 (1993).

37. Semuli, M. Nutritional composition, descriptive sensory analysis and consumer acceptability of products developed from Agave americana flowers. (University of the Free State, 2014).

38. Álvarez, L. Borrachero , cacao sabanero o floripondio (Brugmansia Spp .) un grupo de plantas por redescubrir en la biodiversidad latinoamericana. Cult. y Drog. 13, 77–93 (2008).

39. Cardoso, I., Botrel, N., De-Barros, E., Madeira, N. & De-Castro, R. Caracterização de flores da capuchinha (Tropaeolum majus L.) armazenadas em diferentes temperaturas. in XI Brazilian Meeting on Chemistry of Food and Beverages V Simpósio de Engenharia e Ciência de Alimentos, Brasil 1–6 (2016).

40. Vásquez, G. La Contaminación de los alimentos, un problema por resolver. Rev. Salud Uis 35, 48–57 (2003).

41. Navarro-González, I., González-Barrio, R., García-Valverde, V., Bautista-Ortín, A. B. & Periago, M. J. Nutritional composition and antioxidant capacity in edible flowers: Characterisation of phenolic compounds by HPLC-DAD-ESI/MSn. Int. J. Mol. Sci. 16, 805–822 (2015).

42. Palma, M. & Tamayo, E. Caracterización de la chuquiragua (Chuquiraga jussieui) con perspectivas agroindustriales. (Universidad de las Américas, 2019).

43. Palate, K. Estudio de la composición nutricional de flores comestibles Diente de león (Taraxacum officiale), Tronadora (Tecoma stans), Mastuerzo (Tropaeolum majus), Girasol (Helianthus annuus) para potenciar su consumo. (Universidad Técnica de Ambato, 2021).

44. Coyago-Cruz, E. Estudio sobre el contenido en carotenoides y compuestos fenólicos de tomates y flores en el contexto de la alimentación funcional. (Universidad de Sevilla, Departamento de Ciencias Agroforestales, 2017).

45. Lu, C. et al. Flower color classification and correlation between color space values with pigments in potted multiflora chrysanthemum. Sci. Hortic. (Amsterdam). 283, 110082 (2021).

46. Ko, H., Eom, T., Song, S., Jo, G. & Kim, J. Tyrosinase and α-glucosidase inhibitory activities and antioxidant effects of extracts from different parts of Hypochaeris radicata. Korean J. Med. Crop Sci. 25, 139–145 (2017).

47. Takahashi, J., Guilherme, F., Fidelis, M., Borges, L. & Sande, D. Edible flowers: bioactive profile and its potential to be used in food development. Food Res. Int. 129, 108868 (2020).

9

ARTICLE / INVESTIGACIÓN

Identificación de hongos filamentosos asociados al suelo del bosque protegido de Prosperina
Identification of filamentous fungi associated with the soil of the Prosperina Protected forest

Carreño-Bulgarin Gladys Paola[2], Quijije-Franco Genny[2], Diaz Byron[1], Maridueña-Zavala Maria Gabriela[1] and Cevallos-Cevallos Juan Manuel[1,2]*

DOI. 10.21931/RB/2023.08.01.22

[1] Escuela Superior Politécnica del Litoral, ESPOL, Centro de Investigaciones Biotecnológicas del Ecuador, CIBE, Guayaquil, Ecuador.
[2] Escuela Superior Politécnica del Litoral, ESPOL, Facultad de Ciencias de la Vida, FCV, Guayaquil, Ecuador.
Corresponding author: jmceva@espol.edu.ec

1

Resumen: El Bosque de Prosperina es un área protegida ubicada en la ciudad de Guayaquil-Ecuador donde existe una gran diversidad de plantas, animales y, últimamente, microorganismos que contribuyen a su conservación y mantenimiento. Las muestras de suelo recogidas en las estaciones de Cuevas, Cañas y FCV durante la estación seca se analizaron mediante métodos microbiológicos convencionales. Como resultado, se identificaron 38 especies, y en cada estación se obtuvieron 16, 16 y 16, respectivamente. Los géneros más frecuentes encontrados en las tres estaciones son Aspergillus, Penicillium, Trichoderma y Absidia, con menor frecuencia Fusarium, Cladosporium, Talaromyces, Cur-vularia, Humicola, Gongronella, Clonostachys y Mariannea. Se crioconservaron 38 cepas de hongos filamentosos en la Colección de Cultivos de microorganismos del CIBE (CCM-CIBE), de las cuales 36 eran especies únicas. Los resultados obtenidos sugieren que las especies encontradas. Su desplazamiento puede verse afectado por factores naturales y humanos. Además, confirmamos microorganismos biocontroladores como Purpureocillium, un nematófago y Cladosporium que, pueden tener un alto potencial en actividades de biorremediación de im-portancia para la agricultura y recuperación de suelos, lo que corrobora que el Bosque de Protección es una rica fuente de microorganismos con una gran reputación para su conservación.

Palabras clave: Bosque Protector, microdiversidad del suelo, biocontrol, conservación.

Abstract: The Prosperina Forest is a protected area located in the city of Guayaquil-Ecuador where there is a great diversity of plants, animals and, lately, microorganisms that contribute to its conservation and maintenance. Soil samples collected at the Cuevas, Cañas and FCV stations during the dry season were analyzed by conventional microbiology methods. As a result, 38 species were identified in each station 16, 16 and 16 were obtained, respectively. The most frequent genera found in the three stations are Aspergillus, Penicillium, Trichoderma and Absidia, with less frequency Fusarium, Cladosporium, Talaromyces, Curvularia, Humicola, Gongronella, Clonostachys and Mariannea. Thirty-eight strains of filamentous fungi were cryopreserved in the CIBE Culture Collection of microorganisms (CCM-CIBE), of which 36 were unique species. The results obtained suggest that the species found. Their displacement can be affected by natural and human factors. In addition, we confirm biocontrol microorganism as Purpureocillium, a nematophagous and Cladosporium that, may have a high potential in bioremediation activities of importance for agriculture and soil recovery, which corroborates that the Protected Forest is a rich source of microorganisms with a great reputation for its conservation.

Key words: Protected forest, soil microdiversity, biocontrol, conservation

Introducción

El Bosque protector "Prosperina" (BPP) categorizado como Área de bosque y vegetación protegida desde el 29 de junio de 1994, mediante acuerdo Ministerial N°23 publicada en el registro oficial No. 472, Acuerdo Ministerial No. 144 del Ministerio del Ambiente se encuentra ubicado al oeste del Ecuador en el Campus "Gustavo Galindo" de la Escuela Superior Politécnica del Litoral en la ciudad de Guayaquil, provincia del Guayas y es considerado una zona de reserva que alberga diversas especies de fauna y flora sujeta a investigación por parte de la comunidad científica[1]. El BPP se encuentra rodeada por 5 cuencas hidrográficas y forma parte de la cordillera Chongón Colonche[2]. Además,

estos ecosistemas presentan un clima cálido, con temperaturas que oscilan entre 23 – 27 ºC, lo que coloca al BPP en la categoría de Bosque Seco Tropical, según el criterio de la propuesta preliminar de un sistema de clasificación de vegetación para el Ecuador continental de 1999[3].

Esto significa que el BPP es un área estratégica para la conservación de la biodiversidad biológica ya que poseen árboles nativos caducifolios dadas las dos temporadas seca y lluviosa en la región[4], el BPP realiza programas de protección y concienciación en la conservación de las especies, además busca la valoración de los recursos ambientales mediante visitas y difusión de las principales especies de

Publisher's Note: Bionatura stays neutral with regard to jurisdictional claims in published maps and institutional affiliations.

2

flora y fauna que habitan en el bosque seco. Cerca de sus 332,3 has de bosques en un clima seco tropical favorece el crecimiento de microbiota de suelo rica en consorcios de hongos, como micorrízicos, ectomicorrízicos, micorrízicos arbusculares, patógenos, bacterias y levaduras[5].

El potencial microbiano del BPP puede ser aprovechado para el desarrollo de productos a bases de micotoxinas que pueden actuar como biocontroladores de fitopatógenos en alimentos, también contribuyen en la regeneración de suelos maltratados en la que necesitan incorporarse microorganismos presentes en la materia orgánica de bosques a través de la elaboración de compost[6,7]. Adicionalmente, los hongos filamentosos pueden ser empleados en la biotecnología fúngica porque permiten fomentar la economía circular, mitigar el cambio climático y generar la producción sostenible de alimentos, combustibles, textiles, fármacos, entre otros[8].

Dentro de la microdiversidad que se encuentran en los suelos de bosque podemos encontrar los filo Ascomycota y Basidiomycota, los cuales predominan a escala mundial en los ecosistemas forestales gracias a las condiciones climáticas que permiten su crecimiento[9], tal es así como en el agroecosistema K'iphak'iphani en Bolivia predominan de la división Ascomycota los géneros *Penicillium, Alternaria, Rhizopus, Mucor, Fusarium* y *Trichoderma*[10] algunos con potencial de biorremediación debido a su eficiencia en la degradación de hidrocarburos de petróleo[11].

Según reportes, en el Ecuador entre los géneros de hongos filamentosos representativos de suelos de zonas forestales se encuentran *Aspergillus, Penicillium* y *Trichoderma* los cuales variaban según el tipo de suelo[12]. Así también en el Bosque Protector Aguarongo, se han encontrado los hongos de los Géneros *Aspergillus, Trichoderma* y *Fusarium*[13]. En la región costa se han realizado estudios sobre la diversidad de hongos micorrízicos arbusculares asociados a plantas de cacao que dependen de estos microorganismos para realizar procesos fisiológicos y desarrollar resiliencia al cambio global[14]. No obstante, en el Bosque Protector La Prosperina son pocos los estudios que se han realizado en plantas, pero no contemplan estudios de biodiversidad de hongos filamentosos por lo que es muy importante explorar la biodiversidad microbiana de nuestros bosques que nos ayude a desarrollar técnicas de control microbianas para el control de patógenos en el campo. En función a ello, surge la necesidad de determinar la biodiversidad de hongos filamentosos asociados al suelo del Bosque Protector la Prosperina a través de métodos moleculares y posterior conservación de los mismos.

Materiales y métodos

Zonas de muestreo

Para el muestreo fueron identificadas tres estaciones en la superficie del Bosque Protector La Prosperina: E1) Albarrada Cuevas; E2) Albarrada Cuevas y E3) zona cercana a la Facultad de Ciencias de la Vida en la ESPOL (FCV).

La Estación 1 correspondiente a la "Albarrada Cuevas" se encuentra ubicada a 127 msnm en el núcleo 1 del BPP, específicamente en las coordenadas 2°9'23''S y 79°57'47''W. Posee una alta densidad de especies vegetales herbáceas, especies arbóreas caducifolias que desarrollan hojas al empezar la temporada lluviosa.

La estación 2 correspondiente a la "Albarrada Ca-

ñas" que se ubica en el núcleo 1 del BPP a una altitud de 211msnm y sus coordenadas son 2°9'26''S y 79°57'56''W. Posee una alta densidad de plantas pteridofitas y gramíneas que permanecen con hojas durante todo su ciclo de vida. Dentro de la zona se registró la presencia de anfibios (Epipedobates machalilla) y mamíferos como el oso hormiguero Tamandua tetradactyla.

La estación 3 corresponde a la FCV y se ubica en la zona de protección permanente del BPP, cerca de la Facultad de Ciencias de la Vida (FCV) de la Escuela Superior Politécnica del Litoral (ESPOL). Se encuentra a una altitud de 80 msnm específicamente en las coordenadas 2°9'10''S y 79°56'23''W. El suelo es más compacto que en las otras estaciones y en sus alrededores se encuentra una alta densidad de especies arbóreas y se registra la presencia de diversos grupos de aves y murciélagos.

Recolección de muestras

La recolección de muestras se realizó a una profundidad a 25 cm siguiendo metodología consultada[15], en el que se empleó extractor de núcleos para suelos. En cada estación (E1; E2; E3) se recolectaron 3 réplicas (R1; R2; R3) con equidistancia de 5 metros. Se pesaron 100 g de suelo por réplica y se almacenaron en bolsas plásticas con cierre hermético, previamente esterilizadas con radiación UV, seguido las muestras fueron trasladadas en una nevera portátil el mismo día para su siembra en el laboratorio de Fitopatología del CIBE.

Aislamiento de hongos filamentosos

Para el aislamiento de los hongos se realizaron diluciones seriadas, en las que 10g de suelo por réplica se disolvieron en 90 ml de agua peptonada estéril (10⁻¹), se homogenizó la solución y se dejó reposar durante 5 minutos para que los sólidos decantaran. Seguido a esto, se dispensó una alícuota de 1 ml de la solución de suelo en un tubo Falcón que contenía 9 ml de agua peptonada, se agitó usando el vortex y se continuó con el mismo procedimiento hasta conseguir una dilución de 10⁻⁴. Luego, 2 réplicas por muestras fueron sembradas usando el método de esparcido, en la que 1 ml de cada solución fue esparcido con la ayuda de un asa de Drigalsky en caja petri que contenía medio Agar Papa Dextrosa (PDA), preparado con cloranfenicol (400 ppm). Las muestras fueron incubadas a 25 °C por 7 días y revisadas cada 24 horas para el control de crecimiento y conteo utilizando un estereoscopio BOECO modelo BTB-A. Seguido, las cepas fueron purificadas, trasladando los micelios que estaban creciendo en cajas con medio PDA y cloranfenicol. Una vez que las cepas estaban puras se procedió a la obtención de cultivos monospóricos siguiendo los protocolos previamente reportados[16]. Brevemente, se realizó una solución de esporas en 2 ml de agua estéril, lugo se dispensaron 10 µl de la solución en cajas con medio PDA y se incubó hasta que se observó crecimiento micelial. Luego, con ayuda del bisturí se cortaron secciones de medio donde se encontraban secciones de hifas puras para luego trasladarlas a un nuevo medio y esperar el crecimiento final de micelio para extracción de ADN.

Extracción y amplificación de muestras de ADN

Los cultivos monospóricos fueron utilizados para la extracción de DNA siguiendo el protocolo de extracción de hongos filamentosos reportado en previos estudios[17]. Brevemente, los que a una pequeña porción de micelio se le agregaron 30 µl de NaOH 0,5 M. Luego, se trituró el mi-

Identificación de hongos filamentosos asociados al suelo del bosque protegido de Prosperina
Identification of filamentous fungi associated with the soil of the Prosperina Protected forest

3

celio y se dejó reposar durante 10 minutos. A continuación, a cada tubo se agregaron 150 µl de una solución Tris HCL 100 mM + EDTA 0.5 M, con un pH de 8, seguido de un choque térmico a 95 °C durante 10 minutos. Finalmente, las muestras se centrifugaron durante 5 min a 15000 rpm. Para la amplificación de la región ITS (Internal transcribed spacer) y LSU (Large Subunit) se utilizaron los cebadore ITS1-F (5'CTTGGTCATTTAGAGGAAGTAA3') e ITS4 (5'TCCTCCGCTTATTGATATGC3'), mientras que para LSU se emplearon: LROR (5'ACCCGCTGAACTTAAGC3') y LR5 (5'TCCTGAGGGAAACTTCG3')[18]. Las reacciones de PCR se realizaron con un volumen final de 32 µl compuesto por: 12,72 µl de H2O ultrapura, 16µl de 1X Taq polimerasa, 0,64 µl de cada cebador 0,2 µM y 2 µl de ADN. Las condiciones de amplificación consistieron en una desnaturalización a 95°C durante 10 min, seguido de 35 ciclos de 1 min a 94°C, 2 min a 63 °C y 2 min a 72°C, en base al protocolo[19]. Los amplicones obtenidos fueron separados por electroforesis en gel de agarosa al 2% que se tiñó con SYBR- Safe DNA gel stain. El tamaño de los fragmentos fue verificado por comparación con el marcador de peso molecular correspondiente a 1000 pares de bases. Las condiciones en las que se corrió el gel fueron a 150 V durante 40 minutos. Posteriormente el gel se observó con la ayuda de un transiluminador (trans-UV y epi-white) con Image Lab™ Software, BIO-RAD. Finalmente se cuantificaron los productos de PCR en el NanoDrop 2000c y se enviaron a Macrogen para la secuenciación de las muestras.

Identificación de especies

Para la limpieza de las secuencias se eliminaron los nucleótidos de baja calidad de los extremos de cada secuencia aplicando el software Geneious[20]. Adicionalmente, se descartaron aquellas secuencias con menos de 400 pb. Se realizó la comparación de las secuencias de ADN procesadas con la base de datos de GenBank, mediante Blastn y Blastx (http://www.ncbi.nlm. nih.gov/BLAST). Empleando Geneious, para cada secuencia se obtuvieron los primeros 10 hits considerando que exista un porcentaje de identidad mayor al 98% de acuerdo a lo estipulado para el análisis de unidades taxonómicas operativas empleando las regiones ITS y LSU[21]. Posteriormente, se realizó la selección de secuencias considerando el porcentaje de identidad, el número de gaps, el E-value, la longitud de la secuencia, entre otros. Con el listado de secuencias seleccionadas, se elaboró un listado de las especies identificadas con su respectivo código de acceso a la base de datos de GenBank, paso seguido usando el método Maximun Likelihood se diseñaron arboles filogenéticos para identificar la relación evolutiva entre las especies asociadas al suelo del BPP utilizando el software Mega X[22].

Crioconservación de especies

Para la preservación de los microorganismos obtenidos se siguió el protocolo de conservación empleado en la Colección de Cultivos Microbianos del CIBE[23]. Los procedimientos para el depósito de cepas en la Colección fueron en base a los protocolos internos del Plan de Manejo de microorganismos de la colección. Para garantizar una buena conservación del microorganismo se emplearon cajas Petri con medios PDA con antibiótico en la que el microorganismo se encontraba joven, pero con cuerpos fructíferos de ser el caso, en caso de que el microorganismo solo presentara micelio se debe esperar que esté al menos con un 80% de crecimiento en placa Petri. Una vez alcanzado el tiempo

de crecimiento se realiza la conservación manteniendo 5 tubos criogénicos con medio PDB (Potato dextrosa Broth) y Glicerol para el método de crioconservación, 3 tubos de borosilicato con tapa con medio PDA para el método de aceite mineral y 3 tubos criogénicos con agua para la conservación en agua.

Resultados y discusión

Identificacion de hongos del BPP

En total se obtuvieron 64 aislados de las tres estaciones recolectadas, de la cuales se contabilizaron un total de 38 especies únicas de hongos filamentosos asociados al suelo del BPP. En la estación Cuevas se encontraron 20 aislados, en la Tabla 1 se puede apreciar el listado de cepas identificadas de la estación Cuevas mediante técnicas moleculares con sus respectivos porcentajes de identidad y códigos de acceso para cada cepa. Además, se puede observar los rasgos morfológicos de las cepas en la Figura 1, en esta área predomina el género Aspergillus, seguido de Penicillium.

En la estación Cañas se identificaron 26 cepas, en la Tabla 2 se observa el listado de las cepas identificadas de esta estación por técnicas moleculares junto con su porcentaje de identidad se puede observar también que por la frecuencia de aparición predomina el género Trichoderma, seguido de Penicillium. En la Figura 2 se puede apreciar la morfología de cada cepa identificada.

Finalmente, la estación FCV presentó un total de 18 cepas en total, en la Tabla 3 se puede apreciar el listado de los hongos identificados en esta estación junto con su porcentaje de identidad y en la Figura 3 se observa las características morfológicas de los hongos. De acuerdo con la información obtenida se puede determinar que los géneros que más predominan en esta zona son *Penicillium* y *Aspergillus*.

Con la información de los datos de frecuencias obtenidas de los hongos en cada sitio de recolección se realizó un análisis de los géneros únicos identificados con su respectiva frecuencia por estación. Los principales géneros fueron *Penicillium, Aspergillus* y *Trichoderma* en el BPP. En la Figura 4 se puede observar la frecuencia de aparición por cada género encontrado, es así que para la Estación Cuevas se encontró una mayor abundancia de *Aspergillus, Penicillium, Trichoderma* y *Talaromyces* mientras que otros géneros con menor frecuencia fueron *Absidia, Cladosporium, Curvularia, Gongronella* y *Humicola*. Por otra parte, en la Estación Cañas además de *Trichoderma, Aspergillus* y *Penicillium* se presentaron especies de *Talaromyces, Absidia, Fusarium, Purpureocillium, Curvularia, Clonostachys* y *Mariannaea* con menor frecuencia. Por último, la Estación FCV estuvo dominada por *Penicillium, Aspergillus* y *Fusarium*, y en menor proporción se encontraron especies de *Trichoderma, Absidia, Purpureocillium, Cladosporium* y *Cunninghamella*.

Según lo que se observa las tres estaciones varían muy poco en la clasificación de géneros encontrados, gracias a su cosmopolita distribución y siendo que están en una posición geográfica muy cercana, la poca variación observada en su micro diversidad puede sugerirse que es debido a características del suelo, factores ambientales, la presencia de agua o factores humanos[24], lo que hace que muchos de ellos presenten características dominantes a estos factores

4

Código	Porcentaje de identidad	Código de acceso	Organismo
PITS_A01	99.1%	MH472977	*Aspergillus flavipes*
PLSU_B01	100.0%	OL772705.1	*Aspergillus neoflavipes*
PLSU_D01	99.82%	HQ646592.1	*Penicillium guttulosum*
PITS_E01	99.8%	MK690419	*Curvularia lunata*
PLSU_F01	100.0%	NG_070046.1	*Aspergillus keveii*
PLSU_H01	100.0%	NG_069830.1	*Trichoderma spirale*
PLSU_A02	98.95%	MH870507.1	*Gongronella butleri*
PITS_B02	99.8%	MW757343	*Aspergillus brasiliensis*
PLSU_C02	100.0%	OL772705.1	*Aspergillus neoflavipes*
PLSU_E02	99.8%	NG_069001.1	*Penicillium limosum*
PLSU_F02	100.0%	OL897074	*Talaromyces liani*
PLSU_G02	99.64%	NG_070044.1	*Cladosporium crousii*
PLSU_H02	99.82%	OL711683.1	*Aspergillus pseudonomiae*
PLSU_A03	99.4%	MW671548	*Absidia sp.*
PLSU_B03	99.63%	NG_069973.1	*Trichoderma amazonicum*
PLSU_D03	99.42%	NG_069001.1	*Penicillium limosum*
PITS_E03	100.0%	MT074667	*Talaromyces flavus*
PLSU_F03	99.8%	NG_069001.1	*Penicillium limosum*
PLSU_G03	99.8%	NG_069001.1	*Penicillium limosum*
PITS_C04	99.19%	LT993581.1	*Humicola fuscogrisea*

Tabla 1. Especies identificadas en la Estación Cuevas (E1).
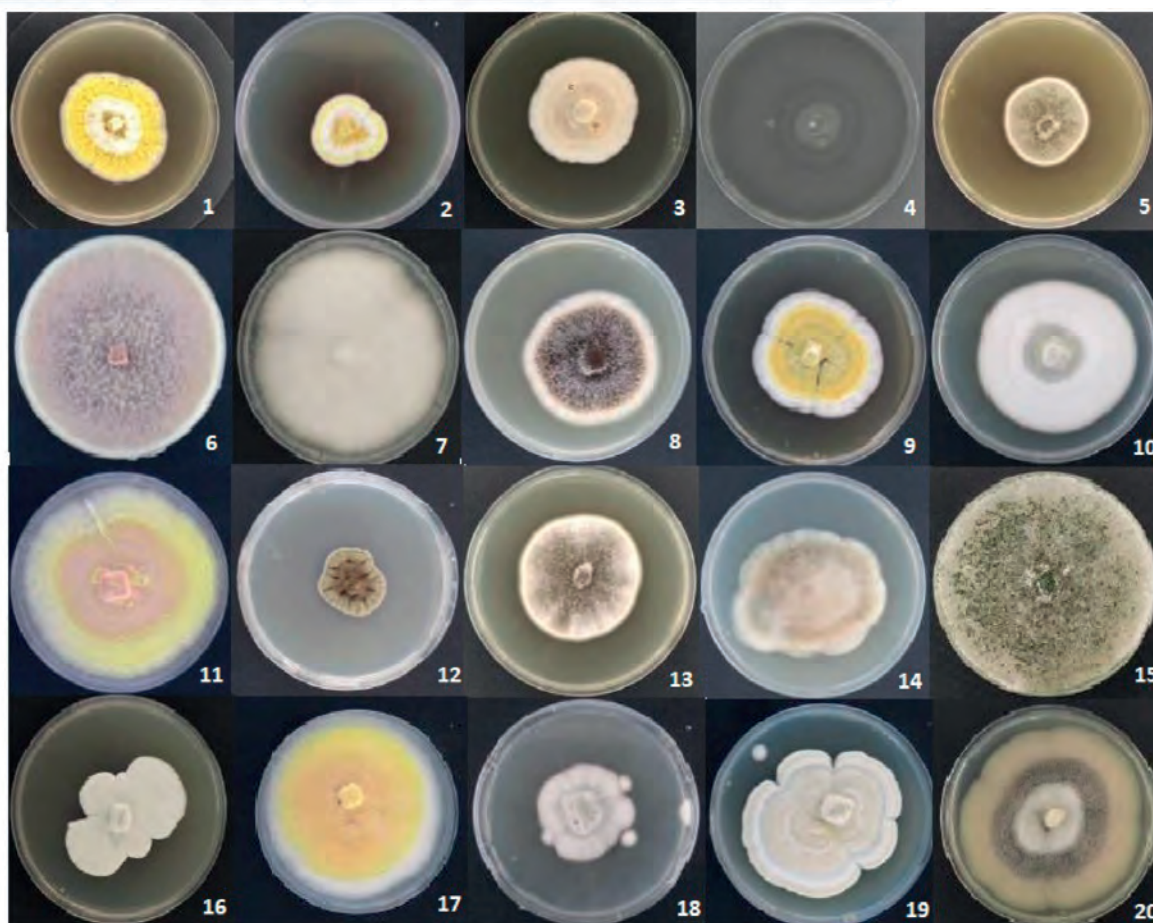
Figura 1. Diversidad de hongos de la Estación 1, *Aspergillus flavipes (1)*, *Aspergillus neoflavipes(2)*, *Penicillium guttulosum(3)*, *Curvularia lunata(4)*, *Aspergillus keveii(5)*, *Trichoderma spirale(6)*, *Gongronella butleri(7)*, *Aspergillus brasiliensis(8)*, *Aspergillus neoflavipes(9)*, *Penicillium limosum(10)*, *Talaromyces liani(11)*, *Cladosporium crousii(12)*, *Aspergillus pseudonomiae(13)*, *Absidia sp.(14)*, *Trichoderma amazonicum(15)*, *Penicillium limosum(16)*, *Talaromyces flavus(17)*, *Penicillium limosum(18)*, *Penicillium limosum(19)*, *Humicola fuscogrisea(20)*.

Código	Porcentaje de identidad	Código de acceso	Organismo
PLSU_E04	100.0%	NG_056277.1	*Purpureocillium lilacinum*
PLSU_F04	99.8%	NG_056277.1	*Purpureocillium lilacinum*
PLSU_G04	100.0%	MN818596	*Curvularia trifolii*
PLSU_H04	100.0%	OL897074	*Talaromyces liani*
PLSU_A05	100.0%	OL772705.1	*Aspergillus neoflavipes*
PITS_B05	99.8%	MW763075	*Absidia sp.*
PLSU_C05	100.0%	NG_069973.1	*Trichoderma amazonicum*
PLSU_D05	99.8%	NG_069973.1	*Trichoderma amazonicum*
PLSU_E05	100.0%	MN017874	*Purpureocillium lilacinum*
PLSU_G05	100.0%	NG_070052	*Aspergillus assiutensis*
PITS_A06	100.0%	MH874891	*Trichoderma pleuroti*
PLSU_B06	99.64%	NG_063999.1	*Penicillium vinaceum*
PLSU_C06	100.0%	NG_069973.1	*Trichoderma amazonicum*
PLSU_D06	99.1%	NG_069831.1	*Trichoderma tomentosum*
PLSU_B03	99.63%	NG_069973.1	*Trichoderma amazonicum*
PLSU_E06	99.6%	NG_069830	*Trichoderma spirale*
PLSU_F06	99.29%	NG_064073.1	*Penicillium sizovae*
PITS_G06	99.1%	MK784067	*Trichoderma harzianum*
PLSU_H06	99.6%	NG_069973.1	*Trichoderma amazonicum*
PLSU_A07	100.0%	MG189915.1	*Fusarium falciforme*
PLSU_D07	99.4%	MW671548.1	*Absidia sp.*
PLSU_E07	100.0%	NG_069973.1	*Trichoderma amazonicum*
PLSU_F07	99.6%	MH874053.1	*Clonostachys rossmaniae*
PLSU_G07	99.29%	NG_064073.1	*Penicillium sizovae*
PLSU_H07	100.0%	NG_069229.1	*Mariannaea humicola*
PLSU_A08	100.0%	NG_070052.1	*Aspergillus assiutensis*

Tabla 2. Especies identificadas en la Estación Cañas (E2).

adversos[25]. El género *Trichoderma* es considerado una especie muy importante debido a su potencial microbiológico que permite ser evaluado frente a otros microorganismos no benéficos gracias a su poder inhibitorio, además de su buen metabolismo puede soportar diversas condiciones ambientales lo que lo categoriza como una especie dominante para muchos de los suelos forestales y agrícolas[26–28], sus beneficios también incluyen a la planta cuándo se ha convertido en unos de sus principales hospederos[29]. Por otro lado, el género *Penicillium* conocido comúnmente por hallarse cerca de materia saprófita es considerado uno de los mayores promotores de crecimiento y fertilidad de suelos, ya que genera metabolitos secundarios que pueden promover el crecimiento de las plantas convirtiéndose en una fuente soluciones para la agricultura[30] y el género *Aspergillius* considerado una especie productora de anflotoxinas, también es reconocida por tener acción antiviral, antibacteria, antifungal[31].

Finalmente, géneros en menor proporción como curvularia, fusarium consideradas especies dominantes al encontrarse en muchos sutratos y en suelos agrícolas pueden llegar a ser desde hongos endófitos hasta patógenos de plantas o suelos en descomposición[32,33], también el género *Purpureocillium* algunos como patógenos de nemátodos pueden actuar produciendo metabolitos tóxicos entre otros[34], el género *Cladosporium* es que ha sido considerado como mohos de interiores y exteriores, también se han

podido encontrar que algunas especies pueden compartir características de endófitos hasta propiedades de biorremediación[35]. Así también, los géneros *Cunninghamella, Clamadomices* y *Absidia* del género mucorales que pueden ser oportunistas y causar afectaciones en la salud humana[36], *Clonostachys* estudiados como posibles agentes de control biológico[37]. En general, los hongos encontrados, aunque en menor proporción sugiere la posibilidad de incorporarlos en pruebas de control biológico para la búsqueda de nuevos inhibidores para el control de plagas.

Arboles filogenéticos

Con la ayuda del programa MEGA y de un análisis Maximun Likelihood, se obtuvo el árbol filogenético de las secuencias analizados. A partir de las especies únicas identificadas, se realizó el estudio de la relación filogenética según de acuerdo a la región ITS y LSU lo que se observa en la Figura 5. Como se puede observar, los géneros con mayor relación evolutiva fueron *Aspergillus* y T*alaromyces. Asimismo, Fusarium* y *Trichoderma* se mantuvieron con estrecha cercanía mientras que *Penicillium, Cladosporium* y *Curvularia* estuvieron como taxones aislados. Además, es necesario notar que aquellas especies con el mismo género o con cercanía evolutiva poseen morfologías y tonalidades similares en su micelio aéreo. Como se puede observar, los géneros con mayor relación evolutiva fueron *Trichoderma, Aspergillus* y *Penicillium*. Por otro lado, *Humicola, Absidia* y

6

Figura 2. Diversidad de hongos de la Estación 2. *Purpureocillium lilacinum (1), Purpureocillium lilacinum(2), Curvularia trifolii(3), Talaromyces liani(4), Aspergillus neoflavipes(5), Absidia sp.(6), Trichoderma amazonicum(7), Trichoderma amazonicum(8), Purpureocillium lilacinum(9), Aspergillus assiutensis(10), Trichoderma pleuroti(11), Penicillium vinaceum(12), Trichoderma amazonicum(13), Trichoderma tomentosum(14), Trichoderma amazonicum(15), Trichoderma spirale(16), Penicillium sizovae(17), Trichoderma harzianum(18), Trichoderma amazonicum (19), Fusarium falciforme (20), Absidia sp.(21), Trichoderma amazonicum(22), Clonostachys rossmaniae(23), Penicillium sizovae (24), Mariannaea humícola (25).*

Código	Porcentaje de identidad	Código de acceso	Organismo
PLSU_C08	100.0%	MH483572	*Penicillium rubidurum*
PLSU_D08	99.6%	MW791866	*Cladosporium cladosporioides*
PLSU_E08	99.8%	OL711761	*Aspergillus keveii*
PLSU_F08	99.8%	LC573561	*Aspergillus aculeatus*
PLSU_G08	99.7%	MG569562	*Cunninghamella echinulata*
PLSU_H08	99.6%	MT560198	*Purpureocillium sp*
PITS_B09	100.0%	NR_164424.1	*Fusarium falciforme*
PITS_C09	99.79%	MH856410.1	*Penicillium vinaceum*
PLSU_D09	99.5%	MH876804	*Penicillium shearii*
PLSU_E09	100.0%	MT533257	*Fusarium solani*
PLSU_H09	99.4%	MH877919	*Trichoderma erinaceum*
PLSU_A10	100.0%	MT582790	*Penicillium steckii*
PITS_B10	98.58%	KU324795.1	*Fusarium solani*
PLSU_C10	100.0%	MN396388	*Aspergillus aculeatus*
PITS_D10	99.6%	MH856410	*Penicillium vinaceum*
PLSU_E10	99.8%	NG_063999	*Penicillium vinaceum*
PLSU_H10	100.0%	MK353174	*Penicillium citrinum*
PITS_A11	98.38%	MN044891.1	*Absidia caatinguensis*

Tabla 3. Especies identificadas en la estación FCV (E3).

7
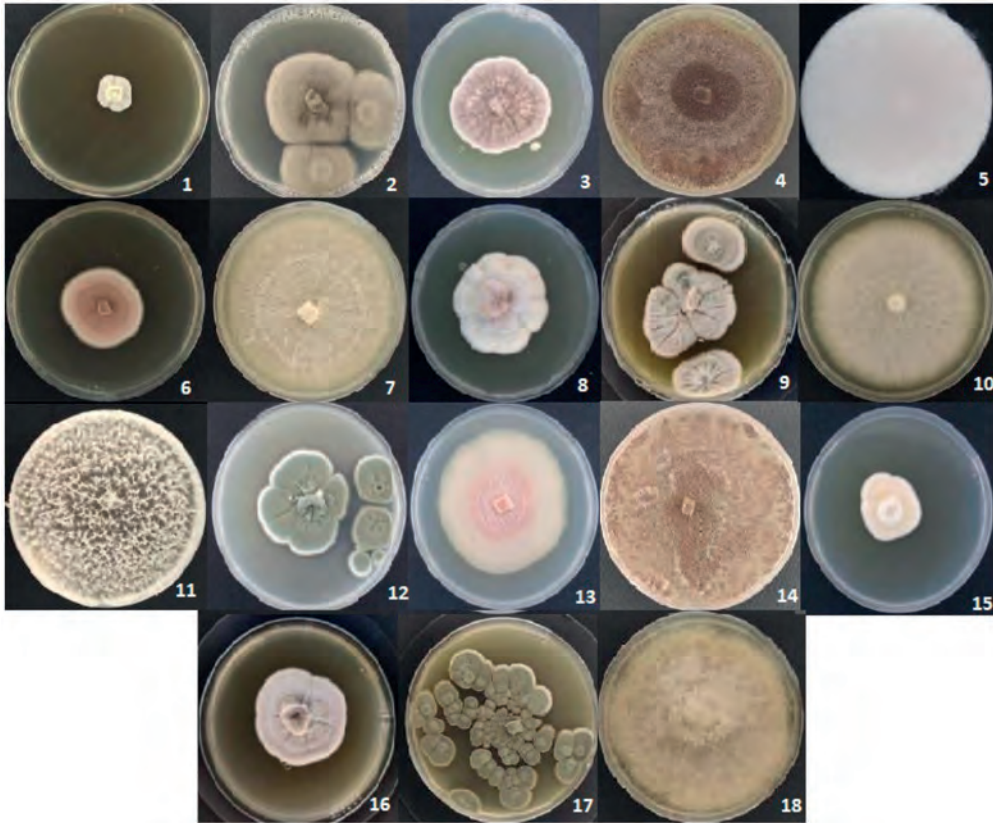
Figura 3. Diversidad de hongos de la Estación 3. *Penicillium rubidurum (1), Cladosporium cladosporioides(2), Aspergillus keveii(3), Aspergillus aculeatus(4), Cunninghamella echinulata(5), Purpureocillium sp(6), Fusarium falciforme(7), Penicillium vinaceum(8), Penicillium shearii(9), Fusarium solani(10), Trichoderma erinaceum(11), Penicillium steckii(12) Aspergillus aculeatus (13), Penicillium vinaceum(14), Penicillium vinaceum(15), Penicillium citrinum(15), Absidia caatinguensis(16).*
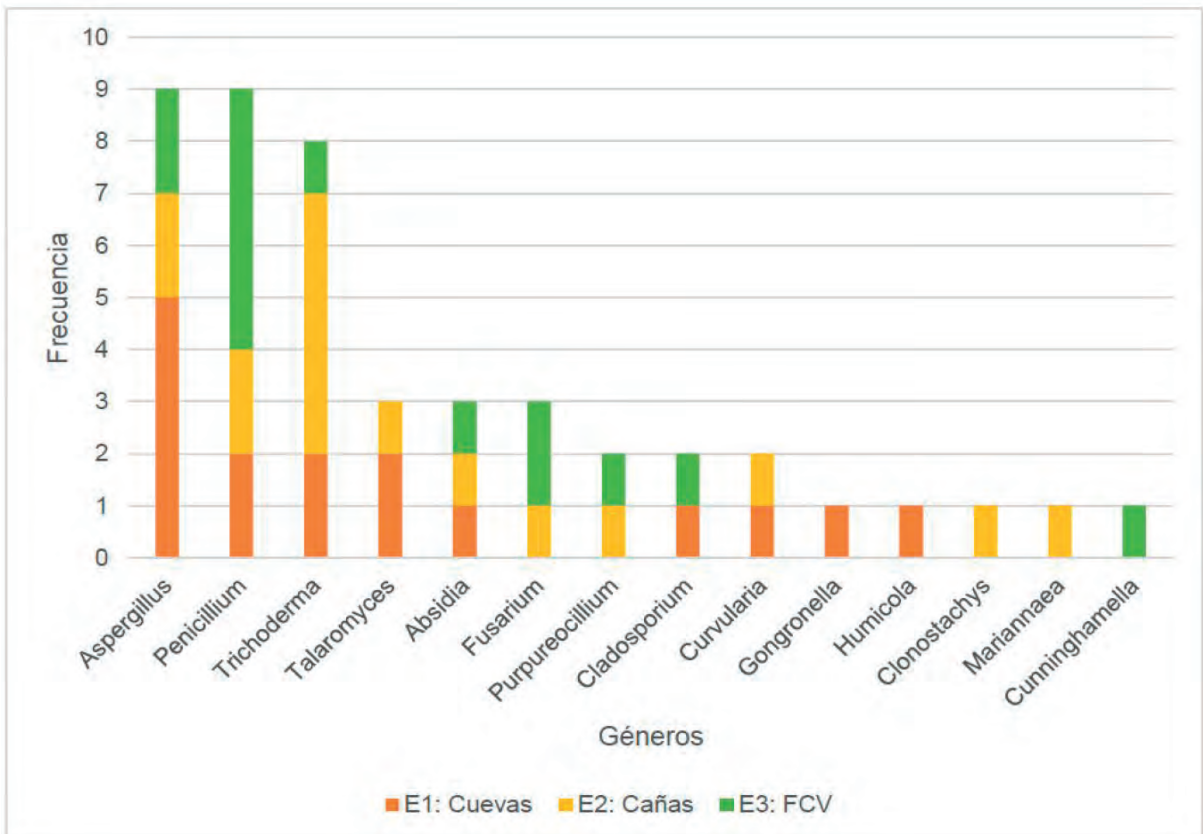
Figura 4. Frecuencia de hongos por estación.
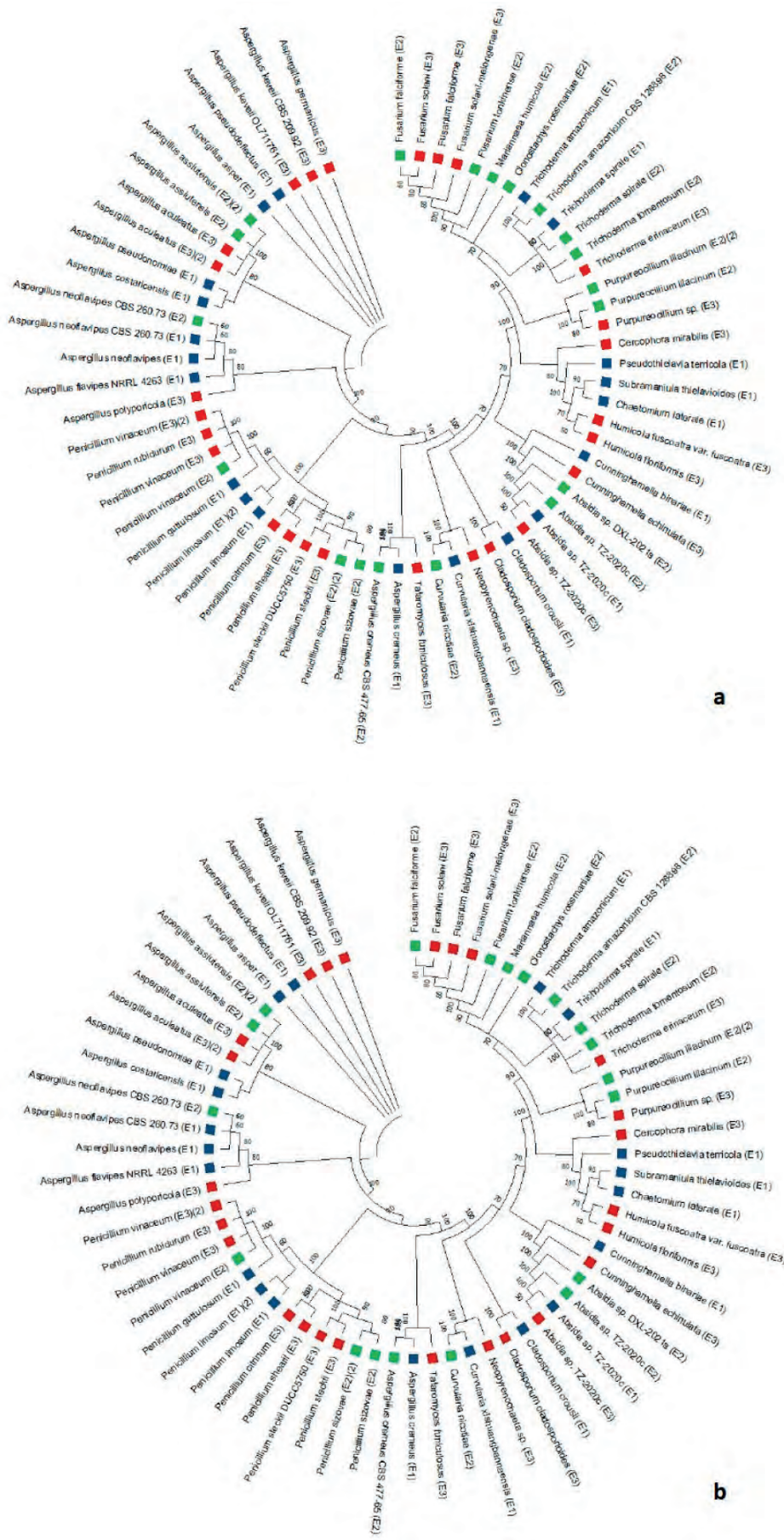
Figura 5. Árbol filogenético de forma circular de las muestras de hongos del Bosque Protector para las regiones ITS (a) y LSU (b).

Cladosporium se presentaron como taxones aislados.

Conservación de microorganismos

Finalmente 38 cepas fueron conservadas en la Colección de Cultivos Microbianos del CIBE bajo los métodos de aceite mineral, crioconservación y agua para fines de investigación. Entre los microorganismos conservados con su respectivo código de depósito tenemos: *Talaromyces liani* (CCMCIBE-H721), *Trichoderma inhamatum* (CCM-CIBE-H722), *Penicillium javanicum* (CCMCIBE-H723), *Curvularia lunata* (CCMCIBE-H724), *Absidia sp.* (CCM-CIBE-H725), *Trichoderma inhamatum* (CCMCIBE-H727), *Trichoderma erinaceum* (CCMCIBE-H728), *Trichoderma saturnisporum* (CCMCIBE-H730), *Penicillium javanicum* (CCMCIBE-H731), *Trichoderma amazonicum* (CCMCIBE-H733), *Trichoderma amazonicum* (CCMCIBE-H734), *Fusarium solani* (CCMCIBE-H735), *Trichoderma spirale* (CCMCIBE-H736), *Cladosporium cladosporioides* (CCMCIBE-H738), *Fusarium solani* (CCMCIBE-H739), *Purpureocillium lilacinum* (CCMCIBE-H740), *Fusarium keratoplasticum* (CCMCIBE-H741), *Cladosporium ramotenellum* (CCMCIBE-H742), *Penicillium vinaceum* (CCMCIBE-H743), *Humicola fuscoatra* (CCMCIBE-H744), *Curvularia trifolii* (CCMCIBE-H745), *Gongronella butleri* (CCMCIBE-H746), *Talaromyces liani* (CCMCIBE-H747), *Purpureocillium sp.* (CCMCIBE-H748), *Talaromyces funiculosus* (CCMCIBE-H750), *Mariannaea aquaticola* (CCMCIBE-H753), *Aspergillus keveii* (CCMCIBE-H754), *Bionectria rossmaniae* (CCMCIBE-H756), *Aspergillus keveii* (CCMCIBE-H757), *Aspergillus germanicus* (CCMCIBE-H758), *Talaromyces flavus* (CCMCIBE-H759), *Penicillium javanicum* (CCMCIBE-H760), *Penicillium javanicum* (CCMCIBE-H762), *Aspergillus flavipes* (CCMCIBE-H763), *Penicillium vinaceum* (CCMCIBE-H764), *Aspergillus flavipes* (CCMCIBE-H765), *Aspergillus keveii* (CCMCIBE-H767), *Penicillium menonorum* (CCMCIBE-H768)

En la actualidad, la conservación de microorganismos está tomando más auge debido a su importancia para el estudio de nuevas especies de hongos y su futura aplicación en el área de la agricultura, farmacología o alimentos[23,38–40]. Muchas de las especies de hongos pueden verse afectadas por condiciones climáticas como la sequía, temperaturas altas o erosión[41] por lo que programas de conservación son necesarios para mantener a través del tiempo biodiversidad que beneficia al ecosistema en general.

La importancia de la implementación de programas de conservación de la biodiversidad en Ecuador corresponden a la preservación del patrimonio natural del país y sus planes de acción ayudan a reducir las presiones antrópicas sobre estos ambientes debido a los constantes desafíos que surgen producto de la expansión urbana. La concientización de preservar las áreas protegidas a través de la investigación científica debe estar incluida en las políticas de los organismos gubernamentales del ambiente puesto que Ecuador forma parte del Convenio de Diversidad Biológica (CBD) y los resultados de estas investigaciones permiten un enfoque ecosistémico en los mecanismos de conservación[42,43].

Conclusiones

El presente trabajo de investigación ha permitido determinar la diversidad microbiana fúngica en tres diferentes zonas del bosque Protector Prosperina. Como resultado se han obtenido 36 especies únicas de hongos filamentosos a través del análisis molecular de las regiones LSU e ITS del ADN, identificando que existe un gran diversidad microbiológica en el BPP que posee un gran potencial biotecnológico. Se encontró que los géneros más abundantes en el BPP fueron Aspergillus, Penicillium y Trichoderma, especificamente en la estación Cuevas se identificaron aquellos géneros acompañados de Cladosporium, Talaromyces, Absidia, Curvularia, Humicola y Gongronella. En la estación Cañas se registraron especies de Talaromyces, Absidia, Fusarium, Curvularia, Purpureocillium, Clonostachys y Mariannea y en la estación FCV también se presentaron los géneros Cladosporium, Absidia, Purpureocillium, Cinninghamella y Cladosporium. La estudios de la biodiversidad del BPP contribuyen al conocimiento de nuestra riqueza microbiana y constituye una base para nuevas investigaciones en la exploración de hongos filamentosos en los bosques secos tropicales de la costa ecuatoriana. Por otro lado, los resultados permitieron la crioconservación de un total de 38 cepas de hongos filamentosos en la Colección de Cultivos Microbianos del CIBE lo que permitirá investigaciones futuras para la búsqueda de enzimas o metabolitos secundarios de interés en la biotecnología y el desarrollo sostenible.

Conflictos de Interés

Los autores declaran no haber conflicto de intereses.

Referencias bibliográficas

1. Delgado-Plaza E, Intriago G, Peralta-Jaramillo J, et al. Autonomous installations for monitoring the 'Protector Prosperina' forest. Applied Sciences (Switzerland); 9. Epub ahead of print October 1 2019. DOI: 10.3390/app9194034.

2. López Remberto, Carrillo Fernando, Pérez C, et al. REVISIÓN DE LA SUSTENTABILIDAD ECOLÓGICA DE LAS ÁREAS VERDES PROTEGIDAS EN LA CIUDAD DE GUAYAQUIL-PROVINCIA DEL GUAYAS-ECUADOR. In: I Congreso Virtual internacional sobre economía social y desarrollo local sostenible . 2018, pp. 1–16.

3. Sierra Rodrigo. Propuesta preliminar de un sistema de clasificación de vegetación para el Ecuador continental. Proyecto INEFAN/GEF-BIRF y EcoCiencia. Quito, 1999.

4. Quinteros Trelles Aleyda, Ramos Plúas Rebeca Betsabé, Rodríguez Almeida Alex. 'EVALUACIÓN DEL USO RECREATIVO BOSQUE PROTECTOR PROSPERINA'. Escuela Superior Politécnica del Litoral, 2010.

5. Wang Y, Liu Y, Li J, et al. Fungal community composition and diversity in the rhizosphere soils of Argentina (syn. Potentilla) anserina, on the Qinghai Plateau. Fungal Ecol; 54. Epub ahead of print December 1 2021. DOI: 10.1016/j.funeco.2021.101107.

6. Gabira MM, da Silva RBG, Bortolheiro FP de AP, et al. Composted sewage sludge as an alternative substrate for forest seedlings production. IForest 2021; 14: 569–575.

7. Llonch L, Gordo C, López M, et al. Agronomic characteristics of the compost-bedded pack made with forest biomass or sawdust. Processes; 9. Epub ahead of print 2021. DOI: 10.3390/pr9030546.

8. Meyer V, Basenko EY, Benz JP, et al. Growing a circular economy with fungal biotechnology: A white paper. Fungal Biology and Biotechnology; 7. Epub ahead of print April 2 2020. DOI: 10.1186/s40694-020-00095-z.

9. Zhou Y, Jia X, Han L, et al. Spatial characteristics of the dominant fungi and their driving factors in forest soils in the Qinling Mountains, China. Catena (Amst); 206. Epub ahead of print November 1 2021. DOI: 10.1016/j.catena.2021.105504.

10. Pacasa-Quisbert Fernando, Loza-Murguia Manuel, Bonifacio-Flores Alejandro, et al. Comunidad de hongos filamentosos en suelos del Agroecosistema de K'iphak'iphani, Comunidad Choquenaira-Viacha. Journal of the Selva Andina Research Society 2017; 8: 2–25.

11. Contreras H, Carreño C. Eficiencia de la biodegradación de hidrocarburos de petróleo por hongos filamentosos aislados de suelo contaminado. Revista de Investigación científica UNTRM: Ciencias Naturales e ingeniería, 2018, pp. 27–33.

12. Delgado Madeleyne. Niveles de Coliformes totales y Escherichia coli en Anadara tuberculosa y Anadara similisen el Recinto El Morro, Provincia Del Guayas. Universidad de Guayaquil, 2017.

13. Ochoa B. SISTEMATIZACIÓN DEL CEPARIO DE HONGOS FILAMENTOSOS DE LA UNIVERSIDAD POLITÉCNICA SALESIANA SEDE CUENCA. Universidad Politécnica Salesiana, 2017.

14. Castillo Celi T, Olaya Villavicencio Angel. Estudio de la diversidad de hongos micorrícicos arbusculares provenientes de dos sistemas agroforestales en plantaciones de cacao, un primer paso hacia la obtención de biofertilizante. 2020.

15. Mendoza RB, Espinoza A. Guía técnica para muestreo de Suelos. 2017.

16. Maridueña-Zavala MG, Villavicencio-Vásquez ME, Cevallos-Cevallos JM, et al. Molecular and morphological characterization of Moniliophthora roreri isolates from cacao in Ecuador. Canadian Journal of Plant Pathology; 38. Epub ahead of print 2016. DOI: 10.1080/07060661.2016.1261372.

17. van Burik J-AH, Schreckhise † R W, White TC, et al. Comparison of six extraction techniques for isolation of DNA from filamentous fungi. 1998.

18. Martin KJ, Rygiewicz PT. Fungal-specific PCR primers developed for analysis of the ITS region of environmental DNA extracts. BMC Microbiol; 5. Epub ahead of print May 18 2005. DOI: 10.1186/1471-2180-5-28.

19. Stielow JB, Lévesque CA, Seifert KA, et al. One fungus, which genes? Development and assessment of universal primers for potential secondary fungal DNA barcodes. Persoonia: Molecular Phylogeny and Evolution of Fungi 2015; 35: 242–263.

20. Kearse M, Moir R, Wilson A, et al. Geneious Basic: An integrated and extendable desktop software platform for the organization and analysis of sequence data. Bioinformatics 2012; 28: 1647–1649.

21. Kõljalg U, Nilsson RH, Abarenkov K, et al. Towards a unified paradigm for sequence-based identification of fungi. Molecular Ecology 2013; 22: 5271–5277.

22. Tamura K, Peterson D, Peterson N, et al. MEGA5: molecular evolutionary genetics analysis using maximum likelihood, evolutionary distance, and maximum parsimony methods. Mol Biol Evol 2011; 28: 2731–9.

23. Maridueña-zavala MG, Quevedo A, Aguaguiña K, et al. Colección de cultivos microbianos CIBE (CCM-CIBE): Una colección para la investigación Microbial Culture Collection from CIBE (CCM-CIBE): A collection for research. Epub ahead of print 2021. DOI: 10.21931/RB/2021.06.01.32.

24. Buée M, Reich M, Murat C, et al. 454 Pyrosequencing analyses of forest soils reveal an unexpectedly high fungal diversity. New Phytologist 2009; 184: 449–456.

25. Totubaeva NE, Shalpykov KT. Dynamics of Microbiological Diversity of Soils in the Chu Valley during Land Use Change in Pastures. Arid Ecosystems 2022; 12: 187–192.

26. Tang GT, Li Y, Zhou Y, et al. Diversity of Trichoderma species associated with soil in the Zoige alpine wetland of Southwest China. Sci Rep; 12. Epub ahead of print December 1 2022. DOI: 10.1038/s41598-022-25223-0.

27. Mulatu A, Megersa N, Abena T, et al. Biodiversity of the Genus Trichoderma in the Rhizosphere of Coffee (Coffea arabica) Plants in Ethiopia and Their Potential Use in Biocontrol of Coffee Wilt Disease. Crops 2022; 2: 120–141.

28. Gams W. Biodiversity of soil-inhabiting fungi. Biodiversity and Conservation 2007; 16: 69–72.

29. Woo SL, Hermosa R, Lorito M, et al. Trichoderma: a multipurpose, plant-beneficial microorganism for eco-sustainable agriculture. Nat Rev Microbiol. Epub ahead of print 2022. DOI: 10.1038/s41579-022-00819-5.

30. Altaf MM, Imran M, Abulreesh HH, et al. Diversity and applications of penicillium spp. in plant-growth promotion. In: New and Future Developments in Microbial Biotechnology and Bioengineering: Penicillium System Properties and Applications. Elsevier, 2017, pp. 261–276.

31. Godinho VM, Gonçalves VN, Santiago IF, et al. Diversity and bioprospection of fungal community present in oligotrophic soil of continental Antarctica. Extremophiles 2015; 19: 585–596.

32. GINTING RCB, SUKARNO N, WIDYASTUTI UTUT, et al. Diversity of Endophytic Fungi from Red Ginger (Zingiber officinale Rosc.) Plant and Their Inhibitory Effect to Fusarium oxysporum Plant Pathogenic Fungi. Hayati 2013; 20: 127–137.

33. Thailand, Seephueak P, Preecha C, et al. The diversity of fungi associated with rice (Oryza sativa L. International Journal of Agricultural Technology 2019; 15: 485–500.

34. Vera-Morales M, López Medina SE, Naranjo-Morán J, et al. Nematophagous Fungi: A Review of Their Phosphorus Solubilization Potential. Microorganisms 2023; 11: 137.

35. Iturrieta-González I, García D, Gené J. Novel species of Cladosporium from environmental sources in Spain. MycoKeys 2021; 77: 1–25.

36. Liang G, Zhang M, Xu W, et al. Characterization of mitogenomes from four Mucorales species and insights into pathogenicity. Mycoses 2022; 65: 45–56.

37. Flores Bazauri Walter, Chico Ruiz Julio, Cerna Rebaza Lisi. Vista de Actividad antagónica in vitro de Clonostachys rosea sobre Fusarium oxysporum, Alternaria solani y Botrytis cinerea. Revista científica de la Facultad de ciencias Biológicas, 2015, pp. 34–42.

38. Sharma SK, Saini S, Verma A, et al. National Agriculturally Important Microbial Culture Collection in the Global Context of Microbial Culture Collection Centres. Proceedings of the National Academy of Sciences India Section B - Biological Sciences 2019; 89: 405–418.

39. Desmeth P, Officer IC. World Federation for Culture Collections Guidelines for the Establishment and Operation of Collections of Cultures of. 2010; 1–19.

40. Sharma A, Shouche Y. Microbial Culture Collection (MCC) and International Depositary Authority (IDA) at National Centre for Cell Science, Pune. Indian J Microbiol 2014; 54: 129–133.

41. Tedersoo L, Mikryukov V, Zizka A, et al. Global patterns in endemicity and vulnerability of soil fungi. Glob Chang Biol. Epub ahead of print 2022. DOI: 10.1111/gcb.16398.

42. Zárate K. Manual para la Gestión Operativa de las Áreas Protegidas de Ecuador. 2013.

43. Delgado-Plaza E, Intriago G, Peralta-Jaramillo J, et al. Autonomous installations for monitoring the 'Protector Prosperina' forest. Applied Sciences (Switzerland); 9. Epub ahead of print October 1 2019. DOI: 10.3390/app9194034.

ARTICLE / INVESTIGACIÓN

Analysis of the Genetic Distance of Several Generations of Barley (*Hordeum valulgare* L) by RAPD-PCR Technique

Raed Salem Alsaffar

DOI. 10.21931/RB/2023.08.01.23

[1] Center of Agrobiotechnological Development and Innovation – CEDAIT, Universidad de Antioquia,Colombia.
[2] Biology Institute, Universidad de Antioquia, Colombia.
Corresponding author: amaria.henao@udea.edu.co

Abstract: Random-amplified-polymorphic-DNA(RAPD) was assayed to detect the genetic variation of 6 barley generations from Iraq. Four primers generated a total of 17 scoreable bands in RAPD analysis) and resolving power, the three polymorphic primers differed (Rp). The use of RAPD marker systems to detect the genetic distance among barley generation was discovered to be beneficial. The RAPD dendrograms indicate a diverse grouping of 6 barely specimens, although we did see that certain groups were identical in several cases. As a result, the RAPD molecular markers reveal two genetic groups in the few specimens examined.

Key words: Barley, Genetic variation, RAPD-PCR.

Introduction

The Barley plant (Hordeum vulgare L.) is the most important crop in the world, and it has been the focus of extensive genetic research. It is considered a diploid plant (2n) species with much DNA that is mostly self-fertilizing[1].

In Iraq, barley is grown on around 450.000 hectares. Early domestication and local expertise have resulted in varied local barley that is mainly utilized for feed. Poorly in terms of food[2].

Sheep owners mainly plant barley in semiarid locations, and it is harvested once or twice as an early winter crop when food and pasture are scarce. Plant genetic resources must be conserved and used and needed for the long-term upkeep and growth of production of agricultural products[3,4].

The preservation of breeders' interests and the documentation of genetic resources have grown increasingly dependent on identifying agricultural plant types. The malting and brewing sectors, respectively, Are critical since various kinds of barley plants have vastly varied characteristics & applications[5,6].

It requires farmers and gardeners to be careful in choosing the seeds of the varieties they want to plant. They must be pure seeds that are not genetically treated and not subject to any additions in order not to affect their genetic sequence[5,8]. Various biochemical methods have been employed to supplement the phenotypic analysis of barley plant cultivation, most of which depend on differences in iso-enzymes and protein storage in the seed seeds. Nonetheless, because of the weak levels of allelic variation for multi-iso-enzymatic loci, the great rank of heredity connection in the middle of the various assortment, and the great extent of variation inside barley plant varieties, characterization with these indicators was not particularly effective for barley varieties[6,7,9].

Molecular and genetic markers have been shown to be effective methods for identifying and assessing genetic variation indoors and across types and societies. Distinct characteristics have been shown to display, unlike types of variation[4,10]. It's linked to the proportion of the DNA surveyed from every kind of genetic indicator, their portioning across the chromosomes, and the size of the purpose target examined by each technique[11].

The adaptation of several molecular methods like RAPD, SSR, STS, RAMP and ISSR was made by the essential technique called the polymerase-chain-reaction-(P-CR)[12,13].

In barley, these molecular markers were utilized to identify genetic distance, detection of genotype and chromosome mapping. The RAPD technique has numerous benefits over other methods, including ease of application, affordable expense, and the utilization of a small quantity of plant matter. Self-pollinating species with little intraspecific diversity, like hexaploid wheat and cultivated barley, are examples., RAPDs have been shown to be helpful as genetic markers[10,14].

Bernard *et al.*[15] utilized the RAPD technique and discovered a lot of variation between wild barley genotypes. They found that comes from the overall diversity of the genetic predicted, 75 percent of the variation was partitioned within genotypes. In contrast, 25% was found to be partitioned within populations., with no significant variations between nations[16].

The ISSR technique shows and detects the genetic sequences of different varieties belonging to certain plants, such as potatoes, through PCR analysis[18].

We use RAPD markers to assess the degree and structure of genetic variation and relationships in complex samples produced in Iraq to provide a baseline for the species' future conservation and breeding initiatives. We also want to show how RAPD may be used to analyze genetic diversity and connections among barley specimens[3,19-21].

2

Materials and methods

Plant-based material In this study, six barley (*Hordeum vulgare* L.) specimens from Iraq's "Ebaa Grain Receiving Center" were utilized.

With few adjustments, total DNA was isolated from fresh leaves using the Genaid kit. And DNA concentration and purity measurement by nanodrop and separated by 2% agarose gel electrophoresis.

Extraction of DNA and Analyzed with RAPD-PCR. Operon molecular for life provided ten decamer random primers for RAPD analysis (Table 1). Total DNA was extracted from grains of 6 Barley using generated kit, and the extracted DNA was diluted to 25 ng /mic by nanodrop technique. Primers were diluted to 10 ng /mic, used for PCR amplification, and separated by 2% agarose gel electrophoresis[1].

Results and discussion

Out of many universal primers utilized for early detection with typical genotypes, just four primers replicate polymorphic specimens. Then these 4 primers were used in the RAPD-PCR technique to analyze all 6 barley plant generations. The PCR bands of the 6 generations with these 4 primers give an overall of 15 different bands. The elevated digit of the band (7) was received by UBC-475 primer, while the little number (3) was received by UBC-490 primer. Several denote the identic distance in their aptitude to determine the genetic variation (100 percent). The 4 polymorphic primers visualize the polymorphism concerning the average band in informativeness (AvIb) and Resolving power (Rp).

Because of its global spread, the genetic variation of barley plant germ cells from divergence homeland has been valuator[7,8,12,22,23]. Bernard *et al.*[15] used RAPD markers to examine the genetic distance of 6 generations from 121 wild barley plant societies from Iraq, Turkey, and Iran. When the overall genetic distance was calculated, 75 percent of the variance was split between the six genotypes and 25% was divided between the social. Because the majority of the very discovered (97 percent) was to part among the 20 societies and the residue across the nations, there were no significant differences between countries when the variation was evaluated[11]. Therefore, the few specimens were joined together regardless of their geographic origin. Dendrograms using RAPD-PCR and ISSR techniques do not indicate geographic profiling among barely plant samples in this investigation[23].

Only a few clusters had comparable classifications based on the makeup of clusters derived using RAPD and ISSR markers separately. Various metrics like the relation of polymorphism, mean band informativeness, resolving power, and clusters produced in the dendrogram were used to assess the performance of these markers[1,7,13,22].

The findings of this study's genetic distance were compared to reports from other RAPD research, such as an assessment of gene distance in the outer covering of a seed of barley plant using phenotypic characteristics and RAPD markers, as well as stored protein analyses[9,14].

Furthermore, it has been observed that the dendrogram created by the RAPD phylogeny meshes best with the barley plant cultivars' genealogy and known pedigree than the dendrogram obtained by the ISSR findings.

On the other hand, data derived from RAPD were shown to be more directly connected to the geographic distribution of the genus Houttuynia Thunb, whilst data derived from the ISSRs technique were found to be intimately related to chromosome number 8-13. It might be accounted for partly by the disparity in the number of informative PCR products. They emphasized the relevance of the real number of locus and their covering of the entire genome once more, as well as obtaining reasonable estimations of genetic relationships among the materials investigated. RAPD-PCR has proven to be the majority polymorphic technique in barley plants, making them extremely useful for various barley applications 19.20. RAPD techniques are a marker used to identify and were also linked to multiple characteristics, including the leaf rust resistance gene Lr 28 in Aegilops speltoides[17,22].

As a result, RAPD analysis might be beneficial for selecting ancestors to cross to generate acceptable populations for genome mapping and breeding[20]. We reach the following deduction depending on the findings of this study: The results showed that RAPD-PCR analysis might be used to assess genetic diversity among Iraqi barley varieties. The findings of this study, based on genetic diversity, will aid breeders in selecting parents for hybridization programs and determining the kind of variation in barley.

Conclusions

Despite the narrow genetic base among the six species used here, RAPD analysis was quite effective in determining the genetic variation among Barley species. It can be used to generate DNA fingerprints for variety identification.

Funding

Primer	Sequence
U-B-C- 402	CCC-GCC-GTT-G
U-B-C-475	CCA-GCG-TAT-T
U-B-C-490	AGT-CGA-CCT-T
U-B-C-534	CAC-CCC-CTG-C

Table 1. Sequence of primers used in the RAPD technique[15].

stage	temperature	time	Cycle number
First denaturation	94	Five min	1
denaturation	94	One min	35
Primer Annealing	37	One min	
Extension of Taq-polymerase	72	Two min	
Final-Extension	72	Seven min	1

Table 2. The PCR condition used in the RAPD technique

3
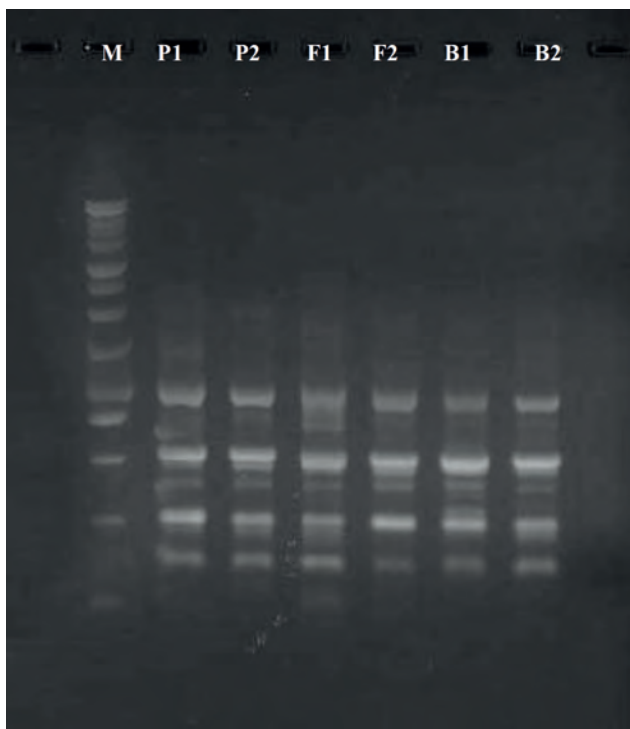
Figure 1. Raped-PCR product for UBC-402 primer. M marker 100 bp.
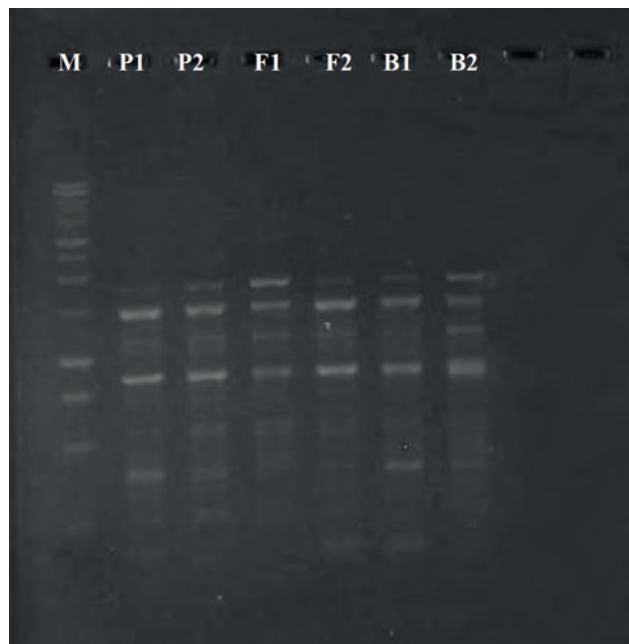
Figure 2. Raped-PCR product for UBC-475 primer. M marker 100 bp.
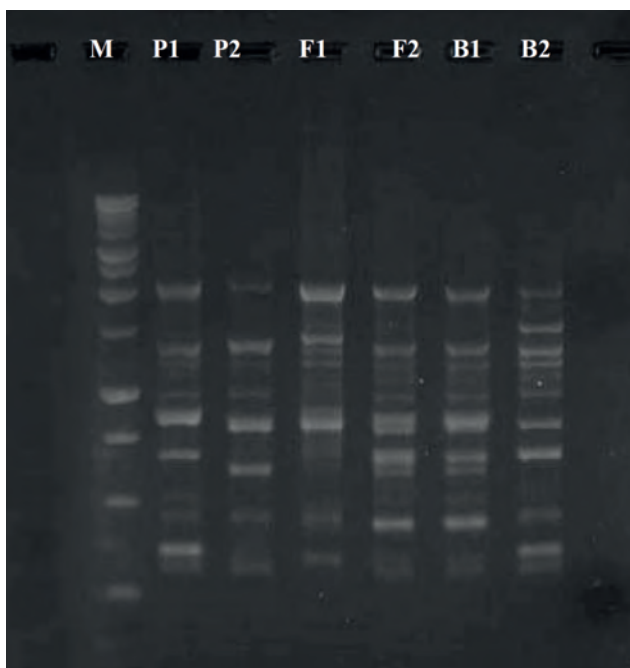
Figure 3. Raped-PCR product for UBC-490 primer. M marker 100 bp.

Acknowledgments

In this section, we acknowledge any person who supports us in completing this project.

Conflicts of Interest

There is no conflict.
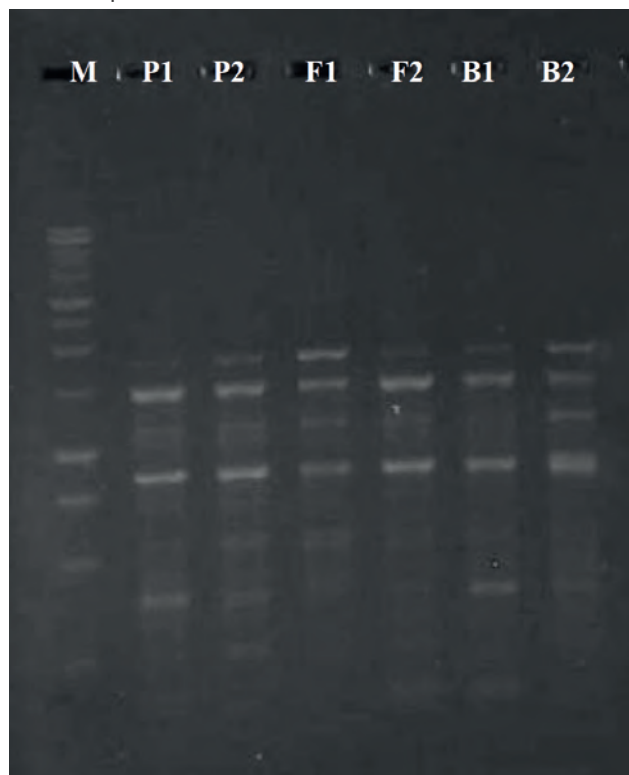
Figure 4. Raped-PCR product for UBC-534 primer. M marker 100 bp.

Bibliographic references

1. S. Laugesen, K. S. Bak-Jensen, P. Hagglund et al. "Barley ¨ peroxidase isozymes. Expression and post-translational modification in mature seeds as identified by two-dimensional gel electrophoresis and mass spectrometry," International Journal of Mass Spectrometry, 2007, vol. 268, no. 2-3, pp. 244–253.

4
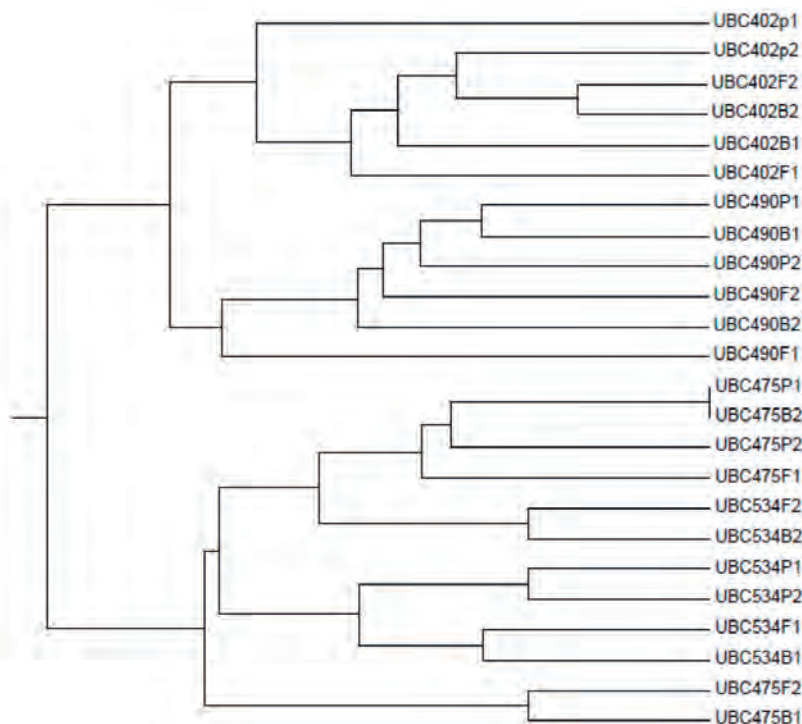
Figure 5. Dendrogram constellates were revealed by six barley plant samples using an RAPD-PCR marker. RAPD-PCR data acquired from the dendrogram show 23 chief clusters (Figure 5).

2. P. C. Canci, L. M. Nduulu, R. Dill-Macky, G. J. Muehlbauer, D. C. Rasmusson, and K. P. Smith. "Genetic relationship between kernel discoloration and grain protein concentration in barley," Crop Science, 2003, vol. 43, no. 5, pp. 1671–1679.

3. X. P. Chen, L. Yan, and Y. Ding. "RAPD analysis and the probable evolutionary route of wild relatives of barley from China," Acta Botanica Sinica, 2000, vol. 42, no. 2, pp. 179–183,.

4. Z. Y. Feng, Y. Z. Zhang, L. L. Zhang, and H. Q. Ling. "Genetic diversity and geographical differentiation of Hordeum vulgare ssp. spontaneum in Tibet using microsatellite markers," High Technology Letters, 2003, vol. 10, pp. 46–53.

5. F. Guasmi, L. Touil, K. Feres, N. Marzougui, W. Elfalleh, and ´ A. Ferchichi. "Variety identification and genetic relationship of some South Tunisian barley accessions using agronomic parameters," Journal of Food, Agriculture and Environment, 2009,vol. 7, no. 2, pp. 522–527.

6. Korol, and E. Nevo. "Microscale ecological stress causes RAPD molecular selection in wild barley, Neve Yaar microsite, Israel," Genetic Resources and Crop Evolution, 2003, vol. 50, no. 2, pp. 213– 224.

7. E.-H. Dakir, M.-L. Ruiz, P. Garc´ıa, and M. Perez de la Vega. "Genetic variability evaluation in a Moroccan collection of barley, Hordeum vulgare L., by means of storage proteins and RAPDS," Genetic Resources and Crop Evolution, 2002, vol. 49, no. 6, pp. 619–631.

8. Y. Q. Yin, D. Q. Ma, and Y. Ding. "Analysis of genetic diversity of hordein in wild close relatives of barley from Tibet," Theoretical and Applied Genetics, 2003,vol. 107, no. 5, pp. 837–842.

9. Zeina S. M. Al-Hadeithi, *Abdul Kareem A. Al-Kazaz, ** Bilal K. Al-Obaidi. Genetic Diversity And Relationships Among Iraqi Barley Cultivars Using RAPD – PCR Technique. The Iraqi Journal of Agricultural Sciences, 2012, 43(6): 117-124.

10. Karim, K.; A. Rawda and C.M. Hatem,. Genetic diversity in barley genetic diversity in local Tunisian barley based on RAPD and SSR analysis. Biological Diversity and Conservation, 2010, Tunisia. ISSN 1308-5301 Print; ISSN 1308-8084 Online.

11. Ciulca, A.; E. Madosa; S. Mihacea, and C. Petolescu. RAPD analysis of genetic variation among some barley cultivars. Romanian Biotechnological Letters, 2010, 15(1):19-24.

12. Mahmood, T.; A.Siddiqua; A.Rasheed, and N.Nazar. Evaluation of genetic diversity in different Pakistani Wheat landraces. Pakistan .Pak. J. Bot., 2011, 43(2): 1233-1239.

13. Eshghi, R. and E. Akhundova. Genetic diversity in hulless barley based on agromorphological traits and RAPD markers and comparison with storage protein analysis. African Journal of Agricultural Research , 2010,5 (1): 97-107.

14. Goswami, S. and V. Tripathi. The use ISSR and RAPD marker for detecting DNA polymorphism, genotype identification and genetic diversity among Trichosanthes dioicaRoxb. Cultivars International Journal of Bio diversityand Conservation. India, 2010,2(12):405-413.

15. R. B. Bernard, E. Nevo, A. J. Douglas, and A. Beiles. "Genetic diversity in wild barley (Hordeum spontaneum C. Koch) in the near east: a molecular analysis using random amplified polymorphic DNA (RAPD) markers," Genetic Resources and Crop Evolution, 1997, vol. 44, no. 2, pp. 147–157.

16. Al- Assei, A. H.A. Analysis of genetic variation of barley cultivated in Iraq using DNA markers. PhD thesis. Biology Department, College of Ibn AlHaithm Education –University of Baghdad, 2002,p:111.

17. Süleyman CENKCİ*, Nevra DOĞAN. Random amplified polymorphic DNA as a method to screen metal-tolerant barley (Hordeum vulgare L.) genotypes. Turk J Bot ,2015, 39: 747-756.

18. s Agarwal M, Shrivastava N, Padh H. Advances in molecular marker techniques and their applications in plant sciences. Plant Cell Rep, 2008, 27: 617–631.

19. Amabile RF, Faleiro FG, Capettini F, Júnior WQR, Peixoto JR, de Almeida BC. Genetic variability of elite barley genotypes for Brazilian savanna irrigated systems based on RAPD markers. Biosci J, 2014, 30: 1118–1126.

20. Aras S, Aydın SS, Körpe DA, Dönmez Ç. Comparative genotoxicity analysis of heavy metal contamination in higher plants. In: Begum G, editor, Ecotoxicology. Rijeka, Croatia: InTech Publications, 2012,pp. 107–124.

21. Cenkci S, Yıldız M, Ciğerci İH, Bozdağ A, Terzi H, Terzi ESA. Evaluation of 2,4-D and Dicamba genotoxicity in bean seedlings using comet and RAPD assays. Ecotox Environ Safe, 2010b, 73: 1558–1564.

22. Cenkci S, Yıldız M, Ciğerci İH, Konuk M, Bozdağ A. Toxic chemicals-induced genotoxicity detected by random amplified polymorphic DNA (RAPD) in bean (Phaseolus vulgaris L.) seedlings. Chemosphere, 2009, 76: 900–906.

23. Cenkci S, Yıldız M, Konuk M, Eren Y. RAPD analyses of some wild Triticum L. and Aegilops L. species and wheat cultivars in Turkey. Acta Biol Cracov Bot, 2008, 50: 35–42.

ARTICLE / INVESTIGACIÓN

Genetic diversity of varieties of barley *Hordum Vulgare* Implanted using RAPD

Shaymaa khaleel alhialy[1]*, Raed Salem Al-Saffar[1], Safa Aldeen Abd. Sulyman[2]

[1] Department of Biology/College of Science/University of Mosul, Iraq.
[2] College of Basic Education/Univ. of Mosul, Iraq.
Corresponding author: drshaymaakhleel@uomosul.edu.iq

Abstract: In the study, a technique of PCR was used, which is the RAPD indicator using nine varieties of the Iraqi barley plant, where the genetic indicators of the implicit sequence were used to determine the level of genetic similarity for the studied varieties and to find the genetic fingerprint for some types. The bundle of varying sizes was 121 in number. The highest number of binding sites was recorded in the R4 primer with 58 bundles, the lowest number of binding sites was given by the R5 initiator with 11 bundles, the highest molecular weight in the binding sites was provided by the R9 initiator 1300pb, and the same initiator gave the lowest molecular weight 125 pb, and from the genetic similarity matrix, the lowest genetic distance was between classes 3 and 4 with a value of 0.8545, while the highest genetic distance was between classes 6 and 7 with a value of 0.4545. The RAPD technique found unique and distinct DNA bundles capable of distinguishing between the studied wheat varieties, meaning that these bundles were found in a particular type and absent in other varieties. It can be used as a distinctive genetic fingerprint to preserve plant breeders' rights. This study showed the efficiency of the RAPD technique in distinguishing between the studied cotton varieties and in determining the degree of genetic proximity and distance between them, which contributed to revealing the genetic diversity among some of the cotton varieties cultivated in Iraq.

Key words: Genetic diversity, RAPD, barly *Hordum Vulgare*.

Introduction

To raise productivity and enhance food security and nutrition, various methods are used to reach the total of diverse and complementary crops and their improved varieties. Among the methods used to improve yields and increase productivity are genetic indicators. Several technologies based on DNA indicators have been developed that are used to detect genetic variations and study genetics. Genetic linkage between species or genetic phenotypes and genetic linkage mapping helped in developing breeding programs and raising their efficiency[1], and it is used effectively in genetic improvement programs, whether in developing breeding programs through Through early detection of the presence of the desired trait in the genetic source, in addition to verifying the degree of mixing or genetic authenticity, identification of varieties and testing their purity is one of the essential processes in the field of the seed industry and biotechnologies based on genetic indicators used to improve yield and shorten the period RAPD Randomly Amplified Polymorphic DNA-PCR[2].

Grain varieties more to biotic and abiotic stresses are now being grown in farmers' fields. The rapid multiplication of high-quality seeds[3] should match the development of more productive grain and feeding regimes

Future scenarios indicate that the pressure to reduce cereal production will disproportionately affect those most at risk, namely, the third world countries and the agriculturally dependent countries, who constitute a large part of the farmers, and the billions of low-income people depend daily on cereals for their survival Alive[4].

With climate change, heat and drought tolerance will become important in cereals, especially in the tropics60. Current research is directed at developing the drought-tolerant wheat project using genetic modification, led by the International Center for Maize and Wheat Improvement, to produce different varieties, including hybrids, that excel. The yield over commercial varieties increased by 25 percent under specific drought conditions. Some are also heat tolerant and produce 27 percent more output than commercial varieties. A heat-tolerant wheat variety based on the genotype maintained by the International Center for Maize and Wheat Improvement and the International Center for Agricultural Research in the Dry Areas (ICARDA center of agriculture) has been released in several countries[5].

Recent years have witnessed a remarkable development in the use of molecular indicators in determining the genetic variation of cultivated plants because of their many advantages. Molecular indicators are of paramount importance in plant breeding, in addition to being helpful indicators in accelerating the selection and breeding processes and reducing material costs. Molecular indicators have been used to determine the genetic variations within plant populations and the genetic relationships between varieties and plant species. Studies have proven that molecular indicators are valuable clues in describing and evaluating genetic diversity within species. deterioration[6].

Among the common and recent indicators are Polymorphic Random Amplified DNA (RAPD) indicators, which are simple, fast, do not require a large amount and can be

Publisher's Note: Bionatura stays neutral with regard to jurisdictional claims in published maps and institutional affiliations.

2

applied to large genetic populations, in addition to the possibility of using random primers. Thus RAPD indicators have applications in the Extensive study of the relationship between clans of the same species or species close to each other. It was also used to determine the genetic identity and to investigate hybrids. It can also help in drawing genetic maps and using them to know the genetic relationship between plants of one species using the same technique. In addition to its use in the field of diagnosis and finding genetic fingerprints, it had applications on various organisms such as humans, animals and bacteria, and the varieties belonging to many plant species were classified[7].

Many researchers used different types of DNA indicators to study genetic variation and molecular characterization of wheat plants in other parts of the world; the study aimed to use RAPD indicators in analyzing genetic variations between some varieties of wheat tri in Iraq to distinguish between all studied sorts, which are the identity of For the variety[8].

Materials and methods

The genealogies of the genotypes and their numbers used in the study(island / Ibaa center / Iraq, Euphrates Abaa Center/Syria, Pool Ebaa Center / Iraq, Rum Ibaa Center / Jordan, Forest Parent Center / Australia, Benedict Parents Center / Sweden. Arafat Parents Center / America, Rayan Parents Center / Syrian, Samir Parents Center / Iraqi).

The amount of rain falling during the growing season was (812.5 mm). Random samples were taken of five spikes of each variety, placed in clean nylon bags, and transferred to the College of Science, Department of Life Sciences - Molecular Biology Laboratory to conduct the laboratory study.

Extraction of DNA from the seeds of wheat under study

The Genomic DNA mini kit supplied by Geneaid Company was used. It included the following (Weigh 0.2 g of wheat seeds, add liquid nitrogen to a ceramic mortar and grind the mixture for 3 seconds until it becomes a homogeneous powder, Transfer the powder to a 1.5 mL tube and add 400 µl of GP1 and 5 µl of RNase and mix using a mixer (Vortex). The tube is incubated at 60°C for 10 minutes. During that time, the tube is turned every 3 minutes, add 100 µl of GP2 Buffer solution mix with Vortex and incubated on ice for 3 minutes, The mixture is transferred to a Filter Column tube, and centrifugation is carried out for 1 minute at a speed of 1000 g, then the filter tube is neglected. The filter is transferred to a 1.5 ml tube, Add 1.5 kg of GP3 solution and mix immediately for 5 seconds. Transfer 700 µl of the key to a GD Column tube and centrifuge for 2 minutes at maximum speed. The filtrate is discarded, and the GD Column is reinstalled into the collection tube. Add 400 µl of solution W1 and centrifuge for 30 seconds at maximum speed. The filtrate is discarded, and the GD Column is reinstalled into the collection tube. Add 600 µl of Wash Buffer solution and centrifuge for 30 seconds at maximum speed, remove the filtrate, and then centrifuge for 3 minutes at full speed. The GD column is fixed in a 1.5 ml tube, and 100 µl of Elution solution is added and left for 3 minutes to allow it to bind with DNA.Centrifuge for 30 seconds at maximum speed. Remove the GD column and store the precipitate at -20°C until use.

Preparation of agarose gel and DNA electrophoresis

For DNA transfer and detection, 1% agarose gel is prepared. To obtain this concentration, 0.5 g of agarose powder is dissolved in (50) ml of X1 TBE, and 3 microliters of safe red dye are added using a heat source with continuous stirring until boiling and left to cool. To a temperature of (60-50) ˚C, Then the gel solution is poured into the basin of the Tray of the relay device after the special comb is fixed to form the Wells at the edges of the gel, taking into account that the pouring is quite to avoid the formation of bubbles. If they are created, they are removed using the pipette, then leave the gel solidifies. The Tray is then placed in an electric relay tank containing an appropriate amount of X1 TBE solution, after which the comb is gently lifted. Migration samples are prepared by mixing (5) µL of the DNA sample with (3) µL of the loading solution. After that, the relay is operated by passing the electric current with a voltage of (5) volts/cm, and the process takes (2-1.5) hours. After that, the gel is photographed under ultraviolet rays using a gel documentation device to see the DNA bundles and the product of the PCR reaction. As shown in the following table (1), ten random starters were used to determine the differences between the wheat cultivars.

T	Primer	Sequence
1	R1	GGTTCGGGAA
2	R2	GAAACGGGTG
3	R3	CACACTCCAG
4	R4	CAAACGTCGG
5	R5	GCATATCCGG
6	R6	CTGACCAGCC
7	R7	ACCAGGTTGG
8	R8	GGACCCCGCC
9	R9	GGCTGCAGAA
10	R10	CTTTCGTGCT

Table 1. Determine the differences between the different wheat cultivars.

PCR reactions

The DNA concentration in all study samples was adjusted by dilution by TE buffer solution to obtain the required concentration for PCR reactions, and it was (25) ng/microliter for each sample. The master reaction mixture was prepared for each PCR reaction by mixing the DNA sample and the special primer for each gene with the components of the Pre-mix inside a 0.2 ml Alpendorf tube supplied by the English company Biolabs. The reaction volume was fixed to 20 µl with distilled water, and the mixture was discarded. In the Microfuge device, for a period between (5-3) seconds, to ensure the mixing of the reaction components, the reaction tubes were inserted into the Thermocycler to conduct the multiplication reaction using the particular program for each response. Adding the volumetric guide DNA Ladder prepared by Biolaps company into one of the holes, the samples are migrated by running the Electrophoresis device for a period ranging from (70-60) minutes, after which the gel is imaged using the Gel Documentation device (Fig. 1).

Statistical analysis

The results of the RAPD prefixes were taken based on the comparison of the presence or absence of a piece of DNA for the studied varieties, which symbolizes the presence of the DNA piece (Band) by (1) and its absence with the number (0), where it was recorded for the company of the DNA band) by the number 1 and for its lack (Band) by the number zero; this table has calculated the number (Band) shown by each prefix in the RAPD and the total number of bundles of genetic varieties of wheat studied, identifying monomorphic and polymorphic bundles, and calculating the degree of variation in the outputs of gene dimension coefficient as well as the similarity coefficient between the analyzed samples using Nei's coefficient 72[9] then he conducted cluster analysis and plotted the genetic dimension using the (UPGMA) method[10].

Statistical analyzes were carried out by computer using the program:

Taxonomy and Multivariate Analysis (NTSYS-pc) Numerical System[11]. The conclusion of the results of this program was based on the (9) to detect genetic similarity by forming a sequential table that includes all the results of the prefixes (for each indicator separately) with all the models studied according to the equation: Ni) + GD=1{2x(Nij/Ni)

Nij: The number of packets shared between the two models i,j

Ni: the number of packages in the i .model Nj: the number of packets in the j. model

---

Results and discussion

Polymorphism results from using the RAPD technique for the studied items

The RAPD technique is one of the old and relatively simple molecular methods, but it is still widely used due to its ease of application. Diagnosing taxa at the DNA level using this technique means finding the genetic fingerprint for each of the taxa, which is how the replicated pieces of the studied taxa are distributed using a specific initiator, i.e., The number of those bundles and their molecular sizes,

which are distinctive for that variety without the rest of the types, and that finding a genetic fingerprint for the array is considered an identity for that variety that can be used[12]. The RAPD technique was applied using ten random primers Table (2) to distinguish nine types of wheat Table (1). The method of analyzing the results of the genetic relationship study depended on the presence or absence of bundles resulting from the duplication of certain pieces of the wheat genome used and on the molecular weights of those bundles that depend on The number and complementary locations of primer sequences on the template DNA strand, the lack of results with some of the primers used is one of the most important foundations that are considered the basis of the differences between taxa[13] primer R1, The number of multiplied pieces of wheat varieties using this starter was 32 bundles whose molecular weights ranged between (300pb-1100pb). Figure (2) The number of multiplicative pieces for cultivars went from 5 to 3; the bundle with a molecular weight of 300 pb appeared in category one to distinguish it. This cultivar used the 1R primer, which represents a genetic indicator for the variety and a guide to facilitate the differentiation task, which was the percentage of the variance between the cultivars using this primer 8, 71.

The R2 primer showed the results of DNA doubling for the cultivars under study using the R2 initiator. Twenty-nine bundles whose molecular weight ranged from 200 pb - 900 pb. The 500 and 900 pb bundles appeared in all varieties. This initiator variety seven was distinguished by the presence of the 700 pb initiator and can be used as a distinctive genetic fingerprint. The variety has a variance ratio of 62.2.

Initiator R3: The number of the resulting bundles reached 28, of which 19 differed between the varieties. The percentage of bundles differed at 67.87; the initiator R3 gave a 200 pb molecular weight that band found in class 5 and not in the rest of the varieties. This confirms the importance of this technique in molecular characterization and genetic fingerprinting.

R4 initiator: The number of bundles using this initiator was 58, of which 40 were different bundles, and the variance ratio between the varieties was 68.97. This initiator did not distinguish a particular variety; the molecular weight of
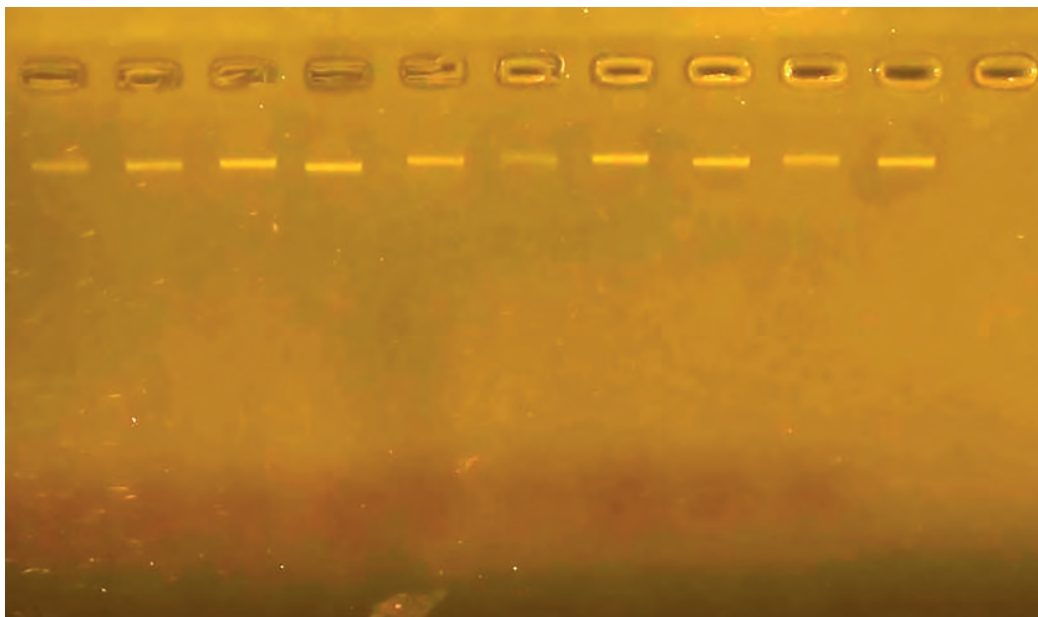
Figure 1. Shows the genome extracted from wheat seed samples and carried over in 2% agarose gel.

3

4
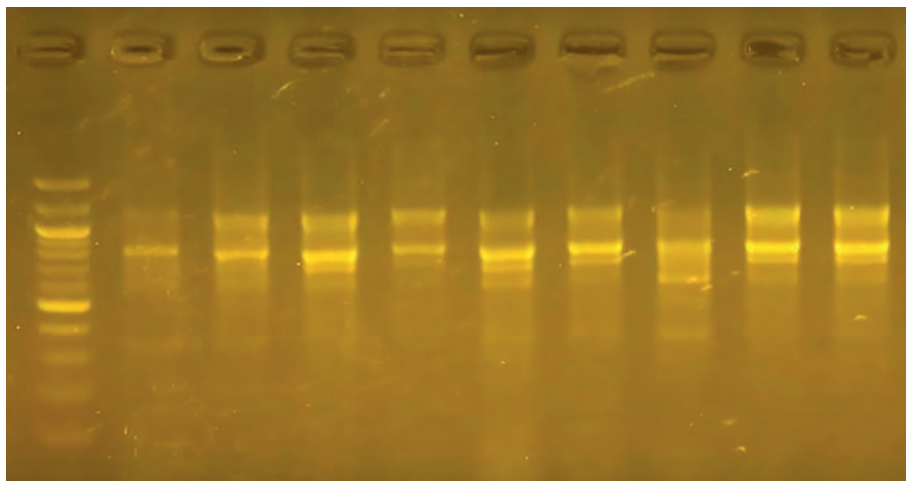
Figure 2. The product of a DNA random amplification reaction using the 1 R . primer.
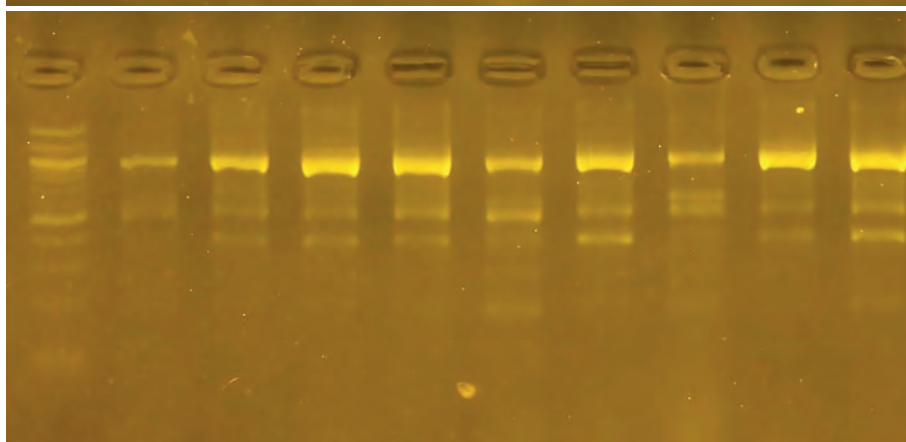
Figure 3. The product of a DNA random amplification reaction using the initiator R2.
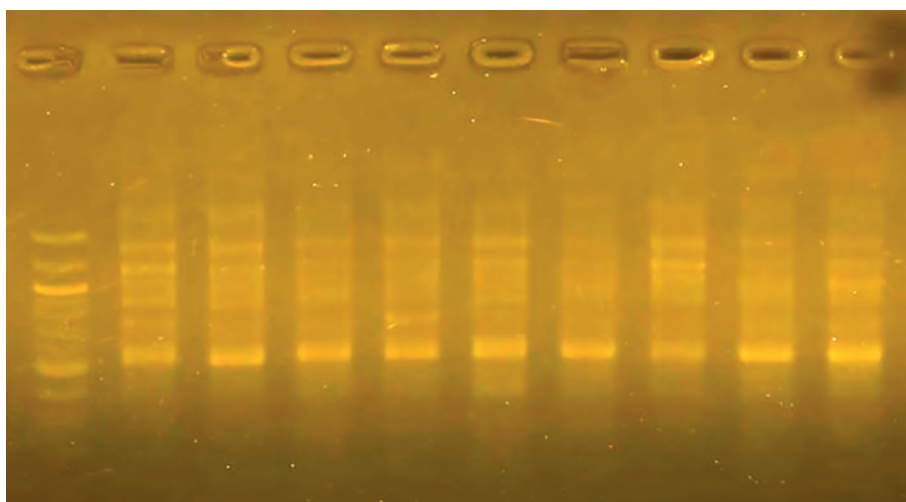
Figure 4. The product of a DNA random amplification reaction using the initiator R3

the bundles ranged from 200pb to 1200pb.

Initiator R5: This initiator gave the least number of bundles, 11 bundles only, did not distinguish any variety, and is considered the least efficient primer. The percentage of variation reached 100, and the molecular weight of the bundles ranged from 600pb to 1200pb.

Starter R6: The number of bundles resulting from using the R6 starter was 34 bundles, and the percentage of the discrepancy between the varieties was 100 because no similar bundles appeared between the varieties. Variety 7 was distinguished by the absence of a bundle with a molecular weight of 400 pb, while it was present in the rest of the varieties. The size of the pieces ranged from 250 pb to 900 pb.

The primer R7, in conjunction with the complementary

sites of the DNA sequences, gave 38 bundles with molecular weights ranging from 500 pb to 1100 pb. No cultivar was distinguished by using this initiator because a unique bundle did not appear for a particular cultivar; the percentage of variance using this primer was 0 zero.

Starter R8: 36 packets produced by this initiator bar interconnected with the complementary sites of DNA, of which 9 bundles are similar. The percentage of the variance between species using this initiator was 75.0. The size of the packets ranged from 400pb to 1200pb

Initiator R9: The number of bundles reached 46 bundles, and their size ranged from 125pb to 1300pb. Class 5 was distinguished by a unique bundle with a molecular weight of 175 pb. The initiator gave a variation ratio of 77.8

Primer 0 1R: The number of bundles produced 48
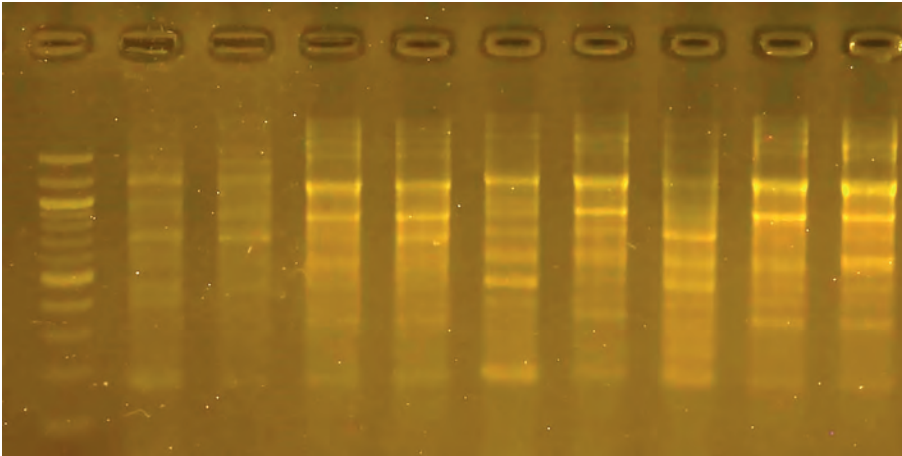
Figure 5. The product of a DNA random amplification reaction using the initiator R4.
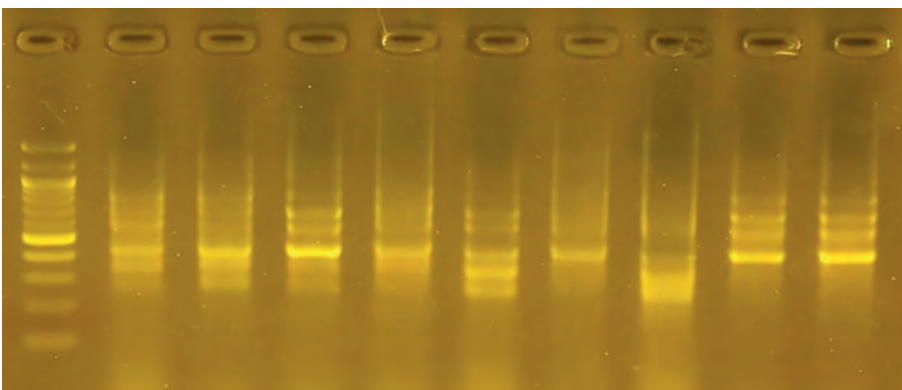
Figure 6. The product of a DNA random amplification reaction using the initiator R5.
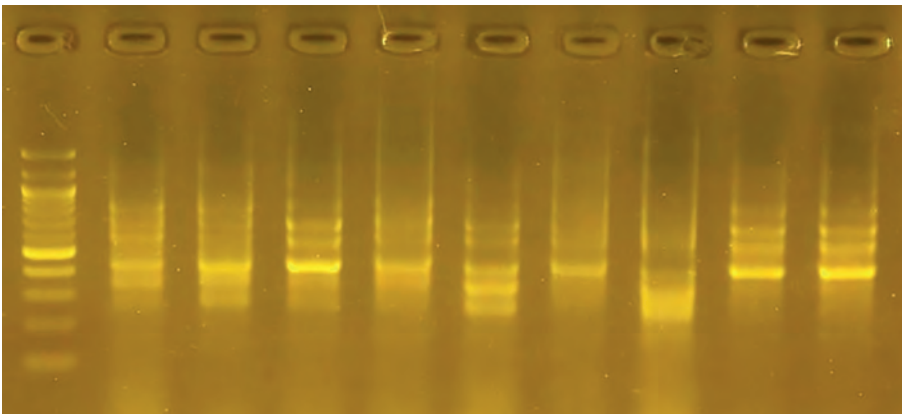
Figure 7. The product of a DNA random amplification reaction using the initiator R6.
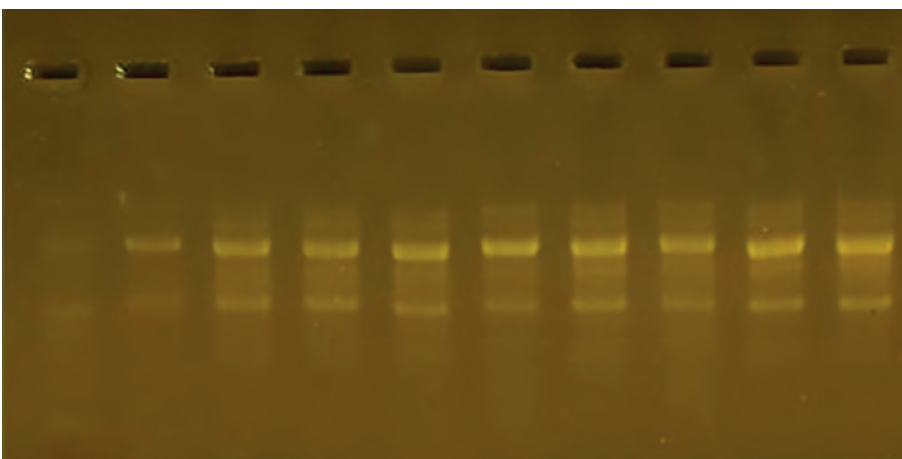
Figure 8. The product of the DNA random amplification reaction using the initiator R7.

6
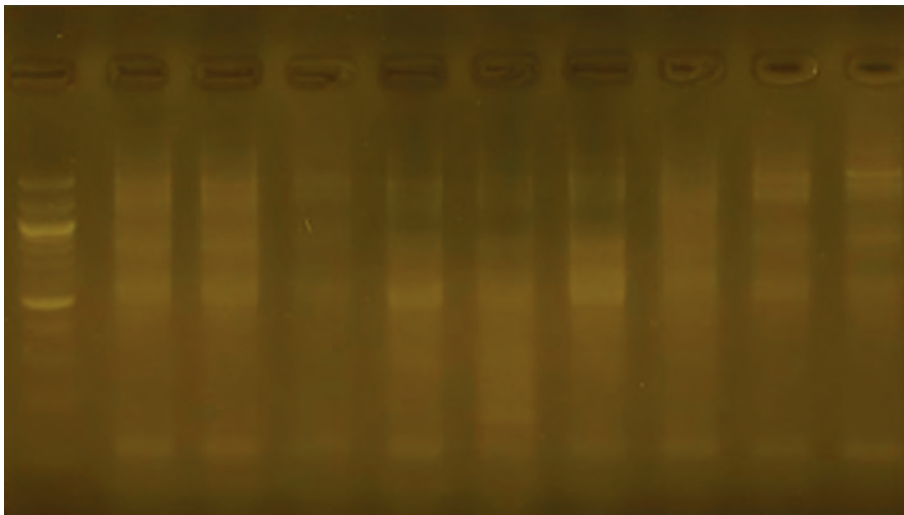
Figure 9. The product of a DNA random amplification reaction using the initiator R8.
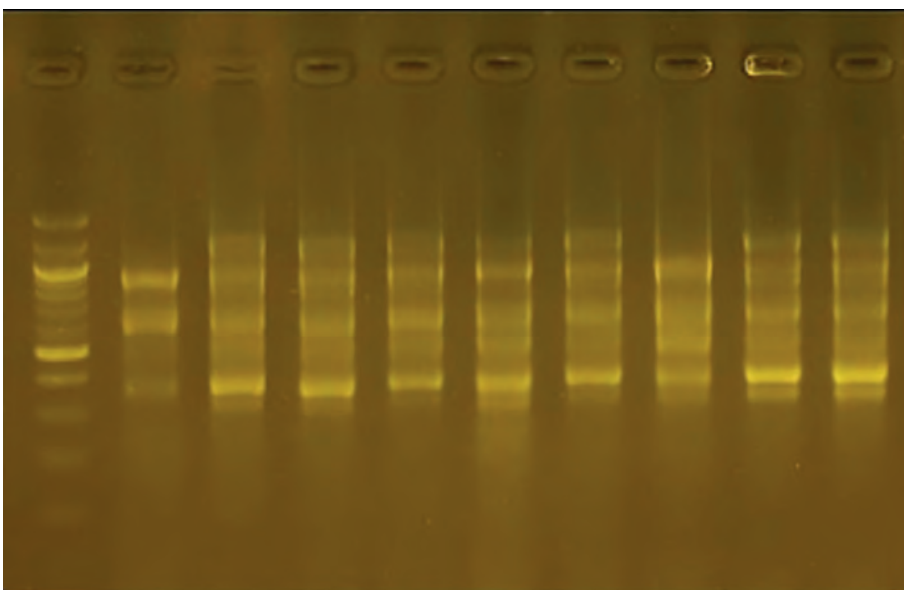
Figure 10. The product of the DNA random amplification reaction using the initiator R9.
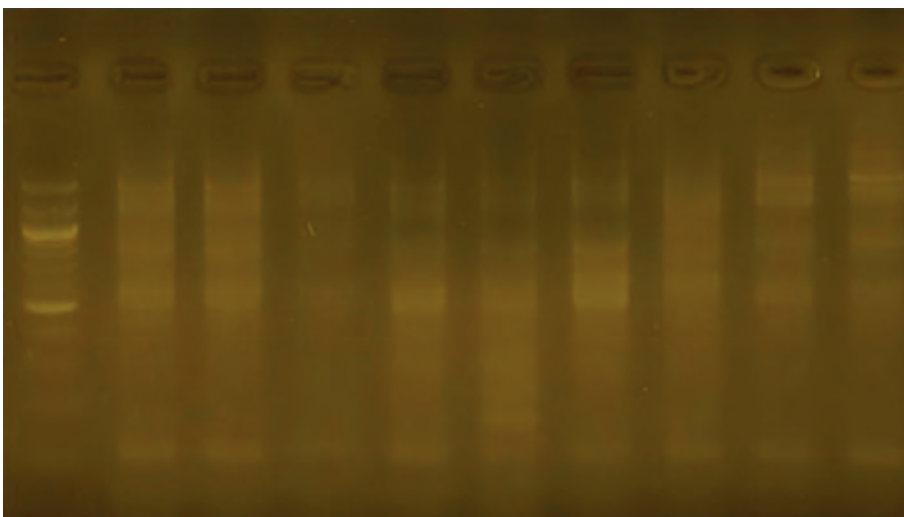
Figure 11. The product of the DNA random amplification reaction using the initiator R10.

bundles; their weight ranged from 300pb to 1100pb. One cultivar was distinguished from the rest of the cultivars by the absence of the bundle. The molecular weight was 300pb, considered a genetic fingerprint for this cultivar. The variance ratio for this cultivar was 25.0.

The relationship genetic tree (Fig. 12) was drawn based on the genetic dimension among the nine varieties.

With a molecular weight of 300 pb, it appeared in cultivar 1, so this cultivar can be distinguished using the 1R primer, which represents a genetic marker for the cultivar and a guide to facilitate the task of differentiation.

Primer 0 1R: The number of bundles produced 48 bundles; their weight ranged from 300pb to 1100pb. One cultivar was distinguished from the rest of the cultivars by the absence of the bundle. The molecular weight was 300pb, which was considered a genetic fingerprint for this cultivar.

The variance ratio for this cultivar was 25.0.

Figure 14 shows the values of genetic dimensions for nine cultivars of wheat, where the values ranged between (0.8727 - 0.4545). Suppose the genetic material is identical between any two cultivars. In that case, the genetic dimension between the two cultivars must be zero. The similarity ratio must be 100%[14], the most significant percentage of similarity appeared between classes 8 and 9 and based on the values of the primers used in the RAPD variants, which means the most similar rate of genetic material between the two classes compared to other varieties, and the reason may be due to their closeness in proportions, while the lowest similarity percentage was between classes 7 and 6 compared to types. This indicates that there are significant differences in the genetic material between them.

The relationship genetic tree (Fig. 12) was drawn based on the genetic dimension among the nine varieties.

Relationship genetic tree

Cluster analysis to build a genetic relationship tree using the UPGMA method depends on the genetic dimension coefficient and allelic frequency. This study drew a genetic relationship tree for nine wheat cultivars using RAPD indicators and ten primers. The aggregate analysis results showed two main groups (Main Cluster). The distance between one group and the other groups indicates their re-lationship. Groups close to each other are placed in close branches within the group, which includes two main groups. The first leading group included two cultivars, class 5 and class 7. The second major group was divided into two minor branches. The first secondary branch included only class 1. The second secondary branch was where the genetic varieties were distributed into two sub-secondary groups. The first sub-secondary branch had two classes, class 8 and class 9. The sub-secondary branch is divided into two groups. The first group was unique to this group by the presence of one category, category 2. The second group was divided into two groups. The first group included classes 3 and 4. In the second group, only category six is included. The importance of determining the genetic relationship by using cluster analysis is due to the possibility of organizing the genetic assets, selecting the parents involved in breeding programs, predicting the best hybrids, and knowing the least possible number of genetic structures that contain the largest possible number of genetic classifications in breeding and improvement programs the plant.

The presence of genetic similarity between varieties of different fathers in the same site may be the reason for their genetic adaptation to the environmental conditions prevailing in that site, so the genetic material is somewhat similar, which led to its reflection in the number of bundles shared between them, or it may have a joint genetic base, and the-
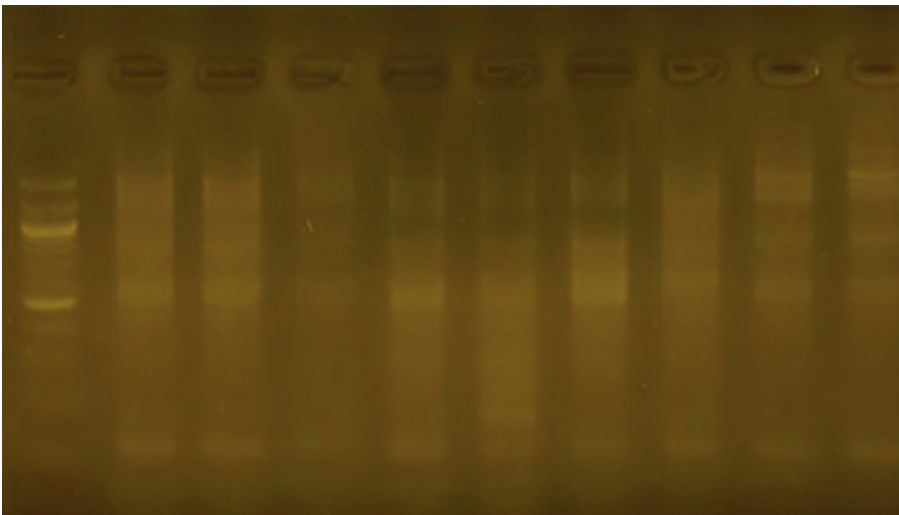
Figure 12. The product of the DNA random amplification reaction using the initiator R9.
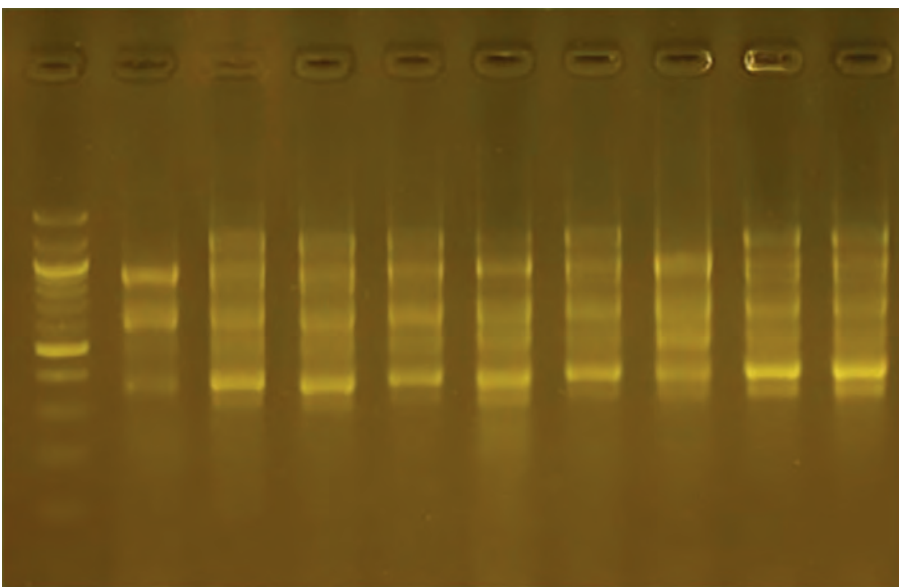
Figure 13. The product of the DNA random amplification reaction using the initiator R10.

```
         A1        A2        A3        A4        A5        A6        A7        A8
      -----------------------------------------------------------------------------
A1 |  1.0000
A2 |  0.7273    1.0000
A3 |  0.7273    0.8182    1.0000
A4 |  0.6909    0.7455    0.8545    1.0000
A5 |  0.5091    0.5636    0.5273    0.4909    1.0000
A6 |  0.6000    0.6909    0.8364    0.8364    0.5091    1.0000
A7 |  0.6364    0.6909    0.5455    0.5455    0.6909    0.4545    1.0000
A8 |  0.7273    0.7091    0.8182    0.7818    0.5273    0.7636    0.5455    1.0000
A9 |  0.6727    0.6909    0.7636    0.6909    0.5091    0.6727    0.5636    0.8727


         A9
      -----------
A9 |  1.0000
```

Figure 14. Similarity matrix computed with Nie coefficient.

refore Genes may flow between different geographic distributions, or the similarity may be due to the common origin of the species 3

Conclusions

Despite the narrow genetic base among the six species used here, RAPD analysis was quite effective in determining the genetic variation among Barley species. It can be used to generate DNA fingerprints for variety identification.

Funding

Acknowledgments

Conflicts of Interest

There is no conflict.

Bibliographic references

1. Behera, T. K ., A. B. Gaikward, A. K. Singh and J. E Staub,. Relative efficiency of DNA markers (RAPD,ISSR and AFLP) in detecting genetic diversity of bitter gourd (Momordica charantia L.) . Short Communication . J Sci Food Agric.2008؛ 88:733–737

2. Dje`,Y, C.G. Tahi, A.I. Zoro Bi, J.-P. Baudoin, and P. Bertin . Use of ISSR markers to assess genetic diversity of African edible seeded Citrullus lanatus landraces . Scientia Horticulturae.2010؛ 124 : 159–164.

3. Ashter, S.Evaluation of some genotyps of the Syrian wheat (hexagonal and quaternary) using biochemical and molecular markers are different. Ph.D. Diss. Agronomy Department. Faculty of Agriculture. University of Tthishreen. Syria.2009؛P:192.

4. Solh, M., Braun, H-J. & Tadesse, W. Save and Grow: Wheat. Paper preparedfor the FAO Technical Consultation on Save and Grow: Maize, Rice and Wheat, Rome, 15–17 December 2014. Rabat,ICARDA. (mimeo).

5. Edmeades, G.O. Maize – Improved varieties. Paper prepared for FAO for Save and Grow: Maize, Rice and Wheat. Rome. (mimeo)2015.

6. JEONG, Jun Seop, et al. Rapid identification of monospecific monoclonal antibodies using a human proteome microarray. Molecular & Cellular Proteomics, 2012, 11.6.

7. MOHAMMED, Bushra MA; KHERAVII, Sarbast KQ. Evaluation of genotoxic potential of Hypericum triquetrifolium extract in somatic and germ cells of male albino mice. Research Opinions in Animal & Veterinary Sciences, 2011.

8. Aydogan, E. and Yagdi, K. Study of genetic diversity in wheat (Triticum aestivum L.) varieties using random amplified polymorphic DNA (RAPD) analysis . Turkish J. Field Crops .,2012؛ 17 : 91-95 .

9. Nei, M. and W.H. Li ¿ Mathematical model for studying genetic variation in terms of restriction endonucleases". Pro. Natl. Acad. Sci. USA.,1976: 74: 5267-527.

10. Sneath P.H.A. and Sokal. Numerical taxonomy-the principals and practice of numerica classification. W.H. Freeman and Co., San Francisco.1973.

11. Rohlf F.J.,. NTSYS-pc: Numerical Taxonomy System. Ver. 2.21.Exeter Software, Setauket, NY, USA.2000: pp. 29-34

12. Tidke, S. D. and Ranawade, P. S. .Genetic Analysis and RAPD Polymorphism in Wheat (Triticum aestivum L.) Genotypes. International Journal of Current Microbiology and Applied Sciences, 2017:6(3): 239-246.

13. Nwangburuka, C.C.; Kehinde, O.B.; Ojo, D.K.; Popoola, A.R.; Oduwaye, O.; Denton, O.A. and Adekoya, M.. Molecular characterization of Twenty-nine Okra Accessions using the random amplified polymorphic DNA (RAPD) molecular marker J.2011 of L. and Ph. 14.

14. Mona, H. A. ; Elrabey, R. M. ; Khalaf, M. H. and Elhalafawi, K. Cytological and Molecular characterization of some Wheat (Triticum aestivum L.) cultivars. Egypt. j.Genet. Cytol.2009:38:235 – 250.

8

ARTICLE / INVESTIGACIÓN

Enhancing salinity tolerance in tomatoes at the reproductive stage by increasing pollen viability

Nasratullah Habibi[1,2]*, Mohammad Yosuf Fakoor[2], Shah Mahomoud Faqiri[2], Zarir Sharaf[2], Mohammad Sadiq Hotak[2], Nelofar Danishyar[2], Mohammad Mustafa Haris[2], Khuwaja Safiullah Osmani[2], Takashi Shinohara[1], Naoki Terada[1], Atsushi Sanada[1], and Kaihei Koshio[1]

DOI. 10.21931/RB/2023.08.01.25

[1] Graduate School of Agriculture, Tokyo University of Agriculture, 1-1-1 Sakuragaoka, Setagaya-ku, Tokyo Japan.
[2] Faculty of Agriculture, Balkh University, Balkh 1701, Afghanistan.
Corresponding author: nasratullah.habibi14@gmail.com

Abstract: This study was conducted to mitigate the adverse effects of sodium chloride stress on the reproductive parameters of tomatoes. This experiment was conducted in the greenhouse of the laboratory of tropical horticultural science, department of International agricultural development, Tokyo University of Agriculture. The design was a factorial CRD (completely randomized design) with five sodium chloride (0 mM, 50 mM, 100 mM, 150 mM, and 200 mM) treatments and four primings (0 MPa, 0.4 MPa, 0.8 MPa, and 1.2 MPa) treatments. Micro-Tom seeds were soaked in polyethylene glycol (PEG6000). Salinity was applied through irrigation water when the first flower bloomed. Reproductive-related parameters such as the number of flowers per plant, pollen viability, pollen germination, pollen tube length, number of fruits per plant, fruits size and yield per plant were measured. It was observed that salinity affected the tomato plants severely during the flowering stage, and many flowers did not bear fruit due to the decrease in pollen viability. In addition, electrolyte leakage increased under salt stress, while priming decreased this parameter. Priming improved the number of flowers, pollen viability, and fruits per plant. The best priming treatments were 0.8 MPa and 1.2 MPa for promoting and enhancing tolerance in the reproductive stage.

Key words: Physiology, priming, pollen viability, reproductive stage, and salinity.

Introduction

Tomato (*Solanum lycopersicum* L.) is one of the essential vegetables around the globe. Countries such as China, the United States, Turkey, Italy, India, and Egypt are the biggest producers of tomatoes[1]. Tomato producers face many challenges and many constraints that limit tomato production[2]. Among abiotic stress factors, salinity is one of the most important abiotic factors that can be found in almost half of the world's soils[3,4]. Salt-affected soils include 63.2 million hectares of topsoil (0-30 cm) and 120.0 million subsoils (30-100 cm)[4]. These soils are formed because of concentrated salts and ions like Na+, which causes degradation[4].

The salt-affected soils are problematic for most plants, and salinity is a high injury factor for vegetable crops like tomatoes worldwide. In some areas, the irrigation source is only seawater. Therefore, further effort is needed to increase water efficiency or plant tolerance[5], but it might be difficult to find a solution for this problem[6] easily.

Salinity affects tomatoes' vegetative and reproductive growth because it slows the absorption of nutrients due to the accumulation of toxic ions like Na+ and Cl-[7]. In vegetables, like tomatoes, the reproductive stage is susceptible, and flowers will be severely affected under salinity[8]. Furthermore, fruits per plant in tomatoes are also harmed due to this factor[9-11], which leads to high leaf surface temperature; thus, stomata start to close, and the cell wall and electrons start to leak from leaf cells[12]. During the reproductive stage, it has been proved that pollen viability and pollen germination are the ideal parameters to be assessed for studying the tolerance of plants against constraints[13] like salinity or heat stress, and both pollen viability and pollen viability and pollen germination decreased under salt stress conditions[14].

There are studies on the breeding and development of salt-tolerant varieties, but most were ineffective for all regions due to climatic fluctuations. Therefore, some easy and effective methods with low cost can increase salt tolerance in the plant before facing stress, one of them is seed priming[9], and it has already been proved that various seed priming agents[10,38] such as polyethylene glycol (PEG) improved growth parameters in tomato plants under sodium chloride stress[11].

In addition, osmo-priming by polyethylene glycol mitigates the toxicity of the ions that are accumulated due to severe salt stress by stabilizing the balance between cations and anions; therefore, polyethylene glycol diminishes the negative effects of Na+ and Cl- ions accumulated in leaves due to sodium chloride salinity stress[13] by increasing the amount of K+ ions[14].

Considering the adverse effects of salinity, tomato is susceptible during their vegetative and reproductive growth, especially in the flowering stage, which is critical against salinity stress[15]. There is no previous study on the comparative effects of PEG6000 and sodium chloride on the reproductive parameters of tomatoes. Thus, the current study was conducted to (a) evaluate the negative effects of salinity on the growth and physiological parameters of tomatoes, (b) evaluate the comparative effectiveness of PEG and salini-

Nasratullah Habibi, Mohammad Yosuf Fakoor, Shah Mahomoud Faqiri, Zarir Sharaf, Mohammad Sadiq Hotak, Nelofar Danishyar, Mohammad Mustafa Haris, Khuwaja Safiullah Osmani, Takashi Shinohara, Naoki Terada, Atsushi Sanada, and Kaihei Koshio

ty on the growth and physiological parameters of tomatoes during flowering and fruit-bearing stages, and (c) study the interaction between PEG and salinity.

Materials and methods

This experiment was conducted at the Tokyo University of Agriculture (Setagaya Campus) in 2021. The experiment was designed as a factorial complete randomized design with 6 replications, having 4 salinity levels and 4 priming treatments, and Micro-Tom seeds were used as plant material. The sodium chloride salinity treatments were (a) control (0 mM), (b) 50 mM, (c) 100 mM, (d) 150 mM, and (e) 200 mM, and priming treatments were (a) control (0 MPa), (b) 0.4 MPa, (c) 0.8 MPa, and (d) 1.2 MPa. PEG6000 was used to prime the seed before cultivation, and the seeds were soaked in the solution for 36 h. Then, the seeds were washed three times with pure water and dried for 3 hours at 25±5°C. The calculation for PEG6000 to be used in osmo-priming was according to Michel & Kaufmann[16] and Aqvila & Carella[17]. The formula 1 was used to calculate the amount of PEG6000 to be dissolved in pure water to prepare priming treatments.

The seeds were cultivated in seed trays at the greenhouse (25±5°C temperature and 60±10 % humidity), and after 30 days, when the plants were 3 to 4 leaves (30 days after germination), they were transplanted to the plant bed made of wool and is called Rockwool.

Salinity was applied at the start of the flowering stage. Salt stress was applied within irrigation water. Irrigation was done using tap water, and we fixed the pH of irrigation to 5.8 – 6, and it was adjusted using sodium hydroxide and hydrochloric acid. Then NaCl was added to the irrigation water in the appropriate molarity and mixed and used for irrigation. Temperature also plays a vital role during salinity stress; therefore, we recorded temperature using a digital thermo-recorder (TR-72WB; ThermoWorks, American Fork, UT, USA). Data were collected hourly, then the average of every 24 hours was taken and represented as daily temperature. The temperature in the greenhouse was adjusted at 25±2 °C by the automatic electric heating system.

Temperature measurement

Temperature is an essential constraint on tomatoes during the reproductive stage. Many researchers have recently reported the negative effects of high and low temperatures on flowering and fruit yield. In the current experiment, temperature data were recorded on an hourly basis from cultivation to harvest. The digital thermometer was used to record the temperature, and the device was kept at least 1 meter from the ground.

Flowers per plant

The number of flowers per plant was counted daily, starting with the first flower blooming and then on the full flowering; the sum of all data was considered as the total number of flowers per plant.

Pollen viability

Pollen viability was determined by MTT (2,5-diphenyl mono-tetrazolium bromide) assay[17]. Some modifications were added to the method. Firstly, 500 mg of agar and 2.5 g of sucrose were poured into a 100 ml beaker, and 47 ml of pure water was added. Then, the solution was kept inside the heater under 70 °C temperature for one minute and mixed well using a strayer. The solution was poured into glassy Petri dishes and covered to avoid contamination. A circle was made in the middle of the medium to keep pollen grains. Then, 50 mg of MTT was taken in a 15 ml falcon, and 5 ml pure water was added and vortexed well. Flowers from all treatments were taken in the morning from 8:00 to 10:00 AM, and pollen was dropped on medium using a sterilized brush. Five flowers were taken from each treatment. The brush was washed using ethanol 100% to be used in each treatment. Then, 0.5 mL of MTT solution was quickly added to pollens using a single channel pipet made by thermos fisher, Japan. Then, the Petri dishes were closed and incubated at 25 °C for one hour. Pollen pictures were taken using CellSense software by microscope (Olympus) with 10x magnification. Pollen with dark colorations was counted as alive and light colorations as dead (Figure 1a). The pollen viability was calculated as formula 2.

$$OP = (-1.18 \times 10^{-2}) \times C - (1.18 \times 10^{-4}) \times C + (2.67 \times 10^{-4}) \times C \times T + (8.39 \times 10^{-7}) \times C^2T \qquad (1)$$

OP is osmotic pressure, C is the PEG concentration, and T is the temperature.
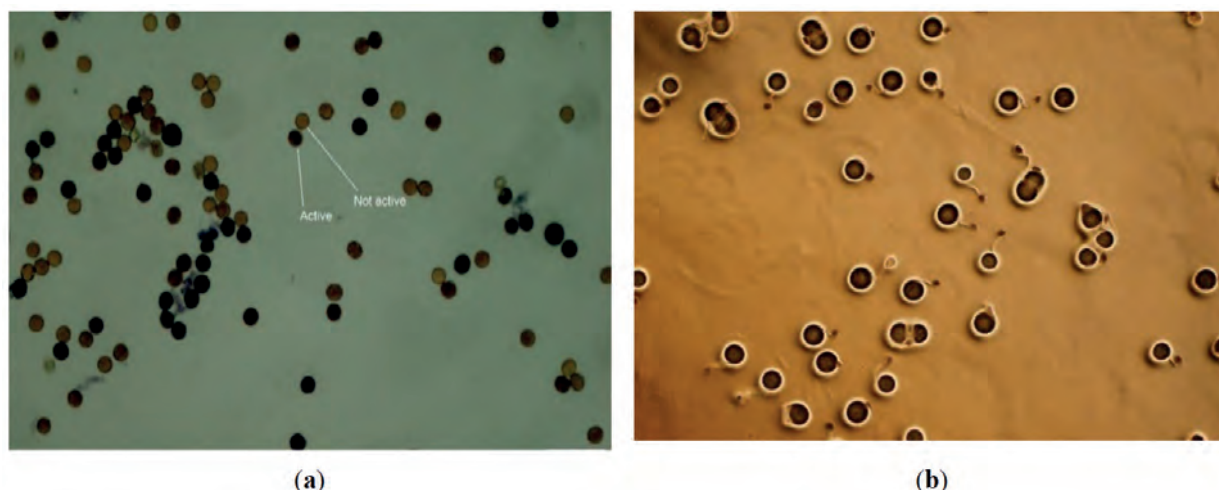
Figure 1. Represents live and dead pollens of tomato flowers (a), and germinated pollens (b).

$$PV\ (\%) = [\ LP\ /\ TP\ ]\ x\ 100 \qquad (2)$$

PV is the pollen viability, LP is the live pollen, and TP is the total number of pollen grains.

Pollen germination

Germinated pollen grains were selected from the pictures taken by a microscope. The number of germinated and non-germinated were counted, and pollen germination percentage was calculated from them (Formula 3) and was measured at 4 hours, 6 hours, 8 hours, and 10 hours after incubation.

Pollen tube length

Pollen tube length was measured using ImageJ software. The pictures taken by the Olympus microscope were analyzed by imageJ for the pollen tube length. Pollen tube Pollen tube length was measured at 4 hours, 6 hours, 8 hours, and 10 hours after incubation.

Leaf injury rate

Leaf injury rate was concluded based on electrolyte leakage (EL) from leaf tissues. A handy meter was used to measure electric conductivity (LAQUATWIN-S070, Horiba Scientific Ltd., Japan), as per the method as described by Habibi[12]. The samples were taken from 15 leaves per treatment and stainless-steel cork-borer with one centimeter diameter was used to make the disk for electric conductivity. Electric conductivity (EC) was measured two times for calculating electrolyte leakage. The first electric conductivity (E1) was measured after keeping the disk inside a vial filled with two milli liter pure water at 25 ± 1 °C temperature for 20 minutes, then the samples were kept under 70 °C for 20 minutes and back cooled to room temperature and electricity was measured for the second time (E2). The following equation was used to calculate the leaf injury:

Yield attributes

The number of fruits per plant was, and these data were taken from six plants in each treatment. Fully ripened fruits were harvested from six plants in each treatment, and then the yield per plant (g) was measured using a digital balance.

Statistical analysis

We used a CRD (complete randomized design) to set up our experiment design. For the data analysis and explanation of the differences, we used two-way, Pearson's correlation analysis, and regression analysis. Analysis of variance was done using the R language, specifically RStudio v3.6.2 statistical software, and correlation analysis with regression analysis and visualization was done using Python software v3.7.4 (Jupyter Notebook, https://api.anaconda.org).

Results

The flowering and reproductive stage was between April 5 to May 10; during this period, the temperature was between 18 to 30 °C, while the fruit growing or harvest stage occurred between May 11 to May 31 with a temperature between 23 to 37 °C. The average daily temperature during the flowering stage was 24 °C, while in the fruit growing and harvest stage, it was 27 °C (Figure 2). The temperature was not considered a factor and was kept constant in the range required for the tomato plant.

Number of flowers per plant

The number of total flowers per plant was significantly affected by salinity and PEG. There was a strongly negative interaction between salinity and PEG; salinity decreased the number of absolute flowers per plant, but PEG increased. Plants under 0.8 MPa and 1.2 MPa PEG produced a more significant number of flowers per plant under all salinity treatments. There is a statistically significant difference between non-primed and primed treatments (Figure 3). The highest number of flowers per plant was recorded at 341 in 0.8 MPa under 50 mM sodium chloride salinity, and 1.2 MPa followed it under the same salinity level, producing 252 flowers per plant.

Pollen viability

In this research, flowers were the most sensitive organ against salinity in the tomato plant. When plants face high salinity stress, most flowers die, and some cannot produce fruits. The reason was that pollens were severely injured by salt stress. The number of life pollens was significantly decreased under salt stress treatments but significantly increased under priming treatments. Furthermore, the interaction between salinity and priming (PEG) was also significant. Only within the groups, the number of life pollen was not significantly different under 50 mM salinity, while for the 100 mM, 150 mM, and 200 mM salinity, 1.2 MPa priming treatment had a more significant number of life pollen compared to the control.

Furthermore, there were more dead pollen grains under salinity treatments with no priming, while the number of dead pollen grains was significantly decreased under priming treatments, and there was a significant negative interaction between salinity and priming. The total number of pollen grains also decreased under salinity, while priming significantly affected it. However, the all-over interaction between salinity and PEG was significant. Finally, pollen viability, considered an important factor for fruit production, was strongly decreased under salinity (p<0.001). However, PEG efficiently improved it; therefore, there was a significant negative interaction between salinity and priming. All PEG treatments had more pollen viability than the control (Table 1).

Figure 4 illustrates a visual comparison of pollen viability in our study. It shows the difference between primed and

$$GP = GPG\ /\ TPG\ *100 \qquad (3)$$

GP is the germination percentage, GPG is the number of germinated pollen grains, and TPG is the total pollen grains.

$$EL\ (\%) = [\ E1\ /\ E2\ ]\ x\ 100 \qquad (4)$$

Nasratullah Habibi, Mohammad Yosuf Fakoor, Shah Mahomoud Faqiri, Zarir Sharaf, Mohammad Sadiq Hotak, Nelofar Danishyar, Mohammad Mustafa Haris, Khuwaja Safiullah Osmani, Takashi Shinohara, Naoki Terada, Atsushi Sanada, and Kaihei Koshio

Figure 2. The average temperature during flowering and fruit-bearing stages.
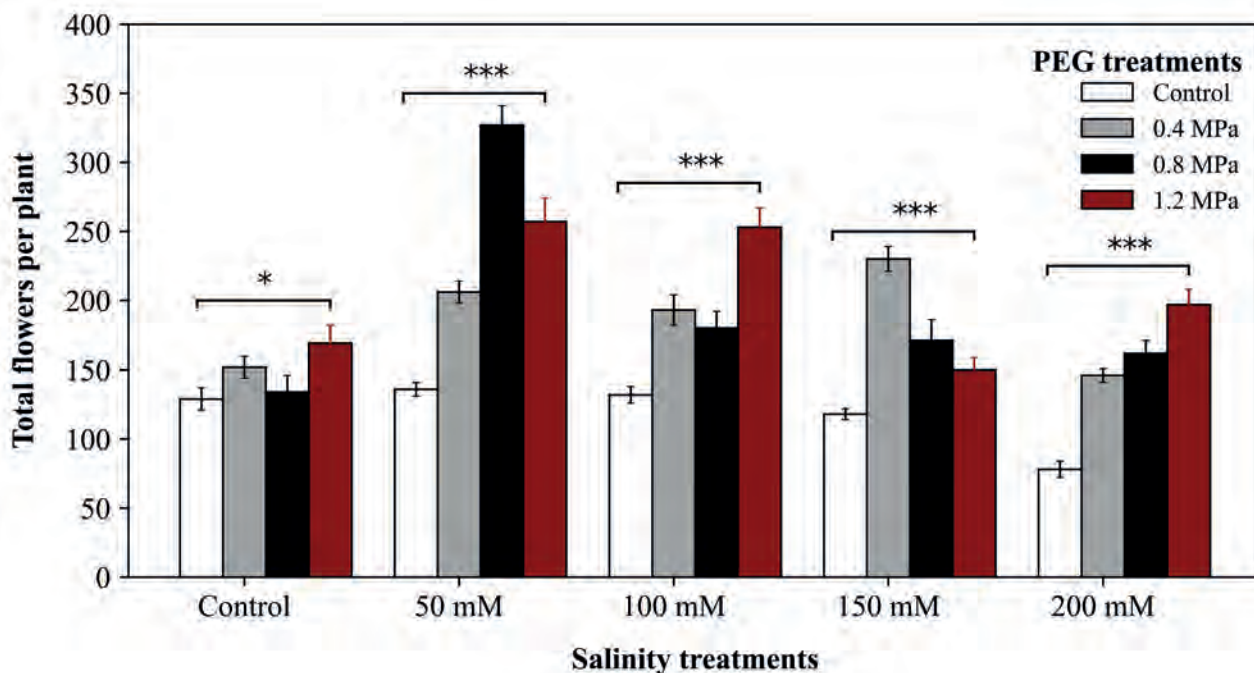
Figure 3. Effect of priming on the total number of flowers per plant under salt stress. *, **, and *** indicate significance levels of P <0.05, P < 0.01, and P < 0.001 respectively.

non-primed tomato plants regarding pollen viability. The top row shows the control (non-primed) plants under different salinity levels, whereas the bottom row shows the pollen viability belonging to the pre-sowing seed-primed plants. This visualization indicates that in non-primed plants, the total number of pollens is sometimes more than in primed ones. However, the flowers belonging to the primed plants had more pollen viability and more living pollen grains. Turning to salt stress conditions, priming treatments increased the total number of pollens compared to the control (Figure 4).

Pollen germination

Pollen germination decreased under salt stress, while priming increased it. Overall, there was a significant difference in pollen germination within each salinity treatment. After 4 hours of incubation, 0.4 MPa and 0.8 MPa priming

treatments showed better performance and the salinity and priming effects were strongly significant, while there was a negative interaction between salinity and priming. After 6 hours after incubation, pollen germination was also affected by both salinity and priming and there was a significant negative interaction between salinity and priming, however, the 0.8 MPa priming treatment was the best one. In addition, the interaction between salinity and priming was negatively significant. Finally, after 10 hours of incubation, primed plants had better pollen germination than the non-primed ones under all salinity treatments (Table 2).

The difference between the highest and lowest pollen germination was 58.4 %, showing a 78,1 % decrease in pollen germination in the salt-stressed plant compared to the normal plants (Table 2). The primed plants with 0.8 MPa of PEG 6000 under no salinity had the highest germination percentage, whereas non-primed plants with 200 mM sa-

Treatments		Pollen viability parameters			
Salinity (S)	PEG (P)	No. of alive pollens	No. of dead pollens	Total No. of pollens	Pollen viability (%)
0 mM	0 MPa	251.2 ± 9.4 b	83.2 ± 9.1 a	334.3 ± 9.2 ab	74.8 ± 4.7 cd
	0.4 MPa	275.7 ± 7.9 ab	18.0 ± 4.8 f	293.7 ± 9.2 bc	94.1 ± 1.3 a
	0.8 MPa	315.7 ± 9.2 a	38.3 ± 5.0 de	354.0 ± 8.1 a	89.3 ± 1.1 ab
	1.2 MPa	293.2 ± 5.8 ab	30.0 ± 2.8 ef	323.2 ± 6.5 ab	90.7 ± 0.8 a
50 mM	0 MPa	172.7 ± 2.4 cd	76.2 ± 6.8 ab	248.8 ± 5.4 cd	69.6 ± 2.3 de
	0.4 MPa	180.2 ± 9.6 cd	59.8 ± 6.5 ab	240.0 ± 8.0 de	74.9 ± 1.3 cd
	0.8 MPa	167.5 ± 5.1 cd	51.2 ± 2.1 cd	218.7 ± 6.0 de	76.6 ± 0.8 cd
	1.2 MPa	199.0 ± 4.4 c	48.2 ± 3.3 de	247.2 ± 4.5 cd	80.5 ± 1.2 bc
100 mM	0 MPa	108.3 ± 1.8 gh	84.2 ± 5.5 a	192.5 ± 6.7 ef	56.5 ± 1.4 g
	0.4 MPa	138.7 ± 4.6 de	64.0 ± 4.3 ab	202.7 ± 6.6 de	68.5 ± 1.5 de
	0.8 MPa	147.3 ± 8.1 de	61.5 ± 4.4 ab	208.8 ± 8.8 de	70.4 ± 1.6 de
	1.2 MPa	155.3 ± 7.0 de	54.2 ± 1.7 bc	209.5 ± 8.3 de	74.1 ± 0.9 cd
150 mM	0 MPa	63.3 ± 1.8 i	84.2 ± 5.5 a	147.5 ± 6.7 hi	43.2 ± 1.3 h
	0.4 MPa	89.0 ± 2.4 hi	64.8 ± 5.5 ab	153.8 ± 6.1 gh	58.2 ± 2.2 g
	0.8 MPa	116.5 ± 6.8 fg	55.2 ± 1.7 bc	171.7 ± 6.5 fg	67.6 ± 1.8 ef
	1.2 MPa	125.7 ± 4.2 ef	55.2 ± 1.7 bc	180.8 ± 5.6 fg	69.5 ± 1.4 de
200 mM	0 MPa	58.3 ± 1.8 i	79.2 ± 5.5 ab	137.5 ± 6.7 i	42.7 ± 1.4 h
	0.4 MPa	84.0 ± 2.4 hi	61.5 ± 4.3 ab	145.5 ± 4.6 hi	57.9 ± 1.9 g
	0.8 MPa	84.2 ± 2.3 hi	50.2 ± 1.7 cd	134.3 ± 2.3 i	62.6 ± 1.2 fg
	1.2 MPa	121.3 ± 3.8 fg	50.2 ± 1.7 cd	171.5 ± 5.2 fg	70.7 ± 1.4 de
Significance	S	***	***	***	***
	P	***	***	*	***
	S : P	**	**	**	***

ns: not significant. *, **, and *** indicate significance levels of $P < 0.05$, $P < 0.01$, and $P < 0.001$ respectively. Data is represented as 'mean ± SE,' and different letters show differences between means.

Table 1. Effect of PEG priming on pollen-related parameters of tomato plants under salt stress.

| (a) | (b) | (c) | (d) | (e) |
| (f) | (g) | (h) | (i) | (j) |
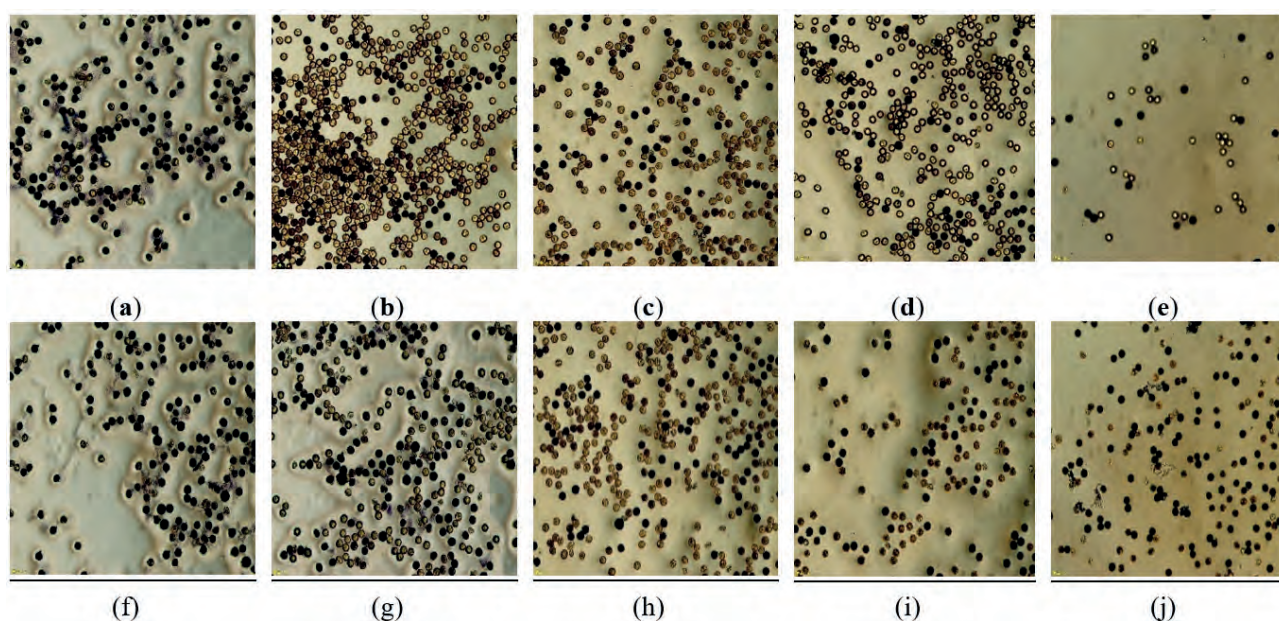
Figure 4. Represents the effects of priming treatments on pollen viability of tomatoes under salt stress compared to ambient conditions. Top row shows pollen viability in control – control (a), 50 mM – control (b), 100 mM – control (c), 150 mM – control (d), 200 mM – control (e) treatments, while the bottom row shows pollen viability in control – 1.2 MPa (f), 50 mM – 0.4 MPa (g), 100 mM – 1.2 MPa (h), 150 mM – 1.2 MPa (i), and 200 mM – 1.2 MPa (j) treatments.

5

Nasratullah Habibi, Mohammad Yosuf Fakoor, Shah Mahomoud Faqiri, Zarir Sharaf, Mohammad Sadiq Hotak, Nelofar Danishyar, Mohammad Mustafa Haris, Khuwaja Safiullah Osmani, Takashi Shinohara, Naoki Terada, Atsushi Sanada, and Kaihei Koshio

Treatments		Pollen germination (%) / hours of incubation			
Salinity (S)	PEG (P)	4 hours	6 hours	8 hours	10 hours
0 mM	0 MPa	64.7 ± 1.0 ab	71.3 ± 1.4 ab	79.3 ± 1.4 ab	84.3 ± 2.5 ab
	0.4 MPa	67.0 ± 1.1 ab	73.7 ± 1.4 ab	84.7 ± 1.4 a	90.0 ± 1.2 a
	0.8 MPa	74.7 ± 1.6 a	82.3 ± 1.2 a	81.3 ± 1.2 a	89.3 ± 2.2 a
	1.2 MPa	71.3 ± 1.2 a	78.3 ± 0.6 ab	86.3 ± 0.6 a	91.0 ± 0.4 a
50 mM	0 MPa	34.0 ± 1.2 de	43.0 ± 1.2 ef	54.0 ± 1.2 d	58.3 ± 1.9 de
	0.4 MPa	61.0 ± 2.0 ab	67.7 ± 1.6 bc	66.7 ± 1.6 c	73.3 ± 1.0 c
	0.8 MPa	56.0 ± 0.4 bc	63.0 ± 0.8 cd	71.0 ± 0.8 bc	76.0 ± 0.7 bc
	1.2 MPa	45.7 ± 0.2 cd	52.7 ± 0.8 de	63.7 ± 0.8 c	67.0 ± 1.1 cd
100 mM	0 MPa	32.7 ± 4.4 de	40.3 ± 3.8 ef	45.3 ± 1.7 de	51.3 ± 1.8 ef
	0.4 MPa	32.7 ± 2.1 de	40.3 ± 2.4 ef	50.3 ± 1.7 de	54.0 ± 1.2 ef
	0.8 MPa	43.7 ± 1.8 cd	51.0 ± 1.5 de	54.0 ± 1.5 d	62.0 ± 2.3 de
	1.2 MPa	41.0 ± 1.5 de	49.0 ± 1.5 ef	54.0 ± 0.8 d	60.7 ± 0.6 de
150 mM	0 MPa	20.3 ± 1.7 gh	28.0 ± 1.8 ij	38.0 ± 1.1 fg	42.3 ± 1.6 hi
	0.4 MPa	31.0 ± 2.5 ef	38.7 ± 2.0 fg	41.7 ± 0.8 ef	50.0 ± 1.3 fg
	0.8 MPa	28.7 ± 1.2 fg	36.3 ± 0.6 gh	44.3 ± 0.6 ef	50.3 ± 0.8 fg
	1.2 MPa	22.3 ± 0.2 gh	29.0 ± 0.4 ij	40.0 ± 0.4 fg	45.0 ± 1.2 gh
200 mM	0 MPa	16.3 ± 3.2 i	25.0 ± 3.2 k	30.0 ± 1.2 h	36.0 ± 0.8 j
	0.4 MPa	18.3 ± 1.9 hi	25.3 ± 1.2 jk	35.3 ± 1.0 gh	39.7 ± 1.2 ij
	0.8 MPa	26.7 ± 2.1 fg	34.3 ± 2.7 hi	37.3 ± 0.8 fg	44.0 ± 1.1 gh
	1.2 MPa	19.3 ± 1.6 hi	26.3 ± 1.0 jk	34.3 ± 1.0 gh	41.3 ± 1.5 hi
Significance	S	***	***	***	***
	P	***	***	***	***
	S : P	***	***	**	*

ns: not significant. *, **, and *** indicate significance levels of P <0.05, P < 0.01, and P < 0.001 respectively.

Data is represented as 'mean ± SE' and different letters show significant differences.

Table 2. Effect of PEG priming on pollen-related parameters of tomato plants under salt stress.

linity had the lowest value. The variation at 6, 8, and 10 hours after incubation was 69.6 %, 65.2 %, and 60.4 %, respectively. The highest pollen germination for 6, 8, and 10 hours after incubation belonged to 0.8 MPa, 1.2 MPa, and 1.2 MPa treatments, whereas under 200 mM salinity had the lowest values under 6, 8, and 10 hours after incubation.

Pollen tube length

Pollen tube length was affected by salinity and priming, where salinity diminished the pollen tube length but oppositely, priming increased the pollen tube length, leading to a higher pollen tube growth speed. There was a significant effect of salinity on pollen tubes after four hours of incubation, while a positive impact of priming was found on pollen tubes. The statistical analysis showed an opposite interaction between salinity and priming treatments.

According to Table 3, after 4 hours of incubation, the 0.4 MPa priming treatment had higher pollen tube length (12.7 μm, 8.5 μm, 7.9 μm, and 6.9 μm) at 0, 50, 100, and 200 mM salinity treatments, while in 150 mM salinity there was no significant differences of pollen tube length between primed and non-primed plants. At 6 hours after incubation, all priming treatments affected the pollen tube length at no salinity treatment (0 mM), while the differences were not significant for salinity treatments. At 8 hours after incubation 0.4 and 0.8 MPa priming treatment had a good performance at 0 mM, 50 mM, 150 mM, and 200 mM salinity, while 1.2 MPa was good at 100 mM and 200 mM salinity compared to the non-primed plants. At 10 hours after incubation, 0.4 MPa priming treatment was the best at all salinity levels.

Leaf injury and survival rate

Leaf injury was decided based on electrons (elec-

trolyte leakage) that were leaked from leaf tissues. There was a positive relation between EL and salinity. A higher EL was observed in saline treatments compared to control during flower blooming and fruiting. Therefore, the flowers wilted, and fewer fruits were formed in saline treatments. Furthermore, salinity decreased the survival rate (%) in tomato plants under saline treatments compared to control, except for 50 mM NaCl stress (Table 4). Seed pre-sowing priming with PEG 6000 decreased EL during both flowering and fruit-bearing. In addition, there was a significant interaction between salinity and priming treatments. In ambient conditions, 0.4 and 1.2 MPa priming treatments significantly decreased the electrolyte leakage of leaves during the flowering stage, while in the fruit-bearing stage, 0.8 and 1.2 MPa priming treatments could dramatically decrease the leaf electrolyte leakage compared to non-primed plants. In 50 mM salinity, 0.4 and 1.2 MPa had the lowest electrolyte leakage in flowering and fruit-bearing stages. In 100 mM salinity, during the flowering stage 0.8 MPa priming treatment and flowering stage, 1.2 MPa priming treatment had lower electrolyte leakage compared to others. In the 200 mM salinity treatment, 0.4 MPa priming treatment was the best treatment during the flowering stage, but during the fruit-bearing stage, 1.2 MPa was the best priming treatment (Table 4).

Number of fruits per plant and plant yield

These two parameters were severely affected by salinity. In this study, the number of fruits per plant decreased under salinity levels, but priming increased them compared to non-primed plants. The treatment of 0 mM salinity and 1.2 MPa priming treatments had a higher number of fruits (45 fruits per plant), while 0.4 and 0.8 MPa were almost

Treatments		Pollen tube length (µm) / hours of incubation			
Salinity (S)	PEG (P)	4 hours	6 hours	8 hours	10 hours
0 mM	0 MPa	9.7 ± 0.3 bcd	11.2 ± 1.3 abc	27.1 ± 2.0 bc	27.9 ± 2.3 bc
	0.4 MPa	12.7 ± 2.1 a	12.7 ± 1.7 a	32.8 ± 1.2 a	4.7 ± 1.1 a
	0.8 MPa	11.5 ± 1.3 ab	11.4 ± 2.2 ab	30.4 ± 1.6 ab	32.1 ± 1.8 ab
	1.2 MPa	10.3 ± 0.5 bc	11.4 ± 2.0 ab	27.1 ± 1.3 bc	28.0 ± 1.1 bc
50 mM	0 MPa	8.1 ± 0.2 de	10.3 ± 0.8 bc	25.5 ± 1.8 c	26.6 ± 2.6 cd
	0.4 MPa	8.5 ± 0.3 cd	11.0 ± 0.4 abc	28.0 ± 0.5 bc	29.9 ± 0.7 bc
	0.8 MPa	8.1 ± 0.2 de	10.9 ± 1.2 abc	26.7 ± 1.2 bc	28.3 ± 1.7 bc
	1.2 MPa	8.3 ± 0.5 de	10.7 ± 2.4 abc	27.6 ± 0.8 bc	29.4 ± 1.0 bc
100 mM	0 MPa	7.5 ± 0.2 efg	10.0 ± 0.2 bcd	24.4 ± 2.0 c	26.1 ± 1.5 cd
	0.4 MPa	7.9 ± 0.3 de	10.5 ± 3.0 bc	25.9 ± 2.1 c	28.4 ± 1.6 bc
	0.8 MPa	7.7 ± 0.4 ef	10.5 ± 0.7 bc	26.0 ± 2.1 c	28.2 ± 1.5 bc
	1.2 MPa	7.6 ± 0.4 ef	10.1 ± 1.1 bc	27.1 ± 0.3 bc	29.0 ± 0.4 bc
150 mM	0 MPa	6.7 ± 0.4 fgh	9.1 ± 2.4 cde	24.8 ± 1.1 cd	28.9 ± 0.4 bc
	0.4 MPa	7.5 ± 0.3 ef	9.7 ± 2.3 bcd	27.0 ± 0.2 bc	27.3 ± 1.4 cd
	0.8 MPa	7.4 ± 0.3 ef	9.7 ± 2.8 bcd	26.1 ± 0.5 bc	28.4 ± 0.6 bc
	1.2 MPa	7.3 ± 0.4 ef	9.4 ± 3.0 bcd	26.6 ± 0.5 bc	26.9 ± 1.7 cd
200 mM	0 MPa	5.8 ± 0.4 g	6.2 ± 2.1 ef	23.8 ± 1.6 d	24.0 ± 1.6 d
	0.4 MPa	6.9 ± 0.4 ef	7.1 ± 0.2 cd	26.4 ± 0.2 bc	28.3 ± 0.3 bc
	0.8 MPa	6.5 ± 0.3 fg	6.9 ± 0.4 de	25.0 ± 2.2 c	27.3 ± 1.6 cd
	1.2 MPa	6.9 ± 0.2 ef	7.0 ± 0.4 cd	25.8 ± 1.0 c	26.4 ± 1.4 cd
Significance	S	***	***	***	***
	P	***	**	**	***
	S : P	*	ns	*	*

ns: not significant. *, **, and *** indicate significance levels of P <0.05, P < 0.01, and P < 0.001 respectively.
Data is represented as 'mean ± SE' and different letters show differences between means.

Table 3. Effect of priming on pollen tube length of tomato under salt stress.

Treatments		Electrolyte leakage (%)	
Salinity (S)	PEG (P)	Flowering stage	Fruit bearing stage
0 mM	0 MPa	26.08 ± 2.31 fgh	28.73 ± 3.98 def
	0.4 MPa	24.00 ± 6.20 h	29.4 ± 0.32 def
	0.8 MPa	28.18 ± 4.65 def	26.75 ± 4.63 fg
	1.2 MPa	24.82 ± 4.39 gh	20.87 ± 10.67 g
50 mM	0 MPa	36.06 ± 2.48 cde	44.31 ± 2.7 ab
	0.4 MPa	27.27 ± 1.79 efg	32.4 ± 3.46 cde
	0.8 MPa	30.27 ± 2.1 def	35.83 ± 1.98 bcd
	1.2 MPa	27.71 ± 1.09 efg	34.83 ± 3.97 cde
100 mM	0 MPa	44.31 ± 1.35 abc	48.91 ± 7.53 a
	0.4 MPa	32.40 ± 1.73 def	33.97 ± 1.39 cde
	0.8 MPa	34.83 ± 1.99 cde	33.61 ± 1.33 cde
	1.2 MPa	35.83 ± 0.99 cde	32.22 ± 1.89 cde
150 mM	0 MPa	48.91 ± 3.77 ab	50.36 ± 2.76 a
	0.4 MPa	33.97 ± 0.7 cde	38.53 ± 1.29 bc
	0.8 MPa	32.22 ± 0.94 def	37.04 ± 1.72 bcd
	1.2 MPa	33.61 ± 0.66 def	36.23 ± 1.72 bcd
200 mM	0 MPa	50.36 ± 1.38 a	36.06 ± 4.97 bcd
	0.4 MPa	36.23 ± 0.86 cde	30.27 ± 4.2 cde
	0.8 MPa	38.53 ± 0.64 bcd	27.71 ± 2.17 efg
	1.2 MPa	37.04 ± 0.86 cde	27.27 ± 3.58 fg
Significance	S	***	***
	P	***	***
	S : P	*	***

ns: not significant. *, **, and *** indicate significance levels of P <0.05, P < 0.01, and P < 0.001 respectively.

Data is represented as 'mean ± SE' and different letters show differences between means.
Table 4. Effect of PEG priming on leaf electrolyte leakage of tomato plants under salt stress.

Nasratullah Habibi, Mohammad Yosuf Fakoor, Shah Mahomoud Faqiri, Zarir Sharaf, Mohammad Sadiq Hotak, Nelofar Danishyar, Mohammad Mustafa Haris, Khuwaja Safiullah Osmani, Takashi Shinohara, Naoki Terada, Atsushi Sanada, and Kaihei Koshio

equal, but all priming treatments were better than non-primed treatments. Priming was effective in all salinity levels, like In 50 mM, 100 mM, and 200 mM salinity level, plants under 1.2 MPa priming treatment had more number fruits per plant, while in 150 mM salinity 0.8 MPa priming treatment was better than others (Figure 5A). Yield per plant was affected by salinity too. There was no significant effect of priming in control, but in 50 mM salinity, the differences between primed and non-primed plants were significant. The 1.2 MPa priming treatment produced more yield than others in all salinity levels (Figure 5B).

Regression analysis

Based on linear regression analysis, the pollen viability and germination model explained 80 % of the variation of the data. Independently, pollen viability and the number of fruits per plant explained 79 %, and pollen viability and yield explained 69 %. It was found that there is a strong relationship between pollen viability and pollen germination, which

means that an increment follows an increment in pollen viability in pollen germination. In addition, in flowers showing more alive, pollens also showed more germinated pollen grains. An increase in pollen viability caused a substantial increment in the number of fruits per plant, meaning that pollen viability directly affects the fruit set. Moreover, pollen viability is directly related to yield per plant (Figure 6).

In addition, there was a negative interaction between EL with pollen viability, number of fruits per plant, and yield. The linear models showed that EL gradually decreased pollen viability, leading to a lower number of fruits per plant and lower yield (Figure 6).

Correlation analysis

Pearson's correlation was conducted to study the relationship between pollen parameters and fruit set. The number of live pollen grains had a strong positive correlation with the total number of flowers, but in high salinity treatments, even if some flowers remained, the number of live
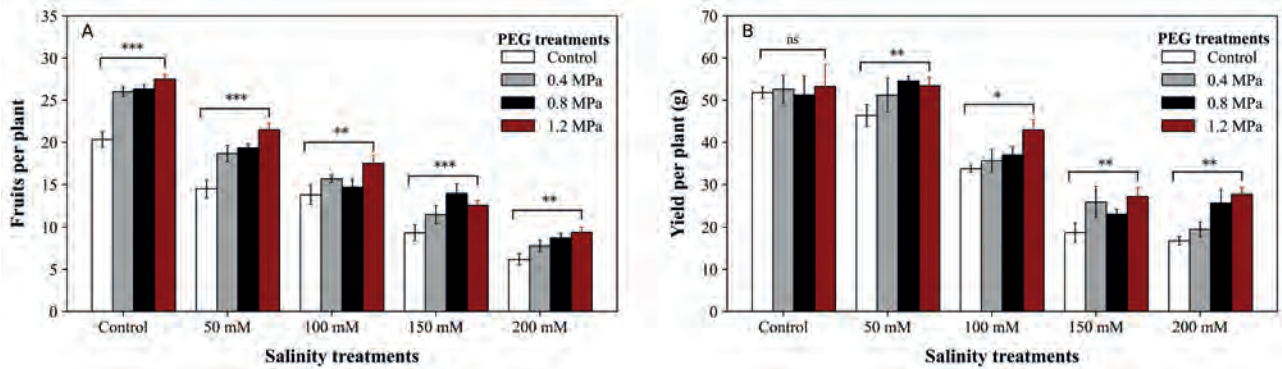
Figure 5. Effect of seed priming on fruits per plant (a) and yield per plant (b) of tomato under salt stress. *, **, and *** indicate significance levels of P <0.05, P < 0.01, and P < 0.001 respectively. ns: not significant.
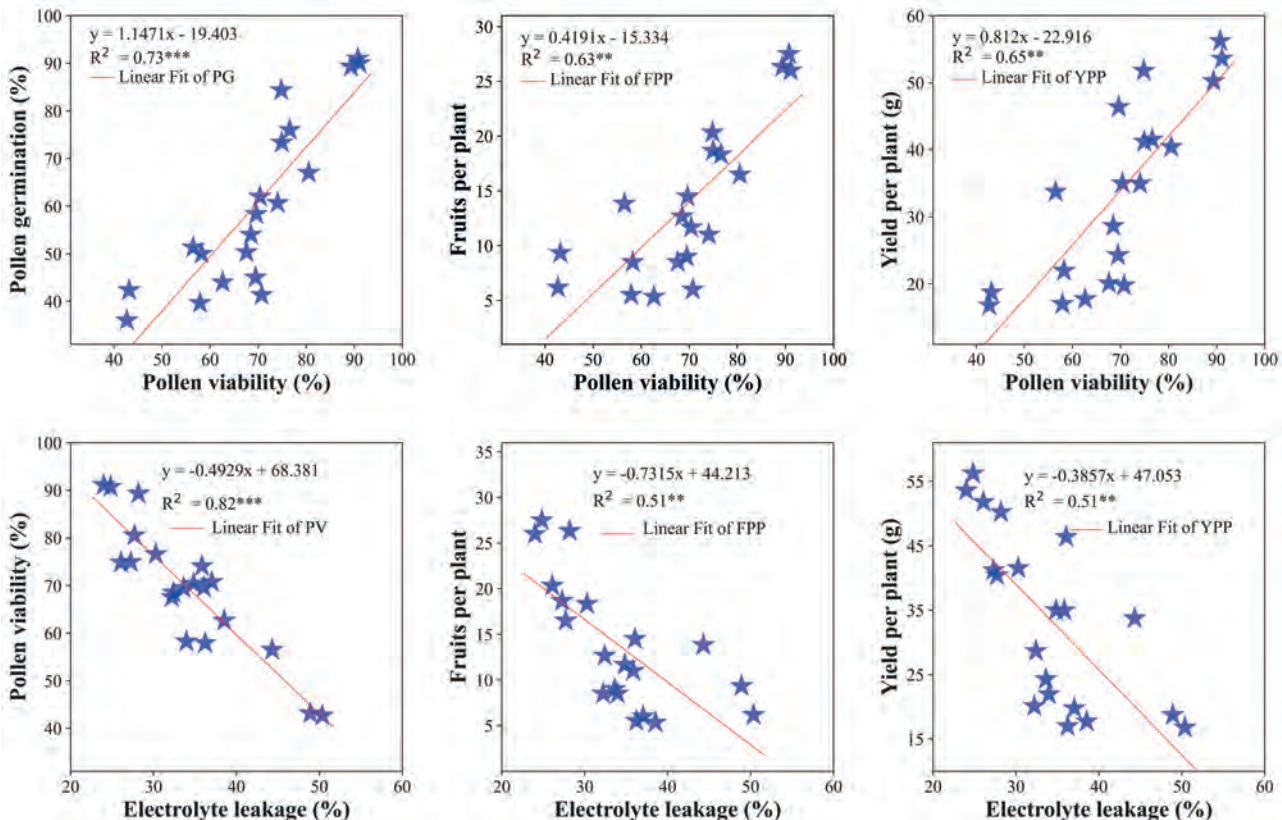
Figure 6. Regression analysis of pollen viability, fruits per plant and yield per plant. PV: pollen viability, PG: pollen germination, FPP: fruits per plant, and YPP: yield per plant.

pollen was less. Furthermore, the number of live pollens and death pollens had a significantly negative correlation. The total number of pollens had a strong positive correlation with the number of flowers per plant and the number of live pollens, which means that if there was a more significant number of flowers in a plant, there was more total number of pollen and more live pollen grains. Moreover, pollen viability had a positive correlation with the number of live pollen grains and the total number of pollen grains but had a negative correlation with the number of death pollen grains. Pollen germination had a strong correlation with flowers per plant, the number of live pollens, the total number of pollens, and pollen viability. Hence, the number of fruits per plant is an important yield parameter had a strong positive correlation with the number of flowers per plant, number of live pollen grains, total number of pollen grains, pollen viability, and pollen germination (Table 5).

Discussion

Temperature is a very important factor besides other constraints on tomato plants during the reproductive stage. Many researchers early up to recently reported the negative effects of high and low temperature[17] on flowering and fruit yield[18].

Flowers are the sensitive organ of plants that can be harmed very quickly due to unboreable environmental conditions. Sodium ions accumulation due to salinity is very harmful to the number of flowers per plant, as previously reported too[12,18]. It's reported that salinity decreases the total number of flowers per plant. Furthermore, according to the previous reported result, sodium chloride salinity delays, the flowering date, and plants under salt stress took more days to produce flowers[8,21]. Moreover, also it's stated that plants under salt stress produce a smaller number of flowers per plant compared to the control plant where no salinity was applied[8,22]. In addition, a delay in production was also reported in tomatoes under salt stress[23]. All the reports are in parallel to our findings except for the effects of priming on the number of flowers per plant under salt stress, where there is very little information about this issue.

Moreover, it is important to be mentioned that some plants can produce flowers under salinity stress, but their flowers don't bear fruits due to inactive pollens. It is also been stated that pollen viability decreases as the salinity concentration increase[24], and this research work was on the effects of salinity on pollen viability and pollen germination of different olive cultivars, and they believe that these parameters can be considered while testing the salt tolerance in plants. And a decrease in pollen viability, pollen germina-

tion, and pollen growth was[25] in Maize while the plants were grown under sodium chloride salinity conditions. Therefore, we conclude that pollen viability is an important factor in explaining the tolerance of plants against abiotic stresses. The difference between their study and ours is, firstly, the plant, and secondly, they just did the screening on the effects of salinity but nothing about increasing the tolerance. At the same time, our study provides enough evidence that seed priming with PEG6000 enhances tomato pollen viability under salt stress.

In high salt stress exposure, pollen viability and pollen germination decrement drastically, and it is reported that pollen viability and pollen germination in tomato plant decreases severely based on type and doses of salinity, and they reported that pollen germination is blocked in over 50 mM. Does of sodium chloride salinity[23,26]. Confirming this result, we also found the same result, but even under more than 50 mM sodium priming could improve our experiment's pollen viability and germination.

It was also found that high sodium chloride salinity decreases the pollen and pollen germination ability for the tomato plant, and they observed that more Na$^+$ was accumulated in flowering organs like style, ovary, and anthers while K$^+$ was decreased[23]. Besides, a significant decrease in pollen viability and pollen germination in chickpeas under 40 mM sodium chloride compared to control was observed[24,27].

Besides, 25 mM sodium chloride could significantly decrease the pollen germination percentage of four olive cultivars[24]. Moreover, it is reported that pollen germination of canola flowers was negatively affected by seawater, where the high salinity treatment decreased the pollen germination to 31-35 % based on varieties[25,28]. In addition, a significant decrease in pollen germination of tomato plant flowers is also reported under 25 and 50 mM of sodium chloride salinity[37], which leads to a low fruit yield. The significance of our study is that we improved the pollen germination of the tomato plant's flowers by pre-sowing seed priming with PEG6000, which is a new finding, and there is no previous report about it. Based on reports[23,26], salinity can decrease the pollen tube length, which confirms our finding, but the difference is that they used olive as plant material, and we used tomato. Furthermore, they used 0, 6.25, 12.5, 18.75 and 25mM of NaCl as salinity treatments, while we used higher concentrations (0, 50, 100, 150, and 200 mM NaCl) in our experiment.

It was observed that salt stress could increase electrolyte leakage in lettuce and spinach[26] because under high salt stress, the cell membrane will be broken and more electrons will come out of tissues, hence, it can the electrolyte leakage could be concluded as cell injury indicator. It means as peroxidation happens in reproductive organs,

	LP	DP	TP	PV	PG	Fr
Fl	0.71***	0.24	0.86***	0.39	0.78***	0.72***
LP		-0.45*	0.96***	0.91***	0.87***	0.94***
DP			-0.18	-0.75***	-0.33	-0.4
TP				0.76***	0.85***	0.92***
PV					0.74***	0.84***
PG						0.91***

Fl: total number of flowers per plant, LP: number of live pollens, DP: number of death pollens, TP: total number of pollens, PV: pollen viability, PG: pollen germination, Fr: total number of fruits per plant. *, **, and *** indicate significance levels of P <0.05, P < 0.01, and P < 0.001 respectively.

Table 5. Correlation Matrix of reproductive-related parameters.

Nasratullah Habibi, Mohammad Yosuf Fakoor, Shah Mahomoud Faqiri, Zarir Sharaf, Mohammad Sadiq Hotak, Nelofar Danishyar, Mohammad Mustafa Haris, Khuwaja Safiullah Osmani, Takashi Shinohara, Naoki Terada, Atsushi Sanada, and Kaihei Koshio

the cell membrane will be damaged, and electrons will leak. Therefore, the pollens will dye, and pollen viability will be decreased. Habibi reported that a decrease follows an increase in electrolyte leakage in flowers per plant and yield per plant[12,27]. However, no research has been conducted before to show that seed priming with PEG6000 was effective on yield parameters of tomato plants und saline conditions, and our result is the first report in this regard.

Moreover, salt stress affects fruits per plant and yield per plant and it is reported that salinity decreases the number of fruits in tomatoes while salinization time was not significantly effective[28,29], but in our study, we found that salinity substantially decreases the number of fruits per plant and fruit yield per plant too. Furthermore, it is reported that a salinity level of more than 150 mM is critical for the tomato plant, and they observe a huge reduction in tomato yield under 200 mM sodium chloride[30]. While we also found that salt stress can severely decrease the number of fruits per plant and the yield per plant, the results from Cano[31] and Harel[32] support our result that seed priming increases tomato yield under salt stress, but they primed the seeds with sodium chloride itself, while we primed the seeds with polyethylene glycol. A 9-10 % yield decrease in tomatoes under salt stress was reported, while seed priming with sodium chloride increased the yield compared to non-primed plants[33].

In the current study, we did the regression analysis to find the relationship between pollen viability, fruits per plant, and yield per plant and consequently found that there was a strong relationship between pollen viability and fruits per plant and yield per plant which proves that more alive pollens will produce a greater number of fruits per plant which leads to higher yield production. Also, it is stated that pollen viability has a strong and direct relationship with fruit set and the number of fruits per plant[34,35]. In addition, it is also reported that a reduction in pollen viability and pollen germination caused the same reduction in fruit set of tomato plants under high temperature[36], while a similar result was reported under high humidity and high temperature[37]. Therefore, the significance of our research is that there is no previous research work on the effect of seed priming by PEG6000 on the reproductive attributes of tomatoes under sodium chloride salinity.

Conclusions

Salinity severely affects the tomato plant during the reproductive stage. It damages the metabolism of the plant by harming physiological processes in the plant, and also it damages the cell wall and increases electrolyte leakage in leaves. Furthermore, the flower, which is a very sensitive organ of the plant, is also affected severely due to cell membrane damage through electrolyte leakage; therefore, many flowers dye under high salinity before bearing fruits, and they have low pollen viability because mostly pollens immediately dye when they face high salt stress. Moreover, the fruits under salinity stress will be smaller in size. However, seed pre-sowing priming with polyethylene glycol (PEG6000) improves the pre-tolerance in plants in a very early young stage. The polyethylene glycol produces a negative pressure around the seed while priming and sucks the inside content of the seed. The same process happens when the plant faces salinity stress. Therefore, the plant adapts to such stress and hereafter, when it faces such stress it can tolerate it.

Author Contributions

Conceptualization, NH, KK, A. S, and NT; Methodology, NH, MYF, TS, and KK; Software, NH, SMF; Validation, NH, AS, ZS, and KK; Formal analysis, NH, MMH, MSH, ND.; Investigation, NH, KK, and TS; Resources, NH, MYF; Data curation, NH, MYF, NT, MMH, KSU, and SMF; Writing-original, N.H.; Writing-reviews and editing, ZS, MSH, SMF, MMH, KSU, and KK Visualization, NH, ND.; Project administration, NH, KK. All authors have read and agreed to the published version of the manuscript.

Institutional Review Board Statement

Not applicable.

Informed Consent Statement

Not applicable.

Conflicts of Interest

The authors declare no conflict of interest.

Bibliographic references

1. Sanower Hossain, M.; Sultan Ahmad Shah, J. Present scenario of global salt affected soils, its management and importance of salinity research . Int. Res. J. Biol. Sci. Pers. 2019, 1(1): 1-3.
2. Jaime D. P. V. Analytical model for the global consumption of tomatoes. Afr. J. Agr. Res 2012, 7(15). doi:10.5897/AJAR11.529
3. Bacha, H.; Tekaya, M.; Drine, S.; Guasmi, F.; Touil, L.; Enneb, H.; Triki, T.; Cheour, F.; Ferchichi. IMPact of salt stress on morpho-physiological and biochemical parameters of Solanum lycopersicum cv . Microtom leaves. Sou. Afr. J. Bot 2017, 108, 364–369. doi:10.1016/j.sajb.2016.08.018
4. Food and agriculture organization for the united nations (FAO). Global map of salt-affected soils. Intergovernmental Technical Panel on Soils (FAO USA) 2021, 1, 1-5.
5. Cuatero, J.; Bolarin, M. C.; Asins, M. J.; Moreno, V. Increasing salt tolerance in the tomato. J. Exp. Bot 2006, 57(5), 1045–1058. doi: 10.1093/jxb/erj102
6. Yeo, A. R.; Flowers, T. J. Variability for some physiological characters affecting salt tolerance in tomato, J. Int. Horti. Sci 2002. 3, 435–441.
7. Caro, M.; Cruz, V.; Cuartero, J.; ESTAN, M. Salinity tolerance of normal-fruited and cherry tomato cultivars. Ind. J. Plant Physiol 1991, 1, 249–255.
8. Rahman, M. M.; Hossain, M.; Hossain, K. F. B.; Sikder, M. T.; Shammi, M.; Rasheduzzaman, M.; Hossain, M. A.; Alam, A. M.; Uddin, M. K. Effects of NaCl-salinity on tomato (Lycopersicon esculentum Mill.) plants in a pot experiment. J. Open Agr. 2018, 3, 578–585. doi:10.1515/opag-2018-0061
9. Pradhan, N.; Prakash, P.; Tiwari, S. K. Osmopriming of tomato genotypes with polyethylene glycol 6000 induces tolerance to salinity stress. J. Tren. Biosc 2014, 7(24): 4412-4417.
10. Hajer, A. S.; Malibari, A. A.; Al-Zahrani, H. S.; Almaghrabi, O. A. Responses of three tomato cultivars to sea water salinity, seedling growth. Afr. J. Biot. 2006, 5(10), 855–861.
11. Kumar, S. Comparative effect of NaCl and PEG on physiological and biochemical attributes during vegetative stage of tomato, Res. J. of Agri. Sci 2021, 12(3), 955-961.

10

12. Habibi, N.; Sediqui, N.; Naoki, T.; Atsushi, S.; Kaihei, K. Effects of salinity on growth , physiological and biochemical responses of tomato. J. ISSAAS 2021, 27(2), 14–28.

13. Sotomayor, A.; Merino, J.; Viera, W. Determining conditions for best pollen quality of red-purple tree tomato (Solanum betaceum Cav.) germplasm. Bionatura; Latin American J. Biot. Life Sci. 2021, 6(4), 2–7. doi: 10.21931/RB/2020.05.01.2

14. Balibrea, M. E.; Parra, M.; Bolarin, M. C.; Perez-Alfocca, F. PEG induced tomato adaptation to salt stress. Aus. J. Plant physiol 1999, 1, 781–786.

15. Farhoudi, R.; Saeedipour, S.; Mohammadreza, D. The effect of NaCl seed priming on salt tolerance , antioxidant enzyme activity, proline and carbohydrate accumulation of muskmelon (Cucumis melo L) under saline condition. Afr. J. Agric. Res. 2011, 6(6), 1363–1370. doi:10.5897/AJAR10.1007

16. Michel, B. E.; Kaufmann, M. R. The osmotic potential of polyethylene glycol 6000. J. Plant Physiol 1973, 51, 914-916.

17. Aqvila, D.; Carella, G. Polyethylene glycol 6000 priming effect on germination of aged wheat seed lots. J. Aur. Agr 1984, 26(3), 166–173.

18. Dafni, A. A new procedure to asses pollen viability. Sex Plant Reprod 2000, 12, 241–244.

19. Maisonneuve, B.; Den Nijs, A. P. M. In vitro pollen germination and tube growth of tomato (Lycopersicon esculentumMill.) and its relation with plant growth. J. Euphytica 1984, 33(3), 833–840.

20. Abdalla, A. A.; Verkerk, K. Growth, flowering and fruit-set of the tomato at high temperature. Neth. J. Agr. Sci 1968, 16(1), 71–76.

21. Panthee, D. R.; Jonathan, P. K.; Ann, P. Heritability of Flower Number and Fruit Set under Heat Stress in Tomato. J. Hort. Sci.2018, 53(9):1294–1299. doi: 10.21273/HORTSCI13317-18

22. Rosadi, R. A. B.; Senge, M.; Suhandy, D.; Tusi, A. The effect of EC levels of nutrient solution on the growth, yield, and quality of tomatoes (Solanum Lycopersicum) under the hydroponic system. J. Agr. Eng. and Biot. 2014, 2(1), 7–12.

23. Ghanem, M. E.; Elteren, J. V.; Albacete, A.; Quinet, M.; Martínez-andújar, C.; Kinet, J.; Pérez-alfocea, F.; Lutts, S. IMPact of salinity on early reproductive physiology of tomato (Solanum lycopersicum) in relation to a heterogeneous distribution of toxic ions in fl ower organs. J. Ind. Hort. 2009, 2, 125–136. doi: 10.1071/FP08256

24. Khaleghi, E.; Karamnezhad, F.; Moallemi, N. Study of pollen morphology and salinity effect on the pollen grains of four olive (Olea europaea) cultivars. Sou. Afr. J. Bot. 2019, 127, 51–57. doi: 10.1016/j.sajb.2019.08.031

25. Dhingra, H. R.; Varghese, T. M. Effect of Salt Stress on Viability, Germination and Endogenous Levels of Some Metabolites and Ions in Maize (Zea mays L.) Pollen. J. Ann. Bot 1985, 55, 415-420.

26. Yokaş, I.; Tuna, A. L.; Bürün, B.; Altunlu, H.; Altan, F.; Kaya, C. Responses of the tomato (Lycopersicon esculentum Mill.) plant to exposure to different salt forms and rates. Turkish J. Agri. Fores. 2008, 32(4), 319–329.

27. Turner, N. C.; Colmer, T. D.; Quealy, J.; Pushpavalli, R.; Krishnamurthy, L. Salinity tolerance and ion accumulation in chickpea (Cicer arietinum L.) subjected to salt stress. J. Int. Horti 2013, 2, 347–361. doi: 10.1007/s11104-012-1387-0

28. Gul, H.; Ahmad, R. Effect of salinity on pollen viability of different canola (Brassica napus L.) cultivars as reflected by the formation of fruits and seeds. Pak. J. Bot. 2006, 38(2), 237–247.

29. Del Amor, F. M.; Martinez, V.; Cerdá, A. Salt tolerance of tomato plants as affected by stage of plant development. J. Hort. Sci 2001, 36(7), 1260–1263.

30. Flowers, T. J. Improving crop salt tolerance. J. Exp. Bot. 2004, 55(396), 307–319. doi: 10.1093/jxb/erh003

31. Cano, E. A.; Moreno, V.; Bolarin, M. C. Pollen viability under salt stress. Plant Cell Reports 1996, 9. 791–794.

32. Harel, D.; Fadida, H.; Slepoy, A.; Gantz, S.; Shilo, K. The effect of mean daily temperature and relative humidity on pollen, fruit set and yield of tomato grown in commercial protected cultivation. Agron 2014, 4(1), 167–177. doi: 10.3390/agronomy4010167

33. Cuatero, J.; Rafael F. M. Tomato and salinity. J. Scientia Hort. 1999, 78, 83-125.

34. Tolessa, K.; Heuvelink, E. P. Pollen viability and fruit set of tomato introgression lines (Solanum esculentum XL. Chmielewskii) at Moderately High Temperature Regimes. J. Plant Physiol 2018, 36(1), 29–38.

35. Abdul-Baki, A. A.; Stommel, J. R. Pollen viability and fruit set of tomato genotypes under optimum- and high-temperature regimes. Hort. Sci 1995, 30(1), 115–117.

36. Wang, S. S.; Lia, Y. L.; Wen, X. Z. Effect of increasing humidity on flowering, fruit-setting and pollen characteristics of tomato under heat stress. Acta Hort. 2018., 1227, 305–311. doi:10.17660/ActaHortic.2018.1227.37

37. Hniličková, H.; Hnilička, F.; Orsák, M.; Hejnák, V. Effect of salt stress on growth, electrolyte leakage, Na + and K+ content in selected plant species. Plant, Soil and Environment 2019., 65(2), 90–96. doi:10.17221/620/2018-PSE

38. Safdary, A. J.; Ahamdi, A. J.; Habibi, N., Rahmani, Z., & Rasooli, S. (2020). The effect of different treatments on seed dormancy breaking and germination inducing in louisiana variety of okra (Abelmoschus esculentus l.). International Journal of Innovative Research and Scientific Studies, 3(4), 124–128. doi: 10.53894/ijirss.v3i4.45

11

Isolation and characterization of fungi and bacteria able to grow on media containing gasoline and diesel fuel

Khadidja Meknassi, Leila Aït Abderrahim*, Khaled Taïbi, Mohamed Sassi, Mohamed Boussaid
Faculty of Life and Natural Sciences, University of Tiaret, 14000, Algeria.
Corresponding author: aitleila-bio@hotmail.com

DOI. 10.21931/RB/2023.08.01.26

Abstract: Petroleum products are significant environmental pollutants. This study aimed to isolate microorganisms able to grow on media containing gasoline and diesel fuel. Microorganisms were isolated from soils sampled near gasoline and diesel pumps. Bacterial isolates were characterized and tested on media containing concentrations ranging from 10 to 100 % gasoline and diesel fuel and combinations of both 50/50 % and 25/25/50 % (gasoline/ diesel/ Mueller Hinton broth). Results showed that microbial isolates belong to the genera *Pseudomonas, Bacillus, Staphylococcus, Micrococcus, Flavobacterium, Actinobacteria, Penicillium, Hansfordia* and *Alternaria. Pseudomonas spp.* and *Bacillus spp.* showed the ability to grow on both products up to the concentration of 80 %. However, no growth was noticed above that concentration and on both mixtures. Throughout this study, it has been shown that using a selective screening method for microorganisms able to grow on pollutants can present a significant advantage for bioremediation.

Key words: Pollution; gasoline; diesel; microorganisms.

Introduction

Petroleum-based products are the primary energy source for industry and daily life; however, they are also considered major environmental toxic pollutants. Leakages and accidental spills occur regularly during large-scale exploration, production, refining, transport, and storage of petroleum and derived products[1]. Pollution due to petroleum hydrocarbons and their derivatives, including diesel fuel, gasoline, heavy oil, motor oil, fuel residues and mineral oil, has an increasing impact on the environment leading to air, soil and groundwater pollution as to the contamination of the food chain[2,3].

Diesel oil spills represent one of the leading environmental pollution problems due to their extensive production and use. Diesel oil, a product of petroleum distillation, is formed of up to 4,000 hydrocarbons. It is a mixture of regular, branched and cyclic alkanes and aromatic compounds (e.g., polycyclic aromatic hydrocarbons PAHs), which are persistent pollutants with high mutagenic, carcinogenic and reprotoxic potential[4].

Petroleum hydrocarbon spills, including diesel oil and gasoline, have been shown to hurt soil's biochemical and physicochemical characteristics and be toxic to plants[5]. They reduce soil fertility and nitrogen fixation and cause erodibility leading to a more significant loss of soil and nutrients and a unbalance in soil fauna and flora[6].

Several physicochemical methods have been developed to treat hydrocarbon-contaminated soil. However, these limitations include expensive costs, incomplete removal of pollutants, and toxic environmental impact[7,8]. Microorganisms can metabolize hydrocarbons, such as diesel oil, as the sole carbon and energy source, into nontoxic, biodegradable products. These microorganisms have catabolic genes that synthesize metabolizing enzymes involved in hydro-

carbon degradation[1]. The initial intracellular reaction is an oxidative process in which the activation and incorporation of oxygen is the key enzymatic reaction catalyzed by oxygenases and peroxidases[9]. Microorganisms have the potential to detoxify hazardous organic compounds using polymerization, mineralization, or transformation[3].

Hydrocarbon degradation by microbial communities depends on the composition of the community and its adaptive response to the presence of petroleum hydrocarbon. The susceptibility of hydrocarbons to microbial degradation can be generally ranked as follows: n-alkanes > branched alkanes > low molecular weight aromatics > cycloalkanes > polyaromatic hydrocarbons (PAHs)[10,11].

Microbial degradation, known as bioremediation, is one of the essential methods of decontamination of pollutants in both terrestrial and aquatic environments[4]. Bioremediation is an efficient, cost-effective, and environmentally friendly approach for decontaminating polluted soils[12].

Microorganisms are critical bioremediation agents and can effectively degrade a wide range of contaminants[13]. Besides, bacteria are the most active agents in petroleum degradation and work as primary degraders of spilled oil in the environment[10].

Moreover, the rate of microbial degradation of hydrocarbons in soils is affected by several physicochemical factors such as soil's particles size, nutrients, oxygen, pH, quality and quantity of the contaminants and temperature, which plays a significant role in controlling the bioavailability of low-solubility hydrocarbons and hence the nature and the extent of microbial metabolism[14].

This study aimed to isolate and identify microorganisms (bacteria and fungus) from polluted soils near gasoline and diesel fuel pumps. Afterward, the isolates were tested for

Publisher's Note: Bionatura stays neutral with regard to jurisdictional claims in published maps and institutional affiliations.

2

their ability to grow on media containing pure gasoline and diesel fuel in a perspective of bioremediation approach.

Materials and methods

Soil and petroleum hydrocarbons samples

Several soil samples were aseptically collected at different depths (5 to 20 cm) from various sites near gasoline and diesel pumps of gas stations in Tiaret, Algeria. The collected samples were kept in sterile bottles and stored in the refrigerator at 4 °C before the manipulation. Samples of gasoline and diesel fuel were obtained directly from a gas station.

Isolation and purification of microorganisms

Suspensions from each soil sample were prepared by mixing 1 g of soil in 10 ml of sterile distilled water. After mixing, the suspensions were left to settle then volumes ranging between 0.1 and 0.5 ml were taken from the supernatant and inoculated into Petri dishes containing culture media i.e., nutrient agar, Sabouraud agar, King A and King B agar[15]. After inoculation, Petri dishes were incubated at 30°C and observed after 24 h, 48 h, until 7 days. Colonies that formed on the culture media were subsequently transferred to new media, and successive subcultures were carried out until pure cultures were obtained.

Identification of isolates

The identification of isolates was based on their morphological and biochemical characteristics.

Morphological characterization

After purification, the microbial isolates are observed macro- and microscopically to check their purity and to visualize colonies and cell structures and disposition as a first step to their identification. The colonies' color, shape, aspect and transparency were examined and recorded as colony morphological characteristics. Whereas the cell's shape, size, arrangement and type of cell wall were examined under the microscope using simple staining and Gram stain for bacteria.

Biochemical characteristics

Several biochemical tests were performed on the microbial isolates to help identify these: citrate utilization, triple sugar iron agar, catalase, oxidase, O-nitrophenyl-β-D-galactopyranoside (ONPG), mannitol mobility tests and respiratory type.

Test of viability of the microbial isolates on diesel and gasoline

After isolation and purification of the microbial strains, each strain is inoculated separately in glass Petri dishes containing different concentrations of gasoline and diesel fuel ranging from 10 % to 100 % mixed with Mueller Hinton agar. Each strain is also inoculated in a mixture of the two hydrocarbons at concentrations of 50/50 % (gasoline/diesel) and 25/25/50 % (gasoline/ diesel/ Mueller Hinton broth) in test tubes. Incubation is done at 37 °C from 24 h to 72 h after microbial growth is recorded.

Results

Microorganisms isolated from polluted soil samples

After the purification and identification of microbial isolates from soil samples (Table 1), we noted the presence of several bacteria belonging mainly to the genera: *Pseudomonas, Bacillus, Staphylococcus, Micrococcus, Flavobacterium* and *Actinobacteria* (Figure 1) whereas the fungal isolates belong to the genera *Penicillium sp.*, *Hansfordia sp.* and *Alternaria sp.* (Figure 2).

Growth of the bacterial isolates on diesel and gasoline

Among the isolated microbial strains, two bacterial strains belonging to the genus Bacillus and two others belonging to the genus Pseudomonas were tested for their ability to grow on gasoline and/or diesel fuel containing media. Results revealed that all the tested bacterial strains are able to grow on concentrations of diesel fuel and gasoline up to 80 % (Figure 3). However, beyond this concentration no bacterial growth was recorded. In addition, the bacterial isolates were not able to grow on both tested concentrations of the mixture gasoline-diesel.

Bacteria/ test	*Bacillus* sp.	*Bacillus* sp.	*Pseudomonas* sp.	*Flavobacterium* sp.	*Staphylococcus* sp.	*Micrococcus* sp.
Catalase	+	+	+	+	+	+
Citrate	+	/	/	+[1]	+	-
Mannitol	+	+	+	+	+	+
ONPG	-	-	-	-	-	-
Oxidase	+	+	+	+	-	-
TSI	/	Glu+, Sac/Lac+	/	Sac and/or Lac+	Glu+, Sac/Lac+	Glu+, Sac/Lac+
Mobility	+	-	+	-	-	-
Gram stain	+	+	-	-	+	+
Respirtory type	Aeroan-aerobe	Aeroan-aerobe	Aerobe	Obligate aerobe	Aeroanaerobe	Aerobe

+ positive result / - negative result

*Glu: glucose, Sac: Saccharose, Lac: Lactose.

Table 1. Results of the biochemical tests on the bacterial isolates.
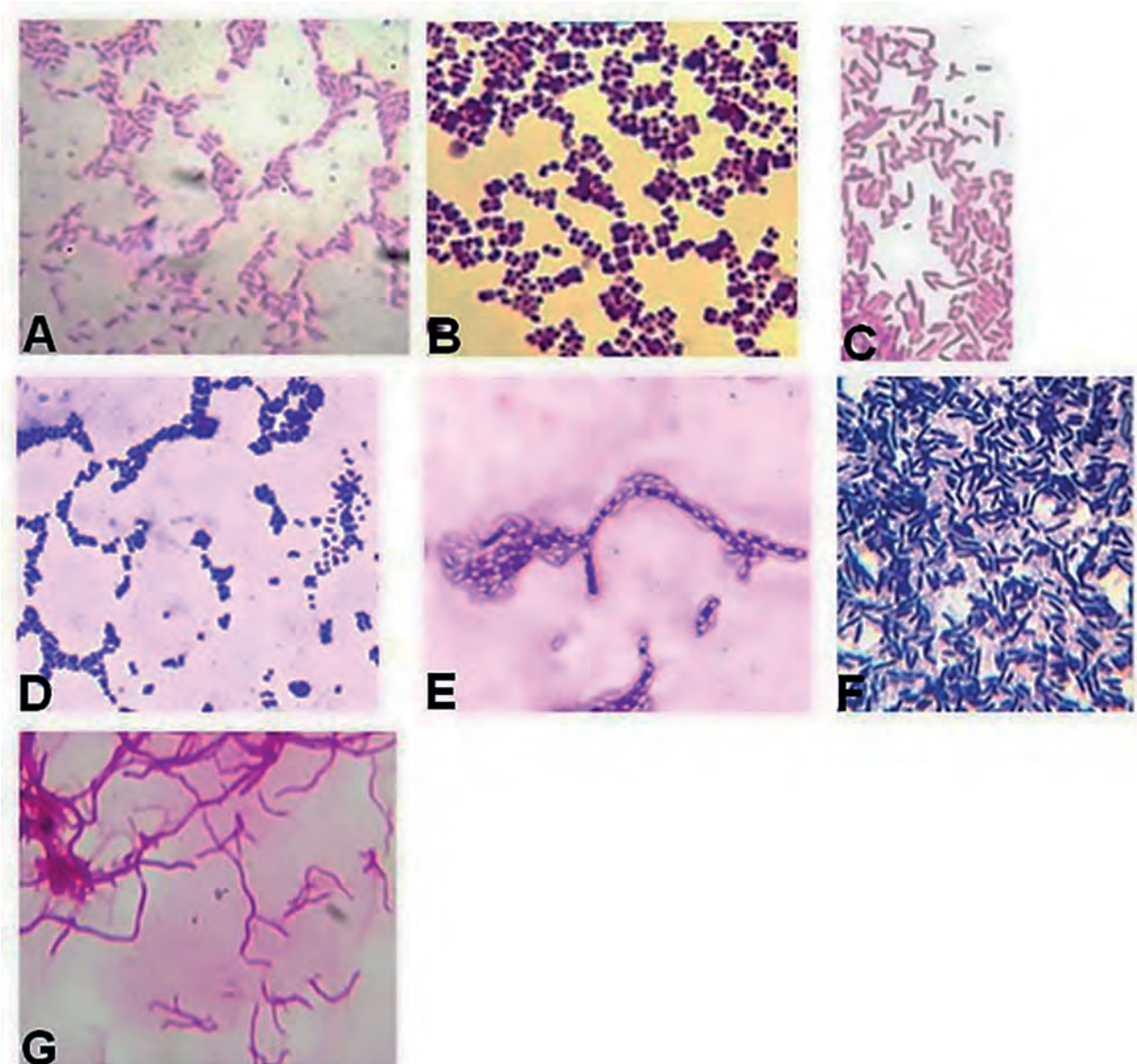
Figure 1. Bacterial isolates; *(A) Flavobacterium sp., (B) Micrococcus sp., (C) Pseudomonas sp., (D) Staphylococcus sp., (E) Bacillus sp., (F) Bacillus sp., (G) Actinobacteria.*
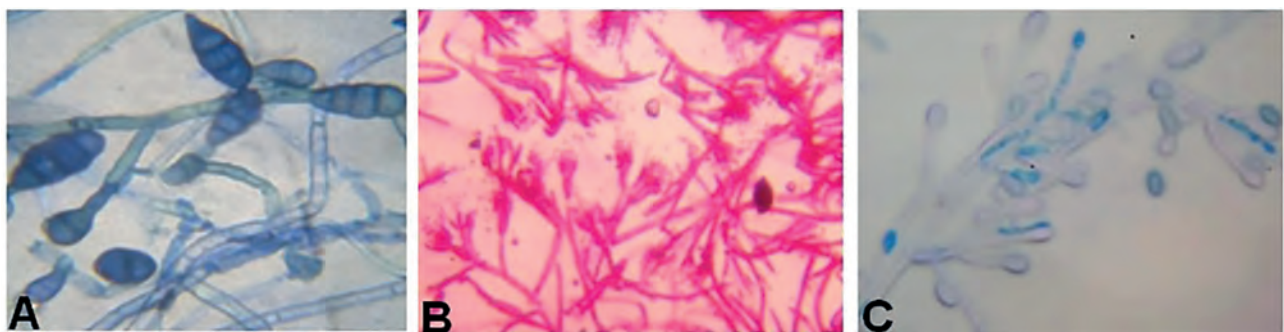
Figure 2. Fungal isolates; (a) *Alternaria sp.*, (b) *Penicillium sp.*, (c) *Hansfordia sp.*

Discussion

Besides the fact that petroleum-derived products are used as the principal source of energy nowadays, they act as a globally environmental toxic pollutant[16]. This study aimed to isolate and characterize microbes capable of using petroleum hydrocarbons for their growth from the perspective of their use in the bioremediation process.

Throughout the present study, we could isolate several bacterial and fungal strains belonging mainly to the genera *Pseudomonas, Bacillus*, and *Staphylococcus* from gasoline and diesel fuel-polluted soils, *Micrococcus, Flavobacterium, Actinobacteria, Penicillium, Hansfordia* and *Alternaria*.

These microorganisms are supposed to be adapted to
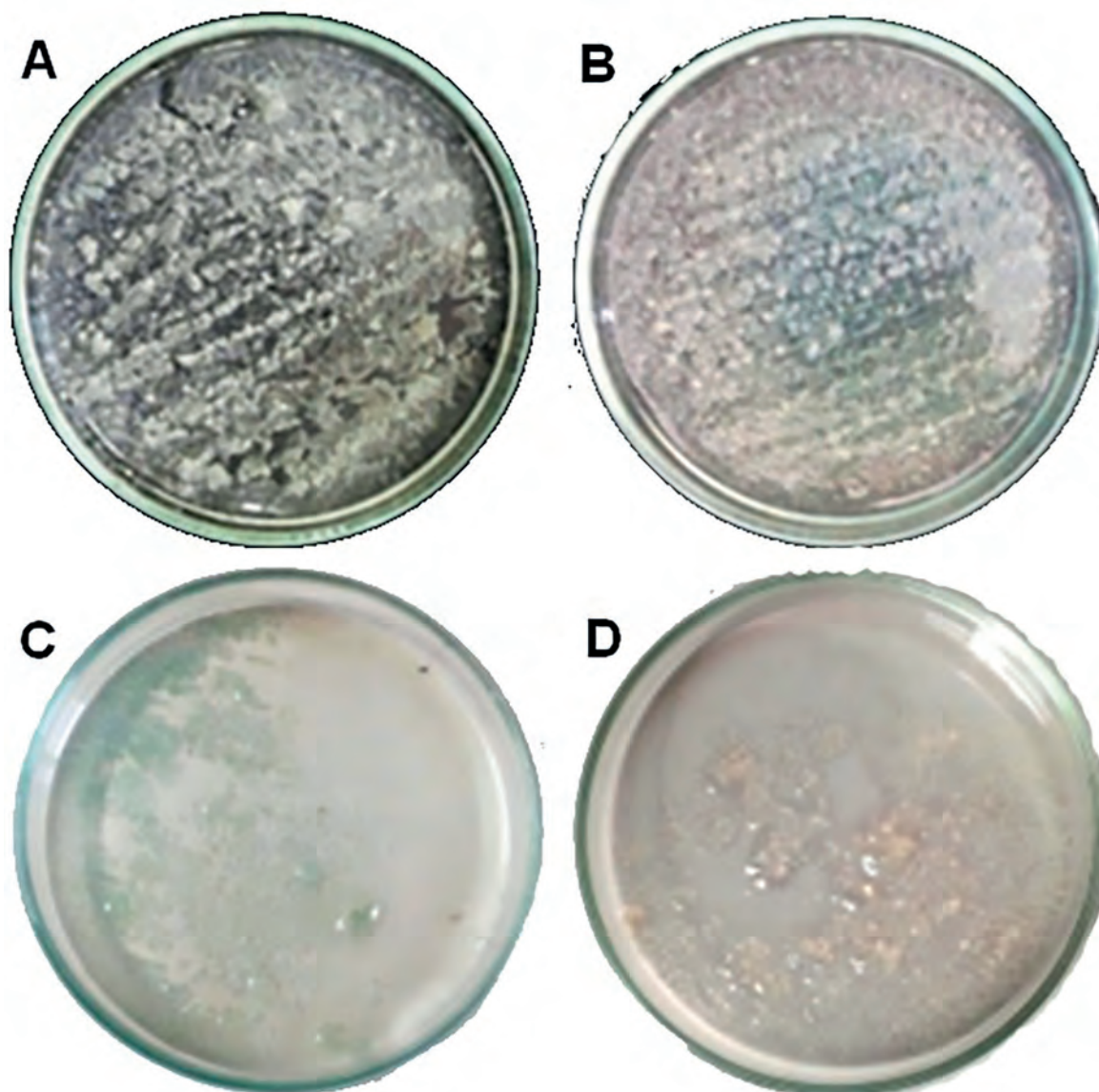
Figure 3. Growth of the bacterial strains on media containing (1) diesel fuel and (2) gasoline. (a) *Bacillus sp.*, (b) *Pseudomonas sp.*

the hydrocarbons present in their living environment. Hydrocarbon degradation by microbial communities depends on the composition of the specific microbial population current and its adaptive response to the presence of petroleum hydrocarbon[10]. Thanks to their enzymatic activity, many microorganisms, such as bacteria, fungi, and yeast, can use hydrocarbons as a sole carbon source. The structural similarities between xenobiotics and complex molecules in living organisms 16 can explain the presence and abundance of microorganisms in polluted environments.

Several studies on the subject demonstrated the presence of many Gram-negative and Gram-positive bacteria in soils polluted with hydrocarbons, such as *Acinetobacter, Pseudomonas, Enterobacter, Corynebacterium, Arrhobacter, Micrococcus, Staphylococcus, Rhodococcus, Bacillus* and *Sphingomonas*[17]. Likewise, several fungal genera and species have been characterized by their ability to propagate in soils and to produce extracellular enzymes allowing the use of hydrocarbons such as *Aspergillus niger*, *Aspergillus terreus*, *Rhizopus sp.*, *Alternaria* and *Penicillium sp.*[18].

Microorganisms play a crucial role in eliminating petroleum hydrocarbons and another organic pollutants from the environment. These pollutants are used as carbon sources to provide energy for microbial growth and are transformed into non-polluting substances or fully mineralized into carbon dioxide and water by microorganisms[19].

The predominance of bacteria over fungi can be explained by the fact that bacteria are much more versatile organisms and have a wider field of action and thus remain qualitatively and quantitatively predominant for metabolizing various substrates even if the fungi, thanks to their hyphae and enzymatic paraphernalia, manage to fix efficiently complex and large amounts of pollutants[20].

Moreover, with their multiple metabolic pathways (both aerobic and anaerobic), bacteria are the most active agents in diesel degradation and act as the main degraders of petroleum hydrocarbons[1,19,21]. Bacteria belonging to the genera *Pseudomonas, Bacillus, Staphylococcus* and *Streptococcus* have been shown to be able to utilize and/or degrade hydrocarbons[22]. Bhuvaneswar *et al.*[23] reported that synergistic mixed culture of Pseudomonas and Staphylococcus could degrade the diesel oil.

Furthermore, Titah *et al.*[24], isolated thirteen bacterial strains from diesel-contaminated areas, of which only *Mi-*

crococcus and *Staphylococcus* displayed the best resistance and highest growth in the diesel-polluted medium at different concentrations.

Al-Dhabaan[15] described hydrocarbon-degrading strains of Bacteria from contaminated sites in Khurais oil field (Dhahran, Saudi Arabia); these are *Bacillus subtilis, Pseudomonas aeruginosa* and *Bacillus cereus*. The ability to form spores when nutrients are limiting makes species of *Bacillus* self-sustainable bioremediation tools[7]. In another study, many species belonging to the genus *Bacillus; B. coagulans, B. subtilis, B. megaterium* and *B. cereus* have been isolated from petroleum–contaminated soils[25].

In this study, fungal strains belonging to the genera *Penicillium, Alternaria* and *Hansfordia* were isolated from diesel fuel and gasoline-contaminated soils. Indeed, several fungal species can use petroleum hydrocarbons as carbon and energy sources and assimilate into fungal biomass[26]. Fungi have several advantages in biodegradation compared to the other microorganisms because of their filamentous form and their ability to cultivate on a large group of substrates by secreting extracellular hydrolytic enzymes, which can penetrate contaminated soil and remove pollutants in a process such as co-metabolism[27]. In addition, fungal cell membranes are permeable to many organic pollutants, and these can be degraded by intracellular enzymes, ex., cytochrome P450 which is considered as an efficient candidate for the potential degradation of polyaromatic hydrocarbons[28].

Numerous studies have shown that fungi, including Penicillium spp., Absidia spinosa and Cladosporium spp. can degrade various hazardous contaminants[29]. Al-Hawash *et al.*[30] reported that *Penicillium* sp. RMA1 and RMA2 isolated from the Rumaila oil field performed effective crude oil-degrading activity and emulsification. Some fungal strains, namely *Alternaria sp., Acromonium sp., Aspergillus terreus* and *Penicillium sp.* were isolated from petroleum-polluted areas of Arak refinery (Iran) where Alternaria sp. showed the highest growth ability in the petroleum-containing media[31]. Mohammadian *et al.*[32] have reported that *Alternaria obovoidea* and *Emericellopsis pallida* were isolated from petroleum contaminated soils in Khuzestan (Iran).

Besides, in this study, we were able to demonstrate that four bacterial strains belonging to the genera *Pseudomonas* and *Bacillus* were able to grow on media containing concentrations up to 80 %; above that concentration, no growth was noticed. This indicates either the ability of bacterial isolates to utilise diesel and gasoline for their growth or at least the tolerance threshold of these bacteria to the toxicity of the pollutant. Raju *et al.*[33] suggested that microbial degradation of diesel is greatly affected by its concentration. They also indicated that two selected strains *B. thuringiensis* B3 and *B. cereus* B6, have great potential in degrading polycyclic aromatic hydrocarbons in diesel. Microorganisms prefer to grow when the concentration of hydrocarbons is low, but every organism has its tolerance level; in addition, bacterial degradation is possible when the concentration of the contaminant is below the threshold of toxicity[34]. Oyewole et al. 21 observed that the highest degradation occurred at a diesel concentration of 1 % and 5 % for both isolates *Bacillus subtilis* and *Bacillus cereus*. The maximum bacterial growth was found in 20 % (v/v) of diesel. The bacterial growth increased with increasing diesel concentration but decreased at 25 % of diesel[34]. *B. cereus* utilizes the hydrocarbons as a sole carbon source for their growth by degrading the hydrocarbon due to the production of biosurfactant[35]. *B. pumilus* produces biosurfactants and has shown very high degradation potential for diesel oil and waste engine oil hydrocarbons[36]. Lipopeptide biosurfactants are commonly produced by bacteria belonging to the genus *Bacillus*[37].

Besides, *Pseudomonas* is among the most typical bacterial genera known for its capacity to degrade hydrocarbons and produce biosurfactants that can increase the solubilization and degradation of hydrophobic compounds[38]. The ability of *Pseudomonas* sp. to degrade petrol, diesel and engine oil was observed by Veerapagu *et al.*[39].

Conclusions

Throughout the present study, several microbial strains were isolated from diesel fuel and gasoline-contaminated soils; these were seven bacterial strains belonging to the genera *Pseudomonas, Flavobacterium, Bacillus, Staphylococcus* and *Actinobacteria*, in addition to three fungal strains belonging to the genera *Penicillium, Alternaria* and *Hansfordia*.

Four bacterial strains belonging to the genera *Pseudomonas* and *Bacillus* have demonstrated their ability to grow on media containing gasoline and diesel fuel up to the concentration of 80 %, showing either their aptitude to use these pollutants for their growth or simply their tolerance threshold to the toxicity of the contaminant.

Further studies should be performed to identify and characterize the degradation potential of the isolates and the tools they use for petroleum hydrocarbon degradation for their future use in the bioremediation process.

Author Contributions

All authors have read and agreed to the published version of the manuscript. All authors have contributed substantially to work reported.

Conflicts of Interest

The authors declare no conflict of interest.

Bibliographic references

1. Pandey, P.; Pathak, H.; Dave, S. Isolation and enrichment of microbes for degradation of diesel oil. Int J Sci Res Sci Technol 2018, 4(5), 1281-1284.
2. Kaboré-Ouédraogo, P.W.; Savadogo, P.W.; Ouattara, C.A.T.; Savadogo, A.; Traoré, J.A.S. Etude de la bio-dépollution de sols contaminés par les hydrocarbures au Burkina Faso. J Soc Ouest-Afr Chim 2010, 30, 19-28.
3. Ibrahim, H.M.M. Biodegradation of used engine oil by novel strains of Ochrobactrum anthropi HM-1 and Citrobacter freundii HM-2 isolated from oil-contaminated soil. 3 Biotech 2016, 6(2), 266. https://doi.org/10.1007/s13205-016-0540-5.
4. Cisneros-de la Cueva, S.; Martinez-Prado, M.A.; Lopez-Miranda, J.; Rojas-Contreras, J.A.; Medrano-Roldan, H. Aerobic degradation of diesel by a pure culture of Aspergillus terreus KP862582. Rev Mex Ing Quím 2016, 15(2), 347-360.
5. Njoku, K.L.; Akinola, M.O.; Taiwo, B.G. Effect of gasoline diesel fuel mixture on the germination and the growth of Vigna unguiculata (Cowpea). Afr J Environ Sci Technol 2009, 3(12), 466-471.
6. Patel, V.; Shah, K. Petroleum hydrocarbon pollution and its biodegradation. International Journal of Chemtech Applications 2011, 2(3), 63-80.
7. Lima, S.D.; Oliveira, A.F.; Golin, R.; Lopes, V.C.P.; Caixeta, D.S.; Lima, Z.M.; Morais, E.B. Isolation and characterization of hydrocarbon-degrading bacteria from gas station leaking-contaminated ground water in the Southern Amazon, Brazil. Braz J Biol 2020, 80(2), 354-361. https://doi.org/10.1590/1519-6984.208611.

5

6

8. Ruley, J.A.; Amoding, A.; Tumuhairwe, J.B.; Basamba, T.A.; Opolot, E.; Oryem-Origa, H. Enhancing the phytoremediation of hydrocarbon-contaminated soils in the Sudd Wetlands, South Sudan, using organic manure. Appl Environ Soil Sci 2020. https://doi.org/10.1155/2020/4614286.

9. Das, N.; Chandran, P. Microbial degradation of petroleum hydrocarbon contaminants: An overview. Biotechnol Res Int 2010. https://doi.org/10.4061/2011/941810.

10. Lakshmi, P.J. Biodegradation of diesel by Aeromonas hydrophila. Int J Pharm Sci Invent 2013, 2(4), 24-36.

11. Erdomus, S.F.; Mutlu, B.; Korcan, S.E.; Güven, K.; Konuk, M. Aromatic hydrocarbon degradation by halophilic Archaea isolated from Çamalti Saltern, Turkey. Water Air Soil Pollut 2013, 224(3), 1449. DOI:10.1007/s11270-013-1449-9.

12. Kuran, P.; Trögl, J.; Novakova, J.; Pilarova, V.; Danova, P.; Pavlorkova, J.; Kozler, J.; Novák, F.; Popelka, J. Biodegradation of spilled diesel fuel in agricultural soil: Effect of humates, zeolite, and bioaugmentation. Sci World J The 2014. http://dx.doi.org/10.1155/2014/642427.

13. Owabor, C.N.; Onwuemene, O.C.; Enaburekhan, I. Bioremediation of polycyclic aromatic hydrocarbon contaminated aqueous-soil matrix: Effect of co-contamination. JASEM 2011, 15(4), 583 – 588.

14. Perfumo, A.; Banat, I.M.; Marchant, R.; Vezzulli, L. Thermally enhanced approaches for bioremediation of hydrocarbon-contaminated soils. Chemosphere 2007, 66(1), 179–184. doi: 10.1016/j.chemosphere.2006.05.006.

15. Al-Dhabaan, F.A. Morphological, biochemical and molecular identification of petroleum hydrocarbons biodegradation bacteria isolated from oil polluted soil in Dhahran, Saud Arabia. Saudi J Biol Sci 2019, 26(6), 1247-1252.

16. Ghanem, K.M.; Al-Gharni, S.M.; Al-Zahrani, M.A. Bioremediation of diesel fuel by fungal consortium using statistical experimental designs. Pol J Environ Stud 2016, 25(1), 97–106. https://doi.org/10.15244/pjoes/42493.

17. Montagnolli, R.N.; Matos Lopes, P.R.; Bidoia, E.D. Assessing Bacillus subtilis biosurfactant effects on the biodegradation of petroleum products. Environ Monit Assess 2015, 187(1), 4116. doi: 10.1007/s10661-014-4116-8.

18. Kurnaz, S.Ü.; Büyükgüngör, H. Bioremediation of total petroleum hydrocarbons in crude oil contaminated soils obtained from southeast Anatoli. Acta Biologica Turcica 2016, 29(2), 57–60.

19. Cui, J.Q.; He, Q.S.; Liu, M.H.; Chen, H.; Sun, M.B.; Wen, J.P. Comparative study on different remediation strategies applied in petroleum-contaminated soils. Int J Environ Res Public Health 2020, 17, 1606. doi:10.3390/ijerph17051606.

20. Chikere, C.B.; Okpokwasili, G.C.; Chikere, B.O. Monitoring of microbial hydrocarbon remediation in the soil. 3 Biotech 2011, 1(3), 117–138.

21. Oyewole, O.A.; Leh-Togi Zobeashia, S.S.; Oladoja, O.E.; Musa, I.O.; Terhemba, I.T. Isolation of bacteria from diesel contaminated soil for diesel remediation. J Biosci 2019, 28, 33-41. https://doi.org/10.3329/jbs.v28i0.44708.

22. Ebakota, O.D.; Osarueme, J.O.; Gift, O.N.; Odoligie, I.; Osazee, J.O. Isolations and characterisation of hydrocarbon-degrading bacteria in top and sub soil of selected mechanic workshops in Benin City Metropolis, Nigeria. J Appl Sci Environ Manag 2017, 21(4), 641-645.

23. Bhuvaneswar, C.; Swathi, G.; Vijaya Bhaskar, B.; Munichandra babu, T.; Rajendra, W. Effective synergetic biodegradation of diesel oil by bacteria. International Journal of Environmental Biology 2012, 2(4), 195-199.

24. Titah, H.S.; Pratikno, H.; Moesriati, A.; Imron, M.F.; Putera, R.I. Isolation and screening of diesel degrading bacteria from ship dismantling facility at Tanjungjati, Madura, Indonesia. J Eng Technol Sci 2018, 50(1), 99-109. DOI:10.5614/j.eng.technol.sci.2018.50.1.7.

25. Dixit, H.; Lowry, M.; Mohsin, U.; Moond, M.; Kumar, S.; Chokriwal, A.; Gupta, S. Screening and identification of diesel oil degrading bacterial isolates from petroleum contaminated soil of Barmer. J Pharm Chem Biol Sci 2018, 6(1), 34-40.

26. Balaji, V.; Arulazhagan, P.; Ebenezer, P. Enzymatic bioremediation of polyaromatic hydrocarbons by fungal consortia enriched from petroleum contaminated soil and oil seeds. J Environ Biol 2014, 35(3), 521-529.

27. Kottb, MR.; El-Agroudy, N.A.; Ali, A.A.E.; Hamed, M.A.; Ezz El-Din, H.M. Biodegradation of some petroleum hydrocarbons by fungi isolated from Gulf of Suez. CATRINA 2019, 18(1), 169-175.

28. Li, Q.; Liu, J.; Gadd, G.M. Fungal bioremediation of soil co-contaminated with petroleum hydrocarbons and toxic metals. Appl Microbiol Biotechnol 2020, 104, 8999–9008. https://doi.org/10.1007/s00253-020-10854-y

29. Savković, Ž.D.; Vukojičić, N.M.; Stupar, M.Č.; Novaković, N.Z.; Unković, N.D.; Ljaljević-Grbić, M.V.; Vukojević, J.B. Assessment of diesel fuel uptake by fungi isolated from petroleum contaminated soil. Matica Srpska J Nat Sci 2017, 133, 221-229.

30. Al-Hawash, A.B.; Alkooranee, J.T.; Abbood, H.A.; Zhang, J.; Sun, J.; Zhang, X.; Ma, F. Isolation and characterization of two crude oil-degrading fungi strains from Rumaila oil field, Iraq. Biotechnol Rep 2018, 17, 104-109.

31. Mohsenzadeh, F.; Rad, A.C.; Akbari, M. Evaluation of oil removal efficiency and enzymatic activity in some fungal strains for bioremediation of petroleum-polluted soils. Iran j environ health sci eng 2012, 9(1), 26. doi: 10.1186/1735-2746-9-26.

32. Mohammadian, E.; Arzanlou, M.; Babai–Ahari, A. Two new hyphomycete species from petroleum–contaminated soils for mycobiota of Iran. Mycol Iran 2016, 3(2), 135-140. DOI: 10.22043/mi.2016.25918.

33. Raju, M.N.; Leo, R.; Herminia, S.S.; Burgos Morán, R.E.; Venkateswarlu, K.; Laura, S. Biodegradation of diesel, crude oil and spent lubricating oil by soil isolates of Bacillus spp. Bull Environ Contam Toxicol 2017, 98, 698–705. https://doi.org/10.1007/s00128-017-2039-0.

34. Ahmed, F.; Fakhruddin, A.N.M. A review on environmental contamination of petroleum hydrocarbons and its biodegradation. Int J Environ Sci Nat Resour 2018,11(3), 63-69.

35. Janaki, S.; Thenmozhi, S.; Muthumari, R. A Study on hydrocarbons degradation by biosurfactant producing Bacillus cereus in oil contaminated soil samples. Int J Life-Sci Sci Res 2016, 2(4), 324-332.

36. Marchut-Mikolajczyk, O.; Drozdzynski, P.; Pietrzyk, D.; Antczak, T. Biosurfactant production and hydrocarbons degradation activity of endophyte bacteria isolated from Chelidonium majus L. Microb Cell Factories 2018, 17, 171. https://doi.org/10.1186/s12934-018-1017-5.

37. Nimrat, S.; Lookchan, S.; Boonthai, T.; Vuthiphandchai, V. Bioremediation of petroleum contaminated soils by lipopeptide producing Bacillus subtilis SE1. Afr J Biotechnol 2019, 18(23), 494-501. https://doi.org/10.5897/AJB2019.16822.

38. Sharma, N.; Lavania, M.; La, B. Microbes and their secondary metabolites: Agents in bioremediation of hydrocarbon contaminated site. Arch Petrol Environ Biotechnol 2019, 4(2), 151. DOI: 10.29011/2574-7614.100051.

39. Veerapagu, M.; Jeya, K.R.; Kalaivani, R.; Jeyanthi, K.A.; Geethanjali, S. Screening of hydrocarbon degrading bacteria isolated from oil contaminated soil. Pharma Innovation 2019, 8(6), 69-72.

ARTICLE / INVESTIGACIÓN

Identificación de inhibidores de las enzimas RdRp y M^pro del virus SARS-CoV-2 mediante homología estructural

Identification of inhibitors of the RdRp and M^pro enzymes of SARS-CoV-2 virus by structural homology

Daysi Espín-Sánchez[1]*, María L. Ramos-Aristimbay[1], Andrés S. Sánchez-Vaca[1], Karen Jaramillo-Guapisaca[1], Carolina Vizueta-Rubio[1], Fernanda Chico-Terán[3], Liliana Cerda-Mejía[2], Mario D. García[1,3]

[1] Carrera de Ingeniería Bioquímica, Facultad de Ciencia e Ingeniería en Alimentos y Biotecnología Universidad Técnica de Ambato, Ambato, Ecuador.
[2] Carrera de Alimentos, Facultad de Ciencia e Ingeniería en Alimentos y Biotecnología Universidad Técnica de Ambato, Ambato, Ecuador.
[3] Carrera de Biotecnología, Facultad de Ciencia e Ingeniería en Alimentos y Biotecnología Universidad Técnica de Ambato, Ambato, Ecuador.
Corresponding author: daysi97espinsanchez@gmail.com

1

Resumen: El COVID-19 ha generado un enorme impacto en la salud pública mundial debido a las altas tasas de contagio y mortalidad asociadas al virus SARS-CoV-2 causante de la enfermedad. Hasta la fecha, la Organización Mundial de la Salud (OMS) ha aprobado el uso de 10 vacunas aparentemente seguras y eficaces. Sin embargo, todavía existen limitaciones importantes para su administración en países en vías de desarrollo y localidades remotas, y la preocupación por la aparición de variantes del virus que puedan evadir la inmunidad adquirida mediante la vacunación se mantiene latente. Además de la prevención de la infección, son necesarios agentes terapéuticos efectivos para tratar a los pacientes diagnosticados con COVID-19. Bajo este contexto, el presente estudio tuvo como objetivo realizar un cribado virtual basado en la estructura de las enzimas proteasa (M^pro) y ARN polimerasa ARN-dependiente (RdRp) del SARS-CoV-2. Para este propósito se ensayaron inhibidores de proteínas homólogas pertenecientes a diferentes virus. El alineamiento múltiple de secuencias de estas enzimas permitió reconocer la presencia de una alta conservación de estas enzimas entre especies, especialmente de las regiones que comprenden los sitios de unión a inhibidores. Por lo tanto, se deduce que es posible emplear un enfoque de redireccionamiento de los inhibidores que fueron diseñados para tratar otras enfermedades virales. Experimentos de acoplamiento molecular permitieron identificar que los inhibidores RTP (afinidad de unión = -7.3 kcal/mol) y V3D (afinidad de unión = -8.0 kcal/mol) son excelentes inhibidores de RdRp y M^pro, respectivamente. Estos resultados sugieren que dichas moléculas son virtualmente capaces de unirse e inhibir la actividad de RdRp y M^pro y por lo tanto constituyen potenciales fármacos para combatir el SARS-CoV-2.

Palabras clave: SARS-CoV-2, COVID-19, inhibidores, RdRp, M^pro.

Abstract: TCOVID-19 has enormously impacted global public health due to the high infection and mortality rates associated with the SARS-CoV-2 virus-causing disease. The World Health Organization (WHO) approved 10 safe and effective vaccines. However, there are still significant limitations to their administration in developing countries and remote locations. Concerns remain about the emergence of virus variants that may evade immunity acquired through vaccination. In addition to preventing infection, effective therapeutic agents are needed to treat patients diagnosed with COVID-19. Under this context, the present study aimed to perform a structure-based virtual screening of the protease (M^pro) and RNA-dependent RNA polymerase (RdRp) enzymes of SARS-CoV-2. For this purpose, homologous protein inhibitors belonging to different viruses were tested. Multiple sequence alignment of these enzymes allowed us to recognize the high conservation of these enzymes between species, especially of the regions comprising the inhibitor binding sites. Therefore, it follows that it is possible to employ a redirection approach to inhibitors that were designed to treat other viral diseases. Molecular docking experiments identified that RTP inhibitors (binding affinity = -7.3 kcal/mol) and V3D (binding affinity = -8.0 kcal/mol) are excellent inhibitors of RdRp and M^pro, respectively. These results suggest that these molecules can virtually bind and inhibit the activity of RdRp and M^pro and thus constitute potential drugs to combat SARS-CoV-2.

Key words: SARS-CoV-2, COVID-19, inhibitors, RdRp, M^pro.

Introducción

La COVID-19, causada por el SARS-CoV-2, es una enfermedad viral emergente de alta preocupación por su elevado impacto sobre la salud pública y la economía global. En Marzo de 2020, la enfermedad fue declarada pandemia tras su rápida propagación alrededor de todo el mundo, llevando a una emergencia sanitaria que continúa vigente[1].

Hasta el momento de redacción de este artículo, según cifras oficiales, a nivel global se han confirmado más 437 millones de casos de COVID-19, incluyendo 5,96 millones muertes[2], estos datos indican que su tasa de mortalidad (CFR) asociada es de 1,36%.

Daysi Espín-Sánchez, María L. Ramos-Aristimbay, Andrés S. Sánchez-Vaca, Karen Jaramillo-Guapisaca, Carolina Vizueta-Rubio, Fernanda Chico-Terán, Liliana Cerda-Mejía, Mario D. García

El SARS-CoV-2 taxonómicamente pertenece al reino *Riboviria*, orden *Nidovirales*, familia *Coronaviridae* y género *Betacoronaviridae*, clasificación correspondiente a virus que poseen ARN de hebra sencilla positiva, envoltura de membrana y que tienen la capacidad de infectar humanos[3]. Análisis filogenéticos del genoma completo del SARS-CoV-2 evidencian su cercanía con coronavirus de murciélago y con el SARS-CoV, presentando entre sí más del 96% de identidad de secuencia[4,5]. Así mismo, se ha revelado que su genoma tiene una longitud aproximada de 30 kb, el cual consiste en dos regiones no traducidas (UTR) y 14 marcos de lectura abierta (ORFs). El primer ORF (Orf 1/ab) abarca más de la mitad del genoma y codifica 16 proteínas no estructurales (NSP) del complejo de replicación-transcripción, mientras que los 13 ORFs restantes codifican cuatro proteínas estructurales y al menos 6 proteínas accesorias[5-8].

Los productos del genoma pueden ser blancos moleculares de agentes antivirales, puesto que se ha demostrado que cumplen funciones críticas en el ciclo de vida de los coronavirus[6]. Las dianas más prometedoras en el SARS-CoV-2 parecen ser las proteínas proteasa principal (Mpro), proteasa de tipo papaína (PLpro) y la ARN polimerasa ARN dependiente (RdRp), ya que comparten el mayor porcentaje de homología con otros coronavirus[9]. También se ha considerado a la proteína espiga (S) como una diana terapéutica, por ser la responsable de la primera interacción del virus con las células del huésped. Sin embargo, esta proteína es altamente susceptible a mutaciones[10].

Tras el ingreso del virus a las células, el genoma viral es transcrito a poliproteínas del complejo de replicación/transcripción (RTC), que son procesadas mediante las proteasas Mpro y PLpro para generar proteínas efectoras funcionales[11], siendo Mpro la enzima predominante en la transformación proteolítica[12]. Un componente clave del RTC es la enzima RdRp, encargada de sintetizar ARN genómico para el ensamblaje de nuevas partículas del virus[13,14]. Tanto Mpro como RdRp presentan más del 95% de similitud de secuencia y estructura con las enzimas del SARS-CoV[14] y se sabe que no poseen homólogos cercanamente relacionados en humanos[15,16] por lo que pueden ser importantes dianas para el desarrollo de inhibidores con alta especificidad[17].

Debido al enorme impacto que ha tenido el COVID-19 en la salud pública mundial, el desarrollo y producción de medicamentos específicos y vacunas es urgente[18]. En la actualidad existen 10 vacunas seguras y eficaces, cuyo uso fue aprobado por la OMS[19]. No obstante, a pesar de la creciente disponibilidad de vacunas contra la COVID-19, aún existen limitaciones importantes para su administración, sobre todo en zonas del planeta con escasos recursos económicos[20,21], y su efectividad contra las nuevas variantes del virus es variable.

Además de la disminución de la transmisión comunitaria del virus y prevención de la infección, son necesarios también agentes terapéuticos efectivos para tratar a los pacientes que han desarrollado cuadros severos de la enfermedad[22]. Debido a la similitud existente entre las enzimas del SARS-CoV-2 con virus como el SARS-CoV e incluso MERS-CoV, los fármacos utilizados para tratar estas y otras infecciones del mismo tipo se encuentran disponibles y pueden ser útiles en la lucha contra el COVID-19[18]. Bajo este contexto, los esfuerzos actuales están enfocados en el redireccionamiento de fármacos con eficacia probada en contra de virus homólogos al SARS-CoV-2[23], lo cual ha conducido a ensayar medicamentos que inhiben a RdRp, tales como Faripiravir y Remdesivir, éste último es un análogo de

nucleósido que a mediados del 2020 obtuvo la aprobación de uso de emergencia por la US FDA en pacientes con COVID-19 severo[24]. Así mismo, otros ejemplos de fármacos son Carmofur y N3, que han demostrado capacidad de inhibición selectiva de Mpro de múltiples coronavirus, lo que los hacen efectivos antivirales con potencial actividad sobre el SARS-CoV-2[25].

El cribado virtual de librerías de compuestos puede ser una estrategia interesante para descubrir antivirales que permitan paliar los efectos adversos de la enfermedad[26]. De este modo, se puede acortar la lista de fármacos con aquellos que parecen unirse con mayor afinidad a las enzimas virales[27] y de los cuales se conocen características como el perfil de seguridad, efectos secundarios y posología[22]. Herramientas de acoplamiento molecular (molecular docking) permiten efectuar el cribado virtual de compuestos previo a su estudio *in-vitro* e *in-vivo*, haciendo posible la predicción de la orientación del fármaco en un receptor particular y su energía de unión. Mediante esta perspectiva, se pueden evaluar cientos de moléculas a un bajo costo y en relativamente poco tiempo[28,29]. En el presente estudio se realizó un cribado virtual de inhibidores basado en la estructura de enzimas Mpro y RdRp pertenecientes a virus estructuralmente homólogos al SARS-CoV-2. Este enfoque tuvo como objetivo identificar fármacos con potencial para ser redireccionados hacia el tratamiento de pacientes diagnosticados con COVID-19, o a su vez, para ser empleados en el diseño racional de nuevos inhibidores específicos de Mpro y RdRp del SARS-CoV-2.

Materiales y métodos

Análisis de homología estructural

A partir de las estructuras 3D de las enzimas RdRp (PDB ID: 6m71) y Mpro (PDB ID: 6yb7) del SARS-CoV-2 se identificó, mediante el uso del servidor PDBeFold[30], enzimas virales que comparten similitud estructural según el parámetro SSE (matched Secondary Structure Elements). En el caso de la polimerasa solo se seleccionó la cadena principal de la proteína (subunidad catalítica nsp12). De los resultados se tomó únicamente las estructuras en complejo con inhibidores.

Construcción de la librería de inhibidores de enzimas Mpro y RdRp

De los datos arrojados por PDBeFold se identificaron inhibidores acoplados a proteínas RdRp y Mpro homólogas a aquellas del SARS-CoV-2. La estructura química de cada inhibidor fue obtenida a partir del complejo enzima-ligando depositado en el PDB[31] y sus coordenadas tridimensionales fueron exportadas mediante PyMOL[32].

Identificación de los sitios de unión de inhibidores

Los sitios de unión de los diferentes inhibidores y sus interacciones con la proteína fueron determinados mediante su superposición con RdRp o Mpro del SARS-CoV-2 en WinCoot[33] y PyMOL[32]. Para el análisis se consideró aquellas interacciones no covalentes en el rango de 2.2 a 4.2 Å.

Alineamiento múltiple de secuencias

Tras la identificación de proteínas homólogas, se realizó un alineamiento múltiple de sus secuencias mediante T-Coffee[34]. El alineamiento fue posteriormente coloreado y

analizado mediante BoxShade de ExPASy[35]. En el alineamiento se establecieron los principales aminoácidos involucrados en el acoplamiento de ligandos de cada enzima.

Preparación de proteínas y ligandos

La preparación de los receptores RdRp (PDB ID: 7bv2) y Mpro (PDB ID: 7bqy), así como de la librería de ligandos (120 compuestos) se realizó utilizando AutoDock Tools versión 1.5.6 rc2[36], obteniendo de este modo las estructuras 3D en formato pdbqt.

Molecular docking

Los ensayos de acoplamiento molecular no covalente rígido se llevaron a cabo usando AutoDock Vina en PyRx[37, 38]. Se utilizó un grid apropiado para cada uno de los ligandos y se usó un valor de exhaustividad igual a 8. Las interacciones enzima-ligando fueron analizadas con Discovery Studio Visualizer[39] y el modo de unión de los compuestos se determinó mediante PyMOL[32]. Las ilustraciones fueron elaboradas mediante PyMOL y Discovery Studio Visualizer.

Resultados y discusión

Análisis de homología estructural

El análisis de homología estructural permitió identificar varias enzimas polimerasas y proteasas que comparten elementos estructurales con la subunidad nsp12 de RdRp y con M^pro del SARS-CoV-2. El valor más alto de %SSE observado para la RdRp corresponde a la polimerasa del virus Zika (ZV), enzima que comparte el 49% de similitud de estructura secundaria con su homóloga del SARS-CoV-2. Por otra parte, las polimerasas del virus de la fiebre aftosa humana (HFMD), Coxsackievirus (CV), Norovirus murino (NVM) y virus Norwalk (NV) presentan un 47% de similitud estructural. Finalmente, se observó un 45% de homología estructural con las RdRp de los virus del Dengue (DV) y de la Hepatitis C (HCV). La baja conservación de los elementos de estructura secundaria entre la RdRp del SARS-CoV-2 y enzimas homólogas se puede deber a la gran diferencia de tamaño que existe entre estas polimerasas. Se conoce que las características principales y la longitud (500 residuos) de las RdRp virales es altamente conservada pese a su baja identidad de secuencia[40]. Sin embargo, la subunidad nsp12 de la RdRp del SARS-CoV-2, con 932 residuos, es significativamente más larga que sus homólogas estructurales que cuentan con secuencias de ~500 aminoácidos. Aquí, hemos observado que la posición y la arquitectura general de los dominios y del sitio activo son altamente similares en las diferentes RdRps, lo que sugiere que los inhibidores de RdRps se unen a estas enzimas de forma similar y que la diferencia en la longitud de los polipéptidos no afecta el modo unión de los inhibidores.

Para M^pro, el análisis estructural determinó que existen enzimas virales de organismos homólogos, como M^pro del SARS-CoV, que comparten hasta un 100% de similitud estructural. De igual forma, el Coronavirus de murciélago HKU4 (HKU4-CoV) comparte un 95% de similitud, mientras que los organismos Coronavirus humano NL63 (HCoV-NL63), MERS-CoV y Virus de la diarrea epidémica porcina (PEDV) muestran hasta un 91% de identidad de estructura secundaria. Por último, los coronavirus de la peritonitis infecciosa felina (FIPV) y de la gastroenteritis transmisible porcina (TGEV) exhiben un 86% y 82% de semejan-

za, respectivamente. A pesar de la evidente conservación de la enzima, un estudio detallado sobre Mpro, basado en análisis de secuencia y estructura, ha revelado que ciertas variantes del virus SARS-CoV-2 presentan unas pocas mutaciones puntuales. Dicho estudio además sugiere que tales cambios probablemente surgieron como respuesta a la evolución adaptativa[41]. En conclusión, el análisis de homología estructural sugiere que los elementos de estructura secundaria son mucho más conservados en M^pro que en RdRp. Sin embargo, las características de sus sitios de unión a inhibidores son altamente conservados en ambas enzimas lo cual sustenta la hipótesis de que es posible redireccionar moléculas diseñadas para inhibir la proteasa o polimerasa de virus homólogos al SARS-CoV-2.

Identificación de inhibidores de enzimas RdRp y M^pro en virus homólogos al SARS-CoV-2

El análisis de homología estructural también permitió identificar un total de 78 moléculas que actúan como inhibidores de las enzimas RdRp de ZV, HFMD, CV, NVM, NV, HCV y DV, donde la mayoría de los inhibidores descritos pertenecen a la polimerasa del HCV (ns5b HCV). Para la enzima M^pro se identificaron 41 inhibidores de los virus SARS-CoV, HKU4-CoV, HCoV-NL63, MERS-CoV, PEDV, FIPV y TGEV. La mayor parte de estos inhibidores pertenecen al SARS-CoV. El listado de ligandos obtenidos del análisis de homología estructural se muestra en la Tabla Suplementaria 1.

En el caso de la RdRp el análisis individual ha mostrado que ciertos inhibidores se unen covalentemente a diferentes aminoácidos o a la plantilla de ARN durante la síntesis. No obstante, la gran mayoría lo hace mediante enlaces no covalentes de tipo puente de hidrógeno y fuerzas de Van der Waals. En Mpro, todos los inhibidores identificados forman contactos con el residuo Cys145, el cual se encuentra altamente conservado entre diferentes especies. La unión se da tanto de forma no covalente y covalente, predominando esta última. Los inhibidores reportados para las dos enzimas muestran amplios rangos de afinidad de unión (IC_{50}, K_i o K_d) en el rango nM a mM (Tabla Suplementaria 1). En cuanto a su estructura química, entre los inhibidores destacan compuestos de diferente índole, como ácidos carboxílicos, ácidos sulfónicos, ácidos benzoicos, cetonas, amidas, aminas y nitrilos. Se identificó varias estructuras químicas relevantes, como las sulfonamidas y carboxamidas. Se conoce que las sulfonamidas constituyen el esqueleto para el diseño de un amplio rango de agentes terapéuticos. A partir de las sulfonamidas se han elaborado antibacteriales, anticancerígenos, anticonvulsionantes, antidiabéticos, diuréticos, antileucémicos, antiinflamatorios y antivirales. De igual forma las carboxamidas son importantes farmacóforos que se encuentran en moléculas de medicamentos usados para regular los niveles de colesterol, hipertensión, enfermedades del corazón y el VIH, entre otras enfermedades[42].

Un gran número de los inhibidores específicos identificados para RdRps y que actúan sobre el sitio activo son análogos de nucleósidos. La enzima RdRp del SARS-CoV-2, al igual que otras polimerasas, posee baja fidelidad, por lo que su propensión a errores durante el proceso de replicación incrementa la posibilidad de aceptación de análogos de nucleótidos como sustratos. Por esta razón, los nucleótidos y nucleósidos modificados son importantes agentes antivirales ya que inhiben la enzima al competir con los ribonucleótidos naturales[15].

Para M^pro, dada su función proteolítica, los primeros

3

Daysi Espín-Sánchez, María L. Ramos-Aristimbay, Andrés S. Sánchez-Vaca, Karen Jaramillo-Guapisaca, Carolina Vizueta-Rubio, Fernanda Chico-Terán, Liliana Cerda-Mejía, Mario D. García

inhibidores reportados con capacidad de unirse covalentemente al sitio activo fueron peptidomiméticos, que son compuestos análogos del sustrato que asemejan una estructura proteica y que además poseen grupos reactivos para atacar al residuo catalítico Cys145[17]. Como era de esperarse, el presente estudio reporta también la aparición de este tipo de moléculas (Tabla Suplementaria 1). Además, aquí identificamos que los carbamatos también constituyen un grupo representativo de inhibidores en diferentes enzimas Mpro. Estos compuestos, en particular los orgánicos, juegan un rol importante en el descubrimiento de fármacos y constituyen elementos estructurales de diversos agentes terapéuticos de funcionalidad probada como ritonavir, amprenavir, atazanavir y darunavir[43]. Algunas de las características que hacen a los carbamatos atractivos para el diseño de fármacos son su elevada estabilidad, permeabilidad a las membranas celulares y su habilidad para regular interacciones con las enzimas objetivo[44].

Definición de los sitios de unión a inhibidores

La enzima RdRp del SARS-CoV-2, a pesar de sus diferencias estructurales con otras del mismo tipo, mantiene la configuración tridimensional típica de polimerasas denominada de "mano derecha", pues comprende los dominios conocidos como Palma (Palm), Dedos (Finger) y Pulgar (Thumb) (Figura 1B). Interesantemente, se ha reportado que varias RdRps pueden ser inhibidas por moléculas que se unen al sitio activo y a múltiples bolsillos alostéricos. El presente estudio permitió determinar que se dispone de una gran cantidad de información estructural de la enzima

ns5b HCV en complejo con diferentes inhibidores. ns5b HCV posee una arquitectura tridimensional característica, donde el sitio activo se ubica en el dominio de la Palma, que implica la cavidad central de la enzima, y donde también se ubican dos sitios adicionales de unión a inhibidores (Palm I site y Palm II site). De igual manera en el dominio del Pulgar se han identificado al menos tres sitios alostéricos (Thumb I site, Thumb II site y Thumb III site) que permiten acoplar ligandos[28,45] (Figura 1A). Respondiendo al grado de conservación estructural de RdRps, en organismos como ZV, NV y NVM también se han reconocido inhibidores alostéricos que se unen en bolsillos cercanos al sitio activo. En contraste, los inhibidores que se han reportado para la nsp12 RdRp actúan únicamente tras su unión en el sitio activo ubicado en dominio de la Palma[46] (Figura 1B).

La superposición estructural de la RdRp del SARS-CoV-2 con su homóloga de referencia (ns5b HCV) (Figura 1C), muestra que en ambas enzimas existe correspondencia de sitios de unión respecto a todos aquellos bolsillos ubicados en la cavidad central de la Palma (Palm I y Palm II), así como de un sitio alostérico en el dominio del Pulgar (Thumb III), pues, aunque se aprecian diferencias en su conformación, estos son visibles en la estructura. Por el contrario, los dos bolsillos alostéricos restantes (Thumb I y Thumb II) prácticamente son inexistentes en la polimerasa del SARS-CoV-2, donde los aminoácidos de la cadena peptídica sobresalen de la estructura impidiendo la formación de cavidades que podrían acoplar inhibidores.

De esta forma, con base en la semejanza estructural con sus enzimas homólogas, en el presente estudio se
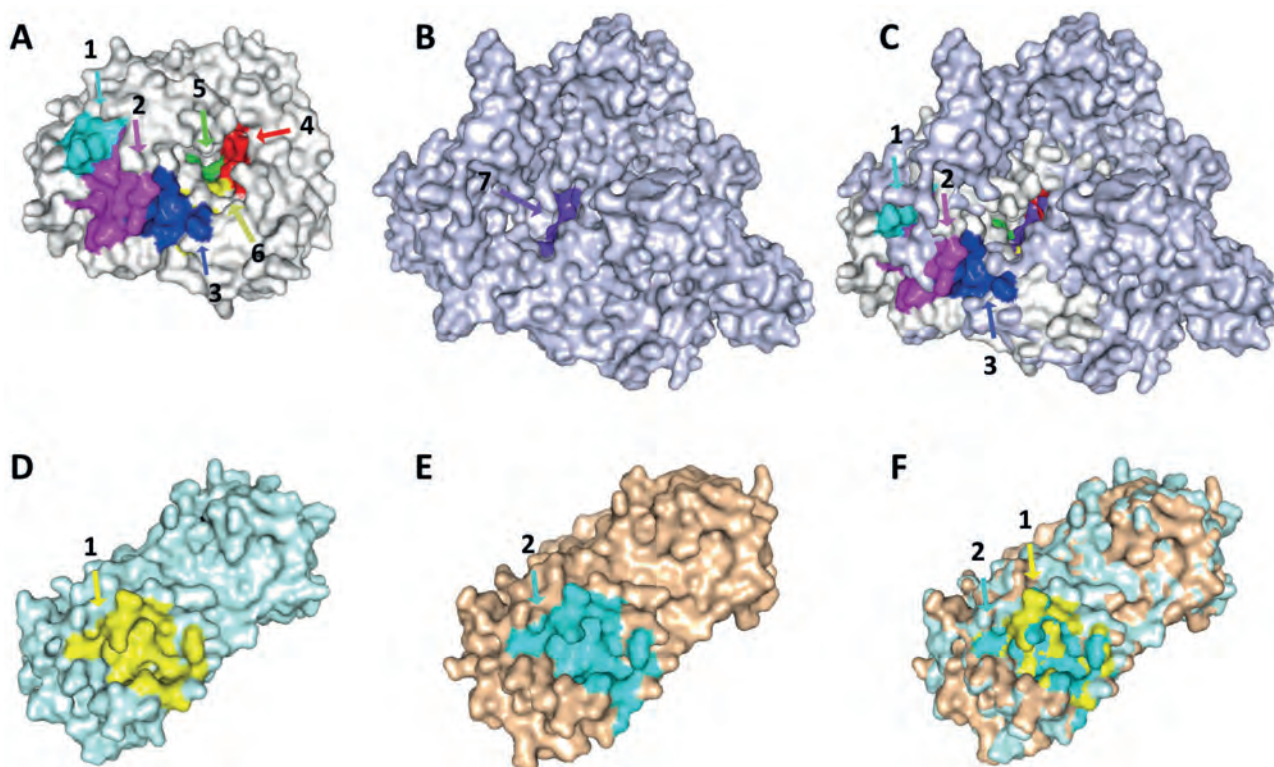
Figura 1. Comparación estructural de sitios de unión a inhibidores en enzimas del SARS-CoV-2. A) Se muestran los 6 bolsillos de unión de la RdRp ns5b HCV: en color cyan el sitio alostérico Thumb I (1), en color magenta el sitio alostérico Thumb II (2), en color azul el sitio alostérico Thumb III (3), en color rojo el sitio activo de la enzima (4), en color verde el sitio alostérico Palm I (5) y en color amarillo el sitio alostérico Palm II (6). B) Se muestra el único bolsillo de unión de la RdRp nsp12 del SARS-CoV: en color morado el sitio activo (7). C) La superposición entre ns5b HCV y nsp12 del SARS-CoV-2. D) Se muestra el sitio activo de la enzima Mpro del SARS-CoV en color amarillo (1). E) Se muestra el sitio activo de la enzima Mpro del SARS-CoV-2 en color cyan (2). F) Superposición entre Mpro del SARS-Co-V y SARS-CoV-2.

5

ensayó el acoplamiento molecular de los ligandos en los bolsillos sitio activo, Palm I site, Palm II site y Thumb III site de RdRp del SARS-CoV-2, asumiendo la posible existencia de estos tres últimos sitios alostéricos. La superposición de ns5b y nsp12 (Figura 1C), permitió determinar de manera visual los aminoácidos que conforman los sitios alostéricos teóricos de la RdRp del SARS-CoV-2, mismos que se indican en la Tabla 1.

Por su parte, Mᵖʳᵒ es una cisteína proteasa cuyo sitio activo está compuesto por cuatro sub-sitios denominados S1´, S1, S2 y S4. Esta enzima consta de tres dominios (I-III) y presenta una diada catalítica Cys-His no canónica localizada en la hendidura que se forma entre los dos primeros dominios[47]. Un estudio de cribado de pequeñas moléculas ha permitido caracterizar compuestos inhibidores alostéricos de Mpro que pueden unirse en un bolsillo distante del sitio activo y que son capaces de modular la actividad enzimática[48]. No obstante, debido a la gran conservación estructural de la enzima, los inhibidores que se unen al sitio activo comparten entre sí numerosas características[47], lo cual es enormemente favorable para el redireccionamiento de fármacos. Por lo tanto, en la presente investigación únicamente se han considerado inhibidores que se acoplan en el sitio activo clásico para los ensayos de docking (Tabla Suplementaria 1). Como se mencionó anteriormente, el análisis de homología estructural mostró que Mᵖʳᵒ del SARS-CoV (Figura 1D) posee una configuración tridimensional virtualmente idéntica con respecto a Mᵖʳᵒ del SARS-CoV-2 (Figura 1E). La superposición de ambas proteasas demostró que sus sitios activos poseen una arquitectura altamente similar (Figura 1F), lo cual sugiere que los inhibidores que tienen como blanco este bolsillo, podrían acoplarse de igual forma a ambas enzimas.

Alineamiento múltiple de secuencias

Para la polimerasa del SARS-CoV-2, el primer inhibidor para el cual se descubrió experimentalmente la estructura del complejo enzima-ligando fue Remdesivir Monofosfato (RMP). Mediante el análisis de sus interacciones con la enzima se determinó que el sitio activo se ubica en los motivos A-G del dominio de la Palma[10], y está conformado principalmente por 14 aminoácidos. El alineamiento múltiple de enzimas RdRp (Figura Suplementaria 1) muestra que la mayoría de los residuos involucrados en el acoplamiento del ligando, tales como Arg555, Asp618, Asp623, Ser682, Thr687, Asn691, Asp760 y Asp761, están altamente conservados entre los diferentes organismos analizados. Por otra parte, Val557 está sólo medianamente conservada, mientras que Arg553, Lys545, Thr680, Ala688 y Ser759 no muestran ningún grado de conservación. Esto señala que a pesar de las diferencias de tamaño de las secuencias de las diferentes RdRps homólogas a la polimerasa del SARS-CoV-2, los principales aminoácidos que intervienen en la unión al sustrato e inhibidores competitivos se mantienen entre especies. Por lo tanto, esto sugiere que los inhibidores competitivos de las polimerasas de ZV, HFMD, CV, NVM, NV, HCV y DV pueden ser alternativas viables para inhibir la replicación del SARS-CoV-2.

La ns5b HCV fue utilizada como referencia debido a la amplia información estructural disponible y cantidad de inhibidores descritos, por lo que los aminoácidos que conforman sus diferentes bolsillos de unión a ligandos también fueron comparados e identificados en nuestro análisis (Figura Suplementaria 1). Esto permitió determinar que 8 (Arg555, Asp618, Asp623, Ser682, Thr687, Asn691, Asp760 y Asp761) de los 13 aminoácidos que conforman el sitio activo de la ns5b están conservados en la nsp12. Estos residuos forman parte del centro catalítico.

Para los 5 bolsillos alostéricos adicionales de la ns5b; sin embargo, no se obtuvo una adecuada correspondencia entre aminoácidos, lo que significa que al menos en términos de secuencia estos no se encuentran conservados. Únicamente para los sitios alostéricos Palm I, Palm II y Thumb III de ns5b se pudo observar la presencia de bolsillos similares en nsp12, considerados aquí como sitios alostéricos teóricos, y por lo tanto incluidos en los estudios de acoplamiento molecular.

En cuanto a la proteasa, tomando como referencia a la estructura de la Mpro del virus SARS-CoV-2 unida al inhibidor N3, en el presente estudio se identificaron un total de 21 aminoácidos que participan en el acoplamiento del sustrato al sitio activo. Estos aminoácidos ayudan a estabilizar la

Sitio de unión	Palm I	Palm II	Thumb III
Residuos	Leu576	Lys593	Glu802
	Lys577	Trp598	Lys807
	Ala580	Met601	Gly808
	Ile589	Leu758	Pro809
	Gly590	Ser759	His810
	Thr591	Asp760	His816
	Ser592	Asp761	Thr817
	Lys593	Phe812	Met818
	Trp598	Cys813	Tyr831
	Met601	Ser814	
	Tyr689	Gln815	
	Leu758	Arg836	
	Cys813	Asp865	
	Gln815		

Tabla 1. Aminoácidos que conforman los bolsillos alostéricos teóricos de la RdRp del SARS-CoV-2.

Daysi Espín-Sánchez, María L. Ramos-Aristimbay, Andrés S. Sánchez-Vaca, Karen Jaramillo-Guapisaca, Carolina Vizueta-Rubio, Fernanda Chico-Terán, Liliana Cerda-Mejía, Mario D. García

unión y a bloquear el compuesto al interior de la cavidad mediante múltiples enlaces no covalentes[25]. Como se indica en la Figura Suplementaria 2, se pudo determinar que todos los organismos incluidos en el alineamiento múltiple de secuencias muestran conservación del sitio de unión de N3. Específicamente, los residuos de Thr26, Leu27, His41, Phe140, Asn142, Gly143, Ser144, Cys145, His163, Met165, Glu166, Pro168, His172, Asp187, Arg188, Thr190 y Glu192 son extremadamente conservados. En este grupo resaltan los aminoácidos catalíticos Cys145 e His41, que por su función central se mantienen conservados en todas las especies. En contraste, solamente 4 residuos, Met49, Leu141, His164 y Gln189, muestran un bajo grado de conservación. De esta forma, el alineamiento múltiple de secuencias demostró que el sitio activo y el bolsillo de unión de N3 es significativamente conservado entre enzimas M^pro de diferentes organismos. Esto sumado a los elevados porcentajes de similitud arrojados por el análisis de homología estructural, permiten deducir que los inhibidores de

las enzimas proteasas de los virus SARS-CoV, HKU4-CoV, HCoV-NL63, MERS-CoV, PEDV, FIPV y TGEV, son excelentes candidatos para el tratamiento del COVID-19, o bien para el diseño racional de nuevos compuestos.

Acoplamiento molecular

El cribado virtual mediante acoplamiento molecular se basó en la determinación de la energía libre de unión (Binding affinity) de los complejos enzima-ligando[38]. Utilizando RdRp como receptor se ensayó el acoplamiento molecular de 78 inhibidores, los cuales mostraron valores de afinidad de unión en el rango de -2 a -7.4 kcal/mol (Tabla suplementaria 2). Los tres mejores resultados fueron XNI (-7.4 kcal/mol), RTP (Ribavirin Trifosfato) (-7.3) y JT1 (JTK-853) (-7.1 kcal/mol) (Tabla 2). La estructura química de estos compuestos se detalla en la Figura 2.

El análisis de las coordenadas tridimensionales generadas mediante el acoplamiento molecular permitió evidenciar que XNI y JT1 se acoplan al sitio de la Palma I, mien-

Nº	RdRp		M^pro	
	PDB ID	Afinidad de unión (kcal/mol)	PDB ID	Afinidad de unión (kcal/mol)
Control	F86 (RMP)	-4,7	N3	-7,5
1.	XNI	-7,4	V3D	-8,0
2.	RTP	-7,3	EOF	-7,9
3.	JT1	-7,1	3A7	-7,8
4.	33F	-7,1	RFM	-7,8
5.	IX6	-7,0	PRD 000815	-7,7
6.	H5U	-7,0	4F4	-7,7
7.	46F	-6,9	PRD_002174	-7,7
8.	888	-6,9	E8E	-7,6
9.	B80	-6,8	ENB	-7,6
10.	XNC	-6,7	SDJ	-7,6
11.	T18	-6,7	ZU4	-7,5
12.	8XV	-6,4	9IN	-7,3
13.	H59	-6,4	CYV	-7,3
14.	26F	-6,3	EJF	-7,3
15.	28M	-6,3	V34	-7,20
16.	1O9	-6,3	PRD 000910	-7,10
17.	054	-6,3	8O5	-7,10
18.	26S	-6,2	PRD1117	-7,10
19.	2AY	-6,2	G81	-7,00
20.	63F	-6,2	I12	-7,00

Tabla 2. Bestranking de resultados del acoplamiento molecular de ligandos obtenidos mediante homología estructural en RdRp y M^pro del virus SARS-CoV-2.

6
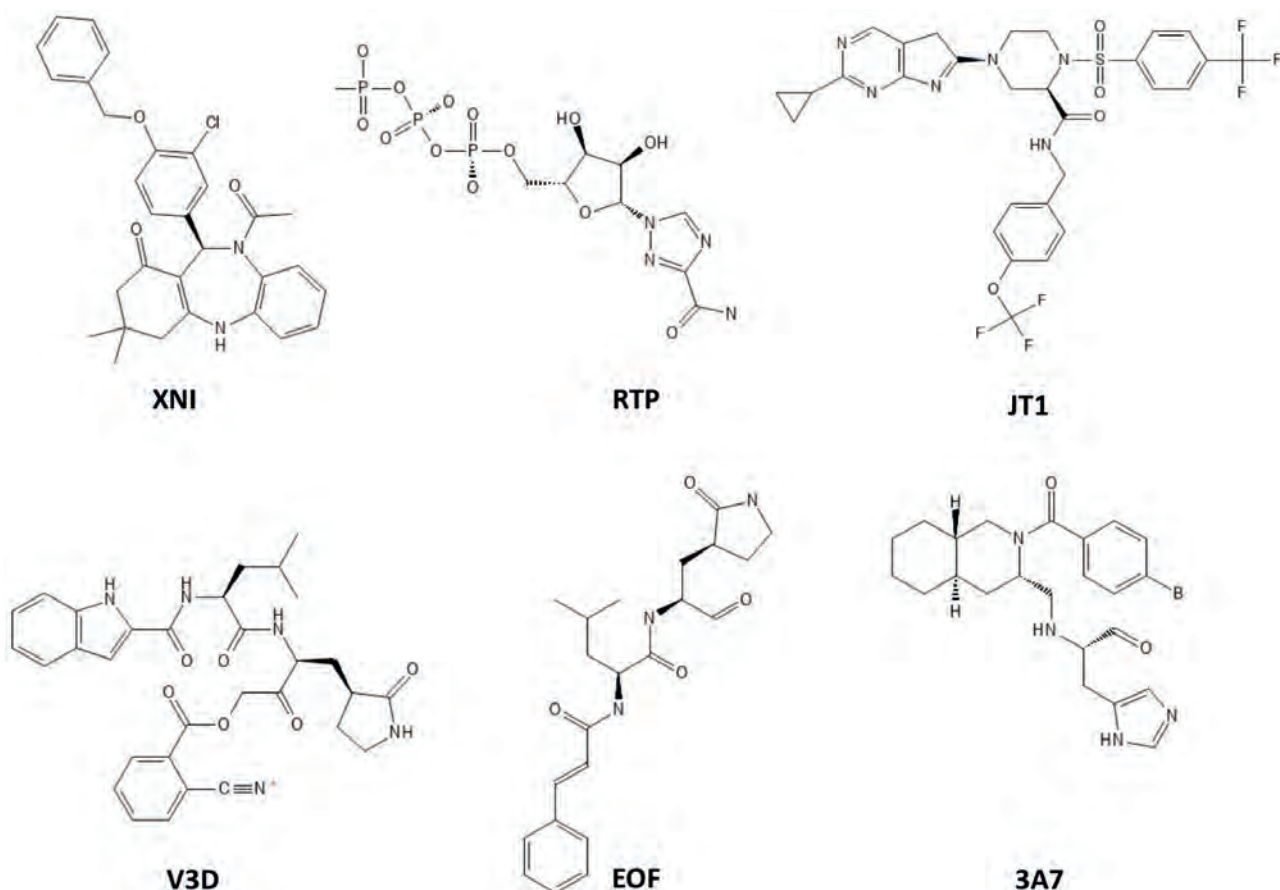
Figura 2. Estructura química de los mejores resultados del acoplamiento molecular en enzimas RdRp y M^pro del SARS-CoV-2. XNI, RTP y JT1 son inhibidores de la RdRp; V3D, EOF y 3A7 son inhibidores de M^pro.

tras que RTP y el control, RMP, se unen al sitio activo de la enzima. Cabe recalcar que los inhibidores de la nsp12 reportados hasta la fecha se unen en al sitio activo y todavía no existe evidencia de inhibidores capaces de unirse a sitios alostéricos adicionales. En este sentido, dada la homología de estructura primaria y secundaria que guardan los sitios activos de las polimerasas del HFMD y SARS-CoV-2 (Figura 4B), RTP puede acoplarse a la nsp12 de forma similar al control, RMP. De hecho, RPT muestra un valor de afinidad superior a aquel observado para el control (-4.7 kcal/mol). Por lo tanto, RTP parece ser el resultado más relevante, pues su modo de unión se asemeja a los compuestos con actividad inhibitoria y antiviral *in-vitro* e *in-vivo*, tales como RMP. RTP es un análogo de guanosina, que difiere de ésta porque la D-ribosa se encuentra unida a un anillo de 1,2,4-triazol-carboxamida en lugar de un anillo de purina, y en su forma activa (trifosfatada), interfiere con la replicación viral49, lo cual explica su afinidad por el sitio activo de la nsp12.

Las poses determinadas para XNI, RTP y JT1 en RdRp del SARS-CoV-2 son altamente similares a aquellas observadas en los complejos XNI-HCV RdRp, JT1-HCV RdRp y RTP-HFMD RdRp. No obstante, se debe recordar que las enzimas RdRp del HCV y HFMD mantienen alrededor de un 46% de homología estructural con la polimerasa del SARS-CoV-2 y menos de 9% de homología de secuencia. Estos porcentajes de similitud se traducen en alteraciones en la configuración de los bolsillos, y consecuentemente en el modo de unión de los ligandos en la nsp12 con respecto a sus targets originales. Las Figuras 5A, 5B y 5C muestran la diferencia entre la posición original del ligando sometido

a cribado y las posiciones adoptadas durante el acoplamiento al sitio de unión en RdRp.

En cuanto al acoplamiento molecular para M^pro, se ensayaron 41 inhibidores en el sitio activo de la enzima. Los valores de afinidad de unión oscilaron entre -6 y -8 kcal/mol (Tabla Suplementaria 3). El mejor resultado se obtuvo con el ligando V3D, seguido por EOF y 3A7, con valores de afinidad de unión de -8, -7.9 y -7.8 kcal/mol, respectivamente, como se indica en la Tabla 2. Todos estos ligandos son inhibidores de la proteasa M^pro del SARS-CoV y sus estructuras químicas se muestran en la Figura 2. V3D es un inhibidor irreversible con un IC_{50} = 53 ± 1 μM. Por otra parte, EOF y 3A7 son inhibidores reversibles con valores de IC_{50} de 0.83 (EOF) y 63 μM (3A7). Como se mencionó anteriormente, las enzimas Mpro del SARS-CoV y SARS-CoV-2 son estructuralmente idénticas (SSE = 100%) y presentan una identidad de secuencia del 96.1%. En cuanto a sus sitios activos, el alineamiento de secuencias muestra la presencia de solo una sustitución (Arg188Ile) en M^pro del SARS-CoV, mientras que el resto de los residuos que contornean el sitio activo se mantienen conservados en ambas enzimas (Figura Suplementaria 2). La superposición de sitios activos de las enzimas Mpro del SARS-CoV y SARS-CoV-2 (Figura 4C) muestra que no solamente existe una alta homología de sus estructuras secundarias, sino que también se encuentran conservadas las conformaciones que adoptan los residuos que contornean su sitio de unión a ligandos de cada enzima. Esta elevada similitud explica por qué los inhibidores de Mpro del SARS-CoV son altamente afines a su enzima homóloga en SARS-CoV-2 en comparación a ligandos provenientes de otras proteasas, así como también

Daysi Espín-Sánchez, María L. Ramos-Aristimbay, Andrés S. Sánchez-Vaca, Karen Jaramillo-Guapisaca, Carolina Vizueta-Rubio, Fernanda Chico-Terán, Liliana Cerda-Mejía, Mario D. García

8
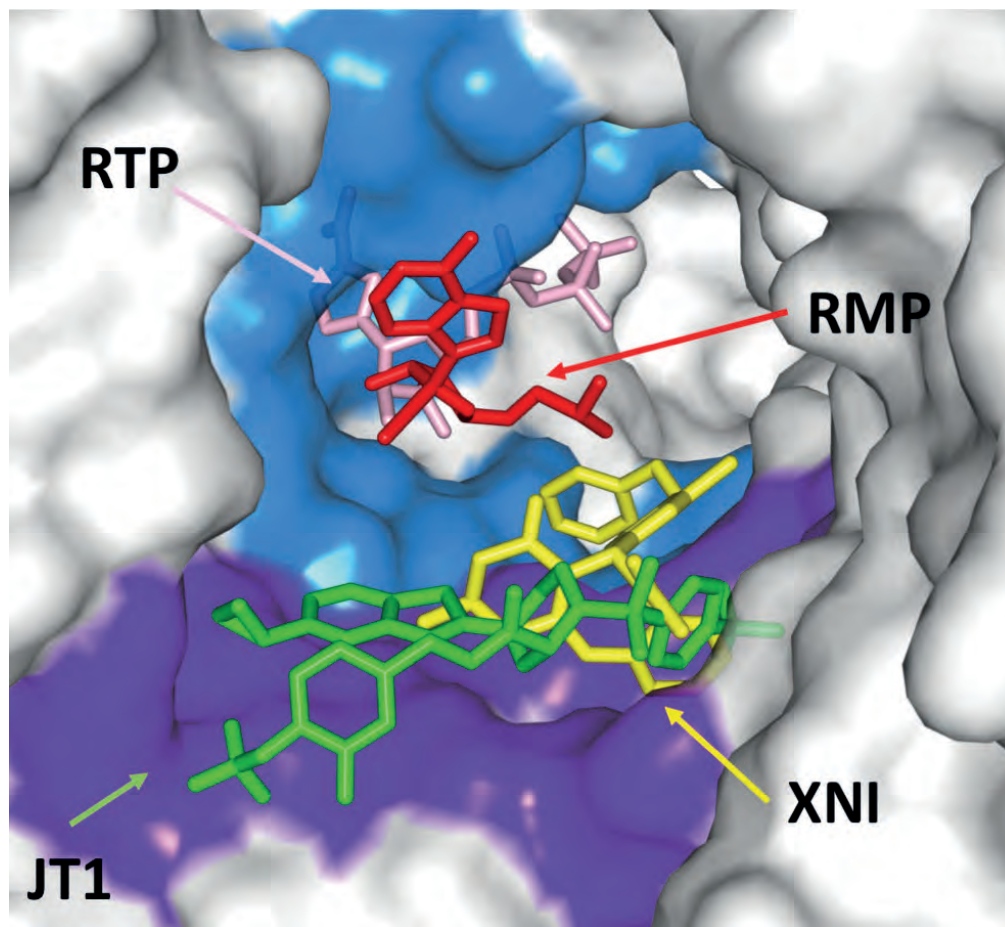
Figura 3. Modo de unión a inhibidores de la enzima RdRp del SARS-CoV-2 según el acoplamiento molecular. Se muestran en palillos los inhibidores XNI, RTP, JT1 y la molécula control Remdesivir Monofosfato (RMP), y en representación de superficie la enzima, en color azul el sitio activo de la enzima y en color morado el sitio alostérico teórico Palm I. Por otra parte, XNI (K_i = 1.7 μM) y JT1 (IC_{50} = 17.8 nM) son inhibidores reversibles que se unen en el sitio alostérico Palm I de la ns5b HCV (Figura 3). Si bien el alineamiento de secuencias demostró que los aminoácidos que componen este bolsillo de unión no se conservan en la nsp12, la superposición del sitio de la Palma I de ns5b junto con la estructura de la nsp12 muestra un bolsillo similar en la polimerasa del SARS-CoV-2 (Figura 4A).
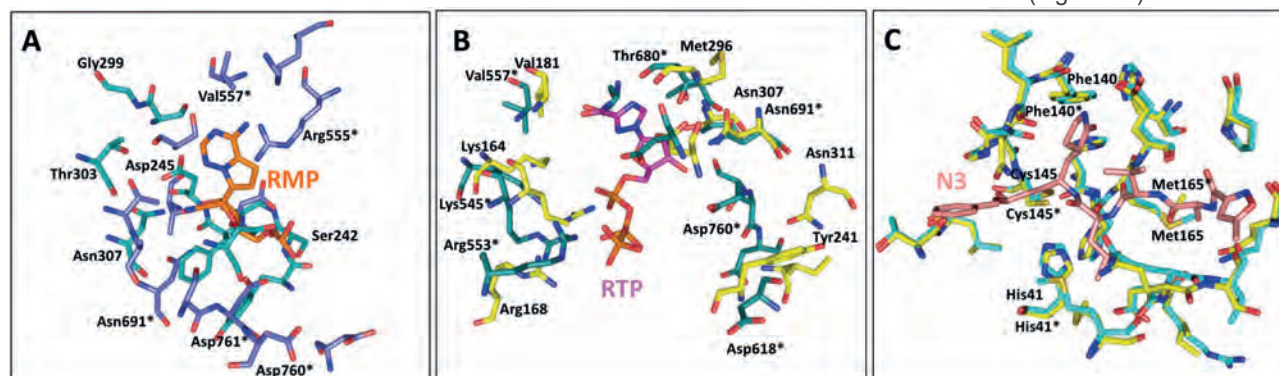
Figura 4. Comparación del sitio de unión a inhibidores entre enzimas del SARS-CoV-2 y sus homólogas de referencia. A) Superposición del sitio alostérico Palm I entre RdRp del HCV en palillos de color verde y del SARS-CoV-2 en palillos de color morado; se indica en palillos de color naranja el inhibidor RMP. B) Superposición del sitio activo de RdRp de HFMD en palillos de color amarillo y del SARS-CoV-2 en palillos de color verde; se indica en palillos de color magenta el inhibidor RTP. C) Superposición del sitio activo de Mpro del SARS-CoV en palillos de color amarillo y del SARS-CoV-2 en palillos de color cyan; se muestra en rosado el inhibidor N3. Los residuos marcados con (*) corresponden al SARS-CoV-2.

explica la razón por la cual la pose adoptada por V3D, EOF y 3A7 en Mpro del SARS-CoV-2 es prácticamente igual a la pose que adoptan estos ligandos en las estructuras cristalinas de M^pro del SARS-CoV (Figura 5D a 5F).

Modo de unión de los complejos RdRp-RTP y M^pro-V3D

El análisis del modo de unión de RTP indica que este inhibidor es capaz de unirse a la RdRp del SARS-CoV-2 por medio de interacciones con 17 residuos de aminoácidos del sitio activo (Figura 6). Entre los más importantes se encuentran los residuos Arg624, Arg553 y Arg555, pues son capaces de generar múltiples interacciones de tipo puente salino y puente de hidrógeno con los átomos de oxígeno de

la porción trifosfato de RTP. En el caso de Arg555, además del puente salino, la cadena lateral forma 3 puentes de hidrógeno con dos oxígenos de la porción trifosfato y uno del anillo de D-ribosa. Los residuos cargados Lys551 y Lys621 también generan puentes salinos con el trifosfato de RTP, mientras que los aminoácidos Asn691, Tyr680 y Tyr456 forman puentes de hidrógeno con la ribosa, el anillo de triazol y el grupo carboxamida, respectivamente. Finalmente, los residuos Thr556, Val557, Cys622, Asp623, Ser681, Ser682, Thr687, Ser759 y Asp760 asisten a la unión del inhibidor mediante enlaces débiles de Van der Waals.

El análisis del modo de unión de V3D en M^pro del SARS-CoV-2 muestra que el modo de unión del inhibidor es prác-
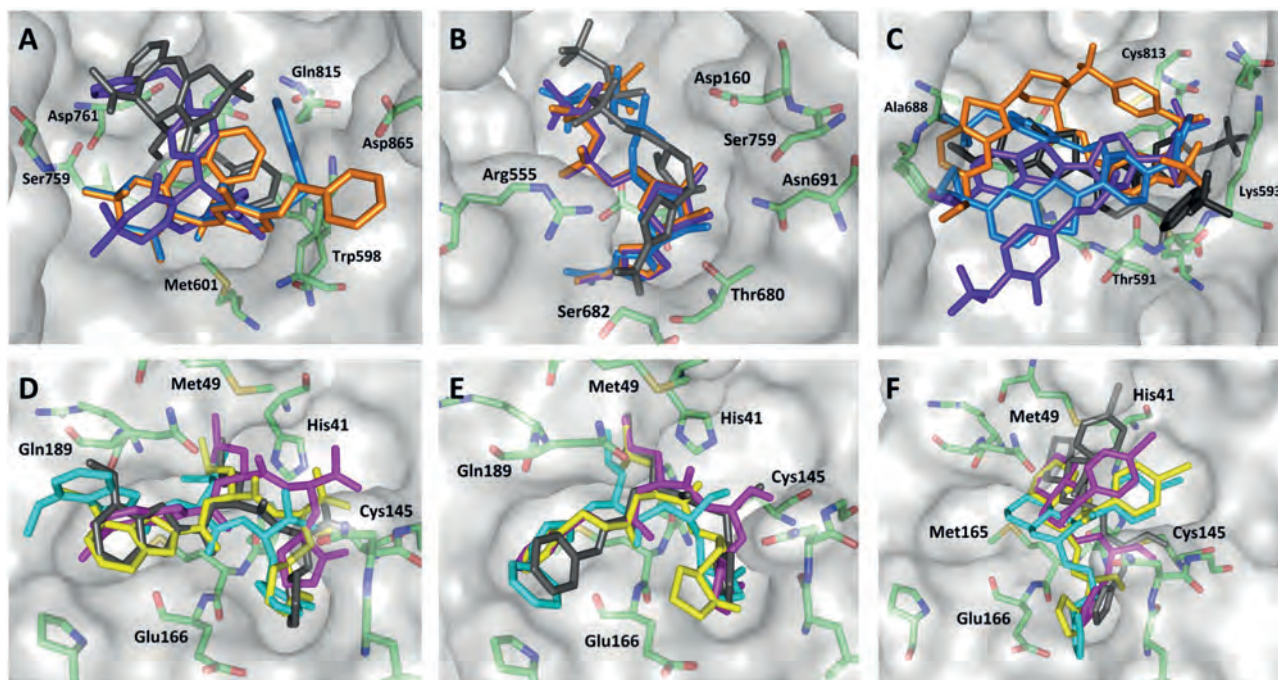
Figura 5. Posiciones adoptadas por los inhibidores de las enzimas del SARS-CoV-2 según el acoplamiento molecular. A) XNI- RdRp. B) RTP-RdRp. C) JT1-RdRp. D) V3D-Mᵖʳᵒ. E) EOF-Mᵖʳᵒ. F) 3A7-Mᵖʳᵒ. Se muestra en palillos de color negro la posición original del ligando y las mejores soluciones de cada resultado están representadas de diferentes colores. La proteína se muestra en superficie de color gris y los aminoácidos que interactúan directamente con los ligandos en el sitio de unión aparecen en palillos de color verde claro.
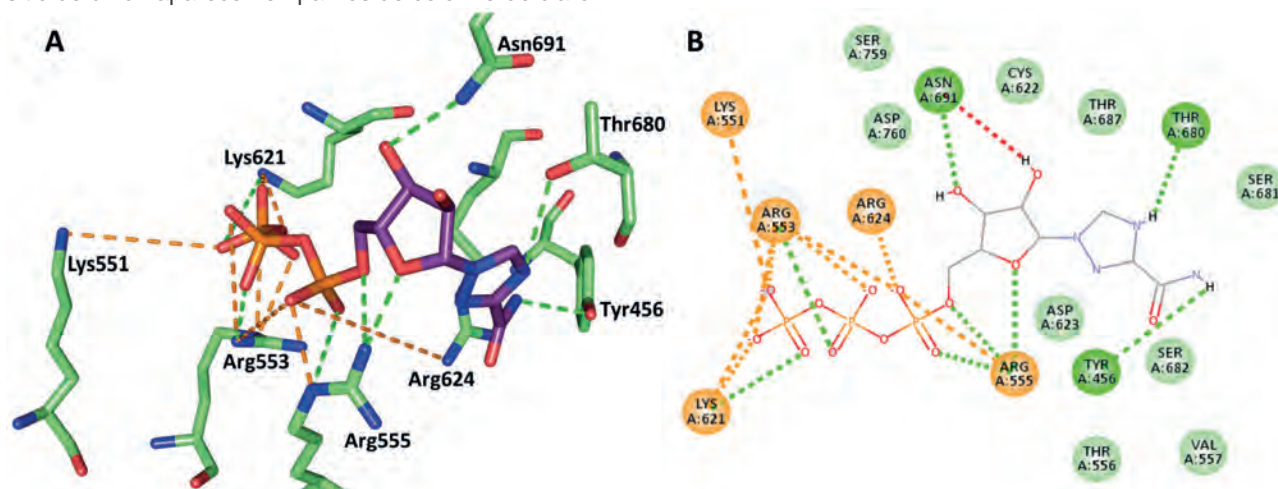
Figura 6. Interacciones entre la enzima RdRp (PDB ID: 7bv2) del SARS-CoV-2 y RTP en el sitio activo. A) Representación 3D. B) Representación 2D. Los puentes salinos y cargas atractivas se muestran en color naranja, los puentes de hidrógeno en color verde y las interacciones donante-donante desfavorables en color rojo.

ticamente igual a cuando se une a Mᵖʳᵒ del SARS-CoV. El anillo de pirrol de la porción indol puede formar un enlace pi-alquil con Met165 y un puente de hidrógeno con Gln189 (Figura 7). Los grupos amino y carbonilo unidos al C-12 forman enlaces de hidrógeno con Gln189 y Glu166, respectivamente. Por su parte, el grupo carbonilo del C-34 forma un puente de hidrógeno con Gly143 mientras que otro puente de hidrógeno se forma entre el H del grupo amino en la porción de la oxopirrolidina y el residuo de Leu141. Adicionalmente, el oxígeno de la oxopirrolidina forma dos puentes de hidrógeno con la cisteína catalítica (Cys 145) y con Ser144. El segundo residuo catalítico, His41, es capaz de formar un enlace pi-catión con el grupo 3S-butil que se une al C-15 y un enlace Pi-alquil con el mismo grupo. Se observan además dos enlaces pi-alquil entre Met49 y 3S-butil. El grupo metoxi del anillo bencénico perteneciente al grupo forma

dos enlaces pi-alquil con Leu167 y Pro168. También se observa numerosos enlaces carbono-hidrógeno entre V3D y los residuos de Thr25, Leu27, Tyr54, Phe140, Asn142, His163, His164, Asp187, Arg188, Thr190 y Gln192. Este modo de unión difiere significativamente del modo de unión de otros inhibidores de Mᵖʳᵒ del SARS-CoV-2, como N3. La estructura cristalina del complejo N3-Mᵖʳᵒ del SARS-CoV-2 muestra que el inhibidor se une al sitio activo con una conformación extendida. La cadena principal del inhibidor forma una hoja antiparalela con los residuos 164-168 de la cadena larga de la proteína, y con los residuos 189-191 del bucle que une a los dominios II y III. La Cys145 juega un rol fundamental, ya que es capaz de formar un enlace covalente con el ligando. Las cadenas laterales de Phe140, Asn142, Glu166, His163, His172 y las cadenas principales de Phe140 y Leu141, conforman el denominado subsitio

Daysi Espín-Sánchez, María L. Ramos-Aristimbay, Andrés S. Sánchez-Vaca, Karen Jaramillo-Guapisaca, Carolina Vizueta-Rubio, Fernanda Chico-Terán, Liliana Cerda-Mejía, Mario D. García
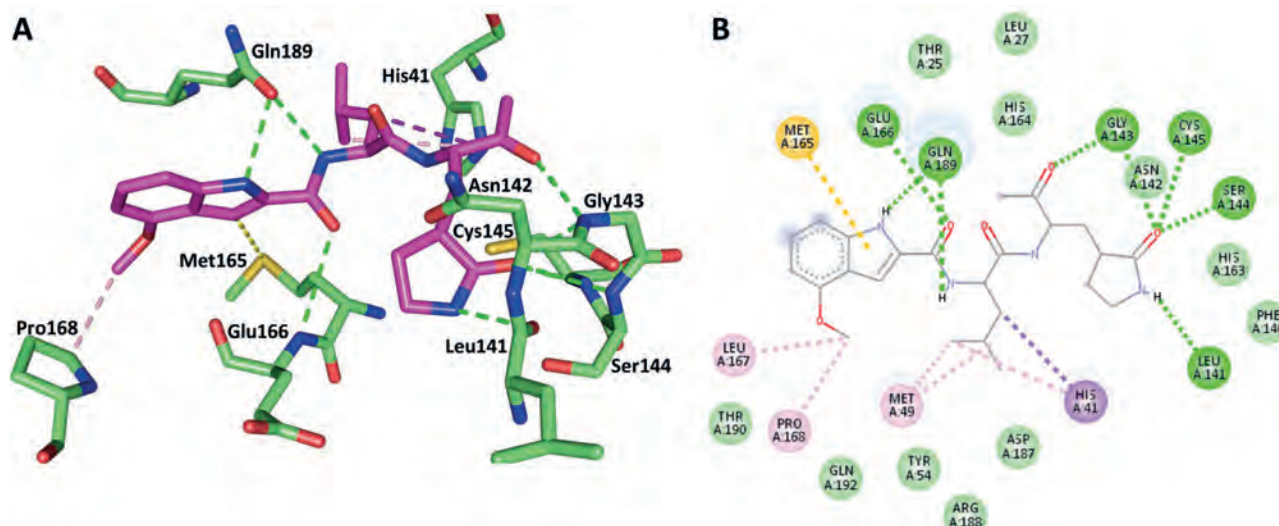
Figura 7. Interacciones entre la enzima M^pro (PDB ID: 7bqy) del SARS-CoV-2 y V3D en el sitio activo. A) Representación 3D. B) Representación 2D. Los enlaces de hidrógeno convencionales y enlaces carbono-hidrógeno se muestran en verde, el enlace Pi-alil en amarillo, los enlaces Pi-amida apilados y Pi-Alquil se muestran en rosado, y el enlace pi-catión en lila.

S1, donde la His163 además crea un puente de hidrógeno con el anillo lactama de N3. En el subsitio hidrofílico S2 se incluyen las cadenas laterales de His41, Met49 y el residuo Leu27 en la región más profunda de la cavidad. Mientras que en el sitio P4, principalmente las cadenas laterales de Met165, Glu192 y Gln189 forman un pequeño bolsillo hidrofóbico. Finalmente, el sitio P5 es capaz de establecer interacciones de tipo Van der Waals con residuos como Pro168 y Thr19025, 47.

Conclusiones

El análisis de homología realizado para enzimas RdRp y M^pro del virus causante del COVID-19 reveló que existen organismos virales que comparten casi el 50% de identidad estructural con la RdRp y hasta el 100% de identidad estructural con M^pro. El posterior alineamiento múltiple de secuencias permitió determinar que el sitio activo de la polimerasa del SARS-CoV-2 está altamente conservado entre organismos a pesar de la diferencia de tamaño entre enzimas. Por su parte, en Mpro también se determinó la conservación del sitio activo enzimático, aunque se han registrado unas pocas mutaciones puntuales. La alta conservación de sus sitios activos, que corresponden los principales bolsillos de unión de inhibidores, se debe al rol central que cumplen ambas enzimas en el ciclo de vida del virus. Por lo tanto, se pudo emplear el enfoque de redireccionamiento de fármacos que inicialmente tenían como blanco a las enzimas de organismos homólogos, para realizar un cribado virtual que permita identificar potenciales inhibidores contra el virus SARS-CoV-2.

Se llevaron a cabo ensayos de acoplamiento molecular en los que se pudo identificar a RTP y V3D como potenciales inhibidores de RdRp y M^pro, respectivamente. Ambas moléculas presentan valores de afinidad de unión inferiores a aquellas determinadas para RMP y N3, los cuales son moléculas con potente actividad *in-vitro* e *in-vivo* contra el SARS-CoV-2. Esto sugiere que RTP y V3D poseen un gran potencial de convertirse en opciones terapéuticas para combatir el SARS-CoV-2.

Conflictos de Interés

Los autores declaran no tener conflicto de interés.

Referencias bibliográficas

1. Pan American Health Organization/World Health Organization. Epidemiological Update: Coronavirus Disease, (2020, accessed 09/02/2021 2021).
2. World Health Organization. WHO Coronavirus (COVID-19) Dashboard. 2020.
3. Gorbalenya AE, Baker SC, Baric RS, et al. The species Severe acute respiratory syndrome-related coronavirus: classifying 2019-nCoV and naming it SARS-CoV-2. 2020; 5: 536.
4. Zhang L, Shen F-m, Chen F, et al. Origin and evolution of the 2019 novel coronavirus. 2020; 71: 882-883.
5. Helmy YA, Fawzy M, Elaswad A, et al. The COVID-19 pandemic: a comprehensive review of taxonomy, genetics, epidemiology, diagnosis, treatment, and control. 2020; 9: 1225.
6. Rangan R, Zheludev IN and Das RJB. RNA genome conservation and secondary structure in SARS-CoV-2 and SARS-related viruses. 2020.
7. Khailany RA, Safdar M and Ozaslan MJGr. Genomic characterization of a novel SARS-CoV-2. 2020; 19: 100682.
8. Gordon DE, Jang GM, Bouhaddou M, et al. A SARS-CoV-2 protein interaction map reveals targets for drug repurposing. 2020; 583: 459-468.
9. Sanders JM, Monogue ML, Jodlowski TZ, et al. Pharmacologic treatments for coronavirus disease 2019 (COVID-19): a review. 2020; 323: 1824-1836.
10. Yin W, Mao C, Luan X, et al. Structural basis for inhibition of the RNA-dependent RNA polymerase from SARS-CoV-2 by remdesivir. Sience 2020; 368: 1499-1504. DOI: 10.1126/science.abc1560.
11. Pastrian-Soto GJIjoo. Bases genéticas y moleculares del COVID-19 (SARS-CoV-2). Mecanismos de patogénesis y de respuesta inmune. 2020; 14: 331-337.
12. Joshi RS, Jagdale SS, Bansode SB, et al. Discovery of potential multi-target-directed ligands by targeting host-specific SARS-CoV-2 structurally conserved main protease. 2020: 1-16.

10

13. Báez-Santos YM, John SES and Mesecar AD. The SARS-coronavirus papain-like protease: structure, function and inhibition by designed antiviral compounds. 2015; 115: 21-38.

14. Liu C, Zhou Q, Li Y, et al. Research and development on therapeutic agents and vaccines for COVID-19 and related human coronavirus diseases. ACS Publications, 2020.

15. Ju J, Li X, Kumar S, et al. Nucleotide analogues as inhibitors of SARS□CoV polymerase. Pharmacology Research & Perspectives 2020; 8: e00674. DOI: 10.1002/prp2.674.

16. Shilatifard A. COVID-19: Rescue by transcriptional inhibition. American Association for the Advancement of Science, 2020.

17. Ullrich S and Nitsche C. The SARS-CoV-2 main protease as drug target. Bioorganic & Medicinal Chemistry Letters 2020; 30. DOI: 10.1016/j.bmcl.2020.127377.

18. Hashemian SM, Farhadi T, Velayati AAJDd, development, et al. A review on remdesivir: a possible promising agent for the treatment of COVID-19. 2020; 14: 3215.

19. OMS. 10 Vaccines Granted Emergency Use Listing (EUL) by WHO. 2022. Organización Mundial de la Salud.

20. Knoll MD and Wonodi CJTL. Oxford–AstraZeneca COVID-19 vaccine efficacy. 2021; 397: 72-74.

21. Kim JH, Marks F and Clemens JDJNm. Looking beyond COVID-19 vaccine phase 3 trials. 2021: 1-7.

22. Gautret P, Lagier J-C, Parola P, et al. Hydroxychloroquine and azithromycin as a treatment of COVID-19: results of an open-label non-randomized clinical trial. 2020; 56: 105949.

23. Dhama K, Sharun K, Tiwari R, et al. COVID-19, an emerging coronavirus infection: advances and prospects in designing and developing vaccines, immunotherapeutics, and therapeutics. 2020; 16: 1232-1238.

24. Lamb YN. Remdesivir: first approval. Springer 2020: 1-9. DOI: https://doi.org/10.6084/m9.figshare.12752432/.

25. Jin Z, Du X, Xu Y, et al. Structure of M pro from SARS-CoV-2 and discovery of its inhibitors. 2020; 582: 289-293.

26. Choudhary S, Malik YS and Tomar SJFii. Identification of SARS-CoV-2 cell entry inhibitors by drug repurposing using in silico structure-based virtual screening approach. 2020; 11: 1664.

27. Śledź P and Caflisch AJCoisb. Protein structure-based drug design: from docking to molecular dynamics. 2018; 48: 93-102.

28. Gupta SP. Chapter 3 - Inhibition of Viruses: Promising Targets and Their Importance. In: Gupta SP (ed) Studies on Hepatitis Viruses. Academic Press, 2018, pp.35-65.

29. Pagadala NS, Syed K and Tuszynski JJBr. Software for molecular docking: a review. 2017; 9: 91-102.

30. Krissinel E and Henrick K. Secondary-structure matching (SSM), a new tool for fast protein structure alignment in three dimensions. Acta Crystallographica Section D: Biological Crystallography 2004; 60: 2256-2268.

31. Berman HM, Westbrook J, Feng Z, et al. The protein data bank. Nucleic acids research 2000; 28: 235-242.

32. Schrödinger L. The PyMOL Molecular Graphics System. 2017.

33. Emsley P, Lohkamp B, Scott WG, et al. Features and development of Coot. Acta Crystallographica Section D 2010; 66: 486-501. DOI: doi:10.1107/S0907444910007493.

34. Di Tommaso P, Moretti S, Xenarios I, et al. T-Coffee: a web server for the multiple sequence alignment of protein and RNA sequences using structural information and homology extension. Nucleic acids research 2011; 39: W13-W17.

35. Artimo P, Jonnalagedda M, Arnold K, et al. ExPASy: SIB bioinformatics resource portal. Nucleic Acids Research 2012; 40: W597-W603. DOI: 10.1093/nar/gks400

36. Forli S, Huey R, Pique ME, et al. Computational protein–ligand docking and virtual drug screening with the AutoDock suite. Nature protocols 2016; 11: 905-919.

37. Trott O and Olson AJ. AutoDock Vina: improving the speed and accuracy of docking with a new scoring function, efficient optimization, and multithreading. Journal of computational chemistry 2010; 31: 455-461.

38. Dallakyan S and Olson AJ. Small-molecule library screening by docking with PyRx. Chemical biology. Springer, 2015, pp.243-250.

39. Biovia DSJR. Materials Studio. 2017.

40. Venkataraman S, Prasad BV and Selvarajan R. RNA dependent RNA polymerases: insights from structure, function and evolution. Viruses 2018; 10: 76.

41. Chuanjun S, Xuan H, Ting H, et al. Potential inhibitors for targeting Mpro and Spike of SARS-CoV-2 based on sequence and structural pharmacology analysis. STEMedicine 2020; 1. DOI: 10.37175/stemedicine.v1i2.41.

42. Ugwu DI, Okoro UC and Ahmad H. New carboxamide derivatives bearing benzenesulphonamide as a selective COX-II inhibitor: design, synthesis and structure-activity relationship. PloS one 2017; 12: e0183807. DOI: 10.1371/journal.pone.0183807.

43. Matošević A and Bosak A. Carbamate group as structural motif in drugs: A review of carbamate derivatives used as therapeutic agents. Archives of Industrial Hygiene Toxicology 2020; 71: 285. DOI: 10.2478/aiht-2020-71-3466.

44. Ghosh AK and Brindisi M. Organic carbamates in drug design and medicinal chemistry. Journal of Medicinal Chemistry 2015; 58: 2895-2940. DOI: 10.1021/jm501371s.

45. Hang JQ, Yang Y, Harris SF, et al. Slow binding inhibition and mechanism of resistance of non-nucleoside polymerase inhibitors of hepatitis C virus. Journal of Biological Chemistry 2009; 284: 15517-15529. DOI: 10.1074/jbc.M808889200.

46. Hillen HS, Kokic G, Farnung L, et al. Structure of replicating SARS-CoV-2 polymerase. Nature 2020; 584: 154-156. DOI: 10.1038/s41586-020-2368-8.

47. Dai W, Zhang B, Jiang X-M, et al. Structure-based design of antiviral drug candidates targeting the SARS-CoV-2 main protease. 2020; 368: 1331-1335.

48. El□Baba TJ, Lutomski CA, Kantsadi AL, et al. Allosteric Inhibition of the SARS□CoV□2 Main Protease: Insights from Mass Spectrometry Based Assays. Angewandte Chemie International Edition 2020; 59: 23544-23548. DOI: doi.org/10.1002/anie.202010316.

49. Gross AE and Bryson ML. Oral ribavirin for the treatment of noninfluenza respiratory viral infections: a systematic review. Annals of Pharmacotherapy 2015; 49: 1125-1135. DOI: https://doi.org/10.1177/1060028015597449.

11

ARTICLE / INVESTIGACIÓN

Production of environmentally friendly attractants for the trap flies *Megaselia halterata* and *Lycoriella ingenue* parasites on edible mushrooms in Iraq

Abdullah Abdulkareem Hassan[1]* and Abier Raouf Mahmoud Al-Qaissi[2]

[1] Department of plant protection, College of Agriculture, University of Tikrit, Iraq.
[2] Agriculture researches office, Ministry of Science and Technology, Iraq.
Corresponding author: drabdullah.has67@tu.edu.iq.

1

Abstract: Among several tested mushroom-related materials, full-grown compost followed by fermented corn cobs and the compost were the best baits for attracting and catching of both insects *M. halterata* and *L. ingenua*. At the same time, there was no effect on attracting insects for the wheat straw, unfermented corn cobs, unfermented bran and water (control). The results proved that the highest attraction in the hunting of the two insects, *M. halterata* and *L. ingenua*, was in the treatment of cut fruit bodies for all studied A. bisporus strains, the highest number was 6.49 and 5.43 insects/bait; in the treatment of cut fruits of A.bisporus B62, respectively, At the level of mushroom species, the brown strain of *A.bisporus* showed the lowest attraction to the studied insects. Chopped fruit bodies and the spawn of some species/strains of oyster mushroom Pleurotus led to the highest interest in insects, followed by the treatment of mashed fruit bodies; the chopped fruits reached the highest attraction of insects for P. eryngii, the number of insects, *M. halterata* and *L. ingenua*, was 6.56 and 5.32 insects/bait, respectively. In the combination baits that were made from mixtures of the most efficient treatments resulting from the media and the fruit bodies of the *A.bisporus* and *Pleurotus spp.*, the results showed that all treatments led to attracting the two insects at a rate of 4.55 - 8.7 insects/bait for *M.halterata* and 4.06 - 7.82 insects/bait for *L. ingenue*. The results also showed that there were significant differences in the reduction of both mushrooms *A.bisporus* and *P. ostreatus* infection rate by all types of tested baits; the lowest infection rates were in the combination bait treatment, resulting in 1.86 and 2.17%, respectively, compared to the control treatment (without bait) in which the infection rate was 87.3 and 91.25%, respectively.

Key words: Plant Tissue culture, Cost analysis, Large-scale production, Biofactory, Monte Carlo Simulation (MCS).

Introduction

The white button mushroom *Agaricus bisporus* and the oyster mushroom *Pleurotus* spp. are mainly edible mushrooms that can provide many essential nutrients, including protein, vitamins and minerals, and medicinal properties that have various health benefits for humans[1]. Mushroom yield is exposed to many pests and diseases that cause losses in the quantity and quality of the product. The mushroom flies belong to some genera, such as *Lycoriella sp.*, *Bradysia sp.*, *Megaselia sp.* and others. They are essential flies that attack most stages of mushroom production, starting from the nutrient medium and ending with the location of producing fruit bodies. These insects also infect most commercially produced edible mushrooms such as *A. bisporus*, *Pleurotus spp.*, *Lentinus edodes* and others[2,3]. Mushroom flies cause damage to the mushroom through various methods, such as direct feeding of the larvae on the developing fruiting bodies and the mycelium growing in compost or substrate (nutrient medium), in addition to competition between the larvae and the grown mycelium to obtain nutrients in the mushroom medium. The indirect harmful effects of the mushroom fly are likely to transmit many pathogens such as bacteria, fungi, viruses and nematodes[2,4]. It is known that a significant decrease in the mushroom yield occurs at a density of only one larva per 125 g of medium[5]. The infection

of mushrooms such as *Agaricus spp.* and *Pleurotus spp.* with the insect pests, especially *Lycoriella sp.* and *Megaselia sp.*, leads to significant losses in the quantity and quality of the mushroom yield. Therefore, many studies have used the applications of control of these insects by chemical, biological and physical methods[4]. Several strategies have been used to control mushroom flies, including the use of chemical pesticides such as diazinon and imadocloprid[6], cyromazine, diflubenzuron, diazinon, endosulfan and chlorfenvinphos[7], sex hormones[8], chitin synthesis inhibitors[9], in addition, biological control has been used against these insects such as entomopathogenic nematodes[10] and larval predators[11]. The biological factors were not widely applied in mushroom farms[3,12]. Therefore, chemical pesticides remain the fastest effective in eradicating mushroom flies, but there are several problems associated with the use of chemicals, such as the impact on human health and the environment as well as the emergence of Pesticide-resistant strains and their effect on natural organisms that beneficial for mushroom growth. Furthermore, spraying pesticides is challenging to apply when insects attack the fruiting bodies because the larvae move after hatching into the fruits and protect themselves from the effects of pesticides[8,13]. Therefore, attention is focused on physical methods, including

color and sticky traps[14], as these traps are considered an inefficient means in the case of mushroom farms because the smell of fruiting bodies attracts insects to them more than the colored traps, in addition to the fact that these traps are not specialized to attract edible mushrooms flies. The use of plants in the form of plant extracts can benefit from some of their insect-repellent, anti-nutritive and growth-regulatory properties[15]. Also, extracts of some plants such as garlic, onion, neem and eucalyptus were used as alternatives to chemical pesticides in the control of *Lycoriella ingenua* that parasitizes *Pleurotus* mushroom. During four weeks, the insect mortality rate was 40-60%, depending on the type of plant[16]. We did not find in the literature the use of mushrooms related materials such as compost or the mycelium and fruit bodies of mushrooms themselves as baits to attract and get rid of the insect. In Iraq, many of these pests and pathogens have been studied previously[17], while mushroom flies, *Megaselia halterata* and *Lycoriella ingenua* were recorded in 2021 for the first time in Iraq[18].

For the importance of mushroom yield, reducing the infection of the mushroom fly, and reducing the use of chemical pesticides in controlling them, this study aimed to evaluate several mixtures of the culture media of these mushrooms and their fruit bodies for studying their attractive role in insect traps.

Materials and methods

Cultivation of the white button mushroom *A. bisporus* and the oyster mushroom *Pleurotus spp.*

A. bisporus was grown on compost in nylon bags 40 cm wide x 80 cm long x 20 cm deep (Fig. 1), while oyster mushroom was grown in bags of 30 cm length and 20 cm width using wheat straw medium supplemented with wheat bran (10%) and calcium carbonate (2%) (Fig. 1). The steps for cultivating mushrooms were carried out in a typical mushroom farm at the College of Agriculture, Tikrit University, including the preparation of the mushroom spawn, compost and all other processes such as spawning, incubation, and the production of fruit bodies according to the previous studies[19-22].

Mushroom flies

The initial identification of the insects was carried out by Prof. Dr. Abdullah A. Hassan based on the insect's morphology and confirmed molecularly based on the nucleotide sequence of the cytochrome oxidase -subunit (1) gene in mitochondria. They were registered in the NCBI Database under accession numbers MZ021516.1 and MZ021517.1 for *Megaselia halterata* and *Lycoriella ingenua*, respectively, in our previous study[18].

Study of insect damage on the mushroom fruit bodies

Fruit bodies of *Agaricus spp.* and *Pleurotus spp.* showed symptoms of infection with the studied insects harvested from the mushroom farm during 2018/2019. The pathological symptoms of fruit bodies were examined morphologically with the longitudinal and transverse sections by a magnifying lens.

Preparation of insects traps and baits

Organic baits

The traps were prepared locally using plastic bottles with a capacity of 2 liters, perforated from the top with holes of a diameter of 0.5 cm and several 20 holes. These bottles (traps) were filled with 100 g of the following media (act as baits) + 100 ml of distilled water then the bottles' nozzles were closed with cotton stoppers. The organic baits include the following treatments: Unfermented wheat straw: It was prepared by soaking the shredded wheat straw (1-2 cm) using a field grinder with tap water. The soaking time was 24 hours, then the straw was filtered from the excess water and pasteurized at 70 °C for one hour[22], then used directly in filling the traps after cooling it to the next day. II; Fermented wheat straw: The same previous steps were followed, but the medium, after cooling, was packed in nylon bags, tightly closed, and incubated for 7 days at a temperature of 30°C to ferment it with natural flora, after which it was filled in traps. III; Unfermented and fermented corn cobs: The same previous steps were followed on the chopped corn cobs (1 cm), replacing wheat straw with corn cobs. IV; *Agaricus spp.* compost: Pasteurized compost prepared ac-

Figure 1. Cultivation of *A. bisporus* and *P. ostreatus* in the growing room with the distribution of treatments for baits experiments.

cording to Hassan and Mahmoud[21] after cooling it to 25° C, it packaged in insect traps. V; Full growth compost: The compost medium was inoculated with the *A.bisporus* spawn of commercial strain A15. The bags were incubated at 25°C for two weeks after the mycelium spread into the compost, it packaged in insect traps. VI; Wheat bran: It was prepared by the steps of preparing the unfermented wheat straw. VII; Wheat bran + yeast and sugar: 50 ml of yeast and sugar solution (1% commercial *Saccharomyces cerevisiae* yeast + 2 g table sugar) were added to 1 kg of pasteurized wheat bran after mixing well, incubated at 25 °C for 7 days and then packed in traps. VIII; Wheat bran + local date vinegar: It was prepared by the same previous steps except adding 100 ml of local date vinegar. IX; Dap fertilizer (Jordanian Fabco Company) The bait consists of 100 g of dab fertilizer and 5 g of *S. cerevisiae* yeast with a liter of water. Use this bait as a positive control for attracting some insects[23]. X; Control treatment: Use only water and XI; The yellow sticky trap for comparison.

Spawn and fruit bodies baits of *Agaricus spp.* and *Pleurotus spp.*

Spawn and fruit bodies of five strains of *A. bisporus* cultured in the mushroom production farm, College of Agriculture / Tikrit University, were used. The strains included brown strain, A15, B62, S11, and the local isolate *A. campestris*. Spawn and fruit bodies of six strains of oyster mushrooms cultured in the same mushroom production farm, including *P. ostreatus, P.florida, P.sajor-caju, P.eryngii, P. pulmonarius* and *P. ostreatus* A19 (local isolate) were used. Traps were filled with 100 g of the following media (act as baits for both mushrooms) + 100 ml of distilled water, then the bottles' nozzles were closed with cotton stoppers; I; The pure spawn has grown on wheat grains prepared according to Hassan[24], II; The dried and ground fruit bodies in a powder form. III; Fresh cut fruit bodies 1-2 cm2. IV; Fresh fruit bodies mashed in a blender in the form of an emulsion and V; Water: control.

Combination of baits

It included various combinations of previous treatments. The best treatments were used in proportions of 50 g for each bait material + 100 ml of distilled water for the binary mixtures.

Insect breeding in the laboratory

100 g of the infected *Pleurotus ostreatus* fruit bodies with both insects, which show necrosis, tunnels, and larvae, were placed in plastic cups, their mouths closed with two layers of gauze, and incubated at 22 °C, 70% humidity and 12:12 light: dark cycle, after 10-14 days the pupation of the larvae is observed (morphologically similar to both insects) , and after 3-6 days the adult insects emerge. Adults were isolated from the pupae separately, placed in plastic cups containing intact (uninfected) pieces of the *P. ostreatus* fruit bodies, and incubated under the above conditions to obtain the insects of both species separately. For the sustainability of the insect culture, fresh fruit bodies are constantly placed in the culture medium. This is the easiest method of breeding the insect recorded for the first time in Iraq, and we did not find it in the international literature.

Execution of the experiment

After cultivation of both *Agaricus spp.* and *Pleurotus*

spp. Mushrooms and the baits were immediately distributed separately in the growing room (Figure 1). 100 adult insect were released in each experiment. After the end of the mushrooms production cycle, the number of insects was recorded in each trap, then the Infestation rate of mushrooms fruit bodies was calculated as the following equation:

Infestation rate = number of fruits infected with the insect / total number of fruits x 100

The fruit was considered infected if there were larvae, necrosis or tunnels caused by the insects in the mushroom fruit bodies.

Statistical Analysis

Statistical analysis of factorial laboratory experiments was carried out using the Mini Tap 18 program, and the means were compared according to Duncan's multiple range test[25] at a probability level of 0.05.

Results

Effect of the type of baits on attracting *M. halterata* and *L. ingenua* in traps

Effect of media

The results of table (1) showed the significant superiority of full-grown compost in attracting and catching both insects *M. halterata* and *L. ingenua*, the number was 8.04 and 7.45 insects/bait, respectively, followed by the fermented corn cobs and the compost, where the number reached (7.7, 6.83) and (6.11 and 5.3) insect/bait for these two insects, respectively, compared with the dab fertilizer (2.78 and 2) and the yellow sticky trap (1.03 and 0.66) insect/bait, while there was no effect on attracting insects for the wheat straw, unfermented corn cobs, unfermented bran and water (control).

Effect of *Agaricus spp.* baits on attracting insects

The results of table (2) proved that the highest attraction in the hunting of the two insects, *M. halterata* and *L. ingenua*, was in the treatment of cut fruit bodies for all studied *A. bisporus* strains, the highest number was 6.49 and 5.43 insects/bait, in the treatment of cut fruits of *A.bisporus* B62, respectively, followed by the attraction of insects in the treatment of the mushroom spawn. The results showed that the lowest number was in the treatment of dried fruit bodies (Table 2), while no insect attraction was recorded in the control treatment (water only). At the level of mushroom species, the brown strain of *A.bisporus* showed the lowest interest to the studied insects.

Effect of oyster mushroom baits on attracting insects

Chopped fruit bodies and the inoculum of some species/strains of oyster mushroom Pleurotus led to the highest attraction to insects, followed by the treatment of mashed fruit bodies, while the treatment of dried fruit bodies was less attractive to insects, while the control treatment (water only) recorded no attraction to insects, the highest attraction of insects was reached by the chopped fruits for *P. eryngii*, the number of insects, *M. halterata* and *L. ingenua*, was 6.56 and 5.32 insects/bait, respectively (Table 3).

Effect of the combination baits

The results of the combination baits were made from mix-

3

Attractant	Number of insects caught	
	M. halterata	*L. ingenua*
Unfermented wheat straw	0.0 h	1.2 g
Fermented wheat straw	4.37 cd	3.33 de
Corn cobs	0.0 h	0.0 h
Provoked corn cobs	7.7 a	6.83 ab
Compost	6.11 bc	5.30 c
Full growth compost	8.04 a	7.54 a
Wheat bran	1.65 g	0 h
Wheat bran+ yeast+ sugar	2.34 e	2.21 ef
Wheat bran+ date vinegar	5.2 c	3.89 d
Dab fertilizer	2.78 e	2.0 fg
sticky trap	1.03 g	0.66 h
Water	0 h	0 h

According to Duncan's multiple range test, the different letters of the alphabet indicate significant differences (P $_{0.05}$).

Table 1. Number of *M. halterata* and *L. ingenua* caught with different baits.

Bait status	*A.capmestrus* A26L		*A.bisporus* brown strain		*A.bisporus* B62		*A.bisporus* S11		*A.bisporus* A15	
	M. h	*L. i*	*M. h*	*L. i*	*M. h*	*L. i*	*M. h*	*L. i*	*M. h*	*L. i*
Dryer	1.2 gh	0 j	0.93 h	1.03 g	1.05 g	1.67 f	1.23 fg	1.65 f	1.40 fg	1.08 g
Chopped	3.8 bc	2.11 ef	0.66 i	1.45 fg	5.43 ab	6.49 a	4.76 b	3.71 bc	4.80 b	4.4 bc
Mashed	2.3 e	1.82 f	0.66 i	1.11 g	2.43 e	3.20 cd	2.12 ef	2.45 e	3.0 de	2.80 e
Spawn	3.0 d	2.06 ef	1.14 g	1.06 g	3.31 c	4.56 b	3.0 d	3.26 cd	3.53 c	3.66 c
Water	0 j	0 j	0 j	0 j	0 j	0 j	0 j	0 j	0 j	0 j

According to Duncan's multiple range test, the different letters of the alphabet indicate significant differences (P $_{0.05}$).

Table 2. Effect of the fruit bodies of *Agaricus spp*. baits on attracting the two insects *M. halterata* and *L. ingenua*.

Bait status	*P. ostreatus*		*P. pulmonarius*		*P.florida*		*P.sajor-caju*		*P.eryngii*		*P. ostreatus A 19*	
	M. h	*L. i*	*M. h*	*L. i*	*M. h*	*L. i*	*M. h*	*L. i*	*M. h*	*L. i*	*M. h*	*L. i*
Dryer	1.12 g	1.33 fg	0 h	0 h	0.66 g	0.66 g	0 h	0 h	2.11 ef	1.98 ef	0.86 g	1.11 fg
Chopped	3.0 d	2.13 ef	3.11 cd	2.52 de	3.93 c	3.87 c	1.68 f	1.99 ef	5.32 b	6.56 a	3.33 c	4.71 bc
Mashed	2.20 def	2.0 ef	1.34 f	1.09 g	2.06 ef	2.21 def	1.55 f	2.0 ef	3.19 cd	3.44 c	2.26 de	2.77 d
Spawn	2.33 de	2.04 ef	1.95 ef	1.66 f	2.93 d	3.11 cd	2.07 ef	2.12 ef	3.0 d	3.16 cd	3.0 d	3.87 c
Water	0 h	0 h	0 h	0 h	0 h	0 h	0 h	0 h	0 h	0 h	0 h	0 h

According to Duncan's multiple range test (P 0.05), the different letters of the alphabet indicate significant differences.

Table 3. Effect of the fruit bodies of *Pleurotus spp*. Baits on attracting the two insects *M. halterata* and *L. ingenue*.

tures of the most efficient treatments resulting from the media and the fruit bodies of the *A.bisporus* and *Pleurotus spp*. Table (4) showed that all treatments attracted the two insects at a rate of 4.55 - 8.7 insects/bait for *M.halterata* and 4.06 - 7.82 insects/bait for L. ingénue. The combinations of (*A.bisporus* B62 + *P.eryngii*), (fermented corn cobs + full-grown compost) and (fermented corn cobs + P.eryngii) achieved the rates of attraction for these two insects (Table 4).

Infection of *A.bisporus* and *P. ostreatus* by *M. halterata* and *L. ingenue* using studied biats

Figure (2) shows the infection rate of the fruit bodies of *A.bisporus* and *P. ostreatus* in the presence of media baits and the fruit bodies of the *A. bisporus* and *Pleurotus spp*. The results showed that there were significant differences in

the reduction of both mushroom *A.bisporus* and *P. ostreatus* infection rate by all types of tested baits; the lowest infection rates were in the combination bait treatment, resulting in 1.86 and 2.17%, respectively, compared to the control treatment (without appeal) in which the infection rate was 87.3 and 91.25%, respectively.

Discussion

M. halterata and *L. ingenua*, cause severe damage to the yield of the edible mushrooms *A. bisporus* and *P. ostreatus*, tunnel digging, necrosis, perforation of fruit bodies with tissue laceration and the presence of larvae wastes are the most critical symptoms of these insects, which causes a

Bait type	*M. halterata*	*L. ingenua*
Fermented corn cobs + Compost	5.2 cd	4.76 d
Fermented corn cobs + full-growth compost	7.23 a	6.55 b
Fermented corn cobs + wheat bran+ date vinegar	5.58 c	5.22 cd
Fermented corn cobs + *P.eryngii* fruit bodies	6.91 ab	6.74 ab
Fermented corn cobs +*A. bisporus b-62* fruit bodies	5.08 d	4.58 d
compost + full-growth compost	4.55 d	4.06 e
Compost + wheat bran+ date vinegar	5.83 c	4.89 d
Compost + *P.eryngii* fruit bodies	5.92 c	5.33 cd
Compost +*A. bisporus b-62* fruit bodies	6.0 bc	6.21 b
Full growth compost+ wheat bran+ date vinegar	5.43 d	5.51 d
Full growth compost + *P.eryngii* fruit bodies	6.11 b	5.60 c
Full growth compost +*A. bisporus b-62* fruit bodies	5.84 c	4.42 d
wheat bran+ date vinegar+ *P.eryngii* fruit bodies	6.76 ab	6.37 b
wheat bran+ date vinegar +*A. bisporus b-62* fruit bodies	6.05 bc	6.19 b
P.eryngii +*A. bisporus b-62* fruit bodies	8.70 a	7.82 a
Water	0 f	0 f

According to Duncan's multiple range test, the different letters of the alphabet indicate significant differences (P $_{0.05}$).

Table 4. Effect of bait combinations on attracting *M. halterata* and *L. ingenua*.
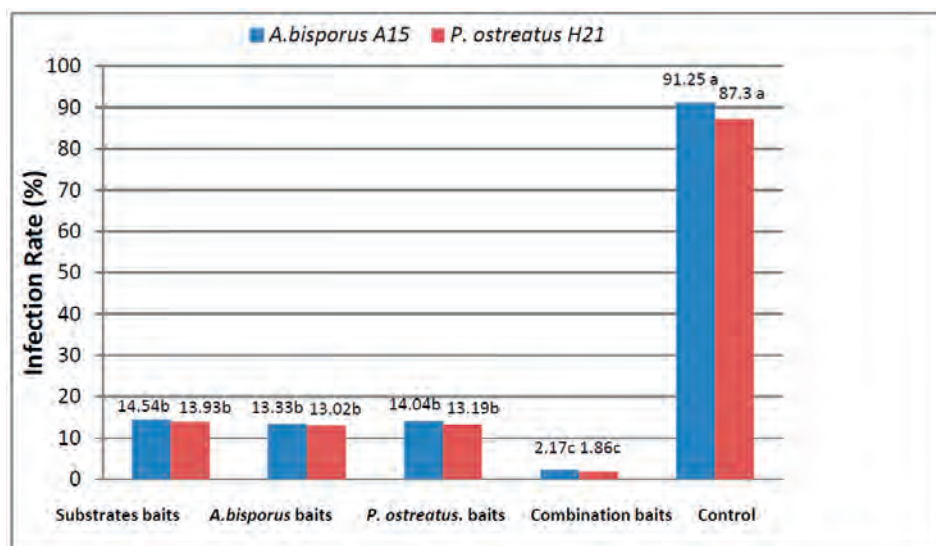
Figure 2. Infection rates of *A. bisporus* and *P. ostreatus* by the insects *M. halterata* and *L. ingenue* in the presence of different baits.

loss of the entire mushroom yield, the infection of the mushroom fruit bodies may be due to the nutritional specialization of these two insects towards feeding on mushroom fruit bodies, this agreed with some relevant studies[26,27]. To avoid chemical pesticides in mushroom production farms, which are among the dangerous factors due to the rapid growth of edible mushrooms and their high efficiency in absorbing materials from the media, the research suggested physical, environmental and biological applications to reduce the impact of these two insects. The synthetic pheromones did not have completely positive effects in attracting these insects[28,29]. In addition, the biological resistance factors are still under ongoing studies. Cloonan et al.[3] mentioned the lack of a wide commercial application of biological agents to control these insects. By tracking the infection of the *A. bisporus* and *Pleurotus spp.* mushrooms by these two insects in several production cycles, we found that they are highly attracted to mushroom growth medium, spawn and fruit bodies, as they are the preferred nutrient sources for these insects[30,31].

The baits used in this study were characterized by their high efficiency in attracting the studied insects. Among the organic materials, fermented corn cobs and compost were distinguished by their highest attraction, which may be attributed to the presence of volatile organic compounds (VOCs) in the compost that attracts insects[32]. In terms of attracting insects to some mushroom species, the bait made from the cutting fruit bodies was more attractive than the dried and mashed fruits; this may be due to the loss of compounds responsible for the distinct aroma and flavor of the mushrooms (*Agaricus*, *Pleurotus*) by drying and mashing process such as benzyl alcohol, benzaldehyde, benzonitrile, methyl benzoate, and phenylacetic acid-like compound, as well as the distinctive smell of the mushroom itself[33,34]. The same effect was recorded in the bait of the mushroom spawn; this is explained by the release of the fungal mycelium that surrounds the spawn grains, the same volatile substances for the smell and flavor compounds in *A. bisporus* and *Pleurotus spp.* mushrooms, conducted by Yin et al.[35] studies, in which he isolated insect-promoting compounds from 6 species of the Pleurotus spp. such as free amino acids and nucleotides, as well as many volatile com-

5

6

pounds, which included 17 aldehyde compounds, 10 ketone compounds, 14 alcohol compounds, 5 hydrocarbons, 10 cyclic aromatic compounds, as well as some organic acids. The same study stated that the most important compounds that distinguish the smell of edible mushrooms are 1-Octen-3-one, 1-octen-3-ol, and 2-octenal.

A study by Nyegue et al.[36] on Pleurotus spp. confirms the isolation of octen-3-ol, often-3-one, octan-3-one, 3-octanol, n-octanal, (E)-2-octenal and n -Octanol, Benzaldehyde (almond odor), benzyl alcohol (sweet-spicy odor), phenylethanol (rose odor), derivatives of monoterpenes such as linalool and linalool oxide, and many aliphatic compounds among the volatile compounds, which explains the attraction of these insects to the mycelium of mushrooms and their fruit bodies.Some mushroom species studied, especially A.bisporus (brown strain) and P.eryngii, were the most attractive, perhaps due to the difference in the genetic composition of these two mushrooms, which is reflected in their physiological activity in producing more concentrated insect-attracting compounds or perhaps other substances that have not been discovered until now. The organic materials, mushroom fruit bodies and the combinations of baits proved their efficiency in reducing the number of insects through a decrease in the infection rate of A. bisporus and Pleurotus spp., which reached a minimum percentage of 1.86-2.17% in the treatments of combinations of baits as a result of the success of attracting insects.

Conclusions

Through the parasitism of the insects M. halterata and L. ingenua on the mushrooms A. bisporus and Pleurotus spp., the most relevant materials for mushrooms were developed as baits to catch these two insects. Each of full-grown compost , fermented corn cobs , compost ,cut fruit bodies and spawn of A. bisporus and Pleurotus spp. strains in addition to the combinations included (A.bisporus B62 + P.eryngii), (fermented corn cobs + full-grown compost) and (fermented corn cobs + P.eryngii) , were the best baits for catching these insects and reducing their harmful effect on mushroom production farms. Using baits to attract and catch mushrooms is one of the safe ways to control these insects instead of insecticides and to avoid losses in the quality and yield of mushrooms.

Availability of data and materials

The data set (table and graphs) supporting this article's conclusion is available.

Ethics approval and consent to participate

All the authors have read and agreed on the ethics for publishing the manuscript.

Consent for publication

The authors approved the consent for publishing the manuscript.

Cometing interests

WThe authors declare that they have no competing interests.

Bibliographic references

1. Cheung P.C.K. (2010) The nutritional and health benefits of mushrooms. Nutr Bull 35:292–299.
2. O'Connor, L. and Keil, C. B. 2005. Mushroom Host Influence on Lycoriella mali (Diptera: Sciaridae) Life Cycle Journal of Economic Entomology, 98(2):342-349.
3. Cloonan, K. R. Stefanos S. Andreadis & Thomas C. Baker. 2016. Attraction of female fungus gnats, Lycoriella ingenua, to mushroom-growing substrates and the green mold Trichoderma aggressivum. Entomologia Experimentalis et Applicata 159: 298–304.
4. Singh. A.U. and Sharma, K. 2016. Pests of Mushroom. Adv. Crop Sci Tech, 4:2
5. White, P.F. (1986) The effect of sciarid larvae (Lycoriella auripila) on cropping of the cultivated mushroom (Agaricus bisporus). Annals of Applied Biology 109: 11–17.
6. Shirvani-Farsani, N., Zamani, A.A., Abbasi, S. and Katayoon Kheradmand. 2013.Toxicity of three insecticides and tobacco extract against the fungus gnat, Lycoriella auripila and the economic injury level of the gnat on button mushroom. J Pest Sci 86, 591–597.
7. Dmoch, J. 1988. Effect of some insecticides on mushroom mycelial growth. Acta Hort. 219: 15-20.
8. Andreadis, S. S., Cloonan, K. R., Myrick, A.J., Chen, H., Baker, T. C. (2015). Isolation of a Female-Emitted Sex Pheromone Component of the Fungus Gnat, Lycoriella ingenua, Attractive to Males. J Chem Ecol. 41:1127–1136
9. Cantelo, W.W. (1983). Control of a mushroom infesting fly (Diptera: Sciaridae) with insecticides applied to the casing layer. Journal of Economic Entomology, 76(6), 1433–1436.
10. Jess S., H. and Kilpatrick M, Mushroom applications, in Nematodes as Biocontrol Agents, ed. by Grewal PS, Ehlers R-U and Shapiro DI. CAB International, Wallingford, Oxon, UK, pp. 191–213 (2005).
11. Lind R. (1993) Control of mushroom flies with the predatory mite, Hypoaspis miles. Contract Report Horticultural Development Council Project M9, Horticultural Development Council, West Malling, Kent, UK, 28 pp.
12. Jessa, S. and Schweizerb, H.. 2009. Biological control of Lycoriella ingénue (Diptera: Sciaridae) in commercial mushroom (Agaricus bisporus) cultivation: a comparison between Hypoaspismiles and Steinernema feltiae. Pest Manag Sci .65: 1195–1200.
13. Bartlett, G.R. and Keil, C.B.O. (1997) Identification and characterization of a permethrin resistance mechanism in populations of the fungus gnat Lycoriella mali (Fitch) (Diptera: Sciaridae). Pesticide Biochemistry and Physiology 58: 173–181.
14. Bellettini, M. B., Bellettini, S., Fiorda, F. A., Pedro, A. C., Bach F., Miriam F., Moron, F. and Hoffmann-Ribani, R. 2018. Diseases and pests noxious to Pleurotus spp. mushroom crops. Rev Argent Microbiol.;50(2):216-226.
15. Smith J, Challen M, White P, Edmondson R, Chandler D (2006) Differential effect of Agaricus host species on the population development of Megaselia halterata (Diptera: Phoridae). Bull Entomol Res 96(6):565
16. Badshah, K., Ullah, F., Ahmad, B. Ahmad, S., Alam, S., Ullah, M., Momana Jamil, M. and Sardar, S. (2021). Management of Lycoriella ingenua (Diptera: Sciaridae) on oyster mushroom (Pleurotus ostreatus) through different botanicals. Int J Trop Insect Sci 41, 1435–1440.

17. Hassan, A. Abdulkareem (2013) . First Report of Diseases and Pests of an Edible Mushroom Agaricus bisporus in Iraq. 1.The Fungal Infections. Journal of Tikrit University For Agriculture Sciences.13(4):60-71.

18. Hassan , A. A., and Al-Qaissi, A. R. (2021). First record of the two insects Megaselia halterata and Lycoriella ingenua parasite on some edible mushrooms in Iraq. Submitted to Arab Journal of Plant Protection.

19. Hassan , A. A.,Natheer , A.M. & Mahmoud, A. R.(2000). effect of application of some organic sources on the oyster mush room Pleurotus ostreatus yield.Iraqi J. Agric.5(4):185-190.

20. Hassan, A. A. Natheer, A. M. and Mahmoud, A. R. (2002). Improvement of agronomic characters and productivity of Agaricus bisporus Lange(Imbach) , using some organic sources . Iraqi J. Agric.7(3): 104-112.

21. Hassan , A. A., and Mahmoud, A. R. (2003). Outdoor cultivation of two white edible mushrooms Agaricus bisporus and Agaricus bitorquis . Iraqi J. Agric. 8(2):59-66.

22. Hassan, A. A. and Mahmoud, A. R. (2008) Outdoor Cultivation Of Oyster Mushroom Pleurotus sp. Using Shaded Plastic Houses. Iraqi J. Agric. 13(1): 48-55.

23. Al-Jubouri, Raghad Khalaf Ibrahim and Al-Jassani, Radi Fadel (2010). Evaluation of the efficiency of some food attractant traps and colored traps in attracting adults of the Mediterranean fruit fly. Anbar Journal of Agricultural Sciences. 8(1): 263-270.

24. Hassan , A. A. (2009). Selection of new isolates from single spore and multispore cultures from two strains of Agaricus bisporus. Tikrit J. of Pure Science. 14(3):1-10.

25. Al-Rawi, K. Mahmoud and Khalaf Allah, A. Muhammad. 1980 . Design and analysis of agricultural experiments. Dar Al-Kutub for Printing and Publishing, University of Mosul.

26. Erler, F., Polat, E., Demir, H., Catal, M. and Tuna G (2011) Control of mushroom Sciarid fly Lycoriella ingenua populations with insect growth regulators applied by soil drench. J Econ Entomol 104:839–844.

27. Park, I. K., Choi, K. S., Kim, D.H., Choi, I.H. Kim, L.S. Bak, W.C. Choi ,J.W. and Shin, S.C. (2006) Fumigant activity of plant essential oils and components from horseradish (Armoracia rusticana), anise (Pimpinella anisum) and garlic (Allium sativum) oils against Lycoriella ingenue (Diptera: Sciaridae). Pest Manag Sci 62:723–728.

28. Gotoh, T., Nakamuta, K., Tokoro, M. and Nakashima, T. (1990) Copulatory behavior and sex pheromones in sciarid fly, Lycoriella mali (Fitch) (Sciaridae: Diptera). Jpn J Appl Entomol Zool 43:181–184

29. Stefanos, S. A. , Kevin R. C., Andrew J. M. Haibin, C. and Thomas C. B.2015. Isolation of a Female-Emitted Sex Pheromone Component of the Fungus Gnat, Lycoriella ingenua, Attractive to Males. J Chem Ecol (2015) 41:1127–1136

30. Lewandowski, M., Sznyk, A. and Bednarek, A. (2004) Biology and morphometry of Lycoriella ingenua (Diptera: Sciaridae). Biol Lett 41:41–50

31. Shamshad, A. (2010) The development of integrated pest management for the control of mushroom sciarid flies, Lycoriella ingenua (Dufour) and Bradysia ocellaris (Comstock), in cultivated mushrooms. Pest Manag Sci 66:1063–107

32. Dhamodharana, K., Varmaa, V. S. , Arivalagan, C. V., Rajendrand, P. K. 2019. Emission of volatile organic compounds from composting: A review on assessment, treatment and perspectives. Science of The Total Environment. 695: 1-33.

33. Chen, C. and Wu, C. 2006. Volatile Components of Mushroom (Agaricus subrufecens) .Journal of Food Science 49(4):1208 – 1209

34. Abend A. M, Chung L , Bibart R T, Brooks M, McCollum DG 2004.Concerning the stability of benzyl alcohol: formation of benzaldehyde dibenzyl acetal under aerobic conditions. J Pharm Biomed Anal. 10;34(5):957-62

35. Yin, C., Fan, X. , Fan, Z ., Shi, D., Yaoa, F. and Gao, H. 2018. Comparison of non￾volatile and volatile flavor compounds in six Pleurotus mushrooms. Journal of the Science of Food and Agriculture 99(4) : 1691–1699.

36. Nyegue, M., Zollo, A., Bessière, J. M. and Sylvie Rapior, S. 2003 . Volatile components of fresh Pleurotus ostreatus and Termitomyces shimperi from Cameroon. Journal of essential oil-bearing plants JEOP 6:153-157.

7

ARTICLE / INVESTIGACIÓN

The efficient procedure of embryogenic callus formation from anther in *Capsicum pubescens* Ruiz & Pav

Alexandra Jherina Pineda-Lázaro, Angel David Hernández-Amasifuen* and Hermila Belba Díaz-Pillasca

Universidad Nacional José Faustino Sánchez Carrión, Laboratorio de Biotecnología Vegetal, Huacho, Perú.
Corresponding author: adhernandz@hotmail.com

1

Abstract: The peppers or ajies (*Capsicum spp.*) are one of Peru's main productive crops, which is why it is among the top ten countries in production and exports. Among the species cultivated in Peru is *Capsicum pubescens* Ruiz & Pav., commonly called rocoto, and represents one of the most critical species in local and national gastronomy. The rocoto ecotype "Selva" or "de Monte" is characterized by its large size and is used to prepare rocoto relleno arequipeño. This crop presents the restriction to obtain homozygous lines for being self-incompatible. Using biotechnology, pure lines can be obtained from the anther culture, and homozygous lines can be obtained. The objective was to induce embryogenic callus formation from anther culture of *Capsicum pubescens* Ruiz & Pav. Ecotype "de Monte". In the results, 74.1% of embryogenic callus was induced in rocoto anthers with a longitudinal ratio of 1.04 mm; the induction was carried out using Murashige and Skoog culture medium added with 2.0 mg/L of 2,4-D. Likewise, the formation of somatic embryos in the globular stage was evidenced after 12 weeks in the culture medium.

Key words: Aji, Biotechnology, Somatic embryos, Self-incompatible, Rocoto, Peppers.

Introduction

The peppers or ajies (*Capsicum spp.*) are a vegetable genus of great importance worldwide, with 31 species reported to date, five of which are cultivated (*C. annuum L., C. chinense Jacq., C. frutescens L., C. baccatum L., C. pubescens* Ruiz & Pav.) and 26 are wild species[1-3]. Peru presents, cultivates and produces the five species of cultivated chili peppers, making it one of the top ten countries in producing and exporting fresh and processed chili peppers[4-6].

The Andean region of Peru is the origin of the rocoto (*C. pubescens* Ruiz & Pav.), with wild relatives still present in these areas, as well as in the highlands and high jungle[7]. The rocoto is a plant species of great national relevance due to its use in gastronomy, based on its two most representative ecotypes[8]. The ecotypes of rocoto in Peru are "Serrano" or "de Huerto" and "Selva" or "de Monte"; the first is the most distributed in the country due to its great adaptation to the different regions, and the second can only be found in the jungle[9]. The Selva ecotype is distinguished by its large size and moderate pungency, which is why it is trendy in the preparation of one of Peru's most representative dishes, rocoto relleno arequipeño (stuffed red pepper)[10]. The Serrano ecotype is smaller in size and has a high pungency, which is why it is widely used as a sauce in many national dishes[11].

The major problem affecting the rocoto crop is related to root rot diseases caused by species of the genus *Fusarium, Phytoptora* and *Rhizoctonia*[7,12,13]. Because of this, rocoto germplasm banks have been implemented with accessions from all over Peru, among the most commercial ecotypes and genotypes with great agronomic potential. Based on the extensive collection of rocoto genetic material, genetic improvement programs have been initiated to obtain defined varieties. Currently, the rocoto crop does not

have a specified variable; therefore, no certified seeds are available in the national market[10]. For this reason, rocoto farmers resort to sources from previous crop seasons, obtaining heterogeneous fruits.

One of the main difficulties in the genetic improvement of rocoto is obtaining homozygous or pure lines because this species is considered self-incompatible; specifically, the genotypes of Peru, Bolivia and Argentina are reported as genotypes with gametophytic self-incompatibility[14]. Likewise, the genetic control of self-incompatibility in rocoto has been identified and measured by the S locus, which is formed by multiple alleles. Therefore, pollen or, in some genotypes, the pollen tube can express enzymatic products that prevent their proliferation on the stigma[15].

Within modern breeding programs, biotechnological tools are being applied through *in vitro* plant tissue culture[16,17]. This allows working with a fragment of selected mother plants for the clonal propagation of these superior genotypes[18]. Likewise, among the methods used in plant tissue culture, anther culture is presented, which allows taking advantage of and working with the male gametes of the plants of interest, thus inducing organogenesis or the formation of somatic embryos directly and indirectly (previous callus formation) for the regeneration of haploid plants, which can be induced to chromosomal duplication and thus obtain pure lines that can be used for crossbreeding between genotypes with a more significant commercial potential[19-21].

In this context, the objective of the present research was to induce the formation of embryogenic callus from anther culture of *Capsicum pubescens* Ruiz & Pav. Ecotype "de Monte".

Materials and methods

Plant material

Flower buds of rocoto of the "de Monte" ecotype were collected from rocoto seedlings in the agricultural zone of Santa Elena Norte, Barranca, Lima, Peru. Flower buds without opening or the presence of pest or disease damage were selected in the early morning hours. The flower buds were then transferred to the facilities of the Plant Biotechnology Laboratory of the Universidad Nacional José Faustino Sánchez Carrión, Huacho, Lima, Peru.

Determination of uninucleate microspores in rocoto anthers

The percentage of microspores in the uninucleate state was evaluated from anthers of rocoto flower buds, which were grouped by size difference and related between petal and sepal, based on the presence of microspores in the uninucleate state. For each sample per group collected, the anthers were extracted, from which the microspores were obtained and stained with 0.5% acetic orcein and observed under the optical microscope at 100X magnification to determine which group had the highest percentage of the indicated stage.

In vitro establishment of rocoto anthers

Once the morphological groups of rocoto flower buds were identified, we continued with the establishment under *in vitro* conditions, determining the optimal concentration of sodium hypochlorite (NaClO) for disinfection and presenting the lowest percentage of oxidation of the plant material. The treatments were set at 1.0%, 1.5%, 2.0%, 2.5%, 3.0%, 3.5%, 4.0%, 4.5% and 5.0% NaClO. Disinfection with the different concentrations of NaClO was carried out for 10 minutes and then washed in sterile distilled water, a process that was repeated three times. Once the flower buds were disinfected, they were dissected to separate the anthers from the rest of the plant material. All anthers were placed in semi-solid culture medium with basal salts Murashige and Skoog 22, and were kept in total darkness, 75% relative humidity and 24° C for two weeks. Evaluations were made after the first and second week of anther introduction into the culture medium to determine the treatment with minor contamination and anther necrosis.

Callus induction in rocoto anthers

For the induction of callus in rocoto anthers, culture medium with Murashige and Skoog[22] basal salts with the addition of vitamins (Table 1), 30 g/L sucrose, 6 g/L agar and treatments with different concentrations of the auxin 2,4-dichloro phenoxy acetic acid (2,4-D) (Table 2) were used. The conditions for maintaining the treatments were 24°C temperature, 75% relative humidity and total darkness. Evaluations were carried out every four weeks to determine the percentage of callus induction and the degree of callus induction[23] (Table 3), maintaining all treatments for a total of 12 weeks.

Vitamin	Concentration (mg/L)
Myoinositol	100.0
Glycine	2.0
Nicotinic acid	0.5
Pyridoxine HCL	0.5
Thiamine HCL	0.1

Table 1. Concentration of vitamins in culture medium.

Treatment	2,4-D (mg/L)
T1	0.00
T2	0.01
T3	0.05
T4	0.10
T5	0.25
T6	0.50
T7	1.00
T8	2.00

Table 2. Treatments for callus induction in *Capsicum pubescens* anthers.

Experimental design and statistical analysis

A completely randomized design (CRD) was used to determine uninucleate microspores, *in vitro* establishment and callus induction in rocoto anthers. Statistical analysis was performed by analysis of variance (ANOVA) and comparison of means with Tukey's test ($p \leq 0.05$). All comments were processed in the R program (version 4.1.3 for Windows) and Rstudio graphical interface (version 2022.07 for Windows).

Results

Determination of uninucleate microspores in rocoto anthers

Five groups of flower buds were obtained by longitudinal relationship (mm) between petal and sepal (Figure 1), and the flower bud group with the highest percentage of uninucleated microspores was also determined (Table 4). Flower buds that presented openings, physical damage and oxidation were discarded for this part of the research and subsequent sections. Flower buds that were grouped by a 1.04 mm sepal to petal length ratio presented 87.31% of microspores in the uninucleate state, representing the appropriate group and, therefore, selected for the next phase of the research focused on callus induction.

In vitro establishment of rocoto anthers

The disinfection of flower buds showed significant differences between treatments for the evaluations of the percentage of contamination and rate of necrosis or oxidation of the explants (Table 5). The NaClO concentrations that presented the lowest percentages of bacterial or fungal contamination were 4.5% and 5.0%, with 11.53% and 8.45% contamination, respectively; these concentrations did not show significant differences between them. In evaluating the percentage of necrosis per explant, the 1% to 4.0% NaClO concentrations presented 0.00%, representing the best treatments to avoid explant oxidation.

Callus induction in rocoto anthers

The response of rocoto anthers in culture medium with the addition of different auxin 2.4-D induced the formation of embryogenic callus (Figure 2) in various degrees of proliferation. In the last evaluation corresponding to week 12, after introducing the anthers into the culture media, the formation of somatic embryos in the globular stage from the embryogenic callus could be recorded (Figure 2). Treatments T7 and T8 induced the highest embryogenic callus formation, with 61.3% and 74.1%, respectively (Table 6). In the degrees of the proliferation of embryogenic callus, the highest percentages were obtained in grade 3 with treatments T7 and T8, with 38% and 59%, respectively (Table 6).

Grade	Callus induction	Observation
0	No callus formation	No cell proliferation
1	Slight callus formation	Weak proliferation in areas of the edge of the explant
2	Callus formation	Proliferation of cells all around the edges of the explant, without forming a mass
3	Abundant callus formation	Formation of a bulky mass of callus

Table 3. Callus induction grades for evaluation in *Capsicum pubescens* anthers.

Figure 1. Flower buds of *Capsicum pubescens* grouped by the longitudinal relationship between sepal and petal.

Group	Sepal (mm)	Petal (mm)	Sepal/petal (mm)	Microspores uninucleated (%)
G1	2.15[a]	0.26[e]	8.26[a]	9.83[d]
G2	2.17[a]	0.72[d]	2.92[b]	17.27[c]
G3	2.52[b]	1.82[c]	1.34[c]	41.43[b]
G4	2.74[b]	2.61[b]	1.04[d]	87.31[a]
G5	3.21[c]	3.84[a]	0.78[e]	23.15[c]

Means followed by the same letter are not significantly different (Tukey test $p \leq 0.05$).

Table 4. Longitudinally related flower bud clusters with uninucleate microspores.

NaClO concentration (%)	Contamination (%)	Necrosis (%)
1.0	78.93[a]	0.00[b]
1.5	52.45[b]	0.00[b]
2.0	48.17[b]	0.00[b]
2.5	32.65[c]	0.00[b]
3.0	28.37[c]	0.00[b]
3.5	22.03[d]	0.00[b]
4.0	19.79[d]	0.00[b]
4.5	11.53[e]	2.42[a]
5.0	8.45[e]	5.26[a]

Table 5. Sodium hypochlorite concentrations in flower bud disinfection.

4
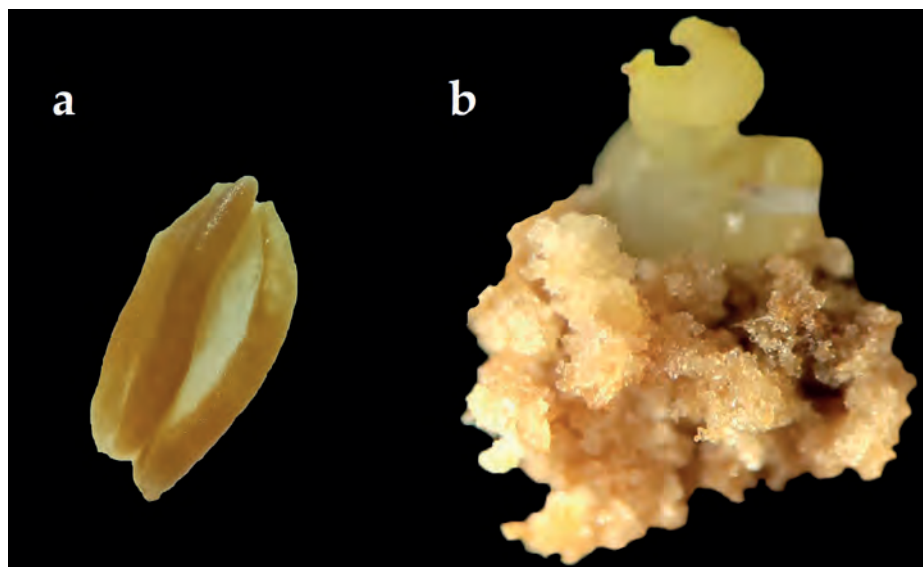
Figure 2. Anther culture of *Capsicum pubescens* ecotype "de Monte"; (a) Anther without response to callus formation. (b) Anther with embryogenic callus formation at twelve weeks of culture and somatic embryo formation.

Treatment	Callus formation (%)	Grades of callus formation			
		0 (%)	1 (%)	2 (%)	3 (%)
T1	0.0[e]	100[a]	0[c]	0[d]	0[d]
T2	0.0[e]	100[a]	0[c]	0[d]	0[d]
T3	8.5[d]	91[a]	9[b]	0[d]	0[d]
T4	22.3[c]	88[b]	15[a]	7[c]	0[d]
T5	28.5[c]	71[b]	8[b]	21[a]	0[d]
T6	38.7[c]	61[c]	16[a]	15[b]	8[c]
T7	61.3[b]	39[d]	7[b]	16[b]	38[b]
T8	74.1[a]	26[d]	0[c]	15[b]	59[a]

Means followed by the same letter are not significantly different (Tukey test p ≤ 0.05).

Table 6. Treatments for callus induction in *Capsicum pubescens* anthers.

Discussion

The group of flower buds G4 had the highest percentage of uninucleate microspores with 87.31% and a ratio of 1.04 sepal/petal. These results validate what was stated by de Vaulx *et al.*[24], who established that in flower buds of *Capsicum annuum* L. the longitudinal size ratio of sepals and petals should be similar to one because in this size ratio, the highest percentages of uninucleated microspores are presented. Compared with the research on anthers of rocoto ecotype "Serrano"[25], the researchers obtained 81.3% of uninucleated microspores in flower buds with a morphological ratio of sepal and petal of 1.09, results lower than those presented in the present research.

In the disinfection of rocoto anthers, the best treatments were 4.5% and 5.0% concentrations of sodium hypochlorite, obtaining contaminations of less than 12%. These results are similar to those obtained by Barroso *et al.*[26], who, for the disinfection of flower buds of *Capsicum annuum* L. used a 2% sodium hypochlorite solution with three drops of Tween 20 for 10 minutes. Koleva *et al.*[27] disinfected nine varieties of *Capsicum annuum* L. using 70% ethanol for thirty seconds and 5% calcium hypochlorite with two to three drops of Tween 20 for 10 minutes and three washes of sterile distilled water.

The induction of callus in rocoto anthers allowed obtaining up to 74.1% in the Murashige and Skoog culture medium added with 2.0 mg/L of 2,4-D, with 59% of callus formation in grade 3 (formation of a voluminous mass of callus). These results are superior to those obtained in rocoto ecotype "Serrano"[25], where 45.75% of callus were obtained in rocoto anthers using Murashige and Skoog culture medium added with 1 mg/L of kinetin and 1 mg/L of 2,4-D. Similarly, the results obtained were superior to those obtained by Koleva *et al.*[27] from their research on anthers of nine varieties of *Capsicum annuum* L., obtained the highest percentages in the varieties 58.88% Feferona variety in Nitch medium supplemented with 1.0 mg/L indole-3-acetic acid (IAA) and 48.90% Slatko Luta variety in Murashige and Skoog medium supplemented with 1.0 mg/L kinetin, 0.01 mg/L 2,4-D and 0.001 mg/L IAA. In the case of, Barroso *et al.*[26], they evaluated the response of anthers of *Capsicum annuum* L. varieties UFPB 134, UFPB 390 and hybrids between both varieties, where they obtained greater results up to 22.0% embryogenic callus in the genotype F2 of hybrids of *Capsicum annuum* L. varieties UFPB 134 and UFPB 390 in Murashige and Skoog culture medium added with 4.65 μM kinetin and 5.73 μM naphthaleneacetic acid (NAA); while for the same genotype, they obtained 14.1% and 20.0% for genotype UFPB 134 using Murashige and Skoog culture medium added with 4.65 μM kinetin and 4.52 μM 2,4-D.

The auxin 2,4-D effectively induces embryogenic callus formation in anthers of rocoto ecotype "de Monte."

The growth regulator 2,4-D is added to the culture media to induce the proliferation of undifferentiated cells, forming the characteristic cell mass called callus[28]. The 2,4-D has a rapid induction effect initially at the edges of the initial explant until it covers the entire structure, depending on the concentrations, combinations with other growth regulators, initial explant and the species with which the research is being carried out[29-31]. From this embryogenic callus, it was possible to observe the formation of somatic embryos after 12 weeks in the culture medium, concerning the fact that some species have the characteristic of inducing the formation of somatic embryos after the formation of callus (indirect somatic embryogenesis), and likewise, remaining in the same culture medium without changing it or refreshing the medium[32].

Conclusions

The formation of embryogenic callus was induced from anther culture of *Capsicum pubescens* Ruiz & Pav. Ecotype "de Monte," using Murashige and Skoog culture medium added with 2.0 mg/L of 2,4-D, obtaining an induction percentage of 74.1% of embryogenic callus, of which 59% represent grade 3 callus, that is, with the voluminous formation of the callus mass. Likewise, the appearance of somatic embryos in the globular stage was evidenced after 12 weeks in the culture medium.

Author Contributions

Conceptualization, AJPL and ADHA; methodology, AJPL; software, ADHA; validation, HBDP; formal analysis, ADHA; investigation, AJPL; resources, HBDP; data curation, ADHA; writing—original draft preparation, AJPL; writing—review and editing, ADHA; visualization, HBDP; supervision, HBDP All authors have read and agreed to the published version of the manuscript.

Funding

This research received no external funding.

Conflicts of Interest

The authors declare no conflict of interest.

Bibliographic references

1. Tripodi, P.; Kumar, S. The Capsicum Crop: An Introduction. The Capsicum Genome 2019, 1, 1-8.
2. Meckelmann, S.; Riegel, D.; van Zonneveld, M.; Rios, L.; Pena, K.; Ugas, R.; Quinonez, L.; Mueller-Seitz, E.; Petz, M. Compositional Characterization of Native Peruvian Chili Peppers (Capsicum spp.). Journal of Agricultural and Food Chemistry 2013, 61(10), 2530-2537.
3. Vera-Guzmán, A.M.; Chávez-Servia, J.L.; Carrillo-Rodríguez, J.C.; López, MG Phytochemical evaluation of wild and cultivated pepper (C. annuum and C. pubescens) from Oaxaca, Mexico. Chilean Journal of Agricultural Research 2011, 71, 578-585.
4. Rojas, J.; Lugo, B.; Pineda, A.; Aguilar, G.; Argüelles, A.; Díaz, H. Establecimiento de un método eficiente de germinación in vitro de arnaucho supano (Capsicum chinense Jacq.). Big Bang Faustiniano 2020, 9(4), 4-7.
5. Hernández, A.; Pineda, A.; Díaz, H. Efecto de la luz y del ácido giberélico en la germinación in vitro de Capsicum annuum L. cv.'Papri King'. Biotecnología Vegetal 2019, 19(3), 165-170.
6. Hernández, A.; Pineda, A.; Rojas, J.; Díaz, H. Regeneración in vitro de arnaucho (Capsicum chinense Jacq.) a partir de yemas apicales. Manglar 2021, 18(1), 71-75.
7. Valdez, I. Caracterización fenotípica de quince accesiones de germoplasma de rocoto (Capsicum pubescens Ruiz & Pavón.) en la estación INIA Santa Rita Arequipa. Bachelor Degree, Universidad Nacional de San Agustín, Arequipa, Peru. 2017.
8. Flores, N. Elaboración de una salsa a base de huacatay (Tagetes minuta) y rocoto (Capsicum pubescens) evaluando sus características fisicoquímicas y sensoriales. Bachelor Degree, Universidad Nacional de Cajamarca, Cajamarca, Peru. 2019.
9. Espinoza, D. Caracterización morfológica de los ajíes de la costa del Perú. Bachelor Degree, Universidad Nacional Agraria la Molina, Lima, Peru. 2017.
10. Sardón, E. Fortalecimiento de la cadena de valor del rocoto fresco (Capsicum pubescens) de la selva central para el mercado de Lima. Bachelor Degree. Universidad Nacional Agraria La Molina, Lima, Peru. 2015.
11. Sánchez, J. Relación de color y características fisiológicas y fisicoquímicas del rocoto (Capsicum pubescens). Bachelor Degree. Universidad Nacional de Trujillo, Trujillo, Perú. 2015.
12. Lucana, C. Respuesta de 5 especies de Capsicum spp. A Phytophthora capsici Leon, bajo condiciones de invernadero, en los laboratorios de fitopatología de la UNALM – Lima. Bachelor Degree. Universidad Nacional de San Antonio Abad del Cusco, Cusco, Peru. 2012.
13. Hernández, A.; Pineda, A.; Díaz, H. Aislamiento e identificación de Fusarium oxysporum obtenidos de zonas productoras de "ají paprika" Capsicum annumm L. (Solanaceae) en el distrito de Barranca, Perú. Arnaldoa 2019, 26(2), 689-698.
14. Saborío, M.; Da Costa, C. Autoincompatibilidad en Caspsicum pubescens. Agronomía Costarricense 1992, 16(2), 279-286.
15. Bo, M.; Cosa, M.; Carrizo, C. Autoincompatibilidad y funciones sexuales en Caspsicum pubescens. XXXIII Jornadas Argentinas de Botánica 2011, 1, 34.
16. Pineda, A.; Argüelles, A.; Rojas, J. Díaz, H. Respuesta en el establecimiento y regeneración in vitro de rocoto (Capsicum pubescens Ruiz & Pav.). Aporte Santiaguino 2021, 14(1), 31-42.
17. Hernández-Amasifuen, A.D.; Pineda-Lázaro, A.J.; Díaz-Pillasca, H.D. In vitro micropropagation of sour orange (Citrus aurantium L.) from nodal segments. Revista Bionatura 2021, 6(4), 2216-2221.
18. Pineda, A.; Hernández, A.; Díaz, H. Multiplicación y reducción del crecimiento in vitro de papa chaucha (Solanum tuberosum L. grupo Phureja). Manglar 2021, 18(2), 123-128.
19. Germaná, M.A. Anther culture for haploid and doubled haploid production. Plant Cell Tissue Organ Cult 2011, 104, 283-300.
20. Seguí-Simarro, J.; Corral-Martínez, P.; Parra-Vega, V.; González-García, B. Androgenesis in recalcitrant solanaceous crops. Plant Cell Reports 2011, 30(5), 765-778.
21. Parra-Vega, V.; González-García, B.; Seguí-Simarro, J.M. Morphological markers to correlate bud and anther development with microsporogenesis and microgametogenesis in pepper (Capsicum annuum L.). Acta Physiol Plant 2013, 35, 627-633.
22. Murashige, T.; Skoog, F. A revised medium for rapid growth and bioassays with tobacco tissue cultures. Physiol Plant 1962, 15, 473-497.
23. Santana, N.B. Determinación de un medio adecuado para la obtención de callos en variedades de caña de azúcar (Saccharum spp) in vitro. Cultivos Tropicales 1982, 4(3), 48-52.
24. de Vaulx, R.D; Chambonnet, D.; Pochard, E. Culture in vitro d'anthères de piment (Capsicum annuum L.): amèlioration des taux d'obtenction de plantes chez différents génotypes par des traitments à +35°C. Agronomie 1981, 1(10), 859-864.
25. Hernández-Amasifuen, A.D.; Pineda-Lázaro, A.J.; Díaz-Pillasca, H.D. In vitro anther culture of rocoto (Capsicum pubescens Ruiz & Pav.). Idesia 2022, 40(1), 115-121.
26. Barroso, P.; Rêgo, M.; Rêgo, E.; Soares, W. Embryogenesis in the anthers of different ornamental pepper (Capsicum annuum L.) genotypes. Genetics and molecular research 2015, 14(4), 13349-13363.

5

6

27. Koleva-Gudeva, L.; Spasenoski, M.; Trajkova, F. Somatic embryogenesis in pepper anther culture: the effect of incubation treatments and different media. Scci Hortic 2007, 11, 114-119.
28. Argüelles, A.; Hernández, A.; Cortez, A.; Díaz, H. Callogénesis in vitro de paprika (Capsicum annuum L.) cv. Papri King a partir de tallos. Big Bang Faustiniano 2020, 9(1), 4-7.
29. Hernández-Amasifuen, A.D.; Argüelles-Curaca, A.; Cortez-Lázaro, A.A.; Díaz-Pillasca, H.B. In vitro induction of callus from foliar explants in rocoto (Capsicum pubescens Ruiz & Pav.). La Granja 2021, 32(2), 127-135.
30. Hernández, A.; Argüelles, A.; Cortez, A.; Díaz, H. Effect of 2,4-dichlorophenoxyacetic concentration on in vitro callus induction using cotyledons of rocoto (Capsicum pubescens Ruiz & Pav.). The Biologist 2020, 17(2), 327-334.
31. Hernández-Amasifuen, A.D.; Cortez-Lázaro, A.A.; Argüelles-Curaca, A.; Díaz-Pillasca, H.B. In vitro callogenesis of peach (Prunus persica L.) var. Huayco rojo from leaf explants. Ciencia Tecnologia Agropecuaria 2021, 23(1), e2032.
32. Zhang, M.; Wang, A.; Qin, M.; Qin, X.; Yang, S.; Su, S.; Sun, Y.; Zhang, L. Direct and Indirect Somatic Embryogenesis Induction in Camellia oleifera Abel. Front. Plant Sci. 2021, 12, 644389.

REVIEW / ARTÍCULO DE REVISIÓN

Manejo odontológico de las manifestaciones orales inducidas por radio-terapia de cabeza y cuello
Dental management of oral manifestations induced by radiotherapy of the head and neck

Nagely J. Mejía-Chuquispuma, Katia V. Flores-Jiménez, Allison C. Castro-Auqui, Manuel A. Mattos-Vela*

Facultad de Odontología, Universidad Nacional Mayor de San Marcos, Lima, Perú.
Corresponding author: mmattosv@unmsm.edu.pe

Resumen: La radioterapia es una de las primeras opciones de tratamiento para el cáncer de cabeza y cuello; sin embargo, puede ocasionar diversas manifestaciones secundarias en la cavidad oral tales como mucositis oral, xerostomía, infecciones orales oportunistas, osteorradionecrosis y trismo. El presente artículo tiene como objetivo describir el manejo preventivo y terapéutico de las complicaciones orales inducidas por radioterapia de cabeza y cuello en la práctica odontológica propuestos hasta la actualidad. Se encontraron diversas medidas que han logrado reducir la incidencia y gravedad de dichas manifestaciones orales; sin embargo, aún existen algunas que requieren de más estudios para confirmar su efectividad.

Palabras clave: Cáncer de cabeza y cuello, manifestaciones bucales, radioterapia, terapéutica.

Abstract: Radiotherapy is one of the first treatment options for head and neck cancer; however, it can cause various secondary manifestations in the oral cavity such as oral mucositis, xerostomia, opportunistic oral infections, osteoradionecrosis and trismus. This article aims to describe the preventive and therapeutic management of oral complications induced by head and neck radiotherapy in dental practice proposed to date. Several actions were found that have managed to reduce the incidence and severity of these oral manifestations; however, there are still some that require further studies to confirm their effectiveness.

Key words: Head and neck neoplasms, oral manifestations, radiotherapy, therapeutics.

Introducción

El cáncer de cabeza y cuello (CCC) es el séptimo tipo de cáncer más común en todo el mundo y representa el 5% de todos los cánceres[1,2]. Según las últimas estimaciones de GLOBOCAN en el 2018, se reportaron un estimado de 887 649 nuevos casos y 453 307 muertes relacionadas con este tipo de cáncer en todo el mundo[3]. Los enfoques terapéuticos más utilizados para estas neoplasias son la cirugía, la radioterapia y la quimioterapia, que se pueden emplear de forma combinada o separada.

La radioterapia consiste en el uso de radiación ionizante y electromagnética para dañar el ADN, molécula necesaria para la replicación celular; por consiguiente, destruye las células cancerosas e inhibe el crecimiento de los tumores[4,5]. Sin embargo, su mecanismo de acción no es selectivo y puede afectar también al tejido sano. Los efectos nocivos en los tejidos biológicos se clasifican en determinísticos y estocásticos[6]. Los efectos determinísticos ocurren cuando se utilizan dosis mayores que el umbral, es decir, por debajo de este, los efectos no se producen; además su severidad aumenta con la dosis y comprende los efectos agudos[7]. Por otro lado, los efectos estocásticos no tienen un umbral de dosis para su manifestación, por lo que pueden aparecer inclusive con dosis bajas e ir aumentando la probabilidad de aparición con el aumento de la dosis de radiación; sin embargo, esta no influye en la gravedad

o severidad del efecto, se manifiestan de forma tardía, es decir, generalmente aparecen años o décadas después de la exposición a la radiación[8].

En el CCC se utiliza, con mayor frecuencia, una dosis de radiación de 2 Gy en solo una fracción al día, durante 5 días y en el transcurso de 7 semanas, alcanzando una dosis acumulativa de 50 Gy a 70 Gy[9]. Esta modalidad de tratamiento es la que provoca mayores complicaciones en la cavidad oral[10,11]. Puede generar manifestaciones orales agudas y tardías; las cuales dependen directamente de la tasa de recambio tisular, el área de tejido expuesto, la dosis total de radiación y la respuesta de cada individuo[12,13]. Los efectos agudos ocurren durante el tratamiento o dentro de 2 a 3 semanas después de finalizar la radioterapia e incluyen la mucositis oral, xerostomía e infecciones secundarias; por otro lado, los efectos tardíos ocurren semanas a años más tarde e incluyen la osteorradionecrosis y trismo[10,14,15].

Las manifestaciones descritas conllevan a la limitación de ciertas funciones básicas como alimentarse, hablar y respirar. Además, de interrumpir el tratamiento antineoplásico, afectando así la calidad de vida del paciente[16]. Por tanto, es necesaria la intervención odontológica antes, durante y después de la radioterapia tanto para disminuir las tasas de incidencia como la gravedad de dichas manifestaciones. Con base a lo mencionado, el presente estudio tuvo

por objetivo describir el manejo preventivo y terapéutico de las complicaciones orales inducidas por radioterapia de cabeza y cuello en la práctica odontológica propuestos hasta la actualidad (Figura 2).

Manejo de las manifestaciones orales inducidas por radioterapia de cabeza y cuello en la práctica odontológica.

Se han reportado una amplia gama de intervenciones para prevenir o tratar las manifestaciones orales inducidas por radioterapia de cabeza y cuello, a continuación, se mencionan algunas de ellas (Tabla 1).

Mucositis oral

La mucositis inducida por radioterapia (RIOM, por sus siglas en inglés) puede involucrar a cualquier persona expuesta a radiación. Su primer signo clínico es el eritema, que aparece en dosis de radiación de aproximadamente 10 Gy, progresando hasta una ulceración cuando las dosis acumulativas son mayores[17,18]. Está acompañada de un espectro de manifestaciones clínicas que incluyen dolor, odinofagia, reducción de la ingesta oral e infecciones secundarias[19]. Es uno de los efectos agudos y determinísticos más frecuentes en pacientes irradiados por CCC, ocurriendo en casi la totalidad de ellos, aproximadamente entre el 85% y 100%[7,10,20,21].

Manejo preventivo para la mucositis oral

Contar con un protocolo de tratamiento oral integral que incluya no solo la evaluación constante de la cavidad oral, sino también la disminución de factores de riesgo predisponentes resulta fundamental para la prevención de la RIOM. Kawashita *et al.*[18] aplicaron un protocolo de atención que consistía en colocar espaciadores (dispositivos intraorales de 3-5 mm de diámetro que cubren la dentición completa) para evitar la radiación dispersa durante la radioterapia, to-

mar clorhidrato de pilocarpina para disminuir la sensación de sequedad oral, aplicar una pomada de dexametasona sobre áreas con enrojecimiento o formación de pseudomembranas y recibir cuidado bucal profesional al menos una vez a la semana; encontraron que dicha intervención se asoció significativamente con una disminución de la incidencia de mucositis oral grave en pacientes que recibían solo radioterapia. Adicionalmente, el estudio de Mallick *et al.*[19] recomendó usar un cepillo de cerdas suaves y evitar el calor, la comida picante, el alcohol y el tabaquismo.

Se han realizado varios estudios acerca de agentes tópicos, principalmente en presentación de enjuagues bucales, utilizados con fines preventivos para la RIOM[18,22-24].

La bencidamina es un agente con propiedades antiinflamatorias, analgésicas y antimicrobianas que tiene fuerte respaldo en la prevención de la RIOM en pacientes que reciben dosis moderadas de radioterapia[22,23]. Sin embargo, tiene poco efecto cuando la dosis de radiación es igual o mayor a 50 Gy y cuando, conjuntamente, se aplica quimioterapia[18].

La curcumina, un agente herbal preventivo con acciones antiinflamatorias, antineoplásicas, analgésicas, antibacterianas y antioxidantes ha mostrado mejores resultados en la prevención de la RIOM[23,24]. Shah *et al.*[23] compararon los efectos del enjuague bucal de curcumina al 0,1% y el de bencidamina al 0,15% y encontraron que, si bien ambos no evitaron la aparición de la RIOM, el enjuague de curcumina logró un mayor efecto en retardar su aparición.

El carácter cicatrizante y antimicrobiano de la miel, además de su fácil accesibilidad y su bajo costo hacen que sea considerado un producto prometedor para prevenir la RIOM[24]. Un estudio encontró que la miel como terapia adyuvante de primera línea es efectiva y segura para pacientes con RIOM moderada-severa, especialmente si se aplica miel local natural pura[25].
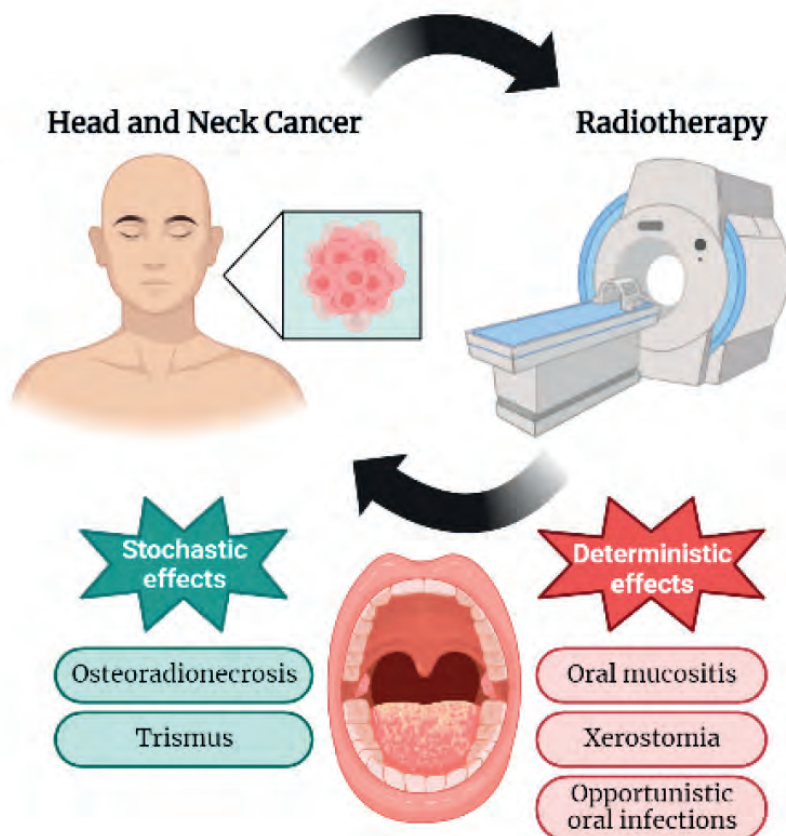
Figura 1. Intervención odontológica para reducir la incidencia y severidad de las manifestaciones orales. Imagen creada con BioRender (https://biorender.com/).

3

Autor y año	Manifestación oral	Manejo de la manifestación oral	Objetivo	Muestra	Protocolo del manejo	Resultado/Conclusión
Kawashita et al. [10] (2019)	Mucositis oral	Protocolo de tratamiento oral integral	Preventivo	124 pacientes	Grupo control: Recibieron solo cuidado bucal profesional al menos una vez a la semana. Grupo intervención: Se colocaron espaciadores en cada sesión de RT. Recibieron 5 mg de clorhidrato de pilocarpina 3 veces al día y se aplicaron ungüento de dexametasona 4 veces al día, además recibieron el cuidado bucal profesional antes mencionado.	La intervención se asoció significativamente con una disminución de la incidencia de mucositis oral grave en pacientes que recibieron solo RT, pero no en los que recibieron quimiorradioterapia.
Shah et al. [15] (2020)		Enjuague bucal de curcumina		74 pacientes	Grupo control: 10 ml de enjuague bucal de bencidamina al 0,15 %, 3 veces al día por 7 días. Grupo intervención: 10 ml de enjuague bucal de curcumina al 0,1 %, 3 veces al día por 7 días.	Ambos enjuagues fueron efectivos para prevenir la RIOM grave. Además, la curcumina retrasó la aparición de la RIOM por 2 semanas.
Yang et al. [17] (2019)		Miel		17 estudios que incluyeron 1265 pacientes	---	La miel natural pura aplicada localmente disminuyó el riesgo de efectos adversos y retrasó el tiempo de aparición de la mucositis oral.
Alsubaie et al. [19] (2021)		Glutamina		11 estudios que incluyeron 922 pacientes	---	La glutamina redujo sustancialmente la incidencia de la RIOM severa.
Yokota et al. [21] (2017)		Rebamipida		94 pacientes	Grupo control: Placebo Grupo A: 5 ml de rebamipida líquida al 2 %, 6 veces al día por 77 días. Grupo B: 5 ml de rebamipida líquida al 4 %, 6 veces al día por 77 días.	La incidencia de mucositis oral de grado mayor o igual a 3 fue menor en el grupo que recibió rebamipida al 4%.
Soutome et al. [22] (2021)		Líquido oral formador de barrera bioadhésiva (Episil)	Terapéutico	15 pacientes	Grupo A: El 1.er día se aplicó una pomada de dexametasona, el 2.do día se realizó un lavado y el 3.er día se aplicó Episil. Grupo B: El 1.er día se aplicó Episil, el 2.do día se realizó un lavado y el 3.er día se aplicó una pomada de dexametasona.	El efecto analgésico de la pomada de dexametasona es comparable o superior al del Episil en pacientes con RIOM.
Peng et al. [26] (2020)		PBMT		29 estudios que incluyeron 1616 pacientes	---	La PBMT disminuyó la duración de la mucositis oral grave, además redujo el grado de severidad medio y la incidencia general del dolor intenso.
Gupta et al. [31] (2020)	Xerostomía	IMRT	Preventivo	60 pacientes	Grupo A: 3D-CRT a una dosis de 70 Gy/35 fracciones durante 7 semanas. Grupo B: IMRT a una dosis de 66 Gy/30 fracciones durante 6 semanas.	La IMRT reduce la incidencia de xerostomía moderada a grave en comparación con la 3D-CRT.
Cao et al. [33] (2021)		IMPT		532 pacientes	Grupo A: IMRT se entregó como fotones de 6 MV usando aceleradores lineales con el sistema de planificación Pinnacle. Grupo B: IMPT se realizó con el sistema de planificación Eclipse.	La xerostomía moderada-grave fue menos frecuente en el grupo IMPT que en el grupo IMRT a los 18-36 meses.
Mercadante et al. [36] (2017)		Fármacos parasimpático miméticos	Terapéutico	20 estudios que incluyeron 1732 pacientes	---	La cevimelina y la pilocarpina pueden reducir los síntomas de xerostomía y aumentar el flujo salival en comparación con el placebo.
Menezes et al. [39] (2021)		Acupuntura		107 pacientes	Grupo control: No recibió intervención. Grupo intervención: En la acupuntura tradicional se aplicaron 18 agujas en sesiones semanales y en la acupuntura auricular se colocaron semillas de mostaza en cada oreja, alternándola semanalmente, durante todo el periodo de tratamiento de RT.	La intervención de acupuntura redujo la xerostomía y aumentó la producción de saliva más del doble en comparación con el grupo control.
Ribeiro et al. [47] (2021)		PBMT		23 pacientes	Se realizaron aplicaciones intraorales y extraorales con láser infrarrojo a una longitud de onda de 808 nm, tres veces por semana en días alternos durante todo el periodo de RT.	La PBMT no interfirió en la xerostomía de los pacientes, pero parece evitar que alcancen grados más altos.
Funahara et al. [61] (2021)	Candidiasis oral	Parche oral de miconazol	Preventivo	28 pacientes	Grupo control: Cuidado bucal, 1 o 2 veces por semana durante el periodo total de RT. Grupo intervención: Se aplicó un parche de miconazol (50 mg de miconazol) en la mucosa cerca de la fosa canina, 1 vez al día durante 14 días, tras la aparición de mucositis oral grado 2.	El parche oral de miconazol suprimió el recuento de Candida albicans en la saliva, por ello, la incidencia de candidiasis oral fue menor en el grupo de intervención.
Doppalapudi et al. [62] (2020)		Terapia con bacterias probióticas		86 pacientes	Grupo probióticos: Utilizaron sobres probióticos (mezcla de 4 cepas probióticas), 3 veces al día, durante 30 días. Grupo cándido: Recibieron un agente antifúngico (Clotrimazol al 1%) durante el tiempo prescrito según el régimen de administración. Grupo combinación: Recibieron sobres probióticos y agente antifúngico.	Se identificó una reducción significativa del recuento de Candida albicans en los tres grupos, además solo el grupo probióticos logró una reducción significativa de Candida glabrata y tropicalis.
Kermani et al. [63] (2021)		Fármacos antimicóticos	Terapéutico	59 pacientes	Se evaluó la actividad in vitro de ocho fármacos antimicóticos comunes (anfotericina B, nistatina, voriconazol, itraconazol, miconazol, clotrimazol y ketoconazol) frente a 55 aislamientos.	El fluconazol es el antimicótico más adecuado para tratar la candidiasis oral extensa.
Zhang et al. [66] (2017)	Osteorradionecrosis	IMPT	Preventivo	534 pacientes	Grupo A: IMRT se entregó como fotones de 6 MV a una dosis media de 41,2 Gy con un sistema de planificación Pinnacle. Grupo B: IMPT a una dosis media de 25,6 Gy con un sistema de planificación Eclipse.	La IMPT redujo el riesgo de ORN, logrando una menor tasa de incidencia.
Aggarwal et al. [68] (2017)		Pentoxifilina y tocoferol		110 pacientes	400 mg de pentoxifilina dos veces al día y 1000 UI de tocoferol (vitamina E) al día, 1 mes antes de la extracción y después de la operación hasta la cicatrización del alvéolo.	La incidencia de ORN fue menor que la normalmente asociada a las extracciones dentales.
Jenwitheesuk et al. [70] (2018)		HBOT	Terapéutico	84 pacientes	Tratamiento diario con HBOT a 2,4 atmósferas absolutas durante 90 min, 20 inmersiones antes y 10 inmersiones después de la cirugía.	HBOT mejoró la cicatrización de heridas en pacientes con ORN en estadios 1 y 2.
Van der Geer et al. [72] (2019)	Trismo	Terapia de ejercicios con dispositivos de estiramiento	Preventivo y terapéutico	12 pacientes	Grupo TheraBite Jaw Motion Rehabilitation System™: Realizaron ejercicios de estiramiento durante 3 meses. Grupo Dynasplint Trismus System®: Realizaron ejercicios de estiramiento durante 3 meses.	Los dispositivos de estiramiento permitieron ganar mm en la apertura bucal, sin embargo, no existió una diferencia significativa entre ambos.

Tabla 1. Estudios sobre el manejo de las manifestaciones orales inducidas por radioterapia de cabeza y cuello. RT: radioterapia, RIOM: mucositis oral inducida por radioterapia, PBMT: terapia de fotobiomodulación, IMRT: radioterapia de intensidad modulada, 3D-CRT: radioterapia convencional tridimensional, IMPT: terapia de protones de intensidad modulada, ORN: osteorradionecrosis, HBOT: oxigenoterapia hiperbárica. (Fuente: creación propia.)

4

La glutamina es un nutriente utilizado para aumentar la proliferación celular, por ende, su deficiencia podría afectar negativamente la función de los tejidos del huésped[26]. Un metaanálisis señaló que, si bien la glutamina no logró una diferencia significativa en la incidencia de mucositis oral en comparación con el grupo control, redujo sustancialmente la gravedad de la RIOM[27]. Davy & Heathcote[20] evaluaron la eficacia de tres intervenciones de bajo costo para mitigar la RIOM y concluyeron que la glutamina oral era la única recomendada para dicho fin.

La rebamipida es un agente mucoprotector que mejora la preservación de las células epiteliales existentes y promueve el reemplazo de tejido perdido[28]. Chaitanya et al.[28] determinaron que las gárgaras con rebamipida son eficaces para aplazar la aparición de mucositis oral, así como para reducir su gravedad. Otro estudio encontró similares resultados y además señaló que, según los perfiles de eficacia y seguridad, la dosis óptima de rebamipida líquida es al 4%[29].

Si bien los agentes preventivos no evitan por completo la aparición de la RIOM, pueden disminuir su gravedad o retrasar su aparición. Sin embargo, hasta la actualidad no existe agente con una total eficacia.

Manejo terapéutico para la mucositis oral

El tratamiento de la RIOM es en gran parte sintomático, basado en el control del dolor y de la infección oral coexistente[10]. Pueden utilizarse agentes tópicos o sistémicos, los cuales están disponibles en diversas presentaciones. Un estudio realizado en pacientes con RIOM comparó el efecto de un líquido oral (Episil), formador de barrera cristalina bioadhesiva superficial que protege a la mucosa, con la pomada de dexametasona para mitigar el dolor relacionado a la mucositis oral y encontró que el Episil alivió el dolor en un 71,4% y la pomada de dexametasona en un 85,7% de los pacientes[30]. Rasic et al.[31] administraron localmente un spray compuesto por lisozima, cetilpiridinio y lidocaína en pacientes con RIOM y encontraron que fue eficaz al disminuir los signos de inflamación y la intensidad del dolor al comer y hablar.

La terapia con láser de baja potencia o fotobiomodulación (PBMT, por sus siglas en inglés) es una de las más efectivas en el tratamiento de la RIOM ya que al poder penetrar en los tejidos blandos tiene efectos cicatrizantes y analgésicos, agilizando el proceso de curación de dicha manifestación[32,33]. Un metaanálisis encontró que la PBMT terapéutica disminuyó significativamente la duración de la mucositis oral grave, además redujo el grado de severidad medio y la incidencia general del dolor intenso[34]. Sin embargo, la implementación de esta intervención en un servicio de atención médica puede incurrir en costos muy altos debido al uso de equipos y a la capacitación del personal[20].

Xerostomía

La xerostomía es definida como la sensación subjetiva de boca seca y es una de las complicaciones más frecuentes, reportándose en un 81-100% de los pacientes durante y después del curso de radioterapia[35]. Si bien esta se correlaciona con la tasa de secreción salival reducida conocida como hiposalivación, ambos fenómenos son independientes[36,37]. El daño de las glándulas salivales es generalmente irreversible a dosis superiores a 50 Gy, por ende, puede ser considerado un efecto determinístico[38]. Existen tres enfoques terapéuticos para su tratamiento: prevención, estimulación y tratamiento sintomático[39].

Manejo preventivo para la xerostomía

La radioterapia de intensidad modulada (IMRT, por sus siglas en inglés) representa una forma avanzada de radioterapia basada en haces de fotones que permite administrar dosis de radiación más altas y precisas al tumor, mientras se reduce considerablemente la irradiación a los tejidos normales circundantes, por consiguiente, tiene un alto potencial para preservar la función de las glándulas salivales[12,40]. Dos estudios clínicos han encontrado que la IMRT proporciona una reducción significativa en la incidencia de xerostomía, en comparación con la radioterapia conformada tridimensional[41,42].

La terapia de protones de intensidad modulada (IMPT, por sus siglas en inglés) proporciona una mejor distribución de la dosis que la radioterapia basada en fotones, gracias a que los protones tienen mejores propiedades físicas y radiobiológicas, depositando alta energía en el tumor y casi ninguna en los tejidos normales[43]. Un estudio realizado en pacientes con cáncer de orofaringe determinó que, 18 a 36 meses después del tratamiento, la xerostomía moderada-grave fue menos frecuente en el grupo que recibió IMPT que en el que recibió IMRT[44].

La amifostina es un agente citoprotector que puede reducir la incidencia de xerostomía, gracias a que se acumula en las glándulas salivales y elimina los radicales libres derivados del oxígeno[12,45]. Riley et al.[45] evaluaron la eficacia de varias intervenciones farmacológicas en la prevención de la disfunción glandular después de radioterapia por CCC y concluyeron que a pesar de la existencia de estudios que demuestran los beneficios de la amifostina, su uso se debe sopesar debido a su alto costo y la existencia de efectos adversos como vómitos, hipotensión, náuseas y respuesta alérgica. (Figura 1).

Manejo terapéutico para la xerostomía

Cuando la capacidad secretora residual de las glándulas salivales aún está presente, puede ser apropiada la estimulación de la secreción salival[46]. Entre las opciones reportadas en la literatura están los fármacos parasimpaticomiméticos, la acupuntura, la fitoterapia, la estimulación nerviosa y la PBMT[38,45-58].

Los fármacos parasimpaticomiméticos, también denominados fármacos agonistas colinérgicos, tienen la capacidad de aumentar la secreción salival, gracias a que actúan a nivel del sistema nervioso parasimpático. Dos metanálisis concluyeron que este tipo de fármacos como la pilocarpina, el betanecol y la cevimelina deberían representar la primera línea de tratamiento en pacientes con CCC y xerostomía inducida por radioterapia[46,47]. Sin embargo, estos sialogogos sistémicos no son totalmente eficaces y pueden generar efectos adversos tales como sudoración, frecuencia urinaria, rinitis, náuseas, astenia y diarrea[45,48].

La acupuntura es una forma de medicina alternativa que consiste en la colocación de agujas en puntos específicos del cuerpo. Se cree que los mecanismos por los cuales aumenta la secreción salival son la estimulación del sistema nervioso parasimpático y simpático a través de la activación neuronal y el aumento del flujo sanguíneo en los acinos glandulares[38]. Menezes et al.[50] demostraron que el protocolo de acupuntura tradicional y acupuntura auricular redujo los síntomas de xerostomía y aumentó el volumen y densidad salival. Otros estudios evidenciaron que la acupuntura es superior que el cuidado bucal estándar para aliviar los síntomas de xerostomía inducida por radioterapia, presentando una incidencia muy baja de efectos adversos[38,49].
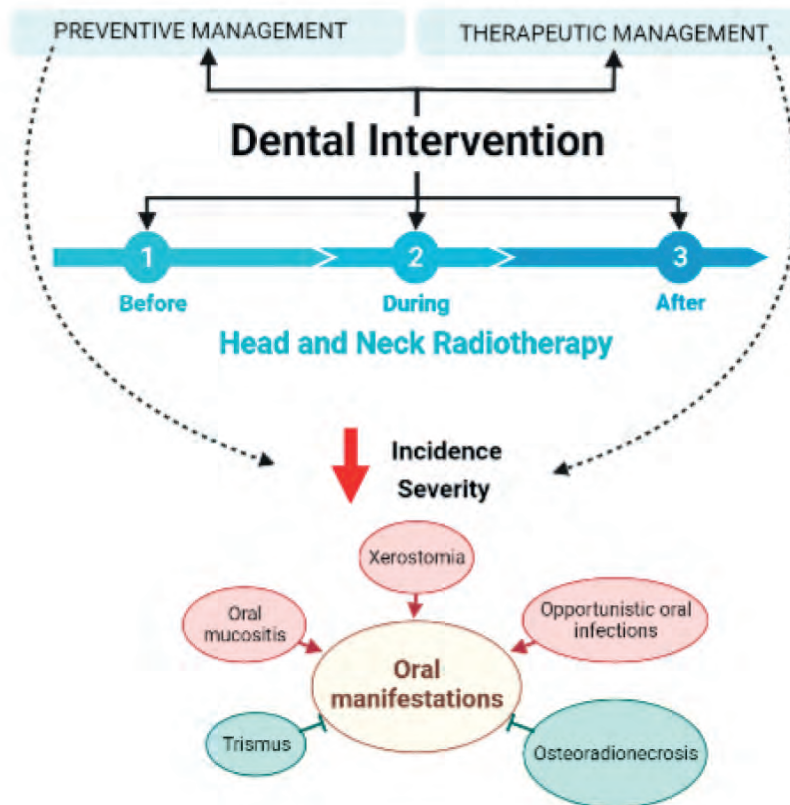
Figura 2. Efectos adversos en la cavidad oral inducidos por radioterapia de cabeza y cuello. Imagen creada con BioRender (https://biorender.com/).

La fitoterapia es otra forma de medicina alternativa y complementaria que se puede utilizar para aliviar la xerostomía. Aunque se desconoce cuál es exactamente el mecanismo de acción de las plantas medicinales utilizadas con dicho fin, es probable que estimulen el movimiento del fluido transcelular y la secreción en las células acinares secretoras[51]. Heydarirad et al.[52] concluyeron que los remedios herbales a base de dos plantas mucilaginosas deben considerarse un tratamiento adecuado para la xerostomía en pacientes irradiados por CCC.

La estimulación nerviosa eléctrica transcutánea (TENS, por sus siglas en inglés) es una técnica no invasiva que transmite corrientes eléctricas sobre la superficie intacta de la piel con el fin de activar los nervios subyacentes. Se ha propuesto como terapia prometedora para la xerostomía ya que logra estimular la función salival[53]. Existen dos tipos de TENS: la TENS convencional que consiste en la estimulación local de las glándulas salivales y la TENS similar a la acupuntura que consiste en la estimulación a distancia[53,54]. Estudios han demostrado que ambos tipos de TENS son eficaces y seguros para disminuir la xerostomía inducida por radioterapia[55,56].

Es bien sabido el papel de la PBMT en el tratamiento de la RIOM; además, debido a su bajo costo y fácil aplicación, se espera que tenga la misma eficacia en reducir la queja de xerostomía reportada por los pacientes con CCC. Ribeiro et al.[57] concluyeron que la PBMT no interfirió significativamente en la incidencia de xerostomía, pero sí parece evitar que esta complicación se agrave. Otra investigación no encontró diferencias significativas en la xerostomía entre el grupo que recibió la PBMT y el grupo control[58]. Por lo tanto, se precisan de más estudios clínicos que confirmen su efectividad.

Otro enfoque terapéutico es el alivio sintomático de la sequedad bucal, para ello existe una gran variedad de productos como chicles sin azúcar, sustitutos salivales, cremas hidratantes y dentífricos[39].

Los sustitutos salivales, también denominados lubricantes orales o saliva artificial, se utilizan como reemplazo de la saliva natural ya que son capaces de imitar sus funciones. Si bien son de aplicación tópica y logran reducir los síntomas de xerostomía, las principales desventajas son que la mayoría de estos no logra proporcionar las funciones antimicrobianas de la saliva normal y sus efectos son de corta duración[12,35,59]. Están disponibles comercialmente en forma de aerosoles, geles, enjuagues bucales y dentífricos, además debido a que contienen conservantes y generan efectos adversos, especialmente reacciones alérgicas, no se recomienda tragarlos[60]. Algunos estudios recomiendan una utilización simultánea de varios agentes tópicos, por ejemplo, Martín et al.[39] encontraron que el uso por 15 días de pasta dental, enjuague bucal, spray y gel, que contenían aceite de oliva, betaína y xilitol, mejoró significativamente los síntomas de boca seca en pacientes tratados con radioterapia por CCC.

En la actualidad, se cuentan con sustitutos salivales comestibles como la jalea humectante oral, la cual ha demostrado tener una eficacia superior al gel comercial tópico para aliviar los síntomas de xerostomía y los problemas de deglución[60].

Candidiasis oral

Las especies de candida forman parte de la microflora bucal normal por lo que, en condiciones normales, no causan enfermedades; sin embargo, cualquier cambio en el ambiente oral y /o sistémico puede generar un aumento en la colonización e infección de estas especies[61,62]. Particularmente, la radioterapia de cabeza y cuello se asocia a

la candidiasis oral debido a factores predisponentes locales como la disminución en la cantidad y calidad de saliva y los daños en la mucosa oral y/o factores predisponentes sistémicos como la inmunosupresión[62-65]. Es la infección oportunista más frecuente en pacientes que reciben radioterapia por CCC, reportándose en un 25-53%[62,66-68].

Manejo preventivo para la candidiasis oral

La modificación de factores predisponentes puede reducir el número de especies de candida y evitar la infección. Lam-Ubol *et al.*[69] reportaron que dos sustitutos salivales fueron eficaces en pacientes con xerostomía inducida por radioterapia de cabeza y cuello ya que disminuyeron significativamente el número de especies de candida entre 1 y 2 meses.

La profilaxis con agentes antimicóticos tópicos ha demostrado ser efectiva para evitar la candidiasis oral durante la radioterapia[14,70]. Funahara *et al.*[70] encontraron que la administración de un parche oral de miconazol 14 días después de la aparición de mucositis oral logró reducir el crecimiento de Candida albicans en pacientes irradiados por CCC. Es por ello, que la presencia de algún factor predisponente debería ser un indicador para aplicar una terapia profiláctica.

La terapia con bacterias probióticas también resulta ser una medida prometedora en la prevención de candidiasis oral. Se ha encontrado que las bacterias probióticas han sido efectivas para reducir la Candida albicans y algunas especies de candida no albicans como Candida glabrata y Candida tropicalis[71].

Manejo terapéutico para la candidiasis oral

Los agentes tópicos se recomiendan como tratamiento de primera línea en las formas más leves de candidiasis oral y se pueden encontrar en diversas presentaciones como pastillas, suspensión oral, crema y enjuagues bucales. Por otro lado, los agentes sistémicos se deben utilizar cuando la terapia tópica haya fracasado o cuando la candidiasis oral sea clínicamente grave[14].

Generalmente, los fármacos antimicóticos utilizados en pacientes irradiados por CCC pertenecen a la familia de los azoles o los polienos. Dos estudios han encontrado que la terapia con fluconazol es la más eficaz y segura en estos pacientes[61,72].

Osteorradionecrosis

La osteorradionecrosis se define como el área de hueso expuesto a la radiación que no cicatriza en un periodo de tiempo de 3 a 6 meses[73]. Las extracciones dentales, el trauma de la dentadura, la infección dental, la inserción de implantes dentales, entre otros, son los responsables de desencadenar la osteorradionecrosis después de la radioterapia[74]. Es una complicación tardía y poco común de la radioterapia en pacientes con CCC, presentándose en ausencia de la neoplasia tratada y con una incidencia de 4-8 %[73,74].

Manejo preventivo para la osteorradionecrosis

La IMPT consiste en la irradiación de energía en tejidos específicos y una disminución de esta en zonas alejadas del punto de irradiación. De este modo, se generan mayores beneficios al proporcionar dosis necesarias para la neoplasia y reducir la exposición de los tejidos sanos, disminuyendo el riesgo de los efectos adversos inducidos por radioterapia como la osteorradionecrosis[75]. Un estudio

realizado en pacientes con CCC que fueron divididos en un grupo que recibió IMPT y otro grupo que recibió IMRT determinó que se desarrollaron menores casos de osteorradionecrosis en los pacientes que recibieron IMPT[75].

La pentoxifilina y el tocoferol actúan como antioxidantes y su manejo se basa en la teoría de la fibrosis inducida por radiación, la cual es considerada como la causa principal de osteorradionecrosis, según Delanian y Lefaix[74,76]. Un estudio realizado en pacientes que recibieron radioterapia por CCC junto a un manejo profiláctico con pentoxifilina y tocoferol antes y después de las extracciones dentales, reportó que solo un paciente desarrolló osteorradionecrosis, evidenciándose una disminución en la incidencia de esta complicación después de las extracciones dentales[74]. Otra investigación realizada en pacientes con tratamiento previo de radioterapia por CCC y que recibieron el tratamiento profiláctico con pentoxifilina y tocoferol un mes antes de la extracción dental hasta la cicatrización del alvéolo, evidenció que dos pacientes desarrollaron osteorradionecrosis, reportándose una incidencia menor que la normalmente asociada[77].

Manejo terapéutico para la osteorradionecrosis

La oxigenoterapia hiperbárica (HBOT, por sus siglas en inglés) consiste en la inhalación de oxígeno (O2) al 100% en una cámara con presión atmosférica superior a la del nivel del mar, con el objetivo de redistribuir el oxígeno a los tejidos hipóxicos ya que estimula la proliferación de fibroblastos, aumenta la angiogénesis y posee mecanismos bactericidas y bacteriostáticos para prevenir infecciones[78]. Algunos estudios han utilizado la HBOT como medida preventiva y terapéutica para la osteorradionecrosis con resultados prometedores[78]. Jenwitheesuk *et al.*[79] evaluaron la eficacia de la HBOT adyuvante en la osteorradionecrosis, los resultados evidenciaron que mejoró la cicatrización de heridas de pacientes con osteorradionecrosis en estadios 1 y 2 que recibieron tratamiento con HBOT antes y después de las extracciones dentales.

La reconstrucción de tejido libre microvascular se realiza en casos graves de osteorradionecrosis, este procedimiento consiste en la resección quirúrgica del hueso necrótico y sus márgenes para posteriormente realizar la reconstrucción con tejido libre vascularizado. Sin embargo, no existe un consenso acerca de la correcta extensión de escisión, lo que conlleva, muchas veces, a casos de recurrencia[78].

Trismo

El trismo se genera cuando la apertura bucal máxima es menor a 35 mm y puede presentarse en pacientes con CCC con una incidencia entre el 5% y el 38%. Presenta diversas causas como la invasión tumoral de los tejidos masticatorios, la inflamación de la mucosa, las infecciones bucales, y además resultar del tratamiento neoplásico como la radioterapia o la cirugía[80].

Manejo preventivo y terapéutico para el trismo

Para tratar el trismo se indica una variedad de terapias de ejercicio. La terapia de ejercicios con dispositivos de estiramiento como TheraBite y Dynasplint Trismus System permiten aumentar la apertura bucal hasta 14 mm, resultando de gran ayuda para estos pacientes[81]. Van der Geer *et al.*[81] atendieron pacientes con trismo inducido por radioterapia de cabeza y cuello e informaron un aumento de la apertura bucal después de realizar la terapia de ejercicios con los dispositivos de estiramiento TheraBite y Dynasplint

Trismus System; además al compararlos, se evidenció que los pacientes que utilizaron el dispositivo TheraBite ganaron 3 mm, mientras que los pacientes que utilizaron Dynasplint Trismus System, 1,5 mm. Otra investigación realizada por Lee et al.[82] demostró que los ejercicios con TheraBite o espátulas de madera antes, durante y después de la radioterapia aliviaron el trismo inducido por radiación en pacientes con CCC en estadios 3 y 4.

Conclusiones

Existen varias alternativas preventivas y terapéuticas para el manejo de las manifestaciones orales inducidas por radioterapia de cabeza y cuello que han resultado ser eficaces y seguras, permitiendo reducir su incidencia y gravedad. Por ello, resulta fundamental la inclusión del odontólogo como parte del equipo multidisciplinario que brinde atención antes, durante y después de la terapia oncológica con la finalidad de mejorar la calidad de vida del paciente.

Contribuciones de los autores

Conceptualización, N.J.M-Ch., K.V.F-J., A.C.C-A. y M.A.M-V.; metodología, M.A.M-V.; investigación, N.J.M-Ch., K.V.F-J. y A.C.C-A.; recursos, N.J.M-Ch., K.V.F-J. y A.C.C-A.; redacción—preparación del borrador original, N.J.M-Ch., K.V.F-J., A.C.C-A. y M.A.M-V.; redacción—revisión y edición, N.J.M-Ch., K.V.F-J., A.C.C-A. y M.A.M-V.; supervisión, M.A.M-V.; administración del proyecto, N.J.M-Ch. Todos los autores han leído y aceptado la versión publicada del manuscrito.

Financiamiento

Esta investigación no recibió financiación externa.

Conflictos de Interés

Los autores declaran no tener conflicto de intereses.

Referencias bibliográficas

1. Dhull A, Atri R, Dhankhar R, Chauhan A, Kaushal V. Major Risk Factors in Head and Neck Cancer: A Retrospective Analysis of 12-Year Experiences. World J Oncol. 2018;9(3):80-4.

2. Liu Z, Dong L, Zheng Z, Liu S, Gong S, Meng L, et al. Mechanism, Prevention, and Treatment of Radiation-Induced Salivary Gland Injury Related to Oxidative Stress. Antioxidants. 2021;10(11):1666-90.

3. Bray F, Ferlay J, Soerjomataram I, Siegel R, Torre L, Jemal A. Global cancer statistics 2018: GLOBOCAN estimates of incidence and mortality worldwide for 36 cancers in 185 countries. CA Cancer J Clin. 2018;68(6):394-424.

4. Sia J, Szmyd R, Hau E, Gee HE. Molecular Mechanisms of Radiation-Induced Cancer Cell Death: A Primer. Frontiers in Cell and Developmental Biology. 2020;8(41):1-8.

5. Liu Y, Zheng C, Huang Y, He M, Xu WW, Li B. Molecular mechanisms of chemo□ and radiotherapy resistance and the potential implications for cancer treatment. MedComm (2020). 2021;2(3):315-40.

6. Aldana VG, Saaibi JF, Medina LA. Tumores cerebrales y lesiones encefálicas por radiación ionizante. Rev Colomb Cardiol. 1 de marzo de 2020;27:79-81.

7. Puerta-Ortiz JA, Morales-Aramburo J. Efectos biológicos de las radiaciones ionizantes. Rev Colomb Cardiol. 1 de marzo de 2020;27:61-71.

8. Barba Ramírez L, Ruiz García de Chacón V, Hidalgo Rivas A, El uso de rayos X en odontología y la importancia de la justificación de exámenes radiográficos. Avances en Odontoestomatología. agosto de 2020;36(3):131-42.

9. Baujat B, Bourhis J, Blanchard P, Overgaard J, Ang KK, Saunders M, et al. Hyperfractionated or accelerated radiotherapy for head and neck cancer. Cochrane Database of Systematic Reviews [Internet]. 2010 [citado 14 de noviembre de 2022];(12). Disponible en: https://www.cochranelibrary.com/es/cdsr/doi/10.1002/14651858.CD002026.pub2/full/es

10. Conceição T, Sanches A, Freire T, Martins G, Marques M, Dantas J. Acute Oral Manifestations in Patients Submitted to Radiotherapy in the Head and Neck Region: Literature Narrative Review. J Health Sci. 2021;23(2):92-8.

11. Coelho L, Silva C, Pedra R, Rosado L, Verner F, Aquino S. Probability of oral complications of radiotherapy and chemotherapy for head and neck cancer. Gen Dent. 2021;69(4):70-4.

12. Jaguar G, Prado J, Campanhã D, Alves F. Clinical features and preventive therapies of radiation-induced xerostomia in head and neck cancer patient: a literature review. Appl Cancer Res. 2017;37(1):31-8.

13. Minicucci EM, da Silva GN, Salvadori DMF. Relationship between head and neck cancer therapy and some genetic endpoints. World J Clin Oncol. 10 de mayo de 2014;5(2):93-102.

14. Sroussi H, Epstein J, Bensadoun R, Saunders D, Lalla R, Migliorati C, et al. Common oral complications of head and neck cancer radiation therapy: mucositis, infections, saliva change, fibrosis, sensory dysfunctions, dental caries, periodontal disease, and osteoradionecrosis. Cancer Med. 2017;6(12):2918-31.

15. Silva E, Oliveira G, Cardoso A, Ferreira I, Brazão M, Guimarães D. Evaluation of Quality of Life and Oral Changes of Patients in Head and Neck Radiotherapy: Observational Study. J Cancer Ther. 2021;12(11):641-53.

16. Nascimento E, Ferreira I, Lajolo P, Paiva C, Paiva Y, Graças G. Health-related quality of life became worse in short-term during treatment in head and neck cancer patients: a prospective study. Health Qual Life Outcomes. 2020;18(1):307-19.

17. Moslemi D, Nokhandani A, Otaghsaraei M, Moghadamnia Y, Kazemi S, Moghadamnia A. Management of chemo/radiation-induced oral mucositis in patients with head and neck cancer: A review of the current literature. Radiother Oncol. 2016;120(1):13-20.

18. Kawashita Y, Koyama Y, Kurita H, Otsuru M, Ota Y, Okura M, et al. effectiveness of a comprehensive oral management protocol for the prevention of severe oral mucositis in patients receiving radiotherapy with or without chemotherapy for oral cancer: a multicentre, phase II, randomized controlled trial. Int J Oral Maxillofac Surg. 2019;48(7):857-64.

19. Mallick S, Benson R, Rath G. Radiation induced oral mucositis: a review of current literature on prevention and management. Eur Arch Otorhinolaryngol. 2016;273(9):2285-93.

20. Davy C, Heathcote S. A systematic review of interventions to mitigate radiotherapy-induced oral mucositis in head and neck cancer patients. Support Care Cancer. 2021;29(4):2187-202.

21. Musha A, Hirai C, Kitada Y, Tsunoda A, Shimada H, Kubo N, et al. Relationship between oral mucositis and the oral bacterial count in patients with head and neck cancer undergoing carbon ion radiotherapy: A prospective study. Radiother Oncol. 2021;167:65-71.

22. Daugélaité G, Užkuraitytė K, Jagelavičienė E, Filipauskas A. Prevention and Treatment of Chemotherapy and Radiotherapy Induced Oral Mucositis. Medicina (Kaunas). 2019;55(2):25-38.

23. Shah S, Rath H, Sharma G, Senapati S, Mishra E. Effectiveness of curcumin mouthwash on radiation-induced oral mucositis among head and neck cancer patients: A triple-blind, pilot randomised controlled trial. Indian J Dent Res. 2020;31(5):718-27.

24. Yarom N, Hovan A, Bossi P, A A, Sb J, M G, et al. Systematic review of natural and miscellaneous agents, for the management of oral mucositis in cancer patients and clinical practice guidelines - part 2: honey, herbal compounds, saliva stimulants, probiotics, and miscellaneous agents. Supportive care in cancer : official journal of the Multinational Association of Supportive Care in Cancer [Internet]. mayo de 2020 [citado 14 de noviembre de 2022];28(5). Disponible en: https://pubmed.ncbi.nlm.nih.gov/32056010/

8

25. Yang C, Gong G, Jin E, Han X, Zhuo Y, Yang S, et al. Topical application of honey in the management of chemo/radiotherapy-induced oral mucositis: A systematic review and network meta-analysis. Int J Nurs Stud. enero de 2019;89:80-7.

26. Yarom N, Hovan A, Bossi P, Ariyawardana A, Jensen S, Gobbo M, et al. Systematic review of natural and miscellaneous agents for the management of oral mucositis in cancer patients and clinical practice guidelines—part 1: vitamins, minerals, and nutritional supplements. Support Care Cancer. 2019;27(10):3997-4010.

27. Alsubaie H, Alsini A, Alsubaie K, Abu-Zaid A, Alzahrani F, Sayed S, et al. Glutamine for prevention and alleviation of radiation-induced oral mucositis in patients with head and neck squamous cell cancer: Systematic review and meta-analysis of controlled trials. Head Neck. 2021;43(10):3199-213.

28. Chaitanya B, Pai K, Yathiraj P, Fernandes D, Chhaparwal Y. Rebamipide gargle in preventive management of chemo-radiotherapy induced oral mucositis. Oral Oncol. 2017;72(9):179-82.

29. Yokota T, Ogawa T, Takahashi S, Okami K, Fujii T, Tanaka K, et al. Efficacy and safety of rebamipide liquid for chemoradiotherapy-induced oral mucositis in patients with head and neck cancer: a multicenter, randomized, double-blind, placebo-controlled, parallel-group phase II study. BMC Cancer. 2017;17:314-21.

30. Soutome S, Yanamoto S, Kawashita Y, Yoshimatsu M, Murata M, Kojima Y, et al. Effects of a bioadhesive barrier-forming oral liquid on pain due to radiation-induced oral mucositis in patients with head and neck cancer: A randomized crossover, preliminary study. J Dent Sci. enero de 2021;16(1):96-100.

31. Rasic A, Kapo B, Avdicevic A, Mekic - Abazovic A, Jankovic SM, Lokvancic A. Efficacy and Safety of Lysozyme, Cetylpyridinium and Lidocaine Fixed Combination for Treatment of Chemotherapy- and Radiotherapy-Induced Oral Mucositis: a Pilot Study. Mater Sociomed. 2019;31(3):166-71.

32. Martins A, Nogueira T, Morais M, Oton A, Valadares M, Batista A, et al. Effect of photobiomodulation on the severity of oral mucositis and molecular changes in head and neck cancer patients undergoing radiotherapy: a study protocol for a cost-effectiveness randomized clinical trial. Trials. 2019;20(1):97-106.

33. Pires Marques EC, Piccolo Lopes F, Nascimento IC, Morelli J, Pereira MV, Machado Meiken VM, et al. Photobiomodulation and photodynamic therapy for the treatment of oral mucositis in patients with cancer. Photodiagnosis Photodyn Ther. marzo de 2020;29:101621.

34. Peng J, Shi Y, Wang J, Wang F, Dan H, Xu H, et al. Low-level laser therapy in the prevention and treatment of oral mucositis: a systematic review and meta-analysis. Oral Surg Oral Med Oral Pathol Oral Radiol. 2020;130(4):387-97.

35. Snider J, Paine C. Sticky stuff: xerostomia in patients undergoing head and neck radiotherapy-prevalence, prevention, and palliative care. Ann Palliat Med. 2020;9(3):1340-50.

36. Lima M, Ribeiro L, Albuquerque R, Carvalho A, Silva I, Leão J. Evaluation of the salivary flow of patients undergoing conventional radiotherapy for head and neck cancer. Gen Dent. 2021;69(5):21-5.

37. Schulz R, Bonzanini L, Ortigara G, Soldera E, Danesi C, Antoniazzi R, et al. Prevalence of hyposalivation and associated factors in survivors of head and neck cancer treated with radiotherapy. J Appl Oral Sci. 2021;29:20200854.

38. Garcia M, Meng Z, Rosenthal D, Shen Y, Chambers M, Yang P, et al. Effect of True and Sham Acupuncture on Radiation-Induced Xerostomia Among Patients With Head and Neck Cancer. JAMA Netw Open. 2019;2(12):1916910.

39. Martín M, Marín A, López M, Liñán O, Alvarenga F, Büchser D, et al. Products based on olive oil, betaine, and xylitol in the post-radiotherapy xerostomia. Rep Pract Oncol Radiother. 2017;22(1):71-6.

40. Jensen S, Vissink A, Limesand K, Reyland M. Salivary Gland Hypofunction and Xerostomia in Head and Neck Radiation Patients. J Natl Cancer Inst Monogr. 2019;2019(53):016.

41. Pan X, Chen K, Huang S, Jiang Y, Ma J, Liang Z, et al. Comparison of the efficacy between intensity-modulated radiotherapy and two-dimensional conventional radiotherapy in stage II nasopharyngeal carcinoma. Oncotarget. 2017;8(44):78096-104.

42. Gupta T, Sinha S, Ghosh S, Budrukkar A, Mummudi N, Swain M, et al. Intensity-modulated radiation therapy versus three-dimensional conformal radiotherapy in head and neck squamous cell carcinoma: long-term and mature outcomes of a prospective randomized trial. Radiat Oncol. 2020;15(1):218-26.

43. Yasuda K, Minatogawa H, Dekura Y, Takao S, Tamura M, Tsushima N, et al. Analysis of acute-phase toxicities of intensity-modulated proton therapy using a model-based approach in pharyngeal cancer patients. J Radiat Res. 2021;62(2):329-37.

44. Cao J, Zhang X, Jiang B, Chen J, Wang X, Wang L, et al. Intensity-modulated proton therapy for oropharyngeal cancer reduces rates of late xerostomia. Radiother Oncol. 2021;160:32-9.

45. Riley P, Glenny A, Hua F, Worthington H. Pharmacological interventions for preventing dry mouth and salivary gland dysfunction following radiotherapy. Cochrane Database Syst Rev. 2017;7(7):012744.

46. Mercadante V, Al Hamad A, Lodi G, Porter S, Fedele S. Interventions for managing radiotherapy-induced xerostomia and hyposalivation: A systematic review and meta-analysis. Oral Oncol. 2017;66:64-74.

47. Johns D. Radiotherapy related xerostomia in head and neck oncology: A systematic review. Ann Oncol. 2017;28(5):390-1.

48. Cheng C, Xu H, Liu L, Wang R, Liu Y, Li J, et al. Efficacy and safety of pilocarpine for radiation-induced xerostomia in patients with head and neck cancer: A systematic review and meta-analysis. J Am Dent Assoc. 2016;147(4):236-43.

49. Ni X, Tian T, Chen D, Liu L, Li X, Li F, et al. Acupuncture for Radiation-Induced Xerostomia in Cancer Patients: A Systematic Review and Meta-Analysis. Integr Cancer Ther. 2020;19:1-14.

50. Menezes A, Sanches G, Gomes E, Soares R, Durães C, Fonseca L, et al. The combination of traditional and auricular acupuncture to prevent xerostomia and anxiety in irradiated patients with HNSCC: a preventive, parallel, single-blind, 2-arm controlled study. Oral Surg Oral Med Oral Pathol Oral Radiol. 2021;131(6):675-83.

51. Nik W, Lim R, Chan S, Lai N, Liew A. A systematic review on Chinese herbal treatment for radiotherapy-induced xerostomia in head and neck cancer patients. Complement Ther Clin Pract. 2018;30:6-13.

52. Heydarirad G, Rezaeizadeh H, Choopani R, Mosavat S, Ameri A. Efficacy of a traditional Persian medicine preparation for radiation-induced xerostomia: a randomized, open-label, active-controlled trial. J Integr Med. 2017;15(3):201-8.

53. Salimi F, Saavedra F, Andrews B, FitzGerald J, Winter S. Trans-cutaneous electrical nerve stimulation to treat dry mouth (xerostomia) following radiotherapy for head and neck cancer. A systematic review. Ann Med Surg. 2021;63:102146.

54. Tulek A, Mulic A, Hogset M, Utheim T, Sehic A. Therapeutic Strategies for Dry Mouth Management with Emphasis on Electrostimulation as a Treatment Option. Int J Dent. 2021;2021:1-21.

55. Iovoli A, Ostrowski A, Rivers C, Hermann G, Groman A, Miller A, et al. Two- Versus Four-Times Weekly Acupuncture-Like Transcutaneous Electrical Nerve Stimulation for Treatment of Radiation-Induced Xerostomia: A Pilot Study. J Altern Complement Med. 2020;26(4):323-8.

56. Paim E, Berbert M, Zanella V, Macagnan F. Electrical stimulation in the treatment of radiotherapy-induced hyposalivationElectrical stimulation in the treatment of radiotherapy-induced hyposalivation. CoDAS. 2019;31(4):2018176.

57. Ribeiro L, Lima M, Carvalho A, Albuquerque R, Leão J, Silva I. Evaluation of the salivary function of patients in treatment with radiotherapy for head and neck cancer submitted to photobiomodulation. Med Oral Patol Oral Cir Bucal. 2021;26(1):14-20.

Manejo odontológico de las manifestaciones orales inducidas por radioterapia de cabeza y cuello
Dental management of oral manifestations induced by radiotherapy of the head and neck

9

58. Louzeiro G, Cherubini K, Figueiredo M, Salum F. Effect of photobiomodulation on salivary flow and composition, xerostomia and quality of life of patients during head and neck radiotherapy in short term follow-up: A randomized controlled clinical trial. J Photochem Photobiol B. 2020;209:111933.

59. Assery M. Efficacy of Artificial Salivary Substitutes in Treatment of Xerostomia: A Systematic Review. J Pharm Bioallied Sci. 2019;11(1):1-12.

60. Nuchit S, Lam-ubol A, Paemuang W, Talungchit S, Chokchaitam O, Mungkung O ong, et al. Alleviation of dry mouth by saliva substitutes improved swallowing ability and clinical nutritional status of post-radiotherapy head and neck cancer patients: a randomized controlled trial. Support Care Cancer. 2020;28(6):2817-28.

61. Jahanshiri Z, Manifar S, Moosa H, Asghari F, Mahmoodzadeh H, Shams M, et al. Oropharyngeal candidiasis in head and neck cancer patients in Iran: Species identification, antifungal susceptibility and pathogenic characterization. J Mycol Med. 2018;28(2):361-6.

62. Kawashita Y, Funahara M, Yoshimatsu M, Nakao N, Soutome S, Saito T, et al. A retrospective study of factors associated with the development of oral candidiasis in patients receiving radiotherapy for head and neck cancer: Is topical steroid therapy a risk factor for oral candidiasis? Medicine. 2018;97(44):13073.

63. Tarapan S, Matangkasombut O, Trachootham D, Sattabanasuk V, Talungchit S, Paemuang W, et al. Oral Candida colonization in xerostomic postradiotherapy head and neck cancer patients. Oral Dis. 2019;25(7):1798-808.

64. Arrifin A, Heidari E, Burke M, Fenlon M, Banerjee A. The Effect of Radiotherapy for Treatment of Head and Neck Cancer on Oral Flora and Saliva. Oral Health Prev Dent. 2018;16(5):425-9.

65. Almhöjd U, Cevik-Aras H, Karlsson N, Chuncheng J, Almståhl A. Stimulated saliva composition in patients with cancer of the head and neck region. BMC Oral Health. 2021;21(1):509-19.

66. Nishii M, Soutome S, Kawakita A, Yutori H, Iwata E, Akashi M, et al. Factors associated with severe oral mucositis and candidiasis in patients undergoing radiotherapy for oral and oropharyngeal carcinomas: a retrospective multicenter study of 326 patients. Support Care Cancer. 2020;28(3):1069-75.

67. Bispo M, Nascimento D, Borges J, Lima H, Medrado A, Pereira M, et al. Frequência de comorbidades associadas ao tratamento radioterápico de cabeça e pescoço. Rev Ciênc Méd Biol. 2018;17(2):185-9.

68. Chitapanarux I, Wongsrita S, Sripan P, Kongsupapsiri P, Phakoetsuk P, Chachvarat S, et al. An underestimated pitfall of oral candidiasis in head and neck cancer patients undergoing radiotherapy: an observation study. BMC Oral Health. 2021;21(1):353-62.

69. Lam-Ubol A, Matangkasombut O, Trachootham D, Tarapan S, Sattabanasuk V, Talungchit S, et al. Efficacy of gel-based artificial saliva on Candida colonization and saliva properties in xerostomic post-radiotherapy head and neck cancer patients: a randomized controlled trial. Clin Oral Investig. 2021;25(4):1815-27.

70. Funahara R, Soutome S, Funahara M, Tsuda S, Hasegawa T, Umeda M, et al. Effects of a miconazole oral patch on preventing development of oral candidiasis in patients with head and neck cancer undergoing radiotherapy: results of a preliminary study quantifying the prevalence of Candida albicans in saliva. Support Care Cancer. 2021;30(1):907-14.

71. Doppalapudi R, Vundavalli S, Prabhat M. Effect of probiotic bacteria on oral Candida in head- and neck-radiotherapy patients: A randomized clinical trial. J Cancer Res Ther. 2020;16(3):470-7.

72. Kermani F, Sadeghian M, Shokohi T, Hashemi S, Moslemi D, Davodian S, et al. Molecular identification and antifungal susceptibility testing of Candida species isolated from oral lesions in patients with head and neck cancer undergoing radiotherapy. Curr Med Mycol. 2021;7(1):44-50.

73. Kubota H, Miyawaki D, Mukumoto N, Ishihara T, Matsumura M, Hasegawa T, et al. Risk factors for osteoradionecrosis of the jaw in patients with head and neck squamous cell carcinoma. Radiat Oncol. 5 de enero de 2021;16:1.

74. Patel V, Gadiwalla Y, Sassoon I, Sproat C, Kwok J, McGurk M. Prophylactic use of pentoxifylline and tocopherol in patients who require dental extractions after radiotherapy for cancer of the head and neck. Br J Oral Maxillofac Surg. junio de 2016;54(5):547-50.

75. Zhang W, Zhang X, Yang P, Blanchard P, Garden AS, Gunn B, et al. Intensity-modulated proton therapy and osteoradionecrosis in oropharyngeal cancer. Radiother Oncol. junio de 2017;123(3):401-5.

76. Rivero JA, Shamji O, Kolokythas A. Osteoradionecrosis: a review of pathophysiology, prevention and pharmacologic management using pentoxifylline, α-tocopherol, and clodronate. Oral Surg Oral Med Oral Pathol Oral Radiol. noviembre de 2017;124(5):464-71.

77. Aggarwal K, Goutam M, Singh M, Kharat N, Singh V, Vyas S, et al. Prophylactic Use of Pentoxifylline and Tocopherol in Patients Undergoing Dental Extractions Following Radiotherapy for Head and Neck Cancer. Niger J Surg. diciembre de 2017;23(2):130-3.

78. Shokri T, Wang W, Vincent A, Cohn JE, Kadakia S, Ducic Y. Osteoradionecrosis of the Maxilla: Conservative Management and Reconstructive Considerations. Semin Plast Surg. mayo de 2020;34(2):106-13.

79. Jenwitheesuk K, Mahakkanukrauh A, Punjaruk W, Jenwitheesuk K, Chowchuen B, Jinaporntham S, et al. Efficacy of Adjunctive Hyperbaric Oxygen Therapy in Osteoradionecrosis. Biores Open Access. 8 de octubre de 2018;7(1):145-9.

80. Martins CA, Goldenberg DC, Narikawa R, Kowalski LP. Trismus and oral health conditions during diagnosis of malignant oral neoplasms. Braz J Otorhinolaryngol. octubre de 2020;86(5):552-7.

81. van der Geer SJ, Reintsema H, Kamstra JI, Roodenburg JLN, Dijkstra PU. The use of stretching devices for treatment of trismus in head and neck cancer patients: a randomized controlled trial. Support Care Cancer. enero de 2020;28(1):9-11.

82. Lee R, Yeo ST, Rogers SN, Caress AL, Molassiotis A, Ryder D, et al. Randomised feasibility study to compare the use of Therabite® with wooden spatulas to relieve and prevent trismus in patients with cancer of the head and neck. Br J Oral Maxillofac Surg. mayo de 2018;56(4):283-91.

ARTICLE / INVESTIGACIÓN

Molecular characterization of national cocoa collection from the leading traditional growing areas in Ecuador

James Quiroz-Vera[1], Eduardo Morillo[2]* Carla Cordoba[2,3] and Johana Buitron

[1] Programa de Cacao. Instituto Nacional de Investigaciones Agropecuarias. Estación Experimental Litoral Sur, Yaguachi, Ecuador.
[2] Departamento de Biotecnología, Instituto Nacional de Investigaciones Agropecuarias, Estación Experimental Santa Catalina, Mejia, Ecuador.
[3] Biology Institute, Universidad de Antioquia, Colombia.
Corresponding author: eduardo.morillo@iniap.gob.ec

DOI. 10.21931/RB/2023.08.01.31

Abstract: Ecuador is the leading producer and exporter of fine cocoa, with plantations over 80 years old, preserving distinctive aroma and flavor characteristics. The research objective was to screen the genetic variability of a collection of National cocoa from Ecuador's leading traditional cocoa growing areas, denominated as Centennial National Cocoa Plants (CCNC). This germplasm collection with 243 accessions was analyzed with 20 microsatellites (SSR) markers. DNA genotyping was highly informative, generating a total of 109 SSR alleles with an average of 5.5 alleles per locus. Only 0.8% of duplicate accessions were identified. The average genetic diversity obtained was 0.447, and the polymorphic content index was 0.414, which shows a high genetic diversity. The clustering, main coordinates, and population assignment analysis revealed that the samples are classified into two subpopulations (GN and GM), differentiated by their level of heterozygosity, with a fixation index value of 0.105. The results showed that microsatellite markers and statistical tools provide useful information that favors managing and conserving genetic variability in CCNC collection.

Key words: Fine and aroma cocoa, Sabor Arriba, DNA genotyping, SSR markers.

Introduction

Theobroma cacao L. is a fruit tree belonging to the genus Theobroma, corresponding to the Malvaceae family1. It is a diploid and allogamous species with a high degree of genetic diversity in its segregating populations[2,3]. Cocoa is an important crop that grows in tropical conditions, mainly in areas ranging from warm to humid, and on continents such as Asia, Africa, and the Americas. It is considered one of the world's most lucrative and commercialized products due to its organoleptic attributes[4,5].

The diversity of cocoa begins with the Criollo cocoa, followed by the Forastero cocoa, and finally, a kind of hybrid cocoa, a result of the mixture between these two kinds of cocoa called Trinitario, based on morphological traits of the crop[6]. Likewise, with more recent molecular data[7], a new classification of cocoa types as proposed in 10 genetic populations called Marañón, Curaray, Criollo, Iquitos, Nanay, Contamana, Amelonado, Purús, Nacional (hereafter National), and Guyana.

In Ecuador, the first plantations of the National cocoa variety date back to the 1600s[8], which were located along the shores of the Guayas River. Until the beginning of the 20th century, National cocoa was the only type of cocoa cultivated in Ecuador. From that time, there are still trees over 100 years old, called Centennial National Cocoa, which still retain the characteristics of fine cocoa and the aroma flavor. Genetic material was introduced between 1916 and 1919 to conserve the crop and reduce the diseases that affected the trees, which resulted in this type of cocoa disappearing from the production area and being replaced by hybrid materials, which nowadays present a high genetic variability[9].

INIAP and the Tenguel Aroma Cocoa Center (CCAT) in Ecuador, in search of the rescue and preservation of these native National trees, established a collection of Centennial trees for study and utilization. Many plants were collected and preserved in ex-situ collections in its leading cocoa germplasm banks.

For the characterization of the cocoa germplasm collected, microsatellite markers or simple sequence repetition (SSR) are often used in cocoa. SSRs are the most commonly used markers in studies of plant genetic diversity, assignment of individuals to their population of origin, and determination of population structure, because they are very polymorphic and codominant, providing more genetic information than other types of markers[10]. There is an excellent variety of cocoa-specific microsatellite markers with sequences previously described[11-14], and ones employed with molecular markers in National cocoa[8,15-19].

The study is part of a broader investigation into preserving Ecuador's National Centenary cocoa collection. It is highlighted that of the samples of trees over 100 years old, their genetic variability is unknown. These trees supposedly preserve their purity (homozygosity) and preserve distinctive characteristics of fine cocoa and aroma. Due to the above, the present study aimed to molecularly characterize a collection of Centenary National cocoa trees from Ecuador's main traditional cocoa growing areas, using a panel of 20 SSR markers.

2

Materials and methods

Biological material

A total of 243 plant samples were collected from the National Centenary cocoa collection (CCNC) of the South Coast Experimental Station of INIAP, located in the Yaguachi canton of the Guayas province. Each sample was coded depending on the origin of the trees from which they were taken: "M" for samples taken from trees from the region of Manabí and "Lr" for those that were taken from trees from the province of Los Rios.

DNA genotyping

DNA was extracted from cocoa leaf tissue by spectrophotometry and stored at -20°C 20, 21. For SSR analysis, 20 cocoa-specific genomic microsatellite markers were used. The forward primers were marked with fluorescent dyes (M13 tailing), and the PCR products were separated by vertical electrophoresis in the LICOR-4300 equipment[22]. The allelic profile obtained was visualized in the SAGA-GT-SSR™ program (LI-COR Biosciences), where the genotyping was performed, and a genotypic matrix was obtained that listed the size of the alleles of each sample for each marker.

Identification of representative accessions

Duplicate samples were identified by pairwise comparisons among the 243 samples based on their available alleles reported in their allelic profile, using the Microsatellite Toolkit program[23]. From the refined genotypic matrix, samples were identified that presented a single allele for at least 16 microsatellite markers of the 20 used, which had a high level of homozygosity (≥80%). These samples are representative since, having this level of homozygosity, they are considered pure samples, and it is estimated that they retain characteristics of fine National cocoa and aroma.

Genetic diversity analysis

The study of the entire population was performed using the PowerMarker v3.25 program[24]. Several statistical parameters were determined, such as the effective number of alleles, allelic frequencies, genotypic frequencies, observed heterozygosity (Ho), expected heterozygosity (He), and the polymorphic information content (PIC)[25]. Using the same program, a bootstrap analysis of 999 permutations and 100 repetitions was performed. These data were used in the PHYLIP 3.67 program to generate a consensus tree. Bayesian clustering analysis using Structure v.2.3.4 software was applied to determine the population structure, with K values from 1 to 6, with a Burnin period of 50000, a Marko v Chain Monte Carlo (MCMC) value of 50000 with 10 simulations. The Structure Harvester software was also used to establish the maximum value of Δk 26. The pairwise distances were indicated in a Principal Coordinate Analysis (PcoA). With the formed subpopulations, a molecular analysis of variance (ANOVA) was performed, and the F statistics, Fis (intrapopulation inbreeding index), Fit (total inbreeding index), and Fst (fixation index) were established using the software GenAlex v6.5 27.

Results

Identification of duplicates

In the pairwise comparison based on the SSR multilocus profile, only two duplicate accessions were identified within the CCNC collection. These two samples shared 38 alleles. Total duplication represents 0.8% of genotyped samples from the CCNC collection.

Identification of representative samples

Thirteen samples were identified as representative samples within the CCNC collection. These samples are those that presented high levels of homozygosity.

Population structure analysis

The population structure simulation established a Δk value equal to 2; that is, the population was divided into two main clusters or subpopulations (Fig. 1). From the Q index, 173 samples were assigned to one of these two subpopulations with a high level of probability (Q index 0.9-1), 99 samples belonging to the subpopulation identified in green color and 74 samples belonging to the subpopulation identified in red. Within the 99 samples grouped in the green subpopulation, 86 presented a homozygosity level of less than 80%, and the remaining 13 samples presented a high level of homozygosity (≥80%), which is why this group was called GN (National Group), and the subpopulation identified in red, made up of the 74 samples, was called GM, referring to the subpopulation of hybrid samples.

This population organization was identified in the PcoA analysis (Fig. 2). The GN subpopulation is more homogeneous since the samples present a high genetic similarity; the GM group is much more diverse since it offers more significant genetic divergence between the samples.

Genetic diversity analysis

A total of 109 alleles were identified for the entire population, with a mean of 5.5 alleles per locus. The mean genetic diversity (He) was 0.447, the observed heterozygosity (Ho) was 0.331, and the polymorphic information index (PIC) was 0.414. The GN subpopulation presented a mean genetic diversity of 29.5%, and the GM subpopulation of 55.4%. Thirty-six exclusive alleles for the GM subpopulation were also identified. The results of the ANOVA and the F statistics for the two subpopulations determined that there is a variability of 70% (Fis=0.178) within the subpopulations and a variability of 30% (Fst=0.105) between the subpopulations.

Discussion

Molecular markers have proven adequate for characterizing genetic variability in T. cocoa[17,18,28-33]. In the present study, samples from a cocoa collection called National Centenarian cocoa collection (NCCC) were used, which is made up of 260 accessions collected from farms where trees with characteristics of National cocoa were found and whose ages were 75-100 years, located in the northern area of the province of Manabí, and in the province of Los Rios in Ecuador.
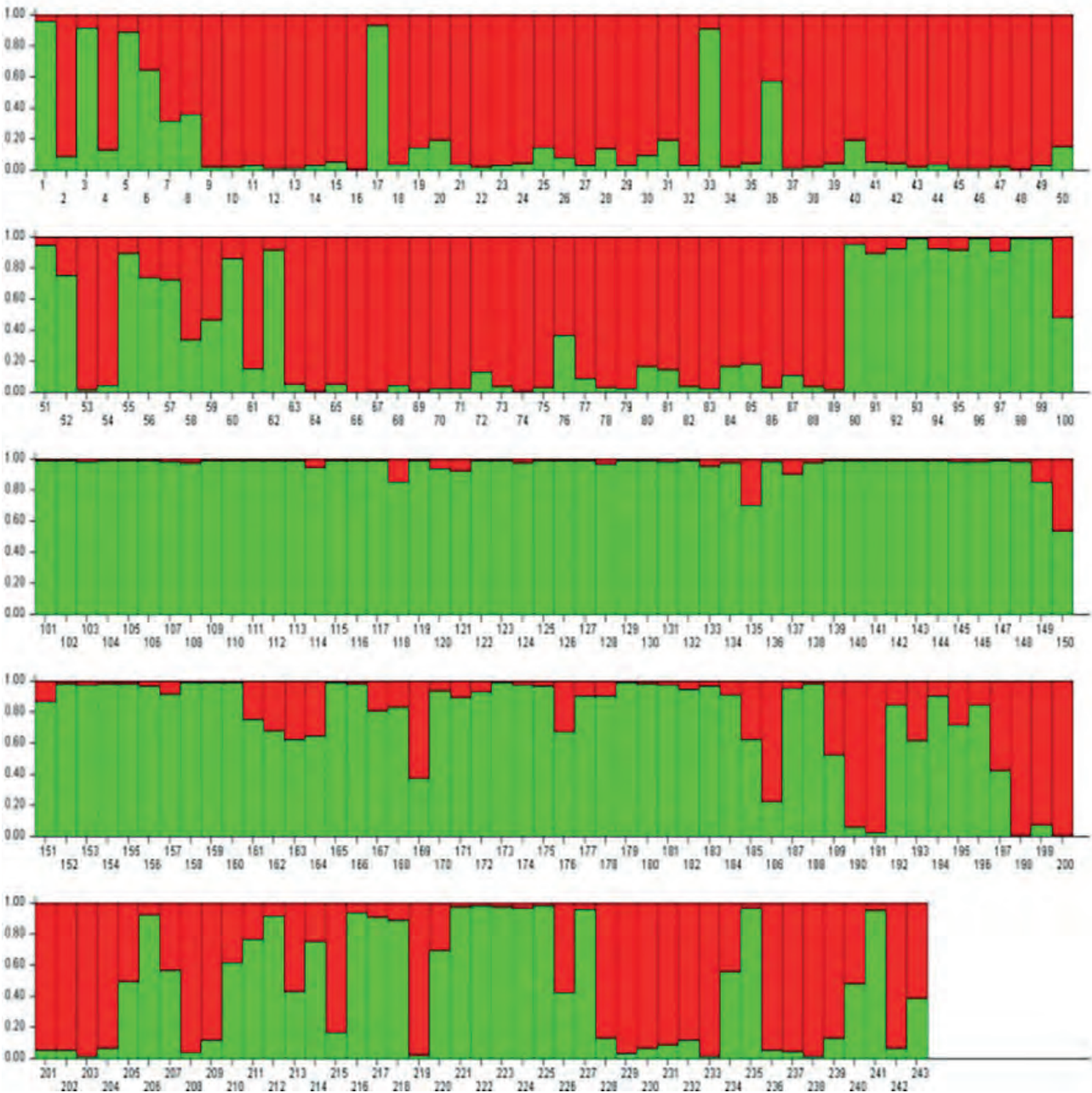
Figure 1. Bayesian population assignment using STRUCTURE (K=2).

In a general context, the CCNC collection presented considerable genetic diversity, taking into account both the level of He and the fact that it was found only one case of duplication among the accessions. This corresponds to 0.8%, much lower than the data reported in other studies, such as 19.6% of duplicates 28, 9.1% 29, and 12.9%[34].

It was shown that CCNC genetic diversity is structured into two groups or subpopulations: the GN and the GM groups. Similar results were reported in previous studies[15] by grouping, and a dendrogram identified two clusters or subpopulations in a population of National cocoa obtained from plantations that were 80 to 100 years old. These two subpopulations showed significant differences based on their average level of heterozygosity; the first subpopulation is characterized by being more homogeneous since it only includes samples of National cocoa and a low level of heterozygosity (5%), and the second presents a high level of heterozygosity (44%) because it is more heterogeneous and includes samples of National cocoa trees from Vene-

zuelan and hybrid models.

Furthermore, results similar to those reported by other researchers were evidenced, showing that Ecuadorian cocoa is divided into two subpopulations[16]: a subpopulation with a low level of heterozygosity (5%), considered to be representative of National cocoa; and a subpopulation with a higher level of heterozygosity (32%), considered to be representative of modern National cocoa, made up of hybrid samples. Previous researchers established that a large part of modern National cocoa cultivation corresponds to the so-called National Trinitarian complex[35], formed from the introduction of Trinitarian-type Venezuelan cocoa at the end of the 19th century and beginning of the 20th century and its subsequent gene flow with the National Centennial cocoa population. It was also established that the high homozygosity of several Ecuadorian cocoa samples may be due to the self-compatibility of the oldest National cocoa from Ecuador[8] and that the compatibility variation of the modern National cocoa is also due to the introgression of

3

4
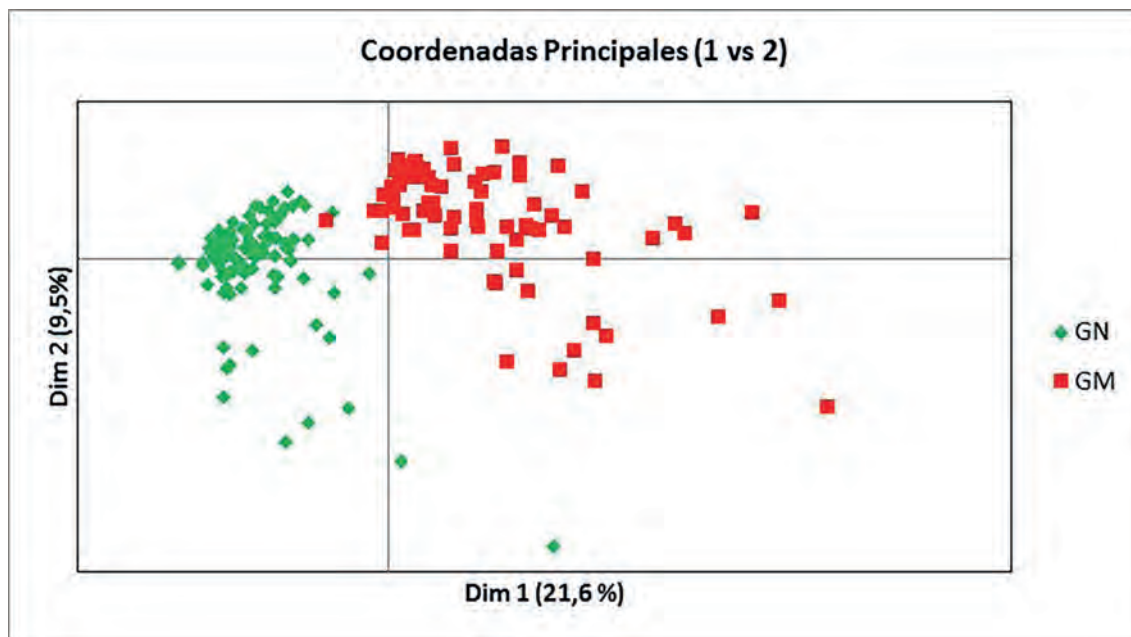
Figure 2. PcoA graph of the 173 accessions assigned to one of the two subpopulations (first coordinate = 18.1% of the total, and the second = 6.1)

the Trinitario cocoa genome. It can be inferred that the GN subpopulation group samples of the purest National type present less gene introgression from other cocoa varieties. On the other hand, the GM subpopulation includes the accessions with the highest level of heterozygosity. The percentage of heterozygosity presented by the GN subpopulation is 29.5%, which is considerably high compared to those published by other researchers[15,16]; this is because only 13 samples belonging to this subpopulation presented a high level of homozygosity. The remaining 86 genotypes did not present the same level of homozygosity but rather a genetic difference with the samples of the GM subpopulation. This genetic differentiation allows these two subpopulations to appear separate from one another in the multivariate PCoA analysis.

The level of genetic diversity of the GM subpopulation was also evidenced due to the presence of the 36 exclusive alleles. It is inferred that the level of heterozygosity of this subpopulation could be the effect of the introgression of genes from various cocoa varieties, not only from Trinitarian cocoa[8]. However, further studies are needed to establish the origin of this genetic diversity. The results obtained in this research are essential and valuable to continue characterization studies in Ecuador cocoa crops since they allow the identification of National cocoa trees with a high level of homozygosity. In addition, the results make it possible to establish genetic improvement programs to recover the characteristics of delicate and aroma cocoa that distinguish Ecuadorian National cocoa as the best worldwide. Improving the quality of this type of cocoa will allow it to be re-activated and commercialized in the international market, giving a new impetus to the country's economy.

Conclusions

We showed the efficiency of the panel of SSR markers used here in the genetic assignment of accessions. The CCNC collection presented a high genetic diversity with little duplication. Genetic diversity was identified in two groups. Firstly, the GN subpopulation includes 99 samples, of which

13 presented homozygosity ≥ 80%; hence they are considered samples of native National cocoa that still conserve their characteristics of fine cocoa and aroma. Likewise, the GM subpopulation includes 74 samples with high diversity, with 36 exclusive alleles, probably due to the introgression of genes from other cocoa varieties.

Author Contributions

Conceptualization, JQ and EM; methodology, EM, JB, CC; software, EM and JB; validation, JB; formal analysis, CC and JB; initial draft preparation, CC and JQ; writing—review and editing, EM and JB; funding acquisition, JQ. All authors have read and agreed to the published version of the manuscript. Please turn to the CRediT taxonomy for the term explanation. Authorship must be limited to those who have contributed substantially to work reported.

Funding

Acknowledgments

Conflicts of Interest

The authors declare no conflict of interest.

Bibliographic references

1. Ballesteros William. Caracterización morfológica de árboles elite de cacao (Theobroma cacao L.) en el municipio de Tumaco, Nariño, Colombia. 2011. Tesis Doctoral. Universidad de Nariño.
2. Argout X, Salse J, Aury J, Guiltinan M, Droc G, Gouzy J, Allegre M, Chaparro C, Legavre T, Maximova S, Abrouk M, Murat F, Fouet O, Poulain J, Ruiz M. Roguet Y, Rodier-Goud M, Barbosa-Neto J. F, Sabot F, Lanaud C. The genome of Theobroma cacao. Nature Genetics. 2011; 43(2), 101–108.

3. López-Hernández, J. A., Ortiz-Mejía, F. N., Parada-Berríos, F. A., Lara-Ascencio, F., & Vásquez-Osegueda, E. A. Caracterización morfoagronómica de cacao criollo (Theobroma cacao L.) y su incidencia en la selección de germoplasma promisorio en áreas de presencia natural en El Salvador. Revista Científica Multidisciplinaria de la Universidad de El Salvador-Revista Minerva, 2019, vol. 2, no 1, p. 31-50.

4. Samaniego, I., Espín, S., Quiroz, J., Rosales, C., Carrillo, W., Mena, P., & García-Viguera, C. Effect of the growing area on the fat content and the fatty acid composition of Ecuadorian cocoa beans. International Journal of Food Sciences and Nutrition. 2021; 72(7), 901-911.

5. Samaniego, I., Espín, S., Quiroz, J., Ortiz, B., Carrillo, W., García-Viguera, C., & Mena, P. Effect of the growing area on the methylxanthines and flavan-3-ols content in cocoa beans from Ecuador. Journal of Food Composition and Analysis, 2020; 88, 103448.

6. Cheesman E. Notes on the nomenclature, classification and possible relationships of cocoa populations. Tropical Agriculture. 1944; 21, 144–159.

7. Motamayor J. C, Lachenaud P, da Silva e Mota J, Loor R, Kuhn D, Brown J, Schnell R. Geographic and genetic population differentiation of the Amazonian chocolate tree (Theobroma cacao L). PLoS ONE. 2008; 3(10).

8. Loor R, Risterucci A, Courtois B, Fouet O, Jeanneau M, Rosenquist E, Amores F, Vasco A, Medina M, Lanaud C. Tracing the native ancestors of the modern Theobroma cacao L. population in Ecuador. Tree Genetics and Genomes. 2009; 5(3), 421–433.

9. Quiroz J, Morillo E, Samaniego I. Estudio de la expresión y diversidad genética para la determinación de la calidad en clones de cacao Nacional centenario del INIAP. 2019. No publicado.

10. Garrido-Cardenas J, Mesa-Valle C, Manzano-Agugliaro F. Trends in plant research using molecular markers. In Planta. 2018; 247(3), 543–557.

11. Lanaud C, Risterucci A, Pieretti I, Falque M, Bouet A, Lagoda P. Isolation and characterization of microsatellites in Theobroma cacao L. Molecular Ecology. 1999; (8), 2141–2152.

12. Risterucci A, Grivet L, N´ Goran J, Pieretti I, Flament M, Lanaud C. A high-density linkage map of Theobroma cacao L. Theoretical and Applied Genetics. 2000; (101), 948–955.

13. Saunders J, Mischke S, Leamy E, Hemeida A. Selection of international molecular standards for DNA fingerprinting of Theobroma cacao. Theoretical and Applied Genetics. 2004; 110(1), 41–47.

14. Pugh T, Fouet O, Risterucci A, Brottier P, Abouladze M, Deletrez C, Courtois B, Clement D, Larmande P, N'Goran J, Lanaud C. A new cacao linkage map based on codominant markers: Development and integration of 201 new microsatellite markers. Theoretical and Applied Genetics. 2004;108(6), 1151–1161.

15. Lerceteau E, Quiroz J, Soria J, Flipo S, Pétiard V, Crouzilat D. Genetic differentiation among Ecuadorian Theobroma cacao L. accessions using DNA and morphological analyses. In Euphytic. 1997; Vol. 95.

16. Crouzillat D, Bellanger L, Rigoreau M, Bucheli P, Pétiard V. Genetic structure, characterisation and selection of nacional cocoa compared to other genetic groups. In F. L. Bekele (Ed.), Proceedings of the international workshop on new technologies and cocoa breeding. INGENIC. 2001.

17. Quiroz J. Caracterización Molecular y Morfológica de Genotipos Superiores con Caracteristicas de Cacao Nacional (Theobroma cacao L.) de Ecuador. Centro Agronómico Tropical de Investigación y Enseñanza. 2002.

18. Loor Rey Gastón. Caracterización Morfológica y Molecular de 37 clones de cacao (Theobroma cacao L.) Nacional de Ecuador 2002. 108 p. INIAP Archivo Historico.

19. Loor-Solorzano R, Fouet O, Lemainque A, Pavek S, Boccara M, Argout X, Amores F, Courtois B, Risterucci A, Lanaud C. Insight into the Wild Origin, Migration and Domestication History of the Fine Flavour Nacional Theobroma cacao L. Variety from Ecuador. PLoS ONE. 2012; 7(11).

20. Doyle J, Doyle J. Rapid DNA isolation procedure for small quantities of fresh leaf tissue. Phytochemical Bulletin. 1987; 19(1), 11–15.

21. Russell A, Samuel R, Rupp B, Barfuss M, Šafran M, Besendorfer V, Chase M, Safran M, Besendorfer V, Chase M. Phylogenetics and cytology of a pantropical orchid genus Polystachya (Polystachyinae, Vandeae, Orchidaceae): Evidence from plastid DNA sequence data. In Source: Taxon. 2010; Vol. 59, Issue 2.

22. Morillo E, Miño G. Marcadores Moleculares en Biotecnología Agrícola: Manual de procedimientos y técnicas en INIAP. Manual No. 91. Instituto Nacional Autónomo de Investigaciones Agropecuarias, Estación Experimental Santa Catalina. 2011; 121 p.

23. Kim K, Sappington T. Microsatellite Data Analysis for Population Genetics. 2013; 271–295.

24. Liu K, Muse S. PowerMaker: An integrated analysis environment for genetic marker analysis. Bioinformatics. 2005; 21(9), 2128–2129.

25. Caruso G, Broglia V, Pocovi M. Diversidad genética. Importancia y aplicaciones en el mejoramiento vegetal. 2015; 4(1), 45–50.

26. Evanno G, Regnaut S, Goudet J. Detecting the number of clusters of individuals using the software STRUCTURE: A simulation study. Molecular Ecology. 2005; 14(8), 2611–2620.

27. Peakall R, Smouse P. GenALEx 6.5: Genetic analysis in Excel. Population genetic software for teaching and research-an update. Bioinformatics. 2012; 28(19), 2537–2539.

28. Zhang D, Mischke S, Johnson E, Phillips-Mora W, Meinhardt L. Molecular characterization of an international cacao collection using microsatellite markers. Tree Genetics and Genomes. 2008; 5(1), 1–10.

29. Irish B, Goenaga R, Zhang D, Schnell R, Brown J, Motamayor J. Microsatellite fingerprinting of the USDA-ARS tropical agriculture research station cacao (Theobroma cacao L.) Germplasm collection. Crop Science. 2010; 50(2), 656–667.

30. Romero C, Bonilla J, Santos E, Peralta E. Identificación Varietal de 41 Plantas Seleccionadas de Cacao (Theobroma cacao L.) Provenientes de Cuatro Cultivares Distintos de la Región Amazónica Ecuatoriana, Mediante el Uso de Marcadores Microsatélites. Revista Tecnológica ESPOL. 2010; 23, 121–128.

31. Lozada-Vargas P. Caracterización molecular de 42 accesiones de la colección de genotipos de cacao Nacional (Theobroma cacao L.) de la EET PICHILINGUE, INIAP, mediante el uso de marcadores microsatélites (SSRs). ESPE. 2014.

32. López-Gómez, P., Avendaño-Arrazate, C. H., Iracheta-Donjuan, L., & del Carmen Ojeda-Zacarías, M.. PCR-SRAP/ITAP para la caracterización molecular del género Theobroma. Revista Fitotecnia Mexicana. 2021; 44(1), 3-3.

33. Ricaño-Rodríguez J, Hipólito-Romero E, Ramos-Prado J, Cocoletzi-Vásquez E. Genotyping-by-Sequencing of native varieties of Theobroma cacao (Malvaceae) from the States of Tabasco and Chiapas, Mexico. Botanical Sciences. 2019; 97 (3): 381-397.

34. Rosero C. Selección estable de marcadores moleculares microsatélites (SSRs) para la identificación de clones comerciales de cacao Nacional (Theobroma cacao L.), recomendados por el INIAP. ESPE. 2013.

35. Amores F, Palacios A, Jiménez J, Zhang D. Entorno ambiental, genética, atributos de calidad y singularización del cacao en el Nor Oriente de la provincia de Esmeraldas. Boletín Técnica. 2009, N°35.

5

ARTICLE / INVESTIGACIÓN

Assessment of the impact of anemia on hematological parameters among hemodialysis patients with chronic kidney disease

Yasamen Raad Humudat

DOI. 10.21931/RB/2023.08.01.32

Environment and Water Directorate, Ministry of Science and Technology, Baghdad, Iraq.
Corresponding author: yasmenraad@yahoo.com

Abstract: Anemia is a common consequence of chronic kidney disease (CKD) that is linked to a decrease in patients' quality of life, a rise in morbidity and mortality, and an acceleration in CKD progression. This study aimed to investigate the hematological profile of chronic renal patients undergoing hemodialysis and to correlate the same with anemia. Fifty (54% males and 46% females) with ages ranging from 18-76 years of patients with CKD and on regular maintenance hemodialysis not less than three months at the Iraqi center for dialysis in Baghdad teaching hospital, and 30 healthy adults were recruited into the study. Hemoglobin concentration, red cell count, white blood cell count, platelet count, ESR, CRP and HCV were assessed for the subjects and controls. Results were analyzed using a t-test independent, and the data were retrieved from the laboratory information system in the hospital. Red blood cell count was reduced in nearly all (96%) of the study patients, while ESR was elevated in (98%) and CRP was elevated in (95%). All patients suffered anemia in HD patients. Most of the patients' WBCs and platelet counts were normal. Anti-HCV antibodies were positive in 15 (30%) of these patients, with non-significant differences in both genders. The study concludes that anemia is a significant comorbidity in hemodialysis patients, with several factors contributing to it, and thorough workup and successful treatment of anemia are essential in this group of patients.

Key words: Anemia, Hematological profile, Hemodialysis, Hepatitis, chronic kidney disease.

Introduction

Chronic kidney disease (CKD) is a type of kidney disease that causes a progressive loss of kidney function which is present for more > 3 months[1]. Anemia is a common characteristic of CKD associated with poor results in hemodialysis (HD) patients[2]. It is related to a decline in patient quality of life, as well as a rise in morbidity and mortality, and accelerates the progression of CKD[3]. In patients with CKD, anemia is when hemoglobin levels are < 13.0 g/dl in adult males and 12.0 g/dl in adult females[4]. Based on the WHO description, approximately 90% of patients with glomerular filtration (GFR) < 25–30 mL/min would have anemia[5].

Kidney disease is the 12th most prevalent cause of death, representing over 1.1 million mortality worldwide per year[6]. According to the Ministry of Health and Environment reports the prevalence of renal failure in Iraq has increased over the last few years. In Iraq, without the Kurdistan region, kidney disease is the fourth among the top ten causes of death at 6.06 %, with 5.9% for males and 5.84% for females[7]. Thus, HD is widely used worldwide, but the effects of HD on patients' blood have not been investigated thoroughly in Iraq.

Patients with CKD undergoing hemodialysis (HD) have higher hepatitis virus compared to individuals with normal renal function[8]. In developing countries, the prevalence of anti-HCV seropositivity among HD maintenance patients varies from 5% to 60%[9]. Therefore, the prevalence of HCV infection in hemodialysis (HD) patients and its associated risk factors is not well established in our country.

This study was carried out on hematological parameters associated with various changes, particularly hemoglobin (Hb) indices, which are most commonly affected, giving rise to anemia. In addition, our country has not well-established the prevalence of HCV infection in hemodialysis (HD) patients and its associated risk factors.

Materials and methods

Patients and Methods

This was a cross-sectional study carried out at the Iraqi center for dialysis in Baghdad teaching hospital, with voluntary participation of 50 (27 males; 23 females) HD patients; it is providing an average of 2 dialysis sessions per week for each patient compared to the control group (30 people non-hepatitis virus without CKD). Inclusion criteria include maintenance HD patients older than 18 years and duration of hemodialysis for more > 3 months.

Ethical Considerations

The local ethics committee of the Ministry of Health and the Environment has approved the research. Written permissions were obtained from the competent authorities based on a description of the study and its objectives, and a signed agreement was reached to treat all individual clinical information as confidential.

2

Blood Collection

Blood samples were collected from the venous port of the hemodialysis catheter before heparin was added to the blood of regular HD patients. The first 5 IU /ml of blood were discarded to prevent the activation of coagulation due to puncture trauma[10], while the second 5 IU/ml were collected and divided into two parts for the following tests:

1. Hematology tests: blood samples were transferred into tubes with EDTA and used for the following parameters by hematology analyze (China): red blood cell count (RBC) and hemoglobin (Hb) concentration, red blood indices – mean corpuscular hemoglobin (MCH), white blood cell count (WBC), lymphocyte, monocyte, neutrocyte, and platelet count.

2. Erythrocyte sedimentation rate (ESR): according to Biosigma, Italy, blood samples.

3. C-reactive protein (CRP): measured after the serum was separated from blood samples using a (CRP kit, Humen/Germany). es were put into tubes with EDTA and utilized for the ESR test.

4. Rapid Hepatitis C virus test: measured by (SD BIO-LINE/ India) after serum separation from blood samples.

Statistical Analysis

Statistical analysis was performed using the Independent sample t-test was utilized to evaluate significant differences. A P-value of 0.05 was considered for the considerable differences between the groups. All statistical analyses were carried out using the Excel 2010 application, and the analyzed data were expressed as a mean ± SD and %.

Results

Hematology Parameters

As indicated in Table-1 for hematology parameters in HD patients, there was no significant difference between males and females in the obtained basic health information, except for the Hb and monocyte at (P<0.05).

The results show that HD patients comprise 27 males and 23 females, aged 58 ±13.9 for males and 50 ±17.7 for females. Similar results, i.e., a higher number of males with higher age values, were reported in HD patients from several studies in Iraq. 13-'14

Concerning RBCs in HD patients, the majority of patients (96%) (3.06±0.67 10^6μL) were lower than in the healthy control group (4.7±0.68 10^6μL). RBCs of patients showed slight differences in 3.2±0.56 10^6μL for males and 2.98 ±0.77 10^6μL for females in both sexes. In general, most of the findings showed that low RBCs are common in patients with hemodialysis[9].

Results appeared all HD patients with Hb levels had anemia (9.05±1.40 g/dL) compared to (13.7±2.7g/dL) in the healthy control group. Hb levels in males (9.2±1.34 g/dL) were slightly higher than in females' dialysis (8.4±1.44 g/dL). At the same time, local standard references are (12 g/dL).

There was a difference compared to the normal value, which might be due to the kidney not making enough of a hormone called erythropoietin that can help the body make red blood cells[8]. In addition, some differences dominated both males and females. Low levels of Hb in females may be due to menstruation every month. For males, the dominant sex hormone is testosterone, and in females, sex hormones are primarily estrogen. Testosterone can increase the rate of metabolism, thereby increasing the rate of Hb formation[15].

Results show that healthy control and hemodialysis patients tend to have average MCH counts of 27.8±4.0 pg and 29.6±2.5 pg, respectively (29.7±2.76 pg males and 29.0±2.2 pg females) relative to the local reference standard (27-33 pg).

In light of the results of this study, it can be concluded that normal MCH in patients during the HD process is due to the administration of several drugs that makes mean capsular hemoglobin normal in HD patients (16). Also, in a previous study done on Chittagong HD patients, Chowdhury et al. showed that MCH was 28.79±3.77 pg[17].

The results of HD patients with WBCs tend to have decreased by 5.3±2.31 10^3μL (4.4±2.25 10^3μL for males and 5±2.35 10^3μL for females) relative to 9.3±2.17 10^3μL for healthy controls. There were 11 (22%) patients with low WBCs, 34 (68%) patients with normal range, and 4 (8%) patients with high WBCs compared to the local standard reference 4-10 10^3μL.

This results in agreement with Kahdina et al., who showed that most patients had normal or even lower WBCs[15].

Furthermore, the majority of patients (68%) with the lymphocyte value (20.6±8.31% for males and 23.7±9.61% for females) were within the normal range, based on local control percentage (20- 40 %). Also, the results show a decrease in monocyte in 44% of HD patients than the local standard reference count (2-8 %). HD patients have a monocyte value of 8.15±3.42 % (8.6±3.66% for males and 7.7 ±3.05% for females), which was higher than 6.03±1.7% in healthy controls. In addition, the results showed that (34 %) of patients had a neutrocyte value (68±21.62 % for males and 68.6±11.17 % for females) above the normal local standard percentage range (40%-60%) in HD people. And there were slight differences in HD patients and the healthy controls group. Overall, HD patients tend to increase the body's defenses, which may be represented by inflammation[15].

In addition, in HD patients, platelet count tends to be reduced in the mean 176.5±66.5 10^3μL, with (166±2710^3μL of males and 187±70.6710^3μL of females) compared with 342±66.9 10^3μL in healthy controls. There were 34% below the local standard reference count (150-4010^3μL). This result is a small percentage relative to another study in which the rate of platelets was estimated at 50 % in HD patients[18].

Furthermore, all HD patients had an ESR of 52±37 mm/hr, which was higher than the usual range according to the local reference standard. The ESR value for HD females was 74±37 mm/hr, which was higher than the 34±27 mm/hr ESR value for males. Statistical analysis showed no significant differences between male and female groups.

In the medical literature, there are just a few reports on the normal range and clinical significance of ESR measurement in HD patients. This is likely because changes in plasma volume caused by dialysis machines have a significant impact on red cell sedimentation[11]. However, ESR levels in hemodialysis blood were enhanced by 98%, whereas Al-somaili et al. found 79.5 % in patients with chronic renal disease[17].

Finally, the number of patients with a CRP concentration below a detection level of ≤6 mg/l was 5%. The maximum positive concentration of CRP (≥48 mg/l) was 30±19 mg/l in male and 38±14 mg/l in female patients. Statistical analysis showed no significant differences between male

and female groups.

The decreased cost and availability of the CRP test are advantages, especially in underdeveloped nations[18]. Although serum CRP concentrations do not alter with changes in kidney function, serum CRP may be linked to serum albumin levels that are impacted by the inflammatory response in the early stages of renal disease[19].

Hepatitis C virus in hemodialysis patients

Table-2 shows the results of the hepatitis C virus in HD patients at Baghdad Educational hospital. In general, there were no observed significant differences between both sexes at (P <0.05).

In this study, 35 (70%) of the dialysis patients who were not infected with hepatitis C were classified as 20 (74%) for males and 15 (65.2%) for females. The number of patients with hepatitis C virus was 15 (30%); the patients comprised 8 (29.6%) males and 7 (30.4%) females.

In the previous study in the same hospital, the anti-HCV was positive for 12 (7.1%); five (4.9%) were male, and seven (10.4%) were female HD patients[9]. Whereas, similar results, i.e., the prevalence of HCV infection were reported in HD patients in Saudi[19]. In addition, these results agree with Sinjari et al., who showed the exact prevalence of HCV in both male and female hemodialysis patients[20]. In general, hemodialysis patients are more vulnerable to such diseases than the general population, which could be returned to blood transfusion is an important factor in the transmission of HCV infection in HD patients, needle sticks, and dialysis workers (if appropriate precautions are not followed)[21].

Correlation of anemia with some hematological parameters in patients with CKD

Results of the current study show significant differences between anemia and some inflammation, namely RBCs, MCH, WBCs, lymphocyte, neutrocyte, and platelets in patients on regular HD therapy. The correlation coefficient was positive in RBCs, WBCs, lymphocytes, monocyte, ESR while HCV infection showed no correlation coefficient for blood samples collected from HD patients at (P<0.05), Table 3.

A previous study by Al-Khayat et al. found that anemia for kidney failure was closely associated with hematological parameters (WBC count and granulocyte)[13]. While Fouad *et al.* found in Egypt research in HD patients with hepatitis C

Parameters	Mean±SD		P value <0.05	Mean±SD		P value <0.05
	Control Group (n=40)	All HD patients (n=50)		Male HD patients (n=27)	Female HD patients (n=23)	
Age years	53±13.9	55±16.3	NS	58±13.9	50±17.7	NS
RBCs $10^6 \mu$L	4.7±0.68	3.06±0.67	Yes	3.2±0.56	3.7±0.59	NS
MCH pg	27.8±4.0	29.6±2.5	Yes	29.7±2.76	29.0±2.2	NS
HB g/dL	13.7±2.7	9.05±1.40	Yes	9.2±1.34	8.4±1.44	NS
WBCs $10^3 \mu$L	9.3±2.17	5.3±2.31	Yes	4.4±2.25	5±2.35	NS
Lymphocyte %	28.3±9.9	21.9±8.84	Yes	20.6±8.31	23.7±9.61	NS
Monocyte %	6.03±1.7	8.15±3.42	Yes	8.6±3.66	7.7±3.05	NS
Neutrocytes %	68±21.62	68.15±17.83	NS	68±21.62	68.6±11.17	NS
Platelets $10^3 \mu$L	342±66.9	176.5±66.5	Yes	166±62.27	187±70.67	NS
ERS mm/hr	33±27	52±37	Yes	34±27	74±37	Yes
CRP mg/l	7±7	34±19	Yes	30±19	38±14	No

NS, non-significant; Yes, significant.

Table 1. Hematology measures of the study patients.

Parameters	All patients (n=50)	Male patients (n=27)	Female patients (n=23)
	Number (%)	Number (%)	Number (%)
Non Hepatitis C virus	35 (70%)	20 (74 %)	15 (65.2%)
Hepatitis C virus	15 (30%)	8 (29.7%)	7 (30.1%)

Table 2. Hepatitis C virus measures for hemodialysis patients.

4

Parameters	Hemodialysis Patients		Control Group	
	Correlation Coefficient-r	Level of Significant	Correlation Coefficient-r	Level of Significant
Hb vs. RBC	0.82	Yes	0.56	Yes
Hb vs. MCH	-0.09	Yes	0.15	Yes
Hb vs. WBC count	0.2	Yes	0.1	Yes
Hb vs. Lymphocyte	0.3	Yes	0.16	Yes
Hb vs. Monocyte	0.21	Yes	0.4	Yes
Hb vs. Neutrocyte	0.06	Yes	0.19	Yes
Hb vs. Platelets	-0.2	Yes	-0.24	Yes
Hb vs. ESR	0.02	Yes	-0.05	Yes
Hb vs. CRP	-0.002	Yes	-0.13	Yes
$P<0.05$				

NS,non-significant; Yes, significant.

Table 3. Correlation of anemia with some hematological parameters in patients with CKD and healthy group.

viral infection appear to have higher hemoglobin[23]. Therefore, further studies with larger sample sizes are recommended to investigate other hematological parameter and their role in renal anemia..

Conclusions

Anemia is a leading cause of morbidity in CKD patients and worsens as the disease progresses. The hemoglobin parameter was positively correlated with in RBCs, WBCs, lymphocytes, monocyte, and ESR. Further analysis is required to understand the underlying nature of the observed relationship.

Acknowledgments

The authors would like to thank the staff of central labs and dialysis centers for their continuous support during the study. The authors report no conflicts of interest in this work.

Conflicts of Interest

There is no conflicts of interest to declare.

Bibliographic references

1. Levin, A and Stevens, P E. Summary of KDIGO 2012 CKD Guideline: behind the scenes, need for guidance, and a framework for moving forward. Kidney International. 2013; 85(1) 49-61.
2. Khadayate, R; Piyush, S; Shilpi , S; Siddhi , K. Study of hematological profile in chronic renal failure patients on hemodialysis in a Tertiary care hospital. International Journal of Health Sciences and Research. 2020; 10(12) 1-7.
3. Cases, A; Egocheaga, M I; Tranche, S; Pallarés, V; Ojeda, R; Górriz, J L; Portolés, J M. Anemia of chronic kidney disease: Protocol of study, management and referral to nephrology. Nefrología (English Edition). 2018; 38(1) 8-12.
4. Kopple, J D. National kidney foundation K/DOQI clinical practice guidelines for nutrition in chronic renal failure. American journal of kidney diseases. 2001; 37(1) S66-S70.
5. Sagheb, M M; Fallahzadeh, M A; Moaref, A; Fallahzadeh, M H; Dormanesh, B. Comparison of hemoglobin levels before and after hemodialysis and their effects on erythropoietin dosing and cost. Nephro-urology monthly. 2016; 8(4) e38495.
6. Neuen, B L; Chadban, S J; Demaio, A R; Johnson, D W; Perkovic, V. Chronic kidney disease and the global NCDs agenda. BMJ Globel Health. 2017, Vol. 2, 2, p. e000380.
7. Iraqi Ministry of Health. Annual statistical report 2017. s.l. : Republic of Iraq, Ministry of Health and Environment, 2018; 322.
8. Khattab, O S. Prevalence and risk factors for Hepatitis C virus infection in hemodialysis patients in an Iraqi renal transplant center. Saudi Journal of Kidney Diseases and Transplantation. 2008; 19(1) 110-115.
9. Etik, D O, Ocal, S and Boyacioglu, A S. Hepatitis C infection in hemodialysis patients: A review. World Journal of Hepatology. 2015; 7 (6) 885-895.
10. Frank RD, Müller U, Lanzmich R, Groeger C, Floege J. Anticoagulant-free Genius® haemodialysis using low molecular weight heparin-coated circuits. Nephrology Dialysis Transplantation. 2005; 21(4) 1013-1018.
11. Humudat, Y R, Al-Naseri, S K and Al-Fatlawy, Y F. Assessment of Inflammation, Comorbidity and Demographic Factors in Patients with Kidney Disease in Baghdad. , . Iraqi Journal of Science. 2019;60 (11) 2418-2425.
12. Alyassin, F F. The patient care and complications of hemodialysis procedure for renal failure patients: A descriptive study at Al Nasiriya city, south of Iraq. Journal of Global Pharma Technology. 2018; 10 (03) 356-365.

13. Al-Khayat , H S, Al-Ameri, A M and Abode, M A. Inflammatory status as a contributor for anemia in patients with chronic kidney disease in Karbala, Iraq. Journal of Contemporary Medical Sciences. 2016; 2(8) 123-125.

14. Kahdina, M, Mardiana, N and Fauziah, D. Levels of hemoglobin, leukocytes, and platelets of chronic kidneydisease patients undergoing hemodialysis in Surabaya. Biomolecular and Health Science Journal. 2018;1(1) 29-33.

15. Mikhail, A; Brown, C; Williams, J A; Mathrani, V; Shrivastava , R; Evans, J; Isaac, H; Bhandari, S. Renal association clinical practice guideline on anaemia of chronic Kidney disease. BMC Nephrology. 2017; 18(1) 1-29.

16. Daugirdas, J T and Bernardo, A A. Hemodialysis effect on platelet count and function and hemodialysis-associated thrombocytopenia. International Society of Nephrology. 2012; 182(2) 147-157.

17. Alsomaili, M I; Yousuf, M; Hejaili, F; Almotairi, W and Al-Sayyari, A A. Erythrocyte sedimentation rate in stable patients on chronic hemodiaysis. Saudi Journal of Kidney Diseases and Transplantation.2015; 26(6) 1149-1153

18. Helal, I, Zerelli, L; Krid, M; ElYounsi, F.; Maiz, HB; Zouari, B; Adelmoula, Jand Kheder, A. Comparison of c-reactive protein and high-sensitivity c-reactive protein levels in patients on hemodialysis. Saudi Journal of Kidney Diseases and Transplantation, 2012; 23(3) 477-483.

19. Heidari, B. C-reactive protein and other markers of inflammation in hemodialysis patients. Caspian Journal of Internal Medicine. 2013; 4(1) 611-616.

20. Alsaran,, K A; Sabry, A A; Alghareeb, A H; Al Sadoon, G. Effect of hepatitis C virus on hemoglobin and hematocrit levels in Saudi hemodialysis patients. Renal Failure. 2009; 31(5) 349-354.

21. Sinjari, H A and Bakr, K A. Prevalence and Risk factors of Hepatitis B and C Virus infections among patients undergoing uemodialysis in Kurdistan. Hepatitis Monthly. 2018; 18, 5.

22. Marinaki, S; Boletis, J N; Sakellariou, S; Delladetsima, I K. Hepatitis C in hemodialysis patients. World Journal of Hepatology. 2015;7(3). 548–558.

23. Fouad, M; Ismail, M I; Mahmoud, A A; Fathy, H; Zidan, A; Mostafa, E. Influence of chronic hepatitis B and C infections on anemia in hemodialysis patients. Enliven: Nephrology Renal Study. 2015; 2(1) 001-006.

ARTICLE / INVESTIGACIÓN

Impact of inflammatory markers, dread diseases and cycle threshold (C$_t$) Values in COVID-19 progression

Thaer A. Abdul Hussein and Hula Y. Fadhil*

Department of Biology, College of Science, University of Baghdad, Al-Jadriya, Baghdad, Iraq.
Corresponding author: hula.younis@sc.uobaghdad.edu.iq

Abstract: The link between the inflammatory marker and SARS-CoV-2 cycle threshold (C$_t$) with disease progression remains undefined, mainly in coronavirus disease-2019 (COVID-19). Therefore, this study aimed to identify several inflammatory markers (Ferritin, LDH, and D-dimer), and C$_t$ values to predict outcomes in hospitalized COVID-19 Iraqi patients. A case study was performed on 426 patients to guess cutoff values of inflammatory markers that were detected by a real-time polymerase chain reaction (RT-PCR) and specific auto-analyzer instrument. Significantly increased levels of inflammatory markers in critical and severe patients compared with mild-moderate ($p < 0.001$). Compared with aging and disease severity, inflammatory markers and C$_t$ values are significantly related to the aging and severity in critical and severe COVID-19 patients ($p < 0.001$). Finding the C$_t$ value was negatively associated with Ferritin, LDH, and D-dimer ($p < 0.001$); moreover, inflammatory markers concentrations and Ct values were significantly higher during the first ten days. The Ct values correlate with some relevant clinical parameters of inflammation. Higher levels of D dimer, S. Ferritin and LDH were associated with older age and the severity of COVID-19. The area under the ROC curve indicates that serum ferritin was the highest and excellent predictor for disease severity.

Key words: Coronavirus disease 2019, Inflammation, D-dimer, Ferritin, Lactate dehydrogenase, Cycle threshold (C$_t$).

Introduction

Coronavirus (CoV) has been linked to outbreaks of severe disease in East Asia and the Middle East in the last two decades. SARS (severe acute respiratory syndrome) and Middle East respiratory syndrome (MERS) first appeared in 2002 and 2012, respectively[1]. In December 2019, a group of patients with unexplained pneumonia appeared in a seafood wholesale market in Wuhan, China, which was identified from a sequence-based analysis of isolates from the patients[2]. The first cases were spread more rapidly, and the epidemic has unevenly affected nearly all continents. The outbreaks of new type pneumonia add to evidence of the SARS-COV-2 (COVID-19) epidemic steadily increasing through person-to-person transmission and involving patients across all age groups and geographic areas[3,4]. One of the nations with the highest number is Iraq for cases of coronavirus disease (COVID-19)[5]. The first confirmed SARS-CoV-2 case was reported on February 24, 2020, from an Iranian student who had traveled from Iran. There has been an upsurge in instances since that time, whether imported or local[6]. COVID-19 has very important clinical manifestations, such as high rates of transmission and mild to critical clinical features, especially with more serious abnormalities found in the elderly and patients with comorbidities; however, young people without obvious underlying diseases may also have life-threatening complications, such as fulminant myocarditis and diffuse intravascular coagulopathy (DIC)[7, 8].

For patients with COVID-19, circulating inflammatory markers representing the immune system and inflammation have been considered a prognostic indicator. Assessing and analyzing several laboratory inflammatory biomarkers of PCR-positive COVID-19 patients, such as plasma D-dimer, serum ferritin, and serum LDH levels, might facilitate early aggressive treatment, thereby reducing mortality and improving hospital resource allocation. In Iraq, biomarkers also show increased D-dimer, Ferritin, LDH and another inflammatory marker in COVID-19 patients[9-11]. Therefore, the current study was conducted to guess the cutoff values of inflammatory markers (Ferritin, LDH, and D-dimer) and clarify their correlation with SARS- COV-2 C$_t$ values and other clinical data variations and severity of the disease.

Materials and methods

Populations studied

The current study involved 426 COVID-19 patients admitted to the Al-Shifa center in Baghdad medical city from December 1, 2020, to the end of April 2021. The practical part of the study was accomplished in Baghdad National Central Public Health Laboratory (CPHL), aged between (18- >70) years old and of both sexes. Those patients included 123 cases with dread disease (83 with hematological disorder and cancer, 36 with renal failure and 4 with autoimmune disease). COVID-19 patients were grouped into mild-moderate (113), severe (231 included 43 hematological disorders and cancer and 15 renal failure) and critical (82 including 38 death cases, 38 hematological disorder and cancer, 21 renal failure and four autoimmune) according to the WHO classification severity. The physical disability of COVID-19 patients with mild-moderate symptoms, no

Publisher's Note: Bionatura stays neutral with regard to jurisdictional claims in published maps and institutional affiliations.

2

evidence of hypoxia or pneumonia; moderate clinical signs of pneumonia (i.e., fever, cough, dyspnea, respiratory distress), but not severe pneumonia with medium oxygen saturation (SpO2) ≥ 90% in room air. For clinically significant signs of severe COVID-19 patients, pneumonia plus one of the following conditions: respiratory rate >30 breaths/minute, extreme breathing difficulty and SpO2 <90% in room air. Meanwhile, the critical condition of COVID-19 patients suffering from other complications such as fatal acute respiratory distress syndrome (ARDS), sepsis or septic shock, acute pulmonary embolism, acute coronary syndrome, acute stroke and delirium[12].

Laboratory tests

Nasopharyngeal (NP) or oropharyngeal (OP) swabs, together with 5 ml of blood samples, were collected from the study groups. Samples were collected from swabs directly put into viral transport media (VTM). A total of 200 μl of each (NP) or (OP) model was used for viral RNA extraction via the ExiprepTMPlus Viral DNA/RNA Kit (Bioneer, Korea). For detection of SARS-CoV-2 infection was performed on swabs samples by specific real-time, reverse transcription polymerase chain reaction (RT-PCR) according to the WHO-approved protocol published by AccuPower® SARS-COV-2 Multiplex Real-Time RT-PCR Kit, and detecting particular sequences in the E, N and RdRp genes. Blood samples were split into two tubes (Sodium Citrate tubes and Gel tubes):

The first part of the blood samples (Sodium Citrate tubes) was centrifuged for 20 minutes at 3500 rpm to obtain plasma which is used for the determination of plasma D-Dimer by using a specific automated protein analyzer (BIO-SENCER STANDARD F200 analyzer) provided by (Suwonsi, Gyeonggi Co., Ltd. Korea 2020). plasma samples for all patients were applied to the instrument then the concentration of D-Dimer was automatically calculated.

The second part of the blood samples (Gel tube) was centrifuged for 10 minutes at 6000 rpm to obtain serum used to determine lactate dehydrogenase (LDH), and Ferritin. Serum concentrations of LDH were evaluated using electro-chemiluminescence immunoassay, Roche Cobas Integra 400 plus (Roche Diagnostics GmbH, Mannheim, Germany). At the same time, the Ferritin was assessed by using a miniVIDAS analyzer for the fluorescent enzymatic detection of β2-microglobulin (β2M) using the technique Enzyme Linked Fluorescent Assay (ELFA) (BioMerieux). Serum samples for all patients were applied to the instrument then the concentration of LDH and Ferritin was automatically calculated.

Statistical analysis

Using the statistical program, data were input, maintained, and evaluated, and variables were presented as mean, standard deviation, frequencies and percentages accordingly. Kolmogorov-Smirnov and Shapiro-Wilk tests were used to determine if continuous variables were standard. The chi-square test was used to assess the association between categorical variables, as Fisher's exact test was used when the chi-square was inapplicable. To compare mean values of a variable/parameter across severity categories, non-parametric Kruskal-Wallis one-way ANOVA test was applied as an alternative test used when the variable did not follow the expected statistical distribution. Receiver operating characteristics curve (ROC) analysis is used to estimate the area under the curve (AUC), 95% confidence interval (CI),

cutoff value, sensitivity and specificity to assess the validity of the significantly different parameters across the disease severity in the prediction of severe or critical disease. The AUC was calculated, and it is an indicator of the validity of a test; an AUC of <0.600 indicates failure of a test as a predictor, 0.600 to 0.700 is a sufficient predictor, 0.700 - 0.800 is good, 0.800 - 0.900 is very good and > 0.900-1.00 indicates excellent predictor test. The optimal cutoff point was identified using the Youden J statistic (also called the Youden Index), which records the effectiveness of a dichotomous diagnostic test. The higher index value indicates the better validity of a test Youden J statistic calculated as an alternative, J = Sensitivity + specificity – 1. The odds ratio (OR) and 95% confidence interval (CI) were determined using logistic regression analysis for two models; I (chronic disease) and II (dread disease). In this analysis, patients were distributed along with and without groups according to mean in without (≤ and > mean, respectively), and the without group was the reference category. Statistical significance was defined as the probability (p) ≤ 0.05. The analytical tool IBM SPSS Statistics 25.0 (Armonk, NY: IBM Corp.) and GraphPad Prism version 8.0.0 were used to perform these analyses.

Results

Baseline characteristics of COVID-19 infection

A total of 426 cases, with male 267(62.7%) and female 159 (37.3%) enrolled in this study. All patients diagnosed with COVID-19 using PCR technique with mild to moderate, severe and critical disease according to the WHO criteria for the classification of disease severity. The distribution of patients according to the severity of diseases it had been found that 113 (26.5 %) patients had mild-moderate disease, 231 (54.2 %) had severe, and 82 (19.3%) had the critical disease and required admission to RCU, including 38 (8.9 % inside the critically ill group) cases were with deterioration for death at admission as shown in Table 1.

The cross-tabulation of patients' age across severity of diseases revealed a statistically significant association between age and severity, younger age patients were more likely to have less severe disease than older ones, (p <0.001). Furthermore, the age of patients with critical disease appeared to be larger than those with severe and those with mild-moderate disease (p <0.001). The association between COVID-19 severity and certain comorbidities (chronic and dread disease) is shown in figure 1. We noticed that the highest prevalence of severe and critical diseases was seen among chronic disease patients (diabetic and hypertension) and dread disease (immunological, cancer, renal and liver disease) patients. Obviously, the prevalence of infection severity is increasing with some comorbidities to reach the highest significant association (p < 0.001).

The distribution of COVID-19 infections by duration from onset of disease to admission. Time from the disease's beginning to access ranged from 1 - 20 days. The first ten days of infection have a significant role (p < 0.001); we noticed that most severe and critical patients were admitted to the hospital in less than ten days from the onset of the disease, as shown in figure 2.

Biomarkers with SARS –COV-2 C_t value

The D-dimer levels, lactate dehydrogenase, and Ferritin showed significant correlations with C_t values of RT-

Age groups/year	Cases Frequency with Severity			Total
	mild-moderate	severe	Critical (dead)	
18-40	68 (60.18%)	92 (39.83%)	12 (1) (15.85%)	173
41-50	17 (15.04%)	59 (25.54%)	14 (8) (26.83%)	98
51-60	17 (15.04%)	52 (22.51%)	7 (16) (28.05%)	92
61->70	11 (9.74%)	28 (12.12%)	11 (13) (29.27%)	63
Total	113(26.5 %)	231(54.2 %)	44 (38) (19.3%)	426
Statistical analysis	Person Chi-Square= 45.94, df=15, $p <0.001$			

Table 1. The age breakdown of the patient population and the severity of the diseases.
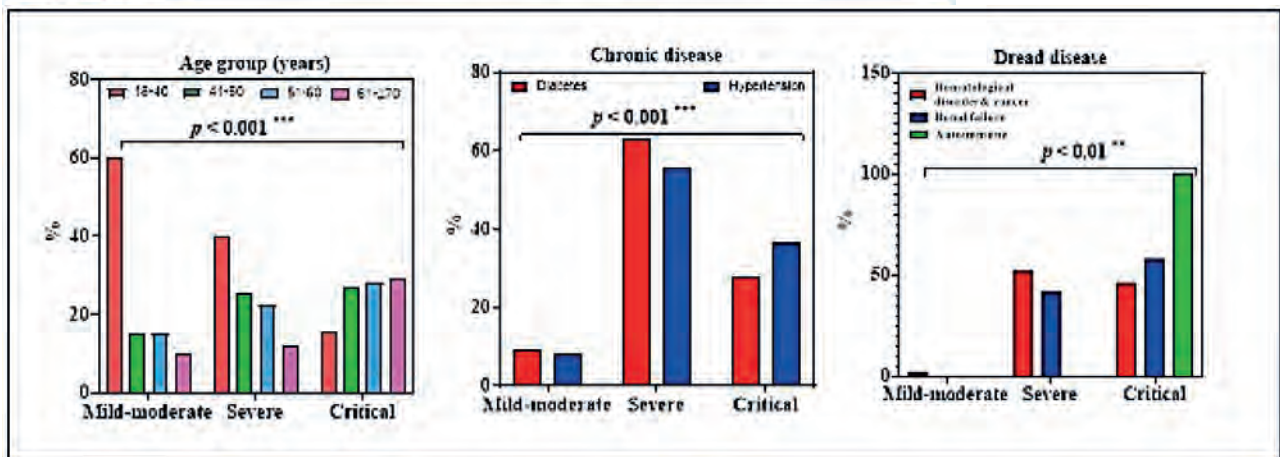
Figure 1. Frequency of severity groups (mild-moderate, severe and critical) of COVID-19 patients stratified to age groups, chronic and dread diseases. Two-tailed Chi-square test was used to compare frequencies.

PCR in COVID-19 patients (p >0.001), as shown in figure 3. Furthermore, the patient's age, severity, sex and duration of infection onset across inflammatory biomarkers (Ferritin, D-dimer and LDH) revealed an increase in the subversive biomarker values that are statistically significant (p <0.001).

Biomarkers with COVID-19 infection

Logistic regression analysis demonstrated that Biomarkers (Ferritin, D. dimer and LDH) were associated with an increased risk of developing COVID-19 whether the study was unadjusted or adjusted for chronic and dread disease. Still, these diseases do not consider an influential factor in increasing levels of biomarkers (Table 2).

To assess the validity of different inflammatory biomarkers in prediction of severity of disease, Receiver Operating Characteristics (ROC) Curve analysis was applied, which is a plot analysis for the true positive rate (sensitivity) against false positive rate (1- specificity), the area under the ROC curve (AUC) was calculated which is an indicator for the validity of a test in prediction of an outcome. As an interpretation, an AUC of less than 0.600 indicates failure of a test as a predictor, 0.600 to 0.700 is a sufficient predictor, 0.700-0.800 is good, 0.800 -0.900 outstanding and > 0.900-1.00 indicates excellent predictor test, according to these cutoff value of AUC, S. Ferritin, was excellent predictors of severe and critical disease with AUC 0.913, LDH and D-dimer were the stronger predictor with AUC of 0.871 and 0.860 respectively, (excellent predictor) (Figure 3).

Model†		OR	95% CI	*p*-value
Ferritin	I	1.2	1.01-1.5	**0.021**
	II	1.02	1.0-1.3	**0.036**
D. dimer	I	1.2	1.03-1.42	**0.025**
	II	1.06	1.001-1.38	**0.042**
LDH	I	1.03	1.0-1.3	**0.041**
	II	1.00	1.01-1.72	**0.022**

†: The reference category is > Mean; OR: Odds ratio; CI: Confidence interval; p: Probability (significant p-value is indicated in bold); I: chronic disease; II: dread disease.

Table 2. Logistic regression analysis of Ferritin, D. dimer and LDH in COVID-19 patients and chronic and dread disease stratified according to the mean of these biomarkers in cases without the desired condition.

4
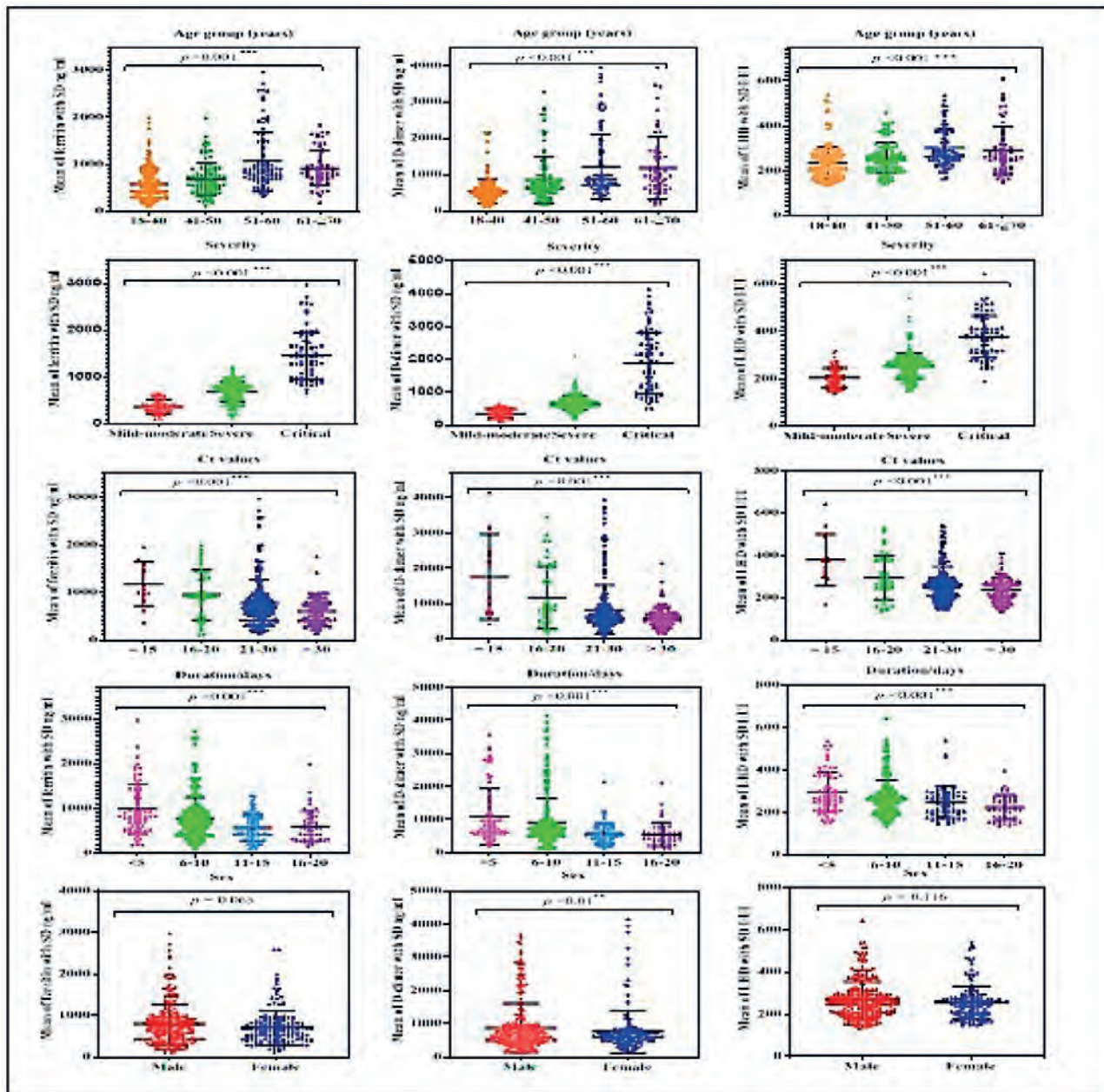
Figure 2. Scatter dot plot (ferritin, D-dimer and L-LDH) graphs of baseline characteristics of COVID–19 patients (age, severity, Ct values, sex, and duration of infection onset). Significant differences were assessed using the One-way ANOVA test (to compare between means).

Discussion

Covid-19 is a significant public health problem; with the number of cases reported daily rising exponentially, no estimate appears adequate for predicting the destruction this disease will cause in death and disability. Covid19 has a more extended incubation period, ranging from 2 to 15 days, and is more contagious than seasonal flu. Following infection, the patient may be asymptomatic or develop flu-like symptoms such as fatigue, myalgia, cough, shortness of breath, and fever[13]. However, some patients may have severe pneumonia or complications such as ARDS, myocarditis, septic shock, venous thromboembolism, and multiorgan failure. Inflammatory biomarker investigation plays an essential role in the management of COVID-19 as it helps not just in diagnosis but also in predicting the disease severity.

The current study aims to identify several inflammatory markers and cycle threshold (Ct) values that predict outcomes in hospitalized COVID-19 Iraqi patients and assess the relationship between the inflammatory markers level and cycle threshold (Ct) values with clinical categories in a diverse group of patients. We analyzed the effect of inflammatory markers and Ct value on COVID-19 disease severity and outcome among 426 COVID-19 patients who were admitted to Al-Shifa center in Baghdad medical city from December 1, 2020, to the end of April 2021. Early detection of inflammatory biomarkers of COVID-19 disease severity and death may assist in focused intervention and patient management. Among the 426 patients studied, 113 had a non-severe disease (26.5 % mild-moderate), the rest, 231 (54.2%), had a severe illness, and 82 (19.2 %) had critical including 38(8.9 %) death cases at admission. The role of gender and age were assessed in covid-19 hospitalized patients; we found that men with COVID-19 were 1.671 times higher than women (62.7 % vs. 37.3%). Elevated incidence of CO-
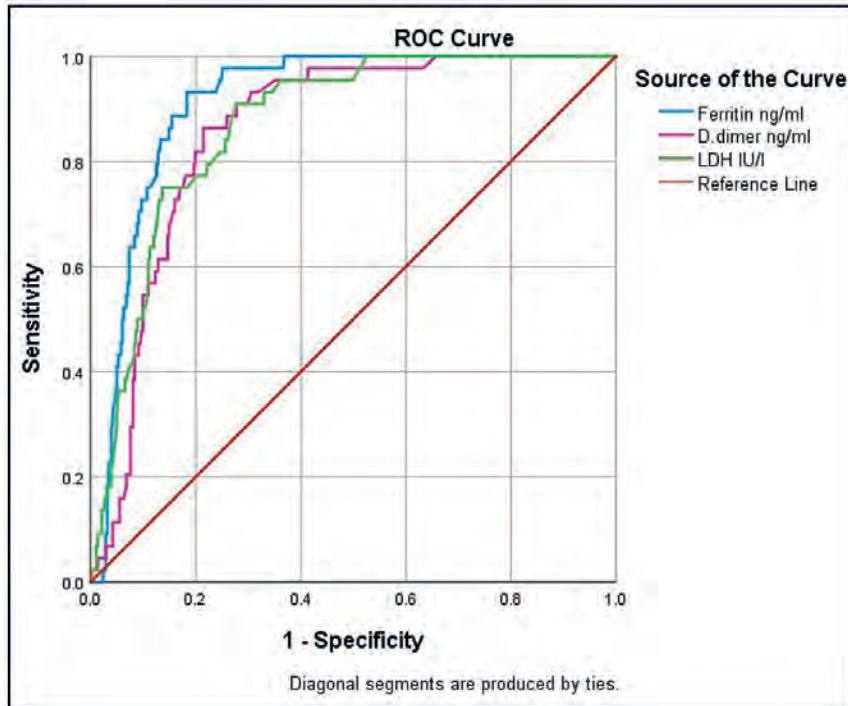
Figure 3. Receiver Operating Characteristics (ROC) curve for the validity of S. Ferritin, D. dimer and S.LDH in the prediction of severity of the disease. Ferritin: area under the curve (AUC) = 0.913; 95% confidence interval (CI) = 0.884 – 0.943; p-value < 0.001; cut–off value > 840.5 ng/ml); sensitivity = 90.9%; specificity = 78.3%. D. dimer: AUC = 0.860; 95% confidence interval (CI) = 0.817 – 0.903; p-value < 0.001; cut–off value > 736 ng/ml); sensitivity = 86.4%; specificity = 76%. S.LDH: AUC = 0.871; 95% confidence interval (CI) = 0.828 – 0.914; p-value < 0.001; cut–off value > 273.5 I/UI); sensitivity = 86.4%; specificity = 76%.

VID-19 in males as they are subjected more than females to certain risk factors, for example, higher expression of angiotensin-converting enzyme-2 (ACE 2; receptors for coronavirus) in males than females, sex-based immunological differences driven by sex hormone (sex-specific steroids) and the activity of X-linked genes, both of which modulate the innate and adaptive immune response to virus infection[14]. our results, in line with previous investigation studies, reported that men with COVID-19 infection were higher than women and reached (56%) in Italy, (52%) in Germany and Sweden, (57%) in Iran, and (51%) in Austria[15]. Differences in susceptibility and inflammation between males and females may be due to chromosomes; for example, the female X chromosome encodes several immune regulatory genes that result in reduced viral load levels. Toll-like receptor 7 (TLR7), higher in females than males, could enhance immune responses and boost the resistance to COVID-19[16].

Furthermore, gender behavior (lifestyle), i.e., higher levels of smoking and drinking among males, lead to less robust immune responses and more susceptibility to various viral infections than females[17].

On the contrary, another study by the Korean Society of Infectious Diseases in 2020 suggested that COVID-19 risk may be greater in females. These variations in COVID-19 gender incidence between studies likely have a complex explanation, including several biological, social, and economic variables[18]. Accordingly, we observed a statistically significant association between age and severity (p <0.001); the chance of acquiring severity was shown to be greater in those 50 years and older. Age is implicated to be related to the seriousness of COVID-19 and outcome in additional research conducted in China, the United States and Europe[7,19]. Similar results are also reported from studies conducted in our country[20-22]. Another study by Terpos et al. described older age and male gender as risk factors for severe disease and death in patients with COVID-19[23]. The reasons for this could be the increased possibility of a reduced immune defense mechanism and co-morbid illnesses, which make older people more susceptible to various diseases with severe progression and the worst outcome.

Comorbidities such as diabetes, hypertension, and dread disease which are unequally distributed among men and women of different ages, may also impact the progression of the disease[24]. The most common comorbidities identified in COVID-19 patients at diagnosis are hypertension, Diabetes Mellitus and dread conditions (immunological, cancer, heart, renal and liver disease). In our study, we noticed that significant predictors of disease severity were seen among comorbidity patients compared to patients with no such comorbidities (p <0.001). Cheema et al. notice that SARS-COV-2 may contribute to an elevated risk of microvascular and macrovascular problems resulting from low-grade vascular inflammation (Vasculitis) in patients that suffered from diabetes mellitus[25]. Similar findings were observed in a study by Jin et al., who noticed that in COVID-19 patients, Increased severity and death were correlated with older age and a significant number of comorbidities[26-28].

The inflammatory markers that are found to be significant determinants of disease outcome were Ferritin, lactate dehydrogenase (LDH) and D-dimer level. An increased level of this inflammatory biomarker indicates the body's stress as an indicator of systemic inflammation. When there is more stress, such as in severe and critical patient states, the level rises to an even higher level. As a result, this inflammatory biomarker indirectly indicates the body's stress level due to the disease's severity. Our study found COVID-19 patients with severe, critical and patients who died (inside the critically ill group) had higher levels of serum ferritin compared with mild to moderate disease; the differences were statistically significant (p <0.001). Ferritin is one of the inflammatory markers that must be present to identify hyperinflammatory syndrome (HI-S) in COVID-19 infection[29]. Systematic review and meta-analysis study done by Szarpak et al. and his colleague for 12 studies show a close association between ferritin levels and the state of the COVID-19 patient. Markedly increased ferritin levels were associated with a more severe patient condition, more intensive care unit exposure, and higher mortality[30]. Also, similar findings from studies conducted showed that COVID-19 association hyperinflammatory criteria (ferritin levels

6

>1500 µg/L) upon admission was linked to a higher fatality rate[29]. Indeed, serum ferritin is affected by hepcidin upregulation, which is stimulated by proinflammatory cytokines, particularly IL-6[31]. Ferritin is highly relevant because it is a mediator of immune dysregulation; it has been proposed that under extreme hyperferritinemia, Ferritin generates direct immunosuppressive and proinflammatory impacts, contributing to the cytokine storm shown in COVID patients 19[32]. Because hyperferritinemia causes regular cell death (RCD), iron oxides interact with serum coagulation cascade proteins. Coagulation disorders are relatively frequently encountered among COVID-19 patients, especially those with the severe disease[33]. The virus may also assault and destroy the hemoglobin, releasing iron from porphyrins and discharging it into the circulatory system, leading to iron overload[34]. furthermore, the activity of the SARS-CoV helicases for viral replication generally requires ATP hydrolysis, which involves the presence of iron. Iron overload complicates the prognosis of HBV and HCV viral infections, and iron supplementation increases mortality in HIV patients. SARS-CoV-2 most likely requires iron for viral RNA replication and function[31]. It's important to note that SARS-CoV-2 is thought to infect macrophages. As a result, elevated iron accumulation in macrophages is expected to boost viral replication. Viruses can also modify other iron-related proteins to speed up their reproduction and spread. Homeostatic iron regulator protein (HFE), a competition of TfR1 for binding to transferrin, is destroyed following binding by US2 protein in the context of human cytomegalovirus (HCMV) infection, resulting in cellular iron overload. The combination between Nef protein and HFE causes cellular iron overload in HIV-1-infected macrophages. TfR1 is also used as a receptor by various viruses during their invasion[35]. When there is a systemic iron overload, there is a higher in cellular oxidative stress, mitochondria dysfunction, cytokine release, a significant decline in cellular oxygen consumption, lipid peroxidation, and a change from aerobic (pyruvate) to anaerobic (lactate) metabolism via lactic dehydrogenase (LDH). This enzyme is stimulated in COVID-19[36]. D-dimer and LDH levels in our findings showed a significant rise across disease severity, with the highest level in critical and severe patients compared with mid-moderate ($p <0.001$). Elevated D-dimer parameters in severe and critical COVID-19 patients have been linked to coagulation activation, dysregulated thrombin generation, impaired natural anticoagulants, and fibrinolysis[37]. Also, several critically ill patients have been reported to develop coagulopathy, antiphospholipid antibodies, and increased arterial and venous thrombotic events such as cerebral infarction[38]. More than 1,800 COVID-19 individuals were studied by Paliogiannis *et al.* line with our results, who found that plasma D-dimer concentrations in those with severe forms of the disease were significantly higher than those in patients with milder forms[39]. LDH is present in lung tissue and is one of the parts mainly affected by COVID-19, so elevated levels of LDH may result from lung tissue degradation. Our findings concur with previous research, which showed high levels of LDH were common in COVID-19 patients in the ICU and indicated a poor outcome[38].

Regarding SARS –CON-2 RNA cycle threshold values (C_T values), we found the lower C_T value was significantly correlated with disease severity and higher inflammatory marker. Among hospitalized patients, those with C_t values <25 had a higher level of Ferritin LDH, D-dimer and higher risk disease severity and mortality rate than patients with C_t values >30. Worsening inflammation demonstrates that a lower C_t value (higher viral RNA concentration) is associated with excessive inflammation, which is highly likely to be a key factor contributing to the induction of cytokine storms and disease progression. This may indicate that the nasopharyngeal or oropharyngeal SARS-CoV-2 lower C_t value directly impacts organ function. Our results are consistent with earlier research that reported the correlation between C_t value and markers of inflammation[32, 40]. In a study conducted by Zheng *et al.*, similar outcomes were seen. Chen *et al.* in their studies reported that low C_t value in samples from the upper respiratory tract in patients with the highly aggressive disease compared to those with mild illness and C_t value associated with an elevated risk of mortality; also, these studies reported the higher lactate dehydrogenase (LDH) is imported marker correlated with lower C_t values[40-42]. Liu *et al.* noticed that Ct values of severe patients with COVID-19 were statically lower compared to mild patients at admission, and the mean viral load of severe patients was 60 times that of mild patients 35. Regarding the duration (time) course of the variation in inflammatory biomarkers, in our results, the first days of infection have a significant role ($p < 0.001$) recorded in severity cases during the first 10 days; we noticed that most of the severe and critical patients were admitted to the hospital in less than ten days from the onset of disease (figure 2). We observed a gradual increase in Ferritin, D-dimer and LDH concentration during the first 10 days of the disease. This result is comparable with previous studies that reported a mean time from symptom onset to hospitalization of 2.62 days in Singapore, 4.41 days in Hong Kong and 5.14 days in the UK[43]. Other studies report means values of time to hospitalization ranging from 5 to 9.7 days[44,45].

Additionally, in the current study, there is no significant differences in serum ferritin and serum LDH ($p = 0.064$) and $p = 0.116$), respectively, between male and female, also D. dimer levels in men were significantly higher than in women (figure 2). Our results disagree with previous studies; for example, a study in Italy reported that serum ferritin and LDH in males are higher than in females[46]. This may be because COVID-19 appears to be determined by the combination of numerous genetic and demographic heterogeneity of the subjects and sex-depending factors. The X chromosome contains approximately 1,200 genes; these genes' differential expression may be partly responsible for the differences in coagulopathy and inflammatory response between males and females[47]. Serum ferritin, LDH, and D-dimer levels were positively correlated with the severity of COVID-19 in both sexes. According to our findings, the area under the ROC curve of serum Ferritin was the highest, with high sensitivity and specificity with AUC of 0.913, followed by the AUC of serum LDH and plasma D. dimer (AUC of 0.871 and 0.860, respectively). The ROC curve analysis confirmed that serum ferritin has excellent prognostic accuracy in males and females with severe clinical conditions (AUC 0.913).

Conclusions

COVID-19 is a widespread systemic infection that substantially impacts the body's immune system. Increased inflammatory biomarkers are a typical side effect of disease with COVID-19. SARS-COV-2 RNA CT value correlates with inflammation marker; it is also essential to consider

viral dynamics; as a result, a more exact assessment of transmissibility would include combining the CT value with the time of evolution (or time since contact in asymptomatic people) clinical course, disease severity, and immunosuppression. Ferritin was the best predictor of mortality, followed by LDH and D. dimer. These parameters should be carefully analyzed at the outset of the study to assist doctors in evaluating primitive risks, and moreover, nearby monitoring can probably reduce mortality. As a result, it is critical to continue conducting virological and immunological studies on this new coronavirus to fully understand the molecular process of viral replication and identify potential markers of disease progression and targets of therapeutic drugs that will allow COVID19 control.

Author Contributions

Thaer A. Abdul Hussein: Designing the experiment, collecting samples with clinical data, analyzing samples, and writing the manuscript. Hula Y. Fadhil: Designing the experiment, supervision, statistical analysis, writing-reviewing, and revision of the manuscript.

Funding

Institutional Review Board Statement

The Ethics Committee of the Iraqi Ministry of Health and Environment and Department of Biology (College of Science, University of Baghdad) (Ref: CSEC/1120/0050) approved the study protocol and written consent was obtained from all participants for collection of blood along with nasopharyngeal swabs.

Acknowledgments

Conflicts of Interest

The authors declare that there were no conflicts of interest.

Bibliographic references

1. Cui J, Li F, Shi Z L. Origin and evolution of pathogenic coronaviruses. Nature reviews. Microbiology. 2019; 17(3): 181–192.
2. Chen X, Kang Y, Luo J, Pang K, Xu X, Wu J, et al. Next-Generation Sequencing Reveals the Progression of COVID-19. Frontiers in cellular and infection microbiology. 2021; 11: 632490.
3. Dallavilla T, Bertelli M, Morresi A, Bushati V, Stuppia L, Beccari T, et al. Bioinformatic analysis indicates that SARS-CoV-2 is unrelated to known artificial coronaviruses. Eur Rev Med Pharmacol Sci. 2020 Apr;24(8):4558-4564.
4. Zhou F, Yu T, Du R. Clinical course and risk factors for mortality of adult inpatients with COVID-19 in Wuhan, China: A retrospective cohort study. Lancet. 2020; 395: 1054–1062.
5. Mahmood ZS, Fadhil HY, Ad'hiah AH. Estimation of Hematological Parameters of Disease Severity in Iraqi Patients with COVID-19. Iraqi Journal of Science. 2021; 62(10): 3487-3496.
6. Dawood AA, Dawood ZA. How will the second wave of the dreadful COVID-19 be with the increasing number of the infected cases and mortality in Iraq? Vacunas. 2021; 22(2): 114–118.
7. Li C, Chen Q, Wang J, Lin H, Lin Y, Peng F, et al. Clinical characteristics of chronic liver disease with coronavirus disease 2019 (COVID-19): a cohort study in Wuhan, China. Aging. 2020; 12(16): 15938–15945.
8. Lippi G, Plebani M. Laboratory abnormalities in patients with COVID-2019 infection. Clin Chem Lab Med. 2020 June 25;58(7):1131-1134.
9. Shnawa IM, Alfatlawi RH, Nemah AH, Abed AS. Determination role of some biomarkers tests for severe SARS-COV-2 infections in babylon province / IRAQ. Materials today. Proceedings, 10.1016/j.matpr.2021.08.225. Advance online publication.
10. Abdullah Y, Al-Badri A, Khallaf SA, Alsaedi RZJ. Serum levels of interleukin – 6, Ferritin, c-reactive protein, lactate dehydrogenase, D-dimer and count of lymphocytes and neutrophils in COVID-19 patients. Its correlation to the disease severity. Annals of the Romanian Society for Cell Biology. 2021; 25: 2220-2228.
11. Ahmed TH, Al-Mousawi NH. Post-hospitalization, levels of D-dimer, C-reactive protein, Ferritin, and lactate dehydrogenase in recovered COVID-19 Iraqi patients. Systematic Reviews in Pharmacy. 2020; 12: 92-99.
12. Beeching F, Fowler A. Beeching NJ, Fletcher TE, Fowler R. BMJ best practice—coronavirus disease 2019 (COVID-19).
13. Singhal T. A Review of Coronavirus Disease-2019 (COVID-19). Indian journal of pediatrics. 2020; 87(4): 281–286.
14. Bwire GM. Coronavirus: Why Men are More Vulnerable to Covid-19 Than Women?. SN comprehensive clinical medicine. 2020; 2(7): 874–876.
15. Dahan S, Segal G, Katz I, Hellou T, Tietel M, Bryk G, et al. Ferritin as a Marker of Severity in COVID-19 Patients: A Fatal Correlation. Isr Med Assoc J. 2020 Aug;22(8):494-500.
16. Conti P, Younes A. Coronavirus COV-19/SARS-CoV-2 affects women less than men: clinical response to viral infection. J Biol Regul Homeost Agents. 2020; 10: 23-33.
17. Gao YD, Ding M, Dong X, Zhang JJ, Kursat Azkur A, Azkur D, et al. Risk factors for severe and critically ill COVID-19 patients: A review. Allergy. 2021 Feb;76(2):428-455.
18. Korean Society of Infectious Diseases, Korean Society of Pediatric Infectious Diseases, et al. Report on the epidemiological features of coronavirus disease 2019 (COVID-19) outbreak in the Republic of Korea from January 19 to March 2, J Korean Med Sci. 2020.
19. Du RH, Liang LR, Yang CQ, Wang W, Cao TZ., Li M, et al. Predictors of mortality for patients with COVID-19 pneumonia caused by SARS-CoV-2: a prospective cohort study. The European respiratory journal. 2020; 55(5): 2000524.
20. Aziz P, Hadi J, Mohammed A, Aziz Sh, Rahman H, Ahmed H, et al. The Strategy for Controlling COVID-19 in Kurdistan Regional Government (KRG)/Iraq: Identification, Epidemiology, Transmission, Treatment, and Recovery. International Journal of Surgery Open. 2020; 25:6-13.
21. Dawood H, Hwayyiz A, Ibrahim I, Abdul Rahman I. The clinical features of COVID - 19 in a group of Iraqi patients: A record review. 2021.
22. Mahmood ZS, Fadhil HY, Abdul Hussein TA, Ad'hiah AH. Severity of coronavirus disease 19: Profile of inflammatory markers and ACE (rs4646994) and ACE2 (rs2285666) gene polymorphisms in Iraqi patients. Meta Gene. 2022; (31): 1-6.
23. Terpos E, Ntanasis-Stathopoulos I, Elalamy I, Kastritis E, Sergentanis TN, Politou M., et al. Hematological findings and complications of COVID-19. American journal of hematology. 2020; 95(7): 834–847.
24. Tibubos AN, Otten D, Ernst M, Beutel ME. A Systematic Review on Sex- and Gender-Sensitive Research in Public Mental Health During the First Wave of the COVID-19 Crisis. Frontiers in psychiatry. 2021; 12: 712-42.
25. Cheema AK, Kaur P, Fadel A, Younes N, Zirie M, Rizk NM. Integrated datasets of proteomic and metabolomic biomarkers to predict its impacts on comorbidities of type 2 diabetes mellitus. Diabetes, Metabolic Syndrome and Obesity: Targets and Therapy. 2020; 13: 2409–2431.

7

8

26. Jin JM, Bai P, He W, Wu F, Liu XF, Han DM, et al. Gender Differences in Patients With COVID-19: Focus on Severity and Mortality. Frontiers in public health. 2020; 8: 152.

27. Huang C, Wang Y, Li X, Ren L, Zhao J, Hu Y, et al. Clinical features of patients infected with 2019 novel coronavirus in Wuhan, China. Lancet (London, England). 2020; 395(10223): 497–506.

28. Sanyaolu A, Okorie C, Marinkovic A. Comorbidity and its Impact on Patients with COVID-19 [published online ahead of print, 2020 June 25]. SN Compr Clin Med.

29. Manson JJ, Crooks C, Naja M, Ledlie A, Goulden B, Liddle T, et al. COVID-19-associated hyperinflammation and escalation of patient care: a retrospective longitudinal cohort study. The Lancet. Rheumatology. 2020; 2(10): e594–e602.

30. Szarpak L, Zaczynski A, Kosior D, Bialka S, Ladny JR, Gilis-Malinowska N, et al. Evidence of diagnostic value of Ferritin in patients with COVID-19. Cardiology journal. 2020; 27(6): 886–887.

31. Perricone C, Bartoloni E, Bursi R, Cafaro G, Guidelli GM, Shoenfeld Y, et al. COVID-19 as part of the hyperferritinemic syndromes: the role of iron depletion therapy. Immunologic research. 2020; 68(4): 213–224.

32. Ramirez-Hinojosa JP, Rodriguez-Sanchez Y, Romero-Gonzalez AK, Chavez-Gutierrez M, Gonzalez-Arenas NR, Ibarra-Arce A, et al. Association between cycle threshold (Ct) values and clinical and laboratory data in inpatients with COVID-19 and asymptomatic health workers. Journal of medical virology. 2021; 93(10): 5969–5976.

33. Ma TL, Zhou Y, Wang C, Wang L, Chen JX, Yang HH, et al. Targeting Ferroptosis for Lung Diseases: Exploring Novel Strategies in Ferroptosis-Associated Mechanisms. Oxidative medicine and cellular longevity. 2021; 1098970.

34. Channappanavar R, Fett C, Mack M, Ten Eyck PP, Meyerholz DK, Perlman S. Sex-Based Differences in Susceptibility to Severe Acute Respiratory Syndrome Coronavirus Infection. Journal of immunology. 2017; 198(10): 4046–4053.

35. Liu W, Zhang S, Nekhai S, Liu S. Depriving Iron Supply to the Virus Represents a Promising Adjuvant Therapeutic Against Viral Survival. Current clinical microbiology reports. 2020; 7(2): 13–19.

36. Zheng S, Fan J, Yu F, Feng B, Lou B, Zou Q, et al. Viral load dynamics and disease severity in patients infected with SARS-CoV-2 in Zhejiang province, China, January-March 2020: retrospective cohort study. BMJ.

37. Zhang Y, Xiao M, Zhang S. Coagulopathy and antiphospholipid antibodies in patients with Covid-19. N Engl J Med. 2020; 16: 64-72.

38. Lippi G, Simundic AM, Plebani M. Potential preanalytical and analytical vulnerabilities in the laboratory diagnosis of coronavirus disease 2019 (COVID-19). Clin Chem Lab Med. 2020 June 25; 58(7):1070-1076.

39. Paliogiannis P, Mangoni AA, Dettori P, Nasrallah GK, Pintus G, Zinellu A. D-Dimer Concentrations and COVID-19 Severity: A Systematic Review and Meta-Analysis. Frontiers in public health. 2020; 8: 432.

40. Rabaan AA, Tirupathi R, Sule AA, Aldali J, Mutair AA, Alhumaid S, et al. Viral Dynamics and Real-Time RT-PCR Ct Values Correlation with Disease Severity in COVID-19. Diagnostics. 2021; 11(6): 1091.

41. Chen J, Qi T, Liu L, Ling Y, Qian Z, Li T, et al. Clinical progression of patients with COVID-19 in Shanghai, China. The Journal of infection. 2020; 80(5): e1–e6.

42. Azzi L, Carcano G, Gianfagna F, Grossi P, Gasperina DD, Genoni A, et al. Saliva is a reliable tool to detect SARS-CoV-2. The Journal of infection. 2020; 81(1): e45–e50.

43. Pellis L, Scarabel F, Stage HB, Overton CE, Chappell L, Fearon E, et al. Challenges in control of COVID-19: short doubling time and long delay to effect of interventions. Biological sciences. 2021; 376(1829): 20200264.

44. Linton NM, Kobayashi T, Yang Y, Hayashi K, Akhmetzhanov AR, Jung S, et al. Incubation period and other epidemiological characteristics of 2019 novel Coronavirus infections with right truncation: A statistical analysis of publicly available case data. J. Clin. Med. 2020 Feb 17;9(2):538.

45. Kraemer MUG, Yang C, Gutierrez B, Wu C, Klein B, Pigott DM, et al. The effect of human mobility and control measures on the COVID-19 epidemic in china. Science. 2020; 368: 493–497.

46. Gandini O, Criniti A, Gagliardi MC, Ballesio L, Giglio S, Balena A, et al. Sex-disaggregated data confirm serum ferritin as an independent predictor of disease severity both in male and female COVID-19 patients. The Journal of infection. 2021; 82(3): 414–451.

47. Marik PE, DePerrior SE, Ahmad Q, Dodani S. Gender-based disparities in COVID-19 patient outcomes. Journal of investigative medicine. 2021; Mar 12:2020-001641.

ARTICLE / INVESTIGACIÓN

Inhibitory effect of Titanium dioxide (TiO$_2$) nanoparticles and their synergistic activity with antibiotics in some types of bacteria

Ashwaq Hazem Najem, Iman Mahmood Khudhur and Ghaydaa M. A. Ali*

Department of Biology, College of Science, Mosul University, Mosul, Iraq.
Corresponding author: ashsbio102@ uomosul.edu.irq

DOI. 10.21931/RB/2023.08.01.34

Abstract: Titanium dioxide nanoparticles (TiO$_2$ NPs) were studied as antibacterial agents at different concentrations against clinical and environmental bacterial isolates without UV or photocatalytic activation. Five TiO$_2$ NPs concentrations (20µg/ml,50µg/ml, 100µg/ml,500µg/ml and 1000µg/ml) were studied against 15 bacterial species:10 clinical isolates and 5 environmental isolates) compared with antibiotics Amikacin(AK)and Levloxacin(LEV).Only500µg/ml concentration of TiO$_2$ NPs was active against 7 bacterial isolates (3 clinical and 4 environmental), and 1000µg/ml concentration of TiO$_2$ NPs was effective against 9 isolates (6 clinical and 3 environmental). These concentrations were mixed with the antibiotics Levloxacin LEV and Amikacin AK to investigate the possibility of synergistic activity against studied bacteria. Bacterial isolate's response or sensitivity to the antibiotic and TiO$_2$ NPs mixture was varied; AK plus 500µg/ml TiO$_2$ NPs concentration showed increased inhibitory activity against 7 isolates (3 clinical, 4 environmental) and 1000µg/ml TiO$_2$ NPs mixed with AK showed increased inhibition activity against one environmental bacterial isolates, where Ak mixed with 500 and Ak plus 1000 µg/ml showed the same effect as the antibiotic alone or less.LEV antibiotic shows no difference in the effect on all 9 bacteria (7 clinical and 2 environmental), while LEV mixed with 500 µg/ml have increased inhibition zones on 4 bacteria (2 clinical, 2 environmental) , and LEV mixed with 1000µg/ml have higher effect than the antibiotic alone on three isolates (2 clinical,1 environmental).

Key words: Antibiotic, titanium nanoparticles dioxide, antibacterial.

Introduction

The mechanical properties of titanium-based implants have improved significantly in recent years thanks to using TiO$_2$ NPs in medical devices. Overcome the bio inertness of the raw metals, corrosion resistance and the rate at which metal ions are released (to prevent aseptic loosening of the implant)[1].

In the early stages of the "race for the surface," the implant may get infested with bacteria. Aseptic loosening of implants and biomaterial-centered infections (BCI) play a significant role in prosthetic implant failure and infection of the implant itself, making them a severe medical problem[2].

In addition to its photocatalytic properties, TiO$_2$ NPs can be used for water separation, energy production, air and water purification and surface sterilizing, organic compound synthesis, and pollution reduction(TiO$_2$ can be used as an adsorbent for environmental pollutants, where it deals with air pollutants such as dust and dust and adsorbs them on the surfaces on which they fall. As for water pollutants, they can be used as a precipitant for contaminants that contain water.)[3] Nanoparticles (NPs) are also employed to make medications, detect infections, proteins, and tumors, and separate and purify biological components and cells[4,5]. Titanium dioxide (TiO$_2$) inorganic nanoparticles have been used for decades due to their non-toxicity, ease of production, and low cost. Furthermore, it may have a universal bactericidal mechanism[6]. The morphological characteristics of titanium dioxide NPs significantly impact their applications[7].

Rutile, anatase, and brookite are all types of TiO$_2$ NPs that can be found in nature. Of the three types of photocatalysts mentioned, anatase NPs are the most commonly used[8,9].

Many people are interested in the antibacterial characteristics of TiO$_2$ in the food industry. TiO$_2$ has been declared nontoxic by the FDA in the United States. TiO$_2$ has been Many people are interested in the antibacterial characteristics of TiO$_2$ in the food industry right now. TiO$_2$ has been declared nontoxic by the FDA in the United States[10]. In addition to its fungicidal activity, TiO$_2$ NPs have been demonstrated to exhibit bactericidal effects on bacteria such as *E. coli, Staphylococcus aureus*, and *Pseudomonas putida*[11,12]. There has been some interest in food packaging with TiO$_2$-coated or incorporated TiO$_2$[13,14]. For food packaging, antimicrobial agents combat germs and enhance traditional packaging functions, such as shelf life extension, quality preservation, and safety assurance[15]. Using an antibacterial agent helps to reduce the spread of hazardous germs and keep food fresh, as shown in figure (1)[16,17]

The anatase form of titanium dioxide nanoparticles (without UV activation or photocatalytic activation) was examined for its antibacterial activity against pathogenic and environmental Gram-positive and Gram-negative bacteria to assess its application as a new antibacterial approach or for ecological health.

Figure 1. Applications of TiO$_2$ NPs and the perspective shortly. DSSC(Dye-sensitized solar cell); PACT (antimicrobial photodynamic therapy); PDT (photodynamic therapy)[18].

Materials and methods

Nanoparticles

The Canadian company MK impex corp supplies commercial TiO2 nanoparticles with a size of 100nm. Were used in this study.

Bacterial Isolates

A total of 15 bacterial isolates were used, which included 7 clinical isolates obtained from wound and urine infections and 6 environmental isolates from water, as shown in table (1).

All isolates were identified by standard microbiological procedures (Gram staining, colonial morphology, catalase test, cytochrome oxidase reaction, motility, and other biochemical tests), which were carried out depending on Bergey's manual of systematic Bacteriology, also by Vitek 2 system[19].

Use of TiO$_2$ NPs as a bactericidal inhibitor of

For testing the antibacterial activity, five concentration of TiO2 NPs were prepared by dissolving the NPs powder in deionized distilled water[20]; different dilution was prepared, including (1000 µg/ml,500 µg/ml,100µg/ml, 50 µg/ml,20 µg/ml)

This preparation was mixed using a vortex for 3 minutes to obtain homogeneous dilution. Whatman no. 1 filter paper discs were saturated with each concentration of TiO$_2$ NPs and used in the sensitivity test.

Antibiotic Amikacin AK (10 mcg) and Lefloxacin LEF (5 mcg) supplied by Bioanalyzer (turkey) were used as positive control for each bacterium.

Bacterial inoculums were prepared by Direct Colony Suspension Method (1-3). Isolation colonies were selected and transferred to a tube of nutrient broth mixed well using a vortex; the bacterial no was fixed at $1.5×10^8$ by comparing the turbidity with the 0.5 McFarland standard[21]. Mueller-Hinton agar plates were inoculated with the suspension of each bacterial strain, then five TiO$_2$ NPs discs, as well as the antibiotic discs, were distributed unit formally on the agar surface, then incubated at 37°C for (20-24) h. Inhibition zones were measured to monitor the effects of TiO$_2$ NPs on bacterial growth[22]. Positive results were scored when a zone of inhibition was observed around the discs after incubation. The experiments were performed in triplicate to obtain means values for each bacterial isolates[9].

Synergistic effects between the active concentrations of TiO$_2$ NPs and the antibiotics against bacteria

The conc.1000 µg/ml and 500 µg/ml were chosen and mixed with the standard antibiotic discs by adding 250 µl from each concentration to 15 antibiotic discs after the experiment in 15 minutes.The antibiotic sensitivity disc was done according to CLSI. Each experiment was repeated three times.

1-	*Aeromonas spp.*	11-	*Staphylococcus aureus 1*
2-	*Staphylococcus aureus 16*	12-	*Staphylococcus aureus 2*
3-	*Klebsiella Oxytoca*	13-	*Staphylococcus aureus 3*
4-	*Enterobacter cloacae*	14-	*Escherichia coli 1*
5-	*burkholderia cepacia*	15-	*Pseudomonas aeruginosa 3*
6-	*Escherichia coli 4*		
7-	*Escherichia coli 3*		
8-	*Pseudomonas aeruginosa*		
9A	*Pseudomonas aeruginosa 2*		
10	*Pseudomonas aeruginosa1*		

Table 1. Bacterial isolates were used in this study.

Results

The activity of five concentrations of TiO$_2$ nanoparticles is shown in table (2), as well as control antibiotics AK and LEV against 15 bacterial isolates from clinical and environmental sources. The concentrations (20, 50, 100) µg/ml didn't show any antibacterial against all bacteria, while the concentration of 500µg/ml of TiO2 nanoparticles shows inhibitory activity against 7 isolates (3 clinical and 4 environmental including *Aeromonas spp., Klebsiella Oxytoca, Pseudomonas aeruginosa* 1.

Staphylococcus aureus 1, Staphylococcus aureus 3, Escherichia coli 1, Pseudomonas aeruginosa 3), the 1000µg/ml showed antibacterial activity against 9 isolates (6 clinical isolates including *Aeromonas spp., Klebsiella oxytoca, Enterobacter cloacae, Burkholderia cepacia, Escherichia coli 4, Escherichia coli 3* and 3 environmental isolates including *Stapylococcus aureus 1, Staphylococcus aureus 3, Escherichia coli 1*).

The inhibitory effect of these two concentrations differs against the different bacterial isolates used, and it also concerns varying the diameters of the inhibitory zone.

The concentration of 500µg/ml of nanoparticles showed a higher inhibition zone than AK antibiotic on 4 isolates (2 clinical including *Staphylococcus aureus 16, Escherichia coli 4* and 2 environmental isolation *Staphylococcus aureus 1, Staphylococcus aureus 3*). In contrast, the antibiotic LEV has the highest inhibitory effect against all bacterial isolates. Also, the concentration 1000 µg/ml showed a higher impact than AK on two bacteria (1 clinical *Aeromonas spp.* and 1 environmental *Escherichia coli 3* isolates). Diagrams (1,2,3 and 4)illustrate the antibacterial activity of different TiO$_2$ NPs concentrations against studied bacteria.

3Study the synergistic activity between antibiotics and TiO2 nanoparticles

500 and 1000µg/ml TiO$_2$ nanoparticles concentrations were mixed with each antibiotic AK and LEV and studied against bacteria.AK plus the concentration 500µg/ml TiO2 showed an increased inhibitory zone against 7 isolates (3 clinical *Staphylococcus aureus 16, Enterobacter cloacae, Pseudomonas aeruginosa*,4 environmental *Staphylococcus aureus 1, Staphylococcus aureus 2, Staphylococcus aureus 3, Escherichia coli 1*) on mixing the concentration 1000µg/ml TiO$_2$ nanoparticles with AK antibiotic shows causes an increase in the inhibition zone against(*Staphylococcus aureus 1, Staphylococcus aureus 2, Staphylococcus aureus 3, Escherichia coli 1, Pseudomonas aeruginosa 3*, where is the other bacterial response to AK.AK mixed with 500 and AK with 1000 µg/ml causes no significant difference.

LEV antibiotic showed no difference in its effect on (7 clinical *Aeromonas spp., Staphylococcus aureus 16, Klebsiella oxytoca, Enterobacter cloacae, Burkholderia cepacia, Escherichia coli 4, Escherichia coli 3* and 3 environmental *Staphylococcus aureus 1, Staphylococcus aureus 2, Staphylococcus aureus 3*), while LEV mixed with 500 µg/ml causes increased inhibitory zones on (*Burkholderia cepacia, Escherichia coli 3, Staphylococcus aureus2, and Pseudomonas aeruginosa 3*) , and LEV mixed with 1000µg/ml increased the effect antibiotic effect on (2 clinical *Burkholderia cepacia, Pseudomonas aeruginosa* and 1 environmental *Pseudomonas aeruginosa3*) and the diagrams (3,4) illustrate the synergistic effect on TiO$_2$ NPs and the chosen concentration of antibiotics.

Fig: (1 and 2) showed the antagonistic effect of AK, LEV and the synergistic effect with concentrations of TiO$_2$ NPs on the *Staphylococcus aureus* and *Klebsiella oxytoca* bacteria as showed in table (3).

No.	Bacterial	Tio2 NP					AK 10 mcg	LEV 5 mcg
		20µg\ml	50µg\ml	100 µg\ml	500 µg\ml	1000 µg\ml		
Clinical isolates								
1-	Aeromonas spp.	--	--	--	30	40	R	22
2-	*Staphylococcus aureus 16*	--	--	--	--	--	25	41
3-	*Klebsiella Oxytoca*	--	--	--	25	18	17	38
4-	*Enterobacter cloacae*	--	--	--	--	37	17	40
5-	*Burkholderia cepacia*	--	--	--	--	25	10	30
6-	*Escherichia coli 4*	--	--	--	--	19	20	40
7-	*Escherichia coli 3*	--	--	--	--	19	17	30
8-	*Pseudomonas aeruginosa*	--	--	--	--	--	16	35
9-	*Pseudomonas aeruginosa 2*	--	--	--	--	--	18	38
10	*Pseudomonas aeruginosa1*	--	--	--	17	--	19	38
Environmental isolates								
11	*Staphylococcus aureus 1*	non	non	non	20	13	40	40
12-	*Staphylococcus aureus 2*	--	--	--	--	--	10	30
13-	*Staphylococcus aureus 3*	--	--	--	20	11	30	40
14-	*Escherichia coli 1*	--	--	--	13	22	17	30
15-	*Pseudomonas aeruginosa 3*	--	--	--	18	--	17	30

Table 2. The effectiveness of different concentrations of TiO$_2$ NP compared with the antibiotics LEV, AK.

4
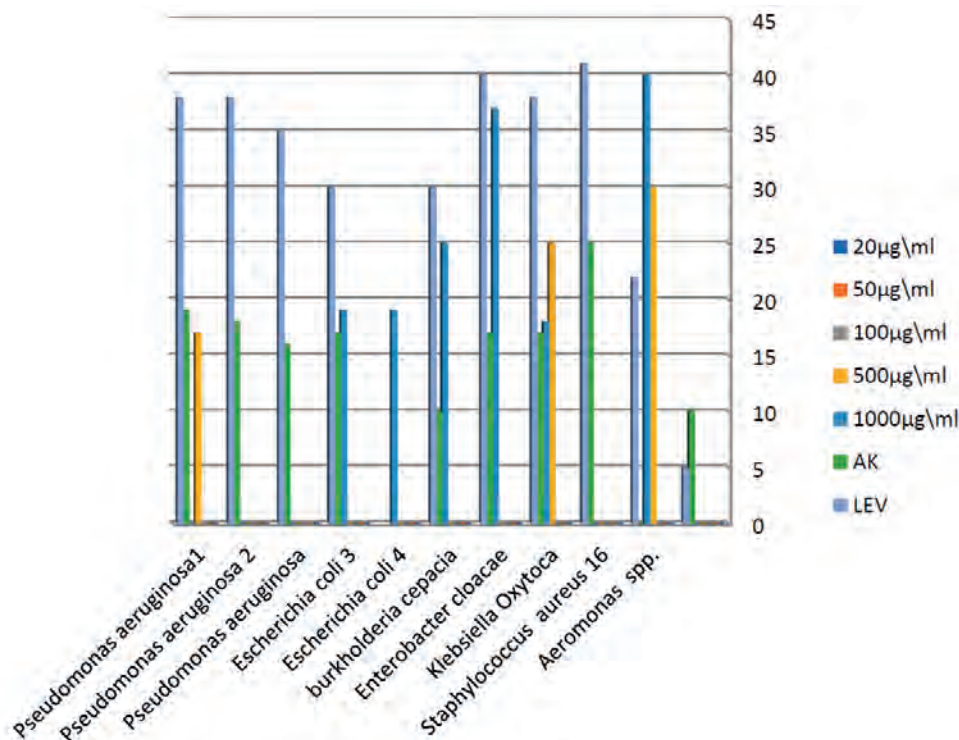
Figure 2. The effect of different concentrations of TIO$_2$ NPs on Clinical bacteria.
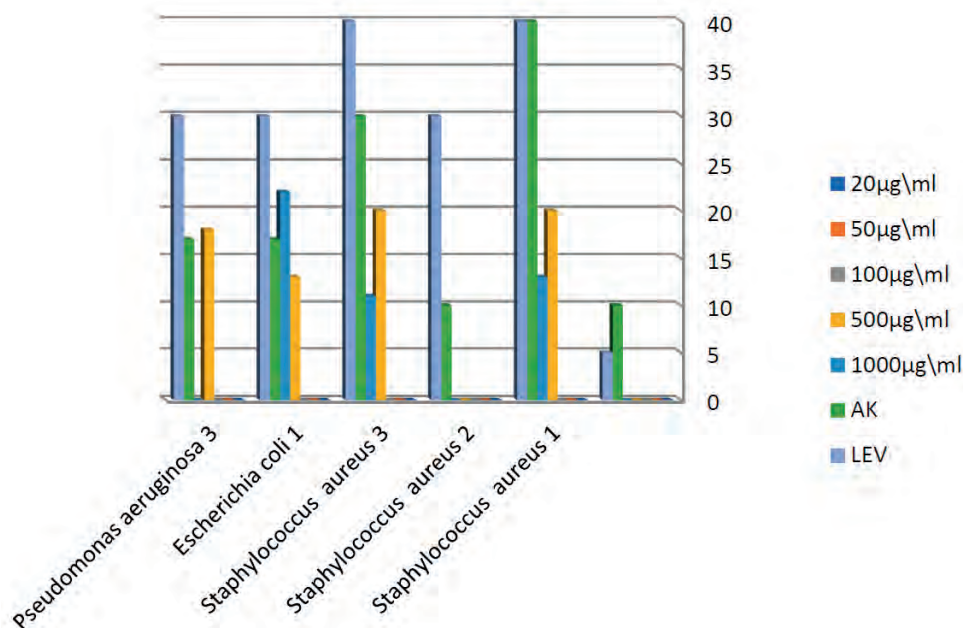
Figure 3. The effect of different concentrations of TiO$_2$ NPs on environmental bacteria.

Discussion

Research has shown that the field of application of NPs in the medical field can increase the performance and effectiveness of therapeutic drugs, and mixing drugs with NPs leads to a process of accumulation in diseased tissues of the mixed substance medicine[23].

Titanium dioxide (TiO$_2$) inorganic nanoparticles have been used in the last decades because they may have a general mechanism of toxicity against bacteria[9,24].

According to several studies, it is believed that the metal oxides carry the positive charge while the microorganisms have negative charges; this causes electromagnetic attraction between microorganisms and the metal oxides, which leads to oxidization and, finally, death of microorganisms[25]. They cause pits or holes, on bacterial cell wall could be associated with internalized particles, leading to increased permeability and cell death[26,27] ((In other words, the difference in electrical charges between polluted metals and living organisms causes a state of attraction between them, which leads to the accumulation of heavy metals in the body of the living organism and it dies.))TiO$_2$ nanoparticles due to their small size and high surface to volume ratio undergo a higher level of interaction with the bacterial cells surface than the larger particles, resulting in a high antibacterial activity[28].

The result of this study may differ from other studies

No.	Bacteria	AK	AK+Ttio2 500µg\ml	AK+ Tio2 1000	LEV	LEV+Tio2 500µg\ml	LEV+Tio2 1000 µg\ml
Clinical isolates							
1-	Aeromonas spp.	20	20	20	40	40	40
2-	Staphylococcus aureus 16	24	28	25	40	40	40
3-	Klebsiella Oxytoca	20	20	20	40	40	40
4-	Enterobacter cloacae	18	24	16	40	40	40
5-	burkholderia cepacia	20	20	20	40	48	44
6-	Escherichia coli 4	20	20	20	40	40	40
7-	Escherichia coli 3	22	22	20	40	50	40
8-	Pseudomonas aeruginosa	30	32	30	48	48	48
9-	Pseudomonas aeruginosa 2	--	--	--	--	--	--
10-	Pseudomonas aeruginosa1	---	17	------	----	38	19
Environmental isolates							
11-	Staphylococcus aureus 1	26	28	26	40	40	40
12-	Staphylococcus aureus 2	30	32	34	40	42	40
13-	Staphylococcus aureus 3	24	26	26	40	40	40
14-	Escherichia coli 1	22	24	22	S	S	S
15-	Pseudomonas aeruginosa 3	20	20	20	36	50	40

Table 3. Synergistic result between TIO₂ and the antibiotics (LEV, AK).

in the response of bacterial species towards TiO₂ NPs at different concentrations because there is no photocatalytic or UV activation; also, the study was done by using the disk diffusion method, whereas many studies done in a liquid medium which may be favoring the close interaction between the suspended nanoparticles and the Gram-positive microbial cells, which could better attach and anchor to the surface of the microbial cells, causing structural changes and damages leading to cell death[29].

TiO₂ NPs can directly oxidize components of cell signaling pathways and even change gene expression by interfering with transcription factors. This result suggested that TiO₂ NPs affect the microorganisms by not only oxidative damage but also bacteria aggregation and biofilm formation, which directly influenced pathogenicity[30].

Conclusions

Antibiotic treatment alone (or sometimes) fails to eradicate microbial infections like a medical device-related biofilm. Combining TiO2 NPs promising agent with antibiotics may be possible to eliminate s in the future.

5

6
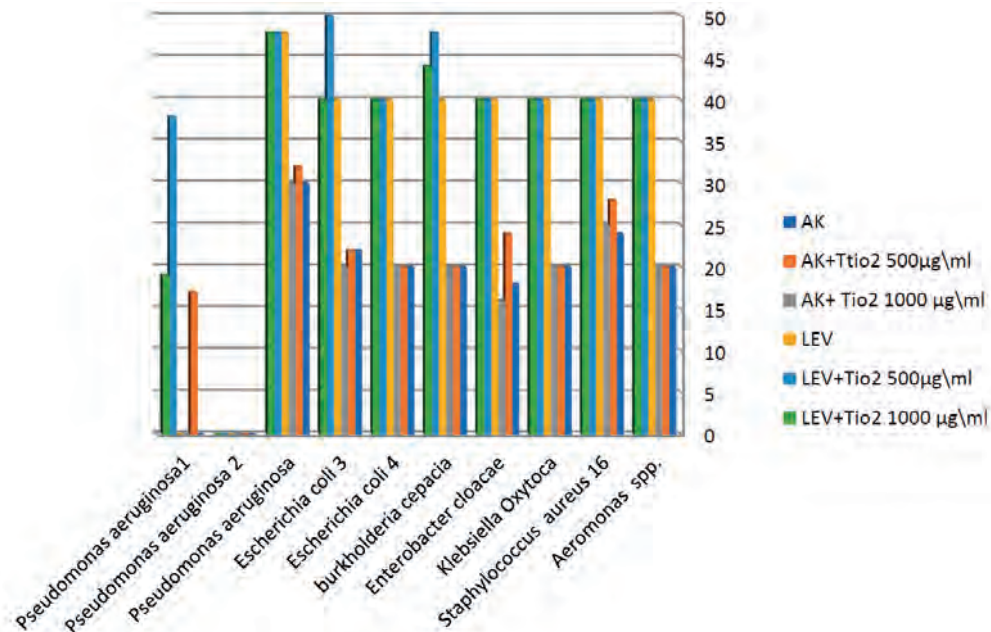
Figure 4. The synergistic effect of at TiO$_2$ NPs a chosen concentration with of antibiotics against clinical bacterial isolates.
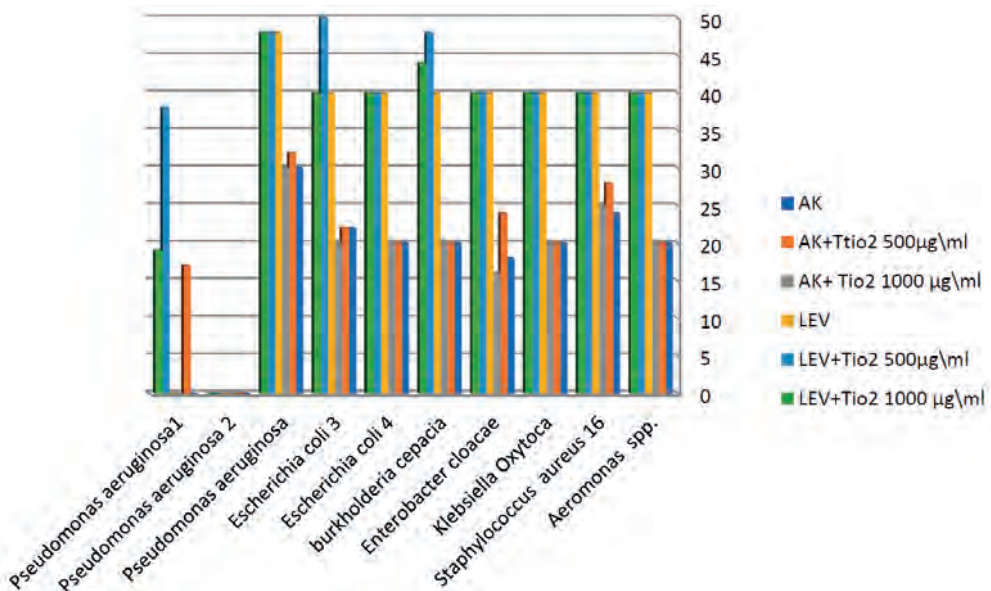
Figure 5. The synergistic effect of TiO$_2$ NPs at a chosen concentration with antibiotics against environmental bacteria.

(a) (b)
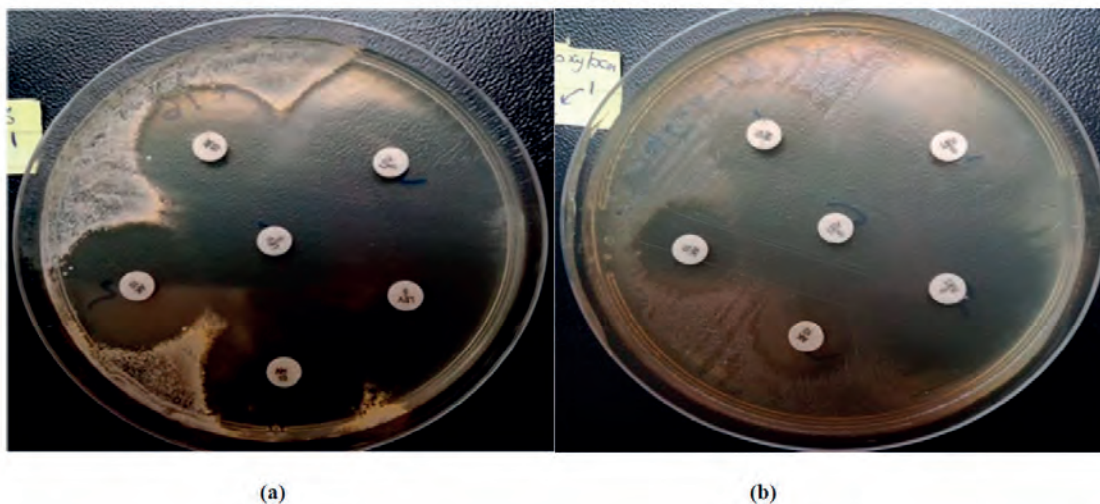
Figure 6. The inhibitory activity of the (Tio$_2$).

Conflicts of Interest

The authors declare that they have no conflict of interest in this study.

Bibliographic references

1. The Influence of Surface Modification on Bacterial Adhesion to Titanium-Based Substrates Martina Lorenzetti, Iztok Dogša,§ Tjaša Stošicki,§ David Stopar,§ Mitjan Kalin,□ Spomenka Kobe, and Saša Novak ACS Appl. Mater. Interfaces 2015, 7, 1644−1651

2. A. Erdem • D. Metzler • D. Cha • C. P. Inhibition of bacteria by photocatalytic nano-TiO2 particles in the absence of light ,Huang 2015.

3. Visai L, De Nardo L, Punta C, Melone L, Cigada A, Imbriani M, Arciola CR. Titanium oxide antibacterial surfaces in biomedical devices. Int J Artif Organs,2011, 34: 929-946.

4. Wang J, Byrne JD, Napier ME, DeSimone JM. More effective nanomedicines through particle design. Small,2011, 7: 1919-1931

5. Xie Y, Heo SH, Yoo SH, Ali G, Cho SO. Synthesis and photocatalytic activity of anatase TiO2 nanoparticles-coated carbon nanotubes. Nanoscale Res Lett,2009, 5: 603–607

6. Taylor E, Webster TJ. Reducing infections through nanotechnology and nanoparticles. Int J Nanomed,2011, 6: 1463-1473

7. Yan M, Chen F, Zhang J, Anpo M. Preparation of controllable crystalline titania and study on the photocatalytic properties. J Phys Chem B,2005, 109:8673–8678

8. Banerjee AN. The design, fabrication, and photocatalytic utility of nanostructured semiconductors: focus on TiO2-based nanostructures. Nanotechnol Sci Applicat,2011, 4: 35–65.

9. Natividad Castro-Alarcón1, José Luis Herrera-Arizmendi, Luis Alberto Marroquín-Carteño1, Iris Paola Guzmán-Guzmán, Armando Pérez-Centeno and Miguel Ángel Santana-Aranda. Antibacterial activity of titanium dioxide nanoparticles, intrinsic and doped with indium and iron.Microbiology Research International Vol. 4(4), pp. 55-62, November 2016.

10. M. Long, J. Wang, H. Zhuang, Y. Zhang, H. Wu, and J. Zhang, "Performance and mechanism of standard nano-TiO2 (P-25) in photocatalytic disinfection of foodborne microorganisms—Salmonella typhimurium and Listeria monocytogenes," Food Control, vol. 39, no. 1, pp. 68–74, 2014.

11. K. Gupta, R. P. Singh, A. Pandey, and A. Pandey, "Photocatalytic antibacterial performance of TiO2 and Ag-doped TiO2 against S. aureus.P. aeruginosa," Beilsten Journal of Nanotechnology, vol. 4, no. 1, pp. 345–351, 2013.

12. S. Bonetta, S. Bonetta, F. Motta, A. Strini, and E. Carraro, "Photocatalytic bacterial inactivation by TiO2-coated surfaces," AMB Express, vol. 3, no. 1, pp. 1–8, 2013.,

13. N. Yao and K. Lun Yeung, "Investigation of the performance of TiO2 photocatalytic coatings," Chemical Engineering Journal, vol. 167, no. 1, pp. 13–21, 2011.].

14. Zhou, J. J., Wang, S. Y., & Gunasekaran, S. Preparation and characterization of whey protein film incorporated with TiO2 nanoparticles. Journal of food science,2009, 74(7), N50–N56.

15. L. Bastarrachea, S. Dhawan, and S. S. Sablani, "Engineering properties of polymeric-based antimicrobial films for food packaging," Food Engineering Reviews, vol. 3, no. 2, pp. 79–93, 2011

16. Siti Hajar Othman, Nurul Raudhah Abd Salam, Norhazlizam Zainal, Roseliza Kadir Basha, Rosnita A. Talib, "Antimicrobial Activity of TiO2 Nanoparticle-Coated Film for Potential Food Packaging Applications", International Journal of Photoenergy, vol. 2014, Article ID 945930, 6 pages, 2014.

17. Thirunavukkarasu Santhoshkumar, Abdul Abdul Rahuman, Chidambaram Jayaseelan, Govindasamy Rajakumar, Sampath Marimuthu, Arivarasan Vishnu Kirthi, Kanayairam Velayutham, John Thomas, Jayachandran Venkatesan, Se-Kwon Kim. Green synthesis of titanium dioxide nanoparticles using Psidium guajava extract and its antibacterial and antioxidant properties, Asian Pacific Journal of Tropical Medicine (2014)968-976

18. Ziental, D., Czarczynska-Goslinska, B., Mlynarczyk, D. T., Glowacka-Sobotta, A., Stanisz, B., Goslinski, T., & Sobotta, L. Titanium Dioxide Nanoparticles: Prospects and Applications in Medicine. Nanomaterials (Basel, Switzerland),2020, 10(2), 387. https://doi.org/10.3390/nano10020387

19. Daniel Ziental, Beata Czarczynska-Goslinska, Dariusz T. Mlynarczyk, Arleta Glowacka-Sobotta, Beata Stanisz, Tomasz Goslinski and Lukasz Sobotta. Titanium Dioxide Nanoparticles: Prospects and Applications in Medicine. Nanomaterials 2020, 10, 387

20. Ansari, M. A., Abdul, H. M., Joshi, G., Opii, W. O., & Butterfield, D. A. Protective effect of quercetin in primary neurons against Abeta(1-42): relevance to Alzheimer's disease. The Journal of nutritional biochemistry,2009, 20(4), 269–275.

21. Melvin P . Weinstein, MD. James S . Lewis II. Clinical and Laboratory Standards Performance Standards for Antimicrobial Susceptibility Testing,2020.

22. P. Nithya Devi1, J. Sathiyabama, S. Rajendran, R. Joseph Rathish and S. Santhana Prabha. Influence of malic acid-Zn2+ system on inhibition of corrosion of mild steel in simulated concrete pore solution prepared in well water,2017.

23. Youssef, Z.; Vanderesse, R.; Colombeau, L.; Baros, F.; Roques-Carmes, T.; Frochot, C.; Wahab, H.; Toufaily, J.; Hamieh, T.; Acherar, S.; et al. The application of titanium dioxide, zinc oxide, fullerene, and graphene nanoparticles in photodynamic therapy. Cancer Nanotechnol. 2017, 8, 6.

24. Taylor, E., & Webster, T. J. Reducing infections through nanotechnology and nanoparticles. International Journal of Nanomedicine,2011, 6, 1463–1473.

25. Zhang H, Chen G. Potent antibacterial activities of Ag/TiO2 nanocomposite powders synthesized by a one-podsol-gel method. Environ Sci Technol 2009;34(8):2905-10.

26. Ravishankar Rai, V. and Jamuna Bai, A. Nanoparticles and Their Potential Application as Antimicrobials, Science against Microbial Pathogens: Communicating Current Research and Technological Advances. In: Méndez-Vilas, A., Ed., Formatex, Microbiology Series,2011, No. 3, Vol. 1, Spain, 197-209;

27. Holt KB, Bard AJ. Interaction of silver (1) ions with the respiratory chain of Escherichia coli: An electrochemical and scanning electrochemical microscopy of micromolar Ag. Biochemistry 2005; 44(39): 13214-23).

28. Morteza Haghi , Mohammad Hekmatafshar Mohammad B. Janipour³, Saman Seyyed gholizadeh, Mohammad kazem Faraz, Farzad Sayyadifar, Marjan Ghaedi. ANTIBACTERIAL EFFECT OF TiO2 NANOPARTICLES ON PATHOGENIC STRAIN OF E. coli. International Journal of Advanced Biotechnology and Research ISSN 0976-2612, 2016.

29. Lane Pineda,1 Andre Chwalibog, ´ 1 Ewa Sawosz,2 Anna Hotowy,1 Jan Elnif,1 and Filip Sawosz1 . Investigating the Effect of In Ovo Injection of Silver Nanoparticles on Fat)Uptake and Development in Broiler and Layer Hatchlings. Hindawi Publishing Corporation Journal of Nanotechnology Volume 2012, Article ID 212486,p7.

30. Carol López de Dicastillo, Matias Guerrero Correa, Fernanda B. Martínez, Camilo Streitt and Maria José Galotto. Antimicrobial Effect of Titanium Dioxide Nanoparticles. Submitted: August 31st, 2019 Reviewed: December 18th, 2019 Published: January 27th, 2020 DOI: 10.5772/intechopen.90891

ARTICLE / INVESTIGACIÓN

Knowledge and awareness of chronic hepatitis C and liver fibrosis among health care personnel and other domains in Iraq

Saja Mohammed Mohsen* and Ghanim Hussein Majeed

Middle Technical University (MTU), Baquba Technical Institute, Baquba, Iraq.
Corresponding author: sajamohammad@mtu.edu.iq

DOI. 10.21931/RB/2023.08.01.35

Abstract: As a significant public health disease, the Hepatitis C virus (HCV) infects more than 185 million worldwide. Chronic infections are led by 170 million illnesses, resulting in 350,000 because of liver and cirrhosis cancer. Injuring of chronic liver from several insults leads to occur fibrosis. For example, metabolic disease (nonalcoholic fatty liver disease), infections (hepatitis B [HBV] and C viruses [HCV]), and toxins (alcohol). This study evaluates the knowledge and awareness about Of Chronic Hepatitis C and Liver Fibrosis among Health Care Workers and other domains of workers in Iraq. This study was carried out as cross-sectional research in Diyala, Iraq, from February / 2021 to January / 2022. In this work, 350 persons participated; the age range was (18-62) years, with a mean age of (25.9 + 9.79). The participants consisted of 100 males and 250 females. Also, they were divided into two groups: groups I and II. I (health care workers group) consists of 200 students studying in the medical department of Baquba technical institute and workers in Diyala hospitals). Group II (other domains Workers) includes (100) participants who work in several domains. Similar to previous studies, a questionnaire was adopted to collect this research data. The outcomes demonstrate higher knowledge about HCV, Liver fibrosis, transmission, and a vaccine was noticed with a statistically significant difference among females compared to males. Regarding residency, the ability of HCV and liver fibrosis in Q1, Q2, and Q5 only among Health Care Workers compared to other domains Workers with a statistically significant difference (P<0.05).

Key words: Chronic Hepatitis C, Liver Fibrosis, Health Care Workers and other domains Workers

Introduction

As a significant public health disease, the Hepatitis C virus (HCV) infects more than 185 million worldwide[1,2]. Chronic infections are led by 170 million infections, resulting in 350,000 because of liver and cirrhosis cancer[3]. In Iran, the rate of tee overall seroprevalence of HCV infection reaches 0.6%[4]. Spontaneously, a few patients (20–30%) recover, while the remaining (70–80%) progress into a chronic infection, of whom 25% lead to hepatocellular carcinoma and cirrhosis[5,6]. There are seven genotypes in the HCV, including more than 65 subtypes[7,8]. Around the world, the most common HCV genotype 1[9–11]. Approximately 1% of Canadians are hepatitis C (HCV)- infected[12,13]. HCV confers a more significant burden regarding reduced functioning and premature mortality among many infectious diseases[14]. Including hepatocellular carcinoma and liver failure, the liver-specific complications of HCV are well developed, and so are the benefits of curative HCV antiviral therapy on these findings[15]. On the other hand, the burden of associated extrahepatic comorbidity is less well known. Many works have established HCV is associated with renal impairment and chronic kidney disease[16 –21].

The most advanced stage of hepatic fibrosis, with 0.1% of the European population affected by cirrhosis, is a continuous growth of the burden of chronic liver disease[22]. Fibrogenesis is the common pathological mechanism that causes cirrhosis, although the disease's etiology varies among countries. Injuring of chronic liver from several insults leads to occur fibrosis. For example, metabolic disease (nonalco-

holic fatty liver disease), infections (hepatitis B [HBV] and C viruses [HCV]), and toxins (alcohol)[23].

Materials and methods

Participants

In this work, 350 persons participated; the age range was (18-62) years, with a mean age of (25.9 + 9.79). The participants consisted of 100 males and 250 females. Also, they were divided into two groups: groups I and II. Specifically, group I (health care workers group) consists of 200 students studying in the medical department of Baquba technical institute and workers in Diyala hospitals). Group II (other domains Workers) includes (100) participants who work in several domains. Similar to previous studies, a questionnaire was used to collect the data for this study.

Measures

Similar to previous works, as listed in table 1, a self-administered questionnaire was used to measure participants' knowledge and awareness of Liver Fibrosis and HCV. In this study, two microbiologist experts (from the microbiology division in the Medicine and Education for Pure Science Colleges) confirmed this questionnaire's validation. The Arabic language was used to write the questionnaire; then, it was translated to English. To collect the data, the questionnaire

Publisher's Note: Bionatura stays neutral with regard to jurisdictional claims in published maps and institutional affiliations.

2

was categorized into two parts:
1.   Demographic characteristics.
2.   Ten questions related to the knowledge of HCV infection and liver fibrosis, the questions evaluating knowledge were "Yes / No / Don't know patterns" shown in table 2 .

N	Socio-demographic characteristic
1	age
2	Six
3	Workers
4	Residence
5	Married

Table 1. Show the Demographic characteristicst.

	Questions	Answer		
1	Have you heard about the Hepatitis C virus before?	Don't know	NO	YES
2	Are you present another type of this virus?	Don't know	NO	YES
3	Is recovery from Hepatitis C virus infection?	Don't know	NO	YES
4	Is this virus infect limited age groups	Don't know	NO	YES
5	Does blood transmit the Hepatitis C virus?	Don't know	NO	YES
6	Is must be a checkup for Hepatitis C virus infection before married	Don't know	NO	YES
7	Is the Hepatitis C virus cause Liver Fibrosis?	Don't know	NO	YES
8	Are you the present relationship between alcohol drinking and Liver Fibrosis?	Don't know	NO	YES
9	Is Hepatitis C virus infection development into liver cancer?	Don't know	NO	YES
10	Is the vaccine for the prevention of the disease available?	Don't know	NO	YES

Table 2. Ten questions related to the knowledge of HCV infection and liver fibrosis.

Procedure

As a cross-sectional study, this work was conducted in Baqubah-Diyala province from February / 2021 to January / 2022. A face-to-face interview was conducted. Before the discussion started, all the participants in this work gave prior approval. After the conversation, the contributors received information about HCV infection and liver fibrosis.

Data Analysis

SPSS software 22nd edition was adopted to perform the statistical analysis. The percentage test used the correct answer only to compare different variables.

Results

Three hundred and fifty (350) members joined in this research. Table 3 illustrates the members' quantitative starting point data: mean age, sex, groups and residence.
Table 4 lists the quantitative results of evaluating participants' liver fibrosis HCV infection knowledge levels.
The results show higher knowledge about HCV, Liver fibrosis, vaccine, and transmission was noticed among women compared to men with a statistically significant difference (P < 0.05) in table 5.
Among health care and other domains Workers, Table 6 compares the percentage knowledge (regarding the residency) of HCV and liver fibrosis in Q1, Q2, and Q5 only with a statistically significant difference (P < 0.05).

Regarding the residency among urban participants, Table 7 shows knowledge about HCV and Liver fibrosis in Q2, Q4, Q5, Q6, Q7, Q8, and Q10 was more significant than in rural participants (P<0.05).

Discussion

To the best of our knowledge, this evaluation is the first study conducted in Diyala society to determine knowledge and awareness about Of Chronic Hepatitis C and Liver Fibrosis among Health Care Workers and other domains of Workers. As listed in table 2, according to Original Bloom's cut-off Points[24], the outcomes revealed good knowledge and awareness about HCV, Liver Fibrosis, infection transmission, risk factors (alcohol drinking), and vaccines. In particular,170 (48.6%) participants said they had heard about HCV. Despite few real works assessing the awareness of hepatitis C in specific populations, the literature states that knowledge about HCV is poor. In a cohort of 3,768 females who were or had at risk for infection of HIV, about (1/4) of those with chronic HCV infection were not aware of their infection status[25]. Black and younger females were less likely to be mindful of the status of their HCV infection.

In contrast, females with a history of injection drugs, past alcohol treatment, or increased liver enzyme (alanine aminotransferase) were more likely to be aware that they were positive for HCV infection. Most participants had very high knowledge about HCV transmission, where 266 (76%) of them correctly answered. These outcomes agree with Stein *et al.* (2001) survey conducted on 306 former IDUs about their knowledge of liver disease risk, HCV transmission, and infection status[26]. By sharing contaminated needles and blood, the authors determined that about all the participants know about how HCV is transmitted. 82% were HCV seropositive among people who did not know their test results or had not been tested. As in other surveys, 1/3 of participants stated that seronegative were seropositive, demonstrating that self-reported infection status is unreliable. In the next ten years, 81% of the respondents anticipated their risk of developing liver disease (specifically cirrhosis) at 50% or greater. The authors in (35,36) reported on healthcare providers' knowledge of HCV transmission. Most healthcare providers identified the main transmission routes in the studies as sharing needles while injecting drugs,

Variables	Frequency	Percentage
Mean age	25.9 $\pm$ 9.79	
Sex		
Male	100	28.6%
Female	250	71.4%
Groups		
Health Care Workers	200	57.1%
Another domain Workers	150	42.9%
Residence		
Urban	240	68.5%
Rural	110	31.5%
Total	350	100%

Table 3. Baseline data of participants.

3

	Questions	Yes No/%	No No/%	Don't know No/%
Q1	Have you heard about the Hepatitis C virus before?	170 (48.6%)	61(17.4%)	119 (34%)
Q2	Are you present another type of this virus?	280 (80%)	8 (2.3%)	62 (17.7%)
Q3	Is recovery from Hepatitis C virus infection?	204 (58.3%)	26 (7.4%)	120 (34.3%)
Q4	Is this virus infect limited age groups	59 (16.9%)	226 (64.6%)	65 (18.5%)
Q5	Does blood transmit the Hepatitis C virus?	266 (76%)	30 (8.6%)	54 (15.4%)
Q6	Is must be checked up for Hepatitis C virus infection before married	246 (70.3%)	43 (12.3%)	61 (17.4%)
Q7	Is the Hepatitis C virus cause Liver Fibrosis?	254 (72.6%)	10 (2.9%)	86 (24.5%)
Q8	Are you the present relationship between alcohol drinking and Liver Fibrosis?	260 (74.3%)	16 (4.6%)	74 (21.1%)
Q9	Is Hepatitis C virus infection development into liver cancer?	218 (62.3%)	21 (6%)	111 (31.7%)
Q10	Is the vaccine for the prevention of the disease available?	181 (51.7%)	79 (22.6%)	90 (25.7%)

Table 4. Knowledge Of Chronic Hepatitis C and Liver Fibrosis among participants.

exposure to blood during sexual activity, and blood transfusions[35,36]. In hemodialysis clinics in Italy, 12% misbelieved kissing in one of the methods that contributed to HCV transmission, 19% of nurses did not know HCV transmitted that getting in tattoo work[35].

Only 254 (72.6%) of the participants' respondents knew that Is Hepatitis C virus cause Liver Fibrosis. The public's knowledge about HCV's natural history[27,28,33] has been published in eight works. In two Canadian works, 83–90% of

participants believed that someone with HCV is unaware of an existing infection[30,32]. Likewise, about (57%) of US baby boomers believed that liver cancer results from HCV infection. Additionally, (61%) stated that no symptoms could be presented to anyone infected with HCV[27]. Another work published previously stated that (1/3) of MSN believed that anyone infected with HCV could lead to liver failure (37%) and liver cancer (31%)[33].

In contrast, a study has been conducted on immigrants

Questions	N	Percentage		Chi-square value
		Male	**Female**	
Q1	170	53(31.2%)	117(68.8%)	1.621(NS)
Q2	280	90(32.1%)	190(67.9%)	9.653*
Q3	204	62(30.4%)	142(69.6%)	1.510(NS)
Q4	59	19(32.2%)	40(67.8%)	1.723(NS)
Q5	266	65(24.4%)	201(75.6%)	23.579*
Q6	246	88(35.8%)	158(64.2%)	25.818*
Q7	254	98(38.6%)	156(61.4%)	45.502*
Q8	260	92(35.4%)	168(64.6%)	23.752*
Q9	218	97(44.5%)	121(55.5%)	71.884*
Q10	181	83(45.9%)	98(54.1%)	54.981*
*(P<0.05)				

Table 5. The effect of sex according to the answer to the question –yes (percentage).

Questions	N	Percentage		Chi-square value
		Health Care Workers	**Another Domain Workers**	
Q1	170	100(58.8%)	70(41.2%)	32.784*
Q2	280	153(54.6%)	127(45.3%)	3.652*
Q3	204	104(51%)	100(49%)	7.813(NS)
Q4	59	44(74.6%)	15(25.4%)	27.384(NS)
Q5	266	144(54.1%)	122(45.9%)	4.305*
Q6	246	123(50%)	123(50%)	17.361(NS)
Q7	254	132(52%)	122(48%)	10.127(NS)
Q8	260	133(51.2%)	127(48.8%)	14.811(NS)
Q9	218	105(48.2%)	113(51.8%)	19.205(NS)
Q10	181	83(45.9%)	98(54.1%)	20.202(NS)
*(P<0.05)				

Table 6. Percentage comparison among healthcare and other domains Workers according to their yes responses.

from Asia stated that there is uncertainty about the natural history of HCV and confusion about the different categories of hepatitis infections[33]. This research demonstrated that females have limited knowledge and awareness that HCV infects limited age groups; only 59(16.9%) correctly answered. Concerning the vaccine for prevention, 181 (51.7%) of participants correctly responded that the vaccine is available to prevent the disease. The authors in (29,31,34) found a misconception about vaccine availability to avoid infection among the general public. (1/2) of the participants interviewed in a Candian study knew about the vaccine availability to prevent the infection[30]. Similarly, 60% of African-American baby boomers and 42% of American baby boomers in two US studies knew about HCV prevention by vaccine[27,29].

Compared with rural participants, the urban showed high knowledge about HCV history, vaccine, type of virus, transmission, liver cancer, and alcohol drinking with statistically significant differences (P). Assessing high-risk populations (such as incarcerated or indigenous peoples)

will likely be included in future works with consistent and clear definitions of knowledge and awareness. Additionally, adopting assessing factors associated with differences in knowledge and awareness (e.g., socioeconomic status). Future knowledge translation and exchange products are the main targets of further studies on healthcare providers' knowledge of the infection. Therefore, there is a need to increase the general public's knowledge and awareness of HCV with healthcare providers to support the discussion of considering HCV tests. This study's obtained gaps and findings can help public health campaigns and future interventions for HCV.

Conclusions

This work showed inadequate knowledge and awareness about HCV, Liver fibrosis, transmission, and vaccine (especially the other domains Workers) among study groups. Such as Liver fibrosis, HCV infection, and its com-

Questions	N	Percentage		Chi-square value
		Urban	**Rural**	
Q1	170	113(66.4%)	57(33.6%)	0.677(NS)
Q2	280	178(63.6%)	102(36.4%)	19.089*
Q3	204	126(61.7%)	78(38.3%)	10.620(NS)
Q4	59	34 (57.6%)	25(42.4%)	4.764*
Q5	266	178(78.8%)	88(21.2%)	2.512*
Q6	246	164(66.7%)	82(33.3%)	1.766*
Q7	254	166(65.3%)	88(34.7%)	4.707*
Q8	260	173(66.5%)	87(33.5%)	1.942*
Q9	218	137(62.8%)	81(37.2%)	11.811(NS)
Q10	181	115(63.5%)	66(36.5%)	5.253*
*(P<0.05)				

Table 7. Percentage of residence effect according to their yes responses.

plications negatively affect all humans. Accordingly, screening programs and Education are crucial to avoiding HCV infections.

Bibliographic references

1. Hajarizadeh B, Razavi-Shearer D, Merat S, Alavian SM, Malekzadeh R, Razavi H. Liver disease burden of hepatitis C virus infection in Iran and the potential impact of various treatment strategies on the disease burden. Hepat Mon. 2016;16(7):e37234.
2. Rahimi P, Solati R, Shokri M, Vahabpour R, Mahmoudizad F, Aghasadeghi M, et al. Evaluation of full length E1 and E2 glycoproteins of HCV expressed in P. pastoris as a protein-based vaccine candidate. Vacc Res. 2015;2(3):74–80.
3. Mirminachi B, Mohammadi Z, Merat S, Neishabouri A, Sharif AH, Alavian SH, et al. Update on the prevalence of hepatitis C virus infection among Iranian general population: a systematic review and meta-analysis. Hepat Mon. 2017;17(2):e42291.
4. Sarvari J, Mansouri M, Hashempoor T, Hosseini SY, Moattari A, Pirbonyeh N, et al. Association of genotype and haplotype of IL-28B gene with hepatitis C infection outcome in Iran: spontaneous clearance versus chronic infection. Hepat Mon. 2017;17(5):e45745.
5. Tameshkel FS, Niya MHK, Sohrabi M, Panahi M, Zamani F, Imanzade F, et al. Polymorphism of IL-28B gene (rs12979860) in HCV genotype 1 patients treated by pegylated interferon and ribavirin. Iran J Pathol. 2016;11(3):216.
6. Sarvari J, Norozian H, Fattahi MR, Pirbonyeh N, Moattari A. The role of inter- feron gamma gene polymorphism (+874A/T, +2109A/G, and −183G/T) in response to treatment among hepatitis C infected patients in Fars Province, Southern Iran. Hepat Mon. 2014;14(1):e14476.
7. Chen Y, Yu C, Yin X, Guo X, Wu S, Hou J. Hepatitis C virus genotypes and sub- types circulating in Mainland China. Emerg Microbes infect. 2017;6(1):1–7.
8. Messina JP, Humphreys I, Flaxman A, Brown A, Cooke GS, Pybus OG, et al. Global distribution and prevalence of hepatitis C virus genotypes. Hepatol- ogy. 2015;61(1):77–87.
9. Mahmud S, Akbarzadeh V, Abu-Raddad LJ. The epidemiology of hepatitis C virus in Iran: systematic review and meta-analyses. Sci Rep. 2018;8(1):150.
10. Ansari N, Doosti M, Ahmadi A, Kakavandi E, Yazdani S, Shayestehpour M. Distribution of hepatitis C virus genotypes in Yazd, Central Province of Iran: increasing the mixed genotypes. Iran J Virol. 2016;10(2):19–24.
11. Ashraf Hafez A, Baharlou R, Mousavi Nasab SD, Ahmadi Vasmehjani A, Shayestehpour M, Joharinia N, et al. Molecular epidemiology of diferent hepatitis C genotypes in serum and peripheral blood mononuclear cells in Jahrom city of Iran. Hepat Mon. 2014;14(5):e16391.
12. Rotermann M, Langlois K, Andonov A, Trubnikov M. Seroprevalence of hepatitis B and C virus infections: results from the 2007 to 2009 and 2009 to 2011 Canadian health measures survey. Health Rep. 2013;24(11):3–13.
13. Payne E, Totten S, Archibald C. Hepatitis C surveillance in Canada. Can Commun Dis Rep. 2014;40(19):421–8.
14. Kwong JC, Ratnasingham S, Campitelli MA, et al. The impact of infection on population health: results of the Ontario burden of infectious diseases study. PLoS One. 2012;7(9):e44103.
15. Myers RP, Krajden M, Bilodeau M, et al. burden of disease and cost of chronic hepatitis C infection in Canada. Can J Gastroenterol Hepatol. 2014; 28(5):243–50.
16. Fabrizi F, Donato FM, Messa P. Association between hepatitis C virus and chronic kidney disease: a systematic review and meta-analysis. Ann Hepatol. 2018;17(3):364–91.
17. Henson JB, Sise ME. The association of hepatitis C infection with the onset of CKD and progression into ESRD. Semin Dial. 2019;32(2):108–18.
18. Kuna L, Jakab J, Smolic R, Wu GY, Smolic M. HCV extrahepatic manifestations. J Clin Transl Hepatol. 2019;7(2):172–82.
19. Park H, Chen C, Wang W, Henry L, Cook RL, Nelson DR. Chronic hepatitis C virus (HCV) increases the risk of chronic kidney disease (CKD) while effective HCV treatment decreases the incidence of CKD. Hepatology. 2018;67(2):492–504.
20. Pol S, Parlati L, Jadoul M. Hepatitis C virus and the kidney. Nat Rev Nephrol. 2019;15(2):73–86.
21. Tsui JI, Vittinghoff E, Shlipak MG, et al. Association of hepatitis C seropositivity with increased risk for developing end-stage renal disease. Arch Intern Med. 2007;167(12):1271–6.
22. Pimpin L et al. Burden of liver disease in Europe: Epidemiology and analysis of risk factors to identify prevention policies. J Hepatol. 2018;69(3):718-35.
23. Pinzani M. Pathophysiology of Liver Fibrosis. Dig Dis. 2015;33(4):492-7.
24. Johon, J. The knowledge and attitudes, practice and perceived barriers towards screening for premalignant cervical lesions among women aged 18 years and above, In Songea Urban, Ruvuma. Thesis. Muhimbili University of Health and Ahied Science. 2011.
25. Cohen, M. H., D. Grey, J. A. Cook, K. Anastos, E. Seaberg, M. Augenbraun, P. Burian, M. Peters, M. Young, and A. French. 2007. Awareness of hepatitis C infection among women with and at risk for HIV. Journal of General Internal Medicine 22(12):1689-1694.

6

26. Stein, M. D., J. Maksad, and J. Clarke. 2001. Hepatitis C disease among injection drug users: Knowledge, perceived risk and willingness to receive treatment. Drug and Alcohol Dependence 61(3):211-215.
27. Allison WE, Chiang W, Rubin A, Oshva L, Carmody E. Knowledge about hepatitis C virus infection and acceptability of testing in the 1945–1965 birth cohort (baby boomers) presenting to a large urban emergency department: a pilot study. J Emerg Med 2016 Jun;50(6):825–831.e2. http://dx.doi.org/10.1016/j.jemermed.2016.02.001.
28. CATIE. Room for improvement: knowledge exchange needs of people living with hepatitis C. Toronto: CATIE; 2015.
29. Crutzen R, Göritz AS. Public awareness and practical knowledge regarding Hepatitis A, B, and C: a two-country survey. J Infect Public Health 2012 Apr;5(2):195–8. http://dx.doi.org/10.1016/j. jiph.2011.12.001.
30. EKOS Research Associates Inc. 2012 HIV/AIDS attitudinal trackingsurvey. Ottawa: EKOS; 2012 Oct. http://www.catie.ca/sites/default/ files/2012-HIV-AIDS-attitudinal-tracking-survey-final-report.pdf
31. Hopwood M, Lea T, Aggleton P. Multiple strategies are required to address the information and support needs of gay and bisexual men with hepatitis C in Australia. J Public Health (Oxf) 2016 Mar;38(1):156–62. http://dx.doi.org/10.1093/pubmed/fdv002.
32. Ipsos Healthcare. Survey on hepatitis C knowledge and perception among Canadians and GP, September 2012. Paris: Ipsos; 2012.
33. Owiti JA, Greenhalgh T, Sweeney L, Foster GR, Bhui KS. Illness perceptions and explanatory models of viral hepatitis B & C among immigrants and refugees: a narrative systematic review. BMC Public Health 2015 Feb;15:151. http://dx.doi.org/10.1186/s12889-015- 1476-0.
34. Rashrash ME, Maneno MK, Wutoh AK, Ettienne EB, Daftary MN. An evaluation of hepatitis C knowledge and correlations with health belief model constructs among African American "baby boomers". J Infect Public Health 2016 Jul-Aug;9(4):436–42. http://dx.doi. org/10.1016/j.jiph.2015.11.005.
35. Bianco A, Bova F, Nobile CG, Pileggi C, Pavia M; Collaborative Working Group. Healthcare workers and prevention of hepatitis C virus transmission: exploring knowledge, attitudes and evidence-based practices in hemodialysis units in Italy. BMC Infect Dis 2013 Feb;13(76):76. http://dx.doi.org/10.1186/1471-2334-13-76.
36. Todorova TT, Tsankova G, Tsankova D, Kostadinova T, Lodozova N. Knowledge and attitude towards hepatitis B and hepatitis C among dental medicine students. J of IMAB 2015;21(3):810–3.

ARTICLE / INVESTIGACIÓN

Evaluating the clinical significance of RBP4, PAI-1, and some trace elements in women with Polycystic Ovary Syndrome

Adnan J. M. Al-Fartosy[1]*, Nadhum Abdul Nabi Awad[1] and Amel Hussein Mohammed[2]

[1] Department of Chemistry, College of Sciences, University of Basrah, Basrah, Iraq.
[2] Al-Kunooze University College, Basrah, Iraq.
Corresponding author: adnan.jassim@uobasrah.edu.iq

DOI. 10.21931/RB/2023.08.01.36

1

Abstract: To assess and compare clinical, hormonal, and metabolic factors with blood levels of RBP4, PAI-1, and trace elements in women with and without polycystic ovarian syndrome (PCOS). A cross-sectional clinical investigation was undertaken. From December 2020 until January 2022, samples were taken at the Basrah Hospital for Obstetrics and Children's infertility center. Significant changes ($p < 0.05$) were in HOMA-IR, E2 and Ts. Levels of PAI-1, RBP4, AMH, LH, LH/FSH, PRL and Cu were significantly ($p<0.01$) increased, and levels of Se, Zn, Mg and E2/T were significantly ($p<0.01$) decreased, between the patient (1o PCOS and 2o PCOS) and control groups, the QUICKI level did not differ significantly ($p>0.05$). Compared to the control group, FSH levels were especially ($p<0.05$) higher in non-obese PCOS patients and lower in obese PCOS patients. Area under the receiver operating characteristics (ROC) curve (AUC) results indicate RBP4 and PAI-1 may be more effective predictors biomarkers for PCOS in expectant women. While trace elements might be considered a protective factor in the emergence of PCOS, metabolic abnormalities and IR in PCOS-affected individuals are associated with the levels of RBP4 and PAI-1, which appear to be a more acceptable diagnostic marker in the early prediction of PCOS.

Key words: Polycystic Ovary Syndrome, RBP4, PAI-1, Trace elements.

Introduction

A diverse hormonal and metabolic condition with only a partially understood pathophysiology, polycystic ovarian syndrome (PCOS) is the most prevalent endocrinopathy among women of reproductive age, with a frequency of up to 15%. In contrast, patients with PCOS who lost 5-7 % of their basal weight showed improvements in insulin resistance, hyperinsulinemia, and hyperandrogenism, which appear to be key factors in at least some causes of PCOS pathogenesis. Therefore, the pathogenesis of PCOS in women may still be largely unknown. Still, it has primarily been linked to increased anti-Mullerian hormone (AMH) levels brought on by oligo-ovulatory cycles or a folliculogenesis disorder, which results in increased preantral and small antral follicle counts[1].

Insulin resistance is a biological misunderstanding in which the body's insulin hormone receptors on cell membranes do not respond to insulin as intended, preventing blood glucose from entering cells and causing a hypoglycemic reaction. Reduced insulin hormone's capacity to control and signal changes in glucose levels in the blood may lead to insulin resistance due to the pancreas pumping out high insulin dosages to get the glucose out of circulation and into cells[2].

Whether PCOS or concomitant obesity is to blame for insulin resistance is still debatable. Any adipose tissue dysfunction may be the primary source of the observed IR and, as a result, the metabolic and cardiovascular effects of the illness. Additionally, some studies suggest that PCOS may cause changes in adipocyte function that affect adipokine release[1].

Retinol-binding protein 4 (RBP4) is an adipokine released by the liver and adipose tissue and is a member of the lipocalin protein family. Its primary function is transporting vitamin A (retinol) from the liver to the peripheral tissues. By attaching to cell surface receptors or acting through retinoic acid on retinoic acid receptors and retinoic acid-X receptors, RBP4 can affect peripheral tissues[3]. Human plasminogen activator inhibitor-1 (PAI-1) is an inhibitor of tissue-type and urokinase-type plasminogen activators (tPA and uPA), which turn plasminogen into plasmin. Because of its capacity to suppress the fibrinolytic activity of tissue-type plasminogen activator (tPA), which produces active plasmin from plasminogen and subsequently eliminates fibrin, PAI-1 is a key regulator of the endogen. Also, it is an essential member of the serine protease inhibitor superfamily, known as Serpin E-1; synthesized by many tissue and cell types, free PAI-1 is relatively inactive in its free form and readily converts into its latent state[4].

The present study examined and compared the association of insulin resistance with mentioned adipokines and trace elements as a clinical predictor for the development of POCS among obese and non-obese women in Basrah province (southern Iraq).

Materials and methods

Study Design and Subjects Recruitment

This study is a clinical case-control trial. Samples were

2

collected between December 2020 and the end of January 2022 from the "infertility center" at Basra Hospital for Obstetrics and Children in Basra Governorate, Iraq. Patient samples from a private clinic were also obtained. Women patients with polycystic ovarian syndrome totaled 124 individuals (PCOS) 60 patients with primary (couples with no prior pregnancies for at least a year after marriage; 28 were obese, and 32 were non-obese); 64 women with secondary (previously pregnant couples) but the pregnancy may not have been successful due to miscarriage, ectopic pregnancy, and other reasons; 31 obese and 33 non-obese); and 56 normal ovulatory women (fertile women presenting at the hospital with a genital prolapsed and history of at least. According to the American College of Obstetricians and Gynecologists criteria, the patients are already PCOS women[5].

Inclusion Criteria

The participants were all from Basrah (Souther of Iraq). The sample populations consist of married women who have been childless for one year and have not used contraception while living with their husbands. Volunteers who voluntarily volunteered to take part in the study served as the controls. It had regular menstrual cycles (26–30 days), had not taken oral contraceptives for at least the previous three months, and showed no symptoms of PCOS or other clinical indicators of hyperandrogenemia. Participants aged 18 to 45 for patients and 20 to 45 for healthy controls. Each participant signed a consent form after receiving complete information.

Exclusion Criteria

Diseases that affected the metabolic status and research eligibility were exclusion criteria. Women with endometriosis, uterine fibroids, breast cancer, epilepsy, migraines, and hormone-dependent cancers were not allowed to participate. Additionally, patients receiving estrogen replacement treatment and those with hyper- and hypothyroidism, diabetes, psychiatric illnesses, and significant diseases involving heart, liver, and kidney malfunction were eliminated.

Samples Preparation

After a 12-hour overnight fast and 30 minutes of rest in the supine position, the morning blood samples (10 ml) were taken. All samples were taken between days two and three of the menstrual cycle and separated into two parts. The first part (1 ml) was placed in polypropylene tubes containing EDTA and gently shaken to be utilized to determine Se concentration. The remaining material was transferred to an untreated plain tube, which could clot for 30 minutes at room temperature. The serum was extracted from the blood by spinning it at 402 x g for 10 minutes after it had clotted. The recovered serum was utilized right away to identify the study's variables, while the rest was kept in deep freezing at (-20 °C) until it was used.

Biochemical Quantification

Blood samples from the controls and PCOS patients were examined for biochemical markers using the following protocols: Body mass index was calculated as the following formula [BMI (kg/m2) = Wt in kg / Ht in m2][6]. The (Abnova-KA0831/Taiwan) kit was used to estimate serum glucose. The quantitative insulin sensitivity check index [QUICKI=1-(Log (insulin, µIU/mL) + Log (glucose, mg/dL)] and the homeostasis model assessment [HOMA-IR=insulin (µIU/mL) × glucose (mg/dL)/405] were used to estimate insulin resistance (IR)[7]. The Insulin was estimated by kit (Abnova-KA0921/Taiwan), (BT-Lab, Shanghai- E1206Hu/China) kit was used to measure serum RBP4 level, and the (BT-Lab, Shanghai- E1159Hu/China) kit was used to measure serum PAI-1 level. The anti-Mullerian hormone was estimated by kit (E-EL-H0317/USA), Follicle stimulating hormone was estimated by kit (Abnova-KA0213/Taiwan), the Luteinizing hormone was estimated by kit (Abnova-KA0214/Taiwan), Testosterone was estimated by kit (Abnova- KA0236/Taiwan), and Estradiol was estimated by kit (Abnova-KA0234/Taiwan), Prolactin was estimated by kit (Abnova- KA0217/Taiwan). All of ELISAs kits were solid phase based on the sandwich principle. While serum copper (Cu) was measured using the 1TAA500-PG flameless AAS (PG Instruments, Leicestershire, England), serum magnesium zinc (Zn) and (Mg) concentrations were measured using the GBC 933 Plus flame atomic absorption spectrometry (AAS) (GBC, Braeside, Australia), and selenium (Se) in whole blood was measured using the hydride generation method AAS (PG Instruments, Leicestershire, England)[8,9].

Statistical analysis

Statistical analysis was performed using SPSS version 26 (IBM Corporation, Armonk, NY, USA). The data were distributed normally, and the comparison between groups was analyzed using the analysis of variance followed by Dunnett's t-test to find the statistical significance. The ROC curve, which is formed by graphing sensitivity (y-axis) against 1- specificity (x-axis) and calculating the area under the curve (AUC), was used to calculate the sensitivities and specificities, as well as the 95% confidence interval. $p < 0.05$ was considered statistically significant, $p < 0.01$ highly substantial, and an AUC value near 0 (or 1) implies a strong diagnostic value; the values of one group are mainly greater (or lower) than the values of the comparison group in this circumstance.

Results

Table 1 summarizes the overall demographics of all the women volunteers who participated in this work.

As indicated in Tables 2 to 4, the findings showed that patients with 1ºPCOS and 2ºPCOS (of both groups of obese and non-obese) HOMA-IR ($p < 0.05$), AMH ($p < 0.01$), LH ($p < 0.01$), LH/FSH ratio ($p < 0.01$), E2, Ts ($p < 0.05$), PRL ($p < 0.01$), PAI-1 ($p < 0.01$), RBP4 ($p < 0.01$), and Cu ($p < 0.01$) were all significantly higher than the control group. Furthermore, patients with PCOS had especially ($p < 0.01$) reduced Se, Zn, Mg, and E2/T ratio levels. In contrast, QUICKI levels between the patients (1ºPCOS and 2ºPCOS) and control groups were not statistically different ($p > 0.05$), as illustrated in Tables 2 to 4.

As shown in Table 3, however, our findings revealed that FSH levels were significantly ($p < 0.05$) higher in non-obese PCOS patients and lower in obese PCOS patients as compared to the control group.

The ROC (receiver operating characteristic) curve's area under (AUC) results obtained indicate that RBP4 and PAI-1 could potentially be used as greater predictive biomarkers in patients women with 1º PCOS (AUC; for obese= 0.909, 1.0 and for non-obese= 0.866, 0.990, respectively) and 2º PCOS (AUC; for obese= 0.905, 1.0 and for non-obese= 0.823, 1.0, respectively), as illustrated in Figure 1.

Characteristics		Control	Patients Women with PCOS	
			Primary (1ºPCOS)	Secondary (2ºPCOS)
Total (No.)		56	124	
			60	64
Age (mean ± SD)		30.44± 4.84	28.88 ± 6.64	29.72 ± 4.62
BMI (Kg/m²)		26.73± 2.54	27.85 ± 1.98	27.685 ± 2.06
Smoking habit	Negative	49	52	58
	Positive	7	8	6
Demographic area	Urban	50	56	57
	Rural	6	4	6
Education	Learned	45	51	49
	Illiterate	11	9	15
Employment	Employed	41	43	44
	Not Employed	15	17	20

Table 1. The main demographic and clinical characteristics of the study population.

Groups		Glucose (mg\dl)	Insulin (mU/L)	HOMAIR±SD	QUIKI±SD
Control	Obese (27)	±3.41 110.35	10.81±1.37	2.94±0.03	0.325±0.04
	Non-obese (29)	±5.19 104.45	±1.13 8.19	2.11±0.04	0.341±0.03
1ºPCOS	Obese (28)	±3.74* 117.32	±1.11 *17.75	±0.07 *5.14	0.301±0.02
	Non-obese (32)	±3.41* 106.74	±1.39 *14.95	±0.04 *3.94	0.312 ±0.06
2ºPCOS	Obese (31)	±4.83* 116.78	±1.13 *16.87	±0.03 *4.86	0.303±0.04
	Non-obese (33)	±3.16* 105.89	±1.04* 14.17	±0.06 *3.70	0.314±0.02

The data is displayed as mean±standard deviation (SD); *p*>0.05: *p*-value not significant, **p*<0.05: *p*-value important;

***p*<0.01: *p*-value highly substantial, indicating the level of significance in comparison with the corresponding control value.
Table 2. Levels of Insulin Resistance Parameters.

Parameters	Patients Women with PCOS				Control 56	
	Primary (1ºPCOS) 60		Secondary (2ºPCOS) 64			
	Obese 28	Non-obese 32	Obese 31	Non-obese 33	Obese 27	Non-obese 29
RBP4 (µg\mL)	± 2.51**36.73	± 3.42**34.98	± 2.73**37.49	± 1.92**35.11	27.12 ± 1.48	25.98 ± 2.31
PAI-1 (AU\l)	± 1.12**10.06	± 2.47**12.79	± 1.91**10.74	± 1.08**13.49	4.07 ± 1.73	6.41 ± 1.22
AMH (mg/mL)	±1.55**19.74	±1.21**17.38	±1.32**20.03	±1.08**16.97	12.43±1.33	10.02± .25
FSH (mU/mL)	5.42*± 0.94	5.52*± 1.07	5.34*± 0.96	5.57*±0 .80	6.35± 1.20	6.71±1.20
LH (mU/mL)	18.86**±0.07	17.06**±0.15	18.92** ±0 .07	17.86**± 0.5	8.64± 0.05	8.37 ± 0.09
LH\FSH ratio	3.47**	3.08**	3.54**	3.20**	1.36	1.24
E2 (pmol/L)	55.28*± 1.8	52.07*± 1.45	55.64*± 1.52	51.98*± 0.81	49.87± 1.55	47.16± 2.10
Ts (nmol\l)	1.89* ± 0.03	1.78* ± 0.05	1.93* ± 0.03	1.81* ± 0.06	0.87 ± 0.03	0.64 ± 0.07
E2\T ratio	29.23**	29.22**	28.81**	28.70**	57.27	73.48
PRL (ng/mL)	18.97*± 0.16	14.59*±1.12	19.24*± 2.40	15.33*± 1.17	10.54±0.36	8.33±0.57

Data are shown as mean and standard deviation (SD); *p*>0.05: *p*-value not significant, **p*<0.05: *p*-value significant; ***p*<0.01: *p*-value highly significant, indicating the level of significance in comparison with the corresponding control value.
Table 3. Levels of RBP4, PAI-1, AMH and some endocrinological hormones in women of healthycontrol and PCOS patients.

Parameters	Patients Women with PCOS				Control 56	
	Primary (1°PCOS) 60		Secondary (2°PCOS) 64			
	Obese 28	Non-obese 32	Obese 31	Non-obese 33	Obese 27	Non-obese 29
Cu (µg\mL)	± 0.02**0.368	± 0.01**0.315	± 0.02**0.377	± 0.04**0.328	0.246 ± 0.03	0.221 ± 0.01
Zn (µg\mL)	± 0.05**0.624	± 0.03**0.645	± 0.04**0.613	± 0.07**0.647	0.715 ± 0.06	0.778 ± 0.07
Mg (µg\mL)	± 2.36**12.304	± 2.51**13.86	± 1.56**12.712	± 1.74**13.65	14.42 ± 2.01	16.741 ± 1.11
Se (ng/mL)	± 4.41**40.12	± 3.16**45.23	± 2.34**41.73	± 2.61**46.32	53.21 ± 3.09	57.34 ± 2.33

Presenting data as mean and standard deviation (SD); $p > 0.05$: p-value not significant, $*p < 0.05$: p-value significant

p-value highly significant, indicating the level of significance in comparison with the corresponding control value.

Table 4. Levels of essential trace elements in women of healthy control and PCOS patients.
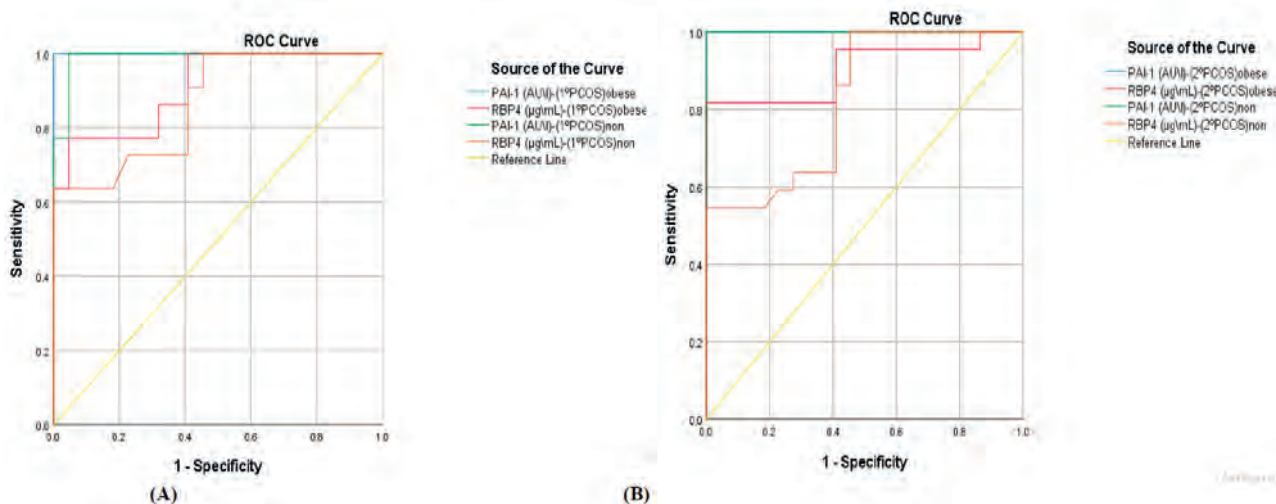
Figure 1. Receiver operating characteristic curve (ROC) for serum RBP4 and PAI-1 levels in obese and non-obese patients women with (A) primary and (B) secondary PCOS.

Discussion

Infertility is the inability to become pregnant after 12 months or more of unprotected sexual activity. As a result, it might be initially assessed after a year of trying to conceive[8]. The inhabitants of urban and rural areas differ significantly in several ways, including those related to food, genetics, social, psychological, environmental factors, pollution, and other environmental and environmental factors. On the other hand, workplace demands could impact women's psychological health. Additionally, tense household circumstances, including childrearing and marital relationships, aggravate the oxidant/antioxidant status issue[10].

A significantly elevated level of RBP4 in women with PCOS may imply a strong correlation between visceral obesity, high levels of circulating and adipose tissue RBP4, and insulin resistance. According to certain studies, the amounts of RBP4 in the blood may be directly linked to how sex hormones affect adiposity expression and secretion. Additionally, RBP4 levels have demonstrated a substantial correlation with serum levels of Testosterone, DHEA-S, FSH, and LH in patients with PCOS[11]. Hyperinsulinemia, insulin resistance, a higher risk of glucose intolerance, diabetes, particularly type 2, and an increased incidence of lipid-related abnormalities are all characteristics of PCOS women.

Although the mechanisms generating PCOS in women are unknown, insulin resistance may play a crucial role in its development. In addition, the prevalence of hyperinsulinemia in women with PCOS patients was previously confirmed, independent of obesity[1]. Contrarily, obesity in PCOS-afflicted women may cause insulin resistance or a greater level of blood insulin, which directly contributes to increased serum RBP4. Previous research has suggested that circulating RBP4 levels may be correlated with the degree of insulin resistance in obese individuals and with the metabolic syndrome's symptoms, such as high body mass index, waist-to-hip ratio, serum triglyceride levels, systolic blood pressure, and decreased levels of HDL cholesterol[12]. The accumulation of Tg in the liver or ectopic fat, which results in hypertriglyceridemia and hyperinsulinemia, prompts RBP4 synthesis and secretion in the liver or ectopic fat and serves as a sign of infertility, according to a theory that suggests impaired free fatty acid metabolism may be a significant factor in controlling RBP4 levels[13]. Additionally, markedly high levels of RBP4 may impede insulin-stimulated glucose uptake in muscle and enhance hepatic glucose synthesis in PCOS women. They may also boost hepatic gluconeogenesis by stimulating phosphoenolpyruvate carboxykinase[14].

Insulin resistance may cause PCOS patients' significantly increased serum levels of (PAI-1) in obese and non-obese PCOS. According to several research, the re-

lationship between PAI-1 and IR in PCOS-affected women patients is independent of body mass and likely reflects insulin-stimulated hepatic PAI-1 production[4]. The association between polycystic ovaries and recurrent miscarriage may be explained by one of the key processes that involves a markedly high level of PAI-1. Women with PCOS frequently exhibit hyperandrogenism, which can inhibit the formation of pores and prevent ovulation. This condition could be brought on by an imbalance in plasminogen levels, which causes theca (interstitium) enlargement and sets off a chain of events that perpetuates the production of the hormone testosterone in men[15]. The etiology of ovarian dysfunction, which eventually leads to disrupted and disordered endothelial, metabolic, and reproductive processes, may be explained by considerably higher levels of PAI-1 in patients with PCOS. The overproduction of PAI-1 brought on by the insulin-driven decrease in the amount of plasmin accessible for extracellular proteolysis may also contribute to folliculogenesis failure in PCOS patients and ovary patients[16]. Additionally, clinical strategies designed to block PAI-1 and lower insulin resistance may be essential to reestablish proteolytic balance in several tissues that have been damaged, such as the ovary, to result in correct ovulation, treatment for PCOS prevention to improve patient fertility, and prevention of its complications that lead to various cardiovascular disease, multiple menstrual irregularities, and infertility in PCOS[17].

Insulin resistance is a biological misunderstanding when the cell membrane insulin hormone receptors do not respond to insulin as expected. As a result, blood glucose cannot enter cells, resulting in a hypoglycemic response. To move the glucose out of the blood and into cells, the pancreas must produce high insulin dosages, which reduces the hormone's capacity to control and communicate variations in blood glucose levels and may lead to insulin resistance[18]. The mechanisms for dramatically increased insulin resistance in patients with PCOS seem too complex; thus, before starting treatment, it is crucial to understand how insulin functions. The insulin hormone has a cell surface receptor with a similar structure to the insulin-like growth factor-1 (IGF-1) receptor that it may bind to. It increases the translocation of the insulin-responsive glucose transporter 4 (GLUT4) from intracellular vesicles to the cell surface in tissues, stimulating the tissue cells to take up glucose. Phosphatidylinositol 3-kinase may be necessary for sharing and mediating this pathway for it to exist (PI3-K). However, because it can activate a cascade of enzymes, including serine/threonine, Raf, MAPK, and MAPK-ERK1/2 of the non-classical models, the MAPK-ERK pathway is involved in the growth and differentiation of cells[19]. The quantitative insulin sensitivity check index (QUICKI) was created to improve fasting measures' sensitivity and precision. QUICKI and clamp measures show a strong correlation in patients with a greater BMI and leanness. A substantial connection with HOMA-IR may also be seen because the euglycemic insulin clamp method is not feasible globally. In clinical settings and population-based research investigations, the HOMA-IR technique is regarded as the standard gold test for assessing insulin resistance[20].

Women with PCOS may have lower whole blood Se levels due to being exposed to oxidative stress, which is known to have a role in the pathophysiology of all known illnesses. The decreased selenium in the blood may indicate increased free radical generation and highly active selenium or glutathione peroxidase enzyme scavengers. According to

several scientific studies, selenium is crucial for the reproductive system to function normally, supporting the link between selenium intake and fertility and procreation-related problems[9]. On the other hand, the pathophysiology of PCOS may be heavily influenced by oxidative stress and insulin resistance. In was reported that found a negative correlation between the blood levels of selenium and the hormones LH and total Testosterone in women with PCOS. This finding may suggest that selenium plays a role in the pathogenesis of PCOS, which is linked to hyperandrogenism. So, through enhanced markers of insulin metabolism and decreased oxidative stress, Se supplementation may lead to reduced levels of serum DHEA and hirsutism. Numerous earlier investigations have demonstrated an association between high androgen levels brought on by PCOS in women and hyperandrogenism, hyperinsulinemia, and insulin resistance[21]. Additionally, insulin resistance and hyperandrogenism, which contribute to endocrine and biochemical changes in women with functional ovarian hyperandrogenism, may be directly connected with oxidative stress (FOH). Se may play a crucial protective role in the active region of enzyme-based antioxidants, including glutathione peroxidase (GPx) and thioredoxin reductase (TrxRs). Therefore, decreased Se level may induce an increased risk factor of cardiovascular disorder, gestational complications, miscarriages, neurodegenerative diseases and increased risk of cancer. Women with PCOS are susceptible to infertility, hirsutism, increased inflammatory factors and increased biomarkers of oxidative stress[22]. Tumor necrosis factor-a (TNF-a), nuclear factor-kappa b (NF-jb), and interleukin-1 (IL-1) are a few examples of inflammatory cytokines that are prevented from being produced and active by selenium, according to numerous research (IL-1 and IL-18). Additionally, the role of reactive oxygen species (ROS) in insulin signaling may impact the imbalance of oxidants and antioxidants. Selenium may be able to lessen ROS and improve insulin resistance due to its significant role as a potent antioxidant[9]. In contrast to a study by Hosseinzadeh et al., who discovered that selenium supplementation might exacerbate insulin resistance in PCOS women, earlier research suggested that selenium intake is linked to lower insulin resistance in PCOS women[21].

The trace elements Zn and Cu play crucial and essential roles as stabilizers, cofactors in several enzymes, and components for healthy and effective hormonal activities. Zn can operate as an antioxidant by shielding the sulfhydryl groups of various proteins and enzymes from free radicals and reducing oxidative stress. In contrast, copper is regarded as a pro-oxidant and oxidant metal in physio-chemistry[23]. One of the trace elements necessary for adequate insulin hormone response is zinc. It is also needed for normal insulin hormone synthesis, storage, and release. In addition, when zinc binds to the insulin receptor, it may have an insulin-like effect[8]. Therefore, acute zinc shortage brought on by oxidative stress may result in severe abnormalities during the per-ovulatory phase that affects egg maturation, cumulus expansion, and ovulation, as well as explain why PCOS patients have higher insulin resistance[21]. On the other hand, higher Cu concentrations in PCOS-affected women's serum may directly impact infertility rates by lowering progesterone levels, which may lead to anovulation, implantation failure, or luteal phase deficit. Furthermore, it is unclear from this research whether elevated copper levels are linked to undiagnosed inflammatory diseases. Ceruloplasmin, regarded as a protein of the acute phase, may

6

also raise serum copper levels while lowering zinc levels[9]. This may suggest that a deficiency in serum copper and zinc may be the primary factor causing infertility. Elevated levels of this element may harm fertility in a variety of ways. For instance, excessive copper levels may disrupt neuronal signaling in the central nervous system (CNS), essential for neuroendocrine fertility regulation[23]. Second, the high serum Cu concentration emphasizes how vital zinc is for controlling ovulation. Therefore, a markedly higher serum Cu level and a significantly lower serum Zn level in pregnant women may hurt fetal brain development and result in minor birth abnormalities. In addition, zinc must be consumed because it is a metal cofactor for many different enzymes (amine oxidase, copper-dependent superoxide dismutase, cytochrome oxidase, and tyrosinase). The enzyme Cu / Zn superoxide dismutase, which reduces superoxide's toxicity by converting it to hydrogen peroxide and oxygen, contains Cu as well[21]. Therefore, a stable balance between the copper-zinc components is responsible for the effectiveness of enzyme function (SOD). Because of enzyme failure, the imbalance in the copper-to-zinc ratio may raise the ratio of dangerous free radicals in the body, which could cause serious harm to cell membranes and walls[22]. In our study, the PCOS group's copper/zinc ratio was noticeably higher than that of the control group. Furthermore, this ratio imbalance may be a significant factor in the disruption of ovarian function, as well as in the lack of follicle maturation persistence, growth of the formation of dominant follicles, and opposition to follicle decay, which may also result in anovulation in polycystic ovarian syndrome[9]. The impact of obesity is another explanation for our findings, higher Cu levels in PCOS. Kurdoglu et al. showed a negative association between copper levels and BMI, but this finding is only valid for PCOS-positive non-obese women. The BMI of PCOS-afflicted women was 28.4 kg/m2, substantially higher than the BMI of the control group (25.6 kg/m^2). However, Li et al. showed no appreciable difference in copper content if BMI was greater than 25 kg/m^2 [23]. Compared to the healthy control group in the current study, the level of Cu in obese and non-obese PCOS patients was significantly significant. Additionally, the obesity shown in some cases may be a symptom of the metabolic syndrome seen in PCOS patients[8]. More research is needed to further understand how zinc or copper contribute to PCOS pathogenicity. This research must consider matched cases and controls for BMI, measure oxidative stress levels, and assess dietary behavior[21].

Women with PCOS demonstrated a statistically significant decline in serum magnesium levels as compared to healthy participants in the current investigation. There have been several research on the physiologic processes, pathological conditions, and therapeutic uses of this necessary metal, including the following: To maintain the structure of ribosomes, nucleic acids, and some proteins-all of which are essential for good health-magnesium, a trace element that is eaten with food or water, is also a crucial cofactor for numerous enzymes involved in glucose metabolism. Second, Mg is thought to have two key functions in biological systems: (i) it can compete with calcium for binding sites on proteins and membranes; and (ii) it can form chelates with significant intracellular anionic ligands, including adenosine triphosphate (ATP)[8]. (iii), the intracellular Mg plays a crucial role as a cofactor for several enzymes involved in the metabolism of carbohydrates, particularly those involved in phosphorylation events like tyrosine kinase. Magnesium contributes significantly to the creation of metal-phosphate

complexes, which may play a crucially important role by triggering the biocatalysts involved in converting triglycerides and glucose[21]. Infertility, spontaneous miscarriages, congenital abnormalities, preeclampsia, placental abruption, preterm rupture of membranes, stillbirths, and low birth weight have all been linked to decreased levels of trace elements like Mg[22]. In addition, lower Mg levels can paradoxically lower the risk of oncogenesis or protect against it. Mg is said to be essential for the cell cycle, and its lack plays a vital role in the development of precancerous cells. On the other hand, too much magnesium can harm the growing fetus, the liver, the kidneys, and the brain[23]. In this study, reduced blood Mg levels in PCOS patients may be related to the prevalence of different metabolic syndrome symptoms or reproductive phenotypes in PCOS-afflicted women of reproductive age, which may increase our understanding of the pathophysiology of PCOS. Therefore, doing dietary research and interventional trials using magnesium supplements becomes sensitive. Despite prior reports of lower serum Mg levels in obese, healthy individuals, we could not detect any differences in serum Mg concentrations between obese and non-obese patients and women with PCOS. The variations may explain this mismatch in eating habits among these various populations. Reduced magnesium absorption as a result of a larger intake of fat and less fiber may be one of the most significant and likely causes of decreased serum Mg in obese PCOS women[24].

Conclusions

From this study, it can be concluded that blood levels of RBP4, PAI-1, and trace elements (Se, Zn, Cu, and Mg) are linked to BMI, metabolic abnormalities and IR, and physical activity in women with PCOS living in Basrah, Iraq. Considering the multivariate regression analysis, RBP4 and PAI-1 seem to be better diagnostic indicators for PCOS early detection, while trace elements may operate as a preventive factor, particularly in people with central obesity. However, more research involving larger sample sizes should be carried out to determine the diagnostic relevance of other biomarkers for the early-stage detection of PCOS and the efficacy of treatments for female infertility issues.

Conflicts of Interest

The authors declared no conflicts of interest.

Bibliographic references

1. Al-Fartosy A.J.M., Awad N.A. and Mohammed A.H. Intelectin-1 and Endocrinological Parameters in Women with Polycystic Ovary Syndrome: Effect of Insulin Resistance. Ewha Med J 2020; 43(1): 1-11. https://doi.org/10.12771/emj.2020.43.1.1.
2. Al-Fartosy A.J.M., Awad N.A. and Abdalemam D.J. Biochemical study of the effect of insulin resistance on adiponectin, lipid profile and some antioxidants elements with relation to obesity in type 2 diabetic patients/Basrah-Iraq. Amer J Biochem 2017;

(7): 73-82. doi: 10.5923/j.ajb.20170704.03.

3. El-Barbary R.H.A., El-Said E.E., Ahmad F. and Al-Wakeel M.E.S. Retinol-binding protein 4, leptin, and insulin resistance in idiopathic hirsutism and hirsute women with polycystic ovary syndrome. Journal of the Egyptian Women's Dermatologic Society 2013, 10: 94–100. doi: 10.1097/01. EWX.0000424171.02538.56.

4. Sahay S., Jain M., Dash D., Choubey L. and Jain S.T.B. Singh Role of plasminogen activator inhibitor type 1 (PAI-1) in PCOS patient. Int J Reprod Contracept Obstet Gynecol 2017; 6(9): 4052-4058. doi: http://dx.doi.org/10.18203/2320-1770.ijrcog20174061.

5. Infertility workup for the women's health specialist. ACOG Committee Opinion No. 781. American College of Obstetricians and Gynecologists. Obstet Gynecol 2019; 133: e377-84.

6. Kumar A.N., Naidu J.N., Satyanarayana U., Anitha M. and Ramalingam K. Association of Insulin Resistance and Serum 25–OH Vitamin-D in Indian Women with Polycystic Ovary Syndrome. Int J Clin Bioch Res 2015; 2(1): 22-26.

7. Gutch M., Kumar S., Razi S.M., Gupta K.K. and Gupta A. Assessment of insulin sensitivity/resistance. Ind J Endoc Metab 2015; 19(1): 160-164. doi: 10.4103/2230-8210.146874.

8. Al-Fartosy A.J.M., Awad N.A. and Mahmood R.A. A Comparative Study of Leptin, Oxidant/Antioxidant Status and Some Trace Elements in Women of Healthy Control and Unexplained Infertility in Basrah-Iraq. Indones Biomed J 2019; 11(3): 327-337. doi: 10.18585/inabj. v11i3.915.

9. Al-Fartosy A.J.M., Shanan S.K. and Awad N.A. Biochemical study of the effects of some heavy metals on oxidant/antioxidant status in gasoline station workers/Basra-Iraq. Int J Sci Res Public 2017; 7: 83-94. www.ijsrp.org.

10. Al-Fartosy A.J.M., Al-Sawaad H.Z. and Al-khazali I.H.A. Seminal Biochemical Markers and Serum Fertility Hormones in Men with or without Infertility/Basrah-Iraq. Inter Med J 2020; 25(4): 2129-2140.

11. Guducu N., Gormus U., Kavak Z.N., Isci H., Yigiter A.B. and Dunder I. Retinol-binding protein 4 is elevated and is associated with free Testosterone and TSH in postmenopausal women. J Endocrinol Invest 2013; 36: 831-834. doi: 10.3275/8948.

12. Yavuz IH, Yavuz G.O., Çokluk E., Kurtoğlu Z. and Bilgili S.G. Investigation of galectin-3, lipocalin 2, retinol binding protein (RBP), small dense low-density lipoprotein (sdLDL) in patients with hirsutism. Advances in Dermatology and Allergology 2019; 36(2):177-183. doi: 10.5114/ada.2019.84593.

13. Zhou Z., Chen H., Ju H. and Sun M. Circulating retinol binding protein 4 levels in nonalcoholic fatty liver disease: a systematic review and meta-analysis. Lipids in Health and Disease 2017; 16:180. doi 10.1186/s12944-017-0566-7.

14. Lingaiah S., Papunen L.M., Piltonen T., Poromaa I.S., Victorin ES and Tapanainen J.S. Serum retinol-binding protein 4 levels in polycystic ovary syndrome. Endocrine Connections 2019; 8, 709–717. doi: 10.1530/EC-19-0116.

15. Ye Y., Vattai A., Zhang X., ZHU J., Thaler C.J., Mahner S., Jeschke U. and Von Schonfeldt V. Role of Plasminogen Activator Inhibitor Type 1 in Pathologies of Female Reproductive Diseases. Int J Mol Sci. 2017; 18(8): 1-17. doi: 10.3390/ijms18081651.

16. Burchall G.F., Pouniotis D.S., Teede H.J., Ranasinha S., Walters K.A. and Piva T.J. Expression of the plasminogen system in the physiological mouse ovary and in the pathological polycystic ovary syndrome (PCOS) state. Reproductive Biology and Endocrinology 2019; 17(33): 2-14. doi: 10.1186/s12958-019-0472-0.

17. Liu Y., Sun M.G., Jiang R., Ding R., Che Z., Chen Y.Y., Yao C.J., Zhu X.X. and Cao J.Y. Plasminogen Activator Inhibitor-1 -675 4G/5G Polymorphism and Polycystic Ovary Syndrome Risk: A meta-analysis. J Assist Reprod Genet 2014; 1-8. doi 10.1007/s10815-013-0171-2

18. Al-Fartosy A.J.M. and Mohammed I.M. Comparison of insulin resistance, prolactin and HbA1c with relation to obesity in men and women of healthy control and diabetic patients/Meisan-Iraq. Int J Cur Res 2017; 9(8): 55643-55648. http://www.journalcra.com.

19. Cakir E., Topaloğlu O., Bozkurt N.O., Bayraktar B.K., Gunguneş A., Arslan M.S., Unsal I.O., Tutal E., Ucan B. and Delibaşi T. Insulin-like growth factor 1, liver enzymes, and insulin resistance in patients with PCOS and hirsutism. Turk J Med Sci 2014; 44: 781-786. doi: 10.3906/sag-1303-80.

20. Tam L.M., Sa L.V.N., Duong L.D., Quoc Huy N.V.Q, Chen C. and Thanh C.N. Exploration of the role of Anti-Mullerian Hormone and LH/FSH ratio in diagnosis of polycystic ovary Syndrome. Clin Endoc 2019; 90(4): 579-585. doi: 10.1111/cen.13934.

21. Al-Fartosy A.J.M. and Mohammed I.M. Biochemical Study of the Effects of Insulin Resistance on Sex Hormones in Men and Women Type-2 Diabetic Patients / Meisan-Iraq. Advances in Biochemistry 2017; 5(5): 79-88. doi:10.11648/j.ab.20170505.11.

22. Mohmmed A.H., Awad N.A. and Al-Fartosy A.J.M. Study of Trace Elements Selenium, Copper, Zinc and Manganese Level in Polycystic Ovary Syndrome (PCOS). Int Res Appl Sci Biotec 2019; 6(6): 16-22. https://doi.org/10.31033/ijrasb.6.6.4.

23. Al-Fartosy A.J.M., Awad N.A. and Alsalimi S.A. Osteoprotegerin and Some Trace Elements in Type 2 Diabetic Patients with or without Nephropathy: Effect of Insulin Resistance. Inter Med J 2020; 25(4): 1771- 1784.

24. Al-Fartosy A.J.M., Awad N.A. and Alsalimi S.A. Clinical markers and some trace elements in patients with type-2 diabetic nephropathy: Impact of insulin resistance. J Med Invest. 2021; 68(1): 76-8.

ARTICLE / INVESTIGACIÓN

Diagnostic and serological study of Breast Cancer in women in Maysan Province, Iraq

Raed Madhi

Department of Biology, College of Science, Misan University, Maysan 62001, Iraq.
Corresponding author: raedsaddam@uomisan.edu.iq

Abstract: The current study was designed to examine the association between breast cancer grading and levels of CA15-3 was studied in addition to the correlation between ABO blood groups and breast cancer. The study involved (140) breast cancer women, and (140) blood samples were collected from healthy women who served as control. The total patients were divided according to their ages into three groups (30-39), (40-49) and (≥50), and ABO blood groups. Moreover, the grades of breast cancer were divided into three groups, and their correlation with serum CA15-3 levels was studied. The current study shows a significant correlation between breast cancer grading and levels of serum CA15-3 antigen. The study also showed that breast cancer is elevated with age. The results demonstrated a great association between the ABO blood groups and breast cancer. Blood group type (A) recorded the highest frequency and percentage (42.14%) of patients with breast cancer. The non-A-blood type (O, B and AB) percentage was as follows (32.14%, 19.29% and 6.43%, respectively). Thus, monitoring breast cancer occurrences in women with blood group A early could be an and excellent strategy to control and facilitate the event of breast cancer.

Key words: Breast cancer, CA15-3, blood groups, breast cancer grading.

Introduction

Breast cancer is one of the most common cancers and the second most commonest that causes cancer death in women. It is well known that breast cancer initiates in breast tissue, which consists of lobules for milk production and ducts that link the lobules to the nipple[1]. Breast cancer can penetrate the duct or gland walls to infiltrate the surrounding fatty tissue of the breast and eventually invade other parts of a woman's body[1]. Many risk factors have been identified to be correlated with breast cancer occurrence, such as family history, obesity, age, diet and environment[2]. It has been shown that breast cancer has a strong association with age and that the occurrence of breast cancer was increased in the age group >45[2].

Different approaches exist to detect and monitor breast cancer incidence and progression. For instance, a breast cancer diagnosis can be seen using blood tumor markers, such as cancer antigen CA15-3 or genetic profiles. CA15-3 has been found to be promising for breast cancer diagnosis[3,4].

ABO blood antigens are carbohydrates that are encoded by one gene with three alleles. These antigens are expressed on the erythrocytes surface[2]. Based on the presence or absence of erythrocyte surface antigens, ABO blood types are classified into four phenotypes: A, B, AB and O[5]. It has been shown that ABO blood type is associated with several diseases such as Hepatitis-B[6], vascular diseases[7], stomach and duodenal ulcer[8], cancer[9] and diabetes mellitus types2[10]. Moreover, ABO blood type has also been documented to be associated with cancer occurrence, such as pancreatic cancer[11-13]. Indeed, antigens of blood types have been found to have an essential role in various conditions such as cell signaling, cell adhesion, tumorigenesis and me-

tastasis[14]. Previous studies have shown that A antigen has similar properties to antigens, A like-antigens, expressed by tumor cells[15]. This could explain why people with A blood type are more susceptible to cancer. This study is aimed to study the association between serum CA15-3 antigen and further confirm the potential connection between blood groups and breast cancer in women.

Materials and methods

Sample collection and study design

The present study was implemented in Maysan province/south of Iraq[R1] . The authorization approval for this study was obtained from Maysan Health Department.

The study included 140 breast cancer patients who attended the AL-Shefaa oncology center in Maysan. The specialist medical staff diagnosed breast cancer according to clinical examinations, evaluations of levels of serum cancer antigen 15-3 (CA15-3), and breast biopsy. Moreover, (140) blood samples were harvested from healthy women and served as control.

CA15-3 measurement

The levels of CA15-3 were measured in the serum of patients and the control group using a commercial kit (EIA-3941, DRG, Germany) and based on the manufacturer's instructions.

Histological examination

A breast biopsy was performed in suspected women

2

with breast cancer for further diagnosis confirmation. Tissue samples were fixed in formaldehyde phosphate buffer[R2] (4%). After dehydration and paraffin embedding, samples were stained (H&E) and examined under light microscopy. The grade of breast cancer was evaluated by using a standard protocol[16].

Identification of ABO blood groups

The conventional slide agglutination method was used to determine blood group phenotypes (A, B, AB, and O) and according to agglutination reactions that were carried out between blood group specific anti-sera and blood group antigens on the cell.

Statistical analysis

Statistical analysis was carried out using Chi-square and T-tests that were analyzed by SigmaStat program 10.0. Data are introduced as mean values±standard error of the mean. Statistical significance between the groups was presented as P<0.05.

Results

Age distribution

The number of patients was exceptionally high in the age group (≥50) years in percent (44.16%), followed by the age group (40-49) years (35%) and then (20.84%) in the age group (30-39) as summarized in table (1).

Levels of CA15-3 antigen in breast cancer and control

CA15-3 antigen has been using commonly as an indicator for breast cancer diagnosis[17]. In this study, breast cancer diagnosis of 140 patients and control wasidentified

based on serum CA15-3 antigen (Figure1). The results showed a significant augmentation in the levels of serum CA15-3 antigen in patient group as compared with healthy group (Figure1).

CA15-3 levels and breast cancer grading

Diagnosis of breast cancer was also confirmed by using another approach, which was histopathological examinations. It was found that tissue architectures and uniform cells in the grade 1 tissues sample are similar to the normal breast tissue (Figure 3). However, tissue architectures and cells in grades 2 and 3 had different features than normal cells. For instance, histological changes in grade 2 show a moderate variability in tissue architecture, cell size, and shape. In addition, histological examinations of grade 3 showed great destruction in tissue architecture and an apparent variation in cell shape and size (Figure 3). Moreover, this study examined the correlation between the CA15-3 antigen and breast cancer grading. The results found an association between serum CA15-3 antigen levels and the grades of breast cancer (Figure 2), which indicated that serum CA15-3 antigen could be used as an indicator even for early diagnosis.

Distribution of ABO blood groups in patients and controls

The overall distribution ratio of blood groups (A, O, B and AB) of 140 patients was (42.14%, 32.14%, 19.29%, and 6.43%) corresponding to blood groups A, O, B and AB, respectively. In contrast, the distribution ratio of blood groups in control subjects was (28.57%, 25%, 39.29% and 7.14%) corresponding to groups A, O, B, and AB, respectively. These findings revealed that blood group A has a significant connection with the occurrence of breast cancer compared to the other blood groups, table (3-3 and 4).

Age group (Years)	Patients		Control	
	Number	%	Number	%
30 – 39	29	20.71	32	22.85
40 – 49	48	34.29	47	33.58
≥ 50	63	45	61	43.57
Total	140	100	140	100

Table 1. Age distribution of patients and controls.
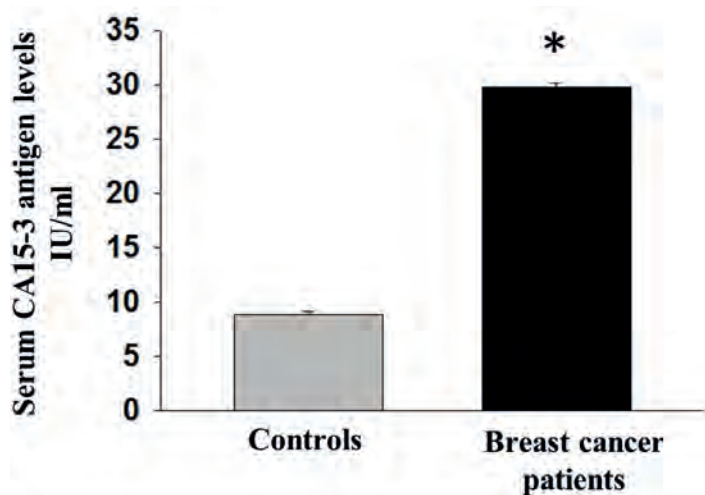
Figure 1. Levels of serum CA15-3 measurements. The black box represents patients with breast cancer. Grey box represents control groups. Data represent means ± SEM. #P <0.05 versus control.
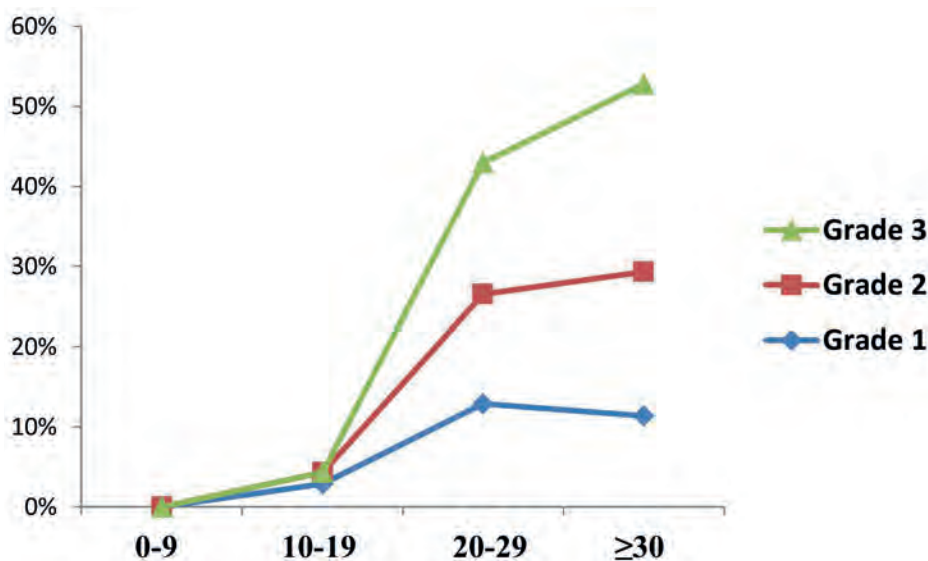
Figure 2. The percentage of CA15-3 antigen and breast cancer grading. Blue line represents grade 1. Red line represents grade 2. Green line represents grade 3. Data described as percentage; comparisons between groups were done using Chi-square test. P-value £ 0.05 used as a significant levels between the groups.

CA15-3 levels (IU/ml)	Grade 1		Grade 2		Grade 3		Total
	NO.	%	NO.	%	NO.	%	NO(%)
0-9	0	0	0	0	0	0	0
10-19	4	2.9	2	1.4	0	0	6(4.3)
20-29	18	12.9	19	13.6	23	16.4	60(42.9)
≥30	16	11.4	25	17.9	33	23.5	74(52.8)
Total	38	27.2	46	32.9	56	39.9	140(100)

Table 2. Association between CA15-3 and breast cancer grading.

Blood group	Patients		Control	
	Frequency	percentage	Frequency	Percentage
A	59	42.14	40	28.57
O	45	32.14	35	25
B	27	19.29	55	39.29
AB	9	6.43	10	7.14
Total	140	100	140	100

Table 3. Blood group distribution of patients and controls.

	Observed	Expected	Difference	Difference Sq.	Diff. Sq. / Exp Fr.
A	59	63	-4.00	16.00	0.25
O	45	61.6	-16.60	275.56	4.47
B	27	11.2	15.80	249.64	22.29
AB	9	4.2	4.80	23.04	5.49
					32.502

Table 4. Statistical differences between ABO blood groups in breast cancer patients using the Chi^2 test.

Discussion

Serum CA15-3 antigen has increased significantly in patients with breast cancer[18]. The findings found that serum CA15-3 antigen levels are associated with breast cancer grades (Figure 2). Moreover, A blood type has been shown to have a great connection with breast cancer incidence compared to non-A blood types. Therefore, serum CA15-3 antigen could be a useful independent indicator in breast cancer patients. In addition, these findings indicate that monitoring the occurrence of breast cancer in women with A blood type, especially in young women, could be a valuable

3

4
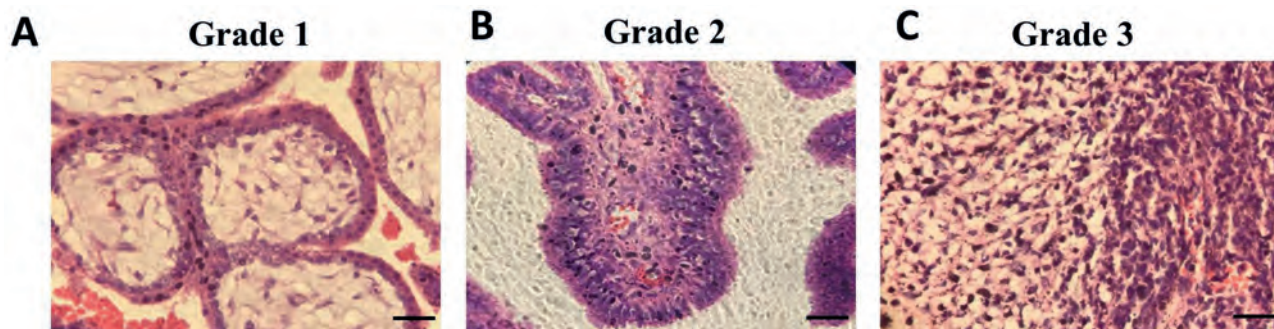
Figure 3. Grades of breast cancer. Hematoxylin & eosin sections from breast tissue of women who had breast cancer. Scale bar = 50 µm. A) grade 1, B) grade 2, C) grade 3.
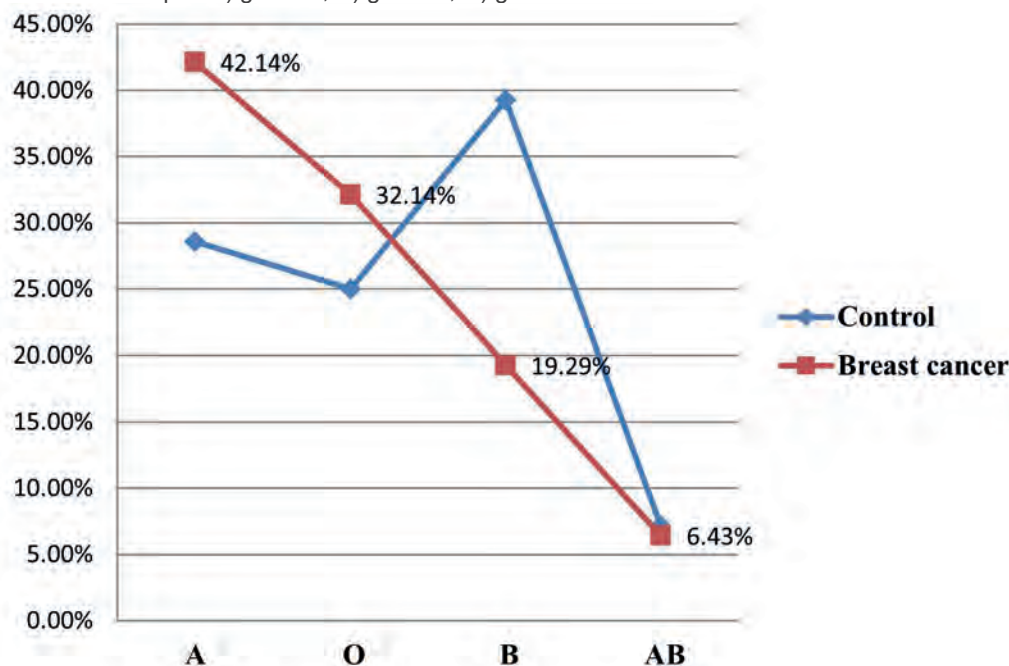
Figure 4. Blood groups distribution of patients and controls. Percentage of ABO blood groups in controls (Blue line) and patients (Red line).

strategy to control breast cancer occurrence.

It is well established that CA15-3 antigen has been used as a marker for different types of cancer. Moreover, CA15-3 antigen has been identified to express breast cancer cells [R4] at higher levels than the standard[17]. The present study found that serum CA15-3 antigen levels increased significantly in the patient's group compared to the healthy group (Figure 1). Moreover, the current findings explored the correlation between serum CA15-3 antigen and breast cancer grading. It was found that serum CA15-3 antigen has a significant correlation with the grades of breast cancer[R5] (Table 2). The findings agree with the previous study by Hashim, Z. M *et al.*[17]. The current results could confirm that identifying serum CA15-3 antigen could be a practical diagnostic approach for early breast cancer diagnosis.

It is well known that cancer can occur at any age; however, many cancer types become common after humans get older. It has been shown that breast cancer incidence has a strong association with age[19]. The present study revealed that patients with breast cancer fall in the age group ≥50 years (Table 1), which gives a clear idea that age is more likely to be associated with breast cancer incidence. In line with that, a previous study has shown that breast cancer incidence increases with age[20]. Moreover, El- Zaemey *et al.*, 2012, have found that breast cancer has a high incidence at age 50 years[21]. It has also been shown that age might be one of the risks of breast cancer occurrence and could be increased at age (60) years or even older[22]. It is assu-

med that the reason beyond this might be an increase in the point mutation in the genetic material of DNA, which causes abnormal changes in the chromosome of the cell. Furthermore, it has shown that breast cancer occurrence rates did not elevate in women under age (40). Still, Ductal Carcinoma "in situ" (DCIS) augmented in women of all ages during the same period[21]. Another explanation is that estrogen levels would be higher in women who start menstruation early and reach menopause at a late age compared to those with a late menarche or early menopause[23]. Moreover, another risk associated with breast cancer development is the age at first pregnancy. For example, the risk of breast cancer is suspected to be reduced in the first full-term pregnancy at a relatively early age compared to those who never have children or those who have their first child relatively late in life[24].

The ABO types are an essential part of transfusion medicine but have been shown to be associated with various diseases[2]. For example, it has been documented that blood group A people are more susceptible to *Pseudomonas aeruginosa* and smallpox[9]. The present study identified that the occurrence of breast cancer was significantly higher in patients with blood group A, compared with non – Groups (O, B, and AB) as shown in (Table 3). These findings were in line with previous studies show that cancer incidences are more suspected to be higher in blood group A people compare to non – A groups (O, B , and AB). For example, it has found that the percentage of cancer occurrence was 64%, 22%, 15%, 28%, 13%, and 11%, of salivary gland, sto-

mach, uterus, ovaries, cervix and colon, which were higher in blood type A people as compared with type O[25]. It is believed that in people with non-A blood type who have tumors, their tumors can be with antigens with the same properties as A antigens. Tumors with A-like antigens were shown to be recognized by anti-A antibodies and subsequently attack the tumors [R6][15]. This could explain why people with A blood type is more susceptible to tumorigenesis.

Conclusions

The present findings show a strong relation between the levels of CA15-3 antigen and breast cancer grading. Moreover, among ABO types, A blood type has a significant association with the occurrence of breast cancer in women compared to other blood types. Accordingly, A blood type has a high risk of breast cancer, so it could be an excellent strategy to monitor breast cancer incidence in young women with blood group A.

Acknowledgments

Conflicts of Interest

The author is declared that there is no conflict of interest in regard of this study.

Bibliographic references

1. Sharma, G.N., et al., Various types and management of breast cancer: an overview. J Adv Pharm Technol Res, 2010. 1(2): p. 109-26.
2. Meo, S.A., et al., Association of ABO and Rh blood groups with breast cancer. Saudi J Biol Sci, 2017. 24(7): p. 1609-1613.
3. Ebeling, F.G., et al., Serum CEA and CA 15-3 as prognostic factors in primary breast cancer. Br J Cancer, 2002. 86(8): p. 1217-22.
4. Duffy, M.J., Serum tumor markers in breast cancer: are they of clinical value? Clin Chem, 2006. 52(3): p. 345-51.
5. Dean, L. and National Center for Biotechnology Information (US), Blood groups and red cell antigens. 2005, NCBI,: Bethesda, Md.
6. Siransy, L.K., et al., ABO/Rh Blood Groups and Risk of HIV Infection and Hepatitis B Among Blood Donors of Abidjan, Côte D'ivoire. Eur J Microbiol Immunol (Bp), 2015. 5(3): p. 205-9.
7. Zakai, NA, et al., ABO blood type and stroke risk: the REasons for Geographic And Racial Differences in Stroke Study. J Thromb Haemost, 2014. 12(4): p. 564-70.
8. Tanikawa, C., et al., A genome-wide association study identifies two susceptibility loci for duodenal ulcer in the Japanese population. Nat Genet, 2012. 44(4): p. 430-4, S1-2.
9. Gates, M.A., et al., ABO blood group and incidence of epithelial ovarian cancer. Int J Cancer, 2011. 128(2): p. 482-6.
10. Meo, S.A., et al., Association of ABO and Rh blood groups with type 2 diabetes mellitus. Eur Rev Med Pharmacol Sci, 2016. 20(2): p. 237-42.
11. Wolpin, B.M., et al., ABO blood group and the risk of pancreatic cancer. J Natl Cancer Inst, 2009. 101(6): p. 424-31.
12. Iodice, S., et al., ABO blood group and cancer. Eur J Cancer, 2010. 46(18): p. 3345-50.
13. Wolpin, B.M., et al., Pancreatic cancer risk and ABO blood group alleles: results from the pancreatic cancer cohort consortium. Cancer Res, 2010. 70(3): p. 1015-23.
14. Weisbrod, A.B., et al., Association of type-O blood with neuroendocrine tumors in multiple endocrine neoplasia type 1. J Clin Endocrinol Metab, 2013. 98(1): p. E109-14.
15. Abegaz, S.B., Human ABO Blood Groups and Their Associations with Different Diseases. Biomed Res Int, 2021. 2021: p. 6629060.
16. Rakha, EA, et al., Breast cancer prognostic classification in the molecular era: the role of histological grade. Breast Cancer Res, 2010. 12(4): p. 207.
17. Hashim, Z.M., The significance of CA15-3 in breast cancer patients and its relationship to HER-2 receptor status. Int J Immunopathol Pharmacol, 2014. 27(1): p. 45-51.
18. Shering, S.G., et al., Preoperative CA 15-3 concentrations predict outcome of patients with breast carcinoma. Cancer, 1998. 83(12): p. 2521-7.
19. Winters, S., et al., Breast Cancer Epidemiology, Prevention, and Screening. Prog Mol Biol Transl Sci, 2017. 151: p. 1-32.
20. Anderson, D.E. and MD. Badzioch, risk of familial breast cancer. Cancer, 1985. 56(2): p. 383-7.
21. El-Zaemey, S., et al., Breast cancer among Yemeni women using the National Oncology Centre Registry 2004-2010. Cancer Epidemiol, 2012. 36(3): p. 249-53.
22. Quinn, M.J., C. Martinez-Garcia, and F. Berrino, Variations in survival from breast cancer in Europe by age and country, 1978-1989. EUROCARE Working Group. Eur J Cancer, 1998. 34(14 Spec No): p. 2204-11.
23. Dall, G.V. and K.L. Britt, Estrogen Effects on the Mammary Gland in Early and Late Life and Breast Cancer Risk. Front Oncol, 2017. 7: p. 110.
24. Susan P. Helmrich et al., Risk factors for breast cancer, American Journal of Epdemiology, Volume 117, Issue 1, January 1983, Page 35-45, https://doi.org/10.1093/oxfordjournals.aje.a113513.
25. Garratty, G., Blood groups and disease: a historical perspective. Transfus Med Rev, 2000. 14(4): p. 291-301.

5

ARTICLE / INVESTIGACIÓN

Assessment of endotoxin levels of water in hemodialysis centers in Iraq

Yasamen Raad Humudat* and Saadi Kadhim Al-Naseri   DOI. 10.21931/RB/2023.08.01.38
Environment and Water Directorate, Ministry of Science and Technology, Baghdad, Iraq.
Corresponding author: yasmenraad@yahoo.com

Abstract: The significance of endotoxin-free, sterile dialysis fluid for long-term, high-quality hemodialysis treatment is obvious and highly desired[MF1] . The current study aimed to determine endotoxin for the water quality used in twenty hemodialysis treatment centers. Eighty samples (40 x dialysates and 40 x dialysis water) were tested for endotoxin using the LAL gel clot method. The results revealed a variation in the quality of the produced water that makes it unaccepted compared to the international standard (ANSI/AAMI/ISO-23500). Endotoxin levels were higher than (0.25 EU/ml) in 40% of dialysis water and 30% of dialysate water, higher than the recommended international standards. The results conclude that systematic water quality monitoring in hemodialysis services is essential for patient safety and health problems.

Key words: Endotoxin, Water quality, Dialysis fluid, LAL test, Hemodialysis patient.

1

Introduction

Water quality is critical for hemodialysis because contaminants in the water can enter the patient's bloodstream and cause significant morbidity and mortality[1]. Chronic inflammation is widespread among dialysis patients but has been linked to poor water quality[2]. To that end, dialysis water is extensively pretreated before use, and most dialysis machines are equipped with endotoxin-retentive filters. One contaminant frequently linked to dialysis water contamination is lipopolysaccharide or endotoxin, which is released primarily from disintegrating gram-negative bacteria GNB[3]. As a result, to prevent the growth of GNB in dialysis systems, dialysis machines must be disinfected regularly and a monitoring program established[4].

The inappropriateness of tap water for a long time is recognized for hemodialysis treatment. The water utilized in hemodialysis centers undergoes additional treatment to decrease pollutants to levels required by national or international standards for dialysis fluids[5]. Although the water treatment stations used in hemodialysis units depend on the quality of the drinking water and the uses of the treated water within the dialysis centers[6], the primary water treatment for the hemodialysis session is divided into three stages. The pretreatment stage's first step removes most suspended particulates, organic matter, and cations (sand filter, softener, brine tank, and carbon filter). The second treatment stage aims to remove any remaining chemical compounds and microbiological contaminants (reverse osmosis). The third stage, known as post-treatment, seeks to ensure that water is distributed to the monitors while considering that circuit designs with external curvatures encourage water stagnation, which can lead to contamination[7].

Recently, the American National Standard Institute (ANSI), Association for the Advancement of Medical Instrumentation (AAMI), and the International Organization for Standardization (ISO) released recommendations for water and dialysis solutions, intending to suggest reasonable procedures for dialysis fluid production and monitoring[3].

Following these guidelines will result in an improvement in dialysis fluid quality. Endotoxin concentration is expressed as Endotoxin Units (EU). Endotoxin content in dialysis water (reverse osmosis water) must be less than 0.25 EU/ml, while the maximum guideline concentration in dialysate water is less than 0.5 EU/ml. In ultrapure dialysate, the guideline concentration is 0.03 EU/ml[8]. Iraq has no national standard for dialysis fluid quality; therefore, the above international criteria will be used to audit and monitor endotoxin content and water quality used to prepare dialysis fluid . This national study aimed to determine the endotoxin level in dialysis water and dialysate in Iraqi hemodialysis centers.

Materials and methods

Work strategy and sampling

The hemodialysis water examined in this study were samples collected for endotoxin analysis during 2021-2022 in 20 Iraqi hemodialysis centers. A total of 80 water samples were analyzed; 40 were examples of dialysis water (reverse osmosis) and 40 samples of dialysate water.

The samples were collected in a sterile, endotoxin-free bottle (100 ml) pre-prepared before sampling in the laboratory. Samples were transported immediately on the same day to the laboratory for testing.

Endotoxin test

Limulus amoebocyte lysate (LAL) and a gel clot were employed to quantify endotoxin in the dialysis fluid. The sensitivity of the measuring kit is (0.015 EU/ml and 0.06 EU/ml)[9]. The examination process includes mixing 0.1 ml of dissolved LAL reagent into the appropriate reaction tube, adding 0.1 ml of the sample, and incubating it using a water bath at 37 ± 1 °C, 60 ± 2 minutes without subjecting it to vibration. When incubation is complete, tilt the tube through

2

180° immediately but gradually. If a gel forms and maintains its integrity without deformation or collapse, the result is positive; if no gel forms, the effect is negative. Samples were analyzed twice using different dilutions.

Statistical analysis

Data analysis was done with Microsoft Excel 2010.

Results

Figures 1 and 2 showed hemodialysis centers' endotoxin levels in dialysis water (n=40) and dialysate (n=40). Endotoxin levels ranged (from>0.03- 0.5 EU/ml (in dialysis water and)<0.015 - 0.5 EU/ml) in dialysate samples. The level of endotoxins was >0.25 EU/ml in samples of dialysis water (n=24) and dialysate (n=22) samples. Overall, the endotoxin level was less than 0.25 EU/ml in 60% of the dialysis water samples and 70% of the dialysate samples. As a result, only those samples complied with the (ANSI/AAMI/ISO) best practice requirements for pure dialysis fluid. Only five Iraqi hemodialysis centers complied with the definition of the (ANSI/AAMI/ISO) best practice limits for ultrapure dialysate.

The dialysis water and dialysate were of poor quality (the level of endotoxin was more significant than 0.25 EU/mL) in 40% and 30% of hemodialysis centers, respectively.

Discussion

The current study is a national survey of the quality of dialysis fluid. Iraq had more than 20 hemodialysis centers in 2021 (according to the Iraqi annual statistical report)[10]. The first attempt to study the quality of dialysis fluid in Iraq was conducted by Al-Naseri et al. It was a small study looking for endotoxin levels in dialysis fluids[11].

The results showed high in 50% pure dialysis and 13% ultrapure hemodialysis water. These endotoxin levels did not comply with international guidelines[8]. This result is consistent with the results of Penne EL *et al.* 2009[12] who confirmed that the ultrafiltration technology might generate online dialysis fluids for an extended period while maintaining consistent quality.

Endotoxin levels in dialysis fluid indicate that the water treatment procedure may be a source of endotoxin contamination[13]. It would be necessary to change the water treatment unit's architecture to include a different phase of controlled ultrafiltration that produces sterile, pyrogen-free fluids suited for infusion.

Excess endotoxin in dialysis fluid from Gram-negative bacteria can produce pyrogenic responses and septicemia[2]. As a result, endotoxin in treated water is a cause for worry in hemodialysis institutions and should be considered when assessing the quality of hemodialysis water. This might be
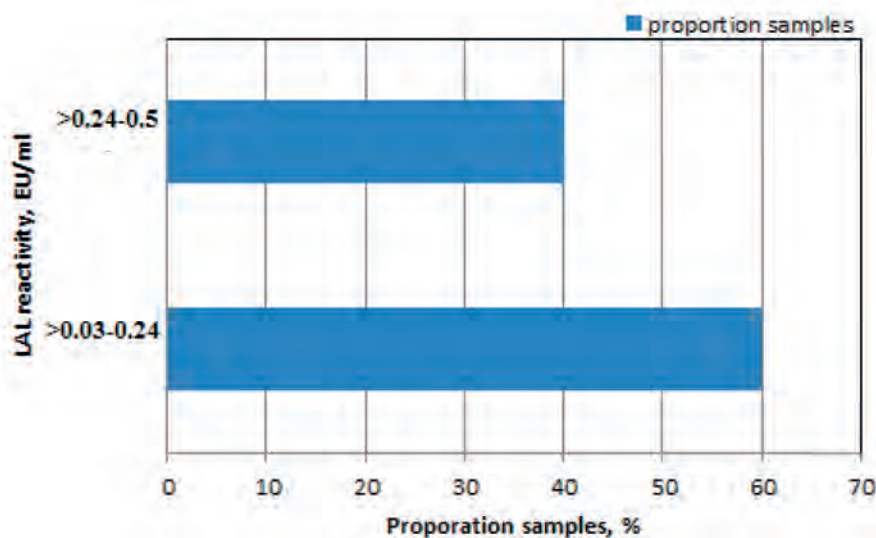
Figure 1. Endotoxin levels in dialysis water of several hemodialysis centers in Iraq.
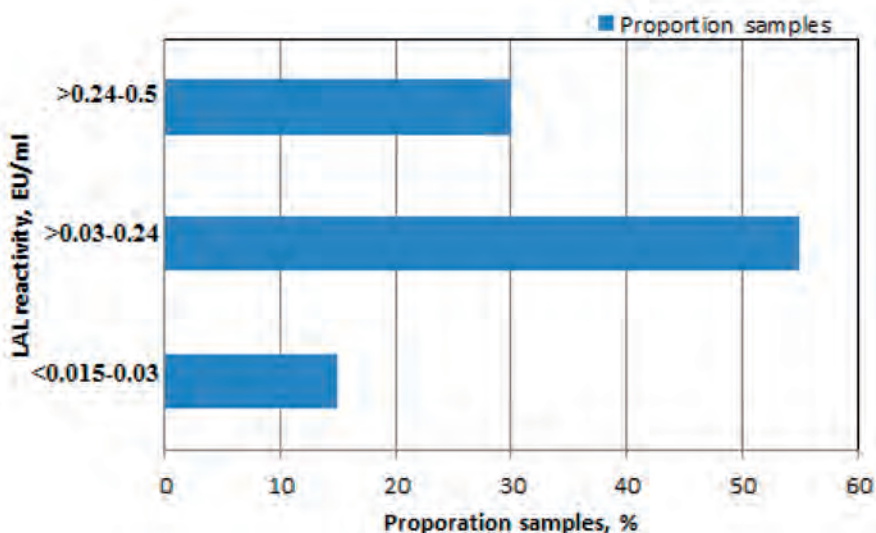
Figure 2. Endotoxin levels in dialysate of several hemodialysis centers in Iraq.

viewed as a potential restriction, given the study's primary goal was not to evaluate clinical symptoms of endotoxemia and inflammatory reactions, which could be investigated further in future studies. This problem was previously addressed in determining the level of endotoxin in hemodialysis patients and its function in generating inflammation[14-16].

Conclusions

Dialysis water should consider a medicinal product by nephrologists. Furthermore, every effort should be taken to guarantee a high-quality liquid. To avoid the formation of bacterial endotoxins, regular disinfection of the entire fluid path is essential, and endotoxin testing should be included in the standard quality control survey.

Acknowledgments

Conflicts of Interest

The author has no conflicts of interest to declare.

Bibliographic references

1. Ahmad, S. Essentials of water treatment in hemodialysis. Hemodialysis International. 2005; 9(2) 127-134.
2. Coulliette, AD. and Arduino, MJ. Hemodialysis and water quality. In Seminars in dialysis. 2013; 26(4) 427-438.
3. Miyamoto, T., Okano, S. and Kasai, N. (2009). Inactivation of Escherichia coli endotoxin by soft hydrothermal processing. Applied and Environmental Microbiology; 2009;75(15). 5058-5063.
4. Humudat, YR., Al-Naseri, SK. and Al-Fatlawy, Y. Assessment of microbial contamination levels of water in hemodialysis centers in Baghdad, Iraq. Water Environment Research; 2020; 92(9)1325-1333.
5. Hoenich, NA. Disinfection of the hospital water supply: a hidden risk to dialysis patients. Critical Care. 2009; 13(61-2.
6. Humudat, YR. Evaluating dialysis fluids properties and its effects on hemodialysis patients at several hospitals in Baghdad. Thesis. Collage of science-University of Baghdad .2020.
7. Gaibor NG, Sacaluga LG, de la Cerda Ojeda F, Cotén JR, Lazo MS. Thermal disinfection in hemodialysis using the A0 concept as dispenser. Nefrología (English Edition). 2019;39(5):482-8.
8. ANSI/AAMI/ISO 23500. American National Standard Institute:Preparation and quality management of fluids for haemodialysis and related therapies. Arlington, Virginia: Association for the Advancement of Medical Instrumentation. 2019.
9. Wako-pyrostar. <85> Bacterial endotoxin test. 2012; 1-36.
10. Iraqi Ministry of Health. . Annual statistical report 2019. Republic of Iraq, Ministry of Health and Environment. 2020; 1-202.
11. Al□Naseri, SK., Mahdi, ZM. and Hashim, MF. Quality of water in hemodialysis centers in B aghdad, I raq. Hemodialysis International. 2013;17(4) 517-522.
12. Penne EL, Visser L, Van Den Dorpel MA, Van Der Weerd NC, Mazairac AH, Van Jaarsveld BC, Koopman MG, Vos P, Feith GW, Hovinga TK, Van Hamersvelt HW. Microbiological quality and quality control of purified water and ultrapure dialysis fluids for online hemodiafiltration in routine clinical practice. Kidney international. 2009 ;76(6):665-72.
13. Skarupskienė, I., Bumblytė, IA., Tamošaitis, D., Venterienė, J and Kuzminskis, V. The level of endotoxins in hemodialysis water and dialysate in Lithuanian hemodialysis centers. Medicina,. 2010; 46(8) 556-560.
14. Abbass, AA., El-Koraie, AF., Hazzah, WA., Omran, EA., and Mahgoub, MA. Microbiological monitoring of ultrapure dialysis fluid in a hemodialysis center in Alexandria, Egypt. Alexandria journal of medicine.; 2018; 54(4) 523-527.
15. Humudat, YR., Al-Naseri, SK. and Al-Fatlawy, YF. Assessment of inflammation, comorbidity and demographic factors in patients with Kidney disease in Baghdad. Iraqi journal of science.; 2019; 60,2418-2425.
16. El-Koraie , AF., Hazzah , WA., Abbass , AA., and El-Shazly, SA. Bacteriological monitoring of dialysis fluid in 2 hemodialysis units in Alexandria, Egypt. Saudi medical journal. 2007; 28(8),1234.

3

Isolation and identification of intestinal parasites from Goats in some areas of Wasit Province, Iraq

Zainab A.Makawi

Iraq Natural History Research Center and Museum, University of Baghdad, Iraq.
Corresponding author: zainab@nhm.uobaghdad.edu.iq

Abstract: The current study was conducted on goats in various parts of Wasit Province, Iraq, from November 2021 to April 2022. The study aims to find and identify intestinal parasites (IPs) in goats in Wasit province. The goat's fresh fecal specimens (n=180) include cysts, eggs, oocysts, trophozoites and larval stages. One hundred eighty sheep feces samples were collected, and more than one parasite was isolated from one sample (mixed infection). According to the data acquired, the overall prevalence of intestinal parasites in goats was 52.77 (95 samples). In the current investigation, eleven distinct (IPs) species with infection rates were identified, including *Toxocara vitulorum* (Goeze, 1782) (16.66 %), *Cryptosporidium sp.*(Tyzzer, 1907) (11.11%), *Amoeba sp.* (8.8%), *Giardia sp.*(Künstler, 1882) (8.8%), *Trichostrongylus sp.*(Looss, 1905) (8.33%), *Cyclospora sp.* (Schneider, 1881) (5.55%), *Dicrocoelium dendriticum* synonym (Distoma dendriticum) (Rudolphi, 1819) (5%), *Paramphistomum cervi* (Zeder, 1790) (4.44%), cercaria larva (2.22%), *Balantidium coli* (Malmsten, 1857) (1.66%), filariae form larvae (1.66%), respectively. This may be the result of infection with various parasites due to the use of Conventional and unsanitary management systems

Key words: Intestinal Parasites, Goats, *Toxocara vitulorum*, *Cryptosporidium spp.*

Introduction

The domestic goat was one of the first animals that humans domesticated. They are found all across the planet, with higher abundance in tropical and dry zones[1]. Gastrointestinal parasitism is one of the most severe diseases affecting goats, particularly nematode infections, among the most significant health issues limiting the animal's productivity[2,3]. However, parasites such as trematode (fluke) and cestode (tapeworm) may also contribute to harmful worm burdens in animals[4]. Protozoan infections such as amoebiasis, giardiasis, and coccidiosis have been documented in Thailand, Costa Rica, and India[5,6]. The distribution of most parasitic diseases has been linked to environmental conditions and vector abundance. Gastrointestinal parasites are ubiquitous in temperate and tropical regions but are more prevalent in warm areas with inadequate sanitation and low living standards[7]. The diversity of parasites affects animal health and causes substantial economic losses to the cattle business. It poses a major health risk and a barrier to small ruminant productivity because of the related morbidity, mortality, treatment costs, and control measures[8]. Small ruminant nematode infections cause low production due to stunted growth, poor weight increase, and poor feed consumption[9]. However, the few available studies on isolating intestinal parasites in goats are uncommon in some areas of Wasit Governorate. As a result, the current study aimed to verify the isolation and identification of infection of goats with intestinal parasites raised in these areas.

Materials and methods

This survey was carried out in Wasit province between November 2021 till April 2022. Fecal samples (n=180) of goats were collected and preserved in transparent, clean, dry, tight-cover sampling containers. Each container was tagged with the relevant data, such as number, time, and date, and maintained in an ice box before being moved to the Natural History Research and Museum Center at the University of Baghdad. The samples were examined microscopically, and parasite data were recorded and maintained at 4 C° until the laboratory exams were completed within 24 hours. The collected fresh feces specimens were tested individually for identifying intestinal parasites utilizing concentration methodology by employing Sugar/salt solution and sedimentation protocol, as reported by (10, 11). In brief, direct smears for eggs/oocysts/ trophozoites were prepared, as well as a sedimentation protocol for eggs and helminths and a flotation method (Scheathers solution) for the detection of nematode eggs and protozoan oocysts.

Results

The overall prevalence of intestinal parasites in goats was 52.77 % over the study period (95 of 180). In Al-Suwaira, the infection rate was 55 percent, while in Al- Shaihemiyh, the infection rate was 50 % (Table 1). This shows the eggs, cysts, oocysts, and larvae of intestinal parasites found in this investigation (Table 2) (Figureures 1 to 11). It included the following: *Toxocara vitulorum* (16.66%), *Cryptosporidium sp.* (11.11%), *Amoeba sp.* (8.8%), *Giardia sp.* (8.8%), *Trichostrongylus sp.* (8.33%), *Cyclospora sp.* (5.55%), *Dicrocoelium dendriticum* (*Distoma dendriticum*) (5%), *Paramphistomum cervi* (4.44%), cercaria (2.22%),

Balantidium coli (Malmsten, 1857) Stein, 1863 (1.66%), filariae form larvae (1.66%), respectively. The infection rate with intestinal parasites, according to months recorded higher infection rate was (70%) in April, while the lower infection rate was (33.33%%) in December (Table 3). Analysis of the data based on sex revealed females higher infection rate than males, as recorded in females (54.63%) and males (50.60%) (Table 4). The data on mixed intestinal parasite infections shows that most investigated goats had mixed conditions (Table 5). Generally, the highest double illnesses among (*Toxocara vitulorum* + *Cryptospordium sp*) with a rate (of 2.22%), while the lowest mix infection was recorded between) *Toxocara vitulorum* + *Giardia sp*) with a rate (of 1.11%).

Discussion

Out of the 180 goat fecal samples were collected (one sample for each animal). From the goats examined, 95 (52.77%) were found positive for one or more parasites from Wasit province. The overall higher prevalence of intestinal parasite infection in the areas studied could be attributed to lower host immunity as a result of malnutrition; grazing of young and adult animals together in poorly drained land provide an ideal environment for the transmission of endoparasite eggs to build up a clinical infestation of the host; this finding is consistent with the findings of many other researchers[12,13].

2

Area	No. of Samples Examined	No. of positive	prevalence (%)
Al-Suwaira	60	33	55%
Al-Aziziyah	60	32	53.33%
Al- Shaihemiyh	60	30	50%
Total	180	95	52.77%

Table 1. The prevalence rate of intestinal parasites in goats in the area.

Intestinal parasite	No. of Samples Examined	Phase	No. of positive	prevalence (%)
Toxocara vitulorum		Egg	30	16.66%
Cryptosporidium sp		Oocyst	20	11.11%
Amoeba sp		Cyst	16	8.8%
Giardia sp		Cyst	16	8.8%
Trichostrongylus sp	180	Egg	15	8.33%
Cyclospora sp		Oocysts	10	5.55%
Dicrocoelium dendriticum(Distoma dendriticum)		Egg	9	5%
Paramphistomum cervi		Egg	8	4.44%
Cercaria		larvae	4	2.22%
Balantidium coli		Cyst	3	1.66%
Filariae		larvae	3	1.66%

Table 2. The prevalence rate with intestinal parasites isolated from 180 fecal samples of goats.

Months/2021	No. of Samples Examined	No. of positive	prevalence (%)
November	30	16	53.33%
December	30	10	33.33%
January	30	15	50%
February	30	15	50%
March	30	18	60%
April	30	21	70%
Total	180	95	52.77%

Table 3. The prevalence rate with intestinal parasites according to months of study.

Sex	No. of Samples Examined	No. of positive	prevalence (%)
Male	83	42	50.60%
Female	97	53	54.63%
Total	180	95	52.77%

Table 4. The prevalence rate with intestinal parasites according to the gender of the goat.

Mix infection	No. of Samples Examined	No. of positive	prevalence (%)
Giardia sp + *Cryptospordium sp*		3	1.66%
Toxocara vitulorum + *Giardia sp*	180	3	1.11%
Toxocara vitulorum + *Cryptospordium sp*		4	2.22%

Table 5. Prevalence of mixed infection intestinal parasite in goat.

3

Figure 1. Oocyst of *Cryptosporidium sp.*

Figure 2. Cyst of *Amoeba sp.*

Figure 3. Cyst of *Giardia sp.*

Figure 4. Egg of *Toxocara vitulorum*.

Figure 5. Egg of *Paramphistomum cervi.*

Figure 6. Egg of *Distoma dendriticum*.

Figure 7. Egg of *Trichostrongylus sp.*

Figure 8. Oocysts of *Cyclospora sp.*

4

Figure 9. Cyst of *Balantidium coli*.

Figure 11. *Filariae*.

According to the data, the prevalence rate of infection with an intestinal parasite is high. It included: *Toxocara vitulorum* (16.66%), *Cryptosporidium spp* (11.11%), *Amoeba sp* (8.8%), *Giardia sp* (8.8%), *Trichostrongylus sp* (8.33%), *Cyclospora sp* (5.55%), *Dicrocoelium dendriticum* (*Distoma dendriticum*) (5%), *Paramphistomum cervi* (4.44%), cercaria larva (2.22%), *Balantidium coli* (1.66%), Filariae form larvae (1.66%), respectively. This study agreed with (14), who found the highest prevalence of Gastrointestinal parasites in goats (91.55 %) in Kirkuk province, Iraq. And (15) found that infection of goats with gastrointestinal parasites was (81.81 %) in Diyala Province, Iraq. In the current study, the lowest infection rate was observed in December (33.33 %), while the highest was in April (70 %). This study is similar to others[8,16,17], which found that the wet months had a higher incidence of infection than the winter months. Maybe a related reason is that reduced grazing hours also reduce the chances of contact between the host and parasites, leading to lower prevalence in the winter season. Further, inclement environmental conditions in winter resulting reduced egg production. According to sex this study recorded infection in females more than in males, agreed with (18), who attributed this variation to a physiological status like pregnancy/ lactation, which causes a dip in natural body resistance in goats against parasites. While (19) and (16) also reported a higher prevalence of gastrointestinal parasites in females than in males. (20) and (21), on the other hand, demonstrated that animal sex did not affect the prevalence of gastrointestinal parasites in small ruminants. In contrast to the current findings, (22) found that males had a higher prevalence and intensity of infection than females. The presence of mixed infection with the gastrointestinal parasites in this study has previously been reported in these animal species[13-15,23]. Perhaps the reason is that goats are

Figure 10. *Cercaria larvae*.

managed in Conventional systems in which large numbers of animals are routinely kept together. This could be due to increased pasture contamination or to poor sanitation and reduced immunity. This may increase the prevalence of intestinal parasites among the animals.

Conclusions

The current study identified several species of intestinal parasites found in goats in Wasit province. This is a significant issue for livestock. As a result, a serious strategy is needed to prevent the spread of more intestinal parasites among local goats And other animals (sheep & cattle) because many parasites may be transmitted between these animals. Furthermore, studies on intestinal parasites in various parts of the country are needed to assess their importance as a source of health hazards. To reduce the parasite burden, some control measures for gastrointestinal parasites in small ruminants must be implemented. Grazing fields should be kept clean and free of animal feces and urine. Education of goat owners on the process of transmission and the influence of these parasites on farm animal productivity should be done regularly.

Acknowledgments

Conflicts of Interest

The authors declare no conflict of interest.

Bibliographic references

1. Di Cerbo, A.R; Manfredi, M.T; Zanzani, S. ; Stradiotto, K. Gastrointestinal infection in goat farm in Lombardy (Northern Italy): Analysis on community and spatial distribution of parasites. Small Ruminants Research, (2010). 88: 102–112.
2. Dimander, SO; Hoglund, J; Sporndly, E; Waller, P.J. The impact of internal parasites on the productivity of young organically reared on semi-natural pastures in Sweden. Veterinary Parasitology, (2000). 90:271-284.
3. Johannes, C; Johan, H; Georg, V.S; Pierre, D; Jozef, V. Gastrointestinal nematode infections in adult dairy cattle: Impact on production, diagnosis and control. Veterinary Parasitology, (2009). 164: 70-79.

4. Rahmann, G ; Seip, H. Alternative strategies to prevent and control endoparasite diseases inorganic sheep and goat farming systems–a review of current scientific knowledge. Ressort forschung furden Okologischen Landbau, (2006). 49-90.

5. Jimenez, AE; Montenegro, V.M; Hernandez, J; Dolz, G; Maranda, L; Galindo, J. Dynamicsof infections with gastrointestinal parasites and Dictyocaulus viviparus in dairy and beef cattle from Costa Rica. Veterinary Parasitology, (2007). 148(3-4): 262-271.

6. Kaur, H; Kaur, D. Prevalence of gastrointestinal parasites in domestic animals of Patiala and its adjoining areas. Journal of Veterinary Parasitology, (2008). 22(2): 25-28.

7. 7-Schmidt, G. D; Roberts, L. S; Janovy, J. Foundation of Parasitology. McGrawhill, Boston, Massachusetts,. Science, (2000). pp670.

8. 8-Nwosu, CO; Madu, PP; Richards, W.S. prevalence and seasonal changes in the population of gastrointestinal nematodes of small ruminants in the semi-arid zone of North-Eastern Nigeria. Veterinary Parasitology, (2007) . 144: 118–124.

9. 9-Pedreira, J; Silva, A.P; Andrade, R.S;Suarez, J.L; Arias, M; Lomba, C; Diaz, P; Lopez, C; Banos, P.D ; Morrondo, P. Prevalence of gastrointestinal parasites in sheep and parasite control practices in North-West Spain. Preventive Veterinary Medicine, (2006) . 75: 56-62.

10. 10-Benson, HJ "Microbiological Application: Laboratory Manual in General Microbiology, Short Version",(2002). Eighth Edition, McGraw Hill, Boston MA, USA.

11. 11-Hendrix, C. M; Robinson, E. "Diagnostic Parasitology for Veterinary Technician", (2006). Third Edition, Elsevier Mosby, St. Louis, U.S.A.

12. 12-Asif, M; Azeem, S; Asif, S; Nazir, S. Prevalence of gastrointestinal parasites of sheep and goats in and around Rawalpindi and Islamabad. Pakistan J. Vet. Anim. Sci. (2008) .(1): 14-17.

13. 13-Gadahi, JA; Arshed, M.J; Ali, Q; Javaid, SB; Shah, S.I. Prevalence of gastrointestinal parasites of sheep and goat in and around Rawalpindi and Islamabad. Pakistan Veterinary World, (2009) . 2(2):51-53.

14. 14-Hassan, HF; Barzinji, A.K. Prevalence of Ruminants Gastrointestinal Parasites in Kirkuk province, Iraq, (2018). 13(3): pp. (96-108)

15. 15-Minnat, TR Detection of gastrointestinal parasite infection of sheep and goats in Diyala Province-Iraq. AL-Qadisiya Journal of Vet. Med. Sci. (2014). 13 (2): 118-123

16. 16-Sharma, DK; Agrawal, N; Mandal, A; Nigam, P; Bhushan, S. Coccidia and gastrointestinal nematode infections in semi-intensively managed Jakhrana goats of semi-arid region of India. Tropical and Subtropical Agroecosystems, (2009). 11: 135- 139.

17. 17-Singh, AK; Das, G; Roy, B; Nath, S; Naresh, R; Kumar, S. Prevalence of gastrointestinal parasitic infections in goat of Madhya Pradesh, India. J. Parasit. Dis., (2015). 39:716-719.

18. 18-Agrawal, N; Sharma, D.K; Mandal, A; Rout, PK; Kushwah, Y.K. Dynamics of faecal egg count in natural infection of Haemonchus Spp. in Indian goats. Vet. World, (2015). 8: 38-41

19. 19-Maqsood, M; Iqbal, Z; Chaudhry, A.H. Prevalence and intensity of haemonchosis with reference to breed, sex and age of sheep and goats. Pak Vet. J., (1996). 16 (1): 41–43.

20. 20-Fikru, R; Teshale, S; Reta, D; Yosef, K. Epidemiology of gastrointestinal parasites of ruminants in Western Oromia, Ethiopia. Int. J. Appl. Res. Vet. M., (2006). 4: 51-57.

21. 21-Tefera, M; Batu, G; Bitew, M. Prevalence of gastrointestinal parasites of sheep and goats in and around Bedelle, South-western Ethiopia. Int. J. Vet. Med., (2009). 8(2): 1-6.

22. 22-Ayaz, MM; Raza, M.A; Murtaza, S; Akhtar, S. Epidemiological survey of helminths of goats in southern Punjab, Pakistan. Trop. Biomed., (2013). 30: 62-71.

23. 23-Bhat, S.A; Rahman Mir, M.U; Qadir, S; Allaie, I.M; Khan, H.M; Husain, I; Sheikh, B.A. Prevalence of gastrointestinal parasitic infections in Sheep of Kashmir valley of India J. Vet. World. (2012) . 5(11):667- 671.

5

ARTICLE / INVESTIGACIÓN

Cost and performance analysis of efficiency, efficacy, and effectiveness of viral RNA isolation with commercial kits and Heat Shock as an alternative method to detect SARS-CoV-2 by RT-PCR

Luis Enrique Calvo Chica[1], Fabian Aguilar-Mora[1,2], Lenin Javier Ramirez Cando[3], Carolina Proaño-Bolaños[1], Andrea Carrera-Gonzalez[1]*

DOI. 10.21931/RB/2023.08.01.40

[1] Faculty of Life Sciences, Universidad Regional Amazonica Ikiam, Tena, Ecuador.
[2] Consejo Nacional de Investigaciones Cientificas y Tecnicas (CONICET), Mendoza, Argentina.
[3] School of Biological Sciences and Engineering. Yachay University for Experimental Technology and Research, Ecuador.
Corresponding author: acarrera88@gmail.com

1

Abstract: In late 2019 a new virus reported in Wuhan, China, identified as SARS-CoV-2, rapidly challenging the healthcare system worldwide. The need for rapid, timely and accurate detection was critical to the prevention of community outbreaks of the virus. However, the high global demand for reagents during the years 2020 and 2021 generated a bottleneck in kits used for detection, significantly affecting developing countries and lagging their ability to diagnose and control the virus in the population. The difficulty in importing reagents, high costs and limited public access to the SARS-CoV-2 detection test led to the search for alternative methods. In this framework, different commercial nucleic acid extraction methodologies were evaluated and compared against heat shock as an alternative method for SARS-CoV-2 detection by RT-PCR to determine the diagnostic yield and its possible low cost compared to other methodologies. Nasopharyngeal samples were used where the diagnostic efficiency of the alternative method was 70 to 73%. The evaluation of the discriminatory efficacy of the technique took the sensitivity and specificity to establish its cut-off point, being 0.73 to 0.817, which allows discrimination between COVID-19 positives and negatives; as for the diagnostic effectiveness expressed as, the proportion of subjects correctly classified is between 80 and 84%. On the other hand, in terms of the costs necessary to carry out the detection, the alternative method is more economical and accessible compared to the commercial methods available in this comparison and evaluation, being possible its implementation in developing countries with high infection rates, allowing access to the diagnostic test with a reliable and low-cost method.

Key words: COVID-19, RT-PCR, Viral RNA.

Introduction

Coronaviruses (CoV) are part of Coronaviridae family with unsegmented single-stranded positive RNA genome belonging 26 to 36 kb length with wide host range, including humans[1-3]. In the history of humankinds have experienced previus infection, during the 1960s CoV-virus have been describe beta-coronavirus like OC43-CoV and HKU1-CoV, and alfa-coronavirus like 229E-CoV and NL63-CoV. Currently are endemic, causes of common colds and mild respiratory infections4. In the last two decades, two beta-coronavirus caused of respiratory illnesses have been monitored, be-tween 2002/2003 the severe cute respiratory syndrome-related human coronavirus 1 (SARS-CoV), and 2012 the middle east respiratory syndrome-related coronavirus (MERS-CoV) both of them produced severe respiratory syndrome[3,5-7]. The novel coronavirus SARS-CoV-2 was reported in Wuhan, China, in December of 2019. SARS-CoV-2 cause COVID-19 challenged the health public system worldwide and genetic sequencing of the virus suggest that SARS-CoV-2 closely linked to SARS-CoV-1, affecting more than 180 countries[8-10]. The most widely used test for detection of SARS-CoV-2 fall into nucleic-acid test, as a multistep that involves, nasopharyngeal swab sample collection, isolation of viral genetic material and Reverse Transcriptase Polymerase Chain Reaction (RT-PCR)[10-13].

During the first few weeks of the COVID-19 pandemic, the global demand for nucleic acid extraction kits and required reagents had already in short supply, making them a limiting source for SARS-CoV-2 testing due to those kits are mainly produced in industrialized countries, which means a disadvantage in the access to COVID-19 testing. Consequently, being a challenge for middle and low-income countries in need of improving SARS-CoV-2 testing fueling the development of alternative SARS-CoV-2 RNA isolation methods and protocols[10,12-16]. Most European countries and the United States have to deal with the accelerated growth of infections and enormous pressure on their health systems, where cases started to grow exponentially[17].

In the case of Latin American countries, their first cases were registered between the end of February and the beginning of March 2020, with Brazil reporting the first cases in the region. COVID-19 poses a significant risk in Latin American countries because countries share many economic, political and health system similarities in controlling COVID-19 outbreaks and deaths[17-19], but the number of IUC beds, prepared medical workers and the robust or fragile public health system between each country created a framework of

2

differences of how control the outbreaks of COVID-19[18-20]. During the implementation of COVID-19 prevention and control measures, the nature and stringency of the response varied from each country based on closed international borders and declaring a national health emergency to ordering a curfew. Despite measures taken in response to the first cases of COVID-19 in Latin America, widespread testing is a crucial strategy to control the spread of the pandemic[19,20]. The need for rapid and accurate detection of SARS-CoV-2 was critical for the prevention and control of communitarian outbreaks. For this reason, the immediate availability of the complete genome of SARS-CoV-2 allowed the development of diagnostic kits employing the Reverse Transcription Polymerase Chain Reaction (RT-PCR) for specific regions of the SARS-CoV-2 genome[1,8,21,22]. The standard molecular method was developed based on the US Center for Disease Control and Prevention (CDC), Charite and World Health Organization (WHO), based on the amplification of specific regions of viral gene N, E and RdRp and the purified RNA isolated from the nasopharyngeal sample[10,23-25].

Nevertheless, the increasing number of tests that were performed worldwide has created a high demand for reagents necessary for SARS-CoV-2 detection, mainly during March-July of 2020In addition, the high need for these reagents has caused a shortage of this product, forcing the public and private health sector in Latin America to prioritize test only for people who have symptoms and signs of COVID-19 increasing the bias, to be left behind in COVID-19 diagnosis and control[21,26-28].

Several commercial SARS-CoV-2 RT-PCR protocols employ manual extraction kits to isolate viral RNA from nasopharyngeal swabs[23,29,30], whereby an accurate extraction, recovery and quantification determine the efficacy of RT-PCR detection[8,31]. The more common methods for viral isolation are (1) silica-based membrane[13,32], also called solid-phase RNA extraction; (2) organic extraction using phenol-guanidineIsothiocyanate (GITC) and (3) magnetic beads[12,33]. All these methods allow cell and viral lysis using registered reagents by trademarks, which has made them a limiting resource for SARS-CoV-2 diagnosis, mainly in the peaks of contagious in the middle of 2020 and 2021[12,34].

The virus's rapid spread in Latin America and the high cost of COVID-19 tests due to shortage of supplies and reagents limits testing access. In March 2020, the cost of the RT-PCR test in Ecuador was between 80 to 120 USD. Later, in June 2021, the cost was reduced to 45 USD[35,36]. This value of 45 USD, according to Trudeau, represents 4.2% of the average monthly income of a middy-class person who would be willing to pay in Latin America in latent demand for COVID-19 tests, concerning other countries where the charges made by private's labs at the beginning of the pandemic scale of up to $70 in Brazil, $140 in Chile, $80 in Colombia and $137 in Uruguay[20,37].

Laboratories across the globe face constraints on equipment and reagents during the COVID-19 pandemic. Here, we compare and evaluate a simple approach causing lysis to the cells by heat shock and using the solution directly to RT-PCR[9,21,38]. This methodology could be an alternative to perform a reliable and rapid diagnosis of SARS-CoV-2, compared with the CDC RT-PCR gold standard that takes about 3 hours to complete, particularly for developing countries where all needed reagents for diagnosis must be imported[10]. These approaches can help to access public or private COVID-19 tests at reasonable prices; however, these data reflected the problem of price variability over time

due to high demand and importation paperwork for reagents and kits for testing in a developing country.

Nucleic acid extraction typically involves three general steps: cell lysis, separation of RNA/DNA from other macromolecules such as DNA/RNA, proteins, and lipids, followed by RNA/DNA elution[34]. Several commercial SARS-CoV-2 RT-PCR protocols employ manual extraction kits to isolate viral RNA from nasopharyngeal swabs[24,35,36], whereby an accurate extraction, recovery and quantification determine the efficacy of RT-PCR detection[9,37]. The more common methods for viral isolation are (1) silica-based membrane[14,38], also called solid-phase RNA extraction; (2) or-ganic extraction using phenol-guanidineIsothiocyanate (GITC) and, (3) magnetic beads[13,39]. All these methods allow cell and viral lysis using registered reagents by trademarks that has made them a limiting resource for SARS-CoV-2 diagnose mainly in the peaks of contagious in middle of 2020 and 2021[13,40].

The most common method for nucleic acid extraction uses Silica-based membrane technology, which relies on the ability of silica particles to adsorb DNA/RNA molecules under certain analytical conditions, and then eluted RNA precipitation using elution special buffers or nuclease-free water[11,34,38]. Another technique for RNA isolation requires the use of magnetic particles, that has several advantages based on (a) hydrogen-binding interaction with an underivatised hydrophilic matrix, typically silica, under chaotropic conditions, (b) ionic exchange under aqueous conditions by means of an anion exchanger, (c) affinity and (d) size exclusion[41]. Although there are numerous ways to extract and isolate RNA, most labs gravitate toward using organic extractions or com-mercially available kits. Acid guanidinium thiocyanate-phenol-chloroform is ongoing used to obtained nucleic acids, where the pH will determine the separation of nucleic acids and proteins. Polar RNA will remain in the upper polar phase, DNA will accumulate in the interphase and de-natured proteins will dissolve in the lower organic phase[34,42-44]. In the face of shortage of kits, re-agents and consumables; it is clear that a huge effort needs to be made to scale up current COVID-19 testing, thus is needed to evaluate alternative protocols, reagents, and approaches to allow a good nucleic-acid isolation for molecular detection of SARS-CoV-2. One of these ap-proaches used is heat-shock technique, that allows free-RNA extraction without purification that can be used directly in RT-PCR.

Considering the context of developing countries, high selling prices and access limitation to the public health system, our aim was to evaluate and compare the efficiency, efficacy and effec-tiveness of using commercial kits with the heat shock as method for extraction of genetic material for molecular detection of SARS-CoV-2 by RT-PCR, in order to propose a low-cost and reliable method.

Materials and methods

The samples were obtained from the project "Molecular diagnosis of SARS-CoV-2 in suspected COVID-19 samples from the Amazon region". In which the guidelines The Strengthening the Reporting of Observational Studies in Epidemiology (STROBE) and the Ecuadorian law of data protection were foll dological analysis. The samples were employed after the diagnosis report was released to the MSP personnel.owed to carry out this observation, wherein no patient data have been included since it is a method.

Samples collection

A nasopharyngeal swab was the reference sampling method used to detect SARS-CoV-2, collected by health-care personnel using synthetic fibber swabs according to World Health Organization (WHO) general guidelines for respiratory sample collection. The samples were stored in 2 mL microtubes with 700 µL of Tris-EDTA buffer, pH 8.0 (46). Samples were received from Molecular Biology and Biochemistry laboratory at Universidad Regional Amazónica Ikiam, the inclusion/exclusion criteria for samples reception were: (1) transportation at 4 °C, (2) triple sealing for samples (collection tube with biofilm in caps, bio-safe bag and external box), (3) epidemiological information of patients, and (4) the samples should not be spilled.

Viral RNA extraction methods

Viral RNA extraction was performed using five different commercial kits, based on their four other technologies, following manufacturers' instructions with minor modifications. A total of 72 samples were selected (Figure 1). The five commercial kits were classified according to the purification method used to isolate viral RNA (Table 1).

The kits were named A, B, C, D, E and F. 35 samples were used with kits A, B and C, while 37 were analyzed with kits D, E, and F. One negative control (nuclease-free water)

Kit	Description of purification method	Required sample volume	RNA elution volume	Processing time	Number of isolated samples
Kit A	Lysis type: Manual lysis using virus binding buffer and proteinase K. Purification method: Silica membrane-based RNA resuspension: Elution Buffer	200 µL	50 µL	2-3 h	Set of 35 samples
Kit B	Lysis type: Manual lysis using guanidine salts Purification method: Silica membrane-based RNA resuspension: Elution buffer	140 µL	60 µL	2-3 h	Set of 35 samples
Kit C	Lysis type: Manual lysis using Viral RNA buffer Purification method: Silica membrane-based RNA resuspension: RNA – free water	200 µL	15 µL	1-2 h	Set of 35 samples
Kit D	Lysis type: Manual lysis by magnetic beads-based Purification method: complementary hybridization between nucleic acid and beads RNA resuspension: RNA-free water	200 µL	50 µL	3-4 h	Set of 37 samples
Kit E	Lysis type: Manual lysis using phenol and guanidine thiocyanate in a mono-phase separation. Purification method: organic phases using chloroform RNA resuspension: RNA – free water	200 µL	-	1-2 h	Set of 37 samples
Kit F	Lysis type: Heat Shock Purification method: N/A RNA resuspension: N/A	10 µL	1 µL	10 min	Set of 72 samples

Table 1. Description of commercial kits to isolate viral RNA according to manufacturers' instruction.
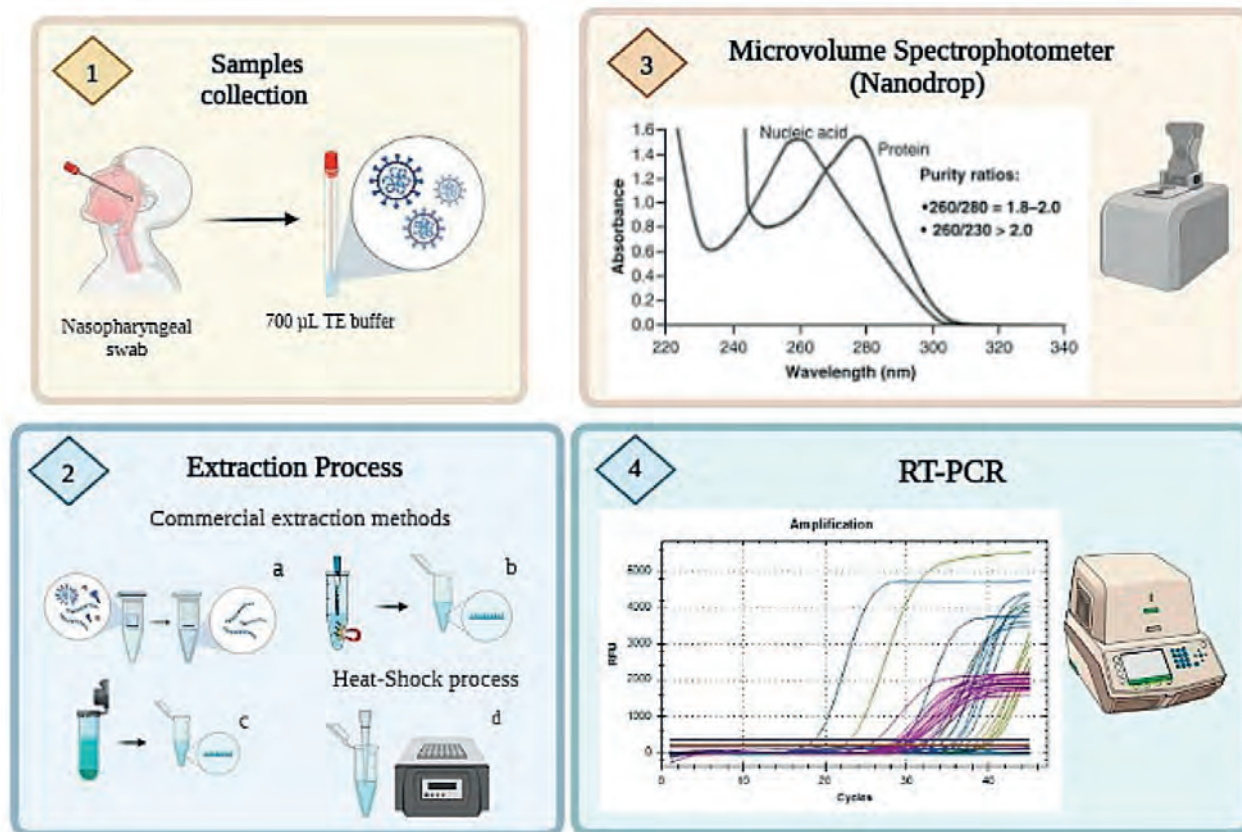
Figure 1. Schematic overview of SARS-CoV-2 RNA extraction and RT-PCR testing procedure. 1). Sample collection. 2). Extraction processes (a.) Silica-based membrane extraction. (b) Magnetic beads extraction. (c.) Mono—phasic organic extraction. (d.) Heat-Shock RNA process. 3). RNA quantification. 4). RNA Amplification by RT-PCR.

was included in each group.

Quantification of viral RNA by Spectrophotometry

The total RNA isolated with the different methods was analyzed to determine the concentration and purity with Na-noDrop™ One/Onec Microvolume UV-Vis Spectrophotometer (Thermo Fisher Scientific, USA). The concentration was obtained in ng/µL of RNA, and purity was calculated using the optical density (OD) ratio at wavelengths of 260/280 and 260/230 (Figure 1). The values used for OD260/280 ranged from 1.8 to 2.0, a good indicator of good-quality RNA, and for OD260/230 in the same range. If these values were out of the range were considered an indicator of organic or chaotropic agents' contamination.

$$Positive \; Likelihood \; Ratio \; = \frac{Sensitivity}{1-Specificity} \quad [1]$$

$$Positive \; Likelihood \; Ratio = \frac{0.700}{1-0.933} = 10.45$$

Heat-Shock of nasopharyngeal swabs samples (kit F)

An alternative extraction method was evaluated in this report, which consisted of an RNA ex-traction using Heat-Shock. The method was performed using stablish samples maintained in re-frigeration at -20 °C, thawed to 4 °C and homogenized, were taken 10 µL of nasopharyngeal swab sample which was heated 95°C for 10 min and then at 4 °C for 10 minutes, until the RT-PCR procedure[10,45-48]. To analyze the alternative method, Bayes' theorem was used to determine the likelihood of sample to be positive, and can be evaluated with Bayesian probability formalism for re-

peated sampling from same patien 11,49 The samples were analyzed by duplicate and triplicate using probability odds conversion for positive likelihood ratio (LR+) [1].

Real-time Retro-Transcriptase Polymerase Chain Reaction (RT-PCR) to detect of SARS-CoV-2

RT-PCR of 72 viral RNA samples was carried out using a commercial one-step detection kit for 2019 Novel Coronavirus (2019-nCoV) RNA (PCR-Fluorescence Probes) by Da An Gene© (Da An Gene Co., Ltda, of Yat-sen University, China) following manufactures' instructions on CFX96 BioRad Touch Real-Time PCR Detection System[2,49,50]. According to the approval of the Chinese Center for Disease Control and Prevention, ORF1ab and N genes were the amplification target regions for SARS-CoV-2 released by WHO to detect SARS-CoV-2 using the PCR kit[51-54]. In addition, this kit includes an endogenous internal standard detection system, which is used for monitoring RNA extraction and PCR amplification, thereby reducing false negative results. The analytical sensitivity of Da An Gene (2019-nCoV) RT-PCR, according to the manufacturer's instruction, was 500 copies/mL as the Limit of Detection(LoD). This kit does not have cross-reaction with other pathogens, including SARS and MERS coronavirus being Open Reading Frame 1ab (ORF1ab) and Nucleocapsid protein (N) target genes in SARS-CoV-2[1,55-57].

Cost analysis

For this report, Activity-Based Costing Model (ABC Model) was performed to analyze the cost of five commercial kits evaluated, including the Heat-Shock reaction (58,59). This analysis was based on elemental material needed to

conduct an RT-PCR response considering direct and indirect costs necessary for the process and their outcome interpretation.

The analysis of the total cost to detect SARS-CoV-2 was established considering (1) direct cost, the raw material (supplies and additional reagents), lab workforce, equipment depreciation, and Personal Protection Equipment (PPE). The cost was obtained through quotes and invoices requested during the years 2020 and 2021.

Statistical analysis

Data such as RNA concentration were represented through the median and interquartile range (IQR), while RNA purity was expressed through the Mean and Standard Deviation (SD) of the optical density (OD) ratio. A non-parametric ANOVA-like Friedman test was applied to analyze the RNA concentration and purity used to detect differences

$$Accuracy = \frac{True\ Positives + True\ Negatives}{True\ Positives + True\ Negatives + False\ Positives + False\ Negatives} \quad [2]$$

$$Sensitivity = \frac{True\ Positive}{True\ Positive + False\ Negative} \quad [3]$$

$$Specificity = \frac{True\ Negatives}{True\ Negatives + False\ Positive} \quad [4]$$

between each extraction methodology.

Accuracy [2], Sensitivity [3] and Specificity [4] were estimated for diagnostic efficiency as indexes using a confusion matrix approach[60-62]. The confusion matrix and confidence interval (95%) were calculated using a diagnostic test evaluation software MedCalc version 20.027 (MedCalc Software Ltd, Ostend, Belgium).). The classification accuracy for SARS-CoV-2 was assessed by the ROC (Receiver Operating Characteristic) curve, which is a useful graphical tool to evaluate the performance of a binary classifier as its discrimination threshold is varied, analysis based on sensitivity as a function of 1-specificity of a diagnostic test, to evaluate the performance of a binary classifier as its discrimination threshold is varied examining the biomarker's discriminative efficacy[61,63], based on how True Positive Rate (TPR) and False Positive Rate (FPR) changes in the classification threshold is varied between infected and non-infected groups.

To summarize and understand the overall discriminative efficacy of the test, the Area Under the Curve (AUC) was used to evaluate the discriminatory effectiveness following the criteria: AUC ranges from 0 to 1, and an AUC of 0.5 suggests no discrimination ability[61]. Although AUC is the most commonly used global index for diagnostic accuracy, the Youden Index, with a range similar to AUC, can provide a

criterion for choosing the "optimal cut-off" value for diagnostic tests[61,64,65]. Finally, a p-value < 0.05 is considered statistically significant in all statistical analyses assessing the kits' effectiveness in isolating SARS-CoV-2 nucleic acids.

For the alternative method to obtain viral RNA (Heat-Shock), Bayes' theorem was used to calculate a posteriori probability based on the confusion matrix results. The idea of a good screening test is a high degree of true positives, high specificity, and a permissive number of false positives. Bayes' theorem allows the provider to convert the results of a test to probability[60,66]. The prevalence, in this calculation, would act as the pre-test or prior probability of disease and combined with the Positive Predictive Value (PPV) would generate a post-test probability for any patient (all-comers) regardless of the individual's risk. Finally, to study the cost necessary to perform a RT-PCR a Multidimensional Scaling was implemented to create a map, which displayed the relative position of variables, given a proximity matrix[67].

Results

RNA Quantification

The RNA extraction yield was calculated based on the median, and visually comparable in Figure 2. The latter was expressed on the mean ratio (OD260/280) as it is represented in Table 2 and Figure 3, where the Friedman test was used to analyze concentration and purity comparing differences of independent but repeated and related variables measure. The average concentration of the straight set of RNAs for kit A shows values between 10.91 and 96.87 ng/μL and a low-value range of 6.75 to 6.91 ng/μL; kit B values between 45.09 and 162.57 ng/μL, while for an unpurified set of RNAs no presented outcome; kit C values between 10.914 and 327.56 ng/μL, while the unpurified set of RNAs presented with a range between 2.988 and 8.945 ng/μL; kit D values between 16.02 and 615.13 ng/μL, while for an unpurified set of RNAs no presented outcome, and finally for kit E values between 14.95 and 160.66 ng/μL, while for an unpurified set of RNAs no given outcome. In the case of kit, F was excluded because it was not purified and concentrated. In our study, the quantity and purity were estimated in 72 samples which were used for all five kits considered for comparison.

The Friedman test was used to analyze concentration and purity; Friedman compares independent variable diffe-

Name of Kit	RNA concentration (ng/μL)		RNA purity (OD$_{260/280}$)	
	Median (IQR)	p-value (Friedman test)	Mean ± SD	p-value (Friedman test)
Kit A	26.71 (18.26 – 42.94)	<0.001	2.54 ± 0.51	<0.001
Kit B	84.12 (73.69 – 88.33)	<0.001	3.12 ± 0.57	<0.001
Kit C	8.97 (5.64 – 19.68)	<0.001	1.85 ± 0.33	<0.001
Kit D	37.30 (30.00 -53.34)	<0.001	1.87 ± 0.11	<0.001
Kit E	32.26 (26.33 – 48.26)	<0.001	1.86 ± 0.12	<0.001
*Kit F	-	-	-	-

Note IQR: Interquartile Range; SD: Standard Deviation; * Quantification of kit F not assessment by the interference of inside cellular substances produced by heat-shock lysis.

Table 2. The median yield of viral RNA concentration and mean A260/280 OD ratio purity of extracted RNA by six extraction kits.

Luis Enrique Calvo Chica, Fabian Aguilar-Mora, Lenin Javier Ramirez Cando, Carolina Proaño-Bolaños, Andrea Carrera-Gonzales

6
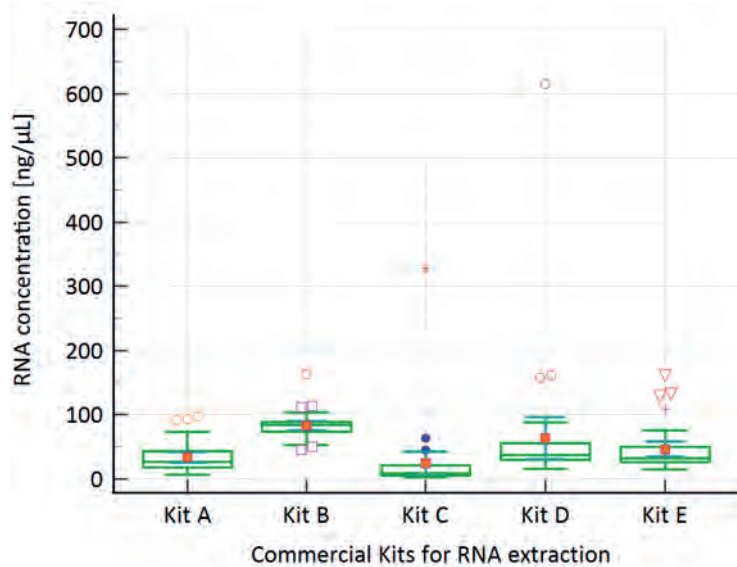
Figure 2. Box-plot of RNA concentration. The use of Friedman's test for concentration was based on the fact that the data failed the ANOVA-MR test. Comparison with each kit shows data with low-dispersion, obtained values that not exceeded in general 100 ng/µL of nucleic acid concentration. Atypical data are seen in all kits; however, kits C (*) and D (o) show extreme outliers compared to each other.
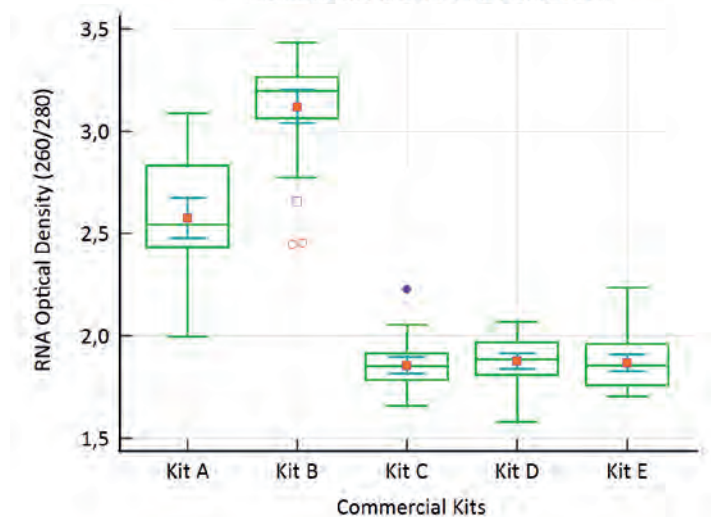
Figure 3. Box-plot of Optical Density. For OD data analyzes, based on the data analysis of concentration, Friedman's test was chosen to visualize the differences between the purity of RNA obtained during the extraction process. Kit A and B shows highest disperse in the interquartile range of the values of each group compared with kit C, D and E, which shows a similar box, low-disperse data and similar mean. In addition, kit B shows extreme outliers, but the nucleic acid purity ratio is better. On the other hand, kit C (•) shows stable values of purity but presents a low outlier compared with kit D and E.

rences for experimental designs involving repeated/related measures. The Friedman test analyzed the observed difference between different kits, and a p-value < 0.001 was considered statistically significant. The concentration and purity of each kit were significantly different from those of the others (Figures 3 and 4).

Heat-Shock inactivation (kit F) analysis

As mentioned above in methodology to evaluate the obtention of nucleic acid using an alternative method called kit F (Heat shock) and use in RT-PCR amplification. Positive Likelihood ratio (LR+) was calculated (LR+= 10.45), and Bayes' theorem uses the LR+ to facilitate the interpretation of a test for a given individual regardless of prevalence by assigning prior probabilities/odds to determine post probabilities/odds for a given data point, in this case, the LR+.

The reach of Bayes' theorem was set in three sceneries: low, moderate, and high pre-test probability of COVID-19 infection according to the exposure grade. To understand the Bayes' theorem, statistical approaches were used, where Individuals in a presumed low prevalence environment would constitute a low pre-test probability between 10–20% of COVID-19 infection, whereas an individual with cough and fever with known cases of COVID-19 may be assigned a moderate pre-test probability 40–60% of disease. A high pre-test probability of 80–90% of COVID-19 may include all known symptoms, with known close contact with confirmed

COVID-19 and an estimated probability pre-test of 22.9% based on data on the prevalence of COVID-19 in the population of Ecuador. For each of these individuals, a positive RT-PCR test result will have different implications, namely post-test odds (which can be converted to a probability for ease of interpretation).

To obtain the pre-test probabilities, LR+ needs to be converted into odds (because LR+ is a ratio of odds) and then to be reverted to possibilities; table 3 and Figure 4 provide a visual gauge of how a LR+ (10.45) changes post-test probabilities based on disease prevalence and a priori probabilities.

RT-PCR analysis

The Da An Gene© kit detects the open reading frame 1a and 1b gene from the region ORF (ORF1ab) and the nucleocapsid protein (N-gene). To validate the results for RT-PCR, the negative control NC (ORF1ab/N) did not show curve for ORF1ab and N genes, but showed an amplification curve for RNAse P gene as internal RT-PCR control, and Ct value under 35 cycles. Positive control PC (ORF1ab/N) showed amplification curves for ORF1ab and N genes, as well as for RNAse P gene as internal control.

To test positive for SARS-CoV-2 in a sample, the result of RT-PCR amplification for ORF1ab gene, N genes, and Ct values need to be under 40 cycles. If the Ct values are up 40 cycles for ORF1ab and N genes, a negative result was

Double sample test				Triplicate sample test			
Pre-test probability	Pre-test odds	Post-test odds	Post-test probability	Pre-test probability	Pre-test odds	Post-test odds	Post-test probability
0.10	0.04	0.42	0.29	0.29	0.41	4.28	0.81
0.20	0.25	2.61	0.72	0.72	2.57	28.85	0.96
0.229	0.30	3.14	0.76	0.76	3.16	33.02	0.97
0.30	0.43	4.49	0.82	0.82	4.55	47.55	0.98
0.40	0.67	7.00	0.88	0.88	7.33	76.60	0.99
0.50	1.00	10.45	0.91	0.91	10.11	105.65	0.99
0.60	1.50	15.68	0.94	0.94	15.66	163.54	0.99
0.70	2.33	24.35	0.96	0.96	24	250.8	0.996
0.80	4.00	41.8	0.98	0.98	49	512.05	0.998
0.90	9.00	94.05	0.99	0.99	99	1034.55	0.999

Note: $odds = \frac{Probability}{1-Probability}$; $Probability = \frac{odds}{odds+1}$; $Post\ test\ odds = pre\ test\ odd \times LR +$

Table 3. Bayesian probabilistic formalism of positive likelihood ratio (LR+) post-test probabilities for low, moderate and high prevalence of COVID-19.
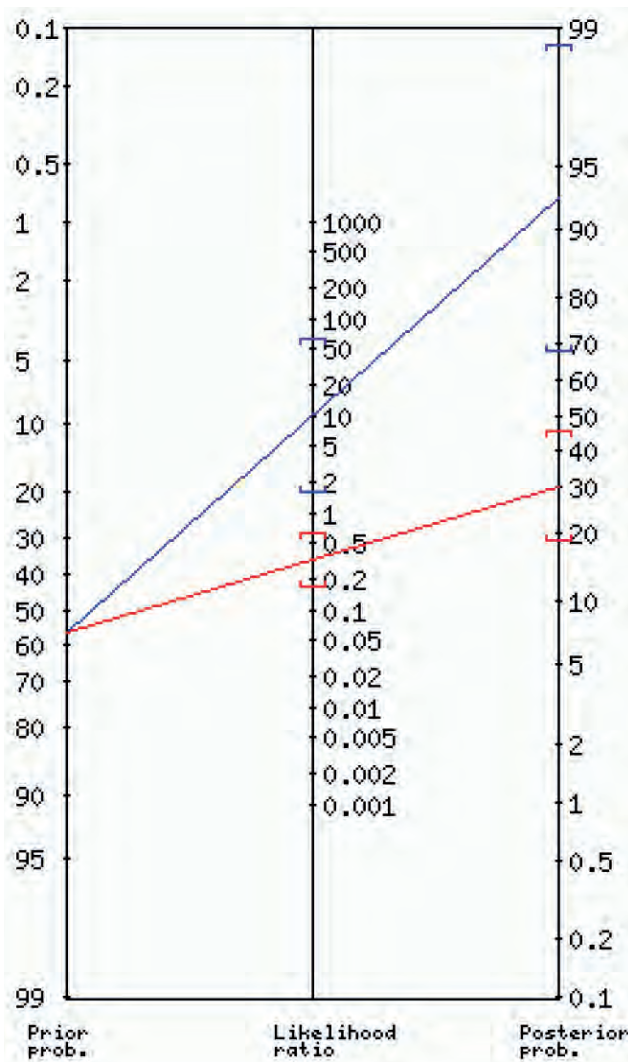
Figure 4. The Fagan nomogram was used to provide a visual estimate of post-test probabilities based on SARS-CoV-2 prevalence and the capacity of evaluate for duplicate and triplicate the samples using heat shock to improve the estimation of a patient's risk of having or contracting the disease when testing positive based on disease prevalence and a priori probabilities. Prevalence, in this graphic and calculation, act as pre-test odd (1.3) or prior pre-test probability (57.14%). For the positive test (blue line), the LR+ was approximately 11 (CI: 1.55 -71), and for the post-test, probability was 94% (odds: 14.7) with CI: 67% -99%. On the other hand, for the negative test (red line), the LR- was 0.32 (CI: 0.16 – 0.64), the post-test probability was 30% (odds: 0.4) with CI: 18% - 46%.

considered. In addition, in both cases the internal control (RNAse P gene) must be presented in amplification curves in RT-PCR. The hole detection time was ap-proximately 90 minutes.

For diagnostic test validation, confirmation of the presence of a disease is important but along with that ruling out the presence of disease in healthy patients, being necessary to care aboid cross contamination of sample and add a control the extraction prior to amplification to reduce false positive an false negatives. Common metrics like accuracy, sensitivity and specificity was calcu-lated using a confusion matrix based on results of True Positives, True Negatives, False Positives and False Negatives. Terms to quantify the diagnostic efficiency and diagnostic effectiveness expres-sed as a proportion of correctly classified samples of any diagnostic test. Table 4 shows the data obtained and used to build a receiver operating characteristic curve (ROC), calculate the area under curve (AUC), and Youden index based on approach as the classification threshold (optimal cut-off point) between the infected and non-infected groups represented in Figure 5.

Cost Analysis for SARS-CoV-2 diagnostic test

An excellent way to analyze the different kits that have been assessed is multidimensional scaling (MDS), a statistical method that provides a graphical representation between objects in multifaceted spaces using distances between them. In cases where the relations between objects are unknown, distances between each other can be calcu-lated. MDS is a technique of interdependence used when any or all of the variables are not dependent and cannot be explained by another when they are involved in the mutual relationship among all variables.

In Figure 6, MDS represents 6 variables (indicators) used in the study of cost analysis between six different methodologies of extraction; the indicators were sensitivi-ty, specificity, direct and indirect cost (for 2020 and 2021), concentration [ng/µL] and Optical Density (A260/280). MDS stress (Goodness of Fit) has been found as 0.9999804 for coordinate 1, and 0.9999804 for coordinate 2, which indi-cates the correct adjustment of latent coordinates created since the original data (indicators), where the grouping and distance adjustment of data concerning coordinate 1 and coordinate 2 indicates a well similarity between each kit, mainly for A, C, D and E by 2020 and considerable similarity by 2021. However, in kits B and F, for 2020 and 2021, there were significant differences between indicators.

In terms of cost, the evaluation of supplements neces-sary for a reaction was divided into direct and indirect costs for the years 2020 and 2021. For kits A and C (Silica-ba-sed), D (magnetic beads) and E (organic extraction), globe cost for the reaction was similar during 2020; meanwhile, for kit B (silica-based), the cost was highest than all methods, values obtained for this evaluation are presented in Table 5. Finally, for kit F, the reaction cost was cheaper than all methods. On the other hand, for 2021, an evident cost re-duction for all kits is appreciable, where the cost of kits A, C, D and E have a clear separation, diverging from each other. However, the economic reduction for kit B is irrelevant since it is still the most expensive at the commercial level. Meanwhile, for kit F the cost for the reaction is more eco-nomical compared to 2020, a method that can be applied for developing countries since its cost allows public access.

Discussion

Around the world, several efforts are being focused on

	Positive samples	Negative Samples	Mean Ct-posi-tive samples	Standard Deviation	Accuracy	Specific-ity	Sensitiv-ity
Kit A	20	15	ORF1ab: 31.89 N: 28.16	ORF1ab: 5.25 N: 5.24	100%	100%	100%
Kit B	18	14	ORF1ab: 35.01 N:31.49	ORF1ab: 6.02 N: 5.66	91%	90%	93%
Kit C	20	14	ORF1ab: 31.24 N:28.83	ORF1ab: 5.71 N: 5.63	97%	93%	100%
Kit D	22	13	ORF1ab: 33.25 N:31.24	ORF1ab: 16.97 N: 16.15	95%	87%	92%
Kit E	18	15	ORF1ab: 32.84 N:27.57	ORF1ab: 10.14 N: 12.62	89%	100%	82%
Kit F	16	15	ORF1ab: 35.39 N:33.04	ORF1ab: 2.23 N: 2.68	82%	93%	70%

Note: Ct: Cycles threshold; SD: Standard deviation

Table 4. Comparison of accuracy, specificity and sensitivity for different RNA extraction kits.
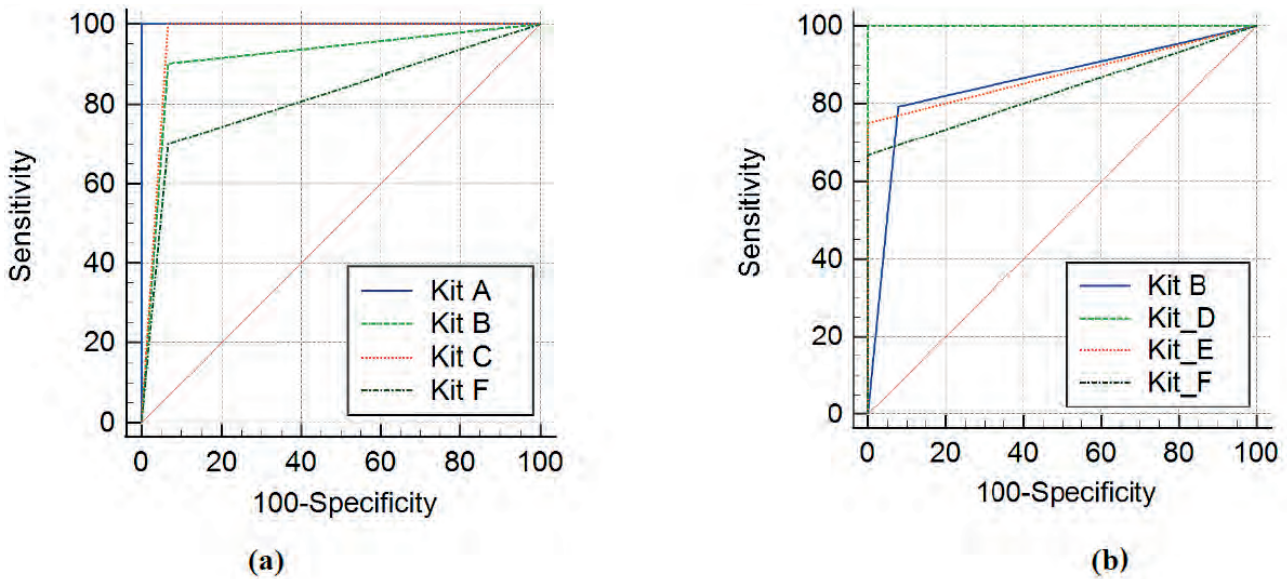
Figure 5. Receiver Operating Characteristic (ROC) curve for different RNA extraction kits. a.) It shows the ROC curve for silica-based extraction and heat shock treatment to obtain the cut-off point for the kit. b.) It shows the ROC curve for non-column extraction and heat shock treatment to get the cut-off point for kits.

Kit	Sensitivity	Specificity	Direct Cost USD (2020)	Indirect Cost USD (2020)	Direct Cost USD (2021)	Indirect Cost USD (2021)	Concentration (ng/µL)	OD 260/280
A	100%	100%	55,00	51,99	62,56	37,11	34,12	2,58
B	90%	93%	64,25	51,97	70,85	37,09	83,27	3,12
C	100%	93%	53,96	51,97	61,37	37,09	24,65	1,86
D	92%	87%	53,12	51,99	60,15	37,11	63,09	1,88
E	82%	100%	52,78	52,05	58,26	37,17	46,05	1,87
F	70%	93%	47,01	50,35	49,16	35,47	N/A	N/A

Table 5. Indicators to cost analysis for six different extraction methodologies.
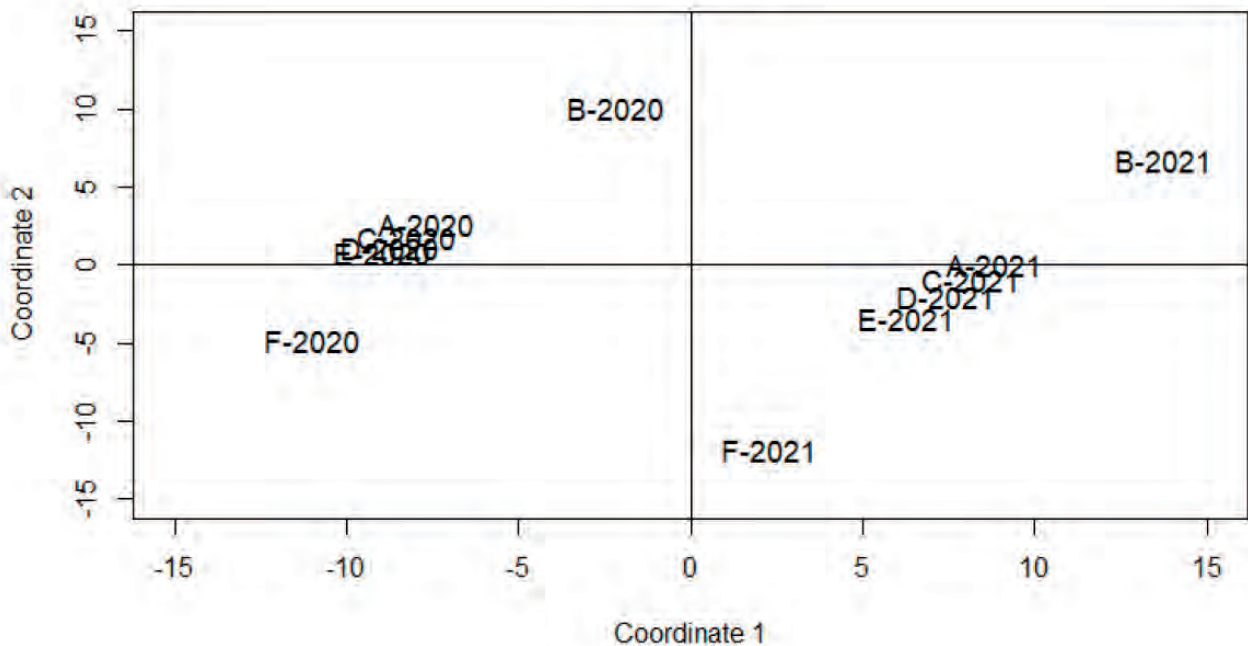
Figure 6. Multidimensional Scaling for different viral RNA extraction kits for 2020 and 2021.

the fast development of novel and reliable diagnostic tests based on nucleic acid kits. However, a severe shortage of nucleic acid extraction kits due to the sudden surge in demand, the reduced production capacity, and delays in shipment challenge the global health system, mainly for developing countries during the first months and the rapid spread of COVID-19 in 2020 and 2021. Management of COVID-19 requires widespread and accessible testing, where the primary step to be diagnosed is to obtain a purified and concentrated viral RNA to be used in the RT-PCR technique to detect SARS-CoV-2. US CDC considers this a "gold standard" technique to its high sensitivity and specificity, significantly faster than other molecular available viral detection techniques[13,68].

Thus, the method used for RNA extraction is the most crucial variable, where the extraction efficiency influence significantly the yield and quality of RNA; thereby, it represents an essential variable in detecting the presence of the SARS-CoV-2 genome by RT-PCR[13]. In this way, many commercial kits use different methods to allow fast, sensitive and reproducible detection of viral RNA. Along this line, reliable protocols are crucial for those molecular laboratories without automated nucleic acid extraction, where the extraction process significantly influences the yield of RNA.

The results obtained from each different kit tested showed that the quantification of RNA is an essential step before RNA-based essays, where the diagnosis requires an accurate RNA quantification to estimate the success of the extraction to determine the appropriate amount of extract for downstream medical applications like RT-PCR for the diagnosis of SARS-CoV-2[31]. Preliminary studies report that direct-to-test addition of unpurified samples allows for SARS-CoV-2 detection of low copy load samples, but may decrease test sensitivity, amplification cycle later and delayed detection of viral RNA[9,10].

The purpose of many diagnostic processes of SARS-CoV-2 after nucleic acid extraction is the efficient detection and successful amplification of the target region in the viral RNA using RT-PCR, where an entire, high amount and good quality of nucleic acid template to be used fundamentally for the downstream molecular process[32]. In this study, a comparison between the six different methodologies for RNA extraction showed variations in the overall performance based on their other technology, where kits B, D and E outcomes obtained show a considerable amount of nucleic acid due to the use of similar required sample volume. However, kits A and C presented results of RNA yields decreased to kits B, D and C, which show extraction efficiency and methodology significantly influence the yield of RNA; despite using similar sample volumes, kit C has the most variable yield and concentration with significant differences in terms of IQR.

In the case of kit F, not having quantified the RNA concentration leaves it out of the comparison with the other commercial kits, given that being a raw genetic material, the generation of interference discriminates the quality of genetic material obtained by the heat shock, which would be used for amplification. However, doing so could have indicated an approximate concentration of RNA, thus evaluating qualitatively if the heat shock is favorable to obtaining quality genetic material.

The commercial kit's wavelength absorbance (OD260/280) shows acceptable purity, so values are proximate to 1.7 – 2.00 and upper 2.2. In this way, kit A and B silica-based membrane extraction present the best purity ra-

tios indicating that the composition of the eluent was RNA. In contrast, kits C (same technology as A and B), D and E show an acceptable purity ratio but lower for optimal density ratios. Although spectroscopy can be used to determine the concentration and purity of RNA it lacks the power to determine the integrity of the RNA, which can affect the RT-PCR to detect nucleic acids for SARS-CoV-2 if the viral load and yield is not highest, being a considerable variable for COVID-19 diagnosis, and make an agarose electrophoresis to view the integrity of extraction would involve an additional cost. So, there are clinical and public health implications for the detection of samples with low levels of SARS-CoV-2 viral RNA. Even though, detection of viral RNA by PCR may not correlate with live transmissible virus for patients presenting early infection[70].

Due to the rapid spread of SARS-CoV-2, studies have tested the use of direct nasopharyngeal samples, indicating that the RNA isolation step could be omitted[12,38]. However, this approach results in reduced sensitivity and specificity of the downstream RT-PCR process. It may require an additional 3 to 7 PCR cycles to reach the detection threshold compared to that of reactions with purified RNA[2,12], compromising the detection of low viral loads. Still, studies reported sensitivity values ranging from 51%[38] to 91.4%[48] as commonly used measures of validity, including specificity. Sensitivity refers to its ability to detect a high proportion of confirmed cases while yielding few false negative results. Meanwhile, specificity, on the other hand, means that a specific test correctly identifies the actual negative and hence yields few false positive cases. Still, this result allowed a gap to increase the presence of False positive and false adverse claims, which can affect the control of spreading COVID-19.

The implementation of alternative methodologies like heat shock to obtain free RNA without concentration and purification, due to the limited supply chains, could be a good way to detect positive cases of SARS-CoV-2. Herein we report this approach as direct RT-PCR, which correctly identified 80 to 84% (diagnostic effectiveness) of samples previously shown to be positive for SARS-CoV-2 by RT-PCR featuring an RNA extraction. Studies that used a similar technique reported approach diagnostic effectiveness of 77.1, 92 and 95% of total positive samples[26,49,69] being the direct detection without RNA extraction, a reliable alternative for commercial kits, especially for kits that based on extraction technology is silica membrane. The advantage to put of sample to thermal treatment is the exposure of viral genome and denatures inhibitors of the PCR; however, the exposure sample to high temperatures above 95ºC for direct RT-PCR (without RNA extraction) may result in the dismissal of diagnostic efficiency in comparison to moderate temperatures 65-70 ºC used in commercial kits which did not affe00ct RT-PCR[38,70]. Also, the use of mild temperatures allows a low capacity to affect their ability to discriminate to classify the healthy as healthy and the sick as sick, in comparison with the use of high temperatures. The Area Under the Curve, called AUC is one of the parameters to evaluate the discriminatory efficacy, obtaining values of 0.73; however, the Youden index can help to determine the highest cut-off, which determines the sensitivity and specificity together, getting a value of 0.817. However, this cut-off point does not necessarily determine the most heightened sensitivity or specificity that the test could achieve[71].

On the other hand, compared to mono-phasic extraction, where the typical extraction involves three general

steps: cell lysis, separation of RNA from DNA, proteins, and lipids, followed by RNA concentration which presents a high yield than heat shock treatment that can be observed in the sensitivity and specificity by RT-PCR[39,42]. Finally, viral RNA extraction using magnetic beads showed similar results with single-stage extraction and silica columns; however, when RT-PCR is performed, sensitivity and specificity vary considerably despite the beads having a certain affinity for RNA and the reagents used being specific.

As for the cost analysis using a multidimensional analysis, a clear difference in prices, concentration and purity of viral RNA obtained for the years 2020 and 2021 can be seen, where the distance between the variables analyzed reflects an increase in direct and indirect costs necessary to perform the RT-PCR process.

Conclusions

In conclusion, for the study presented, the use of alternative techniques such as an extraction RNA method prior to detection of SARS-CoV-2 can improve laboratory workflow. Considering the data, the technique has an acceptable diagnostic capacity for patients with a high viral load but a poor capacity for patients with low viral loads, we considered that the most significant limitation was associated with our inability to evaluate a greater number of samples, which could have made it possible to develop a more robust and extensible protocol. Presenting a clear disadvantage in this process as to diagnostic efficiency and discriminatory efficacy. Although this protocol allows the clinician to significantly reduce processing time, we believe it should only be used in clinical la-boratories where the lack of reagents for RNA extraction is a limiting factor, the main objective being to ensure the quality of the analysis during patient diagnosis. On the other hand, in terms of costs required to perform it, there is a clear advantage, mainly for developing countries where the costs of important inputs and reagents limit the ability to detect SARS-CoV-2 genetic material, and the use of the direct sample with RNase inhibitors can also increase the number of samples that can be processed per day. In terms of other alternatives technologies for extraction of nucleic acid, in this case viral RNA to SARS-CoV-2, low-tech solutions for COVID-19 supply chain crisis can be the implementing self-collected saliva, superficial nasal swabs including dry oral swabs without viral transport medium, being a prospectal technologies with low-invasive for patients that can be ap-plicable for develop countries which use manual extraction methods. Consequently, dedicated biosafety practices need to be implemented to ensure the safety of laboratory personnel and reduce the risk of contamination. So that, heat shock technique could be implemented in cases where the expected positivity rates are high (symptomatic patients) representing an efficient alternative, to subsequently perform the kit extraction technique only in negative samples, which would reduce time and save costs considerably in the diagnosis.

Institutional Review Board Statement

Ethical review and approval were waived for this study due to is an observational study, in which no patient data have been included since it is a methodological analysis.

Informed Consent Statement

Patient consent was waived due to is an observational study, in which no patient data have been included since it is a methodological analysis.

Conflicts of Interest

The authors declare no conflict of interest.

11

Bibliographic references

1. Mollaei HR, Afshar AA, Kalantar-Neyestanaki D, Fazlalipour M, Aflatoonian B. Comparison five primer sets from different genome region of covid-1for detection of virus infection by conventional rt-pcr. Iran J Microbiol. 2020;12(3):185–93.

2. Villota SD, Nipaz VE, Carrazco-Montalvo A, Hernandez S, Waggoner JJ, Ponce P, et al. Alternative RNA extraction-free techniques for the real-time RT-PCR detection of SARS-CoV-2 in nasopharyngeal swab and sputum samples. J Virol Methods. 2021;298(September).

3. Wang H, Li X, Li T, Zhang S, Wang L, Wu X, et al. The genetic sequence, origin, and diagnosis of SARS-CoV-2. European Journal of Clinical Microbiology and Infectious Diseases. 2020;39(9):1629–35.

4. Rodríguez M, León C. Similitudes y diferencias entre el síndrome respiratorio agudo severo causado por SARS-CoV y la COVID-19. Revista Cubana de Pediatrí. 2020;92(1):20.

5. de Groot RJ, Baker SC, Baric RS, Brown CS, Drosten C, Enjuanes L, et al. Middle East Respiratory Syndrome Coronavirus (MERS-CoV): Announcement of the Coronavirus Study Group. J Virol. 2013;87(14):7790–2.

6. Drosten C, Günther S, Preiser W, van der Werf S, Brodt HR, Becker S, et al. Identification of a Novel Coronavirus in Patients with Severe Acute Respiratory Syndrome. New England Journal of Medicine. 2003;348(20):1967–76.

7. Kaye AD, Cornett EM, Brondeel KC, Lerner ZI, Knight HE, Erwin A, et al. Biology of COVID-19 and related viruses: Epidemiology, signs, symptoms, diagnosis, and treatment. Best Pract Res Clin Anaesthesiol [Internet]. 2021;35(3):269–92. Available from: https://doi.org/10.1016/j.bpa.2020.12.003

8. Bruno A, de Mora D, Freire-Paspuel B, Rodriguez AS, Paredes-Espinosa MB, Olmedo M, et al. Analytical and clinical evaluation of a heat shock SARS-CoV-2 detection method without RNA extraction for N and E genes RT-qPCR. International Journal of Infectious Diseases [Internet]. 2021;109:315–20. Available from: https://doi.org/10.1016/j.ijid.2021.06.038

9. Gangwar M, Shukla A, Patel VK, Prakash P, Nath G. Assessment of Successful qRT-PCR of SARS-CoV-2 Assay in Pool Screening Using Isopropyl Alcohol Purification Step in RNA Extraction. Biomed Res Int. 2021;2021.

10. Grant P, Turner M, Shin GY, Nastouli E, Levett L. Extraction-free COVID-19 (SARS-CoV-2) diagnosis by RT-PCR to increase capacity for national testing programmes during a pandemic. 2020;19:6–11.

11. Esbin MN, Whitney ON, Chong S, Maurer A, Darzacq X, Tjian R. Overcoming the bottleneck to widespread testing: A rapid review of nucleic acid testing approaches for COVID-19 detection. Rna. 2020;26(7):771–83.

12

12. Wölfel R, Corman VM, Guggemos W, Seilmaier M, Zange S, Müller MA, et al. Virological assessment of hospitalized patients with COVID-2019. Nature. 2020;581(7809):465–9.

13. Ponce-Rojas JC, Costello MS, Proctor DA, Kosik KS, Wilson MZ, Arias C, et al. A fast and accessible method for the isolation of RNA, DNA, and Protein to Facilitate the Detection of SARS-CoV-2. J Clin Microbiol. 2021;59(4).

14. Ambrosi C, Prezioso C, Checconi P, Scribano D, Sarshar M, Capannari M, et al. SARS-CoV-2: Comparative analysis of different RNA extraction methods. J Virol Methods [Internet]. 2021;287:114008. Available from: https://doi.org/10.1016/j.jviromet.2020.114008

15. Freire-Paspuel B, Morales-Jadan D, Zambrano-Mila M, Perez F, Garcia-Bereguiain MA. Analytical sensitivity and clinical performance of "COVID-19 RT-PCR Real TM FAST (CY5) (AT-Gen, Uruguay) and 'ECUGEN SARS-CoV-2 RT-qPCR' (UD-LA-STARNEWCORP, Ecuador)": High quality-low cost local SARS-CoV-2 tests for South America. PLoS Negl Trop Dis. 2022;16(4):1–9.

16. Santini A. Optimising the assignment of swabs and reagent for PCR testing during a viral epidemic R. Omega (Westport) [Internet]. 2021;102:102341. Available from: https://doi.org/10.1016/j.omega.2020.102341

17. Calvez R, Taylor A, Calvo-bado L, Fraser D, Id CGF. Molecular detection of SARS-CoV-2 using a reagent-free approach. PLoS One [Internet]. 2020;1–11. Available from: http://dx.doi.org/10.1371/journal.pone.0243266

18. González B. Evolution and early government responses to COVID-19 in South. 2021;137.

19. Andrus JK, Evans-gilbert T, Santos JI, Guzman MG, Rosenthal PJ, Toscano C, et al. Perspective Piece Perspectives on Battling COVID-19 in Countries of Latin America and the Caribbean. The American Society of Tropical Medicine and Hygiene. 2020;103(2):593–6.

20. Garcia PJ, Alarc A, Bayer A, Buss P, Guerra G, Ribeiro H, et al. Perspective Piece COVID-19 Response in Latin America. The American Society of Tropical Medicine and Hygiene. 2020;103(5):1765–72.

21. Trudeau JM, Alicea-Planas J, Vásquez WF. The value of COVID-19 tests in Latin America. Econ Hum Biol. 2020;39:1–6.

22. Miranda JP, Osorio J, Videla M, Angel G, Camponovo R, Henríquez-Henríquez M. Analytical and Clinical Validation for RT-qPCR Detection of SARS-CoV-2 Without RNA Extraction. Front Med (Lausanne). 2020;7(October):1–9.

23. Ñique AM, Coronado-Marquina F, Rico JAM, Mendoza MPG, Rojas-Serrano N, Simas PVM, et al. A faster and less costly alternative for RNA extraction of SARS-CoV-2 using proteinase k treatment followed by thermal shock. PLoS One. 2021;16(3 March):1–8.

24. Graham TGW, Darzacq CD, Dailey GM, Nguyenla XH, Dis E van, Esbin MN, et al. Open-source RNA extraction and RT-qPCR methods for SARS-CoV-2 detection. PLoS One [Internet]. 2021;16(2 February):1–24. Available from: http://dx.doi.org/10.1371/journal.pone.0246647

25. Vandenberg O, Martiny D, Rochas O, van Belkum A, Kozlakidis Z. Considerations for diagnostic COVID-19 tests. Nat Rev Microbiol [Internet]. 2021;19(3):171–83. Available from: http://dx.doi.org/10.1038/s41579-020-00461-z

26. Wee SK, Sivalingam SP, Yap EPH. Rapid direct nucleic acid amplification test without rna extraction for sars-cov-2 using a portable pcr thermocycler. Genes (Basel). 2020;11(6):1–13.

27. Chu AWH, Chan WM, Ip JD, Yip CCY, Chan JFW, Yuen KY, et al. Evaluation of simple nucleic acid extraction methods for the detection of SARS-CoV-2 in nasopharyngeal and saliva specimens during global shortage of extraction kits. Journal of Clinical Virology [Internet]. 2020;129(June):104519. Available from: https://doi.org/10.1016/j.jcv.2020.104519

28. Visseaux B, Collin G, Houhou-Fidouh N, le Hingrat Q, Marie Ferré V, Damond F, et al. Evalution of three extraction-free SARS-CoV-2 RT-PCR assays: A feasible alternative approach with low technical requirements. www.archbronconeumol.org Original. 2020;(January).

29. Behnam M, Dey A, Gambell T, Talwar V. COVID-19: Overcoming supply shortages for diagnostic testing. McKinsey and Company [Internet]. 2020;(July):1–8. Available from: https://www.mckinsey.com/industries/pharmaceuticals-and-medical-products/our-insights/covid-19-overcoming-supply-shortages-for-diagnostic-testing#

30. Fomsgaard AS, Rosenstierne MW. An alternative workflow for molecular detection of SARS-CoV-2 – escape from the NA extraction kit-. Eurosurveillance [Internet]. 2020;25(14):1–4. Available from: http://dx.doi.org/10.2807/1560-7917.ES.2020.25.14.2000398

31. Fukumoto T, Iwasaki S, Fujisawa S, Hayasaka K, Sato K, Oguri S, et al. efficacy of a novel SARS-CoV-2 detection kit without RNA extraction and purification. International Journal of Infectious Diseases. 2020;98:16–7.

32. Aranda IV R, Dineen SM, Craig RL, Guerrieri RA, Robertson JM. Comparison and evaluation of RNA quantification methods using viral, prokaryotic, and eukaryotic RNA over a 104 concentration range. Anal Biochem [Internet]. 2009;387(1):122–7. Available from: http://dx.doi.org/10.1016/j.ab.2009.01.003

33. Ali Suliman B. Comparison of five viral nucleic acid extraction kits for the efficient extraction of viral DNA and RNA from cell-free samples. Trends in Medicine. 2019;19(5):1–4.

34. Klein S, Müller TG, Khalid D, Sonntag-Buck V, Heuser AM, Glass B, et al. SARS-CoV-2 RNA extraction using magnetic beads for rapid large-scale testing by RT-qPCR and RT-LAMP. Viruses. 2020;12(8).

35. Sabat J, Subhadra S, Rath S, Ho LM, Kanungo S, Panda S, et al. Yielding quality viral RNA by using two different chemistries: a comparative performance study. Biotechniques. 2021;71(4):510–5.

36. Ministerio de Salud Pública del Ecuador. El costo de las pruebas RT-PCR será de USD 45.08. 2021;19–20. Available from: https://www.salud.gob.ec/comunicado-oficial-el-costo-de-las-pruebas-rt-pcr-sera-de-usd-45-08/

37. Ministerio de Salud Pública del Ecuador. Determinación del costo de las pruebas rápidas y pruebas RT-PCR para detección de Covid-19. 2020;(Mayo):1–3.

38. ¿Cuánto cuesta saber si tienes coronavirus en América Latina? - 31.03.2020, Sputnik Mundo [Internet]. [cited 2022 Aug 27]. Available from: https://sputniknews.lat/20200331/cuanto-cuesta-saber-si-tienes-coronavirus-en-america-latina-1090965827.html

39. Beltrán-Pavez C, Márquez C, Muñoz G, Valiente-Echeverría F, Gaggero A, Soto-Rifo R, et al. SARS-CoV-2 detection from nasopharyngeal swab samples without RNA extraction. 2020;

40. Wozniak A, Cerda A, Ibarra-Henríquez C, Sebastian V, Armijo G, Lamig L, et al. A simple RNA preparation method for SARS-CoV-2 detection by RT-qPCR. Sci Rep [Internet]. 2020;10(1):1–8. Available from: https://doi.org/10.1038/s41598-020-73616-w

41. Berensmeier S. Magnetic particles for the separation and purification of nucleic acids. Appl Microbiol Biotechnol. 2006;73(3):495–504.

42. Chomczynski P, Sacchi N. The single-step method of RNA isolation by acid guanidinium thiocyanate-phenol-chloroform extraction: Twenty-something years on. Nat Protoc. 2006;1(2):581–5.

43. Amirouche A, Ait-Ali D, Nouri H, Boudrahme-Hannou L, Tliba S, Ghidouche A, et al. TRIzol-based RNA extraction for detection protocol for SARS-CoV-2 of coronavirus disease 2019. New Microbes New Infect [Internet]. 2021;41:100874. Available from: https://doi.org/10.1016/j.nmni.2021.100874

44. Escobar MD, Hunt JL. A cost-effective RNA extraction technique from animal cells and tissue using silica columns. J Biol Methods. 2017;4(2):e72.

45. Alvarez FJ, Perez-Cardenas M, Gudiño M, Tellkamp MP. Tips for a reduction of false positives in manual RT-PCR diagnostics of SARS-CoV-2. Revista Bionatura. 2021;6(3):1948–54.

46. Israeli O, Beth-Din A, Paran N, Stein D, Lazar S, Weiss S, et al. Evaluating the efficacy of RT-qPCR SARS-CoV-2 direct approaches in comparison to RNA extraction. International Journal of Infectious Diseases. 2020;99:352–4.

47. Mancini F, Barbanti F, Scaturro M, Errico G, Iacobino A, Bella A, et al. Laboratory management for SARS-CoV-2 detection: a user-friendly combination of the heat treatment approach and rt-Real-time PCR testing. Emerg Microbes Infect. 2020;9(1):1393–6.

48. Smyrlaki I, Ekman M, Lentini A, Rufino de Sousa N, Papanicolaou N, Vondracek M, et al. Massive and rapid COVID-19 testing is feasible by extraction-free SARS-CoV-2 RT-PCR. Nat Commun. 2020;11(1):1–12.

49. Noriega R, Samore MH. Increasing testing throughput and case detection with a pooled-sample Bayesian approach in the context of COVID-19. bioRxiv. 2020;

50. Bruno A, Mora D de, Freire-paspuel B, Rodriguez AS, Paredes-espinosa MB, Olmedo M, et al. Analytical and clinical evaluation of a heat shock SARS-CoV-2 detection method without RNA extraction for N and E genes RT-qPCR. 2020;(January).

51. Freire-Paspuel B, Garcia-Bereguiain MA. Poor sensitivity of "AccuPower SARS-CoV-2 real time RT-PCR kit (Bioneer, South Korea)." Virol J [Internet]. 2020;17(1). Available from: https://doi.org/10.1186/s12985-020-01445-4

52. Cao C, Yu R, Zeng S, Liu D, Gong W, Li R, et al. Genomic variations in SARS-CoV-2 strains at the target sequences of nucleic acid amplification tests. Archives of Medical Science. 2021;2019(January 2020).

53. Davi MJP, Jeronimo SMB, Lima JPMS, Lanza DCF. Design and in silico validation of polymerase chain reaction primers to detect severe acute respiratory syndrome coronavirus 2 (SARS-CoV-2). Sci Rep [Internet]. 2021;11(1):1–10. Available from: https://doi.org/10.1038/s41598-021-91817-9

54. Zhang Y, Wang C, Han M, Ye J, Gao Y, Liu Z, et al. Discrimination of False Negative Results in RT-PCR Detection of SARS-CoV-2 RNAs in Clinical Specimens by Using an Internal Reference. Virol Sin [Internet]. 2020;35(6):758–67. Available from: https://doi.org/10.1007/s12250-020-00273-8

55. Zou L, Ruan F, Huang M, Liang L, Huang H, Hong Z, et al. SARS-CoV-2 Viral Load in Upper Respiratory Specimens of Infected Patients. New England Journal of Medicine. 2020;1–3.

56. Eul T, States M, Emergency PH, Concern I, Eul T, Management Q, et al. WHO Emergency Use Assessment Coronavirus disease (COVID-19) IVDs PUBLIC REPORT Product : Xpert Xpress SARS-CoV-2 EUL Number : EUL-0511-070-00 Outcome : Accepted. 2020;(July).

57. Ruhan A, Wang H, Wang W, Tan W. Summary of the Detection Kits for SARS-CoV-2 Approved by the National Medical Products Administration of China and Their Application for Diagnosis of COVID-19. Virol Sin [Internet]. 2020;35(6):699–712. Available from: https://doi.org/10.1007/s12250-020-00331-1

58. Yi J, Han X, Wang Z, Chen Y, Xu Y, Wu J. Analytical performance evaluation of three commercial rapid nucleic acid assays for sars-cov-2. Infect Drug Resist. 2021;14:3169–74.

59. Parikh NR, Chang EM, Kishan AU, Kaprealian TB, Steinberg ML, Raldow AC. Time-Driven Activity-Based Costing Analysis of Telemedicine Services in Radiation Oncology. Radiation Oncology Biology [Internet]. 2020;108(2):430–4. Available from: https://doi.org/10.1016/j.ijrobp.2020.06.053

60. Sales M, Tobias G, Pinto M, Costa DA, Rocha DA. EFFECTS OF COVID-19 ON WATERWAY TRANSPORT COST STRUCTURE : A MULTIVARIATE ANALYSIS IN AMAZONIA. 2021;204:193–202.

61. Bentley PM. Error rates in SARS-CoV-2 testing examined with Bayes' theorem. Heliyon [Internet]. 2021;7(4):e06905. Available from: https://doi.org/10.1016/j.heliyon.2021.e06905

62. Mandrekar JN. Receiver operating characteristic curve in diagnostic test assessment. Journal of Thoracic Oncology [Internet]. 2010;5(9):1315–6. Available from: http://dx.doi.org/10.1097/JTO.0b013e3181ec173d

63. Yang D, Martinez C, Visuña L, Khandhar H, Bhatt C, Carretero J. Detection and analysis of COVID-19 in medical images using deep learning techniques. Sci Rep [Internet]. 2021;11(1):1–13. Available from: https://doi.org/10.1038/s41598-021-99015-3

64. Perkins NJ, Schisterman EF. The Youden index and the optimal cut-point corrected for measurement error. Biometrical Journal. 2005;47(4):428–41.

65. Fluss R, Faraggi D, Reiser B. Estimation of the Youden Index and its associated cut-off point. Biometrical Journal. 2005;47(4):458–72.

66. Youden WJ. Index for rating diagnostic tests. Cancer. 1950;3(1):32–5.

67. Chan GM. Bayes' theorem, COVID19, and screening tests. American Journal of Emergency Medicine [Internet]. 2020;38(10):2011–3. Available from: https://doi.org/10.1016/j.ajem.2020.06.054

68. Härdle W, Simar L. Multidimensional Scaling. Applied Multivariate Statistical Analysis. 2003;373–92.

69. Zella D, Giovanetti M, Cella E, Borsetti A, Ciotti M, Ceccarelli G, et al. The importance of genomic analysis in cracking the coronavirus pandemic. Expert Rev Mol Diagn [Internet]. 2021;21(6):547–62. Available from: https://doi.org/10.1080/14737159.2021.1917998

70. Lowe CF, Matic N, Ritchie G, Lawson T, Stefanovic A, Champagne S, et al. Detection of low levels of SARS-CoV-2 RNA from nasopharyngeal swabs using three commercial molecular assays. Journal of Clinical Virology. 2020;128(January).

71. Bruce EA, Huang ML, Perchetti GA, Tighe S, Laaguiby P, Hoffman JJ, et al. Direct RT-qPCR detection of SARS-CoV-2 RNA from patient nasopharyngeal swabs without an RNA extraction step. bioRxiv. 2020;1–14.

72. Ulloa S, Bravo C, Parra B, Ramirez E, Acevedo A, Fasce R, et al. A simple method for SARS-CoV-2 detection by rRT-PCR without the use of a commercial RNA extraction kit. J Virol Methods [Internet]. 2020;285(July):113960. Available from: https://doi.org/10.1016/j.jviromet.2020.113960

73. Vizcaíno-Salazar GJ. Importancia del cálculo de la sensibilidad, la especificidad y otros parámetros estadísticos en el uso de las pruebas de diagnóstico clínico y de laboratorio. Medicina y Laboratorio. 2017;23(7–8):365–86.

13

Tumor necrosis factor (TNF)-α-308 gene polymorphism in children of Haemophilia A

Thaer Ali Hussein*, Ali A.H. AL-bakaa, Mohammed Hassan Flaih

DOI. 10.21931/RB/2023.08.01.41

[1] Center of Agrobiotechnological Development and Innovation – CEDAIT, Universidad de Antioquia, Colombia.
[2] Biology Institute, Universidad de Antioquia, Colombia.
Corresponding author: amaria.henao@udea.edu.co

Abstract: Hemophilias are the most common X-linked inherited blood diseases that, if not properly treated, can cause lifelong debilitations. The challenges and problems in babies differ from that in older kids and adults. Blood loss conditions continue to dominate as diagnostic triggers in children, but the locations of blood loss vary with age. The TNF-α-308 gene polymorphism in children with moderate to severe hemophilia correlates with genetic background and with the clinical phenotype of the cases. This study was a case control conducted in fifty hemophilic and fifty age- and sex-matched healthy cases from September 2020 to October 2021. Results; a significant change was found among positive and negative inhibitors regarding the number of factors eight exposure days >20 days (in positive inhibitors was 59.3% compared to adverse inhibitors 27.8%). Conclusion: The (TNF-)308 gene polymorphism is significantly correlated with inhibitor progress in severe Haemophilia A cases. TNF-Alpha gene might be of use as a biomarker as well possible immune response modulator in Haemophilia A patients receiving substitute treatment.

Key words: Polymorphism, TNF-α -308Haemophilia, inhibitor, prophylaxis - intracranial hemorrhage and pediatrics.

Introduction

Haemophilia A (HA) is the most everyday coagulation parameter shortage globally, with elevated treatment costs. It impacts all ethnic inhabitants, and its prevalence fluctuates between various states but is valued at rates of 3 to 20 cases/100k people[1]. According to the World Federation of Hemophilia's (WFH) yearly report for 2016, the estimated total number of cases in Iraq with all types of hemophilia in 2016. There were 1346 cases, for a prevalence of 3.7/100,000 people[2]. Genetically, HA is caused by omitting all or part of the factor VIII gene, a point mutation in the genes or gene regulation. Major inversions of the tip of the X chromosomes, which are adaptive for half of the severe degree of such diversity of abnormalities in the factor-VIII (FVIII) gene, cause a lack of reduced productions of the FVIII molecule, which has no role or decrease of FVIII in plasma[1]. In severe hemophilia, phenotypic changeability is well-known.

Cases of HA have mutable clinical phenotypes that correlate with FVIII plasma levels and other genetic and environmental influences. The precise cause of this clinical heterogeneity remains unknown. The FVIII gene mutation, on the other hand, is regarded as the most critical determinant of the clinical phenotype[3]. TNF is considered a cytokine with multiple functions. TNF- is of an essential role in defense for the host in contradiction of infections and has a primary function in auto-immune disorders. It is also a necessary cytokine for the formation of granulomas. TNF-alpha levels vary from case to case and are genetically determined. A gene encodes TNF-alpha on 6p21, part of the main histocompatibility complex (MHC). The third chromosome was a highly polymorphic region. Several bi-allelic as (SNPs) were found rounding (in or and) the gene of TNF-α. One

G/A polymorphism is situated at the gene -308 upstream and is identified to impact the TNF level. Compared to the allele as TNF—308G, allele A has more excellent transcription activities[4].

We wanted to look into TNF—308 gene polymorphism in children with moderate to severe Haemophilia and see if there was a link between genetics and clinical phenotypes.

Materials and methods

Cases and Methods

This study was a case-control study performed from September 2020 to October 2021 for fifty hemophilic cases& fifty healthy cases of matched age & sex attending hematology at Al-Hussein teaching hospital in Nasiriya.

Inclusion criteria: Age group: > 1 month to18 years old, moderate and severe hemophilic cases, Haemophilia A was sorted regarding the level of serum-FVIII: <1 % of ordinary (severe), 1–5% of regular (moderate), and >5%of every day (mild) and accept to sign the informed consent form

Exclusion criteria: Rather than Haemophilia and associated chronic illness, any associated hematologic disorders.

All cases will be subjected to the following

A- Full history taking including ages, gender, the existence of parental consanguinities, ages at onset of cyanosis, cyanotic conditions and their incidences, blood loss manifestation, thrombocytopenia family history, medication past, family history of Hemophilia, FVIII activity, FVIII brand,

2

ages of first exposures to FVIII.

B- Complete clinical examination: Physical appearance with specific attention to abnormalities of growth, signs of anemia, arterial blood pressure and other vital signs and data such as temp, heart & respiratory rates and BP have been determined.

C- Investigations: 2 ml of venous blood were gathered from all cases and control groups, placed in tubes containing EDTA, and reserved at -20 °C until DNA extraction. DNA was extracted using commercial DNA extracting kits and kept at -20°C.

D- Standard approaches: Southerly blot and wide-range chain reactions (PCR) have been used to analyze the FVIII gene in versional analyzing, PCR and mutation screening approaches.

E- TNFA polymorphisms: The isolated DNA for the polymorphic locations-308 was genotyped for TNF-polymorphism using polymerase chain reactions (PCR) and a thermal cycler. Polymorphisms were studied using the (RFLP) technique and to sites -308 primers specific. The TNF-alpha-308G/A (rs-1800629) polymorphism was discovered using a primer as single, which produces a place as NcoI recognition in the allele as A; therefore, PCR (107 bp) absorption with yields of NcoI being two results (87 and 20 bp). The G-allele is still present. TNF-A amplifications were carried out using a thermal cycler. From blood EDTA-conserved, TNF-A polymorphisms g-DNA was extracted utilizing (Qiagen-genomic tip, Kebo-Lab, Sweden) Kit. The polymorphism as TNFA 308GA (rs1800629) was discovered using primer being single, which generates a site of NcoI-recognizing in the allele as A; therefore, the PCR ingestion (107 bp) along with NcoI (Promega, Germany) yields two results (87 and 20 bp). The G-allele is still present. A thermal cycler (Techne, PHC3 Dri block, and Cambridge, UK) achieved TNF-A amplification amplifications. For 3.5 hours, the digested NcoI samples were exposed to agarose gel electrophoresis in three percent Nu-Sieve GTG at 5-V per cm.

F- Procedure: Extractions of DNA and polymerase chain reactions: DNA was extracted utilizing Gene JET as Total Blood DNA Genomic Purifications Mini Kits (Qiagen genomic tip, Kebo Lab, Stockholm, Sweden) and kept at -20 °C. The primer sequence used is depicted in (Table 1). The reaction volume was 25l: 5l of DNA at 100ngl, 15.0 l Dream Taq Green PCR master mix (thermo-scientific, USA), 0.5 l of every primer (25pmoll), and 4.0l H2O. The reaction was carried out in a thermocycler TC-100 (Biorad, USA) along with the following parameters as cycling: rs1800629: The profile of cycling was as follows: 1st denaturation at 940 degrees Celsius for three minutes, thirty cycles of 94 degrees Celsius for 10 seconds, and appropriate annealing temp. Sixty degrees Celsius for 30 seconds, 72 degrees Celsius for 30 seconds, and ultimate extensions for 5 minutes at 72 degrees Celsius. For checking the products of PCR at 107 bp for rs1800629, ten l of PCR were resolute in agarose gel 2 percent.

DNA concentration, purity and purity: were measured spectro-photometrically utilizing the Thermo Scientific NanoDropTM Spectro-photometer (Nanodrop). Following the formulations: DNA concentration (g per ml) = (A-260–A-320 readings) dilution factor 50g per ml DNA yield (g) = total specimen volume x DNA concentration (ml). The re-activity of every specimen was determined by dividing the average specimen OD by the low positive controls average OD. The final result was multiplied by the number of units assigned to the low positive. After that, samples were labeled being negative (less than 20 units), moderately positive (from 20 to 60 teams) or strongly positive (greater than 60 units).

Statistical analysis: Statistical analysis has been done by SPSS-21 (IBM, USA). The normality of data has been first examined with one-sample Kolmogorov-Smirnov testing. Associations among qualitative variables were done via Chi-square testing, whereas Fischer exact testing and Monte Carlo testing were employed when the expected cell count <5. Comparison between both groups was made by means of Student t-testing for parametric results and Mann-Whitney testing for nonparametric results.

Results

As regards characteristics of studied cases, most of them presented with spontaneous bleeding due to minor trauma (73.3 percent). In addition, most patients (84.4 percent) had negative consanguinity and no Haemophilia family history (55.6 percent). Also, the number of factor exposure days < 20 represents 53.3% of cases. The number of bleeding episodes per month was < one time per month in 57.8%. No first exposure to factor 8 was 55.6% in 25 cases with age < 18 months. All patients in the study were given recombinant factor 8 concentrate therapy on demand at an average dose of 30 iu/kg. 26 of hemophilic cases (57.8%) had factored 8 activities less than 1%. Moderate Haemophilia represents 60% of cases; severe Haemophilia represents 40%. Table (2)

A non-significant change was found among the studied group regarding genotype, but GA distribution was higher in the patient group (15.6%) than in the control group (6.7%). Regarding alleles, the A-allele distribution was higher in the patient group (7.8%) compared to the control group (3.3%). Table (3)

There is no significant difference in positive family history between moderate and severe Haemophilia, but the frequency was higher in severe Haemophilia (61.1%) than in moderate Haemophilia (33.3%). There is a significant difference between average and severe Haemophilia as regards several intensive factors 8 treatment; the frequency was higher in severe Haemophilia (median =8) than in moderate Haemophilia (median =5). There is a significant difference between average and extreme Haemophilia as regards positive consanguinity; frequency was higher in the middle than in severe Haemophilia. Table (4)

A non-significant change was found among moderate and severe Haemophilia regarding genotype, but GA distribution was higher in the middle than severe Haemophilia. Also, the A allele frequency was higher in moderate than powerful Haemophilia. Table (5)

A non-significant change was found among positive and negative inhibitors regarding genotype, but GA distribution was higher in positive inhibitors 22.2% than in adverse inhibitors 5.6%. Also, A allele distribution was increased in positive inhibitors at 11.1%, then in negative inhibitors at 2.8%. Table (6)

Following logistic regression analysis and adjusting for confounding factors, the only independent predictor of positive inhibitors was the number of factors 8 exposure days > 20 days (OR = 3.8) with a 95% CI (1.05-13.7).Table (7).

SNP	Primer sequence		Enzyme
rs1800629	Forward	5`-AGGCAATAGGTTTTGAGGGCCAT-3`	Nco1
	Reverse	5`-TCCTCCCTGCTCCGATTCCG-3`	

Table 1. Primer sequence and PCR-RFLP enzyme.

Cases characteristics	Cases group (n=45)
Positive family history of Haemophilia	
Yes	20 (44.4%)
No	25 (55.6%)
Consanguinity	
Yes	7 (15.6%)
No	38 (84.4%)
No bleeding episodes/month	
<1	26 (57.8%)
1-4	9 (20.0%)
>4	10 (22.2%)
Haemophilia severity	
Moderate	27 (60%)
Severe	18 (40%)
FVIII activity	
Median (IQR)	**1.0 (0.35-2.5)**
<1	26 (57.8%)
>1	19 (42.2%)
Inhibitor	
No	18 (40.0%)
Low	19 (42.2%)
High	8 (17.8%)
Age of 1st exposure to FVIII	
Median (IQR)	**18 (8.5-36)**
<18 m	25 (55.6%)
>18 m	20 (44.4%)
No of FVIII exposure days	
Median (IQR)	**20 (12-38)**
<20 d	24 (53.3%)
>20 d	21 (46.7%)
Reason of 1st exposure to FVIII	
Minor surgery	12 (26.7%)
Hemorrhage	33 (73.3%)
No of intensive FVIII treatment	
Median (IQR)	6 (3.5-10)
Plasma transfusion before factor	
yes	31 (68.9%)
No	14 (31.1%)
Age of 1st exposure to plasma	
Median (IQR)	12 (2-18)

Table 2. Cases characteristics regarding disease.

3

Genotype	Cases group (n=45)	Control group (n=45)	Test of significance	P-value
GG	38 (84.4%)	42 (93.3%)	$\chi^2=1.8$	0.18
GA	7 (15.6%)	3 (6.7%)		
Alleles			$\chi^2=1.69$	0.193
G	83 (92.2%)	87 (96.7%)		
A	7 (7.8%)	3 (3.3%)		

n-number
Mann-Whitney testing
The result is considered significant at p value< 0.05

Table 3. Comparing of Genotype among cases and control groups.

Discussion

TNF—308 promoter gene polymorphism was linked to various auto-immune diseases, counting systemic rheumatoid arthritis, lupus erythematosus, and infections like TB. No studies on TNF- gene polymorphisms in TA were discovered throughout the study writing process. During the manuscript review process, we came across one report that found no TNF- promoter polymorphism in the Han Chinese population. As a result, they conducted this pilot report to investigate TNF—308 polymorphism in TA, a granulomatous vasculitis with an auto-immune basis that is most likely caused by Mycobacterium tuberculosis[5]. This is why this study was chosen to investigate (TNF)—308 gene polymorphisms in Iraqi children with moderate to severe hemophilia and to correlate the genetic background with the clinical phenotypes of the cases. In Iraq, a single Hereditary Blood Disorders Center in every governorate delivers care for these cases, excluding Baghdad, where three centers exist. A case-control study was conducted comprising 50 hemophilic cases& 50 healthy cases of matched age & sex. Total 45 hemophilic cases and 45 controls were screened for participation during this study. There is a non-significant change among the study groups regarding age and sex. Regarding age, the cases group had a median 6 IQR between 5-10 compared to the control group, which had a median 5 IQR between 3-11. Regarding sex, the majority of both groups were males. Our results are supported by the study of Nesheli et al.[6,7] as they reported that the mean age of cases with inhibitors was 10.22 years. Their results revealed that the production of inhibitors in young populations was more significant than in older ones. It might be because of the usage of exogenous FVIII as prophylaxis in some young Haemophilia A cases and the deficiency of use of any factor on demand in the old cases[8,9]. However, Astermark et al.,[10] reported that the median age of the studied group was 24 (3-79)-yrs, and all cases had >100 exposures to FVIII concentrates. The present study shows that as regards characteristics of studied patients. Most of them presented with spontaneous bleeding due to minor trauma (73.3 percent). Furthermore, most cases (84.4 percent) had negative consanguinity and no Haemophilia family history (55.6 percent). Also, the number of factor exposure days < 20 represents 53.3% of cases. The number of bleeding episodes per month was < one time per month in 57.8%. No first exposure to factor 8 was 55.6% in 25 cases with age < 18 months. All cases in the study received recombinant factor 8 concentrate therapy on demand at an average dose of 30IU/kg. Twenty-six hemophilic cases (57.8%) had factor 8 activity less than 1%. Moderate Haemophilia represents 60% of cases; severe Haemophilia represents 40%. Taresh et al.[11] who conducted their study in Basra, Iraq, 39.8-% of enrolled cases with HA had a severe form of the disorder, and more than 33% were >15 years old, while 56% of the cases with HB had a mild grade of the disease, and nearly half were younger than five years old. Our results are supported by the study of Al Tonbary et al.[12] as they reported that moderate presentation represents the majority in 17.2%, followed by severe presentation in 4.7%. The mean presentation symptoms were hemorrhage followed by males' circumcisions at 51.4%, trailed by posttraumatic bleeding at 36.1%. Unplanned detection was revealed to be shared in females.

However, Astermark et al.[10], reported that number of 124 cases, 75.6% have severe (52 cases with HR, 11 cases with LR, 61 patients with no inhibitors), 15.9% were moderate (2 cases with HR, 5 cases with LR, 19 cases with no inhibitors), and 8.5% mild (3cases with HR, 4cases with LR, 7cases with no inhibitor) HA. In the study in our hands, non-significant changes were found among the study groups regarding genotype. However, GA distribution was higher in-patient group (15.6%) than in the control group (6.7%). Regarding alleles, the distribution of the A-allele was high in the patient group (7.8%) compared to the control group (3.3%). Our results are supported by the study of Zhang et al.[13], as they reported that in cases of HA, genotypes as G/A, G/G, and A/A have been found in 12.8%, 84.3% and 2.9% resp.; C/C, C/T and T/T genotypes have been found in 77.2%, 21.4%, and 1.4 %resp. The variance in the genotype incidences among the study groups was non-significant.

Furthermore, Sandhya et al.[14], Three results were obtained after enzyme digestion of the PCR products. A comprehensive NcoI cut for homozygous TNF- (-308G/G), yielding 2 87 and 20 base pair remains; an incomplete cut for heterozygous TNF- (-308G/A), producing 3 107, 87, and 20 base pair remains; and an un-cut homozygous TNF- (-308A/A), yielding 107 base pair fragments. The difference in genotype distribution of the polymorphism between the two groups was not statistically significant. The present work shows that there is non-significant change among moderate and severe Haemophilia regarding genotype, but GA distribution was higher in moderate than severe Haemophilia. Also, A allele frequency was higher in moderate than severe Haemophilia. The study of Astermark et al. su-

Variables	Severity of hemophilia		Significance test	P-value
	Moderate (n=27)	Sever (n=18)		
Age (years)			χ^2=0.24	0.62
<6 y	10 (37%)	8 (44.4%)		
≥6 y	17 (63%)	10 (55.6%)		
Positive FH of Haemophilia			χ^2=3.37	0.066
Yes	9 (33.3%)	11 (61.1%)		
No	18 (66.7%)	7 (38.9%)		
Consanguinity			FET	0.031*
Positive	7 (25.9)	0 (0%)		
Negative	20 (74.1%)	18 (100%)		
No of bleeding episode / month			MC	0.342
<1	17 (63%)	9 (50%)		
1-4	6 (22.2%)	3 (16.7%)		
>4	4 (14.8%)	6 (33.3%)		
Inhibitor			χ^2=0.015	0.901
Negative	11 (40.7%)	7 (38.9%)		
Positive	16 (59.3%)	11(61.1%)		
Age of 1st exposure to FVIII			χ^2=0	1.0
<18 m	15 (55.6%)	10 (55.6%)		
>18 m	12 (44.4%)	8 (44.4%)		
No of FVIII exposure days				0.329
<20 d	16 (59.3%)	8 (44.4%)	χ^2=0.95	
>20 d	11 (40.7%)	10 (55.6%)		
Reason of 1st exposure to FVIII Minor surgery			χ^2=2.29	0.13
Hemorrhage	5 (18.5%)	7 (38.9%)		
	22 (81.5%)	11 (61.1%)		
No of intensive FVIIIttt Median (IQR)	5 (3-7)	8 (5-15)	Z=2.05	0.04*
Plasma transfusion before factor			χ^2=0.069	0.793
yes	19 (70.4%)	12 (66.7%)		
No	8 (29.6%)	6 (33.3%)		
Age of 1st exposure to plasma Median (IQR)	12 (2-24)	9 (2-18)	Z=0.338	0.735
No of joints affected				0.741
No	3 (11.1%)	3 (16.7%)	MC	
<2	18 (66.7%)	10 (55.6%)		
>2	6 (22.2%)	5 (27.8%)		

FET: Fischer exact test, MC: Monte carlo test

n-number

Data are expressed via median (IQR), p value

Table 4. Relation between Haemophilia severity and patient's characteristics.

Genotype	Haemophilia severity		Test of significance	P-value
	Moderate (n=27)	Sever (n=18)		
GG	22 (81.5%)	16 (88.9%)	FET	0.684
GA	5 (18.5%)	2 (11.1%)		
Alleles			χ^2=0.41	0.52
G	49 (90.7%)	34 (94.4%)		
A	5 (9.3%)	2 (5.6%)		

Table 5. Relation between Haemophilia severity and genotype.

Genotype	Inhibitor		P-value
	Positive (n=27)	Negative (n=18)	
GG	21 (77.8%)	17 (94.4%)	0.215
GA	6 (22.2%)	1 (5.6%)	
Alleles			0.148
G	48 (88.9%)	35 (97.2%)	
A	6 (11.1%)	1 (2.8%)	

Table 6. Relation between inhibitor and genotype.

	B	p-value	OR (95%CI)
No FVIII exposure days <20 d (r) >20 d	1.33	0.043*	3.8 (1.05-13.7)
OR: adjusted OR, CI: Confidence interval, (r): reference group Univariate analysis, and 95% confidence interval (CI) odds ratio (OR), is shown			

Table 7. Relation between duration for taking OCS and gingival index.

pports our results[10], They reported that for the current work, Hap 2 (Hap 2-2) homozygous was of significantly greater hazard of inhibitor progression compared to Hap 1-1, and the single variance between such two haplotypes is the uncommon allele being TNFA–308A, which has been linked to pathophysiologic roles in definite antibody-mediated auto-immune disorders. The correlation along with such allele was stronger in the sub-group of cases with HA (OR, 19.2; P value.001) being severe, and it was as well found in the collection of seventy-five cases with overturns—which is, in a group of cases with a similar hazard for inhibitors emergence according to the causal FVIII mutations themselves. This correlation was more than non-dependent on allele-134 of IL-10G[15]. The current work shows that a non-significant change was found among positive and negative inhibitors regarding genotype, but GA distribution was higher in positive inhibitors 22.2% than in negative inhibitors 5.6%. Also, A allele distribution was more increased in positive inhibitors, 11.1%, than in negative inhibitors, 2.8%. Following logistic regression analysis and adjusting for confounding factors, the only independent predictor of positive inhibitors was the number of factors 8 exposure days > 20 days (OR = 3.8) with a 95% CI (1.05-13.7). Zhang et al.[13] reported that cases with homo-zygotes for A-allele had an advanced danger of inhibitors advance compared to those who weren't (OR = 7.519, 95% CI = 3.168 - 17.844). Severe HA cases with homo-zygotes for A-allele had an elevated danger of inhibitors advancing compared to those who weren't (OR = 8.163, 95% CI = 2.521 - 26.434). A non significant change in the danger of inhibitors advance among the cases having or not (OR = 1.586, 95% CI = 0.729 - 3.450). This can be revealing of a causal association of TNFα –308 A/A with inhibitors formations and the elevated incidence connected to the choice of inhibitors cases (47.0%) for the report in the group of MIBS, or to other inherited influences alongside Hap-2 But, the opportunity in which the 308A-allele is additionally predominant in Haemophilia cases with inhibitor compared to such without inhibitor and in controls requisites to be assessed in multi-ethnic populations-built groups. The inhibitory progression of antibodies in response to exogenous FVIII is frequently measured as a Th2-cell-induced immune response, while TNF- is chiefly associated with Th1 cells. But, the cytokine profile obviously shows that inhibitor formations are a mixed Th1 and Th2 cell responding, emphasizing that TNF- levels can similarly moderate the immune response to missing factors in Haemophilia cases. (1). In a study by Wilson et al.[17], The HLA B8, A1, and DR3 alleles were significantly correlated with 17 TNFA –308A. However, while our findings strengthen a link among the polymorphism –308A and such alleles, no one was additionally common in inhibitors cases in their group, with only B44 being the enriched allele of an OR of 2.1—which is analogous to what is defined through Oldenburg et al.[18] (34.5% vs. 16.7%; OR, 2.2).

Conclusions

In cases of severe Haemophilia A, TNFα-308 gene polymorphism is significantly correlated with inhibitor progress. TNF- gene can be a beneficial bio-marker and potential modulator of immune responding to auxiliary therapy in Haemophilia A cases.

Author Contributions

Funding

Bibliographic references

1. Mansouritorghabeh H. Clinical and laboratory approaches to hemophilia A. Iranian journal of medical sciences. 2015 May;40(3):194.

2. Tonbary YA, Elashry R. Descriptive epidemiology of hemophilia and other coagulation disorders in mansoura, egypt: retrospective analysis. Mediterranean journal of hematology and infectious diseases. 2010 Aug 13;2(3):e2010025-.

3. Carcao MD, et.al. Correlation between phenotype and genotype in a large unselected cohort of children with severe hemophilia A. Blood, The Journal of the American Society of Hematology. 2013 May 9;121(19):3946-52.

4. Astermark J, et.al. MIBS Study Group. Polymorphisms in the TNFA gene and the risk of inhibitor development in patients with hemophilia A. Blood. 2006 Dec 1;108(12):3739-45.

5. Lv N, et.al. The role of tumor necrosis factor-α promoter genetic variation in Takayasu arteritis susceptibility and medical treatment. The Journal of rheumatology. 2011 Dec 1;38(12):2602-7.

6. Nesheli HM, Hadizadeh A, Bijani A. Evaluation of inhibitor antibody in hemophiliaA population. Caspian journal of internal medicine. 2013;4(3):727.

7. SAl-Shaheeb, H Kamil Hashim, A Kadhim Mohammed, H Abdulkareem Almashhadani, A Al Fandi. Assessment of lipid profile with HbA1c in type 2 diabetic Iraqi patients. Revis Bionatura 2022;7(3) 29.

8. Franchini M, Tagliaferri A, Mengoli C, Cruciani M. Cumulative inhibitor incidence in previously untreated patients with severe hemophilia A treated with plasma-derived versus recombinant factor VIII concentrates: a critical systematic review. Critical reviews in oncology/hematology. 2012 Jan 1;81(1):82-93.

9. Al Gburi RH, Hashim RD, Kadhim HA, Adam Ş, Almashhadani HA. Correlation of Angiotensin-converting enzyme inhibitors and angiotensin II receptor blockers with serum GDF-15 in a group of hypertensive Iraqi patients. 2022 Aug 30;52(13.96):13-96.

10. Astermark J, Oldenburg J, Carlson J, Pavlova A, Kavakli K, Berntorp E, Lefvert AK, MIBS Study Group. Polymorphisms in the TNFA gene and the risk of inhibitor development in patients with hemophilia A. Blood. 2006 Dec 1;108(12):3739-45.

11. Taresh AK, Hassan MK. Inhibitors among patients with hemophilia in Basra, Iraq–A single center experience. Nigerian journal of clinical practice. 2019 Mar 1;22(3):416-.

12. Tonbary YA, Elashry R. Descriptive epidemiology of hemophilia and other coagulation disorders in mansoura, egypt: retrospective analysis. Mediterranean journal of hematology and infectious diseases. 2010 Aug 13;2(3):e2010025-.

13. Zhang LL, Yu ZQ, Zhang W, Cao LJ, Su J, Bai X, Ruan CG. Relationship between factor VIII inhibitor development and polymorphisms of TNFα and CTLA-4 gene in Chinese Han patients with hemophilia A. Zhonghua xue ye xue za zhi= Zhonghua Xueyexue Zazhi. 2011 Mar 1;32(3):168-72.

14. Sandhya P, Danda S, Danda D, Lonarkar S, Luke SS, Sinha S, Joseph G. Tumour necrosis factor (TNF)-α-308 gene polymorphism in Indian patients with Takayasu's arteritis-A pilot study. The Indian journal of medical research. 2013 Apr;137(4):749.

15. Astermark J, Oldenburg J, Pavlova A, Berntorp E, Lefvert AK, MIBS Study Group. Polymorphisms in the IL10 but not in the IL1beta and IL4 genes are associated with inhibitor development in patients with hemophilia A. Blood. 2006 Apr 15;107(8):3167-72.

16. Reding MT, Lei S, Lei H, Green D, Gill J, Conti-Fine BM. Distribution of Th1-and Th2-induced anti-factor VIII IgG subclasses in congenital and acquired hemophilia patients. Thrombosis and haemostasis. 2002;88(10):568-75.

17. Wilson AG, De Vries N, Pociot FD, Di Giovine FS, Van der Putte LB, Duff GW. An allelic polymorphism within the human tumor necrosis factor alpha promoter region is strongly associated with HLA A1, B8, and DR3 alleles. The Journal of experimental medicine. 1993 Feb 1;177(2):557-60.

18. Oldenburg J, Picard JK, Schwaab R, Brackmann HH, Tuddenham EG, Simpson E. HLA genotype of patients with severe haemophilia A due to intron 22 inversion with and without inhibitors of factor VIII. Thrombosis and haemostasis. 1997;77(02):238-42.

ARTICLE / INVESTIGACIÓN

Isolation and molecular identification of washing machine bacteria and study of the effect of some detergents on their growth

Amina G.O. Al-Ani, Khansa Mohammed Younis, Sura M.Y. Al-Taee*
Department of Biology, College of Science, Mosul University, Mosul, Iraq
Corresponding author: amesbio115@uomosul.edu.iq.

DOI. 10.21931/RB/2023.08.01.42

1

Abstract: This study aimed to isolate, molecular identify, and evaluate the antimicrobial activity of the three commercial types of household detergents; Persil (P), Arial (A), and Peros (Pe) in both forms of gel liquid and (Tate) powder and antibiotics susceptibility test to assessed against isolates from used washing machines in Mosul city/ Iraq. A total of 46 bacterial isolates were isolated. Five isolates were designated as Kh-Am1, Kh-Am4 from the Drum part, Kh-Am3, Kh-Am6 from the Rubber door seal part and Kh-Am5 from Drain dictum; these isolates were selected for molecular identification by 16S rRNA. The 16S rRNA gene of Kh-Am1, Kh-Am3, Kh-Am4, Kh-Am5 and Kh-Am6. The disc agar diffusion method was adopted for each selected isolate using stock and diluted concentrations. After incubation at $37_{o}C$ for 24 hours, inhibition of Aerea was recorded. The results showed that the powder and gel form detergent stock solution has more inhibitory efficacy for the assayed isolates than dilutions. Susceptibility to antibiotics assay revealed that almost all the selected isolates were resistant. Even though infectious strains were not found, opportunistic pathogens were detected. However, because many bacteria have been detected in wash water, washing items at home with it may result in microbial contamination.

Key words: Washing machine bacteria, Washing machine environment, Detergents effect on bacteria, Antibiotic Susceptibility of washing machine bacteria.

Introduction

Within the home environment, there are many opportunities for microbial transmission and laundry service at home. Cleaning agents have been used since time immemorial to eliminate dust and odour for hygienic or medical purposes. These items include a wide variety of items.

Laundry machines are among the most widely used household application for maintaining domestic hygiene. As a result of its extensive use, laundry is one of the most popular housework tasks[1]. The washing drum's technical rotation determines a washing machine's clean efficiency, the quantity of cloth with water and cleaners, and the suitable washing duration and water temperature[2].

Bacteria were decreased but not wholly destroyed throughout wash cycles after entering the washing machine via contaminated clothing and influent water. In the washing machines, the washing process generates a microbiological exchange of influent water, microorganisms, biofilm-related bacteria and skin – clothing related bacteria[3,4]. Surviving bacteria live inside the washing machine, attaching to various surfaces or being spread in the wash load throughout the wash cycle. Suppose bacteria such as Escherichia coli or Staphylococcus aureus are prevalent. In that case, household members may be at risk of complications[5,6] describe an occurrence in a newborn intensive care unit caused by a single species of multidrug-resistant bacteria *Klebsiella oxytoca* ST201, which has only been controlled whenever the washing machine was removed. Moreover, the researchers indicated that modifications in washing machine design and processing are needed to reduce the accumulation of water vapor, which might contribute to the establishment of bacterial growth.

A detergent(washing powders) is a synthetic surfactant, a chemical substance used for Cleaning. Since it includes one or more surfactants, a detergent is an efficient cleaning product. A disinfectant detergent that effectively kills harmful bacteria can help people stay healthy[7,8].

Materials and methods

Isolation of Bacteria

Samples were taken from four different types of washing machines used by other families in Mosul/ Iraq, for periods ranging from months to years and where various common detergents were used. Briefly, washing machine samples were taken from three parts: Rubber door seal , Drum and Drain ditch[9]. Samples were taken from the previous four locations of each washing machine using sterile swab sticks (BIONOVO, Poland) and then cultured on Tryp-to Soy Agar (TSA),

Then the plates were incubated for 24-48 hours at 37°C; the isolates were constantly purified until pure colonies were obtained.

The Gram-staining method was used to determine microbiological properties. The total quantity of Gram-negative and gram-positive bacteria and the phenotypic form of the cells were determined by using a light microscope after preparing slides of isolates.

Five isolates were designated as Kh-Am1, Kh-Am4 from the Drum part, Kh-Am3, Kh-Am6 from Rubber door seal part and Kh-Am5 from the Drain ditch; by analyzing

2

colony appearance and cell morphology, they matched the definition of the genera Bacillus and Lactobacillus in Bergey's Manual of Systemic Bacteriology, The 16S rRNA sequencing was used for more molecular identification.

Amplification of the 16S rRNA gene and phylogenetic trees

The isolates Kh-Am1, Kh-Am3, Kh-Am4, Kh-Am5, and Kh-Am6 were cultivated for 24 hours at 37°C using a rotary shaker with 250 rpm in falcon tube containing (20 ml) of Tryptic Soy Broth (TSB).

Then the G- spin DNA extraction kit was used to carry out the DNA extraction procedure (intron biotechnology, Korea). Using the Maxime PCR PreMix kit approach, the genes of 16S rRNA were amplified from the genomic DNA of selected isolates by polymerase chain reaction (PCR) (i-Taq).

Each reaction of PCR used Taq PCR PreMix (5µl), 1µl of 10 picomols/µl of each conserved primer 1250 F (5'-AGAGTTTGATCCTGGCTCAG- 3') and 1250R (5'- GGT-TACCTTGTTACGACTT- 3') from IDT (Integrated DNA Technologies company, Canada) , DNA template(1.5µl) and ddH2O (16.5 µl) for a 25µl total volume.

The optimal setting for the cycle of PCR amplification for gene detection is mentioned in (Table 1). To determine the outcome of PCR interactions in the presence of standard DNA and to identify the bundle size of the PCR interaction product on the agarose gel, amplification products were electrophoresed in a 1 percent (w/v) agarose gel.

PCR Products Purification

The products of the PCR were purified by utilizing the PCR kit of QIAquik (QIAGEN) following the manufacturer's instructions. To mix the components, five parts of the binding buffer were added to one part of the PCR product. The mixture was placed onto a QIAquick spin column after complete mixing. The flow-through was removed, and the collecting tube was refilled with the column. DNA was cleaned using wash buffer (0.75 ml) and centrifuged (30 to 60 seconds). After removing the flow-through, the tube underwent another minute of centrifugation. The column was then placed in a centrifuge tube (1.5 ml). 50 mL Elution Buffer solution was then added to the central of the QIAquik membrane for DNA elution. For a minute, the tube was centrifuged. Finally, the PCR product was purified and then sequenced by the Macro gene and the Korea Sequencing Service.

Phylogenetic relationships

The sequences of DNA collected have been compared to the database sequences of the gene bank (http://www.ncbi.nlm.nih.gov). By internet bioinformatics tools, BLAST (www.ncbi.nlm.nih.gov/BLAST), homolog surveys have been performed . Sequences shared the highest similarity with *Bacillus tropicus* Kh-Am1, *Lacticaseibacillus rhamnosus* Kh-Am3, *Bacillus subtilis* Kh-Am4, *Lacticaseibacillus rhamnosus* Kh-Am5 and *Lactobacillus zeae* Kh-Am6. In the format of FASTA, all the isolates have been downloaded. A maximal likelihood[10] Multiple Sequence Comparative via

No.	Phase	Tm (ºC)	Time	No. of cycle
1-	Initial Denaturation	95ºC	5 min.	cycle 1
2-	Denaturation -2	95ºC	45sec	cycle 35
3-	Annealing	58ºC	45sec	
4-	Extension-1	72ºC	45sec	
5-	Extension -2	72ºC	7 min.	cycle 1

Table 1. The PCR amplification cycles under ideal conditions.
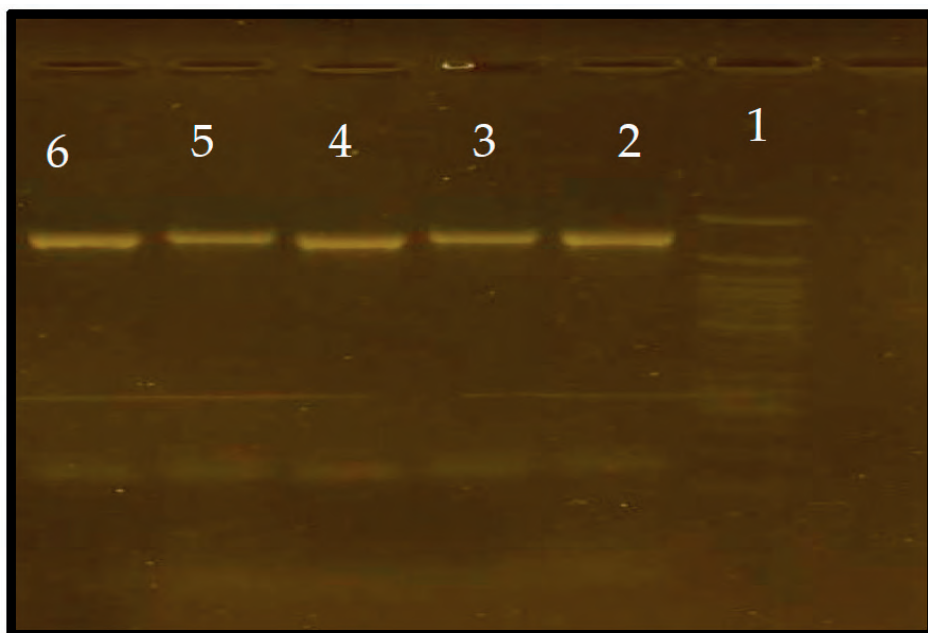
Figure 1. Electrophoresis gel of 16S rRNA gene amplified from isolates Kh-Am1, Kh-Am3, Kh-Am4, Kh-Am5, Kh-Am6, Kh-Am7. Lane 1: 1,500 bp DNA ladder; lane 2: Kh-Am1 isolate; lane 3: Kh-Am3 isolate; lane 4: Kh-Am4 isolate; lane 5: Kh-Am5 isolate; lane 6: Kh-Am6 isolate.

Log Expectation (MUSCLE) software was used to create phylogenetic trees with each 16S gene of isolates via using matched sequence and MEGA version 7.0 program. One thousand bootstrap copies of the original sequences have been used to calculate the confidence value for every branch. The complete series of 16S rRNA genes were entered into the GenBank database.

Assay of detergents activity

Microorganisms Used in the Experiment

Isolates of Kh-Am1, Kh-Am3, Kh-Am4, Kh-Am5 and Kh-Am6 bacteria were used in the experiment. Before the microbiological assay, the isolates were standardized to get the cell population of (0.5 Mac Farland standard).

Detergents

The antimicrobial potential of the detergents manufactured by different companies was investigated, and three types of detergents: Persil (P), Arial (A), and Peros (Pe) in both forms, gel liquid and (Tate) powder, were used.

Powder (Tate) solution of the three detergent types was prepared by dissolving 0.5 g/ml to form the concentrated mixture.

(stock solution), five –fold dilutions of all the stock were then used for the following tests. Gel detergents from the original packages were considered absolute concentration (100%), andfive–fold dilutions of all the stock solution Gel were then used for the following tests.

Screening for Sensitivity

The disc agar diffusion method was adopted; for each isolate, three plates were used. One for the dilutions and two for the stock solutions (i.e., duplicated). 1 ml of the bacterial suspension for each of the following isolates: - Kh-Am1, Kh-Am3, Kh-Am4, Kh-Am5 and Kh-Am6 were placed in each sterile Petri dish, at 45°C, 19 ml sterile molten Muller-Hinton agar was poured into each of the plates that contain the suspension isolates. These were thoroughly combined and allowed to sit for a while timer: 20 minutes. Boring holes were made with a 6 mm cup borer. Each plate was divided into parts, each of which was numbered suitably. 50 mL of each stock and dilution solution was poured into the dug wells. Before incubation at 37°C for 24 hours, the plates remained at room temperature for 30 minutes.

The inhibition zone diameters that resulted were calculated and registered[7,11].

Assay of antibiotic activity

The selected isolates were tested for antimicrobial susceptibility on Mueller–Hinton agar (Merck, Germany) using the disk diffusion (Kirby Bauer's) technique. Standard antibiotics were used: Penicillin G (P10 U) , Cephalexin (CL30 mcg) , Ceftazidime (CAZ 30 mcg), Vancomycin(VA 30 mcg), Cefixime (CFM 5 mcg) from (Bioanalyse). Amount of 0.1ml from 1 ml selected isolates suspension: Kh-Am1, Kh-Am3, Kh-Am4, Kh-Am5 and Kh-Am6, using the 0.5 McFarland reference, the concentration was adjusted to roughly 1 × 10^8 CFU/mL were spread onto molten Muller-Hinton agar. Antibiotic discs were loaded onto the agar. After a 24-hour incubation period at 37°C, the diameter of each antibiotic's inhibitory zone was measured[12].

Results

Swabs for attached microorganisms from the three parts of the washing machine were done. Streaking on cultured media plates revealed that the parts of the washing machine are filled with a variety of bacterial communities, table 2, with gram-positive bacteria dominating. Forty-six isolates of bacteria were collected, all of which revealed that they were more cultivable bacteria.

Accession numbers for nucleotide sequences

Designated isolates as the Kh-Am1, Kh-Am3, Kh-Am4, Kh-Am5, Kh-Am6 and their ribosomal 16S gene sequences were deposited in the NCBI Genbank database under the accession numbers MW447497.1, MW447499.1, MW448431.1, MW448432.1 and MW460243.1 respectively.

Phylogenetic studies of the selected isolates

When the 16S rRNA genes of the chosen isolates were amplified and analyzed using a 1 percent agarose gel-electrophoretic method, PCR products were a size of 1500 bp (Figure 1). (http://www.ncbi.nlm.nih.gov) the search engine performed BLAST analyses on sequences of partial 16S r RNA for each isolate. All of the isolates had 98 to 100 percent sequences compared to those in the NCBI GenBank database. Neighbor-joining tree (NJ) for isolation as built-in MEGA version 7 (Fig. 2, 3). For each nucleotide position, the

Parts of the washing machine	The total number of isolates	Gr +	Gr -
Rubber door seal (R)	15	9	6
Drum (D)	14	10	4
Drain ditch (Dr)	17	9	8
Total number	46	28 The highest number of Gram-positive bacteria	18

Table 2. Microflora in the washing machine parts: Rubber door seal, Drum and Drain ditch (imaging for microscope by using Gram stain).

scale represents 0.01 substitution. *P. mirabilis* (KX898582) was used as an outgroup.

For the Bacillus tree (Figure 2), a neighbor-joining tree based on the sequences of 16S rRNA gene with the highest similarity showed that *Bacillus tropicus* Kh-Am1 and *Bacillus subtilis* Kh-Am4 were the most closely related to *Bacillus paranthracis* strain MCCC 1A00395, *Bacillus nitratireducens* strain MCCC 1A00732 and *Bacillus tropicus* strain MCCC 1A01406.

Lacticaseibacillus isolates tree (Figure 3), showed that a neighbor-joining tree depending on the highest similarity sequences for 16S rRNA gene for *Lactobacillus* **zeae** Kh-Am6 is the most closely related to *Lactobacillus zeae* strain LT678023.1, while *Lacticaseibacillus rhamnosus* Kh-Am3 and *Lacticaseibacillus rhamnosus* strain Kh-Am5 were the most closely related to *Lacticaseibacillus rhamnosus* strain

19590 and *Lacticaseibacillus rhamnosus* strain 46 respectively.

Assay of detergents activity

The results of Table (3) showed that stock solution for powder has more inhibitory efficacy for five isolates than dilutions, as stock for Persil powder showed the highest inhibition of isolate Kh-Am6 with a diameter equal to 32 mm compared to other types, the lowest inhibitory diameter was for Kh-Am3 separate with a diameter equal to 13 mm for a stock for Ariel. In contrast, all the bacterial isolates showed resistance to dilutions for three types of powder detergents.

The results of Table (4) showed that stock solution for gel has more inhibitory efficacy than dilutions, as stock for Ariel gel showed the highest inhibition of isolate Kh-Am3 with a diameter equal to 15 mm compared to other types,
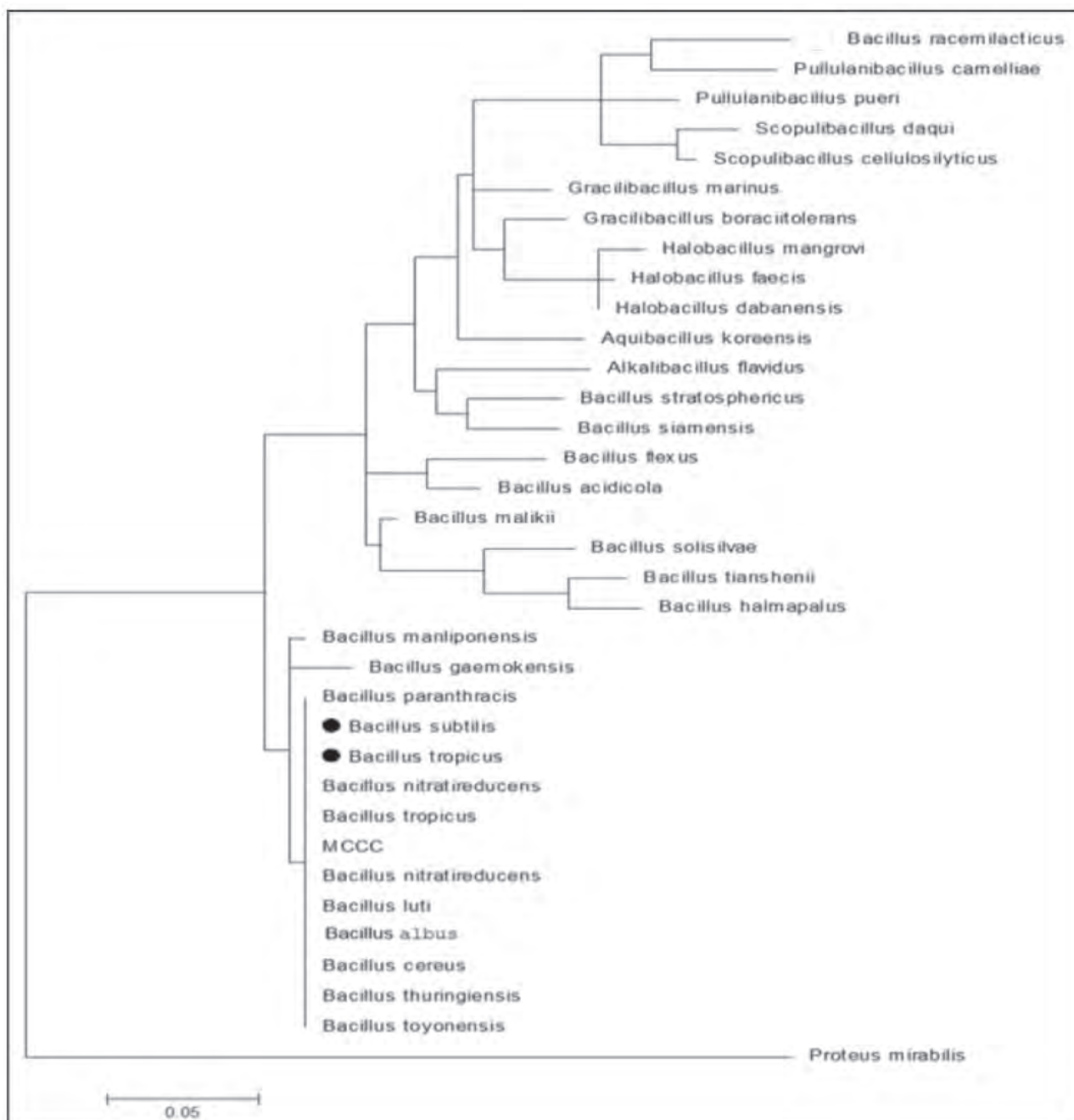
Figure 2. Neighbor-joining phylogenetic tree (1000 bootstrap) by using MEGA7 from (31)16S rRNA sequences homologous to that of *Bacillus subtilis* Kh-Am4 and *Bacillus tropicus* Kh-Am1, respectively (indicated by black Circle).

Figure 3. MEGA7 tool was used to create a neighbor-joining phylogenetic tree (1000 bootstrap) from 30 16S rRNA sequences homologous to that of *Lactobacillus zeae* Kh-Am6, *Lacticaseibacillus rhamnosus* Kh-Am3 and *Lacticaseibacillus rhamnosus* Kh-Am5, respectively (indicated by black rhombus).

Isolates	Peros		Ariel		Persil	
	Stock	**Dilutions**	**Stock**	**Dilutions**	**Stock**	**Dilutions**
Kh-Am1	14	0	14	0	0	0
Kh-Am3	15	0	13	0	20	0
Kh-Am4	24	0	14	0	20	0
Kh-Am5	20	0	22	0	0	0
Kh-Am6	28	0	30	0	32	0

Table 3. Sensitivity (in mm) of Kh-Am1, Kh-Am3, Kh-Am4, Kh-Am5 and Kh-Am6 bacteria to the powder detergents.

while all isolates showed resistance against the dilute concentration of three types for gel detergents except for Kh-Am6 at (15) mm inhibition diameter for gel Ariel.

Assay of antibiotic activity

Table (5) shows that Kh-Am1and Kh-Am5 isolates are more resistant to the antibiotics used than other isolates, the Kh-Am4 isolate is more sensitive to antibiotics, and all isolates showed resistance to both CFM5 and CAZ 30 antibiotics.

Discussion

Bacteria that colonies the extreme environment of ancient washing machines that have been in use for more than five years with commonly used washing machine de-

5

Isolates	Peros		Ariel		Persil	
	Stock	Dilutions	Stock	Dilutions	Stock	Dilutions
Kh-Am1	0	0	0	0	0	0
Kh-Am3	10	0	15	0	0	0
Kh-Am4	0	0	11	0	0	0
Kh-Am5	0	0	10	0	8	0
Kh-Am6	0	0	8	15	0	0

Table 4. Sensitivity (in mm) of Kh-Am1, Kh-Am3, Kh-Am4, Kh-Am5 and Kh-Am6 bacteria to the powder detergents.

6

isolates	VA 30	CL30	CFM5	CAZ30	P10
Kh-Am1	R	R	R	R	R
Kh-Am3	S	R	R	R	S
Kh-Am4	S	S	R	R	S
Kh-Am5	R	R	R	R	R
Kh-Am6	S	R	R	R	S

Table 5. Antibiotic susceptibility: Sensitivity of Kh-Am1, Kh-Am3, Kh-Am4, Kh-Am5 and Kh-Am6 bacteria to Vancomycin(VA 30 mcg), Cephalexin (CL30 mcg) , Cefixime (CFM 5 mcg), Ceftazidime (CAZ 30 mcg), Penicillin G (P10 U).

tergents were investigated. Using cultivation-dependent approaches, swab collection from household washing machine parts (Rubber door seal, Drum and Drain ditch) was picked.

Sample collection sites were carefully selected, as they provide surfaces for collecting microbes in addition to being in contact with the washing water.

The largest number of isolates were obtained in the Drain ditch part, which is evident as it accumulates an amount of the washing water, thus forming a moist environment that helps the growth of microbes. The collected washing water is rich in elements that support the development of microbes[9].

The three most contaminated parts of the washing machine are Gram-positive bacteria compared to Gram-negative bacteria Table (1). The reasons are probably due to the ability of some bacteria, such as *Bacillus*, to form spores, ensuring their survival for a more extended period.

Spores are one of the most resistant life forms known to date. One of the key factors contributing to these organisms' resistance to various difficulties, such as chemicals and extreme physical conditions, is their distinctive spore structure, which can withstand temperatures 40–45 0C higher than those experienced by their vegetative cells. The inner spore membrane, the peptidoglycan cortex, and the outer protein coat surround the dehydrated spore core, with the cortex playing a crucial role in the preservation of resistance[13]. Also, some bacteria such as *Lactobacillus* inhibit the growth of gram-negative bacteria[14]. In contrast, the studies of (15,16) mentioned that the negative bacteria are prevalent within the washing clothes and dishwasher machine community as they are more resistant to detergents

(without bleaching agent), while the Gram positive bacteria are more resistant to high temperatures.

A polyphasic taxonomic analysis was used to explore five novel Gram-stain positive bacteria. These isolates belonged to the *Bacillus* and *Lactobacillus* families, according to 16S rRNA gene sequence analyses, with over 97 percent identity to recognized *Bacillus* and *Lactobacillus* species. They well-separated branches from species were recorded, according to multilocus sequence typing analyses. The neighbor-joining tree depending on the highest similarty sequences for the 16S rRNA gene, showed that the *Bacillus* tropicus Kh-Am1 and *Bacillus* subtilis Kh-Am4 were the most closely related to *Bacillus* paranthracis strain MCCC 1A00395, *Bacillus* nitratireducens strain MCCC 1A00732 and *Bacillus tropicus* strain MCCC 1A01406, all have been deposited in GenBank, but represent unpublished data.

Furthermore, a split network tree based on the concatenated sequences of the highest similar 16S rRNA gene was performed, and three isolates of the *Lacticaseibacillus* group were divided into two principal clusters: *Lactobacillus zeae* which *Lactobacillus zeae* Kh-Am6 was deposit and *Lacticaseibacillus rhamnosus* were *Lacticaseibacillus rhamnosus* Kh-Am3 and Kh-Am5 were the most closely related.

In this study, results of the detergent's sensitivity (tables 2 and 3) showed that isolates vary in their response to three different types of commercial brands tide (Peros, Ariel, Persil) for both powder and liquid forms. The stock solution of the powder and gel for the three types of the wave has more inhibitory efficacy for five isolates than dilutions; this is consistent with what researcher[17] indicated in his study, where the maximum microbial growth at the lowest concentration of detergents, and the minimum microbial growth was recorded at the higher concentration, as the detergents contain several chemicals that enhance their antimicrobial properties.

As stock for Persil powder showed the highest inhibition of isolate Kh-Am6 with a diameter equal to 32 mm compared to other types, the lowest inhibitory diameter was for Kh-Am3 separate with a diameter equal to 13 mm for the stock for Ariel. In contrast, store for Ariel gel showed the highest inhibition of isolating Kh-Am3 with a diameter equal to 15 mm compared to other types; the study of 7 mentioned that the Ariel detergent was found to be the most active, in concentrated in addition to dilute solutions. Streptococcus pneumonia showed the highest inhibition with a diameter equal to 29 mm.

All the isolates of this study showed resistance against the dilute concentration of three types for powder and gel detergents except for Kh-Am6 at 15 mm inhibition diame-

ter for gel Ariel. Another study of (11) mentioned that the effect of detergents does not depend only on the type of detergent; it also depends on the period of immersion and temperature, in addition to the fact that bacteria can develop biofilms since they do so frequently in washing machine[18]. It is recommended to increase the washing machine program, meaning extending the drying, washing and spinning time, to get rid of the films and some plankton that may remain in the body of the washing machine, which may result in a fertile environment for the growth of microbes.

For the antibiotic activity, the study showed that most of the isolates were resistant to antibiotics, as shown in Table (4); kh-am1 and Kh-Am5 isolates showed resistance to all used antibiotics, while the Kh-Am4 isolate was more sensitive to used antibiotics. The high temperatures and continuous exposure to various types of detergents in washing led to the development of antibiotic resistance by stimulating mutations in the genetic material.

(19) stated that the resistance of bacteria to antibiotics is due to chromosome mutations or direct transfer of genes encoding a resistance mechanism. Resistance genes can be transferred in various ways, including conjugation (mobile genetic elements), transduction or transformation. The conjugation between the *Bacillus* genus and clinically relevant pathogens is possible, resulting in the transfer of antibiotic-resistance genes[20]. Perhaps the plasmid transfer in the biofilms enhances the resistance of bacteria to antibiotics and chemicals because the biofilm community is the dominant environment in washing machines[21].

The antibiotics used in this study have a common mechanism of action: to inhibit the synthesis of the peptidoglycan layer of the bacterial cell wall. Therefore these antibiotics are resistant by one of the two mechanisms, either by the enzymatic inhibition in some penicillin-resistant bacteria by synthesis of the enzyme beta-lactamase that breaks the beta-lactam ring in antibiotics or antibiotic resistance is developed through a change in the target site (antibiotic site of action) such as alteration in penicillin-binding proteins (PBP) and thus preventing binding of the antibiotic to the active site[22].

Conclusions

The study revealed that the washing machine was contaminated with gram-negative and gram-positive bacteria, with gram-positive bacteria dominating. This could be due to some bacteria's ability to form sporulation, which is the most life-resistant form of life that can withstand a variety of challenges, including chemicals, heat, and other harsh conditions where possible in addition to the Lactobacillus' ability to produce anti-growth of gram-negative bacteria, as well as its ability to resist temperatures surpassing 40-45° C.

Bacterial isolates had varying levels of resistance to both types of detergents, Tate and Gel, and from several commercial brands (Peros, Ariel, Persil) and also Perose cleaner is better at removing bacteria, then Ariel and Persil.

The stock solution for each powder and gel inhibited the bacteria, although all of the isolates were resistant.

Thus, the washing machine cleans the garments rather than sterilizes them. It may play a part in providing a sterile environment by lengthening the washing time, selecting the proper temperature, or selecting the detergent to minimize microbial growth in the washing machine environment.

Supplementary Materials

The following are available in this PDF, Table S1: Composition culture medium, Sheet 1 S2: Total cost, Sheet 2 S2: Stages of production, Sheet 3 S2: Direct and indirect labor, Sheet 4 S2: Culture medium, Sheet 5 S2: IMC, Sheet 6 S2: 6. Assumptions.

Author Contributions

Conceptualization, Ana María Henao Ramírez and Aura Inés Urrea Trujillo; methodology and software, Hernando David Palacio Hajduck and Ana María Henao Ramírez; validation anf formal analysis, Ana María Henao Ramírez; investigation, resources, data curation, writing—original draft prepara-tion, Ana María Henao Ramírez; writing—review and editing and supervision, Aura Inés Urrea Trujillo. All authors have read and agreed to the published version of the manuscript.

Conflicts of Interest

The authors declare no conflict of interest.

Bibliographic references

1. Bao, W., Gong, R. H., Ding, X., Xue, Y., Li, P., & Fan, W. Optimizing a laundering program for textiles in a front-loading washing machine and saving energy. Journal of cleaner production,2017: 148, 415-421.

2. Bloomfield, S. F., Exner, M., Signorelli, C., & Scott, E. A. Effectiveness of laundering processes used in domestic (home) settings October 2013. In IntSci Forum Home Hyg (pp. 1-62).

3. Callewaert, C., Van Nevel, S., Kerckhof, F. M., Granitsiotis, M. S., & Boon, N. Bacterial exchange in household washing machines. Frontiers in microbiology,2015: 6, 1381.

4. Teufel, L., Pipal, A., Schuster, K. C., Staudinger, T., &Redl, B. Material dependent growth of human skin bacteria on textiles investigated using challenge tests and DNA genotyping. Journal of applied microbiology,2010: 108(2), 450-461.

5. Bloomfield, S., Exner, M., Flemming, H. C., Goroncy-Bermes, P., Hartemann, P., Heeg, P., ...&Trautmann, M. Lesser-known or hidden reservoirs of infection and implications for adequate prevention strategies: Where to look and what to look for. GMS hygiene and infection control,2015: 10.

6. Schmithausen, R. M., Sib, E., Exner, M., Hack, S., Rösing, C., Ciorba, P., ...&Exner, D. The washing machine as a reservoir for transmission of extended-spectrum-beta-lactamase (CTX-M-15)-producing Klebsiellaoxytoca ST201 to newborns. Applied and environmental microbiology,2019: 85(22).

7. Ikegbunam, M. N., Metuh, R. C., Anagu, L. O., & Awah, N. S. Antimicrobial activity of some cleaning products against selected bacteria. International Research Journal of Pharmaceutical and Applied Sciences,2013: 3, 133-135.

8. Wang, Z., Shen, Y., Ma, J., &Haapasalo, M. The effect of detergents on the antibacterial activity of disinfecting solutions in dentin. Journal of endodontics,2012: 38(7), 948-953.

9. Tabata, A., Zhang, D., Maeda, T., Nagamune, H., & Kourai, H. Microbial contamination in home laundry operations in Japan. Biocontrol Science,2003: 8(1), 9-18.

10. Felsenstein, J. Evolutionary trees from DNA sequences: a maximum likelihood approach. Journal of molecular evolution,1981: 17(6), 368-376.

7

8

11. Jouda, M. M., Dardona, Z., & Albayoumi, M. The Antibacterial Effect of Some Household Detergents Againts Staphylococcus Aureus. Int J Curr Microbiol App Sci,2016: 5(2), 459-463.
12. Zulkhairi Amin, F. A., Sabri, S., Ismail, M., Chan, K. W., Ismail, N., Mohd Esa, N., & Zawawi, N. Probiotic properties of Bacillus strains isolated from stingless bee (Heterotrigona itama) honey collected across Malaysia.2020: International journal of
13. Robinson, R. K. Encyclopedia of food microbiology. Academic press.2014.
14. Bordignon Junior, S. E., Miyaoka, M. F., Spier, M. R., Rubel, R., Soccol, V. T., & Soccol, C. R. Production biomolecule with inhibitory activity against Gram-negative bacteria isolated from faeces of broilers and swine. Brazilian Archives of Biology and Technology,2011: 54(4), 723-731.
15. Nix, I. D., Frontzek, A., & Bockmühl, D. P. Characterization of microbial communities in household washing machines. Tenside Surfactants Detergents,2015: 52(6), 432-440.
16. Younis, K. M., Matter, I. R., & AL-Omari, A. W. Isolation and Molecular Identification of Bacillus boroniphilus sp. nov., Isolated from Dishwasher. Annals of the Romanian Society for Cell Biology,2021: 12286-12295.
17. Bhat, R., Prajna, P. S., Menezez, V. P., & Shetty, P. Antimicrobial activities of soap and detergents. Adv Biores,2011: 2(2), 52-62.
18. Gattlen, J., Amberg, C., Zinn, M., & Mauclaire, L. Biofilms isolated from washing machines from three continents and their tolerance to a standard detergent. Biofouling,2010: 26(8), 873-882.
19. Banoon, S., Ali, Z., & Salih, T. Antibiotic resistance profile of local thermophilic Bacillus licheniformis isolated from Maysan province soil. Comunicata Scientiae,2020: 11, e3921-e3921.
20. Dworkin, M. The Prokaryotes: Vol. 3: Archaea. Bacteria: Firmicutes, Actinomycetes. Springer Science & Business Media.2006.
21. Stalder, T., & Top, E. Plasmid transfer in biofilms: a perspective on limitations and opportunities. NPJ biofilms and microbiomes,2016:2(1), 1-5.
22. Drawz, S. M., & Bonomo, R. A. Three decades of β-lactamase inhibitors. Clinical microbiology reviews,2010: 23(1), 160-201.

ARTICLE / INVESTIGACIÓN

Calculation of soil pollution indices with elements in residential areas of Baghdad city

Rashid K. Al-Dahar1, Adel M. Rabee2*, Riyam J. Mohammed2

DOI. 10.21931/RB/2023.08.01.43

[1] Department of Medical Physics, College of Medical Sciences Techniques, University of Mashreq, Baghdad, Iraq.
[2] Department of Biology, College of Science, Baghdad University, Baghdad, Iraq.
Corresponding author: adel.mashaan@sc.uobaghdad.edu.iq

Abstract: Estimation of elements: Pb, Zn, Mn, Cd, and Cu, which were conducted seasonally from October-2021 till March-2022 in residential areas of Baghdad City using Geoaccumulation index (Igeo), enrichment factor ratios (EF), the factor of contamination (CF), contamination degree (Cd), index of pollution load (PLI) and index of potential ecological risk (Eif). The overall contamination factor in the research area is limited from low contamination with Cu, Mn, and Zn, moderately contaminated to very high contamination with Pb and Cd, while the assessment according to the I-geo index shows categories that vary from a slightly polluted to unpolluted by those examined heavy metals. The pollution load index indicates that the soils in some residential areas in Baghdad City have high levels of contamination by certain heavy metals. According to the EF results, the areas were moderately to significantly enriched with Pb and Cd and minimally enriched with Mn, Zn, and Cu. The potential for ecological risk had an irregular distribution, and the overall ecological risk level ranged from moderate to low. The PLI depicts the research area's vulnerability to soil heavy metal contamination and associated ecological concerns, particularly from lead and cadmium.

Key words: Pollution Index, Enrichment Factor, PLI index, Potential ecological risk.

Introduction

Soil is the habitat of many organisms, the skeleton of the terrestrial ecosystem and the most threatening factor of our environment due to the likely influences of various pollutants from human actions such as agricultural, industrial, etc[1]. Soil acts as a tank for heavy metals through surface complexation, ion exchange and surface precipitation[2]. Elements have been the topic of specific interest among pollutants due to their long-standing toxicity when the thresholds are exceeded and become one of the major environmental problems. These element ions are non-degradable and persistent in the environment[3]. Thus, the ecological issue of sediments and soil pollution by elements has increased in interest in the last decades in each developed and developing country worldwide[4]. Understanding the levels, degree and sources of elements contamination is fundamental for managing the environment[5].

Various methods of calculation based on the foundation of multiple algorithms may lead to a discrepancy in pollution estimation; simultaneously, these methods are estimating the soil quality or/and ecological sediment geochemistry. Thus, choosing an acceptable procedure to estimate sediment and soil quality is essential for urban planning decision-making[6]. This work aims to be a foundation for future studies of activities leading up to temporal changes in the metal concentrations within the soil of Baghdad City.

Materials and methods

Study area

Baghdad is the capital of Iraq and covers each side of the Tigris River. It lies around longitude 33.35° north and latitude 44.45° east. The municipality of Baghdad encompasses 40 administrative units, six in Karkh (west of the Tigris River) and eight in Rusafa (east of the Tigris River). The area of the municipality of Baghdad is 870 Km[2]. Baghdad's climate is semi-arid, continental and subtropical; cool winters and short springs; hot and dry long summers; few precipitations, little relative humidity, and high sun brightness. The rainfall duration is from December to April, with an annual average of 100 and 180 mm[7]. The Baghdad area has streets with intensive automobile traffic and many industrial activities located in this area.

Soil sampling and processing

Soil samples were collected seasonally from October-2021 till March-2022. A control soil sample was collected from a rural area (Abu-Ghuraib). In contrast, other sites represent the urban regions in Baghdad City (Doura, Ameriya, Ghazaliya, Jaderia, Adhamiyah, Karadah, Jamia and Zafaraniya). Soil samples were taken to a depth of 10 cm from each experimental site, taken with plastic tools, and then stored using polyethylene sample bags. The samples

2

Figure 1. Baghdad City with the sampling sites[7].

were oven-dried in the laboratory at 105°C for 24 h and passed through a 2-mm sieve. Then these samples were digested with a 3: 2: 2 mixture of HNO_3- H_2SO_4 – HCl. The digested soil samples were analyzed for their total Pb, Zn, Cu, Mn, and Cd concentrations by using atomic absorption spectrophotometer (Perkin-Elemer model 5000). While electrical conductivity, TDS and pH were measured as the method mentioned by Tandon[8] defined by making (1:2) soil and water solution for one hour was placed in a rotary shaker. Soil texture has been identified by the soil texture triangle method.

Soil pollution indices

To assess elements contamination in soils, some ecological indexes of soil pollution were calculated by using the following formulas:

Index of Geo-accumulation (I_{geo})

According to Muller,1969[9] procedure I_{geo}= log2 (Cn / Bn .1.5)

where Cn = Measured concentration of heavy metal in soil, Bn= Geochemical background value in average shale of element n. The seven proposed descriptive classes for I-geo deals are as follows: <0 = practically unpolluted; 0 – 1= unpolluted to slightly polluted, 1 – 2 = moderately polluted; 2 – 3= moderately to strongly polluted; 3 – 4= strongly polluted; 4 – 5 = strongly to very strongly polluted and >5 = very strongly polluted.

Degree of Contamination and Contamination Factor

Values of Cf are proposed to define the factor of contamination which is calculated by the formula[9]:
CF = C metal / C background value
Where C metal= concentration of metal
C background value= Reference value for each element.

The following terminologies are used to describe the contamination factor: CF <1, low contamination factor; 1≤CF<3, moderate contamination factors; 3≤CF<6, important contamination factors; and CF≥6, very high contamination factor. The degree of contamination (Cd) was defined as the sum of all contamination factors. The following terminology was adopted to describe the degree of contamination (Cd values) for the selected metals. Cd< 6: low degree of contamination; 6 = Cd< 12: moderate degree of contamination; 12= Cd< 24: considerable degree of contamination; Cd= 24: very high degree of contamination indicating serious anthropogenic pollution[9].

Pollution Load Index (PLI)

All sites were estimated for the range of metal pollution using the formula submitted by Thomilson *et al.* 1980[10].
PLI = (CF1 ✕ CF2 ✕ CF3 ✕…✕ CFn) 1/n
Where n is the number of metals studied (five in this study), and CF is the contamination factor calculated as described in the equation mentioned above. The PLI provides simple but comparative means for assessing a site quality, where a value of PLI < 1 denote perfection; PLI = 1 presents that only baseline levels of pollutants are present, and PLI > 1 would indicate deterioration of site quality.

The enrichment Factor (EF) is calculated by comparing each tested metal concentration with that of a reference metal submitted by Sinex and Helz[11.]

Enrichment Factor (EF) = (C_x / CFe) sample / (C_x / CFe) reference soil

Where: Cx/CFe sample of the heavy metal to the Fe ratio in the same sample and Cx/CFe reference is the natural background value of the metal ratio to Fe. Iron was chosen as a reference element because it is one of the most significant parts of soil, and iron is difficult to change by other human sources.

Six contamination categories were recognized because

of the enrichment factor. As the enrichment factor increases, the anthropogenic origins' contributions also increase. Therefore, this study used Mn as the reference metal because it was found most abundantly in the soil and environment.

Potential Ecological Risk Index (Eif)

The potential ecological risk for a given contaminant was calculated according to Hakanson[12].

$$E_f^i = C_f^i * T_f^i$$

Where T_f^i is the toxic response factor for a given heavy metal, C_f^i is the contamination factor.

T_f^i for Pb, Zn, Cu, Mn and Cd are 5, 1, 5, 5 and 30, respectively. The potential ecological risk of heavy metals is classified into five levels, according to the values of E_f^i:< 20 →low, 20-40 → moderate, 40-80 → considerable, 80-160 → high and > 160 →very high.

Statistical analyses

All statistical analyses were performed using SPSS version 12 for Windows. The significance level was set at P ≤ 0.05. One-way ANOVA was done to estimate significant differences between the concentrations of heavy metals in the study area, followed by Tukey's honesty test to compare the mean soil contamination levels. Correlation coefficients were also tested in this study.

Results and discussion

Soil characteristics and texture

The values of soil textures taken from residential areas are given in Table 1.

The texture of most samples is sandy clay loam. Clay loam soil has a tremendous nutrient-holding capacity and a great water-holding capacity[13]. Its aeration and permeability might be a little restricted. The soil texture taken from Jaderia and Zafaraniya is loam. Loamy soil composes clay,

silt, sand and organic matter in equally mixed particles of different sizes. Loamy soil is porous, which permits the better keeping of moisture and air circulation. During this work, the pH of the ground was reported to be alkaline (7.1-8.7). Charman and Murphy[14] recorded that the basic soil pH decreases the solubility of all micronutrients (excluding boron, chlorine and molybdenum), particularly those of copper, zinc, manganese and iron.

However, the minimum values of EC (458 μS/cm) and TDS (200 ppm) were found in the Karadah site, and the maximum values of EC (2500 μS/cm) and TDS(1220 ppm) were in the Doura site respectively, with significant (p ≤0.05) difference reported in all study sites (Table 2). The regions of high EC readings are represented by the area of Al-Doura that was recorded (1503-2500 μS/cm).

Elements concentration

The range of elements concentration Pb, Zn, Cu, Mn, and Cd in the studied sites are shown in Table-2.

The lead concentration in different regions ranged between a maximum value of 220 ppm in the Al-Jaderia site during the Summer and a minimum value of 40 ppm in the Abu-Ghuraib site during the Winter (Fig.2).

A significant variation (P ≤0.05) in Zn content during the investigation period in all the regions, which varied from 20 ppm in the Abu-Ghuraib site to 115 ppm in the Karadah site in Autumn (Fig.3). Regarding Cu, the current study has shown that the highest value was 60 ppm in the Doura site in the Summer, and the lowest value was 17ppm in the Adhamiyah site during winter (Fig.4). The results of Mn in the current study have shown that the highest value was 511 ppm in the Adhamiyah site during Summer, while the lowest mean data was 147 ppm in the Karadah region during Summer(Fig.5). Among the ten study sites, the Cd content of the soil was found to be the highest in the Doura region (1.1ppm) in Summer, and the lowest value (0.33 ppm) was found in the Zafaraniya site during the Autumn (Fig 6).

Sites	pH	EC(μS/cm)	TDS (ppm)	Soil texture
Abu-Ghuraib	7.6-7.8 7.7[a]	1126-1800 1400[c]	269-480 380[c]	Sand clay loam
Doura	7.1-7.7 7.6[a]	1503-2500 2000[a]	760-1220 800[a]	Sand clay
Ameriya	7.3-7.8 7.6[a]	841-1780 1200[c]	568-1200 807[a]	Sand clay loam
Ghazaliya	7.7-8.2 7.9[a]	860-1800 1234[c]	450-900 742[b]	Sand clay loam
Jaderia	7.7-8.2 7.9[a]	1400-2180 1800[b]	700-1120 890[a]	loam
Adhamiyah	7.8-8.7 8.2[b]	950-1740 1367[c]	450-870 600[b]	sand
Karadah	7.4-7.6 7.5[a]	458-790 600[d]	200-410 370[c]	Sand loam
Jamia	7.7-8.2 7.9[a]	463-1300 980[e]	300-777 521[b]	Sand clay loam
Zafaraniya	7.6-7.9 7.8[a]	1000-1300 1120[e]	400-700 532[b]	loam

Different superscript letters (a,b,c and d) in a row show significant differences (P < 0.05) indicated by Tukey Honest (HSD) significant difference tests

Table 1. Basic statistical data (range and mean) of the soil characteristics measured in the present study.

Sites	Pb ppm	Zn ppm	Cu ppm	Mn ppm	Cd ppm
Abu-Ghuraib	40-140 $78^b \pm 53$	25-53 $37^c \pm$	20-30 $25^b \pm 4$	200-337 $262^d \pm 69$	0.4-0.6 $0.49^c \pm 0.12$
Doura	110-137 $119^a \pm 15$	95-130 $102^a \pm$	39-60 $45^a \pm 10$	255-440 $303^c \pm 100$	0.6-1 $0.8^a \pm 0.19$
Ameriya	50-120 $83^b \pm 35$	40-75 $55^c \pm$	26-33 $29^b \pm 2.8$	200-330 $239^b \pm 61$	0.43-1.1 $0.6^b \pm 0.2$
Ghazaliya	80-102 $90^b \pm 13$	44-110 $68^b \pm$	20-50 $33^b \pm 12$	140-300 $215^d \pm 66$	0.75-0.9 $0.8^a \pm 0.06$
Jaderia	90-220 $136^a \pm 72$	60-115 $82^a \pm$	23-55 $35^a \pm 13$	190-390 $235^b \pm 59$	0.43-1 $0.78^a \pm 0.28$
Adhamiyah	47-120 $82^b \pm 36$	60-75 $68^b \pm$	17-50 $25^b \pm 15$	180-511 $290^a \pm 153$	0.7-1 $0.88^a \pm 0.1$
Karadah	55-112 $92^b \pm 32$	40-60 $46^c \pm$	22-29 $35^a \pm 3$	147-340 $235^b \pm 86$	0.4-1 $0.82^a \pm 0.23$
Jamia	60-120 $80^b \pm 34$	37-65 $47^c \pm$	20-30 $25^b \pm 4$	200-220 $211^d \pm 10$	0.43-1 $0.68^b \pm 0.28$
Zafaraniya	50-95 $66^c \pm 24$	29-70 $49^c \pm$	26-33 $28^b \pm 1.7$	150-212 $190^d \pm 27$	0.3-0.9 $0.62^b \pm 0.23$
Reference value [9]	20	95	45	900	0.3
EPA soil quality guidelines	40	110	64	-	0.6

Different superscript letters (a,b,c and d) in a row show significant differences ($P < 0.05$) indicated by Tukey Honest (HSD) significant difference tests

Table 2. Basic statistical data of the five elements measured in the present study (Range, mean ± standard deviation).
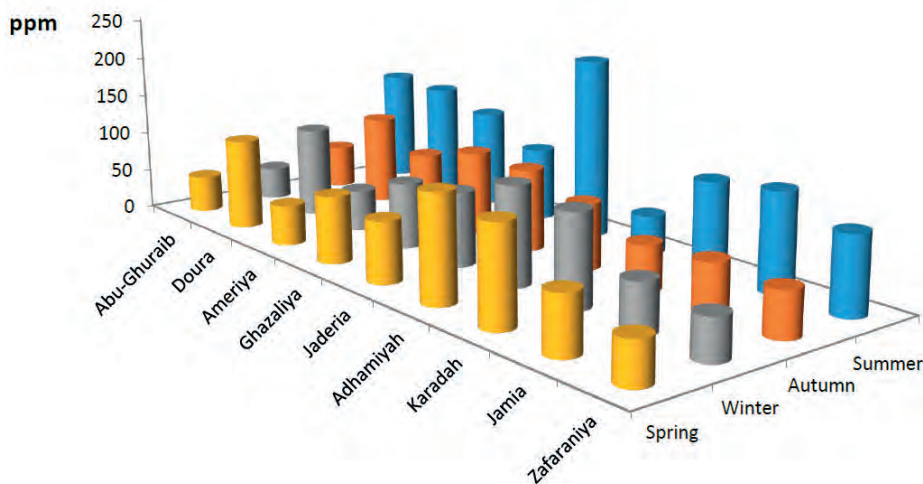
Figure 2. Seasonal variations of Pb in various residential areas of the Baghdad City.
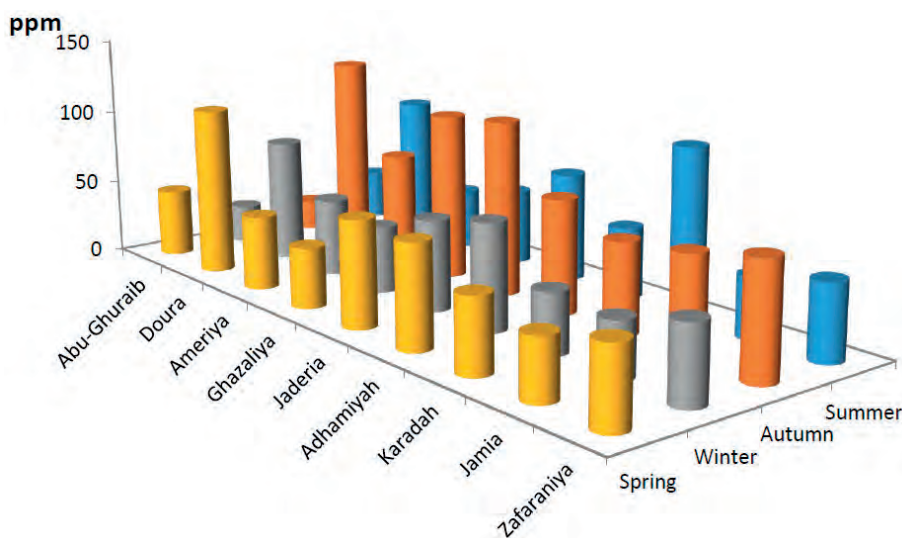
Figure 3. Seasonal variations of Zn in various residential areas of the Baghdad City.
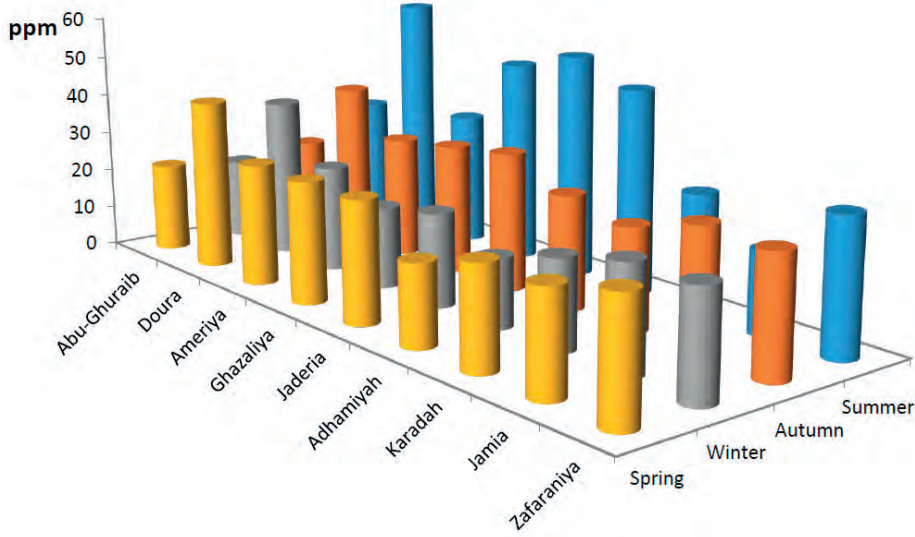
Figure 4. Seasonal variations of Cu in various residential areas of the Baghdad City.
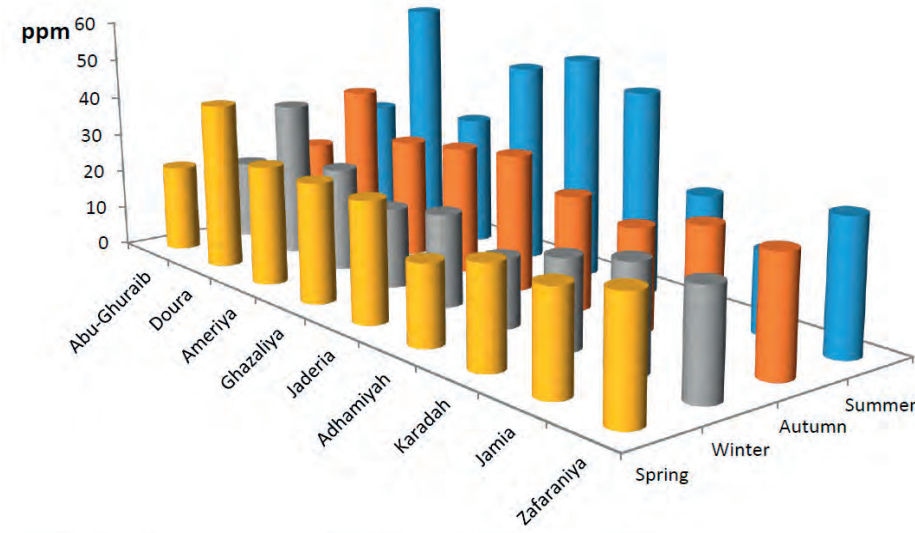
Figure 5. Seasonal variations of Mn in various residential areas of the Baghdad City.
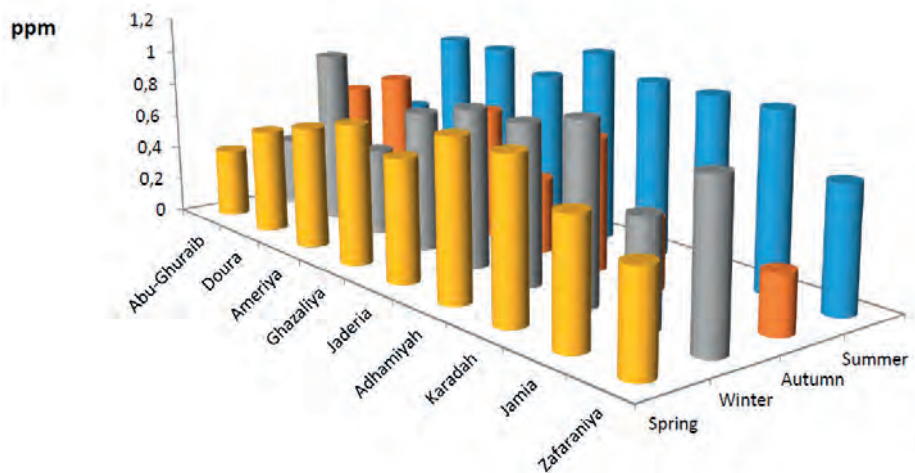
Figure 6. Seasonal variations of Cd in various residential areas of the Baghdad City.

The order of the heavy metals in this study is Mn>Pb >Zn>Cu>Cd. Manganese is comparatively affluent, with an average upper earth crust and a bulk continental crust mean of 1400 mg/kg[15].

Low concentrations of examined heavy metals were recorded in the Abu-Ghuraib site, a rural area, compared to other regions that represent urban areas. As well as, the metropolitan area has intensive anthropogenic activities, and high population density, which means urban surfaces collect different sources like industrial discharges, vehicle

emissions, waste disposal, and other human anthropogenic actions[16].

Seasonally, the results reflect that the highest concentrations of heavy metals were recorded in the Summer, while the minimum values were recorded in the winter. This may be due to the effect of the rainfall factor. The descriptive statistics affecting the heavy metals concentrations, taken from soils in Baghdad residential areas, displayed the values of the heavy metals. Compared with their background values, except for Pb and Cd, they were lower and were more than

their background value. This result showed that lead and Cd in Baghdad City pollute soils. Similar results were recorded in previous studies in Baghdad City[17] and Al-Hila City[18] in Iraq.

The selected sites display a significant difference ($P \leq 0.05$) between the group means of the elements. A significant correlation was found between the contaminants of Cu and Mn ($r = 0.6$), Pb and Cd ($r = 0.57$). Pb and EC($r=0.770$). EC and Zn($r=0.540$), TDS and Cu ($r = 0.880$), Cu and TDS($r=0.840$), Pb and TDS($r=0.868$). These results suggest that mixed origins of pollution sources include different human activities. Mn, Cu and Zn are of mixed origins of pollutants, with Mn being predominant lithogenic and emissions of vehicular characterized by Pb. The comparison of the contents of heavy metals in urban soils (residential areas) with the rural area (Abu-Ghuraib) reveals that the contamination levels of the metals in urban are higher than that in rural soils.

Assessment of elements contamination

The actual results of the calculation for I-geo in various soil samples are displayed in Table 3.

Studying geo-accumulation index (I-geo) values showed that the soils in residential areas in Baghdad City are unpolluted with Zn, Cu and Mn but slightly polluted with lead and cadmium.

Soils in Baghdad City were assessed for another contamination factor: factor of concentration, contamination degree, and pollution load index. The results are displayed in Table 4. Based on the CF values, the overall contamination of soils in Baghdad residential areas indicates that soils were low contaminated with Cu, Zn and Mn, moderately contaminated to very high contamination with Pb and Cd.

The degree of contamination varied from 6.3 in Abu-Ghuraib to 11.3 in the Jaderia area. The PLI values for Pb, Mn, Zn, Cu and Cd were more than 1 in Doura, Ghazaliya and Jaderia, indicating a high contamination level. Using the contamination factor categories previously described, residential areas of Baghdad suffered from a moderate degree of contamination by all heavy metals. The contamination index highlighted the harm that each element may have to the ecosystem and the human body. Alternatively, the pollution load index reflected the effects of the heavy metals in the soil and stressed the overall environmental impact of high concentrations of heavy metals.

In this work, we used the enrichment factor to estimate the possible anthropogenic impact and contamination in Baghdad soils (Table 5).

Therefore, to define the degree of metal contamination relatively, comparisons were made to background concentrations in the crust of the earth's using Mn as (a reference element). This index was used to quantify the pollution level and the potential of anthropogenic results in urban soils. Ultimately, while the enrichment factor values are rising, the anthropogenic sources' contributions are increasing too. Suppose the factor of enrichment is more significant than unity. In that case, it references that the richness of the heavy metal in the soil might not appear from the background of localized ground but from other natural or/and anthropogenic sources in urbanized areas, including industrial discharge, vehicle emissions, and other actions[19]. The results of EF indicated that the soils taken from residential areas of Baghdad City were moderately enriched to significantly enriched with Pb and Cd and minimally enriched with Zn and Cu. Mn was chosen as a fixed element that calculated the single enrichment index and was ignored in other counting methods.

	I-geo Pb	I-geo Zn	I-geo Cu	I-geo Mn	I-geo Cd
Abu-Ghuraib	0.9	-1.3	-0.9	-1.6	1
Doura	1.3	-0.3	-0.3	-1.4	1.7
Ameriya	1	-0.9	-0.8	-1.7	1.2
Ghazaliya	1	-0.73	-0.7	-1.6	1.7
Jaderia	1.5	-0.54	-0.5	-1.7	1.7
Adhamiyah	1	-0.72	-0.98	-1.5	1.8
Karadah	1.1	-1.1	-0.96	-1.4	1.7
Jamia	0.9	-1	-0.98	-1.8	1.4
Zafaraniya	0.7	-1.1	-0.95	-1.9	1.4

Table 3. Geo-accumulation index (I-geo) values of elements in residential areas in Baghdad City.

Sites	CF-Pb	CF-Zn	CF-Cu	CF-Mn	CF-Cd	Cd index	PLI-index
Abu-Ghuraib	3.9	0.3	0.5	0.29	1.5	6.4	0.67
Doura	5.6	1	1	0.33	2	9.9	1.2
Ameriya	4	0.5	0.4	0.33	2	7.2	0.88
Ghazaliya	4.5	0.7	0.7	0.26	2.6	8.7	1
Jaderia	6.8	0.8	0.6	0.62	2.5	11.3	1.1
Adhamiyah	4	0.48	0.5	0.32	2.5	7.7	0.91
Karadah	4.6	0.48	0.7	0.26	2.3	8.2	0.98
Jamia	4	0.47	0.5	0.23	2	7.1	0.84
Zafaraniya	3.1	0.5	0.6	0.2	2	6.4	0.82

Table 4. Contamination Factor, Degree of Contamination and PLI index values of heavy metals in residential areas of Baghdad City.

Sites	EF-Pb	EF-Zn	EF-Cu	EF-Cd
Abu-Ghuraib	13	1	1.7	5
Doura	16	3	3	6
Ameriya	12	1.3	1.2	6
Ghazaliya	17	2.6	2.3	4
Jaderia	10	1.3	1	4
Adhamiyah	12	1.1	1.8	7.8
Karadah	17	1.7	2.5	8.8
Jamia	17	2.1	2	8.6
Zafaraniya	15	2.5	3	10

Table 5. Enrichment Factor (EF) values of heavy metals in residential areas of Baghdad City.

7

It is possible to conclude that Pb, followed by Cd, was the most critical enriched element in the residential areas of Baghdad. It can observe that the values of enrichment factors significantly higher than one indicate an area of heavy metals and do not come from the background of localized soil but from other (anthropogenic or/and natural) sources in urbanized areas, including industrial discharges, vehicle emissions and other actions[20]. Well, as the presence of a large number of private generators. In environmental contamination studies, a popular strategy to assess how much soil is affected anthropogenic or naturally with elements is to estimate the enrichment factor for metal concentrations above uncontaminated background or levels of reference[21].

Assessment according to the potential ecological risk index

Meanwhile, the soil is contaminated with elements. It will be able to enter the body of humans through different exposure routes[22]. High toxic levels of heavy metals in soil can cause critical health and ecological risks[23,24]. The potential ecological risk index estimated their ecological potentiality and environmental impacts on toxicology in soil. The Hakanson potential ecological risk index is based on careful consideration of the heavy metals' ecological and environmental effects and toxicology in soils. The Hakanson index also provides a quantitative method of directly isolating the extent of potential hazards[25]. According to the ecological potentiality risk index, all examined locations have moderate potential ecological risk with lead, considerable potential environmental risk with cadmium, and low potential ecological risk with Zn, Cu, and Mn, respectively (Table 6). The chances of each element based on the likely environmental risk index were various, especially for the Cd. The possi-

ble reason may be the higher values of toxicity for Cd. The potential ecological risk index (RI) values are classified as the severe environmental risk for Cd in other Iraqi local studies[26].

Relatively high values for each Cd and Pb, which were recorded by the potential ecological risk index, indicate the seriousness of these metals and may threaten the people of Baghdad. There is a rising environmental interest in Cd as one of the most eco-toxic metals that shows a high level of adverse effects on soil's biological activity, plant metabolism, and the health of both animals and humans. One of the most important symptoms of exposure to cadmium (Cd) anemia is resistance to treatment and osteomalacia and urinary tract problems, kidney problems, prostate and lung cancer, and the loss of sense of smell[24]. Cd's other health complications in humans include kidney dysfunction, hepatic damage, and hypertension[26]. The poisonous (Lead) makes combinations with Oxo-groups in enzymes to impact practically all steps in the process of hemoglobin synthesis and porphyria metabolism. The levels of lead toxicity in the human body are connected with seizures, mental retardation and encephalopathy[27,28].

Conclusions

The investigation of soil elements content in the Residential Areas of Baghdad City indicated that the concentrations of Cd and Pb often exceeded the calculated average mean for the world scale of unpolluted soil. The pollution indices spatial Potential Ecological Risk Index (Eif) is vital for analyzing, treating, and transferring basic environmental information to managers, technicians, decision-makers, and their partners.

Sites	Eif -Pb	Eif -Zn	Eif -Cu	Eif -Mn	Eif -Cd
Abu-Ghuraib	19.5	0.3	2.5	1.4	45
Doura	28	1	5	1.6	60
Ameriya	20	0.5	2	1.6	60
Ghazaliya	22.5	0.7	3.5	1.3	78
Jaderia	34	0.8	3	3.1	75
Adhamiyah	20	0.48	2.5	1.6	75
Karadah	23	0.48	3.5	1.3	69
Jamia	20	0.47	2.5	1.1	60
Zafaraniya	15	0.5	3	1	60

Table 6. Potential Ecological Risk Index (Eif) values of elements in residential areas of Baghdad City.

Conflicts of Interest

The authors declare no conflict of interest.

Bibliographic references

1. Morton-Bermea, O.; Hernandez Alvarez, E.; Gaso, I., Segovia, N. Heavy metal concentrations in surface soil from Mexico City.Bull. Environ. Contam. Toxicol. 2002, 68,pp.383–388.
2. Yong, R. N. Mohamed, A.-M. O. and Warkentin, B. P. Principles of contaminant transport in soils, Elsevier, Amsterdam, First Edition, 1992 , pp. 327.
3. Wang, J. and Chen, C. Biosorbents for heavy metals removal and their future. Biotechnol. Adv. 2009, vol. 27, no 2, pp. 195–226.
4. Zhang L. Xin Y., Huan F., Youhai J., Tong O., Xingtian Y., Rongyuan L., Chengtie G., and Weiqi C.. Heavy metal contamination in western Xiamen Bay sediments and its vicinity, China. Mar. Pollut. Bull., 2007, vol. 54, no7, pp. 974–982.
5. Guan, Y.; Shao, C. and Ju, M. Heavy metal contamination assessment and partition for industrial and mining gathering areas, Int. J. Environ. Res. Public Health. . 2014, vol.11, no.7, pp. 7286–7303.
6. Caeiro, S. .Costa, M.H. Ramos, T.B., Fernandes, F..Silveira, N. , Coimbra, N. Medeiros, G. and Painho, M . Assessing heavy metal contamination in Sado Estuary sediment: an index analysis approach. Ecol. Indic. 2005, vol.2, pp. 151–169.
7. Al-Adili, A. Geotechnical evaluation of Baghdad soil subsidence and their treatments. Ph.D.Thesis University of Baghdad, Baghdad, Iraq. 1988.
8. Tandon, H. L. S. Methods of analysis of soil, plants, water and fertilizers. 1993. Publ. Fertiliser Development and Consultation Organisation 204-204A Bhanot Corner, 1-2 Pamposh Enclave New Delhi - 110048 (India),1993, Pp. 144.
9. Muller, G. Index of geo-accumulation in sediments of the Rhine river. Geol. J. 1969, vol. 2, no.3, pp. 108–118.
10. Tomlinson, D. L. ; Wilson, J. G.; Harris, C. R. and Jeffrey, D. W. Problems in the assessment of heavy-metal levels in estuaries and the formation of a pollution index. Helgolnder Meeresunters.1980, vol. 33, no. 1, pp. 566–575.
11. Sinex, S. A. and Helz, G. R. Regional geochemistry of trace elements in Chesapeake Bay sediments," Environ. Geol. 1981, vol. 3, no. 6, pp. 315–323.
12. Hakanson L. An ecological risk index for aquatic pollution control: A sedimentological approach. Water Resear. 1980, vol. 14,pp. 975-1001.
13. Maral, N. Soil and water analysis techniques for agricultural production.2010, thesis, Graduate school of natural and applied sciences, Middle East Technical University. Pp.108.
14. Charman P. E. V ; and Murphy, B. W. Soils, their properties and management. 3rd edition, Oxford University Press, 2007.
15. Taylor, S. R. and McLennan, S. M. The geochemical evolution of the continental crust. Rev. Geophys. 1995, vol. 33, no. 2, pp. 241–265.
16. Biasioli, M. ; Barberis, R. and Ajmone-Marsan F. The influence of a large city on some soil properties and metals content. Sci. Total Environ. 2006, vol. 356, no. 1–3, pp. 154–164.
17. Al Obaidy, A.M and Al Mashhadi A. A. M. Heavy metal Contaminations in urban soil within Baghdad City, Iraq.. J. of Environ.Protec. 2013, vol. 4, pp. 72-82.
18. Al-Rubaiee, A. H. and Al-Owaidi, M. R. A. Assessment of Heavy Metal Contamination in Urban Soils of selected areas in Hilla City, Babylon, Iraq. Iraqi J. of Sci., 2022,vol. 63, no. 4, pp. 1627-1641
19. Cabrera, F. ; Clemente, L., Barrientos, E. D. ; López, R. and Murillo, J. M. Heavy metal pollution of soils affected by the Guadiamar toxic flood. Sci. Total Environ., 1999, vol. 242, no. 1–3, pp. 117–129.
20. Thornton, I. Metal contamination of soils in urban areas. Soils urban Environ., 1991, pp. 47–75.
21. Bade, R. ; Oh, S. Shin, W. S. and Hwang, I. Human health risk assessment of soils contaminated with metal (loid) s by using DGT uptake: A case study of a former Korean metal refinery site. Hum. Ecol. Risk Assess. An Int. J. 2013, vol. 19, no. 3, pp. 767–777.
22. Dong, X. ; Li, C. ; Li, J. ; Wang, J. ; Liu, S. and Ye, B. A novel approach for soil contamination assessment from heavy metal pollution: A linkage between discharge and adsorption. J. Hazard. Mater. 2010, vol. 175, no. 1–3, pp. 1022–1030.
23. Dinelli E. and Tateo, F. Factors controlling heavy-metal dispersion in mining areas: the case of Vigonzano (northern Italy), a Fe-Cu sulphide deposit associated with ophiolitic rocks. Environ. Geol. 2001, vol. 40, no. 9, pp. 1138–1150.
24. Hashim, B. M. Measurement and study concentrations some air pollutants in Baghdad city. MSc. Thesis, College of Science ,Al-Mustansiriyah University, 2009, pp.95.
25. Klaassen, C. D. Heavy metals and heavy-metal antagonists. Pharmacol. Basis Ther. 1996, vol. 12, pp. 1851–1875.
26. AL-Heety L. F.D., Hasan, O.M. and Al-Heety, E. A. M. S. Heavy metal pollution and ecological risk assessment in soils adjacent to electrical generators in Ramadi City, Iraq. Iraqi J. of Sci. 2021, vol. 62, no. 4, pp. 1077-1087.
27. Ademoroti, C. M. A. Environmental chemistry and toxicology. Ibadan Foludex Press Ltd, 1996.
28. Schumann, K. The toxicological estimation of the heavy metal content (Cd, Hg, Pb) in food for infants and small children

8

Long survival of *Neisseria meningitidis* in freeze-dried cultures maintained in potentially unsuitable conditions

Oderay Gutierrez[1], Isabel Martínez[2], Onelkis Feliciano[1], Luis Jerez[1], Rafael Llanes[1*]

[1] Centro de Investigaciones, Diagnóstico y Referencia. Instituto de Medicina Tropical Pedro Kourí (IPK), La Habana, Cuba.
[2] Departamento de Investigaciones. Escuela Latinoamericana de Medicina (ELAM), La Habana, Cuba.
Corresponding author: llanes@ipk.sld.cu

Currently, diagnosis of *Neisseria meningitidis* in nasopharyngeal samples can be made by culture and nucleic acid amplification techniques[1]. In Cuba, molecular diagnosis of meningococcal meningitis was introduced at the National Reference Laboratory for Neisseria (NRLN), in 2010, through a PCR that amplifies a fragment of the ctrA gene using the protocol described by Taha, 2000[2]. This gene codes for a capsule protein that regulates the adhesion of *N. meningitidis* to the host, and 16 to 28% of meningococci isolates, especially in the nasopharynx, lack this gene[2]. In contrast, the sodC gene, related to the production of superoxide-dismutase of this organism, is less sensitive to antigenic variation, hence its importance for molecular diagnosis in patients and asymptomatic carriers[3]. Information on the meningococcal carriage is essential for public health policy[4]. Still, the high number of invasive meningococci disease (IMD) affecting Cuba during the 1980s and the absence of molecular tools prevented its accurate microbiological diagnosis in carriers[5]. This study aimed to identify

In Ciego de Avila province, *N. meningitidis*, by conventional and molecular methods in freeze-dried nasopharyngeal cultures of 50 *Neisseria spp.*, recovered from carriers during 1987-1988, one of the most affected by a large epidemic of IMD in Cuba[5]. Lyophilized material, which was preserved for 30 years, was reconstituted in 2 mL of nuclease-free sterile distilled water (Promega, USA). One milliliter was subcultured onto chocolate agar and incubated at 36.5-37°C for 18-24 hours, with 5-10% CO_2, and the other milliliter was used to perform DNA extraction. Conventional methods used as sugar utilization and Vitek®2 automated system (bioMérieux, France) identified Neisseria species. QIAamp®DNA Mini and Blood Mini method, QIAGEN, Germany made 1 DNA extraction. Two PCR systems were used for molecular identification of meningococci, a simple PCR test that amplifies a 523 bp fragment of the *ctrA* gene[2], and a real-time PCR (rt-PCR) that amplifies a 127 bp fragment of the *sodC* gene[3]. Serogroup identification of *Neisseria meningitidis* isolates was developed by slide agglutination using Remel™ Agglutinating Sera (Lenexa, USA). In addition, the main serogroups (A, B, C, W135, Y, X) of meningococci were investigated by rt-PCR[6], in positive samples identified by both simple and rt-PCR systems.

Pharyngeal carriage of *N. meningitidis* has been considered a prerequisite for the development of IMD and is known to be essential for transmission[4]. In this study, ten isolates (20%) recovered from lyophilized material of nasopharyngeal carriers were identified as meningococci by

culture, the standard gold method for detecting bacterial carriage[7]. Nine of ten isolates were serogroup B, which was predominant during the epidemic of IMD in Cuba[5], and the other isolate was non-groupable.

Freeze-drying is more practical for the long-term preservation of

N. meningitidis cultures and optimal conditions for its conservation are refrigeration

(2-8°C) or freezing (-30 -70°C) temperatures, ampules are protected from the action of light and placed in an environment without humidity[8,9]. These conditions produce good genetic stability of the product, with a longevity of up to 20 years[8]. Moreira *et al.*, in Cuba, obtained a 46.3% of survival of N. meningitidis lyophilized cultures after one year of storage at 4°C[10]. Lyophilization is a very complex physical process affected by many parameters and variables such as growth medium, cell concentration, freezing rate, lyoprotectant, reconstitution medium, and time[11]. In the current investigation, freeze-dried ampules were stored at room temperature and unprotected from light. However, its more prolonged survival of 30 years is noteworthy under these unsuitable conditions[8,9]. Recently, Swain et al. demonstrated the relatively prolonged survival of the Cuban, New Zealand and Norwegian epidemic *N. meningitidis* serogroup B strains on inanimate surfaces for up to 8 days, depending on temperature and humidity, in comparison to other meningococci strains belonging to serogroup W135. In addition, carriage isolates appeared to survive better than invasive isolates, with a statistically significant difference (P = 0.002)[12].

Some authors recommend molecular tests for the identification and serogrouping of

N. meningitidis in cultures from carriers and lyophilized material[4,11]. The end point-PCR results that amplify a fragment of *ctrA* gene detected *N. meningitidis* in 76% of cell suspensions of *Neisseria spp.* Investigated (Figure 1). Meanwhile, the rt-PCR that amplified a 127 bp fragment of the *sodC* gene identified meningococci in 100% of cell suspensions (Figure 2), which highlights the capacity of this rt-PCR system for the definitive identification of *N. meningitidis*. There are few studies on using *sodC* gene in nasopharyngeal cultures from carriers[3,4]. Dolan *et al.* reported that sodC rt-PCR effectively identified 99.7% (624/626) of invasive and carriage *N. meningitidis* strains and was superior to the *ctrA* rt-PCR assay (71.6% 448/626)[3]. Jones *et al.* recently investigated three target genes (*ctrA, sodC* and *porA*) by whole-genome sequencing and rt-PCR. The *ctrA*

2

gene was absent in a large percentage (58%, 54/93) of carriage isolates. However, both *porA* and *sodC* genes were well represented in the carriage collection (99% and 97%)[13]. In addition, Jordens & Heckels reported the development of a *porA* rt-PCR assay that identified several *N. meningitidis* isolates from carriers that were missed by using only the *ctrA* gene[7].

In the current study, 68.4% (26/38) of cell suspension positive to *N. meningitidis* by both PCR belonged to serogroup B, 5.3% was serogroup C, and the remainder (26.3%) were non-groupable. Martínez *et al.*, in a longitudinal study carried out on meningococci strains corresponding to nasopharyngeal carriers of the epidemic (1982-1992) and post-epidemic (1993-2002) stage in Cuba, detected a predominance of serogroup B (67.3%) in the epidemic phase and the non-agglutinable strains during the post-epidemic stage (70.7%)[14]. In Colombia, Moreno *et al.* also report a predominance of *N. meningitidis* serogroup B in carriers[15].

The absence of comprehensive information for carriage in developing countries limits clarification of the epidemiology of IMD16. In the case of the Caribbean region, in particular, there is no previous report about the use of molecular methods for identifying or seron-grouping *N. meningitidis* in patients or carriers. The current study supports the usefulness of molecular tools in future studies of nasopharyngeal carriers in the Cuban population. In addition, this genetic material is helpful for further genomic characterization of Cuban meningococci strains by multi-locus sequence typing and/or other sequence methods. Genomic surveillance for *N. meningitidis* is fundamental for understanding pathogen evolution and disease epidemiology and can be significantly improved using culture-free methods[17].

Conclusions

This study represents the first international report about a more prolonged survival of *N. meningitidis* in freeze-dried cultures from nasopharyngeal carriers that were kept under potentially unsuitable temperature, humidity and light
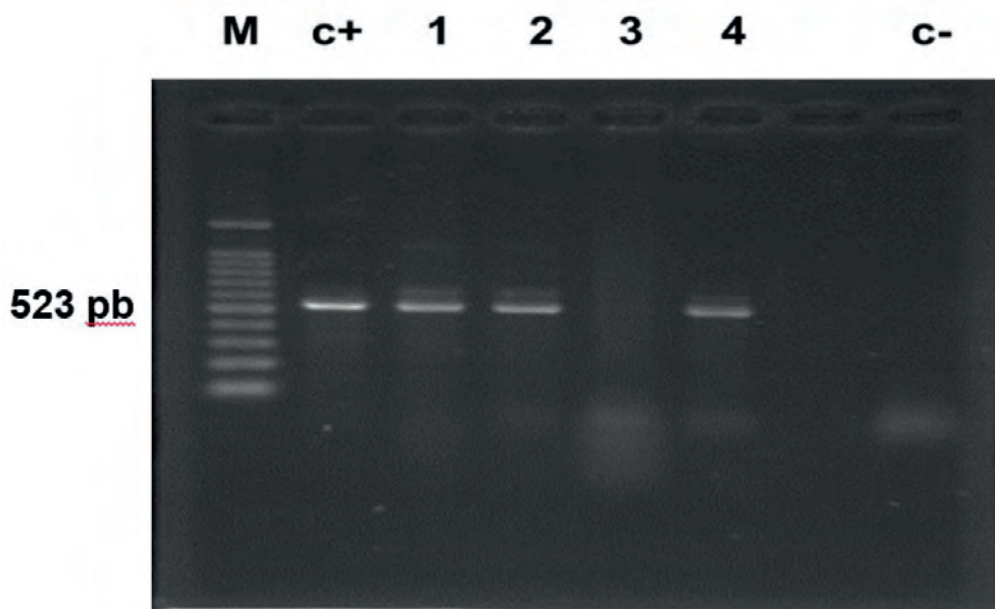
Figure 1. Amplifying *Neisseria meningitidis ctrA* gene in freeze-dried cultures of *Neisseria spp.* from carriers using a PCR with DNA extraction shown in 2% agarose gel stained with ethidium bromide, giving a 523 bp amplicon. Lanes: M: 100 bp DNA ladder; c+: positive control DNA of *N. meningitidis* ATCC 26195; lanes 1-4: DNA from carriers; c-: negative internal control (distilled water).

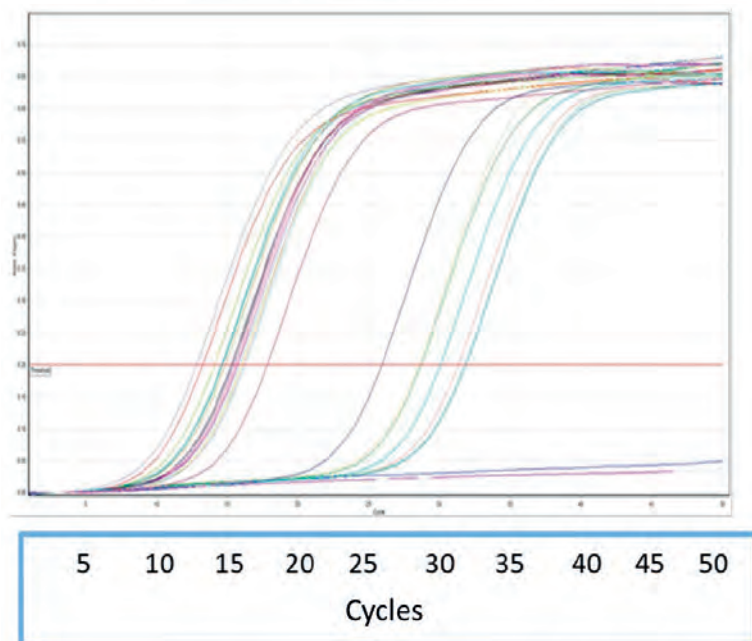**Figure 2.** Specific amplification curves for real-time PCR with TaqMan that amplifies a 127 bp fragment of *Neisseria meningitides sodC* gene obtained from freeze-dried cultures of *Neisseria spp* in carriers. The horizontal line is the threshold.

exposure conditions. The sodC-based rt-PCR assay had an advantage over *ctrA* gene for detecting meningococci in cell suspensions of *Neisseria spp.* from lyophilized material obtained during the extensive epidemic of IMD in Cuba in the 1980s.

Acknowledgments

The authors acknowledged Dr. Yaxier de Armas and Prof. Imti Choonara for comments about the manuscript and Dr. Eldy Machado for English revision.

Conflicts of Interest

None.

Bibliographic references

1. Rizek CF, Luiz AM, Assis GR, Figueiredo F, Levin AS, Lopes ME. Comparison of methods to identify Neisseria meningitidis in asymptomatic carriers. Rev Inst Med Trop Sao Paulo. 2016; 58: 60. doi: 10.1590/S1678-9946201658060. Last accessed [June 28 2022]

2. Taha MK. Simultaneous approach for nonculture PCR-based identification and serogroup prediction of Neisseria meningitidis. J Clin Microbiol. 2000; 38: 855-7. doi: 10.1128/JCM.38.2.855-857.2000. Last accessed [June 28 2022]

3. Dolan T, Hatcher CP, Satterfield DA, Jordan M, Bach MC, Linskot KB, et al. SodC-based real-time PCR for detection of Neisseria meningitidis. PloS one. 2011; 6: e19361. https://doi.org/10.1371/journal.pone.0019361. Last accessed [June 28 2022]

4. Coch CA, Silva de Lemos AP, Outeiro MC, Mendoza RA, Ballester T, Von Groll A, et al. Detection of Neisseria meningitidis in asymptomatic carriers in a university hospital from Brazil. Rev Argentina Microbiol. 2015; 47: 322-7. doi: 10.1016/j.ram.2015.08.004. Last accessed [June 28 2022]

5. Sierra-González VG. Vacuna cubana antimeningocócica VA-MENGOC-BC®: Treinta años de uso y potencialidades vigentes. VacciMonitor. 2020; 29(1):32-43. ISSN 1025-028X. Last accessed [27 June 2022].

6. World Health Organization. PCR for Detection and Characterization of Bacterial Meningitis Pathogens: Neisseria meningitidis, Haemophilus influenzae, and Streptococcus pneumoniae. Chapter 10. In: Laboratory Methods for the Diagnosis of Meningitis caused by Neisseria meningitidis, Streptococcus pneumoniae, and Haemophilus influenzae. 2nd ed. WHO/IVB.11.09, 2011. 323 pp.

7. Jordens JZ, Williams JN, Jones GR, Heckels JE. Detection of Meningococcal Carriage by Culture and PCR of Throat Swabs and Mouth Gargles. J Clin Microbiol. 2002; 40 (1): 75-9. doi: 10.1128/JCM.40.1.75-79.2002. Last accessed [June 27 2022]

8. Green LH. Culturing and Preserving Microorganisms. In: Goldman E & Green LH. Practical Handbook of Microbiology. 2015. Chapter 3. CRC Press, London. https://www.routledgehandbooks.com/doi/10.1201/b17871-5. Last accessed April 22 2022.

9. Del Puerto CA, Iglesias E, Morales T, Baños N, Nocedo MD, Carnota G, et al. Organización y manejo de la colección de cepas de referencia del Instituto Finlay. Vaccimonitor. 2009; 18: 20-4. ISSN 1025-028X. Last accessed [27 June 2022]

10. Moreira T, Iglesias E, Delgado H. Preservation of Neisseria meningitidis group B by freeze-drying. J Microbiol Meth. 1995; 23: 343-6.

11. Peiren J, Buyse J, De Vos P, Lang E, Clermont D, Hamon S, et al. Improving survival and storage stability of bacteria recalcitrant to freeze-drying: a coordinated study by European culture collections. Appl Microbiol Biotechnol 2015; 99: 3559–71. doi: 10.1007/s00253-015-6476-6 Last accessed [June 27 2022]

12. Swain CL, Martin DR, Sim D, Jordan TW, MacKishan JK. Survival of Neisseria meningitidis outside of the host: environmental effects and differences among strains. Epidemiol. Infect. 2017; 145, 3525–3534. doi:10.1017/S0950268817002473. Last accessed [June 27 2022]

13. Jones CH, Mohamed N, Rojas E, Andrews L, Hoyos J, Hackins JC, et al. comparison of phenotypic approaches to capsule typing of Neisseria meningitidis by use of invasive and carriage isolate collections. J Clin Microbiol 2016; 45: 25-34. doi: 10.1128/JCM.01447-15

14. Martinez I. Neisseria meningitidis: contribución al transporte-conservación y caracterización de cepas aisladas en Cuba (1982-1992). Tesis presentada en opción al grado científico de doctor en ciencias médicas. Ciudad de La Habana, 2004. http://scielo.sld.cu › pdf › mtr05206. Last accessed [27 June 2022]

15. Moreno J, Sanabria O, Saavedra S, Rodríguez K, Duarte C. Caracterización fenotípica y genotípica de Neisseria meningitidis serogrupo B aisladas en Cartagena, Colombia, 2012-2014. Biomédica. 2014; 35(1): 138-43. doi: http://dx.doi.org/10.7705/biomedica.v35i1.2414. Last accessed [27 June 2022]

16. Serra L, Presa J, Christensen H, Trotter C. Carriage of Neisseria meningitidis in low and middle income countries of the Americas and Asia: A Review of the Literature. Infect Dis Ther. 2020; 9(2): 209–40. doi: 10.1007/s40121-020-00291-9. Last accessed [June 27 2022]

17. Itsko M, Topaz N, Ousmane-Traoré S, Popoola M, Ouedraogo R, Gamougam K, et al. Enhancing Meningococcal Genomic Surveillance in the Meningitis Belt Using High-Resolution Culture-Free Whole-Genome Sequencing. J Infect Dis 2022; 226: 729-37. doi: 10.1093/infdis/jiac1042022;226:729–37. Last accessed November 2, 2022

3

ARTICLE / INVESTIGACIÓN

Molecular analysis of Fungi: *Malasseziarestricta* from Felidae

Afkar Muslim Hadi*, Hani Saber Khalif
Iraq Natural History Research Center and Museum, University of Baghdad, Iraq.
Corresponding author: afkar_hadi_iraq@yahoo.com

DOI. 10.21931/RB/2023.08.01.46

1

Abstract: A total of 9 samples of wild cat *Felischausfurax* (de Winton, 1898) and 13 (11 positives) samples of domestic cat *Feliscattus* (Linnaeus, 1758) belong to Family Felidae. All cats were trapped and used hair and skin scrapings by forceps and surgical blades. The areas of the collection were: Mosul province (north of Iraq); Baghdad, Al-Rashidiya, Tharthar, Nahrawan, AL-Mahmoudiya (middle of Iraq) and AL-Haretha (south of Iraq). The current study revealed that the sensitive and specific PCR assay allowing rapid and reliable identification of *Malasseziarestricta* by the fragment size amplified was 500bp in the ITS1 gene in one sample of wild cats. The current study recorded a new strain of *Malasseziarestricta* that called AF2013 strain "small subunit ribosomal RNA gene, partial sequence; internal transcribed spacer 1", complete sequence; and 5.8S ribosomal RNA gene, partial sequence. Which was inserted in GenBank: MW376484.1 from wild cat *Felischausfurax* for the first time in Iraq. Sequencing revealed close matching of the phylogenetic tree to an isolate from Korea (CP030254). The compression was performed using NCBI – the based nucleotides website.

Key words: Dermatitis, Cutaneous microflora, fungi, Genotype, *Malasseziarestricta*.

Introduction

The taxonomy of *Malasseziarestricta* (E.Guého, J.Guillot&Midgley) according to GBIF[1]:

Kingdom: Fungi
Phylum: Basidiomycota
Class: Malasseziomycetes
Order: Malassezialess
Family: Malasseziaceae
Genus: *MalasseziaBaill*, (1889)
Synonyms: *PityrosporumSabour* (1904)

The genus of *Malassezia* includes seven species comprising the three former taxa *M. furfur, M. pachydermatis* and *M.sympodialis*, and four new taxa *M. globosa*, *M. obtuse, M. restricta* and *M. slooffiae*[2].

Molecular techniques have increased research in this field, such that revealed the infection with *Malassezia* spp. to man for over 150 years, and seven new species have been added to this genus[3].

The skin colonization with *Malassezia* spp. depends on the skin's body site, the host's age, and other comorbid skin conditions, as the geographic area. It is found in the highest density in sebaceous regions such as the scalp, face, and upper trunk. It is seen in higher densities in young adults, who tend to have relatively oily skin[4].

Malassezia spp. is naturally found on the skin surfaces of many animals, including humans. It can cause hypopigmentation or hyperpigmentation on the trunk and other locations in humans[5]. The knowledge about *Malassezia* spp. has expanded remarkably since the 1990s in dogs and cats[6]. *Malassezia* furfurwas isolated from cats in 1999 by Crespo[7].

The epidemiological map of the spread of fungi Malassezia from animals to humans is unclear, as Morris[8] indicated that *M. pachydermatis* was transmitted from pet dogs to humans. This is an important indicator that prompts us to re-

search further the transmission of *Malassezia* spp. from domestic and wild animals. In Poland, along with surveys from 2008 to 2018 for many groups of animals like dogs, cats, rodents, riding horses, birds and other pet animals (reptiles and mammals), Bozena[9] revealed to fungal species involved and evaluated the risk of their transmission to humans.

The study aims to spotlight the species of Malasseziarestrictathat infected domestic and wild cats through molecular analysis for the first time in Iraq.

Materials and methods

Collection of samples

A total of 9 samples of wild cat *Felischausfurax* (de Winton, 1898) and 13 (11 positives) samples of domestic cat *Feliscattus* (Linnaeus, 1758) of Felidae Family were trapped and used as hair and skin scrapings by forceps and surgical blades. The scales were collected in sterile empty Petri dishes[10]. The areas of the collection were: Mosul province (north of Iraq); Baghdad, Al-Rashidiya, Tharthar, Nahrawan, AL-Mahmoudiya (middle of Iraq) and AL-Haretha (south of Iraq).

DNA Extraction

Genomic DNA was isolated from two samples according to the QIAamp DNA Mini Kit protocol, QIAGEN.

Primer preparation

Lyophilized primers (Macrogen Company) were dissolved in nuclease-free water to give a final concentration of 100 pmol/µl as a stock solution. A working solution of these primers was prepared by adding 10µl of primer stock solu-

Publisher's Note: Bionatura stays neutral with regard to jurisdictional claims in published maps and institutional affiliations.

2

tion (stored at freezer -20 C) to 90µl of nuclease-free water to obtain a working primer solution of 10 pmol/µl. Tables 1, 2 and 3.

complete sequence; and 5.8S ribosomal RNA gene, partial sequence, which inserted in GenBank: MW376484.1 from wild cat *Felischausfuraxfor* the first time in Iraq—fig. 3.

Primer Name	Vol. of nuclease-free water (µl)	Concentration (pmol/µl)
ITS1-F	300	100
ITS1-R	300	100
ITS2-F	300	100
ITS2-R	300	100

Table 1. Primer preparation as Macrogen Company protocol.

PCR Component Calculation				
No. of Reaction	2	rxn	Annealing temperature of primers	54
Reaction Volume /run	25	µl	Length of PCR product (bp)	≈500
Safety Margin	5	%	No. of PCR Cycles	30

Table 2. Reaction Setup and Thermal Cycling Protocol.

Master mix components	Stock	Unit	Final	Unit	Volume
					1 Sample
Master Mix	2	X	1	X	12.5
Forward primer	10	µM	1	µM	1
Reverse primer	10	µM	1	µM	1
Nuclease Free Water					5.5
DNA		ng/µl		ng/µl	5
Total volume					25
Aliquot per single rxn	20	µl of Master mix per tube and add		5	µl of Template

Table 3. PCR Program.

Agarose Gel Electrophoresis was adopted to confirm the presence of PCR amplification.PCR products were loaded directly. The Ethidium bromide-stained bands in gel were visualized using a Gel imaging system. Standard Sequencing APPLIED IN KOREA (MACROGEN CORPORATION) BY SANGER USING (ABI3730XL).

Results and discussion

Summary of Data Production: the results of DNA concentration for two samples were concluded in table 4.

Sample	Conc.
01	1
02	1.26

Table 3. DNA Concentration (ng/µl).

PCR amplification of two samples, ITS1 and ITS2, as in Figures 1 and 2.

The current study revealed that the sensitive and specific PCR assay allowing rapid and reliable identification of Malasseziarestricta by the fragment size amplified was 500bp in ITS1 gene in one sample of the wild cat as in Figure 1. And there is no results shown in the ITS2 gene as in figure 2.

Data Analysis

The current study recorded a new strain of *Malassezia-restricta* that called AF2013 strain "small subunit ribosomal RNA gene, partial sequence; internal transcribed spacer 1",

The current result of recording *Malasseziarestricta* cat indicates that it is a common disease between humans and animals, where it was found by Sugita[11] revealed that *M. restrict* commonly colonizes both AD (Atopic Dermatitis) patients and healthy subjects. And more, Annabelle[12] described the case of a pediatric oncology patient with splenic lesions secondary to *Malasseziarestricta*. Males and females are affected by the infection of (PV) PityriasisVersicolor, especially individuals between (10-20) years[13]. No significant correlation was reported between economic status; type of job; or water source with the infection of *Malassezia* spp.[14], which increases the risk.

Awad[14] revealed that patients who have contact with dogs only were equally exposed to *Malassezia spp.*, which reflects that dogs are not only the source of infection. Bond[6] reviewed 18 types of fungus *Malassezia* and their locations between animals and humans and mentioned *Malassezia-restricta* only in humans.

Phylogenetic tree

The current sequencing data has reported *Malassezia-restricta* from Iraq (MW376484); their host is a wild cat; this species revealed close matching on the phylogenetic tree to an isolate of *Malasseziarestricta* strain KCTC 27527 chromosome IV, complete sequence from Korea (CP030254); their host is Homo sapiens. On the other hand, it matches the isolation of *Malasseziarestricta* strain Y. H. Yeh I0610 "small subunit ribosomal RNA gene, partial sequence; internal transcribed spacer 1", "5.8S ribosomal RNA gene and
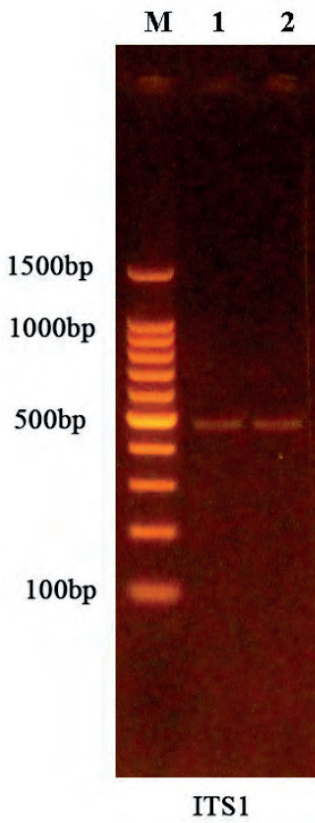
Figure 1. Results of the amplification of *ITS1* gene were fractionated on 1.5% agarose gel electrophoresis stained with Eth.Br. M: 100bp ladder marker. Lanes 1-2 resemble ≈500bp PCR products.
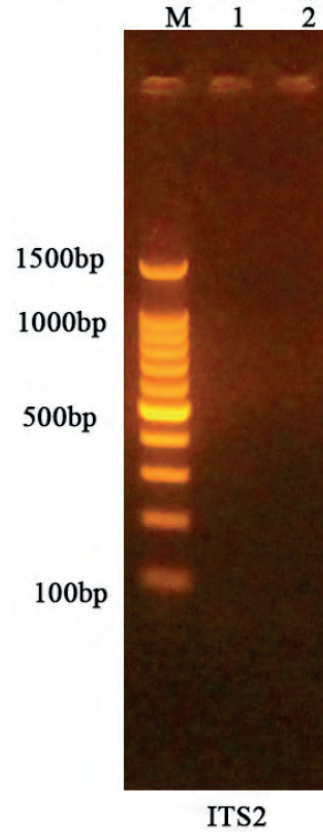

Figure 2. No Results of the amplification of the *ITS2* gene were fractionated on 1.5% agarose gel electrophoresis stained with Eth. Br. M: 100bp ladder marker.

3

Description	Common Name	Max Score	Total Score	Query Cover	E value	Per. Ident	Acc Len
Malassezia restricta CBS 7877 chromosome V, complete sequence	Malassezia rest...	761	761	100%	0.0	99.76%	794021
Malassezia restricta strain KCTC 27527 chromosome IV, complete sequence	Malassezia rest...	761	5333	100%	0.0	99.76%	846651
Uncultured fungus clone CMH139 18S ribosomal RNA gene, partial sequence; internal transcribed spacer 1, 5.8S...	uncultured fungus	761	761	100%	0.0	99.76%	942
Uncultured basidiomycete ITS region including 18S rRNA gene, ITS1, 5.8S rRNA gene, ITS2 and 28S rRNA gene...	uncultured Basi...	761	761	100%	0.0	99.76%	905
Uncultured fungus clone CMH030 18S ribosomal RNA gene, partial sequence; internal transcribed spacer 1, 5.8S...	uncultured fungus	756	756	100%	0.0	99.52%	943
Uncultured basidiomycete ITS region including 18S rRNA gene, ITS1, 5.8S rRNA gene, ITS2 and 28S rRNA gene...	uncultured Basi...	745	745	100%	0.0	99.04%	909
Uncultured basidiomycete ITS region including 18S rRNA gene, ITS1, 5.8S rRNA gene, ITS2 and 28S rRNA gene...	uncultured Basi...	737	737	100%	0.0	98.80%	901
Malassezia sp. LCP-2008a 18S ribosomal RNA gene, partial sequence; internal transcribed spacer 1 and 5.8S rib...	Malassezia sp. ...	736	736	100%	0.0	98.56%	2111
Fungal sp. isolate OTU_882_22 small subunit ribosomal RNA gene, partial sequence; internal transcribed spacer ...	fungal sp.	730	730	96%	0.0	99.50%	411
Uncultured basidiomycete ITS region including 18S rRNA gene, ITS1, 5.8S rRNA gene, ITS2 and 28S rRNA gene...	uncultured Basi...	728	728	100%	0.0	98.32%	909
Uncultured basidiomycete ITS region including 18S rRNA gene, ITS1, 5.8S rRNA gene, ITS2 and 28S rRNA gene...	uncultured Basi...	717	717	100%	0.0	97.84%	909
Uncultured basidiomycete ITS region including 18S rRNA gene, ITS1, 5.8S rRNA gene, ITS2 and 28S rRNA gene...	uncultured Basi...	713	713	95%	0 0	99 00%	825
Uncultured Malassezia clone 252_K3_A3ov small subunit ribosomal RNA gene, partial sequence; internal transcri...	uncultured Mal ...	592	592	77%	8e-165	99.69%	913
Uncultured Malassezia clone IBL157f 18S ribosomal RNA gene, partial sequence; internal transcribed spacer 1, 5...	uncultured Mal...	592	592	77%	8e-165	99.69%	762
Uncultured Malassezia clone WT-1-4 18S ribosomal RNA gene, partial sequence; internal transcribed spacer 1, 5...	uncultured Mal...	592	592	77%	8e-165	99.69%	748
Uncultured Malassezia clone CHiv68 18S ribosomal RNA gene, internal transcribed spacer 1, 5.8S ribosomal RN...	uncultured Mal...	592	592	77%	8e-165	99.69%	771
Uncultured fungus clone F68 18S ribosomal RNA gene, partial sequence; internal transcribed spacer 1, 5.8S ribo...	uncultured fungus	592	592	77%	8e-165	99.69%	677
Uncultured fungus clone ABP_38 18S ribosomal RNA gene, partial sequence; internal transcribed spacer 1, 5.8S ...	uncultured fungus	592	592	77%	8e-165	99.69%	771
Uncultured Malassezia clone CEobase392 18S ribosomal RNA gene, partial sequence; internal transcribed spac...	uncultured Mal...	590	590	77%	3e-164	99.69%	769
Uncultured fungus clone OTU_113 small subunit ribosomal RNA gene, partial sequence; internal transcribed spa...	uncultured fungus	586	586	77%	4e-163	99.38%	328
Uncultured Malassezia clone IM-L-1-6724 18S ribosomal RNA gene, partial sequence; internal transcribed space...	uncultured Mal...	586	586	77%	4e-163	99.38%	437
Uncultured fungus isolate DGGE gel band F1-5-1 18S ribosomal RNA gene, partial sequence; internal transcribe...	uncultured fungus	586	586	77%	4e-163	99.38%	326
Malassezia restricta isolate KCTC 27527 small subunit ribosomal RNA gene, partial sequence; internal transcribe...	Malassezia rest...	584	584	77%	1e-162	99.38%	328

Figure 3. BLAST 2 results of sequences revealed to *Malasseziarestricta* from wild cat in Iraq.

internal transcribed spacer 2 , the complete sequence" and large subunit ribosomal RNA gene, partial sequence from Taiwan (MK336446) their host is a goat (Ipomoea pes-caprae). Then, it matches the isolation of *Malasseziarestricta* CBS 7877 chromosome V, complete sequence from the United Kingdom: Bristol (CP033152); their host is Homo sapiens. Fig. 4.[13] revealed that the evidence shown by the phylogenetic tree showed that all species of *Malasseziaspp.* have high similarity with each other.

Conclusions

The current study spotlighted the species of *Malasseziarestricta* that infected domestic and wild cats by mo-

4
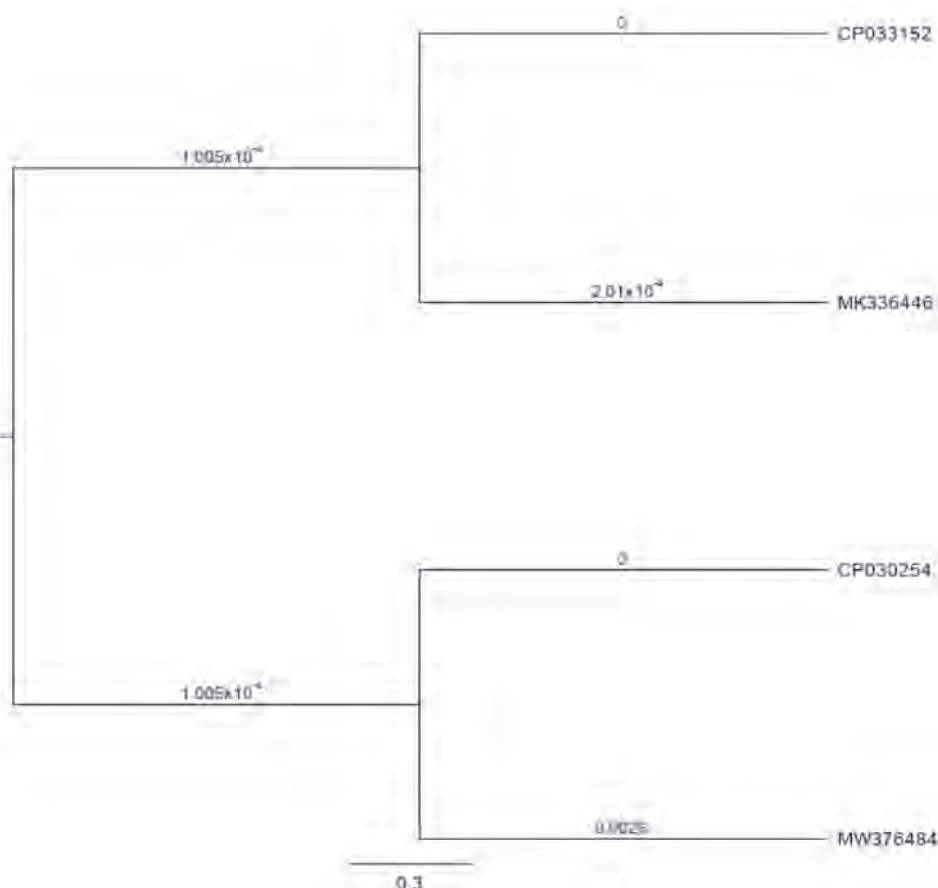
Figure 4. Phylogenetic tree analysis relied on the *ITS1* gene-specific region of *Malasseziarestrictafrom* Iraq (MW376484); their host is a wild cat. Sequencing revealed close matching of the phylogenetic tree to an isolate from Korea (CP030254). The compression was performed using NCBI – the based nucleotides website.

lecular analysis for the first time in Iraq, which was inserted in GenBank: MW376484.1 from wild cat *Felischausfurax*. This is a significant result as it proves that the fungus *Malasseziarestricta* is a common infection between humans and animals (zoonotic infection) and that cats can play this role.

Ethical approval

The trial was registered in "The Iraq Natural History Research Center and Museum INHM" (Email: info@nhm.uobhdad.edu.iq). The research proposal was approved by the Scientific Affairs Department of Baghdad University (SH.A.923/17/2/2021).

Conflicts of Interest

The authors declare no conflict of interest related to the work in a manuscript.

Bibliographic references

1. GBIF, Global Biodiversity Information Facility, 2021. https://www.gbif.org/species/2518093
2. Guého, E., Midgley, G. and Guillot, J. ,"The genus Malassezia with description of four new species", Antonie van Leeuwenhoek , 1996 (69): 337–355.
3. Thayikkannu, A. B. ,Kindo, A. J., andVeeraraghavan,M., " Malassezia-Can it be ignored", Indian JDermatol, 2015;(60): 332-339
4. Levin, N.A., and Delano, S., " Evaluation and treatment of Malassezia related skin disorders", Cosmet. Dermatol. , 2011; (24):137-145
5. Ran, Y., "Observation of Fungi, Bacteria, and Parasites in Clinical Skin Samples Using Scanning Electron Microscopy". In Janecek, Milos; Kral, Robert (eds.). Modern Electron Microscopy in Physical and Life Sciences.InTech. 2016.
6. Bond,R., Daniel, O., Morris, J. G., Emmanuel, J., Bensignors, D. R., Kenneth, V. M., Rui, K., and Peter B. H.,"Biology, diagnosis and treatment of Malassezia dermatitis in dogs and cats Clinical Consensus Guidelines of the World Association for Veterinary Dermatology, Veterinary Dermatology, 2020; 31 (27 –e4):1-49.
7. Crespo, M. J.,Abarca, M. L., and Caban˜es, F. J., "Isolation of Malassezia furfur from a Cat", Journal of Clinical Microbiology, vol. 37, no.5, pp. 1573–1574, 1999.
8. Morris, D.O., O'Shea, K., Shofer, F.S., Rankin, S., "Malasseziapachydermatis carriage in dog owners" , Emerg. Infect. Dis. [serial on the Internet].,2005:11(1): 83-88.
9. Bożena, D. K., Małgorzata, J. B., and Iwona, D.,"Occurrence of various pathogenic and opportunistic fungi in skin diseases of domestic animals: a retrospective study", BMC Veterinary Research, 2020;(16): 248 .
10. Khosravi, A., Eidi, S., Katiraee, F., Ziglari, T., Bayat, M., Nissiani, M., "Identification of different Malassezia species isolated from patients with Malassezia infections" , World Journal of Zoology, 2009; 4(2): 85-89.
11. Sugita, T., Mami, T., Misato, A., Ryoji, T., and Akemi, N. , "Genotype Analysis of Malasseziarestrictaas the Major Cutaneous Flora in Patients with Atopic Dermatitis and Healthy Subjects" Microbiol. Immunol., 2004;48(10): 755–75.
12. Annabelle, M., Haydar, F., Alice, C., and John, V. W. "Prolonged Fever and Splenic Lesions Caused by Malasseziarestrictain an Immunocompromised Patient", Author manuscript, Pediatr Transplant, 2014; 18(8): 283-286.
13. Al-Jabry, A. T., and Alsudani, A. A., "Survey of Malasseziaspp. that causing PityriasisVersicolor in Al-Diwaniyah city, Iraq", European Journal of Molecular & Clinical Medicine, 2020;7(2): 4416- 4428 .
14. Awad, A.K., Al-Ezzy, A. I., and Jameel, GH., " Phenotypic Identification and Molecular Characterization of Malassezia Spp. Isolated from PityriasisVersicolor Patients with Special Emphasis to Risk Factors in Diyala Province, Iraq", Open AccessMaced. J.Med. Sci., 2019 ; 7(5):707-714.

ARTICLE / INVESTIGACIÓN

Detection of *lukf-pv* gene in *Staphylococcus aureus* isolated from pregnant women with Urinary tract infection

Hiba Qasim Hameed[1], Inas Ahmed Saeed[2], Enas Abdalhadi Hussain[2]*

[1] Department of Biology, College of Education for pure science Ibn-Al Haitham, University of Baghdad, Baghdad, Iraq.
[2] Department of Microbiology ,Collage of Medicine, University of Babylon, Iraq.
Corresponding author: enas.ah.h@ihcoedu.uobaghdad.edu.iq

DOI. 10.21931/RB/2023.08.01.47

Abstract: *Staphylococcus aureus* is a human pathogen as well as commensal bacteria. *S. aureus* has colonized around 30% of the human population. This study aimed to diagnose *Staphylococcus aureus* by molecular techniques, correlate the resistance against selected antimicrobial substances with the presence of the *lukf-pv* gene, and find the sequence of *lukf-pv* gene for the isolates obtained to investigate the mutations of those obtained isolates. This study included 60 patients diagnosed by the hospital with a urinary tract infection in Teaching Medical City Hospital, Baghdad, and Al-Yarmouk Teaching Hospital, between January 2021 and July 2021. The isolates were cultured on a blood agar overnight; then, isolates were diagnosed by VITEK as *S. aureus.* DNA has been isolated from all the included samples. A specific region of the *16SRNA* gene has been amplified to diagnose *S. aureus* by molecular techniques. Then possession of the *lukf-pv* gene was tested by PCR, then amplified products were sequenced to detect the mutations within the *lukf-pv* gene. The finding appeared that blood group O+ has the highest rate of bacterial infection, the lowest is O- (1.7%), and the highest rate is shown within people not suffering from complicated diseases (65%). Of the 60 isolates, 60 (100%) were confirmed by *16sRNA* gene amplification and were positive, among which 37 (61.6%) were *lukf-pv* positive. Results of the *lukf-pv* gene sequences showed around 501 bits score and 96% compatibility (ID: CP076105.1). The current study showed that antibiotics Cefoxitin, Benzylpenicillin, Oxacillin, Clindamycin, Fusidic acid, Rifampicin, Erythromycin, Vancomycin, and Teicoplanin had the highest resistance to antibiotics and as follow;100 %, 100 %, 40.54 %, 27.03 %, 27.03 %, 16.22 %, 13.51 %, and 10.81 %, respectively.

Key words: *Staphylococcus aureus*, 16sRNA and *lukf-pv* genes.

Introduction

Staphylococcus aureus (*S. aureus*) is a common human pathogen that causes infections ranging from minor skin and soft-tissue infections to life-threatening sepsis. It has been linked to significant morbidity and mortality in community-acquired (CA) and healthcare-associated (HA) infections[1,2].

Surface colonization is a significant risk factor for infection; *S. aureus* colonization of the skin and mucus membranes is estimated in 30% of healthy people, with another 30% being temporary carriers[3]. Because of the widespread use of beta-lactams in infection treatment, *S. aureus* can acquire methicillin resistance, first in hospitals and, more recently, in community strains[4].

Several cell surface and secreted virulence factors contribute to the pathogenesis of *S. aureus*. For example, panton-Valentine leukocidin (pvl encodes lukS-PV/lukF-PV genes) is a two-component toxin that causes hole development in complement receptors on leukocyte cell membranes[5]. pl-associated *S. aureus* (*pvl-sa*) infection is most typically associated with community-acquired methicillin-resistant *S. aureus* (CA-MRSA) infection[6]; however, outbreaks due to pvl-positivity's methicillin-susceptible *S. aureus* (MSSA) strains have been observed in close community settings[7]. This study aimed to identify *Staphylococcus aureus* by molecular techniques by the *16sRNA* gene, then correlate the resistance against selected antimicrobial substances with the presence of the luk gene; this gene has been further investigated by sequencing to investigate the mutations of those obtained isolates.

Materials and methods

Sample Collection

The current research included 60 swabs isolated from pregnant women suffering from UTI attending Teaching Medical City Hospital, Baghdad Teaching Hospital, and Al-Yarmouk Teaching Hospital between January 2021 and July 2021. The bacteria from all 60 nasal swabs were grown on blood agar using the streak way and incubated for 24 hours at 37°C. Standard sterile saline was introduced to the test tube (3.0 mL). An application stick or sterile brush was employed to transfer enough pure-crop colonies and suspend the isolated colonies in normal saline. McFarland's turbidity (0.5-0.63) was adjusted, and Densi ChekTM was employed. The transmission tube is then inserted into the matching suspension tube, while the test tube is placed in the next slot. Suspension cards for bacteria before loading are inoculated by a process that cuts the transfer tube and seals it

2

to the incubator. There is room for up to 60 cards or up to 30 cards. Each card was incubated at 35,5+ 1,0°C for 15 minutes before being removed from the incubator and transferred to the optical system for reaction measurements.

Additionally, a single algorithm is used to remove bogus measures from tiny bubbles. Raw data calculations are performed and compared for each test to evaluate reactions. The test reaction results are displayed on the VITEK 2 Compact as "+," "(-)," or "(+)." Test results of an unknown organism were compared to the associated database to generate a quantitative nearness value for each database taxonomy. Antimicrobial resistance patterns were determined using the VITEK-2 AST.

Detection of 16sRNA and *lukf-pv* gene by Polymerase Chain Reaction (PCR)

The 16s rRNA and *lukf-pv* gene were detected using PCR on all *S. aureus* isolates. For the amplification of 16sRNA gene, a specific primer has been used; the sequence of sense primer, 5′-AACTCTGTTATTAGGGGAA-GAACA-3′ and the antisense; 5′-CCACCTTCCTCCGG TTTGTCACC-3′ (8). The reaction mixture has been set to 25 µl and contains; Taq PCR PreMix 5µl, Forward primer 10 picomols/µl (1µl), Reverse primer 10 picomols/µl (1µl) DNA 1.5µl (2ng/µl), and Nuclease – Free Water 16.5 µl. The cycling conditions of amplification were as follows; Initial Denaturation at 94°C for 5 min, then 30 cycles of Denaturation -2 at 94°C for 1min, annealing at 55°C for 1min, and extension at 72°C for 2min. Then one cycle of extension at 72°C for 10min. Amplification of lukf-pv gene was done by using the sense primer; 5′- ATCATTAGGTAAAATGTCTGGACAT-GATCCA-3′, and the antisense primer, 5′-GCATCAAGT-GTATTGGATAGCAAAAGC-3′ 8. The reaction mixture is composed of the same components of 16sRNA except for primers. The cycling condition was as follows; Initial Denaturation at 94°C for 3 min. Then 35 cycles of Denaturation at 94°C for 30 seconds, followed by annealing at 55°C for 30 seconds, then extension at 72°C for 30sec. Then one step of extension at 72°C for 7 min. The Macrogen company then sequenced the amplified products.

Results and discussion

The results appeared 60 samples isolated from pregnant were diagnosed as *S. aureus*. It examined the resistance of 37 isolates against antibiotics studies; according to the effects of Viteck, these isolates were resistant to Oxacillin; therefore, *S. aureus* was considered methicillin-resistant. The percentage of infection with *S. aureus* has been classified according to the patient's job, and the results are shown (Table 1). The housewife had the highest rate of bacterial illness, 31 (51.7%), followed by 26 Employees (43.3%) and 3 Students (5%), respectively. The difference between the percentage of infection is significant (p<0.0001).

Jobs	No. (%)	Probability
Employee	26 (43.3)	<0.0001
Housewife	31 (51.7)	
Student	3 (5.0)	
Total	60 (100.0)	

Table 1. The percentage of samples distribution according to jobs.

Antigen expression differences between blood groups can increase or decrease a host's susceptibility to various illnesses. Blood groups can play a direct role in infection by acting as receptors or co-receptors for bacteria, parasites, and viruses. This study showed that blood group O+ has the highest bacterial infection rate, and the lowest is O- (1.7%), as shown in table (Table 2).

Blood groups	No. (%)	Probability
A+	11 (18.3)	<0.0001
A-	2 (3.3)	
B+	7 (11.7)	
B-	4 (6.7)	
AB+	11 (18.3)	
AB-	5 (8.3)	
O+	19 (31.7)	
O-	1 (1.7)	
Total	60 (100.0)	

Table 2. Distribution of samples according to Blood groups.

The infection rate differed among the different diseases, as shown in table (3); the highest rate is shown among people that are not suffering from any complicated diseases (65%), followed by people with blood pressure (13.3%), diabetes (11.7) and the lower rate with the Joints infection (10%).

Other diseases	No. (%)	Probability
Non	39 (65.0)	<0.0001
Blood pressure	8 (13.3)	
Joints pain	6 (10.0)	
Diabetes	7 (11.7)	
Total	60 (100.0)	

Table 3. Distribution of samples according to diseases.

The electrophoresis results of the amplified product of the *16sRNA* region are shown in figure (1). The results showed a clear, sharp band at 756bp for the positive samples, and the results showed the 37 (61.6%) *S. aureus* isolates under study have the gene *lukf-pv* from all 60 isolates. In contrast, the results of electrophoresis of the amplified *lukf-pv* gene showed 433bp in Figure 2.

To demonstrate the resistance of bacterial strains against the antibiotic, the antibacterial sensitivity of *S. aureus* isolates for 19 antibiotics was tested using the Vitek-AST methods, and the results of the current investigation revealed that some *S. aureus* isolates had a clear difference in the antibiotic resistance utilized in this study (Table 4). It was observed from the results of the present study that the highest resistance to antibiotics was to the antibiotics *Cefoxitin, Benzylpenicillin, Oxacillin, Clindamycin*, *Fusidic acid, Rifampicin, Erythromycin, Vancomycin* and *Teicoplanin*; 100%,100%, 100%, 40.54%, 27.03%, 27.03%, 16.22%,13.51%, 10.81% respectively.

luk-pvl gene sequences around 501 bits sore showed 96% compatibility (ID: CP076105.1), as seen in figure (3), while varied in 1%. And this percentage of difference includes 14 variations; two Transition A>G, the first one is 81bp ,
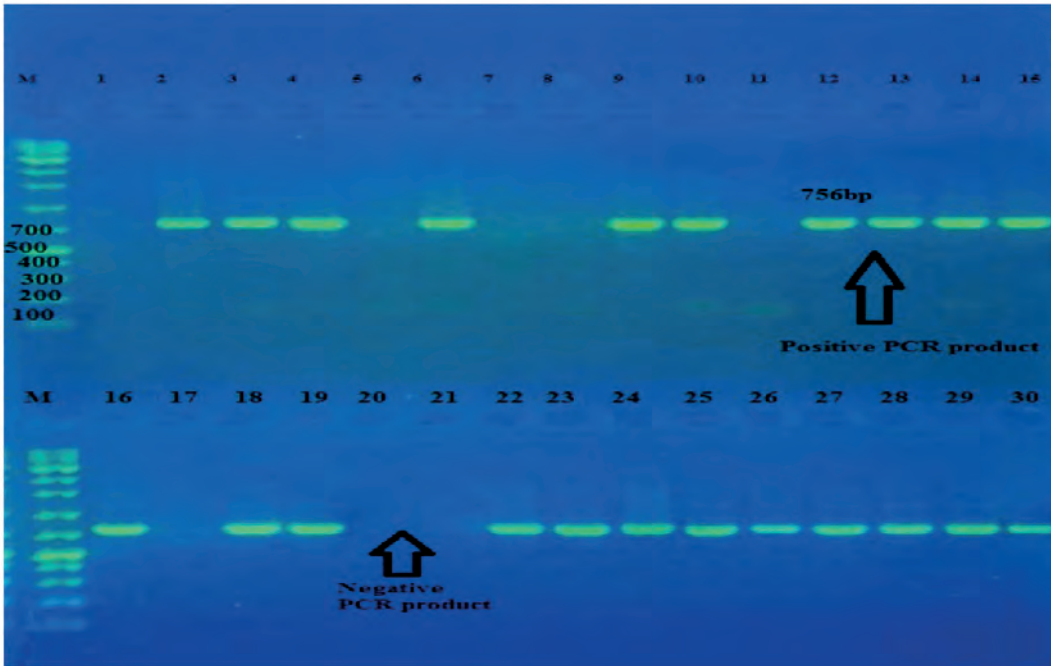
Figure 1. The PCR product (756bp) of *16sRNA* gene was electrophoresis on 2% agarose at 5 volt/cm². 1x TBE buffer for 1:30 hours. N: DNA ladder (1000bp).
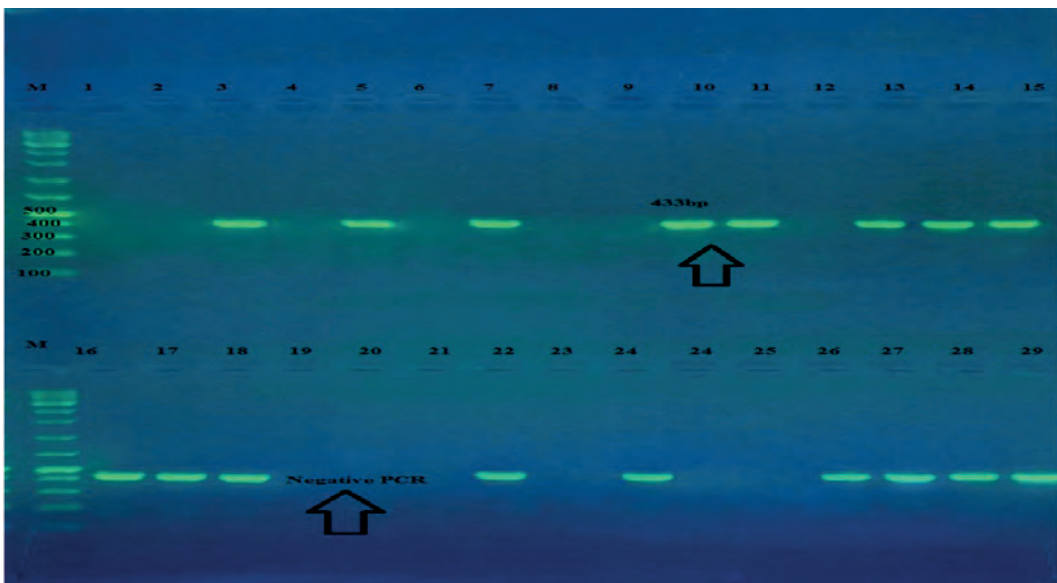
Figure 2. The PCR product (433bp) of *lukf-pv* gene was electrophoresis on 2% agarose at 5 volt/cm². 1x TBE buffer for 1:30 hours. N: DNA ladder (1000bp).

and the second transition is 105bp.Two Transversion share the same changing code, which is T>A and located in (49, 76 nucleotide), and Three Transversions T>G in locations (51, 77,110 nucleotide) , as well as one Transversion G>C in location (45 nucleotide), also three deletion C\-,A\-, C\- in locations (24,40,44nucleotide), and one Insertion -\G in location (9nucleotide).

In the present study, the results showed for *S. aureus* carriers, 61.6% of the isolates were identified as MRSA that carried the *Luk-pv-1* gene, disagreeing with Hussein *et al.*[9] the results showed 22.5% in Iraq's Kurdistan Region; this agreement with findings of a prior study conducted in Duhok in 2016[10].

In Iran, the prevalence of MRSA was 16 - 35% (6,7). The MRSA rate was 10.1% in Jordan[11], and 73% in Saudi Arabia[12]; in another study in Iraq that was conducted in rural and urban schools, the rates of nasal infection by isolates of *S. aureus* and MRSA were 17.75% and 10%, respectively[13].

MRSA strains obtained from hospitals in the Netherlands had a pvl positive 8% of the isolates carrying the *pvl* gene. In Iran, MRSA, the *pvl* gene, and MRSA-*pvl* isolates were found in 19-32, and10 %, of the population, respectively[14]. In this study *pvl* prevalence (61.6%) was extremely high, but similar to that reported in Ghana (75 %)[15], and higher than that recorded in Senegal (47 %), elsewhere in Africa, and around the world[1,3]. According to research by Akanbi *et al.*[16] Antibiotic resistance in *S. aureus* varied greatly, with the highest rates of resistance to rifampicin and clindamycin (80 %), and erythromycin (70 percent) disagree with our findings, whereas Oxacillin (73.3%) and cefoxitin (76.7%) this agree with our study. Multiple antibiotic-resistant patterns were found in all 37 *S. aureus* isolates (resistant to three or more antibiotics). In a survey conducted by Velasco *et al.*[8], a nasal infections rate of 7.6% for *S. aureus* was detected, which is significantly lower than the prevalence reported, contradicting our findings agree with those of other studies[17,18] *S. aureus* bacteria are resistant to three or more antibiotics.

Hiba Qasim Hameed, Inas Ahmed Saeed, Enas Abdalhadi Hussain
Volume 8 / Issue 1 / 47 • http://www.revistabionatura.com

Antibiotic	Results	Screen	Chi-square	P- Value
Cefoxitin	R	37 (100.0)	74	<0.0001
	S	0 (0.0)		
Benzylpenicillin	R	37 (100.0)	74	<0.0001
	S	0 (0.0)		
Oxacillin	R	37 (100.0)	74	<0.0001
	S	0 (0.0)		
Gentamicin	R	0 (0.0)	74	<0,0001
	S	37 (100.0)		
Tobramycin	R	0 (0.0)	74	<0.0001
	S	37 (100.0)		
Levofloxacin	R	0 (0.0)	74	<0.0001
	S	37 (100.0)		
Moxifloxacin	R	0 (0.0)	74	<0.0001
	S	37 (100.0)		
Inducible Clindamycin Resistance	R	0 (0.0)	39.41	<0.0001
	S	37 (100.0)		
Erythromycin	R	6 (16.22)	33.74	<0.0001
	S	31 (83.78)		
Clindamycin	R	15 (40.54)	2.65	0.104
	S	22 (59.46)		
Linezolid	R	0 (0.0)	74	<0.0001
	S	37 (100.0)		
Teicoplanin	R	4 (10.81)	45.46	<0.0001
	S	33 (89.19)		
Vancomycin	R	5 (13.51)	39.41	<0.0001
	S	32 (86.49)		
Tetracycline	R	5 (13.51)	39.41	<0.0001
	S	32 (86.49)		
Tigecycline	R	0 (0.0)	74.0	<0.0001
	S	37 (100.0)		
Nitrofurantoin	R	0 (0.0)	74.0	<0.0001
	S	37 (100.0)		
Fusidic acid	R	10 (27.03)	15.62	<0.0001
	S	27 (72.97)		
Rifampicin	R	10 (27.03)	15.62	<0.0001
	S	27 (72.97)		
Trimethoprim / Sulfamethoxazole	R	0 (0.0)	74.0	<0.0001
	S	37 (100.0)		

R, resistant; S; Sensitive.

Table 4. The percentages of antibiotic resistance of *S. aureus* isolates

Conclusions

It was concluded that *Staphylococcus aureus* isolated from pregnant with urinary infections were resistant to antibiotics studied. Thirty-seven isolates were resistant against antibiotics studies and resistant to Oxacillin; therefore, *S. aureus* was considered methicillin-resistant. Moreover, *S. aureus* isolates have the gene *lukf-pv*.

Funding

No.

Conflicts of Interest

There are no conflicts.

Bibliographic references

1. Breurec S, Fall C, Pouillot R, Boisier P, Brisse S, Diene-Sarr F, Djibo S, Etienne J, Fonkoua MC, Perrier-Gros-Claude JD, Ramarokoto CE. Epidemiology of methicillin-susceptible Staphylococcus aureus lineages in five major African towns: high prevalence of Panton-Valentine leukocidin genes. Clinical Microbiology and Infection. 2011 Apr 1;17(4):633-9.
2. Özekinci T, Dal T, Yanık K, Özcan N, Can Ş, Tekin A, Yıldırım Hİ, Kandemir İ. Panton-Valentine leukocidin in community and hospital-acquired Staphylococcus aureus strains. Biotechnology & Biotechnological Equipment. 2014 Nov 2;28(6):1089-94.
3. Shallcross LJ, Fragaszy E, Johnson AM, Hayward AC. The role of the Panton-Valentine leucocidin toxin in staphylococcal disease: a systematic review and meta-analysis. The Lancet infectious diseases. 2013 Jan 1;13(1):43-54.
4. Cosgrove SE, Sakoulas G, Perencevich EN, Schwaber MJ, Karchmer AW, Carmeli Y. Comparison of mortality associated with methicillin-resistant and methicillin-susceptible Staphylococcus aureus bacteremia: a meta-analysis. Clinical infectious diseases. 2003 Jan 1;36(1):53-9.
5. Rasigade JP, Laurent F, Lina G, Meugnier H, Bes M, Vandenesch F, Etienne J, Tristan A. Global distribution and evolution of Panton-Valentine leukocidin-positive methicillin-susceptible Staphylococcus aureus, 1981–2007. The Journal of infectious diseases. 2010 May 15;201(10):1589-97.
6. Asiimwe BB, Baldan R, Trovato A, Cirillo DM. Molecular epidemiology of Panton-Valentine Leukocidin-positive community-acquired methicillin resistant Staphylococcus aureus isolates in pastoral communities of rural south western Uganda. BMC infectious diseases. 2017 Dec;17(1):1-7.

Figure 3. Alignment analysis *luk-pv-1* gene of *S. aureus.* Query symbolizes the gene sequence of the sample; Subject represents the gene sequence by the database of NCBI.

7. Rasigade JP, Laurent F, Lina G, Meugnier H, Bes M, Vandenesch F, Etienne J, Tristan A. Global distribution and evolution of Panton-Valentine leukocidin-positive methicillin-susceptible Staphylococcus aureus, 1981–2007. The Journal of infectious diseases. 2010 May 15;201(10):1589-97.

8. Velasco V, Buyukcangaz E, Sherwood JS, Stepan RM, Koslofsky RJ, Logue CM. Characterization of Staphylococcus aureus from humans and a comparison with isolates of animal origin, in North Dakota, United States. PloS one. 2015 Oct 20;10(10):e0140497.

9. Hussein N, Salih RS, Rasheed NA. Prevalence of methicillin-resistant Staphylococcus aureus in hospitals and community in Duhok, Kurdistan region of Iraq. International Journal of Infection. 2019 Apr 30;6(2).

10. Hussein NR. Prevalent genotypes of Staphylococcus aureus strains isolated from healthcare workers in Duhok City, Kurdistan Region, Iraq. International Journal of Infection. 2016 Apr 1;3(2).

11. Aqel AA, Alzoubi HM, Vickers A, Pichon B, Kearns AM. Molecular epidemiology of nasal isolates of methicillin-resistant Staphylococcus aureus from Jordan. Journal of Infection and Public Health. 2015 Jan 1;8(1):90-7.

12. Iyer A, Kumosani T, Azhar E, Barbour E, Harakeh S. High incidence rate of methicillin-resistant Staphylococcus aureus (MRSA) among healthcare workers in Saudi Arabia. The Journal of Infection in Developing Countries. 2014 Mar 13;8(03):372-8.

13. Hussein NR, Basharat Z, Muhammed AH, Al-Dabbagh SA. Comparative evaluation of MRSA nasal colonization epidemiology in the urban and rural secondary school community of Kurdistan, Iraq. PLoS One. 2015 May 1;10(5):e0124920.

14. Lari AR, Pourmand MR, Ohadian Moghadam S, Abdossamadi Z, Namvar AE, Asghari B. Prevalence of PVL-containing MRSA isolates among hospital staff nasal carriers. Laboratory Medicine. 2011 May 1;42(5):283-6.

15. Dekker D, Wolters M, Mertens E, Boahen KG, Krumkamp R, Eibach D, Schwarz NG, Adu-Sarkodie Y, Rohde H, Christner M, Marks F. Antibiotic resistance and clonal diversity of invasive Staphylococcus aureus in the rural Ashanti Region, Ghana. BMC Infectious Diseases. 2016 Dec;16(1):1-6.

16. Akanbi OE, Njom HA, Fri J, Otigbu AC, Clarke AM. Antimicrobial susceptibility of Staphylococcus aureus isolated from recreational waters and beach sand in Eastern Cape Province of South Africa. International journal of environmental research and public health. 2017 Sep;14(9):1001.

17. Gorwitz RJ, Kruszon-Moran D, McAllister SK, McQuillan G, McDougal LK, Fosheim GE, Jensen BJ, Killgore G, Tenover FC, Kuehnert MJ. Changes in the prevalence of nasal colonization with Staphylococcus aureus in the United States, 2001–2004. The Journal of infectious diseases. 2008 May 1;197(9):1226-34.

18. Mainous AG, Hueston WJ, Everett CJ, Diaz VA. Nasal carriage of Staphylococcus aureus and methicillin-resistant S aureus in the United States, 2001–2002. The Annals of Family Medicine. 2006 Mar 1;4(2):132-7.

5

ARTICLE / INVESTIGACIÓN

Farmacovigilancia de los efectos asociados a la vacunación contra el SARS-CoV-2 en el personal sanitario de un hospital de atención exclusiva de pacientes con COVID-19

Pharmacovigilance of the effects associated with vaccination against SARS-CoV-2 in the health personnel of a hospital for the exclusive care of patients with COVID-19

Jorge Luis Vélez-Páez[1,2], Yuan Kuonqui-Vera[1,3], Juan-Pablo Castelo[1,4], Gabriela Rivadeneira-Bonifaz[1,4], Cristina Chango-Salas[1,5], Jhoana Parreño[1,3], Cristina Barriga[1,5]

[1] Hospital Pablo Arturo Suárez, Comisión Técnica de Farmacovigilancia, Quito, Ecuador.
[2] Unidad de Cuidado Crítico, Hospital Pablo Arturo Suárez, Quito, Ecuador.
[3] Departamento de Medicina Interna, Hospital Pablo Arturo Suárez, Quito, Ecuador.
[4] Departamento de Farmacia Institucional, Hospital Pablo Arturo Suárez, Quito, Ecuador.
[5] Enfermeras de Hospital Pablo Arturo Suárez, Quito, Ecuador.
Corresponding author: jlvelez@uce.edu.ec

1

Resumen: El Hospital Pablo Arturo Suárez, ubicado en Quito, la capital de Ecuador, se convirtió en un hospital de atención exclusiva para pacientes COVID-19 desde marzo de 2020, y fue uno de los primeros centros en inmunizar a su personal con un solo tipo de vacuna, la de Pfizer-BioNTech. Se realizó un estudio de farmacovigilancia en 1304 trabajadores sanitarios de este centro que fueron inmunizados entre enero y marzo del 2021. Los vacunados tuvieron una media de edad de 38,7 años y predominó el sexo femenino (63%). Reportaron efectos adversos 81 (6%) inmunizados, su media de edad fue de 38,8 años y predominaron las mujeres (69%), similar a la población total. Se reportaron 305 efectos adversos relacionados a las vacunas, de ellos, solo 1 (0,3%) fue grave y requirió hospitalización, el resto (23%) fueron no graves. La cefalea, el malestar general, el dolor en el sitio de inyección fueron los efectos más reportados. Los resultados obtenidos muestran un paralelismo de lo reportado a nivel mundial sobre la seguridad de las vacunas contra el COVID-19 en general y la Pfizer-BioNTech en particular. La relevancia de nuestro trabajo radica en que es uno de los primeros reportes de reactogenicidad de esta vacuna en una ciudad de altitud a inicios de la pandemia, en una corte de personal sanitario directamente dedicado a la atención de este tipo de pacientes.

Palabras clave: Farmacovigilancia, virus del SARS, vacunación masiva. (Fuente: DeCS-BIREME).

Abstract: The Pablo Arturo Suárez Hospital, located in Quito, the capital of Ecuador, became an exclusive care hospital for COVID-19 patients in March 2020. It was one of the first centers to immunize its staff with a single type of vaccine, that of Pfizer-BioNTech. A pharmacovigilance study was conducted on 1304 health workers from this center who were immunized between January and March 2021. The vaccinated had an average age of 38.7 years, and the female sex predominated (63%). 81 (6%) immunized reported adverse effects, and their mean age was 38.8 years; women (69%) predominated, similar to the total population. Three hundred five adverse effects related to vaccines were reported; of them, only 1 (0.3%) was severe and required hospitalization, and the rest (23%) were non-serious. The most reported effects were headache, malaise, and pain at the injection site. The results show a parallel with what has been said worldwide on the safety of vaccines against COVID-19 in general and Pfizer-BioNTech in particular. The relevance of our work lies in the fact that it is one of the first reports of the reactogenicity of this vaccine in a high-altitude city at the beginning of the pandemic, in a court of health personnel directly dedicated to the care of this type of patient.

Key words: Pharmacovigilance, SARS virus, mass vaccination. (Source: MeSH-NLM).

Introducción

El 31 de diciembre de 2019 en Wuhan-China se reportó algunos casos de una neumonía atípica que no fue causada por ningún agente etiológico usual[1]. Se descubrió un nuevo agente viral, un coronavirus beta, que se designó como coronavirus del síndrome respiratorio agudo severo tipo 2 (SARS-CoV-2)[2]. La OMS lo proclamó pandemia el 11 de marzo de 2020, y la enfermedad provocada por este virus se denominó COVID-19[3]. Las tasas de mortalidad por COVID-19 fueron considerablemente altas en América Latina, una región con niveles notables de desigualdad socioeconómica, especialmente entre los pobres[4]. Los recursos financieros limitados en los sistemas de salud y las pruebas

2

de diagnóstico insuficientes hicieron que el control de los brotes de enfermedades a nivel comunitario fuera una tarea ardua, lo que resultó en un alto número de ingresos hospitalarios a las unidades de cuidados intensivos[5].

La creación de una vacuna avanzó de manera vertiginosa y la aprobación para el inicio de la fase 4 de las vacunas candidatas contra el SARS-CoV-2 por parte de agencias nacionales e internacionales de regulación, masificó la distribución y administración de las mismas a nivel mundial, con la aparición de efectos adversos no observados en las fases previas. Trombosis autoinmune, síndrome de Guillain-Barré, entre otros, fueron eventos notificados[4,5].

La farmacovigilancia, es una rama de la farmacología que estudia las relaciones causales de los eventos adversos asociados a fármacos y vacunas, que ha tomado importancia fundamental notificando e investigando las reacciones presentadas posvacunales en tiempos de inmunizaciones contra el COVID-19 a gran escala[6].

El Hospital Pablo Arturo Suárez, ubicado en Quito, la capital de Ecuador se convirtió en un hospital de atención exclusiva para pacientes COVID-19 desde marzo de 2020[7], y fue uno de los primeros centros en inmunizar a su personal con un solo tipo de vacuna, la de Pfizer-BioNTech.

En el presente trabajo, mostramos las características epidemiológicas y la incidencia basada en el reporte de efectos adversos relacionados con la vacuna de Pfizer-BioNTech contra el SRAS-CoV-2, en el personal sanitario de este centro, hasta dónde sabemos éste es uno de los primeros reportes de reactogenicidad de esta vacuna, en una ciudad e altitud, a inicios de la pandemia, en una corte de personal sanitario directamente dedicado a la atención de éste tipo de pacientes.

Materiales y métodos

Lugar

El estudio se realizó en el Hospital Pablo Arturo Suárez, exclusivo para la atención de COVID-19 en Quito-Ecuador.

Diseño del estudio

Estudio de cohorte retrospectivo, con datos secundarios tomados de una base de datos de vigilancia clínica epidemiológica de las personas inmunizadas en el hospital.

Población y tamaño de la muestra

Se incluyó en el estudio a todos los pacientes adultos que fueron inmunizados con la vacuna de Pfizer-BioNTech (única vacuna administrada), desde el 21 de enero hasta el 19 de marzo del 2021.

Criterios de inclusión

Se incluyó en el estudio a todos los pacientes adultos que recibieron las dos dosis completas de la vacuna Pfizer-BioNTech.

Criterio de exclusión

Se excluyeron a los pacientes no inmunizados.

Variables y medidas

Nuestro equipo revisó los registros electrónicos de todos los pacientes vacunados y las fichas de reportes de eventos adversos relacionados con la inmunización y se obtuvo las variables edad, sexo, comorbilidades, efectos adversos reportados.

Análisis estadístico

Realizamos un análisis estadístico descriptivo completo, valores absolutos y relativos de cada variable cualitativa y medidas de tendencia central para las variables cuantitativas.

Consideraciones éticas

De acuerdo con los principios bioéticos locales de la investigación en humanos, los datos anonimizados y no identificables de los registros clínicos, excluidos los informes de casos, no requieren la aprobación de las juntas de revisión internas.

Resultados

Se analizó a 1304 pacientes que fueron inmunizados, tuvieron una media de edad de 38,7 años y predominó el sexo femenino (63%). Reportaron efectos adversos 81 (6%) inmunizados, su media de edad fue de 38,8 años y predominaron las mujeres (69%), similar a la población total. (Tabla 1)

En cuanto a las comorbilidades, 60 pacientes (4%) del total de inmunizados declararon enfermedades preexistentes, la hipertensión arterial fue la más prevalente, seguida de la diabetes y trastornos tiroideos. (Tabla 2)

En los pacientes vacunados que reportaron efectos adversos, cuatro de cada 10 (40%) tenían comorbilidades, la HTA, la patología tiroidea como el hipotiroidismo y las neoplasias tiroideas; el lupus eritematoso sistémico y la diabetes fueron las enfermedades preexistentes más frecuentes.

Se reportaron 305 efectos adversos relacionados a las vacunas en 81 pacientes, de ellos, solo 1 (0,3%) fue grave y requirió hospitalización, el resto (23%) fueron no graves. La cefalea, el malestar general, el dolor en el sitio de inyección, la fiebre y las artralgias fueron los más frecuentes reportados. (Tabla 4)

	TOTAL DE VACUNADOS	VACUNADOS CON EFECTOS ADVERSOS
Frecuencia	1304	81
Porcentaje	100%	6%
Edad (promedio)	38,7 años	38,8 años
Sexo (M/F)	490 (37%)/813 (63%)	25 (31%)/56 (69%)
Comorbilidades	60 (4%)	33 (40,7%)

Abreviaturas: M: masculino, F: femenino.

Tabla 1. Características básicas de la población vacunada y que reportó efectos adversos.

COMORBILIDADES EN VACUNADOS	FRECUENCIA	PORCENTAJE
HTA	12	20%
Diabetes miellitus II	6	10%
Hipotiroidismo	5	8,3%
Neoplasia tiroidea	5	8,3%
Asma	4	6,6%
Neoplasia de mama	3	5%
LES/AR	3	5%
Trastornos depresivos/ansiosos	3	5%
Inmunodeficiencias secundarias	2	3,3%
Obesidad	2	3,3%
Dermatitis atópica	2	3,3%
Otros	13	21%

Abreviaturas: HTA: hipertensión arterial, LES: Lupus eritematoso sistémico, AR: Artritis Reumatoidea

Tabla 2. Comorbilidades en pacientes vacunados

3

COMORBILIDADES EN VACUNADOS CON EFECTOS ADVERSOS	FRECUENCIA	PORCENTAJE
HTA	10	30%
Patologías tiroideas	10	30%
Diabetes miellitus II	4	12%
LES	2	6%
Otros	7	21%

Abreviaturas: HTA: hipertensión arterial, LES: Lupus eritematoso sistémico

Tabla 3. Comorbilidades en los pacientes vacunados que reportaron efectos adversos.

Discusión

El personal sanitario inmunizado del Hospital Pablo Arturo Suárez es en promedio adulto joven, con predominio del sexo femenino similar a reportes de Argentina donde el promedio de edad fue de 40 años y de igual manera predominó el sexo femenino con 68%[8], difiere de un gran estudió israelí realizado en población general sobre seguridad de la vacuna donde de 1,736,832 personas fueron inmunizadas con una edad promedio de 38 años, con ligero predominio del sexo masculino[9].

Las comorbilidades en el presente estudio fueron bastante bajas (4%), en comparación con otros estudios realizados en población general en las que se encontró una condición mórbida preexistente entre el 23 hasta el 44%[8-12]. Sin embargo, la presencia de enfermedades preexistentes en los inmunizados que reportaron efectos adversos en nuestra serie fue alta (40%), aunque no podemos afirmar una relación causal.

Ochenta y un pacientes reportaron efectos adversos (6%), un porcentaje bajo comparado con Israel, dónde se notificó 70% de reacciones[9] o si comparamos con otras vacunas como la Novavax que llegó hasta el 79%[11]; pero alto, al compararlo con el reporte de farmacovigilancia realizado en Estados Unidos con la vacuna Pfizer en la población general en casi dos millones de receptores, en dónde, solo 4393 (0,2%) reportaron dichos eventos al VAERS (Vaccine Event Report System)[13]. La posibilidad de un subregistro de notificaciones en nuestro estudio existe, ya que, al tratarse de personal sanitario, es posible, que se hayan automedicado sin buscar otro tipo de atención.

Los efectos adversos más frecuentes en nuestra serie fueron cefalea, malestar general, dolor en el sitio de la inyección, fiebre y artralgias, similares a los indicados por el fabricante, pero diferentes a otras series como la estudiada en Israel, en dónde, se observó frecuentemente linfadenopatías, parestesias, síncope e infección por herpes zóster[9]; por otro lado, se encuentran coincidencias con los reportes de la vacuna Novavax, en dónde, los eventos más frecuentes fueron dolor en el sitio de la inyección, cefalea, mialgias y fatiga[12]. Consideramos que la heterogeneidad de los reportes tiene casusas multifactoriales como la vacuna utilizada, la etnia, el tipo de población y la no notificación de los mismos, entre otros.

Solo un evento adverso grave fue reportado en nuestro estudio (0,07%), un episodio de broncoespamo severo, que requirió hospitalización. A diferencia de otras series, como la de Estados Unidos con las vacunas de ARN, en dónde las reacciones alérgicas eran lo más notificado, reportándose 22 casos de anafilaxia en casi 2 millones de vacunados y ninguno requirió hospitalización[13], y la de Israel, en donde el evento adverso grave más frecuente fue la miocarditis[13] que tuvo hasta el triple de riesgo de presentar esta complicación en el grupo vacunado. En nuestra población no fue reportado ninguna complicación cardiaca, los autores de dicha publicación israelí sugieren que se presentó con más frecuencia en hombres jóvenes, en nuestro estudio el rango de edad fue bastante similar, sin embargo, no se registró dicha complicación; existió una persona en nuestra serie que presentó taquicardia que se resolvió espontáneamente, pero no tenemos datos si existió evaluación médica para descartar asociación con miocarditis.

4

EFECTO ADVERSO	CANTIDAD	SEVERIDAD
Broncoespasmo severo	1	Grave
Cefalea	47	No grave
Malestar general	39	No grave
Dolor en el sitio de inyección	21	No grave
Fiebre	17	No grave
Artralgias	17	No grave
Escalofrío	14	No grave
Edema	14	No grave
Diarrea	13	No grave
Dolor en brazo	12	No grave
Mialgia	11	No grave
Nausea	9	No grave
Vómito	8	No grave
Disnea	7	No grave
Adenopatía axilar	7	No grave
Mareo	6	No grave
Epigastralgia	6	No grave
Dolor de espalda	6	No grave
Eritema	5	No grave
Hipertensión	3	No grave
Fatiga	3	No grave
Dolor lumbar	3	No grave
Dolor en ojos	5	No grave
Odinofagia	3	No grave
Adenopatía occipital	3	No grave
Somnolencia	2	No grave
Rash alérgico	2	No grave
Prurito	2	No grave
Hipotensión	2	No grave
Diaforesis	2	No grave
Astenia	2	No grave
Taquicardia	1	No grave
Sensibilidad al tacto	1	No grave
Parestesia en piernas	1	No grave
Febrícula	1	No grave
Espasmo muscular en espalda	1	No grave
Espasmo muscular en brazo	1	No grave
Dolor en hombro	1	No grave
Dolor de pies	1	No grave
Dolor de cuello	1	No grave
Dolor abdominal	1	No grave
Disfagia	1	No grave
Congestión nasal	1	No grave
Adenopatía inguinal	1	No grave

Tabla 4. Frecuencia y gravedad de los efectos adversos reportados en los pacientes vacunados.

Conclusiones

Hay varios estudios que se han publicado sobre factores de riesgo y biomarcadores de mortalidad en pacientes con COVID-19 que habitan en altitud 14-20; sin embargo, éste estudio es relevante ya que es uno de los primeros reportes sobre la reactogenicidad de la vacuna de Pfizer-Biontech, en una población específica que habita en elevada altitud a inicios de la pandemia por SARS-CoV-2. La farmacovigilancia de la inmunización con esta vacuna en nuestro centro de atención COVID-19 exclusivo, arrojó un porcentaje de 6% de eventos adversos, la mayoría leves y sin ningún evento fatal lo que habla de la seguridad de las vacunas de ARN mensajero.

Referencias bibliográficas

1. International Society for Infectious Diseases. PRO/AH/EDR> COVID-19 update (59): global, cruise ship. WHO [Internet]. 2020 [cited 2022 Jun 13]. Available from: https://promedmail.org/promed-post/?id=20200813.7673720

2. Coronavirus disease (COVID-19) [Internet]. [cited 2022 Jun 13]. Available from: https://www.who.int/emergencies/diseases/novel-coronavirus-2019/question-and-answers-hub/q-a-detail/coronavirus-disease-covid-19

3. COVID-19: cronología de la actuación de la OMS [Internet]. [cited 2022 Jun 13]. Available from: https://www.who.int/es/news/item/27-04-2020-who-timeline---covid-19

4. Ortiz-Prado E, Cevallos-Sierra G, Henriquez-Trujillo A, Lowe R, Lister A. COVID-19 in Latin America [Internet]. 2020. Available from: https://www.who.int/emergencies/diseases/novel-coronavirus-

5. Decerf B, Ferreira FHG, Mahler DG, Sterck O. Lives and livelihoods: Estimates of the global mortality and poverty effects of the Covid-19 pandemic. World Development. 2021 Oct 1;146.

6. Sáenz-López J, Sierra Rodríguez M, García Salcedo J. Predictores se Mortalidad en Pacientes con COVID-19Mortality Predictors in Patients with COVID-19. Archivos de Medicina [Internet]. 2020 May 20;16(2):6. Available from: www.archivosdemedicina.com

7. Ecuador, El Comercio. «Dos hospitales atienden casos de covid-19 en Quito». El Comercio Ecuador. Consultado el 31 de marzo de 2020.

8. Tortosa F, Parodi V, Carrasco G, et al. Estudio de seroprevalencia en personal de salud: Relación de la vacunación con la presencia de infección previa por SARS- COV-2 en el contexto de la campaña nacional de vacunación para coronavirus luego de la primera dosis Gam-COVID-VAc (Sputnik-V). Scielo pre-prints. Published online 2021. https://doi.org/10.1590/SciELOPreprints.1790

9. Barda N, Dagan N, Ben-Shlomo Y, et al. Safety of the BNT162b2 mRNA Covid-19 Vaccine in a Nationwide Setting. N Engl J Med. 2021;385(12):1078-1090. doi:10.1056/nejmoa2110475

10. Polack FP, Thomas SJ, Kitchin N, et al. Safety and Efficacy of the BNT162b2 mRNA Covid-19 Vaccine. N Engl J Med. 2020;383(27):2603-2615. doi:10.1056/nejmoa2034577

11. Heath PT, Galiza EP, Baxter DN, et al. Safety and Efficacy of NVX-CoV2373 Covid-19 Vaccine. N Engl J Med. 2021;385(13):1172-1183. doi:10.1056/nejmoa2107659

12. Luzuriaga JP, Marsico F, Garcia E, et al. Impacto de la aplicación de vacunas contra COVID-19 sobre la incidencia de nuevas infecciones por SARS-COV-2 en PS de la Provincia de Buenos Aires. Scielo. Published online 2021:1-13. https://preprints.scielo.org/index.php/scielo/preprint/view/2068/3406

13. Shimabukuro T, Nair N. Allergic Reactions including Anaphylaxis after Receipt of the First Dose of Pfizer-BioNTech COVID-19 Vaccine. JAMA - J Am Med Assoc. 2021;325(8):780-781. doi:10.1001/jama.2021.0600

14. Campos A, Scheveck B, Parikh J, Hernandez-Bojorge S, Terán E, Izurieta R. Effect of altitude on COVID-19 mortality in Ecuador: an ecological study. BMC Public Health. 2021 Dec 1;21(1).

15. Simbaña-Rivera K, Morocho Jaramillo PR, Velastegui Silva J v., Gómez-Barreno L, Ventimilla Campoverde AB, Novillo Cevallos JF, et al. High-altitude is associated with better short-term survival in critically ill COVID-19 patients admitted to the ICU. PLoS ONE. 2022 Mar 1;17(3 March).

16. Jibaja M, Roldan-Vasquez E, Rello J, Shen H, Maldonado N, Grunauer M, et al. Effect of High Altitude on the Survival of COVID-19 Patients in Intensive Care Unit: A Cohort Study. Journal of Intensive Care Medicine. 2022 May 9;088506662210998. Ç

17. Vélez-Paez, J.L.; Montalvo, M.P.; Jara, F.E.; Aguayo-Moscoso, S.; Tercero-Martínez, W.; Saltos, L.S.; Jiménez-Alulima, G.; Irigoyen-Mogro, E.; Castro-Reyes, E.; Mora-Coello, C.; et al. Predicting Mortality in Critically Ill Patients with COVID-19 in the ICU from a Secondary-Level Hospital in Ecuador. Revista Bionatura 2022.

18. Ortiz-Prado E, Cevallos-Sierra G, Henriquez-Trujillo A, Lowe R, Lister A. COVID-19 in Latin America [Internet]. 2020. Available from: https://www.who.int/emergencies/diseases/novel-coronavirus-

19. Ortiz-Prado E, Fernandez Naranjo RP, Vasconez E, Simbaña-Rivera K, Correa-Sancho T, Lister A, et al. Analysis of Excess Mortality Data at Different Altitudes during the COVID-19 Outbreak in Ecuador. High Altitude Medicine and Biology. 2021 Dec 1;22(4):406–16.

20. Vélez-Páez JL, Tercero-Martínez W, Jiménez-Alulima G, Navarrete-Domínguez J, Cornejo-Loor L, Castro-Bustamante C, Cabanillas-Lazo M, Barboza JJ, Rodriguez-Morales AJ. Neutrophil-to-lymphocyte ratio and mean platelet volume in the diagnosis of bacterial infections in COVID-19 patients. A preliminary analysis from Ecuador. Infez Med 2021; 29(4):530-537. https://doi.org/10.53854/liim-2904-5 PMID: 35146361

Neutralizing antibodies as a correlate of protection against classical swine fever in Porvac® vaccinated pigs

Marisela Suárez-Pedroso[1]*, Yusmel Sordo-Puga[1], María Pilar Rodríguez-Moltó[1], Paula Naranjo-Valdés[2], Danny Pérez-Pérez[1], Iliana Sosa-Teste[3], Carlos Montero-Espinosa[1], Yohandy Fuentes-Rodríguez[1], Talía Sardina-González[1], Elaine Santana-Rodríguez[1], Milagros Vargas-Hernández[1], Ayme Oliva-Cárdenas[1], Nemecio González-Fernández[4], Eddy Bover-Fuentes[4], Carlos A. Duarte[1], Mario Pablo Estrada-García[1]

DOI. 10.21931/RB/2023.08.01.49

[1] Departamento de Biotecnología Animal, Centro de Ingeniería Genética y Biotecnología, La Habana, Cuba.
[2] Unidad de Laboratorio Central para Salud Agropecuaria (ULCSA), La Habana, Cuba.
[3] Centro de Toxicología Experimental (CETEX), Centro Nacional para la Producción de Animales de Laboratorio (CENPALAB), Cuba.
[4] Departamento de Investigación Desarrollo, Centro de Ingeniería Genética y Biotecnología, Camagüey, Cuba.
Corresponding author: marisela.suarez@cigb.edu.cu

Abstract: Porvac is a classical swine fever (CSF) subunit vaccine. It is safe and induces a robust neutralizing antibody response, sterilizing immunity, and early protection, and it prevents vertical transmission in pregnant sows. The methodology to approve Porvac batches is a challenging experiment in pigs with a virulent CSF virus strain. However, there is an ethical reason to reduce, at minimum, the use of animals in these lethal experiments. The knowledge indicates that neutralizing antibody titers in the blood could be a good correlate of protection. The results of 22 challenge experiments involving 116 Porvac vaccinated and 38 unvaccinated animals were analyzed. All vaccinated animals remained free from CSF clinical signs and pathological lesions and were negative for viral isolation after the challenge. In contrast, all unvaccinated pigs developed clinical and pathological signs of the disease and had to be euthanized eight days post-challenge. All vaccinated pigs exhibited high neutralizing antibody titers, with a geometric mean value of 1: 5153. The lower titer registered was 1: 800. A complete correspondence between neutralizing antibody titers and protection was demonstrated. These results support substituting the viral challenge test for the neutralizing peroxidase-linked assay in the release of Porvac® batches.

Key words: Classical swine fever, virus, subunit vaccine, viral challenge, neutralizing antibodies.

Introduction

Classical Swine Fever (CSF) is a highly contagious and devastating viral disease with a severe socio-economic impact on the pig industry worldwide[1]. The etiological agent, CSF virus (CSFV), is icosahedral and enveloped positive-stranded RNA virus member of the Pestivirus genus of the *Flaviviridae family*[2].

In endemic areas, vaccination using modified live vaccines (MLV) is mainly directed to limit the effects of the disease or as a first step within a general program for the control and eradication of the virus[3]. However, MLV can't discriminate between infected and vaccinated animals, require a cold distribution chain, and maternal-derived neutralizing antibodies compromise its immunogenicity in the piglets[4]. These drawbacks have limited the application of MLV in disease-free regions. Several subunit vaccines have been developed to substitute MLV, but they show a late onset of protection compared to MLV and provide incomplete protection against vertical transmission[3,5-7].

Porvac® is a novel subunit marker vaccine against CSFV. It is based on a chimeric antigen (E2-CD154), comprising the E2 protein of CSFV and the molecular adjuvant CD154. This vaccine has been safe and capable of inducing an unusually rapid onset of protection against a challenge with a highly pathogenic CSFV strain, similar to the one described for MLV[8-10]. The animals immunized with Porvac® develop high neutralizing antibodies (NAb) titers and cell-mediated immune responses. Furthermore, the administration of Porvac® to pregnant sows interferes with the transplacental transmission of the virus[11].

Porvac® has been registered in Cuba since 2017 (Sanitary Registry 763) and has currently been used in large state-owned pig production units, genetic units, and small private farms. A potency test, consisting in the challenge of the vaccinated animals with 10^5 PLD_{50} of a highly virulent strain, has been established to release the batches of Porvac®. This test has been previously used in the batch release process for MLV[12,13]. However, it involves suffering for control animals, which would have to die to ensure vaccine quality. Furthermore, it requires the handling of large amounts of virus, and, therefore, special contention facilities are needed to avoid dissemination of the virus, increasing the costs of quality control.

As stated in the last edition of the Manual of Diagnostic Tests and Vaccines for Terrestrial Animals[14], the efficacy of veterinary vaccines should be demonstrated through accurate statistical analysis of the host species. Nevertheless, challenge experiments in the final species may be unnecessary if data on the predictive value of serological tests are available. Wherever possible, applying procedures to replace, reduce and refine (the three R rule) the animals in-

Marisela Suárez-Pedroso, Yusmel Sordo-Puga, María Pilar Rodríguez-Moltó, Paula Naranjo-Valdés, Danny Pérez-Pérez, Iliana Sosa-Teste, Carlos Montero-Espinosa, Yohandy Fuentes-Rodríguez, Talía Sardina-González, Elaine Santana-Rodríguez, Milagros Vargas-Hernández, Ayme Oliva-Cárdenas, Nemecio González-Fernández, Eddy Bover-Fuentes, Carlos A. Duarte, Mario Pablo Estrada-García

volved in such studies should be encouraged. The potency tests required for the approval of each vaccine batch must correlate with the vaccine's efficacy in the host species[15].

Previous work has established that neutralizing antibody (NAb) titers are a good correlate of protection against CSFV in swine. A NAb titer equal to or higher than 1:50 is considered protective[16-18]. In line with these experimental data, the chapter of the OIE Terrestrial Manual about protein subunit vaccines based on the CSFV E2 protein recommends that the induction of specific anti-E2 antibodies in vaccinated pigs can be used to confirm the potency of each batch once the title has been correlated with the results of the efficacy test[14].

Therefore, this study aimed to demonstrate the correspondence between the NAb titers in the serum of Porvac-vaccinated animals and protection from lethal viral challenges. The final goal is replacing the viral challenge test for the neutralizing peroxidase-linked assay in the routine release of Porvac® batches.

Materials and methods

Vaccine

Five batches of the Porvac® were evaluated (P51031, P61011-1, P61021-1, P71011-1, P81011-1). Each 2 mL dose contains 50 µg of E2-CD154 antigen (25 µg/mL) in Montanide™ ISA 50V2 oil adjuvant (SEPPIC, Paris). The vaccine was kept at 2-8 C until use. Vaccination and viral challenge were repeated every six months for some batches, which increased the number of animals evaluated in this analysis to a total of 116 vaccinated animals and 38 unvaccinated control animals.

Experimental animals

Nine weeks old Crossbred Duroc/Yorkshire swine (25-30 Kg) (CENPALAB, Cuba), belonging to an unvaccinated, CSF-free herd, were used. A total of 154 animals were used, 116 were vaccinated with Porvac®, and the other 38 were used as unvaccinated controls for the challenge. The animals were housed in separate experimental boxes, following the animal welfare regulations and standards established by the Animal Health Department of the Ministry of Agriculture in Cuba. Vaccination/challenge experiments were conducted under appropriate high containment facilities, following the animal welfare regulations and standards according to EU Directive 2010/63/EU and Good Clinical Practices[14]. The Ethical and Animal Welfare Committee of CENPALAB, Cuba, approved and supervised the protocols.

Vaccination and challenge schedules

A two-dose vaccination schedule was conducted, with 21 days interval between injections. A volume of 2 ml was administered intramuscularly in the neck. The animals were challenged between 8 and 10 days post-vaccination (dpv) with 10^5 PLD_{50} of the highly virulent CSFV "Margarita" strain, belonging to subgenotype 1.4[19,20], by intramuscular injection in the neck.

The clinical signs compatible with CSFV infection in the animals after viral challenge were scored from 0 to 18, according to Mittelholzer et al.[21], with some modifications. The changes consisted of eliminating three parameters (body tension, body shape, and breathing), and adding the rectal temperature. The pigs were visually inspected for at least 15 minutes per day before and during the feeding and cleaning of the boxes. A dairy registry was filled for each animal with all the relevant clinical signs (rectal temperature, dullness, anorexia, prostration, constipation, diarrhea, cutaneous hyperemia, posterior paralysis and paresis, conjunctivitis, unsteady gait, convulsions, lack of response to stimulus, and presence of cutaneous or mucosal lesions. For ethical reasons, control animals were euthanized eight days post-challenge (dpc) when they reached clinical scores higher than 10. Vaccinated animals were evaluated until 21 dpc. The macroscopic anatomopathological analysis was conducted immediately after the sacrifice. Samples from the spleen and tonsils were collected in some cases. Some of these samples were processed for virus detection through the viral isolation technique (VI).

The challenge test for Porvac® includes several acceptance criteria, which are listed below:
● All control animals must get the disease severely or die after the challenge.
● More than 80 % of the animals vaccinated with the full schedule must show clinical protection.
● No vaccinated animal must develop a fever (temperature above 40 ºC) for 3 or more consecutive days.
● After the viral challenge, vaccinated animals should be free from CSF-compatible macroscopic lesions.

Blood samples

Blood samples were taken in the presence or absence of an anticoagulant. Whole blood and serum samples were stored at -70 °C or -20 °C, respectively, until their use for virus isolation or antibody detection. The samples were taken on day 0 (before vaccination), day 21 (after one immunization), at 28-30 days (7-10 days after the second administration), and 7 and 21 days after the challenge.

Cell line

The PK-15 cell line (ATCC CCL-33TM) was used for the Neutralizing Peroxidase Linked Assay (NPLA)[22] and viral isolation[23]. A cell culture-adapted variant of the highly virulent CSFV strain Margarita, gently provided by the Centro Nacional de Sanidad Agropecuaria, Mayabeque Cuba, was used in NPLA.

CSFV NAb detection (NPLA test)

NAb titers in the serum were determined by the Neutralizing Peroxidase Linked Assay (NPLA)[22]. Titers were expressed as the reciprocal of the higher dilution of serum that neutralized 100 $TCID_{50}$ of Margarita strain in 50% of the culture replicates. The virus was detected by incubation with the anti-E2 Mab CBSSE2.3 (CIGB-SS, Cuba) conjugated to horseradish peroxidase, followed by 3-amino-9-ethyl carbazole substrate and hydrogen peroxide.

Viral isolation

For viral isolation, organs of vaccinated and control animals were taken at sacrifice, and blood samples at different post-challenge moments. One cubic centimeter of each organ was macerated in a mortar with 1 mL of DMEM medium. The macerated material was suspended in 4 mL of DMEM medium and allowed to stand for one hour at room temperature, then centrifuged for 15 min at 1200 g. The supernatant was collected and stored at -70 °C. Two successive passages of this supernatant were made in the PK15 cell line (ATTC CCL-33). After the last incubation, the cells were fixed with heat. The presence of CSFV antigens

in the cells was detected by incubation with the anti-E2 Mab CBSSE2.3 (CIGB-SS, Cuba) conjugated to horseradish peroxidase, followed by 3-amino-9-ethyl carbazole substrate and hydrogen peroxide.

Statistical analysis

The software GraphPad Prism v6.0 (GraphPad Software, Inc., La Jolla, USA) was used for statistical analysis. The geometric mean (GM) of the NAb titers and the confidence intervals of the GM were calculated for each vaccine batch and all vaccinated animals after one or two administrations of the vaccine. The Kolmogorov-Smirnov test and variance homogeneity determined normality by the Levene test. Mann-Whitney test was used to compare the NPLA titers between two experimental groups and the Kruskal-Wallis test, followed by the Dunn test, was applied to compare the GM of the NAb titers among several experimental groups.

Results and discussion

NAb response in Porvac® vaccinated animals

The 116 Porvac-vaccinated pigs seroconverted after the first administration of the vaccine (Figure 1). The GM of the NAb at day 21 after the first immunization was 1: 358.6, and the GM's lower and upper 95% confidence intervals

(CI) were 302.3 and 425.4, respectively. The lowest NAb titer observed was 1:10 (in only one pig), and the highest was 1:1600.

A strong anamnestic response was observed after the second immunization (Figure 1). The GM of the NAb titers increased to 1: 5217, with CI of 4571 and 5954. Those NAb titers are significantly higher than those observed after day 21 after the first immunization (Mann-Whitney, p = 0.0001). The lowest individual NAb titer was 1:800, and the highest was 1:25600. Moreover, 78 % of the NAb titers were more increased than 1:3200.

The frequency distribution of the NAb titers at 21 and 28 dpv is presented in Figure 2. The marked differences between one and two doses of Porvac® are evident. From these results, and based on the published data that indicate that a NAb titer of 1:50 is sufficient to protect pigs from CSFV challenge[16-18], it is possible to predict that all animals should be protected after the challenge experiments.

Even after a single immunization, only one animal out of 116 showed NAb titers below the protective threshold. Therefore, it is very likely that the protective status of the animals can be achieved after only one dose in the 99.14% of vaccinated animals. This is an advantageous property for a vaccine that is intended to be applied in an endemic region where a rapid onset of immunity is needed. Other recombinant subunit vaccines have conferred only incomplete protection after one administration[18,24,25].
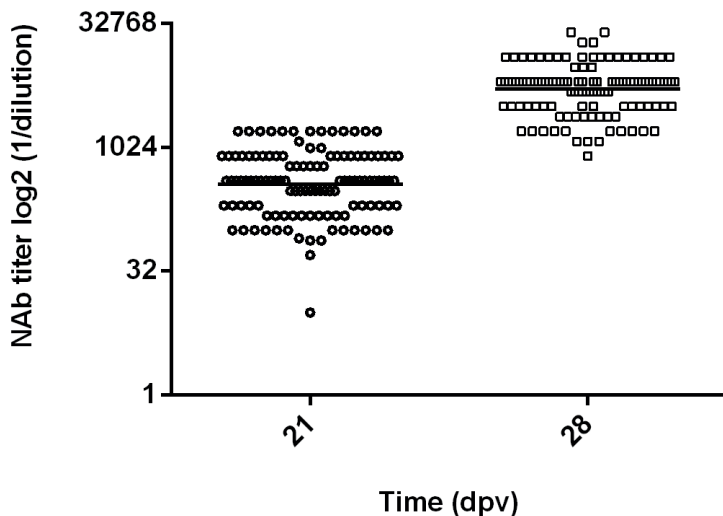
Figure 1. NAb titers in Porvac® vaccinated pigs. The X-axis scale is log2. Dpv: days post-vaccination. NAb was measured at 21 dpv (1 immunization) and 28 dpv (2 immunizations). n = 116. Horizontal lines represent the geometric mean of each group. Significant statistical differences were found between the two groups (Mann-Whitney, p = < 0.0001).
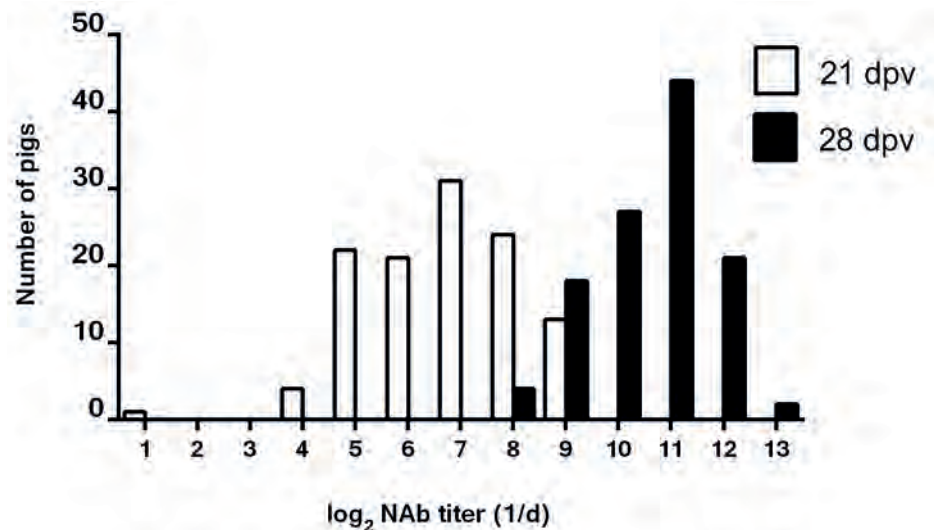
Figure 2. Frequency distribution of the NAb titers in pigs with 1 or 2 immunizations with Porvac®. Dpv: days post vaccination, 21 dpv (1 dose), 28 dpv (2 doses), n = 116.

3

Marisela Suárez-Pedroso, Yusmel Sordo-Puga, María Pilar Rodríguez-Moltó, Paula Naranjo-Valdés, Danny Pérez-Pérez, Iliana Sosa-Teste, Carlos Montero-Espinosa, Yohandy Fuentes-Rodríguez, Talía Sardina-González, Elaine Santana-Rodríguez, Milagros Vargas-Hernández, Ayme Oliva-Cárdenas, Nemecio González-Fernández, Eddy Bover-Fuentes, Carlos A. Duarte, Mario Pablo Estrada-García

The five batches of Porvac® studied induced similar levels of NAb

Figure 3 shows the NAb titers induced by the five batches of Porvac looked at 28 dpv. No statistically significant differences were observed among the five batches (Kruskal-Wallis, p = 0.4207). These results demonstrate the robustness and stability of the Porvac® production process.

All Porvac vaccinated pigs were protected against the CSFV challenge

All 22 independent challenge assays fulfilled the success criteria established for the test. All 116 vaccinated animals were protected from the viral challenge. They remain with good health status and appetite and without clinical signs of the disease. All pigs gain weight during the post-challenge period. Even the pig with the lowest NAb titer on the day of the challenge (1:800) was fully protected. The macroscopic examination of the main target organs conducted after the sacrifice at 21 dpc showed no pathological lesions in the vaccinated animals.

95 % of the vaccinated animals show typical temperature values after the challenge. The average temperature of the animals during the 21 dpc, did not exceed 39.6 ºC, within the physiological values for species[26] (Figure 4). Temperature values above 40 ºC were observed in 6 out of 116 animals in the study (5%) in punctual days after the challenge. However, the vaccines passed the test since the acceptance criterion established that temperature must be above 40 ºC for 3 consecutive days to be considered as relevant fever. Therefore, these transient temperature increases were supposed to be related to other punctual health issues in the animals.

Moreover, all samples from vaccinated animals analyzed in these studies were negative for viral isolation.

These results correspond with o the animals' good health after the viral challenge and the examination of the target organs after the necropsy.

In contrast, control animals experience a rapid rise in the rectal temperature (Figure 4) and CSF-compatible clinical signs from 3 dpc. In this group, the temperature raised sustainably above 40 ºC up to values above 41.4 ºC. From six dpc, a marked deterioration in the animal health was observed (>10 points in the clinical score), therefore, all control animals were sacrificed at 8 dpc to avoid unnecessary suffering. The pigs suffered diarrhea, conjunctivitis, respiratory disorders, anorexia, ataxia, and prostration due to severe nervous symptoms. Figure 5 shows the time course of the clinical score in vaccinated and control animals after the viral challenge.

Moreover, CSF-compatible macroscopic lesions were also observed in the target organs. Histological examination of the immune system in unvaccinated animals exposed to the virus shows peripheral and local depression (lymphopenia in the spleen, mesenteric lymph nodes, and Peyer's patches in the ileum). An inflammatory reaction (diffuse and perivascular) in the central nervous system with the predominance of lymphocytes at the cortex level and meninges was observed in the control animals evaluated. These lesions corresponded with this group's clinical score and the disease's development.

Finally, and in agreement with the lesions found in the target organs, 100 % of blood samples and organs analyzed from control pigs were positive for viral isolation.

These findings confirm that the viral challenge was effective in all the independent experiments conducted and, therefore, the high NAb titers developed in Porvac® vaccinated pigs conferred full protection against a lethal CSFV challenge. NAb are capable of sequestering the virus outsi-
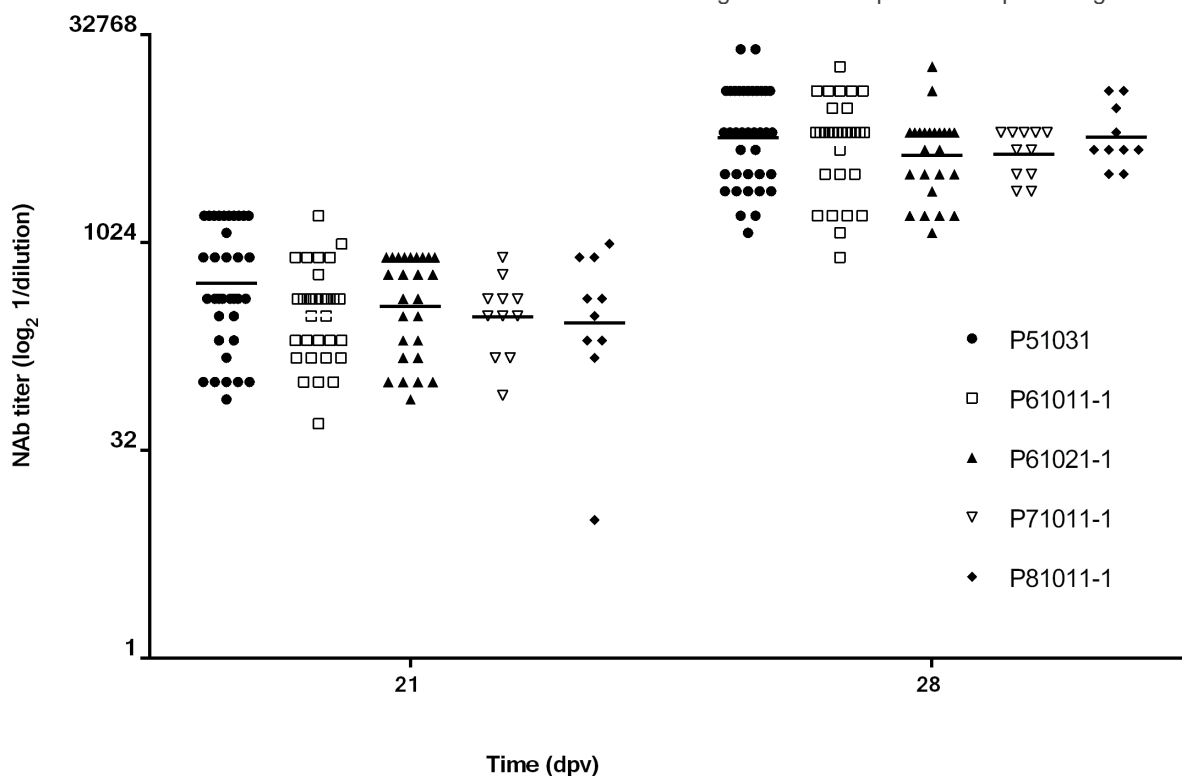
Figure 3. NAb titers induced by five production batches of Porvac. NAb titers were measured at 21 dpv (1 dose) and 28 dpv (2 doses). Horizontal lines represent the geometric mean of each group. Batches: P51031, n=37; P610111-1, n=32; P61021-1, n=26; P71011-1, n =11; P81011-1, n=10). No significant differences were found among the different batches after one or two immunizations (Kruskal-Wallis p>0.05).
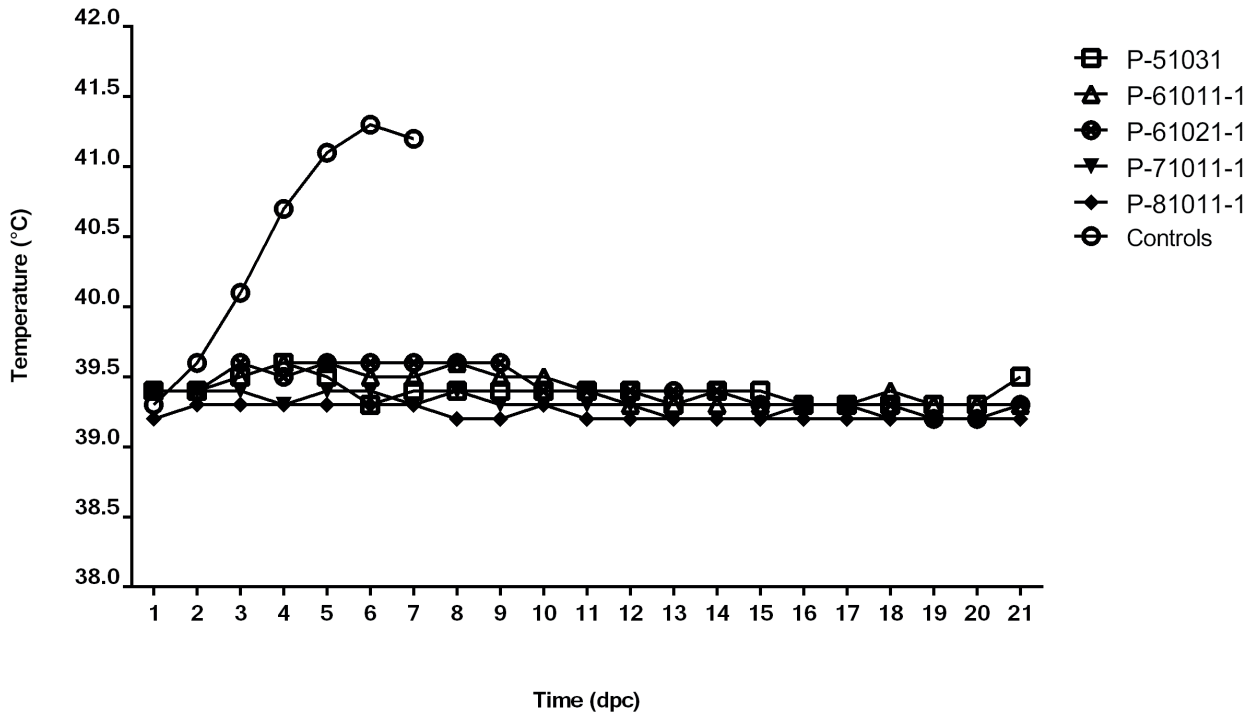
Figure 4. Time course of the average body temperature after the challenge. The average temperatures in the five groups of animals vaccinated with different batches of Porvac® and in control animals are represented. Vaccinated pigs were monitored during 21 dpc. All control pigs were euthanized at 8 dpc. dpc, days post challenge.
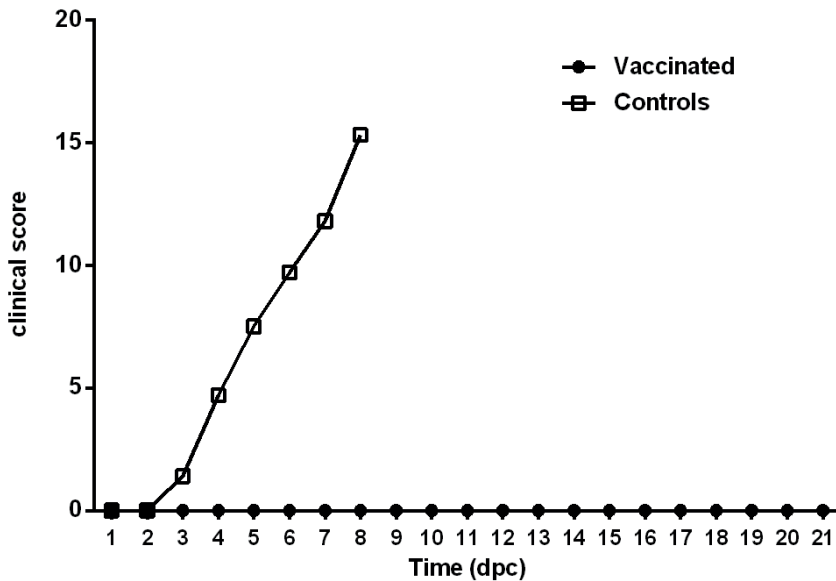
Figure 5. Time course of the clinical score after the challenge. The average clinical scores in vaccinated and control animals after the challenge are represented. Vaccinated pigs were monitored for 21 dpc. All control pigs were euthanized at 8 dpc. dpc, days post challenge.

de the target cells and arresting its multiplication.

Table 1 summarizes the results of the 22 challenge experiments conducted. There is an absolute correspondence between the presence of CSFV NAb in the serum of Porvac® vaccinated animals and protection against the viral challenge. Taking together, these results demonstrate for the first time that NAb elicited by immunization with Porvac® is a good correlate of protection against CSFV infection, as reported by other authors for MLV or other subunit vaccines in vaccinated/challenge animals.

Therefore, a potency test consisting of vaccinating pigs with Porvac® and measuring the NAb titers with the NPLA test can be proposed as a surrogate for the viral challenge experiment.

A NAb titer of 1:400 could be established as a cutoff value for approval of the production batches. This value is well above the 1:50 titer proposed by others as the cutoff for protection, implying a safety margin for a vaccine intended to be used in CSFV-endemic regions.

The following acceptance criteria would be considered for each production batch:
● All animals must develop NAb titers equal to or higher than 1: 400 after completing the vaccination schedule (21-day interval between the two doses)
● The geometric mean of the NAb titers of all vaccinated animals must be greater than 1: 1000.

By eliminating the viral challenge, the suffering of the animals will be reduced, as well as the risk of dissemination of the high-virulence strain used. The duration of the test and the costs will also be reduced.

Marisela Suárez-Pedroso, Yusmel Sordo-Puga, María Pilar Rodríguez-Moltó, Paula Naranjo-Valdés, Danny Pérez-Pérez, Iliana Sosa-Teste, Carlos Montero-Espinosa, Yohandy Fuentes-Rodríguez, Talía Sardina-González, Elaine Santana-Rodríguez, Milagros Vargas-Hernández, Ayme Oliva-Cárdenas, Nemecio González-Fernández, Eddy Bover-Fuentes, Carlos A. Duarte, Mario Pablo Estrada-García

Summary of the viral challenge potency tests					
Batch	Challenged animals	Protected animals	GM of NAb titers at 28 dpv	Lower 95% CI of GM	Upper 95% CI of GM
P51031	37	37	1: 5902	4523	7702
P61011-1	32	32	1: 5257	3964	6975
P61021-1	26	26	1: 4397	3341	5788
P71011-1	11	11	1: 4480	3410	4118
P81011-1	10	10	1: 5940	5886	8569
All vaccinated animals	116	116	1: 5217	4571	5954
Unvaccinated controls	38	0	< 1:5	-	-

NAb, neutralizing antibodies; dpv, days post-vaccination; GM, geometric mean; CI, confidence intervals of the geometric mean

Table 1. Summary of the challenge experiments with Porvac® vaccinated pigs.

Discussion

In Colombia, approximately 176,000 cultivated hectares benefit 52,000 families in 422 municipalities of 30 departments,

Monte Carlo Simulation Analysis (MCS)

After structuring costs, the most influential cost component was direct labor, representing 53% of the total cost. The cost of culture media was 12% of the total, IMC represented 5%, and operating expenses, including administrative expenses and infrastructure, were 30% (Figure 2).

Conclusions

In summary, a complete correspondence between the neutralizing antibody titer in the sera of Porvac© vaccinated pigs and protection from CSFV challenge have been demonstrated in a large set of experimental data. These results support substituting the viral challenge test for the neutralizing peroxidase-linked assay in the release of Porvac© batches. By eliminating the viral challenge, the suffering of the animals will be alleviated, as well as the risk of dissemination of the high-virulence strain used in those experiments. The duration of the test and the associated costs will also be reduced.

Acknowledgments

Ethics

The Center for Genetic Engineering and Biotechnology ethics committee approved the study design.

Conflicts of Interest

The authors declare no conflicts of interest regarding the results presented in this article.

Funding

Bibliographic references

1. Moennig V, Greiser-Wilke I. Classical swine fever virus. In: Mahy B, Van Regenmortel M, eds. Encyclopedia of Virology Third Edition ed: Oxford: Academic Press; 2008: 525-32.
2. Blome S, Staubach C, Henke J, Carlson J, Beer M. Classical swine fever—an updated review. Viruses 2017;9:86.
3. Van Oirschot J. Vaccinology of classical swine fever: from lab to field. Veterinary microbiology 2003;96:367-84.
4. Coronado L, Perera CL, Rios L, Frías MT, Pérez LJ. A Critical Review about Different Vaccines against Classical Swine Fever Virus and Their Repercussions in Endemic Regions. Vaccines 2021;9:154.
5. Dong XN, Chen YH. Marker vaccine strategies and candidate CSFV marker vaccines. Vaccine 2007;25:205-30.
6. Bouma A, De Smit A, De Jong M, De Kluijver E, Moormann R. Determination of the onset of the herd-immunity induced by the E2 sub-unit vaccine against classical swine fever virus. Vaccine 2000;18:1374-81.
7. Uttenthal A, Le Potier MF, Romero L, De Mia GM, Floegel-Niesmann G. Classical swine fever (CSF) marker vaccine. Trial I. Challenge studies in weaner pigs. Vet Microbiol 2001;83:85-106.
8. Sordo-Puga Y, Suárez-Pedroso M, Naranjo-Valdéz P, et al. Porvac® Subunit Vaccine E2-CD154 Induces Remarkable Rapid Protection against Classical Swine Fever Virus. Vaccines 2021;9:167.
9. Suárez M, Sordo Y, Prieto Y, et al. A single dose of the novel chimeric subunit vaccine E2-CD154 confers early full protection against classical swine fever virus. Vaccine 2017.
10. Suárez-Pedroso M, Sordo-Puga Y, Sosa-Teste I, et al. Novel chimeric E2CD154 subunit vaccine is safe and confers long lasting protection against classical swine fever virus. Veteri-

nary Immunology and Immunopathology 2021;234:110222.

11. Muñoz-González S, Sordo Y, Pérez-Simó M, et al. Efficacy of E2 glycoprotein fused to porcine CD154 as a novel chimeric subunit vaccine to prevent classical swine fever virus vertical transmission in pregnant sows. Veterinary microbiology 2017;205:110-6.

12. OIE. Manual of Diagnostic Tests and Vaccines for Terrestrial Animals, 5th Edition, Chapter 2.8.3. 2018;1.

13. Blome S, Meindl-Bohmer A, Loeffen W, Thuer B, Moennig V. Assessment of classical swine fever diagnostics and vaccine performance. Revue Scientifique et Technique-Office International des Epizooties 2006;25:1025-38.

14. Manual of Diagnostic Tests and Vaccines for Terrestrial Animals, Chapter 3.8.3. Classical swine fever (hog cholera) infection with classical swine fever virus. OIE, 2019. (Accessed 3/4/2020, 2020, at http://www.oie.int/fileadmin/Home/eng/Health_standards/tahm/2.08.03_CSF.pdf; .)

15. Manual of Diagnostic Tests and Vaccines for Terrestrial Animals, Chapter 1.1.8. Principles of Veterinary Vaccine. 2019. (Accessed 3/7/2020, 2020, at https://www.oie.int/fileadmin/Home/eng/Health_standards/tahm/1.01.08_VACCINE_PRODUCTION.pdf.)

16. Biront P, Leunen J, Vandeputte J. Inhibition of virus replication in the tonsils of pigs previously vaccinated with a Chinese strain vaccine and challenged oronasally with a virulent strain of classical swine fever virus. Veterinary microbiology 1987;14:105-13.

17. Terpstra C, Wensvoort G. The protective value of vaccine-induced neutralising antibody titres in swine fever. Vet Microbiol 1988;16:123-8.

18. Bouma A, de Smit AJ, de Kluijver EP, Terpstra C, Moormann RJ. Efficacy and stability of a subunit vaccine based on glycoprotein E2 of classical swine fever virus. Vet Microbiol 1999;66:101-14.

19. Ganges L, Barrera M, Díaz de Arce H, et al. Antigenic, biological and molecular characterization of the Cuban CSFV isolate "Margarita". Rev Salud Anim Vol 2007;29:182-92.

20. Postel A, Schmeiser S, Perera CL, Rodríguez LJP, Frias-Lepoureau MT, Becher P. Classical swine fever virus isolates from Cuba form a new subgenotype 1.4. Veterinary microbiology 2013;161:334-8.

21. Mittelholzer C, Moser C, Tratschin JD, Hofmann MA. Analysis of classical swine fever virus replication kinetics allows differentiation of highly virulent from avirulent strains. Vet Microbiol 2000;74:293-308.

22. Terpstra C, Bloemraad M, Gielkens AL. The neutralizing peroxidase-linked assay for detection of antibody against swine fever virus. Vet Microbiol 1984;9:113-20.

23. De Smit A, Terpstra C, Wensvoort G. Comparison of virus isolation methods from whole blood or blood components for early diagnosis of CSF. Report on Meeting of the EU National Swine Fever Laboratories, Brussels; 1994. p. 22-4.

24. De Smit A, Bourne A, De Kluijver E, Terpstra C, Moormann R. Prevention of transplacental transmission of moderatevirulent classical swine fever virus after single or double vaccination with an E2 subunit vaccine. Veterinary Quarterly 2000;22:150-3.

25. Ziegler U, Kaden V. Vaccination of weaner pigs against classical swine fever with the subunit vaccine" Porcilis Pesti": influence of different immunization plans on excretion and transmission of challenge virus. Berliner und Munchener tierarztliche Wochenschrift 2002;115:267-73.

26. Zhang Z, Zhang H, Liu T. Study on body temperature detection of pig based on infrared technology: A review. Artificial Intelligence in Agriculture 2019;1:14-26.

7

ARTICLE / INVESTIGACIÓN

Role of Vitamin D in the diagnosis of acute Myeloid Leukemia

Noor Thair Tahir[1], N. A Thamer[2]*, Noah A .Mahmood[3]
[1] National Diabetes Center, Muatansiriyah University, Baghdad, Iraq.
[2] Medical Technical College, Al-Farahidi University, Al-Jadiriyah Bridge, Baghdad, Iraq.
[3] Iraqi Center for Cancer and Medical Genetics Research, Muatansiriyah University, Baghdad, Iraq.
Corresponding author: neran.technical@gmail.com

DOI. 10.21931/RB/2023.08.01.50

Abstract: A range of hematological and biochemical markers have been investigated in Acute Myeloid Leukemia (AML) patients to determine the relationship between cancer growth and metabolic problems. This study aimed to determine the effects of vitamin D deficiency in Iraqi patients with acute myeloid leukemia who had recently been diagnosed. There was a significant inverse correlation between the total serum cholesterol (TC) level of acute myeloid leukemia (AML) patients group [(148.77±12.2) for males, (165.29±9.64) for females] and the control group [(164.50±7.26) for males, (180.05±7.31) for females], also an inverse correlation between high-density lipoprotein (HDL) level of acute myeloid leukemia (AML) patients group [(46.00±2.04) for males, (46.18±1.08) for females] and control group [(54.25±1.86) for males,(51.94±1.37) for females]. A significant difference was between the serum triglyceride (TG) level of acute myeloid leukemia (AML) patients group [(128.71±13.07) for males, (152.48±10.6) for females] and control group [85.12±11.30) for male, (90.50±10.90) for females], also between vitamin D level of acute myeloid leukemia (AML) patients group [(17.23±1.18) for males, (12.96±0.74) for females] and control group [(42.62±1.43) for males, (40.76±0.82) for females]. A statistically significant difference was between the serum calcium levels of individuals with acute myeloid leukemia [(8.99±0.32) for males, (8.91±0.23) for females]   and the control group [(13.13±1.16) for males, (10.73±0.28) for females].   AML patients can benefit from vitamin D treatment, according to a pairwise analysis of receiver operating characteristic (ROC) curves. The above results are related to concluding that Vitamin D can be utilized as a diagnostic test for AML patients.

Key words: Acute myeloid leukemia (AML), Hypereosinophilia, ROC curve, hypocholesterolemia, vitamin D.

Introduction

Leukemia is a type of cancer that affects the blood and blood-forming tissues, such as the bone marrow and the lymphatic system. Several risk factors for leukemia have been identified, including smoking, a genetic disorder such as Down syndrome, exposure to a large amount of radiation or exposure to specific chemical compounds such as benzene, certain chemotherapy used to treat previous cancer, and having a family history of leukemia[1]. Chronic leukemia progresses more slowly than acute leukemia. Patients have a higher proportion of mature cells. In acute leukemia, the immature cells are rapidly advancing, and these cells cannot perform their normal functions[2]. Malignancy myeloid cells lead to myeloid leukemia, whereas that including T and B lymphocytes leads to lymphocytic leukemia[3]. Acute myeloid leukemia (AML) is a cancer that develops when long-lived myeloid blasts in the bone marrow and peripheral blood undergo unchecked transformation and proliferation. Normal cells are replaced by malignant ones, lowering the number of healthy cells[4].

Lipid metabolism disorders are characterized by anomalies of lipids and lipid metabolites occurring mostly in plasma and other tissues, which cause genetic or acquired factors[5]. Several related genes, hormones and enzymes organize the level of lipids. Abnormalities of these factors lead to lipids metabolism disorders, which cause cardiovascular disorders, metabolic diseases and cancers[6]. Different studies have indicated that abnormal levels of lipids are closely related to carcinogenesis and cancer metastasis. Malignant cancer cell proliferation requires high energy to transform and accelerate, leading to lipid metabolism alterations[7]. Some studies showed a decrease in plasma lipid levels in patients with cancer. This may result in increased utilization of blood lipids by malignant cells as a competing factor[8]. Despite these positive correlations between hypercholesterolemia and carcinogenesis, some epidemiologic observations suggest no association exists between cholesterol and cancer progression[9].

Different studies have reported a relationship between Vitamin D deficiency and AML[10]. An inverse relationship exists between circulating vitamin D levels and malignancy for colorectal[11] and breast cancer[12]. This research sought to determine the levels of lipids, high-density lipoprotein (HDL), calcium, vitamin D, and various aspects of the hematological picture in newly diagnosed Acute Myeloid Leukemia (AML) patients in Iraq, with the ultimate goal of improving treatment outcomes.
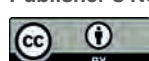
Materials and methods

This study proceeded at the National Center for Hematology of Al-Mustansiriyah University in Baghdad from April 2019 until November 2019. This research enrolled 55 newly diagnosed AML patients before any specific medication was administered. Their ages ranged from (33-80) years and were compared to 26 healthy people who served as a con-

trol group. Body mass index was determined as weight in kilograms divided by the square of height (kg/m^2). Before starting therapy for AML, blood samples were taken from patients at diagnosis and before they were treated for AML. The separated serum was used for total cholesterol, triglycerides and HDL measurements by Auto Analyzer Kenza 240 TX (Biolabo, France). Vitamin D3 was determined by a mini vidas analyzer (biomerieux, France). Serum Ca was measured by the easy kit analyzer. (Beckman Coulter, Ireland) were used to analyze the Complete Blood Count (CBC).

Statistical Analysis

SAS was used to analyze the data statistically (Statistical Analysis System - version 9.1). To determine if there were any statistically significant differences between means, a one-way ANOVA and the Least Significant Differences (LSD) post hoc test were used. The p-value (P < 0.05) is regarded as statistically significant when it is less than one. The receiver operation characteristic (ROC) curve was used to determine the validity of markers as indicators of illness in a particular population. The area under the curve (AUC) of the features was calculated and compared (AUC). The analysis was completed with the help of the Med Calc software[13,14].

Results

This study reported different parameters for patients with AML compared with the control. In table (1), some of the baseline characteristics showed no change in an age when compared between patients and controls; there were increases in the weight of male patients and base mass index. Moreover, some of the hematological studies showed no change in values of Red blood cells (RBC), Basophils but increased Eosinophil values when compared between

patients and controls.

Table 2 determined total serum cholesterol, triglyceride, high-density lipoprotein lipids, serum calcium and vitamin D for AML compared with the control. There was a decrease in TC, HDL,D 3 and calcium, while there was an increase in TG.

Figures 1 (A and B) illustrate the receiver operating characteristic curve (ROC) for calcium (A) and vitamin D (B).

Figure hows the area under the curve (AUC) for vitamin D and calcium. While in table 3 shows the AUC, standard error (SE) and confidence interval (CI) for vitamin D and calcium.

Discussion

There was no statistically significant difference in age between the patients and the control group. However, there was a statistically significant difference in male weight between the control and the patients (Table 1) and a significant difference in BMI among males and females. Being overweight was related to raised risk of AML. Adipose tissue is one of the active and complex endocrine organs. Recent studies highlighted the bidirectional interactions, based on adipokines and lipids, between white adipose tissue and tumors and their role in cancer progression (later, "adipose tissue" will refer to white adipose tissue). In addition, adipocyte-secreted factors have been shown to regulate the expression of genes associated with cancer progression (adhesion, invasion, angiogenesis, signal transduction and apoptosis) in non-cancerous mammary cells suggesting a role in cancer initiation[15]; they may also participate to the leukemogenesis of AML[16].

Hypereosinophilia is classified to Primary (Chronic eosinophilic leukemia, Familial eosinophilia, Clonal hypereosinophilia, and Idiopathic hypereosinophilia) and secondary (Infections, autoimmune diseases, allergic diseases, drugs

		Age	Weight	BMI	RBC	BAS	EO
control	Male no=8	36.00±1.19 a	69.62±4.54 b	24.75±1.44 b	5.67±0.49 a	0.02±0.001 a	0.26±0.04 b
	Female no=17	39.05±1.52 a	74.58±2.63 ab	25.86±0.79 b	5.47±0.32 a	0.04±0.02 a	0.28±0.04 b
patients	Male no=26	42.15±2.82 a	81.15±2.25 a	29.05±0.95 a	5.67±0.49 a	0.03±0.01 a	0.49±0.06 a
	Female no=27	42.55±2.81 a	74.92±2.32 ab	27.00±0.64 ab	5.21±0.24 a	0.06±0.02 a	0.41±0.04 a
	LSD	8.9252	8.396	2.8467	0.8996	0.0657	0.1385

Small letters within a single column represent the comparison between the control and patients. Different letters mean significant results.

Table 1. Baseline characteristics and some hematological parameters in AML patients and controls.

		TC	TG	HDL	D3	Ca
control	Male no=8	164.50±7.26 a	85.12±11.30 b	54.25±1.86 a	42.62±1.43 a	13.13±1.16 a
	Female no=17	180.05±7.31 a	90.50±10.90 b	51.94±1.37 a	40.76±0.82 a	10.73±0.28 b
patients	Male no=26	148.77±12.2 b	128.71±13.07 a	46.00±2.04 b	17.23±1.18 b	8.99±0.32 c
	Female no=27	165.29±9.64 b	152.48±10.6 a	46.18±1.08 b	12.96±0.74 b	8.91±0.23 c
	LSD	5.17	5.68	5.4416	3.3389	1.1895

D3= vitamin D, TC =total cholesterol, TG = triglyceride, HDL= high-density lipoprotein. Small letters within a single column represent the comparison between the control and patients. Different letters mean significant results.

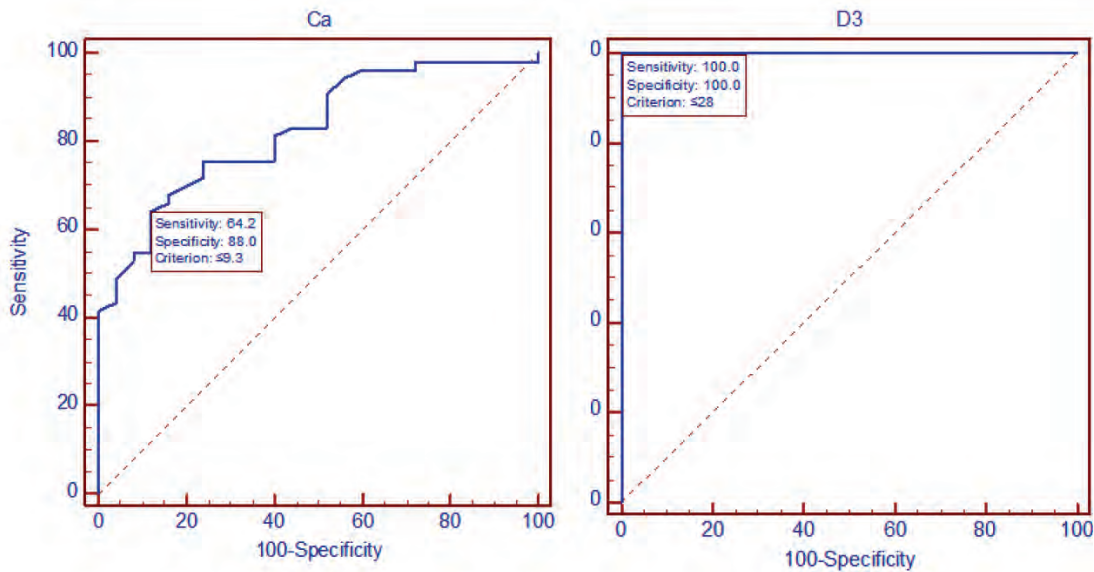**Table 2.** Some biochemical studies for AML and control.

Figure 1. ROC curve for identifying optimal calcium (left) and vitamin D (right) cutoff points.
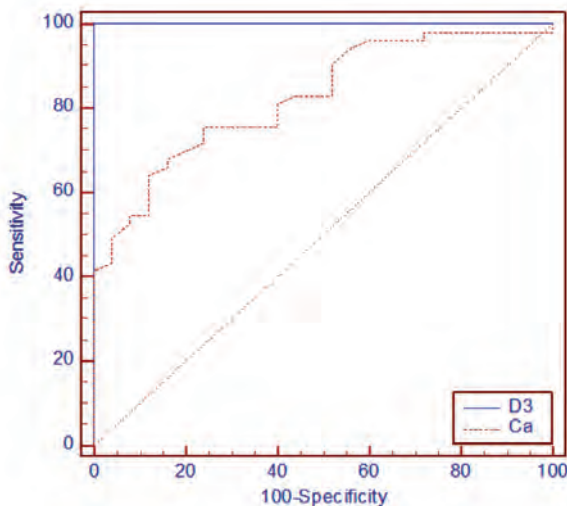

Figure 2. The ROC curves with different areas under the curve.

Variable	AUC	SE [a]	95% CI [b]
D3	1.000	0.000	0.954 to 1.000
Ca	0.826	0.0465	0.724 to 0.903
Pairwise comparison of ROC curves			
D3 ~ Ca Significance level		P = 0.0002	

Table 3. AUC, SE and CI for vitamin D and calcium.

and Malignancies)[17]. Through search in articles, we found similar results were matched with our results[18,19]. Many surveys have been performed considering the serum lipids abnormalities[20]; in table 2, no statistically significant variations in plasma total cholesterol, triglycerides, or high-density lipoprotein were detected between men and females, neither for AML patients nor controls. There was a considerable decrease(p<0.05) in cholesterol and HDL, whereas triglycerides value a significantly elevated(P<0.05) when compared with males between(patients and controls) and females between (patients and power). This results in agreement with the other findings[21]. Different researchers explained the relation between hypocholesterolemia and the stage of maturation of leukemic blast cells in acute myeloid leukemia[22]. The elevated LDL receptor in AML patients was caused by hypocholesterolemia[23]. Several research has been conduc-

ted to characterize HDL's potential to boost proliferation, immigration, and survival in cancer cell cultures[24]. According to many studies, HDL-C is related to an increased risk of cancer because it continues to provide extra cholesterol to and fuel the development of the tumor[25].

In this study, we found a low level of Vitamin D in newly diagnosed AML patients before the beginning of their treatment. In the Middle East, different factors cause Vitamin D deficiency, such as Low exposure to sunlight, lack of Vitamin D in food, the nature of clothes, type of skin, and lack of complements[26]. But, recently, the use of Vitamin D supplements has obtained great interest among older adults; they essentially have sufficient levels of Vitamin D[27]. Different epidemiological and experimental studies support that Vitamin D deficiency has increased the risk of developing several cancers[28]. Various studies have indicated that Vitamin D can usually modify several critical cellular methods, involving suppression of carcinogenesis by creating cellular differentiation, suppression of proliferation and promoting apoptosis[29,30]. Vitamin D has other significant effects, such as inhibiting tumor angiogenesis, invasion and metastasis[31].

On the other hand, a previous study showed a positive correlation between low vitamin D levels and higher BMI or obesity[32]. Hypocalcemia is unusual in hematoma malignancy. Various factors, including low albumin, inadequate nutrition, low vitamin D, low magnesium, or persistent respiratory alkalosis, may cause it. In tumor lysis, increased serum phosphorous may cause calcium-phosphate deposition, decreasing serum calcium[33]. Figures 1 (A and B) illustrate the receiver operating characteristic (ROC) curves. Generally, the ROC curve measures a test's effectiveness by establishing appropriate cutoff points. The graph depicts calcium sensitivity, and specificity (A) was 64.2. % and 88.0%, then sensitivity and specificity for vitamin D (B) were 100.0% and 100.0%, respectively.

Table 3 shows that AUC for vitamin D was 1.000 (95% CI = 0.954–1.000), and AUC for calcium was 0.826 (95% CI = 0.724 –0.903). The AUC is a standard measure of the accuracy of a diagnostic test. Tests are often classed based on the area under the ROC curve (figure 2). The bigger the AUC, the higher the test's total score. The positive and false favorable rates for the vitamin D test (figure 1) are greater than those for calcium test A at all cutoffs, making

4

it the better choice. The AUC for vitamin D is larger than the area under the curve for the calcium test. The pairwise comparison of the ROC curves revealed a statistically significant difference (P= 0.0002) for vitamin D and calcium parameters. In a paired ROC analysis, the vitamin D measure was shown to be more discriminatory than the calcium measure. A perfect test has an AUC of 1.0. So that vitamin D is an ideal test for diagnostic AML patients than calcium. Recently, cancer disease can be diagnosed by PCR, such as CML[34] and Adenocarcinoma[35,36]. This molecular technique was also employed to diagnosis different microorganisms that caused pathogenicity in human such as *Clostridium perfringens*[37], *Brucella melitensis*[38], *Proteus vulgaris*[39,40], *Staphylococcus aureus*[41], *Pseudomonas aeruginosa*[42,43], and *Toxoplasma spp*[44,45].

Conclusions

The pairwise comparison among the ROC curves for vitamin D and calcium showed that the vitamin D measure was more discriminative than calcium. So vitamin D is a perfect test for early diagnosis of AML patients.

Conflicts of Interest

No conflict.

Bibliographic references

1. Lupatsch JE, Kreis C, Konstantinoudis G, Ansari M, Kuehni CE, Spycher BD. Birth characteristics and childhood leukemia in Switzerland: a register-based case–control study. Cancer Causes & Control. 2021; 32(7):713-23.

2. Jabbour E, Kantarjian H. Chronic myeloid leukemia: 2020 update on diagnosis, therapy and monitoring. American journal of hematology. 2020;95(6):691-709..

3. Juárez-Avendaño G, Méndez-Ramírez N, Luna-Silva NC, Gómez-Almaguer D, Pelayo R, Balandrán JC. Molecular and cellular markers for measurable residual disease in acute lymphoblastic leukemia. Boletín médico del Hospital Infantil de México. 2021;78(3):159-70.

4. Aitken MJ, Ravandi F, Patel KP, Short NJ. Prognostic and therapeutic implications of measurable residual disease in acute myeloid leukemia. Journal of Hematology & Oncology. 2021;14(1):1-5.

5. Tian L, Yu X. Lipid metabolism disorders and bone dysfunction-interrelated and mutually regulated. Molecular Medicine Reports. 2015;12(1):783-94.

6. Kansal R. Acute myeloid leukemia in the era of precision medicine: recent advances in diagnostic classification and risk stratification. Cancer biology & medicine. 2016;13(1):41-54.

7. Agrawal AG, Nagarajappa AK, Bandela V, Agrawal G, Chaturvedi SS, Patil SR. Alteration in Serum Lipid Profile Pattern in Oral Squamous Cell Carcinoma and Potentially Malignant Disorders. Pesquisa Brasileira em Odontopediatria e Clínica Integrada. 2021;14;21.

8. Saha SP, Kalathiya RJ, Davenport DL, Ferraris VA, Mullett TW, Zwischenberger JB. Survival after pneumonectomy for stage III non-small cell lung cancer. Oman Medical Journal. 2014;29(1):24.

9. Cholesterol Treatment Trialists'(CTT) Collaboration. Lack of effect of lowering LDL cholesterol on cancer: meta-analysis of individual data from 175,000 people in 27 randomised trials of statin therapy. PloS one. 2012 ;7(1):e29849.

10. Swords R, Sznol J, Elias R, Watts J, Zelent A, Martin E, Vargas F, Bethel-Ellison S, Kobetz E. Acute leukemia in adult Hispanic Americans: a large-population study. Blood cancer journal. 2016;6(10):e484-

11. Roth DE, Abrams SA, Aloia J, Bergeron G, Bourassa MW, Brown KH, Calvo MS, Cashman KD, Combs G, De☐Regil LM, Jefferds ME. Global prevalence and disease burden of vitamin D deficiency: a roadmap for action in low☐and middle☐income countries. Ann. N.Y. Acad. Sci., 2018;1430:44–79.

12. Zhang L, Zou H, Zhao Y, Hu C, Atanda A, Qin X, Jia P, Jiang Y, Qi Z. Association between blood circulating vitamin D and colorectal cancer risk in Asian countries: a systematic review and dose-response meta-analysis. BMJ open. 2019;9(12):e030513.

13. MedCalc Statistical Software version 16.4.3 (MedCalc Software bvba, Ostend, Belgium; https://www.medcalc.org; 2016.

14. SAS.2010.SAS/STAT Users Guide for Personal Computer. Release 9.13.SAS Institute, Inc., Cary, N.C., USA.

15. Tahergorabi Z, Khazaei M, Moodi M, Chamani E. From obesity to cancer: a review on proposed mechanisms. Cell biochemistry and function. 2016 ;34(8):533-45.

16. Li S, Chen L, Jin W, Ma X, Ma Y, Dong F, Zhu H, Li J, Wang K. Influence of body mass index on incidence and prognosis of acute myeloid leukemia and acute promyelocytic leukemia: A meta-analysis. Scientific reports. 2017 ;7(1):1-10.

17. Kolobovnikova YV, Dmitrieva AI, Yankovich KI, Vasil'eva OA, Purlik IL, Poletika VS, Novitskii VV, Urazova OI. Expression of galectins-1 and galectin-3 in stomach and colorectal cancer with tissue eosinophilia. Bulletin of Experimental Biology and Medicine. 2018;165(2):256-258.

18. Reiter A, Gotlib J. Myeloid neoplasms with eosinophilia. Blood, The Journal of the American Society of Hematology. 2017;129(6):704-714.

19. Zhang X, Wang B, Zhang R, Chai X, Chao H. Hypereosinophilia (HE) in acute myeloid leukemia (AML) with normal karyotype: A report of two cases. Nigerian Journal of Clinical Practice. 2020;23(1):116-.117.

20. Zhao L, Zhan H, Jiang X, Li Y, Zeng H. The role of cholesterol metabolism in leukemia. Blood Science. 2019;1(1):44-49.

21. Ozturk E. The Relationship Between Hematological Malignancy and Lipid Profile. Medeniyet Medical Journal. 2021;36(2):146.

22. Parsa N, Taravatmanesh S, Trevisan M. Is low cholesterol a risk factor for cancer mortality?. European Journal of Cancer Prevention. 2018;27(6):570-576.

23. Oztas Y. Hypocholesterolemia: a neglected laboratory finding. Acta Medica. 2016;47(1):19-22.

24. Panchoo M, Lacko A. Scavenger receptor class B type 1 regulates neuroblastoma cell proliferation, migration and invasion. Biochemical and biophysical research communications. 2018 ;495(1):614-20.

25. Morin EE, Li XA, Schwendeman A. HDL in Endocrine carcinomas: biomarker, drug carrier, and potential therapeutic. Frontiers in endocrinology. 2018;9:715.

26. Lips P, Cashman KD, Lamberg-Allardt C, Bischoff-Ferrari HA, Obermayer-Pietsch B, Bianchi ML, Stepan J, Fuleihan GE, Bouillon R. Current vitamin D status in European and Middle East countries and strategies to prevent vitamin D deficiency: a position statement of the European Calcified Tissue Society. European journal of endocrinology. 2019;180(4): 23-54.

27. Alizadeh N, Khalili H, Mohammadi M, Abdollahi A. Serum vitamin D levels at admission predict the length of intensive care unit stay but not in-hospital mortality of critically ill surgical patients. Journal of research in pharmacy practice. 2015;4(4):193.

28. Ma Y, Johnson CS, Trump DL. Mechanistic insights of vitamin D anticancer effects. Vitamins & Hormones. 2016;100:395-431.

29. Thompson T, Andreeff M, Studzinski GP, Vassilev LT. 1, 25-Dihydroxyvitamin D3 Enhances the Apoptotic Activity of MDM2 Antagonist Nutlin-3a in Acute Myeloid Leukemia Cells Expressing Wild-type p531, 25D Accelerates Apoptosis in AML Cells. Molecular cancer therapeutics. 2010;9(5):1158-68.

30. Fernández-Barral A, Bustamante-Madrid P, Ferrer-Mayorga G, Barbáchano A, Larriba MJ, Muñoz A. Vitamin D effects on cell differentiation and stemness in cancer. Cancers. 2020;12(9):2413.

31. Skrajnowska D, Bobrowska-Korczak B. Potential molecular mechanisms of the anti-cancer activity of vitamin D. Anticancer research. 2019;39(7):3353-3363.

32. Wortsman J, Matsuoka LY, Chen TC, Lu Z, Holick MF. Decreased bioavailability of vitamin D in obesity. The American journal of clinical nutrition. 2000 ;72(3):690-693.

33. Luciano RL, Brewster UC. Kidney involvement in leukemia and lymphoma. Advances in Chronic Kidney Disease. 2014;21(1):27-35.

34. Ahmed AA, Khaleel KJ, Fadhel AA, Al-Rubaii BA. Chronic Myeloid Leukemia: A retrospective study of clinical and pathological features. Bionatura. 7(3):41. DOI. 10.21931/RB/2022.07.03.41.

35. Ali SM, Lafta BA, Al-Shammary AM, Salih HS. In vivo oncolytic activity of non-virulent newcastle disease virus Iraqi strain against mouse mammary adenocarcinoma. InAIP Conference Proceedings 2021; 2372(1):030010. AIP Publishing LLC.

36. Ali SM, Laftah BA, Al-Shammary AM, Salih HS. Study the role of bacterial neuraminidase against adenocarcinoma cells in vivo. InAIP Conference Proceedings 2021; 2372: 030009). AIP Publishing LLC.

37. Hashim ST, Fakhry SS, Rasoul LM, Saleh TH, ALRubaii BA. Tropical Journal of Natural Product Research. 2021; 5(4):613-616.

38. abdulkaliq Awadh H, Hammed ZN, Hamzah SS, Saleh TH, AL-Rubaii BA. Molecular identification of intracellular survival related Brucella melitensis virulence factors. Biomedicine. 2022;42(4):761-765.

39. Abdul-Gani MN, Laftaah BA. Purification and characterization of chondroitinase ABC from Proteus vulgaris, an Iraqi clinically isolate. Current Science. 2017;113(11):2134-2140.

40. kadhim AL-Imam MJ, AL-Rubaii BA. The influence of some amino acids, vitamins and anti-inflammatory drugs on activity of chondroitinase produced by Proteus vulgaris caused urinary tract infection. Iraqi Journal of Science. 2016; 57(4A):2412-2421.

41. Sabah Fakhry S, Noori Hammed Z, Abdul-elah Bakir W, Abdullah Laftaah ALRubaii B. Identification of methicillin-resistant strains of Staphylococcus aureus isolated from humans and food sources by Use of mecA 1 and mecA 2 genes in Pulsed-field gel electrophoresis (PFGE (technique. Revis Bionatura 2022; 7 (2) 44. Doi: 10.21931/RB/2022.07.02.44.

42. Shehab ZH, AL-Rubaii BA. Effect of D-mannose on gene expression of neuraminidase produced from different clinical isolates of Pseudomonas aeruginosa. Baghdad Science Journal. 2019;16(2):291-298.

43. Shehab ZH, Laftah BA. Correlation of nan1 (Neuraminidase) and production of some type III secretion system in clinical isolates of Pseudomonas aeruginosa. BIOSCIENCE RESEARCH. 2018; 15(3):1729-1738.

44. Abdulla L, Ismael MK, Salih TA, Malik SN, Al-Rubaii BA. Genotyping and evaluation of interleukin-10 and soluble HLA-G in abortion due to toxoplasmosis and HSV-2 infections. Annals of parasitology. 2022;68(2):385-390.

45. Jiad¹ AL, Ismael MK, Muhsin SS, Al-Rubaii BA. ND2 Gene Sequencing of Subfertile Patients Recovered from COVID-19 in Association with Toxoplasmosis. Bionatura, 7(3): 45. http://dx.doi.org/10.21931/RB/2022.07.03.45.

5

Studying the toxicity of polluted water with polyaromatic hydrocarbon compound (Anthracene) by using micronucleus assay in fish

Milad A.Hussein, Estabraq N, Abdul Lateef, Sarab R. Mustafa, Noor Nihad Baqer*, Suha A. Ali, Maha M Taen, Nora Saheab

DOI. 10.21931/RB/2023.08.01.51

Ministry of Science and Technology, Environment And Water Director, Baghdad, Iraq.
Corresponding author: noornihadbaqer@gmail.com

Abstract: Polycyclic aromatic hydrocarbons mainly originate from the incomplete combustion of fossil fuels such as petroleum, natural gas and coal. Also, biomass burning has attracted much attention due to its mutagenic, allergenic and carcinogenic properties. Anthracene, a three-ringed polycyclic aromatic hydrocarbon, is widely known as a common hazardous ubiquitous environmental pollutant. Anthracene is used to make dyes, plastics and pesticides. The present study aims to evaluate the risks of Anthracene to fish using a micronucleus (MN) assay; the test has been used successfully as a mutagenic assay. Ninety fishes were adapted and acclimated to the laboratory conditions for one week before starting the experiment, then were exposed to (7.5mg/L, 10mg/L, and 12.5mg/L) of Anthracene for 72 hours. Results demonstrated that the LD50 of Anthracene in fish was (10 mg/L). Based on the values of LC50, the fish were then exposed for 72 h to three concentrations of sub-lethal Anthracene (2.5 mg/L, 5 mg/L and 7.5 mg/L) and control (0.00 mg/L) after (72 hours, 10 days, 20 days). Peripheral blood samples smears were collected from each group, the sample was stained by Giemsa stain, and frequencies of MNs were counted. The study showed an increase in micronuclei with concentration and period. In conclusion, it can use of the micronucleus assay in erythrocytes of fish as a sensible index for the assessment and evaluation of aquatic environmental pollution.

Key words: PAH, Anthracene, Micro nucleus assay, Carp.

Introduction

Polycyclic aromatic hydrocarbons (PAH) are a group of hydrophobic organic compounds that are widespread pollutants. Crude oil drops out, industrial, refinery activities, and civil wastes are essential sources of (PAH) in aquatic ecosystems.PAH are potentially carcinogenic agent[1] and a significant interest because of widespread contaminants in coastal and freshwater zones[2]. PAH contamination is significant near industrialized areas[3].

Anthracene ($C_6H_4.C_2H_2.C_6H_4$) is a rigid polycyclic aromatic hydrocarbon with a low molecular weight derived from coal tar consisting of three fused benzene rings. Anthracene, Para naphthalene, is a Green Oil that accompanies naphthalene in the final steps of coal tar percolation. Anthracene is used in the artificial production of the red dye alizarin. It is also used in insecticides, coating materials and preservatives of wood. Moreover, Anthracene is colorless but exhibits blue fluorescence under ultraviolet light. If Anthracene is released into water, it will be expected to absorb particulate and sediments strongly. It was not hydrolyzed but may be bio-concentrated in aquatic organisms, which causes loss or reduction of microsomal oxidase (this enzyme enables the rapid metabolism of polyaromatic hydrocarbons). It undergoes immediate photolysis close to the surface of natural waters and maybe follows significant biodegradation based on laboratory experiments. Besides, industrial and agricultural activities have raised pollution in the aquatic environment, which is contaminated by different chemicals toxic from the discharge of waste waters and agriculture; these are accountable for several effects on the organisms, including humans[4]. PAHs are absorbed by the fish body surface and via the gills. It also enters through food intake or contaminated materials[5].

Fish are an excellent topic for studying the mutagenic and/or carcinogenic possibility of contaminants in water samples since they can metabolize, concentrate and store waterborne pollutants[6]. Since fish often react to toxicants in a similar way to higher vertebrates, they can be used to screen for chemicals that are potentially teratogenic and carcinogenic in humans. The main application of fish used as a test model is to mark the distribution and effects of chemical contaminants in the watery environment[7]. Micronucleus assay was viable to freshwater and marine fishes and showed that gill cells are more sensitive than hematopoietic cells to micronucleus-inducing agents. The micronucleus assay is an in vivo and in vitro short-time screening procedure that is openly used to discover genotoxic effects. It is one of the most straightforward, dependable, low expenses and fast screening systems[8]. The MN test, one of the most common tests of environmental genotoxicity, has served as an indicator of cytogenetic hurt[9]. Micronuclei are cytoplasmic chromatin masses with the appearance of small nuclei that emerge from chromosome fragments or intact total chromosomes lagging in the anaphase phase of cell division. Their existence in cells reflects structural and numerical chromosomal aberrations arising through mitosis[10]. These compounds may create hepatic lesions and physiological and biochemical disorders in fish. Contaminated fish may then be used to bio-observe the existence and impor-

tance of these pollutants. The present study aims to evalua- te the risks of Anthracene to fish by using a micronucleus (MN) assay,

Materials and methods

There are 90 fish of common carp (Cyprinus carpio) ranging between 7-9 cm in total length and 60-80 gm. in body weight, with no visible signs of disease or morbidity. Fish were kept in an aquarium with aerated tap water; they were fed on commercial feed and adapted to laboratory conditions for one week before the experiments were complete.

The experiment was conducted in a 20 L aquarium and gently aerated tap water. A set of 10 fish specimens were randomly exposed to anthracene concentrations (7.5, 10.0 and 12.5mg/L); after 72 h, the value of LC50 of Anthracene for C. carpio was specified as 10.0 mg/L.

Based on the LD50 values, the fish were then exposed for 72 h to three concentrations of sub-lethal Anthracene (2.5mg/L, 5mg/L and 7.5 mg/L) and control (0.00 mg/L). The mortalities did not occur in all groups following the period of exposure. After 72 h (Acute exposure), the water was exchanged, and the blood was collected from the caudal

vein for a micronucleus test after 72 hrs, 10 and 20 days of the experiment. Statistical analysis was performed by using Excel word 2019

Micronucleus Test

The smear of peripheral blood pulled from the caudal vein by a syringe coated with heparin was prepared, and well-dried slides were stained with 10% Giemsa stain solu- tion for a half hour following the method of (11). (1000 cells/ slide) for micro-nuclei were scored.

Results

The results of this study showed that the MN was in- creased, correspondingly with the increasing anthracene concentrations (2.5%, 5%, and 7.5%) than that control group in all the anthracene concentrations (Figure 1).

Micronucleus was calculated in the acute group (after 72 hrs), and the chronic group (after 10 and 20 days of the experimental period) showed an increase of micronuclei with the increase in concentration, and also when compa- red within the group according to the period of exposure as in Figure (2,3,4,5).
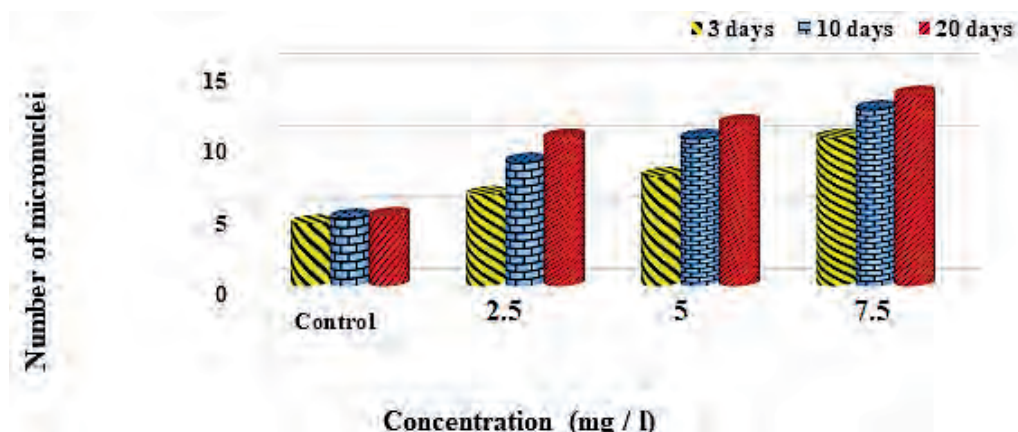
Figure 1. The number of micronuclei at diffe- rent times and concen- trations of Anthracene (mg/L).
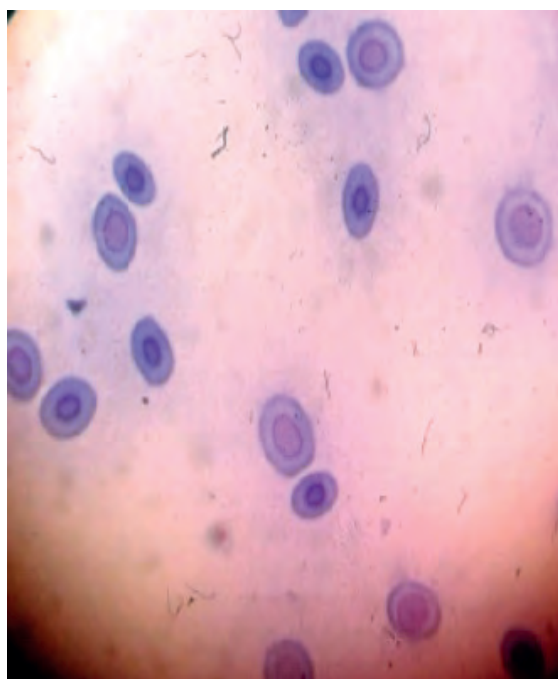
Figure 2. Normal red blood cells without micronuclei.
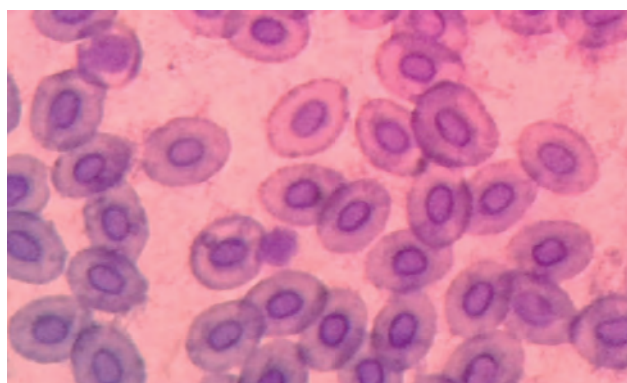
Figure 3. Micronuclei in Red Blood Cells of Fish
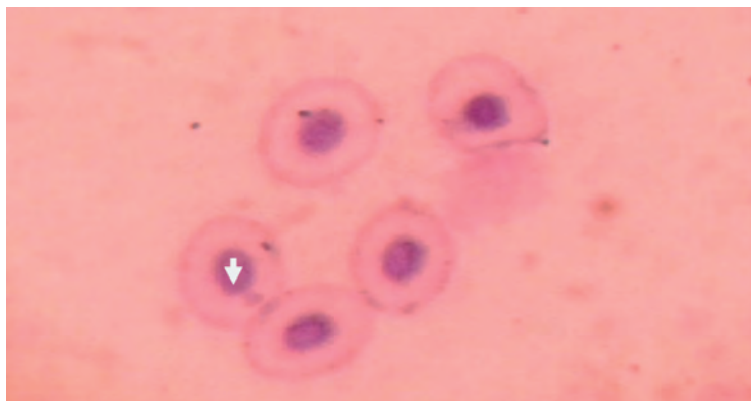
Figure 4. Micronuclei in Red Blood Cells of Fish.
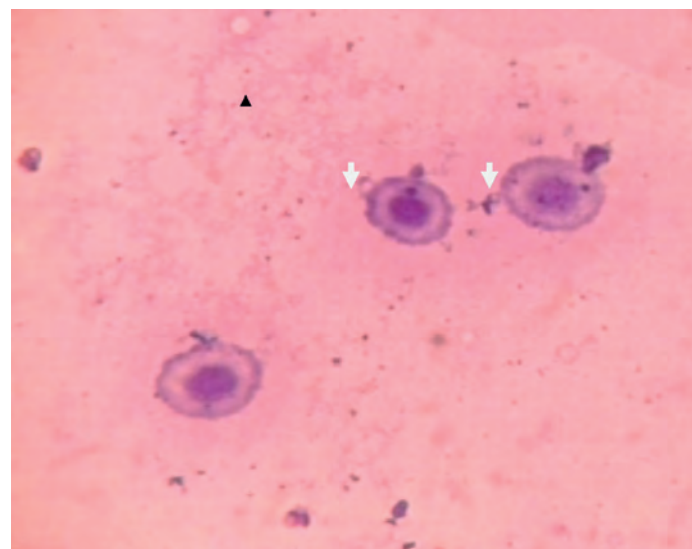
Figure 5. Micronuclei in Red Blood Cells of Fish.

Discussion

The results agreed with the development of Carlos *et al.*[12], who observed an increase in clastogenic accidents, and submission of the formation of MN when considering nuclear alterations and micronuclei together; group xenobiotic exposure and controls were significantly different.

Micronuclei occur due to exposure to different concentrations of benzene and Anthracene. The effect of these structures on the chromosome to form chromosome fragments or loss of centromere lead to delay of these fragments in the anaphase stage cell mitosis. After the telophase stage, these chromosome fragments are turned around to form Micronuclei[13,14].

Differing from other organisms belonging to the trophic chain, fishes are sensitive to relatively small concentrations of environmental Pollutants (with the possibility of mutagenic effects); thus, fishes are considered excellent bioindicators of environmental biomonitoring[15].

MNs assay, initially developed in mammalian species, has been widely used to evaluate the genotoxic effect of many chemical agents[16].

MNs assay can be considered a useful bioindicator of genotoxic and cytotoxic effects of contaminants in aquatic organisms[17-20].

The results showed the importance of MNs assay in mutagenic altered assessment in fishes, which can be used as sentinel organisms to indicate the potential for human exposure to genotoxic chemicals in drinking water. The concentrations of contaminants in fish reverse the situation of contamination of the environment, and thus, the observed levels of total PAHs in fish indicate high levels of PAHs contamination. However, the Consumption rate of 1 g/day appears to be protective from the carcinogenic effects of the PAHs levels. This is because the (Predicted Environmental Concentration) PEC values associated with a consumption rate of 1 g/day are found to be less than the screening value[21].

The present study showed that high PAH levels affect the health of fish and, thus, consumption of these fish may cause a significant health risk.

Conclusions

The present study showed that high PAH levels affect the health of fish and, thus, consumption of these fish may cause a significant health risk. It can use the micronucleus assay in erythrocytes of fish as a sensible index for assessing and evaluating aquatic environmental pollution.

Author Contributions

All authors contributed to the design methodology, analysis results and writing manuscript.

Funding

No funding.

Milad A.Hussein, Estabraq N, Abdul Lateef, Sarab R. Mustafa, Noor Nihad Baqer, Suha A. Ali, Maha M Taen, Nora Saheab

4

Conflicts of Interest

There is no conflict.

Bibliographic references

1. Shailaja MS, D'Silva C. Evaluation of impact of PAH on a tropical fish, Oreochromis mossambicus using multiple biomarkers. Chemosphere. 2003 Dec 1;53(8):835-41.
2. Akaishi FM, Silva de Assis HC, Jakobi SC, Eiras-Stofella DR, St-Jean SD, Courtenay SC, Lima EF, Wagener AL, Scofield AL, Oliveira Ribeiro CA. Morphological and neurotoxicological findings in tropical freshwater fish (Astyanax sp.) after waterborne and acute exposure to water soluble fraction (WSF) of crude oil. Archives of environmental contamination and toxicology. 2004 Feb;46(2):244-53.
3. Aas A, Beyer J, Goksoyr A. Fixed wavelength fluorescence (FF) of bile as a monitoring tool for polyaromatic hydrocarbon exposure in fish: an evaluation of compound specificity, inner filter effect and signal interpretation. Biomarkers. 2000 Jan 1;5(1):9-23.
4. Isani G, Andreani G, Cocchioni F, Fedeli D, Carpene E, Falcioni G. Cadmium accumulation and biochemical responses in Sparus aurata following sub-lethal Cd exposure. Ecotoxicology and environmental safety. 2009 January 1;72(1):224-30.
5. Vasanth S, Ganesh A, Vijayakumar TS, Karthikeyeni S, Manimegalai M, Subramanian P. Assessment of Anthracene on hepatic and antioxidant enzyme activities in Labeo rohita (Hamilton, 1822). International Journal of Pharmacy & Life Sciences. 2012 May 1;3(5).
6. Al-Sabti K, Metcalfe CD. Fish micronuclei for assessing genotoxicity in water. Mutation Research/Genetic Toxicology. 1995 Jun 1;343(2-3):121-35..
7. Al-Sabti K. Handbook of genotoxic effects and fish chromosomes. Handbook of genotoxic effects and fish chromosomes.. 1991.
8. Hayashi M, Ueda T, Uyeno K, Wada K, Kinae N, Saotome K, Tanaka N, Takai A, Sasaki YF, Asano N, Sofuni T. Development of genotoxicity assay systems that use aquatic organisms. Mutation Research/Fundamental and Molecular Mechanisms of Mutagenesis. 1998 Mar 20;399(2):125-33.
9. Baršienė J, Dedonytė V, Rybakovas A, Andreikėnaitė L, Andersen OK. Investigation of micronuclei and other nuclear abnormalities in peripheral blood and kidney of marine fish treated with crude oil. Aquatic Toxicology. 2006 Jun 1;78:S99-104.
10. Bolognesi C, Hayashi M. Micronucleus assay in aquatic animals. Mutagenesis. 2011 Jan;26(1):205-13.
11. Schmid W. The micronucleus test. Mutat Res. 1975 Feb;31(1):9-15.
12. Da Rocha CA, Dos Santos RA, Bahia MD, Da Cunha LA, Ribeiro HF, Burbano RM. The micronucleus assay in fish species as an important tool for xenobiotic exposure risk assessment—a brief review and an example using neotropical fish exposed to methylmercury. Reviews in Fisheries Science. 2009 Oct 2;17(4):478-84.
13. Heddle JA, Salamone MF. Chromosomal aberrations and bone marrow toxicity. Environmental Health Perspectives. 1981 Jun;39:23-7.
14. Al-Aadhhami SM .Studying Chromosomal abnormality of human induced by petroleum by product. Master thesis, college of Science, Baghdad University.2000.
15. Minissi S, Ciccotti E, Rizzoni M. Micronucleus test in erythrocytes of Barbus plebejus (Teleostei, Pisces) from two natural environments: a bioassay for the in situ detection of mutagens in freshwater. Mutation Research/Genetic Toxicology. 1996 Apr 6;367(4):245-51.
16. Dailianis S, Domouhtsidou GP, Raftopoulou E, Kaloyianni M, Dimitriadis VK. Evaluation of neutral red retention assay, micronucleus test, acetylcholinesterase activity and a signal transduction molecule (cAMP) in tissues of Mytilus galloprovincialis (L.), in pollution monitoring. Marine Environmental Research. 2003 Oct 1;56(4):443-70.
17. Ferraro MV, Fenocchio AS, Mantovani MS, Ribeiro CD, Cestari MM. Mutagenic effects of tributyltin and inorganic lead (Pb II) on the fish H. malabaricus as evaluated using the comet assay and the piscine micronucleus and chromosome aberration tests. Genetics and Molecular Biology. 2004;27:103-7.
18. Cavas T, Garanko NN, Arkhipchuk VV. Induction of micronuclei and binuclei in blood, gill and liver cells of fishes subchronically exposed to cadmium chloride and copper sulphate. Food and Chemical Toxicology. 2005 Apr 1;43(4):569-74.
19. Matsumoto ST, Mantovani MS, Malaguttii MI, Dias AL, Fonseca IC, Marin-Morales MA. Genotoxicity and mutagenicity of water contaminated with tannery effluents, as evaluated by the micronucleus test and comet assay using the fish Oreochromis niloticus and chromosome aberrations in onion root-tips. Genetics and Molecular Biology. 2006;29:148-58.
20. Lanfranchi AL, Menone ML, Miglioranza KS, Janiot LJ, Aizpun JE, Moreno VJ. Striped weakfish (Cynoscion guatucupa): a biomonitor of organochlorine pesticides in estuarine and near-coastal zones. Marine Pollution Bulletin. 2006 Jan 1;52(1):74-80.
21. Nyarko E, Klubi BE. Polycyclic aromatic hydrocarbons (PAHs) levels in two commercially important fish species from the coastal waters of Ghana and their carcinogenic health risks. West African Journal of Applied Ecology. 2011;19(1).

The inhibitory effect of some plant essential oils on the growth of some bacterial species

Mohammed Abdullah Mahmood[1], Shaker Gazi Gergees[2], Alaa Taha Younis AL-Hammadi[1]*   DOI. 10.21931/RB/2023.08.01.52

[1] Biology Department, College of Education Pure Science, Mosul University, Mosul, Iraq.
[2] Biology Department, College of Science, Mosul University, Mosul, Iraq.
Corresponding author: alaatyounis@uomosul.edu.iq

Abstract: This research is aimed at investigating the inhibitory essential oils activity of thyme, clove, cinnamon, ginger and garlic plants against some positive and negative gram pathogenic bacteria (*Escherichia coli, proteus spp., Staphylococcus epidermidis, Staphylococcus aureus*) by using the disk diffusion method And compares this activity with the activity of standard antibiotics, then study the synergistic and antagonistic effect between these essential oils with the antibiotics used against these bacteria. The results represented the effectiveness of all essential oils on the studied bacteria to varying degrees, except the clove oil, which doesn't show any inhibitory effect on *E.coli* and *S.epidermidis*. In contrast, cinnamon oil had the most inhibiting impact on all the bacteria studied. While garlic and ginger oil showed the lowest Inhibitory, thyme oil showed a strong inhibitory effect on *E.coli* and a moderate effect on other studied bacteria. Also, the results showed the synergistic effect between most essential plant oils and most antibiotics against most bacterial strains. The antagonistic effect was between essential oils with a few studied antibiotics toward some bacterial strains.

Key words: Plant, essential oils, bacteria, the inhibitory effect.

Introduction

The essential oil has been used medically throughout history to treat various disease infections over a long period, such as skin treatment, burns, cancers and other diseases. The widespread interest in the use of essential oils has emerged in the modern with the emergence of the department of aromatherapy as an alternative medicine based on other compounds and oil that has shown good treatment effects, The emergence of bacterial resistance to conventional antibiotics and drugs have led other researchers to search for alternative therapeutic biocidal Sources against different pathogenic bacteria[1].

The antimicrobial activity of essential oils (Eos) has been known through research and tested in vitro towards a wide range of pathogens; these oils are secondary metabolites enriched in chemical compounds[2,3]. It has been used recently in food preservation and treatment for types of cancers[4-7]. The main components of (essential oils) are phenolics, alcoholics, hydrocarbons, aldehydes and ketones which are answerable for medicinal plant biological activities. The cell membrane of bacterial cells is the main target of the mechanism oils[8,9]. Medicinal plants and their oils were used in folk medicine. Naturally, essential oils play a significant role in producing plants against pathogens. The essential oils contain secondary metabolic substances that can inhibit and kill many bacteria, yeasts and molds. The bacterial cell membrane is the main target for making these oils and other targets in bacteria[10]. The inhibitory efficacy of essential oils against pathogenic pathogens has been investigated because of the emergence of multiple resistances to these pathogens to conventional antibiotics, which is a significant problem in treating many bacterial diseases[11].

People in various parts of the world have historically used ginger, thyme, clove, cinnamon and garlic for various purposes, so the purpose of this research is to examine in vitro behavior of the oils toward two Gram-negative bacterial strains and two Gram-positive bacterial strains and study a mixing of such essential oils and standard antibiotics in vitro action.

Materials and methods

Essential Oils

Five essential oils were collected from local markets equipped by the Itimad Company, Iraq (Table 1). Such oils have been selected based on survey literature and used for medical purposes.

Local name	Name Botanical
Thyme	*Thumus vulgaris*
Clove	*Syzygium aromaticum*
Cinnamon	*Cinnamomum Cassia*
Ginger oil	*Zingiberofficinableg*
Garlic oil	*Allium sativum*

Table 1. Essential oils used in this study.

Bacteria isolates

Two types of Gram-negative bacteria (*Escherichia coli, Proteus spp.*), and two types of Gram-positive bacteria (*Staphylococcus epidermidis, Staphylococcus aureus*). These isolates were obtained as pure identifiable isolates from the biology department/college of science/ Mosul University. The bacteria cultures were stored at 4 ° C in their appropriate agar slants and used as stock cultures throughout the study. Mueller Hinton agar (MHA).

2

Antibiotics

Five disks of antibiotics were used-manufactured by *Bioanalyses* (Turkey). Amoxicillin Clavulanic acid(AMC 30µg), Ceftriaxone (CTX 30µg), Trimethoprim- Sulphamethoxazole (SXT 25µg), Gentamicin (CN 10µg) and Ciprofloxacin(CIP 10µg).

The Antibiotics sensitivity test

Antibiotics sensitivity test against studied bacterial isolates was conducted according to the modified method of Kirby-Bauer[12].

Antibacterial activity of Essential oils Test

The method of diffusion of discs was used in this research. An overnight culture has been calibrated to 0.5 McFarland requirements 10^8 CFU/ml for each microbial strain. Five hundred µL suspensions were spread out Mueller-Hinton agar (MHA) plates. With aseptic conditions, 10 µL of essential oil was impregnated with empty sterilized filter paper disks (6 mm diameter) of five types and placed on the surface of the agar. For 18-24h, the inoculated plaques were incubated at 37 ° C. Antimicrobial activity was measured against the test species by calculating the inhibition zone (mm). Every assay has been repeated 2 times[13].

Results and discussion

The Antibiotics sensitivity test

The results of the sensitivity of the (*E.coli, Proteus spp., S.aureus, and S.epidermidis*) to a group of antibiotics were shown in Table 2 and Figure 1 (A-D), where contrasts between these isolates can be noticed in the manner of their resistance to antibiotics.

The antiprogram of different isolates showed that all tested isolates were sensitive toward the selected standard antibiotics; the antibiotic sensitivity test was performed to compare the antibacterial activities of tested essential oils with the inhibitory action of antibiotics.

Antibacterial activity of Essential oils

Antibacterial activities of five "essential oils" toward four bacterial species are shown in Table 3.

These results showed that the oil of cinnamon exhibits superior antibacterial activity toward all bacteria, with inhibition zones (12 to 25 mm). This demonstrated the highest antibacterial activities in *E.coli* (25 mm), and the lowest inhibition effect observed in both *S.epidermidis* (12 mm), as shown in Figure 2 (A-D). Depending on the susceptibility of the bacteria studied, clove oil produced an inhibition zone toward *E.coli* and *S.aureus* only (12mm, 7mm), respectively, as shown in Figure 2 (A-D). In contrast, the location of inhibition produced by garlic and ginger essential oils varies from (8mm to 12mm). For garlic oil, the lowest inhibitory zone was observed against *S.epidermidis* (8mm), but the lowest inhibitory area was *E.coli* and *S.aureus* (12 mm), as shown in figures(B 1-4); for ginger oil, the lowest inhibitory zone was observed against *S.aureus* (8mm), but the top inhibitory zone was showed toward *E.coli*, and *S.epidermidis* (12mm) as shown in Figure 2 (A-D) and the inhibition zone of essential oil Thyme produced differs from (8mm to 20mm). The minimal inhibition zone was observed against *Proteus spp.* and *S.aureus* (8mm). In comparison, the optimum inhibition zone was for E.coli (20 mm) as shown in Figure 2 (A-D).

In vitro experiments in this study have shown that the essential oils of Ginger, Clove, Thyme, Cinnamon and Garlic show antibacterial activity toward the studied bacteria, but their activities varied. Many studies on the antimicrobial activity of plant compounds toward various types of microbes have been released, including food pathogthese[14] Clove and Thyme oils demonstrated solid antibacterial activity with inhibition zones at (8-20mm) and (7-12mm).
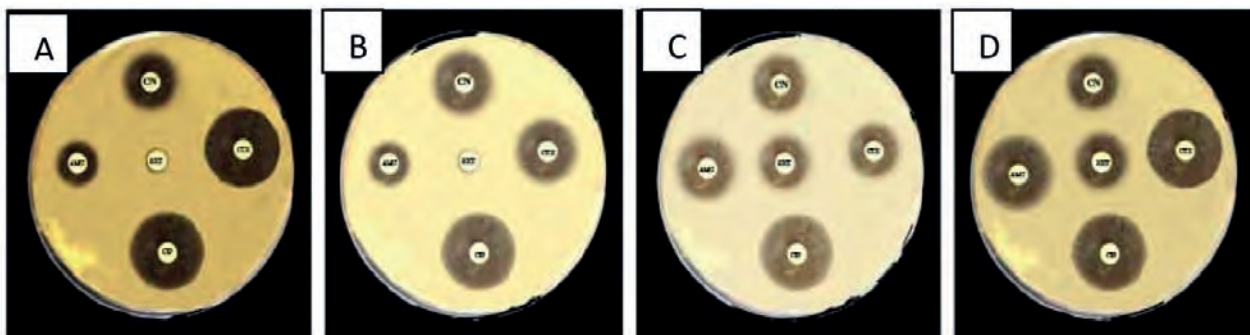
Figure 1. Results of antibiotic sensitivity test. *(A): E.coli; (B): proteus spp. (C) S.epidermidis; (D) S.aureus).*

Bacteria	CN (10) µg	SXT (25) µg	CTX(30)	CIP(10) µg	AMC(30) µg
E. coli	15	-	23	23	10
Proteus spp.	20	-	20	25	10
S.epidermidis	15	15	20	23	20
S.aureus	15	18	15	25	20

(-): NO Inhibitory effect

Table 2. Result of the standard antibiotics sensitivity test against the bacterial isolates, inhibition zones in mm.

Bacteria	Clove	Thyme	Cinnamon	Garlic	Ginger
E. coli	-	20	25	12	12
Proteus spp.	12	8	14	10	10
S.epidermidis	-	12	12	8	8
S.aureus	7	8	15	12	12

(-): NO Inhibitory effect

Table 3. Antibacterial activities of "essential oils" (10µl / disc) toward bacterial strains.
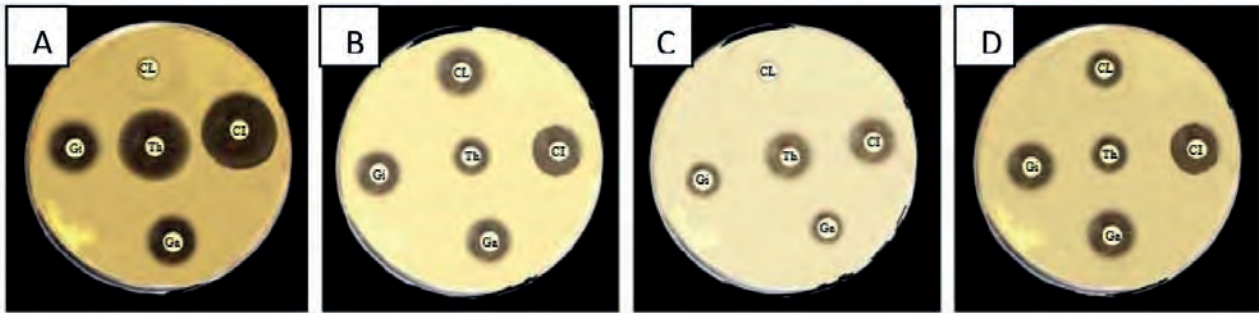
Figure 2. Antibacterial activity of five tested Essential oils. (Th-Thyme, Cl-Clove, Ci-Cinnamon, Gi-Ginger, Ga-Garlic). *(A): E.coli; (B): proteus spp. (C) S.epidermidis; (D): S.aureus.*

Accordingly, such results consent with[15] Clove oil is active against foodborne "Gram-positive" bacteria (*Bacillus cereus, Staphylococcus aureus, Enterococcus faecalis and Listeria monocytogenes*). And "Gram-negative" bacteria (*P.aeruginosa, E.coli, Yersinia enterocolitica, Salmonella choleraesuis*). And Clove oil had the highest activity with a measured inhibition zone (23.7 mm) towards *V.cholerae*[16,17] the essential thyme oil was reported to have better activity against E.coli. Toward results were in agreement with the results of (18), which indicated that essential oil of thyme exhibited higher activity against *S.aureus* (20.1 mm), *B.subtilis*, and *S.aureus* (Gram-positive bacteria) and were much more sensitive than Gram-negative bacteria to the essential oils. The combined effect of the compounds results in the antimicrobial activities of essential oils.

The "antimicrobial activity" of essential oil of thyme and thymol was assessed in other tests, like (19), where the substantial activity of thyme toward *E.coli* and *Salmonella spp.* has been documented. An essential thyme oil antimicrobial effect was also recorded toward *E.coli* and other foodborne bacteria[20].

The cinnamon essential oil has shown the best antibacterial activity toward whole bacterial species studied; these results are by (21), in which cinnamon oil exhibited potent activity against bacterial strains selected. And the other side, multiple studies showed that cinnamon and clove oils have precise and reliable effects on different pathogens and bacteria[22].

Several studies have shown that oils' activity can be attributed to their hydrophobicity as a feature of "essential oils" and their components, which allow them to separate bacterial cell membrane lipids, challenge the cell well structures and make them more permeable[23]. And the exit of critical ions and molecules will lead to death[24].

Aromatogram test for combinations of essential oils with antibiotics

Applying Cinnamon oil with all standard antibiotics tested, the antimicrobial activity of all antibiotics increased against the four bacterial strains tested, as shown in Table 4 and Figures 3 (A-D).

The application of thyme with all standard antibiotics tested led to enhance the antibacterial activities of these antibiotics, except the combination with (AMC and SXT) resulted in a decrease in the inhibition zone exerted by the antibiotics when used alone against *S.epidermidis* as shown in Table 5 and Figures 4 (A-D). Toroglu said combining basic Thyme oil and standard in vitro antibiotics resulted in an

**Figure 3.** (A): Inhibitory activity of Combination between cinnamon oil with tested antibiotics against *E.coli*. (B): Inhibitory activity of Combination between cinnamon oil with tested antibiotics against *proteus spp.* (C): Inhibitory activity of Combination between cinnamon oil with tested antibiotics against *S.epidermidis*. (D): Inhibitory activity of Combination between cinnamon oil with tested antibiotics against *S.aureus*.

Bacteria	Essential oil	Standard antibiotic discs					Standard antibiotic discs with essential oil				
		CN	SXT	CTX	CIP	AMC	CN	SXT	CTX	CIP	AMC
E. coli	25	15	-	23	23	10	25	20	25	25	25
Proteus spp.	14	20	-	20	25	10	25	25	25	25	25
S.epidermidis	12	15	15	20	23	20	25	22	25	30	20
S.aureus	15	15	18	15	25	20	18	20	30	30	20

(-): NO Inhibitory effect

Table 4. The antibacterial activities (inhibition zones) of Cinnamon essential oil and its synergistic with antibiotic effects.

Figure 4. (A) Inhibitory activity of Combination between Thyme oil with tested antibiotics against *E.coli*. (B) Inhibitory activity of Combination between Thyme oil with tested antibiotics against *proteus spp*. (C): Inhibitory activity of Combination between Thyme oil with tested antibiotics against *S.epidermidis*. (D): Inhibitory activity of Combination between Thyme oil with tested antibiotics against *S.aureus.*

Bacteria	Essential oil	Standard antibiotic discs					Standard antibiotic discs with essential oil				
		CN	SXT	CTX	CIP	AMC	CN	SXT	CTX	CIP	AMC
E. coli	20	15	-	23	23	10	20	17	23	30	15
Proteus spp.	8	20	-	20	25	10	22	20	22	30	15
S.epidermidis	12	15	15	20	23	20	15	9	25	30	12
S.aureus	8	15	18	15	25	20	25	25	25	25	25

(-): NO Inhibitory effect

Table 5. The antimicrobial activities (inhibition zones) of Thyme essential oil and its synergistic with antibiotic effects. Mm antagonistic effect on bacteria[25].

Applying Ginger oil with all tested standard antibiotics led to the antagonistic effect of these antibiotics against all bacteria tested except the combination of (SXT) against *E. coli, Proteus spp.* , and (CTX) against *S.epidermidis , S.aureus* . And (AMC) against *Proteus spp.*, and (CN) against *S.aureus*, which led to a synergistic effect as shown in Table 6 Figure 5 (A-D).

The combination of Garlic oil with all tested standard antibiotics resulted in a synergistic effect against all tested bacteria except the case of applying this oil with (CXT) against *E.coli, Proteus spp.*, which led to a decrease in the antimicrobial activity of this antibiotic compared when used as alone, also antagonistic effect occurred with (SXT) against the *S.epidermidis* as shown in Table 7 Figure 6 (A-D).

Applying Clove oil with all tested standard antibiotics resulted in a synergistic effect with most antibiotics against most tested bacteria except in the case of applying this oil with (SXT, AMC) against *S.epidermidis* only, as shown in Table 8 and Figure 7 (A-D).

Figure 5. (A): Inhibitory activity of Combination between Ginger oil with tested antibiotics against *E.coli*. (B): Inhibitory activity of Combination between Ginger oil with tested antibiotics against *proteus spp*. (C): Inhibitory activity of Combination between Ginger oil with tested antibiotics against *S.epidermidis*. (D): Inhibitory activity of Combination between Ginger oil with tested antibiotics against *S.aureus.*

Bacteria	Essential oil	Standard antibiotic discs					Standard antibiotic discs with essential oil				
		CN	SXT	CTX	CIP	AMC	CN	SXT	CTX	CIP	AMC
E. coli	12	15	-	23	23	10	14	8	18	20	7
Proteus spp.	10	20	-	20	25	10	16	11	11	22	10
S.epidermidis	12	15	15	20	23	20	13	8	20	16	9
S.aureus	8	15	18	15	25	20	16	9	18	23	9

(-): NO Inhibitory effect

Table 6. The antimicrobial activities (inhibition zones) of ginger essential oil and its synergistic with antibiotic effects. Mm
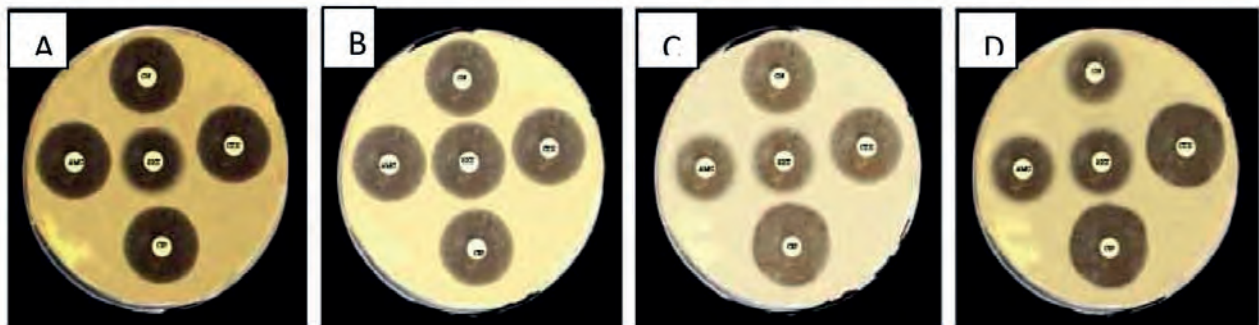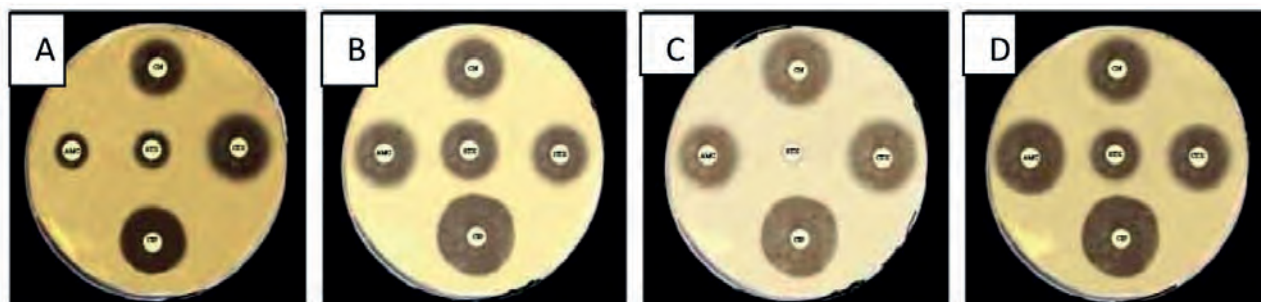
Figure 6. (A) Inhibitory activity of Combination between Garlic oil with tested antibiotics against *E.coli.* (B) Inhibitory activity of Combination between Garlic oil with tested antibiotics against *proteus spp.* (C) Inhibitory activity of Combination between Garlic oil with tested antibiotics against *S.epidermidis.* (D)Inhibitory activity of Combination between Garlic oil with tested antibiotics against *S.aureus.*

Bacteria	Essential oil	Standard antibiotic discs					Standard antibiotic discs with essential oil				
		CN	SXT	CTX	CIP	AMC	CN	SXT	CTX	CIP	AMC
E. coli	12	15	-	23	23	10	15	8	18	25	10
Proteus spp.	10	20	-	20	25	10	22	21	15	28	18
S.epidermidis	8	15	15	20	23	20	26	-	26	30	23
S.aureus	12	15	18	15	25	20	18	15	18	27	25

Table 7. The antimicrobial activities (inhibition zones) of essential garlic oil and its synergistic with antibiotic effects. Mm
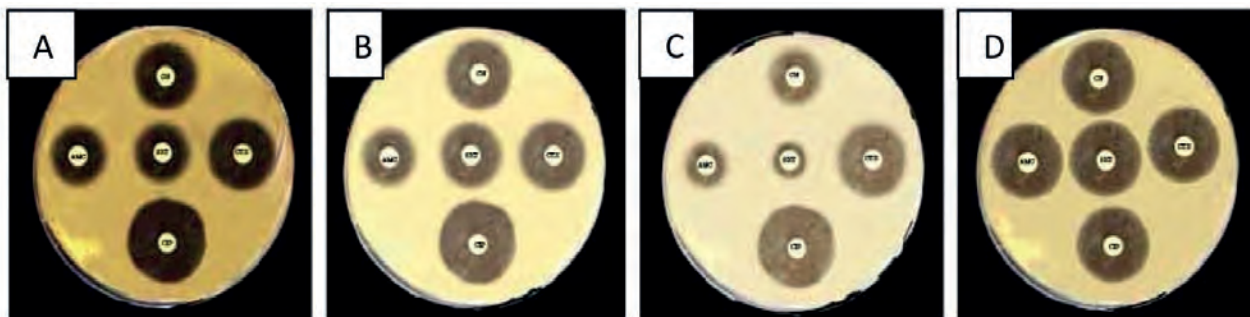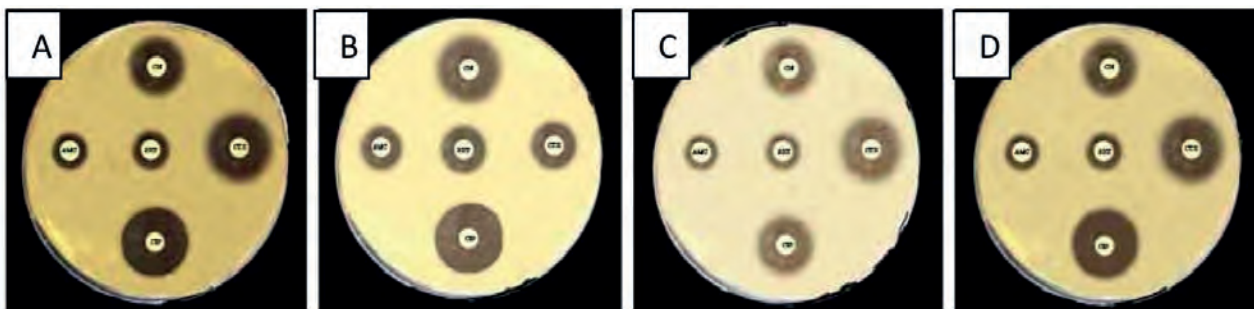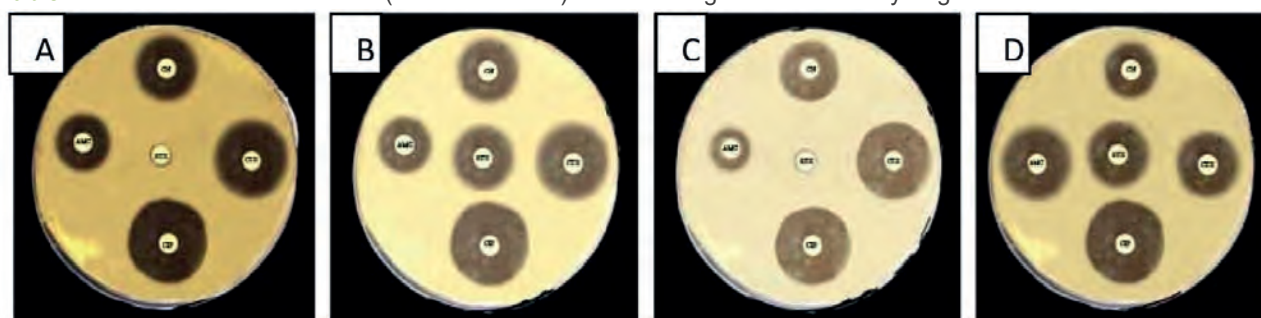

Figure 7. (A): Inhibitory activity of Combination between Ginger oil with tested antibiotics against *E.coli.* (B): Inhibitory activity of Combination between Ginger oil with tested antibiotics against *proteus spp.* (C): Inhibitory activity of Combination between Ginger oil with tested antibiotics against *S.epidermidis.* (D): Inhibitory activity of Combination between Ginger oil with tested antibiotics against *S.aureus.*

Bacteria	Essential oil	Standard antibiotic discs					Standard antibiotic discs with essential oil				
		CN	SXT	CTX	CIP	AMC	CN	SXT	CTX	CIP	AMC
E. coli	-	15	-	23	23	10	20	-	25	30	15
Proteus spp.	12	20	-	20	25	10	22	22	23	30	15
S.epidermidis	-	15	15	20	23	20	16	-	24	23	11
S.aureus	7	15	18	15	25	20	15	20	20	30	25

Table 8. The antimicrobial activities (inhibition zones) of Clove essential oil and its synergistic with antibiotic effects. Mm

Conclusions

The study shows that combining "essential oils" from these medicinal plants with traditional antibiotics has considerable potential for producing and eliminating new antimicrobial treatments for many microorganism-caused diseases. Based on the results obtained, the essential oils function with the standard antibiotics studied. This collaboration could result in new treatment options for infectious diseases and increasing drug resistance. More molecular-based studies of synergistic interaction are required to understand the synergistic mechanism, which is fundamental to ggggggggg pharmacological agents for treating bacterial infections using medicinal plants. The research will also focus on finding medicinal plants with synergistic activity in that direction.

Conflicts of Interest

The authors declare that there is no conflict of interest.

Author Contributions

All authors contributed equally to this work.

Funding

This is self-funding research.

Ethics Statement

Not applicable.

6

Bibliographic references

1. Abad. M, J, Ansuategui., M and Bermejo., P.(2007) .Active antifungal substances from natural sources.ARCHIVOC; 2007, 116–145.
2. Kalemba., D, and Kunicka. A. (2003) .Antibacterial and antifungal properties of essential oils. Current Medicinal Chemistry, 10: 813–829.
3. Al-Bayati, F. (2009). Isolation and identification of antimicrobial compound from menthe longifolia l, leaves grown wild in Iraq. Annals of clinical microbiology and antimicrobials 8:20.
4. Faid., M, Bakhy., K, Anchad., M, Tantaoui-Elaraki., AandAlomondpaste.,A.(1995).Physicochemical and microbiological characterizations and preservation with sorbic acid and cinnamon Food Prod 1995; 58:547-550.
5. Buttner., M,P, Willeke., K, Grinshpun., S,A.(1996) Sampling and analysis of airborne microorganisms. In Manual of Environmental Microbiology Edited by: Hurst CJ, Knudsen GR, McInerney MJ, Stetzenbach LD, Walter MV. ASM Press: Washington, DC: 629-640.
6. Van de Braak., S, A, A, J and Leijten. G,C,J,J. Essential Oils and Oleoresins: A Survey in the Netherlands and other Major Markets in the European Union. CBI, Centre for the Promotion of Imports from Developing Countries, Rotterdam. 1999: 116.
7. Sylvestre., M, Pichette.,A, Longtin., A, Nagau.,F.andLegault., J.(2006).Essential oil analysis and anticancer activity of leaf essential oil of Croton flavens L. from Guadeloupe.J Ethnopharmacol; 103:99-102.
8. Di Pasqua., R, Betts., G, Hoskins., N, Edwards., M, Ercolini., D andMauriello., G. (2007).Membrane toxicity of antimicrobial compounds from essential oils.Journal of Agricultural and Food Chemistry; 55, 4863–4870.
9. Mahmood, M. A., & Essa, M. A. (2021). Antimicrobial activity of peptides extracted from camels' blood neutrophils against some pathogenic bacteria. Iraqi Journal of Veterinary Sciences, 35(1), 33-37.
10. Nazzaro., F.; Fratianni. F, De Martino., L, Coppola R and De Feo. , V (2013). Effect of Essential Oils on Pathogenic Bacteria, Pharmaceuticals, 6;1451-1474
11. Andradea.,B, F ,M,Barbosaa., L ,N,Probsta I da &Júniora.,A. F .(2014)Journal of Essential Oil Research 26:1, 34-40 .
12. Clinical and Laboratory Standards Institute/National Comitee for clinical Laboratory Standards (CLSI/ NCCLS). (2012). In: Performance Standards for Antimicrobial Susceptibility Testing; Fifteenth Information Supplement. CLSI/NCCLS document M 100–S15. Wayne, PA,
13. Oulkheir .,S, Aghrouch.,M , El Mourabit.,F, Dalha.,F, Graich.,H , Amouch.,F, Ouzaid.,K, Moukale., A and S. Chadli.(2017). Antibacterial Activity of Essential Oils Extracts from Cinnamon, Thyme, Clove and Geranium Against a Gram Negative and Gram Positive Pathogenic Bacteria. Journal of Diseases and Medicinal Plants; 3(2-1): 1-5
14. Friedman., M, Henika., R,P, Mandrell., E,R.(2002).Bactericidal activities of plant essential oils and some of their isolated constituents against Campylobacter jejuni, Escherichia coli, Listeria monocytogenes, and Salmonella enterica.J. Food Protect. 65:1545-1560.
15. Lopez., P, Sanchez. Batlle., R, Nerin., C .(2005). Solid- and Vapor-phase antimicrobial activities of six essential oils: susceptibility of selected food borne bacterial and fungal strains. J. Agric. Food Chem., 53 (17): 6939-6946.
16. Sabahat., S and Perween., T. (2008). In vitro antibacterial activity of Clove against Gram negative bacterial Pak. J. Bot.; 40(5): 2157-2160.
17. Deise., F,S, Francielli., P,K,J, Régis., A, Z, Karine., B, S, Andressa., F and Leadir., L,M, F.(2014).Antimicrobial Activity of the Essential Oil of Thyme and of Thymol against Escherichia coli Strains.Acta Scientiae Veterinariae.; 42: 1234
18. Bosnić., T, Softić., D, and Grujić-Vasić. J, (2006). Antimicrobial Activity of Some Essential Oils and Major Constituents of Essential Oils.Acta MedicaAcademica ;35:19-22 .
19. Ivanovic., J, Misic., D, Zizovic., I and Ristic., M.(2012) In vitro control of multiplication of some food-associated bacteria by thyme, rosemary and sage isolates. Food Control. 25(1): 110116.
20. Silva N, Alves S, Gonçalves A, Amaral JS, Poeta P. (2013). Antimicrobial activity of essential oils from Mediterranean aromatic plants against several foodborne and spoilage bacteria. Food Science and Technology International. 19(6): 503-510.
21. Rabuseenivasan., S, Jayakumar. M and Ignacimuthu.,S. (2006) In vitro antibacterial activity of some plant essential oils. BMC Complementary and Alternative Medicine, 6:39.
22. Matan., N, Rimkeeree., H, Mawson., A, J, Chompreeda., P, Haruthaithanasan., V and Parker M.(2006) Antimicrobial activity of cinnamon and clove oils under modified atmosphere conditions. Into J Food Microbial; 107:180-185.
23. Sikkema., J., de Bont, J.A.M. and Poolman, B. (1994) Interactions of Cyclic Hydrocarbons with Biological Membranes. Journal of Biological Chemistry, 269, 8022-8028.
24. Denyer., S.P (1995) Mechanisms of action of antibacterial biocides international-biodeterioration-and-biodegradation Volume 36 Issues 3–4 Pages 195-475
25. Toroglu.,S.(2007). In vitro antimicrobial activity and antagonistic effect of essential oils from plant species.J.Environ Biol.;28:551-9

ARTICLE / INVESTIGACIÓN

Evaluation of serum Interleukin 36 in Iraqi patients with Rheumatoid arthritis

Wafaa Talib Mohammed[1]*, Alia Essam Mahmood Alubadi[1], Mohammed Hadi Munshed Alosami[2]   DOI. 10.21931/RB/2023.08.01.53

[1] Department of Biology, College of Science, Mustansiriyah University, Baghdad, Iraq.
[2] College of Medicine, University of Baghdad, Baghdad, Iraq.
Corresponding author: wafaatialp@yahoo.com

Abstract: Rheumatoid arthritis is a worldwide inflammatory chronic autoimmune disease with varying severity. Due to no definitive cure for this disease, current therapies aim to decrease the pain and slow further damage. The interleukin (IL)□36 cytokine was little known for its role in rheumatoid arthritis; this research aimed to evaluate the serum IL36 levels in RA patients compared to healthy controls. This study included 80 patients with rheumatoid arthritis registered at the Rheumatology Clinic in Baghdad teaching hospital. The patients were divided into three groups based on the treatments received. Group 1 included patients treated with biological therapy (etanercept, adalimumab), Group2 patients with non-biological treatment (methotrexate hydroxychloroquine and prednisone), Group3 patients without any treatment and compared with Group 4 healthy control group. Patients is all groups were assessed for their serum IL-36 concentration; the mean IL-36 serum level was significantly higher in three groups of RA patients which include the group of patients treated with biological therapy (Enbrel (etanercept) and Humira (adalimumab) means were (1132.41±475.2,), and group of non-biological therapy patients (Methotrexate hydroxychloroquine and prednisone) (G2) means was 553.95±307, than patients' group without any treatment (G3) means was 1044.01±575.3 compared to the control (341.38±113.1) p-value> 0.00001. The patient's age and BMI were not significantly different between three groups of patient Rheumatoid arthritis. Parameters for this disease also were tested which include RF, CRP, ESR, anti-CCP and disease activity score-28 (DAS 28), there were significant differences when compared with the control group. IL-36 serum level was significantly higher in three groups of rheumatoid arthritis than those in controls, and when compared between three patients groups there was less concentration in the non-biological therapy treatment group means was 553.95±307 than in the rest of the patient groups,biology tratment, without any treatment, means were (1132.41±475.2, 1044.01±575.3) respectively. This study found that Rheumatoid arthritis patients' serum IL36 levels increased, where a non-biologic therapies reduced this cytokine. IL-36's pathogenic involvement in Rheumatoid arthritis needs more study.

Key words: Rheumatoid arthritis, IL-36, IL-1,C-reactive protein, RF, ESR and anti-CCP.

Introduction

Rheumatoid arthritis (RA) is a worldwide inflammatory chronic autoimmune disease with varying severity, and due to no definitive cure for this disease, the goals of current therapies are to decrease the pain and slow further damage[1]. Rheumatoid arthritis affects small joints after that, larger joints, finally leading the tendons and ligaments weaken, and the cartilage and bone of joints are distortion and erosion which cause severe pain for a patient, and affects on heart, kidneys, lungs skin, and eyes[2]. Commonly autoimmune diseases are characterized by an excessive immune response and cause deterioration of specific or multiple tissues and organs[3], and generally believed that cytokines implicated in each phase of the pathogenesis of RA, such as IL-18, IL-17, IL-16, IL-12, IL-10, IL-8, IL-7, IL-6, IL-1, IFN-gamma, etc[4]. Interleukin 36 is an inflammatory cytokine, a member of the IL1 family, composed of agonists IL36α, IL36β, IL36γ, antagonist IL-36 receptor IL36Ra and accessory protein (IL-1RAcP)[5], chromosome 2 carries the genes of the IL-36 family[6], expressed and act on the barrier sites of the body on a variety of cells including epithelial (synoviocytes, keratinocytes, and skin, lung, and gut cells) and immune cells (T lymphocytes, antigen-presenting cells)[7]. IL-36 cytokines are regulated immune responses in a specific tissue; the upregulation of IL36 through CD80, CD86, MHCII of dendritic cells induces the production of several proinflammatory cytokines[3] such asIL-L1β, IL6, IL8, IL17, and TNFα and IFNγ in the pathogenesis of inflammatory diseases, in lung tissue, joint synovium (arthritis), colonic mucosa tissues (bowel diseases)and skin lesion[8] and may have diagnostic and/or therapeutic relations with inflammatory diseases[7]. In RA patients, IL-36α, IL-36R, and IL-36Ra were detected in the synovial tissues and may be correlated with its pathogenesis[6,8]. In the synovium of RA patients, IL-36α, IL-36β, IL-36γ, and IL-36Ra are correlated and upregulated with the expression of IL-1β, Chemokine ligand 3, Chemokine ligands 4 and Macrophage colony-stimulating factor[8], detected the IL-36 cytokines in the synovium of RA patients which induce production of proinflammatory mediators by synovial fibroblasts. Still, there were no effects when the blockade of IL-36 receptors in the arthritis of mouse models the production of proinflammatory mediators by synovial fibroblasts[9]. Found the circulating IL-36 levels were significantly higher among Juvenile Idiopathic Arthritis children10. The present study examined the serum concentration of IL-36 in rheumatoid arthritis patients.

Wafaa Talib Mohammed, Alia Essam Mahmood Alubadi, Mohammed Hadi Munshed Alosami

2

Materials and methods

All serum samples of 80 rheumatoid arthritis patients (11 males and 69 females) who attended the Rheumatology Clinic in Baghdad teaching hospital and diagnosis was under the supervision of Dr. Muhammad Hadi Al-Assami, Consultant Rheumatologist, according to the revised American College of Rheumatology 2010 criteria, based on 4 factors which are the distribution of affected joints number tender joint and swollen, Serology test results rheumatoid factor (RF), anti-cyclic citrullinated protein antibody (ACCP), Acute-phase reactant test results(such as ESR, CRP etc.), the duration of symptoms, the score >6weak constitutes a classification of RA

Clinicians used criteria to diagnose rheumatoid arthritis. Presence of at least one clinical tumor in the participant), up to three points are assigned depending[11]; it was done by the consultant medical staff at the clinic, in addition to using the kits for laboratory tests to confirm the presence of arthritis such as anti-cyclic citrullinated peptide antibodies (anti-CCP) kit (commercially available kits by indirect enzyme-linked immunosorbent assay MyBioSource, USA), rheumatoid factor (RF) and C-reactive protein (CRP) kits (latex slide agglutination tests by Agappe Diagnostics Switzerland GmbH for semi-quantitative detection). The serum concentrations of IL-36 were measured by using the Competitive ELISA kit (MyBioSource, USA, sensitivity = 1.0 ng/ml)) according to the manufacturer's instructions.

Disease Activity Score were measured based on the estimation of 28 of joints (DAS28) with the number of swollen joints and erythrocyte sedimentation rate (ESR)(by the Westergren method), and it was calculated using the following equation:

DAS 28 = 0.56 × √(tender 28 joint count) + 0.28 × √(swollen 28 joint counts) + 0.70 × ln(erythrocyte sedimentation rate (ESR), mm/hr) + 0.014 × general health[12-14],

after obtaining all patients' data, patients were categorized into patients treated with biological treatment(Enbrel (etanercept) and Humira (adalimumab)G1(38), non-biological treatment (Methotrexate hydroxychloroquine and prednisone) G2 (26), and without treatment G3 (16), also patients identified 2 specific groups: first, patients with positive anti-CCP test and second, patients who had the negative anti-CCP test. While 36 healthy control group G4 individuals were selected according to strict conditions, they didn't suffer from any disease symptoms and were negative for CRP, RF, ESR and anti-CCP tests.

Patients and control individuals were obtained under the Ministry of Health and Mustansiriyah University approved protocols, informed consent was obtained from the ministry of health, and a written all participants acceptance.

Statistical analysis

The statistical analyses were performed using the SPSS 20 (2022))Statistical Package For the Social Sciences, also known as IBM SPSS Statistics) analysis of variance (ANOVA) test to compare various groups with each other for numerical variables, which were expressed as mean + standard error (SE), and the LSD test was used to calculate the significant differences between the tested mean, the letters (A, B, C, and D for column and a, b, c and d rows) represented the levels of significant, highly significant start from the letter (A or a) and decreasing with the last one. Similar letters mean no significant differences between the tested mean; all data showed normal distribution using the Shapiro-Wilk test. The categorical variables were expressed as a percentage and used chi-square tests of goodness of fit and independence.

Results

The demographic and clinical features of the 80 patients with rheumatoid arthritis included in this study are displayed in Table 1 according to the above-mentioned division in the materials and methods. There were no significant differences observed in the age at sample collection between the patients with RA and the healthy control group (P > .05). The mean age of the three patient groups: treated with the biological treatment group was 43.8±2.3, the non-biological treatment group was 46.1±2.2, and the non-treatment group was 40.3±3.2 and36 healthy controls with a mean age of 46.7±2.9 years (Table 1).

The selection of patients, according to what was mentioned in the materials and methods, from patients who visit a specialized center for rheumatic diseases and who were diagnosed according to the revised American College of Rheumatology 2010 criteria by specialists and the general parameters for this disease also were tested which include RF, CRP, ESR, anti-CCP and disease activity score-28 (DAS 28), and there were significant differences when compared with the control group because the latter was chosen with great caution table 2. It excluded anyone who gave a positive result to any of those above to confirm that the control group members were free from RA table 2.

The mean IL-36 serum level was significantly higher in three groups of RA patients which include the group of patients treated with biological therapy (Enbrel (etanercept) and Humira (adalimumab)) (G1), the group of non-biological therapy patients (Methotrexate hydroxychloroquine and prednisone) (G2), and the patients' group without any treatment (G3) (1132.41±475.2, 553.95±307, 1044.01±575.3) respectively, compared to the control (341.38±113.1), (Fig. 1).

Variables	G1	G2	G3	G4	P value
Age(Mean±SD)	3.8±2.3	46.1±2.2	40.3±3.2	46.7±2.9	NS
Total patient	38	26	16	36	
Female	31	24	14	18	0.0008
Male	7	2	2	18	
Sex M/F	4/1	12/1	7/1	1/1	

G1) patients treated with biological treatment (38), (G2) patients with non-biological treatment (26), (G3) patients without any treatment (16), and (G4) control group (36). P value < 0.05* is significant, while P value < 0.01** is highly substantial and NS not significant.

Table 1. Demographic characteristics of RA patients and healthy controls.

Variables	G1	G2	G3	G4	
Anti-CCP	0.34±0.05	0.23±0.05	0.48±0.09	0.12±0.004	0.009
ESR	40.2±4.4	41.3±3.5	41.1±6.1	15.2±1.2	0.0004
DAS 28	4.9±0.09	5.06±0.07	4.42±0.13	0	0.0006**
CRP Positive (No.)	19	16	10	0	0.0002** (chi square= 19.86)
Positive RF(No.)	17	7	8	0	0.004** (chi-square =13.83)
IL-36	1132.41±475.2	553.95±307	1044.01±575.3	341.38±113.1	0.00001**

(G1) patients treated with biological treatment (38), (G2) patients with non-biological treatment (26), (G3) patients without any treatment (16), and (G4) control group(36), CRP: C-Reactive Protein; Anti-CCP antibody: Anti-cyclic Citrullinated Peptide Antibody, RF: Rheumatoid Factor, ESR: Erythrocyte Sedimentation Rate, and DAS 28. P value < 0.05* is significant, while P value < 0.01** is highly significant, and NS not significant

Table 2. Laboratory characteristics of the rheumatoid arthritis.
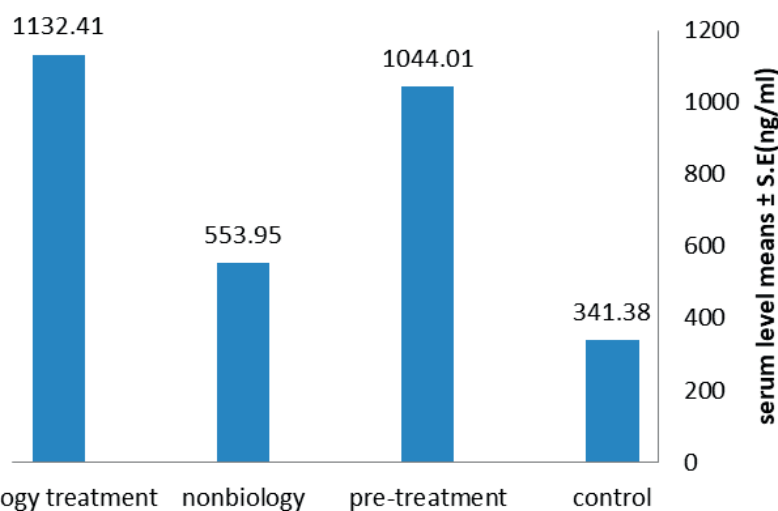
Figure 1. Distribution of serum levels IL 36 in three patients versus controlIL-36 concentration in the studied groups; patients treated with biological treatment, non-biological treatment, pre-treatment, and control group.

Discussion

There were significant differences between patients with rheumatoid arthritis and normal controls in terms of sex (Table I); the ratio of female to male was 6:1 in this study, and in general, according to previous studies, women are about three times more likely to suffer from this disease, and the effect of the disease is also different between the two sexes, and this may be due to physiological differences between the sexes, such as the difference in hormonal content, the difference in behavior, and the role of genes and heredity[15,16]. RA can be triggered by the production of autoantibodies (anti-citrullinated protein antibodies ACPA) against citrullinated peptides which are distributed throughout the whole body that activate MHC class II-dependent T cells that induce B cells to produce more ACPA[17]. The mean IL-36 serum level was significantly higher in three groups of RA patients, these results are in line with a previous study, soon published, where it was found that interleukin-36 increases in patients with Juvenile Idiopathic Arthritis[10], High levels of interleukin36 were observed in patients and mouse models with osteoarthritis through joint destruction and found that transforming growth factor-beta (TGF-β) receptor type 2 signaling dampened IL-36 signaling in healthy joints[18], found that IL-36 upregulated in the synovial tissue of patients with RA and they added that particularly linked to the inflammatory processes in the synovial tissue throu-

gh promotes the expression of proinflammatory cytokines[19], this confirmed by found that the serum IL-36 higher in SLE patients with arthritis than in those without arthritis[20], IL-36 acts as a proinflammatory by magnifying inflammatory responses and triggering further inflammatory mediators and causing excessive immune infiltration and tissue damage[21,22]. Also noted in table 1 interleukin-36 was less concentrated in the non-biological therapy (hydroxychloroquine and prednisone) treatment group (553.95±307) than the rest of the patient groups (1132.41±475.2, 1044.01±575.3) figure 1, (methotraxate ,prednisone) decreases inflammation and suppresses the immune system through binding with specific nuclear receptors and cause altered gene expression and inhibition of proinflammatory cytokine production[23] while hydroxychloroquine treatment prevents trained immunity Many causes depend on the severity of the disease, the stage of the disease , the effect of the treatment and the dose, the physiological factors, the age[24] and this confirmed recently by Devarajan and Vaseghi in their study that hydroxychloroquine impair host immunity in response to SARS-CoV-2[25] and that demonstrates this results.

According to previous articles, the uses of these two treatments lead to a decrease in the production of inflammatory cytokines; prednisone has a significant effect on inhibiting the immune response through its effect on immune cells and also can reduce the concentration of inflammatory cytokines[26] and hydroxychloroquine is an antimalarial drug

3

and, is now used as an immunomodulator agent for rheumatic autoimmune disorders, such as primary Sjögren's syndrome, systemic lupus erythematosus and rheumatoid arthritis through the inhibition of antigen presentation, B- and T-cell activation, NOX signaling and rebalances Treg/Th17 cell ratio and these effects on different immune cells cause decreased in production and release of proinflammatory cytokines[27,28].

Conclusions

This study demonstrated that RA patients displayed increasing in serum IL□36 and it was also found that non-biological treatments have a role in reducing this cytokine. Further studies are needed to explain a more detailed IL-36 pathogenic role in RA.

Abbreviations

Rheumatoid arthritis (RA), Anti-Cyclic Citrullinated Peptide antibodies (Anti-CCP), anti-citrullinated protein antibodies (ACPA), Disease active score (DAS 28), Cluster of Differentiation (CD), C-Reactive Protein (CRP), Interleukin (IL), Major Histocompatibility Complex (MHC), Rheumatoid factor (RF), erythrocyte sedimentation rate (ESR), Systemic Lupus Erythematosus (SLE), Intreleukin-1 receptor accessory protein (IL-1RAcP).

Funding

No fund received: for this article.

Informed consent to publish

Not applicable.

Ethical statements for human/animal experiments

The study was approved by institutional ethics committee "University of Mustansiriyah" and informed consent was obtained in written by each individual participants. Each participant was known about the study follow up before enrolling for the study.

Declaration of competing interest

The authors declare that they have no known competing financial interests or personal relationships that could have appeared to influence the work reported in this paper.

Acknowledgments

We thank Mustansiriyah University in Baghdad /Iraq) for its support to achievement this work.

Bibliographic references

1. Bullock J, Rizvi SA, Saleh AM, Ahmed SS, Do DP, Ansari RA, Ahmed J. Rheumatoid arthritis: a brief overview of the treatment. Medical Principles and Practice. 2018;27(6):501-507. https://doi.org/10.1159/000493390
2. Lee JE, Kim IJ, Cho MS, Lee J. A case of rheumatoid vasculitis involving hepatic artery in early rheumatoid arthritis. Journal of Korean medical science. 2017 Jul 1;32(7):1207-10.
3. Chen WJ, Yu X, Yuan XR, Chen BJ, Cai N, Zeng S, Sun YS, Li HW. The Role of IL-36 in the Pathophysiological Processes of Autoimmune Diseases. Frontiers in Pharmacology. 2021:2643..https://doi.org/10.3389/fphar.2021.727956
4. Burska A, Boissinot M, Ponchel F. Cytokines as biomarkers in rheumatoid arthritis. Mediators of inflammation. 2014 Mar 9;2014, 545493. https://doi.org/10.1155/2014/545493.
5. Zhou L, Todorovic V. Interleukin-36: structure, signaling and function. Protein Reviews. 2020:191-210.
6. Yuan ZC, Xu WD, Liu XY, Liu XY, Huang AF, Su LC. Biology of IL-36 signaling and its role in systemic inflammatory diseases. Frontiers in immunology. 2019:2532.
7. Buhl AL, Wenzel J. Interleukin-36 in infectious and inflammatory skin diseases. Frontiers in Immunology. 2019:1162.
8. Ding L, Wang X, Hong X, Lu L, Liu D. IL-36 cytokines in autoimmunity and inflammatory disease. Oncotarget. 2018 Jan 5;9(2):2895.
9. Schmitt V, Hahn M, Kästele V, Wagner O, Wiendl M, Derer A, Taddeo A, Hahne S, Radbruch A, Jäck HM, Schuh W. Interleukin□36 receptor mediates the crosstalk between plasma cells and synovial fibroblasts. European journal of immunology. 2017 Dec;47(12):2101-12.
10. Jamal QW, Alubaidi G, Humadi Y. Level of Interleukin-35, Interleukin-36, and the Interleukin-35/Interleukin-36 Ratio in Juvenile Idiopathic Arthritis. Open Access Macedonian Journal of Medical Sciences. 2021 Sep 2;9(A):741-7.
11. Aletaha D, Neogi T, Silman AJ, Funovits J, Felson DT, Bingham III CO, Birnbaum NS, Burmester GR, Bykerk VP, Cohen MD, Combe B. 2010 rheumatoid arthritis classification criteria: an American College of Rheumatology/European League Against Rheumatism collaborative initiative. Arthritis & rheumatism. 2010 Sep;62(9):2569-81.
12. Prevoo ML, Van'T Hof M, Kuper HH, Van Leeuwen MA, Van De Putte LB, Van Riel PL. Modified disease activity scores that include twenty□eight□joint counts development and validation in a prospective longitudinal study of patients with rheumatoid arthritis. Arthritis & Rheumatism: Official Journal of the American College of Rheumatology. 1995 Jan;38(1):44-8.
13. Balsa A, Carmona L, González-Alvaro I, Belmonte MA, Tena X, Sanmartí R, EMECAR Study Group. Value of Disease Activity Score 28 (DAS28) and DAS28-3 compared to American College of Rheumatology-defined remission in rheumatoid arthritis. The Journal of rheumatology. 2004 Jan 1;31(1):40-6.
14. Schmitt V, Hahn M, Kästele V, Wagner O, Wiendl M, Derer A, Taddeo A, Hahne S, Radbruch A, Jäck HM, Schuh W. Interleukin□36 receptor mediates the crosstalk between plasma cells and synovial fibroblasts. European journal of immunology. 2017 Dec;47(12):2101-12.
15. Nourisson C, Soubrier M, Mulliez A, Baillet A, Bardin T, Cantagrel A, Combe B, Dougados M, Flipo RM, Schaeverbeke T, Sibilia J. Impact of gender on the response and tolerance to abatacept in patients with rheumatoid arthritis: results from the 'ORA'registry. RMD open. 2017 Nov 1;3(2):e000515.
16. Intriago M, Maldonado G, Cárdenas J, Ríos C. Clinical characteristics in patients with rheumatoid arthritis: differences between genders. The Scientific World Journal. 2019 Jul 3;2019.
17. Guo Q, Wang Y, Xu D, Nossent J, Pavlos NJ, Xu J. Rheumatoid arthritis: pathological mechanisms and modern pharmacologic therapies. Bone research. 2018 Apr 27;6(1):1-4.
18. Li T, Chubinskaya S, Esposito A, Jin X, Tagliafierro L, Loeser R, Hakimiyan AA, Longobardi L, Ozkan H, Spagnoli A. TGF-β type 2 receptor–mediated modulation of the IL-36 family can be therapeutically targeted in osteoarthritis. Science translational medicine. 2019 May 8;11(491):eaan2585.
19. Frey S, Derer A, Messbacher ME, Baeten DL, Bugatti S, Montecucco C, Schett G, Hueber AJ. The novel cytokine interleukin-36α is expressed in psoriatic and rheumatoid arthritis synovium. Annals of the rheumatic diseases. 2013 Sep 1;72(9):1569-74.
20. Mai SZ, Li CJ, Xie XY, Xiong H, Xu M, Zeng FQ, Guo Q, Han YF. Increased serum IL-36α and IL-36γ levels in patients with systemic lupus erythematosus: association with disease activity and arthritis. International immunopharmacology. 2018 May 1;58:103-8.
21. Aoyagi T, Newstead MW, Zeng X, Nanjo Y, Peters-Golden M, Kaku M, Standiford TJ. Interleukin-36γ and IL-36 receptor signaling mediate impaired host immunity and lung injury in cytotoxic Pseudomonas aeruginosa pulmonary infection: Role of prostaglandin E2. PLoS pathogens. 2017 Nov 22;13(11):e1006737.

4

22. Hahn M, Frey S, Hueber AJ. The novel interleukin-1 cytokine family members in inflammatory diseases. Current opinion in rheumatology. 2017 Mar 1;29(2):208-13.
23. Heming N, Sivanandamoorthy S, Meng P, Bounab R, Annane D. Immune effects of corticosteroids in sepsis. Frontiers in Immunology. 2018:1736.
24. Devarajan A, Vaseghi M. Hydroxychloroquine can potentially interfere with immune function in COVID-19 patients: Mechanisms and insights. Redox Biology. 2021 Jan 1;38:101810.
25. Rother N, Yanginlar C, Lindeboom RG, Bekkering S, van Leent MM, Buijsers B, Jonkman I, de Graaf M, Baltissen M, Lamers LA, Riksen NP. Hydroxychloroquine Inhibits the trained innate immune response to interferons. Cell Reports Medicine. 2020 Dec 22;1(9):100146.
26. Shams S, Martinez JM, Dawson JR, Flores J, Gabriel M, Garcia G, Guevara A, Murray K, Pacifici N, Vargas MV, Voelker T. The therapeutic landscape of rheumatoid arthritis: current state and future directions. Frontiers in Pharmacology. 2021 May 28;12:1233.
27. Mohammadpour F, Kargar M, Hadjibabaie M. The role of hydroxychloroquine as a steroid-sparing agent in the treatment of immune thrombocytopenia: a review of the literature. Journal of research in pharmacy practice. 2018 Jan;7(1):4.
28. Nirk EL, Reggiori F, Mauthe M. Hydroxychloroquine in rheumatic autoimmune disorders and beyond. EMBO molecular medicine. 2020 Aug 7;12(8):e12476.

5

ARTICLE / INVESTIGACIÓN

Estado nutricional, comorbilidades y factores de riesgo asociados a la seguridad alimentaria y nutricional en niños, Francisco Morazán, Honduras

Nilda Suyapa Barahona Aguilar[1]*, Maylin Yesenia Alvarado García[1], Dayanna Michelle Alvarado Barahona[1], María Victoria Zelaya[1], Manuel Alejandro DelCid Barahona[2]

DOI. 10.21931/RB/2023.08.01.54

[1] Facultad de Ciencias Químicas y Farmacia, Universidad Nacional Autónoma de Honduras (UNAH), Tegucigalpa, Honduras.
[2] Doctor en Medicina y Cirugía, Médicos del Mundo Honduras, Tegucigalpa, Honduras.
Corresponding author: nilda.barahona@unah.edu.hn

Resumen: A nivel mundial 52 millones de niños presentan desnutrición aguda, 155 millones sufren desnutrición crónica, mientras que 41 millones tienen sobrepeso u obesidad. En Honduras, el 1.9% de los niños presentan desnutrición aguda, 19% sufren desnutrición crónica y el 4.5% tiene sobrepeso u obesidad. Es necesario analizar la situación de seguridad alimentaria y nutricional (SAN) de las poblaciones, para prevenir las enfermedades crónicas no transmisibles y garantizar el derecho humano a la alimentación adecuada. Caracterizar el estado nutricional, incidencia de comorbilidades y factores de riesgo asociados a la situación de seguridad alimentaria y nutricional en los niños que asisten a los Centros de Desarrollo Integral (CDI). Métodos: Estudio cuantitativo tipo descriptivo transversal realizado entre enero y junio de 2019. Se obtuvo una muestra de 170 niños posterior a un tamizaje nutricional de una población de 1,150 niños. La recolección de datos se realizó mediante la aplicación de dos instrumentos, instrumento 1 recolectó los datos antropométricos y el instrumento 2 recolectó los datos que corresponden a la determinación de la calidad y diversidad de la dieta e índice de SAN. El estudio fue socializado en los CDI obteniendo su aprobación, se solicitó consentimiento informado a los padres y asentimiento informado a los niños participantes. Resultados: La categorización de la malnutrición fue de: 24.0% (41) con desnutrición, 38.0% (64) con sobrepeso y 38.0% (65) con obesidad, con un 61.2% (104) de incidencia de comorbilidades. Conclusiones. La prevalencia de la malnutrición fue del 16.0% (179), la calidad de la dieta de los niños es intermedia y la diversidad de la dieta se categorizó predominantemente como media. La población infantil con malnutrición reflejó inseguridad alimentaria en un 70.0% (119) relacionado a un nivel pobre de acceso a los alimentos y a un consumo deficiente de alimentos.

Palabras claves: Calidad dieta, comorbilidades, malnutrición, seguridad alimentaria y nutricional.

Abstract: Worldwide, 52 million children are acutely malnourished, 155 million are chronically malnourished, and 41 million are overweight or obese. In Honduras, 1.9% of children are acutely malnourished, 19% are chronically malnourished, and 4.5% are overweight or obese. It is necessary to analyze the food and nutrition security (FNS) of the populations, to prevent chronic non-communicable diseases and guarantee the human right to adequate food. Goals. To characterize the nutritional status, the incidence of comorbidities, and risk factors associated with food and nutritional security in children who attend Integral Development Centers (CDI). Methods: Quantitative, descriptive, cross-sectional study carried out between January and June 2019. A sample of 170 children was obtained after the nutritional screen of 1,150 children. The data collection was carried out through the application of two instruments, instrument 1 collected the anthropometric data, and instrument 2 collected the data corresponding to the determination of the quality and diversity of the diet and the SAN index. The study was disseminated in the CDI obtaining their approval, informed consent was authorized to the parents, and informed assent was to the participating children. Results: The categorization of malnutrition was: 24.0% (41) with malnutrition, 38.0% (64) with overweight, and 38.0% (65) with obesity, with 61.2% (104) incidence of comorbidities. conclusions. The prevalence of malnutrition was 16.0% (179), the quality of the children's diet is intermediate, and the diversity of the diet was categorized predominantly as the medium. The child population with malnutrition reflected food insecurity in 70.0% (119) related to a poor level of access to food and deficient food consumption.

Key words: Diet quality, comorbidities, malnutrition, food and nutrition security.

Introduction

En el año 2019, se estimó una falta parcial o total de alimentos que afecta a 187 millones de personas en América Latina y el Caribe en la cual el hambre es la consecuencia individual más severa de la inseguridad alimentaria y nutricional (INSAN), que afecta a 820 millones de personas en el mundo y a 42,5 millones en Latinoamérica, de las cuales 11 millones se encontraban en Centroamérica[1].

El sobrepeso y obesidad en niños se está convirtiendo en un problema creciente a nivel mundial, en el cual la seguridad alimentaria juega un papel determinante en los

Nilda Suyapa Barahona Aguilar, Maylin Yesenia Alvarado García, Dayanna Michelle Alvarado Barahona, María Victoria Zelaya, Manuel Alejandro DelCid Barahona

resultados nutricionales de los niños[2,3]. Con este panorama alarmante, en la década del 70 surge el concepto de SAN, fundamentado en la producción y disponibilidad de alimentos, en los años 80, se introdujo la idea del acceso tanto económico y físico de los alimentos. Posteriormente en la década del 90, se conformó el concepto actual que incluye la inocuidad y las preferencias culturales en el consumo de alimentos y finalmente en la actualidad, la SAN es un derecho humano a nivel mundial[4]. Por lo cual, la agenda 2030 para el Desarrollo Sostenible reconoce que la población mundial debe vivir sin hambre, sin inseguridad alimentaria y sin malnutrición, garantizando el acceso a alimentos suficientes, sino también nutritivos que constituyan una dieta saludable para la población[5].

La situación de seguridad alimentaria a nivel mundial se encuentra ligada a factores preponderantes como ser los recursos asignados a las políticas y programas nacionales de nutrición de madres y niños, factores sociodemográficos, el empleo, el alcance económico, el acceso a agua limpia, saneamiento básico, servicios de salud de calidad, el entorno alimentario, la cultura, entre otros[6,7].

Considerando la importancia de estos factores, la premisa de que "Una nutrición adecuada contribuye de manera fundamental a la realización del derecho al disfrute del más alto nivel posible de salud física y mental de niños y niñas"[8] y que la población de Honduras se caracteriza por ser joven, ya que el 41.9% está representada por niños y adolescentes menores de 18 años en los que la desnutrición es un problema de gran impacto[9], sumado a esto, actualmente la población hondureña es afectada por el aumento alarmante de la incidencia y prevalencia de las Enfermedades Crónicas No Transmisibles (ECNT), las cuales están relacionadas intrínsecamente con la malnutrición y el sedentarismo[10,11] y la situación económica del país que influye en forma determinante en la disponibilidad, acceso y consumo de los alimentos[12]. Por lo cual, este estudio se enfatiza en la prevención, diagnóstico y tratamiento oportuno de la obesidad infantil con el fin de prevenir las comorbilidades, en especial el desarrollo del síndrome metabólico en la edad pediátrica, influir en las políticas públicas de SAN y en la toma de decisiones que beneficien a la población estudiada. Para lo cual se caracterizó el estado nutricional de los niños que asisten a los Centros de Desarrollo Integral (CDI) ubicados en los municipios del Distrito Central y Valle de Ángeles, Francisco Morazán, Honduras. Estos centros brindan asistencia social a familias en riesgo social, no cuentan con estudios ni datos estadísticos que muestren una tendencia del estado nutricional de su población infantil. En el estudio se analizó en su primera etapa el estado nutricional, con el fin de categorizar según el tipo y grado de malnutrición presente en los niños. En una segunda etapa el estudio determinó factores de riesgo nutricional asociados con el acceso y consumo de alimentos, con el fin de determinar la diversidad y calidad de la dieta, y la situación e índice de seguridad alimentaria de la población estudiada.

Materials and methods

Objetivos

Caracterizar el estado nutricional, incidencia de comorbilidades y factores de riesgo asociados a la situación de seguridad alimentaria y nutricional en los niños que asisten a los Centros de Desarrollo Integral (CDI).

Área de estudio

Este estudio se desarrolló en cinco Centros de Desarrollo Integral (CDI) adscritos a iglesias evangélicas con patrocinio de Compassion Honduras, a través de ellos se brinda ayuda social y asistencial a niños como a sus familias que se encuentran en riesgo social, estos centros se ubican en las colonias: Sagastume, 3 de mayo, El Sitio y Aldea El Guanábano (municipio del Distrito Central) y el CDI ubicado en el sector urbano del municipio de Valle de Ángeles.

Tipo de estudio y muestra

Estudio con enfoque cuantitativo y descriptivo, realizado en el Distrito Central y Valle de Ángeles, Honduras, durante una cohorte transversal de enero a junio de 2019. La muestra es no probabilística e intencionada, para la selección de esta se partió de una población de 1,150 niños en edades de 3 - 18 años, quedando como muestra final un total de 170 niños con diagnóstico de malnutrición fundamentada en un tamizaje nutricional y posterior a una evaluación médica y nutricional.

Recolección de datos

La información se recolectó en dos etapas mediante 2 instrumentos. En la primera, se recolectó los datos antropométricos para caracterizar el estado nutricional, detallados en los expedientes clínicos de los niños beneficiarios de los CDI. Así mismo, se identificó las características sociodemográficas, manifestaciones clínicas de malnutrición y las comorbilidades relacionadas, mientras en la segunda etapa, se aplicó el instrumento 2, que incluyó un cuestionario que contenía el registro de la ingesta de alimentos durante 24 horas y la frecuencia semanal de alimentos de la dieta, dirigido a un familiar de los niños que conformaron la muestra seleccionada.

Aspectos éticos

Para la ejecución de la investigación se contó con la aprobación y consentimiento de los directores de cada CDI y la facilitadora de Compassion Honduras. A su vez, se socializó el proyecto de investigación con la facilitadora y directores de cada CDI para establecer los mecanismos de comunicación para la ejecución del estudio, se obtuvo el consentimiento informado de los familiares y el asentimiento informado de los niños participantes en el estudio.

Análisis de Datos

ELas medidas antropométricas obtenidas en la primera etapa con el instrumento 1 se incorporaron en el software OMS Anthro versión 3.2.2, mientras que los datos de manifestaciones clínicas de malnutrición y las comorbilidades relacionadas se identificaron en los expedientes clínicos. Los datos recolectados con el instrumento 2 se tabularon a través del programa Microsoft Excel versión 2013, para realizar el análisis de la información recolectada que corresponde a los factores de riesgo nutricional asociados al acceso y consumo de alimentos, se emplearon múltiples herramientas: indicadores del Instituto de Nutrición de Centroamérica y Panamá (INCAP), el Puntaje de la Diversidad Alimentaria Individual (IDDS) propuesto por la Organización de las Naciones Unidas para la Alimentación y la Agricultura – Food and Nutrition Technical Assistence (FAO-FANTA), el Puntaje de Consumo de Alimentos (PCA) y el índice de seguridad alimentaria propuesto por el Programa Mundial de Alimentos (PMA), con el objetivo de determinar la diver-

sidad y calidad de la dieta, y la situación e índice de seguridad alimentaria y nutricional.

Results

Caracterización del estado nutricional, incidencia de comorbilidades y factores de riesgo asociados

La edad promedio fue de 10 años, siendo la edad pediátrica escolar la más frecuente con un 61.0% (104), con rango de edad de 6 – 11 años. El sexo predominante fue el femenino con un 55.0% (93) y el nivel de educación con mayor frecuencia fue el de primaria con un 68.0% (116). (ver tabla 1).

Características	n	(%)
Sexo		
Femenino	93	(55.0)
Masculino	77	(45.0)
Edad (años)		
3 - 5 años	16	(9.4)
6 - 11 años	104	(61.2)
12 - 18 años	50	(29.4)
Promedio	10	
Nivel de educación		
Ninguna	1	(0.6)
Kinder	16	(9.4)
Primaria	116	(68.0)
Secundaria	37	(22.0)

Table 1. Características sociodemográficas de niños con malnutrición en edades de 3 – 18 años, Distrito Central y Valle de Ángeles, enero – junio 2019. n=170.

Durante el período del estudio se intervino un total de 1,150 niños, realizándose un tamizaje nutricional de esta población, donde se identificó una prevalencia de malnutrición del 15.0 % (170) y un 84.4% (971) con normopeso. La población con malnutrición que participó en el estudio se categorizó en 24.0% (41) niños con desnutrición, 38.0% (64) con sobrepeso y 38.0% (65) con obesidad.

La desnutrición se categorizó según el tipo y el grado. En relación al tipo de desnutrición se identificó un 36.6% (15) desnutrición aguda y un 63.4% (26) desnutrición crónica. Con respecto al grado de desnutrición, se encontró que el 41.5% (17) tenia desnutrición leve, el 46.3% (19) moderada y el 12.2% (5) severa.

El sobrepeso se categorizó según el grado de riesgo nutricional que presentaban, siendo que el 29.7% (19) tenía riesgo moderado mientras que el 70.3% (45) riesgo alto. En relación a la obesidad, se clasificó según el grado, se encontró en grado 1 al 32.3% (21), en grado 2 al 44.7% (29), en grado 3 al 21.5% (14) y en grado 4 al 1.50% (1). (ver tabla 2).

Entre las manifestaciones clínicas de la población infantil con desnutrición predominaron las musculo-esqueléticas en un 92.7% (38) y las neurológicas-cognitivas con un 65.9% (27). En relación a las manifestaciones clinicas de

niños con sobrepeso y obesidad, las endocrinas fueron las mas frecuentes en ambas, con un 100.0% (64) en sobrepeso y con un 100.0% (65) en obesidad. (ver tabla 3).

Las comorbilidades relacionadas con desnutrición, prevaleció la enfermedad infecciosa con un 65.9% (27), talla baja y trastornos cognitivos con un 63.4% (26). (ver tabla 4) En las comorbilidades relacionadas con sobrepeso y obesidad, los desordénes psicosociales prevalecieron como los de mayor frecuencia en ambas, con un 31.2% (20) y un 87.7% (57) respectivamente. (ver tabla 5).

En los Antecedentes Patológicos Familiares (AFP) de la poblacion infantil con malnutrición, se identificaron los factores asociados categorizandose según el grado de consanguinidad afectado. Se identificó que el 70.0% (119) del total de la población de este estudio presentaba al menos un antecedente patológico familiar, siendo la Diabetes Mellitus (DM) y la obesidad las patologías más frecuentes con un 50.4% (60). El grado de consanguinidad afectado con mayor frecuencia fue el de primer grado con un 63.0% (75). (ver tabla 6).

Situación de la seguridad alimentaria y nutricional y factores de riesgo nutricional asociados al accesso y consumos de alimentos

Acceso a los alimentos

Las características sociodemográficas de los familiares de los niños con malnutrición determinaron que la edad promedio fue de 33 años, el sexo predominante fue el femenino con un 94.1% (160) y el nivel de educación más frecuente fue el de primaria completa con un 25.9% (44). 68.8% (117) de la población se identificó en condición de desempleo, con un ingreso económico familiar de mayor frecuencia en-

Caracterización del estado nutricional	n	(%)
Malnutrición		
Desnutrición	24.0	(41)
Sobrepeso	38.0	(64)
Obesidad	38.0	(65)
Tipo de desnutrición		
Desnutrición aguda	36.6	(15)
desnutrición crónica	63.4	(26)
Grado de desnutrición		
Desnutrición leve	41.5	(17)
Desnutrición moderada	46.3	(19)
Desnutrición severa	12.2	(5)
Sobrepeso-riesgo nutricional		
Riesgo moderado	29.7	(19)
Riesgo alto	70.3	(45)
Grado de obesidad		
Grado 1	32.3	(21)
Grado 2	44.7	(29)
Grado 3	21.5	(14)
Grado 4	1.50	(1)

Table 2. Caracterización del estado nutricional en niños con 3-18 años, Distrito Central y Valle de Ángeles, enero – junio 2019. n=170.

3

Nilda Suyapa Barahona Aguilar, Maylin Yesenia Alvarado García, Dayanna Michelle Alvarado Barahona, María Victoria Zelaya, Manuel Alejandro DelCid Barahona

4

Manifestaciones clínicas	Desnutrición		Sobrepeso		Obesidad	
	n=41	(%)	n=64	(%)	n=65	(%)
Dermatológicas	20	(48.8)	8	(12.5)	57	(87.7)
Músculo esqueléticas	38	(92.7)	5	(7.8)	33	(50.8)
Gastrointestinales	10	(24.4)	0	(0.0)	22	(33.8)
Neurológicas - cognitivas	27	(65.9)	20	(31.3)	34	(52.3)
Cardiovasculares	23	(56.1)	0	(0.0)	2	(3.1)
Endocrinas	26	(63.4)	64	(100.0)	65	(100.0)

Table 3. Manifestaciones clínicas según el tipo de malnutrición en niños con 3-18 años, Distrito Central y Valle de Ángeles, enero – junio 2019.

Comorbilidades	n	(%)
Enfermedad infecciosa	27	(65.9)
Parasitismo intestinal	10	(24.4)
Síndrome anémico	24	(58.5)
Síndrome de malabsorción	3	(7.3)
Talla baja	26	(63.4)
Trastornos cognitivos	26	(63.4)

Table 4. Comorbilidades relacionadas a la población con desnutrición en edades de 3-18 años, Distrito Central y Valle de Ángeles, enero – junio 2019. n=41

Comorbilidades	Sobrepeso		Obesidad	
	n=64	(%)	n=65	(%)
Sospecha de resistencia a insulina	0	(0.0)	28	(43.1)
Apnea obstructiva del sueño	2	(3.1)	13	(20.0)
Asma bronquial	5	(7.8)	6	(9.2)
Trastornos menstruales	5	(7.8)	15	(23.1)
Pseudomicropene/ginecomastia	0	(0.0)	21	(32.2)
Desordenes psicosociales	20	(31.2)	57	(87.7)
Síndrome de ovario poliquístico	5	(7.8)	8	(12.3)
Enfermedad infecciosa	2	(3.1)	5	(7.7)

Table 5. Comorbilidades relacionadas a la población con sobrepeso y obesidad en edades de 3-18 años, Distrito Central y Valle de Ángeles, enero – junio 2019.

Antecedentes Patológicos Familiares	n	(%)
Patología		
Diabetes mellitus	60	(50.4)
Hipertensión arterial	56	(47.1)
Dislipidemias	22	(18.5)
Cardiopatías	5	(4.2)
Enfermedades tiroideas	10	(8.4)
Obesidad	60	(50.4)
Grado de consanguinidad del familiar		
Primer grado	75	(63.0)
Segundo grado	37	(31.1)
Tercer grado	7	(5.9)

Table 6. Antecedentes patológicos familiares en la población con malnutrición en edades de 3-18 años, Distrito Central y Valle de Ángeles, enero – junio 2019. n=119

tre el rango de L. 4,640 – 9,443 ($188.83 – 384.30) con un 45.3% (77) y el promedio de número de fuentes de ingreso económico fue de un solo ingreso. (ver tabla 7).

Las características sociodemográficas de los hogares de la población infantil estudiada se encontró que el 52.0% (89) de los hogares contaba con acceso a agua potable y un 99.0% (168) con acceso a luz eléctrica. Del total de hogares, se identificó que el 86.0% (147) contaban con condiciones de habitabilidad, mientras que el 46.0% (78) presentaron condiciones de hacinamiento con una frecuencia predominante de 2 dormitorios por hogar y 5 convivientes por hogar. (ver tabla 8).

En relación al acceso a los alimentos que corresponde al ingreso económico familiar y al número de fuentes de ingreso, se encontró que el 42.4% (72) tenía un nivel de acceso pobre, un 45.3% (77) presentó un nivel promedio y el 12.3% (21) restante tenía un acceso bueno.

Consumo de alimentos

En cuanto a la historia diética y nutricional de los niños con malnutrición, se identificó que el 46.0% (78) recibió lactancia materna exclusiva durante los primeros 6 meses de vida y el 61.0% (104) presentó transgresión alimentaria durante esta etapa pediátrica. Con respecto al registro de bebidas y alimentos consumidos, se encontró que el 67.0% (114) consumía comida con bajo valor nutritivo, a su vez se identificó que el método de preparación de alimentos más utilizado es la fritura con un 98.0% (168), haciendo uso de grasas saturadas en un 53.0% (90) de los niños. (ver tabla 9).

La diversidad de la dieta se categorizó a través del registro de alimentos y bebidas en 24 horas, en el cual se identificó que el 69.4% (118) de la población tenía una dieta con diversidad media, el 30.0% (51) con diversidad alta y únicamente el 0.6% (1) presentó una diversidad baja. En el grafico 1, se detallan los grupos de alimentos consumidos por la población con malnutrición, donde se refleja que los grupos predominantes son el grupo de granos, raíces y tubérculos con un 100.0% (170) y el grupo de aceites y grasas con un 99.0% (168).

Con respecto al factor de riesgo nutricional relacionado al consumo de alimentos, él cual se estimó a partir del Puntaje de Consumo de Alimentos (PCA), se identificó la frecuencia de ingesta de grupos de alimentos mediante la determinación de la moda; de manera que se determinó un PCA total de 76 puntos en la población con malnutrición, evidenciando un consumo de alimentos aceptable en las familias del estudio. (ver tabla 10).

Características	n	(%)
Edad (años)		
15 - 30	76	(44.7)
31 - 59	92	(54.1)
≥ 60	2	(1.2)
Promedio	33	
Sexo		
Femenino	160	(94.1)
Masculino	10	(5.9)
Nivel de educación		
Analfabeto	8	(4.7)
Primaria incompleta	39	(22.9)
Primaria completa	44	(25.9)
Secundaria incompleta	39	(22.9)
Secundaria completa	34	(20)
Universitaria incompleta	5	(3.0)
Universitaria completa	1	(0.6)
Condición de trabajo		
Empleo	53	(31.2)
Desempleo	117	(68.8)
Ingreso económico familiar		
< L. 4,640	72	(42.4)
L. 4,640 - 9,443	77	(45.3)
> L. 9,443	21	(12.3)
Remesas		
Si	39	(23.0)
No	131	(77.0)
Fuentes de ingreso económico		
1 fuente	122	(71.8)
≥ 2 fuentes	48	(28.2)
Promedio	1	

Table 7. Características sociodemográficas de familiares de los niños con malnutrición en edades mayores de 15 años, Distrito Central y Valle de Ángeles, enero – junio 2019. n=170

La calidad de la dieta de los niños con malnutrición se identificó como intermedia, ya que el consumo diario de alimentos se basa en carbohidratos y grasas, con una ingesta moderada de proteinas de origen animal y una pobre ingesta de alimentos ricos en vitaminas y minerales.

El índice de seguridad alimentaria de la población infantil con malnutrición se estimó a partir del nivel de acceso y consumo de alimentos (Figura 2).

Discussion

En este estudio se categorizó la población infantil según el tipo y grado de malnutrición, detallando sus características desde un enfoque nutricional, clínico, sociodemográfico

Características	n	(%)
Acceso a servicios públicos		
Agua potable	89	(52.0)
Luz eléctrica	168	(99.0)
Aguas negras/alcantarillado	71	(42.0)
Tren de aseo	157	(92.0)
Características de la vivienda		
Techo de madera o metal	165	(97.0)
Paredes de madera, ladrillo o bloque	147	(86.0)
Estufa eléctrica / gas	146	(86.0)
Inodoro lavable	130	(76.0)
Número de dormitorios		
Promedio	2	
No. de convivientes en el hogar		
Promedio	5	
Hacinamiento	78	(46.0)
Tipo de familia		
Monoparental	57	(34.0)
Biparental	113	(66.0)

Table 8. Características sociodemográficas de los hogares de la población infantil con malnutrición en edades de 3-18 años, Distrito Central y Valle de Ángeles, enero – junio 2019. n=170.

Historia dietética y nutricional	n	(%)
Antecedentes nutricionales		
Lactancia materna exclusiva 6 meses	78	(46.0)
Ablactación a los 6 meses	71	(42.0)
Transgresión alimentaria	104	(61.0)
Destete después de los 2 años	85	(50.0)
Registro de alimentos y bebidas		
Consumo de bebidas azucaradas	137	(81.0)
Consumo de comida "chatarra"	114	(67.0)
Tipo de aceite utilizado		
Grasa saturada	90	(53.0)
Grasa insaturada	80	(47.0)
Preparación de los alimentos		
Hervida	164	(96.0)
Frita	166	(98.0)
Horneada	121	(71.0)
Crudo / Fresco	116	(68.0)

Table 9. Historia dietética y nutricional en la población con malnutrición en edades de 3-18 años, Distrito Central y Valle de Ángeles, enero – junio 2019. n=170.

Nilda Suyapa Barahona Aguilar, Maylin Yesenia Alvarado García, Dayanna Michelle Alvarado Barahona, María Victoria Zelaya, Manuel Alejandro DelCid Barahona

Grupo de alimentos	Frecuencia semanal de consumo	
	Moda (Ẋ)	Puntaje
Cereales y tubérculos	7	14
Leguminosas	7	21
Vegetales	2	2
Frutas	0	0
Carnes, pescados y mariscos	5	12
Leche y derivados	5	20
Azúcar y productos derivados	7	3.5
Aceites y grasas	7	3.5
	PCA Total	76

Table 10. Puntaje de Consumo de Alimentos (PCA) de la dieta de los niños con malnutrición en edades de 3-18 años, Distrito Central y Valle de Ángeles, enero – junio 2019.

y epidemiológico. Se identificó que el tipo de malnutrición con mayor prevalencia es el sobrepeso y obesidad con un 75.9% (129), siendo el grupo más vulnerable ya que se encontró que el 100.0% (129) tenía manifestaciones clínicas endocrinas, las cuales se ven reflejadas en el 43.1% (28) que presentó sospecha de resistencia a la insulina, siendo esta comorbilidad la de mayor riesgo para el desarrollo del síndrome metabólico en la infancia. En congruencia con el estudio del estado nutricional y condiciones de vida de niños y jóvenes rurales, realizado por Salazar y Oyhenart en Argentina en el 2021, se evidenció el impacto que agrava la situación en salud por las carencias socioeconómicas y condiciones epidemiológicas que afectan de alguna manera u otra los procesos de transición nutricional[13,14]. De manera similar, Calceto en su estudio realizado en Ecuador en el 2019 llamado relación del estado nutricional con el desarrollo cognitivo y psicomotor de los niños en la primera infancia, destacó que la influencia significativa del factor socioeconómico en la malnutrición[15].

Estos resultados son alarmantes ya que la población estudiada tiene un riesgo elevado de desarrollar comorbilidades dentro del grupo de las ECNT en la edad pediátrica.
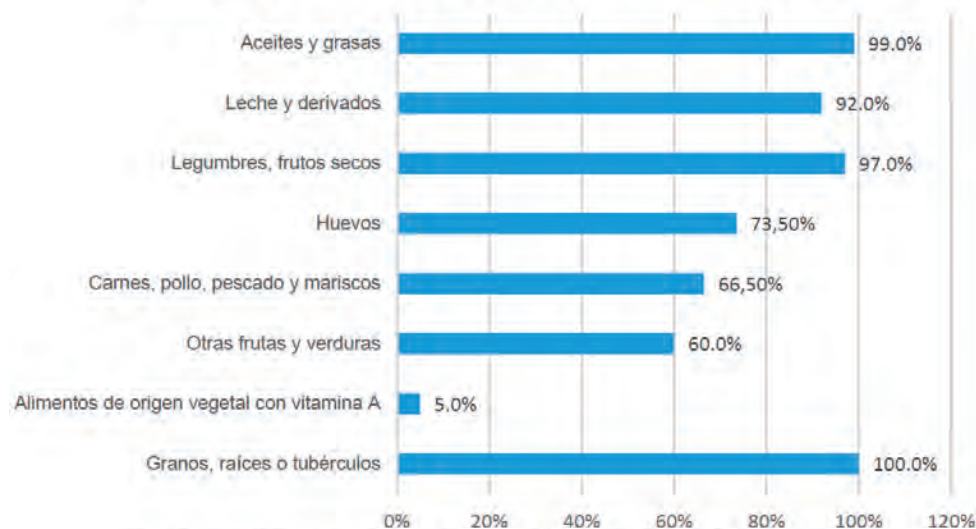

Figure 1. Diversidad dietética de la población infantil con malnutrición en edades de 3-18 años, Distrito Central y Valle de Ángeles, enero – junio 2019.
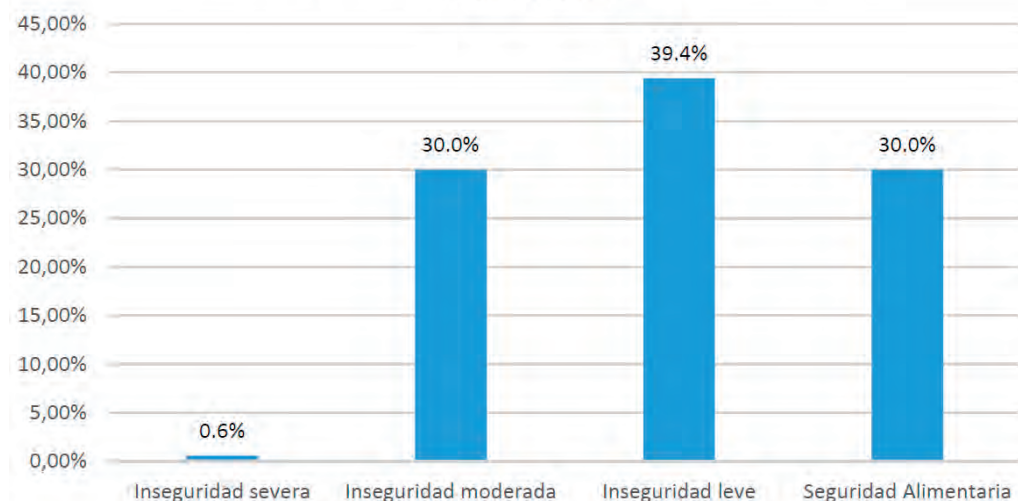

Figure 2. Índice de seguridad alimentaria de la población infantil con malnutrición en edades de 3-18 años, Distrito Central y Valle de Ángeles, enero – junio 2019.

En comparación con el estudio de valoración nutricional de Deossa, realizado en el 2021 en estudiantes universitarios de México, se determinó que las enfermedades como la diabetes mellitus (DM), hipertensión arterial (HTA), cáncer y obesidad tenían el factor influyente de una conducta alimentaria deficiente hacia una dieta no equilibrada y balanceada independiente del ciclo de vida y que se relacionó con el desarrollo de ECNT[16].

Contrastado con el estudio de Sánchez en 2017 realizado en una población con edad pediátrica escolar en el municipio de Cienfuegos, Cuba, donde reportó que el 56.4% de los niños tenía sobrepeso y obesidad, 41.0% normopeso y un 2.6% tenía desnutrición. También encontrándose que el 41.0% de los niños con obesidad tenía riesgo de desarrollar síndrome metabólico, ya que presentaron manifestaciones clínicas de resistencia a la insulina y alteraciones en las cifras tensionales; y se evidenció que en relación con los AFP predominó la obesidad con un 42.0%, la HTA con un 44.2% y la DM con un 21.0%[17]. Dichos resultados son similares en tendencia a los de nuestro estudio, donde encontramos como AFP predominantes la HTA en un 47.1% (56), la DM y la obesidad en un 50.4% (60).

Este estudio evidenció que el 70.0% (119) de la población infantil vivía con algún grado de inseguridad alimentaria, debido a un nivel de acceso pobre a los alimentos en el que se identificó que un 66.8% (117) de la población se encontraba en condición de desempleo, y un 45.3% (77) de las familias contaban con un ingreso económico familiar menor al salario mínimo, oscilando entre el rango de L. 4,640 – 9,443 ($188.83 – 384.30) y se identificó que el promedio de número de fuentes de ingreso económico fue de una sola fuente. Datos que dejan en evidencia lo que García describió en relación con el factor económico versus al acceso ante el recurso monetario, en su estudio realizado en 2020, donde enfatizó que los factores económicos son los de mayor influencia en la seguridad alimentaria y nutricional, identificándose una división social y pobre acceso a alimentos de calidad para una alimentación adecuada. Así mismo, en su estudio identificó un consumo de alimentos caracterizado por una ingesta prioritaria de grupos de alimentos ricos en carbohidratos y grasas, y siendo deficiente en alimentos ricos en vitaminas y proteínas, teniendo como diversidad dietética predominante la diversidad media con un 69.4% (118)[18]. Comparado al estudio de Mundo en el 2014, realizado en México en una población de 955 niños y sus hogares, en el cual se reportó que el 77.6% de la población estudiada vivía en inseguridad alimentaria en el hogar, y también se evidenció una diversidad dietética media como predominante en la población con un 43.6%[19]. También de manera similar, en el estudio de Sagastume realizado en México sobre seguridad alimentaria familiar y hogares sustentables de alumnos practicantes de nutrición durante la pandemia de Covid-19 en el año 2021, en el cual determinó una muestra de 67 familias donde identificó que aproximadamente el 91.8% de las familias de los alumnos se encontraba en inseguridad y vulnerabilidad alimentaria siendo uno de los factores el consumo de alimentos[20]. Ambos estudios evidencian la inseguridad alimentaria en diferentes hogares y poblaciones.

Conclusions

El estado nutricional de los niños se caracterizó con una prevalencia de malnutrición del 16.0% (179), predominando el sobrepeso u obesidad con la presencia de manifestaciones clínicas endocrinas que evidencian sospecha de resistencia a la insulina, generando un alto riesgo de desarrollar síndrome metabólico en la infancia como comorbilidad incidente relacionada al estado nutricional.

La calidad de la dieta de los niños con malnutrición es intermedia y la diversidad de la dieta predominantemente se categorizó como media con un promedio de consumo de 5 grupos alimenticios, caracterizándose por una ingesta deficiente en proteínas y vitaminas, con un alto grado de consumo de carbohidratos y grasas, siendo factor de riesgo nutricional para el desarrollo de ECNT.

La situación de SAN de la población infantil con malnutrición reflejó inseguridad alimentaria en un 70.0% (119), relacionado a un nivel pobre de acceso a los alimentos y a un consumo deficiente de alimentos que no garantiza una alimentación adecuada y saludable.

Bibliographic references

1. Bernal, J.; Agudelo Martínez, A. Medición de inseguridad alimentaria-nutricional, hambre y estrategias de afrontamiento de niños y adolescentes en Medellín-Colombia. ALAN, 2020, 70, 20-29. Disponible en: https://doi.org/10.37527/2020.70.1.003
2. FAO; FIDA; UNICEF; PMA; OMS. El estado de la seguridad alimentaria y la nutrición en el mundo. Fomentando la resiliencia climática en aras de la seguridad alimentaria y la nutrición. FAO, Roma. 2018.
3. Montenegro Coral, FA.; Rosero Galindo, CY.; Hernández Arteaga, I.; Lasso Portilla, N. Evaluación del estado nutricional en población infantil del municipio de Pasto, Colombia. Revista Cubana Salud Pública 2021, 47, e1333.
4. FAO. Seguridad Alimentaria y Nutricional, Conceptos Básicos. 3rd ed.; Programa Especial para la Seguridad Alimentaria (PESA) Centroamérica. Proyecto Food Facility Honduras. 2015; pp. 1-3.
5. Ramírez, Roberth F.; Vargas, Pablo L., Cárdenas; Olimpo S. La seguridad alimentaria: una revisión sistemática con análisis no convencional. Revista espacios 2020, 41, 319-328. Disponible en: 10.48082/espacios-a20v41n45p25
6. FAO. EL estado de la seguridad alimentaria y la nutrición en el mundo: Fomento de la resiliencia en aras de la paz y la seguridad alimentaria. FOOD & AGRICULTURE ORG, Roma, 2017.
7. Salvador Castell G.; Ngo de la Cruz J.; Pérez Rodrigo C.; Aranceta J. Escalas de evaluación de la inseguridad alimentaria en el hogar. Revista Española de Nutrición Comunitaria 2015, 21, 270-276. Disponible en: 10.14642/RENC.2015.21.sup1.5074
8. Naciones Unidas-CEPAL. Disponible en línea: https://www.cepal.org/es/enfoques/malnutricion-ninos-ninas-america-latina-caribe (acceso el 24 julio 2019).
9. Instituto Nacional de Estadística. Disponible en línea: http://181.115.7.199/binhnd/RpWebEngine.exe/Portal?BASE=EPH2017&lang=ESP (acceso el 24 septiembre 2019).
10. OPS; OMS; FAO; INCAP; Visión Mundial. Guía Alimentaria Basada en Alimentos (GABA) para Honduras. Tegucigalpa, Honduras. 2014.
11. Secretaría de estado en el despacho de salud; Instituto Hondureño de Seguridad Social. Plan Nacional de Salud 2021, Honduras, 2005; pp. 22-23.

7

Nilda Suyapa Barahona Aguilar, Maylin Yesenia Alvarado García, Dayanna Michelle Alvarado Barahona, María Victoria Zelaya, Manuel Alejandro DelCid Barahona

8

12. Lara-Árevalo, J.; Escobar-Burgos, L. Malnutrición en Honduras durante la COVID-19: el ambiente obesogénico y el hambre oculta. Innovare 2020, 9, 120-122. Disponible en: https://doi.org/10.5377/innovare.v9i2.10203

13. Salazar-Burgos R.; Oyhenart, E. Estado nutricional y condiciones de vida de niños y jóvenes rurales de Tucumán, Argentina. Revista Española de Nutrición humana y Dietética 2021, 25, 111-120. Disponible en: https://doi.org/10.14306/renhyd.25.1.1162

14. Delcid Morazán, AF.; Delcid Morazán, LE.; Barcan Batchvaroff, ME.; Leiva Molina, FA.; Barahona Andrade, DS. Estado nutricional en escolares de primero a sexto grado en La Paz, Honduras. Revista Científica de la Escuela Universitaria de las Ciencias de la Salud 2017, 4, 27-33.

15. Calceto-Garavito, L.; Garzón, S.; Bonilla, G.; Cala-Martínez, D. Relación Del Estado Nutricional Con El Desarrollo Cognitivo y Psicomotor De Los Niños En La Primera Infancia. Revista Scielo 2019, 28, 50-58.

16. Deossa Restrepo, G.; Segura Buján, M.; Restrepo Betancur, L. Evaluación del estado nutricional y estilo de vida en universitarias de Nutrición y Dietética de México y Colombia. Revista Habanera de Ciencias Médicas 2021, 20.

17. Sánchez, V.; García, B.; González Hermida, K.; González Hermida, A.; Saura Naranjo, C. Sobrepeso y obesidad en niños de 5 a 12 años. Revista Finlay 2017, 7, 47-53.

18. Martínez-Valdés, G., et al. Aspectos que influyen en el desarrollo de la seguridad alimentaria en el sector social. Revista Scielo 2020, 26. Disponible en: https://doi.org/10.18004/pdf-ce/2076-054x/2020.026.51.051

19. Mundo Rosas, V.; Cruz Góngora, V.; Jiménez Aguilar, A.; Shamah Levy, T. Salud pública de México. Diversidad de la dieta y consumo de nutrimentos en niños de 24 a 59 meses de edad y su asociación con inseguridad alimentaria. Revista Scielo 2014, 56, s39-s46.

20. Crocker Sagastume, R., et al. Seguridad alimentaria familiar y hogares sustentables de alumnos practicantes de nutrición durante la pandemia de COVID 19. Revista salud pública y nutrición 2021, 20, 1-10.

LETTER TO EDITOR / CARTA AL EDITOR

Producción científica de la Universidad Nacional Autónoma de Honduras (UNAH) en la revista Bionatura durante el segundo semestre del año 2022

Dely Ramírez[1,3], Lilian Sosa[2,3*] , Santiago Ruiz[3]

[1] Facultad de Ciencias Económicas, Administrativas y Contables, Universidad Nacional Autónoma de Honduras.
[2] Grupo de Investigación en Tecnología Farmacéutica, Facultad de Ciencias Químicas y Farmacia, Universidad Nacional Autónoma de Honduras (UNAH).
[3] Dirección de Investigación Científica, Humanística y Tecnológica (DICIHT), Universidad Nacional Autónoma de Honduras (UNAH)
Corresponding author: lilian.sosa@unah.edu.hn

Las autoridades de la Universidad Nacional Autónoma de Honduras (UNAH), desde el año 2019, asumieron el reto de colocar a la UNAH dentro del ranking SCIMAGO, siendo esta una plataforma que clasifica a las instituciones académicas de acuerdo a tres conjuntos de datos basados en: la investigación (50% de la puntuación final), la innovación (30% de la puntuación final) y el impacto social medido en base a la visibilidad de las webs (20% de la puntuación final)[1]. El SCImago Journal & Country Rank provee una serie de indicadores sobre la calidad y el impacto de publicaciones y revistas a partir de información de Scopus de Elsevier[2].

Scopus es una base de datos de referencias bibliográficas, citas de literatura, revision por pares y contenido web de calidad, con herramientas para el seguimiento, análisis y visualización de la investigación[3].

Para que la UNAH pudiese entrar en el ranking SCIMAGO, se propuso que los investigadores de esta institución publicaran al menos 100 artículos en revistas indizadas en la base de datos SCOPUS. Para ello, en los años 2020 y 2021, la Dirección de Investigación Científica, Humanística y Tecnológica (DICIHT) se planteó entrenar, mediante programas de capacitación a los investigadores, con el objetivo de que estos pudiesen escribir sus resultados de investigaciónes cientificas (muchos de ellos derivados de tesis de grado y posgrado) en formato paper. Lo anterior, en atención a lo establecido en la política de investigación científica, desarrollo tecnológico e innovación UNAH 2015 – 2019, inciso F, punto 4[4]. Esto no solo involucró el entrenamiento en redacción, también en la busqueda de referencias bibliográficas que pudieran enriquecer el contenido de los manuscritos, surgiendo así, la preocupación por acceder a la literatura científica de alto impacto puesto que la UNAH no cuenta con los suficientes recursos para pagar el acceso a bases de datos donde se publican artículos científicos. Lo anterior, impedía citar artículos de calidad, por lo que fue necesario hacer busqueda de aquellas revistas de acceso abierto y de reconocido prestigio.

El acceso abierto debe ser gratuito y sin restricciones por parte de todas las personas, especialmente en paises como Honduras donde la limitación presupuestaria para investigar es enorme. El contenido de esta literatura debe ser de manera libre y universal, sin costo alguno para el lector, a través de Internet o cualquier otro medio. Sin esto, se vuelve difícil y hasta imposible investigar y publicar resultados de calidad. Así mismo, publicar en este tipo de revistas genera una mejor visualización por área del conocimiento, así como la actividad académica y científica de un investigador, permitiendo que más personas tengan acceso al conocimiento y a la aplicación de estas en la resolución de los problemas de la sociedad, mejorando así la calidad de vida de los habitantes de un país . Asi mismo, esto conlleva a un mayor difusión y numero de citaciones ya que se promueve el acceso abierto a la información y se utillizan una variedad de herramientas para promocionar y difundir el contenido, además tienen un mayor impacto a menor costo beneficiando aquellos paises que tienen recursos limitados.

Para poner en practica lo anteriormente expuesto, en el año 2022, se implementó como estrategia, realizar un congreso titulado "Congreso Internacional SCOPUS XIV - Congreso de investigación científica, UNAH 2022: a la luz de la agenda 2030 para el desarrollo humano sostenible"; donde el requisito fundamental para participar era la escritura de al menos un artículo científico que se sometiera a una revisión por pares para asegurar la calidad e impacto de los mismos.

El congreso se dividió en dos partes: 1. Ciencia, Desarrollo y Vida y 2. Ciencias, Salud y Vida. Esta última contó con producción científica que fue publicada en la revista Bionatura en el volumen 7, Números 3 y 4.

La revista Bionatura es una revista de acceso abierto que se dedica a la publicación de manuscritos sobre temas relacionados con todos los aspectos de la biotecnología y las ciencias de la vida. Los temas incluyen: Agricultura, Bioinformática, Biomedicina, Biociencia, Biotecnología, Epidemiología, Inmunología, Insectos, Informe de casos médicos, Microbiología, Micología, Nanomedicina, Nanopartículas, Parasitología, Investigación farmacológica, Plantas (Botánica), Contaminación, Polímeros, Virología, tambien acepta artículos de revisión sobre los aspectos éticos de la investigación biomédica y la práctica clínica (Bioética)[5].

En la presente nota al editor se puede ver la clasificación de la producción científica por carrera (Figura 1) y temas de investigación (figura 2) realizada por los investigadores de la UNAH en la revista Bionatura durante el segundo semestre del 2022. Así mismo, se mencionan las universidades y/o entes externos nacionales e internacionales que apoyaron a estas publicaciones.

Se publicó un total de veintinueve artículos científicos en la revista Bionatura durante el segundo semestre del 2022, de los cuales, veintiocho se publicaron en el volumen número 3 y uno en el volumen número 4.

2

Número de publicaciones por carrera

Figure 1. Número de publicaciones de la UNAH en revista Bionatura durante el segundo semestre del 2022 clasificado por carreras. IHCIT: Instituto Hondureño de Ciencias de la Tierra (Facultad de Ciencias). DICIHT: Dirección de Investigación Científica, Humanística y Tecnológica, de la UNAH.

Número de publicaciones por área del conocimiento
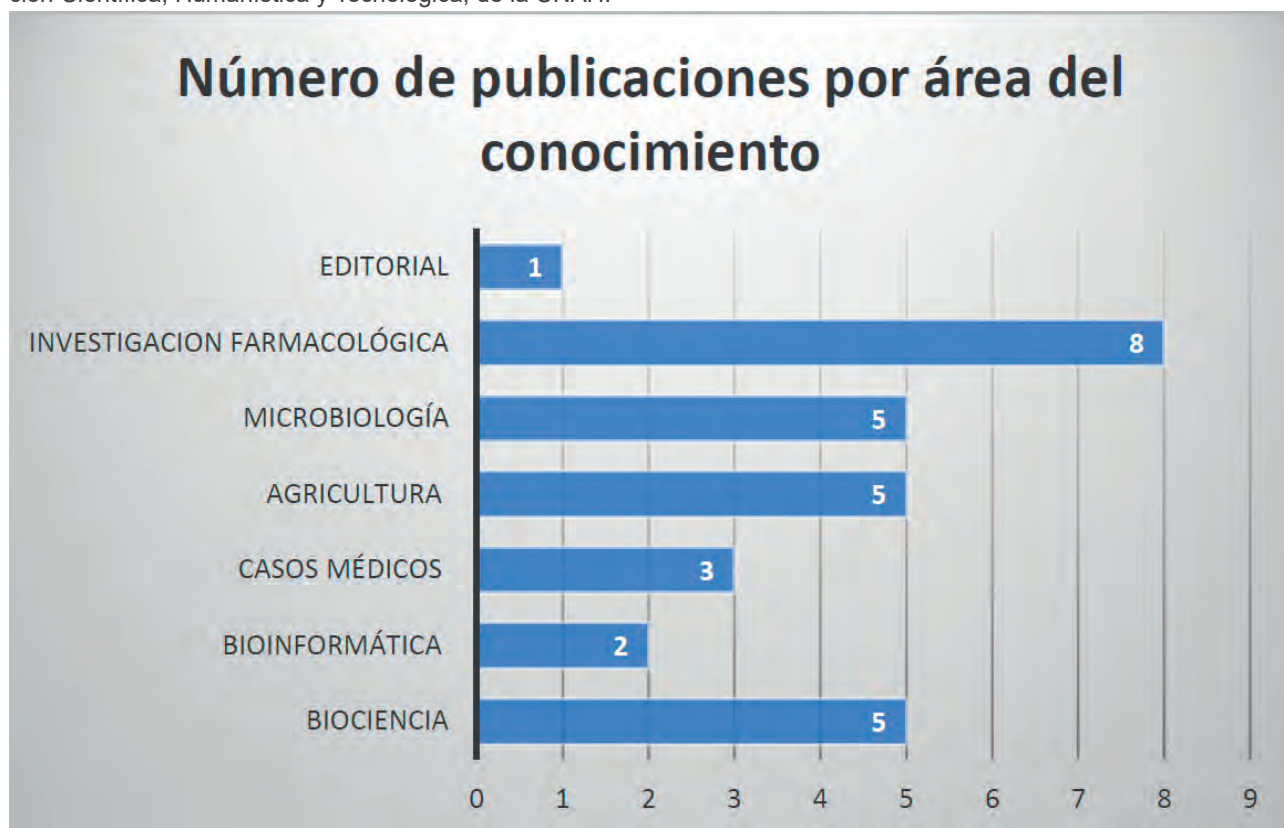
Figure 2. Número de publicaciones por área del conocimiento en la revista Bionatura.

*Cabe destacar que varios de los artículos publicados fueron colaboración de dos facultades y/o carreras. Por ejemplo, de los 8 artículos que provenían de la Facultad de Ciencias Químicas y Farmacia, 1 de ellos fue una colaboración con la Escuela de Microbiología, para hacer un total de 5 artículos publicados de esta última carrea. Otro caso similar, se dio con los artículos que provenían de la carrera de ingeniería agronómica, donde 4 de los artículos publicados se hicieron en conjunto con la facultad de Ciencias Químicas y Farmacia, para hacer un total de 12 artículos científicos publicados para esta última carrera.

La clasificación, por área temática, de los 29 artículos científicos se puede observar en la figura 2. Varios de estos artículos pueden sub agruparse, por ejemplo, de los 8 ar-

tículos del área de investigación farmacológica, 1 de ellos habla de la nanomedicina y su aplicación en la parasitología. Así mismo, otro artículo del área de investigación farmacológica se combina con la microbiología. Por otro lado, de los 5 artículos del área de la agricultura, todos se combinan con la química.

Las facultades que tuvieron más proyección referente a las publicaciones científicas fue: la Facultad de Ciencias Químicas y Farmacia (12)*, la Facultad de Ciencias con las carreras de Microbiología (5)*, Biología (2) y el IHCIT (2).

Los 29 artículos científicos contaron con la autoría de investigadores provenientes de universidades nacionales como: la Universidad Nacional de Agricultura (UNAG), Universidad Tecnológica Centroamericana (UNITEC), Escuela Agrícola Panamericana (ZAMORANO) y organismos nacionales como: Instituto Nacional de Conservación y Desarrollo Forestal, Áreas Protegidas y Vida Silvestre e Instituto Hondureño del Café (IHCAFE). También se contó con la participación de investigadores de universidades internacionales como: Universidad de Valladolid (UVa), Universidad de la Habana (UH), Universidad de Costa Rica (UCR), Universidad Santiago de Compostela (USC), Universidad Técnica Particular de Loja (UTPL), Universidad de Barcelona (UB) y Queen´s University Belfast. Aquí queda evidenciado que los lazos o conformación de redes entre universidades, genera una mejor conocimiento y producción científica con contenido de elevada calidad.

El pago por acceso a los artículos científicos se ha convertido en un ¨negocio¨ ya que muchos investigadores requieren publicar ¨si o si¨para mantener su puesto de profesor titular y/o subir de categoria y mantener su ¨status¨, lo que los obliga a caer es esta tentadora oferta. Es indispensable contar con revistas de acceso abierto como lo es Bionatura Journal ya que su contenido es de libre acceso y reconocida reputación, significando un ¨ respiro¨ para la comunidad científica evitando pagar hasta 40 dolares para leer un artículo, promoviendo la transparencia y la integridad en la publicación científica.

Agradecemos la excelente gestión realizada por Bionatura Journal y los lazos generados con nuestra institución.

Bibliographic references

1. Universidad de Murcia, Ranking Scimago, disponible en: https://www.um.es/web/umu-en-cifras/ranquines/scimago (accedido el 06 de febrero de 2022).
2. SCImago. Form. Univ., La Serena, v. 5, n. 5, p. 1, 2012.
3. Base de datos de SCOPUS, FECYT, recursos científicos, disponible en: https://www.recursoscientificos.fecyt.es/licencias/productos-contratados/scopus (accedido el 10 de febrero de 2022).
4. Compendios de investigación Científica, Universidad Nacional Autónoma de Honduras (UNAH), Inciso F, Punto 4, Pg. 19.
5. Journal Scope, Bionatura Journal, disponible en: https://revistabionatura.com/ (accedido el 23 de febrero de 2022).
6. Livia, José; Merino-Soto, Cesar y Livia Ortíz, Rodrigo. Producción científica en la base de datos Scopus de una Universidad privada del Perú. Rev. Digit. Invest. Docencia Univ. 2022, vol.16, n.1.

ARTICLE / INVESTIGACIÓN

Estudio de la variabilidad en el tiempo y espacio de la actividad antioxidante y composición bioquímica de Kappaphycus alvarezii en diferentes densidades de siembra

Study of the variability in time and space of the antioxidant activity and biochemical composition of Kappaphycus alvarezii at different stocking densities

Estefany Lema Ch[1], Iván Chóez-Guaranda[1,2], Omar Ruíz-Barzola[3], Lorena I.Jaramillo[4], Ángela Pacheco Flores de Valgaz[1,5], Sofie Van Den Hende[6] and Patricia Manzano[1,2,3]*

DOI. 10.21931/RB/2023.08.01.13

1   Facultad de Ciencias de la Vida (FCV); Campus Gustavo Galindo; Escuela Superior Politécnica del Litoral; Km. 30.5 vía Perimetral; Guayaquil P.O. Box 09-01-5863; Ecuador; ealema@espol.edu.ec. ; angvapac@espol.edu.ec.
2   Centro de Investigaciones Biotecnológicas del Ecuador (CIBE), Campus Gustavo Galindo; Km 30.5 vía Perimetral; Guayaquil P.O. Box 09-01-5863; Ecuador; iachoez@espol.edu.ec.; pmanzano@espol.edu,ec.
3   Facultad de Ciencias Naturales y Matemáticas (FCNM); Campus Gustavo Galindo; Escuela Superior Politécnica del Litoral (ESPOL), Km. 30.5 vía Perimetral; Guayaquil P.O. Box 09-01-5863; Ecuador; oruiz@espol.edu.ec.
4   Departamento de Ingeniería Química y Agroindustria; Facultad de Ingeniería Química y Agroindustria; Ladrón de Guevara E11-253; Quito 170525 ; Ecuador;
5   Laboratorio de Instrumental; Ingeniería en Biotecnología; Facultad de Ciencias de la Vida; Campus María Auxiliadora; Universidad Politécnica Salesiana (UPS); Km 19.5 vía a la Costa; Guayaquil P.O. Box 09-01-2074, Ecuador. apachecof@ups.edu.ec.
6   Centro Nacional de Acuicultura e Investigaciones Marinas (CENAIM), Escuela Superior Politécnica del Litoral (ESPOL), San Pedro de Manglaralto, P.O. Box 09-01-5863, Santa Elena, Ecuador. shende@espol.edu.ec.
*   Corresponding author: ealema@espol.edu.ec
Available from: http://dx.doi.org/10.21931/RB/2023.08.01.13

Resumen: *Kappaphycus alvarezii* es una de las especies de algas más cultivadas en el mundo, debido a su alto contenido de compuestos bioactivos con reportes antioxidantes y bioestimulantes. El presente estudio evaluó el efecto de las densidades de plantación sobre la composición bioquímica y antioxidante de K. alvarezii cultivada en un sistema de línea larga durante las estaciones seca y húmeda, con el fin de proporcionar una base científica para una cosecha óptima. Se midieron el contenido de humedad, cenizas, grasa, fibra, auxinas, fenoles, flavonoides, DPPH y ABTS. Los datos se analizaron mediante pruebas t, Wilcoxon, Kruskal-Wallis y ANOVA unidireccional. Los resultados mostraron un mayor contenido de grasa (2,01 % P.s), fibra bruta (5,21% P.s), contenido total de fenoles (324,09 μg GAE/g P.s) y ABTS (9,32 μg GAE/g P.s) durante la estación seca. Con respecto a la densidad de plantación, se produjo un aumento significativo del contenido en cenizas, fenoles totales y ABTS con una densidad de 10 líneas.célula^{-1} al mismo tiempo. Los contenidos de flavonoides, DPPH y auxina mostraron una tendencia estacional opuesta, alcanzando los niveles máximos en la estación húmeda. Este estudio aporta nueva información sobre las condiciones ambientales que pueden provocar cambios en la actividad antioxidante y la composición bioquímica de esta especie con vistas al desarrollo de bioproductos para diferentes sectores industriales como el alimentario, el farmacéutico y el de los fertilizantes en Ecuador.
Palabras clave: Alga roja, Fenoles, Flavonoides, Antioxidante, Composición bioquímica, Variación estacional, densidad de siembra.

Abstract: Kappaphycus alvarezii is a species of algae most cultivated in the world, due to its high content of bioactive compounds with reported antioxidant and biostimulant activities. The present study evaluated the effect of stocking densities on the biochemical and antioxidant composition of K. alvarezii cultivated in a long-line system, during the dry and wet seasons to provide a scientific basis for optimal harvesting. Moisture content, ash, fat, fiber, auxins, phenols, flavonoids, DPPH, and ABTS were measured. Data were analyzed using t-tests, Wilcoxon, Kruskal-Wallis, and one-way ANOVA. The results showed a higher fat content (2.01% P.s), crude fiber (5.21% P.s), total phenol content (324.09 μg GAE/g P.s), and ABTS (9.32 μg GAE/g P.s) during the dry season. Concerning the stocking density, a significant increase in the content of ash, total phenols, and ABTS was evidenced in the density of 10 lines.cell-1 at the same time. On the other hand, the content of flavonoids, DPPH, and auxins showed an opposite seasonal trend, reaching maximum levels in the wet season. This study provides new information on the environmental conditions that can lead to changes in the antioxidant activity and biochemical composition of this species to develop bioproducts for different industrial sectors such as food, pharmaceutical, and fertilizer in Ecuador.
Keywords: Red algae; Phenols; Flavonoids; antioxidants; Biochemical composition; Seasonal variation; stocking **density.**

Introducción

En los últimas décadas, se ha incrementado el interés por la búsqueda de nuevos compuestos naturales con actividades potenciales para la alimentación y aplicaciones tanto biomédica como agrícola por parte de las industrias dedicadas al desarrollo de nuevos alimentos funcionales, fármacos y fertilizantes[1,2]. Algunas excelentes candidatas

Estefany Lema Ch, Iván Chóez-Guaranda, Omar Ruíz-Barzola, Lorena Jaramillo, Ángela Pacheco Flores de Valgaz, Sofie Van Der Hende and Patricia Manzano

son las macroalgas que han sido utilizadas para la alimentación humana en los países asiáticos durante siglos, mientras que en América constituyen un recurso infraexplotado, empleado especialmente como materia prima para la industria de los ficoloides[3,4]. En el 2019, las algas marinas alcanzaron los 34,7 millones de toneladas en peso fresco que representan el 28,9 % de la producción acuícola mundial del total de todas las especies[5]. Como resultado de la creciente demanda, las especies de macroalgas comestibles se han producido con éxito en los sistema agrícolas como las macroalgas pardas a mencionar: *Saccharina japónica*, *Undaria pinnatifda* y las macroalgas rojas *Porphyra capensis*, *Kappaphycus alvarezii* y *Gracilaria fusiforme*[6].

K. alvarezii (Doty) Doty ex P.C. Silva. conocida como "cottonii", es una especie de macroalgas roja originaria de Filipinas, que ha sido cultivada con éxito en más de 20 países desde que la demanda de materias primas de carragenina aumentó rápidamente por parte de una industria que dependía de la explotación de lechos naturales[7]. Esta especie contiene un alto contenido de proteínas, minerales, fibra dietética, ácidos grasos poliinsaturados[8,9], reguladores de crecimiento como giberelinas, auxinas y citoquininas[10,11], así como otros metabolitos secundarios que han reportado propiedades antioxidantes, antibacterianas[12,13], antiabéticas y antihiperlipidémicas[14] entre otras.

En particular, los antioxidantes se han asociado con la prevención o el tratamiento de enfermedades de origen cardiaco e inmunológico, debido a su capacidad para mitigar el envejecimiento celular en el organismo cuando se exponen a condiciones de estrés oxidativos[2,15]. Se ha informado que los compuestos antioxidantes extraídos de las algas son muy utilizados como materiales biodegradable de empaque de alimentos por su propiedades formadoras de películas[16]. Asimismo han sido usados como estabilizadores o conservantes en productos alimenticios enriquecidos con lípidos para atenuar el deterioro de su calidad y prolongar su vida de anaquel, sustituyendo el uso indiscriminado de antioxidantes artificiales, los cuales se han vuelto controversiales, debido a su toxicidad sobre la salud[17-19]. También se ha descrito en la literatura la eficacia de la savia de *K. alvarezii* como bioestimulante o fuentes de potasio empleados en diversos cultivos, fomentando su aplicación en las industrias alimenticias, farmacéuticas y de fertilizantes[20-22].

Considerando una mejor utilización de esta especie es importante comprender las variaciones en el contenido y la diversidad de los metabolitos de las algas como producto de varios factores tales como la temporada, calidad de agua,estado reproductivo, período de cultivo, densidad de siembra, profundidad de cultivo y la zona geográfica que pueden estimular o inhibir la biosíntesis de varios nutrientes[23-25].

Se han informado cambios estacionales en el perfil químico y de antioxidantes en *K.alvarezii* y de otras especies de macroalgas cultivadas en diferentes partes del mundo[8,26-28]. Del mismo modo, se ha indicado que el contenido de polifenoles, proteínas, lípidos, fibras y carbohidratos se ven afectados por los niveles de irradiación UV, temperatura del agua, precipitación, salinidad y nutrientes[29-32].

Dentro de la información resultante de varias investigaciones que abarca la caracterización de compuestos bioactivos de varias algas marinas[33], no se ha reportado estudios en Ecuador sobre la influencia que ejerce la variación estacional y la densidad de siembra sobre la composición bioquímica y la actividad antioxidante en *K. alvarezii*.

Por lo que el presente proyecto de investigación tiene como objetivo evaluar los efectos de la época humeda, época seca y la densidad de siembra sobre el perfil bioquímico y las propiedades antioxidantes de *K.alvarezii* cultivada en las zonas costeras del Ecuador, a fin de proporcionar una base científica para una recolección óptima.

Los resultados sugieren que *K. alvarezii* es una fuente sustentable de compuestos bioactivos para su aplicación comercial como antioxidante y bioestimulante natural en productos alimenticios, nutracéuticos y fertilizantes.

Materiales y métodos

Ubicación, recolección y procesamiento

Kappapycus alvarezii fue recolectada en las cosechas de enero y agosto del 2021, que representa la época húmeda y seca en el cantón Santa Rosa (S2°13'34.39"O80°51'31.43"), de la provincia de Santa Elena, Ecuador, durante la marea baja. La determinación del estudio de las densidades de siembra sólo se realizó en la época seca (agosto) debido a las restricciones de movilidad por pandemia, las cuales impidieron que se realice el cultivo en diferentes densidades en la época húmeda (enero). La siembra y la cosecha en diferentes densidades de población se realizó de la siguiente manera (fig.1 y 2): En la balsa flotante (long-line) se cultivaron bajo tres diferentes densidades de siembra (6,8 y 10 líneas.celda^{-1}) que constituye el número de líneas que está conformada una celda. En cada celda de 3x5 m, se colocaron cada una de las redes tubulares inoculadas con las plántulas previamente libres de impurezas a lo largo de cada cuerda de polipropileno (líneas), luego de 45 días se procedió a tomar 1,5kg de muestra fresca de cada línea correspondiente a las tres densidades de siembra (n = 24). Todas las muestras se lavaron minuciosamente con agua potable para la eliminación total de epífitas,congeladas a -80 °C y liofilizadas (Labconco). Las muestras secas se trituraron en un molino de

Figura 1. Método de siembra por red tubular. A-B)Inoculación de plántulas de algas en malla tubular a través de un tubo PVC de 75 mm con 1 m de longitud. C)Atamiento de cada una de las redes tubulares con algas en el sistema de cultivo long-line.
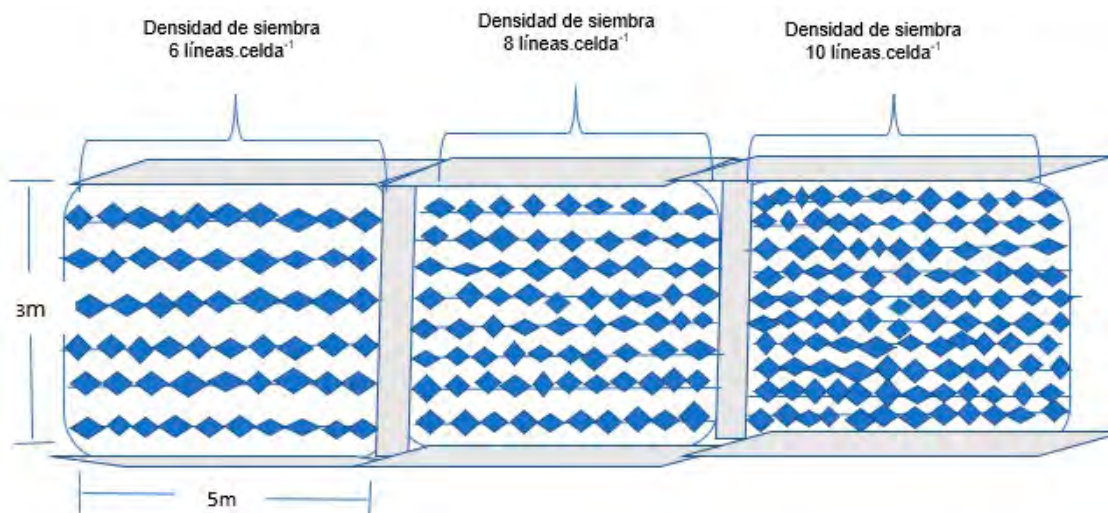
Figura 2. Esquema que conforma la balsa utilizadas para el cultivo de *Kappaphycus alvarezii*, con las líneas de cultivo que representan cada densidad de siembra.

café a un tamaño de partícula de 250 μm y se almacenaron en un desecador hasta su posterior análisis.

Disolvente y reactivo

Todos los reactivos químicos y solventes utilizados se obtuvieron de Sigma-Aldrich.

Composición proximal

Los contenidos de humedad, cenizas, lípidos y fibra en las algas marinas se analizaron de acuerdo al método estándar oficial de la AOAC (2003)[34] con algunas modificaciones.

La humedad se analizó utilizando muestras frescas, pesadas y secadas en una estufa a 105°C durante 2 horas hasta obtener un peso constante. El contenido de humedad se expresó como porcentaje de peso fresco.

La ceniza total se obtuvo por calcinación de la biomasa seca en una mufla a 750°C por 4 horas y los resultados se expresaron como porcentaje del peso seco.

Los lípidos del polvo de alga fueron (aprox.4g) extraídos durante 4 horas en un extractor de Soxhlet empleando hexano como disolvente.

La fibra cruda se cuantificó en muestras desgrasadas de 2g previamente hervidas con 200 ml de H_2SO_4 al 1,25 %. La mezcla se filtró y se lavó con agua hirviendo hasta un pH 7. El residuo obtenido se volvió a extraer con 200 ml de NaOH al 1,25 %, luego se lavó con agua destilada hirviendo y finalmente se secó a 105°C hasta peso constante. El residuo seco se incineró a 600°C durante 1 hora y los resultados se expresaron como porcentaje del peso seco.

Extracción y purificación de auxinas

La extracción y purificación de auxinas se basó de acuerdo con la metodología adoptada por Díaz *et al.*[35] y Prasad *et al.*[36] con algunas modificaciones. Cada gramo de muestra seca se combinó con 10 ml de etanol. La mezcla se digestó utilizando una plancha de calentamiento (Fisher Scientific) a 47°C a 48 minutos. El sobrenadante obtenido se rotavaporó hasta sequedad y se mezclaron 400 uL de agua acidificada de pH 3 con 1,2 ml de acetato de etilo formandose dos fases. Se procedió a extraer, rotavaporar hasta sequedad la fase de acetato y después se resuspendió en metanol.

Extracción de antioxidante

El proceso de extracción de los antioxidantes se basó de acuerdo a la metodología adoptada por Diyana *et al.*[37]. El polvo liofilizado del alga fue extraído con etanol al 50 %, se maceraron en agitador rotatorio durante 72 horas a temperatura ambiente, luego los extractos se filtraron y se almacenaron en frascos ambar de 10 ml a -17 °C hasta su análisis.

Análisis espectrométricos

Detección y cuantificación de auxinas

La determinación de auxinas totales se realizó con el reactivo de Salkowsky según lo descrito por Weber *et al.*[38] con algunas modificaciones. Para la preparación del reactivo se basó de acuerdo con Gang *et al.*[39]. Se hizo reaccionar 50 μL de muestra con 100 μL de la solución del reactivo de Salkowsky (v/v) en una placa de 96 pocillos y se incubó durante 30 minutos en la oscuridad a temperatura ambiente. La absorbancia se midió a una longitud de onda de 540 nm mediante un espectrofotómetro UV-VIS. El contenido auxinas totales se expresó en mg equivalente de ácido indolacético por gramo de peso seco de la muestra (mg AIA/g P.s).

Contenido de fenoles totales

La estimación de fenoles totales en los extractos se realizó con el reactivo de Folin-Ciocalteu por el método colorimétrico descrito por Zhon *et al.*[37]. Se mezcló 25 μL de extracto con 25 μL de la solución del reactivo de Folin y 200 μL de agua destilada en una placa de 96 pocillos y se dejó reposar a temperatura ambiente durante 5 minutos. Se añadio a la mezcla, 25 μL de una solución de Na2CO3 al 10 % y se incubó en la oscuridad durante 60 minutos. La absorbancia se midió a 765 nm en un espectrofotómetro UV-Vis (Synergy™ 5, BioTek). El contenido fenólico se expresó como mg equivalente de ácido gálico por gramo de peso seco de la muestra (mg GAE/g Ps).

Contenido de flavonoides totales

El contenido de flavonoides se estimó según el método de Avramova *et al.*[40]. Se hicieron reaccionar 20 μL de muestra con 200 μl de la mezcla de reactivos preparado por separado con etanol absoluto, cloruro de aluminio al 10 %,

3

Estefany Lema Ch, Iván Chóez-Guaranda, Omar Ruíz-Barzola, Lorena Jaramillo, Ángela Pacheco Flores de Valgaz, Sofie Van Der Hende and Patricia Manzano

acetato de potasio 1 M y agua destilada en una microplaca de 96 pocillos durante 30 minutos a temperatura ambiente lejos de la luz. La absorbancia se midió a 415 nm en un espectrofotómetro UV-Vis (Synergy™ 5, BioTek). Los resultados se expresaron como mg equivalente de quercetina por gramo de peso seco de la muestra (mg QE/g P.s).

Actividad de eliminación de radicales DPPH

La actividad secuestrante de radicales DPPH se analizó con el método descrito por Viteris et al.41 con ligeras modificación. A 50 μL de muestra se añadio 150 μL de una solución de DPPH etanólico (0,15 mM) en una microplaca de 96 pocillos. La mezcla se incubó a temperatura ambiente durante 30 minutos y se midió la absorbancia a 517 nm en un espectrofotómetro UV-Vis (Synergy™ 5, BioTek). La actividad antioxidante se expresó en mg equivalente de trolox por gramo de peso seco de la muestra (mg TE/g P.s).

Actividad de eliminación de radicales ABTS

El método utilizado fue descrito por Viteris et al.41 con ligeras variaciones. La solución de ABTS•+ se preparó mezclando ABTS (7 mM) y persulfato de potasio (3,6 mM) en agua destilada, luego la solución se agitó y se mantuvo en reposo en la oscuridad a 4°C,durante 18 horas para permitir la generación de radicales libres. Se diluyó 610 μL de la solución ABTS•+ en 25 ml de etanol absoluto. Se agregó 50 μL de muestra o las soluciones estándar diluidas en cada pocillo de la microplaca por triplicado y se añadió 150 μL de ABTS. La mezcla de la reacción se incubó durante 30 minutos en la oscuridad a temperatura ambiente y se midió la absorbancia a 732 nm en un espectrofotómetro UV-Vis (Synergy™ 5, BioTek). Los resultados se expresaron en mg equivalente de trolox por gramo de peso seco de la muestra (mg TE/g Ps).

Análisis estadístico

El contenido de humedad, cenizas y fibras, al igual que las auxinas totales fueron analizados con la prueba paramétrica t, después de comprobar la normalidad de los datos. Los compuestos fenólicos y antioxidantes (DPPH y ABTS) fueron analizados a través de la prueba no paramétrica de Wilcoxon, debido a que no se cumplieron los supuestos estadísticos; considerando dos momentos de cosechas (Enero y agosto). En cuanto al estudio de densidades de siembra, los datos del contenido de humedad, cenizas, lípidos y fibras, así como los compuestos antioxidantes se analizaron mediante la prueba de Kruskal-Wallis debido a la heterogeneidad de las varianzas. Por otro lado, el contenido de auxinas se determinó mediante ANOVA unidireccional utilizando Tukey para determinar la diferencia entre los tratamientos. Todas las pruebas estadísticas fueron realizadas con un nivel de significación del 5%. Los análisis estadísticos se realizaron utilizando el software R versión 4.2.0.

Resultados

Composición química de *K. alvarezii*

La Tabla 1 muestra el contenido de humedad, cenizas, lípidos y fibras de *K. alvarezii*, recolectada en Santa Rosa, Ecuador en los meses de enero y agosto del 2021. Los contenidos de humedad y cenizas no fueron muy diferentes entre las dos estaciones. Según las pruebas t y Tukey mostraron que ambos parámetros no se vieron afectados significativamente por la estacionalidad . Por lo general, las algas marinas contienen concentraciones más altas de fibras. Sin embargo, el contenido de fibra de está rodófita fueron relativamente bajos entre las dos épocas. Los niveles de fibras y lípidos mostraron diferencias estadísticamente significativas.

La variación de las diferentes densidades de siembra sobre los contenidos de humedad, cenizas, grasas y fibras en *K. alvarezii* se presentan en la tabla 2.

Las pruebas de Mann-Whitney y Kruskal-Wallis que el contenido de humedad, lípidos y fibras no mostraron diferencias significativas entre las tres densidades de siembra mientras que el contenido de cenizas tuvo hubo un efecto significativo.

Contenido de auxinas totales en *K. alvarezii*

La variación estacional sobre el contenido endógeno

Temporada	n_i	Humedad (%)[1]	Cenizas (%)[2]	Lípidos (%)[2]	Fibras (%)[2]
Enero 2021 (Época húmeda)	5	83,73 ± 0,70 [a]	20,78 ± 0,35 [a]	0,81 ± 0,06 [a]	4,34 ± 0,11 [a]
Agosto 2021 (Época seca)	10	84,88 ± 0,68 [a]	21,60 ± 0,61 [a]	2,01± 0,04 [b]	5,21 ± 0,11 [b]

Los datos se presentan como media ± error estándar de los tratamientos. n_i = tamaño de muestra en cada mes de colecta. Las mismas letras dentro de las columnas indican que no hubo diferencias significativas ($p > 0,05$). Las diferentes letras dentro de las columnas indican diferencias significativas ($p < 0,05$) según la prueba de Tukey. [1]En base de peso húmedo. [2]En base del peso seco.

Tabla 1. Variación estacional del contenido de humedad, cenizas, lípidos y fibra en *K.alvarezii* correspondiente en la densidad 10 líneas.celda[-1].

Densidades de siembra (líneas.celda[-1])	n_i	Humedad (%)[1]	Cenizas (%)[2]	Lípidos (%)[2]	Fibras (%)[2]
6	6	83,19 (5,17) [a]	19,37 (2,50) [a]	2,06 (0,76) [a]	4,92 (0,90) [a]
8	8	85,62 (1,54) [a]	19,69 (1,88) [a]	2,02 (0,37) [a]	5,43 (0,59) [a]
10	10	85,27(5,34) [a]	21,27 (1,70) [b]	2,03 (0,20) [a]	5,22 (0,60) [a]

Los valores se presentan como mediana (rango intercuartil) de los tratamientos. n_i = tamaño de la muestra tomada en cada densidad de siembra. Las letras similares dentro de las columnas indican que no hay diferencias significativas ($p > 0,05$). Las letras diferentes dentro de las columnas indican diferencias significativas ($p < 0,05$) de acuerdo con la prueba de Mann-Whitney. [1]En base de peso húmedo .[2] En base de peso seco.

Tabla 2. Composición química de *K. alvarezii* cultivada en diferentes densidades de siembra en el agosto (época seca).

de auxinas en *K. alvarezii* se muestran en la Tabla 3 y bajo tres diferentes densidades de siembra en la tabla 4.

Contenido fenólico y antioxidante en *K. alvarezii*

Se prepararon ABTS y DPPH para estimar las actividades antioxidantes en extractos etanólico al 50%. El uso de solventes orgánicos combinados con agua puede producir un medio moderadamente polar que aumentará la extracción de antioxidantes[42,43]. Los altos valores de actividad antioxidante en extractos acuosos con 50% de solvente se deben al alto contenido de moléculas fenólicas presentes en los tejidos vegetales, puesto que al adicionar agua al disolvente orgánico facilita la extracción de químicos que son solubles en agua y/o solvente orgánico. Se empleo del etanol al 50% para extracción de compuestos fenólicos y antioxidantes por considerarse dentro de los grupos de solventes no tóxicos, se ha informado que la mezcla eta-

nol-agua, particularmente 50% de etanol, es la más idónea para mantener una alta actividad antioxidante en algas marinas[44,45]. La variación estacional sobre la composición fenólica y antioxidante de *K. alvarezii* se resume en la tabla 5 y su contenido en tres diferentes densidades de siembra en el mes de agosto (época seca) en la tabla 6.

Discusión

Composición química de *Kappaphycus alvarezii*

En general, las algas frescas exhiben un alto contenido de humedad que oscila entre 70 y 90%[46-48], rango que encajan perfectamente con los valores encontrados en este estudio (Tabla 1). Aun cuando, tuvo un mayor contenido de humedad en agosto (84,88 %) que en enero (83,73 %), la diferencia no fue significativa (p > 0,05) entre las dos

Fitohormona (ppm)	Temporada	
	Enero 2021 (Época húmeda)	Agosto 2021 (Época seca)
Auxina totales	0,05 ± 0,003 [b]	0,04 ± 0,002 [a]

Los valores se presentan como media ± error estándar de los tratamientos. n_i = tamaño de muestra en cada mes de colecta. Las letras diferentes dentro de las columnas son significativamente diferentes ($p < 0,05$) de acuerdo con la prueba de Tukey. P.s = peso seco de la muestra. ppm= parte por millón.

Tabla 3. Variación estacional del contenido de auxinas de *K. alvarezii* en la densidad 10 líneas.celda[-1].

Fitohormona (ppm)	Densidades de siembra		
	6 Líneas.celda[-1]	8 Líneas.celda[-1]	10 Líneas.celda[-1]
Auxinas totales	0,04 ± 0,003 [a]	0,04 ± 0,001 [a]	0,04 ± 0,002 [a]

Los valores se presentan como media ± error estándar de los tratamientos. Las letras dentro de las columnas seguidas por las diferentes similares no son significativamente diferentes ($p > 0,05$) de acuerdo con la prueba de Tukey. P.s = peso seco de la muestra. ppm = parte por millón.

Tabla 4. Auxinas totales en *K. alvarezii* cultivada en diferentes densidades de siembra en el mes de agosto (Época seca).

Temporada	Extracto	n_i	Fenoles totales (µg GAE/g P.s)	Flavonoides totales (µg GAE/g P.s)	ABTS (µmol TE/g P.s)	DPPH (µmol TE/g P.s)
Enero 2021 (Época húmeda)	Hidroetanólico (50:50,v/v)	5	60,59 (25,89) [a]	151,95 (14,04) [a]	6,09 (1,29) [a]	0,89 (0,21) [a]
Agosto 2021 (Época seca)		10	324,09 (85,30) [b]	73,96 (27,25) [b]	9,32 (0,60) [b]	0,30 (0,15) [b]

Los valores se presentan como mediana (rango intercuartil) de los tratamientos. n_i = tamaño de la muestra tomada en cada mes de colecta. Las letras diferentes dentro de las columnas indican diferencias significativas (P < 0.05) de acuerdo con la prueba de Mann-Withney. P.s= peso seco de la muestra; GAE=equivalente de ácido gálico; QE=equivalente de quercetina; TE=equivalente de trolox.

Tabla 5. Variación estacional del contenido fenólico y antioxidante en *K. alvarezii* correspondiente a la densidad 10 línea.celda[-1].

Extracción	Densidades de siembra (líneas.celda[-1])	n_i	Fenoles totales (µg GAE/g P.s)	Flavonoides totales (µg GAE/g P.s)	ABTS (µmol TE/g P.s)	DPPH (µmol TE/g P.s)
Hidroetanólico (50:50,v/v)	6	6	286,89 (116,49) [a]	76,95 (28,62) [a]	8,95 (1,23) [b]	0,34 (0,16) [a]
	8	8	252,33 (113,35) [ab]	80,48 (14,09) [a]	8,04 (1,05) [a]	0,29 (0,18) [a]
	10	10	324,09 (79,50) [b]	73,95 (27,89) [a]	9,32 (0,55) [b]	0,30 (0,14) [a]

Los valores se presentan como mediana (rango intercuartil) de los tratamientos. n_i = tamaño de muestra tomadas en cada densidad de siembra. Las letras similares dentro de las columnas indican que no hay diferencias significativas (P > 0,05). Las letras diferentes dentro de las columnas indican diferencias significativas (P < 0,05) de acuerdo con la prueba de Mann-Whitney ; P.s = peso seco de la muestra; GAE=equivalente de ácido gálico; QE=equivalente de quercetina; TE=equivalente de trolox.

Tabla 6. Composición fenólica y antioxidante de *K.alvarezii* cultivada en diferentes densidades de siembra en el mes de agosto (época seca).

Estefany Lema Ch, Iván Chóez-Guaranda, Omar Ruíz-Barzola, Lorena Jaramillo, Ángela Pacheco Flores de Valgaz, Sofie Van Der Hende and Patricia Manzano

épocas de estudio. Aroyehun et al.[49] informaron un patrón similar al no hallar diferencias significativas entre las estaciones en el contenido de humedad en la macroalga roja *G. manilaensis*. Alternativamente, Schiener et al.[50] reportaron un mayor contenido de humedad en 4 especies de macroalgas pardas *Laminaria digitata*, *Laminaria hyperborea*, *Saccharina latissima* y *Alaria esculenta* durante los meses de invierno y menor en los meses de otoño. Los resultados difieren con el estudio de las macroalgas pardas, debido a las distintas especies, ubicación de muestreo, ya que las muestras fueron cultivadas y no se recolectadas en zonas intermareales en donde frecuentemente están expuestas a ciclos de desecación y rehidratación del mar[51].

Los resultados también mostraron un alto contenido de cenizas en ambos períodos (Tabla 1) lo cual puede deberse a la presencia de sal en los talos (tejido vegetativo de las algas), como resultado de una alta salinidad en el sitio de muestreo[52,53]. En este sentido, el alto porcentaje de cenizas refleja su riqueza considerable de minerales, especialmente potasio y sodio encontrados en está alga[8]. El contenido de cenizas de *K. alvarezii* se ubica dentro del amplio rango descrito en la literatura para macroalgas rojas (5,8-46,2 % P.s)[51]. A pesar de que los valores de cenizas aumentaron ligeramente de enero a agosto, esto no fue estadísticamente significativo ($p > 0,05$), por lo que los cambios estacionales no parecieron afectar este parámetro. Sin embargo, esto se debería confirmar ampliando el número de períodos de muestreo. Kumar et al.[8] informó una tendencia opuesta para la variación de cenizas de *K.alvarezii* recolectada en la costa noroeste de India, con altos niveles de cenizas registrado en verano y los más bajos en invierno. De manera similar, Araujo et al.[26] registraron un mayor porcentaje de cenizas en esta misma especie de alga durante el verano en la costa de San Paulo, Brazil. Estas diferencias se deben a las flutuaciones meterológicas y ambientales.

En cuando al contenido de lípidos, en las dos estaciones fueron relativamente bajos, alcanzando un mayor contenido en agosto (época seca) en comparación con enero (época húmeda) cuyo contenido se reduce en menos de la mitad (Tabla 1). De acuerdo con los análisis estadísticos mostraron diferencias estacionales significativos en el contenido de lípido ($p < 0,05$). Se ha evidenciado que la mayoría de algas rojas contiene un bajo porcentaje de lípido que varía entre 0,3 y 3,8 % P.s, lo que indica un bajo contenido calórico, en comparación con los vegetales terrestres[54]. Khairy et al.[55] informaron un patrón similar en el que reportaron una mayor concentración de lípidos durante la temporada de baja temperatura, así como otros autores al determinar el contenido de lípidos en macroalgas del género *Ulva sp*[56-58]. En contraste a los resultados presentados en este estudio, otros autores han registrado un mayor contenido de lípidos en *Fucus sp.* durante el verano en diferentes localidades del continente europeo, donde las temperaturas son muy altas[47,59]. Aunque estos resultados puedan parecer discordante con los casos anteriores, es presumible que estos variaciones en los niveles de lípidos no solo dependieron de la temperatura, sino que puedan deberse a la etapa del ciclo de vida, como factores fisiológicos o incluso biológicos[60,61].

El contenido de fibra cruda varió en menor grado, pero con significativas ($p < 0,05$) diferencias entre los meses de estudio (Tabla 1). Estos resultados coinciden con los niveles de fibras reportados previamente para otras especies de macroalgas incluida *K.alvarezii* recolectadas en la zona costera de Ecuador (0,9-5 % P.s)[33] en los meses de marzo y mayo del 2017, pero inferior a los valores informado para *K. alvarezii*, la cual fluctuó entre 9,68 y 18,57 % P.s, durante el transcurso de tres años en Okha, noroeste de India. Por otro lado, se encontró un mayor contenido de fibra para diferentes especies de macroalgas durante el invierno (42,5 % P.s) y un menor contenido durante el verano y otoño (33,1 % P.s) en las costa del Mar Rojo[62]. Esto puede suscitarse debido a factores como: la etapa de crecimiento, la actividad fotosintética y la absorción de nutrientes, como señalan Rajauria et al.[63] respecto al contenido de fibra en las algas marinas.

El contenido de humedad presentó un incremento a medida que la densidad de siembra aumentó, pero sin significación estadística ($p > 0,05$) (Tabla 2). Este hecho pudo deberse a que las muestras estuvieron expuestas a las mismas condiciones ambientales. Cabe señalar, que estos datos no pudieron ser comparables con otros trabajos, ya que, no hay información disponible en la literatura donde evalúen la variabilidad de humedad en *K.alvarezii*, ni en otras especies de algas semejantes en función a la densidad de siembra, por lo que este es el primer informe que evalúa este parámetro en condiciones naturales de cultivo.

En lo concerniente al contenido de cenizas, se evidenció un mayor porcentaje a medida que la densidad de siembra aumentaba (Tabla 2), encontrándose diferencias significativas ($p < 0,05$). Esta tendencia es diferente con lo reportado por otros estudios, donde se registró un mayor contenido de cenizas en otra alga del género *Ulva* cuando la densidad de cultivo disminuyó[64,65]. Estos investigadores alegan que el contenido de ceniza está influenciado por la densidad de siembra debido a que al existir una menor población la tasa de competencia disminuye, por lo tanto, hay una mayor exposición de la luz solar y absorción de nutrientes sobre las poblaciones de algas, lo que deriva a un aumento sustancial de cenizas en las mismas. Sin embargo, esta teoría no concuerda con este estudio, por lo que se especula que podría estar más asociado a factores geográficos y ambientales como la temperatura, salinidad y los nutrientes. Se sugiere corroborar tal hipótesis extendiendo el muestreo por varios meses del año en diferentes densidades, considerando estos parámetros ambientes.

En cuanto a los niveles de lípidos entre las tres densidades, fueron relativamente similares; alrededor de 2,00 % P.s (Tabla 2), análogos con el rango reportado para *K.alvarezii* cultivada en la zona costera de Indonesia[66] (0,73-2,08 % P.s) pero superiores para los especímenes cosechados en diferentes sitios de la zona costera del continente asiático (0,03-1,0 % P.s)[32,67,89]. Es posible que las diferencias del contenido de lípidos en la misma especie se deban a la variedad de cepas, regiones geográficas y las estaciones[61,68]. Según los resultados estadísticos, la interacción entre las densidades de siembra y los niveles de lípidos no fue estadísticamente diferente ($p > 0,05$). Se registró un comportamiento similar en los niveles de lípidos para la macroalga *D.tenuissima*, puesto que, no tuvieron un efecto significativo en las cinco diferentes densidades de siembra probadas[69]. Por el contrario, otro estudio[64] observaron un aumento sustancial en el contenido de lípidos en *Ulva rigida* cuando se exponían a un déficit de nitrógeno y a una alta densidad de población, condiciones que favorecieron al mecanismo de almacenamiento de energía y la síntesis de lípidos en donde el exceso de carbono en vez de transformarse en proteína se almacena en forma de grasa[59]. En complemento, Khotimchenko et al.[70] indicaron que las condiciones subóptima de luz, favorecen al aumento de lípidos

en las membranas fotosintéticas de las macroalgas como consecuencia de la acumulación de glicolípidos en las mismas. Factores como la condición fisiológicas de los talos, etapa de vida o incluso los procedimientos de extracción pudieron haber contribuido en estos resultados[71].

En el contenido de fibra cruda no se encontró diferencias significativas entre las tres densidades de siembra (p > 0,05) (Tabla 2). Se ha informado valores similares a los obtenidos para *K.alvarezii* cultivada en diferentes sitios de Indonesia (4,3–6,6 % P.s)[72] , y particularmente superior a lo registrado para las muestras de Gorontalo, Indonesia (0,40-0,87%)[32]. Marinho *et al.*[23]. y Denis *et al.*[73] reportaron un alto porcentaje fibra en las rodófitas Gracilaria cervicornis (56,54 %) de Brazil y Grateloupia turuturu (60 %) de Francia. De acuerdo a estos hallazgos, el contenido de fibra en algas rojas pueden diferir según los taxones, ubicación geográfica, madurez y los factores abióticos[51]. No se encontraron en la literatura revisada una evaluación comparable sobre la influencia de la densidad de siembra sobre el contenido de fibra en *K.alvarezii*. Este enfoque solo ha sido planteado previamente por Queiros *et al.*[64] en *Ulva rigida*, donde evaluaron los cambios en la composición de polisacáridos de *U. rigida* en función a la densidad de siembra. En su estudio los autores no detectaron ninguna diferencia entre los niveles de fibras y la densidad de siembra, aunque varios investigadores han manifestado que el contenido de fibra está asociado con la limitación de nutrientes en el medio como el nitrógeno, etapa de crecimiento y la actividad fotosintética entre las especies de algas[74].

Contenido de auxinas totales en *K. alvarezii*

El contenido endógeno de auxinas totales de esta especie, mostraron un ligero aumento durante enero con un 0,05 ppm en comparación con agosto que tuvo un valor de 0,04 ppm (Tabla 3). La variación estacional de auxinas totales fue estadísticamente significativa (p < 0,05). Como sabemos no hay trabajos publicados que evalúen la influencia de la estacionalidad en el contenido de auxinas de *K.alvarezii*, ni otros especímenes de macroalgas. A pesar de sus diferencias taxonómicas, siguió la misma tendencia reportada por Sivaci y Yalcin *et al.*[75] quienes registraron una mayor concentracción de AIA en diferentes variedades manzanas (*Malus syvestris* Miller) durante la primavera como resultado de una mayor actividad fotosintética producida durante este período. Cabe indicar que las algas como las plantas terrestres realizan las mismas funciones metabólicas, puesto que ambas son organismos fotosintéticos. Los datos de este estudio podrían atribuirse al período de crecimiento como consecuencia de las condiciones ambientales a las que estuvieron expuestas durante su ciclo de reproducción[10], dado que las auxinas intervienen en el crecimiento, desarrollo y metabolismo de las algas marinas[76-78], siendo este el primer estudio en determinar el efecto de la estacionalidad sobre la concentración auxinas.

Como se evidenció en la tabla 4, las tres densidades obtuvieron similares concentraciones de auxinas, sin encontrarse diferencias significativas entre ellas (p > 0,05). Se cree que el rango de valores de densidad de siembra puede tratarse de un rango no influyente sobre el contenido de auxinas totales a las condiciones ambientales (temperatura del agua, salinidad y nutrientes) correspondientes al sitio de cultivo y cosecha. Sin embargo, se necesitarían más datos relacionados con este tema para confirmar está presunción. Otros estudios también han encontrado valores más altos de auxinas en distintas especies de macroalgas

como *Caulerpa racemosa* (10 ppm), *Hipnea corona* (6,70 ppm) y *Ulva lacinulata* (2,30 ppm)[79,80] pero hay que tener en cuenta que los autores no efectuaron ensayos de densidades en su investigación, lo cual pudiera ser debido factores como la densidad de siembra y los procedimientos de análisis utilizados, ya que las muestras del presente estudio se determinaron por espectofotometría UV-visible, en lugar del análisis por cromatografía de alta resolución que fueron empleados por los estudios mencionados anteriormente. La escasez de investigaciones orientadas a estos parámetros dificulta el aprovechamiento de este tipo de biomoléculas de interés biotecnológico de una fuente comercial explotable como el cultivo de *K. alvarezzii*.

Contenido fenólico y antioxidante en *K. alvarezii*

El contenido fenólico de los extractos hidroetanólicos (50:50,v/v) de *K. alvarezii* reflejaron variaciones estacionalmente significativas. El contenido se quintuplica en la época seca en comparación con la época húmeda (Tabla 5). Estos resultados fueron mayores a los reportado previamente para los extractos de etanólico al 50% (173,2 µg GAE g^{-1}P.s)[37] y menor para los extractos metanólicos al 50% (1.150 µg GAE g^{-1}P.s)[12] para la misma especie recolectada en Malasia, aunque los investigadores no mencionan el mes de cosecha. Lo más probable, es que estas diferencias se deban a la polaridad de los disolventes aplicados (el metanol es un disolvente más polar que el etanol) y la solubilidad de los compuestos antioxidantes presentes en las algas. Por otro lado, Araújo *et al.*[26] informaron alto contenido fenólico en *K. alvarezii* durante el otoño (101,39 mg GAE g^{-1} P.s) y más bajos en verano (46,26 mg GAE g^{-1} P.s) en donde la temperatura alcanzan los 30°C. En otras algas rojas también se han reportado el efecto de la estacionalidad y el solvente empleado[81] registrando un mayor contenido fenólico durante el otoño, época que se caracteriza por temperaturas suaves y lluvias escasas.

El contenido de flavonoides varió estacionalmente, reduciéndose su contenido a la mitad en agosto en comparación a enero (Tabla 5). Una tendencia similar fue encontrada en los extractos metanólicos del alga parda *F. spiralis*[4] y *S. latissima*[3], los cuales presentaron niveles superiores de flavonoides durante la temporada de verano en comparación con el invierno. Esto se puede atribuir a los diferentes factores ecológicos, como la temperatura, precipitaciones y la duración e intensidad de la luz solar[42], y que a medida que avanzamos de enero a agosto, el clima se vuelve gradualmente más cálido en el transcurso del día[82]. Es decir, las algas marinas están expuestas a una luz solar más intensa durante varias horas al día, lo que induce una biosíntesis mejorada de flavonoides que, al ser antioxidantes, juegan un papel importante en el sistema de defensa de las algas para resistir a los depredadores y a los desafíos ambientales[83-85].

Con respecto al DPPH, se ha registrado cerca del triple de actividad en enero en comparación a agosto (Tabla 5). Es decir, hubo una reducción en su contenido entre ambas estaciones, lo cual representa una diferencia significativa en el contenido antioxidante de *K.alvarezii* (p < 0,05) respecto a la temporada. Esta observación está de acuerdo con Araujo *et al.*[26] quienes obtuvieron un alto nivel de inhibición de DPPH de *K. alvarezii* durante el verano período que coincide con un aumento notable en la temperatura en las costas de San Paulo, Brazil, y que en general, son calurosos y secos. Según Pedro *et al.*[86], quienes registran una mayor actividad depurativa de DPPH en extractos

etanólicos del alga verde *Codium sp.* durante el verano, este aumento podría estar relacionado a un mecanismo fotoprotector, para resistir el estrés lumínico en respuesta a la radiación UV intensificada[87]. Otros autores han reportado valores superiores de DPPH en diferentes extractos de *K.alvarezii*, aunque no informaron datos de la fecha de cosecha[88,89], lo que puede estar asociado a la participación de otros parámetros, tales como los diferentes métodos de extracción, los solventes aplicados y las diferentes cepas existentes de *K.alvarezii*.

Con lo concerniente al ABTS, los resultados reflejaron variaciones estacionales significativas, registrándose un aumento del 30% en su actividad en agosto en comparación a enero (Tabla 5). Pese a las diferencias taxonómicas y geográficas, estos resultados se asemejan con lo reportado por Pedro *et al.*[86] quienes registraron un mayor contenido de actividad antioxidante ABTS en los extractos etanólicos del alga *Codium sp.* durante el invierno (11,0 μmol TE g^{-1} P.s) y menor en el verano (8,9 μmol TE g^{-1} P.s), lo que se presume que estos resultados obtenidos, guardan una relación con el momento de la cosecha y los solventes empleados para su extracción[44]. Esta fue la única referencia que se asocia el contenido de ABTS con relación a la estacionalidad en especies de macroalgas.

El contenido fenólico presenta su valor máximo en la densidad 10 líneas.celda^{-1}, mientras que los más bajos se registraron en la densidad 8 líneas.celda^{-1}, seguido de la densidad 6 líneas.celda^{-1}. Estos resultados no fueron directamente comparables con los de la literatura, puesto que, hasta la fecha, no hay información reportada sobre la influencia que ejerce la densidad de siembra en el contenido de compuestos fenólico de *K. alvarezii*, incluso en otras especies de macroalgas cultivadas en el mar. Sin embargo, esta tendencia concuerda con la reportada por estudios en otros organismos fotosintéticos, observándose un aumento sustancial en los niveles de ácidos fenólicos a medida que aumentaba la densidad de siembra de hortalizas como: coliflor[90], alcachofas globo[85] y la col rizada[91]. Pese a las diferencias taxonómicas las hortalizas y las algas guardan una similitud debido a que ambas dependen del proceso de la fotosíntesis para su sobrevivencia. En estos estudios de hortalizas los investigadores plantearon la hipótesis de que los altos niveles de compuestos fenólicos podría estar relacionado con la respuesta bioquímica de las plantas como resultado de la competencia intraespecífica por los recursos fotosintéticos[92].

El contenido de flavonoides totales presenta una diferencia no estadísticamente significativa (p >0,05), denotando un efecto nulo sobre el contenido de flavonoides dentro de ese rango de densidad de siembra (Tabla 6). Un estudio comparó la composición química de los brotes de otro organismo fotosintético bajo cinco densidades de siembra diferentes[93] obteniendo un mayor contenido de flavonoide a una baja densidad. Cheng *et al.*[94] han informado que el anabolismo de los flavonoides puede estar estrechamente relacionado con el proceso fotosintético. Por este motivo, no son aconsejables las sobrepoblaciones de siembra, ya que cuando la densidad de cultivo se multiplica se genera mayor competencia por iluminación y ventilación entre la población[95]. Esto podría causar una disminución sustancial de producción.

En cuanto al DPPH tampoco presentó diferencias significativas (p > 0,05) (Tabla 6). Magnusson *et al.*[96] reportó resultados afines en la macroalga *Derbesia tenuissima* cultivada en un sistema terrestre. Las algas han desarrollado mecanismos de defensa como respuesta a estreses abióticos como la intensidad de luz solar en el ambiente que están expuestas durante la fotosíntesis y el transporte de electrones, por lo que se especula que cuando la densidad de población es baja, mayor es la incidencia de la luz sobre los cultivos, lo que desencadena una mayor proliferación de los compuestos antioxidantes[97]. Sin embargo, es meritorio más investigaciones que comparen y contrasten estos valores reportados en *K. alvarezii* en las condiciones dadas de las costas ecuatorianas.

El contenido de ABTS se encuentra dentro del rango reportado en la literatura para algas pardas y rojas recolectadas en la isla de Faial, Portugal (5 y 60 μmol TE g^{-1} P.s)[98]. En este estudio se detectó diferencias entre las densidades de siembra, alcanzando una mayor actividad de 9.32 μmol TE g^{-1} P.s en la densidad de siembra 10 línea.celda^{-1} (Tabla 6). Sin embargo, es difícil determinar que factor ambiental incidió en las variaciones evidenciadas en este estudio, ya que los cambios son pequeños e irregulares, teniendo en cuenta que la macroalga *K.alvarezii* fue recolectada en condiciones naturales, por lo que no es fácil separar los efectos de los factores individuales de la influencia multifactorial del medio ambiente. Por esta razón, se recomienda realizar más ensayos experimentaciones con otras densidades de siembra considerando otras condiciones ecológicas como la irradiación UV, corriente del mar, puesto que estos factores podrían influir en gran medida en la actividad antioxidante de ABTS.

Conclusiones

El contenido de grasas, fibras, fenoles totales y ABTS reflejaron cambios estacionales, obteniéndose un mayor contenido en la época seca (agosto), mientras que en la época húmeda (enero) se registró una alta concentración de flavonoides, auxinas totales y DPPH. La presencia de cada uno de estos componentes hace de *K. alvarezii* un alga muy prometedora para el desarrollo de nuevas industrias mediante el aprovechamiento de sus distintos componentes.

Con respecto a la densidad de siembra, se evidenció un aumento significativo de cenizas, fenoles totales y ABTS en la medida que la densidad aumentó dentro del rango estudiado. En base a estos resultados obtenidos se concluye que la composición bioquímica, así como los valores de bioactividad funcional mostrado en el extracto etanólico de *K. alvarezii* en dos épocas del año, proporcionaron información valiosa sobre el efecto de tres densidades de siembra y dos épocas de cosecha para la recolectar esta alga con perspectiva de desarrollar nuevos bioproductos funcionales en diferentes sectores industriales.

Estos parámetros deben estudiarse en mayores rangos de densidades de siembra y en períodos más largos de tiempo, ya que dependiendo del fin comercial que se le dé al alga, se podrá climatizar las condiciones de cultivo a fin de promover el desarrollo del metabolito de interés. Esta información sobre el efecto de la estacionalidad sobre el contenido de DPPH, compuestos fenólicos, flavonoides, fibras, ABTS es parte de los primeros acercamientos hacia el aprovechamiento comercial de los distintos metabolitos que contiene *K. alvarezii* en países neófitos en su cultivo y en vía desarrollo, ya sea para su uso en condiciones aclimatadas en piscinas o a mar abierto.

Conflictos de Interés

Los autores declaran no tener conflicto de intereses.

Referencias bibliográficas

1. Mekinić, I. G. et al. Phenolic content of brown algae (Pheophyceae) species: Extraction, identification, and quantification. Biomolecules 9, (2019).
2. Choudhary, B., Chauhan, O. P. & Mishra, A. Edible Seaweeds: A Potential Novel Source of Bioactive Metabolites and Nutraceuticals With Human Health Benefits. Front. Mar. Sci. 8, (2021).
3. Marinho, G. S., Sørensen, A. D. M., Safafar, H., Pedersen, A. H. & Holdt, S. L. Antioxidant content and activity of the seaweed Saccharina latissima: a seasonal perspective. J. Appl. Phycol. 31, 1343-1354 (2019).
4. Alemañ, A. E., Robledo, D. & Hayashi, L. Development of seaweed cultivation in Latin America: current trends and future prospects. Phycologia 58, 462-471 (2019).
5. F A O. Seaweeds and microalgae: an overview for unlocking their potential in global aquaculture development. vol. 1229 (2021).
6. Buschmann, A. H. et al. emerging research activity Seaweed production : overview of the global state of exploitation , farming and emerging research activity. Eur. J. Phycol. 52, 391-406 (2017).
7. Hurtado, A. Q., Gerung, G. S., Yasir, S. & Critchley, A. T. Cultivation of tropical red seaweeds in the BIMP-EAGA region. 707-718 (2014) doi:10.1007/s10811-013-0116-Kumar, K. S., Ganesan, K. & Rao, P. V. S. Seasonal variation in nutritional composition of Kappaphycus alvarezii (Doty) Doty — an edible seaweed. 52, 2751-2760 (2015).
8. Aminah, A. & Xiren, G. K. Proximate composition and total amino acid composition of Kappaphycus alvarezii found in the waters of Langkawi and Sabah, Malaysia. Int. Food Res. J. 24, 1255-1260 (2017).
9. Fadilah, S., Alimuddin, Pong-Masak, P. R., Santoso, J. & Parenrengi, A. Growth, Morphology and Growth Related Hormone Level in Kappaphycus alvarezii Produced by Mass Selection in Gorontalo Waters, Indonesia. HAYATI J. Biosci. 23, 29-34 (2016).
10. Mondal, D. et al. Elimination of gibberellin from Kappaphycus alvarezii seaweed sap foliar spray enhances corn stover production without compromising the grain yield advantage. Plant Growth Regul. 75, 657-666 (2015).
11. Chew, Y. L., Lim, Y. Y., Omar, M. & Khoo, K. S. Antioxidant activity of three edible seaweeds from two areas in South East Asia. LWT - Food Sci. Technol. 41, 1067-1072 (2008).
12. Bhuyar, P., Rahim, M. H., Sundararaju, S., Maniam, G. P. & Govindan, N. Antioxidant and antibacterial activity of red seaweed; Kappaphycus alvarezii against pathogenic bacteria. Glob. J. Environ. Sci. Manag. 6, 47-58 (2020).
13. Matanjun, P. & Muhammad, K. Functional Food Laboratory, Faculty of Food Science and Technology and 2 School of Food Science and Nutrition, University of Malaysia Sabah, Kota Kinabalu, Sabah; and 3 Faculty of Veterinary Medicine, University of Putra Malaysia, Serdang, Selangor, Malay. J. Med. Food 13, 1-10 (2010).
14. Karimzadeh, K. & Zahmatkesh, A. Phytochemical screening, antioxidant potential, and cytotoxic effects of different extracts of red algae (Laurencia snyderiae) on HT29 cells. Res. Pharm. Sci. 16, 400-413 (2021).
15. R. Kanatt, S., Lahare, P., P. Chawla, S. & Sharma, A. Kappaphycus alvarezii : Its antioxidant potential and use in bioactive packaging films. J. Microbiol. Biotechnol. food Sci. 5, 1-6 (2015).
16. Shahidi, F. & Zhong, Y. Novel antioxidants in food quality preservation and health promotion. Eur. J. Lipid Sci. Technol. 112, 930-940 (2010).
17. Jerez-Martel, I. et al. Phenolic profile and antioxidant activity of crude extracts from microalgae and Cyanobacteria strains. J. Food Qual. 2017, (2017).
18. Liu, R. & Mabury, S. A. Synthetic Phenolic Antioxidants: A Review of Environmental Occurrence, Fate, Human Exposure, and Toxicity. Environ. Sci. Technol. 54, 11706-11719 (2020).
19. Singh, S., Singh, M. K., Singh, A. K. & Singh, C. S. Application of Seaweed Sap (Kappaphycusalvarezii and Gracilariaedulis) for Higher Productivity of Maize (Zea mays L.). Res. Pap. Res. J. Agric. Sci. 6, 232-234 (2015).
20. Matheus, A. da C. et al. Kappaphycus alvarezii extract used for the seed treatment of soybean culture. African J. Agric. Res. 12, 1054-1058 (2017).
21. Garai, S. et al. Impact of seaweed sap foliar application on growth, yield, and tuber quality of potato (Solanum tuberosum L.). J. Appl. Phycol. 33, 1893-1904 (2021).
22. Marinho-Soriano, E., Fonseca, P. C., Carneiro, M. A. A. & Moreira, W. S. C. Seasonal variation in the chemical composition of two tropical seaweeds. Bioresour. Technol. 97, 2402-2406 (2006).
23. Tirtawijaya, G. et al. Neurotrophic activity of the carrageenophyte Kappaphycus alvarezii cultivated at different depths and for different growth periods in various areas of Indonesia. Evidence-based Complement. Altern. Med. 2018, (2018).
24. Cotas, J. et al. Seaweed phenolics: From extraction to applications. Mar. Drugs 18, (2020).
25. Araújo, P. G. et al. Seasonal variation of nutritional and antioxidant properties of different Kappaphycus alvarezii strains (Rhodophyta) farmed in Brazil. J. Appl. Phycol. 34, 1677-1691 (2022).
26. Francavilla, M., Franchi, M., Monteleone, M. & Caroppo, C. The red seaweed gracilaria gracilis as a multi products source. Mar. Drugs 11, 3754-3776 (2013).
27. Sampath-Wiley, P., Neefus, C. D. & Jahnke, L. S. Seasonal effects of sun exposure and emersion on intertidal seaweed physiology: Fluctuations in antioxidant contents, photosynthetic pigments and photosynthetic efficiency in the red alga Porphyra umbilicalis Kützing (Rhodophyta, Bangiales). J. Exp. Mar. Bio. Ecol. 361, 83-91 (2008).
28. Khairy, H. M. & El-Sheikh, M. A. Antioxidant activity and mineral

Estefany Lema Ch, Iván Chóez-Guaranda, Omar Ruíz-Barzola, Lorena Jaramillo, Ángela Pacheco Flores de Valgaz, Sofie Van Der Hende and Patricia Manzano

composition of three Mediterranean common seaweeds from Abu-Qir Bay, Egypt. Saudi J. Biol. Sci. 22, 623-630 (2015).

29. Parys, S. et al. Seasonal variation of polyphenolics in Ascophyllum nodosum (Phaeophyceae). Eur. J. Phycol. 44, 331-338 (2009).

30. Mannino, A. M., Vaglica, V. & Oddo, E. Seasonal variation in total phenolic content of Dictyopteris polypodioides (Dictyotaceae) and Cystoseira amentacea (Sargassaceae) from the Sicilian coast. Flora Mediterr. 24, 39-50 (2014).

31. Adharini, R. I., Setyawan, A. R., Suadi & Jayanti, A. D. Comparison of Nutritional Composition in Red and Green Strains of Kappaphycus Alvarezii Cultivated in Gorontalo Province, Indonesia. E3S Web Conf. 147, 3-7 (2020).

32. D'Armas, H., Jaramillo, C., D'Armas, M., Echavarría, A. & Valverde, P. Proximate composition of several green, brown and red seaweeds from the coast of Ecuador. Rev. Biol. Trop. 67, 61-68 (2019).

33. AOAC Official Metods of Analysis. Association of Official Analytical Chemists, Washington DC. en (ed. Helrich, K.) vol. 1 73-80 (2003).

34. Sisalema, Á. C. D. Evaluación de la actividad fitorreguladora de auxinas obtenidas a partir de un extracto de tallos de fréjol común (Phaseolus vulgaris L.) en cultivos de plantas in vitro. vol. 10 (Universidad Técnica de Ambato, 2018).

35. Prasad, K. et al. Detection and quantification of some plant growth regulators in a seaweed-based foliar spray employing a mass spectrometric technique sans chromatographic separation. J. Agric. Food Chem. 58, 4594-4601 (2010).

36. Diyana, F., Hisham, S., Chan, K. . & Abdullah, A. Antioxidant activity of red algae Kappaphycus alvarezii and Kappaphycus striatum. Int. Food Res. J. 22, 1977-1984 (2015).

37. Gordon, S. A. & Weber, R. P. Colorimetric estimation of indoleacetic acid. 192-195 (1951).

38. Gang, S., Sharma, S., Saraf, M., Buck, M. & Schumacher, J. Analysis of indole-3-acetic acid (IAA) production in Klebsiella by LC-MS/MS and the Salkowski method. Bio-Protocol 9, 1-9 (2019).

39. Avramova, V. et al. High antioxidant activity facilitates maintenance of cell division in leaves of drought tolerant maize hybrids. Front. Plant Sci. 8, (2017).

40. Viteri, R., Giordano, A., Montenegro, G. & Zacconi, F. Extractos de Eucryphia cordifolia : Cribado fitoquímico , actividades antibacterianas y antioxidantes. 5-8 (2022).

41. Čagalj, M., Skroza, D., Tabanelli, G., Özogul, F. & Šimat, V. Maximizing the antioxidant capacity of Padina pavonica by Choosing the Right drying and extraction methods. Processes 9, 1-15 (2021).

42. Musa, K. H. & Abdullah, A. Antioxidant Activity of Pink-Flesh Guava (Psidium guajava L .): Effect of Extraction Techniques and Solvents. 100-107 (2011) doi:10.1007/s12161-010-9139-3.

43. Almeida, B. et al. Seasonal evaluation of phlorotannin-enriched extracts from brown macroalgae fucus spiralis. Molecules 26, 1-21 (2021).

44. Getachew, A. T., Jacobsen, C. & Holdt, S. L. Emerging technologies for the extraction of marine phenolics: Opportunities and challenges. Mar. Drugs 18, 1-22 (2020).

45. del Olmo, A., Picon, A. & Nuñez, M. Preservation of five edible seaweeds by high pressure processing: effect on microbiota, shelf life, colour, texture and antioxidant capacity. Algal Res. 49, (2020).

46. Paiva, L., Lima, E., Neto, A. I. & Baptista, J. Seasonal variability of the biochemical composition and antioxidant properties of fucus spiralis at two Azorean Islands. Mar. Drugs 16, (2018).

47. Ito, K. & Hori, K. Seaweed: Chemical composmon and potential food uses. Food Rev. Int. 5, 101-144 (1989).

48. Aroyehun, A. Q., Planieveloo, K. & Farid Ghazali, M. R.-I. and A. R. Effects of seasonal variability on the physicochemical,biochemical,and nutritional composition of Western Peninsular Malaysia Gracilaria manilaensis. molecules (2019).

49. Schiener, P., Black, K. D., Stanley, M. S. & Green, D. H. The seasonal variation in the chemical composition of the kelp species Laminaria digitata, Laminaria hyperborea, Saccharina latissima and Alaria esculenta. J. Appl. Phycol. 27, 363-373 (2015).

50. Afonso, C. et al. Seasonal changes in the nutritional composition of agarophyton vermiculophyllum (Rhodophyta, gracilariales) from the center of Portugal. Foods 10, (2021).

51. Wahidatul Husna Zuldin, R. S. Performance of red seaweed (Kappaphycus sp.)cultivates using tank culture system. J. Fish. Aquat. Sci. 8, 80-86 (2015).

52. Msuya, F. E. Effects of stocking density and additional nutrients on growth of the commercially farmed seaweeds Eucheuma denticulatum and Kappaphycus alvarezii in Zanzibar Tanzania. Tanzania J. Nat. Appl. Sci. 4, 605-612 (2013).

53. Makkar, H. P. S. et al. Seaweeds for livestock diets: A review. Anim. Feed Sci. Technol. 212, 1-17 (2016).

54. Khairy, H. M. & El-Shafay, S. M. Seasonal variations in the biochemical composition of some common seaweed species from the coast of Abu Qir Bay, Alexandria, Egypt. Oceanologia 55, 435-452 (2013).

55. Floreto, E. A. T., Hirata, H., Yamasaki, S. & Castro, S. C. Effect of Salinity on the Growth and Fatty Acid Composition of Ulva pertusa Kjellman (Chlorophyta). Bot. Mar. 37, 151-156 (1994).

56. Moreira, A. S. P. et al. Seasonal plasticity of the polar lipidome of Ulva rigida cultivated in a sustainable integrated multi-trophic aquaculture. Algal Res. 49, 101958 (2020).

57. El Maghraby, D. M. & Fakhry, E. M. Lipid content and fatty acid composition of Mediterranean macro-algae as dynamic factors for biodiesel production. Oceanologia 57, 86-92 (2015).

58. Kim, M. K., Dubacq, J. P., Thomas, J. C. & Giraud, G. Seasonal variations of triacylglycerols and fatty acids in Fucus serratus. Phytochemistry 43, 49-55 (1996).

59. Madden, M., Mitra, M., Ruby, D. & Schwarz, J. Seasonality of selected nutritional constituents of edible delmarva seaweeds. J. Phycol. 48, 1289-1298 (2012).

60. Moreira, A. S. P. et al. Polar Lipids of Commercial Ulva spp . of Different Origins : Profiling and Relevance for Seaweed Valorization. mdpi J. food (2021).

61. El-Manawy, I., Nassar, M. & Rashedy, S. Spatial and temporal variations in the nutritional composition of some seaweeds from the Red Sea, Egypt. Egypt. J. Phycol. 20, 29-50 (2019).

62. Rajauria, G., Cornish, L., Ometto, F., Msuya, F. E. & Villa, R. Identification and selection of algae for food, feed, and fuel applications. en Seaweed Sustainability 315-346 (Elsevier Inc., 2015). doi:10.1016/B978-0-12-418697-2/00012-X.

63. Queirós, A. S. et al. Valuable nutrients from ulva rigida: Modulation by seasonal and cultivation factors. Appl. Sci. 11, (2021).

64. Masaló, I.; Oca, J.; Ferrer, J.; Cremades, J.; Pintado, J.; Jiménez, P. Influence of Growing Conditions on Ulva Ohnoi Composition Cultivated in an IMTA-RAS System. 6-8 (2016).

65. Dewi, E. N., Darmanto, D. & Ambariyanto, A. Nutrition of Edible Seaweed Kappaphycus alvarezii Related to Different Environmental Coastal Water Condition. Omni-Akuatika 14, 59-65 (2018).

66. Abirami, R. G. & Kowsalya, S. Nutrient and nutraceutical potentials of seaweed biomass Ulva lactuca and Kappaphycus alvarezii. Agric. Sci. Technol. 5, 1-7 (2011).

67. Hurtado, A. Q., Reis, R. P. & Loureiro, R. Kappaphycus (Rhodophyta) Cultivation : Problems and the Impacts of Acadian Marine Plant Extract Powder. (2014) doi:10.1201/b17540-9.

68. Magnusson, M., Mata, L., de Nys, R. & Paul, N. A. Biomass, Lipid and Fatty Acid Production in Large-Scale Cultures of the Marine Macroalga Derbesia tenuissima (Chlorophyta). Mar. Biotechnol. 16, 456-464 (2014).

69. Khotimchenko, S. V. & Yakovleva, I. M. Lipid composition of the red alga Tichocarpus crinitus exposed to different levels of photon irradiance. Phytochemistry 66, 73-79 (2005).

70. Schmid, M., Guihéneuf, F. & Stengel, D. B. Plasticity and remodelling of lipids support acclimation potential in two species of low-intertidal macroalgae, Fucus serratus (Phaeophyceae)

10

and Palmaria palmata (Rhodophyta). Algal Res. 26, 104-114 (2017).

71. Simatupang, N. F. et al. Growth and product quality of the seaweed Kappaphycus alvarezii from different farming locations in Indonesia. Aquac. Reports 20, 100685 (2021).

72. Denis, C. et al. Study of the chemical composition of edible red macroalgae Grateloupia turuturu from Brittany (France). Food Chem. 119, 913-917 (2010).

73. Lahaye, M., Jimenez, M. & Garcia-reina, G. Natural Decoloration , Composition and Increase in Dietary Fibre & tent of an Edible Marine Algae , Ulva rigida (Chlorophyta), Grown under Different Nitrogen Conditions. 99-104 (1995).

74. Yalcin, A. S. and I. The seasonal changes in endogenous levels of Iindole-3-Acetic acid,Gibberellic Acid,Zeatin and Abscisic Acid in Stems of some apple varieties(Malus sylvestris Miller).pdf. Asian J. Plant Sci. (2008).

75. Layek, J. et al. Seaweed extract as organic bio-stimulant improves productivity and quality of rice in eastern Himalayas. J. Appl. Phycol. 30, 547-558 (2018).

76. Pan, X. et al. Effects of gibberellin A 3 on growth and microcystin production in Microcystis aeruginosa (cyanophyta). 165, (2008).

77. Agarwal, P., Patel, K., Das, A. K., Ghosh, A. & Agarwal, P. K. Insights into the role of seaweed Kappaphycus alvarezii sap towards phytohormone signalling and regulating defence responsive genes in Lycopersicon esculentum. J. Appl. Phycol. 28, 2529-2537 (2016).

78. Dumale, J. V., Gamoso, G. R., Manangkil, J. M. & Divina, C. C. Detection and quantification of auxin and gibberellic acid in Caulerpa racemosa. Int. J. Agric. Technol. 14, 653-660 (2018).

79. Spagnuolo, D. et al. Screening on the Presence of Plant Growth Regulators in High Biomass Forming Seaweeds from the Ionian Sea (Mediterranean Sea). Sustain. 14, (2022).

80. Fellah, F., Louaileche, H., Dehbi-Zebboudj, A. & Touati, N. Seasonal variations in the phenolic compound content and antioxidant activities of three selected species of seaweeds from Tiskerth islet, Bejaia, Algeria. J. Mater. Environ. Sci. 8, 4451-4456 (2017).

81. Siatka, T. & Kašparová, M. Seasonal variation in total phenolic and flavonoid contents and DPPH scavenging activity of Bellis perennis L. flowers. Molecules 15, 9450-9461 (2010).

82. Ahmed, D., Baig, H. & Zara, S. Seasonal variation of phenolics, flavonoids, antioxidant and lipid peroxidation inhibitory activity of methanolic extract of Melilotus indicus and its sub-fractions in different solvents. Int. J. Phytomedicine 4, 326-332 (2012).

83. Farasat, M., Khavari-Nejad, R. A., Nabavi, S. M. B. & Namjooyan, F. Antioxidant activity, total phenolics and flavonoid contents of some edible green seaweeds from northern coasts of the Persian gulf. Iran. J. Pharm. Res. 13, 163-170 (2014).

84. Lombardo, S., Pandino, G., Mauro, R. & Mauromicale, G. Variation of phenolic content in globe artichoke in relation to biological, technical and environmental factors. Ital. J. Agron. 4, 181-189 (2009).

85. Pedro, J., Cardoso, C., Afonso, F. & Bandarra, N. M. Season affects three insufficiently studied seaweed species (Bifurcaria bifurcata , Codium sp ., Ericaria selaginoides): bioactivity alterations. Appl. Phycol. 3, 98-108 (2022).

86. Nenadis, N. et al. Interactive effects of UV radiation and reduced precipitation on the seasonal leaf phenolic content/composition and the antioxidant activity of naturally growing Arbutus unedo plants. J. Photochem. Photobiol. B Biol. 153, 435-444 (2015).

87. Mohamed, N. & Abdullah, A. Comparison of total phenolic content and antioxidant activity of Kappaphycus alvarezii from Langkawi and Semporna. AIP Conf. Proc. 1784, (2016).

88. Sobuj, M. K. A. et al. Effect of solvents on bioactive compounds and antioxidant activity of Padina tetrastromatica and Gracilaria tenuistipitata seaweeds collected from Bangladesh. Sci. Rep. 11, 1-13 (2021).

89. Kałużewicz, A. et al. The effects of plant density and irrigation on phenolic content in cauliflower. Hortic. Sci. 44, 178-185 (2017).

90. Danesi, F., Valli, V., Elementi, S. & D'Antuono, L. F. The Agronomic Techniques as Determinants of the Phenolic Content and the Biological Antioxidant Effect of Palm-Tree Kale. Food Nutr. Sci. 05, 1-7 (2014).

91. Björkman, M. et al. Phytochemicals of Brassicaceae in plant protection and human health - Influences of climate, environment and agronomic practice. Phytochemistry 72, 538-556 (2011).

92. Wu, L., Deng, Z., Cao, L. & Meng, L. Effect of plant density on yield and Quality of Perilla sprouts. Sci. Rep. 10, 1-8 (2020).

93. Cheng, S. Y., Xu, F. & Wang, Y. Advances in the study of flavonoids in Ginkgo biloba leaves. J. Med. Plants Res. 3, 1248-1252 (2009).

94. Ball, R. A., Purcell, L. C. & Vories, E. D. Short-season soybean yield compensation in response to population and water regime. Crop Sci. 40, 1070-1078 (2000).

95. Magnusson, M. et al. Manipulating antioxidant content in macroalgae in intensive land-based cultivation systems for functional food applications. Algal Res. 8, 153-160 (2015).

96. Tretiak, S. et al. Optimizing antioxidant activity in Agarophyton vermiculophyllum for functional packaging. Algal Res. 54, 102232 (2021).

97. Campos, A. M. et al. Azorean macroalgae (Petalonia binghamiae, Halopteris scoparia and Osmundea pinnatifida) bioprospection: a study of fatty acid profiles and bioactivity. Int. J. Food Sci. Technol. 54, 880-890 (2019).